WOODHEAD PUBLISHING SERIES IN ENERGY

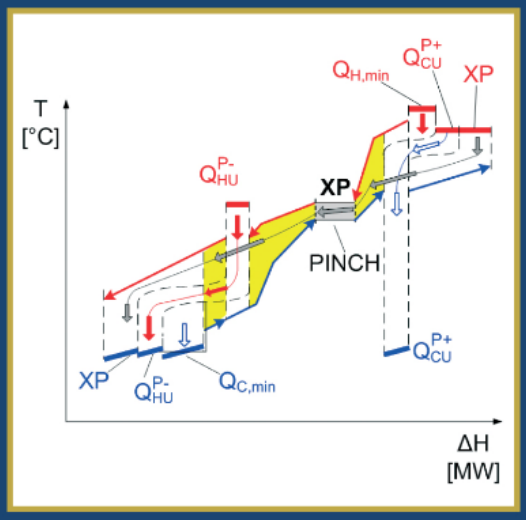

Handbook of Process Integration (PI)

Minimisation of energy and water use, waste and emissions

Edited by Jiří J. Klemeš

WP
WOODHEAD PUBLISHING

Handbook of Process Integration (PI)

© Woodhead Publishing Limited, 2013

Related titles:

Handbook of water and energy management in food processing
(ISBN 978-1-84569-195-0)

The coal handbook: Towards cleaner production: Coal production (Volume 1)
(ISBN 978-0-85709-422-3)

The coal handbook: Towards cleaner production: Coal utilisation (Volume 2)
(ISBN 978-1-78242-116-0)

Details of these books and a complete list of titles from Woodhead Publishing can be obtained by:

- visiting our web site at www.woodheadpublishing.com
- contacting Customer Services (e-mail: sales@woodheadpublishing.com; fax: +44 (0) 1223 832819; tel.: +44 (0) 1223 499140 ext. 130; address: Woodhead Publishing Limited, 80, High Street, Sawston, Cambridge CB22 3HJ, UK)
- in North America, contacting our US office (e-mail: usmarketing@woodheadpublishing.com; tel.: (215) 928 9112; address: Woodhead Publishing, 1518 Walnut Street, Suite 1100, Philadelphia, PA 19102–3406, USA)

If you would like e-versions of our content, please visit our online platform: www.woodheadpublishingonline.com. Please recommend it to your librarian so that everyone in your institution can benefit from the wealth of content on the site.

We are always happy to receive suggestions for new books from potential editors. To enquire about contributing to our Energy series, please send your name, contact address and details of the topic/s you are interested in to sarah.hughes@woodheadpublishing.com. We look forward to hearing from you.

The team responsible for publishing this book:

Commissioning Editor: Sarah Hughes
Publications Coordinator: Steven Mathews
Project Editor: Rachel Cox
Editorial and Production Manager: Mary Campbell
Production Editor: Richard Fairclough
Project Manager: Newgen Knowledge Works Pvt Ltd
Copyeditor: Newgen Knowledge Works Pvt Ltd
Proofreader: Newgen Knowledge Works Pvt Ltd
Cover Designer: Terry Callanan

© Woodhead Publishing Limited, 2013

Woodhead Publishing Series in Energy: Number 61

Handbook of Process Integration (PI)

Minimisation of Energy and Water Use, Waste and Emissions

Edited by
Jiří J. Klemeš

Oxford Cambridge Philadelphia New Delhi

© Woodhead Publishing Limited, 2013

Published by Woodhead Publishing Limited,
80 High Street, Sawston, Cambridge CB22 3HJ, UK
www.woodheadpublishing.com
www.woodheadpublishingonline.com

Woodhead Publishing, 1518 Walnut Street, Suite 1100,
Philadelphia, PA 19102-3406, USA

Woodhead Publishing India Private Limited, 303 Vardaan House, 7/28 Ansari Road,
Daryaganj, New Delhi – 110002, India
www.woodheadpublishingindia.com

First published 2013, Woodhead Publishing Limited
© Woodhead Publishing Limited, 2013. Note: the publisher has made every effort to ensure that permission for copyright material has been obtained by authors wishing to use such material. The authors and the publisher will be glad to hear from any copyright holder it has not been possible to contact.
The authors have asserted their moral rights.

This book contains information obtained from authentic and highly regarded sources. Reprinted material is quoted with permission, and sources are indicated. Reasonable efforts have been made to publish reliable data and information, but the authors and the publisher cannot assume responsibility for the validity of all materials. Neither the authors nor the publisher, nor anyone else associated with this publication, shall be liable for any loss, damage or liability directly or indirectly caused or alleged to be caused by this book.

Neither this book nor any part may be reproduced or transmitted in any form or by any means, electronic or mechanical, including photocopying, microfilming and recording, or by any information storage or retrieval system, without permission in writing from Woodhead Publishing Limited.

The consent of Woodhead Publishing Limited does not extend to copying for general distribution, for promotion, for creating new works, or for resale. Specific permission must be obtained in writing from Woodhead Publishing Limited for such copying.

Trademark notice: Product or corporate names may be trademarks or registered trademarks, and are used only for identification and explanation, without intent to infringe.

British Library Cataloguing in Publication Data
A catalogue record for this book is available from the British Library.

Library of Congress Control Number: 2013940962

ISBN 978-0-85709-593-0 (print)
ISBN 978-0-85709-725-5 (online)
ISSN 2044-9364 Woodhead Publishing Series in Energy (print)
ISSN 2044-9372 Woodhead Publishing Series in Energy (online)

The publisher's policy is to use permanent paper from mills that operate a sustainable forestry policy, and which has been manufactured from pulp which is processed using acid-free and elemental chlorine-free practices. Furthermore, the publisher ensures that the text paper and cover board used have met acceptable environmental accreditation standards.

Cover artwork: Petar S. Varbanov

Typeset by Newgen Knowledge Works Pvt Ltd, India
Printed by Lightning Source

© Woodhead Publishing Limited, 2013

Contents

Contributor contact details *xviii*
Woodhead Publishing Series in Energy *xliii*
Foreword *xlvii*

Part I Overview of Process Integration and Analysis 1

1 Process Integration (PI): An Introduction 3
Jiři Jaromir Klemeš, University of Pannonia, Veszprém, Hungary

1.1 Introduction 3
1.2 A Short History of Process Integration (PI) 7
1.3 Current Centres of Expertise in PI 12
1.4 Sources of Further Information 21
1.5 References 22

2 Basic Process Integration Terminology 28
Petar Sabev Varbanov, University of Pannonia, Veszprém, Hungary

2.1 Introduction 28
2.2 Process Integration Terms: The Importance of Context 29
2.3 Fundamental Process Integration Terms 30
2.4 Conventions: Symbols for Heaters and Coolers 74
2.5 References 75
2.6 Appendix: Nomenclature 76

3 Process Design, Integration and Optimisation: Advantages, Challenges and Drivers 79
Vasile Lavric, University 'Politehnica' of Bucharest, Romania

3.1 Introduction 79
3.2 Grassroots Design versus Retrofit Design 84

© Woodhead Publishing Limited, 2013

3.3 Process Integration 90
3.4 Integration versus Intensification 97
3.5 Process Integration Techniques 98
3.6 Optimisation of Integrated Processes 102
3.7 Controllability of Integrated Processes 106
3.8 Process Integration under Disturbances 112
3.9 References 113

Part II Heat Integration 127

4 Heat Integration: Targets and Heat Exchanger Network Design 129
Truls Gundersen, Norwegian University of Science and Technology, Trondheim, Norway

4.1 Introduction 129
4.2 Stages in the Design of Heat Recovery Systems 132
4.3 Data Extraction 134
4.4 Performance Targets 138
4.5 Process Modifications 146
4.6 Network Design 153
4.7 Design Evolution 159
4.8 Conclusion 165
4.9 Sources of Further Information 166
4.10 References 166

5 Application of Process Integration to the Synthesis of Heat and Power Utility Systems Including Combined Heat and Power (CHP) and Industrial Heat Pumps 168
Thore Berntsson, Simon Harvey and Matteo Morandin, Chalmers University of Technology, Gothenburg, Sweden

5.1 Introduction 168
5.2 Targeting Utility Loads and Temperature Levels 169
5.3 Integration of Advanced Energy Conversion Cycles as Process Utilities: Basic Concepts 176
5.4 Process Integration of Heat Engines 181
5.5 Process Integration of Heat Pumps 190
5.6 Sources of Further Information and Advice 196
5.7 References 198

© Woodhead Publishing Limited, 2013

6 Total Site Methodology 201
Simon Perry, The , UK

6.1 Introduction 201
6.2 Data Extraction for Total Sites 203
6.3 Total Site Profiles and Total Site Composite Curves 212
6.4 Site Utility Grand Composite Curve (SUGCC) 219
6.5 Conclusion 222
6.6 Sources of Further Information 223
6.7 References 224

7 Extending Total Site Methodology to Address Varying Energy Supply and Demand 226
Petar Sabev Varbanov, University of Pannonia, Veszprém Hungary

7.1 Introduction 226
7.2 Characteristics of Energy Supply and Demand 228
7.3 Thermal Energy Storage and Integrated Architecture 232
7.4 Terminology for Process Streams and Utilities 235
7.5 Identification of Time Slices 236
7.6 Heat Cascades for the Evaluation of Total Site Targets When There Is Variation in Supply and Demand 239
7.7 Case Study: Integration of Solar Thermal Energy into a Locally Integrated Energy Sector (LIES) 250
7.8 Conclusion 256
7.9 Sources of Further Information 256
7.10 References 258
7.11 Appendix: Nomenclature 260

8 Analysis and Design of Heat Recovery Systems for Grassroots and Retrofit Situations 262
Truls Gundersen, Norwegian University of Science and Technology, Trondheim, Norway

8.1 Introduction 262
8.2 Extended Procedures for Grassroots Analysis 264
8.3 Extended Procedures for Grassroots Design 273
8.4 Retrofit Analysis and Design 281
8.5 Use of Optimisation for Heat Exchanger Network Synthesis 295

© Woodhead Publishing Limited, 2013

8.6 Conclusion 303
8.7 Sources of Further Information 304
8.8 References 306

9 Heat Integration in Batch Processes 310
Thokozani Majozi, University of Pretoria, South Africa and Council for Scientific and Industrial Research, South Africa

9.1 Introduction 310
9.2 Graphical Technique for Heat Integration in Batch Process 313
9.3 Mathematical Technique for Heat Integration of Batch Plants 324
9.4 Case Study of a Multipurpose Batch Facility 335
9.5 Industrial Case Study 339
9.6 Conclusion 346
9.7 Sources of Further Information 346
9.8 References 347
9.9 Appendix: Glover Transformation 349

Part III Mass Integration 351

10 Water Pinch Analysis for Water Management and Minimisation: An Introduction 353
Sharifah Rafidah Wan Alwi and Zainuddin Abdul Manan, Process Systems Engineering Centre (PROSPECT), Faculty of Chemical Engineering, Universiti Teknologi Malaysia, Johor Bahru, Malaysia

10.1 Approaches for Water Management and Minimisation 353
10.2 Water Integration and Water Pinch Analysis 355
10.3 Water Pinch Analysis Steps 357
10.4 Examples of Successful Case Studies 374
10.5 Sources of Further Information and Advice 378
10.6 References 379
10.7 Appendix: Nomenclature 381

11 Using Systematic Design Methods to Minimise Water Use in Process Industries 383
Jin-Kuk Kim, Hanyang University, Seoul, South Korea

11.1 Introduction 383
11.2 Water Use in Process Industries 386
11.3 Process Integration for Water Systems 388

© Woodhead Publishing Limited, 2013

11.4 Conclusion and Future Trends 397
11.5 Sources of Further Information 398
11.6 References 399

12 Synthesis of Water Networks with Water Loss and Gain via an Extended Pinch Analysis Technique 401
Xiao Feng and Chun Deng, China University of Petroleum, Beijing, China

12.1 Introduction 401
12.2 Targeting a Single Water-Using Process 405
12.3 Process-based Graphical Approach (PGA) for Synthesis of Direct Reuse Water Networks 411
12.4 Conclusion 419
12.5 Sources of Further Information and Advice 419
12.6 Acknowledgements 419
12.7 References 420
12.8 Appendix: Nomenclature 421

13 Conserving Material Resources through Process Integration: Material Conservation Networks 422
Mahmoud M. El-Halwagi, Texas A&M University, USA

13.1 Introduction 422
13.2 Overall Targeting of Material Conservation Networks 424
13.3 Mass Exchange Networks 426
13.4 Water-Pinch Analysis 429
13.5 Direct Recycle and Material Recycle Pinch Diagram 431
13.6 Property-Based Material Recycle Pinch Diagram 433
13.7 References 437
13.8 Appendix: Nomenclature 439

Part IV Extended Process Integration 441

14 Process Integration for Cleaner Process Design 443
Dominic C. Y. Foo and Denny K. S. Ng, University of Nottingham Malaysia, Selangor, Malaysia

14.1 Introduction 443
14.2 A Revised 'Onion Diagram' 443
14.3 Different Models for Total Material Network (TMN) 446
14.4 Case Study: Water Minimisation in a Water Fabrication Plant 451

© Woodhead Publishing Limited, 2013

14.5 Conclusion 457
14.6 Sources of Further Information 457
14.7 References 458
14.8 Appendix: Nomenclature 459

15 Process Integration Concepts for Combined Energy and Water Integration 461
Luciana Elena Savulescu, Natural Resources Canada – Varennes, Canada and Alberto Alva-Argaez, Process Ecology Inc., Canada

15.1 Introduction 461
15.2 Water–Energy Specifics and Challenges 463
15.3 Water Path Concept 466
15.4 State-of-the-Art Methodology for Combined Energy and Water Integration 468
15.5 Sequential, Simultaneous, Mathematical Programming 476
15.6 Conclusion 478
15.7 Sources of Further Information 479
15.8 References 480

16 Process Integration Techniques for Cogeneration and Trigeneration Systems 484
Martín Picón-Núñez, University of Guanajuato, México and José Martín Medina-Flores, Polytechnic University of Guanajuato, México

16.1 Introduction 484
16.2 Combined Heat and Power 485
16.3 Heat Integration of Trigeneration Systems 488
16.4 Conclusions 500
16.5 Sources of Further Information 501
16.6 References 501
16.7 Appendix: Nomenclature 502

17 Pinch Analysis for Sustainable Energy Planning Using Diverse Quality Measures 505
Raymond R. Tan, De La Salle University, Manila, Philippines and Dominic C. Y. Foo, University of Nottingham, Selangor, Malaysia

17.1 Introduction 505
17.2 Generalised Problem Statement 508

© Woodhead Publishing Limited, 2013

17.3 Graphical Targeting Procedure 510
17.4 Case Studies 513
17.5 Conclusion 519
17.6 Sources of Further Information 519
17.7 References 520
17.8 Appendix 522

18 A Unified Targeting Algorithm for Diverse Process Integration Problems 524
Uday V. Shenoy, Synew Technologies, India

18.1 Introduction to Targeting Algorithms 524
18.2 Unified Approach to Diverse Resource Optimisation Problems 525
18.3 Basis for Unification 527
18.4 Unified Targeting Algorithm (UTA) 532
18.5 Heat Exchange Networks (HENs) and Mass Exchange Networks (MENs) 541
18.6 Water Networks: Case Study of a Specialty Chemical Plant 548
18.7 Hydrogen and Other Gas Networks 550
18.8 Property-Based Material Reuse Networks 558
18.9 Alternative Approaches to Targeting 561
18.10 Conclusion 564
18.11 Sources of Further Information 565
18.12 References 565
18.13 Appendix: Nomenclature 569

19 A Process Integration Approach for Supply Chain Development 571
Hon Loong Lam and W. P. Q. Ng, The University of Nottingham, Malaysia, Selangor, Malaysia

19.1 Introduction 571
19.2 Supply Chain Characteristics and Performance Measurement 572
19.3 Supply Chain Development with Process Integration 576
19.4 Case Studies 584
19.5 Future Trends 592
19.6 Sources of Further Information 592
19.7 References 593

© Woodhead Publishing Limited, 2013

20 Application of Heat Recovery Loops to Semi-continuous Processes for Process Integration 594
Michael R. W. Walmsley, Martin John Atkins and Timothy G. Walmsley, University of Waikato, New Zealand

20.1 Introduction 594
20.2 Indirect Heat Recovery Systems 595
20.3 Application of Heat Recovery Loops to Semi-continuous Plants 600
20.4 A More Complex Example of a Heat Recovery Loop (HRL) 613
20.5 Case Study: Semi-continuous Multi-plant Dairy Factory 618
20.6 Conclusion and Future Trends 626
20.7 Sources of Further Information 627
20.8 References 627

Part V Applications and Case Studies 631

21 Applications of Energy and Water Process Integration Methodologies in Oil Refineries and Petrochemical Complexes 633
M. Hassan Panjeshahi, University of Tehran, Iran

21.1 Introduction 633
21.2 Heat and Power Integration 634
21.3 Water and Wastewater Minimisation 667
21.4 Effluent Treatment and Regeneration 686
21.5 Conclusion 699
21.6 Sources of Further Information 701
21.7 References 702

22 Process Integration of an Oil Refinery Hydrogen Network 705
Nan Zhang, Process Integration Limited Manchester, UK

22.1 Introduction 705
22.2 Technology Review 706
22.3 An Industrial Case Study 711
22.4 Hydrogen Management in the Wider Context of Process Integration: Future Trends 718
22.5 Conclusion 722
22.6 Sources of Further Information 722
22.7 References 723

© Woodhead Publishing Limited, 2013

23 Retrofit Mass Integration of Acid Gas Removal Systems in Petrochemical Plants 725
Duncan McKenzie Fraser, University of Cape Town, South Africa

23.1 Introduction 725
23.2 Review of Previous Work on Mass Exchanger Network Synthesis (MENS) and Retrofit of Existing Systems 727
23.3 Systems Studied: Venturi Scrubber System and Ethanolamine Absorber System 734
23.4 Pinch Approach 736
23.5 Hybrid Approach 741
23.6 Solution Equilibria 744
23.7 Results and Discussion 746
23.8 Conclusions and Sources of Further Information 749
23.9 Acknowledgements 749
23.10 References 750
23.11 Appendix: Nomenclature 751

24 Applications of Pinch Technology to Total Sites: A Heavy Chemical Industrial Complex and a Steel Plant 752
Kazuo Matsuda, Chiyoda Corporation, Japan

24.1 Introduction 752
24.2 Case Study of a Heavy Chemical Complex 753
24.3 Case Study of a Steel Plant 757
24.4 Conclusion 761
24.5 Sources of Further Information 762
24.6 Acknowledgements 762
24.7 References 762

25 Applications of Process Integration Methodologies in the Pulp and Paper Industry 765
Jean-Christophe Bonhivers and Paul R. Stuart, École Polytechnique – Montreal, Canada

25.1 Introduction 765
25.2 Energy Demands and Sources in the Kraft Pulping Process 767
25.3 Relations between the Heat Exchanger and Water Networks 773
25.4 Increasing Energy Efficiency in Existing Mills 777
25.5 Methodological Developments for Heat Integration in Existing Mills 783

© Woodhead Publishing Limited, 2013

25.6 Evolution of Pulp and Paper Mills 789
25.7 Conclusion 794
25.8 Sources of Further Information 796
25.9 References 797

26 Application of Process Integration Methodologies to the Thermal Processing of Waste 799
Petr Stehlík, Brno University of Technology, Czech Republic

26.1 Introduction 799
26.2 Types of Waste Thermal Processing Plants 802
26.3 Analysis of Energy Efficiency in the TERMIZO Plant 804
26.4 Application of Heat Integration Technology 811
26.5 Conclusion 816
26.6 Sources of Further Information and Advice 816
26.7 References 817
26.8 Appendix: Nomenclature 818

27 Application of Process Integration Methodologies in the Brewing Industry 820
François Marechal, Anurag Kumar Sachan and Leandro Salgueiro, Ecole Polytechnique Fédérale de Lausanne (EPFL), Switzerland

27.1 Introduction 820
27.2 Process Flowsheet Analysis 823
27.3 Calculating Maximum Heat Recovery in the System 837
27.4 Defining the Energy Conversion System 839
27.5 Conclusion 858
27.6 Sources of Further Information 860
27.7 References 860
27.8 Appendix A: Complementary Tables 861
27.9 Appendix B: Nomenclature 862

28 Applications of Process Integration Methodologies in Dairy and Cheese Production 864
Martin John Atkins and Michael R. W. Walmsley, University of Waikato, New Zealand

28.1 Introduction 864
28.2 Application of Process Integration Methodologies 866
28.3 Selected Case Studies 873
28.4 Future Trends 879

© Woodhead Publishing Limited, 2013

28.5 Sources of Further Information 879
28.6 References 880

29 Applications of Process Integration Methodologies in Beet Sugar Plants 883
Krzysztof Urbaniec, Mirosław Grabowski and Jacek Wernik, Warsaw University of Technology, Plock Campus, Poland

29.1 Introduction 883
29.2 Sugar Production from Sugar Beet 884
29.3 Identification of Opportunities to Improve Energy and Water Use in Sugar Plants 885
29.4 Reduction of Energy Consumption 887
29.5 Reduction of Water Consumption 893
29.6 Energy and Water Use in Sugar Production Directly from Raw Beet Juice 898
29.7 Future Trends 909
29.8 Sources of Further Information and Advice 911
29.9 References 912

30 Application of Process Integration Techniques for the Efficient Use of Energy in a Urea Fertiliser Plant: A Case Study 914
Martín Picón-Núñez, University of Guanajuato, Mexico

30.1 Introduction 914
30.2 Process Description 916
30.3 Opportunities for the Reduction of Energy Consumption 924
30.4 Conclusion 932
30.5 Sources of Further Information 934
30.6 References 935
30.7 Appendix: Nomenclature 936

31 Process Integration for Energy Saving in Buildings and Building Complexes 938
Petro O. Kapustenko and Olga P. Arsenyeva, National Technical University – Kharkiv Polytechnical Institute, Ukraine

31.1 Introduction 938
31.2 Buildings as Consumers and Producers of Energy 939
31.3 Commercial and Public Buildings and Building Complexes 942
31.4 District Energy (DE) Systems and Total Site Analysis (TSA) 947
31.5 The Use of Industrial Waste Heat 951

© Woodhead Publishing Limited, 2013

31.6 Renewable Energy for Buildings 956
31.7 Conclusion 961
31.8 Sources of Further Information and Advice 961
31.9 References 962

32 Heat Transfer Enhancement in Heat Exchanger Networks 966
Robin Smith, Ming Pan and Igor Bulatov, The University of Manchester, UK

32.1 Introduction to Shell-and-Tube Heat Exchangers 966
32.2 Heat Transfer Enhancement Techniques 979
32.3 Heat Transfer Enhancement in Heat Exchanger Network Retrofit 996
32.4 Heat Transfer Enhancement in Heat Exchanger Network Retrofit with Fouling Consideration 1017
32.5 Sources of Further Information 1027
32.6 Nomenclature 1029
32.7 References 1033

33 Applications of Pinch Analysis in the Design of Isolated Energy Systems 1038
Santanu Bandyopadhyay, Indian Institute of Technology, Bombay, India

33.1 Introduction 1038
33.2 Isolated Energy Systems: Descriptions and Models 1040
33.3 Grand Composite Curve and Storage Sizing 1043
33.4 Design Space 1046
33.5 Illustrative Applications 1048
33.6 Sources of Further Information and Advice 1053
33.7 References 1054

Part VI Software Tools and Epilogue 1057

34 Software Tools for Heat Integration 1059
Igor Bulatov, The , UK

34.1 Heat Integration Software Tools 1059
34.2 Sources of Further Information and Advice 1081
34.3 References 1084

© Woodhead Publishing Limited, 2013

35 Mass and Water Integration Software Tools 1086
Igor Bulatov, The , UK

35.1 Mass and Water Integration Software Tools 1086
35.2 Sources of Further Information and Advice 1095
35.3 References 1096

36 Epilogue: The Importance of Problem Formulation and Data Extraction in Process Integration 1099
Jiří Jaromir Klemeš, University of Pannonia, Veszprém, Hungary

36.1 Introduction: Process Integration – from its Roots to its Present Strong Position 1099
36.2 Successful Applications of Process Integration 1101
36.3 Methods of Obtaining Credible High Integration (HI) Solutions 1103
36.4 Data Extraction 1104
36.5 Integration of Renewables – Fluctuating Demand and Supply 1109
36.6 Results Interpretation 1110
36.7 Conclusion: Making It Happen 1110
36.8 Sources of Further Information 1111
36.9 Acknowledgements 1111
36.10 References 1112

Index *1117*

© Woodhead Publishing Limited, 2013

(*=main contact)

Preface

Professor Dr Bodo **Linnhoff** retired from chemical engineering in 2002. In his early work at the ETH Zurich (1972) and Leeds University (PhD 1979) he developed the basics of Pinch Analysis. He worked for ICI from 1977 to 1982, took a Chafir at Inštfitute of Scfience and Technology (UMIST) in 1982 and set up Linnhoff March Ltd in 1983. Across the three organisations he set up teams for ongoing development and practical applications of Pinch Analysis. At UMIST he established the 'Research Consortium' of sponsoring companies (founder members included Shell, Exxon, BP and BASF) and later the (first ever) Department of Process Integration. He left UMIST in 1994 and built up his company Linnhoff March into a dominant worldwide supplier. He sold Linnhoff March in 2002 to KBC (FTSE listed). Bodo Linnhoff's work was recognised through many honours and awards. These include a Royal Society Gold Medal (UK, 1982), the AIChE Lifetime Achievement Award (USA, 1990) and the Ahlström Prize (now Millennium Technology Prize) (Finland, 1994).

Editor, Chapter 1 and Chapter 36

Professor Dr Jiří Jaromír **Klemeš**, DSc, is the head of the Centre for Process Integration and Intensification CPI^2 at the Research Institute of Chemical and Process Engineering, University of Pannonia, Veszprém, Hungary. After graduating from VUT Brno in Czechoslovakia, he worked for CHEPOS, a large chemical equipment manufacturing company. He was awarded a UNDP Scholarship and in 1977 he spent a period at the University of Leeds, UK where he met Bodo Linnhoff. His research interests developed from flowsheeting simulation to Heat Exchanger Network synthesis and finally to Process Integration. He has collaborated with John Flower at Leeds and Jack Ponton at the University of Edinburgh, UK. He spent nearly 20 years

© Woodhead Publishing Limited, 2013

at DPI UMIST and The wfith Bodo Lfinnhoff,
Jiři Klemeš and the DPI group. He has coordinated and continues to collaborate in numerous research projects supported by NATO and especially the EC. In 2007 he was awarded EC Marie Curie Chair of Excellence to move to Veszprém where he works jointly with Petar Varbanov and Ferenc Friedler. He is a founder and President of the PRES conference – Process Integration, Modelling and Optimisation for Energy Saving and Pollution Reduction and a Chair of the CAPE-WP of the European Federation of Chemical Engineering (EFCE).

Professor Jiří Jaromír Klemeš
Centre for Process Integration and Intensification – CPI^2
Research Institute of Chemical and Process Engineering
University of Pannonia
Egyetem utca 10
Veszprém H-8200
Hungary

Email: klemes@cpi.uni-pannon.hu

Chapters 2 and 7

Dr Petar Sabev **Varbanov**, is the deputy head of the Centre for Process Integration and Intensification CPI^2 at the Research Institute of Chemical and Process Engineering, University of Pannonia, Veszprém, Hungary.

He graduated from the University of Chemical Technology and Metallurgy – Sofia, Bulgaria, worked for Bulgarian Academy of Sciences and a Bulgarian IT Company. In September 2000 he was awarded a PhD scholarship in Process Integration at DPI UMIST supervised by Robin Smith. He won a Research Fellowship at Tyndall Centre for Research in Climate Change in Manchester. After graduation he was awarded a Marie Curie Intra-European Fellowship at Technische Universität Berlin, Germany running two years research with Gűnter Wozny. In 2007 he won another EC Marie Curie European Reintegration Grant and joined Jiří Klemeš and Ferenc Friedler in Veszprém. He is a Scientific Secretary of PRES conferences and CAPE-WP of EFCE.

Dr Petar Sabev Varbanov
Centre for Process Integration and Intensification – CPI^2
Research Institute of Chemical and Process Engineering
University of Pannonia
Egyetem utca 10
Veszprém H-8200
Hungary

Email: varbanov@cpi.uni-pannon.hu

© Woodhead Publishing Limited, 2013

Chapter 3

Professor Dr Vasile **Lavric**, is member of the Council of the Faculty of Applied Chemistry and Material Science, University 'Politehnica' of Bucharest, Romania.

He graduated University 'Politehnica' of Bucharest and worked 2 years for large complex manufacturing company ELECTROAPARATAJ. After that, he entered University 'Politehnica' of Bucharest where he is still working. His interest in Process Integration dates from 2000, with the project devoted to Chemical Reactor's Energy Integration (Chemical Pinch), in collaboration with Jacques De Ruyck, from Vrije Universiteit Brussel, and Danielle Baetens, from Vlaamse Instelling voor Technologisch Onderzoek, Belgium. Another major contribution in Process Integration is represented by the techniques developed for water/wastewater industrial networks optimisation – continuous, semi-continuous or pure batch, jointly with Prof Valentin Pleşu and Petrica Iancu. He is the recipient of 'Nicolae Teclu' award of Chemical Division of Romanian Academy.

Professor Vasile Lavric
University 'Politehnica' of Bucharest
Chemical and Biochemical Engineering Department
RO-011061, Polizu 1–7
Bucharest
Romania

Email: v_lavric@chim.upb.ro

Chapters 4 and 8

Professor Dr Truls **Gundersen**, is currently affiliated with the Department of Energy and Process Engineering, Norwegian University of Science and Technology, Trondheim, Norway.

He graduated from the Norwegian University of Science and Technology in 1982 and became involved in Process Integration in 1983 while working for Norsk Hydro. In the 1980s he was involved in software prototyping (SuperTarget), industrial applications and scientific publications in the area of Process Integration. He served as chairman of the advisory board for the Process Integration Research Consortium at UMIST 1990–1992, and he was operating agent for an Implementing Agreement on Process Integration in the IEA 1995–2002. After 12 years with Norsk Hydro, Research Centre in Porsgrunn, and 3 years at Telemark Institute of Technology in Porsgrunn, he joined the Norwegian University of Science and Technology in 1996. Process Integration has remained the main activity in research (PhDs and Postdocs), education (PI course with nearly 200 students) and publications.

© Woodhead Publishing Limited, 2013

Professor Truls Gundersen
Department of Energy and Process Engineering
Norwegian University of Science and Technology
Kolbjoern Hejes vei 1.A
NO-7491 Trondheim
Norway

Email: truls.gundersen@ntnu.no

Chapter 5

Thore **Berntsson** is professor in energy in the Process Industry at Chalmers University of Technology in Gothenburg, Sweden, Division of Heat and Power Technology. He graduated at Chalmers University. His research areas were new energy technologies, especially heat pumps, in industrial processes and systems. He then moved into the general area of Process Integration in the late 1980s. His contributions were initially connected to the pulp and paper industry, but have later been broadened to, for example, the petrochemical and refinery industries. Today biorefinery concepts in all industrial sectors are a core area in his research. In his group, methodologies for retrofitting of Heat Exchanger Networks, piping and complex industrial systems, optimisation of water amounts and temperature levels in the pulp and paper industry, integration of CCS systems in industry as well as optimisation of biorefinery systems under uncertainty have been developed. Numerous applied studies and industrial case studies have been carried out. He has been a member of the Board of the Swedish Energy Agency and has been very active internationally with direct cooperation with many groups, for example, in Canada, UK, Norway, Finland, Switzerland, Portugal, and Denmark, in EU and in IEA. In IEA, International Energy Agency, he was chair of the implementing agreement on Process Integration between 2002 and 2005 and of the implementing agreement of Pulp and Paper Industry. When these two merged into IETS, Industrial Energy Related Technologies and Systems, he was chair there and is currently vice-chair in that implementing agreement.

Professor Simon **Harvey** is the head of the Division of Heat and Power Technology at the Department of Energy and Environment, Chalmers University of Technology, Göteborg, Sweden.

He graduated in Mechanical Engineering from the Catholic University of Louvain-La-Neuve, Belgium. He received his MSc and PhD at Thayer School of Engineering, Dartmouth College, NH, USA. His research efforts were initially directed towards simulation and exergy analysis of advanced gas turbine cycles. After a period as assistant professor at the Department of Energy Systems and Environment at the Ecole des Mines in Nantes, France,

© Woodhead Publishing Limited, 2013

he moved to his current location at Chalmers University of Technology, where he was appointed full professor in Industrial Energy Systems. His current research is focused on Process Integration of biorefinery concepts at industrial process sites, with a focus on host sites in the pulping industry and the petrochemical industry. He is also active in the area of application of Total Site Analysis methodology to large industrial process sites. Another focus area is methodology for evaluation of the long-term impact of energy efficiency measures on process cash flows and Carbon Footprints. He is also very active in teaching, and is the main examiner for an MSc module in Heat Integration Methodology. He has been involved in numerous research projects in Sweden and Scandinavia. He is a member of the PRES International Scientific Committee, and is a reviewer for many international publications.

Dr Matteo **Morandin** is assistant professor at the Division of Heat and Power Technology at Department of Energy and Environment, Chalmers University of Technology, Gothenburg, Sweden.

He graduated in Mechanical Engineering from the University of Padova, Italy, on advanced exergy analysis of a cogeneration system under the co-supervision of Andrea Lazzaretto (University of Padova) and George Tsatsaronis (Berlin Technical University, Germany). His PhD studies were at the Department of Mechanical Engineering, University of Padova, under the supervision of Andrea Lazzaretto, with a focus on the synthesis and design optimisation of thermal energy systems and of energy intensive industrial processes. He obtained his PhD degree with the award of Doctor Europaeus. He has been collaborating with François Maréchal and Daniel Favrat at the Industrial Energy System Laboratory, EPFL, Lausanne, Switzerland, where he was also employed as scientific assistant. During this period he collaborated with ABB in Baden, Switzerland, for the conceptual design of a thermo-electric energy storage system. In 2011 he joined Chalmers University of Technology where he is currently carrying out research activities on synthesis and design optimisation of multi-product biorefineries and on their integration with large industrial sites.

Professor Thore Berntsson, Professor Simon Harvey* and Dr Matteo Morandin
Heat and Power Technology Division
Department of Energy and Environment
Chalmers University of Technology
412 96 Göteborg
Sweden

Email: thore.berntsson@chalmers.se; simon.harvey@chalmers.se; matteo.morandin@chalmers.se

© Woodhead Publishing Limited, 2013

Chapter 6

Simon **Perry** is a senior lecturer in the School of Chemical Engineering and Analytfical Scfience, The . He graduated wfith a Bachelor of Science in Atmospheric and Geophysical Sciences from the University of London and undertook research in urban and industrial influenced atmospheric systems at London and at UMIST.

He joined the Centre for Process Integration at UMIST in 1986, and has taught Process Integration courses at UMIST and The University of Manchester, both at undergraduate and postgraduate levels. He has also taught similar courses worldwide, both in universities and industry. His research interests have focused on improvements in efficiency in heat recovery systems and site utility systems, and he has published widely in these areas. More recent research has focused on Locally Integrated Energy Systems and the integration of renewable and waste energy in distributed systems. He has been involved in numerous research projects in the UK and the EC. He is a member of the PRES International Scientific Committee, and is a reviewer for many international publications.

Dr Simon Perry
Centre for Process Integration
School of Chemical Engineering and Analytical Science
The
Manchester M13 9PL
UK

Email: simon.perry@manchester.ac.uk

Chapter 9

Professor Thokozani **Majozi,** the Department of Chemical Engineering at the University of Pretoria (UP), South Africa. He has BScEng and MScEng degree (Chemical) from the University of Natal, South Africa. His PhD in Process Integration is from UMIST, Manchester, UK.

His main research interest is Batch Chemical Process Integration including the development of a continuous-time framework for the synthesis of batch plants and a novel technique for near zero-effluent batch chemical facilities.

He štarted hfiš profeššfional career at . Later he waš appofinted aš a senior process engineer at Dow AgroSciences and in 2002 he joined Sasol Technology as a technology leader for optimisation and integration. In 2004 he joined the University of Pretoria. He was also an associate professor in Computer Science at the University of Pannonia in Hungary (2005–2009). He is a fellow of various institutions, including Academy of Sciences of South Africa (ASSAf), Council for Scientific and Industrial Research (CSIR) and

© Woodhead Publishing Limited, 2013

the Academy of Engineering of South Africa. He was awarded the S2A3 British Association Medal (Silver) and the South African Institution of Chemical Engineers Bill Neal-May Gold Medal for his scientific contributions. He is author and co-author of numerous publications, including a book in Batch Chemical Process Integration published by Springer 2010.

Professor Thokozani Majozi
Department of Chemical Engineering
University of Pretoria
Lynnwood Road
Pretoria 0002
South Africa

Email: thoko.majozi@up.ac.za

Chapter 10

Associate Professor Dr Sharifah Rafidah **Wan Alwi,** CEng, MIChemE, is the Director of Process Systems Engineering Centre (PROSPECT) of Universiti Teknologi Malaysia (UTM), Johor Bahru, Malaysia.

She graduated from UMIST, Manchester in 2003 and later completed her PhD study on Water Integration studies in 2006. Her PhD work has won the Prince Sultan Abdul Aziz International Water Award. She also won the Green Talents 2009 Award from the Federal Ministry of Research Germany for her excellence in environmental research and was also among the five shortlisted candidates for IChemE Young Engineer Award 2009. She was awarded Highly Commended Sir Frederick Warner Prize 2011 from IChemE UK. Her main research area is in Process Integration, specifically towards Pinch analysis, where she has embarked on various Resource Conservation minimisation for heat, water, mass, gas, carbon and very recently power. She is also a certified energy manager trainer and an energy professional under Green Technology Malaysia (GTM). She has been extensively involved as a consultant in eleven consultancy projects for various companies and government agencies and has trained engineers from more than 50 companies in the field of energy and water minimisation.

Professor Dr Zainuddin **Abdul Manan** is the dean of the Faculty of Chemical Engineering, Universiti Teknologi Malaysia (UTM). He is the founding director of UTM-Process Systems Engineering Centre (PROSPECT). He holds a BSc in Chemical Engineering from the University of Houston, USA, MSc in Process Integration from the Department of Process Integration, UMIST, UK, and PhD in Chemical Engineering from the University of Edinburgh, Scotland. He was an engineer in PETRONAS and Hume Industries and has been extensively involved as a researcher, consultant and trainer for 20 years. He is a chartered professional engineer, a certified energy manager

© Woodhead Publishing Limited, 2013

and currently the certified lead trainer for Malaysia's energy managers' accreditation under the ASEAN Energy Management Accreditation Scheme (AEMAS). He was the co-winner of 2008 Prince Sultan Abdul Aziz International Award for Water and a vice-chairman of the Board of Judges for ASEAN Energy Awards program until 2011. He spearheaded the implementation of Sustainable Energy Management Program in UTM, and led UTM to win the 2012 ASEAN Energy Awards.

Associate Professor Ir Dr Sharifah Rafidah Wan Alwi* and Professor Zainuddin Abdul Manan
Process Systems Engineering Centre (PROSPECT)
Faculty of Chemical Engineering
Universiti Teknologi Malaysia
81310 Johor Bahru
Johor
Malaysia

Email: shasha@cheme.utm.my; zain@cheme.utm.my

Chapter 11

Dr Jin-Kuk **Kim** is an associate professor in Chemical Engineering, Hanyang University, Seoul, Republic of Korea. He completed his PhD under the supervision of Robin Smith in 2001 from the Centre for Process Integration (CPI), UMIST and his association with CPI had been continued after his PhD. He had worked within the group as a lecturer and later a senior lecturer, before joining Hanyang University in 2011. He has gained significant research experience in the wide range of Process Integration area, including design of energy systems, utility systems, separation systems, water systems and carbon capture systems from various industry-focused development and projects, especially through PIRC (Process Integration Research Consortium). His research focuses on the systematic investigation of design interactions between elements of processes, and exploits synergetic benefits from integrated design with the application of process modelling, simulation and optimisation, which is the heart of Process Integration.

Dr Jin-Kuk Kim
Department of Chemical Engineering
Hanyang University
Wangsimni-ro 222
Seongdong-gu
Seoul
Republic of Korea

Email: jinkukkim@hanyang.ac.kr

© Woodhead Publishing Limited, 2013

Chapter 12

Professor Xiao **Feng**, is a professor in College of Chemical Engineering, China University of Petroleum, Beijing, China.

She graduated from Xi'an Jiaotong University and got her BSc (1982), MSc (1985) and PhD (2000) there. She worked in Xi'an Jiaotong University from 1985 to 2009, and in 2009, she moved to China University of Petroleum. Her research interest includes Process Integration, including water, energy, and hydrogen system integration.

Dr Chun **Deng**, is an assistant professor in State Key Laboratory of Heavy Oil Processing, College of Chemical Engineering, China University of Petroleum, Beijing, China.

He graduated from Xi'an Jiaotong University, Xi'an, China in 2006 and got the BSc of Engineering. In 2006 he joined Xiao Feng's group and worked on Water System Integration. In 2007 he visited Dominic Foo's group at the University of Nottingham at Malaysia. In 2009 he visited El-Halwagi's group in Texas A&M University at College Station as a joint PhD student. He got his PhD from Xi'an Jiaotong University in 2011 and joined China University of Petroleum, Beijing.

Professor Xiao Feng* and Dr C. Deng
State Key Laboratory of Heavy Oil Processing
College of Chemical Engineering
China University of Petroleum, Beijing
18 Fuxue Road
Changping
Beijing 102249
P. R. China

Email: xfeng@cup.edu.cn

Chapter 13

Professor Dr Mahmoud M. **El-Halwagi** is holder of the McFerrin Professorship at the Artie McFerrin Department of Chemical Engineering, Texas A&M University, USA.

Professor El-Halwagi has a BS and MS from Cairo University and a PhD from the University of California, Los Angeles, all in chemical engineering. His main research interests involve sustainable design through Process Integration. He is the author of three textbooks on Process Integration, the co-editor of five books, and the co-author of more than 200 papers and book chapters. He has served as a consultant to a wide variety of chemical, petrochemical, petroleum, pharmaceutical, biorefining, and metal finishing

© Woodhead Publishing Limited, 2013

industries. He is the recipient of several awards including the American Institute of Chemical Engineers Sustainable Engineering Forum (AIChE SEF) Research Excellence Award, the Fluor Distinguished Teaching Award, and the US National Science Foundation's National Young Investigator Award.

Professor Mahmoud M. El-Halwagi
Department of Chemical Engineering
Texas A&M University
College Station
Texas 77843
USA

Email: El-Halwagi@tamu.edu

Chapter 14

Professor Dr Dominic C. Y. Foo is the professor of Process Design and Integration, and founding director for the Centre of Excellence for Green Technologies (CEGT) at the University of Nottingham Malaysia Campus. He is a professional engineer at Malaysia and chartered engineer at the UK. He is also a fellow for both the Institution of Chemical Engineers (IChemE) and Higher Education Academy (HEA) UK.

He obtained his BEng, MEng and PhD at Universiti Teknologi Malaysia, where he learned the fundamental knowledge of Process Integration. During his PhD, he went for a short-term research attachment with Mahmoud M. El-Halwagi at Texas A&M University, USA. His research interest in Process Integration began with Mass Integration, and later extended into Water Minimisation, and other Resource Conservation areas, covering both continuous and batch processes. He then established carbon-constrained energy planning. He is member of the editorial board of *Trans IChemE Part B* (*Process Safety & Environmental Protection*) and *Chemical Engineering Transactions*, author of the book *Process Integration for Resource Conservation* and co-editor of the book *Recent Advances in Sustainable Process Design and Optimization*. He won the Innovator of the Year Award 2009 of Institution of Chemical Engineers UK (IChemE), Young Engineer Award 2010 of the Institution of Engineers Malaysia (IEM), as well as the Outstanding Young Malaysian Award 2012.

Dr Denny K. S. Ng, is the associate professor at the Department of Chemical & Environmental Engineering and Manager of Professional Training at the Centre of Excellence for Green Technologies (CEGT), the University of Nottingham Malaysia Campus.

© Woodhead Publishing Limited, 2013

He graduated his BEng from Universiti Teknologi Malaysia, and obtained his PhD from the University of Nottingham. During his PhD, he went for several short-term research attachments with Mahmoud M. El-Halwagi at Texas A&M University, USA, Raymond R. Tan at De La Salle University, Philippines, Cheng-Liang Chen at National Taiwan University, Taiwan. He learned the fundamental knowledge of Process Integration during his undergraduate study, and further explored into water minimisation and resource conservation during his PhD. He later extended Process Integration techniques for synthesis and optimisation of integrated biorefinery, carbon-constrained energy planning, carbon capture and storage (CCS) as well as production planning. Recently, he applied his R&D output in industrial consultation projects, both in Resource Conservation and palm-oil-based integrated biorefinery. He is the recipient of World Federation of Scientists (Malaysia National Scholarship) award in 2007 and IChemE Young Chemical Engineer of the Year 2012.

Professor Dominic C. Y. Foo* and Dr Denny K. S. Ng
Department of Chemical and Environmental Engineering
Centre of Excellence for Green Technologies (CEGT)
University of Nottingham Malaysia Campus
Broga Road
43500 Semenyih
Selangor
Malaysia

Email: Dominic.Foo@nottingham.edu.my; Denny.Ng@nottingham.edu.my

Chapter 15

Dr Luciana Elena **Savulescu**, research scientist in the Industrial Systems Optimisation Group at CanmetENERGY, Natural Resources Canada, Varennes, Canada.

She graduated with a BSc degree in Chemical Engineering from the University Politehnica of Bucharest, Romania. In 1995 she joined the Department of Proceßß Integratfion (DPI) at the
Institute of Science and Technology – UMIST, UK. She was awarded the DPI PhD scholarship and the Overseas Research Students Award from the Committee of Vice-Chancellors and Principals of the Universities of the United Kingdom. She completed her PhD work on Simultaneous Energy and Water Minimisation under the supervision of Robin Smith in 1999. Since then, she is the scientific leader for research and development activities in the area of combined water and energy system integration with the Industrial Systems Optimisation Group at CanmetENERGY, Natural Resources Canada. She also provides scientific and technical

© Woodhead Publishing Limited, 2013

guidance as part of large collaborative projects involving universities such as Ecole Politechnique, Canada; EPFL, Switzerland; industries and research institutions like FPInnovations, Canada; VTT, Finland, in the field of Process Integration.

Dr Alberto **Alva-Argaez**, DSc, is a principal and senior project manager at Process Ecology Inc. With over 18 years of experience in chemical engineering research and process optimisation for sustainability, Dr Alva-Argaez has worked across multiple industries to help operating companies become more efficient in their use of energy and water. He started his career as a production engineer with Bayer and then spent ten years in Academia as research scientist and lecturer. In 1999 he joined Hyprotech/Aspentech in Calgary, AB as product manager for conceptual design software tools and thermodynamics. He later worked for seven years with Natural Resources Canada performing R&D and supporting energy-intensive industrial sectors through Process Integration and optimisation projects. With Process Ecology he has specialised in modelling and optimisation for emissions reduction in the oil and gas sector. Dr Alva-Argaez is a Biochemical Engineer who graduated from UAMI in Mexico City and holds MSc and PhD degrees from UMIST, UK.

Dr Luciana Savulescu
Industrial Systems Optimisation Group
Natural Resources Canada
1615 Lionel-Boulet, C.P. 4800
Varennes
Quebec J3X 1S6
Canada

Email: Luciana.Savulescu@RNCan-NRCan.gc.ca

Dr Alberto Alva-Argaez
Senior Project Manager
Process Ecology Inc.
105-150 Crowfoot Cr. NW
Calgary, Alberta T3G 3T2
Canada

Email: alberto@processecology.com

Chapter 16 and Chapter 30

Dr Martín **Picón-Núñez** is currently at the Department of Chemical Engineering of the University of Guanajuato in México.

He graduated as a Chemical Engineer from the University of Guanajuato and in 1989 studied the MSc course in Process Integration and the University of Manchester Institute of Science and Technology (UMIST). Upon

© Woodhead Publishing Limited, 2013

completion of this degree he continued PhD studies at the Department of Chemical Engineering of UMIST working under the supervision of Graham T. Polley, obtaining his degree in 1995. In his research, he developed techniques based on Process Integration principles for the design of multistream heat exchangers and techniques for the operability analysis of Heat Exchanger Networks. He has worked as a consultant to a number of private chemical and petrochemical companies in México in energy issues, ranging for improved heat recovery, design of cogeneration systems and optimisation of water cooling systems. Among his research interest is the development of shortcut techniques for the design of compact heat exchangers and utility systems.

Dr José Martín **Medina Flores** (Chapter 16 only) is the head of the BSc program in Energy Engineering at the Polytechnic University of Guanajuato, Cortazar, México.

He holds a PhD degree from the Department of Mechanical Engineering of the University of Guanajuato supervised by Dr Martín Picón-Núñez. He worked as a performance engineer for three years at the General Electric Centre for Research and Technological Assistance in Queretaro, México. His research interests involve the optimal design and integration of utility and heat recovery systems. He is currently collaborating with Martín Picón-Núñez from the University of Guanajuato, in projects related to the optimal integration of trigeneration systems in process plants and optimal design and selection of steam systems.

Profesor Martín Picón-Núñez*
Department of Chemical Engineering
University of Guanajuato
Noria Alta s/n
Guanajuato, Gto.
México

Email: picon@ugto.mx; piconnunez@gmail.com

Dr José Martín Medina-Flores
Department of Energy Engineering
Polytechnic University of Guanajuato
Av. Universidad
Norte s/n
Localidad Juan Alonso
Cortázar, Gto.
C.P. 38483
México

Email: jmedina@upgto.edu.mx

© Woodhead Publishing Limited, 2013

Chapter 17

Professor Raymond R. **Tan** is a university fellow and professor of Chemical Engineering as well as the director of the Centre for Engineering and Sustainable Development Research (CESDR) at De La Salle University, Manila, Philippines.

He is the author of numerous papers with an h-index of 20. Among his most important contributions are extensions of Process Integration techniques to various non-conventional areas, such as Carbon Emissions Pinch Analysis (CEPA), which he developed jointly with Dominic **Foo** of the University of Nottingham in Malaysia. His current work focuses on optimal deployment of low-carbon energy systems, such as bioenergy and CO_2 capture and storage. He is member of the editorial board of *Clean Technologies and Environmental Policy*, co-editor of the book *Recent Advances in Sustainable Process Design and Optimization* and the recipient of multiple awards from the Philippine National Academy of Science and Technology (NAST) and the National Research Council of the Philippines (NRCP).

Professor Dr Dominic C. Y. **Foo** is the professor of Process Design and Integration, and founding director for the Centre of Excellence for Green Technologies (CEGT) at the University of Nottingham Malaysia Campus. He is a professional engineer at Malaysia and chartered engineer at the UK. He is also a fellow for both the Institution of Chemical Engineers (IChemE) and Higher Education Academy (HEA) UK.

He obtained his BEng, MEng and PhD at Universiti Teknologi Malaysia, where he learned the fundamental knowledge of Process Integration. During his PhD, he went for a short-term research attachment with Mahmoud M. El-Halwagi at Texas A&M University, USA. His research interest in Process Integration began with Mass Integration, and later extended into Water Minimisation, and other Resource Conservation areas, covering both continuous and batch processes. He then established carbon-constrained energy planning. He is member of the editorial board of *Trans IChemE Part B* (*Process Safety & Environmental Protection*) and *Chemical Engineering Transactions*, author of the book *Process Integration for Resource Conservation* and co-editor of the book *Recent Advances in Sustainable Process Design and Optimization*. He won the Innovator of the Year Award 2009 of Institution of Chemical Engineers UK (IChemE), Young Engineer Award 2010 of the Institution of Engineers Malaysia (IEM), as well as the Outstanding Young Malaysian Award 2012.

Professor Raymond R. Tan*
Chemical Engineering Department
Center for Engineering and Sustainable Development Research
De La Salle University
2401 Taft Avenue

© Woodhead Publishing Limited, 2013

1004 Manila
Philippines

Email: raymond.tan@dlsu.edu.ph; natdnomyar@gmail.com

Professor Dominic C. Y. Foo
Department of Chemical and Environmental Engineering
Centre of Excellence for Green Technologies (CEGT)
University of Nottingham Malaysia
Broga Road
43500 Semenyih
Selangor
Malaysia

Email: Dominic.Foo@nottingham.edu.my
Please refer to Prof. Dominic C. Y. Foo's profile in p. xxviii.

Chapter 18

Dr Uday V. **Shenoy** is co-founder and Strategic Advisor of Syvum Technologies Inc., Canada and Synew Technologies, India. From 1988 to 2006, he was at the Indian Institute of Technology (IIT-Bombay) as professor in the Chemical Engineering Department and the Computer Aided Design Centre.

He graduated with a BTech from IIT-Bombay and a PhD from Carnegie Mellon University, USA. His research interests include Process Integration, resource optimisation, energy management, transport phenomena, polymer engineering and computer applications. He has published several research papers in reputed international journals, conducted numerous intensive courses for industry and undertaken consultancy projects in these areas. He is the sole author of a 642-page book with software titled 'Heat Exchanger Network Synthesis' published by Gulf Publishing Company, USA in 1995. He received the Amar Dye Chem Award from the Indian Institute of Chemical Engineers for excellence in R&D, and the ISTE-IPCL National Award from the Indian Society for Technical Education. He has also received the Excellence in Teaching Award, the Manudhane Best Undergraduate Teacher Award and the Manudhane Best Postgraduate Teacher Award in 2006 from IIT-Bombay. He is a full member of Sigma Xi and the New York Academy of Sciences.

Dr Uday V. Shenoy
Synew Technologies
A 502 Galleria
Hiranandani Gardens
Powai
Mumbai 400 076
India

Email: shenoys@vsnl.com

© Woodhead Publishing Limited, 2013

Chapter 19

Dr Hon Loong **Lam** is the assistant professor at the Department of Chemical and Environmental Engineering and Manager of Conference at Centre of Excellence for Green Technologies (CEGT), University of Nottingham Malaysia Campus.

He obtained double PhDs from two well-known Process Integration centres: Centre for Process Integration and Intensification CPI^2, University of Pannonia, Veszprém, Hungary and The Laboratory for Process System Engineering and Sustainable Development, University of Maribor, Slovenia. His research works are mainly related to the application of Process Integration approach in supply chain optimisation. Recently, he received several industrial and international research grants to develop the Green Supply Chain for unutilised biomass.

Dr Hon Loong Lam
Department of Chemical and Environmental Engineering
University of Nottingham Malaysia
Jalan Broga
43500 Semenyih
Selangor Darul Ehsan
Malaysia

Email: HonLoong.Lam@nottingham.edu.my; honloong.lam@gmail.com

Chapters 20 and 28

Dr Michael R. W. **Walmsley** is a senior researcher and senior lecturer in the Energy Research Centre and School of Engineering at the University of Waikato, Hamilton, New Zealand.

He graduated from the University of Auckland in Chemical Engineering in 1988, took up an academic position at Monash University, Melbourne, Australia from 1988 to 1995 and, while there, helped set up the Australian Pulp and Paper Institute. He returned to New Zealand in 1995 to take up an academic position at the University of Waikato where he has helped establish a School of Engineering and an Energy Research Centre with expertise in Process Integration applied to multi-plant semi-continuous processes, such as dairy processes.

Dr Martin John **Atkins**, is a senior research fellow for the Energy Research Group at the School of Engineering, University of Waikato, Hamilton, New Zealand.

He graduated from the University of Waikato with a PhD in Materials and Process Engineering in 2008. He then joined the Energy Research Group at the University of Waikato where he is the lead researcher in a major research programme that focuses on Process Integration of non-continuous processes and on improving the energy efficiency of the dairy industry through optimising thermal energy use and maximising heat

© Woodhead Publishing Limited, 2013

recovery. He has worked extensively and successfully with industrial end-users in industries as diverse as diary processing to pulp and paper.

Chapter 20

Mr Timothy G. **Walmsley** is a PhD candidate in the Energy Research Centre and School of Engineering at the University of Waikato, Hamilton, New Zealand.

He graduated from the University of Waikato in Materials and Process Engineering in 2011. He was awarded the Todd Foundation PhD scholarship in 2011 for research to be undertaken in the field of energy. His research focus has been devoted to the fields of fouling in gas heat recovery exchangers and Process Integration of multiple semi-continuous processes.

Dr Michael R. W. Walmsley,* Dr Martin J. Atkins and Mr Timothy G. Walmsley
Energy Research Group – Industrial Energy Efficiency Division
Faculty of Science & Engineering
The University of Waikato
Private bag 3105
Hamilton 3240
New Zealand

Email: walmsley@waikato.ac.nz; matkins@waikato.ac.nz

Chapter 21

Professor Dr M. Hassan **Panjeshahi**, Department of Chemical Engineering, the University of Tehran, Iran. He is also adjunct professor in the Department of Chemical and Petroleum Engineering, University of Calgary, Canada.

He studied his BSc at Sharif University of Technology in Iran and the MSc and PhD at the UMIST in the UK. He is a member of editorial board of six scientific journals and member of several scientific societies and institutions, including Iran Academy of Sciences. He is the founder and the first president of the Iran Energy Association and also the founder and the first editor-in-chief of the *Iranian Journal of Energy* affiliated to the World Energy Council. For five years he was chancellor of the Petroleum University of Technology in Iran. He has been working in the field of Process Integration over the past 25 years, dealing with Process Optimisation, Energy Conservation, Emission Reduction, Water and Waste Water Minimisation in Process Industries. He has performed many consultancy services for different process industries and carried out numerous applied research projects in different aspects of Process Integration. He has developed five engineering software tools in the field of Process Integration, delivered many keynote lectures in conferences and seminars

© Woodhead Publishing Limited, 2013

and also published extensively. He was the recipient of the 1990 Moulton Gold Medal awarded by the IChemE UK for the best paper written in Chemical Engineering, about 'Retrofit of Heat Exchanger Networks' and also 2003 Behsaman Prize by The 4th Iranian Energy Congress as 'Premier Researcher'.

Professor Mohammad Hassan Panjeshahi
Department of Chemical Engineering
University of Tehran
Iran

Email: mhpanj@ut.ac.ir

Chapter 22

Dr Nan **Zhang** is the chief executive officer at Process Integration Limited, and a lecturer at the Centre for Process Integration, The University of Manchester, UK.

He graduated with BSc in Chemical Engineering from Tsinghua University in Beijing, China, and with PhD from DPI, UMIST. In between, he spent five years as a process engineer with Sinopec. Since working as an academic at DPI, UMIST from 2000, his research interest includes refinery optimisation, refinery hydrogen management, refinery process modelling, emissions reduction and reliability, availability and maintainability. In 2007 he co-founded Process Integration Limited with Robin Smith and other colleagueš at the Centre for Procešš Integratfion, the .
Since then he has also been active in commercial development and applications of Process Integration technologies.

Dr Nan Zhang
Process Integration Limited
One Central Park
Northampton Road
Monsall
Manchester M40 5BP
UK

Email: nan.zhang@processint.com

Chapter 23

Professor Emeritus Duncan McKenzie **Fraser**, University of Cape Town (UCT), South Africa.

He obtained a BSc(Eng) in Chemical Engineering with first class honours and a PhD on turbulent air flow from UCT. He was a process

© Woodhead Publishing Limited, 2013

engineer at the Caltex Refinery in Cape Town. In 1979 he was appointed as a senior lecturer in the Chemical Engineering Department at UCT, later promoted to associate professor and in 2007 to Professor. He was elected an emeritus professor when he retired in 2012. His research interests are in Process Synthesis and Engineering Education. In Process Synthesis, his work started in Heat Exchanger Network Synthesis, making use of Pinch Technology. He then extended this work into the field of Mass Exchange Network Synthesis and to the use of Mathematical Programming for the optimisation of Heat and Mass Exchange Network Designs. He has collaborated with colleagues in Hungary, India, Malaysia and Slovenia in this research. He has also run workshops in this area for industry in India, Malaysia and South Africa.

Professor Duncan McKenzie Fraser
Department of Chemical Engineering
University of Cape Town
7701 Rondebosch
South Africa

Email: Duncan.Fraser@uct.ac.za

Chapter 24

Kazuo **Matsuda** is a leader in Sustainable Business Development Section, Chiyoda Corporation, Japan.

He graduated with a Bachelor of Science in Hydrocarbon Chemistry from Kyoto University in 1977. He has been working for one of the leading engineering company, Chiyoda. He has been responsible for a great number of Energy Conservation studies at heavy chemical complexes with government fund for long years. Through such studies, he was able to establish a way of diagnosis of Energy Conservation, engineering of Energy Conservation and verification of Energy Conservation for plant. He is a member of the PRES International Scientific Committee, and is a reviewer for many international publications.

Mr Kazuo Matsuda
Sustainable Business Development Section
Chiyoda Corporation
4–6-2 Minatomirai
Nishi-ku
Yokohama 220–8765
Japan

Email: kmatsuda@ykh.chiyoda.co.jp

© Woodhead Publishing Limited, 2013

Chapter 25

Professor Paul R. **Stuart** is a professor in the Chemical Engineering Department at École Polytechnique of the University of Montréal, where he is also senior chair holder of the first Natural Sciences and Engineering Research Council of Canada (NSERC) Design Engineering Chair entitled *Process Integration in the Pulp & Paper Industry*.

He received his PhD in Chemical Engineering from McGill University in Montréal. He is a fellow of the Canadian Academy of Engineering, and a past president of the Canadian Society of Chemical Engineering (CSChE). He is founder and principal consultant for his one-man consulting company – Processys Inc. – and co-founder and principal consultant of EnVertis Inc. The latter company focuses upon, amongst other things, the application of Process Integration and process systems engineering for improving the competitive position of forestry companies, including their transformation to improved business models such as the biorefinery.

Dr Jean-Christophe **Bonhivers** is a graduate of the University of Louvain and University of Liege (Belgium), and received his PhD in Chemical Engineering at École Polytechnique de Montréal (Canada) in the NSERC Design Engineering Chair for Process Integration for the pulp and paper industry.

Dr Jean-Christophe Bonhivers and Professor Paul Stuart*
NSERC Chair in Design Engineering
Department of Chemical Engineering
École Polytechnique de Montréal
University of Montreal
P.O. Box 6079, Station Centre-Ville
Montreal
Quebec H3C 3A7
Canada

Email: jean-christophe.bonhivers@polymtl.ca; paul.stuart@polymtl.ca;

Chapter 26

Professor Petr **Stehlík** is a director of the Institute of Process and Environmental Engineering at Brno University of Technology in the Czech Republic. He currently holds the position of vice president of the Czech Society of Chemical Engineers.

He had several years of experience in engineering practice before joining the university, and at present he is also a director of research and development of a certified engineering and contracting company with activities aimed especially at waste to energy technologies. Some of his main activities include: executive editor of Heat Transfer Engineering and guest editor of

© Woodhead Publishing Limited, 2013

other journals, coordinator/contractor of national and international research projects. His research and application activities are aimed at waste to energy systems, applied heat transfer, Process Integration of special cases, energy saving and environmental protection. He has founded a research and development NETME Centre (New Technologies for Mechanical Engineering). He is a co-founder and vice president of PRES conference – Process Integration, Modelling and Optimisation for Energy Saving and Pollution Reduction.

Professor Petr Stehlík
Institute of Process and Environmental Engineering
Faculty of Mechanical Engineering
Brno University of Technology
Technicka 2
616 69 Brno
Czech Republic

Email: stehlik@fme.vutbr.cz

Chapter 27

Professor Dr François Marechal holds a Process Engineering degree and a PhD from University of Liège in Belgium in Process Integration of industrial sites under the supervision of Boris Kalitventzeff. In 2001 he moved to Ecole Polytechnique Fédérale de Lausanne (EPFL) in Switzerland where he joined the Industrial Energy Systems Laboratory. He is now heading the Industrial Process and Energy Systems Engineering (IPESE) group conducting research in the field of analysis and design of sustainable industrial energy systems. His activities focus on the development of Computer Aided Methods applying Process Integration and optimisation techniques. He has published widely in the field of energy efficiency in the industry, process system design for biofuels and electricity production, industrial ecology and sustainable energy systems in urban areas studying the optimal integration of renewable energy resources. He is a member of the scientific committee of IFP Energies Nouvelles and representative of Switzerland in the CAPE-WP of the European Federation of Chemical Engineering.

Prof. François Marechal,* Anurag Kumar Sachan and Dr Leandro Salgueiro
Industrial Energy Systems Laboratory
IPESE – IGM – STI
Ecole Polytechnique Fédérale de Lausanne
Station 9

© Woodhead Publishing Limited, 2013

CH 1015, Lausanne
Switzerland

Email: Francois.Marechal@epfl.ch; leandro.salgueiro@epfl.ch

Chapter 29

Professor Dr Krzysztof **Urbaniec**, DSc is the head of Centre of Excellence in the Reduction of Environmental Impact of Process Industries CERED at the Plock Campus of Warsaw University of Technology (WUT), Poland.

He graduated from WUT and started his professional career at WUT but after receiving his PhD he joined the engineering company CHEMADEX, Warsaw, Poland where he had served seven years as head of R&D. He returned to academic activities in 1986 when he took the post of lecturer at Lund University, Sweden and in 1989 he assumed his professorship at Plock Campus of WUT. His research interests are in the design and optimisation of process equipment and systems for thermal processes. He has supervised several PhDs including Mirosław Grabowski and Jacek Wernik. He is the winner of the Research Excellence Award of the Polish Academy of Sciences for his work on rational energy use in the sugar industry. He has contributed to ten EU supported projects; two coordinated, in the fields of university-level education, technological research and technology transfer. Through these projects he has established research cooperation with Robin Smith and Jiří Klemeš, and other personalities of the Process Integration scene.

Dr Mirosław **Grabowski** is the manager of the Laboratory of Thermal Engineering in Plock Campus of Warsaw University of Technology, Poland.

After graduating from WUT, he gained industrial experience through five-year business activity as the owner and manager of a small company that produced laboratory and medical equipment. In 1994 he joined WUT and later received training on Process Integration methods at DPI UMIST. As a member of the team of project SUCLEAN, he took a research internship at the Institute of Chemical Technology Prague, Czech Republic. Working under supervision of Krzysztof Urbaniec, in 2002 he completed his PhD on the energy demand of a novel sugar production process. He later carried out research for a sugar manufacturing company and he had been member of the team of project TOSSIE (Towards Sustainable Sugar Industry in Europe).

Dr Jacek **Wernik** is the deputy director of the Institute of Mechanical Engineering in Plock Campus of Warsaw University of Technology, Poland.

He graduated from WUT in 1997 and subsequently joined the team of EU supported research project SUCLEAN devoted to the minimisation of energy and water use in a novel sugar manufacturing process (a collaborative effort by DPI UMIST, WUT and four other partners from Italy and

© Woodhead Publishing Limited, 2013

Czech Republic). He completed his PhD under supervision of Krzysztof Urbaniec on the rational water use in beet sugar factories. He has been member of the project team of EU supported project TOSSIE coordinated by Krzysztof Urbaniec.

Professor K. Urbaniec,* Dr M. Grabowski and Dr J. Wernik
Warsaw University of Technology
Płock Branch
Jachowicza 2/4
09–402 Płock
Poland

Email: k.urbaniec@mbox.pw.edu.pl; gstku@mbox.pw.edu.pl

Chapter 31

Professor Dr Petro O. **Kapustenko**, is the deputy head of Centre for Energy Saving Process Integration at National Technical University 'Kharkiv Polytechnic Institute', Kharkiv, Ukraine.

He graduated from the National Technical University 'Kharkiv Polytechnic Institute', Kharkiv, Ukraine and received his PhD at Mendeleev Russian Chemical Technology University. The Centre for Energy Saving Process Integration at National Technical University 'Kharkiv Polytechnic Institute' with support of DPI of UMIST, Manchester and British Council Link project. He is chief executive of Sodrugestvo-T, which he cofounded engineering company and is its. The company was involved in a number of EC and World Bank funded projects aimed on renovation of District Heating networks and industry, using Process Integration methods and advanced energy saving equipment such as CHP units, heat pumps, modern DH substations and others, mostly in Ukraine and Russia. Petro Kapustenko is also Member of Ukrainian Building Construction Academy.

Dr Olga P. **Arsenyeva**, is the associate professor in Department of Integrated Technologies, Processes and Aparatuses at the National Technical University 'Kharkiv Polytechnic Institute', Kharkiv, Ukraine.

She graduated the Kharkiv and did her PhD under the supervision of Leonid Tovazhnyianskyy. In 2005 she joined Professor Petro Kapustenko in Spivdruzhnist-T Engineering Company (Kharkiv, Ukraine). Both CESPI and Spivdruzhnist-T had close relations with DPI UMIST (now CPI, The) and Centre for Procešš Integratfion and
Intensification CPI[2] of Pannonia University. Her research interests are plate heat exchangers design and application, Process Integration.

© Woodhead Publishing Limited, 2013

Professor Petro O. Kapustenko* and Dr Olga P. Arsenyeva
Department of Integrated Technologies Processes and Apparatuses
National Technical University – Kharkiv Polytechnical Institute
21 Ulica Frunze
61002, Kharkiv
Ukraine

Email: petro.kapustenko@kpi.kharkov.ua

Chapter 32

Professor Dr Robin **Smith** is director of the Centre for Process Integration in the School of Chemical Engineering and Analytical Science of The University of Manchester. He is also president of Process Integration Limited. He has extensive industrial experience with Rohm & Haas in process investigation, production and process design, and with ICI in process modelling and Process Integration. He has acted extensively as a consultant to industry in Process Integration projects. He has published widely in the field of Process Integration and is author of 'Chemical Process Design and Integration', published by Wiley. He is a fellow of the Royal Academy of Engineering, a fellow of the Institution of Chemical Engineers in the UK and a Chartered Engineer. In 1992 he was awarded the Hanson Medal of the Institution of Chemical Engineers for his work on waste minimisation. He currently has an active research programme in the design, retrofit and optimisation of heat recovery systems, process utility systems, distributed energy systems and separation systems, and the design of sustainable processes.

Professor Robin Smith,* Dr Ming Pan and Dr Igor Bulatov
Centre for Process Integration
School of Chemical Engineering and Analytical Science
The
Manchester M13 9PL
UK

Email: robin.smith@manchester.ac.uk

Chapter 33

Professor Santanu **Bandyopadhyay** is the head of Department of Energy Science and Engineering at the Indian Institute of Technology (IIT) Bombay, Powai, Mumbai, India.

He obtained his BTech (Hons) in Energy Engineering from IIT Kharagpur in 1992, and MTech in Energy Systems Engineering from IIT Bombay in 1995. In 1999 he was awarded PhD from IIT Bombay. He

© Woodhead Publishing Limited, 2013

then worked for Heat and Mass Transfer Division of Engineers India Limited, New Delhi. In 2001, he joined Department of Energy Science and Engineering (formally Energy Systems Engineering), IIT Bombay. His research interests include Process Integration, Pinch Analysis, Industrial Energy Conservation, Modelling and Simulation of Energy Systems, Design and optimisation of renewable energy systems, etc. Since 1994, he has been associated with and contributed towards various developmental, industrial and research activities involving different structured approaches to process design, resource (including energy and water) integration and conservation as well as renewable energy systems design.

Professor Santanu Bandyopadhyay
Department of Energy Science and Engineering
Indian Institute of Technology, Bombay
Powai
Mumbai, 400076
India

Email: santanub@iitb.ac.in

Chapters 32, 34 and 35

Dr Igor **Bulatov** is a project officer in the School of Chemical Engineering and Analytical Science, United Kingdom.

He graduated from Mendeleev University of Chemical Technology of Russia in Moscow. His PhD was separation and heat transfer. In 2002 he was awarded a Royal Society/NATO scholarship and spent a year at DPI, UMIST doing research on plate-fin heat exchanger design under the supervision of Robin Smith. From 2003 he was a researcher at the DPI, UMIST (later CPI, The) partficfipatfing fin a number of
European and national projects on Process Integration, energy saving and optimisation coordinated by Jiří Klemeš and Robin Smith. From 2009 he is a Project Officer, the position which enables him to combine research and scientific managerial responsibilities.

Dr Igor Bulatov
Centre for Process Integration
School of Chemical Engineering and Analytical Science
The
Manchester M13 9PL
UK

Email: igor.bulatov@manchester.ac.uk

© Woodhead Publishing Limited, 2013

Woodhead Publishing Series in Energy

1 **Generating power at high efficiency: Combined cycle technology for sustainable energy production**
Eric Jeffs
2 **Advanced separation techniques for nuclear fuel reprocessing and radioactive waste treatment**
Edited by Kenneth L. Nash and Gregg J. Lumetta
3 **Bioalcohol production: Biochemical conversion of lignocellulosic biomass**
Edited by K. W. Waldron
4 **Understanding and mitigating ageing in nuclear power plants: Materials and operational aspects of plant life management (PLiM)**
Edited by Philip G. Tipping
5 **Advanced power plant materials, design and technology**
Edited by Dermot Roddy
6 **Stand-alone and hybrid wind energy systems: Technology, energy storage and applications**
Edited by J. K. Kaldellis
7 **Biodiesel science and technology: From soil to oil**
Jan C. J. Bart, Natale Palmeri and Stefano Cavallaro
8 **Developments and innovation in carbon dioxide (CO_2) capture and storage technology Volume 1: Carbon dioxide (CO_2) capture, transport and industrial applications**
Edited by M. Mercedes Maroto-Valer
9 **Geological repository systems for safe disposal of spent nuclear fuels and radioactive waste**
Edited by Joonhong Ahn and Michael J. Apted
10 **Wind energy systems: Optimising design and construction for safe and reliable operation**
Edited by John D. Sørensen and Jens N. Sørensen
11 **Solid oxide fuel cell technology: Principles, performance and operations**
Kevin Huang and John Bannister Goodenough

© Woodhead Publishing Limited, 2013

12 **Handbook of advanced radioactive waste conditioning technologies**
Edited by Michael I. Ojovan
13 **Membranes for clean and renewable power applications**
Edited by Annarosa Gugliuzza and Angelo Basile
14 **Materials for energy efficiency and thermal comfort in buildings**
Edited by Matthew R. Hall
15 **Handbook of biofuels production: Processes and technologies**
Edited by Rafael Luque, Juan Campelo and James Clark
16 **Developments and innovation in carbon dioxide (CO_2) capture and storage technology Volume 2: Carbon dioxide (CO_2) storage and utilisation**
Edited by M. Mercedes Maroto-Valer
17 **Oxy-fuel combustion for power generation and carbon dioxide (CO_2) capture**
Edited by Ligang Zheng
18 **Small and micro combined heat and power (CHP) systems: Advanced design, performance, materials and applications**
Edited by Robert Beith
19 **Advances in clean hydrocarbon fuel processing: Science and technology**
Edited by M. Rashid Khan
20 **Modern gas turbine systems: High efficiency, low emission, fuel flexible power generation**
Edited by Peter Jansohn
21 **Concentrating solar power technology: Principles, developments and applications**
Edited by Keith Lovegrove and Wes Stein
22 **Nuclear corrosion science and engineering**
Edited by Damien Féron
23 **Power plant life management and performance improvement**
Edited by John E. Oakey
24 **Electrical drives for direct drive renewable energy systems**
Edited by Markus Mueller and Henk Polinder
25 **Advanced membrane science and technology for sustainable energy and environmental applications**
Edited by Angelo Basile and Suzana Pereira Nunes
26 **Irradiation embrittlement of reactor pressure vessels (RPVs) in nuclear power plants**
Edited by Naoki Soneda
27 **High temperature superconductors (HTS) for energy applications**
Edited by Ziad Melhem
28 **Infrastructure and methodologies for the justification of nuclear power programmes**
Edited by Agustín Alonso

© Woodhead Publishing Limited, 2013

29 **Waste to energy conversion technology**
Edited by Naomi B. Klinghoffer and Marco J. Castaldi

30 **Polymer electrolyte membrane and direct methanol fuel cell technology Volume 1: Fundamentals and performance of low temperature fuel cells**
Edited by Christoph Hartnig and Christina Roth

31 **Polymer electrolyte membrane and direct methanol fuel cell technology Volume 2: *In situ* characterization techniques for low temperature fuel cells**
Edited by Christoph Hartnig and Christina Roth

32 **Combined cycle systems for near-zero emission power generation**
Edited by Ashok D. Rao

33 **Modern earth buildings: Materials, engineering, construction and applications**
Edited by Matthew R. Hall, Rick Lindsay and Meror Krayenhoff

34 **Metropolitan sustainability: Understanding and improving the urban environment**
Edited by Frank Zeman

35 **Functional materials for sustainable energy applications**
Edited by John A. Kilner, Stephen J. Skinner, Stuart J. C. Irvine and Peter P. Edwards

36 **Nuclear decommissioning: Planning, execution and international experience**
Edited by Michele Laraia

37 **Nuclear fuel cycle science and engineering**
Edited by Ian Crossland

38 **Electricity transmission, distribution and storage systems**
Edited by Ziad Melhem

39 **Advances in biodiesel production: Processes and technologies**
Edited by Rafael Luque and Juan A. Melero

40 **Biomass combustion science, technology and engineering**
Edited by Lasse Rosendahl

41 **Ultra-supercritical coal power plant: Materials, technologies and optimisation**
Edited by Dongke Zhang

42 **Radionuclide behaviour in the natural environment: Science, implications and lessons for the nuclear industry**
Edited by Christophe Poinssot and Horst Geckeis

43 **Calcium and chemical looping technology for power generation and carbon dioxide (CO_2) capture: Solid oxygen- and CO_2-carriers**
P. Fennell and E. J. Anthony

44 **Materials' ageing and degradation in light water reactors: Mechanisms, and management**
Edited by K. L. Murty

© Woodhead Publishing Limited, 2013

45 **Structural alloys for power plants: Operational challenges and high-temperature materials**
Edited by Amir Shirzadi, Rob Wallach and Susan Jackson
46 **Biolubricants: Science and technology**
Jan C. J. Bart, Emanuele Gucciardi and Stefano Cavallaro
47 **Wind turbine blade design and materials: Improving reliability, cost and performance**
Edited by Povl Brøndsted and Rogier Nijssen
48 **Radioactive waste management and contaminated site clean-up: Processes, technologies and international experience**
Edited by William E. Lee, Michael I. Ojovan, Carol M. Jantzen
49 **Probabilistic safety assessment for optimum nuclear power plant life management (PLiM): Theory and application of reliability analysis methods for major power plant components**
Gennadij V. Arkadov, Alexander F. Getman and Andrei N. Rodionov
50 **The coal handbook Volume I: Towards cleaner production**
Edited by D. G. Osborne
51 **The coal handbook Volume II: Coal utilisation**
Edited by D. G. Osborne
52 **The biogas handbook: Science, production and applications**
Edited by Arthur Wellinger, Jerry Murphy and David Baxter
53 **Advances in biorefineries: Biomass and waste supply chain exploitation**
Edited by K. W. Waldron
54 **Geoscience of carbon dioxide (CO_2) storage**
Edited by Jon Gluyas and Simon Mathias
55 **Handbook of membrane reactors Volume 1: Fundamental materials science, design and optimisation**
Edited by Angelo Basile
56 **Handbook of membrane reactors Volume 2: Reactor types and industrial applications**
Edited by Angelo Basile
57 **Alternative fuels and advanced vehicle technologies: Towards zero carbon transportation**
Edited by Richard Folkson
58 **Handbook of microalgal bioprocess engineering**
Christopher Lan and Bei Wang
59 **Fluidized bed technologies for near-zero emission combustion and gasification**
Edited by Fabrizio Scala
60 **Managing nuclear projects: A comprehensive management resource**
Edited by Jas Devgun
61 **Handbook of Process Integration (PI): Minimisation of energy and water use, waste and emissions**
Edited by Jiří Klemeš

© Woodhead Publishing Limited, 2013

Foreword

When Professor Klemeš called me early in 2012 to ask me to write a foreword for his *Handbook of Process Integration* (*PI*) it seemed like a call from a previous life. I said I had not been involved in the process industries for about ten years, so how could I do justice to some of the latest work in the field? Jiří Klemeš was just as I always remembered him: he never gives up. So here we are.

The agreement reached was that I would attempt to put the contributions in this handbook in context with the early days. This I'm happy to do.

Anyone opening this book will likely know that Pinch Technology goes back almost 40 years. Originally, it was all about 'Heat Exchanger Network Design' – the words 'process' and 'integration' came later. Also, it was about energy savings – capital and other costs came later.

I remember a conference in the 1970s when an elder statesman academic colleague commented after my paper: '… it seems you struck lucky with heat exchangers. But you will never find an equivalent solution for heat and power systems …'. I don't mention this to prove this colleague wrong. I mention it because his was an opinion shared by many people at the time. If I am honest, didn't I hear a little voice sometimes whispering in my ear that he might be right? The challenge to develop definitive insights and methods for the systematic design of optimised whole processes in real life seemed formidable.

Three decades on, the doubters are proven wrong. There exists much evidence for this and Professor Klemeš's handbook proves it yet again. Perhaps we still cannot solve every problem in process design but we have moved on considerably from the culture of 'design by inspection' so prevalent in the 1970s. In this handbook, authors from more than 20 countries from all parts of the world cover a wide range of process design and integration topics ranging from the 'classics' such as heat and utility systems to water, recycling, waste and hydrogen systems addressing not just operating and capital cost but also equipment design and operability issues through to buildings and supply chains, etc. I assume that some of this work is still forward looking but it is clear that Process Integration has matured into a discipline extending beyond Heat Integration.

© Woodhead Publishing Limited, 2013

What the doubters have not anticipated is the combined effect that many people pursuing a common goal can have. The dream of bringing understanding and method to the task of process design was shared by many and I recognise amongst the authors in this handbook at least seven 'old warriors' from the early days. You know who you are. You stuck to it longer than I did and I salute you for it. It is this consistency and sense of mission that has ultimately allowed Process Integration to become both established and mature.

Bodo Linnhoff
Berlin, 4.10.2012

© Woodhead Publishing Limited, 2013

1

Process Integration (PI): An Introduction

JIŘI JAROMIR KLEMEŠ, University of Pannonia, Veszprém, Hungary

DOI: 10.1533/9780857097255.1.3

Abstract: This chapter provides an introduction to Process Integration (PI). PI methodology dates back to the 1970s and was conceived and developed as a response to the oil crisis, which had caused fuel to become expensive and scarce. The first developments were naturally in the Heat Integration (HI) field and targeted energy efficiency and energy savings. HI proved to be a great success and was successfully implemented in the oil, chemical and energy industry. Based on this success, further developments into several other related fields, such as Mass Integration and Water Integration followed. More than 40 years later PI is still at the forefront of energy research and industrial interest, and new directions for the development of its applications continue to be found. After a brief history of PI, the following sections review current centres of expertise in this area and sources of further information and advice.

Key words: Process Integration, history of the development, PI Research Consortium, Heat Integration, Mass Integration and Water Integration, Centres of PI Research.

1.1 Introduction

Process Integration (PI) methodology dates back to the 1970s and was conceived and developed as a response to the oil crisis, which had caused fuel to become expensive and scarce. The first developments were naturally in the HI field and targeted energy efficiency and energy savings. Heat Integration methodology still provides the design foundations for Combined Heat and Power (CHP) systems, refrigeration, air conditioning and heating with pump systems. It is equally applicable for small, medium and large industrial sites, such as power stations and oil refineries, which use petrochemical production. The technology provides the answer to one of the major challenges in the design of heating and cooling systems, namely, the complexity of Energy and Power Integration, by providing a mapping strategy based on thermodynamically derived upper bounds on the system thermal and power performance. The efficient use of available heating and cooling resources for serving complex systems of various sizes and designations can significantly reduce energy consumption and emissions. This methodology can also be

© Woodhead Publishing Limited, 2013

used to integrate renewable energy sources such as biomass, solar PV (photovoltaic) and solar thermal into the combined heating and cooling cycles.

1.1.1 Global Energy Demand and Consumption

The BP Statistical Review of World Energy (2012) declared that world primary energy consumption – which in 2012 for the first time included a time series for commercial renewable energy – grew by 5.6% in 2010, the largest increase (in percentage terms) since 1973. Consumption in OECD countries grew by 3.5%, the strongest growth rate since 1984, although the level of OECD consumption remains roughly in line with that seen ten years ago. Non-OECD consumption grew by 7.5% and was 63% above the level in 2000. Consumption growth accelerated in 2010 for all regions, and growth was above average in all regions. Chinese energy consumption grew by 11.2%, and China surpassed the USA as the world's largest energy consumer. Oil remains the world's leading fuel, accounting for 33.6% of the global energy consumption, but oil has continued to lose market share for the 11th consecutive year.

Global hydroelectric and nuclear output, meanwhile, have each seen their strongest increases since 2004. The hydroelectric output grew by 5.3%, with China accounting for more than 60% of the global growth due to a combination of new capacity and wet weather. The worldwide nuclear output grew by 2%, with three-quarters of the increase coming from OECD countries. The French nuclear output rose by 4.4%, accounting for the largest volumetric increase in the world.

Other renewable energy sources continued to grow rapidly. Global biofuel production in 2010 grew by 13.8%, which is equivalent to 240,000 b/d, constituting one of the largest sources of liquid-production growth in the world. Growth was driven by the USA (+140,000 b/d, representing 17%) and Brazil (+50,000 b/d, representing 11.5%). Renewable energy used in power generation grew by 15.5%, driven by continued robust growth in wind energy (+22.7%). The increase in wind energy in turn was driven by China and the USA, who together accounted for nearly 70% of the global growth. Even with those growing figures, however, these forms of renewable energy still only accounted for 1.8% of the global energy consumption, which was up from 0.6% in 2000.

In 2012, when the world economy was hit by the crises in a number of countries, energy consumption stagnated or was lowered. Overall trends have been growing, however – see Fig. 1.1 for electricity, Fig. 1.2 for oil and Fig. 1.3 for natural gas. Coal consumption grew by 7.6% in 2010, the fastest global growth since 2003. Coal now accounts for 29.6% of the global energy consumption and is up from 25.6% ten years ago.

When considering the environmental effect imposed by the growing energy consumption of fossil fuels and, to a certain extent, even by renewable

© Woodhead Publishing Limited, 2013

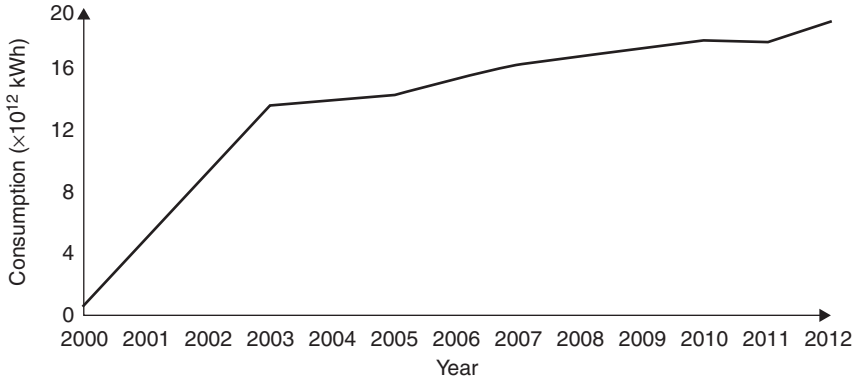

y	2000	2003	2004	2005	2006	2007	2008	2009	2010	2011	2012
10^{12} kWh	0.3427	13.81	13.94	14.28	15.45	16.33	16.88	17.48	17.93	17.78	19.09

1.1 Development of the World Consumption of Electricity (after Index Mudi, 2012). Definition of electricity consumption: This entry consists of total electricity generated annually plus imports and minus exports. The discrepancy between the amount of electricity generated and/or imported and the amount consumed is accounted for as loss in transmission and distribution.

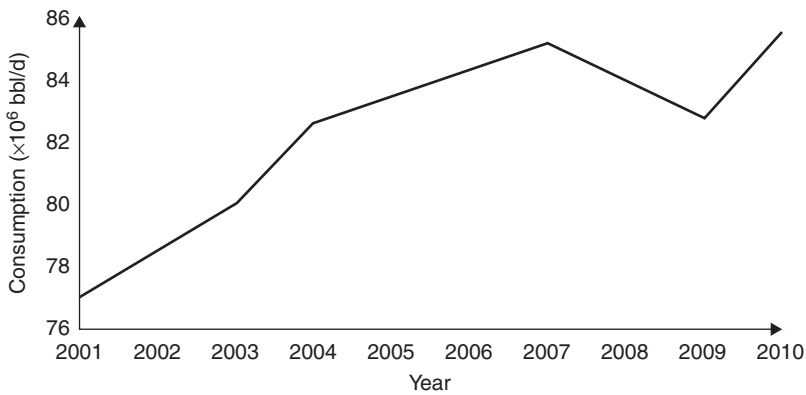

y	2001	2003	2004	2007	2009	2010
10^{6} bbl/d	77,040	80,100	82,590	85,220	82,780	85,510

1.2 Development of the world consumption of oil (Index Mudi, 2012). Definition of Oil Consumption: This entry is the total oil consumed in bbl/d. The discrepancy between the amount of oil produced and/or imported and the amount consumed and/or exported is due to the omission of stock changes, refinery gains, and other complicated factors.

© Woodhead Publishing Limited, 2013

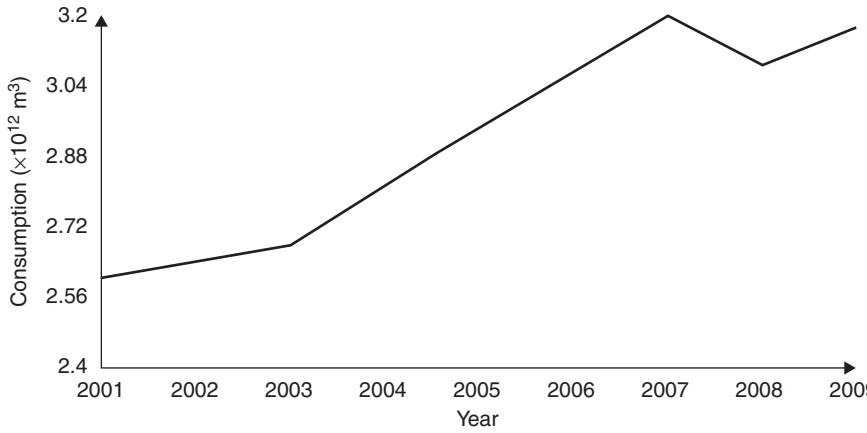

y	2001	2003	2004	2007	2008	2009
10^{12} m^3	2,599	2,675	2,819	3,198	3,085	3,172

1.3 Development of the world consumption of natural gas (Index Mudi, 2012).
Definition of Natural Gas consumption: This entry is the total natural gas consumed. The discrepancy between the amount of natural gas produced and/or imported and the amount consumed and/or exported is due to the omission of stock changes and other complicated factors.

energy sources – since they do have some impact on the environment as well, obviously the aim is to decrease the global demand on energy supplies and to save energy, either by increasing the efficiency of current energy resources or by producing new sustainable energy sources.

As mentioned above, research demand into PI was originally triggered by the energy crisis in the 1970s. This strong incentive is still present and, to some extent, growing. This is one of the key reasons why PI has continuously attracted the attention of researchers on the one hand, and users on the other – in various fields and industries including business, services, residential and even the agricultural sector. This was one of the main motivations for writing this handbook. The PI story started with energy, but the success and size of its implementation has encouraged the extension of this methodology to include Mass, Water, Hydrogen and Property Integrations, to mention at least some of the recent areas of development, which are also covered in this handbook.

1.1.2 About This Handbook

Various guides, books and handbooks have been published, mapping the development of PI methodology at different stages of its development (details of these can be found in Section 1.4). Some of them were written by

© Woodhead Publishing Limited, 2013

a single researcher, others by groups of authors, and many of them provide very valuable state-of-the-art information for the time period up to when they were written and published. This handbook, however, is (as far as the editor is aware) the first attempt to bring together the leading scientists and researchers currently contributing to PI development. The aim is to pool their expertise and specialist knowledge to provide readers with a comprehensive and upto date guide to the latest PI research and applications. The unified terminology, conventions and graphical representations have been a challenge and it is for the readers to assess to what extent this attempt has succeeded.

This handbook provides a comprehensive guide to PI for graduate and postgraduate teaching, as well as for further professional development and training courses. It is supported by a collection of case studies of varying complexity completed over years and benefitting from the considerable expertise stemming from the work of the world's leading experts in the field. The extensive material used in this handbook has been collected over years of postgraduate and further career development courses and training for the industry. Verification of the effectiveness of PI applications in the industry plays an extremely important role in the development of the methodology. The authors of this handbook run their research and industrial applications in eight European Union countries as well as in Norway, Canada, China, India, Japan, Korea, Malaysia, Mexico, New Zealand, Philippines, South Africa, Ukraine and the USA. They were invited to provide as much detailed information regarding the implementation of PI in various industrial, business and geographical conditions as possible.

The vast majority of leading PI experts positively answered the invitation to write and joined forces to provide the first comprehensive *Handbook of Process Integration*. As editor, I have been delighted at this collaboration with all the contributors and would like to express my unreserved appreciation and thanks.

1.2 A Short History of Process Integration (PI)

The development of PI started with Heat Exchanger Network (HEN) Synthesis. A number of various approaches dealing with the optimum HEN Synthesis have been published, several of which have become very popular, such as Ponton and Donaldson (1974). The comprehensive overview of HEN Synthesis presented by Gundersen and Naess (1990) and the overview of process synthesis presented earlier by Nishida *et al*. (1981) provided considerable impulse for further research and development in the field – as can be witnessed in the more recent overview by Furman and Sahinidis (2002).

In most literature sources, such as Gundersen (2000), the concept of HI based on a Recovery Pinch was described, which aimed to independently curtail the levels and parts discovered by Hohmann (1971) and by research groups in the following publications: (i) the two parts paper by Linnhoff and

© Woodhead Publishing Limited, 2013

Flower (1978) and Flower and Linnhoff (1978) and followed up by a PhD thesis from Linnhoff (1979), and (ii) by Umeda *et al*. (1978). Gundersen (2000) also stated that Hohmann (1971) was the first to provide a systematic method for obtaining energy targets using his feasibility table.

In 1971 Hohmann completed his PhD in which some basic principles, later further developed into HI, were included. With the exception of a conference PhD presentation in 1976 (Hohmann and Lockhart, 1976), however, he has not published these results in a way which would attract a wider audience. Moreover, the less well-known work, including important information on the Problem Table Algorithm, was also published at around the same time by MSc student Bodo Linnhoof at ETH Zūrich (Linnhoff, 1972). In that pre-information-technology time, the interactions amongst researchers were not as swift and simple as they are today. Finding what the other researchers are working on was usually only possible after acquiring the printed publications.

During the later years of the 1970s it was again Bodo Linnhoff (at that time a PhD student at the University of Leeds) who continued to investigate HI and realised its potential. His first paper Linnhoff and Flower (1978), which later became very highly cited, was initially nearly rejected by the leading journal of that time. It is only due to Bodo's strong will and persistence that the paper was successfully published and the idea of using HI got off the ground. After the first paper's difficult start, Linnhoff's further papers – Flower and Linnhoff (1978) and Flower and Linnhoff (1979) shortly followed and were published more smoothly.

Another group which produced interesting contributions to the field at the time was from Japan working at Chiyoda Chemical Engineering & Construction Co. Ltd., Tsurumi, Yokohama. They published a series of publications dealing with PI issues and HEN Synthesis – Umeda *et al*. (1978, 1979), optimum water reallocation in a refinery – Takama *et al*. (1980) and applications of the T-Q diagram to heat integrated system synthesis – Itoh *et al*. (1986).

1.2.1 DPI UMIST and CPI The

After obtaining his PhD in 1979, Linnhoff settled at The University of Manchester Institute of Science and Technology (UMIST) and created a group which later became the Department of Process Integration. The Department owed much of its success to the pioneering work of this group, which developed the concept of PI into an industrial technology in the 1980s and 1990s.

The basic idea of PI began by drawing the total heating and the cooling requirements of a process separately in a cumulative manner in a temperature–enthalpy diagram, commonly referred to as Composite Curves. Gundersen (2000) acknowledged that similar drawings had already been used

© Woodhead Publishing Limited, 2013

by designers for low temperature processes such as air separation (Linde AG in Germany) to design multi-stream heat exchangers. The Linde AG drawings had not, however, been developed into the completed methodology.

The graphical representations are referred to as Composite and Grand Composite Curves (see Chapter 2). There are also several numerical methods of presentation, such as the Problem Table Algorithm published in related papers (Flower and Linnhoff, 1978; Linnhoff and Flower, 1978) and the Heat Cascade (Linnhoff, 1979) – an early development which lasted until 1984 and which was summarised by Linnhoff (1984) in his paper on HENs with process modifications. The Heat Cascade is used as an HI methodology because it (i) provides a useful illustration of the heat flows and decompositions in heat recovery systems, and (ii) provides the necessary information to construct the Grand Composite Curve.

Dhole (1994) in his PhD thesis made the important extension into sub-ambient temperatures. The feature of having a heat-deficit region above the Process Pinch and a heat-surplus region below the Process Pinch provided the guidelines for modifying the process to increase the potential for heat recovery. These guidelines later coined the Plus/Minus Principle and have been discussed by Umeda *et al*. (1979), and further developed by Linnhoff and Parker (1984) and Linnhoff and Vredeveld (1984).

This concept was later expanded into new areas using various analogies. Linnhoff (1993) in his overview summarised the eight developments, which are: pressure drop optimisation; batch PI; multiple base case design; water and wastewater minimisation; distillation column profiles; Total Site Integration; low temperature process design; and emissions targeting. Those developments were further extended and developed by the UMIST and The GROUP, AŠ WELL AŠ BY ŠEVERAL OTHER AUTHORŠ, AND ARE described in more detail described in Chapters 4–9.

A considerable contribution to the field came from DPI UMIST in Total Site Integration. The idea published by Dhole and Linnhoff (1993) has been further developed in the PhD thesis of Raissi (1994) and another progress was made under the EC funded project '*Targeting and Planning for Reduction of Fuel, Power and CO_2 on Total Sites*' (Klemeš *et al*., 1997). The inclusion of renewable energy sources and the extension of the Total Sites to the surrounding locally distributed areas were started in the work of Perry *et al*. (2008).

Another important contribution was the development of utility system optimisation methodologies. This was based on Total Site Integration works and especially on co-generation targeting (Raissi, 1994). This series of developments initially directed efforts toward steam network modelling and optimisation in the case of network synthesis (Mavromatis and Kokossis, 1998a, 1998b). This was developed further by Shang (2000), who has developed hardware models for fired steam boilers and for gas turbines. He established

© Woodhead Publishing Limited, 2013

a framework for steam level selection, superstructure construction and subsequent optimisation of the resulting utility system configuration. The overall framework was completed by Varbanov (2004), who revised hardware models and devised overall procedures for the most important cases of utility system optimisation: operation optimisation (Varbanov *et al*., 2004a), synthesis (Varbanov *et al*., 2005), thermodynamic analysis using power-to-heat ratio and Top-Level Analysis (Varbanov *et al*., 2004b).

Asante (1996) was a contribution to the automated and interactive retrofit design of practical HENs. This methodology was later developed and presented by Zhu (1997). Further development resulted in an EC project *Sustainable Development by Retrofit and Debottlenecking for Energy Based System – REDBAS* (2001).

A joint EC development *Design and Operation of Energy Efficient Batch Processes* lead by UMIST (Klemeš *et al*., 1994) further extended previous works in Batch Heat Integration by Kemp and Deakin (1989a) 'Calculation of Energy Targets'; (1989b) 'Network Design and Process Scheduling'; (1989c) 'Network Design and Process Scheduling', and also on the research and training courses from Linnhoff March Ltd. (1998).

1.2.2 PI Development by Other Research Groups

A valuable overview was provided in one of the earliest handbooks – *A Process Integration PRIMER* (Gundersen, 2000). This was the result of an International Energy Agency initiative.

The most obvious analogy to heat transfer is provided by mass transfer. In heat transfer, heat is transferred with temperature difference as the driving force. Similarly, in mass transfer, mass (or certain components) is transferred using concentration difference as the driving force. The corresponding Mass Pinch, developed by El-Halwagi and Manousiouthakis (1989), has a number of industrial applications whenever process streams are exchanging mass in a number of mass transfer units, such as absorbers, extractors, etc.

One specific application of the Mass Pinch is in the area of wastewater minimisation, where the optimal use of water and wastewater is achieved through reuse, regeneration and possibly recycling. The corresponding Water Pinch, developed by Wang and Smith (1994), can also be applied to the design of distributed effluent treatment processes. Prakash and Shenoy (2005) made an important contribution with their targeting and design of water networks for fixed flow rate and fixed contaminant load operations. These restrictions were later relaxed following further research.

Oxygen Pinch Analysis (Zhelev and Ntlhakana, 1999) represents a further extension of PI. The idea here is to analyse the system so that targets

© Woodhead Publishing Limited, 2013

are derived prior to designing a system for minimising the oxygen consumption of the micro-organisms used for waste degradation. The next step is to design a flowsheet that achieves these targets. In most cases, oxygen is supplied through agitation. Aeration requires energy, so an analysis based on the Oxygen Pinch eventually leads back to the original application of energy conservation.

Several attempts have been made to combine Pinch Analysis for related domains. These combinations include energy–water, oxygen–water and Pinch–energy. When the problems of energy and water conservation are considered jointly, finding the best energy-recovery options and water-reuse schemes is an extremely complex task, because there are strong design interactions between the systems used for water and energy. Both the Water Pinch and the Energy Pinch concepts have been accommodated in separate single-design frameworks. However, the methodological procedure is changed slightly when the interactions between water reuse and energy recovery have to be considered. Based on the PhD thesis of Savulescu (2003), a two-paper work has been published (Savulescu *et al*., 2005a, 2005b). Zhelev and Bhaw (2000) attempted to combine the Water–Oxygen Pinch Analysis better in order to improve wastewater treatment management. The Composite Curve in energy-transformity coordinates were published by Zhelev and Ridolfi (2006).

The composition of a stream or a mixture is only one of several chemical and physical properties that are essential in a chemical process. Other common properties include acidity and alkalinity (as measured by pH), density, viscosity, reflectivity, turbidity, colour and solubility. The process network synthesis associated with these chemical properties cannot be addressed by conventional Mass Integration techniques, so another generic approach has been developed to deal with this problem, firstly by Shelley and El-Halwagi (2000), then further extended by El-Halwagi *et al*. (2003). For systems that are characterised by one key property, Kazantzi and El-Halwagi (2005) introduced a Pinch-based graphical targeting technique that establishes rigorous targets for minimum usage of fresh materials, maximum recycling and minimum waste discharge.

Foo *et al*. (2006) focused on developing an algebraic technique to solve the problem of identifying rigorous targets for property-based recycling and the reuse of materials. A key element of these techniques is the concept of a material surplus, which generalises the analogous concept developed for the tasks of synthesising hydrogen and water networks. It was based on research conducted in his PhD work by Hallale (1998), later published by Hallale (2002), as well as on another PhD thesis by Alves (1996), later published by Alves and Towler (2002). Manan *et al.* (2004) developed an algebraic approach called Property Cascade A (PCA) to identify various performance targets for a Maximum Resource Recovery (MRR) network.

© Woodhead Publishing Limited, 2013

Foo *et al*. (2006) wrote a paper introducing network design techniques for the synthesis of an MRR network as well as a systematic procedure for identifying optimum process modification strategies. The problem of designing a Property-Based Material Reuse network was formulated. The Property-Based Material Reuse Pinch diagram combines fresh usages to determine minimum fresh consumption (Kazantzi and El-Halwagi, 2005). Bandyopadhyay (2006) suggested an interesting extension into the field of waste treatment – the Source Composite Curve for waste reduction.

The power of Pinch Analysis, which combines quality (e.g., temperature, concentration) with quantity (e.g., heat duty, mass flow), has been successfully applied to analysing supply chains. In this case, (reduced) time is the 'quality' and the amount of material (e.g., number of units, mass) is the 'quantity'. Singhvi and Shenoy (2002) formulated the aggregate planning problem, and Singhvi *et al*. (2004) extended this suggested methodology to the case of planning for multiple-product scenarios.

An approach using PI methodology for regional resource management has been developed and simultaneously tackles the two most important issues with biomass supply chains: transportation and land use. The biomass supply-chain problem is complex due to the distributed nature of biomass resources and their low energy density, which necessitates large transportation capacity. Growing biomass requires considerable land area, often leading to competition with food production. To address these problems, a two-level approach to biomass supply-chain synthesis – based on a novel Regional Energy Clustering (REC) approach – was proposed by Lam *et al*. (2010b) and extended to minimise the carbon footprint (Lam *et al*., 2010b) and optimise the region's biomass supply by means of P-graphs (Lam *et al*., 2010c).

Other important issues, not directly part of PI methodology but nonetheless having a substantial influence on the quality of the PI results, is data collection – see Klemeš and Varbanov (2010), reconciliation for example, Heyen and Kalitventzeff (2007), results interpretation and training provided – see Klemeš *et al*. (2013).

Those are just a few examples of how widely PI has spread into various applications. Further examples, of these and of the applications of PI in other areas, are covered by the chapters in this handbook.

1.3 Current Centres of Expertise in PI

Over the years, several very strong centres of expertise developed over the world. With initial development in Western Europe, USA and Japan, further spread out presently covers most parts of the world dealing with power production and consumption as well as industrial production. Very recent developments show a very strong interest in Asia, Latin America and Africa.

© Woodhead Publishing Limited, 2013

1.3.1 PI Research Consortium

The Process Integration Research Consortium (PIRC, 2012) has had a major influence on the industrial penetration of PI. It was founded in 1984 by four founding members – Shell, Exxon, BP and BASF. The origins of the research programme in the early 1980s were rooted in energy conservation. Today the programme has expanded to take account of the drive towards greater efficiency in the use of raw materials in general, and of the increasing pressure to design environmentally friendly processes – see Table 1.1. An objective, which runs through all aspects of the programme, is the efficient use of capital. Despite the fact that the programme has broadened in its scope and objectives, the traditions and values, which were established in the early days of the programme in the field of energy conservation, have been maintained. The programme's objective is to develop as deep an understanding as possible of the physical principles that underlie PI problems. Once these principles have been understood, the objective is to then develop these into practical methodologies, employing the necessary mathematical algorithms.

PIRC methods attempt, where possible, to maintain a two-step approach to solving PI problems. The first step sets targets without having to carry out design. Such targets can be used to scope and screen many design options quickly and efficiently. The second step provides systematic design methods to allow the targets to be achieved in practice.

The PIRC traditionally follows CPI methodologies through to their first applications, to ensure that they are indeed practical and meet the requirements of the process designers. To enable this, the academics in the PIRC work closely with the Consortium's member companies. PIRC welcomes enquiries from major companies across the whole process, manufacturing, water and power generation sectors of industry. The PIRC membership reflects many multi-national companies with a diverse range of interests. The exchange of concepts, experiences and ideas, over a powerful cross-section of industry worldwide, is one of the most fascinating aspects of the Consortium. For it to stay this way, members need to be active and enthusiastic. Membership is by formal agreement and on an annual basis (Table 1.2).

Based on the PIRC funding, the Department of Process Integration at UMIST, and later at The , haš produced a large
number of graduates in PI both at MSc and especially at PhD level.

1.3.2 Courses and Projects Funded by the European Community

Further distribution of the technology has been via franchised courses and further professional development courses. The UK Know How

© Woodhead Publishing Limited, 2013

Table 1.1 The PIRC membership beneΔ ts

Software	Provision of software packages developed for the members.
Workshop	'Hands on' training is given in a series of workshops both at The , in Japan, UK, USA and in-house. The workshops are often based around their software. Distance learning formats are also available.
Conferences	Participation in the Annual Conference for as many delegates as the company wishes to send.
Research Results	Are presented at the Annual Conference giving at least 2–3 years lead-time before they appear in the public domain.
Publications	Advance copies of all our publications.
Consulting and Training	Discounts on consulting services and training courses.
Direct Interface	A forum and network that facilitates direct personal contact between the major users of the technology and the research team.
Newsletters	Quarterly newsletters keep members regularly up to date.
Quality Assurance	Through knowledge of the state of the art in PI, the quality of designs and design and software services can be assessed.
Advisory Board Membership	Each member has a nominated representative on the Consortium Advisory Board, which reviews and advises the Department on research direction, expectations, software and training needs. The Chairman of the board is elected by the members.
Software details	The PIRC develops software programs in the Centre for the use of our Consortium members. This facilitates rapid and effective technology transfer. The packages are updated each year to include our latest research results. They have an easy to use MS WINDOWS interface and are backed by technical and workshop support along with effective documentation. Packages currently available and under further development are (for more details see Chapters 34 and 35): REACTOR, COLOM, STAR, WORK, SPRINT, WATER, HYDRO

Source: Process Integration Research Consortium (2012).

funding projects via Academic Links administered by the British Council has had considerable impact in the field. Finally, the European Community has been very considerably involved in supporting research and teaching projects. These projects have promoted PI around the world and have led to widespread interest in the field. A selection of participants in projects funded by the European Community is listed in Tables 1.3 and 1.4.

© Woodhead Publishing Limited, 2013

Table 1.2 Process Integration Research Consortium Members – present and past (in alphabetical order)

1. AEA Technology Engng Software, UK
2. Air Products, US
3. ARCO, US
4. Aspentech, US
5. BASF, DE
6. Bayer, DE
7. Bechtel, US
8. BOC Cryoplant, UK
9. BP, UK
10. British Nuclear Fuels plc, UK
11. British Gas, UK
12. Brown & Root Braun, US
13. CANMET, CA
14. Chevron UK Ltd, UK
15. Degussa-Hüls AG, DE
16. Dow Chemicals, US
17. DSM Research, NL
18. Du Pont, US
19. Eastman Chemical Corp, US
20. E A Technology, UK
21. EDF, F
22. Elf, F
23. Engineers India Ltd, IN
24. ENN Science and Technology Ltd, CN
25. EPRI, USA
26. Essochem, UK
27. Exxon, USA
28. Fluor Daniel BV, US
29. Fortum Power and Heat Oy, FI
30. Foster Wheeler Energy, US and UK
31. Hyprotech, US and UK
32. IChemE, UK
33. ICI, UK
34. Institute Françoise du Petrol, F
35. JGC Corp, JP
36. KBC, US
37. Keuken, Keuken & de Koning, NL
38. KTI (Kinetics Technology Int), US
39. Liege University, BE
40. Linnhoff March, UK
41. Lummus, US
42. M.W. Kellogg, UK and US
43. Mitsubishi, JP
44. Mitsubishi Heavy Industries, JP
45. MOL, Hungarian Oil Comp, HU
46. National Oil Corp (PETROM), RO
47. National Power plc, UK
48. Neste Oy, FI
49. Norsk Hydro, NO
50. Parsons Energy and Chemicals, US
51. Petramina, Indonesia
52. Petrobras, BR
53. Petroleum Research Centre, US
54. Petronas UT, MY
55. PowerGen, UK
56. Procter & Gamble, US
57. Rafinaria Astra Romana S.A., RO
58. Rio Tinto Technology Develop. BR
59. Romanian Oil Comp PETROM, RO
60. SABIC, SA
61. Saudi Aramco, SA
62. SERC, UK
63. Shell, NL and UK
64. Sinopec Tech, CN
65. Technip Benelux, NL
66. UCC (Union Carbide Corp), US
67. UMIST Ventures, UK
68. , US
69. Union Carbide, US
70. University Politechnica Bucharest, RO
71. UOP, US
72. VITO, BE

Source: Courtesy of Centre of Process Integration, The University of Manchester, UK.

1.3.3 Other Important Centres of PI Research, Development and Application

The increasing interest in PI has led to the creation of many strong research centres around the world, the main ones of which are listed in Table 1.5.

© Woodhead Publishing Limited, 2013

Table 1.3 Spreading the PI message to industry – contractors and consultancies (a selection)

Linnhoff March/KBC US	March Consulting Group, UK
ASPEN Tech, US and UK	Hyprotech, US and UK
CANMET, Natural Resources CA	Shell Global Solution, NL and UK
VTT Energy, FI	Sodrugestvo-T, UA
Process Integration Ltd, UK	ICI (Imperial Chemical Industries), UK
Dow Chemical Canada Inc, CN	Monsanto, US
SLOVNAFT Bratislava, SK	MOL Group, HU
NORSK HYDRO, NO	US Environmental Protection Agency, US
ECOPETROL Colombia, CO	PETROBRAS, BR
EVECO Brno, CZ	PETRONAS, MY CHEMOPETROL Litvínov, CZ
ACHEMA JONAVA, LI	Chemical Works NOVAKY, SK
BUTiH, PL	Council for Scientific and Industrial Research Pretoria, ZA
ALDARIS Brewery Riga, LA	KREMENCHUG Refinery, UA
European Pulp and Paper Industry Ass	SINTEF Trondheim, NO
Ministry of Environ Protection, SI	Johnson & Johnson, East London, ZA
Nuclear Energy Corp of South Africa, ZA	Norwich BioScience Institutes, UK

Table 1.4 Spreading the message to academia and education sector (a selection)

University of Pannonia, HU	Univ POLITEHNICA Bucharest, RO
Monash University, AU	Libyan Petroleum Institute, LY
University of Tehran, IR	Politecnico 'Leonardo da Vinci', Milan, IT
Warsaw University of Technology, PL	Brno University of Technology, CZ
Budapest University of Technology and Economics, HU	Universitat Politecnica de Catalunya, ES
National Technical University - Kharkov Polytechnical Institute, UA	University of Western Macedonia, GR
University of Maribor, SI	Technical University Graz, AT
Riga Technical University, LI	Technical University of Kaunas, LT
University of Tallinn, ES	Technical University Bishkek, KY
von Karman Institute of Fluid Dynamics, BE	South African Inst of Chem Eng, ZA
University of Durban, ZA	University of Pretoria, ZA
Tula State University, RF	Seoul National University, KR
Mendeleev University of Chemical Techechnology of Russia, RF	Waikato University, Hamilton, NZ
University of Zagreb, HR	Xi'an Jiaotong University, CN
Technical University of Minsk, BY	University of Liege, BE
South China University of Technology, CN	Kazan University, RF
University of Graz, AT	Slovak Technical University, SK

© Woodhead Publishing Limited, 2013

Table 1.5 World centres of research, application and expertise in PI (in alphabetical order)

Institution	Address	Contact	Web address
Brno University of Technology (UPEI VUT)	Institute of Process and Environmental Engineering, Faculty of Mechanical Engineering, Brno University of Technology (UPEI VUT), Brno, Technická 2896/2, 616 69, Brno, Czech Republic	Petr Stehlík stehlik@fme.vutbr.cz	<www.fme.vutbr.cz/index.html?lang=1>
Chalmers University of Technology	Chalmers University of Technology, Heat and Power Technology Division, Department of Energy and Environment, 412 96 Göteborg, Sweden	Thore Berntsson Simon Harvey: simon.harvey@chalmers.se	<www.chalmers.se/en>
China University of Petroleum State Key Laboratory of Heavy Oil Processing	China University of Petroleum State Key Laboratory of Heavy Oil Processing, Beijing, China	Xiao Feng, Chun Deng xfeng@cup.edu.cn	<www.cup.edu.cn/internationaloffice/en>
COWI A/S	COWI A/S, Parallelvej 2, DK-2800, Kongens Lyngby, Denmark	John Jørgensen, Communication Manager (DJ): jhj@cowi.dk	<www.cowi.com>
Ecole Polytechnique Federale de Lausanne	Laboratory for Industrial Energy Systems, Ecole Polytechnique Federale de Lausanne, Bat. ME A2. Station 9, CH-1015 Lausanne, Switzerland	Francois Marechal francois.marechal@epfl.ch	<leniwww.epfl.ch/>
EVECO Brno	EVECO Brno Ltd, Březinova 42, 616 00 Brno, Czech Republic	Jaroslav Oral eveco@evecobrno.cz	<www.evecobrno.cz/index.php/english>
Hanyang University	Hanyang University, Department of Chemical Engineering, Wangsimni-ro 222, Seongdong-gu, Seoul, Republic of Korea	Jin-Kuk Kim jinkukkim@hanyang.ac.kr	

(*Continued*)

© Woodhead Publishing Limited, 2013

Table 1.5 Continued

Institution	Address	Contact	Web address
HRC Consultants Ltd	HRC Consultants Ltd, a Leafield Road, Disley, Cheshire, SK12 2JF, UK	Harry Cripps: hrc@hrcconsultants.co.uk; +44(0)1663 765080	<www.hrcconsultants.co.uk>
Indian Institute of Technology Bombay	Energy Science and Engineering, Indian Institute of Technology Bombay, Powai, Mumbai, 400076, India	Santanu Bandyopadhyay santanu.bandyopadhyay@gmail.com	<www.me.iitb.ac.in>
KBC Energy Services (Formerly Linnhoff March)	KBC Energy Services (Formerly Linnhoff March), Targeting House, Gadbrook Park, Northwich, Cheshire CW9 7UZ, UK		<www.kbcenergyservices.com>
National Taiwan University	National Taiwan University, Department of Chemical Engineering	Cheng-Liang Chen: CCL@ntu.edu.tw	<www.ntu.edu.tw/english>
National Technical University – Kharkov Polytechnical Institute	National Technical University – Kharkov Polytechnical Institute Department of Integrated Technologies Processes and Apparatuses, 21 Ulica Frunze, 61002, Kharkiv, Ukraine	Petro O. Kapustenko: petro.kapustenko@kpi.kharkov.ua	<www.kpi.kharkov.ua/en>
Norwegian University of Science and Technology	Thermal Energy, Department of Energy and Process Engineering, Norwegian University of Science and Technology, NO-7491, Trondheim, Norway	Truls Gundersen truls.gundersen@ntnu.no	<www.ntnu.no>
Process Integration Limited	Process Integration Limited, One Central Park, Northampton Road, Monsall, Manchester, M40 5BP, UK	Nan Zhang: nan.zhang@processint.com	<www.processint.com>

© Woodhead Publishing Limited, 2013

Institution	Address	Contact	Web address
Synew Technologies	Synew Technologies, A 502, Galleria, Hiranandani Gardens, Powai, Mumbai 400 076, India	Uday V. Shenoy: shenoys@vsnl.com	<www.vsnl.com>
Texas A&M University	Artie McFerrin Department of Chemical Engineering, Texas A&M University, College Station, TX 77843, USA	Mahmoud M. El-Halwagi: El-Halwagi@tamu.edu	<www.che.tamu.edu>
The University of Manchester (formerly UMIST)	Manchester, Centre for Process Integration, CEAS, The University of Manchester (formerly UMIST) Manchester, M13 9PL, UK	Robin Smith robin.smith@manchester.ac.uk	<www.ceas.manchester.ac.uk/research/researchcentres/centreforprocessintegration/>
The University of Nottingham, Malaysia Campus	The University of Nottingham, Malaysia Campus, Department of Chemical and Environmental Engineering, Jalan Broga, 43500 Semenyih, Selangor Darul Ehsan, Malaysia	Dominic C. Y. Foo: Dominic.Foo@nottingham.eed.my; Denny K. S. Ng: Denny.Ng@nottingham.edu.my; Hon Loong Lam: HonLoong.Lam@nottingham.edu.my	<www.nottingham.edu.my/Faculties/ Engineering/Chemical/Pages/default.aspx>
The University of Waikato	The University of Waikato, Energy Research Group – Industrial Energy Efficiency Division, Faculty of Science and Engineering, Hamilton 3240, New Zealand	Michael Walmsley: m.walmsley@waikato.ac.nz Martin Atkins	<sci.waikato.ac.nz/atee>
Universiti Teknologi Malaysia	Universiti Teknologi Malaysia, Faculty of Chemical Engineering, Professor and Founder, Process Systems Engineering Centre (PROSPECT), UTM Johor Bahru 81310, Johor, Malaysia	Zainuddin Abdul Manan: zain@cheme.utm.my; Sharifah Rafidah Wan Alwi: shasha@cheme.utm.my	<www.cheme.utm.my/prospect>

(*Continued*)

© Woodhead Publishing Limited, 2013

Table 1.5 Continued

Institution	Address	Contact	Web address
University of Cape Town	University of Cape Town Department of Chemical Engineering, 7701 Rondebosch, South Africa	Duncan Fraser: Duncan.Fraser@uct.ac.za	
University of Guanajuato	University of Guanajuato, Department of Chemical Engineering, Noria Alta s/n, Guanajuato, Gto., México	Martín Picón-Núñez: picon@ugto.mx	
University of Montreal/Ecole Polytechnique de Montreal	University of Montreal/Ecole Polytechnique de Montreal, Department of Chemical Engineering, P.O. Box 6079, Station Centre-Ville, Montreal, Quebec H3C 3A7, Canada	Paul Stuart: paul.stuart@polymtl.ca	
University of Pannonia	Centre for Process Integration and Intensification – CPI^2, Research Institute of Chemical and Process Engineering, MÜKKI, Faculty of Information Technology, University of Pannonia, Egyetem u.10, Veszprém, H-8200, Hungary	Jiří Jaromír Klemeš: klemes@cpi.uni-pannon.hu Petar Sabev Varbanov: varbanov@cpi-uni.pannon.hu	<cpi.uni-pannon.hu>
University POLITEHNICA of Bucharest	Centre for Technology Transfer for the Process Industries Department of Chemical Engineering University POLITEHNICA of Bucharest 1, Gh. POLIZU Street, RO-011061 BUCHAREST ROMANIA	Professor Valentin PLESU: v_plesu@webmail.chim.upb.ro	<www.chim.upb.ro>
Warsaw University of Technology	Warsaw University of Technology, Płock Campus, Poland	Krzysztof Urbaniec K.Urbaniec@mbox.pw.edu.pl	<www.pw.plock.pl>

© Woodhead Publishing Limited, 2013

1.4 Sources of Further Information

Sources of further information have been provided for each chapter covering the specific topic or, in some cases, group of subjects. In this introductory chapter, only works covering the general aspects of PI have been listed. They fall into two main categories: (i) overview books, textbooks and handbooks, and (ii) review papers. Several very high quality books have been published on PI, the authors of which have contributed considerably to the development of the methodology and/or possess unique skills for providing an overview of the current state of the art. It is, however, important to remember that each of them, for natural reasons, could cover only the period up until the date when it was written, and for the most recent developments it is necessary to look at more recently published sources.

The first and very popular 'Red Book' was a joint work by a number of authors lead by Bodo Linnhoff (Linnhoff *et al*., 1982). This highly successful book has been reprinted many times, and the last edition covering developments up until 1994 is especially useful (Linnhoff *et al*., 1994). Kemp (2007) presented a second comprehensively upgraded edition of this book called 'Black Book', which utilised UMIST MSc Course documentation (CPI, 2004, 2005).

Shenoy's 1995 book dealt with HEN Synthesis and included a considerable section dealing with PI (Shenoy, 1995).

The 'Blue Book', by Robin Smith (2000) was another highly successful PI text and was later further developed by Smith (2005). A developed and extended version was also produced for Russian-speaking readers, in collaboration with Ukrainian co-authors (Smith *et al*., 2000).

El-Halwagi has also produced three valuable books on PI; the first focuses on pollution prevention through PI (El-Halwagi, 1997), the second is a more general discussion on PI (El-Halwagi, 2006) and the most recent book investigates sustainable design through PI (El-Halwagi, 2012).

Klemeš *et al*. (2008) produced an edited book specialising in water and energy management in food processing, which included chapters dedicated to PI. Sieniutycz and Jeżowski (2009) presented a book on energy optimisation in process systems, which included a section dealing with PI.

Of the more recent publications containing key information about developments in PI, it is possible to recommend Klemeš *et al*. (2010). Foo (2012) recently published a book focusing on PI for resource conservation, and was the editor of another book dealing with recent advances in sustainable process design and optimisation (Foo *et al*., 2012).

There have been several chapters in edited books which are of special interest: El-Halwagi (1999) deals with sustainable pollution prevention through Mass Integration; Klemeš and Perry (2007) investigates process

© Woodhead Publishing Limited, 2013

optimisation to minimise water use and wastage; Klemeš *et al*. (2010) provides information about water recycling and recovery in the food and drink industry using the application of Water Integration.

There are numerous useful sources related to PI available on the web – such as CANMET (2003) and ASPNTECH (2009). Details of the recent technology are available from for example web PIL (2012), including various descriptions and documents. Several other web-links relating to PI software are in detail discussed in Chapters 34 and 35.

1.5 References

Alves, J. J. (1999). Analysis and design of refinery hydrogen distribution systems. PhD thesis, UMIST, Manchester, UK.

Alves, J. J., Towler, G. P. (2002). Analysis of refinery hydrogen distribution systems. *Industry and Engineering Chemistry Research*, **41**, 5759–5769.

Asante, N. D. K. (1996). Automated and interactive retrofit design of practical heat exchanger networks. PhD thesis, UMIST, Manchester, UK.

AspenTech. (2009). *Aspen Energy Analyser* – Reference Guide, <www.aspentech.com> accessed 16/08/2012.

Bandyopadhyay, S. (2006). Source composite curve for waste reduction, *Chemical Engineering Journal*, **125**, 99–110.

BP Statistical Review of World Energy, <www.bp.com/assets/bp_internet/globalbp/globalbp_uk_english/reports_and_publications/statistical_energy_review_2011/staging/local_assets/pdf/statistical_review_of_world_energy_full_report_2012.pdf> accessed 20/06/2012.

CANMET Energy Technology Centre. (2003). *Pinch Analysis: For the Efficient Use of Energy, Water and Hydrogen.* ISBN: 0–662–34964–4, <cetc-varennes.nrcan.gc.ca> accessed 12/08/2012.

CPI [Centre for Process Integration]. (2004). Heat integration and energy systems. MSc course, UMIST, Manchester, UK.

Dhole, V. R. (1991). Distillation column integration and overall design of subambient plants. PhD Thesis, UMIST, UK.

Dhole, V. R., Linnhoff, B. (1993b). Total site targets for fuel, co-generation, emissions and cooling. *Computers & Chemical Engineering*, **17**(Suppl.), 101–109.

El-Halwagi, M. M. (1997). *Pollution Prevention through Process Integration: Systematic Design Tools*. Academic Press, San Diego, USA.

El-Halwagi, M. M. (1999). Sustainable pollution prevention through mass integration. In: Sikdar, S., Diwekar, U. (eds), *Tools and Methods for Pollution Prevention.* Kluwer Pub., Norwell, USA, pp. 233–275.

El-Halwagi, M. M. (2006). *Process Integration*. Academic Press, Amsterdam, The Netherlands.

El-Halwagi, M. M. (2012). *Sustainable Design through Process Integration: Fundamentals and Applications to Industrial Pollution Prevention, Resource Conservation, and Profitability Enhancement.* Butterworth-Heinemann/Elsevier, Oxford, USA.

El-Halwagi, M. M., Gabriel, F., Harell, D. (2003). Rigorous graphical targeting for resource conservation via material recycle/reuse networks. *Industrial and Engineering Chemistry Research,* **42**(19), 4319–4328.

© Woodhead Publishing Limited, 2013

El-Halwagi, M. M., Manousiouthakis, V. (1989). Synthesis of mass exchange networks. *AIChE Journal*, **35**(8), 1233–1244.

Flower, J., Linnhoff, B. (1979). Thermodynamic analysis in the design of process networks. *Computers & Chemical Engineering,* **3**(1–4), 283–291.

Flower, J. R., Linnhoff, B. (1978). Synthesis of heat exchanger networks: II. Evolutionary generation of networks with various criteria of optimality. *AIChE Journal*, **24**, 642–654.

Foo, D., Kazantzi, V., El-Halwagi, M., Manan, Z. A. (2006). Surplus diagram and cascade analysis technique for targeting property-based material reuse network. *Chemical Engineering Science*, **61**, 2626–2642.

Foo, D. C. Y. (2012). *Process Integration for Resource Conservation.* CRC Press, Boca Raton, Florida, USA.

Foo, D.C.Y. (2009). State-of-the-art review of pinch analysis techniques for water network synthesis. *Industrial and Engineering Chemistry Research*, **48**(11), 5125–5159.

Foo, D. C. Y., El-Halwagi, M. M., Tan, R. R. (eds). (2012). *Recent Advances in Sustainable Process Design and Optimization.* World Scientific Publishing Co., London, UK.

Friedler, F. (2009). Process integration, modelling and optimisation for energy saving and pollution reduction. *Chemical Engineering Transactions*, **18**, 1–26.

Friedler, F. (2010). Process integration, modelling and optimisation for energy saving and pollution reduction. *Applied Thermal Engineering,* **30**, 2270–2280.

Furman, K. C., Sahinidis, N. V. (2002). A critical review and annotated bibliography for heat exchanger network synthesis in the 20th century. *Industrial & Engineering Chemistry Research*, **41**, 2335–2370.

Gundersen, T. (2000). *A Process Integration Primer – Implementing Agreement on Process Integration*. International Energy Agency, SINTEF Energy Research, Trondheim, Norway.

Gundersen, T., Naess, L. (1988). The synthesis of cost optimal heat exchanger networks – an industrial review of the state of the art. *Computers & Chemical Engineering*, **12**(6), 503–530.

Hallale, N. (1998). Capital cost targets for the optimum synthesis of mass exchange networks. PhD thesis, Department of Chemical Engineering, University of Cape Town, South Africa.

Heyen, G., Kalitventzeff, B. (2007). Process monitoring and data reconciliation. In: Puigjaner, L., Heyen, G. (eds), *Computer Aided Process and Product Engineering,* Vol. **2**. Wiley, New York, USA, pp. 517–540.

Hohmann, E. C. (1971). Optimum networks for heat exchange. PhD thesis, University of Southern California, Los Angeles, USA.

Hohmann, E. C., Lockhart, F. J. (1976). Optimum heat exchanger network synthesis. AIChE 82nd National Meeting, Atlantic City, NJ, USA, Paper No 22a.

INDEX MUNDI Electricity <www.indexmundi.com/g/g.aspx?c=xx&v=81> accessed 20/06/2012.

INDEX MUNDI Gas <www.indexmundi.com/g/g.aspx?c=xx&v=137> accessed 20/0962012.

INDEX MUNDI Oil <www.indexmundi.com/g/g.aspx?c=xx&v=91> accessed 20/06/2012.

Itoh, J., Shiroko, K., Umeda, T. (1986). Extensive applications of the T-Q diagram to heat integrated system synthesis. *Computers & Chemical Engineering*, **10**(1), 59–66.

© Woodhead Publishing Limited, 2013

Jezowski, J. (2010). Review of water network design methods with literature annotations. *Industrial & Engineering Chemistry Research,* **49**, 4475–4516.

Kemp, I. C. (2007). *Pinch Analysis and Process Integration*, 2nd ed. Butterworth-Heinemann (Elsevier), Oxford, UK (authors of the first edition: Linnhoff, B., Townsend, D. W., Boland, D., Hewitt, G. F., Thomas, B. E. A., Guy, A. R., Marsland, R. H. (1982 and 1994). *A User Guide on Process Integration for the Efficient Use of Energy*, IChemE, Rugby, UK).

Kemp, I. C., Deakin, A. W. (1989a). The cascade analysis for energy and process integration of batch processes. Part 1: calculation of energy targets. *Chemical Engineering Research and Design*, **67**, 495–509.

Kemp, I. C., Deakin, A. W. (1989b). Cascade analysis for energy and process integration of batch processes. Part 2: network design and process scheduling. *Chemical Engineering Research and Design*, **67**(5), 510–516.

Kemp, I. C., Deakin, A. W. (1989c). The cascade analysis for energy and process integration of batch processes. Part 3: network design and process scheduling. *Chemical Engineering Research and Design*, **67**, 510–516.

Klemeš, J., Smith, R., Kim, J.-K. (eds) (2008). *Handbook of Water and Energy Management in Food Processing*. Woodhead Publishing Limited, Cambridge, England, **195**(4), 1029. ISBN 9781845691950. E-ISBN 9781845694678.

Klemeš, J., Dhole, V. R., Raissi, K., Perry, S. J., Puigjaner, L. (1997). Targeting and design methodology for reduction of fuel, power and CO_2 on total sites. *Applied Thermal Engineering,* **7**, 993–1003.

Klemeš, J., Friedler, F., Bulatov, I., Varbanov, P. (2010). *Sustainability in the Process Industry – Integration and Optimization.* McGraw-Hill, New York, USA.

Klemeš, J., Kravanja, Z., Varbanov, P. S., Lam, H. L. (2013). Advanced multimedia engineering education in energy, process integration and optimisation. *Applied Energy,* **101**, 26–32. DOI:10.1016/j.apenergy.2012.01.039

Klemeš, J., Lam, H. L., Foo, D. C. Y. (2010). Water recycling and recovery in food and drink industry. In: Waldron, K., Moates, G. K., Faulds, C. B. (eds), *Total Food, Sustainability of the Agri-Foot Chain*. Royal Society of Chemistry, Cambridge, pp. 186–195.

Klemeš, J., Linnhoff, B., Kotjabasakis, E., Zhelev, T. K., Gremouti, I., Kaliventzeff, B., Heyen, G., Maréchal, F., Lebon, M., Puigjaner, L., Espuca, A., Graells, M., Santos, G., Prokopakis, G. J., Ashton, G. J., Murphy, N., Paor, de A. M., and Kemp, I. C. (1994). Design and operation of energy efficient batch processes. Final Report, Commission of the European Communities. Brussels, Belgium.

Klemeš, J., Perry, S. J. (2007). Process optimisation to minimise water use and wastage. In: Waldron, K. (ed). *Waste Management and Co-product Recovery in Food Processing*. Woodhead Publishing Limited, Cambridge, pp. 90–118.

Klemeš, J., Varbanov, P. (2010). Process Integration – successful implementation and possible pitfalls. *Chemical Engineering Transactions*, **21**, 1369–1374. DOI: 10.3303/CET1021229.

Klemeš, J. J. (2012). Industrial water recycle/reuse. *Current Opinion in Chemical Engineering*, **1**(3), 238–245.

Lam, H. L., Varbanov, P. S., Klemeš, J. (2010a). Regional resource management composite curve. *Chemical Engineering Transactions*, **18**, 303–308.

Lam, H. L., Varbanov, P., Klemeš, J. (2010b). Minimising carbon footprint of regional biomass supply chains. *Resources, Conservation & Recycling*, **54**(5), 303–309.

© Woodhead Publishing Limited, 2013

Lam, H. L., Varbanov, P., Klemeš, J. (2010c). Optimisation of regional energy supply chain utilising renewables: P-graph approach. *Computers and Chemical Engineering*, **34**(5), 782–792.

Linnhoff, B., Parker, S. (1984). Heat Exchanger Networks with Process Modifications. Paper presented at the IChemE Conference in Bath. L 6. Available from <www.cpi.umist.ac.uk/publicat/Dept_publications1.asp?TypePubPaper=Paper&DPID=31a&YearPub=&Surname=&Keyword=&Page=3> accessed 18/11/2012.

Linnhoff, B. (1972). Thermodynamic analysis of the cement burning process (Thermodynamische Analyse des Zementbrennprozesses). Diploma work, Abteilung IIIa, ETH Zurich (1972) (in German).

Linnhoff, B. (1979). Thermodynamic analysis in the design of process networks. PhD thesis, University of Leeds, Leeds, UK.

Linnhoff, B. (1993). Pinch analysis – a state-of-the-art overview. *Chemical Engineering Research and Design*, **71**(A5), 503–522.

Linnhoff, B., Flower, J. R. (1978). Synthesis of heat exchanger networks: I. Systematic generation of energy optimal networks. *AIChE Journal*, **24**, 633–642.

Linnhoff, B., Mason, D. R., Wardle, I. (1979). Understanding heat exchanger networks. *Computer & Chemical Engineering*, **3**, 295–302.

Linnhoff, B., Townsend, D. W., Boland, D., Hewitt, G. F., Thomas, B. E. A., Guy, A. R., Marsland, R. H. (1982). *A User Guide on Process Integration for the Efficient Use of Energy.* IChemE, Rugby, UK.

Linnhoff, B., Townsend, D. W., Boland, D., Hewitt, G. F., Thomas, B. E. A., Guy, A. R., Marsland, R. H. (1994). *A User Guide on Process Integration for the Efficient Use of Energy.* IChemE, Rugby, UK.

Linnhoff, B., Vredeveld, D. R. (1984). Pinch technology has come of age. *Chemical Engineering Progress*, **80**(7), 33–40.

Linnhoff March Ltd. (1998). *Introduction to Pinch Technology*. Linnhoff March Ltd. now part of KBC Advanced Technologies plc., UK.

Manan, Z. A., Tan, Y. L., Foo, D. C. Y. (2004). Targeting the minimum water flow rate using water cascade analysis technique. *AIChE Journal*, **50**, 3169–3183.

Mavromatis, S. P., Kokossis, A. C. (1998a). Conceptual optimisation of utility networks for operational variations – I. Targets and level optimisation. *Chemical Engineering Science,* **53**(8), 1585–1608.

Nishida, N., Stephanopoulos, G., Westerberg, A. W. (1981). A review of process synthesis. *AIChE Journal*, **27**, 321–351.

NRCan (Natural Resources Canada). (2012). *Pinch analysis: for the efficient use of energy, water & hydrogen.* cetc-varennes.nrcan.gc.ca/en/indus/agroa_fd/ip_pi/ap_pa.html, accessed 15/08/2012, 61 pages.

Ponton, J. W., Donaldson, R. A. B. (1974). A fast method for the synthesis of optimal heat exchanger networks. *Chemical Engineering Science*, **29**(12), 2375–2377.

Prakash, R., Shenoy, U. V. (2005). Targeting and design of water networks for fixed flowrate and fixed contaminant load operations. *Chemical Engineering Science*, **60**(1), 255–268.

PIL, Process Integration Ltd. Manchester, UK <www.processint.com and www.processint.com/download/documents> accessed 20/10/2012.

Proceßß Integratfion Reßearch Conßortfium. The , UK, 2012, <www.cpi.umist.ac.uk/ consortium/ consortium_page.asp?page=membership.asp>, accessed 6/7/2012.

© Woodhead Publishing Limited, 2013

REDBAS 'EU Programme INCO-COPERNICUS *Sustainable Development by Retrofit and Debottlenecking for Energy Based System*'. Research & Technology Development Project " – PL 5046".2001. Final Publishable Report, < European Commission, Brussels, Belgium.

Savulescu, L. (1999). Simultaneous energy and water minimisation. PhD thesis, UMIST, Manchester, UK.

Savulescu, L., Kim, J., Smith, R. (2005a). Studies on simultaneous energy and water minimisation – Part I: systems with no water re-use. *Chemical Engineering Science*, **60**(12), 3279–3290.

Savulescu, L., Kim, J., Smith, R. (2005b). Studies on simultaneous energy and water minimisation – Part II: systems with maximum re-use of water. *Chemical Engineering Science,* **60**(12), 3291–3308.

Shenoy, U. V. (1995). *Heat Exchanger Network Synthesis – Process Optimization by Energy and Resource Analysis*. Gulf Publishing, Houston, USA.

Sieniutycz, S., Jeżowski, J. (2009). *Energy Optimization in Process Systems*. Elsevier Science, Dordrecht, The Netherlands.

Singhvi, A., Madhavan, K. P., Shenoy, U. V. (2004). Pinch analysis for aggregate production planning in supply chains. *Computers & Chemical Engineering*, **28**(6–7), 993–999.

Singhvi, A., Shenoy, U. V. (2002). Aggregate planning in supply chains by pinch analysis. *Chemical Engineering Research and Design*, **80**(6), 597–605.

Smith, R. (2005). *Chemical Process Design and Integration.* John Wiley & Sons, Chichester, West Sussex, UK.

Smith, R., 1995. *Chemical Process Design*. McGraw-Hill, New York, USA.

Smith, R., Klemeš, J., Tovazhnyansky, L. L., Kapustenko, P. A., Uliev, L. M. (2000). *Foundations of Heat Processes Integration*. NTU KhPI, Kharkiv, Ukraine (in Russian).

Takama, N., Kuriyama, T., Shiroko, K., Umeda, T. (1980). Optimal water allocation in a petroleum refinery. *Computers and Chemical Engineering*, **4**(4), 251–258.

Umeda, T., Itoh, J., Shiroko, K. (1978). Heat exchanger systems synthesis. *Chemical Engineering Progress,* **74**(7), 70–76.

Umeda, T., Harada, T., Shiroko, K. A. (1979). Thermodynamic approach to the synthesis of heat integration systems in chemical processes. *Computers and Chemical Engineering*, **3**(1–4), 273–282.

Umeda, T., Niida, K., Shiroko, K. (1979). A thermodynamic approach to heat integration systems. *AIChE Journal*, **25**, 423.

Varbanov, P. (2004). Optimisation and synthesis of process utility systems. PhD thesis, UMIST, Manchester, UK.

Varbanov, P. S., Doyle, S., Smith, R. (2004a). Modelling and optimisation of utility systems. *Transactions on IChemE, Chemical Engineering Research and Design*, **82**(A5), 561–578.

Varbanov, P., Perry, S., Makwana, Y., Zhu, X. X., Smith, R. (2004b). Top-level analysis of site utility systems. *Transactions on IChemE, Chemical Engineering Research and Design*, **82**(A6), 784–795.

Varbanov, P., Perry, S., Klemeš, J., Smith, R. (2005). Synthesis of industrial utility systems: cost-effective de-carbonization. *Applied Thermal Engineering*, **25**(7), 985–1001.

Wang, Y. P., Smith, R., 1994. Wastewater minimisation. *Chemical Engineering Science*, **49**(7), 981–1006.

© Woodhead Publishing Limited, 2013

Zhelev, T. K., Bhaw, N. (2000). Combined water–oxygen pinch analysis for better wastewater treatment management. *Waste Management*, **20**(8), 665–670.

Zhelev, T., Ntlhakana, L. (1999). Energy-environment closed loop through oxygen pinch. *Computers & Chemical Engineering*, **23**(Suppl.), 79–83.

Zhelev, T. K., Ridolfi, R. (2006). Energy recovery and environmental concerns addressed through energy–pinch analysis. *Energy*, **31**, 2486–2498.

Zhu, X. X. (1997). Automated design method for heat exchanger networks using block decomposition and heuristic rules. *Computers & Chemical Engineering*, **21**(10), 1095–1104.

© Woodhead Publishing Limited, 2013

2

Basic Process Integration Terminology

PETAR SABEV VARBANOV, University of Pannonia, Veszprém, Hungary

DOI: 10.1533/9780857097255.1.28

Abstract: This chapter establishes a framework for systematically reading the handbook by defining the basic terms associated with Process Integration. It begins by defining Process Integration and its applications, and then continues with definitions of core Process Integration phases and terms. The main section then defines other significant terms associated with Process Integration in alphabetical order.

Key words: Process Integration, basic terms, glossary.

2.1 Introduction

Process Integration (PI) has developed enormously since its conception in the 1970s. The method was originally used mainly for heat recovery as Heat Integration (HI). Subsequently, it has been applied to many areas for resource minimisation. As a result, there are currently many concepts and terms associated with PI, some of which are sometimes difficult to distinguish from one another. The present chapter provides definitions for most common, fundamental PI terms, and also explains the context in which they are used whenever this is relevant.

Process Integration

The first term to define is ***PI*** itself. PI is a family of methodologies for combining operations within a process or several processes to reduce consumption of resources and/or harmful emissions. Many definitions of PI are possible. The one adopted by the International Energy Agency (Gundersen, 2000) is: '*Systematic and general methods for designing integrated production systems ranging from individual Processes to Total Sites and with special emphasis on the efficient use of energy and reducing environmental effects.*'

A list of the most well-known PI applications follows (definitions for terms in boldface and italic are provided in this chapter):

- ***Heat Integration*** deals with heat recovery in a group of operations termed a ***Process***.

© Woodhead Publishing Limited, 2013

- ***Total Site Integration*** for heat recovery and Combined Heat and Power (CHP) generation (Dhole and Linnhoff, 1993); and extended by Klemeš *et al*. (1997) over ***Total Sites***. A ***Total Site*** includes a collection of energy use and generation areas, termed ***Processes***, and a central ***utility system***, recently extended to a power system as well (Wan Alwi, 2012).
- ***Mass Integration and Resource Conservation*** (El-Halwagi and Manousiouthakis, 1989), of which ***water minimisation*** (***waste water minimisation***) is the most common branch (Wang and Smith, 1994). It has also been combined with HI in studies without water reuse (Savulescu *et al*., 2005a) and maximum reuse (Savulescu *et al*., 2005a, 2005b).
- ***Hydrogen Pinch*** for managing hydrogen in refineries (Alves, 1999), extended in Alves and Towler (2002).
- ***Oxygen Pinch Analysis*** (Zhelev and Ntlhakana, 1999) also combined with water minimisation (Zhelev and Bhaw, 2000).
- ***Targeting Supply Chains performance*** applications to classical supply chains (Singhvi and Shenoy, 2002) and also to regional resource management (Lam *et al*., 2010b) have been developed.
- ***Targeting Property-Based Material Reuse*** (Foo *et al*., 2006).
- ***Targeting Carbon Footprint Reduction*** (Tjan *et al*., 2010).

Other applications have also been presented over the years, and some of them are reviewed in following chapters of this handbook.

2.2 Process Integration Terms: The Importance of Context

A significant number of the terms can be used in different contexts and in some cases their meaning changes depending on the context. Where this is the case, the context in which a term is defined is specified in bold within square brackets.

A list of the contexts in which some of the terms in this chapter are used is below.

(i) ***HI***. As a context it is used for all matters concerning HI – also including Heat Exchanger Networks (HENs).
(ii) ***MI (Mass Integration) – referring to Mass Exchanger Networks and Mass Integration.***
(iii) **Water**. This refers to the context of *water networks*.
(iv) **Resource**. This refers to the context of a general resource.
(v) **Total Site**. This is a collection of entities having heating demands and offering heat supply, which are linked by a common infrastructure. The entities are most commonly referred to as processes and the common infrastructure as a utility system.

© Woodhead Publishing Limited, 2013

(vi) **Hydrogen**. This refers to the context of hydrogen networks.
(vii) ***Grand Composite Curve (GCC)***. Identifies the context of the *GCC* in *HI*.
(viii) ***Total Site Profiles (TSP)***. Identify the context of TSP in *Total Site Integration*.
(ix) **Regional Energy Supply**. This is a relatively new area of PI, dealing with the evaluation of energy supply for regions, emphasising on renewable energy sources.

2.3 Fundamental Process Integration Terms

This section defines the fundamental concepts and terms, serving as a basis for the definitions of more elaborate concepts used in PI.

Isothermal and Non-isothermal Utilities [HI]

In HENs the utilities for heating or cooling supply or absorb heat. As a result, the enthalpy contents of the utility streams reduce or increase. If a utility is used at phase change conditions (evaporation, condensation) its temperature does not change and such a utility is referred to as ***Isothermal***. Examples include steam use via its condensation or steam generation by evaporating saturated liquid water. Outside such conditions, the utility streams do change their temperatures and are termed ***Non-isothermal***. Examples include heating utilities – such as hot oil or flue gas.

Operating Unit

The implementation of a *unit operation* is a facility frequently called an ***Operating Unit***.

Primary Resource

An important concept is that of ***Primary Resource***. This is any resource taken from the environment and exploited for the purpose of human activities – including industrial operations.

Process and Process Flowsheet

A ***Process*** (***Processing Plant***) is a collection of related *modules* and *unit operations* which are put together for generating a certain final or intermediate product. The *unit operations* in a *process* can be viewed as forming a network, which is usually represented by a block-type diagram, termed a ***Process Flowsheet*** (short – ***Flowsheet***). A *flowsheet* contains pictorial representations of *operating units*, connected by *process streams*.

© Woodhead Publishing Limited, 2013

Process Streams

In the *general process context*, a ***Process Stream*** is a flow of material or energy which may be a system input (entering an *operating unit*), output (leaving an *operating unit*) or an intermediate (connecting two *operating units*) of a *process (system)*.

Resource Conservation

This is a goal or a strategy for preserving the reserves of a certain *primary resource*. Examples of such reserves are the underground deposits of coal, crude oil or natural gas, which are fuels having high energy values. Therefore, the preservation of such deposits is also frequently referred to as ***Energy conservation***.

Resource Recovery

The goal of *resource conservation*, which is implemented by actions and facilities, is the reduction of the intake of the targeted resource. This is performed by extracting from a product or waste stream the resource or a material containing it, followed by the use/application of the latter. This forms a closed Loop in the Path of the resource. As a result, the actions and facilities used are termed *reuse*, *recycling*, *regeneration*, etc.

Resource Recovery Network

This is a *process*, or part of a *process*, aimed at the recovery of certain resources. Examples include ***Heat Exchange Network*** (***Heat Recovery Network***) and ***Water Reuse Network***.

Unit Operations and Modules

The overall processing plants are implemented in functional steps, termed ***Modules***. Examples include reactor, separator (distillation column, adsorption column, membrane), boiler, Heat Recovery Steam Generator (HRSG), cooling tower, furnace, refrigeration, heat pump, utility mains (steam mains, water mains, power mains), heat engines (gas turbine, steam turbine, fuel cell), heat exchangers (recovery / process-to-process, heater, cooler). When the module constitutes a unit, which cannot be subdivided further into parts, it is referred to as a ***Unit Operation***. According to these definitions, a reactor is viewed as a unit operation, while a fuel cell or a gas turbine can be viewed as a unit operation when considered in the context of a larger system or as a complete system itself, since it consists of other modules and unit operations.

© Woodhead Publishing Limited, 2013

Utility

This is a resource stream provided via a material or electric (electrical power) carrier. Examples of utilities from HENs include heating utilities: steam supply or flue gas (from a furnace or a gas turbine); cooling utilities – such as steam generation or cooling water. As another example, the *electricity grid* is a supplier of electrical power utility.

2.3.1 Main Process Integration Phases and Related Terms

PI involves several phases (Gundersen, 2000), which can be applied in full sequence, partially, or even within the framework of a more elaborate or iterative process optimisation algorithm. The main phases are:

(1) ***Data Extraction***. This involves first identifying the correct ***PI Interface*** for the relevant PI domain (e.g. HI, Water Minimisation, and Supply Chains). Further, the relevant data are collected from the problem formulation at hand and represented in the standardised way for the application domain. For HEN Synthesis the interface is termed a ***Process Stream***. A process stream [HI] represents a heating or a cooling demand in the process and contains items for supply (or starting) temperature (TS), target (or ending) temperature (TT) and either enthalpy change (ΔH) or heat-capacity flowrate (CP).
(2) ***Targeting***. This is the process of obtaining the targets.
(3) ***Process Modifications.***
(4) ***Network Design***. This is the process of obtaining the relevant process network for reusing/recovering the resources tracked by the application domain. The design may proceed by various algorithms and involve sub-phases. One of the possible algorithms is the ***Pinch Design Algorithm***, which involves an initial construction of a ***HEN*** featuring ***Maximum Energy Recovery*** (MER) and further evolving it by trading off the energy costs for utilities versus the investment costs for heat exchangers and piping.

2.3.2 Further Process Integration Terms

Above the Pinch

This refers to the location point of an *operating unit* or utility supply in the *Composite Curves* (usually thermodynamic) representation of a *resource recovery network*. It means that, on the axis corresponding to the intensive

© Woodhead Publishing Limited, 2013

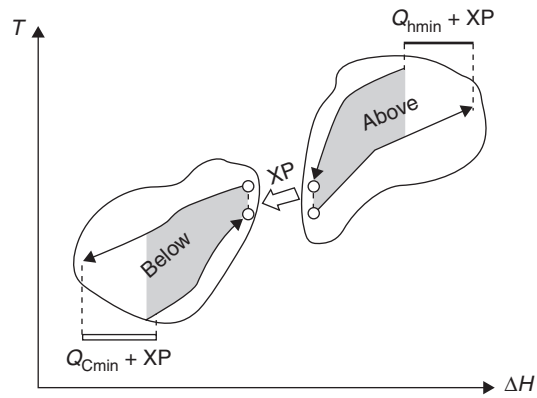

2.1 Positions relative to the Heat Recovery Pinch.

variable in the analysis, the reference point is located at a higher value than the Pinch. Examples include: (a) for HENs a utility, a heat exchanger, or a heat-intensive operation (e.g. a distillation column) may be placed Above the Pinch, meaning all its temperatures are higher than that of the *Heat Recovery Pinch* (Fig. 2.1); (b) for water networks, when tracking a single contaminant, a water-using operation Above the Pinch means having concentrations higher than the *Water Pinch*.

Annualisation Factor

When a new process design is evaluated, it is necessary to account for both operating and capital (investment) costs. Both these are components of: $/y, €/y (i.e. on an annual basis). To convert the *capital cost* from a finite amount of money ($ or €) to annual form, it is multiplied by a parameter termed an ***Annualisation Factor***. The value of this parameter is derived based on the project life time (*Plant Life Time*). The most straightforward calculation is to take the inverse of the project life time:

$$AF = 1 / PLF \qquad [2.1]$$

There are other, more elaborate, ways of calculating the annualisation factor accounting for loan interest rates and other economic variables. An example can be found in Smith (2005), which also includes a derivation.

Appropriate Placement Principle [HI]

Certain *operating units* or subsystems, featuring intensive energy demands for heating and/or cooling, can be integrated with a set of process streams

© Woodhead Publishing Limited, 2013

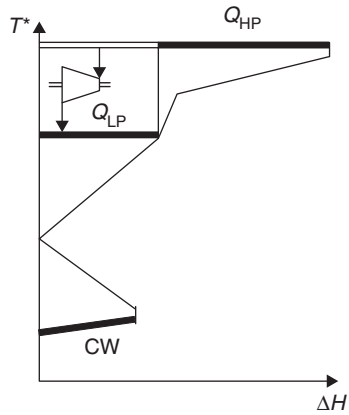

2.2 Appropriate placement of a steam turbine.

(a *process*). To integrate such a unit with the process, Pinch Analysis of the *process* is performed, and the unit heat sources and sinks are placed against the GCC of the *process*. When placing the unit, the goal is to reduce the utility requirements for the combined system, including the *process* and the unit. These goals constitute the ***Appropriate Placement Principle***, and the achieved integration is termed ***Appropriate Placement***. An example is the integration of a steam turbine with a heat recovery problem. In Fig. 2.2 the steam turbine is placed Above the Pinch, resulting in a saving of steam for running the turbine.

Automated Network Design/Synthesis

The synthesis of a process network is performed based on a particular algorithm. The steps in that algorithm may be performed by a system designer (a person) or by a computer. When all, or all significant, steps in the synthesis are performed by the computer, eliminating extensive interventions by the system designer into the solution process, the algorithm is referred to as automated, giving rise to ***Automated Network Design (Synthesis)***. This definition applies, for example, to the design of HENs, water networks, hydrogen management networks, supply chains, etc.

Area Efficiency

This is the ratio of the *area target* and the *heat transfer area* of a particular HEN. It expresses how well the considered HEN performs compared to the *area target*.

© Woodhead Publishing Limited, 2013

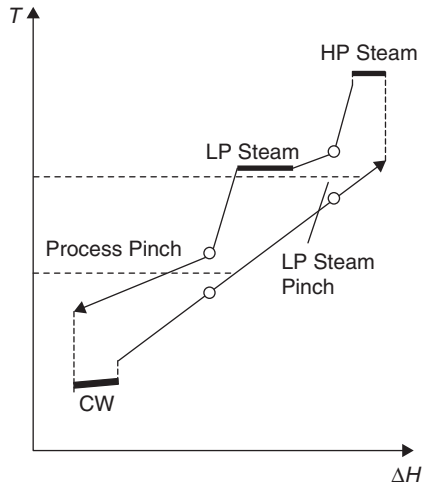

2.3 Balanced Composite Curves.

Balanced Composite Curves [HI] (BCC)

The plot of the ***Balanced Composite Curves*** is a variation of the Composite Curves, which include the various utilities (Fig. 2.3) placed after targeting with the *Problem Table Algorithm* (Linnhoff and Flower, 1978) and the *GCC*. For obtaining the plot, hot utilities are treated as hot streams and cold utilities as cold streams.

Batch Process

A manufacturing process can be arranged to produce its main outputs (products) in finite quantities of material. In such cases, the finite quantities of material are referred to as ***Batches*** and the process is termed a ***Batch Process***. Any process which is a consequence of discrete tasks that have to follow a predefined sequence from raw materials to final products is a batch process. For example, *batch processes* are used in pharmaceutical production, specialty chemicals and beer manufacturing.

Bath Formula

This is an equation for evaluating the targets for the heat transfer area in a HEN, presented at the 1984 annual IChemE meeting in Bath, UK (Townsend and Linnhoff, 1984). The equation is based on a number of assumptions. The derivation starts by dividing the enthalpy axis of the Composite Curves into Enthalpy Intervals (EI) to ensure vertical heat transfer. Next, all hot streams in each EI are allowed to match with all cold streams in the same

© Woodhead Publishing Limited, 2013

interval, while making sure that the outlet temperature for each match is the same as the interval temperature. This is further discussed in Chapter 8.

Below the Pinch

This refers to a location point of an *operating unit* or utility supply in the thermodynamic representation of a resource recovery network. It means that, on the axis corresponding to the intensive variable in the analysis, the reference point is located at a lower value than the Pinch. An example of Below–Above the Pinch division for heat recovery problems is shown in Fig. 2.1. This situation is the opposite of '*Above the Pinch*'.

Capital Cost

Capital cost is the cost of purchasing or developing assets during the initial construction of a plant or during retrofit. Assets include, for example, buildings, hardware (the equipment for the *operating units*) and software. The initial value of the asset is then depreciated over a period of time (usually the useful life of the asset).

CHP – Combined Heat and Power

CHP usually means 'Combined Heat and Power Generation'. Another synonym is '***Co-Generation***'. A *co-generation* plant produces both power and useful heat from the same primary energy resource. By this definition, a Gas Turbine Combined Cycle power station is not a *co-generation* plant, but merely a simple generation one. On the other hand, even a simple steam turbine, supplying heat to users in addition to the power, is a *co-generation* (CHP) plant.

Cold Stream [HI]

The term *cold stream* is used to denote a heating requirement in a process. It is more often associated with a material *process stream*, but for the purpose of *HI* heating, requirements of chemical reactors are also extracted as cold streams from a *process*.

Column Grand Composite Curve (CGCC)

The CGCC is analogous to the GCC for a general process, but constructed for a distillation column. It shows the heat load which can be added or removed at a given temperature (stage) in order to maintain acceptable thermodynamic operating conditions. The calculation procedure for the CGCC involves determination of the net enthalpy deficit at each stage by

© Woodhead Publishing Limited, 2013

generating envelopes from either the condenser end (top-down approach) or the reboiler end (bottom-up approach).

Composite Curve (CC)

A ***CC*** is a combined representation of the use of a certain resource in a process network. A distinctive feature of such a curve is that it represents the cumulative resource use or supply versus another problem variable – either intensive (temperature or concentration) or extensive (cumulative area or distance). CCs can be built for various applications and can represent different facets of the analysed problem, as described next.

Composite Curve [HI]

For the analysis of heat recovery problems, *CC*s are constructed in coordinates of temperature versus enthalpy change. There are two main types: ***Composite Curves*** (Hot and Cold) and ***GCC***. The CCs represent composite hot and cold streams, matched in terms of temperature, and they show the amounts of heat recovery and utility needs according to the temperature. The name derives from combining the heat flows and temperatures of a number of hot and cold process streams into the *Hot and Cold CCs*. The GCC is defined separately.

Composite Curve [Water], Limiting Composite Curve

This is a *CC* constructed from *Limiting Water Profiles* of a number of water-using operations, representing water use in terms of the contaminant concentrations versus contaminant load. This applies to water networks with a single contaminant. The construction of the ***Limiting CC*** for water reuse is based on combining the individual operations in terms of their contaminant loads and concentrations, in a way similar to the construction of the *CCs* for HENs.

Concentration (of Contaminant), C [ppm]

This is the amount of a contaminant present in a water volume (in a stream flow or in a vessel) expressed per unit of mass or volume. In water network applications the convention is to express the contaminant concentration as the contaminant mass per unit mass of pure water.

Concentration Difference

There are two contexts defining a ***Concentration Difference***. One is the difference between concentrations of two mass exchanging streams at a point

© Woodhead Publishing Limited, 2013

in a mass exchanger. Another is the change in the concentration in the same stream (not to be confused with mass-exchange driving force). The most usual example of the latter is the change in the contaminant concentration in a water stream when interacting with a water-using operation or when being cleaned in a water treatment facility.

Contaminant mass flow (load) [kg/h]

This is the amount of contaminant carried with a water flow passing through a certain location per unit time.

Cooling Duty

The heat flow removed in a *heat exchanger* from a *hot process stream* is referred to as a ***Cooling Duty***, usually implying that the corresponding *cold stream* is a *utility* and the *heat exchanger* is a *cooler*.

Cooling System

In industry, the term cooling system denotes a network of equipment items and resource supplies for providing utility cooling to the main production processes in an industrial site (Smith, 2005). The used utilities are usually water and various refrigerants. In the latter case, the cooling is referred to as *refrigeration* and is used to achieve sub-ambient temperatures. The cooling system can be centralised using the above-mentioned utility carriers. It can also be distributed, meaning that the utilities can be generated/regenerated at the locations of use, or close to them, and not originate from a single central location. An example of this is air cooling.

COP – Coefficient of Performance (of a Heat Pump)

An important characteristic of heat pumps is their COP. This metric for device efficiency is defined (Fig. 2.4) as the ratio between the heat delivered to the heat sink and the consumed Shaft Work (mechanical power).

CP Tables

In applying the Pinch Design Method for HEN Synthesis, the choice of *Essential Matches* is assisted by a tool called ***CP Tables***. This is a set of two tables – one for the design *Above the Pinch* and another for the design *Below the Pinch*. Each table has two columns: in one column are listed the *CPs* of the *hot streams*, while in the other are listed those for the *cold streams*. All values are sorted in descending order.

© Woodhead Publishing Limited, 2013

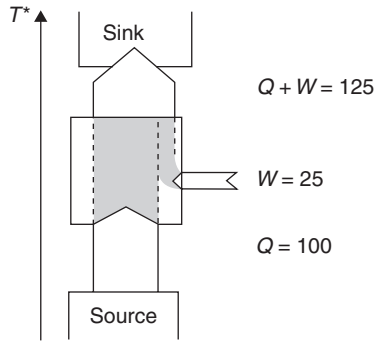

$$\text{COP} = \frac{Q + W}{W} = f(\Delta T)$$

2.4 Heat pump configuration.

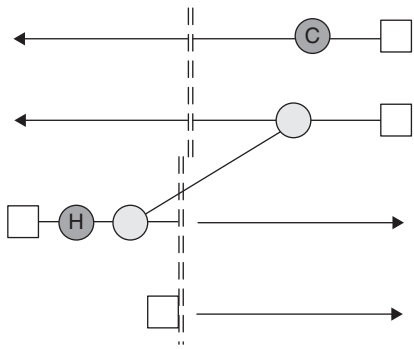

2.5 Cross-Pinch Heat Exchanger.

Cross-Pinch Heat Transfer

This is heat transfer in a *heat exchanger* where heat is transferred from *Above the Pinch* to *Below the Pinch*. Figure 2.5 shows a *Grid Diagram* representation of another case, where the *hot stream*, while inside the *heat exchanger*, is located *Above the Pinch* and heat is transferred to a part of a cold stream, which is *Below the Pinch*.

More complicated situations are possible, where the hot and cold streams both cross the Pinch inside the heat exchanger. In such situations Cross-Pinch heat transfer should be detected by more detailed analysis, identifying how much of the heat transfer in the exchanger takes place *Above the Pinch*, *Below the Pinch* and ***Across the Pinch***.

© Woodhead Publishing Limited, 2013

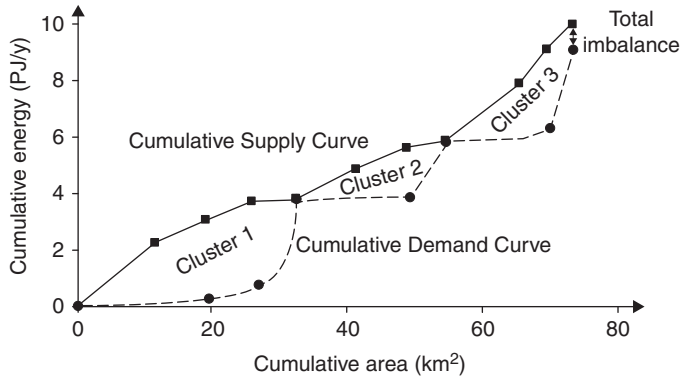

2.6 Regional Energy Supply-Deficit Curves (after Lam *et al.*, 2010a).

Cryogenic Processes

These are *processes* operating at very low temperatures. The cryogenic temperature range is defined as from –150°C (123.15 K) down to close to absolute zero (0 K) (Britannica, 2012).

Cumulative Demand Curve

This is a curve expressing the overall energy demand in a region in terms of cumulative area versus cumulative energy demand (Fig. 2.6). It is constructed by performing summations of the areas and the energy demands of all zones in a region (Lam *et al.*, 2010a). The *Cumulative Demand Curve* is constructed and used in combination with the *Cumulative Supply Curve*.

Cumulative Supply Curve

This is a curve expressing the overall renewable energy supply in a region in terms of cumulative area versus cumulative energy supply (Fig. 2.6). It is constructed by performing summations of the areas and the energy supply flows of all zones in a region (Lam *et al.*, 2010a). The *Cumulative Supply Curve* is constructed and used in combination with the *Cumulative Demand Curve*.

Data Extraction

As discussed previously, data extraction is an activity for obtaining only the relevant data for the relevant PI domain (HI, water minimisation, Supply Chains, etc.) and presenting the data in a standardised format suitable for further analysis.

© Woodhead Publishing Limited, 2013

Data – Soft and Hard

Distinguishing soft data from hard data is one of the most important aspects of data extraction. When data specifications for heating and cooling demand are extracted from a process flow sheet, those process entities, which can take specifications with some flexibility over an interval (e.g. a temperature), are termed ***Soft Data***. On the other hand, when the specifications must be closely matched, these are ***Hard Data***.

Driving Force: Temperature Difference, Minimum Allowed Temperature Difference, ΔT_{min}

The ***Driving Force*** in heat- and mass-transfer phenomena is the deviation of the tracked intensive variable (temperature or concentration) from its equilibrium value. For resource recovery networks involving heat and mass transfer, these deviations are represented by the differences in the variable values of the streams exchanging heat or mass. For heat transfer, the *driving force* is represented by ***Temperature Differences*** between the streams in a heat exchanger, and for a mass-exchange operation by ***concentration differences*** between the streams and the corresponding equilibrium concentrations for those streams in the mass exchanger.

In the context of heat recovery networks (*HENs*), to ensure that an excessively large heat transfer area is not selected, the *temperature differences* between the hot and the cold streams in each heat exchanger are kept larger than a certain lower bound. In the HEN design, the concept of the ***Minimum Allowed Temperature Difference*** ($\Delta T_{\min}$) is introduced, representing this lower bound. $\Delta T_{\min}$ is a design parameter, determined by exploring the trade-offs between larger heat recovery and the larger heat transfer area requirement.

Effluent Composite Curve

This is a variation of a Hot CC, constructed from the cooling requirements of the effluents from an industrial plant, which need cooling down to a specified temperature before being disposed of – Kim *et al*. (2001). The curve also draws upon an analogy with the *Limiting CC* for targeting *water networks*.

Electricity Grid (Electrical Grid, Power Grid)

This is a network of power generators, distribution facilities and transmission lines for generating and distributing electrical power to final users.

© Woodhead Publishing Limited, 2013

End Time, t^T [h]

Batch or other dynamic processes are characterised by periods of activity and absence of certain process streams, heating or cooling requirements. The point in time when the activity expires/stops is the ***End Time*** of the associated stream or other process feature.

Energy–Capital Trade-off

This is a trade-off between the costs spent for energy and those invested in energy-efficiency equipment. The usual trends are that smaller investment would result in lower system capital costs and increased the cost for energy via utilities, while increasing the investment would tend to reduce the energy cost. In combining both cost items (capital and energy), the overall trend, in the simplest case, would produce a convex curve with a minimum. An illustrative sketch of such trends is shown in Fig. 2.7.

An example can be given from the HEN Synthesis where the investment is allocated to heat exchangers and the connected pipes. The trade-off is between this investment on the one hand and the cost for heating and cooling utilities on the other.

Enthalpy

Enthalpy (H) can be defined (Towler and Sinnott, 2008) as a measure of the total energy of a process fluid or a stream, where the kinetic and potential energy components are assumed negligible. It comprises the *internal* (U) and *external* (P·V) energy components (H = U + P·V). This is an extensive property measured in e.g. [kJ]. The *enthalpy* per unit mass

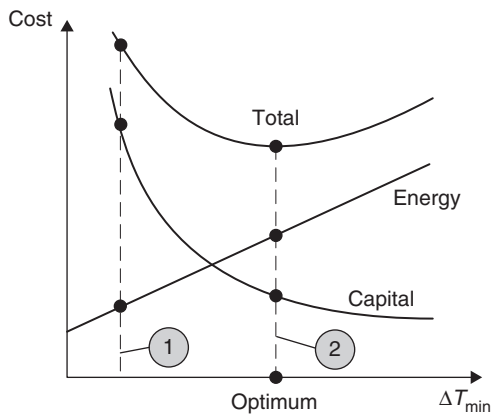

2.7 Capital–Energy trade-off.

© Woodhead Publishing Limited, 2013

is an intensive property, termed *Specific Enthalpy* (h) and is measured in [kJ/kg]. The product of the specific enthalpy of a process stream and its mass flowrate can be considered as enthalpy flowrate measured in [kW]. In thermodynamics enthalpy refers to the finite amount of energy in a system as just described.

Enthalpy Change, Enthalpy Difference

In HI, enthalpy is usually meant as 'enthalpy flow' under the terms enthalpy change and enthalpy difference. They are used to denote the enthalpy flow defined by a process stream ($\Delta H = m \cdot (h_2 - h_1)$).

Emission Targeting

This is an activity for evaluating the minimum possible emissions of certain compounds into the atmosphere. Usual compounds tracked are CO_2, SO_2, NO_x, other toxins, and particulates. *Emissions Targeting* can be applied to various systems. Examples include local heating systems, industrial utility systems, energy supply chains, and even an entire energy sector within a country.

Exergy Composite Curves

A pair of curves plotting the ***Carnot Factor*** versus *enthalpy change* for *cold process streams* and the *hot process streams*. They are derived from the CCs for the same *process streams*.

Exergy Grand Composite Curve

This is a plot derived from the GCC by replacing the temperature with the *Carnot Factor*.

Flowrate, F [t/h], [kg/s], [m^3/h] or [m^3/s]

This is the amount of material flowing through a certain location (e.g. cross-section of a pipe) per unit time. Depending on the needs, it can be represented on a mass basis in [t/h] or [kg/s] or volume basis in [m^3/s, m^3/h].

Footprints: Carbon Footprint, Water Footprint

Any *process*, in addition to using resources, also affects the environment, when being built, started, operating, and being decommissioned. There can be various impacts from a single process. In the case of biomass utilisation, besides greenhouse gas (GHG) emissions, other negative impacts may result from biomass production and use for energy generation – water

© Woodhead Publishing Limited, 2013

pollution and shortage, as well as food and land scarcity, to name a few. These give rise to the relevant environmental footprints such as:

- ***Carbon Footprint*** – CFP. The total amount of CO_2 and the equivalent amount of other greenhouse gases emitted over the full life cycle of a process or product (POST, 2006).
- ***Energy Footprint*** – EFP (Palmer and Pete, 1998). One of its definitions is that it represents the demand for non-renewable energy resources.
- ***Water Footprint*** – WFP (Hoekstra and Chapagain, 2007), defined as the total volume of direct and indirect freshwater used, consumed and/or polluted.
- ***Agricultural Land Footprint*** – LFP (Kissinger and Gottlieb, 2010) (the agricultural land area used for growing biomass for both food and energy).
- ***Water Pollution Footprint*** – WPFP (Sánchez-Chóliz and Duarte, 2005) (the amount of substances emitted to water in the environment).

Fouling Factor

This is a dimensionless parameter (value in the range [0,1]) that shows the decrease of the film transfer rates in heat exchangers in fouling conditions compared with in a clean condition.

Grand Composite Curve [HI]

GCC is the graphical representation of the *Heat Cascade*, which is obtained by plotting the values of the temperature boundaries versus the heat flows across the boundaries (Fig. 2.8). The Grand Composite Curve can be directly related to the *Shifted Composite Curves* (SCCs), which are the result of shifting the CCs toward each other by $\Delta T_{min}/2$ so that the curves touch each other at the Pinch (Klemeš *et al*., 2010).

Grid Diagram

The heat- and mass-transfer operations in a resource recovery network are frequently represented by specialised flowsheets. For HENs, the ***Grid Diagram*** (Linnhoff and Flower, 1978) (Fig. 2.9) is mainly used. This is an efficient HEN representation, which allows both intuitive visualisation and easy manipulation of the network elements. This is achieved by showing only heat-transfer operations and the introduction of a temperature scale where the temperature increases from left to right in the grid, which is intuitive, and makes (re)sequencing heat exchangers straightforward.

Other variations besides the example in Fig. 2.9 are also used – also including the utilities as streams and/or indicating the Pinch location. They have been two versions in stream direction orientation. In this handbook it has been decided to follow the orientation used for CCs – the hot streams run from the right to the left and cold streams in the opposite direction.

© Woodhead Publishing Limited, 2013

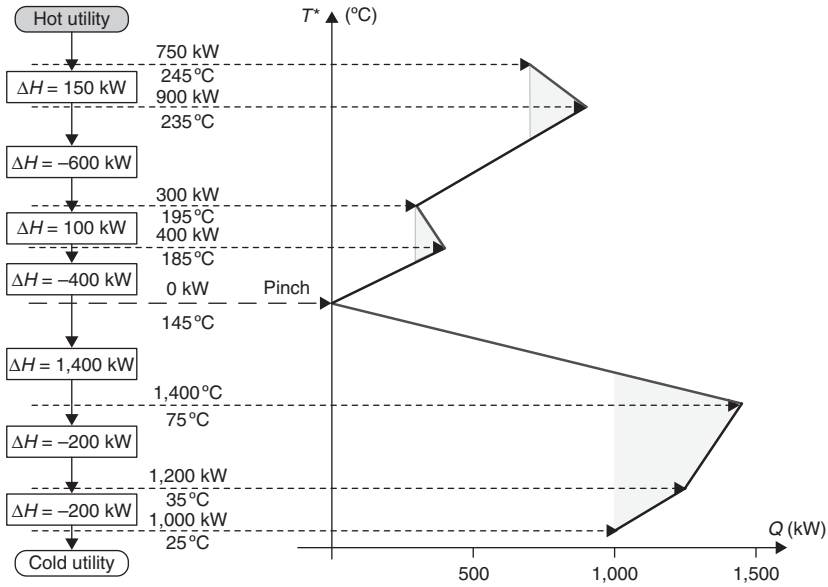

2.8 Construction of the GCC.

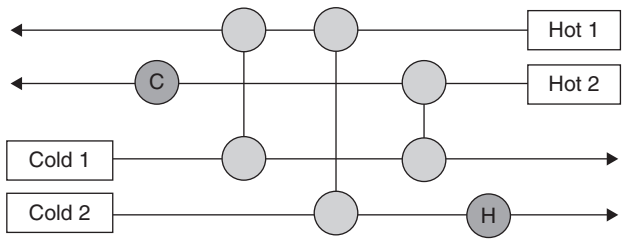

2.9 Grid Diagram for HENs.

Heat-Capacity Flowrate, $CP = M \cdot C_p$ [kW/°C]

This is the product of the mass flowrate and the specific heat capacity (C_p) of a material *process stream*. It is used for convenient representation of process streams for HI and for the calculations on HENs, where the product of the *CP* and temperature difference for a *process stream* is the heat load of the stream.

Heat Cascade

The ***Heat Cascade*** (Fig. 2.10) is a flowchart defined over a number of temperature intervals starting from higher and moving to lower temperatures, where utility heating is supplied at higher temperatures and heat is cascaded

© Woodhead Publishing Limited, 2013

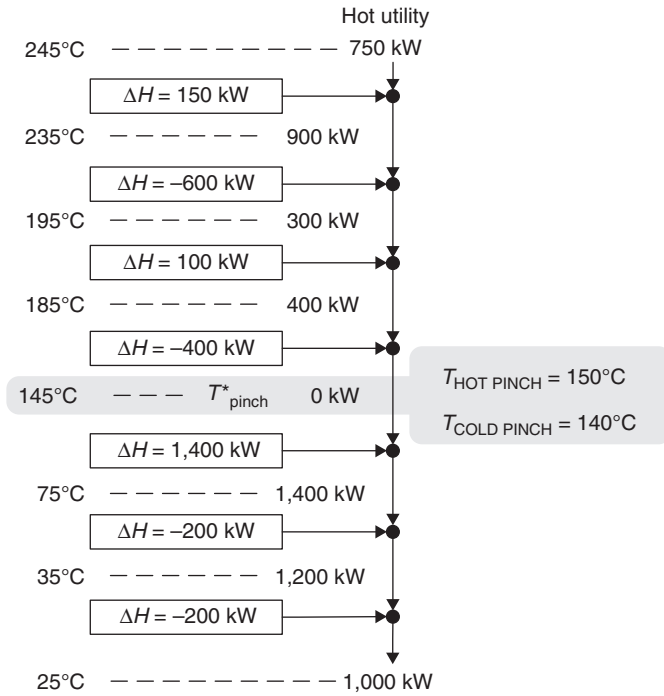

2.10 Heat Cascade example.

between successive temperature intervals by the decreasing temperature. The output from the bottommost temperature interval is directed to a cooling utility. The cascade, when properly constructed, also indicates the location of the *Heat Recovery Pinch*.

Heat Engine

A Heat Engine is a facility or equipment item which takes a heat flow from a higher temperature source, produces mechanical power, and rejects another heat flow at a lower temperature than the source (Fig. 2.11). Examples include steam turbines and gas turbines.

Heat Exchanger

Heat transfer takes place in ***Heat Exchangers***. A *heat exchanger* is an equipment unit where heat transfer takes place either via mixing or via heat transfer through a wall. Examples of heat exchangers include shell-and-tube, double pipe, and plate heat exchangers, all referred to as ***surface heat exchangers***. In contrast, the simple mixing of streams at different temperatures in a

© Woodhead Publishing Limited, 2013

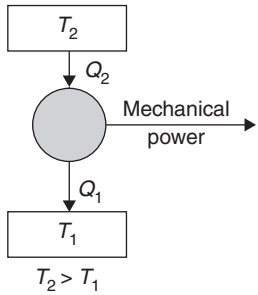

2.11 Heat engine.

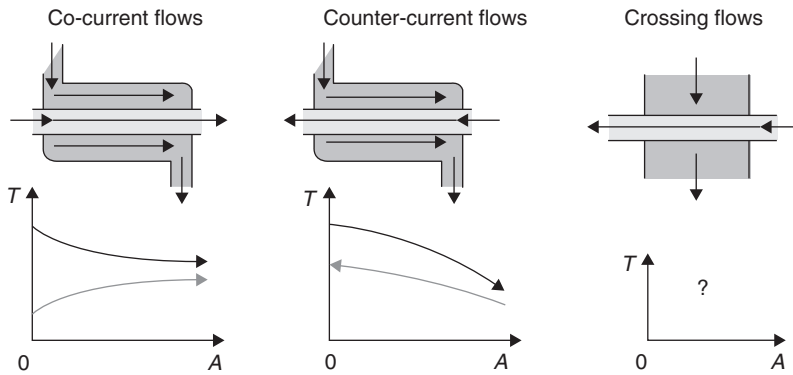

2.12 Heat exchanger types by flow arrangement.

mixer gives rise to *non-isothermal mixing*, and such mixers are sometimes referred to as ***mixing heat exchangers***.

By the configuration of the heat exchanging streams, in surface heat exchangers there can be three main *heat exchanger* configurations: co-current, counter-current and cross-flow (Fig. 2.12).

The most widely used surface heat exchangers are shell-and-tube heat exchangers, which can have either single shell-and-tube pass (***single-pass heat exchanger***) or more than one stream pass on the tube and/or the shell side (***multi-pass heat exchanger***).

Heat Exchanger Network – HEN

The network formed by connecting the heat exchangers for a certain *process* for the purpose of heat recovery is termed a ***HEN*** (more rarely – ***heat recovery network***). HENs can be represented by various diagram types, but the most common currently is the *grid diagram* (Fig. 2.9).

© Woodhead Publishing Limited, 2013

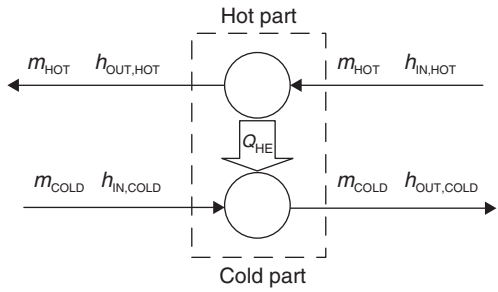

2.13 Flow diagram of a Heat Exchange Match.

HEN Design

This is the activity of constructing a *HEN* topology by selecting and sizing the *Heat Exchange Matches* in the constructed network. Another synonym of this activity is ***HEN Synthesis***.

Heat Exchange Match, Essential Match (Pinch Match) [HI]

A *hot process stream* can supply heat to a *cold process stream* when paired in one or several consecutive heat exchangers. Each such pairing is referred to as a Heat Exchange Match (Fig. 2.13). The Heat Exchange Matches are often viewed as being identical to heat exchangers, but this is not always the case. A given Heat Exchange Match may be implemented by devices of different construction or by a combination of devices – for example, two counter-current heat exchangers in sequence may implement a single Heat Exchange Match.

At the *Pinch*, the driving force restrictions reduce the degrees of freedom and certain matches must be made if the design is to achieve minimum utility usage without violating the ΔT_{min} constraint. These are referred to as ***Essential Matches (synonym: Pinch Matches)***.

Heat Flow/Heat Load, Q [kW] or [MW]

Heat Flow represents an amount of heat flowing through a certain area per unit time. ***Heat Load*** of a heat exchanger refers to the heat flow through the total heat transfer area of the exchanger.

Heat Flux

This is the specific *heat flow* – i.e. *heat flow* per unit area.

© Woodhead Publishing Limited, 2013

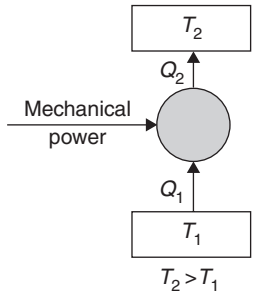

2.14 Heat pump.

Heat Integration

This is the founding discipline of *PI*. It refers to a collection of systematic methods for combining the heating and cooling demands in a *process* for minimising the use of heating and cooling *utilities* through maximising the heat recovery.

Heat Pump

A Heat Pump takes heat flow from a lower temperature source, upgrades it by applying mechanical power, and then delivers another heat flow (approximately equal to the sum of the inlet heat flow and applied power) to a higher temperature heat sink (Fig. 2.14).

Heat Recovery and Maximum Heat Recovery

The reuse of heat from hot to cold streams in a HEN is referred to as ***Heat Recovery*** (prevention of heat waste). When a HEN achieves the state of *minimum energy consumption*, the *heat recovery* is maximised and referred to as ***Maximum Heat Recovery*** (*maximum energy recovery*).

Heat Sinks

The term ***heat sink*** refers to a part of a *process* which presents a heat demand. Examples include a *cold process stream*, a segment in a *Cold CC* or in certain parts of a *GCC* (Fig. 2.15).

In the context of constructing the *TSP*, a *heat sink* is a segment extracted from a *GCC* (and further shifted to the relevant *Total Site* temperature level), which needs heating.

© Woodhead Publishing Limited, 2013

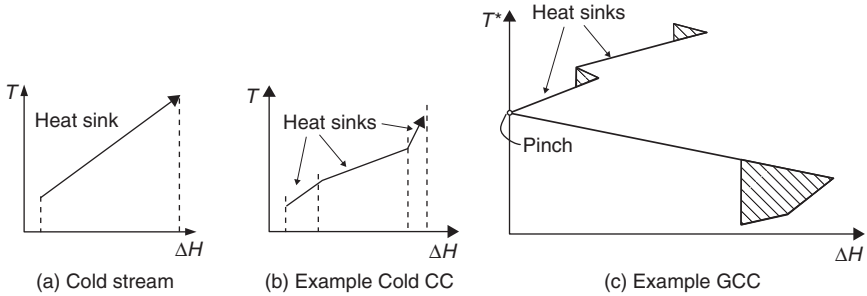

(a) Cold stream (b) Example Cold CC (c) Example GCC

2.15 Heat sink examples.

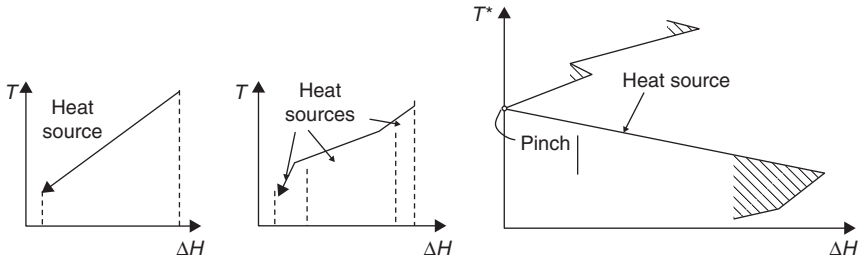

(a) Hot stream (b) Example Hot CC (c) Example GCC

2.16 Heat source examples.

Heat Sink Profile

This is a composite profile constructed from *heat sinks* (*Heat Sink Segments*), in turn derived from the *GCCs* of the *Site Process*. It represents the overall utility heating demand for the entire *Total Site*, before any utility recovery is performed. It is one of the two *TSP*s (Fig. 2.22).

Heat Source

The term ***Heat Source*** refers to a part of a *process* which presents a cooling demand (heat supply). Examples include a *hot process stream*, a segment in a *Hot CC* or in certain parts of a *GCC* (Fig. 2.16).

Heat Source Profile

This is a composite profile constructed from *heat sources* (*heat source segments*), in turn derived from the *GCCs* of the *Site Processes*. It represents the overall utility cooling demand for the entire *Total Site*, before any utility recovery is performed. It is one of the two *TSP*s (Fig. 2.22).

© Woodhead Publishing Limited, 2013

Heat Storage

Various forms of energy can be stored in devices and facilities. ***Heat Storage*** refers to a facility storing heat. Heat can be stored based on various features of the employed materials. The most common *heat storage* is a hot water tank storing heat in a sensible form. It is also possible to store heat in molten salts or other *Phase Change Materials* (*PCM*s) or cold in ice.

Heat Transfer Area

Usually heat is transferred in *heat exchangers* over a certain ***Heat Transfer Area***. The latter is formed differently in the various *heat exchanger* types. For instance, in *shell-and-tube heat exchangers* the *heat transfer area* is formed by the outside surface area of all tubes.

Heat Transfer Area Target

When the *Balanced CC*s for a heat recovery (HEN) problem are constructed, they allow the estimation of the lower bound on the total *heat transfer area* for the HEN by dividing the curves into *EI*s, estimating the minimum area inside each interval and performing a summation. The estimate obtained is the ***Heat Transfer Area Target***.

Heat Transfer Coefficient, h and U

This can be defined as the amount of heat that would pass through a unit area of a medium or system over a unit time when the temperature difference between the boundaries of the system is one degree (in terms of temperature). Since heat can flow through several layers from one fluid to another, each of these layers has its own *Heat Transfer Coefficient*. The usual layers considered in heat transfer engineering are the laminar boundary layers of the fluids on the two sides of the heat transfer surface, as well as the heat transfer surface itself. This gives rise to *partial (film-) heat transfer coefficients* characterising the heat transfer kinetics in the laminar fluid layers (films) on both sides of the surface. The heat transfer surface is usually made of a solid non-permeable material. The heat transfer coefficient for this layer is characterised by the ratio of its thickness and the conductivity of the solid material. When all these partial coefficients are combined, this results in the *overall heat transfer coefficient*.

Heat Transfer Enhancement

This is an activity which aims at improving the heat transfer coefficients within heat exchangers through changing the characteristics of the stream

© Woodhead Publishing Limited, 2013

flows in the passages (tubes, shells, channels). Measures for achieving this for shell-and-tube heat exchangers include modifications of the tube surfaces (inner and outer) or adding/modifying baffles on the shell side. Fins or studs are also added on the outside surfaces of the tubes in the convection section of furnaces and in air coolers.

Heating Duty/Load

When a *heat sink* is satisfied in a *heat exchanger*, the ***Heat Load*** of that exchanger is referred to as ***Heating Duty*** or ***Heating Load***.

Hot Oil Circuit

This is a utility system or subsystem providing high-temperature heating (above 300°C) through a mineral hot oil carrier. The usual pattern is that the oil is heated in a furnace and then, termed as ***hot oil***, is directed to the processes with heating demands. There a large fraction of the heat in the oil is transferred to the process cold streams. As a result, the temperature of the *hot oil* drops and the carrier is returned to the furnace. Since the path of the *hot oil* forms a closed loop, the overall arrangement is referred to as a ***Hot Oil Circuit***.

Hot Stream

The term *Hot Stream* is used to denote a cooling requirement in a *process*. It is more often associated with a material *process stream*. However, for the purpose of *HI* cooling requirements of chemical reactors are also extracted as hot streams from a *process*.

Hydrogen Pinch

Hydrogen Pinch is the purity (of H_2) at which the hydrogen network has neither hydrogen surplus nor deficit. This point shows the bottleneck for how much hydrogen can be recovered and reused in the system. This was first developed by Alves (1999) and extended in Alves and Towler (2002).

Hydrogen Surplus Diagram

This is a plot of hydrogen purity versus hydrogen surplus for a network serving hydrogen sinks and sources. It is obtained by establishing the hydrogen surplus balances within a set of purity intervals. This plot is analogous to the *GCC* in *HI*.

Gas Turbine

This is an internal combustion engine having, beside other components, a compressor (for compressing inlet air), a combustion chamber and an

© Woodhead Publishing Limited, 2013

expander (the turbine component). It generates power and heat at the expense of burning fuel (usually gaseous or liquid).

Limiting Inlet Concentration, C_{in} [ppm]

This is the highest possible contaminant concentration in the incoming water stream which a water-using operation in a water network would accept.

Limiting Outlet Concentration, C_{out} [ppm]

This is the highest possible contaminant concentration in an out-flowing water stream to be expected from a water-using operation.

Limiting Water Flowrate, F [t/h]

This is the water flowrate required by a water-using operation, derived from the limiting inlet and outlet contaminant concentrations and the contaminant load imposed by the corresponding water-using operation.

Locally Integrated Energy Sectors and Extended Total Sites

Traditionally, *Total Site* has been defined as a collection of only industrial *processes* connected by a common utility system supplied by fossil fuels as energy sources. A broader view of the concept is presented by allowing the integration of more process types alongside industrial plants – residential customers and the service-sector energy systems, for example. For the energy sources, renewables are also considered, including solar thermal and photovoltaic capture, wind power and geothermal sources. This type of extension has been developed by various authors e.g. Perry *et al*. (2008) who added residential and service-building processes (hospitals, hotels, offices) to the traditional scope of *Total Sites*, allowing low-grade industrial heat, waste to heat, and renewables to be utilised. This conceptual extension, referred to as ***Locally Integrated Energy Sector***, allows applying the *Total Site* integration strategy to local communities involving a larger number of smaller-scale entities.

Logarithmic Mean Temperature Difference

The *heat transfer area* for a (two-stream) *heat exchanger* is calculated using a single variable for temperature difference. However, in a *heat exchanger* there is a range of temperature differences between the hot and the cold stream, over the device surface. To overcome this, a single temperature difference is used to represent the *heat exchanger*. This role is played by the ***Logarithmic Mean Temperature Difference***. It is usually derived based on

© Woodhead Publishing Limited, 2013

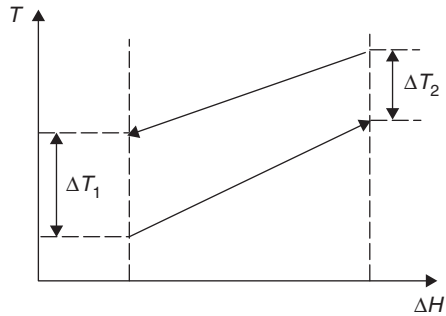

2.17 Temperature differences at heat exchanger ends.

solving the differential equations for a heat exchanger with constant parameters (C_p for the hot and cold streams and the overall heat transfer coefficient). It can be defined as follows:

$$\Delta T_{LM} = \frac{\Delta T_1 - \Delta T_2}{\ln\left(\Delta T_1 / \Delta T_2\right)} \qquad [2.2]$$

where the symbols ΔT_1 and ΔT_2 are shown in Fig. 2.17.

Loops and Paths [HI]

In a HEN topology, a ***Path*** is a set of heat exchanger units – including both recovery and utility – which are connected via process streams. A ***Loop*** is a circular closed Path connecting two or more heat exchangers. A Utility Path connects a hot with a cold utility or connects two utilities of the same type. Figure 2.18 shows a HEN *loop* and a *utility path*. A network may contain many such *loops* and *paths*.

For HEN Synthesis, if the Pinch Design Method is used, after the initial stage of producing a MER HEN, the capital–energy trade-off is addressed by explicit identification of Loops and Paths. Some such methodologies rely on identification of a HEN Loop and eliminating it by removing one or several of the heat exchangers forming the Loop. This action is referred to as ***Loop Breaking*** and tends to decrease the HEN capital cost. Another approach is the identification of a *utility path* and exploiting it for the elimination of very small recovery heat exchangers via reasonable increase in both hot and cold utility demands. The exploited *utility path* can be also termed ***Energy Relaxation Path***.

For HEN retrofit only, utility paths are used for identifying the HEN bottleneck referred to as the ***Network Pinch*** (Asante and Zhu, 1997).

© Woodhead Publishing Limited, 2013

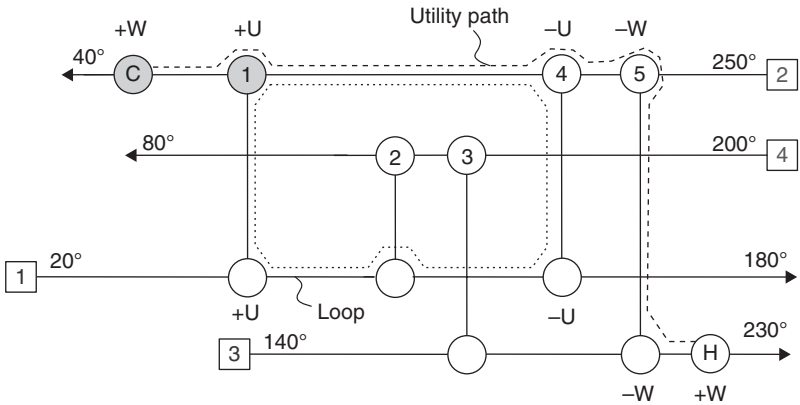

2.18 A loop and a path in a HEN. The numbers inside the square boxes represent stream identifiers. The numbers inside the circles represent heat exchanger match identifiers.

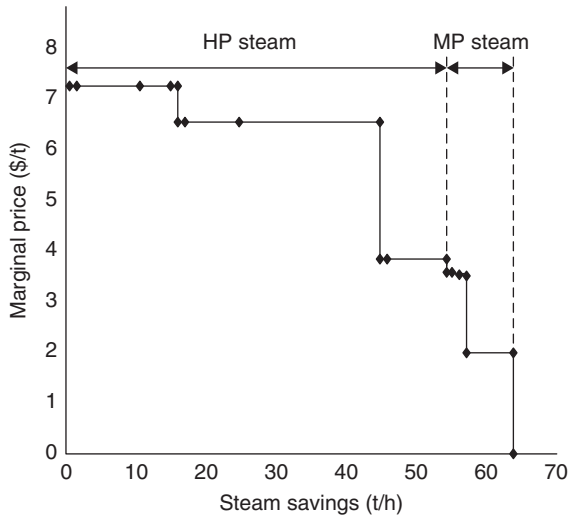

2.19 A typical Marginal Steam Price Plot for a site utility system (after Smith and Varbanov, 2005).

Marginal Steam Price

This is a metric that captures the change in a utility system's energy cost per unit change in steam demand, and it is specific to a given combination of steam header and operating conditions. By optimising a utility system at gradual successive reductions of potential steam demand on the headers, it is possible to obtain a curve of the Marginal Steam Price versus the savings that could be achieved. An example of such plot is shown in Fig. 2.19.

© Woodhead Publishing Limited, 2013

Mass Exchange Network (MEN)

This is a network of *mass exchangers*, which is used for transferring certain chemical components from a set of rich streams to a set of lean ones, minimising the use of external mass separating agents (utilities for cleaning and fresh materials).

Mass Exchange Pinch Diagram

This is a plot of exchanged component mass load (Y-axis) versus concentration (X-axis), consisting of two *CC*s – one for component sources and another for sinks. It is analogous to the *CC*s from *HI*, but the intensive variable is on the X-axis rather than the Y-axis.

Mass Exchange Cascade Diagram

This is a cascade of the mass flow of a certain component, over a series of concentration intervals, where each interval is considered as a mass-exchange system with two component flow inlets – from a higher concentration and from rich process streams (waste streams), as well as with two outlets – one to a lower concentration interval and another to the lean streams. In this way the contaminant is allowed to be cascaded from higher concentration intervals to lower concentration ones, giving rise to the cascade name.

Mass Exchanger

This is a direct-contact mass-transfer unit that employs a Mass Separating Agent (MSA), usually the lean stream, to selectively remove certain components (e.g., impurities, pollutants, by-products, products) from a rich stream. The term 'rich' stream implies that it is the source of the exchanged component, while 'lean' refers to the stream accepting the component and playing the role of a sink.

Mass Flowrate

This is a property of a process stream, representing the amount of the overall stream mass carried with the stream per unit time over a certain control point (e.g. pipe cross-section).

Mass Separating Agent

In MENs, particular components (often pollutants) are removed from rich process streams using lean process streams in units such as absorbers, strippers, ion exchange columns, adsorbers and mixer-settlers. Often external utility streams are used as the lean streams, termed MSAs.

© Woodhead Publishing Limited, 2013

Maximum Energy Recovery Network (MER) [HI]

This term refers to a HEN achieving maximum heat recovery, i.e. achieving the heat recovery targets identified by the Pinch Analysis.

Mechanical Work, Work, Power

The work can be viewed as a finite amount of energy spent (or available to be spent) for a useful purpose. Power is defined as the rate of energy transfer or the rate of performing work. It can be viewed as the work performed per unit time. The useful purpose may be to move an object over a certain distance applying a certain force. An example is the propulsion of a ship, where the engine performs ***Work*** for moving the ship. In this case the work is the product of the applied force and the distance of movement:

$$W = F \cdot \Delta L \qquad [2.3]$$

When a fluid has to be moved through a pipe, *Mechanical Work* is converted by a pump or a compressor into an external energy (via pressure increase). When movement is achieved, the fluid contains both pressure- and kinetic-energy as per the Bernoulli Equation (Bird *et al*., 2007).

The examples provided so far are of ***mechanical work***. It is also possible to perform other kinds of work in operating chemical and thermo-chemical processes – for instance the work done on a charged particle by an electric field (electrical work).

Minimum Allowed Stack Temperature

This is a parameter specification for applications of fuel combustion followed by heat recovery from the resulting flue gas. As heat is transferred from the flue gas to the recipient fluid (usually steam generation or hot oil heating) the temperature of the flue gas drops. The flue gas usually contains a number of chemical species (CO_2, SO_2, NO_2, water) which can form acids in liquid form, causing corrosion. The temperature at which droplets of liquid acid start forming in the flue gas is called the gas ***Acid Dew Point***. Below this temperature the acid formation is even faster. Therefore, the flue gas is allowed to deliver heat to other fluids to a usually slightly higher temperature, termed ***Minimum Allowed Stack Temperature***.

Minimum Energy Consumption: Minimum External Heating ($Q_{H,min}$), Minimum External Cooling ($Q_{C,min}$) [HI]

When *Pinch Analysis* of a system is completed, it produces thermodynamic targets for HEN performance. The targets are based on a system condition

© Woodhead Publishing Limited, 2013

characterised by ***Minimum Energy Consumption***. This is the steady state of a HEN in which both the total utility heating and the total utility cooling are the smallest possible. Therefore they are referred to as ***Minimum External (Utility) Heating*** and ***Minimum External (Utility) Cooling***.

Minimum Number of Units

It is possible to synthesise a HEN employing different number of heat exchanger units (recovery, heaters and coolers). Using connectivity considerations and the Euler's rule from *Graph Theory*, a lower bound on this number can be calculated via a simple expression involving the sum of the number of all streams (process and utilities). This lower bound is termed the ***Minimum Number of Units*** and is an important target for guiding HEN Synthesis (Linnhoff *et al.*, 1982).

Minimum Number of Shells

This is a PI target, representing the smallest number of heat exchanger shells for a heat recovery problem. This target becomes important if the anticipated heat exchanger types would yield significant deviation from the pure counter-current heat exchange configuration. More details can be found in Chapter 8.

Multiple Pinches

This term denotes a situation where the *CC*s or *Balanced CC*s of a heat recovery problem define more than one *Pinch Point*. In such cases, the set of *Pinch Points* is referred to as ***Multiple Pinch Points***.

Multiple Utilities

For a heat recovery problem, when the temperatures for placing heating and cooling utilities span large intervals, more than one heating and/or cooling utility could be placed against the GCC. This is a practice denoted as ***Multiple Utility Use/Placement***.

Multiple Utility Targeting

The estimation of the targets for more than one heating and/or cooling utility via the *multiple utility placement* constitutes ***Multiple Utility Targeting***.

Multi-Stream Heat Exchanger

This is a *heat exchanger* type involving more than one hot and one cold stream.

© Woodhead Publishing Limited, 2013

Network Evolution [HI or MI]

After a *MER HEN* is synthesised, it is usually modified in several steps for removing some heat exchanger units. The units to remove should be involved in loops or utility paths. Usually smaller-load units are removed. The *HEN* operating variables – heat loads and temperatures – are recalculated before or after the removal. Such steps may be repeated more than once. The described procedure is referred to as ***Network Evolution***. A more sophisticated variant of *Network Evolution* involves steps of Linear Programming (LP) optimisations of the HEN operating variables, followed by the removal of all zero-load *Heat Exchanger Matches* and zero-flow branches.

Network Pinch, Pinching Match

These terms apply to HEN retrofit. ***Network Pinch*** (Asante and Zhu, 1997) is a point in a particular *HEN* topology, defined by a *Heat Exchange Match*, where the temperature difference at one or both ends of the match are equal to the Minimum Allowed Temperature Difference. Such a match is referred to as ***Pinching Match***. This condition is achieved by manipulating the loads of some *Heat Exchange Matches* in the *HEN* for increasing the heat recovery without modifying the topology.

Non-isothermal Mixing

This is a case of mixing two physical streams corresponding to two process streams or their branches, where the temperatures of the mixed streams are different. As a result, the resulting mixed stream has a temperature generally different from any of the inlet streams. Such an operation is referred to as ***Non-isothermal Mixing***.

Number of Streams [HI]

In a heat recovery problem, the number of *process streams* plays an important role. Depending on the exact problem part (context), one can distinguish the following classifications:

- The ***overall number of streams*** includes the count of all *process streams* in the problem regardless of their type or location relative to the *Pinch*.
- The ***number of the hot streams*** includes the count of all *hot streams* in the process regardless of their location relative to the *Pinch*.
- The ***number of the cold streams*** includes the count of all *cold streams* in the process regardless of their location relative to the *Pinch*.
- The ***number of streams Above the Pinch*** includes the count of all *process streams Above the Pinch* regardless of their type.
- The ***number of streams Below the Pinch*** includes the count of all *process streams Below the Pinch* regardless of their type.

© Woodhead Publishing Limited, 2013

It is also possible to combine the above criteria deriving numbers of *hot/cold streams Below/Above the Pinch*.

When obtaining the target for *Minimum Number of Units*, the concept of 'number of streams' is used in a slightly different meaning. That notion includes both process streams and utilities, as utilities are also considered a variation of the *Stream* concept.

Onion Diagram (Onion Model)

This is a diagram consisting of consecutively embedded circles representing the various subsystems of a *process* as layers, thus underlining the hierarchical nature of *process design* (Douglas, 1988). It is termed as the ***Onion Diagram*** because the layers resemble those of an onion bulb.

Operating Cost (Energy Cost, Fresh Water Cost)

The cost for running a *process*, which is dependent on the rates of consumed resources, is referred to as ***Operating Cost***. The *operating cost* items most frequently considered in *PI* are ***Energy Cost*** and ***Water Cost***.

Payback Time

This is the time for which an investment in a retrofit project would be recovered from the monetary savings realised as a result of the retrofit.

Pinch [HI], Pinch Temperatures (Shifted, Hot, Cold), Heat Recovery Pinch, Utility Pinch, Water Pinch

In *PI*, ***Pinch Point*** ('***Pinch***' for short) refers to a location in the problem where the process driving force is equal to the minimum allowed. For *HI* (*HEN Design*), the *Pinch* is located using the temperature as the intensive variable and temperature difference as a driving force. ***HI Pinch*** is defined as a location in the heat recovery problem where the temperature differences between the streams are equal to $\Delta T_{\min}$. For the different representations of the problem it is identified in different ways:

- In a *CC*s plot, each point with a temperature distance between the *CC*s equal to $\Delta T_{\min}$ indicates a *Pinch Point* ('Process Pinch' in Fig. 2.3).
- On a *Heat Cascade* or a *GCC* a *Pinch* is indicated by a point with zero heat flow (Fig. 2.8).

A *Pinch Point* [**HI**] is characterised by several ***Pinch Temperatures***:

- A single *Shifted Temperature* derived from a *Heat Cascade* or a *GCC* (Fig. 2.8).

© Woodhead Publishing Limited, 2013

- A pair of temperatures corresponding to the process streams (not shifted), one *Pinch Temperature* for the hot streams and another for the cold streams.

Depending on the cause of the *Pinch* one can distinguish two main types:

(i) ***Heat Recovery Pinch*** (***Process Pinch***) – caused by the combination of the process streams, their temperatures and heating/cooling demands.
(ii) ***Utility Pinch*** – caused by placing a heating or cooling utility.

There may be one or more instances of both *Pinch* types in a heat recovery problem. The most common situation is to have one *Process Pinch* and several *Utility Pinches* (Fig. 2.8).

In the context of *water networks*, the *Pinch Point*-Water Pinch (Wang and Smith, 1994), is indicated by the touch of the *Water CC* and the line for fresh water supply (Fig. 2.20) or can be found as a zero water flow on a *Water Cascade*.

For other Mass Exchanger Networks, ***Mass Pinch*** is indicated as the closest approach of the *Composite Streams* (*Lean and Rich*). On the *Mass Exchange Pinch Diagram* it is usually a touch point. For the MEN y-x (vapour–liquid composition) diagram, it is a point where the rich and lean CCs are Δy_{min} apart, as for HEN CCs. Hydrogen Pinch is indicated in the Hydrogen Surplus Diagram, on the Surplus CC, as a point with zero hydrogen flow.

Pinch Match

This term denotes a *Heat Exchange Match* placed at the *Pinch*, in such a way that the temperatures at one of the match ends are exactly equal to the *Pinch* Temperatures for hot and cold streams.

Plant Life Time

This is the time duration that is expected for a plant to operate with full capacity.

Plus/Minus Principle [HI]

This is a principle for identifying *process modifications* based on the *CCs* for a heat recovery problem. It stipulates that modifications should be made such that:

(i) Above the *Pinch* to increase the Heat Load of hot streams (+) or decrease the Heat Load of cold streams (–).
(ii) Below the *Pinch* to increase the Heat Load of cold streams (+) or decrease the Heat Load of hot streams (–).

© Woodhead Publishing Limited, 2013

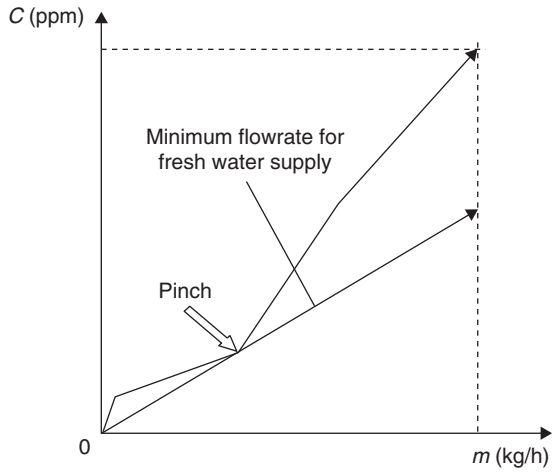

2.20 Water Pinch (after Wang and Smith, 1994).

Ideally, both of the above objectives should be reached resulting in transferring heat from *Below* to *Above the Pinch*.

Pocket [GCC, Water]

This is a part of a curve in PI plots, where the curve forms a closed area by repeating values on one axis while progressing on the other axis. Examples can be given from HI – the GCC (Fig. 2.8) and from the Limiting CC (Fig. 2.20). Of these two, the GCC pockets are more commonly known and have a well-defined meaning – they mark the areas of the heat recovery problem, where the hot and the cold process streams are in enthalpy balance.

Pressure Drop, Stream Pressure Drop

Pressure drop denotes the decrease in pressure of a fluid flowing through a device (pipe, heat exchanger or reactor). It is caused by the forces of friction with the containing vessels and equipment as well as by the internal fluid friction, resulting in the loss of kinetic energy. The lost energy is usually dissipated as heat. When the pressure drop occurs over a process stream, it can be also referred to as stream pressure drop.

Problem Table Algorithm

This is the numerical targeting procedure for obtaining the heat recovery targets for a HEN Synthesis problem (Linnhoff and Flower, 1978). It

© Woodhead Publishing Limited, 2013

involves obtaining *Shifted Temperatures*, *Temperature Boundaries*, temperature intervals, enthalpy balances within those intervals and finally obtaining the correct *Heat Cascade* and the relevant *heat recovery targets*.

Process Analysis

This is an activity involving collection of flowsheet and operating data about a *process* and analysing them with some goal. The goal can be *data extraction* for *PI*, preparation for an optimisation study, or merely obtaining the current status of the *process*.

Process Flowsheet

A diagram showing the operating units involved in a *process* and their interconnections is referred to as a ***Process Flowsheet*** (***Flowsheet*** for short). Another synonym for this is ***Process Flow Diagram***. It is used to indicate the flows of the various streams in the *process*, also frequently supplemented by other stream properties (composition, temperature, pressure), as well as properties of the operating units (throughput, physical dimensions/size, valves, location including height).

Process Intensification

A term denoting techniques or actions aimed at increasing the rate of heat- and/or mass-transfer in a process and/or the production more intensive, making the process more productive (intensive).

Process Modifications

The general term means any changes to a *process* whether to a new design or an existing operating plant. The changes may concern operating specifications such as pressures and temperatures of operating units, as well as changes modifying the topology of the *process* (the *Process Flowsheet*). In the context of *HI* the term means changes to a *process* aiming at improving its *heat recovery targets*.

Process Stream

HEN: abstracting the information about a *Flowsheet Stream* for the purpose of *HI* leaves a bundle of only three items: *supply temperature*, *target temperature*, and either *heat-capacity flowrate* or *enthalpy change*. This data bundle

© Woodhead Publishing Limited, 2013

is referred to as a ***process stream*** in *HI* and *HEN synthesis*. *Process streams* are of two types – ***hot streams*** requiring cooling and ***cold streams*** requiring heating.

Process Stream Branch

When a certain *process stream* is split, after the splitter it forms two or more branches, each of which is referred to as a *Process Stream Branch*. This is used mainly in the context of *HEN*s.

Process Synthesis and Process Design

This is an activity for constructing *process flowsheets*. The involved choices also include selection of *operating units*, their connectivity, sizes and throughputs, while the inputs to and the outputs from the system are provided as fixed specifications. Sometimes the term ***Process Design*** is used as a synonym, although the latter can be also defined as obtaining the finer properties of the system components after the synthesis.

Process Retrofit, Retrofit

The activity of planning, selecting and implementing modifications to an existing (running) *process* is termed ***Process Retrofit***. The actions usually involve adding or removing *operating units*, changing the connections among existing *operating units*, modifying the throughput (e.g. maximum crude oil flowrate to be processed by an atmospheric distillation unit) or efficiency (e.g. *heat transfer enhancement* of a *heat exchanger*) of the *operating units*.

One of the reasons for *retrofit* is ***debottlenecking***, where the focus of the activity is on increasing throughput or production volume.

Prohibited Matches [HI, MI]

When synthesising *resource recovery networks*, certain matches between *process streams* are not allowed – usually for reasons of safety or product quality. These are usually referred to as ***Prohibited Matches***. A synonym to this term is ***Forbidden Matches***.

Property-Based Material Reuse

Recycling of process and waste streams is important for resource conservation and waste reduction. In many cases recycling and reuse are limited by sink constraints on properties of the recycled streams. By applying the source-sink partitioning of the problem and combining the sources

© Woodhead Publishing Limited, 2013

and sinks in property-based, Resource Cascade allows one to implement such a strategy termed ***Property-Based Material Reuse***.

Refrigeration

This is a specialised form of cooling – removal of heat from a *stream* or a *process*, taking place at temperatures lower than that of the ambient – usually below 0°C.

Refrigeration System

This is a network of refrigerators and auxiliary equipment providing *refrigeration* utilities for achieving sub-ambient temperature cooling.

Regional Resource Management Composite Curve

This kind of *CC* provides straightforward and valuable information for energy surplus/deficit planning as well as land use management. The quantity of the energy and the area of the zone are showing on the X-axis and Y-axis, respectively. The zones with positive slope supply biomass to the demanding zones which have negative slope. Each of the left-hand turning points (could be also called a ***Cluster Pinch***) indicates the start of a new *Cluster*. A ***Cluster*** is a collection of zones in a region, which interact closer with each other than with other zones.

Resource Cascade: Heat Cascade, Renewable Energy Cascade, Generalised property cascades

When a resource recovery network is evaluated and targeted, the consumption of the evaluated fresh resource (heat, biomass, water, and other properties) is usually minimised by reusing or recycling the same or another resource form. This is achieved by constructing a Resource Cascade. The latter is a diagram consisting of resource intervals and flows connecting the intervals, where the intervals usually form a gradient of descending quality of the resource. A typical special case of this is the *Heat Cascade*. Other examples include cascades for renewable energy used for supply chain synthesis (Lam *et al*., 2010b) and for general regional analysis (Lam *et al*., 2011), water, as well as for generalised properties (Foo *et al*., 2006).

Resource Deficit

This is a condition at which a certain system, part of a *process* or a *resource interval* features insufficient balance of a resource. This may result from lack of supply or from a situation of demand exceeding the supply.

© Woodhead Publishing Limited, 2013

Resource Surplus

This is a condition at which a certain system, part of a *process* or a *resource interval* features excess balance of a resource. This may result from lack of demand or from a situation of the supply exceeding the demand.

Semicontinuous Process

A batch process using a utility continuously is termed a Semicontinuous Process. For example, a batch reactor (batch process) cooled by a water stream which flows continuously through the jacket.

Sensitivity Analysis

This is an operation of a numerical experiment for determining the sensitivity of a *process* or its model toward the variation of key specifications. A typical example from utility system is the determination of the *Marginal Steam Price* in order to motivate the need for process *HEN* retrofit. In this case, the sensitivity factor is the potential for steam saving and the sensitivity indicator is the *Marginal Steam Price* calculated as a ratio of the change in energy costs over the hypothetical step change in steam demand.

Shaft work – Mechanical Power

This refers to a mechanical work (finite amount of spent or delivered energy) performed by the shaft of a heat engine or an electrical motor. In some cases '*Shaft Work*' is used with the meaning of mechanical power (energy flow) delivered by the engine shaft.

Shifted Composite Curves [HI]

For a heat recovery problem the Shifted Composite Curves (SCC) are obtained by shifting the CCs toward each other by $\Delta T_{min}/2$ so that the curves touch each other at the Pinch (Fig. 2.21).

Sink [Resource]

Resource Sink is an *operating unit*, a *process stream* or another part of a *process*, consuming the resource. Examples include:

- Heat sink: cold process stream, heat sink segment from a GCC or from a heat sink profile [**Total Site**].

© Woodhead Publishing Limited, 2013

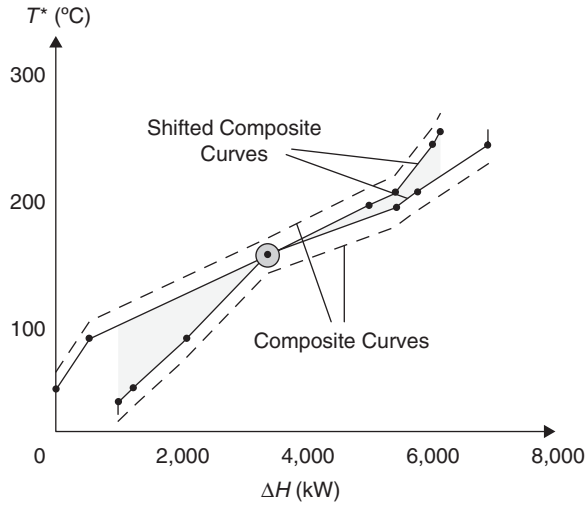

2.21 Example SCCs.

Sink Composite Curve [Total Site]

This is a *CC* representing the potential for using hot utilities for a *Total Site* (Fig. 2.22). It is generated from the *Site Sink Profile* by intersecting it with the temperature levels of the defined site utilities.

Site Composite Curves [Total Site]

This is a pair of *CC*s including the *Sink CC* and the *Source CC* (Fig. 2.22).

Site Sink Profile [Total Site]

This is a composite profile combining all *heat sinks* on a *Total Site* (Fig. 2.22). The *heat sinks* are usually obtained from the *GCC*s of all *processes* on the site.

Site Source Profile [Total Site]

This is a composite profile combining all *heat sources* on a *Total Site* (Fig. 2.22). The *heat sources* are usually obtained from the *GCC*s of all *processes* on the site.

Site Utility Composite Curves [Total Site]

This is a synonym for *Site CCs*.

© Woodhead Publishing Limited, 2013

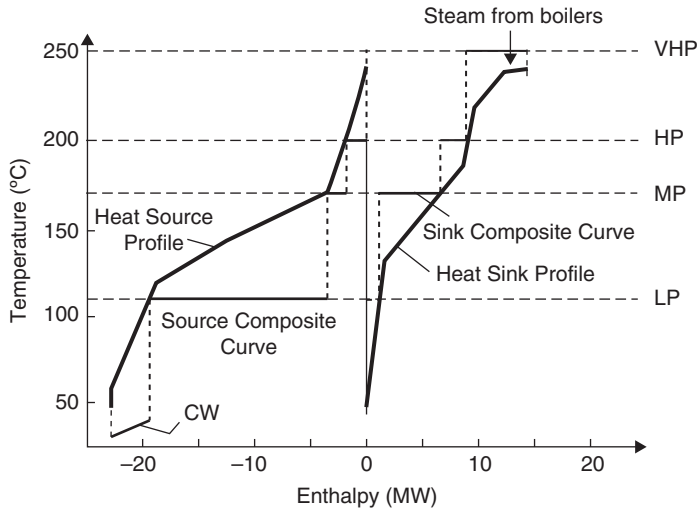

2.22 An example of TSP.

Source Composite Curve [Total Site]

This is a *CC* representing the potential for generating hot utilities for a *Total Site* (Fig. 2.22). It is generated from the *Site Source Profile* by intersecting it with the temperature levels of the defined site utilities.

Specific Heat Capacity, Cp [kJ/(kg·°C)]

This is the amount of heat absorbed or released by a material when its temperature is increased or decreased by a unit temperature difference.

Starting Time, t^S [h]

This term is used to denote the time point when an operation begins, when a certain process stream becomes active, when a demand for a resource comes online, or when a resource supply becomes available.

Stream Splitting

The activity or action involving the division of a *process stream* into two or more branches is termed ***Stream Splitting***.

Steam Turbine

Steam turbine is a heat engine in which steam at a higher pressure and temperature is expanded through a series of bladed wheels producing

© Woodhead Publishing Limited, 2013

mechanical power and exhausting the expanded steam at a lower pressure and temperature.

Superstructure

The topological representation of more than one structural option for designing a process network is referred to as a Superstructure. If the superstructure includes all possible structural alternatives, it is also referred to as Maximal Structure or a Hyperstructure.

Supertargeting

This is a procedure for obtaining simultaneously targets for heat recovery and heat transfer area of a *HEN*, ultimately producing also a *Total Cost Target*. The procedure involves evaluation of these targets for various values of the *Minimum Allowed Temperature Difference* specification (ΔT_{min}).

Supply Temperature, T_S [°C] [HI]

This is a temperature at which a process stream in a heat recovery problem is supplied. It is also sometimes referred to as *Starting Temperature*.

Surplus Composite Curve [Hydrogen]

The plot of the hydrogen purity versus hydrogen surplus for a refinery operation problem is referred to as a Surplus CC. The overall diagram is referred to as a Hydrogen Surplus Diagram.

Targets and Targeting

Estimating the key performance indicators for a process is termed ***Targeting*** and the obtained estimates are termed ***Targets***. With proper techniques, it is possible to obtain targets representing an upper bound on system performance and/or a lower bound on the system cost. It is also possible to calculate practically achievable targets, resulting in estimation of the system's best performance (similar in essence to Best Available Technology). These properties make targeting the perfect tool of applying the iterative design strategy described above. Examples of targeting include:

- For water systems, current targeting practices mainly yield the first type of estimate: the maximum possible amount of water reduction.
- For HEN Synthesis, the *MER* targets can be established and HENs achieving them also feature reasonable costs. However, this is seldom the global minimum for the total annualised cost.

© Woodhead Publishing Limited, 2013

Usually the engineer aims either to achieve the targets exactly or to approach them closely with the final design. If the targeting model is too idealised, then the targets will serve as loose performance or cost bounds, not as tight ones. Yet in many cases this strategy results in a simple design procedure and a nearly optimal outcome.

If the targeting model is exact, as in Pinch Analysis for HI (Linnhoff and Flower, 1978), or if it at least captures all key factors at the corresponding design stage, as with ***Regional Energy Clustering*** (Lam *et al*., 2010a), then the targeting procedure also provides a convenient partitioning of the original design space. This makes it easier to decompose the problem and to simplify the remaining actions.

Target Temperature, T_T [°C] [HI]

This is a temperature which a process stream in a heat recovery problem is required to reach. It is also sometimes referred to as *Ending Temperature*.

Temperature–Enthalpy Diagram

Representing *enthalpy change* (*difference*) for a *process stream* or a heat recovery problem is performed in the coordinates of *Temperature* (T) on the Y-axis versus *enthalpy change* (ΔH) on the X-axis. Such a plot is referred to as a ***Temperature–Enthalpy Diagram***.

Temperature Lift (of a Heat Pump)

A heat pump takes heat flow from a lower temperature source, upgrades it by applying mechanical power, and then delivers another heat flow (approximately equal to the sum of the inlet heat flow and applied power) to a higher temperature heat sink (Fig. 2.14). The difference between the higher and the lower temperatures for a *heat pump* is termed as ***Temperature Lift***.

Temperatures [HI]: Process Temperature, Shifted Temperature [GCC], Shifted Temperature [TSP]

In obtaining targets for heat recovery in a single *process*, the procedure starts from the real temperatures of the *process streams*, referred to as ***Process Temperatures***. For the purpose of obtaining the temperature intervals of the *Heat Cascade*, ***Shifted Temperatures [GCC]*** are derived from the *process temperatures* by shifting the temperatures of *hot process streams* down and those of the *cold process streams* up – in both cases by half ΔT_{min}.

© Woodhead Publishing Limited, 2013

When the GCC data is used for further Total Site Targeting in constructing the *TSP*, heat source and sink segments are extracted from the GCC of each process and shifted further to the temperature levels of the site utilities, which results in further ***Shifted Temperatures [TSP]***.

Threshold Problem

Threshold Problem is a special case of a heat recovery problem, featuring targets where only one utility type is required – either hot or cold. They are important mostly because they often result in no utility–capital trade-off below a certain value of ΔT_{min}, since the minimum utility demand (hot or cold) becomes invariant.

Time Average Composite Curves

In *HI* of batch and other variable processes the *CC*s obtained by applying the *Time Average Model* can be referred to as ***Time Average CC*s**.

Time Average Model (TAM)

The method applied in HI of batch processes that averages the heat flows of process streams over the duration of a batch or the operating horizon.

Time Slice Composite Curves

In *HI* of batch and other variable processes the *CC*s obtained by applying the *Time Slice Model* can be referred to as ***Time Slice CC*s**. One pair of such curves is generated per each *Time Slice*.

Time Slices

In *HI* of batch and other variable processes, to model the heat load variations in time, the operation horizon is divided into time intervals termed ***Time Slices***. They are obtained by combining the starting and ending times of the *process streams*.

Top-Level Analysis

For the purpose of determining the scope for energy saving projects on a Total Site, a sensitivity analysis of potential steam savings is frequently used, termed ***Top-Level Analysis***. It employs a number of operation optimisation runs on a model of the site utility system obtaining the marginal steam price for the site and identifying sets of processes with higher marginal prices as the more economic for HEN retrofit.

© Woodhead Publishing Limited, 2013

Topology Traps

This term refers to the sharp (non-continuous) and generally counter-intuitive changes in the values of the HEN utility targets, as well as in the optimal HEN topology with varying the value of ΔT_{min}. Factors playing major role in the occurrence of this phenomenon are usually process streams with large latent heat loads over relatively narrow temperature ranges.

Total Annualised Cost, TAC [currency unit/y, e.g. $/y, €/y, £/y]

The sum of the operating and the annualised investment (capital) costs constitutes the ***Total Annualised Cost***. It applies to a *unit operation*, a *process* or a *Total Site*. The operating cost is usually taken on an annual basis directly, while the investment cost is annualised using an annualisation factor based on the life time of the project.

Total Site

An industrial ***Total Site*** includes a collection of energy use and generation areas, termed *processes* and a central *utility system*. An extension of the *Total Site* concept is the one of *Locally Integrated Energy Sector*, which considers other energy use and generation *processes*, beside industrial.

Total Site Composite Curves

This is a pair of *CC*s including the *Sink CC* and the *Source CC* (Fig. 2.22). The term is a synonym to *Site CC*s.

Total Site Pinch

The area, where the *Total Site Composite Curves* touch, is usually confined between two steam levels. This is referred to as the ***Total Site Pinch***.

Total Site Profiles

This is a pair of composite profiles (Fig. 2.22) – the Site Source Profile (combining heat sources) and the Site Sink Profile (combining heat sinks).

Utility Path

This is a path in a HEN connecting a heater and a cooler via recovery heat exchangers (see Fig. 2.18).

© Woodhead Publishing Limited, 2013

Utility Pinch [HI]

When utilities are placed against the *GCC*, this changes the thermodynamic configuration of the problem. When a utility line or profile touches the *GCC*, a new *Pinch Point* is created, termed a ***Utility Pinch***. *Utility Pinches* are best visualised using the *Balanced Composite Curves*. Figure 2.3 illustrates a *Utility Pinch* resulting from the placement of LP steam as an intermediate-temperature heating utility.

Utility System

Utility system is a collection of *unit operations* on an industrial site, intended to provide the site *processes* with utilities. Examples include heating utilities: steam, hot oil, flue gas (furnace gas); cooling utilities: cooling water, refrigeration, cooling air; as well as other utilities – electrical power, mechanical power, fresh process water, compressed air. The *utility system* is usually the main interconnection hub of all processes on the site.

Water Network [Water]

This is a network involving water-using operations, fresh water sources, end-of-pipe water treatment (purification) operations, water regeneration operations, and water sinks (including effluents).

Water Sink

In a *water network*, a ***Water Sink*** is a connection requiring water of certain purity. An example is the input to a *water-using operation*.

Water Sources

In a *water network*, a ***Water Source*** is a connection supplying water of certain purity. An example is the output from a *water-using operation*.

Water Recycling

In a *water network*, feeding water from the output of a *water-using operation* to its input is referred to as ***Water Recycling***. The usual arrangement in this case is to apply *water regeneration* before feeding it to the operation input.

Water Regeneration

This is a process of contaminant removal (purification) from a water stream. It is usually combined with *water reuse* or *water recycling*.

© Woodhead Publishing Limited, 2013

Water Reuse

This is a connection arrangement in a *water network* where the output of one *water-using operation* is feed to the input to another. *Water Reuse* is sometimes combined with *water regeneration*.

Water-Using Operation

This is a *unit operation* which requires water input stream of certain purity and may produce a water output stream with usually lower purity (higher contamination).

Zone Targeting

This may be considered in different contexts. Examples include *HI* and *Regional Energy Supply*.

- **[HI]**: Zone Targeting is a procedure for partitioning a larger set of process streams into subsets based on location proximity or operational considerations, with further evaluation of the heat recovery targets and their comparison for variations of the partitioning and for the whole initial set. This procedure is used to decide whether to allocate certain process streams to one or to several processes.
- **[Regional Energy Supply]**: ***Zone Targeting*** is a procedure for evaluating the optimal configuration of renewable energy (biomass) exchange among zones in a region, where the optimality criterion is usually minimum energy loss or minimum *Carbon Footprint*.

2.4 Conventions: Symbols for Heaters and Coolers

When adding arrows to the symbols for heat exchange units for providing external utilities (heaters and coolers), the arrows are drawn indicating the temperature change occurring with the utility carrier (Fig. 2.23). For a cooler, the arrow is drawn from bottom left to top right, indicating that the cooling fluid absorbs heat. Similarly, for a heater, the arrow starts from top left and progresses to bottom right, indicating that the heating fluid loses heat.

2.23 Convention for drawing utility exchangers.

© Woodhead Publishing Limited, 2013

2.5 References

Alves, J. (1999). Analysis and design of refinery hydrogen distribution systems. PhD thesis, UMIST, Manchester, UK.

Alves, J. J., Towler, G. P. (2002). Analysis of refinery hydrogen distribution systems, *Industry and Engineering Chemistry Research*, **41**, 5759–5769.

Asante, N. D. K., Zhu, X. X. (1997). An automated and interactive approach for heat exchanger network retrofit. *Chemical Engineering Research and Design*, **75**(part A), 349–360.

Bird, R. B., Stewart, W. E., Lightfoot, E. N. (2007). *Transport Phenomena*, 2nd ed. John Wiley and Sons, New York, United States, ISBN 0470115394.

Britannica., (2012). Cryogenics (physics) – Britannica Online Encyclopaedia <www.britannica.com/EBchecked/topic/144945/cryogenics> accessed 01/03/2012.

Dhole, V. R., Linnhoff, B. (1993b). Total site targets for fuel, co-generation, emissions and cooling. *Computers & Chemical Engineering*, **17**(Suppl.), 101–109.

Douglas, J. M. (1988). *Conceptual Design of Chemical Processes*. McGraw-Hill, New York, US.

El-Halwagi, M., Manousiouthakis, V. (1989). Synthesis of mass exchange networks. *AIChE Journal*, **35**(8), 1233–1244.

Foo, D. C. Y., Kazantzi, V., El-Halwagi, M. M., Manan, Z. A. (2006). Surplus diagram and cascade analysis technique for targeting property-based material reuse network. *Chemical Engineering Science*, **61**, 2626–2642.

Geldermann, J., Schollenberger, H., Treitz, M., Rentz, O. (2005). Multi Objective Pinch Analysis (MOPA) for integrated process design. Operations Research Proceedings, 2005, Volume 2004, Part 17, pp. 461–469, DOI: 10.1007/3-540-27679-3_57.

Hoekstra, A.Y., Chapagain, A.K., (2007). Water footprints of nations: water use by people as a function of their consumption pattern. Water Resources Management, 21, 35–48, doi:10.1007/s11269-006-9039-x.

Kim, J.-K., Savulescu, L., Smith, R. (2001). Design of cooling systems for effluent temperature reduction. *Chemical Engineering Science*, **56**(5), 1811–1830.

Kissinger, M., Gottlieb, D., (2010). Place oriented ecological footprint analysis. The case of Israel's grain supply. Ecological Economics **69**, 1639–1645.

Klemeš, J., Dhole, V. R., Raissi, K., Perry, S. J., Puigjaner, L., (1997). Targeting and design methodology for reduction of fuel, power and CO_2 on total sites. *Applied Thermal Engineering*, **7**, 993–1003.

Klemeš J., Friedler F., Bulatov I., Varbanov P., (2010). Sustainability in the Process Industry: Integration and Optimization, McGraw Hill Companies Inc, USA, ISBN 978-0-07-160554-0, 362 ps.

Lam, H. L., Varbanov, P., Klemeš, J., (2010a). Minimising carbon footprint of regional biomass supply chains, *Resources, Conservation & Recycling*, **54**(5), 303–309.

Lam, H. L., Varbanov, P., Klemeš, J. (2010b). Optimisation of regional energy supply chain utilising renewables: P-graph approach. *Computers and Chemical Engineering*, **34**, 782–792.

Lam, H. L., Varbanov, P., Klemeš, J. (2011). Regional renewable energy and resource planning, *Applied Energy*, **88**(2), 545–550.

Linnhoff, B., Flower, J. R. (1978). Synthesis of heat exchanger networks: I. Systematic generation of energy optimal networks. *AIChE Journal*, **24**(4), 633–642.

Palmer, A. R. Pete, (1998). Evaluating ecological footprints. Electronic Green Journal **1**(9). <escholarship.org/uc/item/05k183c9>.

© Woodhead Publishing Limited, 2013

Parliamentary Office for Science and Technology (POST), London, UK, (2006). Carbon footprint of electricity generation. <www.parliament.uk/documents/upload/postpn268.pdf> accessed 22/02/2012.

Perry, S., Klemeš, J., Bulatov, I. (2008). Integrating waste and renewable energy to reduce the carbon footprint of locally integrated energy sectors. *Energy*, **33**(10), 1489–1497.

Sánchez-Chóliz, J., Duarte, R. (2005). Water pollution in the Spanish economy: analysis of sensitivity to production and environmental constraints. Ecological Economics **53**, 325–338.

Savulescu, L., Kim, J., Smith, R. (2005a). Studies on simultaneous energy and water minimisation – Part I: Systems with no water re-use. *Chemical Engineering Science*, **60**(12), 3279–3290.

Savulescu, L., Kim, J., Smith, R. (2005b). Studies on simultaneous energy and water minimisation – Part II: Systems with maximum re-use of water. *Chemical Engineering Science*, **60**(12), 3291–3308.

Singhvi, A., Shenoy, U. V. (2002). Aggregate planning in supply chains by pinch analysis. *Chemical Engineering Research and Design*, **80**(6), 597–605.

Smith, R., Varbanov, P. (2005). What's the price of steam?, *Chemical Engineering Progress*, **101**(7), 29–33.

Smith, R., (2005). *Chemical Process Design and Integration*, Wiley, Chichester, UK.

Tjan W., Tan R. R., Foo D. C. Y., (2010). A graphical representation of carbon footprint reduction for chemical processes. *Journal of Cleaner Production*, **18**(9), 848–856.

Towler G., Sinnott R. (eds) (2008). *Chemical Engineering Design, Principles, Practice and Economics of Plant and Process Design*. Elsevier, Amsterdam, The Netherlands.

Townsend, D. W., Linnhoff, B. (1984). Surface area targets for heat exchanger networks. *IChemE Annl. Res. Mtg*., Bath, UK, Lecture 6A.

Wan Alwi, S. R., Mohammad Rozali, N. E., Abdul-Manan, Z., Klemeš, J. J. (2012). A process integration targeting method for hybrid power systems. *Energy*, **44**(1), 6–10

Wang, Y. P., Smith, R. (1994). Wastewater minimisation. *Chemical Engineering Science*, **49**(7), 981–1006.

Zhelev, T., Ntlhakana, L. (1999). Energy-environment closed loop through oxygen pinch. *Computers & Chemical Engineering*, **23**(Suppl.), 79–83.

Zhelev, T. K., Bhaw, N. (2000). Combined water–oxygen pinch analysis for better wastewater treatment management. *Waste Management*, **20**(8), 665–670.

2.6 Appendix: Nomenclature

A number of the terms can be used in different contexts and in some cases their meaning changes depending on the context. Where this is the case, the context in which a term is defined is specified [**in bold**] within square brackets.

A	heat transfer area, m^2
AF	Annualisation Factor, y^{-1}
C	cooler [**heat exchanger**]

© Woodhead Publishing Limited, 2013

C	concentration (of contaminant) [**Water**], ppm
CCs	Composite Curves
CGCC	Column GCC
CHP	Combined Heat and Power
C_{in}	limiting inlet concentration, ppm
COP	Coefficient of Performance (of a heat pump)
C_{out}	limiting outlet concentration, ppm
CP	heat-capacity flowrate, kW/°C or MW/°C
C_p	specific heat capacity, kJ/(kg·°C)
CW	cooling water
EFP	Energy Footprint
F	limiting water flowrate [**Water**], t/h
F	force [**Physics**], N
GCC	Grand Composite Curve
GHG	Greenhouse gas
H	heater [**heat exchanger**]
H	enthalpy [**HI**], kJ or MJ
	enthalpy [**flow**], kW or MW
h	specific Enthalpy [**thermodynamics, HI**], kJ/kg or MJ/kg
h	film heat transfer coefficient [**heat transfer**], kW/(m^2·°C)
HEN	Heat Exchanger Network
HI	Heat Integration
$h_{IN,COLD}$	specific enthalpy of a cold stream entering a heat exchanger, kJ/kg
$h_{IN,HOT}$	specific enthalpy of a hot stream entering a heat exchanger, kJ/kg
$h_{OUT,COLD}$	specific enthalpy of a cold stream leaving a heat exchanger, kJ/kg
$h_{OUT,HOT}$	specific enthalpy of a hot stream leaving a heat exchanger, kJ/kg
HP	high pressure
LFP	Agricultural Land Footprint
LP	low pressure [**Total Site**]
LP	Linear Programming [**Optimisation**]
m	mass flowrate, kg/s or t/h, or kg/h
m_{COLD}	mass flowrate of a cold stream flowing through a heat exchanger, kg/s or t/h
MEN	Mass Exchange Network
MER	Maximum Energy Recovery
m_{HOT}	mass flowrate of a hot stream flowing through a heat exchanger, kg/s or t/h
MI	Mass Integration
MOPA	Multi-Objective Pinch Analysis
MP	medium pressure
MSA	Mass Separating Agent
PCM	Phase Change Material
PI	Process Integration

© Woodhead Publishing Limited, 2013

PLF	project life time, y
Q	a heat flow, kW or MW. May have various subscripts defining the context.
$Q_{C,min}$	minimum external (utility) cooling, kW or MW
$Q_{H,min}$	minimum external (utility) heating, kW or MW
Q_{HE}	heat load of a heat exchanger, kW or MW
Q_{HP}	enthalpy flow in high pressure steam, kW or MW
Q_{LP}	enthalpy flow in low pressure steam, kW or MW
SCCs	Shifted Composite Curves
T	temperature, °C
TAC	Total Annualised Cost, $/y, €/y, £/y or other currency/y
T_S	supply (or starting) temperature, °C
t^S	starting time, h
TSP	Total Site Profiles
T_T	target (or ending) temperature, °C
t^T	end time of an operation, h
U	internal energy [**thermodynamics**], kJ or MJ
U	overall heat transfer coefficient [**heat transfer**], kW/(m²·°C)
V	volume, m³
VHP	very high pressure
W	power, kW or MW
W	mechanical work, kJ
WFP	Water Footprint
WPFP	Water Pollution Footprint
XP	Cross-Pinch
ΔH	enthalpy change [**flow**], kW or MW
ΔL	distance, m
ΔT	temperature difference, °C
ΔT_{LM}	Logarithmic Mean Temperature Difference, °C
ΔT_{min}	Minimum Allowed Temperature Difference, °C

© Woodhead Publishing Limited, 2013

3

Process Design, Integration and Optimisation: Advantages, Challenges and Drivers

VASILE LAVRIC, University 'Politehnica' of Bucharest, Romania

DOI: 10.1533/9780857097255.1.79

Abstract: This chapter begins with a short history of process design, and then presents a hierarchical approach to the main currents: heuristic approach, phenomena-driven design, conflict-based approach, case-based reasoning, driving force method and axiomatic design. The main similarities and differences between design and retrofit are emphasised. Process Integration definitions and main tools are introduced, the integration techniques are detailed, and the distinction between integration and intensification is clarified. The main optimisation techniques are shown, emphasising that different scalar/vector objective functions applied to the same mathematical model give different topologies. Lastly, simultaneous integration and control is advocated.

Key words: process design, Process Integration, process optimisation, Process Intensification, Pinch Analysis, integration and control, Process Retrofit, Pareto optimisation, driving force method, integration techniques.

3.1 Introduction

An industrial process, aimed at producing, both sustainably and economically, some valuable end-products – and, simultaneously, by-products which can be used in other processes – should, when possible, take some important steps in its journey from cradle-to-grave (Harmsen, 2004): chemical processes synthesis, conceptual/systematic process design/synthesis, process development, process engineering, process and/or site integration, detailed engineering, plant operation and, finally, end of life.

During this journey, innovation should be the key driving factor, while sustainability should be the paradigm (Dimian and Bildea, 2008). There is no universally accepted definition for sustainability; according to Stiglitz (1974), sustainability is 'the optimal growth path that maintains economic development while protecting the environment and optimising the social conditions with the boundary of relying on limited, exhaustive natural resources',

© Woodhead Publishing Limited, 2013

which emphasises the need for responsible development, and not simple preservation. A truly sustainable development means embracing the opportunities and managing the risks deriving from economic, environmental and social aspects, taking into account all the interactions among them (Cano-Ruiz and Mcrae, 1998). For a thorough discussion related to process design under the sustainability paradigm, see the excellent book of Klemeš *et al.* (2010), which explains how to optimise Process Integration (PI) for improving the energy and water efficiency of industrial as well as non-industrial energy users, formulating sustainable tasks as optimisation problems. In a recent approach, Upadhye *et al.* (2011) showed how this paradigm is essential in developing renewable energy technologies.

Although the steps related to process aspects (design/synthesis, development, engineering, integration and detailed engineering) were traditionally considered sequentially, though taking into account the interdependencies between them through local loops, there is a growing tendency in the academic world to approach both design and integration processes simultaneously owing, especially, to affordable computational power. Yet industry is still reluctant to fully embrace this trend, due to the lack of well-established procedures, the huge complexity and the difficulty in interpreting the optimisation results (Harmsen, 2004).

The ultimate goal of process design is to come up with flowsheet alternatives of the raw material processing according to the chemical transformations envisaged. To this end, either knowledge-based (Cecelja *et al.*, 2011) or systematic approaches could be used (Grossmann and Hooker, 2000). The former, known also as conceptual design, is based upon hierarchical decomposition, using heuristics and engineering experience, while the latter encompasses the optimisation of a superstructure of alternatives, based on mathematical programming techniques (Grossmann and Daichendt, 1996).

Knowledge-based methods concentrate on the representation and knowledge organisation of the design problem. The process design begins with identifying existing or novel process units which integrate the functions (tasks) associated with raw material transformation. The functions are combined as much as possible by shifting to common pressure and temperature ranges. A set of multi-functional equipment should be defined, including new equipment where functions operating at the same temperature and pressure range can be combined, provided that in this way the capital expenditure and exergy losses are reduced (Li and Kraslawski, 2004).

Systematic design can be approached in two ways: (i) targeting for the optimum profile of the process driving forces, ahead of detailed design and without commitment to the final system configuration (Klemeš *et al.*, 2010), or (ii) putting the alternative flowsheets in the form of an optimisation problem, using a superstructure which should be reduced to the optimal solution,

© Woodhead Publishing Limited, 2013

irrespective of whether the system at hand is time dependent (Li *et al.*, 2010) or in steady state (Khor and Elkamel, 2010).

Generally speaking, systematic design based on superstructures contains six steps (Biegler *et al.*, 1997):

1. The process engineer generates all conceivable unit operations.
2. The necessary simplifying assumptions are acknowledged, to suitably reduce the complexity of the process.
3. A superstructure connecting all individual units in all possible ways is built up, according to those simplifying assumptions.
4. The complex mathematical model corresponding to this superstructure is written, including the components, mass and enthalpy flows, together with the cost expressions associated with feed stocks, investments in buildings and equipment, and operations.
5. An objective function is defined, together with all constraints of the variables – traditionally, it is either a cost-based function, or an operating one (productivity, specific energy consumption, etc.); currently, a vector of dichotomic objective functions is being used, to obtain a set of optimally equivalent solutions (Alhammadi *et al.*, 2002).
6. Using an appropriate optimisation algorithm (direct or stochastic), the optimum selection of equipment and conditions is undertaken.

The methods of choice for the optimisation of the mathematical model associated with the superstructure are based upon NLP/mixed-integer non-linear programming (MINLP), where the objective function is convex or the concave objective function is replaced by its piecewise convex approximation. When the mathematical model is linearised and the objective function is linear, the algorithms are of MILP or LP type (Klemeš *et al.*, 2010). Although the deterministic algorithms can under some conditions guarantee the global optimum, they strongly depend upon a good starting point. Moreover, the approximations implied by linearisation render the solution suboptimal. In order to avoid these drawbacks, stochastic/evolutionary algorithms are used; among the latest, a joint disjunctive-genetic algorithmic approach is proposed, for the synthesis of process networks involving discrete/discontinuous functions, or for the selection of different equipment, units or processes, given a set of alternatives. This approach eliminates the reformulation into a direct MINLP problem step, thus allowing the solution of the original problem as a continuous optimisation problem but only at each individual discrete and reduced search space (Odjo *et al.*, 2011).

There are some important weaknesses of optimisation-based methods:

(a) The lack of the ability to automatically generate a flowsheet superstructure.
(b) The huge computational effort.

© Woodhead Publishing Limited, 2013

(c) The optimality of the solution can only be guaranteed with respect to the alternatives that have been considered a priori.

3.1.1 Hierarchical approach

The hierarchical heuristic approach combines the long-term experience of engineers and researchers with the evolutionary techniques to end up with a set of flowsheet alternatives (Zhelev, 2007). The hierarchical heuristic approach is a top-down flowsheet synthesis, identifying common tasks and grouping them in layers. For each layer, an evolutionary approach is envisaged (Douglas, 1988). First, a possible previous solution is sought for this new problem, using the similarity functions as metrics for the distance between the solutions to the most similar and the actual problems. If there is no predefined solution for the present requirements, a new solution should be created (Li and Kraslawski, 2004). According to Dimian (2003), this approach identifies the optimal design space for each alternative.

The hierarchical heuristic approach could be systematised into the following steps, according to the communality of tasks, as presented in Fig. 3.1, which, in the author's opinion, synthesises the latest trends in this field:

1. Opportunity assessment – evaluate if the proposed process is sustainable (health, safety and environmental risks), then gather the fundamental technological and economic data for a sustainable conceptual design (Dimian and Bildea, 2008).
2. Detailed study of the chemistry, thermodynamics and kinetics – evaluate chemical equilibrium limitations, state parameters for fastest process rates and separation techniques discrimination through feasibility.
3. Input/output structure of the process – performs the overall material balance using raw materials as input, and products, by-products and waste as output. Based on similar processes, a crude energy balance could be made, together with an estimate of necessary utilities. A primary economic analysis should be envisaged, to estimate the profitability of a sustainable process.
4. Reactors' network – the operating mode for the reactors (batch versus continuous) is selected, together with their type and the overall performance of the reaction train; the variability of raw materials and several scenarios regarding the production rate should delimit an 'operation window' for the state and operating parameters. The non-linearities induced by external recycles from the separation trains should be addressed, to emphasise possible problems with reactors' control and stability (Labrador-Darder *et al.*, 2009). A rough estimation of the utility allocation could be done, based upon the heat of the reaction.

© Woodhead Publishing Limited, 2013

5. Separation system synthesis – generate viable separation sequences for each phase of the process; the characteristic property concept will be used to rank separation techniques. The recycle structure of the flowsheet candidates should be established, with direct impact upon the controllability of the reactors' network.
6. Process Integration and Intensification – reduce, through local and flowsheet recycle, reuse and local regeneration, the consumption of utilities such as energy (heat, power), material (water, solvent), using well-established Process Integration techniques (Smith, 2005); obtain faster processes or compact and complex units using Process Intensification guidelines (Klemeš *et al.*, 2010).
7. Risk assessment – evaluate quantitatively the risks associated with key tasks and the associated containment measures, to ensure sustainability (Hossain *et al.*, 2008).
8. Process control architecture – define local and process levels of hierarchical control, taking into account the fundamental process-control principles; local levels should be designed concomitantly with the controlled subsystems, while the process level should be designed as the last task concluding the flowsheet (Vasudevan and Rangaiah, 2011).

The hierarchical heuristic method emphasises the strategy of decomposition and screening. It allows for the quick location of flowsheet structures that are often 'near' optimal solutions. This method has evolved from a true sequential nature, where the interactions between different design levels were minimal, to an algorithmic sequence of steps, some of them being executed iteratively till certain criteria are met (Fig. 3.1). In order to increase sustainability, Steps 1 to 3 should be sequentially executed till some of the sustainability metrics have acceptable values (Dimian and Bildea, 2008). Then, Steps 4 and 5 have to be implemented iteratively till the whole reactor/separation trains network performs flawlessly and its controllability is ensured. Step 6 could have repercussions upon the previous two, since integration reduces the degrees of freedom, rendering control more difficult. This is why there is a growing tendency to design the control architecture simultaneously with the integration step (Patel *et al.*, 2008). More information can be found in the excellent papers of Ricardez-Sandoval *et al.* (2009) for a review of the literature, or Jogwar *et al.* (2010) for theoretical approaches. Risk analysis is intimately related to sustainability, being one of its major tools in taking the right measures to curb the probability of accidental contamination of the environment due to some process malfunctions (Dimian and Bildea, 2008). The results of risk analysis could imply re-execution of any engineering step (4 to 6), in the search for a safer solution. The final step encompasses the design of the control architecture at the process level, which should ensure the optimal set-points for the local control systems.

© Woodhead Publishing Limited, 2013

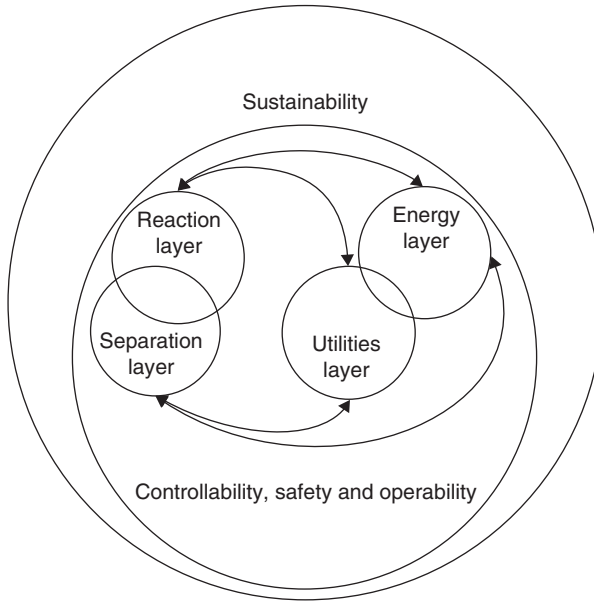

3.1 Layers' interactions during flowsheet alternatives' generation by hierarchical heuristic approach – a personal view by the author of this chapter.

However, despite its evolution toward an algorithmic method, the hierarchical heuristic approach offers no guarantee of finding the best possible design (Klemeš *et al.*, 2010).

3.2 Grassroots Design versus Retrofit Design

Grassroots process design, meaning producing the blueprint of a new process/plant, represents the topic of choice for the vast majority of the research efforts and published papers, since a good process design makes the difference between success and failure. Systematic, or heuristic, grassroots design continuously improves with new or enhanced tools aimed at better solutions to the problems specific to each design stage. On the other hand, retrofit design, known also as revamp design or debottlenecking, meaning modifying an existing plant to improve its performance (Enriquez *et al.*, 2011), receives substantially less attention, for several reasons: significantly lower scientific appeal, a tacit acceptance that many tools developed for grassroots design are readily available for retrofit, and the reluctance of industry to debottleneck unless the profitability is sufficient. Even then, industry prefers to revamp using proprietary knowhow, tools and procedures, verified by a long practice.

© Woodhead Publishing Limited, 2013

There could be several motivations in retrofitting an existing plant: a permanent change in feed or product specifications, an increase in foreseeable demand – insufficient to build a new plant, but high enough to raise the capacity of an existing one – improved safety, significantly reduced operating costs, or accommodating new environmental specifications aimed at curbing emissions (Smith, 2005). Although there are many similarities between grassroots and retrofit design, given by the common methodologies used to analyse reactors and separation networks, integration and control or risks associated with the process, the main difference is that debottlenecking works on an existing plant and, thus, the existing equipment and piping system should be used effectively, avoiding unnecessary investment, even if it does not perform optimally (Smith, 2005). The Golden Rule states that the fewer the modifications to either the connections and the equipment, the better. The major economic objectives of any retrofit design should be to maximise:

(a) The cost-saving on utilities minus the annualised capital cost.
(b) The net present value of the retrofit.
(c) The return on the investment.
(d) The utility cost-savings, subject to a certain capital investment limit.

When the incentive of the revamp is to increase the capacity, a thorough analysis should be undertaken concerning the spare capacities of the existing units, focusing on either replacing or modifying the items performing below the new expected capacities, or placing new items, in parallel or series with the existing ones. Either way, the piping system should be revisited to accommodate these changes (Smith, 2005).

The retrofit design of chemical-engineering processes could benefit from the simultaneous application of process simulation and Response Surface Methodology (RSM), although it is not often straightforward to build a robust simulation and optimisation framework and apply it (Enriquez *et al.*, 2011). This new method reduces the complexity of the original model, approximating its response surface with an acceptable level of confidence. The proposed Retrofit Design Approach (RDA) has three main stages (Enriquez *et al.*, 2011):

1. Diagnosis, with its strategic elements *Key Design Variables' Selection* and *Conceptual Understanding*, aiming to eliminate variables that do not show effect on the performance index of the process.
2. Evaluation, which has two main parts *Preliminary screening* and *RSM*.
3. Optimisation, where the reduced model derived from the RSM is optimised to obtain the optimal values of the response within the ranges of parameters studied. A final retrofit portfolio from the RDA includes all the changes to be made and their techno-economic benefits.

© Woodhead Publishing Limited, 2013

A retrofitting holistic approach is depicted by Liu *et al.* (2006), aiming at fully resynthesising the entire process by incorporating the operating units with enhanced performance and the inevitable restructuring of the flowsheet's network. With the combinatorial feasibility of most operating units largely predetermined, the approach detects easily any changes in the flowsheet's network structure incurred by retrofitting.

Uerdingen *et al.* (2005) analyse a systematic retrofit design method for screening, identifying and evaluating the options to improve the cost-efficiency of a continuous chemical process. The method is organised in five steps: (1) base case analysis, (2) generation of retrofit options, (3) rough economic evaluation of the retrofit options, (4) process optimisation with regard to retrofit options that do not require investment, and (5) feasibility study as well as the economic profitability of the retrofit options that require investment. This method is a continuation of Uerdingen *et al.'s* (2003) work, where the first three steps were extensively presented and discussed.

Water and wastewater networks, including here water-using, treatment and regeneration units together with the piping and pumping systems, were subjected to fewer retrofit studies, despite its practical significance. No optimisation approach for water networks retrofit accounts for parameter optimisation of water-using processes and selection of their type. It should be pointed out that criteria that are valid for the retrofit scenario are important, because they generally differ from those for a grassroots design (Jeżowski, 2010).

Tokos *et al.* (2012) developed an approach to retrofit a large-scale brewery water system, which integrates water-using operations and wastewater-treatment units in different production sections within the same network. They used an MINLP model for water reuse and regeneration reuse in batch and semicontinuous processes, proposing two alternative multilevel strategies to solve such problems by means of temporal decomposition. The results obtained show that, despite the high piping cost, integration of both sections yields a better result than the separate Water Network Design in each section.

Khor *et al.* (2012) developed an optimisation framework for refinery water network systems design and retrofit that integrates the complementary advantageous features of Water Pinch Analysis. The framework explicitly incorporates water minimisation strategies by first postulating a superstructure representation that embeds all feasible flowsheet alternatives for implementing water reuse, regeneration and recycling opportunities. Subsequently, an NLP model was formulated and then solved. Post-optimality analysis on the numerical results was performed to achieve the desired water reuse quality.

Sotelo-Pichardo *et al.* (2011) analysed the optimal retrofit of water conservation networks considering recycle, reuse and regeneration schemes,

© Woodhead Publishing Limited, 2013

simultaneously taking into account economic (because of the reduction of fresh sources costs) and environmental (because of the reduction of waste stream discharge into the environment and with better quality) improvements. A good retrofit formulation should consider: (a) the environmental regulations for waste stream discharge (additional treatment), (b) the maximisation of the mass exchanged at the least cost, (c) the repiping costs, which is a key issue, and (d) the possibility of simultaneously modifying existing or installing new treatment units and of reconfiguring the piping system as options for the retrofit network.

Faria and Bagajewicz (2011) present a planning model, flexible enough to be used for the systematic grassroots design and/or retrofit of industrial water systems, aiming at addressing an increase in plant capacity associated with new water-using units to be added through time and/or higher mass loads for the existing water-using units.

Sujo-Nava *et al.* (2009) presented their case study on retrofitting of sour water networks in oil refineries, while Iancu *et al.* (2009b) discussed wastewater network retrofitting through optimal placement of the regeneration unit, whereas Alva-Argaez and Savulescu (2009) argued that the selection of retrofit projects to increase water productivity has to account for the limitations imposed by the existing process configuration and utility infrastructure. Their methodology is based on analogies with the transhipment model.

Tan and Manan (2008) discussed a systematic technique for retrofit of water network based on Pinch Analysis with three main steps:

1. Network Diagnosis, which provides a good understanding of the existing water network through the use of the Concentration Block Diagram.
2. Network Retrofit, which provides the preliminary retrofit design based on a set of Pinch rules performed on the existing water network.
3. Network Evolution, which generates the final retrofit scheme.

Tan *et al.* (2007b) demonstrated the use of Water Pinch Analysis to build a two-step systematic technique for the retrofit of a water network with regeneration:

1. Retrofit Targeting, where retrofit targets (utility savings and capital investment) were determined for a range of process parameters (total flow rate and/or outlet concentration of the regeneration unit) to obtain a savings-versus-investment curve, and.
2. Design for a water network with regeneration unit(s), where the existing water network is redesigned according to the chosen targets.

This is a continuation of the Tan and Manan (2006) work, where retrofit of a water network is done optimising the existing regeneration units.

© Woodhead Publishing Limited, 2013

Chen and Hung (2005) presented a simultaneous optimisation method for the retrofit of existing mass-exchange networks, represented as a stage-wise superstructure according to which a mixed-integer non-linear programming model is formulated, which considers the costs of mass separating agents, the reassignment of existing exchange units to different process stream matches and their need for additional tray numbers, column height, or both, and the creation and installation of new units.

There are several other published results presenting different aspects of revamping water and wastewater networks that the reader could consult: Dantus and High (1996) introduced economic evaluation for the retrofit of chemical processes through waste minimisation and Process Integration; Kim and Smith (2003) presented a methodology for automated retrofit design of cooling-water systems, while Tan and Cruz (2004) used symmetric fuzzy linear programming for the synthesis of robust water reuse networks for single-component retrofit problems.

Due to the historical development, the retrofit of heat/energy networks has been better studied. There are many more papers published in this domain than devoted to water and wastewater network retrofit. The excellent review of Smith *et al.* (2010) presents the developments in the retrofit of Heat Exchanger Networks (HENs), in a very pleasing and systematic way. Apart from this, another very useful paper is the review of Morar and Agachi (2010), covering complementarily the problem of heat/energy network retrofitting. Useful information related to both heat/energy and water and wastewater network retrofitting could be also found in Friedler (2010). From then, other papers have been published in this respect, worth being mentioned.

Bakhtiari *et al.* (2010) developed a systematic methodology for the integration of absorption heat pumps (AHP) in industrial processes; guidelines are formulated for the proper selection of heat sources and sinks that will maximise the benefit derived from heat pumping while respecting process constraints and operating requirements of the AHP. The principles of AHP operation and its efficient Process Integration are thus described. The methodology relies on data extracted from a Pinch Analysis of the plant.

Coletti *et al.* (2010) develop a dynamic, distributed mathematical model for shell-and-tube heat exchangers undergoing crude-oil fouling (validated against refinery data) thus including the time effect in the design or retrofit of HEN to maximise energy-recovery performance. Simulation results show that network designs that maximise energy recovery in clean conditions (following traditional Pinch rules) may not be best when fouling occurs, and that a proper retrofit design must include consideration of time-varying fouling effects.

Kralj (2010) proposes the extension of a stage-wise model of superstructure representation, which includes additional equations and

© Woodhead Publishing Limited, 2013

limitations with respect to the grassroots variant, to retrofit a HEN through Process Integration. This model can be easily solved regarding both trivial and complex industrial problems. The method of the stage-wise model for a retrofitted HEN provides solutions that are sufficiently good over a short time.

Li and Chang (2010) argued that, due to the rapid growth of oil prices in recent years, there is an urgent need to retrofit the existing 'optimal' networks, using smaller driving forces than in the original designs, so as to reduce the current utility consumption rates. Accordingly, a simple Pinch-based approach is proposed, while keeping additional capital investment to a reasonable level. In particular, every Cross-Pinch match is removed, and its heat loads on the hot and cold streams are both divided into two according to the Pinch Temperatures. At either side of the Pinch, the divided heat loads on each stream are combined and then matched according to a systematic procedure derived from simple Pinch Analysis.

Mejia-Suarez *et al.* (2010) proposed an MINLP model, together with the associated superstructure, for the simultaneous retrofit of HENs which takes into account: (a) the placement, modification and reassignment of existing exchangers, (b) additional exchangers, (c) HEN topology, (d) utility costs, and (e) investment cost. In addition, the model formulation incorporates repiping costs that limit the number of reassignments of the available equipment. A methodology to facilitate the search for good alternative solutions is detailed, so the designer will have diverse options to consider and, besides the total annualised cost, different network features can be taken into account in the final selection of the retrofit design.

For the retrofit, Nguyen *et al.* (2010) consider both addition and relocation of heat exchangers, allowing control of repiping costs as well as splitting, together with the cost associated to area reduction and/or increase of the existing exchangers and all the costs associated with new shells, area addition to existing shells, relocation and piping changes. They advocate the superiority of step-by-step changes that allow better planning around turnarounds as opposed to an all-at-once solution. Also, they claim that their model offers a good level of flexibility.

Feng *et al.* (2011a) propose some principles to define a boundary for Heat Integration in systems composed of several interconnected processing units. Accordingly, they develop some Heat Integration strategies offering significant energy saving potential and simplicity in implementation to obtain reliable retrofit schemes. The boundary for Heat Integration can be the whole process or its individual units, the choice of which is determined by their energy saving potentials.

Liang and Feng (2011) utilised Pinch Technology to analyse and optimise the HEN of a certain continuous reforming process, identifying the unreasonable heat exchanges, which are mainly the heat transfer across the Pinch.

© Woodhead Publishing Limited, 2013

The retrofit is then undertaken on the existing network by removing the heat exchangers with large heat duties, major contributors to overall generated entropy.

Khalilpour and Abbas (2011) recommend a procedure of reducing the energy penalty imposed by integration of pulverised coal-fired power plants with solvent-based post-combustion carbon capture (PCC) processes via HEN optimisation, through the diminution of utility and operating cost.

Piacentino (2011) proposes a procedure for the retrofit of existing networks, based on an integrated use of several techniques, in the framework of Pinch Analysis. The preliminary step of the retrofit study is the diagnosis of the existing network resulting in a *minimum energy requirement* configuration. Then, an innovative spider-type diagram is presented to identify a hierarchic order among a set of retrofit topologies and the most promising relaxation paths for each network topology. The procedure helps to identify preferential routes in networks' retrofit and to exclude the least promising improvement directions of the existing network, as an alternative to algorithms for automatic optimisation of HENs. The methodology enables the energy analyst to identify solutions achieving near-minimum total costs focus, analysing the energy performance of the different schemes.

3.3 Process Integration

Process Integration, grown nowadays into a family of methodologies for combining several processes to reduce consumption of resources and/or harmful emissions to the environment, and thus becoming an important asset in ensuring the sustainability of chemical, biochemical and power generating industrial processes (Friedler, 2010), emerged during 1970s as Pinch Technology, a collection of Heat-Integration techniques, aiming at reducing hot and cold utility consumption. These targets are then used in the HEN Synthesis (Linnhoff *et al.*, 1982). Later on, Pinch Technology became Pinch Analysis, applying the Pinch concepts to an ever increasing variety of processes wherever an imbalance between sources and sinks exists which should be compensated by a convenient utility: energy (heat, power and pressure), material (water, hydrogen, oxygen and carbon dioxide), etc. Klemeš *et al.* (2010) published an excellent book devoted to PI, covering all aspects of this complex paradigm and emphasising its essential contribution to ensuring the sustainability of industrial processes.

According to El-Halwagi (1997), PI is a framework permitting a deeper understanding of the insights of the strong interaction among process units, streams and objectives in order to methodically determine its attainable performance targets, and systematically make decisions leading to the realisation of these targets. PI has three main interconnected stages: synthesis, analysis and optimisation.

© Woodhead Publishing Limited, 2013

From a thermodynamic perspective, *PI is a paradigm having as core the concept of optimal distribution of the driving force or forces along the process, thus minimising the process generated entropy*.

PI can roughly be divided into insight-based, evolved from Pinch Analysis concepts (Klemeš *et al.*, 2010), and mathematical modelling techniques, based upon superstructures and their associated first-principle equations and restrictions. The former always consists of a two-step approach (Smith, 2005):

1. *Targeting*, during which the optimal driving force over the whole process is sought (temperature, concentration, pressure, or any gap between a source and a sink), and
2. *Design*, aiming at building an irreducible structure, using heuristics (Dimian and Bildea, 2008).

The irreducibility is guaranteed by systematically avoiding the introduction of redundancies in the flowsheet. The mathematical modelling techniques, on the other hand, start from a superstructure, meant to be reducible from the beginning, which embeds within it all feasible process options and interconnections, including the redundant ones that are candidates for the final integrated process (El-Halwagi, 1997). Then, the associated mathematical model is built, based upon first-principle equations; afterward all sorts of restrictions are added, to help in discriminating between candidate solutions. Finally, a scalar or vector objective function is used to reduce the superstructure to the optimal network, using direct or stochastic/evolutionary optimisation algorithms, provided that this optimum was embedded in the original superstructure.

PI heavily relies on thorough use of Process Simulation, as a mean to rapidly screen the candidate flowsheets, to better understand the behaviour of complex systems, and on this basis to propose effective innovative solutions (Klemeš *et al.*, 2010).

There are two main directions in which PI has developed according to its potential, namely Heat/Enthalpy Integration (sometimes redefined as Energy Integration) and Water Integration. Apart from these, other domains where Process Integration is applied are: *power*, combined or not with *Heat Integration* – Bolliger *et al.* (2005) used Process Integration multi-objective thermoeconomic optimisation for advanced power plant design, Zhelev and Ridolfi (2006) proposed the Emergy-Pinch Analysis to address energy recovery under environmental concerns, Martinez-Patino *et al.* (2010) developed a methodology for the integration of power, heat and water in industrial processes, while Crilly and Zhelev (2010) used Pinch Analysis to curb CO_2 emissions through energy targeting; *hydrogen* – Bealing and Hutton (2002) presented the framework of Hydrogen-Pinch Analysis, applied by Li

© Woodhead Publishing Limited, 2013

to refineries (2003), Nelson and Liu (2008) revisited the Hydrogen-Pinch Analysis, Domenichini *et al.* (2010) used Pinch Analysis, thermodynamic and economic evaluations to combine the production of hydrogen and power, Liao *et al.*, in a paper in two parts, presented some rigorous algorithmic targeting methods for hydrogen networks – in the first, purification of hydrogen is disregarded (Liao *et al.*, 2011a), whereas in the second, it is allowed (Liao *et al.*, 2011b), while Zhang *et al.* (2011b) developed a graphical method for the integration of hydrogen distribution systems with purification reuse; *oxygen* – the group of Zhelev used combined Water–Oxygen–Thermal Pinch Analysis to improve wastewater treatment management (Zhelev, 2002); and *solid systems* – Kit *et al.* (2011) developed a new graphical approach for simultaneous targeting and design of a paper recycling network.

There are several reviews devoted to Heat Integration, one of the last (Morar and Agachi, 2010) focusing on the papers representing the turning points and the emerging trends in developing and improving of Heat Integration and HENs methods. This paper presents, in an easy understood visual format through diagrams, the relationships between domains, authors/research groups, and journals, related by their fields of research. Another review paper worth mentioning is owed to Friedler (2010), which covers the whole aforementioned domains of PI, emphasising the exemplary role played by the series of conferences 'Process Integration, Modelling and Optimisation for Energy Saving and Pollution Reduction' (PRES) in contributing to the solution of PI problems as a forum where new or improved dedicated methodologies are presented and cooperation among participants are made possible that often result in international projects.

From the time these two papers and the book of Klemeš *et al.* (2010) appeared, other contributions to the field of Combined Heat and Power research had appeared, with a clear trend to Total Site or interplant integration.

Söderman and Ahtila (2010) developed an optimisation model for the integration of cooling and heating systems with power generation in large industrial plants with hundreds of heating and cooling heat exchangers. The costs of pipelines and the pumping costs of the streams are included in the model. The model can be used in the design of green grass and retrofit investments and in versatile what-if analyses.

Raskovic *et al.* (2010) studied the Process Integration of the bioprocess plant for production of yeast and alcohol, using Pinch Analysis as a primary tool; the results show considerable energy savings in a short payback period.

The reduction of CO/CO_2 emissions through carbon capture and storage in integrated gasification combined cycle power generation systems, known for their high Combined Heat and Power (CHP) generation efficiency and flexibility, was studied by Ng *et al.* (2010b). Strategies for designing

© Woodhead Publishing Limited, 2013

high-efficiency CHP networks have been proposed based on thermodynamic heuristics and Pinch theory.

Dias *et al.* (2011) carried out simulations of an autonomous distillery, along with utilities demand-optimisation using Pinch Analysis concepts to discriminate between different cogeneration systems: a traditional Rankine Cycle, with steam of high temperature and pressure/back pressure and condensing steam turbines configuration, and a biomass integrated gasification combined cycle (gas turbine set operating with biomass gas produced in a gasifier using sugarcane bagasse as raw material).

Lai and Hui (2010) focused on the design of a flexible and economical thermal energy production system by integrating tri-generation (electricity, heating and cooling) and cold-storage techniques, analysing the capacity determination of the main equipment units, their interconnections and operating conditions during different demand periods and electricity costs. Although a high degree of flexibility in meeting demand changes is usually introduced with a tri-generation system, its expensive investment cost makes it less economically attractive under the discounted electricity tariff. A hybrid system which produces thermal energy via both electricity and town gas is examined.

CO_2 recovery rate in a supercritical pulverised coal power plant was emphasised as an important factor for the net power efficiency by Fu and Gundersen (2010) through a detailed exergy analysis of an oxy-combustion process. The Composite Curves are applied to study the sub-ambient heat exchangers in the air separation unit and compression unit, seeking for the Heat Integration between them.

Becker *et al.* (2010) studied the influence of restricted matches imposed by the industrial constraints upon heat recovery and optimal energy conversion in industrial processes given by Pinch Analysis. Intermediate heat transfer systems are integrated so that restricted heat exchanges become possible and heat recovery penalties, created by those constraints, can be reduced.

Atkins *et al.* (2010) focused on solar-thermal systems that are especially suited for low Pinch Temperature processes (food, beverage and textile sectors), despite their difficult integration into industrial processes due to the non-continuous nature of the supply. Using a thorough Pinch Analysis, they derived a systematic method to account for the non-continuous operating rates of the solar-thermal systems in evaluating the utility-demand profile, which leads to improved design and an optimal operating strategy. The appropriate placement of the solar heat is analogous to the placement of a hot utility source, and an energy penalty is incurred when the solar-thermal system provides heat Below the Pinch Temperature.

Total Site Integration is addressed by Zhang *et al.* (2011a) to improve the energy-use efficiency, introducing the concept of up-plants with multiple hot discharges and down-plants with multiple hot feeds together with

© Woodhead Publishing Limited, 2013

a T-Q graphic method to target the temperature of multiple hot discharges/feeds between plants. The T-Q diagram is composed of a Grand Composite Curve (GCC) and a Composite Curve that only involves process streams employed for hot discharge/feed.

In order to increase the technological and economic feasibility of the bio-oil integrated gasification and methanol synthesis systems, Ng and Sadhukhan (2011b) developed a method to process material and Heat Integration strategies for a cryogenic air separation unit and a water electrolyser.

A systematic and automatic design procedure for optimal integration of HENs, using a software platform, is presented by Jiang *et al.* (2011), based on diverse Pinch/Composite Curves, due to the effect of the dissimilar film heat transfer coefficients on the Area Target, and mathematical programming.

The problematic of polygeneration of Synthetic Natural Gas (SNG), power and heat by catalytic hydrothermal gasification of biomass and biomass wastes in supercritical water is addressed by Gassner *et al.* (2011) following a systematic process-design methodology to build up a general superstructure; thermodynamic property models and thermoeconomic process models for hydrolysis, salt separation, gasification and the separation of methane, CO_2, hydrogen and water at high pressure are developed and validated with experimental data.

Galvez *et al.* (2011) advocate the use of grey-system theory (grey linear/mixed-integer linear programming), a simple technique to consider uncertainty, for HEN Design, as against the mathematical programming techniques; complete methodologies are developed, which include the Grey Composite Curve, the determination of the grey minimum utility consumption and the determination of grey number of exchanger units.

Drobež *et al.* (2011) performed simultaneous Heat Integration and the synthesis of a biogas process based on a mixed-integer non-linear programming model, saving almost totally the cost of the hot utility and 1/3 of cold utility by converting environmentally harmful organic and animal waste into valuable products, and thus most of the electricity and heat produced in the cogeneration system from biogas can be sold as surplus to the distribution networks.

Beninca *et al.* (2011) explore a two-step complexity reducing methodology, to analyse Heat Integration opportunities of an existing plant, identify and quantify reductions of energy consumption, and propose changes to implement them. Initially, the whole plant gets evaluated with traditional Pinch Analysis tools. Then, the proposed modifications were segregated to represent small and independent portions of the original process, allowing the mathematical methodologies to synthesise flexible solutions.

A thermochemically based process superstructure is used by Baliban *et al.* (2011) to consider various process alternatives to convert biomass, coal and

© Woodhead Publishing Limited, 2013

natural gas to liquid transportation fuels, taking into account simultaneous Heat and Power Integration which uses a series of heat engines to recover electricity from the process waste heat; a MINLP model is developed to determine the topology of the refinery that produced the lowest-cost fuels, together with carbon dioxide sequestration and greenhouse gas reduction.

Atuonwu *et al.* (2011) present a one-step Pinch-based optimisation methodology for an energy-efficient adsorption dryer design that considers sensible and latent heat recovery as an integral part of drying system design. Energy balances are written above and below various Pinch Point alternatives, the optimum corresponding to the minimisation of the amount of external heating utility required while satisfying drying and thermodynamic constraints.

Based on mathematical modelling, Quijera *et al.* (2011) evaluate the viability of integrating a solar-thermal system, operating at low and middle temperatures, to the conventional energy structure of a dairy plant, using Pinch Analysis.

Baliban *et al.* (2012) extended their work, introducing a comprehensive wastewater network into a thermochemically based process superstructure to convert biomass, coal, and natural gas to liquid transportation fuels. The MINLP model includes simultaneous Heat, Power, and Water Integration – heat engines are used to recover electricity from waste heat and several treatment units are considered for processing and recycling wastewater.

Although Water Integration, known also as Water Pinch, emerged later than Energy/Heat Integration, to which it owes many of its methods, it has developed massively over the last decade, covering both operating modes: continuous and batch networks, the latter being devised in pure batch and semicontinuous. In a semicontinuous network, water flows continuously through the units, whereas the raw materials are processed discontinuously (Dogaru and Lavric, 2011).

Stringent regulations on wastewater discharge, increasing public concern at scarce water resources, and the increasing price of fossil fuels, demanding emphasis on the need for energy consumption, have given rise to a great number of publications over recent years focusing on water conservation. This concerns both networks of water-using units and wastewater treatment processes, for which better and more rigorous process models are needed.

The excellent review of Jeżowski (2010), devoted to Water Network Design methods, presents the state of the art in this domain, together with his personal view of the perspectives and directions in which there is still need for improvement.

Another very good review was published by Gouws *et al.* (2010) where various water minimisation methodologies for Batch Processes, namely

© Woodhead Publishing Limited, 2013

insight-based and mathematical techniques, the latter considering or not the scheduling, are discussed and comparisons are made among them.

From the moment that these two fine papers appeared, some other contributions were published in the field of water network optimisation, with emphasis on the combined Energy/Heat and Water Integration.

George *et al.* (2011) proposed a methodology to reduce utility consumption in heat-integrated process water networks. Heat Integration is based on an LP model applicable to fixed flow rate water allocation networks, for both single and multiple contaminants, incorporating isothermal or non-isothermal mixing of streams, the latter being formulated as a discontinuous NLP. The number of required heat exchangers is less in heat-integrated water allocation problems with non-isothermal mixing.

A complex problem, the increase of process sustainability through the simultaneous integration of power, heat and mass-exchange systems, is addressed by Martinez-Patino *et al.* (2010), who show that there is a direct relationship between the consumption of these three utilities, and present a series of steps for their design integration. They could be better controlled if these relationships among them were known.

Another study devoted to the design of heat-integrated water utilisation networks was published by Liao *et al.* (2011c), who acknowledged its increased complexity, compared to the design of HENs, due to the non-isothermal mixing and freely splitting nature of hot and cold streams. The resultant MTLP model matches heat exchanges between hot and cold streams ahead of the detailed network design, for which a stage-wise HEN superstructure is introduced.

Bandyopadhyay and Sahu (2011) developed a methodology to target the minimum energy requirement with isothermal mixing in Heat-Integrated Water Networks, prior to the detailed design of both the water allocation network as well as the HEN.

Boix *et al.* (2012b) developed a framework for the design of water and heat exchangers networks based on a two-step methodology: (i) an MILP technique is used to solve the water and energy allocation problem, minimising simultaneously two objectives (fresh water consumption and interconnection number), which leads to several Pareto fronts for fixed numbers of connections and heat exchangers, and (ii) another MINLP procedure is used to improve the best results of (i) with Energy Integration into the water network, minimising an objective cost function which takes into account the energy consumption and the number of heat exchangers.

The means of obtaining a good process design, characterised by efficient use of raw materials, low capital cost and good operability, is presented by Polley *et al.* (2010) as a set of procedures applicable for processes in which water and energy consumption form a large part of the operating cost ('Pinch' or 'Threshold' problems). An integrated water and energy system

© Woodhead Publishing Limited, 2013

should minimise: (a) water consumption, (b) energy consumption, and (c) network structure. The first two problems can be de-coupled and the water conservation options should be established first. Then, the design of the Heat Recovery Network itself is usually simple and straightforward.

3.4 Integration versus Intensification

Process Intensification means designing innovative operating conditions, relative phase circulation, and a combination of simultaneous physical and chemical processes, with the aim of obtaining faster global kinetics, substantially decreasing equipment–size/production–capacity ratio, energy consumption or waste production and, ultimately, resulting in cheaper, sustainable technologies (Grossmann and Westerberg, 2000). This could be done in two ways: Process Intensification equipment and Process Intensification methods.

Contrary to PI, which deals with networks/systems of units/equipment, trying to curb utility consumption through optimal distribution of the process driving force, Process Intensification's goal is to make processes faster, increasing at least one of the terms of the generic mass/heat transfer equation $P = K \cdot A \cdot \Delta F$, where P is either mass or heat flow, K is the kinetic term, A stands for the contact area and ΔF means the overall driving force, which show the distance between the actual state of the process and its thermodynamic equilibrium.

The kinetic term roughly depends upon the local fluid circulation, so any change in the direction, orientation and magnitude of the velocity vector will disrupt the boundary layer, with beneficial effects upon the transfer rates.

The transfer area could be increased differently for direct or indirect contact. In the former case:

(a) Size reduction methods could be applied for bubbles or drops while ensuring a quiescent flow for the continuous phase, curbing the coalescence probability.
(b) Fluidisation exposes completely the dispersed phase to the continuous one.
(c) Promoting high levels of local turbulence in the continuous phase increases the probability of both coalescence and breaking phenomena.

The overall driving force tends to diminish as the process accomplishes. In the case of reversible chemical processes, keeping the overall driving force at high values means combining a physical separation process with the chemical one in a hybrid innovative fashion, aimed at moving the valuable product away from the reaction phase.

© Woodhead Publishing Limited, 2013

3.5 Process Integration Techniques

PI techniques have experienced a massive development, from the emergence of Pinch Technology to today. Some of the newest developments will be presented, according to the accepted clustering into inside-based and mathematical modelling techniques, but after acknowledging the latest reviews and books which systematise this development into an accessible and easy understandable way.

3.5.1 Property-based Techniques

Starting from the seminal work of Shelley and El-Halwagi (2000), where they introduced the notion of clusters that act as surrogate properties and enable the conserved tracking of functionalities instead of components, Property Integration became a distinct Process Integration methodology, aiming especially at Material Integration. They argued that there are many design problems that are not component-based; instead, they are property based (e.g., pH, density, viscosity, chemical oxygen demand, basic oxygen demand, toxicity). Additionally, thermal constraints (e.g., stream temperature) may be required to identify acceptable recycles, thus the need to work with properties instead of component-related measures. Property integration is defined as a functionality-based, holistic approach to the allocation and manipulation of streams and processing units, which is based on tracking, adjusting, assigning and matching functionalities throughout the process (El-Halwagi *et al.*, 2004). After that, an algebraic technique for Property Integration via componentless design was devised (Qin *et al.*, 2004). An important step in enlarging the capability of Property Integration techniques was extending it to the synthesis and scheduling of hybrid dynamic/steady-state networks (Grooms *et al.*, 2005), improved afterwards by introducing interception into the batch (Ng *et al.*, 2008) and continuous (Napoles-Rivera *et al.*, 2010) networks. The concepts of surplus diagram and cascade analysis technique were tailored for use in Property Integration of a material-reuse network (Foo *et al.*, 2006). Ng *et al.* (2009) solved the problems of automated targeting for both total property-based network integration, and conventional and bilateral property-based resource conservation network integration (Ng *et al.*, 2010a). Another notable evolution in Property-Based Integration is the synthesis of a unified model for batch and continuous processes (Chen *et al.*, 2010). Chen *et al.* (2011) extended this technique to the synthesis of a property-based resource conservation network with time-varying process disturbance. Another step towards a complete integration of networks was made by Kheireddine *et al.* (2011), who considered the simultaneous property, mass and thermal effects. Ponce-Ortega *et al.* (2010a) included environmental constraints in their optimal synthesis of property-based recycle

© Woodhead Publishing Limited, 2013

and reuse networks, extended further to the synthesis of material conservation networks with economic objectives (Ponce-Ortega *et al.*, 2011a).

3.5.2 Pinch Analysis Derived Energy Integration

The book of Klemeš *et al.* (2010) covers in detail the techniques derived from Pinch Analysis aimed to improve the energy efficiency of industrial processes, with emphasis on continuous processes. For batch or semicontinuous processes, there are several newly-published papers synthesising the specific techniques, which should take into account the effects induced upon the process by the time irreversibility. Foo (2010) proposes a targeting technique generic in nature and formulated as a mathematical optimisation model to determine the minimum resource and waste targets for Batch Process Integration problems. The technique, which is built on the insight-based Pinch Analysis, handles fixed-schedule batch heat and mass exchange, as well as water networks, enabling the identification of the minimum resource/cost targets prior to the detailed design. Foo *et al.* (2008) extend the minimum units targeting and network evolution techniques that were developed for batch mass-exchange networks into batch HENs. Isafiade and Fraser (2007) use a Pinch Technology approach, combining the optimisation of Heat and Mass Exchanger Networks, to target for their simultaneous design.

3.5.3 Pinch Analysis Derived Material Integration

The state of the art of Pinch Analysis techniques for water network synthesis is reviewed in a complex and complete paper by Foo (2009), which is continued by another synthesis paper, especially devoted to automated targeting technique for Batch Process Integration (Foo, 2010). Also, a wealth of information related to Mass Integration through Water Pinch and derived methods can be found in (Klemeš *et al.*, 2010).

From the time these major contributions were published, other methods had appeared. Saw *et al.* (2011) present a technique which improves the surplus diagram for water and hydrogen networks, making it possible to determine rigorous fresh resource and waste generation flow rate targets for different resource conservation network problems. Another approach, designed to simultaneously locate the minimum freshwater and wastewater flow rate targets, and synthesise the water network that corresponds to the minimum flow rate targets, is presented by Deng *et al.* (2011). The proposed approach handles both fixed load (including operations with water loss and/or gain) and fixed flow rate problems, considering also regeneration in the process of total water network synthesis.

© Woodhead Publishing Limited, 2013

3.5.4 Mathematical Modelling of Energy Integration

Morar and Agachi (2010) presented in their review contributions in the development and improvement of the mathematical modelling-based Heat Integration techniques, together with the interdependencies between the research groups active in this domain. The book of Klemeš *et al.* (2010) represents another source of information related to the mathematical modelling-based Heat Integration techniques. Ponce-Ortega *et al.* (2010b) developed a model based on a stage-wise superstructure that contains all possible matches between hot and cold streams in every stage to synthesise HENs with optimal placement of multiple utilities. Söderman and Ahtila (2010) derived a model for the integration of cooling and heating systems in large industrial plants, while complex integration via mathematical modelling was considered by Gassner *et al.* (2011) for optimal process design for the polygeneration of SNG, power and heat by hydrothermal gasification of waste biomass, by Liang and Feng (2011) for Heat Integration of a continuous reforming process and by Ponce-Ortega *et al.* (2011b) for integration of renewable energy with industrial absorption refrigeration systems observing some technical, economic and environmental objectives.

3.5.5 Mathematical Modelling of Material Integration

The starting point in making an inventory of the methods used in Material Integration through mathematical modelling is the excellent review with personal annotations of Jezowski (2010); it provides an analysis of water network problem formulation together with the associated solution techniques, and, at the same time, some statistics and classifications of the literature annotations. As seen in the case of process synthesis, the vast majority of the mathematical models used in Material Integration are based upon superstructures, while the objective functions are of an economic nature. Thus, with few exceptions, the overall model is of the NLP type, the main concern being how to reduce its complexity to MINLP without compromising its adequacy.

Bai *et al.* (2010) used the effect of process decomposition upon a water-using process, and further on a regeneration reuse water system, to build a superstructure and three sequential mathematical models to optimise single-contaminant regeneration reuse water systems, showing that decomposition multiplies optimising variables and increases model dimensions, which incur a series of solving difficulties. Handani *et al.* (2010) used a representative superstructure based on the water management hierarchy options, which considers all conceivable methods to holistically reduce fresh

© Woodhead Publishing Limited, 2013

water usage through elimination, reduction, reuse/outsourcing and regeneration, and solved the optimisation using the MINLP technique. Later on, Handani *et al.* (2011) developed a water network superstructure and, on its base, a generic linear programming model which simultaneously sets the targets and design of the maximum water recovery network, for both mass transfer-based and non-mass transfer-based problems.

Ahmetović and Grossmann (2011) used a complex superstructure, encompassing one or multiple sources of water of different quality, water-using processes and wastewater treatment operations, with all feasible connections between them, to optimise an integrated process water network. A different approach to solving the same problem of integrated water/wastewater networks optimisation was used by Tudor and Lavric (2011), who regard the water-using and water-treatment networks as two oriented graphs – a special structure where the recycle is forbidden *ab initio* and each water-using unit receives wastewater from the previous units and sends wastewater for reuse to the next units in the network (Tudor and Lavric, 2010). The treatment units are seen as contaminated sources (Lavric *et al.*, 2004), thus closing the external recycle; the approach can be easily extended to the zero-discharge case. The oriented graph concept, developed earlier by Lavric *et al.* (2005), was used also by Iancu *et al.* (2009a) to prove that the internal streams regeneration is an effective tool for wastewater network optimisation and wastewater network retrofitting through optimal placement of regeneration units. The same concept of the oriented graph was used by Dogaru and Lavric (2011) to search for the optimal dynamic water network topology of semicontinuous processes, with respect to the water throughput, but batch when it comes to the raw materials processed. For each time-interval, the water sub-network could be abstracted as pseudo-stationary, and optimised accordingly. The concentration of the contaminants in the storage tank, though, is dynamic by nature, so adjustments should be made with respect to the freshwater consumption when violations of water-using restrictions are possible (Dogaru and Lavric, 2012).

Pan *et al.* (2012) showed that, when the regeneration recycling implies known regeneration ratios, the design of a water-using network is an iterative process, starting from the initial regenerated concentrations, determined based on the features of the network and the regeneration process, then using these as the initial starting point for the next iteration.

Boix *et al.* (2012a) approached the problem of optimisation of the pending water network of an eco-industrial park, which was formulated as a MILP and solved by the ε-constraint method. Regeneration units could be of three types, and the MILP is solved under two kinds of conditions: limited or unlimited number of connections, same or different gains for each company belonging to the eco-industrial park.

© Woodhead Publishing Limited, 2013

3.5.6 Combined Energy and Material

One of the latest approaches regarding network utilities refers to combined energy and material optimisation, for which the annotated review of Jezowski (2010) represents a good starting point.

Grossmann and Martín (2010) proposed a strategy based on mathematical programming techniques to model and optimise the structure of the processes, and perform Heat Integration including the use of multi-effect distillation columns and integrated water networks, to show that energy efficiency and water consumption in bioethanol plants can be significantly improved. Later, Čuček *et al.* (2011) extended the scale of the optimisation to the simultaneous production of ethanol and food from the entire corn plant through energy, water and process technologies integration. The same school (Li *et al.*, 2011) approached the problem of simultaneous synthesis of the integrated separation network, where both mass and energy separating agents are taken into account, through a novel state-space superstructure with multi-stream mixings, capturing all possible network configurations.

George *et al.* (2011) proposed a mathematical optimisation approach for targeting the minimum utility consumption in heat-integrated process water networks. Heat Integration in fixed flow rate water allocation networks is addressed through LP models, for both single and multiple contaminants, incorporating isothermal mixing; non-isothermal mixing gives a discontinuous NLP model.

3.6 Optimisation of Integrated Processes

Applying the methodologies based upon mathematical modelling generally leads to non-convex NLP or non-convex MINLP problems. One way of optimising these models is to approximate them as convex NLP or MINLP problems, through a series of linear transformations. Then, traditional solvers proposed in commercial software are used. Another approach takes into account that, in order to obtain the global optimality of the non-convex NLP and MINLP problems, it is important to be able to obtain tight lower bounds on the variables as general equations obtained by physical inspection of the superstructure, and to incorporate the cut by Karuppiah and Grossmann (2006) to obtain tight lower bounds on the objective (Ahmetović and Grossmann, 2011). Excellent sources of information regarding the optimisation of an integrated process are the textbook of Klemeš *et al.* (2010) and the reviews of Jeżowski (2010) and Morar and Agachi (2010).

Although they cannot guarantee global optimality, meaning the true optimum point, evolutionary algorithms are more and more used due to

© Woodhead Publishing Limited, 2013

their ability to avoid local traps when multimodal objective functions are used and their capacity to provide a sufficiently accurate global optimum. Mimicking the biological evolution, *the mono-objective GAs* were used by: Brand and Ostfeld (2011) for the optimal design of regional wastewater systems comprising transmission gravitational and pumping sewer pipelines, decentralised treatment plants and end users of reclaimed wastewater; Thunyawart *et al.* (2011) to develop a mass-exchange networks module for a minimum freshwater usage target; Gorji-Bandpy *et al.* (2011) for the optimisation of Heat Exchanger Networks, in tandem with Sequential Quadratic Programming; Lotfi and Boozarjomehry (2010) for the synthesis of HENS, based on *GAs* coupled with a commercial process simulator through the ActiveX capability of the simulator; and *the multi-objective GAs* were used by: Dogaru and Lavric (2012) for searching for the particular successions of topologies and operating conditions for a semicontinuous water network (batch with respect to the raw materials) that minimise both the freshwater consumption and the investment and operating costs; Hajabdollahi *et al.* (2011) for obtaining maximum exergy efficiency with minimum total annual cost per produced steam exergy; Tudor and Lavric (2011) for minimising fresh water consumption and operating costs of an integrated water/wastewater network; they both became the optimiser of choice.

Other evolutionary algorithms applied in PI optimisation are:

- The disjunctive-genetic programming (Odjo *et al.*, 2011).
- The elitist non-dominated sorting genetic algorithm with continuous and discrete variables (Hajabdollahi *et al.*, 2011).
- Simulated annealing, in conjunction or not with *GAs* – Athier *et al.* (1997) developed a two-level procedure for HEN Synthesis problems, related to structural optimisation; Yu *et al.* (2000) solved a large-scale system Energy Integration problem; Wei *et al.* (2004) applied it to the multi-stream HEN Synthesis, with non-linear constraints and a non-convex objective function; An and Yuan (2009) used it for synthesis of multi-component distillation systems.
- Particle swarm – Silva *et al.* (2010) determined the HEN that minimises the total annualised cost, accounting for capital costs of heat exchangers and the energy costs for utilities and pumping duties; Luo and Yuan (2008) minimised the total cost of fresh water and wastewater treatment of an integrated water system, where water-using processes and water-treatment operations are combined into a single network; Tan *et al.* (2008) designed industrial material reuse/recycle networks using a zero-one programming or 'knapsack' formulation; Seingheng *et al.* (2007) solved the problem of water network synthesis by considering physical

© Woodhead Publishing Limited, 2013

stream properties such as pH or resistivity; Hul *et al.* (2007) solved MINLP models for water network synthesis using a mutation-enhanced particle swarm algorithm.

- Ant colony – Schluter *et al.* (2009) presented an extension of the ant colony optimisation metaheuristic, in order to solve the problem of integrated process and control system design, which is frequently non-convex and, therefore, local optimisation techniques usually fail to locate the global solution; Maier *et al.* (2003) used this technique for the optimal design of water distribution systems, showing that it outperformed *GAs* for the case studies considered, both in terms of computational efficiency and ability to find near global optimal solutions.
- Shuffled frog leaping algorithm – Chung and Lansey (2009) minimised the total system cost of a general large-scale water supply system model, consisting of networks of pipes, canals and storage and treatment facilities that collect, treat, store and distribute water to consumers; Eusuff and Lansey (2003) used it to solve discrete optimisation problems such as optimal pipe sizes for new pipe networks and for network expansions.
- Multi-objective evolutionary strategy – Girardin *et al.* (2009) integrate steam cycles in the power plant industry, using PI techniques and a multi-objective optimisation procedure to generate optimal steam cycle configurations ordered by complexity-cost and efficiency, aiming to optimise the conversion of the available heat into mechanical power; Bolliger *et al.* (2005) optimised power plant designs using a thermodynamic model for the energy flows of the energy conversion units, a special steam cycle model to represent all the possible heat exchange interactions and to compute the optimal flow rates in the system with a minimum of structural information.
- Fuzzy optimisation – is one of the newest approaches, promoted especially by the school of Tan (more than ten papers and communications already published), from the early attempts to minimise the utility water consumption and effluent generation of process plants through the implementation of reuse or recycle networks (Tan and Cruz, 2004), to the use of energy-based fuzzy optimisation approach for water reuse in an eco-industrial park (Taskhiri *et al.*, 2011), or to Water Footprint constraints optimisation of eco-industrial supply chains (Aviso *et al.*, 2011a), or even to the optimisation of topologically constrained eco-industrial resource conservation networks with incomplete information (Aviso *et al.*, 2011b).

Poplewski *et al.* (2011) used as an optimiser the adaptive random search method, a precursor of evolutionary algorithms, which descends rather from the direct search algorithms, with shrinking radius and random search discs.

© Woodhead Publishing Limited, 2013

3.6.1 Objective Functions Shape Topology

The process-related objective functions used to integrate a process, considering or not its control structure during this process, could be split into two main categories: direct and indirect.

Direct process-related objective functions embed any of the variables governing the process, expressed either in its measuring units, or in a normalised form implying a reference value. Pumping power (kW), heat reused internally (kJ), utility consumption (t/h for material, kW for power or kJ for heat/energy) and length of the active piping system (km) are several examples which help in clarifying the ideas. Another direct process-related objective functions are thermodynamic in nature, generated like entropy (kJ/K) or lost exergy (kJ). Although these latter are more difficult to compute, they could reveal important insights as to where the flaws of the process are, and hints about the strategy to adopt in removing these flaws. The very important characteristic of any direct process-related objective function is that the topology and the related operating conditions resulting from an optimisation process are time independent, unless some technological improvements are introduced, when a retrofit could be envisaged.

The indirect process-related objective functions are cost based, thus the topology and operating conditions they lead to through optimisation are heavily time dependent, being affected by the current market prices. The effects are two-fold:

(a) The use of direct or indirect process-related objective functions generally leads not only to different results, with respect to the optimised topology and operating conditions, but also to different degrees of fulfilment of the intended goal.
(b) The retrofit of the cost optimised process should be done every time the markets' costs embedded in the objective function change significantly.

As an example which illustrates the former effect, if the goal is greenhouse gas reduction but the market value of the product is high enough, the optimisation result could advocate the acceptance of larger emissions, despite the penalty fees incurred, against a slight decrease in production. When the competition brings down the product market value, the penalty fees could become unbearable, rendering the process prone to retrofit. This is not the case when the pollutant gas flow rate is directly used as an objective function to be minimised; unless there are major technological breakthroughs, the process ensuring the minimum greenhouse gas emissions will not be retrofitted.

© Woodhead Publishing Limited, 2013

The same process, abstracted into a mathematical model, could be subjected to optimisation using different objective functions and, regardless of whether they are direct or indirect process related, the results could differ, especially when there is a pronounced dichotomy between them. A way of solving this problem is to aggregate them into a single objective function, weighting their contribution according to some previous knowledge. This is a rather subjective solution, since choosing the particular weights is a matter of personal experience and knowledge. A better alternative is the multi-objective Pareto optimisation approach, as the way of having a set of equally optimal solutions, to choose from using hardly quantifiable criteria.

3.7 Controllability of Integrated Processes

The tendency of integrating as much as possible the industrial processes, beginning with the reaction-separation subsystems and ending with Total Site or eco-industrial parks, renders them more difficult to control (Fig. 3.1). This is because, on the one hand, the degrees of freedom diminish severely, and, on the other, the number of multiple interconnections between non-linear processes increases, altering profoundly the time-scales (Morud and Skogestad, 1996) and thus the plantwide process dynamics (Yuan *et al.*, 2012). According to Morud and Skogestad (1996), an interconnection, whether it be internal or external, can be classified as either: (a) feedback – any secondary effect that modifies the original dynamic, (b) feedforward (parallel paths) – any system where an input affects an output through several independent subsystems or mechanisms, and (c) series – the output of one subsystem is the input to the next (no feedback between subsystems). Any feedback, such as mass and/or energy recycle, disturbs the poles and thus possibly the plant stability, whereas any feedforward changes the zeros and thus the achievable performance of the plant under feedback control. These, in turn, could give rise to instability or oscillatory behaviour (limit cycles), even when the individual processing units are stable by themselves (Marquardt and Mönnigmann, 2005). Recognising as early as possible the inherent characteristics that can jeopardise both process behaviour and controllability becomes a must to guarantee it remains robust and safe, without compromising its profitability (Yuan *et al.*, 2011).

A process is plantwide controllable if there is a plantwide control system, as given by the set of the controlled variable set-points, so that a steady state is feasible for all allowable values of system parameters and disturbances. This means that all of the energy and material balances are satisfied under the process constraints (Chodavarapu and Zheng, 2002).

There are two main design methods for improving the controllability characteristics of a process: the optimisation-based method, including here the robust control, and the controllability indices-based anticipating sequential

© Woodhead Publishing Limited, 2013

method. Both types are reviewed by Yuan *et al.* (2011), who discussed their advantages and disadvantages. Rojas *et al.* (2009) advocate the use of the dissipativity of each process unit and the topology of the process network to assess the plantwide operability, solving numerically the associated dynamic performance optimisation problem. The topology of the process network can be modelled efficiently with a suitable interaction matrix, although Marquardt and Mönnigmann (2005) argue that using it complicates the study. To ease the analysis, a hierarchical approach is recommended. In order to quantify the performance of a dynamic system, Rico-Ramirez *et al.* (2010) recommend Fisher information not only as a measure of the degree of variability of a dynamic system, but also as source of useful insights with potential application in process control; Fisher information could be seen as a controller tuning criterion.

Although very important, few papers have been devoted to controllability analysis of the energy/heat and/or material integrated networks, under its various aspects. The former class of problems is illustrated by Li and Chang (2011), who proposed a systematic flexibility assessment procedure to analyse and modify a given network so as to achieve the desired level of operational resiliency, and by Young *et al.* (2006) who proposed a methodology for the design of heat-integrated chemical processes, particularly HENs, where controllability and energy recovery are both balanced during the design synthesis stage. The latter class of problems had been followed by Feng *et al.* (2011b), who presented a methodology for a water allocation network design with process disturbance taken into account; the synthesised network structure can guarantee that the water system consumes minimum freshwater under both normal and disturbance conditions and with the minimum number of control streams under disturbance, and also, by Li and Chang (2011) who proposed a systematic flexibility assessment procedure to analyse and modify a given network so as to achieve the desired level of operational resiliency.

Due to the complexity of heat-integrated passive or reactive distillation columns, their sustainability analysis is the subject of several distinct papers – Vazquez-Ojeda *et al.* (2011) observed that the energy requirements and the total annual cost of the complex distillation sequences with a minimum number of reboilers are reduced significantly in comparison with the conventional reactive distillation process and can be also achieved without significant control problems; Zhang *et al.* (2011c) demonstrated that the asymmetrical configuration should generally be favoured over the symmetrical for the development of the externally heat-integrated double distillation columns; Zhu *et al.* (2009) have shown that strengthening internal Heat Integration within a reactive distillation column involving reactions with high thermal effect is really effective for the reduction of utility consumption and capital investment, besides the improvement in process dynamics

© Woodhead Publishing Limited, 2013

and operation; moreover, a favourable effect is again observed upon the process dynamics and operability; Kaymak and Luyben (2006) explored the effectiveness of the two-temperature control structure to quantify the impact of design on controllability, and found that the locations of the temperature control trays should be made such that the two temperature controllers both have direct action (an increase in temperature increases feed), which requires negative open-loop process gains for both loops; Meeuse and Grievink (2002) have shown how non-equilibrium thermodynamics can be used to include controllability in the synthesis phase, addressing both lumped and approach systems.

The flexibility/resiliency of networks should be addressed in more depth, searching for criteria motivating when and how a topological network change would be beneficial, and not only some change in parameters (Jeżowski, 2010).

Brendel and Dhurjati (2010) developed a simple transfer function-based method to compare the dynamic behaviour of candidate heat-integrated flowsheets, which allows for identification of dynamic characteristics ignored by the steady-state analysis alone. The heat-integrated process dynamics is represented as two separate interacting sections, making the analysis easier in the early design stage. The process decomposition is logical in that it follows the typical work sequence of process design steps. The block-diagram format makes apparent the source of positive feedback that can result from adding Heat Integration to a process.

Yan *et al.* (2006) approached the process controllability analysis during the process synthesis phase of Heat Integration systems, to avoid choosing designs with poor structural controllability. Their systematic process synthesis methodology involved utilisation of system disturbance propagation models, synthesising cost-effective and highly controllable HENs.

Westphalen *et al.* (2003) propose an index as a measure of HEN controllability, which can be used during the conceptual design stage of a chemical process to avoid obtaining process structures that are difficult to control. At the same time, the controllability index easily identifies the trade-offs between controllability and Heat Integration.

The design of water networks generally assume that process data are fixed and well-defined (Tan *et al.*, 2007a), although the actual water flow rates, concentrations and/or mass loads may fluctuate over time. These fluctuations in processing conditions can lead to process disruptions and product-quality problems. Tan *et al.* (2007a) made use of Monte Carlo simulations to emphasise the vulnerability of water networks to noisy mass loads, chosen since they tend to have greater variability than stream flow rates, which can be controlled with pumps and valves. The methodology allows the designer to select a network configuration with the lowest probability of failure.

© Woodhead Publishing Limited, 2013

The non-linear analysis of large-scale waste water-treatment plants (WWTPs), together with the controllability implications, was done by Flores-Tlacuahuac *et al.* (2009), motivated by the strong interactions among the main processing variables – highly non-linear kinetic relationships and positive feedback induced by activated sludge recycle. Bifurcation analysis was used to emphasise the complex interactions among potential controlled, manipulated and disturbance variables, showing that non-linear behaviour was only present when considering disturbances in the main flow rate of the polluted stream. Consequently, WWTPs could be properly controlled with simple proportional, integral and derivative controllers making probably unnecessary the use of advanced control systems.

A systematic approach to the synthesis of highly controllable mass-exchange networks was proposed by Shoaib (2011), to avoid propagation of severe disturbances of concentration or mass flow rate of an inlet stream to the outlet streams. The approach is based upon four heuristics: (i) if the high-disturbance rich/lean stream is matched with a lean/rich stream with high control precision, then the former stream must be split, (ii) if the load of the rich/lean stream cannot be ticked off with any of the lean/rich streams Above or Below the Pinch, then the former stream must be split, (iii) when a rich/lean stream is split Above or Below the Pinch, then one of the matches must tick off the part of lean/rich streams Above or Below the Pinch, and (iv) if the high-disturbance propagation rich/lean stream is not split, then it must be matched with lower-level control precision lean/rich stream that it is preferred to be split.

3.7.1 Process Integration and Control

Although recognised as a better approach than the sequential methodology consisting of initial process design based on steady-state economic calculations followed by the synthesis of a control strategy that is generally based on heuristic controllability measures, simultaneous Process Integration and control lagged behind due to mainly the lack of adequate mathematical tools (Dimian, 2003), solving strategies and computational power (Dimian and Bildea, 2008). As these tools developed, the simultaneous approach starts showing its merits, as shown in the review of Ricardez-Sandoval *et al.* (2009), i.e. the controller and the system's design parameters are optimised together, addressing the trade-offs between conflicting design and control objectives.

Some methods are based on controllability indices such as the relative gain array, the condition number, the disturbance condition number and the integral error criterion, used to quantify the process dynamic performance. The controllability of the closed loop is estimated using either steady-state

© Woodhead Publishing Limited, 2013

or linear dynamic models, thus limiting the applicability of these calculations to a small neighbourhood of a nominal steady state. Even more, the use of controllability indices which cannot be directly correlated to the economics of the process, combined with the assumptions of linearity, may result in suboptimal solutions (Ricardez-Sandoval *et al.*, 2010).

A better approach is based upon dynamic optimisation, which captures the evaluation of the variability by means of simulations based on the full non-linear dynamic model of the process. Thus, it is possible to identify the worst-case scenario, when the largest process output variability is obtained for a given set of nominal operating conditions. There are several drawbacks: the computational complexity, the unclear relationship between variability and the overall cost function, as for the case of capital and operating cost, and the lack of regard for system stability, and consequently some designs could be unstable (Ricardez-Sandoval *et al.*, 2009). Ricardez-Sandoval *et al.* (2010) came with a structured singular value norm calculation to estimate the worst-case disturbance profile, used to simulate the closed-loop non-linear dynamic process model for obtaining the worst-case output variability and to test the process feasibility constraints. In order to guarantee that the final design is stable, a stability test is included in the analysis. Instead of variability, Malcolm *et al.* (2007) promote the use of dynamic flexibility analysis for integrating system's design and control. A two-stage problem decomposition leading to a massive reduction of problem size and complexity is presented as a novel embedded control, which is expected to have a broad impact on high-performance systems operating close to their limits. Patel *et al.* (2008) present a bi-level dynamic optimisation approach to achieving integration of process design and control. First, an optimal controller (a modified linear quadratic regulator) is used to evaluate the best achievable control performance for each candidate flowsheet. Then the process superstructure can be augmented with the closed-loop system, thus enabling consideration of both cost and controllability in design. In order to ease the solving strategy of the complex problem of simultaneously designing an integrated process and its control system, which is frequently non-convex, an extended ant-colony optimisation algorithm was proposed by Schluter *et al.* (2009), as a global optimisation algorithm capable of solving this challenging class of problems in an efficient and robust way. The aim is to simultaneously find the static variables of the process design as well as the operating conditions and the controllers' parameters which optimise a combined measure of the plant economics and its controllability, subject to a set of constraints which ensure appropriate dynamic behaviour and process specifications. Hamid *et al.* (2010) present a methodology that makes use of thermodynamic-process insights, to identify a bounded search space, and the reverse design approach to arrive at the final simultaneous

© Woodhead Publishing Limited, 2013

process-controller design. The optimisation problem is decomposed into four sub-problems: (i) pre-analysis – the concepts of attainable region (AR) and driving force (DF) are used to locate the optimal process controller design solution, (ii) design analysis, (iii) controller-design analysis, and (iv) final selection and verification. The final design is verified through rigorous simulation.

Zhang *et al.* (2010) developed a plantwide control structure for the ammonia synthesis process using the integrated framework of simulation and heuristics, which is then compared with the results obtained using the self-optimising control procedure.

Dynamic optimisation problems are difficult to solve, so robust control analysis tools are proposed instead, which lead a non-linear optimisation model that is significantly easier to solve. This is an extension of the problem of finding the robust control for the safest trajectory of a process between two steady states (Marquardt and Mönnigmann, 2005). The optimal design provides a feasible asymptotically stable design against any amplitude-bounded external perturbations and/or process parametric uncertainty, while meeting the proposed process production and operational constraints (Ricardez-Sandoval *et al.*, 2009). These bounds, accounted for through their maximal magnitude, are calculated based on linear models with uncertainty and therefore do not require the use of the full non-linear dynamic model of the system. This is also the drawback of the approach, since it produces potentially conservative and suboptimal designs as compared to dynamic optimisation-based methodologies. Marquardt and Mönnigmann (2005) introduced the concept of the critical manifold that separates regions of the design space with desired process behaviour from those with undesired process behaviour, permitting a unifying approach to robust stability and feasibility. Stability is acknowledged during the process design stage, which thus accounts for uncertainty. As the new approach allows optimisation of a process model with respect to a profit function and to simultaneously take constraints on the dynamics into account, it is ideally suited for the integration of design and control.

A generic class of integrated networks with significant energy flows which generate multi-time-scale dynamic analysed by Jogwar *et al.* (2010), is a generalisation of a previous study (Jogwar *et al.*, 2008). Such networks encompass individual units with fast dynamics embedded in the entire network, which is characterised by slow dynamics. Jogwar *et al.* (2010) advocate that tight Energy Integration and the presence of significant energy flows can facilitate, rather than hinder, control structure design and performance. Consequently, a hierarchical control approach is proposed: fast, distributed control for the individual units and non-linear supervisory control for the entire network.

© Woodhead Publishing Limited, 2013

3.8 Process Integration under Disturbances

When integrating into the process design the control network as well, the tractability of the problem worsens, and the result cannot be as robust as intended. To gain in robustness, while still keeping the problem at hand sufficiently simple, a special type of Process Integration has been developed, during which the disturbances are accounted for. This approach is based upon the known distribution of disturbances, which permits design of the integrated process under nominal and worst-case scenarios and deciding how the nominal topology and/or operating parameters should be modified in order to cope with the latter case, obtaining a resilient integrated process. Another purpose of analysing the integrated process under disturbance is to emphasise its complex dynamic behaviour under the effect of the main disturbances and to develop an optimal advanced control scheme.

HEN Targeting, when stream heat capacity flow rates are affected by stochastic disturbances within given ranges, was approached by Jezowski *et al.* (2000). A rigorous approach, based on recursive solution of an MILP model, has been developed for calculating all feasible locations of Pinches that can occur in the minimum utility cost of HENs operating under disturbances.

The problem of endowing a HEN consuming minimum total utility with a desired operational flexibility was solved by Konukman *et al.* (2002) via a non-iterative, superstructure-based, simultaneous-MILP formulation, assuming that the feasible region in the space of uncertain input parameters is convex. When the target-flexibility value is set to zero, the optimal HEN is the same as predicted by Pinch Analysis, under the constraint of minimum total utility consumption. The same problem of providing a HEN with flexibility from the synthesis stage is dealt with by Chen and Hung (2004), considering that specified uncertainties in the source-stream temperatures and flow rates are present. First, a HEN topology is designed under minimum total annual cost constraint. Then, a flexibility analysis is performed for the full disturbance range to test the feasibility of this network. Afterwards, the exclusion of those networks not passing the flexibility analysis is done, thus narrowing the search space used for further HEN Synthesis.

The implementation of a model predictive control using the complex dynamic behaviour of the heat-integrated plant under the effect of the main disturbances is analysed by Iancu and Agachi (2010), aiming at the improvement of plant safety in operation and the increase of product quality. The implemented MPC strategy focused on the response of the heat-integrated process in terms of operation, product quality and cost reduction of the heat-integrated plant.

The modelling methodology for characterising disturbance propagation and predicting the worst scenario to occur in a MEN during synthesis was proposed by Yan and Huang (2002), together with a model-based

© Woodhead Publishing Limited, 2013

design procedure for optimally placing recycles for disturbance rejection. Dumping/rejecting disturbances by recycles optimally placed represent a helpful Process Integration technique for designing cost-effective and highly controllable integrated process systems.

Tan (2011) presents a fuzzy mathematical programming model for the synthesis of water networks when the model parameters exhibit fuzzy uncertainties in order to design and install a water network for the optimal reuse, recycle and regeneration of water streams within a process plant or an eco-industrial park, balancing the risks associated with process data uncertainties. The parametric uncertainties regard the quality level of source streams, the quality tolerances of stream sinks and in all the stream flowrates.

Li and Chang (2011) developed a NLP flexibility index for single-contaminant water networks, using a single critical point instead of the entire region of uncertain parameters, thus ensuring a faster convergence rate for the iterative optimisation process. A systematic flexibility assessment procedure permits the analysis of a given network and emphasises the modifications needed to achieve the desired level of operational resiliency; namely, either to relax the upper limit of freshwater capacity, or to add new pipelines and/or remove existing ones.

3.9 References

Ahmetović, E., Grossmann, I. E. (2011). Global superstructure optimization for the design of integrated process water networks. *AIChE Journal,* **57**, 434–457.

Alhammadi, H., Barton, G. W., Romagnoli, J. A., Alexander, B. (2002). An integrated framework for multi-objective optimisation in process synthesis and design. *Computer-Aided Chemical Engineering,* **10**, 817–822.

Alva-Argaez, A., Savulescu, L. (2009). Water Reuse Project Selection: A retrofit path to water and energy savings. *Chemical Engineering Transactions*, **18**, 403–408.

An, W.-Z., Yuan, X.-G. (2009). A simulated annealing-based approach to the optimal synthesis of heat-integrated distillation sequences. *Computers & Chemical Engineering*, **33**, 199–212.

Antonio Quijera, J., Gonzalez Alriols, M., Labidi, J. (2011). Integration of a solar thermal system in a dairy process. *Renewable Energy*, **36**, 1843–1853.

Athier, G., Floquet, P., Pibouleau, L., Domenech, S. (1997). Synthesis of heat-exchanger network by simulated annealing and NLP procedures. *AIChE Journal*, **43**, 3007–3020.

Atkins, M. J., Walmsley, M. R. W., Morrison, A. S. (2010). Integration of solar thermal for improved energy efficiency in low-temperature-pinch industrial processes. *Energy*, **35**, 1867–1873.

Atuonwu, J. C., Van Straten, G., Van Deventer, H. C., Van Boxtel, A. J. B. (2011). Improving adsorption dryer energy efficiency by simultaneous optimization and heat integration. *Drying Technology*, **29**, 1459–1471.

© Woodhead Publishing Limited, 2013

Aviso, K. B., Tan, R. R., Culaba, A. B., Cruz, J. B. (2011a). Fuzzy input–output model for optimizing eco-industrial supply chains under water footprint constraints. *Journal of Cleaner Production*, **19**, 187–196.

Aviso, K. B., Tan, R. R., Culaba, A. B., Foo, D. C. Y., Hallale, N. (2011b). Fuzzy optimization of topologically constrained eco-industrial resource conservation networks with incomplete information. *Engineering Optimization*, **43**, 257–279.

Bai, J., Feng, X., Deng, C. (2010). Optimal design of single-contaminant regeneration reuse water networks with process decomposition. *AIChE Journal*, **56**, 915–929.

Bakhtiari, B., Fradette, L., Legros, R., Paris, J. (2010). Retrofit of absorption heat pumps into manufacturing processes: implementation guidelines. *Canadian Journal of Chemical Engineering*, **88**, 839–848.

Baliban, R. C., Elia, J. A., Floudas, C. A. (2011). Optimization framework for the simultaneous process synthesis, heat and power integration of a thermochemical hybrid biomass, coal, and natural gas facility. *Computers & Chemical Engineering*, **35**, 1647–1690.

Baliban, R. C., Elia, J. A., Floudas, C. A. (2012). Simultaneous process synthesis, heat, power, and water integration of thermochemical hybrid biomass, coal, and natural gas facilities. *Computers & Chemical Engineering*, **37**, 297–327.

Bandyopadhyay, S., Sahu, G. C. (2011). Energy targeting in heat integrated water networks with isothermal mixing. *Computer-Aided Chemical Engineering*, **29**, 1989–1993.

Bealing, C., Hutton, D. (2002). Hydrogen-pinch analysis. *Chemical Engineering*, **109**, 56–61.

Becker, H., Girardin, L., Marechal, F. (2010). Energy integration of industrial sites with heat exchange restrictions. *Computer-Aided Chemical Engineering*, 28, 1141–1146.

Beninca, M., Trierweiler, J. O., Secchi, A. R. (2011). Heat integration of an olefins plant: pinch analysis and mathematical optimization working together. *Brazilian Journal of Chemical Engineering*, **28**, 101–116.

Biegler, L. T., Grossmann, I. E., Westerberg, A. W. (1997) *Systematic Methods of Chemical Process Design.* Prentice Hall, New York, USA.

Boix, M., Montastruc, L., Pibouleau, L., Azzaro-Pantel, C., Domenech, S. (2012a). Industrial water management by multiobjective optimization: from individual to collective solution through eco-industrial parks. *Journal of Cleaner Production*, **22**, 85–97.

Boix, M., Pibouleau, L., Montastruc, L., Azzaro-Pantel, C., Domenech, S. (2012b). Minimizing water and energy consumptions in water and heat exchange networks. *Applied Thermal Engineering*, **36**, 442–455.

Bolliger, R., Marechal, F., Favrat, D. (2005). Advanced power plant design methodology using process integration and multi-objective thermo-economic optimisation. In: Kjelstrup, S., Hustad, J. E., Gundersen, T., Rosjorde, A., Tsatsaronis, G. (eds.) *Proceedings of ECOS 2005, Vols 1–3: Shaping Our Future Energy Systems*, ECOS 2005, June 20–22, 2005, Trondheim, Norway, vol. **2**, pp. 777–784.

Brand, N., Ostfeld, A. (2011). Optimal design of regional wastewater pipelines and treatment plant systems. *Water Environment Research*, **83**, 53–64.

© Woodhead Publishing Limited, 2013

Brendel, R. J., Dhurjati, P. S. (2010). Design methodology for screening dynamic characteristics of candidate heat-integrated flowsheets. *Industrial & Engineering Chemistry Research*, **49**, 9877–9886.

Cano-Ruiz, J. A., Mcrae, G. J. (1998). Environmentally conscious chemical process design. *Annual Review of Energy and the Environment*, **23**, 499–536.

Cecelja, F., Kokossis, A., Du, D. (2011). Integration of ontology and knowledge-based optimization in process synthesis applications. *Computer-Aided Chemical Engineering*, **29**, 427–431.

Chen, C.-L., Lee, J.-Y., Denny Kok Sum, N., Foo, D. C. Y. (2011). Synthesis of property-based resource conservation network in palm oil mills with time-varying process disturbance. *Clean Technologies and Environmental Policy*, **13**, 625–632.

Chen, C.-L., Lee, J.-Y., Ng, D. K. S., Foo, D. C. Y. (2010). A Unified Model of Property Integration for Batch and Continuous Processes. *AIChE Journal*, **56**, 1845–1858.

Chen, C. L., Hung, P. S. (2004). Simultaneous synthesis of flexible heat-exchange networks with uncertain source-stream temperatures and flow rates. *Industrial & Engineering Chemistry Research*, **43**, 5916–5928.

Chen, C. L., Hung, P. S. (2005). Retrofit of mass-exchange networks with superstructure-based MINLP formulation. *Industrial & Engineering Chemistry Research*, **44**, 7189–7199.

Chodavarapu, S. K., Zheng, A. (2002). A definition of steady-state plantwide controllability. *Industrial & Engineering Chemistry Research*, **41**, 4338–4345.

Chung, G. H., Lansey, K. (2009). Application of the shuffled frog leaping algorithm for the optimization of a general large-scale water supply system. *Water Resources Management*, **23**, 797–823.

Coletti, F., Macchietto, S., Polley, G. T. (2010). Effects of fouling on performance of retrofitted heat exchanger networks: a thermo-hydraulic based analysis. *Computer-Aided Chemical Engineering*, **28**, 19–24.

Crilly, D., Zhelev, T. (2010). Further emissions and energy targeting: an application of CO_2 emissions pinch analysis to the Irish electricity generation sector. *Clean Technologies and Environmental Policy*, **12**, 177–189.

Čuček, L., Martин, M., Grossmann, I. E., Kravanja, Z. (2011). Energy, water and process technologies integration for the simultaneous production of ethanol and food from the entire corn plant. *Computers & Chemical Engineering*, **35**, 1547–1557.

Dantus, M. M., High, K. A. (1996). Economic evaluation for the retrofit of chemical processes through waste minimization and process integration. *Industrial & Engineering Chemistry Research*, **35**, 4566–4578.

Deng, C., Feng, X., Ng, D. K. S., Foo, D. C. Y. (2011). Process-based graphical approach for simultaneous targeting and design of water network. *AIChE Journal*, **57**, 3085–3104.

Dias, M. O. S., Modesto, M., Ensinas, A. V., Nebra, S. A., Maciel Filho, R., Rossell, C. E. V. (2011). Improving bioethanol production from sugarcane: evaluation of distillation, thermal integration and cogeneration systems. *Energy*, **36**, 3691–3703.

Dimian, A. (2003). *Integrated Design and Simulation of Chemical Processes.* Elsevier, Amsterdam, The Netherlands.

Dimian, A., Bildea, C. S. (2008). *Chemical Process Design.* Wiley-VCH Verlag GmbH & Co. KgaA, Weinheim, Germany.

© Woodhead Publishing Limited, 2013

Dogaru, E.-L., Lavric, V. (2011). Dynamic water network topology optimization of batch processes. *Industrial & Engineering Chemistry Research*, **50**, 3636–3652.

Dogaru, E. L., Lavric, V. (2012). Pareto approach in designing optimal semicontinuous water networks. *Industrial & Engineering Chemistry Research*, **51**, 6116–6136.

Domenichini, R., Gallio, M., Lazzaretto, A. (2010). Combined production of hydrogen and power from heavy oil gasification: pinch analysis, thermodynamic and economic evaluations. *Energy*, **35**, 2184–2193.

Douglas, J. M. (1988). *Conceptual Design of Chemical Processes.* McGraw-Hill, New York, USA.

Drobez, R., Pintaric, Z. N., Pahor, B., Kravanja, Z. (2011). Simultaneous heat integration and the synthesis of biogas processes from animal waste. *Asia-Pacific Journal of Chemical Engineering*, **6**, 734–749.

El-Halwagi, M. (1997). *Pollution Prevention through Process Integration.* Academic Press, Amsterdam, The Netherlands.

El-Halwagi, M. M., Glasgow, I. M., Qin, X. Y., Eden, M. R. (2004). Property integration: componentless design techniques and visualization tools. *AIChE Journal*, **50**, 1854–1869.

Enriquez, A. H., Tanco, M., Kim, J. K. (2011). Simulation-based process design and integration for the sustainable retrofit of chemical processes. *Industrial & Engineering Chemistry Research*, **50**, 12067–12079.

Eusuff, M. M., Lansey, K. E. (2003). Optimization of water distribution network design using the shuffled frog leaping algorithm. *Journal of Water Resources Planning and Management-Asce*, **129**, 210–225.

Faria, D. B. C., Bagajewicz, M. J. (2011). Planning model for the design and/or retrofit of industrial water systems. *Industrial & Engineering Chemistry Research*, **50**, 3788–3797.

Feng, X., Pu, J., Yang, J., Chu, K. H. (2011a). Energy recovery in petrochemical complexes through heat integration retrofit analysis. *Applied Energy*, **88**, 1965–1982.

Feng, X., Shen, R., Zheng, X., Lu, C. (2011b). Water allocation network design concerning process disturbance. *Industrial & Engineering Chemistry Research*, **50**, 3675–3685.

Flores-Tlacuahuac, A., Esparza, M. H. N., LyPez-Negrete De La Fuente, R. (2009). Bifurcation behavior of a large scale waste water treatment plant. *Industrial and Engineering Chemistry Research*, **48**, 2605–2615.

Foo, D. C. Y. (2009). State-of-the-art review of pinch analysis techniques for water network synthesis. *Industrial & Engineering Chemistry Research*, **48**, 5125–5159.

Foo, D. C. Y. (2010). Automated targeting technique for batch process integration. *Industrial & Engineering Chemistry Research*, **49**, 9899–9916.

Foo, D. C. Y., Chew, Y. H., Lee, C. T. (2008). Minimum units targeting and network evolution for batch heat exchanger network. *Applied Thermal Engineering*, **28**, 2089–2099.

Foo, D. C. Y., Kazantzi, V., El-Halwagi, M. M., Manan, Z. A. (2006). Surplus diagram and cascade analysis technique for targeting property-based material reuse network. *Chemical Engineering Science*, **61**, 2626–2642.

Friedler, F. (2010). Process integration, modelling and optimisation for energy saving and pollution reduction. *Applied Thermal Engineering*, **30**, 2270–2280.

© Woodhead Publishing Limited, 2013

Fu, C., Gundersen, T. (2010). Heat Integration of an oxy-combustion process for coal-fired power plants with CO(2) capture by pinch analysis. *Chemical Engineering Transactions*, **21**, 181–186.

Galvez, E. D., Mellado, M. E., Patino, P. S., Ossandon, K. L., Cisternas, L. C. (2011). Grey heat integration. *Revista Mexicana De Ingenieria Quimica*, **10**, 521–528.

Gassner, M., Vogel, F., Heyen, G., Maréchal, F. (2011). Optimal process design for the polygeneration of SNG, power and heat by hydrothermal gasification of waste biomass: thermo-economic process modelling and integration. *Energy & Environmental Science*, **4**, 1726–1741.

George, J., Sahu, G. C., Bandyopadhyay, S. (2011). Heat integration in process water networks. *Industrial & Engineering Chemistry Research*, **50**, 3695–3704.

Girardin, L., Bolliger, R., Marechal, F. (2009). On the use of process integration techniques to generate optimal steam cycle configurations for the power plant industry. *Chemical Engineering Transactions*, **18**, 171–176.

Gorji-Bandpy, M., Yahyazadeh-Jelodar, H., Khalili, M. (2011). Optimization of heat exchanger network. *Applied Thermal Engineering*, **31**, 779–784.

Gouws, J. F., Majozi, T., Foo, D. C. Y., Chen, C.-L., Lee, J.-Y. (2010). Water minimization techniques for batch processes. *Industrial & Engineering Chemistry Research*, **49**, 8877–8893.

Grooms, D., Kazantzi, V., El-Halwagi, M. (2005). Optimal synthesis and scheduling of hybrid dynamic/steady-state property integration networks. *Computers & Chemical Engineering*, **29**, 2318–2325.

Grossmann, I. E., Daichendt, M. M. (1996). New trends in optimization-based approaches to process synthesis. *Computers & Chemical Engineering*, **20**, 665–683.

Grossmann, I. E., Hooker, J. (2000). Logic based approaches for mixed integer programming models and their application in process synthesis. In: Malone, M. F., Trainham, J. A. (eds.) *Fifth International Conference on Foundations of Computer-Aided Process Design*, AICHE Symposium Series, 96 No. 323, pp. 70–83.

Grossmann, I. E., Martín, M. (2010). Energy and water optimization in biofuel plants. *Chinese Journal of Chemical Engineering*, **18**, 914–922.

Grossmann, L. E., Westerberg, A. W. (2000). Research challenges in process systems engineering. *AIChE Journal*, **46**, 1700–1703.

Hajabdollahi, H., Ahmadi, P., Dincer, I. (2011). An exergy-based multi-objective optimization of a heat recovery steam generator (HRSG) in a combined cycle power plant (CCPP) using evolutionary algorithm. *International Journal of Green Energy*, **8**, 44–64.

Hamid, M. K. A., Sin, G., Gani, R. (2010). Integration of process design and controller design for chemical processes using model-based methodology. *Computers & Chemical Engineering*, **34**, 683–699.

Handani, Z. B., Alwi, S. R. W., Hashim, H., Manan, Z. A. (2010). Holistic approach for design of minimum water networks using the mixed integer linear programming (MILP) technique. *Industrial & Engineering Chemistry Research*, **49**, 5742–5751.

Handani, Z. B., Alwi, S. R. W., Hashim, H., Manan, Z. A., Abdullah, S. H. Y. S. (2011). Optimal design of water networks involving multiple contaminants for global water operations. *Asia-Pacific Journal of Chemical Engineering*, **6**, 771–777.

© Woodhead Publishing Limited, 2013

Harmsen, G. J. (2004). Industrial best practices of conceptual process design. *Chemical Engineering and Processing*, **43**, 671–675.

Hossain, K. A., Khan, F. I., Hawboldt, K. (2008). Sustainable development of process facilities: state-of-the-art review of pollution prevention frameworks. *Journal of Hazardous Materials*, **150**, 4–20.

Hul, S., Tan, R. R., Auresenia, J., Fuchino, T., Foo, D. C. Y. (2007). Water network synthesis using mutation-enhanced particle swarm optimization. *Process Safety and Environmental Protection*, **85**, 507–514.

Iancu, M., Agachi, P. S. (2010). Optimal process control and operation of an industrial heat integrated fluid catalytic cracking plant using model predictive control. *Computer-Aided Chemical Engineering*, **28**, 505–510.

Iancu, P., Plesu, V., Lavric, V. (2009a). Regeneration of internal streams as an effective tool for wastewater network optimisation. *Computers & Chemical Engineering*, **33**, 731–742.

Iancu, P., Plesu, V., Lavric, V. (2009b). Waste water network retrofitting through optimal placement of regeneration unit. *Chemical Engineering Transactions*, **18**, 851–856.

Isafiade, A., Fraser, D. (2007). Optimization of combined heat and mass exchanger networks using pinch technology. *Asia-Pacific Journal of Chemical Engineering*, **2**, 554–565.

Jezowski, J. (2010). Review of water network design methods with literature annotations. *Industrial & Engineering Chemistry Research*, **49**, 4475–4516.

Jezowski, J., Bochenek, R., Jezowska, A. (2000). Pinch locations at heat capacity flow-rate disturbances of streams for minimum utility cost heat exchanger networks. *Applied Thermal Engineering*, **20**, 1481–1494.

Jiang, N., Bao, S., Gao, Z. (2011). Heat exchanger network integration using diverse pinch point and mathematical programming. *Chemical Engineering & Technology*, **34**, 985–990.

Jogwar, S. S., Baldea, M., Daoutidis, P. (2010). Tight energy integration: dynamic impact and control advantages. *Computers & Chemical Engineering*, **34**, 1457–1466.

Jogwar, S. S., Baldea, M., Daoutidis, P., IEEE (2008), 'Dynamics and control of reactor – feed effluent heat exchanger networks. *2008 American Control Conference, Vols* 1–12, Seattle, Washington, USA, June 11–13, pp. 1481–1486.

Karuppiah, R., Grossmann, I. E. (2006). Global optimization for the synthesis of integrated water systems in chemical processes. *Computers & Chemical Engineering*, **30**, 650–673.

Kaymak, D. B., Luyben, W. L. (2006). Evaluation of a two-temperature control structure for a two-reactant/two-product type of reactive distillation column. *Chemical Engineering Science*, **61**, 4432–4450.

Khalilpour, R., Abbas, A. (2011). HEN optimization for efficient retrofitting of coal-fired power plants with post-combustion carbon capture. *International Journal of Greenhouse Gas Control*, **5**, 189–199.

Kheireddine, H., Dadmohammadi, Y., Deng, C., Feng, X. A., El-Halwagi, M. (2011). Optimization of direct recycle networks with the simultaneous consideration of property, mass, and thermal effects. *Industrial & Engineering Chemistry Research*, **50**, 3754–3762.

© Woodhead Publishing Limited, 2013

Khor, C. S., Elkamel, A. (2010). Superstructure optimization for oil refinery design. *Petroleum Science and Technology*, **28**, 1457–1465.

Khor, C. S., Shah, N., Mahadzir, S., Elkamel, A. (2012). Optimisation of petroleum refinery water network systems retrofit incorporating reuse, regeneration and recycle strategies. *Canadian Journal of Chemical Engineering*, **90**, 137–143.

Kim, J.-K., Smith, R. (2003). Automated retrofit design of cooling-water systems. *AIChE Journal*, **49**, 1712–1730.

Kit, S. G., Alwi, S. R. W., Manan, Z. A. (2011). A new graphical approach for simultaneous targeting and design of a paper recycling network. *Asia-Pacific Journal of Chemical Engineering*, **6**, 778–786.

Klemeš, J. J., Friedler, F., Bulatov, I. S., Varbanov, P. S. (2010) *Sustainability in the Process Industry: Integration and Optimization.* McGraw Hill, New York, USA.

Konukman, A. E. S., Camurdan, M. C., Akman, U. (2002). Simultaneous flexibility targeting and synthesis of minimum-utility heat-exchanger networks with superstructure-based MILP formulation. *Chemical Engineering and Processing*, **41**, 501–518.

Kralj, A. K. (2010). Optimization of an industrial retrofitted heat exchanger network, using a stage-wise model. *Energy*, **35**, 4748–4753.

Labrador-Darder, C., Cecelja, F., Kokossis, A. C., Linke, P. (2009). Integration of superstructure-based optimization and semantic models for the synthesis of reactor networks. *Computer-Aided Chemical Engineering*, **26**, 865–870.

Lai, S. M., Hui, C. W. (2010). Integration of trigeneration system and thermal storage under demand uncertainties. *Applied Energy*, **87**, 2868–2880.

Lavric, V., Iancu, P., Plesu, V. (2004). Optimal water system topology through genetic algorithm under multiple contaminated-water sources constraint. *Computer-Aided Chemical Engineering*, **18**, 433–438.

Lavric, V., Iancu, P., Plesu, V. (2005). Genetic algorithm optimisation of water consumption and wastewater network topology. *Journal of Cleaner Production*, **13**, 1405–1415.

Li, B.-H., Chang, C.-T. (2010). Retrofitting heat exchanger networks based on simple pinch analysis. *Industrial & Engineering Chemistry Research*, **49**, 3967–3971.

Li, B.-H., Chang, C.-T. (2011). Efficient flexibility assessment procedure for water network designs. *Industrial & Engineering Chemistry Research*, **50**, 3763–3774.

Li, L.-J., Zhou, R.-J., Dong, H.-G. (2010). State-time-space superstructure-based minlp formulation for batch water-allocation network design. *Industrial & Engineering Chemistry Research*, **49**, 236–251.

Li, L.-J., Zhou, R.-J., Dong, H.-G., Grossmann, I. E. (2011). Separation network design with mass and energy separating agents. *Computers & Chemical Engineering*, **35**, 2005–2016.

Li, X., Kraslawski, A. (2004). Conceptual process synthesis: past and current trends. *Chemical Engineering and Processing: Process Intensification*, **43**, 583–594.

Li, Z. M. (2003). Pinch analysis of hydrogen system in refineries. *Computer-Aided Chemical Engineering*, **15**, 952–955.

© Woodhead Publishing Limited, 2013

Liang, C., Feng, X. (2011). Heat integration of a continuous reforming process. *Chemical Engineering Transactions*, **25**, 213–218.

Liao, Z.-W., Rong, G., Wang, J.-D., Yang, Y.-R. (2011a). Rigorous algorithmic targeting methods for hydrogen networks-Part I: systems with no hydrogen purification. *Chemical Engineering Science*, **66**, 813–820.

Liao, Z.-W., Rong, G., Wang, J.-D., Yang, Y.-R. (2011b). Rigorous algorithmic targeting methods for hydrogen networks-Part II: systems with one hydrogen purification unit. *Chemical Engineering Science*, **66**, 821–833.

Liao, Z., Rong, G., Wang, J., Yang, Y. (2011c). Systematic optimization of heat-integrated water allocation networks. *Industrial & Engineering Chemistry Research*, **50**, 6713–6727.

Linnhoff, B., Townsend, D. W., Boland, D., Hewitt, G. F., Thomas, B. E. A., Guy, A. R., Marsland, R. H. (1982). *A User Guide on Process Integration for the Efficient Use of Energy*. IChemE, Rugby, UK.

Liu, J. H., Fan, L. T., Seib, P., Friedler, F., Bertok, B. (2006). Holistic approach to process retrofitting: application to downstream process for biochemical production of organics. *Industrial & Engineering Chemistry Research*, **45**, 4200–4207.

Lotfi, R., Boozarjomehry, R. B. (2010). Superstructure optimization in heat exchanger network (HEN) synthesis using modular simulators and a genetic algorithm framework. *Industrial & Engineering Chemistry Research*, **49**, 4731–4737.

Luo, Y. Q., Yuan, X. G. (2008). Global optimization for the synthesis of integrated water systems with particle swarm optimization algorithm. *Chinese Journal of Chemical Engineering*, **16**, 11–15.

Maier, H. R., Simpson, A. R., Zecchin, A. C., Foong, W. K., Phang, K. Y., Seah, H. Y., Tan, C. L. (2003). Ant colony optimization for design of water distribution systems. *Journal of Water Resources Planning and Management-ASCE*, **129**, 200–209.

Malcolm, A., Polan, J., Zhang, L., Ogunnaike, B. A., Linninger, A. A. (2007). Integrating systems design and control using dynamic flexibility analysis. *AIChE Journal*, **53**, 2048–2061.

Marquardt, W., Mцnnigmann, M. (2005). Constructive nonlinear dynamics in process systems engineering. *Computers & Chemical Engineering*, **29**, 1265–1275.

Martinez-Patino, J., Picon-Nunez, M., Hernandez-Figueroa, M. A., Verda, V., Serra, L. M. (2010). On the integration of power, heat and water in industrial processes. *Chemical Engineering Transactions*, **21**, 253–258.

Meeuse, F. M., Grievink, J. (2002). Optimum controllability of distributed systems based on non-equilibrium thermodynamics. *Computer-Aided Chemical Engineering*, **10**, 259–264.

Mejia-Suarez, D. A., Zamora-Mata, J. M., Serna-Gonzalez, M., Lugo-Leyte, R., Ponce-Ortega, J. M. (2010). Synthesis of alternative designs in the retrofit of heat exchanger networks. *Revista Mexicana De Ingenieria Quimica*, **9**, 99–123.

Morar, M., Agachi, P. S. (2010). Review: important contributions in development and improvement of the heat integration techniques. *Computers & Chemical Engineering*, **34**, 1171–1179.

Morud, J., Skogestad, S. (1996). Dynamic behaviour of integrated plants. *Journal of Process Control*, **6**, 145–156.

© Woodhead Publishing Limited, 2013

Napoles-Rivera, F., Ponce-Ortega, J. M., El-Halwagi, M. M., Jimenez-Gutierrez, A. (2010). Global optimization of mass and property integration networks with in-plant property interceptors. *Chemical Engineering Science*, **65**, 4363–4377.

Nelson, A. M., Liu, Y. A. (2008). Hydrogen-pinch analysis made easy. *Chemical Engineering*, **115**, 56–61.

Ng, D. K. S., Foo, D. C. Y., Rabie, A., El-Halwagi, M. M. (2008). Simultaneous synthesis of property-based water reuse/recycle and interception networks for batch processes. *AIChE Journal*, **54**, 2624–2632.

Ng, D. K. S., Foo, D. C. Y., Tan, R. R., El-Halwagi, M. (2009). Automated targeting for total property-based network. *Computer-Aided Chemical Engineering*, **26**, 1189–1195.

Ng, D. K. S., Foo, D. C. Y., Tan, R. R., El-Halwagi, M. (2010a). Automated targeting technique for concentration- and property-based total resource conservation network. *Computers & Chemical Engineering*, **34**, 825–845.

Ng, K. S., Lopez, Y., Campbell, G. M., Sadhukhan, J. (2010b). Heat integration and analysis of decarbonised IGCC sites. *Chemical Engineering Research & Design*, **88**, 170–188.

Nguyen, D. Q., Barbaro, A., Vipanurat, N., Bagajewicz, M. J. (2010). All-at-once and step-wise detailed retrofit of heat exchanger networks using an MILP model. *Industrial & Engineering Chemistry Research*, **49**, 6080–6103.

Odjo, A. O., Sammons, N. E., Jr., Yuan, W., Marcilla, A., Eden, M. R., Caballero, J. A. (2011). A disjunctive-genetic programming approach to synthesis of process networks. *Industrial & Engineering Chemistry Research*, **50**, 6213–6228.

Pan, C., Shi, J., Liu, Z.-Y. (2012). An iterative method for design of water-using networks with regeneration recycling. *AIChE Journal*, **58**, 456–465.

Patel, J., Uygun, K., Huang, Y. (2008). A path constrained method for integration of process design and control. *Computers & Chemical Engineering*, **32**, 1373–1384.

Piacentino, A. (2011). Thermal analysis and new insights to support decision making in retrofit and relaxation of heat exchanger networks. *Applied Thermal Engineering*, **31**, 3479–3499.

Ponce-Ortega, J. M., El-Halwagi, M. M., Jimenez-Gutierrez, A. (2010a). Global optimization for the synthesis of property-based recycle and reuse networks including environmental constraints. *Computers & Chemical Engineering*, **34**, 318–330.

Ponce-Ortega, J. M., Mosqueda-Jimenez, F. W., Serna-Gonzalez, M., Jimenez-Gutierrez, A., El-Halwagi, M. M. (2011a). A property-based approach to the synthesis of material conservation networks with economic and environmental objectives. *AIChE Journal*, **57**, 2369–2387.

Ponce-Ortega, J. M., Serna-Gonzalez, M., Jimenez-Gutierrez, A. (2010b). Synthesis of heat exchanger networks with optimal placement of multiple utilities. *Industrial & Engineering Chemistry Research*, **49**, 2849–2856.

Ponce-Ortega, J. M., Tora, E. A., Gonalez-Campos, B., El-Halwagi, M. M. (2011b). Integration of renewable energy with industrial absorption refrigeration systems: systematic design and operation with technical, economic, and environmental objectives. *Industrial & Engineering Chemistry Research*, **50**, 9667–9684.

© Woodhead Publishing Limited, 2013

Poplewski, G., Jeżowski, J. M., Jeżowska, A. (2011). Water network design with stochastic optimization approach. *Chemical Engineering Research & Design*, **89**, 2085–2101.

Qin, X., Gabriel, F., Harell, D., El-Halwagi, M. M. (2004). Algebraic techniques for property integration via componentless design. *Industrial & Engineering Chemistry Research*, **43**, 3792–3798.

Raskovic, P., Anastasovski, A., Markovska, L., Mesko, V. (2010). Process integration in bioprocess industry: waste heat recovery in yeast and ethyl alcohol plant. *Energy*, **35**, 704–717.

Ricardez-Sandoval, L. A., Budman, H. M., Douglas, P. L. (2009). Integration of design and control for chemical processes: a review of the literature and some recent results. *Annual Reviews in Control*, **33**, 158–171.

Ricardez-Sandoval, L. A., Budman, H. M., Douglas, P. L. (2010). Simultaneous design and control: a new approach and comparisons with existing methodologies. *Industrial & Engineering Chemistry Research*, **49**, 2822–2833.

Rico-Ramirez, V., Reyes-Mendoza, M. A., Quintana-Hernandez, P. A., Ortiz-Cruz, J. A., Hernandez-Castro, S., Diwekar, U. M. (2010). Fisher information on the performance of dynamic systems. *Industrial & Engineering Chemistry Research*, **49**, 1812–1821.

Rojas, O. J., Setiawan, R., Bao, J., Lee, P. L. (2009). Dynamic operability analysis of nonlinear process networks based on dissipativity. *AIChE Journal*, **55**, 963–982.

Saw, S. Y., Lee, L., Lim, M. H., Foo, D. C. Y., Chew, I. M. L., Tan, R. R., Klemeš, J. J. (2011). An extended graphical targeting technique for direct reuse/recycle in concentration and property-based resource conservation networks. *Clean Technologies and Environmental Policy*, **13**, 347–357.

Schluter, M., Egea, J. A., Antelo, L. T., Alonso, A. A., Banga, J. R. (2009). An extended ant colony optimization algorithm for integrated process and control system design. *Industrial & Engineering Chemistry Research*, **48**, 6723–6738.

Seingheng, H., Tan, R. R., Auresenia, J., Fuchino, T., Foo, D. C. Y. (2007). Synthesis of near-optimal topologically constrained property-based water network using swarm intelligence. *Clean Technologies and Environmental Policy*, **9**, 27–36.

Shelley, M. D., El-Halwagi, M. M. (2000). Component-less design of recovery and allocation systems: a functionality-based clustering approach. *Computers & Chemical Engineering*, **24**, 2081–2091.

Shoaib, A. M. (2011). A systematic approach for the synthesis of highly controllable mass exchange networks. *Industrial & Engineering Chemistry Research*, **50**, 10872–10877.

Silva, A. P., Ravagnani, M. a. S. S., Biscaia, E. C., Jr., Caballero, J. A. (2010). Optimal heat exchanger network synthesis using particle swarm optimization. *Optimization and Engineering*, **11**, 459–470.

Smith, R. (2005). *Chemical Process Design and Integration.* John Wiley & Sons Ltd, Chichester, UK.

Smith, R., Jobson, M., Chen, L. (2010). Recent development in the retrofit of heat exchanger networks. *Applied Thermal Engineering*, **30**, 2281–2289.

Söderman, J., Ahtila, P. (2010). Optimisation model for integration of cooling and heating systems in large industrial plants. *Applied Thermal Engineering*, **30**, 15–22.

© Woodhead Publishing Limited, 2013

Sotelo-Pichardo, C., Ponce-Ortega, J. M., El-Halwagi, M. M., Frausto-Hernбndez, S. (2011). Optimal retrofit of water conservation networks. *Journal of Cleaner Production*, **19**, 1560–1581.

Stiglitz, J. (1974). Growth with exhaustible natural resources: efficient and optimal growth pats. *Review of Economic Studies*, **41**, 139–152.

Sujo-Nava, D., Scodari, L. A., Slater, C. S., Dahm, L., Savelski, M. J. (2009). Retrofit of sour water networks in oil refineries: a case study. *Chemical Engineering and Processing*, **48**, 892–901.

Tan, R. R. (2011). Fuzzy optimization model for source-sink water network synthesis with parametric uncertainties. *Industrial & Engineering Chemistry Research*, **50**, 3686–3694.

Tan, R. R., Col-Long, K. J., Foo, D. C. Y., Hul, S., Ng, D. K. S. (2008). A methodology for the design of efficient resource conservation networks using adaptive swarm intelligence. *Journal of Cleaner Production*, **16**, 822–832.

Tan, R. R., Cruz, D. E. (2004). Synthesis of robust water reuse networks for single-component retrofit problems using symmetric fuzzy linear programming. *Computers & Chemical Engineering*, **28**, 2547–2551.

Tan, R. R., Foo, D. C. Y., Manan, Z. A. (2007a). Assessing the sensitivity of water networks to noisy mass loads using Monte Carlo simulation. *Computers & Chemical Engineering*, **31**, 1355–1363.

Tan, Y. L., Manan, Z. A. (2006). Retrofit of water network with optimization of existing regeneration units. *Industrial & Engineering Chemistry Research*, **45**, 7592–7602.

Tan, Y. L., Manan, Z. A., Foo, D. C. Y. (2007b). Retrofit of water network with regeneration using water pinch analysis. *Process Safety and Environmental Protection*, **85**, 305–317.

Tan, Y. L., Manan, Z. A. (2008). A new systematic technique for retrofit of water network. *International Journal of Environment and Pollution*, **32**, 519–526.

Taskhiri, M. S., Tan, R. R., Chiu, A. S. F. (2011). Emergy-based fuzzy optimization approach for water reuse in an eco-industrial park. *Resources Conservation and Recycling*, **55**, 730–737.

Thomas Polley, G., Picon-Nunez, M., De Jesus Lopez-Maciel, J. (2010). Design of water and heat recovery networks for the simultaneous minimisation of water and energy consumption. *Applied Thermal Engineering*, **30**, 2290–2299.

Thunyawart, J., Srinophakun, T., Henwatthana, W. (2011). Simulation of mass exchange networks using modified genetic algorithms. *Korean Journal of Chemical Engineering*, **28**, 332–341.

Tokos, H., Pintarič, Z. N., Yang, Y., Kravanja, Z. (2012). Multilevel strategies for the retrofit of large-scale industrial water system: a brewery case study. *AIChE Journal*, **58**, 884–898.

Tudor, R., Lavric, V. (2010). Optimization of total networks of water-using and treatment units by genetic algorithms. *Industrial & Engineering Chemistry Research*, **49**, 3715–3731.

Tudor, R., Lavric, V. (2011). Dual-objective optimization of integrated water/wastewater networks. *Computers & Chemical Engineering*, **35**, 2853–2866.

Uerdingen, E., Fischer, U., Gani, R., Hungerbuhler, K. (2005). A new retrofit design methodology for identifying, developing, and evaluating retrofit projects for

© Woodhead Publishing Limited, 2013

cost-efficiency improvements in continuous chemical processes. *Industrial & Engineering Chemistry Research*, **44**, 1842–1853.

Uerdingen, E., Fischer, U., Hungerbuhler, K., Gani, R. (2003). Screening for profitable retrofit options of chemical processes: a new method. *AIChE Journal*, **49**, 2400–2418.

Upadhye, A. A., Qi, W., Huber, G. W. (2011). Conceptual process design: a systematic method to evaluate and develop renewable energy technologies. *AIChE Journal*, **57**, 2292–2301.

Vasudevan, S., Rangaiah, G. P. (2011). Integrated framework incorporating optimization for plant-wide control of industrial processes. *Industrial & Engineering Chemistry Research*, **50**, 8122–8137.

Vazquez-Ojeda, M., Segovia-Hernandez, J. G., Hernandez, S., Hernandez-Aguirre, A., Maya-Yescas, R. (2011). Optimization and controllability analysis of thermally coupled reactive distillation arrangements with minimum use of reboilers. *Industrial & Engineering Chemistry Research,* **51**(17), 5856–5865.

Wei, G. F., Yao, P. J., Luo, X., Roetzel, W. (2004). Study on multi-stream heat exchanger network synthesis with parallel genetic/simulated annealing algorithm. *Chinese Journal of Chemical Engineering*, **12**, 66–77.

Westphalen, D. L., Young, B. R., Svrcek, W. Y. (2003). A controllability index for heat exchanger networks. *Industrial & Engineering Chemistry Research*, **42**, 4659–4667.

Yan, Q., Xiao, J., Huang, Y. (2006). Synthesis of highly controllable heat integration systems. *Journal of the Chinese Institute of Chemical Engineers*, **37**, 457–465.

Yan, Q. Z., Huang, Y. L. (2002). A disturbance rejection model for designing a structurally controllable mass exchanger network with recycles. *Chemical Engineering Research & Design*, **80**, 513–528.

Young, B. R., Tellez, R., Svrcek, W. Y. (2006). Towards integrated process and control system synthesis for heat-integrated plants. *Canadian Journal of Chemical Engineering*, **84**, 219–229.

Yu, H. M., Fang, H. P., Yao, P. J., Yuan, Y. (2000). A combined genetic algorithm/simulated annealing algorithm for large scale system energy integration. *Computers & Chemical Engineering*, **24**, 2023–2035.

Yuan, Z., Chen, B., Zhao, J. (2011). An overview on controllability analysis of chemical processes. *AIChE Journal*, **57**, 1185–1201.

Yuan, Z., Zhang, N., Chen, B., Zhao, J. (2012). Systematic controllability analysis for chemical processes. *AIChE Journal,* **58**(10), 3096–3109, DOI: 10.1002/aic.13722.

Zhang, B. J., Luo, X. L., Chen, Q. L., Hui, C.-W. (2011a). Heat integration by multiple hot discharges/feeds between plants. *Industrial & Engineering Chemistry Research*, **50**, 10744–10754.

Zhang, C., Vasudevan, S., Rangaiah, G. P. (2010). Plantwide control system design and performance evaluation for ammonia synthesis process. *Industrial & Engineering Chemistry Research*, **49**, 12538–12547.

Zhang, Q., Feng, X., Liu, G., Chu, K. H. (2011b). A novel graphical method for the integration of hydrogen distribution systems with purification reuse. *Chemical Engineering Science*, **66**, 797–809.

© Woodhead Publishing Limited, 2013

Zhang, X., Huang, K., Chen, H., Wang, S. (2011c). Comparing three configurations of the externally heat-integrated double distillation columns (EHIDDiCs). *Computers & Chemical Engineering*, **35**, 2017–2033.

Zhelev, T. (2007). The conceptual design approach – a process integration approach on the move. *Resources Conservation and Recycling*, **50**, 143–157.

Zhelev, T. K. (2002). Wastewater treatment management using combined water-oxygen-thermal pinch analysis. *Computer-Aided Chemical Engineering*, **10**, 391–396.

Zhelev, T. K., Ridolfi, R. (2006). Energy recovery and environmental concerns addressed through emergy-pinch analysis. *Energy*, **31**, 2486–2498.

Zhu, F., Huang, K., Wang, S., Shan, L., Zhu, Q. (2009). Towards further internal heat integration in design of reactive distillation columns-Part IV: application to a high-purity ethylene glycol reactive distillation column. *Chemical Engineering Science*, **64**, 3498–3509.

© Woodhead Publishing Limited, 2013

4

Heat Integration: Targets and Heat Exchanger Network Design

TRULS GUNDERSEN, Norwegian University of Science and Technology, Trondheim, Norway

DOI: 10.1533/9780857097255.2.129

Abstract: This chapter describes the basic steps of Pinch Analysis for heat recovery that made Process Integration a methodology employed by numerous designers and engineers worldwide and made industrial leaders in the 1980s claim these concepts to be the results of academic research that had the largest impact on industrial thinking in relation to design and operation in the process industries. Key elements of the chapter are the Heat Recovery Pinch, Performance Targets ahead of design, and a step-wise and systematic procedure for Heat Exchanger Network Design. One of the main characteristics of Pinch Analysis is the extensive use of graphical diagrams and representations, which give the designer a good overview of even the most complex processes. These tools provide insight and ease the communication between designers and engineers.

Key words: Heat Recovery Pinch, Composite Curves, Performance Targets, Pinch Design Method, design evolution.

4.1 Introduction

This section provides a brief introduction to the history, major topics and key concepts of Heat Integration, while subsequent sections provide more detail about Performance Targets, graphical diagrams and representations, as well as design procedures that form the basis of the methodology, with a few simple, illustrative examples to assist the explanations in the text. The section repeats and expands parts of Chapter 2 on Basic Terminology of Process Integration. Heat Integration was an early ('pioneering') activity and is still an important part of the 'discipline' that today is referred to as Process Integration.

The term Heat Integration has two meanings. First, it refers to the physical arrangement of equipment, process sections, production plants, entire sites and even the surroundings in the cases of district heating or district cooling. Second, it refers to an area of Process Synthesis, with methods and tools aimed at increased energy efficiency in industrial processes and energy

© Woodhead Publishing Limited, 2013

plants. Such improved energy efficiency can be achieved by combining (i.e. integrating) heating and cooling demands and thereby reducing the need for external heating and cooling utilities. Efficient use of equipment is of course also part of the scope, since energy efficiency only becomes interesting, and will only be implemented, if it is economically feasible.

The birth of Process Integration as a systems-orientated design activity is related to the discovery of the concept referred to as the ***Heat Recovery Pinch***. A methodology termed Pinch Analysis was developed in the late 1970s and early 1980s, which resulted in a departure from traditional design practice that had been based on extending and improving process technologies by the use of operating and engineering insight (i.e. following the 'learning curve') and by choosing the best design from a set of case studies. Of course, there would occasionally be discoveries and breakthroughs that made step changes possible, but the uncertainty whether designs could be further improved, and by how much, was still left with the designer. Most of the text in this chapter on Heat Integration will focus on increasing the Energy Efficiency of processing systems, using Pinch Analysis as the main methodology.

The most important new feature in Pinch Analysis was the ability to establish ***Performance Targets*** ahead of design based only on information about the change in thermodynamic state for the Process Streams, described in table form and hereafter referred to as Stream Data. These targets were first developed for thermal energy (external heating and cooling) and were later extended to mechanical energy (power or shaft work), number of heat exchangers and total Heat Transfer Area. In fact, by use of analogies, the original Heat Pinch concept and the idea of Targeting ahead of design have been reused (as indicated in Chapter 2 and several other chapters of this handbook) in other areas, such as mass exchange processes (Mass Pinch), wastewater minimisation and distributed effluent treatment systems (Water Pinch), hydrogen management in oil refineries (Hydrogen Pinch) and oxygen-consuming processes (Oxygen Pinch). Similar ideas have also been applied to study for example Supply Chains and Carbon Emission reductions.

The concept of a Heat Recovery Pinch was independently discovered and developed step by step by Hohmann (1971), Huang and Elshout (1976), Linnhoff *et al*. (1978, 1979) and Umeda *et al*. (1978) – for details see Chapter 1. The basic idea is to draw separately the total heating and the total cooling requirements of a process cumulatively in a Temperature–Enthalpy Diagram, commonly referred to as ***Composite Curves***. Similar drawings had already been used by designers of low temperature processes such as air separation (Linde AG in Germany) to design multi-stream heat exchangers (Gundersen, 2000). The graphical construction of Composite Curves is explained with an example in Section 4.4.1.

© Woodhead Publishing Limited, 2013

Heat recovery between hot and cold streams is restricted by the shape of the Composite Curves and the fact that heat can only be transferred from higher to lower temperature. The Minimum Allowed Temperature Difference (ΔT_{min}) is an economic parameter that indicates a near-optimal ***trade-off*** between Investment Cost (heat exchangers) and Operating Cost (energy). The point of smallest vertical distance (equal to ΔT_{min}) between the Composite Curves represents a bottleneck for heat recovery and is referred to as the Heat Recovery Pinch.

An alternative representation of the overall heating and cooling demands in a process is the ***Heat Cascade***, a special case of the Transshipment Model from Operations Research. Here, hot streams (i.e. 'sources' of heat) contribute to a set of temperature intervals (i.e. 'warehouses' of heat), while cold streams (i.e. 'sinks' of heat) draw heat from the same intervals. The temperature intervals are established on the basis of the Supply and Target Temperatures of all process streams. A heat balance is made for each temperature interval, and any heat surplus in one interval is cascaded (thus the name) down to the next interval with lower temperatures. The Heat Cascade also forms the basis of the ***Grand Composite Curve*** (also referred to as the Heat Surplus Diagram), a very important tool for studying the interface between the process and the Utility System (consumption and generation of various types of utilities, both load and level) and for evaluating heat integration of special equipment such as Distillation Columns, Evaporators, Heat Pumps and Heat Engines. The graphical construction of Heat Cascades and the Grand Composite Curve is explained with an example in Section 4.5.2.

Perhaps the most important property of the Heat Recovery Pinch is that it decomposes the process into a heat deficit region above Pinch and a heat surplus region below Pinch. There is not enough heat available in the hot streams above Pinch to satisfy the overall heating demand of the cold streams, and external heating is required. Below Pinch, there is not enough cooling available in the cold streams to satisfy the overall cooling demand of the hot streams, and external cooling is required. Based on this insight about ***Pinch Decomposition***, systematic, general and step-wise design procedures have been developed for Heat Exchanger Networks with Minimum Energy Consumption.

Pinch Decomposition also forms the basis of more general rules for design modifications, as well as integration of special equipment, heat and power considerations and beyond. The ***Plus/Minus Principle*** states that any design modification aiming to reduce external heating and cooling should result in (1) an increase ('Plus') in the duty of hot streams above Pinch or cold streams below Pinch, and/or (2) a decrease ('Minus') in the duty of colds streams above Pinch or hot streams below Pinch, where (1) and (2) can often be combined. The ***Appropriate Placement*** concept is based on the

© Woodhead Publishing Limited, 2013

same philosophy, and can be stated in general terms as the placement (or integration) of heat sources above Pinch and Heat Sinks below Pinch.

As indicated above, Pinch Decomposition is the basis for the ***Pinch Design Method*** (PDM), adopted and extensively used in a large number of industrial sectors such as, but not limited to, oil and gas, chemical and petrochemical, pulp and paper, metal production, dairies, breweries and pharmaceuticals. Any heat leakage from the higher temperature region above Pinch (with heat deficit) to the lower temperature region below Pinch (with heat surplus) results in an increase of both hot and cold utilities; thus there is a ***Double Penalty*** associated with such heat transfer. The main philosophy behind the PDM (Linnhoff and Hindmarsh, 1983) is thus to avoid any Cross-Pinch heat transfer by designing separate Heat Exchanger Networks above and below Pinch. PDM is a step-wise (sequential) design procedure that provides rules for the selection of hot and cold streams to be matched in heat exchangers, the sequence and duty of the heat exchangers, the need for stream splitting, etc.

This chapter describes tools and methods for designing new plants, often referred to as ***Grassroots Design***, while a much more common activity in industry is the improvement of existing plants by making investments that increase production volumes and/or process efficiency. The latter is often referred to as ***Retrofit Design*** where, as explained in Chapter 8, Section 8.4, the main objective is to reduce energy consumption in existing process plants by increasing the Level of Heat Recovery. The design project then focuses on investing in some new equipment, repiping or changing internals in heat exchangers, while making maximum use of existing units. Heat exchangers are tailor-made, and thus there is no second-hand market and equipment that is purchased and installed should be kept as part of the modified design.

4.2 Stages in the Design of Heat Recovery Systems

As indicated above, there is a fundamental difference between designing Heat Exchanger Networks for new designs ('grassroots') and modifying heat recovery systems for existing plants ('retrofit'). At the same time, the design process contains the same stages for the two cases, although with quite different content, as will be explained in Section 4.3.2 and Chapter 8, Section 8.4. More specifically, the stages in design of heat recovery systems are:

- Data Extraction
- Performance Targets
- Process Modifications
- Network Design

© Woodhead Publishing Limited, 2013

- Design Evolution
- Process Simulation

Data extraction refers to collecting and processing data about heating and cooling requirements, as well as to the need for evaporation and condensation of process streams, often referred to as Stream Data. Similar data must be collected for systems available for external heating and cooling, often referred to as Utility Data. Finally, Economic Data are needed, such as the cost of heat exchangers and utilities, economic parameters, etc. For grassroots, consistent data are normally available from rigorous mass and energy balances established by process simulators; however, the quality of the data depends on whether or not the simulation model is a good representation of the actual process. For retrofit, data could also be taken from process simulations; alternatively, data collected from measurements could be used. In the latter case, some data reconciliation is required after removing obvious (or 'gross') errors.

Performance targets refer to establishing measures for best performance ahead of design based only on information available in the stream data, utility data and economic data (the type of data that are needed depends on the actual target(s) to be obtained). Typical targets for Heat Exchanger Networks include minimum external heating ($Q_{H,min}$) and cooling ($Q_{C,min}$) demands, minimum number of heat exchangers (U_{min}), and minimum total heat transfer area (A_{min}). With Multiple Utilities, targets can also be established for the cost-optimal utility mix.

Process modifications refer to the consideration of making changes in the basic process (reactor system, separation system, recycle system, etc.) in such a way that the scope for heat recovery is improved. The indicator for the potential advantage of making such process changes is the Composite Curves established during the Performance Targets stage, and the tool for suggesting these changes is the Plus/Minus Principle mentioned in Section 4.1.

Network design in this chapter refers to establishing a network of heat exchangers that achieves the Performance Targets for energy consumption and number of heat exchangers, referred to as a Maximum Energy Recovery (MER) design. The primary tool for network design is the PDM mentioned in Section 4.1, which is fundamentally based on the Pinch Decomposition principle. Separate networks are established above and below Pinch based on firm rules for matching Hot and Cold process streams in heat exchangers, rules for the sequencing of these units, and a strategy for stream splitting when favourable or required.

Design evolution primarily refers to refining MER designs by removing small heat exchangers resulting from the use of the PDM, where separate

© Woodhead Publishing Limited, 2013

networks are developed above and below Pinch. This activity is also referred to as Energy Relaxation, since the removal of units will require more utilities (energy) and possibly also more heat transfer area. The motivation for this stage is cost reduction as well as reduction in network complexity (fewer units, which is often followed by fewer stream splits). The tools are the degrees of freedom in the network, referred to as Stream Splits, Heat Load Loops and Heat Load Paths, that will be described in Section 4.7.1.

Finally, ***process simulation*** in this context refers to testing the feasibility of the Heat Exchanger Network that has been designed and optimised in the previous stages of the design process. This stage may also involve switching from simplified models of pure counter-current heat exchangers to more practical and realistic design configurations. However, to fully describe the process simulation stage is beyond the scope of this chapter.

4.3 Data Extraction

Data extraction is a very time consuming and critical activity, since the quality and realism of the design solutions depend heavily on the correctness of the data. The saying 'garbage in means garbage out' also applies here.

4.3.1 Data Required for Basic Heat Integration

The type of data required for Heat Integration projects obviously relates to the need for heating, cooling, evaporation and condensation in the process. In short, what is needed is a quantification of the required enthalpy changes of the process streams. From thermodynamics, the change in the total enthalpy flow, H (kW), that a process stream undergoes when changing conditions can be obtained from Equation [4.1].

$$\Delta H = \int m \cdot \mathrm{d}h \qquad [4.1]$$

where m is mass flowrate (kg/s) and h is specific enthalpy (kJ/kg), giving change in enthalpy flow in the units (kJ/s = kW). Enthalpy is in general a complicated function of stream pressure, temperature and composition. In Heat Integration, a process stream is defined as one that does not change mass flowrate or composition. Whenever such changes take place, a new process stream is introduced. If we assume constant mass flowrate and stream composition, and ignore the effect of pressure on enthalpy, then Equation [4.1] can be simplified to Equation [4.2].

$$\Delta H = m \cdot \int c_p \cdot \mathrm{d}T \qquad [4.2]$$

© Woodhead Publishing Limited, 2013

where c_p is the Specific Heat Capacity at constant pressure (kJ/kgK). In order to replace numerical integration by simple summation, the assumption of a constant c_p or a piece-wise linear relation between temperature and enthalpy has been extensively used in Pinch Analysis. If c_p is assumed constant, and the supply and target temperatures of a process stream are denoted T_S and T_T, respectively, then Equation [4.2] is simplified even further to Equation [4.3].

$$\Delta H = m \cdot c_p \cdot \int_{T_S}^{T_T} \mathrm{d}T = CP \cdot (T_T - T_S) \qquad [4.3]$$

where CP is a lumped parameter (the product of m and c_p) referred to as the 'Heat Capacity Flowrate' with units (kW/K). For process streams changing phase, information about the latent heat of such phase changes would be required. It should be emphasised that in this chapter, no formal sign convention is made, rather common sense is applied. This means that both hot and cold streams have changes in enthalpy flow that are positive as indicated in Equation [4.4], where subscripts h and c refer to hot and cold process streams, respectively. By definition, a hot process stream is one that is being cooled and/or condensed, while a cold process stream is one being heated and/or evaporated.

$$\Delta H_h = CP_h \cdot (T_{S,h} - T_{T,h}) \text{ and } \Delta H_c = CP_c \cdot (T_{T,c} - T_{S,c}) \qquad [4.4]$$

If the relationship between temperature and enthalpy is non-linear, either caused by a non-constant c_p or a phase change, improved accuracy in the analysis can be obtained by dividing process streams into piece-wise linear substreams often referred to as stream segments. This improves the Targeting part (Section 4.4), but it adds complexity to the network design (Section 4.6) since one needs to keep track of the relationship between stream segments and the original process streams when suggesting heat exchangers in the network.

The data described above are sufficient to establish targets for minimum external heating and cooling in the process, as soon as a value for the minimum allowed temperature difference mentioned in Section 4.1, ΔT_{min}, is established. When information about the Utility System (the number of different utility types for external heating and cooling) is available, targets for the Minimum Number of Heat Exchangers (often referred to as units) can be established. In order to calculate targets for the minimum total heat transfer area in heat recovery systems, data for film heat transfer coefficients, h (kW/m^{2}K), for process streams and utilities are also required.

© Woodhead Publishing Limited, 2013

4.3.2 Major Challenges in Data Extraction

There are two very different types of challenges related to data extraction for a Heat Integration project:

(i) To establish the most correct set of data related to flowrates and thermodynamic conditions of process streams used as input to heat recovery analysis and design.
(ii) To represent the heating, cooling, evaporation and condensation needs of the process streams in such a way that the degrees of freedom are kept open for network design .

While activity (i) is fairly straightforward (but involves a lot of work), activity (ii) requires skill and experience. It has often been stated that data extraction (in particular the second part) is ***more art than science***, and most of the attempts to provide procedures and guidelines for this activity have failed, including the development of knowledge-based systems (also referred to as expert systems). Some of the commercial general-purpose process simulators have features for automatic stream data extraction on the basis of a converged steady-state mass and energy-balance calculation. While these procedures enable easy generation of Composite and Grand Composite Curves, they do not keep the degrees of freedom open.

Despite the importance of data extraction, the topic has not been much discussed in the literature beyond textbooks on Process Integration, such as Linnhoff *et al*. (1982), Smith (2005) and Kemp (2007). The topic is also thoroughly covered in the recent book by Klemeš *et al*. (2010). Interestingly, rather detailed literature on data extraction has been provided in the form of reports from research institutes (such as CANMET, 2003), software vendors (such as AspenTech, 2009) and consulting companies (such as Linnhoff March, 1998), which again illustrates the importance of proper data extraction for a successful Heat Integration project.

For manual data extraction, the following guidelines can be useful:

(a) Do not copy all features of the conceptual flowsheet or an existing design.
(b) Do not mix streams at different temperatures.
(c) Do not include utilities as stream data.
(d) Do not accept the prejudice of colleagues against Heat Integration.
(e) Do not ignore true practical constraints.
(f) Distinguish between soft and hard stream data.

Rule (a) refers to the issue of keeping the degrees of freedom open in order not to overlook promising solutions for heat recovery systems. Rule

© Woodhead Publishing Limited, 2013

(b) involves several aspects, and should be discussed in more depth. First, a mixer can act as a heat exchanger, thus saving Capital Cost; however, mixing streams of different compositions is only an option if the streams are entering the same unit operation, such as a chemical reactor. Second, mixing streams at different temperatures introduces exergy losses and should be avoided. Third, mixing streams may eliminate potential heat recovery solutions. Finally, mixing streams may be required from a practical point of view, such as adding steam to hydrocarbon streams to avoid coking inside pipes and equipment, or it may be forbidden from a safety point of view, such as mixing oxygen-rich streams with hydrocarbon streams. Rule (c) is rather obvious, since the goal of the exercise is to establish minimum utility requirements; however, there are cases where it is not so easy to distinguish whether a stream is a process stream or is acting as a utility.

Rule (d) relates to the common reluctance in the process industries to accept Heat Integration solutions from an operational point of view; however, it is a fact that most industrial processes are heavily integrated, and rather than focusing on Maximum Heat Recovery, one should focus on correct or appropriate Heat Integration. In addition, it should be mentioned that when the economic potential of Heat Integration is established and well documented, it is often easier to get acceptance for such projects. Rule (e) means that, even though one should try to keep the degrees of freedom open, obviously one should not forget that some practical constraints cannot be ignored. One example is related to metal dusting, a severe form of corrosive degradation of metals that happens in some temperature ranges when CO is present. This is a problem in synthesis gas production, and in order to keep the metal temperature at a sufficiently low level, the boiler is placed upstream of the steam superheater, which is not the best solution from a thermodynamic point of view as conveyed in Pinch Analysis.

Finally, Rule (f) is quite important in the sense that some stream data must be considered as hard specifications, while others can be adjusted if that improves or simplifies the heat recovery system (as discussed in Chapter 2 on Basic Process Integration Terminology). An inlet temperature to a reactor or distillation column must often be regarded as a hard specification, while the target temperature of a process stream going to some sort of storage is an example of soft process data. Specifying a low target temperature for a hot product stream going to storage in order to increase the heat recovery potential will only result in increased need for external cooling if the target temperature is below the Pinch Temperature. Instead, this cooling could have been taken care of by nature itself through convective heat loss to the environment.

Returning to activity (i) of the data extraction exercise, there are two distinctly different situations. For grassroots design, there is normally a simulation model available for the process providing stream data as part of a

© Woodhead Publishing Limited, 2013

steady-state material and energy balance calculation. The advantage in this case is that the data are consistent. As an example, the hot and cold side of a heat exchanger will always be in balance for a converged simulation. The quality of the data, however, depends on to what extent the simulation models describes the behaviour of the real process.

For retrofit design, in addition to using a simulation model if available, one could resort to the original specification sheets for the process, or one could use measurements from the plant. However, the plant may have been modified several times since its start-up, and flowsheets and specification sheets are not always updated. Regarding the use of measurements, the typical situation is that some measurements are missing, and instruments may be either not functioning at all, or they may give incorrect readings. In such cases, the task of data reconciliation can be enormous, and a key to success is to work very closely with operators and plant engineers.

4.4 Performance Targets

In order to illustrate the different stages in the design of heat recovery systems, consider the very simple process example in Fig. 4.1, where two feed streams (A and B) are heated before entering a chemical reactor where a product and a by-product are produced. The main product is then recovered in the bottom stream from a distillation column, while the by-product and traces of unreacted raw material (feed) is taken from the top of the same distillation column. Figure 4.1 also indicates the supply and target temperatures of the process streams as well as the lumped parameter *CP* ('heat capacity flowrate') in brackets with units (kW/K). Notice that heat exchangers are not included, since these will be the result of the Heat Integration study.

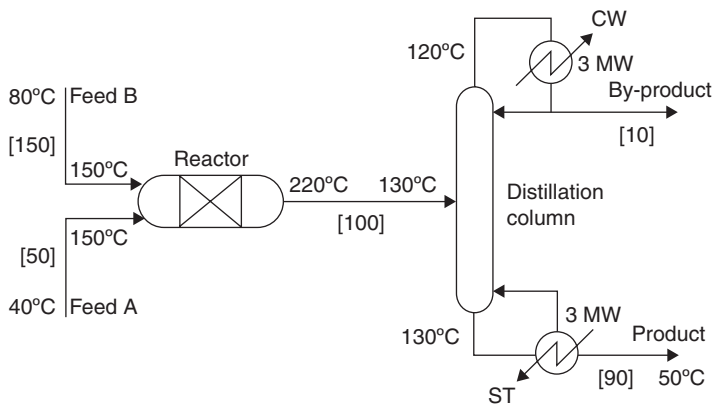

4.1 Simple process used as an illustrative example.

© Woodhead Publishing Limited, 2013

Table 4.1 Stream data for the simple process in Fig. 4.1

ID	Description	T_S (°C)	T_T (°C)	CP (kW/°C)	ΔH (kW)
H1	Reactor effluent	220	130	100	9,000
H2	Main product	130	50	90	7,200
C1	Feed A	40	150	50	5,500
C2	Feed B	80	150	150	10,500
CON	Column condenser	120	120	n.a.	3,000
REB	Column reboiler	130	130	n.a.	3,000
ST	Steam for heating	250	250	n.a.	Variable
CW	Cooling Water	20	30	n.a.	Variable

It is important at this stage to emphasise that 'heat capacity flowrate' ($CP = mCp$) is different from mass flowrate (m). This is why the reactor effluent ($CP = 100$) is less than the sum of the reactor inlets ($CP = 50 + 150 = 200$). The explanation in this case is that feed stream B is subject to evaporation before entering the reactor. Since the outlet temperature from the reactor is higher than the inlet temperature, the chemical reactions taking place must be exothermic. Based on the flowsheet in Fig. 4.1 and the given data for temperatures, heat capacity flowrates and duties for the distillation column reboiler and condenser, the stream data resulting from data extraction (Section 4.3) are listed in Table 4.1.

For distillation columns, the heating and cooling requirements are normally given as the duties of the reboiler and the condenser. The reflux and boil-up are circulating internal streams in the column and therefore normally not measured. This means that the CP values are not available (n.a.) as indicated in Table 4.1. The duties of steam and cooling water are listed as 'variable' in Table 4.1, which is obvious since these are the unknowns that will be found as a result of the Energy Targeting exercise.

4.4.1 Minimum External Heating and Cooling

As mentioned in Section 4.1, targets for heat recovery systems depend on the specification of a minimum allowed temperature difference for heat transfer, $\Delta T_{\min}$, which is an economic parameter for the trade-off between investment cost (heat exchangers) and operating cost (energy). Given a value for this parameter, targets for minimum external heating, $Q_{H,\min}$, and minimum external cooling, $Q_{C,\min}$, can be obtained by graphical or numerical methods established in the early period of Pinch Analysis. The graphical representations are referred to as Composite and Grand Composite Curves, while there are several numerical methods such as the Problem Table Algorithm (Linnhoff and Flower, 1978) and the Heat Cascade (Linnhoff, 1979). Actually, Hohmann (1971) was the first to provide a systematic way

© Woodhead Publishing Limited, 2013

to obtain energy targets by his Feasibility Table. The Heat Cascade will be used in this chapter since it (i) provides a nice illustration of the heat flows and decompositions in heat recovery systems and (ii) provides the necessary information to construct the Grand Composite Curve.

Optimisation techniques, such as Linear and Mixed Integer Programming (LP and MILP), can also be used to obtain targets for minimum external heating and cooling as well as targets for the fewest number of heat exchangers, especially in more complicated situations such as for example when there are Forbidden Matches between hot and cold process streams. These optimisation techniques will be briefly discussed in Chapter 8, Section 8.5.

Composite Curves

Composite Curves have been described and applied by a number of authors, such as Huang and Elshout (1976), Umeda *et al*. (1978) and Linnhoff *et al*. (1982). The Composite Curves (*T-H* diagram) are constructed by dividing the temperature axis into intervals based on the supply (T_S) and target (T_T) temperatures of the process streams, and to add together the enthalpy contributions (hot streams) and requirements (cold streams) in each temperature interval. Finally, these enthalpies are drawn cumulatively against the corresponding temperatures, resulting in one curve for the hot streams and one curve for the cold streams.

These curves are then positioned relative to each other in such a way that the Hot Composite Curve (the cooling curve) is always above the Cold Composite Curve (the heating curve). In this way, heat can be recovered in the overlapping region of the Composite Curves. This 'positioning' in the *T-H* diagram is obtained by shifting the two curves horizontally. Moving the curves closer together means increased heat recovery, and the economic limit is the point where the smallest vertical distance between the curves becomes equal to $\Delta T_{\min}$, while the thermodynamic limit is the point where this vertical distance becomes zero. The point where the vertical distance between the Composite Curves is at its minimum (and equal to $\Delta T_{\min}$) acts as a bottleneck against increased Heat Integration and has therefore been referred to as the Heat Recovery Pinch.

Composite Curves for the stream data in Table 4.1 are shown in Fig. 4.2 for $\Delta T_{\min} = 20°C$. Key information about the heat recovery system can be obtained from this graphical diagram, such as the Process Pinch, Maximum Heat Recovery, and the corresponding minimum external heating and cooling requirements. Reading accurate information from such diagrams can be somewhat difficult, which is why numerical methods are often preferred. The real advantage of such graphical diagrams, however, is that they provide an overview of the system and they contribute strongly to the

© Woodhead Publishing Limited, 2013

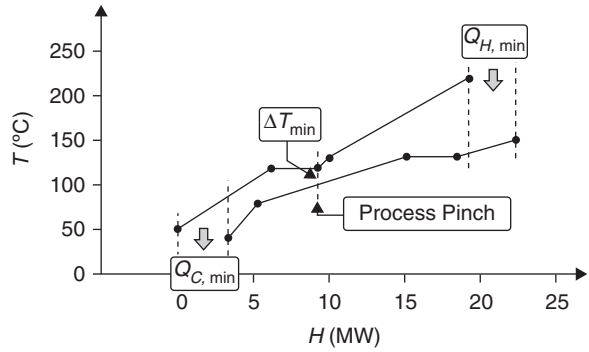

4.2 Composite Curves for the illustrative example.

understanding of the problem. One such insight is that any heat leakage from the region above Pinch to the region below Pinch (cross-Pinch heat transfer) will result in increased need for both hot and cold utilities (i.e. double penalty).

Based on the Composite Curves in Fig. 4.2, approximate targets for minimum external heating and cooling seem to be in the range 3.0–3.5 MW. As indicated above, there are also a number of numerical methods that can be applied to obtain these targets more accurately. Figure 4.3 shows the Heat Cascade for the same illustrative example with stream data in Table 4.1. The reboiler (REB) and the condenser (CON) of the distillation column add two rather strange temperature intervals to the Heat Cascade, since it is assumed that condensation and evaporation in these units take place at constant temperature. This means that the streams with sensible heat (H1, H2, C1 and C2) do not deliver or extract any heat from these intervals that are marked with a '+' and a '–' for the corresponding temperatures.

Heat Cascade

The Heat Cascade is an example of the Transshipment Model from Operations Research, with sources, warehouses and sinks. The hot streams are drawn as sources of heat on the left-hand side of the cascade, with corresponding hot stream temperatures. The cold streams are drawn as sinks of heat on the right-hand side of the cascade, with corresponding cold stream temperatures. All supply and target temperatures of the process streams should be represented as interval temperatures in the cascade; in addition, there will be 'corresponding' temperatures on the 'opposite' side obtained by adding ΔT_{min} to the supply and target temperatures of cold process streams and subtracting ΔT_{min} from the supply and target temperatures of hot process streams. This means that the specification of a minimum temperature

© Woodhead Publishing Limited, 2013

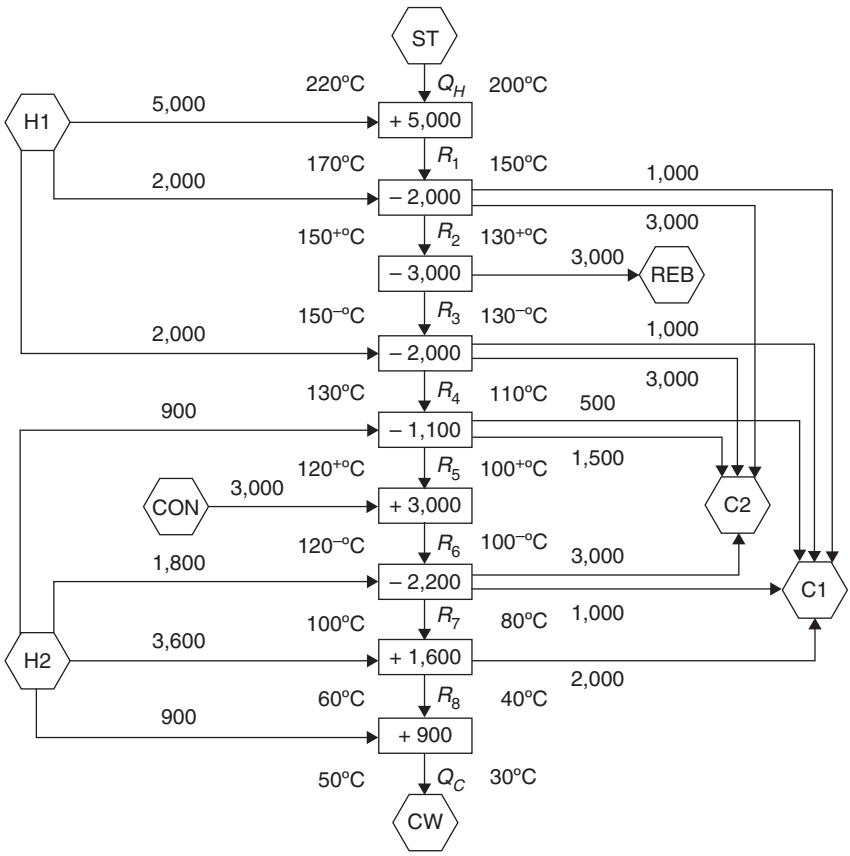

4.3 Heat Cascade for the illustrative example.

difference is built into the Heat Cascade. Any heat exchange taking place in the temperature intervals of Fig. 4.3 will be feasible and satisfy the requirement that $\Delta T \geq \Delta T_{\min}$.

As indicated in Fig. 4.3, the hot streams provide heat to the temperature intervals according to their cooling requirements, and the cold streams extract heat from the temperature intervals according to their heating requirements. Heat balances are established for each interval, and any surplus of heat in one interval is cascaded (thus the name 'Heat Cascade') as a heat residual (R_k) to the next interval with lower temperatures. Since none of these residuals can be negative (which would indicate transfer of heat from lower to higher temperatures, infeasible with heat exchangers), the minimum external heating requirement can be identified as the minimum heat needed to make these residuals non-negative.

© Woodhead Publishing Limited, 2013

A simple, yet powerful way to establish values for $Q_{H,\min}$ and $Q_{C,\min}$ is to start by assuming Q_H = 0 kW in Fig. 4.3. The heat residuals can then be obtained for the entire Heat Cascade sequentially as follows:

$$R_1 = Q_H + 5{,}000 = +5{,}000 \text{ kW} \quad R_2 = R_1 - 2{,}000 = +3{,}000 \text{ kW} \quad R_3 = R_2 - 3{,}000 = 0 \text{ kW}$$
$$R_4 = R_3 - 2{,}000 = -2{,}000 \text{ kW} \quad R_5 = R_4 - 1{,}100 = -3{,}100 \text{ kW} \quad R_6 = R_5 + 3{,}000 = -100 \text{ kW}$$
$$R_7 = R_6 - 2{,}200 = -2{,}300 \text{ kW} \quad R_8 = R_7 + 1{,}600 = -700 \text{ kW} \quad Q_C = R_8 + 900 = 200 \text{ kW}$$

As mentioned above, negative residuals are infeasible when designing a system of heat exchangers, and residual R_5 has the largest negative value of the entire Heat Cascade. This residual then becomes the bottleneck (i.e. Heat Recovery Pinch), and minimum external cooling is found to be $Q_{H,\min}$ = 3,100 kW. The corresponding minimum external heating is then $Q_{C,\min}$ = 3,300 kW, and the Process Pinch is defined by the temperatures 120°C (for hot streams) and 100°C (for cold streams). Since the residual R_5 actually is related to the temperatures 120^{+}°C and 100^{+}°C, it means that the column condenser (CON) is supplying heat below Pinch. The implications of this will be discussed in Sections 4.5.1 and 4.5.2.

4.4.2 Minimum Number of Heat Exchangers

The next logical step in a Heat Integration project is to establish targets for the minimum number of heat exchangers, also referred to as units. This is done by the so-called (N – 1) rule, used for the first time by Hohmann (1971). Linnhoff *et al*. (1979) explained that the (N – 1) rule is a simplification of Euler's Rule from Graph Theory ($U = N + L - S$). The analogy between graphs and Heat Exchanger Networks is that nodes represent streams, while edges represent heat exchangers. Thus N is the total number of process streams and utility types, U is the number of heat exchangers (units), L is the number of independent loops and S is the number of subnetworks (or subgraphs). Since the objective is to establish a target for the number of units *ahead* of design, network related features, such as loops and subnetworks, are not known. This is overcome by setting $L = 0$ (loops can be removed, as will be shown in Section 4.7.2) and $S = 1$ (conservative, since the presence of subnetworks reduces the number of units). As a result, Euler's Rule reduces to $U = N - 1$. As pointed out in Section 4.1, however, separate networks must be designed above and below Pinch in order to achieve the targets for minimum external heating and cooling. Thus, the (N – 1) rule has to be applied separately above and below Pinch in order to have a target for the number of units that is compatible with the heating and cooling targets. A Targeting formula for the minimum

© Woodhead Publishing Limited, 2013

number of units in a Heat Exchanger Network achieving MER is then given by Equation [4.5].

$$U_{\min,\mathrm{MER}} = (N_{\mathrm{above}} - 1) + (N_{\mathrm{below}} - 1) \quad [4.5]$$

As will become evident in Section 4.7.2, the Minimum Number of Units in heat recovery systems that relax the MER requirement (do not decompose at the Pinch) is another useful target value and is given by Equation [4.6].

$$U_{\min,\mathrm{global}} = (N_{\mathrm{total}} - 1) = (N_H + N_C + N_{\mathrm{Util}} - 1) \quad [4.6]$$

Grid Diagram

Another invention from the pioneering period of Pinch Analysis is the Grid Diagram, which is an alternative way to draw Heat Exchanger Networks. While the Grid Diagram is a departure from standard ways of representing process flowsheets, it has the important advantage that it mimics the desirable counter-current flow of heat exchangers and thereby makes it easy to implement Pinch Decomposition in Heat Exchanger Networks as well as to study cross-Pinch heat transfer. Figure 4.4 shows the Grid Diagram for the illustrative example presented in Figs 4.1–4.3. Contrary to the first version of this representation proposed by Linnhoff (1979), the handbook follows the more logical form, where temperatures increase from left to right, as they would do in any *xy* diagram. This then defines the directions of the hot and cold process streams in the diagram. It should also be emphasised that no linear temperature scale is applied; rather, the main focus is on whether a stream is present above, across or below Pinch.

While the Grid Diagram will act as a 'drawing board' for network design in subsequent sections, the first use of this representation is to establish targets for the minimum number of heat exchangers. In this respect, heat exchangers (or units) refer to process-to-process heat exchangers as well as utility exchangers (such as steam heaters and water coolers). The dashed lines in Fig. 4.4 indicate the 'position' of the Process Pinch, and all streams are drawn relative to these Pinch Temperatures. Thus, similar to the Heat Cascade, the Grid Diagram also keeps track of both hot and cold stream temperatures. Utilities could also have been included in the Grid Diagram (particularly useful with multiple utilities), but has been left out for the sake of simplicity. It should be emphasised that Targeting for units takes place after Targeting for energy, thus the types and amounts of different utilities needed are known and fixed.

© Woodhead Publishing Limited, 2013

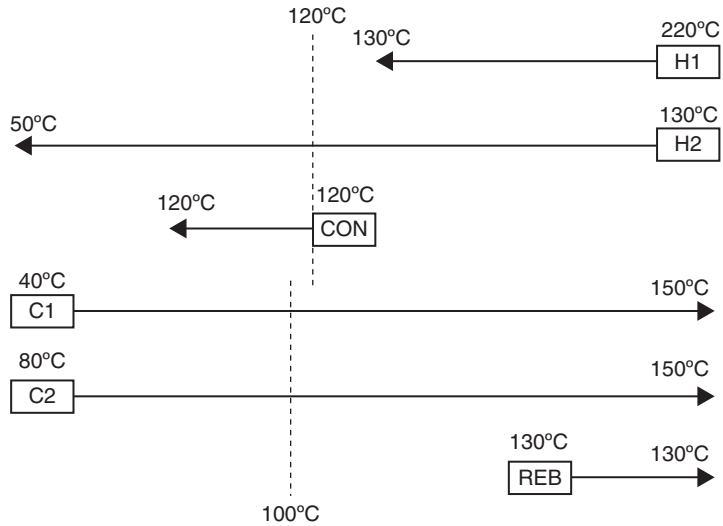

4.4 Grid Diagram for the illustrative example.

The Grid Diagram can be used to set targets for the minimum number of units as follows: for an MER design, Pinch Decomposition must be obeyed, and Equation [4.5] can be applied. Energy targeting established the need for both steam (3,100 kW) and cooling water (3,300 kW). Above the Pinch, there are two hot streams (H1 and H2), three cold streams (C1, C2 and REB) and one hot utility (ST). Below the Pinch, there are two hot streams (H2 and CON), two cold streams (C1 and C2) and one cold utility (CW). The MER target for the minimum number of units then becomes:

$$U_{\min,\mathrm{MER}} = (N_{\mathrm{above}} - 1) + (N_{\mathrm{below}} - 1) = (2+3+1-1) + (2+2+1-1) = 5+4 = 9$$

Similarly, the target for the fewest number of units when strict Pinch Decomposition is relaxed, can be found by Equation [4.6]:

$$U_{\min,\mathrm{global}} = (N_{\mathrm{total}} - 1) = (3+3+2-1) = 7$$

This means that the penalty for MER (and strict Pinch Decomposition) is that two (i.e. 9 – 7) more heat exchangers are likely to be required in the network. This issue will be further discussed in Section 4.7.2.

Targeting methods have also been developed for minimum total heat transfer area, the minimum number of heat exchanger shells (rather than units) for situations where shell-and-tube exchangers are dominating, and Total Annual Cost. The latter can be used to identify a reasonable value for

© Woodhead Publishing Limited, 2013

ΔT_{min} (also referred to as pre-optimisation or SuperTargeting). These more advanced targets will be presented in Chapter 8. Further targets that will be discussed in other chapters of the handbook involve mechanical energy, such as shaft work targets and targets for total sites (both heat and power).

4.5 Process Modifications

With Composite Curves established and Performance Targets calculated, it makes sense to consider options for process modifications before continuing with network design. The shape of the Composite Curves indicates whether potentials for increased heat recovery exist, and what actions are needed to reduce external heating and cooling for the process. Ideally, the Composite Curves should be as parallel as possible, since this allows for a high level of heat recovery. In reality, the Composite Curves will have kinks or 'knees' that act as bottlenecks (Pinch Points), which will limit heat recovery. One way to make the Composite Curves more parallel is to move some of these kinks to other temperatures, or to remove some of the kinks completely, with main focus on the near Pinch Region of the process.

In addition, the fundamental feature of having a heat deficit region above the Process Pinch and a heat surplus region below the Process Pinch provides guidelines for how the process should be modified to increase the potential for heat recovery. These guidelines, later coined the Plus/Minus Principle, have been discussed again in various ways by Umeda *et al*. (1979) and Linnhoff and Parker (1984) and in a most systematic and applicable way by Linnhoff and Vredeveld (1984). The Plus/Minus Principle suggests that, above Pinch, one should try to increase the amount of heat provided by hot streams (+) or decrease the amount of heat required by cold streams (−). Likewise, below Pinch, one should try to increase the amount of heat required by cold streams (+) or decrease the amount of heat provided by hot streams (−). This means that if a hot stream (or part of it) is moved from below to above Pinch or a cold stream (or part of it) is moved from above to below Pinch, the situation improves in both regions. Such 'moves' can be realised by changing the temperature of streams, which in some cases results from changing the stream pressure. Another possibility is to increase or reduce the enthalpy change of a stream.

Some obvious examples of process modifications include:

- Decrease the pressure and thus the boiling point temperature of an evaporator (cold stream) to move the operation from above to below Pinch.
- Split an evaporator into several stages in series (i.e. multi-effect).
- Decrease the pressure of a distillation column to move the reboiler (a cold stream) from above to below Pinch.

© Woodhead Publishing Limited, 2013

- Increase the pressure of a distillation column to move the condenser (a hot stream) from below to above Pinch.
- Change the reflux of a distillation column.
- Change the feed preheating or precooling of a distillation column.
- Change the operating conditions of a reactor.

4.5.1 Plus/Minus Principle and Appropriate Placement

The Plus/Minus Principle also provides guidelines for integration (or Appropriate Placement) of special equipment such as distillation columns (Linnhoff *et al.*, 1983), evaporators (Smith and Linnhoff, 1988), and heat pumps and heat engines (Linnhoff and Townsend, 1982). The background is that such equipment should not be integrated unless there are considerable energy savings involved that will compensate for additional operating problems as well as any increase in investment cost. The term Correct Integration has also been used, and the issue can be addressed simply by considering the different units as sources and sinks of heat. For obvious reasons, energy savings will only be made if one integrates a source of heat with a sink of heat, and simple thermodynamic principles require that the source must have a higher temperature than the sink. The following classification can be made for some of the typical equipment mentioned above as well as for the 'background' (or remaining) process:

- The background process as represented by its Heat Cascade is a Heat Sink above the Process Pinch and a Heat Source below the same Pinch.
- A distillation column represents a Heat Sink in the reboiler and a Heat Source in the condenser.
- An evaporator represents a heat sink in the evaporation stage (boiler) and a Heat Source in the condenser.
- A heat pump represents a Heat Sink at lower temperature (evaporator) and a Heat Source at higher temperature (condenser), while consuming mechanical energy.
- A heat engine represents a Heat Sink at higher temperature and a Heat Source at lower temperature, while producing mechanical energy.

Correct use of a heat pump, to reduce external heating in the background process, then means to integrate the source of the process below Pinch with the Sink of the heat pump (evaporator) as well as to integrate the source of the heat pump (condenser) with the sink of the process above Pinch. In short, this means that the heat pump should be integrated across Pinch, in the sense that it utilises heat from the surplus region below Pinch and supplies it to the deficit region above Pinch. Such integration (or use) of a heat

© Woodhead Publishing Limited, 2013

pump reduces both hot and cold utility consumption. If a heat pump is integrated entirely above Pinch, the only result from an energy point of view is that mechanical energy usage is converted into thermal energy savings on a 1:1 basis, which is not a good idea, since mechanical energy has a higher value. If a heat pump is integrated below Pinch, however, a much worse scenario can be drawn: use of mechanical energy in the heat pump only results in an increased consumption of cold utility.

Correct Integration of a distillation column with the background process requires integration of the condenser (Heat Source) with cold streams above Pinch (Heat Sink) or integration of the reboiler (Heat Sink) with hot streams below Pinch (Heat Source). Since the reboiler temperature is always higher than the condenser temperature, only one of these options is available for a single column. For a condenser integrated above Pinch, the maximum savings in both hot and cold utilities are equal to the duty of the condenser, Q_{cond}. Likewise, for a reboiler integrated below Pinch, the maximum savings in both hot and cold utilities are equal to the duty of the reboiler, Q_{reb}. In summary, there are three distinct cases with very simple rules for integration:

(1) $T_{\text{reb}} > T_{\text{cond}} > T_{\text{Pinch}}$: the condenser of the distillation column should be integrated with the background process above Pinch, and the savings are $\Delta Q_H = \Delta Q_C \leq Q_{\text{cond}}$.
(2) $T_{\text{reb}} > T_{\text{Pinch}} > T_{\text{cond}}$: the distillation column should not be integrated with the background process, since no energy savings will be obtained.
(3) $T_{\text{Pinch}} > T_{\text{reb}} > T_{\text{cond}}$: the reboiler of the distillation column should be integrated with the background process below Pinch, and the savings are $\Delta Q_H = \Delta Q_C \leq Q_{\text{reb}}$.

Returning to the simple process example in Fig. 4.1, with corresponding Composite Curves in Fig. 4.2 and Heat Cascade in Fig. 4.3, the principles of Appropriate Placement can be applied to the distillation column that is part of the process. Both Figs 4.2 and 4.3 indicate that the Process Pinch is caused by the condenser of the distillation column. According to the simple rules mentioned above, the illustrative process example falls into category (2), which means that one should not integrate the distillation column in this case. However, the background process can be established and analysed by removing the column reboiler and condenser from the stream data. The resulting Heat Cascade for the background process is given in Fig. 4.5. By analysing the temperature intervals in this case, it is obvious that the third interval will be the limiting one, thus minimum external heating is given by the need to make R_3 non-negative. For the background process, the energy targeting exercise provides the following results:

© Woodhead Publishing Limited, 2013

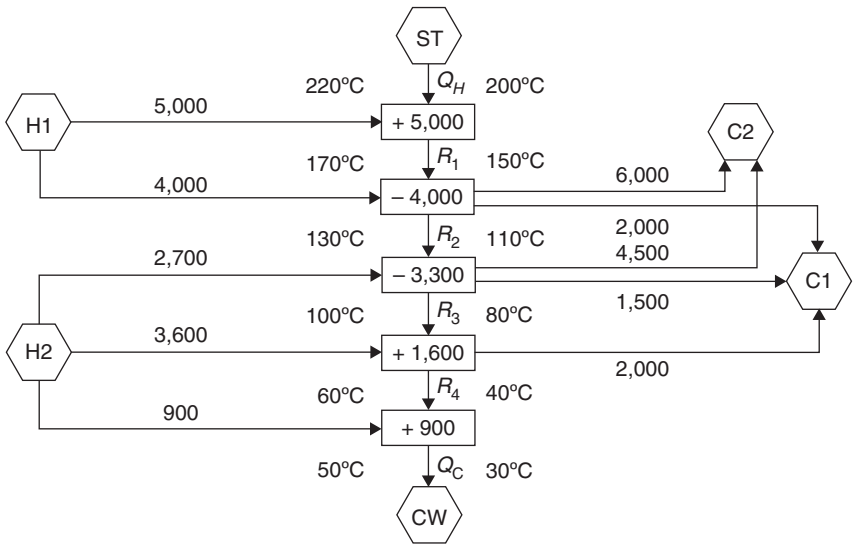

4.5 Heat Cascade for the background process.

- Process Pinch is given by $R_3 = 0$, $T_{\text{Pinch}} = 100°C/80°C$ (for hot/cold streams).
- Minimum external heating is given by $Q_{H,\min} = 3{,}300 + 4{,}000 - 5{,}000 = 2{,}300$ kW.
- Minimum external cooling is given by $Q_{C,\min} = 1{,}600 + 900 = 2{,}500$ kW.

These results are surprising and should be analysed and explained. The simple rule applied above indicated that no savings would be obtained by integrating the distillation column. The background process needs 2,300 kW of external heating, while the reboiler of the column needs 3,000 kW. In the non-integrated case, the total need for hot utility is then 2,300 + 3,000 = 5,300 kW. The assumption behind the Composite Curves (Fig. 4.2) and the total Heat Cascade (Fig. 4.3) is that the distillation column is integrated with the background process. The background for this statement is that the condenser and the reboiler are included in the stream data in Table 4.1, which is the basis for Figs 4.2 and 4.3. In the integrated case, the calculated minimum external heating requirements are 3,100 kW, which means that despite the predictions of the simple analysis above, Heat Integration of the column actually saves 5,300 – 3,100 = 2,200 kW. The reason for this apparent contradiction is that the Pinch for the background process (100°C/80°C) is different from that when the distillation column is integrated (120°C/100°C). In fact, distillation columns often cause Pinch Points due to their large duties at near constant temperature, a feature that results in marked 'knees' on the

© Woodhead Publishing Limited, 2013

Composite Curves. With reference to the Pinch of the background process, the distillation column operates entirely above Pinch and the example falls into category (1) above.

Another important result is that the savings are less than the duty of the integrated condenser ($2{,}200 < 3{,}000 = Q_{cond}$). Explaining this result requires use of another graphical diagram – the Grand Composite Curve. While the simple rules can be used in a qualitative way to establish whether Appropriate Placement is feasible or not, the Grand Composite Curve provides quantitative information about the amount of heat that can be correctly integrated, and thus how much heating and cooling can be saved by Correct Integration.

4.5.2 Grand Composite Curve and Correct Integration

As mentioned when introducing the Heat Cascade in Section 4.1, one of its advantages is that it provides the necessary information (or data) to construct the Grand Composite Curve (Linnhoff *et al.*, 1982). This is a diagram that shows the net accumulated heat surplus and heat deficit in the process, and provides an excellent interface between the process and the Utility System. It can also be used to evaluate the integration of special equipment such as distillation columns, heat pumps, etc. While the Composite Curves show two independent curves for hot and cold process streams using real temperatures, the Grand Composite Curve (which is another *T-H* diagram) shows the residual of heat in the Heat Cascade as a single curve. Thus, there is a need for a common temperature scale that can be used for both hot and cold process streams, which is why the so-called 'modified' temperatures have been introduced. The simplest way to establish such modified temperatures is to subtract half of ΔT_{min} from hot stream temperatures and likewise add half of ΔT_{min} to cold stream temperatures.

Considering the Heat Cascade in Fig. 4.5, this means that the average values of the hot and cold interval temperatures will be used as the new temperature scale. A more advanced way to establish modified temperatures is to introduce individual stream contributions to ΔT_{min} This allows for a more realistic approach to industrial problems where film heat transfer coefficients may vary by one or two orders of magnitude. In such cases, the use of a single global value for ΔT_{min} is a gross over-simplification. Modified temperatures for hot streams (i) and cold streams (j) are established by Equation [4.7], where ΔT_i and ΔT_j are individual contributions for hot and cold streams. The simple approach used in this chapter, however, is that $\Delta T_i = \Delta T_j = 0.5\ \Delta T_{min}$.

$$\begin{aligned} T^*_{Hi} &= T_{Hi} - \Delta T_i \\ T^*_{Cj} &= T_{Cj} + \Delta T_j \end{aligned} \qquad [4.7]$$

© Woodhead Publishing Limited, 2013

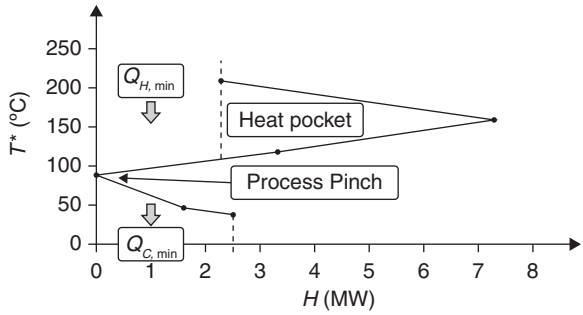

4.6 GCC for the background process.

The Grand Composite Curve for the background process is shown in Fig. 4.6. This diagram provides the same fundamental information as the Composite Curves (i.e. location of the Pinch and minimum external heating and cooling), but it also hides information related to process-to-process heat transfer. As a net Heat Surplus/Deficit Curve, the only process-to-process heat transfer shown in the Grand Composite Curve is the transfer of surplus heat from one interval to another interval at lower temperature with heat deficit. This is referred to as heat 'pockets', and the Grand Composite Curve in Fig. 4.6 has one such pocket.

The Grand Composite Curve not only shows the required external heating and cooling, it also shows at what temperatures such external heating and cooling is required. This combination of load and level is of course important information for utility placement, and can be used to identify near-optimal consumption and possible production of various utility types. In addition, as mentioned above, the Grand Composite Curve can be used to quantify how much energy savings can be made by integrating distillation columns, evaporators, heat pumps and heat engines with the background process. Focusing on the illustrative example, Fig. 4.6 shows that the need for external heating is in the range from 90°C to 110.9°C (found by interpolation) in modified temperatures, which means that the hot utility must have temperatures between 120.9°C and 100°C to satisfy the specified $\Delta T_{\min}$ of 20°C. Using steam at 250°C as indicated in Table 4.1 would be a real waste of energy quality in this case, since for example very low pressure steam at 121°C or hot water (or hot oil) operating between 121°C and 100°C would be sufficient.

As already stated, the Grand Composite Curve can be used to quantitatively address the issue of Correct Integration. Since the simple process example in Fig. 4.1 includes a distillation column, it will be used to illustrate how the Grand Composite Curve can be used to identify the scope for integrating the column with the background process. A distillation column can

© Woodhead Publishing Limited, 2013

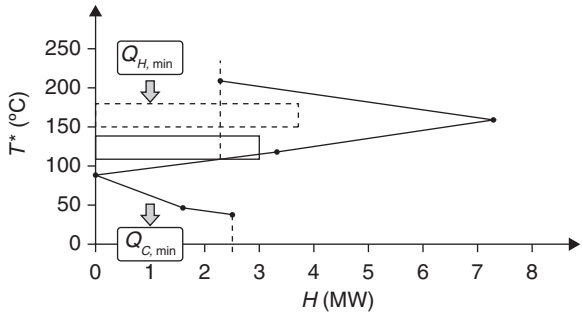

4.7 Background Process GCC and distillation column.

be plotted as a box in *TH* diagrams, where temperature profile and duty are plotted for the condenser and the reboiler. In the illustrative example, condensation (120°C) and evaporation (130°C) take place at constant temperature, and the duty of these units are equal (3 MW). The box representation in a *TH* diagram then becomes a simple rectangle. When plotted together with the Grand Composite Curve, modified temperatures must be used, which means that for $\Delta T_{min} = 20°C$, the condenser (hot stream) should be plotted at 110°C, while the reboiler (cold stream) should be plotted at 140°C. Figure 4.7 shows the Grand Composite Curve (GCC) for the background process and the distillation column plotted in the same *TH* diagram.

The solid rectangle in Fig. 4.7 is in conflict with the GCC, and feasible heat transfer (meaning $\Delta T \geq \Delta T_{min}$) between the condenser and the background process is limited to 2,200 kW (found by interpolation in the GCC for a modified temperature of 110°C). If, however, the pressure of the column is increased slightly, the condenser and reboiler temperatures will increase accordingly, and the enthalpy box representing the column would fit into the heat pocket of the GCC. Increasing pressure will in most cases make the separation more difficult, and thus there is a need for more equilibrium stages in the column or more reflux (with a balanced trade-off, this normally means an increase in both number of stages and reflux). This is indicated in Fig. 4.7 by making the dashed rectangle for the column after pressure increase somewhat wider along the enthalpy axis, since reboiler and condenser duties are proportional to the reflux.

In summary for this example, the background process requires 2,300 kW of external heating while the distillation column needs 3,000 kW heating in the reboiler, a total of 5,300 kW. Total cooling is correspondingly 2,500 + 3,000 = 5,500 kW. By integrating the column condenser with cold streams above the Pinch, it is possible to utilise 2,200 kW of the condenser duty. This means that 2,200 kW of savings are made in external heating (41.5%) as well as cooling (40%). However, using process modifications, in this case

© Woodhead Publishing Limited, 2013

a slight increase in the column pressure, makes it possible to integrate the entire condenser and save 3,000 kW of external heating (56.6%) and cooling (54.6%). The disadvantage with this last scheme, which saves an additional 800 kW, is the need to integrate both the condenser (totally) and the reboiler (partly) with corresponding operational challenges related to the control of the column.

4.6 Network Design

With Performance Targets for energy and units, the next step is the actual design of the Heat Exchanger Network. One of the most significant features of Pinch Analysis is that the insight obtained in establishing Performance Targets ahead of design actually forms the core of the design methodology. The discovery of the Heat Recovery Pinch in the early and late 1970s was followed by the understanding that in order to design Heat Exchanger Networks with minimum external heating and cooling requirements, decomposition at the Pinch, and the development of two independent networks were absolute requirements.

4.6.1 The Pinch Design Method (PDM)

The PDM was outlined by Linnhoff and Turner (1981) and also by Linnhoff *et al*. (1982) before it was comprehensively described by Linnhoff and Hindmarsh (1983). The PDM provides a strategy for developing the network sequentially, deciding on one heat exchanger at a time with rules for matching hot and cold streams for these heat exchangers. The method also indicates when and how stream splitting should be applied. The key elements of a simplified version of the PDM are the following design actions and rules:

- Decompose the heat recovery problem at the Pinch.
- Develop separate networks above and below Pinch, starting at the Pinch.
- Start network design immediately above and immediately below Pinch, since this is where the problem is most constrained (small driving forces) and thus where the degrees of freedom to match hot and cold process streams are most limited.
- Assign Pinch Exchangers first (units that bring hot streams to Pinch Temperature above Pinch and cold streams to Pinch Temperatures below Pinch), then assign the other process-to-process units, and finally install utility exchangers where required to reach the target temperatures for the streams.

© Woodhead Publishing Limited, 2013

- Use the *CP* rules (see Equation [4.8]) to decide on the matching between hot and cold process streams in the Pinch Exchangers.
- Whenever the *CP* rules cannot be applied or the topology rules (see Equation [4.9]) are broken, stream splitting has to be considered.
- For each accepted match, maximise the duty of the heat exchanger to increase the probability of reaching the target for fewest number of units (i.e. the 'tick-off' rule).

Pinch Exchangers will have minimum allowed driving forces ($\Delta T_{\min}$) in the cold end (units above Pinch) or the hot end (units below Pinch) of the heat exchanger. Since the driving forces are at the minimum, there can be no further reduction, and the *CP* rules assure exactly that. Also, there has to be at least one stream (or branch of a stream) of the opposite type to bring the hot streams (above Pinch) and cold streams (below Pinch) to the Pinch Temperature. The resulting *CP* rules and topology rules are fundamental when applying the PDM:

$$\text{Above Pinch:} \quad CP_{Cj} \geq CP_{Hi} \qquad \text{Below Pinch:} \quad CP_{Hi} \geq CP_{Cj} \qquad [4.8]$$

$$\text{Above Pinch:} \quad N_C \geq N_H \qquad \text{Below Pinch:} \quad N_H \geq N_C \qquad [4.9]$$

If either the topology rules Equation [4.9] are not satisfied for the entire set of streams, or the CP rules Equation [4.8] are not satisfied for each and all of the Pinch Exchangers, then stream splitting is required, and a detailed discussion on this topic is provided in Section 4.6.3.

When the Pinch Exchangers are installed, the next important task is to utilise any remaining heat in the hot streams above Pinch and any remaining cooling in the cold streams below Pinch. This can be achieved by adding more process-to-process units, and in this case the matches are no longer restricted by the *CP* rules, since the driving forces have opened up when moving away from the Pinch. Whenever a match violates the *CP* rules, however, the temperature difference of the heat exchanger must be checked.

In this simplified version of the PDM, it is assumed that utility exchangers are placed last where necessary, to obtain the target temperatures of the streams. With multiple utilities at different temperature levels, this is obviously not a good strategy as will be shown in Chapter 8.

4.6.2 Developing an Initial MER Design

Next, the actual use of the PDM will be demonstrated using the simple process example presented in Fig. 4.1 with stream data in Table 4.1. The results

© Woodhead Publishing Limited, 2013

from the Targeting stage and the subsequent process modification stage can be summarised as follows:

- Increasing the pressure of the distillation column would allow complete integration of the column condenser with cold streams above the background Process Pinch saving 3 MW of external heating and cooling; however, this change will not be made here in order to keep the case study simple, and the stream data of Table 4.1 will be used.
- Integration of the distillation column without process modifications will save 2,200 kW of external heating and cooling, and the Grid Diagram in Fig. 4.4 will be used to design the Heat Exchanger Network.
- When the condenser and reboiler are included in the stream data (with the intention to partly or fully integrate the column), the following Targeting results were obtained:
  - Overall Process Pinch (with background process and distillation column): $T_{\text{pinch}} = 120°\text{C}/100°\text{C}$ for hot/cold process streams.
  - Minimum external heating: $Q_{H,\min} = 3{,}100$ kW.
  - Minimum external cooling: $Q_{C,\min} = 3{,}300$ kW.
  - Minimum number of units that is compatible with MER: $U_{\min,}\text{MER} = 5 + 4 = 9$ (five units above and four units below Pinch).
  - Minimum number of units when relaxing Pinch Decomposition: $U_{\min,\text{global}} = 7$.

The Grid Diagram in Fig. 4.8 is the same as in Fig. 4.4, however with additional information about CP and ΔH to make the design process easier. The heat exchangers have been numbered according to the sequence they were introduced into the network. Utility exchangers are marked H for heaters and C for coolers. Notice that since hot stream H1 is cooled to 130°C, which is above the hot Pinch Temperature (120°C), there is only one Pinch Exchanger above Pinch (for hot stream H2). Below Pinch, both cold streams C1 and C2 require Pinch Exchangers. In Fig. 4.8, all relevant duties (in kW) and temperatures are provided.

The Grid Diagram with the MER design in Fig. 4.8 clearly illustrates the advantages of this representation, compared to the traditional way to draw the process flowsheet. The Pinch Point location and the decomposition into two separate Heat Exchanger Networks above and below Pinch can be easily seen. For each heat exchanger it is very easy to check the driving forces, since the process streams are drawn in a counter-current way. This means that the hot inlet to a heat exchanger is drawn vertically above the cold outlet from the same unit, with easily available information about the hot end of the exchanger. Likewise, the hot outlet from the heat exchanger is drawn vertically above the cold inlet to the same unit, with easily available information about the cold end of the exchanger. Further, as will become

© Woodhead Publishing Limited, 2013

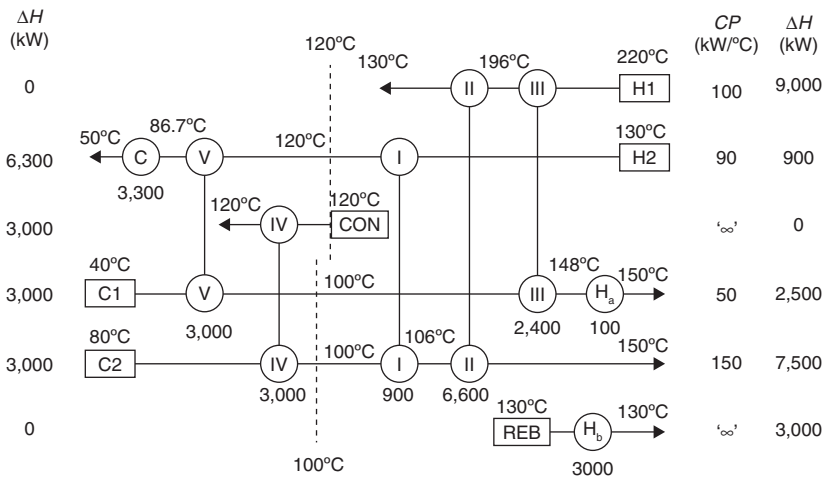

4.8 MER Network for the illustrative example.

evident in the retrofit design case described in Chapter 8 (Section 8.4), if the four temperatures for each exchanger are logically positioned relative to the vertical dashed line that marks the Pinch (above/below or right/left), then cross-Pinch heat transfer is easily identified graphically.

When an MER design is established using the PDM, one should always check the developed network versus the Performance Targets calculated at earlier stages of the Heat Integration project. From Fig. 4.8, the following can be established:

- External heating: $Q_H = 100 + 3{,}000 = 3{,}100 = Q_{H,\min}$
- External cooling: $Q_C = 3{,}300 = Q_{C,\min}$
- Number of units: $U = 5+2+1 = 8 < 9 = U_{\min,\mathrm{MER}}$

Since the PDM decomposes the design problem at the Pinch, the resulting network will always meet the energy targets, unless errors are made during design. Such errors can be use of hot utility below Pinch or use of cold utility above Pinch. For industrial size problems there will be cases where it is not straightforward to develop an MER design, especially if the Composite Curves have a parallel shape or if there are Near-Pinches. Some of these problems will be addressed in Chapter 8 (Section 8.3). It could also be argued that the target values for minimum external heating and cooling are firmly based on thermodynamics and therefore represent rigorous targets.

The situation is quite different for the number of heat exchangers in the resulting network. The $(N - 1)$ rule that forms the basis for the Targeting formulas for the minimum number of units (Equations [4.5] and [4.6]) is a

© Woodhead Publishing Limited, 2013

simplification of Euler's Rule from graph theory ($U = N + L - S$). As explained in Section 4.4.2, in order to establish a formula that could be applied ahead of design, assumptions had to be made regarding loops ($L = 0$) and subnetworks ($S = 1$). Of course, this means that the target formulas are not rigorous, and there will be cases where the number of heat exchangers in the network can be both larger and smaller than the number of units obtained by the ($N - 1$) rule. The network in Fig. 4.8 has one unit less than the target value, and the reason is that there is a perfect match between the cooling requirements (3,000 kW) in the condenser (CON) and the heating requirements (3,000 kW) of cold stream C2 below Pinch, thus introducing subnetworks. This means that below Pinch, the number of units becomes ($N - 2$) rather than ($N - 1$). This perfect match saves one unit, and the two subnetworks are [H2, C1, CW] and [CON, C2].

4.6.3 A Strategy for Stream Splitting

In Heat Exchanger Networks there are three different reasons why it is often beneficial and profitable to split process streams into two or more branches:

- Reduce energy consumption.
- Reduce total heat transfer area.
- Reduce the number of units.

In this section, focus will be on the relation between stream splitting and energy consumption (external heating and cooling). In Chapter 8, Section 8.3.3, the effect of splitting streams on heat transfer area will be discussed. The last of these three situations will not be discussed in detail, but refers to cases where there is a single or a few streams of one type (hot or cold) and many streams of the opposite type (cold or hot). The best process example is in oil refining, where the crude oil is preheated by a considerable number of hot streams coming from the main fractionator (distillation column) and elsewhere in the plant. In order to fully utilise these hot streams with much smaller CP values, cyclic matching has been used, resulting in a large number of heat exchangers. When the crude is split into several branches, each of the hot streams can be utilised in a single match, and the number of heat exchangers can be considerably reduced. This is in fact what has happened over the years in these so-called crude preheat trains.

In the application of the PDM, situations are commonly encountered where stream splitting is an absolute requirement in order to design Heat Exchanger Networks that achieve minimum external heating and cooling. Figure 4.9 illustrates two such cases where stream splitting is required to develop an

© Woodhead Publishing Limited, 2013

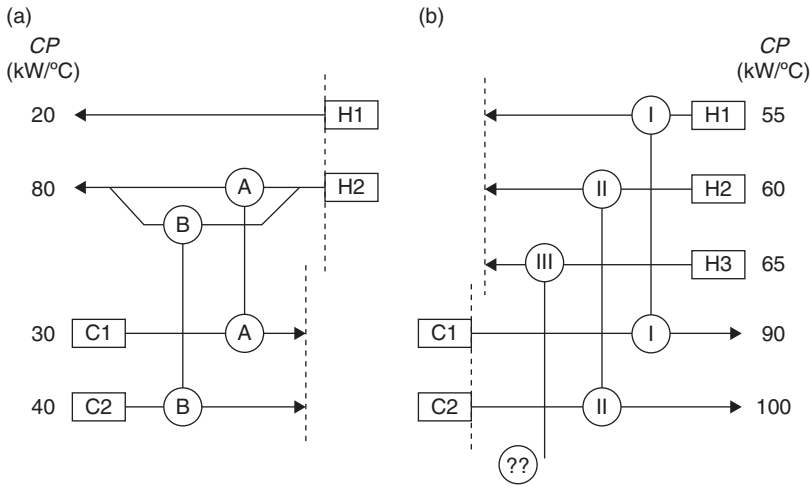

4.9 Stream Splitting Situations (a) Below Pinch and (b) Above Pinch.

MER design. In Fig. 4.9a, hot stream H1 cannot be used in a Pinch Exchanger with any of the cold streams, since the *CP* value of H1 is too small. Splitting one of the cold streams to make it possible for H1 to participate in a Pinch Exchanger is not a good idea, since then the topology rule would be broken (three cold stream branches and only two hot streams). Since, however, hot stream H2 has a *CP* value that is larger than the sum of the *CP* values for the two cold streams, a split of H2 results in two branches that can bring the two cold streams to Pinch Temperature and the problem is solved.

In Fig. 4.9b, there are three hot streams above Pinch, while there are only two cold streams available to bring these hot streams down to Pinch Temperature. In this case, the topology rule Equation [4.9] is broken, and a cold stream has to be split in order to have three cold streams (including branches). Considering the *CP* values in this case, however, it is not possible to split any of the cold streams into two branches that both have *CP* values large enough to bring a hot stream to Pinch Temperature. This means that the *CP* rule Equation [4.8] cannot be satisfied for all the Pinch Exchangers, and one of the hot streams will have to be split. The result then is a return to the original problem, where the number of hot streams is greater than the number of cold streams, thus violating the topology rule, and further stream splitting is required.

At this stage, one may question whether it is always possible to split a number of hot and cold streams in such a way that all Pinch Exchangers satisfy the *CP* rule, while at the same time not violating the topology rule. The key to this question is an understanding of the concept of the Heat Recovery Pinch. The definition of the Pinch is that temperature driving forces are at

© Woodhead Publishing Limited, 2013

its minimum, and in the immediate vicinity of the Pinch (just above and just below), the Composite Curves are opening up when moving towards higher and lower temperatures. This means that relations exist (Equation [4.10]) between the *CP* value for the sum of the hot streams and the *CP* value for the sum of the cold streams that are present close to the Pinch. Equality in Equation [4.10] only occurs when the Composite Curves are parallel, and the Pinch Point expands into a Pinch Region.

$$\text{Above Pinch: } \sum_j CP_{Cj} \geq \sum_i CP_{Hi} \quad \text{Below Pinch: } \sum_i CP_{Hi} \geq \sum_j CP_{Cj} \qquad [4.10]$$

Above the Pinch, the total *CP* 'resource' for the cold streams is large enough to allow the *CP* rule to be satisfied for all Pinch Exchangers bringing hot streams down to Pinch Temperature. Similarly, below the Pinch, the total *CP* 'resource' for the hot streams is large enough to allow the *CP* rule to be satisfied for all Pinch Exchangers bringing cold streams up to Pinch Temperature. The reason why it seemed difficult to find a good splitting scheme for the case in Fig. 4.9b (above Pinch) is that the total *CP* resource for the cold streams (190 kW/°C) is only slightly larger than the total *CP* value for the hot streams (180 kW/°C). As mentioned in Section 4.6.2, network design is more complicated when the Composite Curves have a near-parallel shape.

4.7 Design Evolution

While Pinch Decomposition guarantees the development of Heat Exchanger Networks with minimum external heating and cooling (relative to a specified value of $\Delta T_{\min}$), it also tends to produce networks in which some of the heat exchangers have a rather small duty. Since heat exchangers have an economy-of-scale type cost law as indicated in Equation [4.11], such small units will be quite expensive in capital cost for the limited amount of heat transferred or recovered.

$$\text{Cost}_{\text{hex}} = a + b \cdot A^c \qquad [4.11]$$

In Equation [4.11], a is the so-called fixed charge term, b is a cost coefficient, A is the heat transfer area (for some exchanger types, volume could be used instead of area) and c is the exponent in this power-law type cost equation. The economy-of-scale effect results from the fact that c is typically less than one, which means that the cost/area ratio reduces with increasing area. The fixed charge term is another economic argument for removing small heat exchangers.

© Woodhead Publishing Limited, 2013

The Pinch Decomposition also tends to produce networks with a considerable number of stream splits (although this was not the case for the small process example in Fig. 4.1, with corresponding Heat Exchanger Network in Fig. 4.8). However, the MER design should only be considered as an initial design that can be improved, both with respect to economy and network complexity. This section on design evolution will investigate the removal of small units by accepting a modest increase in external heating and cooling (energy relaxation). While the removal of small units has the potential to reduce total annual cost for the network, it may have the additional benefit of removing some of the stream splits. This is the case if the removed heat exchanger is located on a branch of a split stream. The effect will be reduced network complexity and cost and, in most cases, improved process operability.

4.7.1 A Three-Way Trade-off in Network Design

Similar to any design activity, Heat Exchanger Network Design involves a number of economic trade-offs. The three most important cost elements are external heating and cooling (Energy), total heat transfer area and the number of heat exchangers (Units). This three-way trade-off between Energy, Area and Units is to a large extent affected by the selected value of ΔT_{min}, and the optimum trade-off is the point at which the total annual cost of the network is minimised. Other elements that should be considered during optimisation are piping, control valves for stream splitting, network complexity, issues related to operability (including start-up and shut-down) and controllability; however, these aspects are beyond the scope of this chapter.

Design evolution is a simplified form of network optimisation, since the basic structure of the network is maintained while smaller changes are made to the network by removing small heat exchangers. As in any optimisation, design evolution also needs degrees of freedom. In Heat Exchanger Networks, the degrees of freedom that can be used to optimise the three-way trade-off mentioned above belong to one of three categories:

- Heat Load Loops
- Heat Load Paths
- Stream Splits.

Heat Load Loops in the network are a result of Pinch Decomposition and represent a relation between an even number of heat exchangers (two, four, six, etc.) in the sense that their duties can be modified without changing the enthalpy balance of the affected streams. The number of independent loops is equal to the difference between the actual number of heat

© Woodhead Publishing Limited, 2013

exchangers in the network (U) and the minimum number of units without Pinch Decomposition (U_{min}). Heat Load Paths in the network represent a relation between an odd number of units (three, five, seven, etc.) in the sense that their duties can be modified similarly to the Heat Load Loops. A major difference is that a path starts with a hot utility exchanger and ends with a cold utility exchanger. While loops are primarily used to remove small units from the network, paths are primarily used to restore violations of ΔT_{min} in the network that result from manipulating loops. Stream Splits in the network allow mass flowrates in the stream branches to be varied in order to minimise heat transfer area and thereby minimise cost.

4.7.2 Using Loops and Paths to Evolve Network Design

In Fig. 4.8 there is a very small heater (H_a) with a duty of only 100 kW, while the smallest process-to-process heat exchanger is 900 kW. The number of units in this MER design is eight, while the minimum number of units without Pinch Decomposition as calculated in Section 4.4.2 is seven. Using Euler's Rule from graph theory, the number of independent Loops can be found by Equation [4.12], when the number of subnetworks for the overall problem is assumed to be $S = 1$.

$$U = N + L - S \Rightarrow L = U - (N - S) = U - (N - 1) = U - U_{min} \qquad [4.12]$$

The number of independent loops in the MER design in Fig. 4.8 is then 8 – 7 = 1. This single loop (here referred to as L1) can be found by inspection to be:

$$\text{(L1):} \quad H1 \rightarrow (III) \rightarrow C1 \rightarrow (V) \rightarrow H2 \rightarrow (I) \rightarrow C2 \rightarrow (II) \rightarrow H1$$

A Heat Load Loop represents a degree of freedom, in the sense that the duties of the heat exchangers that are involved in the loop can be varied within limits. Another characteristic of such a loop is that the process streams involved in the loop flow through two of the units in the loop. This means that if the duty of one of these units is increased, then the duty of the other unit can (and has to) be reduced by the same amount, so that the enthalpy change for the stream remains unchanged, and the stream will reach its target temperature. It should be emphasised that utility exchangers can also be part of such Heat Load Loops, as long as these units operate with the same type of utility. This means that HP steam must be distinguished from LP steam, and cooling water must be distinguished from refrigeration, etc.

For loop L1, assume that the duty of the participating units is changed by x kW. In order to satisfy the enthalpy change for the participating streams

© Woodhead Publishing Limited, 2013

(H1, H2, C1 and C2), the change in duty for these heat exchangers must follow the scheme given in Equation [4.13].

$$Q_{III} = 2,400 + x, Q_V = 3,000 - x, Q_I = 900 + x, Q_{II} = 6,600 - x \quad [4.13]$$

Since heat exchangers with negative duties are infeasible, the optimisation variable x that represents the degree of freedom for this loop is bounded by: $-900 \leq x \leq 3{,}000$. While in principle one could optimise the network (i.e. minimise its total cost) by varying x in this region, the main objective of design evolution (which distinguishes it from optimisation) is to reduce cost and complexity in the MER design by removing small heat exchangers. For this particular case, unit I with the smallest duty in the loop can be removed if $x = -900$ kW.

The resulting network with updated duties and temperatures is shown in Fig. 4.10. Changing duties for the exchangers in loop L1 will actually violate Pinch Decomposition that was the basis for the MER design in Fig. 4.8. It should thus not come as a surprise that there is a penalty involved in removing one of the heat exchangers in the network. As indicated in Fig. 4.10, the temperature driving forces ($\Delta T_{min} = 20°C$) are violated in heat exchanger V, since the hot inlet temperature is 130°C while the cold outlet is 118°C, i.e. the temperature difference in the hot end of this unit is reduced to 12°C. One option is to accept this situation, which means that the penalty for removing unit I is an increase in heat transfer area for unit V. Alternatively, one could require that the driving forces in the network should be restored to ΔT_{min}, which means that

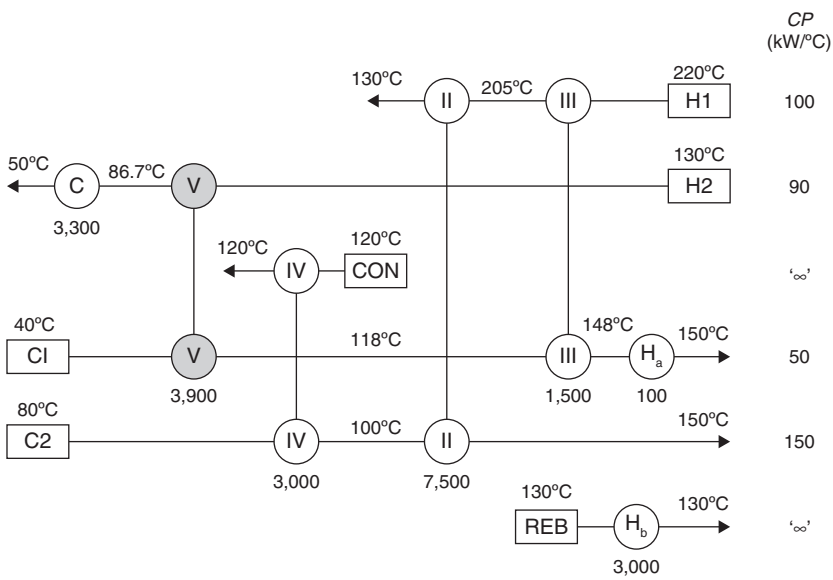

4.10 Evolved Networks for the illustrative example.

© Woodhead Publishing Limited, 2013

the penalty will be increased energy consumption. In an industrial setting, the penalty will be split into some additional heat transfer area and some additional external heating and cooling, dictated by the trade-off between capital cost and operating cost. For illustration purposes in this case, a Heat Load Path from hot utility to cold utility will be used to restore the temperature driving forces. The selected path has to affect the heat exchanger with too small ΔT in such a way that the driving forces will be restored.

For the network in Fig. 4.10, there is only one Heat Load Path:

$$\text{(P1): ST} \rightarrow (\text{H}_\text{a}) \rightarrow \text{C1} \rightarrow (\text{V}) \rightarrow \text{H2} \rightarrow (\text{C}) \rightarrow \text{CW}$$

It should be obvious that more steam and cooling water must be used to restore the driving forces. This is in line with the Composite Curves in Fig. 4.2, where increased external heating and cooling will move the two curves apart and increase the temperature driving forces. The change in duty for the units in the Heat Load Path should follow the scheme given in Equation [4.14].

$$Q_{\text{Ha}} = 100 + y,\ Q_{\text{V}} = 3,900 - y,\ Q_C = 3,300 + y \qquad [4.14]$$

The hot inlet temperature to heat exchanger V will remain at 130°C, which means that the cold outlet temperature must be reduced to 110°C to restore ΔT_{min} for this unit. This observation will determine the minimum value of the energy penalty y. By following cold stream C1 through heat exchanger V, the relation in Equation [4.15] can be established.

$$40 + \frac{(3,900 - y)}{50} = 110 \qquad \Rightarrow y = 400 \text{ kW} \qquad [4.15]$$

This means that the energy penalty for removing a heat exchanger with duty $x = 900$ kW is considerably less, i.e. $y = 400$ kW. The general relation between x and y is given by Equation [4.16].

$$0 < y \leq x \qquad [4.16]$$

The fact that $y < x$ for the example above can be explained as follows: when unit V (a Pinch Exchanger) is increased in duty from 3,000 to 3,900 kW, both the hot inlet and the cold outlet temperatures are changed (increased). This means that the duty of this heat exchanger does not have to be reduced to its original value of 3,000 kW in order to restore the driving forces. The resulting network (Design A) has the same structure as the design in Fig. 4.10 and will not be shown here. The units in the Heat Load Path (Equation [4.14]) will have their duties changed by 400 kW, with corresponding changes of the internal network temperatures for streams H2 and C1.

© Woodhead Publishing Limited, 2013

While the initial MER network is typically designed under stringent conditions of Pinch Decomposition and $\Delta T \geq \Delta T_{min}$ for all heat exchangers, the design evolution stage allows for relaxation and creative solutions. One should also keep in mind the distinction between hard and soft stream data discussed in Section 4.3.2. In the MER network in Fig. 4.8, there is a very small steam heater with a duty of only 100 kW in order to increase the temperature of cold stream C1 from 148°C to 150°C. If there is some 'softness' in the target temperature for C1, then this heater should not be installed, and one would accept 148°C as the modified target temperature for C1. If the original target temperature of 150°C is a hard specification, then this temperature can still be reached without installing such a small heater. The clue to this rather creative solution is to use the Heat Load Path P1 in the 'opposite' direction (see Equation [4.17]) to remove the small heater H_a rather than to use Heat Load Loop L1 to remove heat exchanger I.

$$Q_{Ha} = 100 - y, \quad Q_V = 3,000 + y, \; Q_C = 3,300 - y \qquad [4.17]$$

By choosing $y = 100$ kW, the resulting network uses 100 kW less steam and cooling water and it has one unit less than the MER design. Of course, this does not come without a penalty, and in the final network for this alternative (Design B) shown in Fig. 4.11, heat exchanger V has a temperature difference of 18°C in the hot end, which is a very small violation of ΔT_{min}.

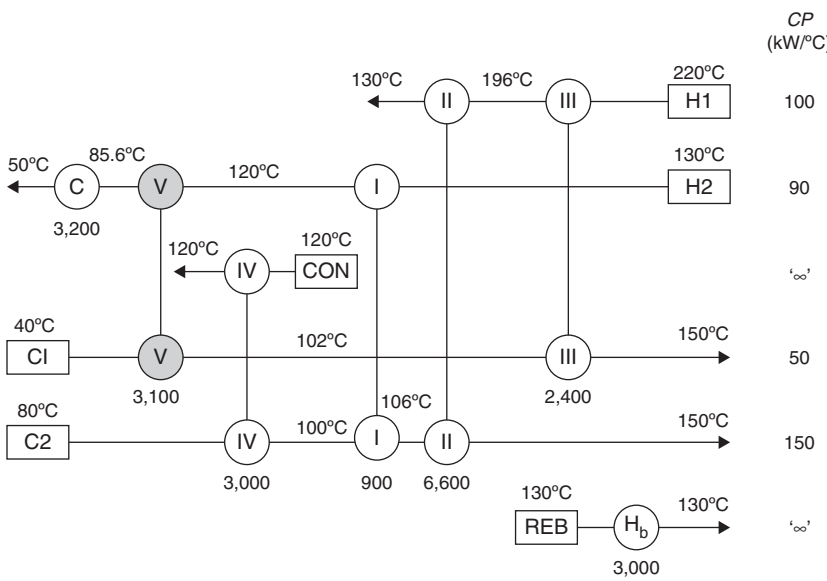

4.11 An Alternative Network (Design B) for the illustrative example.

© Woodhead Publishing Limited, 2013

Table 4.2 Alternative networks for the simple process in Fig. 4.1

Design	Q_H (kW)	Q_C (kW)	Units	ΔT_V (°C)
MER	3,100	3,300	8	20
A	3,500	3,700	7	20
B	3,000	3,200	7	18
C	3,000	3,200	6	10

Finally, when removing both heat exchanger I and heater H_a from the initial MER design, it is not possible to restore ΔT_{min} in the network, since there is no Heat Load Path. The only ΔT_{min} violation in this case is again heat exchanger V that has a temperature difference of 10°C in the hot end. This design is referred to as Design C and is shown together with the other network alternatives in Table 4.2. While focus in Table 4.2 is on ΔT_{min} violation in heat exchanger V, it should not be forgotten that the driving forces for some of the other heat exchangers in the network are also affected, but these effects are marginal for this particular example, and there are no other units that violate the ΔT_{min} specification.

In summary, even for very small processes (as in Fig. 4.1), there are a large number of different Heat Exchanger Networks that can be designed, with differences both in network topology and network parameters (stream temperatures and heat transfer area for the heat exchangers).

4.8 Conclusion

In this chapter, the main concepts, representations, procedures and graphical diagrams of basic Pinch Analysis for Heat Integration have been defined and illustrated with application to a small and simple process example. The most important topics covered in this chapter are:

- Data extraction and process modifications
- Plus/Minus Principle, Appropriate Placement and Correct Integration
- Performance Targets for Heating, Cooling and Number of Units
- Heat Recovery Pinch and Pinch Decomposition
- Composite Curves, Heat Cascade and Grand Composite Curve
- Grid Diagram and Pinch Design Method with Matching Rules
- Design evolution with Heat Load Loops and Paths
- Differences between grassroots and retrofit design

The treatment of the topics in this chapter has been kept on a fairly simple level to convey the most important concepts and provide insight and understanding that will hopefully make the reading of the other chapters

© Woodhead Publishing Limited, 2013

in the Handbook easier. For more reading material on these topics, readers are referred to textbooks published over the last 15 years by Shenoy (1995), Smith (2005), Kemp (2007) and Klemeš *et al*. (2010). Each book provides the state-of-the-art until the year when it was published.

For a more detailed and advanced approach to Heat Integration with focus on Heat Exchanger Network Design for both grassroots cases and retrofit projects, readers are referred to Chapter 8. A number of issues will be discussed and described in Chapter 8 that will add industrial realism to the material. Examples of topics that will be treated are targets for heat transfer area and total annual cost, multiple utilities, forbidden matches, different heat exchanger types and a brief introduction to the use of Optimisation in Heat Integration. The different stages in retrofit design of Heat Recovery Systems will also be described.

4.9 Sources of Further Information

The primary objective of this chapter has been to introduce the basics of Pinch Analysis as a foundation and core technology in the discipline of Process Integration. For further and more detailed information, the reader is advised to consult Chapter 8 on 'Analysis and Design of Heat Recovery Systems for Grassroots and Retrofit Situations' as well as all the other chapters of this handbook.

4.10 References

AspenTech. (2009). *Aspen Energy Analyser* – Reference Guide <www.aspentech.com> accessed 16.08.2012.

CANMET Energy Technology Centre. (2003). *Pinch Analysis: For the Efficient Use of Energy, Water and Hydrogen.* ISBN: 0–662–34964–4, <cetc-varennes.nrcan.gc.ca> accessed 12.08.2012.

Gundersen, T. (2000). A process integration primer. IEA Report, SINTEF Energy Research, Trondheim, Norway.

Hohmann, E.C. (1971). Optimum networks for heat exchange. PhD thesis, University of Southern California, Los Angeles, USA.

Huang, F., Elshout, R. V. (1976). Optimizing the heat recovery of crude units. *Chemical Engineering Progress*, **72**, 68–74.

Kemp, I. C. (2007). *Pinch Analysis and Process Integration*, 2nd ed. Butterworth-Heinemann (Elsevier), Oxford, UK (authors of the first edition: Linnhoff, B., Townsend, D. W., Boland, D., Hewitt, G. F., Thomas, B. E. A., Guy, A. R., Marsland, R. H. (1982 and 1994). *A User Guide on Process Integration for the Efficient Use of Energy.* IChemE, Rugby, UK).

Klemeš, J., Friedler, F., Bulatov, I., Varbanov, P. (2010). *Sustainability in the Process Industry – Integration and Optimization.* McGraw-Hill, New York, USA.

Linnhoff, B. (1979). Thermodynamic analysis in the design of process networks. PhD thesis, University of Leeds, UK.

© Woodhead Publishing Limited, 2013

Linnhoff, B., Dunford, H., Smith, R. (1983). Heat integration of distillation columns into overall processes. *Chemical Engineering Science*, **38**, 1175–1188.
Linnhoff, B., Flower, J. R. (1978). Synthesis of heat exchanger networks: I. Systematic generation of energy optimal networks, *AIChE Journal*, **24**, 633–642.
Linnhoff, B., Hindmarsh, E. (1983). The pinch design method for heat exchanger networks. *Chemical Engineering Science*, **38**, 745–763.
Linnhoff, B., Mason, D. R., Wardle, I. (1979). Understanding heat exchanger networks, *Computers and Chemical Engineering*, **3**, 295–302.
Linnhoff, B., Parker, S. (1984). Heat exchanger networks with process modification. IChemE Annual Research Meeting, Bath, UK, lecture.
Linnhoff, B., Townsend, D. W. (1982). Designing total energy systems. Chemical Engineering Progress, **78**, 72–80.
Linnhoff, B., Townsend, D. W., Boland, D., Hewitt, G. F., Thomas, B. E. A., Guy, A. R., Marsland, R. H. (1982). *A User Guide on Process Integration for the Efficient Use of Energy*, 1st ed. IChemE, Rugby, UK. Revised edition 1994.
Linnhoff, B., Turner, J. A. (1981). Heat-recovery networks: new insights yield big savings. *Chemical Engineering*, **88**, 56–70.
Linnhoff, B., Vredeveld, D. R. (1984). Pinch Technology has come of age. *Chemical Engineering Progress*, **80**, 33–40.
Linnhoff March Ltd. (1998). *Introduction to Pinch Technology*. Linnhoff March Ltd. Now part of KBC Advanced Technologies plc., UK.
Shenoy U. V. (1995). *Heat Exchanger Network Synthesis – Process Optimization by Energy and Resource Analysis.* Gulf Publishing, Houston, USA.
Smith, R. (2005). *Chemical Process Design and Integration*. John Wiley & Sons, Chichester, West Sussex, UK.
Smith, R., Linnhoff, B. (1988). The design of separators in the context of overall processes. *Chemical Engineering* Research and Design, **66**, 195–228.
Umeda, T., Itoh, J., Shiroko, K. (1978). Heat exchange system synthesis. *Chemical Engineering Progress*, **74**, 70–76.
Umeda, T., Niida, K., Shiroko, K. (1979). A thermodynamic approach to heat integration in distillation systems. *AIChE Journal*, **25**, 423–429.

© Woodhead Publishing Limited, 2013

5

Application of Process Integration to the Synthesis of Heat and Power Utility Systems Including Combined Heat and Power (CHP) and Industrial Heat Pumps

THORE BERNTSSON, SIMON HARVEY and MATTEO MORANDIN, Chalmers University of Technology, Gothenburg, Sweden

DOI: 10.1533/9780857097255.2.168

Abstract: This chapter discusses the main aspects of application of Pinch Analysis to the analysis and synthesis of heat and power utility systems for industrial processes. The chapter first reviews the basic concepts for the use of the Process Grand Composite Curve as a targeting tool. The chapter then discusses the application of this tool for synthesis and design of utility systems of main relevance in industrial practice, such as centralised heating systems, Combined Heat and Power (CHP) production system and industrial heat pumps.

Key words: Heat Integration, utility, synthesis, steam, CHP, heat pump.

5.1 Introduction

A chemical engineering *process* is commonly defined as a set of unit operations performing the core physical and chemical transformations of incoming feedstock into desired products. Such transformations usually require heating or cooling, and thus the process net energy requirements has to be balanced by *utilities*, which usually represent one of the major operating costs. The graphical representations provided by Pinch Analysis, in particular the Grand Composite Curve (GCC), can be used as powerful tools for obtaining qualitative and quantitative indications of the optimal choice of utility technologies (see Chapter 2).

The concept of Minimum Energy Requirement for an industrial process has been introduced in Chapter 2. The minimum utility loads are obtained through the solution of the Problem Table, and can be read directly from the Composite Curves. Such results give a first indication of how energy-demanding the process under investigation is, but still constitute rather abstract information since the utility costs depend ultimately

© Woodhead Publishing Limited, 2013

on the specific technology selected to satisfy the given loads at the required temperature levels. For this reason, it is more appropriate to treat hot and cold utilities as real thermal streams with given characteristic heat capacities, temperature ranges and Minimum Temperature Difference contributions. In this chapter, and in particular in Section 5.2, the basic notions as well as some illustrative examples are provided to identify such information correctly.

Heating and cooling are often products of the degradation of an energy carrier of much higher quality, such as the chemical energy of a fuel or the electricity required to run a heat pump or a refrigeration cycle. Achieving low-cost hot and cold utilities is therefore intrinsically related to the efficient use of high-quality energy carriers. For example, if a net cooling demand exists under the ambient temperature, it is necessary to use refrigeration cycles, which are electricity consumers. Similarly, if a net heating demand appears at relatively low temperatures compared to fuel combustion, it can be of interest to cascade such heat through a heat engine cycle, thereby producing electricity and maximising the conversion of the chemical energy of the fuel. In this respect it is appropriate to treat process hot and cold utilities as the cold or the hot side of thermodynamic cycles. In this chapter, and in particular in Section 5.3, basic notions and some examples of the correct choice and placement of advanced power, refrigeration and heat engine cycles are provided.

Many of the methodological aspects described in this chapter were introduced for the first time more than thirty years ago by two independent research groups, one in the UK (Linnhoff and Flower, 1978) and another a little later in Japan (Umeda *et al*., 1979) followed by Nishio *et al*. (1980). Much literature has been produced since then on further methodological developments (including mathematical programming) and applications. The main reference works are cited in the following text as key concepts are introduced; however, an exhaustive literature survey in the field of synthesis and design of process utility systems is beyond the scope of the present chapter. The reader is referred to the last section (Section 5.6) for a selection of sources of further information.

5.2 Targeting Utility Loads and Temperature Levels

In this section, hot and cold utilities are treated as thermal streams to be integrated with the *process*. We introduce a graphical methodology for obtaining qualitative and quantitative information about appropriate heating and cooling technologies based on interpretation of the process GCC as described in Townsend and Linnhoff (1983b) and also later in Itoh *et al*. (1986).

© Woodhead Publishing Limited, 2013

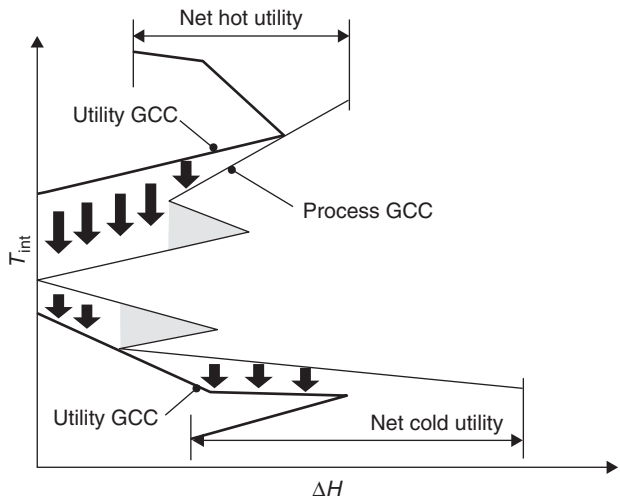

5.1 Principle of foreground/background representation of integration between a process and its utility system.

5.2.1 Basic Concepts

The idea is to graphically superimpose the utility thermal streams onto the GCC as shown in Fig. 5.1. The graphical representation of the utility thermal streams should be 'read' in the opposite way to the GCC of the 'background' process, since utilities are used to balance the process heating or cooling requirements (i.e. where the process is heated up the utility is cooled down, and vice versa). This graphical approach by which the utility thermal profiles are mirrored in the process GCC is also referred to as the 'foreground/background' or 'Integrated Grand Composite Curve' representation, which is used here to discuss the integration between utilities (foreground or Utility Curve) and process (background), but can also be used in discussing the integration between any subsets of a system's thermal streams.

Basic thermodynamic considerations indicate that the hot utility load, as well as the temperature level at which the heat is supplied, should both be minimised. This can be explained by considering that Maximum Energy Recovery for the total system is achieved by reducing the temperature difference (until a Pinch Point is activated) between the system (process plus utility) cold and hot thermal streams. However, it is important to note that the utility temperatures can be adjusted (by choosing the appropriate type and size of utility) whereas the temperatures of the process streams are imposed by the operating conditions of the background process equipment (e.g. reaction and separation temperatures). As discussed in the introduction to this chapter, this principle is justified by the idea of

© Woodhead Publishing Limited, 2013

maximising the conversion efficiency of high-quality energy carriers such as fuel or electricity.

However, industrial practice is based on economic considerations. Targeting maximum thermodynamic efficiency often results in high capital cost, and thus is usually not profitable. Therefore, energy conversion processes are often limited by the economic factors of the specific technology that is adopted as the utility system. This leads us to distinguish between several typical cases in industrial practice.

Hot utility generally implies fuel combustion. It is useful to differentiate between local (distributed) and centralised heat supply technologies. In local heating devices such as furnaces or immersed heaters, process streams are very close to the high-temperature heating source, thus limiting the required heat transfer surface. Alternatively, the same heating requirement can be covered by a centralised boiler in which the heat of combustion is transferred to a fluid that is then used to distribute the heat to the various process units through a network of headers and heat exchangers. These latter heating networks are of interest here, as these are the cases in which decisions on temperature levels can be taken with the help of the process GCC.

5.2.2 Steam Utility Systems

Steam is a very common fluid for heating purposes (Babcock & Wilcox, 1992). In Fig. 5.2 an example of a typical industrial steam network is shown. Water is heated up and evaporated in a centralised steam boiler. The energy required for this phase change is provided through fuel combustion. Steam is delivered to the process by means of headers. Heat is transferred to the process by means of heat exchangers where steam condenses at the saturation temperature corresponding to the header pressure. The condensate is then returned to the boiler.

In general, process heating is required at different temperature levels, therefore steam is delivered at different pressures, typically at medium (1–2 MPa) and low pressures (0.3–0.6 MPa). Although it might seem reasonable from a thermodynamic perspective to minimise the steam pressures and temperatures, adopting boiler technology for steam production implies that the heat is ultimately produced by fuel combustion. Thus high-quality fuel energy is substantially degraded due to the rather low temperatures at which the heat is delivered to the process. Accordingly, there are no thermodynamic reasons for reducing the pressure and the temperature of the steam network. Conversely, the design of a steam network is substantially driven by equipment-cost reasons, in particular by the cost of pressurised equipment and of the necessary safety devices and let-down valves. The diameters of medium or high pressure headers are also often smaller than

© Woodhead Publishing Limited, 2013

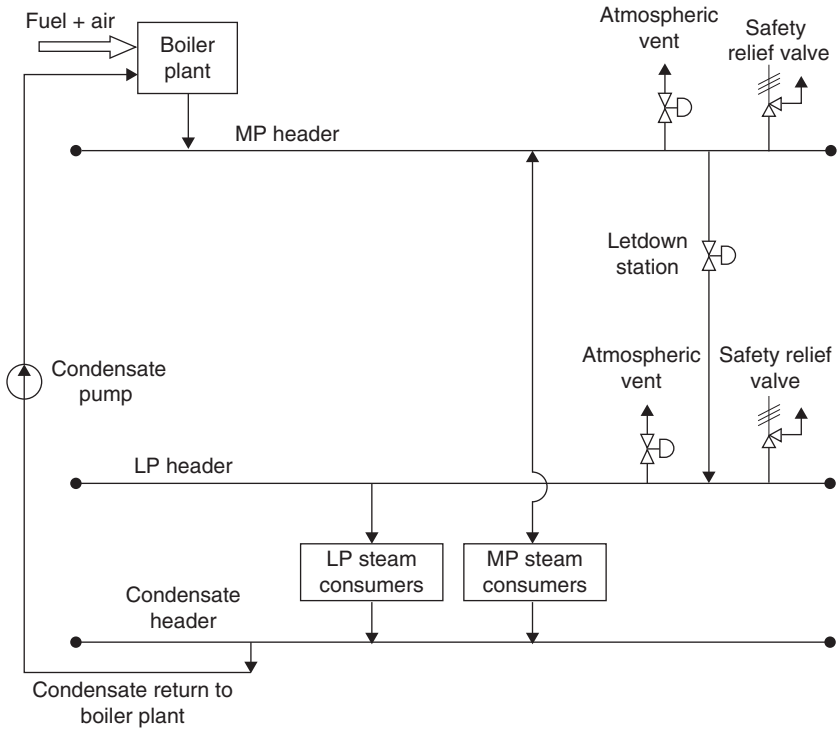

5.2 Example of industrial steam network with a MP and LP headers.

for low pressure ones, due to the greater steam density which reduces the amount of piping material. For this reason, medium pressure headers are sometimes preferred even though the heat is in this way delivered at much higher temperature than the minimum level at which is required by the process. In addition, different boiler technologies (water tube, fire tubes, etc.) are indicated for different pressure specifications.

Even though the steam network design parameters are ultimately chosen to achieve the best trade-off between the above equipment cost, the GCC can provide useful indications about the minimum quantities of medium pressure (MP) and low pressure (LP) steam required by a process.

In the example in Fig. 5.3, the MP and LP steam thermal profiles are represented against the GCC of a *background* process. The temperature scale on the y-axis is the corrected temperature (actual temperature adjusted by the Minimum Temperature Difference contribution) whereby the *Utility Pinch Point* (*UP*) is located where the GCCs for the background process and utility system touch each other. Such a representation is particularly useful when dealing with the appropriate placement of a utility. If LP steam is less expensive than MP steam, utility cost can

© Woodhead Publishing Limited, 2013

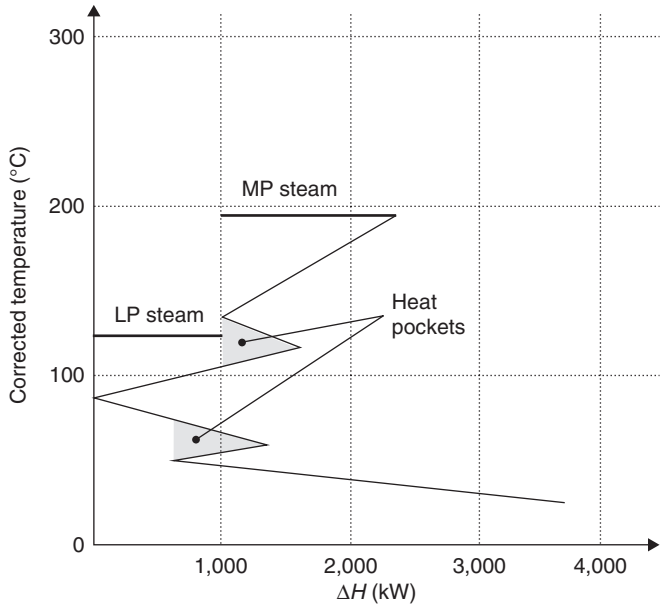

5.3 Graphical assessment of MP and LP steam loads for a given process based on GCC.

be minimised by targeting for maximum LP steam load, as described in Chapter 2.

In general, it is important to avoid supplying heat in heat pockets. Heat pockets represent self-sufficient parts of the process heat cascade so that any heating provided with hot a utility within such pockets constitutes a heat surplus that will ultimately be cascaded to the cold utility and should therefore be avoided. This is the case in Fig. 5.3 where the maximum LP steam load (1 MW) is constrained by a heat pocket. For this simple example, the MP steam load can be estimated by subtracting the LP steam load from the total hot utility load, given that the temperature of the MP steam is higher than that of the maximum process temperature. The maximum utility load at a given temperature is ultimately constrained by the heat transfer feasibility, i.e. the activation of a Pinch Point between the utility stream and the process GCC, commonly referred to as a *UP*.

5.2.3 Hot Oil Utility Systems

The heat transfer properties of superheated steam are poor compared to other types of heat transfer fluids. In addition, reheating low temperature steam in a boiler is usually prohibitively expensive. For this reason, steam is usually only used for latent-heat type of heating. The steam pressure sets

© Woodhead Publishing Limited, 2013

the temperature level at which steam heating is possible. Theoretically, pressures up to the water critical point (22 MPa, 374°C) are possible but, for cost reasons, pressures above 10 MPa are seldom implemented and pressures between 4 and 10 MPa are usually justified only if work-recovery steam turbines are also adopted.

As shown in Fig. 5.3, due to the discrete number of temperature levels at which steam heating is available, the temperature difference between the process and the steam can in some cases be quite large. For process reasons, such large temperature differences are sometimes not acceptable, so that a different type of heating technology is sought, preferably based on sensible heating. Pressurised water is an option but its application is limited to a maximum of 200°C. Mineral oils are often chosen for sensible heating at higher temperatures. The use of oils is advantageous compared to steam, mainly because oils remain in liquid state at atmospheric pressure for temperatures up to 320°C, after which thermal cracking can incur. The cost of oils is, however, much higher, so that they are used mainly for local heating or in small distribution systems. Synthetic oils, with better tolerance to high temperatures compared to mineral oils, can also be used for the same purpose, with the drawback of being more expensive. At very high temperatures, liquid alkali metals or molten salts are also sometimes used, generally as cooling media. Usage of such heat transfer media is generally imposed by the technological requirements of high-temperature energy conversion technologies such as nuclear reactors or solar concentrators.

Under the assumption that the amount of oil must be minimised, the Process GCC provides useful information about the oil temperatures required to cover the process hot utility. The Process GCC in Fig. 5.3 is taken again as an example in Fig. 5.4a where oil is now used as the hot utility instead of steam.

To minimise the cost of the oil charge it is of interest to evaluate the minimum mass flow rate necessary to provide the required process hot utility while respecting the Minimum Temperature Difference. This is usually limited by the activation of a *UP*. For the case in Fig. 5.4b, this occurs when the minimum oil temperature is equal to the Process Pinch Point (*PP*) temperature. For a given value of process heat requirement, a decrease in oil mass flow rate (assuming a constant oil specific heat) has to be counter-balanced by an increase in difference between the initial and final oil temperatures.

5.2.4 Delivery of Excess Process Heat to a District Heating Network

In the previous sections, practical examples of the use of the process GCC to target heat loads and temperatures of hot utility systems are given. The

© Woodhead Publishing Limited, 2013

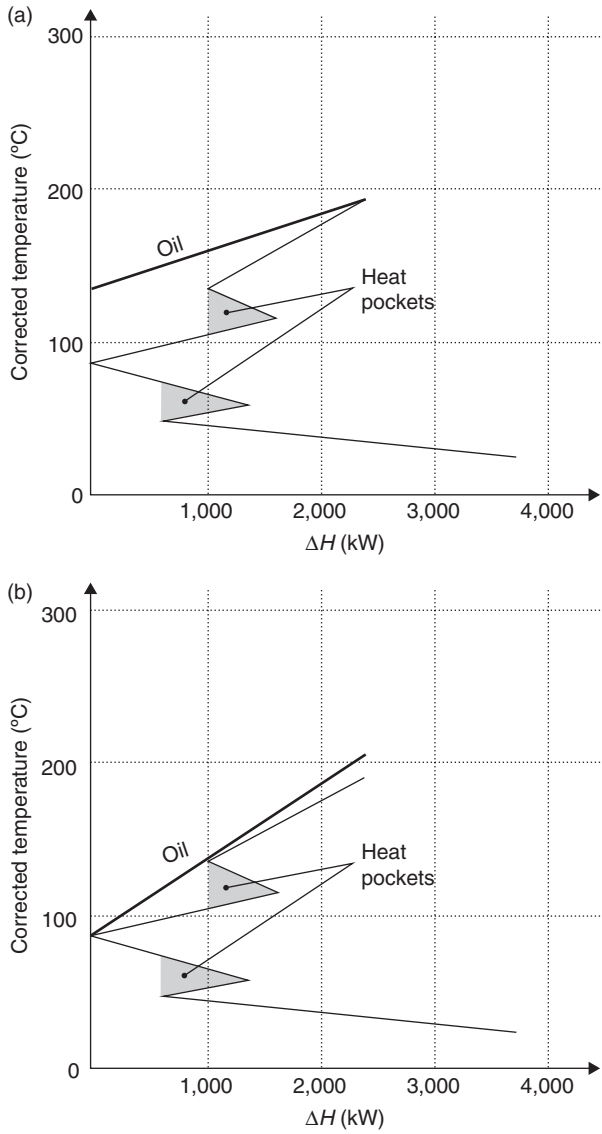

5.4 Graphical assessment of the hot oil temperatures for a given process GCC: (a) General case; (b) Case of minimum hot oil charge (minimum mass flow rate).

concept of the *UP* can be applied in similar way to target heat loads and temperatures for cold utility systems.

The case of the cold utility is usually not that relevant compared to the hot utility case, since in most of the industrial cases the hot utility is ultimately provided by expensive fuel combustion while the cold utility (unless under

© Woodhead Publishing Limited, 2013

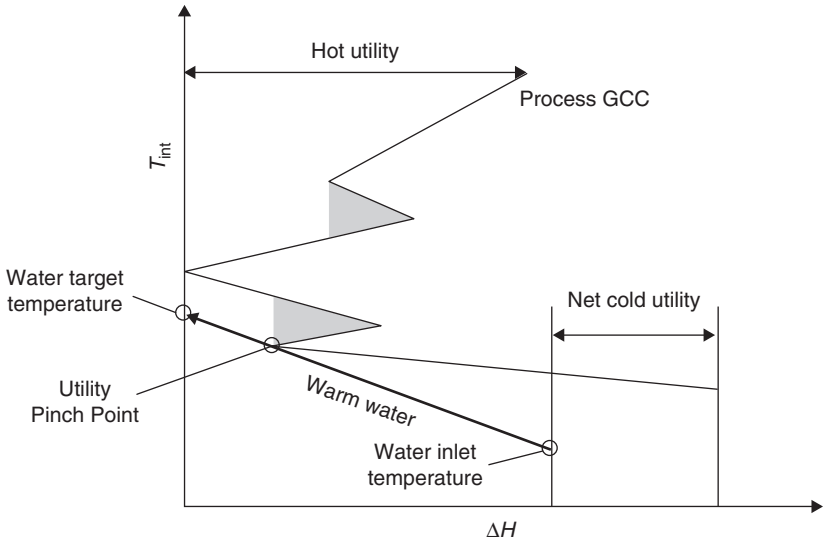

5.5 Principle of Heat Integration of a district heating system.

ambient conditions) is provided by cooling water at a relatively low cost. This implies that the cold utility end-temperatures are usually not that important unless the water is used further. This would be the case when an industry decides to produce hot water for internal use or for district heating delivery.

To estimate the maximum potential for hot water production it is necessary to specify the range of operating temperatures (supply and return) required by the specific end-use of the water (space heating, hot water for cleaning purposes, etc.). The maximum hot water mass flow rate can be estimated directly from the process GCC by identifying the hot water heat profile within the specified temperature range that activates the *UP* as illustrated in Fig. 5.5.

5.3 Integration of Advanced Energy Conversion Cycles as Process Utilities: Basic Concepts

Power and heat pump/refrigeration cycle devices convert heat energy into Mechanical Work or vice versa. The underlying principle is the change in properties of a thermodynamic medium that undergoes a cycle of transformations involving pressure changes (compression and expansion) and temperature changes (heating and cooling). The Second Law of thermodynamics indicates that this implies degradation of an energy carrier, thus producing not only the desired effect but also transfer of heat between two temperatures (Bejan, 1997).

© Woodhead Publishing Limited, 2013

Such devices are used in industry for power production, heating, cooling, or a combination thereof. For the case of cooling below ambient temperature, the use of a refrigeration cycle is necessary. The use of heat engines is justified mainly by a simultaneous need for heating and power for the process. As all thermodynamic cycles are based on the conversion of a high-quality energy carrier (such as fuel chemical energy or electricity), it is desirable to maximise the efficiency of such a conversion. The Heat Cascade of the energy conversion cycle should not significantly affect the Process Heat Cascade. In Pinch Analysis terms, this means that the increase in utility requirement with respect to the case with heating and cooling only should be very close to the net power input or output of the heat pump or power cycle. This means, for instance, that the increase in fuel chemical energy supply rate due to implementation of a heat engine power cycle should not significantly exceed the net engine electrical power output thereby maximising the co-generation marginal electrical efficiency. The principle of correct placement of heat engines and heat pumps with respect to a Process Heat Cascade were first introduced in two papers published by Townsend and Linnhoff (1983a, 1983b). To estimate size and energy targets, the heat cascade or the thermodynamic cycle can be compared with the process GCC, using the foreground/background analysis procedure as shown in Fig. 5.1. Such a representation can provide important indications about the type, size and operating parameters of appropriate cycles.

Figure 5.6 shows the thermal cascade characteristics of heat engines and heat pumps. Heat engines convert the heat available from a heat source (e.g. heat of fuel combustion) to Mechanical Work and heat which is rejected to a heat sink at a lower temperature. Heat pumps convert Mechanical Work (generally available by means of an electrical motor) into a heat flow from a heat source to a heat sink at a higher temperature. This is also the working principle of a refrigeration machine, with the only difference that the desired effect (cooling at lower temperature) is the opposite of a heat pump (heating at higher temperature).

The appropriate placement of such energy conversion cycles with respect to a Process Heat Cascade results from the working principles of heat engines and heat pumps. For a typical process thermal cascade, the Pinch Point divides the cascade into two parts with opposite heat behaviours: the process behaves as a heat sink (hot utility required) above the Pinch Point, and as a heat source (cold utility required) below the Pinch Point.

A heat engine can be integrated in two ways, as shown in Fig. 5.7. The integration with the process can occur by using the heat rejected by the engine to heat up the process above its Pinch Point (e.g. exhaust gases from a gas turbine are used for process heating). Alternatively, the heat available

© Woodhead Publishing Limited, 2013

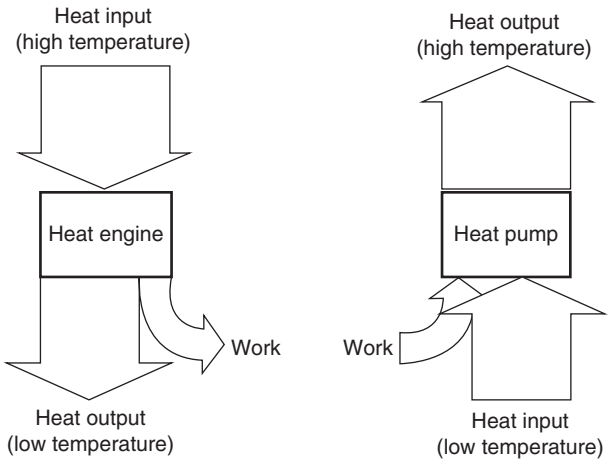

5.6 Energy flows for heat machines.

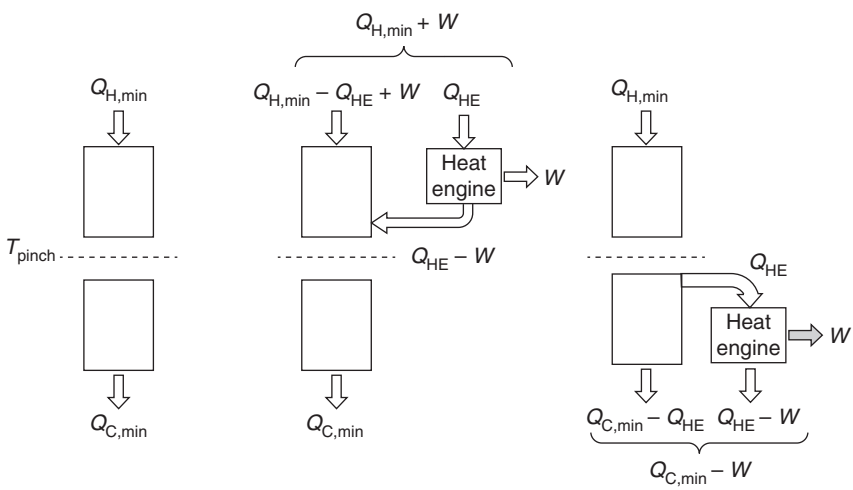

5.7 Optimum thermodynamic integration of a heat engine.

below the *PP* can be supplied to drive a heat engine (e.g. hot process effluents are used to run an organic Rankine cycle).

In the case in which the engine and the process are not integrated, the engine heat efficiency is equal to W/Q_{HE} and the total combined hot utility demand of the process and engine is therefore equal to the sum of heat demands of the constituting processes ($Q_{H,min} + Q_{HE}$). For an ideally integrated CHP system above the *PP*, the total system hot utility demand corresponds only to the power produced ($Q_{H,min} + W$). If correctly placed below

© Woodhead Publishing Limited, 2013

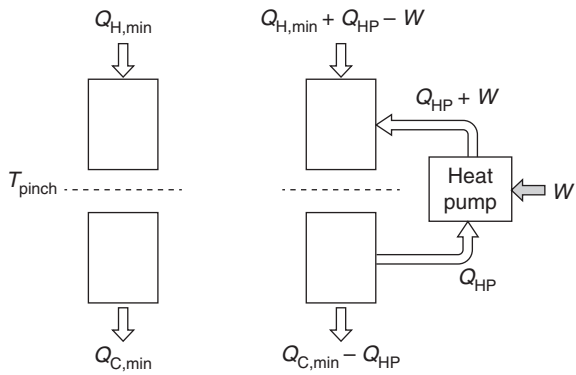

5.8 Optimum thermodynamic integration of a heat pump.

the Pinch, the engine uses the process heat to produce power, so that the heat cascaded to the cold utility is reduced by the same amount of mechanical energy ($Q_{C,\min} - W$). For such ideal integration, maximum conversion of heat into work is achieved. This is possible until the heat from the engine saturates the Process Heat Cascade (activation of one, or more, *UP*s), which determines the maximum amount of work that can be generated at maximum efficiency. To generate more work, the heat flow has to increase further and a Pinch Point violation appears, thereby cascading some heat through the Pinch Point and progressively reducing the conversion efficiency of the fuel energy.

The direction of the heat flow achieved by a heat pump is opposite to that of the background process heat cascade, as illustrated in Figure 5.8. Thus, appropriate heat pump integration is achieved by placing the machine 'across' the *PP* (Townsend and Linnhoff, 1983a). The benefit of such a machine is clear, given that the reduction in hot utility is larger than the spent Mechanical Work (W), part of the process cascade being balanced by 'recycling' heat (Q_{HP}) from below to above the Pinch. As for a heat engine, the maximum size of such a heat pump is achieved when a *UP* is activated, i.e. when the heat removed below the Pinch or the heat pumped above the Pinch saturates the Process Heat Cascade.

The criterion for appropriate placement of a heat pump applies also for a refrigeration machine, since they are based upon the same thermodynamic cycle (Linnhoff and Dhole, 1992). However, the Second Law indicates that the performances of heat pump and refrigeration cycles depend on the temperature levels of the heat sink and heat source required for their operation. In the case of a heat pump, the coefficient of performance $(Q_{HP}+W)/W$ is significantly affected by the temperature difference between the hot and cold sides, and this effect increases at low temperatures. This makes the use

© Woodhead Publishing Limited, 2013

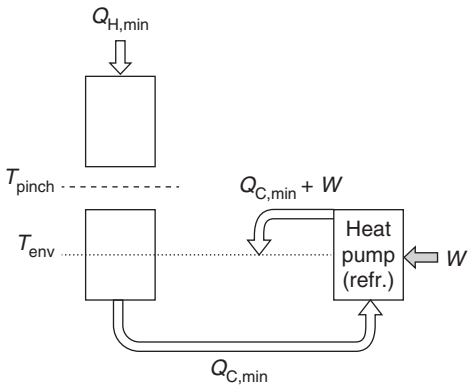

5.9 Principle of refrigeration.

of the heat pump profitable only if the process cascade presents a large heat deficit immediately above the Pinch Point and a large heat surplus immediately below the Pinch Point.

When cooling is required at sub-ambient temperatures, refrigeration is needed. In theory, an appropriate placement of a refrigeration machine would require recovering the heat from the condenser for process heating. This arrangement corresponds to a double-effect heat pump (refrigeration and heating). In fact, the temperature departure between the *PP* and the temperature at which refrigeration is required is often so large that the resulting low performance makes this type of machine unprofitable, with only few exceptions in residential applications.

For this reason, pure refrigeration machines are often preferred, in which the heat is pumped up to a temperature at which ambient heat sinks are available (cooling water or ambient air). As shown with a simple energy balance in Fig. 5.9, this is the case in which the process cold utility does not itself represent a consequence of the heat cascade, as thermodynamics (Second Law) shows that any form of energy degrades towards the temperature level of the environment. In fact, refrigeration occurs when an inappropriately placed heat pump is required for process reasons and therefore represents a total degradation of high-quality energy (e.g. electricity). The size and the operating temperature of such machines are therefore fully specified by the required refrigeration effect and no specific attention needs to be put on the activation of *UP* for the maximisation of Total Site performance.

The thermodynamic principles highlighted above have a general validity. However, as shown in Section 5.2, the integration of specific utility technologies might impose further considerations on the feasible temperature levels and heat capacities, which vary according to the different technologies.

© Woodhead Publishing Limited, 2013

In the following sections, examples of integration are given for advanced energy conversion systems that are commonly used in industry.

5.4 Process Integration of Heat Engines

5.4.1 Steam Turbine CHP

In Section 5.2, the use of a steam network for heating-only purposes was introduced. It was shown that steam can be delivered at different pressure levels according to the temperature level at which process heating is required. It was also shown that, when steam is produced by fuel combustion, the energy cost of process heating is in principle independent of the pressure level of the steam network. The choice of the pressure level, if not dictated strictly by process reasons, generally takes into account only the cost of piping and pressurised equipment.

It is clear that steam at high pressure and temperature has a higher potential for work production than saturated steam at MP or LP. For this reason, if the process has a simultaneous requirement for heat and power, it is profitable to produce power by expanding the steam from HP to LP in turbines before the steam is further used for process heating (Babcock and Wilcox, 2006). Alternatively, the cogenerated power can be sold to the power grid.

According to the principle of appropriate placement (and sizing) of heat engines discussed above, the conversion of fuel into work and heat can occur at maximum efficiency until the engine heat discharged at low temperature saturates the process heat cascade. This implies that expansion in the steam turbine has to stop at the pressure level at which steam condensation can be used for process heating. This steam system configuration is generally referred to as the back-pressure turbine.

For constant pressure levels of the steam network and steam superheating end-temperature, the efficiency of the steam cycle is unaffected by the steam flow rate. To increase power production, it is necessary to increase the fuel rate and the steam mass flow rate. Once the flow rate of the steam cycle is sufficient to activate the *UP*, the extra steam produced cannot be converted totally into power, since the process heating requirement is already satisfied. Thus, all the extra steam can be expanded down to the minimum technically achievable pressure (temperature) at which condensation with the cold utility can take place. This configuration is usually referred to as an *extraction/condensing* steam co-generation system. With the increase in size, the plant becomes increasingly similar to a condensing plant where only power is produced and significant amounts of low-grade heat are discharged to the environment.

As the focus of our discussion is the use of heat engines for high-efficiency CHP purposes, the case of back-pressure turbines is hereafter discussed in

© Woodhead Publishing Limited, 2013

more detail. The principles for Process Integration for this type of system are illustrated in Fig. 5.10, together with the corresponding graphical representation of its Heat Integration with a background process. High pressure steam is produced in a boiler. The steam expands through a turbine, thereby producing work W_{ST}. The LP turbine exhaust steam supplies heat (Q_{ST}) to the process above the Pinch. The recovered condensate is returned to the boiler. An energy balance for the boiler yields that the amount of fuel energy Q_{fuel} that has to be supplied to the boiler is equal to $Q_{ST} + W_{ST} + Q_{loss}$. If there were no losses in the boiler, the fuel energy supplied to the boiler in addition to that required to satisfy the process steam demand only would be converted at 100% efficiency.

For a Process Integrated steam turbine CHP, the choice of steam pressure (temperature) at which heat is delivered to the process influences the possibilities for electricity production. If there is only one distribution level (as in Fig. 5.10), the whole heating demand has to be satisfied with steam that temperature-wise satisfies the heating demand at the highest temperature in the process. The back-pressure in the steam turbine thus becomes relatively high. If several steam levels are used, the amount and temperature of these levels can be set so that heat is transferred to the process at lower temperatures. The steam is extracted from the turbine at the appropriate steam levels and as much steam as possible can be expanded to the back-pressure. In this way more heat expands in the turbine and increases the electricity production. This is the case in the example in Fig. 5.11 where the same process heating is divided into two temperature levels corresponding to the minimum pressures at which steam can be used for process heating.

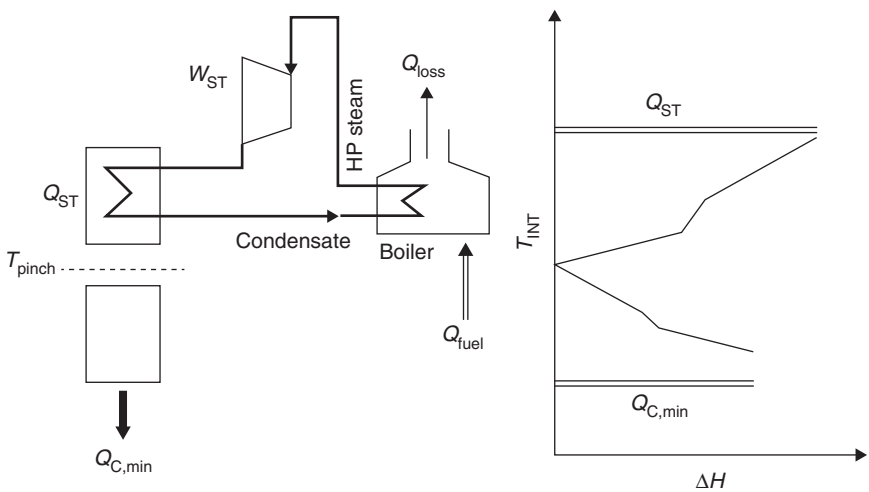

5.10 Integration of steam turbine CHP – the principles.

© Woodhead Publishing Limited, 2013

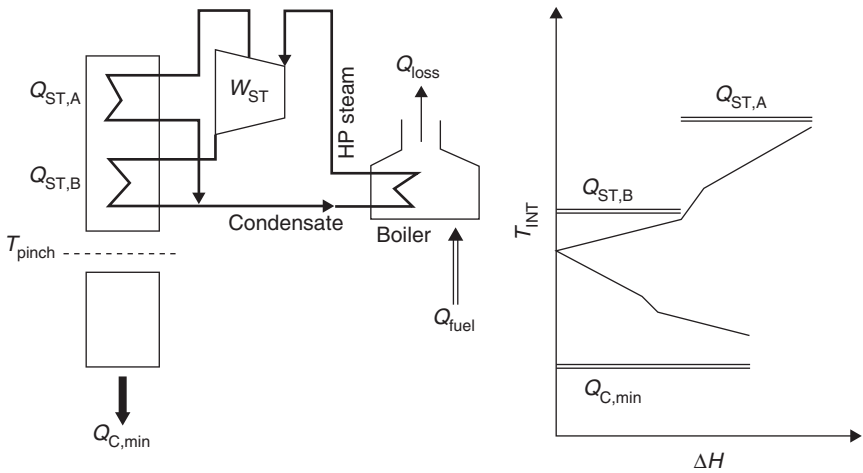

5.11 Steam turbine CHP with two back-pressure levels.

Steam networks with CHP production can also be used as heat recovery cycles. This is the case in which a background process presents a relatively high amount of waste heat at high temperatures. In these cases, the steam cycle behaves as a heat engine below the *PP*, which has therefore to occur at a temperature level that is sufficiently high to allow for MP or HP steam to be produced. This application is typical of the gas processing industry, where high-temperature synthesis gas is produced in a reactor and has to be cooled down before further processing. It is also typical that subsequent process steps (e.g. separation processes) require some heat at lower temperature for which low temperature steam is used.

As shown in Fig. 5.12, this leads to a hybrid configuration in which a steam network is used for heat recovery at high temperature and for process heating at low temperature. If the relative position of the heat engine with respect to the process thermal cascade is 'below the Pinch', the heat engine does not behave here only as a heat sink. The appropriate sizing of the steam network is therefore done by accurately evaluating the amount of steam at different levels in order to saturate the process heat cascade at several temperature levels, resulting in the activation of multiple *UP*s. In Fig. 5.12, in particular, due to the relatively low heating required at the LP level, further expansion of the steam at very low pressure through a condensing turbine stage is also considered.

5.4.2 Gas Turbine CHP

In a plant with a gas turbine, the hot exhaust gases from the turbine can be used to heat the process (Boyce, 2002). The principles for Process

© Woodhead Publishing Limited, 2013

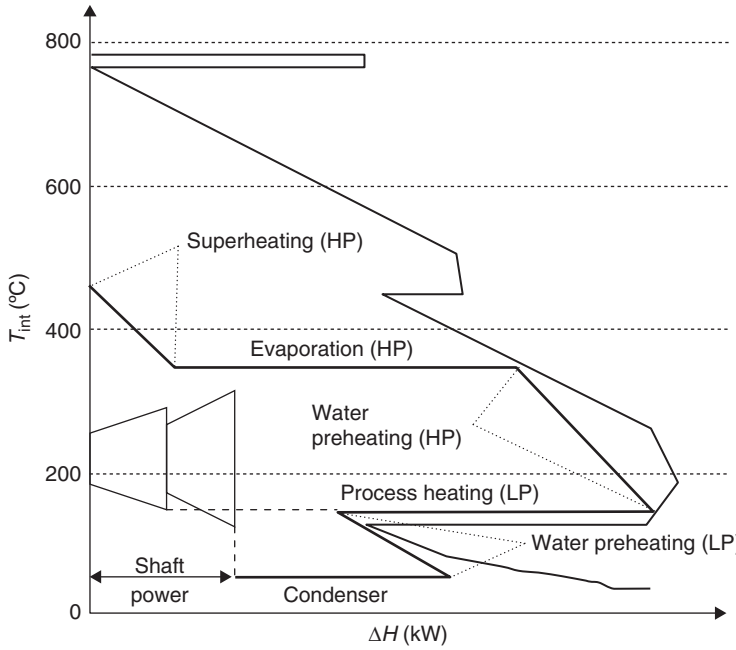

5.12 Heat recovery steam cycle with extraction (LP) and condensation.

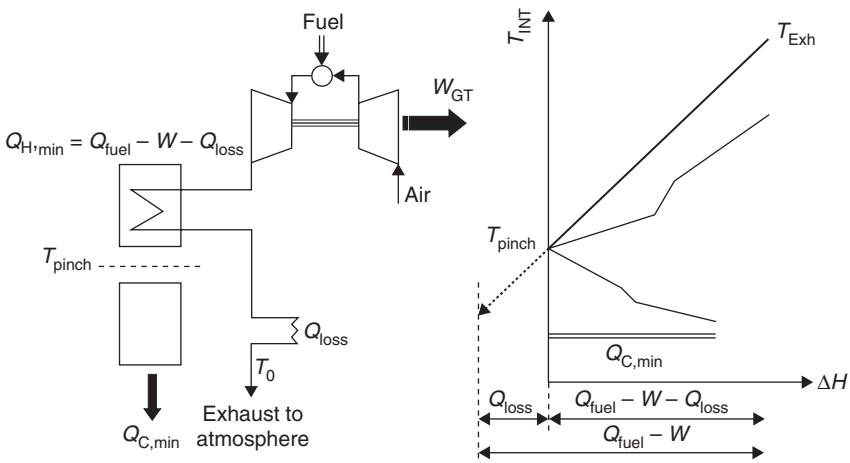

5.13 Integration of gas turbine CHP – the principles.

Integration for this type of system are illustrated in Fig. 5.13, together with the corresponding representation of its Heat Integration with a background process. Air enters a compressor where it is compressed before entering a combustion chamber, in which combustion of fuel increases its temperature.

© Woodhead Publishing Limited, 2013

The combustion gases are expanded in the turbine, which produces enough shaft work to drive the compressor and produce useful work (to drive an electricity generator for example). Heat can then be recovered from the expanded gas stream (turbine exhaust) to heat the process, and thereafter the gas stream is discharged to the atmosphere. Gas turbine CHP systems are normally only used for medium to large scale applications. Similarly to steam turbine CHP concepts, if there were no exhaust loss to the atmosphere (i.e. if Q_{loss} was zero), fuel energy would be converted at 100% efficiency. In practice, the amount of heat lost to the atmosphere depends on the turbine exhaust profile, the Pinch Temperature level and the shape of the process GCC.

For these reasons, the appropriate size and, to some extent, the appropriate gas turbine cycle parameters, can be studied using the principles of Pinch Analysis.

As discussed above, process heating can be done through centralised systems (furnace plus heat distribution network), or by means of a combination of several local heating devices (small furnaces, etc.). Direct process heating with gas turbine exhaust gases is one of these latter cases, and due to the high temperature and large volumes of the gases, it is in fact implemented only in special situations, e.g. furnace heating in a refinery or drying.

A gas turbine produces exhaust gases of a given temperature, T_{Exh} (see Fig. 5.13), and this determines the temperature level at which the heat is available for the process. Usually, the lower the exhaust temperature the higher is the gas turbine electrical efficiency as a result of high expansion ratios.

Heat transfer with the process occurs through convection, so the exhaust gases are cooled down while exchanging heat with the process. The exhaust gas end-temperature is, however, limited by technical reasons to be at least above 100°C approximately. Following the general rule for Heat Integration of utility systems, the minimum size of gas turbine can be therefore estimated by identifying the appropriate heat capacity (i.e. exhaust mass flow rate) that activates a *UP* with the background process, while respecting the technical constraints on exhaust temperatures (so no *UP*s are activated below the stack temperature). This leads in some cases to evaluating integration opportunities for different gas turbines with varying efficiencies and sizes. The final choice is determined by profitability criteria accounting for both capital and operating cost.

The general principles of the use of process GCC for such evaluations are explained graphically in Fig. 5.14.

If the *PP* is at a temperature higher than the minimum allowable stack temperature (Fig. 5.14 left), the *PP* determines the temperature below which all the heat available is lost to the stack. Therefore, to maximise the efficiency of fuel conversion into heat and power, the exhaust gas profile

© Woodhead Publishing Limited, 2013

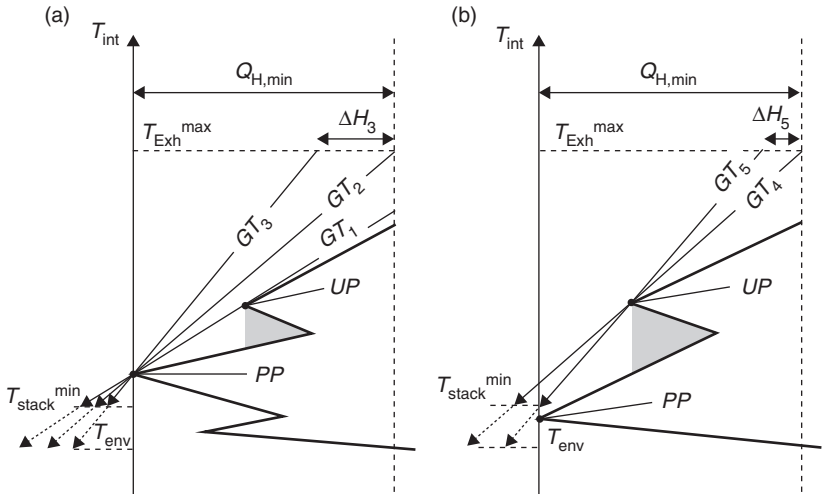

5.14 Energy consequences of different choices of gas turbine for process heating. (a) Minimum allowable stack temperature is below the *PP*. (b) *PP* is below the minimum allowable stack temperature.

should activate a *UP* at the *PP*. Gas turbines with different values of turbine outlet temperature can be chosen. In this example, GT_1 has the lowest T_{Exh} which still enables the full process heating requirements to be satisfied. Note that the GT_1 exhaust gas profile activates a second *UP*. A smaller size gas turbine requires a higher value of T_{Exh} (GT_2 in the figure). Note also that since T_{Exh} is directly related to the gas turbine's electrical efficiency and other thermal material constraints in the hot sections of the engine, there is a maximum temperature level at which gas turbines are available on the market (T_{Exh}^{max}, currently approximately 600°C). In the example, the size of GT_2 is therefore the minimum size for which a gas turbine is still able to deliver the required heat to the process. A further decrease in gas turbine size (case GT_3) implies that a portion of the process hot utility (ΔH_3 in figure) must be satisfied with a separate heat source.

It can be observed that if most of the process heating is required at high temperatures (Fig. 5.14, right), the high-temperature *UP* substantially hinders the total heat recovery from gas turbine exhaust gases even if the *PP* is at a temperature lower than the stack temperature. In such a situation, to minimise the stack losses while achieving maximum possible efficiency of fuel conversion, a heat deficit ΔH_5 appears. which has to be covered with a separate high-temperature heating device. Although the investment in separate heating equipment is sometimes preferred for backup reasons, profitability evaluation might suggest reducing the capital cost by investing in the gas turbine only (case GT_4) even if this implies higher stack losses.

© Woodhead Publishing Limited, 2013

5.4.3 Combined Gas Turbine and Steam Network CHP

Direct heat exchange between the exhaust gases and the process streams is, in reality, only possible in certain special industrial situations. In most cases the heat distribution to the different consumers within a plant is most commonly achieved using steam distribution systems at one or several pressure levels. Due to the advantages of a centralised system, a more common gas turbine CHP configuration consists in using the heat from the exhaust gases to produce steam which is then distributed to the process through a network (Boyce, 2002).

This is here referred to as a 'combined' configuration since this technology consists of a combination of gas turbine and steam network. In such arrangements the utility system resembles steam systems with a boiler and turbine, with the only difference that a gas turbine is used instead of a boiler. Due to the much lower temperatures at which the exhaust gas heat is available compared to fuel combustion in a furnace, the estimation of optimal pressure levels of the steam network is of high importance, as it does not influence only the costs of the piping and of the pressurised equipment but also CHP targets, due to the possible activation of multiple *UP*s.

It is worth noting that if the steam system is equipped with an expansion turbine for additional power generation, a 'combined cycle' configuration is obtained (topping gas turbine cycle plus bottoming steam cycle), which allows in general very high electrical efficiency (up to 60% in condensing mode operation). In such an arrangement, however, the gas turbine and the steam cycle parameters are chosen in order to optimise the Hat Integration between the top and bottom cycle in order to maximise the power generation. This implies for instance building special gas turbines with rather low compression ratios (almost half that of commercial stand-alone gas turbines) in order to achieve higher exhaust gas temperatures. To recover most of the heat, multiple steam pressure levels and very high pressures are also implemented. Such design choices are fully justified by the increase in electrical efficiency for condensing power plant applications but are essentially non-existent in CHP plants. Due to the tight constraints imposed by the relatively low temperature of the hot gases compared to a furnace, the most typical CHP application of a gas turbine is in combination with a steam network in which no steam turbines are considered.

The principles are shown in Fig. 5.15, in which three steam pressure levels (LP, MP, HP) are assumed. The introduction of intermediate distribution systems is viable only with an increase of total temperature differences between the gas turbine exhaust profile and the process. This is particularly true for the case of steam networks in which steam condensation occurs at discrete temperature intervals (latent heat) as shown in the example in Fig. 5.15. This implies that the stack temperature is determined by the steam

© Woodhead Publishing Limited, 2013

temperature at the lowest pressure level (LP in the figure), or possibly by feed-water preheating if the condensate returns at a temperature much below saturation. In the example shown in the figure, if only the MP and HP levels were adopted, the MP steam would need to cover the remaining heating demand that is currently covered by the LP steam, with an increase in the minimum stack temperature and therefore an increase in gas turbine size. To obtain the lowest possible size of the gas turbine (i.e. to increase the fuel conversion efficiency), several steam levels can be therefore adopted, with the drawback of an increase of investment on the steam network. A profitability analysis has to be carried out to find the best trade-off between capital cost and the fuel conversion efficiency.

5.4.4 Organic Rankine Cycle CHP

Steam networks and gas turbine based CHP plants are examples of heat engine applications in which the engine operates as a heat source for the process, i.e. its position with respect to the process heat cascade is 'above the Pinch'. The particular case of a heat recovery steam cycle 'below the Process Pinch' has been introduced previously in this chapter. In industrial practice, this case still involves some process heating at low temperature levels.

The case in which a heat engine 'below the Pinch' is used strictly for power generation is in reality not as common as the above cases, the waste heat (heat that is not recovered) that is eventually discharged to the cold utility being usually available at low temperature levels where the Heat Integration of a heat engine becomes technically challenging. In the cases in which a nearby district heating infrastructure is available, the option of waste heat recovery for district heating is the preferred solution, as discussed previously.

Due to the increase in electricity prices, the use of low temperature power generating equipment has recently received attention from the industrial sector, especially from the cement industry. It is also worth pointing out that for techno-economic reasons total process heat recovery is often not viable. Even if the total process thermal cascade suggests recovering process heat for low temperature heating, this is not done as it would result in unacceptable process complexity (high Heat Exchanger Network (HEN) capital cost and complex process control). In such cases, low temperature power production can appear as an interesting solution for waste heat utilisation.

Low temperature power cycles (below 200°C) are usually of the Rankine Cycle type, in particular with organic working fluids, hereafter denoted Organic Rankine Cycles (ORC). The underlying thermodynamic cycle is described in most standard texts on engineering thermodynamics, see for example (Bejan, 1997). Hung *et al*. (1997) provide a review of the related

© Woodhead Publishing Limited, 2013

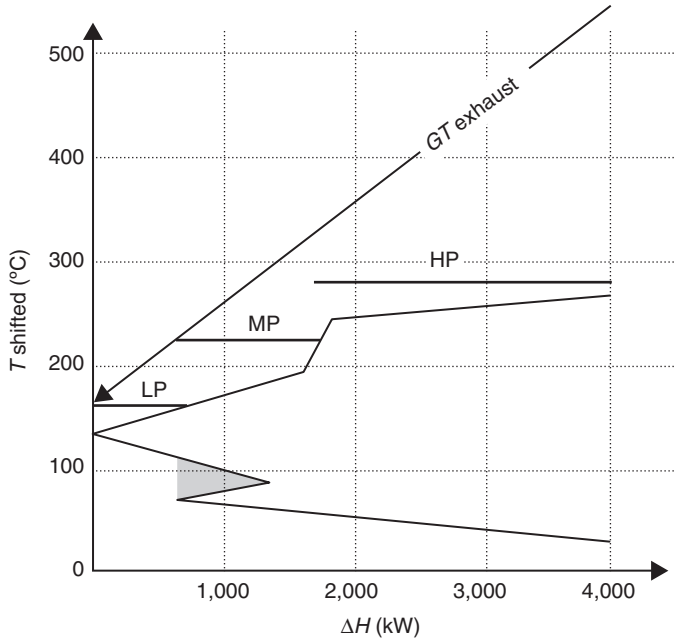

5.15 Introduction of a *GT* into a process with three steam distribution systems.

technology, and a discussion of Heat Integration issues for this type of heat engine is provided in Desai and Bandyopadhyay (2009). These fluids feature saturation temperatures that are much lower for given pressure levels compared to steam. Furthermore, to achieve maximum thermodynamic cycle efficiency, transcritical cycles with dry fluids are particularly appropriate for such applications.

As shown in Fig. 5.16, the Heat Integration of an ORC cycle does not differ conceptually from the integration of Steam Rankine Cycles, with the only difference that much lower temperature levels are involved. For Process Integration purposes, it is important to correctly estimate the thermal profile of the supercritical evaporation, which features a smooth transition from liquid to superheated condition, unlike steam CHP cycles which are most usually subcritical and therefore present a sharp change of the heat capacity at the saturated liquid condition (at which the *UP* commonly occurs). For background–foreground analysis purposes, the supercritical heat profile can be discretised in a sequence of small temperature intervals.

Another possible difference compared to the steam cycle can occur when the working fluid is a mixture of refrigerants (e.g. propane and isobutane), in which case the phase transition within the vapour–liquid region is non-isothermal. In addition, ORC cycles often feature LP ratios which,

© Woodhead Publishing Limited, 2013

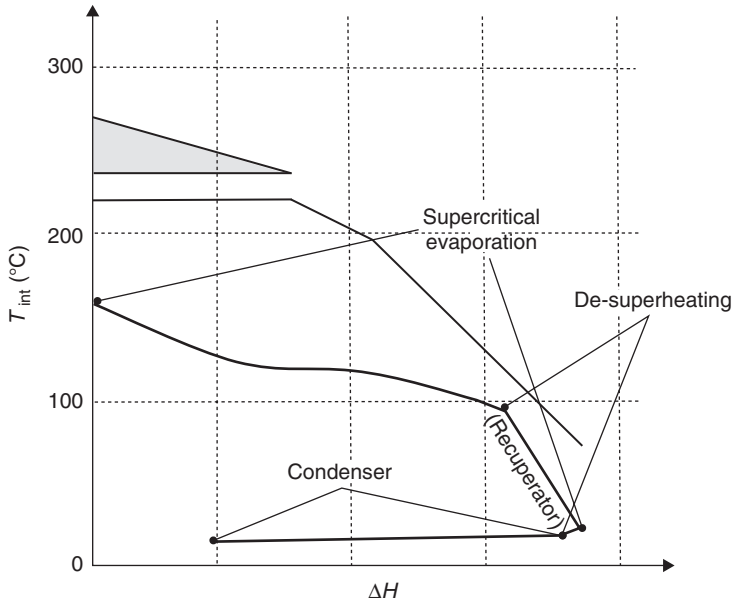

5.16 Principle of Heat Integration of an ORC for waste heat electricity production.

together with the dry characteristics of the refrigerant, result in the working fluid being highly superheated at the expander outlet, thereby requiring de-superheating. Such de-superheating represents therefore a great opportunity for cycle internal heat recovery, thus increasing the cycle efficiency.

5.5 Process Integration of Heat Pumps

The basic concept of heat pump integration, as introduced above, is to 'pump' the heat from below the Pinch to a temperature level above the Pinch at which process heating is required.

Similarly to heat engines, different heat pump cycles are possible and two general groups can be identified: Brayton-Joule Cycles, in which the working fluid remains in gas phase throughout the cycle, and Rankine Cycles, in which the working fluid undergoes a phase change (von Cube and Steimle, 1981). This latter group is commonly applied in many industrial and domestic cases and, as mentioned before, is essentially based on the same technology used for refrigeration cycles, with the only difference that the temperature levels of interest are much higher than in the refrigeration case so different working fluids can be used.

Heat and power targets for three main types of heat pump machines are discussed in the following with the help of Pinch Analysis graphical tools.

© Woodhead Publishing Limited, 2013

5.5.1 Closed-Cycle Compression Machines

The most common heat pump machine is based on the closed Rankine Cycle in which the working fluid undergoes compression, condensation, expansion and evaporation. Condensation and evaporation occur on the hot and cold sides of the machine with respect to the process (they take place in heat exchangers where the working fluid exchanges heat with process thermal streams).

According to the heat pump principles discussed previously and illustrated in Fig. 5.6, the heat available on the condenser side (above the Pinch) corresponds to the heat required on the evaporator side (below the Pinch Point) plus the net compression work (this is equal to the compressor shaft power in simple machines with throttling expansion valve or to the net compression work for machines with work-recovery liquid expanders). The theoretical performance for such machines is given by $COP_{th} = T_{cond}/(T_{cond} - T_{evap})$. Due to compressor inefficiencies and pressure drops, actual performance is usually around half of COP_{th}. For these reasons, not only is the heat available at the condenser side always larger than the evaporator heat, but the difference (i.e. the heat pump work) increases exponentially with increase in temperature difference between the hot and cold sides of the cycle.

As shown in Fig. 5.17, this implies that heat pump targeting has to take into account the effect of temperature rise to be achieved. In the left side of Fig. 5.17 for instance, only part of the process heat is covered by the heat pump condenser and only the part of the load occurring just above the Pinch Point. In the case illustrated, a lot of process heat is still available that could be supplied to the heat pump evaporator. It is reasonable, therefore, to investigate the possible savings to be obtained by an increase in heat pump size. In the example the heat pump activates a *UP* with the process heat pocket at the current condenser temperature, thus an increase in heat pump size is only appropriate if the condenser temperature (pressure) is increased. For the above-mentioned thermodynamic effects, this implies a progressively lower performance with an increase in compression work. In the right side of Fig. 5.17, the condenser temperature and the heat pump size have been adjusted in order to fully match the process heat requirement. It is clear that much more work has to be expended in this case per unit of pumped heat.

The right choice of compression heat pump has to include the total investment cost and the cost of compression work. However, energy calculations can provide first indications about the suitability of such machines. It is important that the primary energy required to generate the electricity needed to run the heat pump does not exceed the fuel savings achieved for process hot utility production. For example, if the average (national mix)

© Woodhead Publishing Limited, 2013

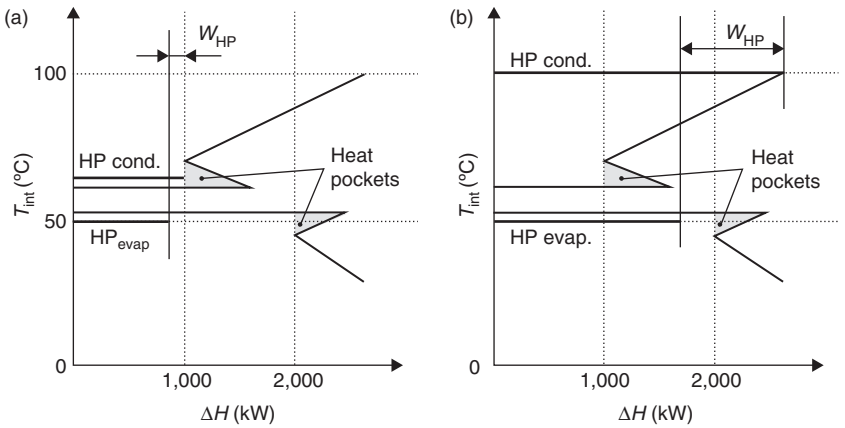

5.17 Examples of integration of compression heat pumps (for visualisation purposes the heat pump profiles do not overlap the Process GCC as it may be done to reduce compression work). (a) High efficiency system with lowest possible heat pump temperature lift. (b) Heat pump sized to completely cover the heat load.

thermal efficiency of electricity production is around 35%, heat pumping results in primary energy savings if COP is higher than 2.85. Given the relative market price differences between boiler fuel and electricity, the heat pump COP value necessary to achieve profitability for installing a heat pump may be even higher. Thus, a very efficient heat pump, such as shown on the left-hand side of Fig. 5.17, should be preferred to larger ones with rather low performance, such as shown on the right side of Fig. 5.17, even if this implies that some additional heating at higher temperatures must be covered by a separate hot utility system.

5.5.2 Mechanical Vapour Recompression Heat Pumps

In conventional closed-cycle compression heat pumps, the working fluid is a refrigerant selected on the basis of the temperature ranges required for the specific application.

Appropriate integration of a heat pump is often achieved if the background process has a large heat demand and heat availability immediately above and below the Pinch Point. Such is often the case for evaporation and condensation processes, for instance in the case of evaporation in the food industry or pulp and paper processes and any separation process involving distillation.

When a process stream is available in vapour phase close to the *PP*, direct mechanical vapour recompression (MVR) can offer an interesting alternative to traditional close cycle compression machines (von Cube and Steimle,

© Woodhead Publishing Limited, 2013

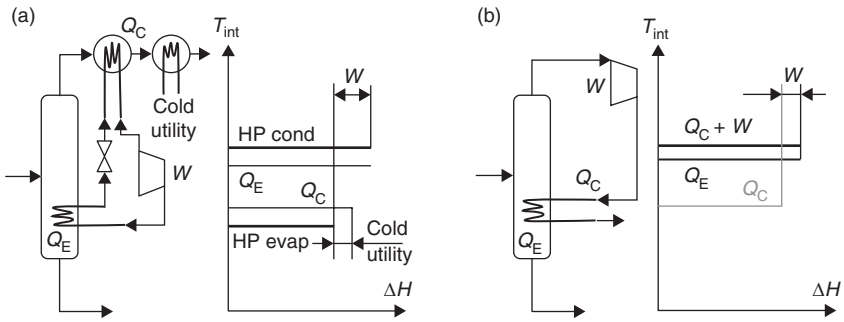

5.18 Comparison of Heat Integration of compression heat pumps: (a) closed-cycle compression machine; (b) MVR machine.

1981). As shown in Fig. 5.18, MVR can sometimes lead to a much lower work requirement, as indirect heat transfer between the heat pump working fluid and the process streams is avoided, the fluid achieving the heat pump effect being the process stream itself. Given that the performance of a heat pump is significantly affected by the temperature difference between the hot and cold sides, MVR can generate substantial savings. Compared to an ideal heat pump machine, the only energy loss of an actual MVR machine is due to the hydraulic efficiency of the compressor (around 0.8).

There are two major differences between MVR machines and conventional compression machines. In the closed-cycle heat pump machine, the refrigerant is chosen independently of the process (although the refrigerant selected has to be chosen in accordance with the desired temperature levels), while in MVR the working fluid is the process stream, which can feature very high specific volumes, or be particularly corrosive, which requires large and expensive compressors.

5.5.3 Absorption Units

Absorption machines are a special type of heat pump/refrigeration unit in which heat from a hot source (e.g. combustion or waste heat) is the main form of energy to be spent for the heat pumping process, and not mechanical power as in the more common compression machines. This apparent contradiction is justified by the fact that the desired cooling or heating effects have a greater value (either bigger load or higher temperature) than the required heat input. In practice, such units are sometime preferred to compression ones given their very small electricity requirement (still necessary for pumping a certain amount of liquid), so their application is often limited to cases where electricity is very expensive compared to heat or when a significant amount of waste heat is available at a temperature level compatible with the absorption technology.

© Woodhead Publishing Limited, 2013

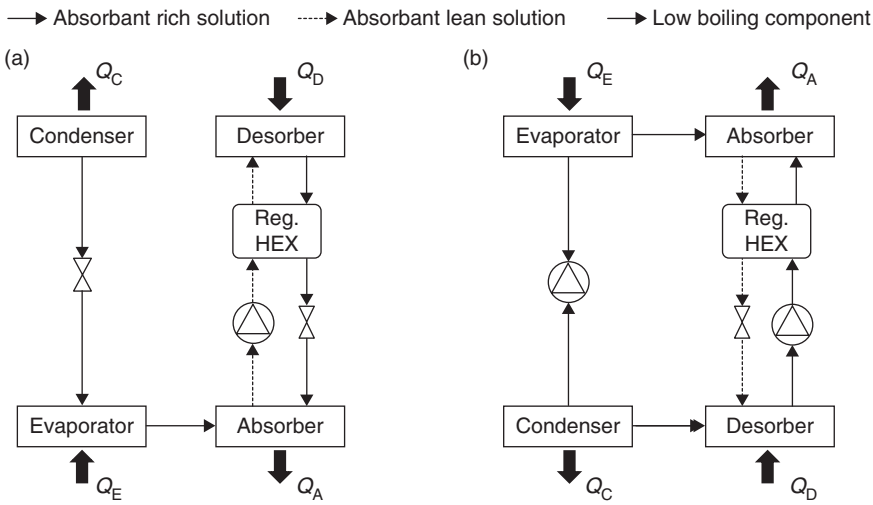

5.19 Single-effect absorption heat pumps configurations: (a) Type 1 (refrigeration); (b) Type 2 (heat transformer). Q_E: Evaporator heat load. Q_A: Absorber heat load. Q_D: Desorber heat load. Q_C: Condenser heat load (energy balance: $Q_E + Q_D = Q_A + Q_C$).

The underlying thermodynamic cycle is based on the use of a mixture as working fluid, which undergoes a cyclic change of concentration by means of sorption and separation processes, as discussed by Herold *et al*. (1996). Due to vapour–liquid equilibrium of multi-component mixtures, at a given pressure, different concentrations correspond to different temperatures. As heat is supplied to the desorber, the temperature of the mixture increases, thus leading to an increase of concentration of the high-boiling component (absorbent) with a release of vapour rich in the low boiling component (refrigerant), which is subsequently condensed.

As shown in Fig. 5.19, in absorption heat pumps this latter condensate (which corresponds to almost pure low boiling component) can subsequently follow two different sequences of transformation, so that two general heat pump configurations can be achieved (more complex system configurations can also be obtained with a combination of the two but their description are beyond the scope of this chapter). In the first case (type 1, also referred to as the absorption refrigeration machine), the low boiling component is expanded (through a throttling valve) and evaporated (LP, low temperature), thus achieving the common refrigeration effect. The refrigerant in the vapour phase is then absorbed in the mixture, rich in absorbent coming from the desorber and subsequently pumped again to the desorber. In the second case (type 2, also referred to as heat transformer), the refrigerant is pumped and evaporated before entering the

© Woodhead Publishing Limited, 2013

high-temperature absorber, where it is absorbed by producing the desired heating effect. The mixture is then throttled to the LP desorber in order to restart the cycle.

In principle, several types of mixture can be used in an absorption machine. However, only two are commonly used: ammonia/water and water/lithium–bromide. The ammonia/water machines are commercially available only for small sizes (a few kW) and are essentially limited to residential applications. Only the water/lithium–bromide systems have a broad application range in industry, with sizes ranging between tens of kW and several MW so the following discussion is hereafter limited to this technology.

In water/lithium–bromide heat pumps, for technical reasons, the temperature levels of the different effects are not that variable and the two configurations in Fig. 5.19 correspond in reality to two distinct application cases. In the first case (type 1) for example, chilled water is evaporated at a temperature immediately above 0°C, in order to prevent icing while achieving a desired refrigeration effect. In the case of the heat transformer (type 2), water vapour at 100°C is absorbed thus increasing the temperature of the mixture to around 150°C, where absorption heat can be used for process heating.

Understanding the corresponding Heat Cascade representation of this type of complex thermodynamic system may help the practitioner to decide whether to select a machine of this type rather than a more conventional compression machine.

Absorption heat pumps are often referred to as three-temperature level cycles (Herold *et al*., 1996). In type 1, the driving heat is at high temperature (desorber) and the desired effect is refrigeration (evaporator) at low temperature and heating (condenser) at intermediate temperature. In type 2, the driving heat is at intermediate temperature (evaporator) and the desired effect is heating at higher temperature (absorber) and heating at lower temperature (condenser). The first type is the most common, and it is usually used as an alternative refrigeration system to traditional compression machines. As mentioned in the introduction, the use of heat pump machines for refrigeration does not need to follow the rule of appropriate placement, as refrigeration is in principle pure degradation of high-quality primary energy. In such cases, therefore, absorption heat pumps compete in the market with stand-alone compression machines, so the absorption machines are often operated by burning fuel to provide the required desorption heat. In some circumstances of combined heat power and cooling, low temperature steam or water (e.g. from engine jacket cooling) may be used in place of fuel combustion.

Nevertheless, an energy-wise appropriate placement of absorption heat pumps is still possible although it is quite limited to special features of the surrounding process. The principle of application of two types of absorption

© Woodhead Publishing Limited, 2013

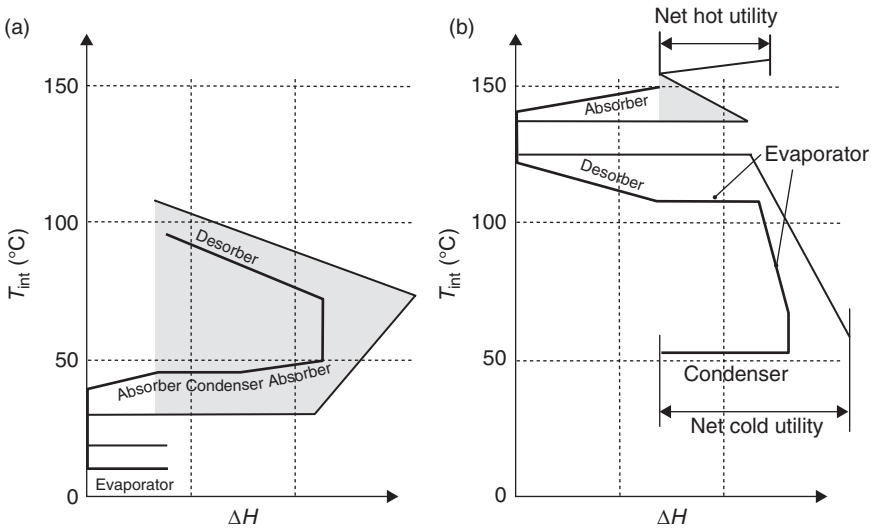

Fig. *5.20* Principles of Heat Integration of absorption machines: (a) Type 1; (b) Type 2 – heat transformer.

machines (type 1 and 2) are given in Fig. 5.17 in which the heat pump thermal cascades (foreground) are represented against background processes.

In both cases, the integration is beneficial only if the background process features an almost complementary heat cascade. As shown in Fig. 5.20, in the case of type 1 machines, this requires a heat pocket available immediately above the *PP*. For heat transformers, a considerable amount of waste heat is required under the *PP*. In both cases, the absorption heat pump achieves the effect (either refrigeration or heating or a combination of the two) that would otherwise require a compression machine with consequent use of mechanical energy.

Compared to compression heat pumps, absorption heat pumps are far more complex machines requiring, in the simplest case, five heat exchangers (four for heat exchangers with process and utility streams plus one internal recuperator). In addition, as the desired effects are obtained either with the refrigerant cycle part (condenser and evaporator) or with the absorption/desorption heat, with the two parts substantially featuring two opposite heat cascades, a much larger machine is required with respect to compression heat pumps.

5.6 Sources of Further Information and Advice

This chapter discussed how Pinch Analysis graphical tools, in particular the Process GCC, can be used for the estimation of optimal size and parameters of advanced energy conversion technologies. It is worth noting that the

© Woodhead Publishing Limited, 2013

success of the targeting methodology introduced in Linnhoff and Flower (1978) is mainly due to the simple graphical tools, which avoid dealing with complex mathematical formulation of engineering problems. The success of this methodology in the field of synthesis and design of utility systems is confirmed by a large body of literature, of which only a few examples are provided in the following, which is primarily a historical overview of some of the more important contributions.

Løken (1985) implemented the process heat cascade calculation in one of the earliest computer programs for automatic estimation of the net energy consequences of using heat pumps in industrial processes. Ranade (1988) further contributed to methods for investigating the benefit of heat pump integration by proposing an economic targeting methodology based on Pinch Analysis. Benstead and Sharman (1990) proposed a computer program for graphical interactive Process Integration synthesis with specific reference to appropriate placement of heat pumps. Wallin and Berntsson (1994) extended the targeting methodology to the estimation of economic consequences of heat pump implementation in process retrofitting. The targeting procedure was further extended by Klemeš *et al*. (1997) to include fuel power and emission reductions for Total Sites. New developments related to establishing power generation targets for Total Sites are presented by Ghannadzadeh *et al*. (2012). For integration of refrigeration systems, recent developments include e.g. a new design methodology for cascaded mixed refrigerant systems with multistage heat exchanges proposed by Nogal *et al*. (2008). Methodology extensions using exergy based curves for low temperature applications have been recently presented by e.g. Marmolejo-Correa and Gundersen (2012). The same authors discuss general recommendations for appropriate placement of compressors and expanders – see Gundersen and Marmolejo-Correa (2012). For further information about recent developments in the area of Process Integration of technologies using low-grade heat, the reader is referred to e.g. Kapil *et al*. (2011).

Indeed, Pinch Analysis has the merit of formulating a basic thermodynamic principle (heat cascades only in presence of a temperature departure between a hot and a cold stream) through a simple algebraic procedure (Problem Table) by adjusting the real temperatures of a Minimum Temperature Difference contribution (i.e. the Pinch Point appears when the Composite Curves with interval temperatures touch each other). In this sense, the Problem Table, instead of being used to generate targeting graphical representations of heat flows within the process, can be used to impose physical constraints in process synthesis and design optimisation problems. If the thermodynamic states of system material streams are defined (fixed temperature and pressures), heating and cooling loads can be expressed as linear functions of mass flow rates, thereby leading to simple mathematical formulations of the targeting problems analysed above, which can be solved

© Woodhead Publishing Limited, 2013

through linear programming. In this context, the Problem Table Algorithm is therefore used to impose the heat transfer feasibility constraint (positive cumulative heat load at any system temperature level). This formulation of integration of utility systems constitutes the basis of several works, of which only few are cited here. Colmenares and Seider (1987) used the cascade principle to set a heat transfer feasibility constraint in a non-linear programming method for heat and power integration in industrial processes. Swaney (1989) formulated the economic optimum integration of heat engine and heat pumps through a transhipment method. Maréchal and Kalitvenzeff (1996) proposed a combination of Pinch Analysis and mathematical tools for synthesis and design of utility systems, based on mixed-integer programming in which the thermal cascade is used to set the heat transfer feasibility constraints between process and utility systems thermal streams. The methodology is further developed for the specific case of steam utility networks, see Maréchal and Kalitventzeff (1999). More recent work by the group of Maréchal (2012) includes e.g. the ability to handle integration of industrial heat pumps in connection with multi-period problems (Becker and Maréchal, 2012).

Mathematical programming may in fact represent the ultimate approach to tackle rigorous synthesis and design optimisation of complex utility systems in which the heat match between process streams and utility streams is solved explicitly in a single mixed-integer linear programming procedure, as suggested in Papoulias and Grossmann (1983) or by decomposing the synthesis problem into a sequence of integer and linear programming procedures as suggested in Petroulas and Reklaitis (1984). Recent developments include, for example, the application of mathematical programming to synthesis of mechanical driver and power generation configurations (Del Nogal *et al.*, 2010). Mathematical programming methods are applied by Martelli *et al.* (2011) for optimising the design of integrated heat recovery steam generators together with the heat recovery steam network. Aguilar *et al.* (2007) present a modelling framework for design and optimisation of flexible utility systems subject to variable conditions.

Pinch Analysis remains, however, a powerful targeting graphical tool for preliminary design, especially for large industrial processes. The insights achieved by applying Pinch Analysis tools can help to identify promising solutions that can be refined subsequently using more rigorous procedures, as suggested in Pintarič and Glavič (2002).

5.7 References

Aguilar, O., Perry, S. J., Kim, J.-K., Smith, R. (2007). Design and optimization of flexible utility systems subject to variable conditions: Part 1: Modelling framework. *Chemical Engineering Research and Design*, **85** (8A), 1136–1148.

© Woodhead Publishing Limited, 2013

Babcock & Wilcox. (2006). *Steam: Its Generation and Use,* 41st edn. Babcock and Wilcox Company, Charlotte, North Carolina, USA.

Becker, H., Maréchal, F. (2012). Targeting industrial heat pump integration in multi-period problems. *Computer Aided Chemical Engineering*, **31**, 415–419.

Bejan, A. (1997). *Advanced Engineering Thermodynamics.* John Wiley & Sons, New York, NY, USA.

Benstead, R., Sharman, F. W. (1990). Heat pumps and pinch technology. *Heat Recovery Systems & CHP,* **10**, 387–398.

Boyce, M. P. (2002). *Handbook for Cogeneration and Combined Cycle Power Plants.* American Society of Mechanical Engineers, New York, NY, USA.

Colmenares, T., Seider, W. (1987). Heat and power integration of chemical processes. *AIChE Journal,* **33**, 898–915.

Del Nogal, F. L., Kim, J.-K., Perry, S., Smith, R. (2010). Synthesis of mechanical driver and power generation configurations, Part 1: Optimization framework. *AIChE Journal*, **56**(9), 2356–2376.

Desai, N. B., Bandyopadhyay, S. (2009). Process integration of organic Rankine cycles. *Energy,* **34**, 1674–1686.

Ghannadzadeh, A., Perry, S., Smith, R. (2012). Cogeneration targeting for site utility systems. *Applied Thermal Engineering*, **43**, 60–66

Gundersen, T., Marmolejo-Correa, D. (2012). Appropriate placement of compressors and expanders. *AIChE Spring Meeting and 8th Global Congress on Process Safety*. Houston, TX, USA.

Herold, K., Radermacher, R., Klein, S. (1996). *Absorption Chillers and Heat Pumps.* CRC Press, Inc., Boca Raton, FL, USA.

Hung, T. C., Shai, T. Y., Wang, S. K. (1997). A review of Organic Rankine Cycles (ORCs) for the recovery of low-grade waste heat. *Energy,* **22**, 661–667.

Itoh, J., Shiroko, K., Umeda, T. (1986). Extensive applications of the TQ diagram to heat integrated system synthesis. *Computers & Chemical Engineering,* **10**, 59–66.

Kapil, A., Bulatov, I., Smith, R., Kim, J.-K. (2011). Site-wide process integration for low grade heat recovery. *Computer Aided Chemical Engineering*, **29**, 1859–1863

Klemeš, J., Dhole, V. R., Raissi, K., Perry, S. J., Puigjaner, L. (1997). Targeting and design methodology for reduction of fuel, power and CO_2 on total sites. *Applied Thermal Engineering*, **7**, 993–1003.

Linnhoff, B., Flower, J. R. (1978). Synthesis of heat exchanger networks: I. Systematic generation of energy optimal networks. *AIChE Journal*, **24**, 633–642.

Linnhoff, B., Dhole, V. R. (1992). Shaftwork targets for low-temperature process design. *Chemical Engineering Science,* **47**, 2081–2091.

Linnhoff, B., Townsend, D. W., Boland, D., Hewitt, G. F., Thomas, B. E. A., Guy, A. R., Marsland, R. H. (1982). A *User Guide on Process Integration for the Efficient Use of Energy*, IChemE, Rugby, UK.

Løken, P. A. (1985). Process integration of heat pumps. *Heat Recovery Systems,* **5**, 39–49.

Maréchal, F., Kalitventzeff, B. (1996). Targeting the minimum cost of energy requirement: a new graphical technique for evaluating the integration of utility systems. *Computers & Chemical Engineering,* **20**, 225–230.

Maréchal, F., Kalitventzeff, B. (1999). Targeting the optimal integration of steam networks: mathematical tools and methodology. *Computers & Chemical Engineering,* Supplement, 133–136.

© Woodhead Publishing Limited, 2013

Marmolejo-Correa, D., Gundersen, T. (2012). A new graphical representation of exergy applied to low temperature process design. *Computer Aided Chemical Engineering*, **31**, 1180–1184.

Nishio, M., Itoh, J., Shiroko, K., Umeda, T. (1980). A thermodynamic approach to steam-power system design. *Industrial & Engineering Chemistry Process Design and Development,* **19**, 306–312.

Martelli, E., Amaldi, E., Consonni, S. (2011). Numerical optimization of heat recovery steam cycles: Mathematical model, two-stage algorithm and applications. *Computers and Chemical Engineering*, **35**(12), 2799–2823.

Nogal, F. D., Kim, J.-K., Perry, S., Smith, R. (2008). Synthesis of cryogenic energy systems. *Computer Aided Chemical Engineering*, **25**, 67–72

Papoulias, S. A., Grossmann, I. E. (1983). A structural optimization approach in process synthesis – I Utility Systems. *Computers and Chemical Engineering*, **7**, 695.

Petroulas, T., Reklaitis, G. (1984). Computer-aided synthesis and design of plant utility systems. *AIChE Journal,* **30**, 69–78.

Pintarič, Z. N., Glavič, P. (2002). Integration of flue gas into the process flowsheet by combined pinch-MINLP approach. *Chemical Engineering Research and Design*, **80**, 606–614.

Ranade, S. M. (1988). New insights on optimal integration of heat pumps in industrial sites. *Heat Recovery Systems & CHP,* **8**, 255–263.

Swaney, R. E. (1989). Thermal integration of processes with heat engines and heat pumps. *AIChE Journal,* **35**, 1003–1016.

Townsend, D. W. Linnhoff, B. (1983a). Heat and power networks in process design. Part I Criteria for placement of heat engines and heat pump in process networks. *AIChE Journal,* **29**, 742–748.

Townsend, D. W. Linnhoff, B. (1983b). Heat and power networks in process design. Part II Design procedure for equipment selection and process matching. *AIChE Journal,* **29**, 748–771.

Umeda, T., Harada, T., Shiroko, K. (1979). A thermodynamic approach to the synthesis of heat integration systems in chemical processes. *Computers & Chemical Engineering,* **3**, 273–282.

Von Cube, H. L., Steimle, F. (1981). *Heat Pump Technology.* Butterworth-Heinemann, Woburn, MA, USA.

Wallin, E., Berntsson, T. (1994). Integration of heat pumps in industrial processes. *Heat Recovery Systems & CHP,* **14**, 287–296.

© Woodhead Publishing Limited, 2013

6

Total Site Methodology

SIMON PERRY, The University of Manchester, UK

DOI: 10.1533/9780857097255.2.201

Abstract: The optimal design of large scale utility systems is complex, as these systems are required to provide the heat and power requirements for individual processes contained within the total processing site. targeting methods have been proposed which enable engineers to fully scope options prior to more detailed design. Targeting for Total Sites is an extension of the established Pinch Technology Targeting methodologies and has been used extensively in industry. The Total Site Targeting methodology includes data extraction methods, the formation of Total Site Profiles, Total Site Composite Curves and the Site Utility Grand Composite Curve.

Key words: Total Sites, targeting, process heat sources, process heat sinks, steam generation, steam use, steam recovery, boiler steam reduction.

6.1 Introduction

The optimal design of large scale utility systems that serve large chemical processing sites, such as refineries, is extremely complex, as these systems are required to provide the heat and power for the processes within the site. In order to simplify the process of design, targeting methods have been put forward which enable engineers to fully scope options prior to more detailed design methods. Targeting for Total Sites has gained worldwide acceptance since it was established as an extension of the already well-known Pinch Technology Targeting methodologies, and consequently it has been used extensively in industry. The Total Site Targeting methodology forms part of an extensive overall procedure required to synthesise the entire Total Site system, which includes process utility and Heat Exchanger Network Design integrated with the site utility system.

Total Site Targeting was advanced as a means of integrating the heating and cooling requirements of individual process units in a Total Site (Dhole and Linnhoff, 1993). The heat source and heat sink information was extracted from the chemical processes comprising the Total Site, and targets for steam supply and demand were derived. Dhole and Linnhoff

© Woodhead Publishing Limited, 2013

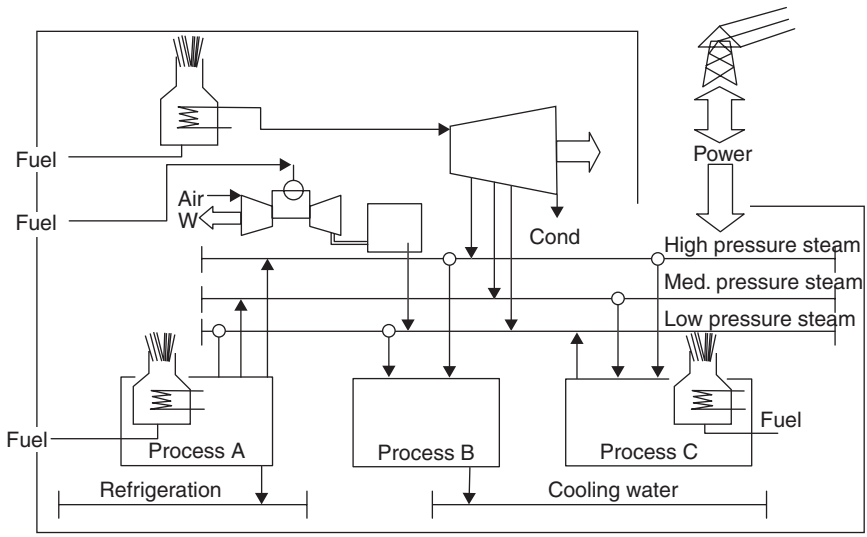

6.1 Integration of process heating and cooling demands with supporting site utility system. (Source: Adapted from Klemeš *et al.*, 1997.)

also considered shaft work co-generation, making use of the Carnot Factor and exergy to produce targets. Raissi (1994) extended this work, and examined shaft work co-generation without considering conversions to Carnot factors, and also examined the trade-off between minimum fuel requirements and minimum utilities cost in determining the correct pressure for the steam-distribution mains on the Total Site. In both cases, information from individual processes on the site can produce targets for the overall heating and cooling demands which have to be met by the Total Site Utility System. The Total Site Targeting method allows waste heat from processes to be used as a source of heat in other processes. The waste heat sources are converted to steam, and then passed to processes that are in heat deficit through the steam system infrastructure. The targeting methodology can determine the amounts of steam used and generated by the combined individual processes, the amount of heat recovery that can be achieved through the steam system, the amount of steam that has to be supplied by the utility system steam generators, and the potential co-generation that can be produced by distributing the stream through the Total Site system (Klemeš *et al.*, 1997). The Total Site Analysis methods were then related to the overall design of the site utility system by Smith (2005). A representation of this Total Site system is given in Fig. 6.1.

© Woodhead Publishing Limited, 2013

6.2 Data Extraction for Total Sites

In order to demonstrate the methodology of producing targets for Total Sites, we will consider a Total Site which comprises two site processes, Process A and Process B. The heating and cooling demands of these processes are represented by their respective Grand Composite Curves. The Grand Composite Curve represents heating and cooling demands of the process remaining after heat recovery has taken place within the process. These curves show the heat remaining (on a temperature basis) after heat exchange has taken place between the process hot streams (those process streams that need cooling) and the process cold streams (those process streams that need heating), taking into account an appropriate Minimum Approach Temperature ($\Delta T_{\min}$) for heat exchange between the hot streams and the cold streams. The temperature scale on the Grand Composite Curve is in terms of the shifted temperature T^*. The shifted temperature scale is produced by shifting the supply and target temperatures of hot streams downwards in temperature by $0.5\,\Delta T_{\min}$, and shifting the supply and target temperatures of the cold streams upwards by $0.5\,\Delta T_{\min}$, thereby building feasible heat exchange (at the selected value of the Minimum Approach Temperature) in the heat exchangers into the curve. The Pinch location (which splits the process between a heat sink region and a heat source region) is also readily seen in the Grand Composite Curve. Additionally, the overall heating ($Q_{H\min}$) and cooling ($Q_{C\min}$) requirements which have to be supplied by external sources of heating and cooling are also readily apparent.

For Process A the $\Delta T_{\min}$ has been set at 30°C, and the Grand Composite Curve is shown in Fig. 6.2. The Problem Table data for Process A is given in Table 6.1. The Grand Composite Curve in Fig. 6.2 has been produced from the STAR (2012) software available from the Centre for Process Integration, , UK, and fiš dfišcuššed more fully fin Chapter 34.

The minimum heating demand for Process A at the specified $\Delta T_{\min}$ of 30°C ($Q_{H\min}$) is 1,999.5 kW and the minimum cooling demand ($Q_{C\min}$) is 358.5 kW. The location of the Pinch is at an interval temperature of 120°C, equivalent to 135°C for the hot streams and 105°C for the cold streams.

The equivalent information for Process B is given in Fig. 6.3 and Table 6.2. In this case the Minimum Approach Temperature, $\Delta T_{\min}$, is 10°C. In Process B the minimum heating requirement, $Q_{H\min}$, is 300 kW, and the minimum cooling demand is 1,590 kW. The Pinch is at 250°C interval temperature, which represents 245°C for the cold streams and 255°C for the hot streams.

Prior to the extraction of the temperature/enthalpy information from the Grand Composite Curves, a decision has to be made regarding the 'pockets' in the Grand Composite Curves of both processes. A 'pocket' is an area of additional process heat recovery in the process, where heat at

© Woodhead Publishing Limited, 2013

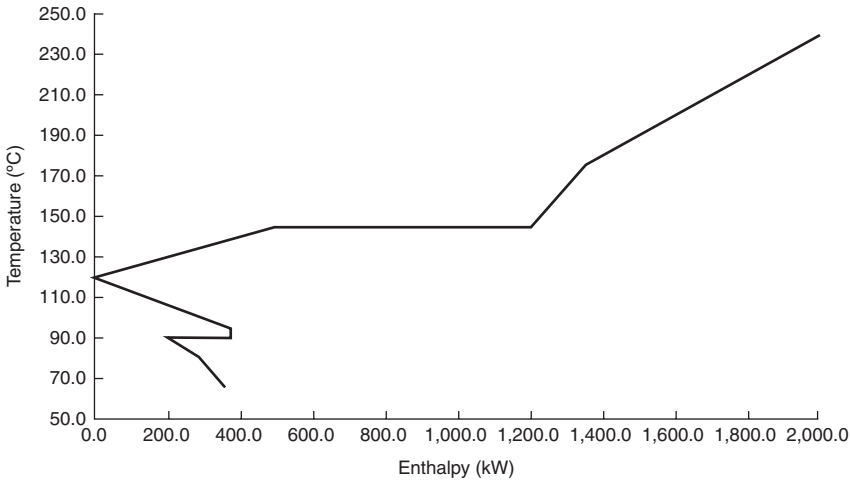

6.2 The Grand Composite Curve for Process A with a ΔT_{min} of 30°C.

Table 6.1 Problem Table for Process A with a ΔT_{min} of 30°C

Interval temperature, T^* (°C)	Enthalpy (kW)
240.0	1,999.5
175.0	1,349.5
145.1	1,200.0
145.0	500.0
120.0	0.0
95.0	375.0
90.1	375.0
90.0	191.0
80.0	291.0
65.0	358.5

a higher temperature can be made available to a cold stream at a lower temperature. In the case of Process A, there is a 'pocket' between the interval temperatures of 107.3°C and 95°C. The choice is to either retain the 'pocket' in the process for heat recovery, or to extract the pocket as a heat source and a cold sink to be met by external utilities provided by the site utility system. If the pocket is to be extracted from the process, then the heat source of the pocket (a hot stream segment) will need to be able to generate a hot utility, normally steam, and the cold sink will have to be heated by an external hot utility, again normally steam, provided by the site utility system. If this extraction is to be worthwhile, two conditions should be met, as illustrated by Fig. 6.4a and 6.4b. Initially only HP steam generation is considered for the process (Fig. 6.4a). In this case there is

© Woodhead Publishing Limited, 2013

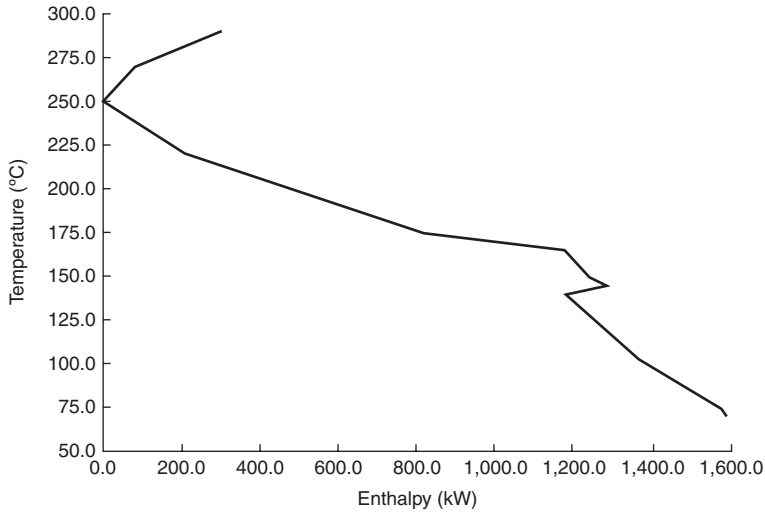

6.3 The Grand Composite Curve for Process B with a ΔT_{min} of 10°C.

Table 6.2 Problem Table for Process B with a ΔT_{min} of 10°C

Interval temperature, T^* (°C)	Enthalpy (kW)
290.0	300.0
270.0	80.0
250.0	0.0
220.0	210.0
185.0	665.0
175.0	815.0
165.0	1,175.0
150.0	1,235.0
145.0	1,280.0
140.0	1,175.0
100.0	1,375.0
75.0	1,575.0
70.0	1,590.0

process heat recovery in the pocket on the left of the figure. However, as the pocket has a considerable temperature difference (Fig. 6.4b), it can support generating a hot utility (steam) by the heat source in the pocket, and using a lower temperature hot utility (steam) to supply the cold sink. The heat source should be reasonably large, greater than a few hundred kW, in order to justify the cost of capital required to transform it to a hot utility that can be used elsewhere on the Total Site. This, of course, can only be properly determined using a full economic analysis. In the case of Process A, the heat source exists at an interval temperature of 107.3°C, or

© Woodhead Publishing Limited, 2013

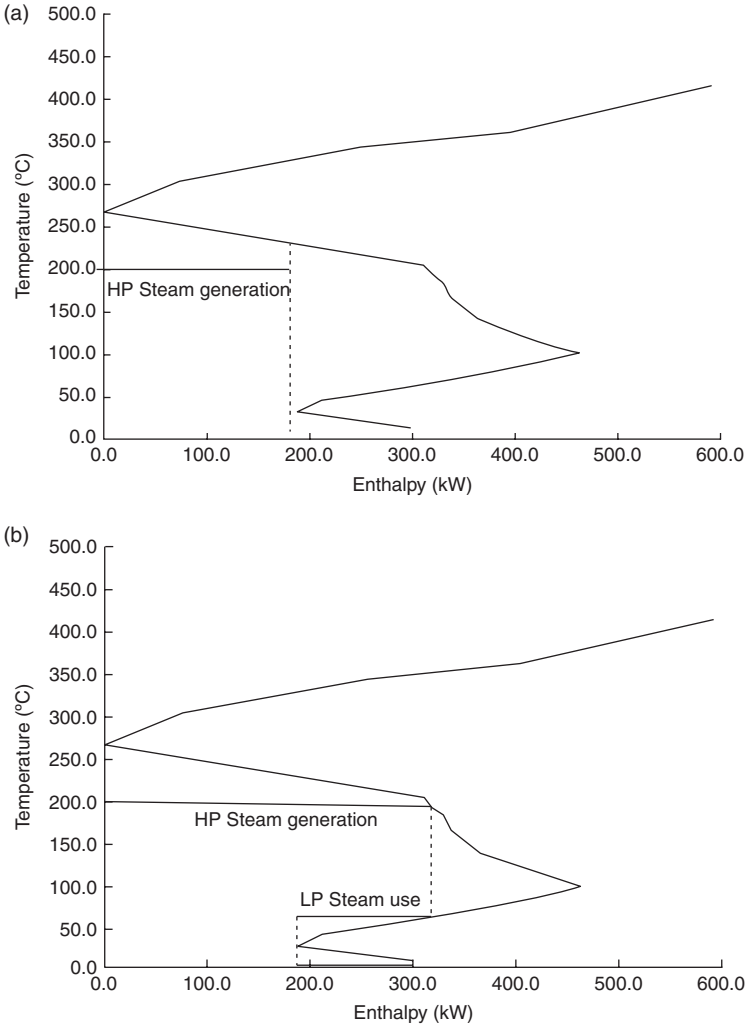

6.4 (a) Grand Composite Curves with HP steam generation and heat recovery retained in the process. (b) Grand Composite Curves with HP steam generation and LP steam use instead of process heat recovery. Some heat recovery still retained in the process.

122.3°C real temperature. At this temperature it is unlikely to be able to produce a low-pressure, low-temperature steam which could be used elsewhere on the Total Site. The amount of heat available, 184 kW, is also likely to be unworthwhile in relation to the capital cost of the generating equipment. However, to determine the trade-off with greater accuracy would require more extensive costing data.

© Woodhead Publishing Limited, 2013

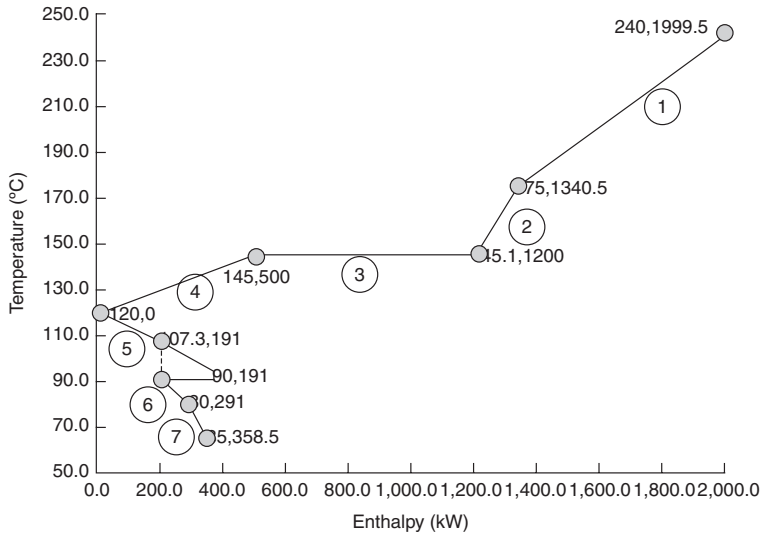

6.5 Process A Grand Composite Curve with stream segments shown.

A similar situation exists for Process B (Fig. 6.3). In this case a small pocket exists between 165°C and 140°C. The amount of heat available from the heat source (stream segment) is 105 kW. The same reasoning can be applied to the pocket in this process as in the case in Process A. Here the pocket heat source and heat sink information should not be extracted and left as process heat recovery in Process B.

The information needed for data extraction for Process A is now transposed from the Problem Table and superimposed on the Grand Composite Curve (Fig. 6.5). Each start- and end-point of the stream segments making up the Grand Composite Curve is shown, and in addition the co-ordinates of each point are shown in terms of temperature and enthalpy values. Each stream segment is also numbered for easier reference.

The heat source and heat sink information extracted from the process via the Grand Composite Curve for Process A is shown in Table 6.3. The information provided includes the stream segment number, the stream segment type (either hot or cold), the shifted supply temperature (T_S*), the shifted target temperature (T_T*), the amount of heat (ΔH) and the *CP*. Also included are the real supply and target temperatures of the stream segments (T_S and T_T), and their supply and target temperatures shifted in temperature by a whole $\Delta T_{\min}$ instead of 0.5 $\Delta T_{\min}$ (T_S** and T_T**).

It can be seen from the Grand Composite Curve for Process A in Fig. 6.5 that stream segment 1 is a heat sink. This means that this stream segment is a cold stream and that the supply temperature of the segment in terms of shifted temperature given by the Grand Composite Curve is 175°C. The

© Woodhead Publishing Limited, 2013

Table 6.3 Stream segment data extracted from Process A with a ΔT_{min} of 30°C

NO.	Type	T_S* (°C)	T_S (°C)	T_S** (°C)	T_T* (°C)	T_T (°C)	T_T** (°C)	ΔH (kW)	CP (kW.°C^{-1})
1	C	175	160	190	240	225	255	650	10
2	C	145.1	130.1	160.1	175	160	190	149.5	5
3	C	145	130	160	145.1	130.1	160.1	700	7,000
4	C	120	105	135	145	130	160	500	20
5	H	120	135	105	107.3	122.3	93.3	191	15
6	H	90	105	75	80	95	65	100	10
7	H	80	95	65	65	80	50	67.5	4.5

shifted target temperature is 240°C. As the ΔT_{min} of the process is 30°C, the real supply temperature of the cold stream segment is 175°C–0.5 ΔT_{min}, giving a supply temperature of 160°C. From previous chapters, a cold stream is shifted upwards in terms of temperature when using the Problem Table Algorithm and constructing the Grand Composite Curve. Consequently, the real target temperature of segment 1 is 225°C. The amount of heat that this stream segment requires to raise its temperature from the supply to target temperature is 1,999.5–1,349.5 kW (from the enthalpy co-ordinates in Fig. 6.5), giving a value of 650 kW of required heating. From the Grand Composite Curve it can be seen that segments 2, 3 and 4 are also cold stream segments and the required information representing these stream segments is produced in the same way.

Below the process Pinch for Process A, shown by the interval temperature of 120°C and zero enthalpy, we have a heat source area dominated by hot stream segments. The first segment below the Process Pinch (segment 5 in Fig. 6.5) should have a shifted supply temperature of 120°C and a shifted target temperature of 95°C. The stream should also lose 375 kW of heat in moving from its shifted supply temperature to shifted target temperature. However, part of this stream segment is involved in the pocket heat recovery, and consequently only a part of this heat source is required to be extracted. The amount of heat from this segment that can be extracted is 191 kW, and consequently the shifted target temperature of this segment is 107.3°C.

The extraction procedure described above can also be applied to Process B, but in this case the ΔT_{min} is 10°C. Figure 6.6 shows the Grand Composite Curve with the required stream segments to be extracted, and Table 6.4 shows the extracted stream segment data. In this case the stream segment heat sources from 165°C to 145°C are not extracted, along with the stream segment heat sink data from 145°C to 140°C.

© Woodhead Publishing Limited, 2013

Table 6.4 Stream segment data extracted from Process B with a ΔT_{min} of 10°C

NO.	Type	T_S* (°C)	T_S (°C)	T_S** (°C)	T_T* (°C)	T_T (°C)	T_T** (°C)	ΔH (kW)	CP (kW.°C^{-1})
1	C	270	265	275	290	285	295	220	11
2	C	250	245	255	270	265	275	80	4
3	H	250	255	245	220	225	215	210	7
4	H	220	225	215	185	190	180	455	13
5	H	185	190	180	175	180	170	150	15
6	H	175	180	170	165	170	160	360	36
7	H	140	145	135	100	105	95	200	5
8	H	100	105	95	75	80	70	200	8
9	H	75	80	70	70	75	65	15	3

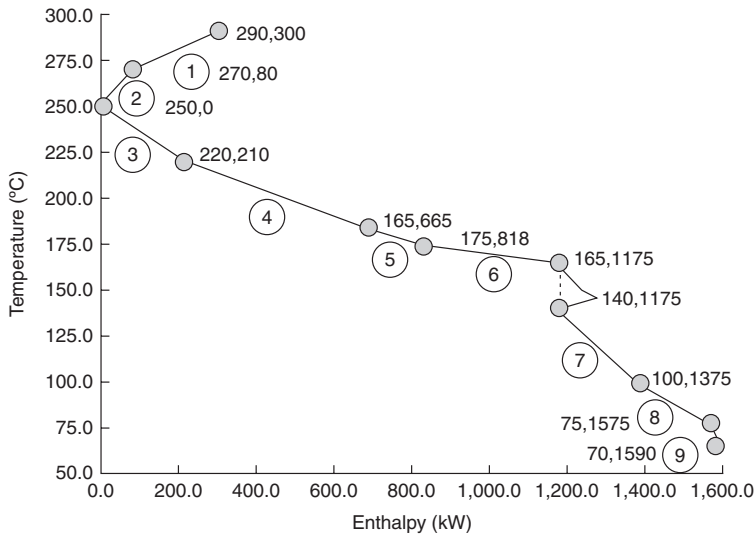

6.6 Process B Grand Composite Curve with stream segments shown.

The next stage in the development of the Total Site Targeting procedure is the combination of the heat source information from the Total Site processes (Process A and Process B) into a Composite Site Source Profile. From the information on available stream segments from Table 6.3 and from Table 6.4 we can see that the heat source segments from Process A are segments 5, 6, and 7 and from Process B are segments 3, 4, 5, 6, 7, 8 and 9. These are combined into a Composite Curve using the double-shifted supply and target temperatures of the stream segments (T_S** and T_T**). The reason for using the double-shifted temperatures is in order that feasible heat transfer from

© Woodhead Publishing Limited, 2013

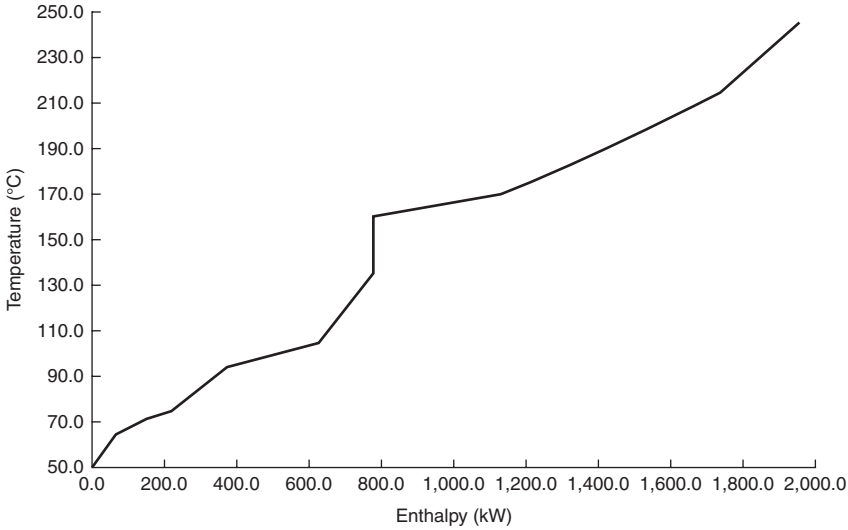

6.7 Combined heat source information or Site Source Profile.

these stream segments can take place when they are used for the generation of steam (represented by their real unshifted saturated temperatures) or the use of steam. The resultant Composite Curve of the heat source stream segments or Site Source Profile is shown in Fig. 6.7.

The same combination procedure can be applied to the heat sink segments from Process A and Process B. The stream segments from Process A that need to be included are segments 1, 2, 3 and 4 and, from Process B, stream segments 1 and 2. Again the double-shifted supply and target temperatures are used to construct the Composite Curves. However, in this case the temperatures are shifted upwards in comparison to their real temperatures. The Site Sink Profile is shown in Fig. 6.8.

The final stage in the procedure of creating the Site Profiles representing the external heating and cooling duties of the site processes, which cannot be met by process heat recovery within each process, is combining the Site Source Profile and Site Sink Profile on one graph. This is shown in Fig. 6.9.

The Site Profiles therefore depict the total heat source available from all the contributing processes in the Total Site (the curve on the left of Fig. 6.9) and the total heat sink that has to be satisfied from external heat sources (the curve on the right of Fig. 6.9).

At this stage the Total Site Profiles show us that the total amount of heat that has to be supplied to the process on the site from an external heat source is 2,299.5 kW. The amount of excess heat that has to be removed is 1,948.5 kW. However, the principal concept behind the Total

© Woodhead Publishing Limited, 2013

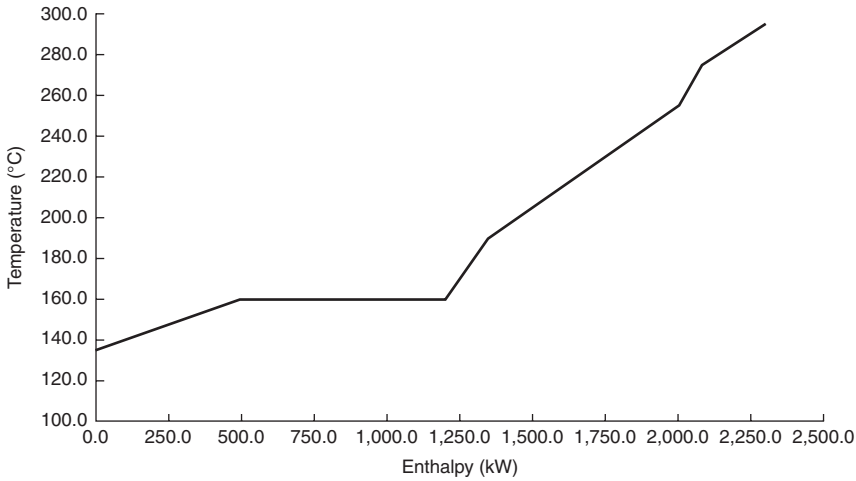

6.8 Combined heat sink information or Site Sink Profile.

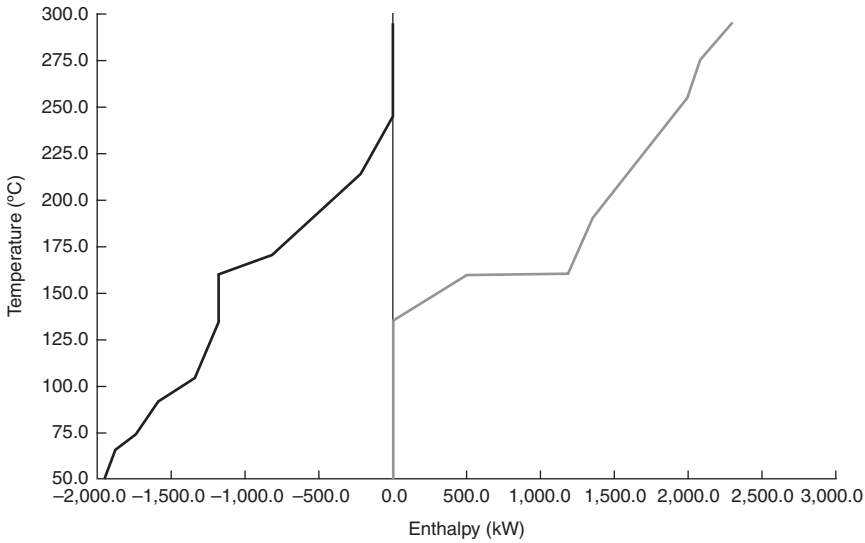

6.9 Total Site Profiles.

Site Technology is that the heat sources from the site processes can be used to provide heat to the heat sinks of the site processes via the generation and use of steam. The steam consequently is used as an intermediate form of heat transfer between the site heat sources and the site heat sinks. In this way the total amount of external heating and cooling which is required to be supplied to the Total Site is reduced, thereby reducing fuel needed

© Woodhead Publishing Limited, 2013

to raise the heat needed and so reducing the overall operating cost of the Total Site system.

6.3 Total Site Profiles and Total Site Composite Curves

To create the Total Site Profiles we need to target the amount of steam that can be generated from the heat sources across the Total Site, and additionally to target the amount of steam that has to be used to meet the heat sinks across the Total Site. Consequently, we need to decide the number of steam mains that will be used to distribute steam across the Total Site, and the pressures (and consequently temperature) of these steam mains. In order to simplify this selection in the first instance, we shall represent the steam mains at their saturation temperatures. The number of steam mains and their pressures/temperatures can be determined in a number of ways, but again for simplification in the first instance, we will consider three mains for steam distribution (generation and use) and a cooling utility for heat sources that are at a temperature below the temperatures for steam generation. The chosen steam mains and cooling main are given in Table 6.5.

It should be noted that the pressure of the HP steam mains may be considered to be at too high a pressure at 86 bar. In many cases steam is distributed to site process heat sinks at a maximum of 40 bar, representing a saturated steam temperature of 250°C. If this was the case, then the extraction of heat sinks in a Site Process Grand Composite Curve would have to be limited to this temperature. Any heat sinks which required a higher temperature utility would need to remain in the process and be met by a local hot utility such as hot oil.

These steam mains and cooling water main are then added to the graph representing the Site Profiles and are shown at their real saturated temperatures. This new graph is known as the Total Site Profiles and is shown in Fig. 6.10. As the steam mains have been shown at their real

Table 6.5 Steam mains information and cooling main for the Total Site

Steam main	Saturated temperature (°C)	Mains pressure (bar)
HP	300	86
MP	200	15.5
LP	160	6.2
Cooling Water	20	1

© Woodhead Publishing Limited, 2013

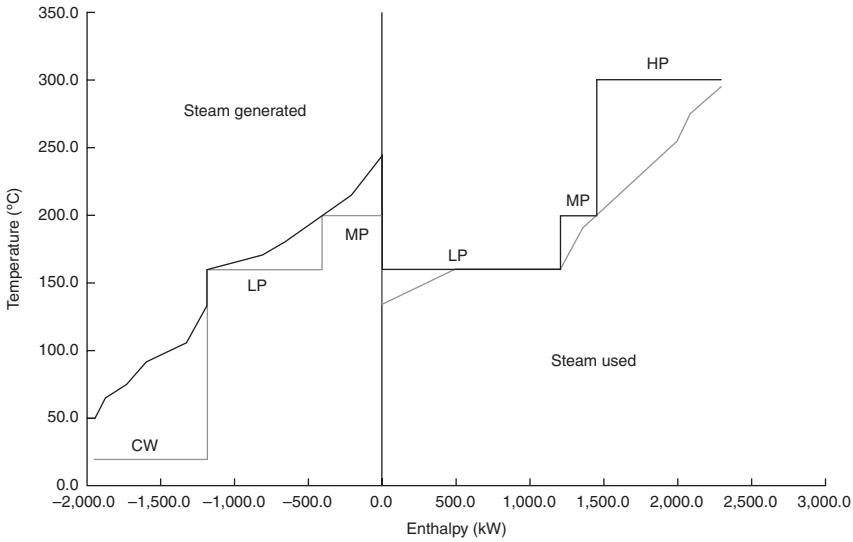

6.10 Total Site Profiles with steam levels.

Table 6.6 Steam used and steam generated across the Total Site

Steam main	Steam used (kW)	Steam generated (kW)
HP	849	0
MP	250.5	405.9
LP	1,200	769.1
Cooling water	0	773.5

temperatures, and because of the double shift in heat source and heat sink temperatures, feasible heat transfer is ensured. When a horizontal line representing the steam main temperature touches the Site Profile, the shift in temperature of the extracted process stream segments and the real temperatures of the steam mains means that heat exchange will take place at the appropriate Minimum Approach Temperature (ΔT_{min}) for that process. In other words, if steam has to be supplied to Process A at that point then the steam temperature supplying the heat will be 30°C higher than the stream segment from Process A at this point, because the real temperature of this cold stream segment is ΔT_{min} below the depicted temperature shown by the Heat Sink Profile. For the Process B stream segment, the real temperature of the stream segment is 10°C below that of the steam temperature providing heat to that segment. The amount of steam used at each steam mains saturated temperature level to satisfy the heat sinks of the site processes, and the amount of steam generated

© Woodhead Publishing Limited, 2013

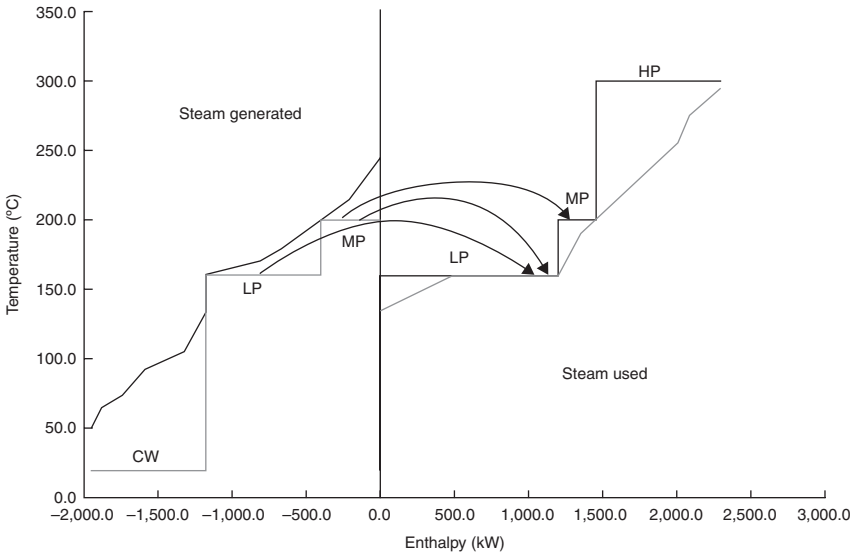

6.11 Total Site Profiles with potential steam heat recovery.

from the heat sources of the site processes, are easily extracted from the Total Site Profiles and are given in Table 6.6.

The amount of steam that has to be provided by the HP, MP and LP steam mains equals the amount of total heat that has to be supplied to the heat sinks in the site processes, 2,299.5 kW. The amount of steam that can be generated, or that has to be disposed of to cooling water, equals the total amount of heat contained by the heat source segments, 1,948.5 kW.

At this stage the Total Site Profiles are only an intermediate stage in the final targeting of the amount of external heat in the form of steam that needs to be supplied to the site processes. At this stage, the Total Site Profiles show that the amount of heat in the form of steam that has to be supplied from the site steam supply boilers is 2,299.5 kW. Again, at this stage, none of the steam generated by the site process heat sources is being used to compensate for the steam being supplied by these boilers. To determine or target the final requirements for steam from the boilers we need to make use of the Total Site Composite Curves.

The Total Site Composite Curves can be achieved by making use of the steam generation from the Total Site Source Profile to satisfy the heating requirements of the Total Site Sink Profile. The potential is illustrated in Fig. 6.11. The generation of steam at any level can be used to provide heating at the same temperature level, or at a lower temperature, by letting down steam

© Woodhead Publishing Limited, 2013

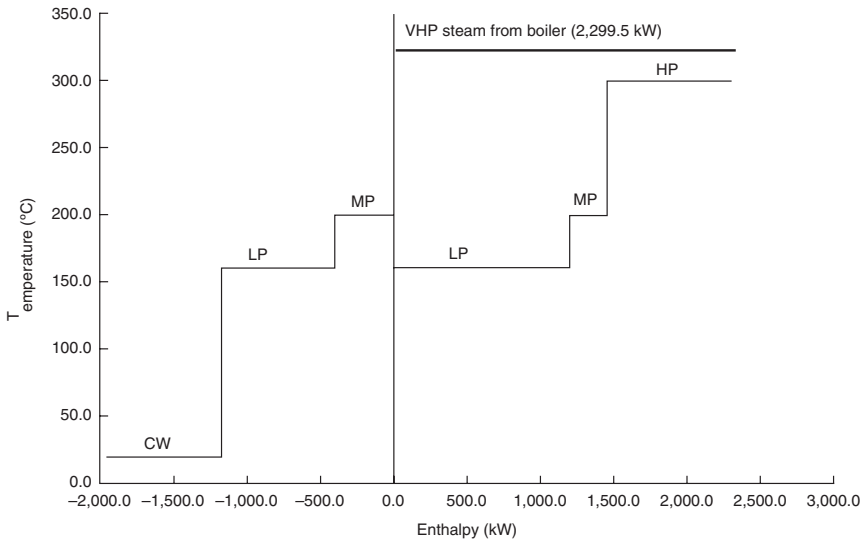

6.12 Steam Profiles with steam boilers providing VHP steam.

to the reduced pressure (with the potential of producing co-generation shaft work as shown by the arrows in Fig. 6.11).

To determine the amount of final VHP steam to be supplied by the boilers, we need to overlap the sink side of the Total Site Profiles with the source side of the Total Site Profiles. This is best achieved by separating the Steam Profiles from the Total Site Profiles as shown in Fig. 6.12.

In the situation shown in Fig. 6.12, the steam required by the site processes at HP, MP and LP steam levels has to be supplied by the steam boilers. The use of steam by the processes is not compensated in any way by the steam generated by the site processes. To achieve some degree of compensation we need to determine this by overlapping the Source and Sink Profiles as shown in Fig. 6.12.

Figure 6.13 shows some overlap between the Sink and Source Profiles. The Sink Profile has been pushed towards the Source Profile so that the VHP steam needed from the boilers has been reduced from 2,299.5 to 1,600 kW. The amount of steam used and generated at the various steam pressure levels in the system has not changed. However, with this amount of overlap, 699.5 kW of steam generation is now being used by the site processes in preference to steam supplied by the boilers.

The maximum amount of overlap between the Source and Sink Profiles is shown in Fig. 6.14. In this situation the Sink Profile cannot be pushed any

© Woodhead Publishing Limited, 2013

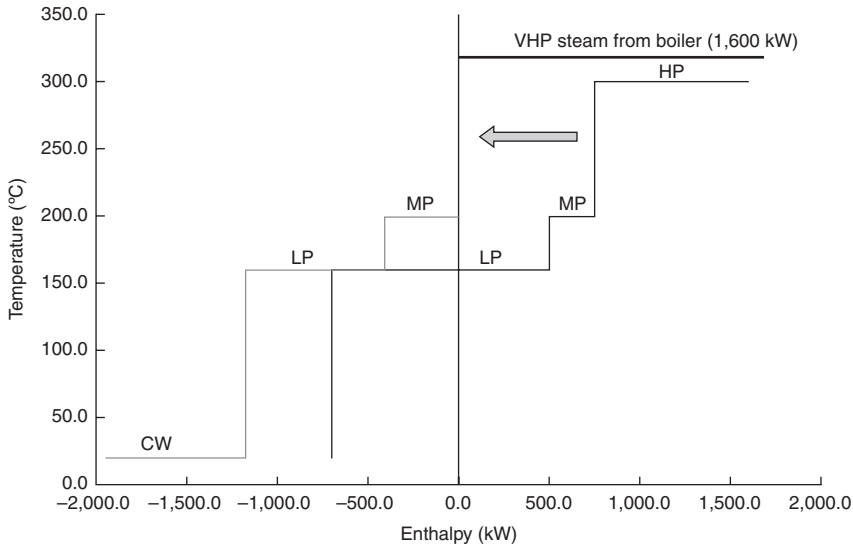

6.13 Steam Profiles showing VHP reduction to 1,600 kW.

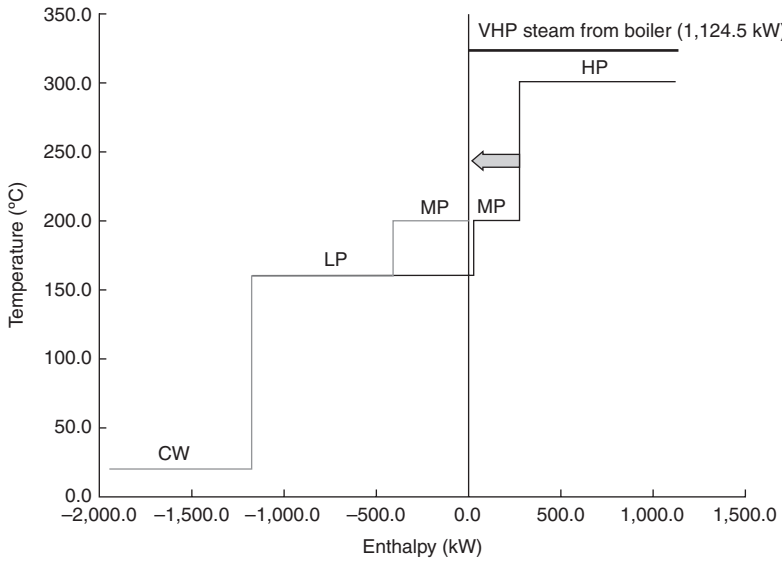

6.14 Maximum overlap between the Source and Sink Profile and minimum VHP demand from boilers.

further towards the Source Profile. The inhibiting factor is the trade-off between the amount of LP steam generated and the amount of LP steam being used by the site processes. At this position of maximum overlap, the amount of VHP steam to be supplied by the boilers has been reduced to 1,124.5 kW. The amount of heat recovery through the steam system is 1,175 kW.

© Woodhead Publishing Limited, 2013

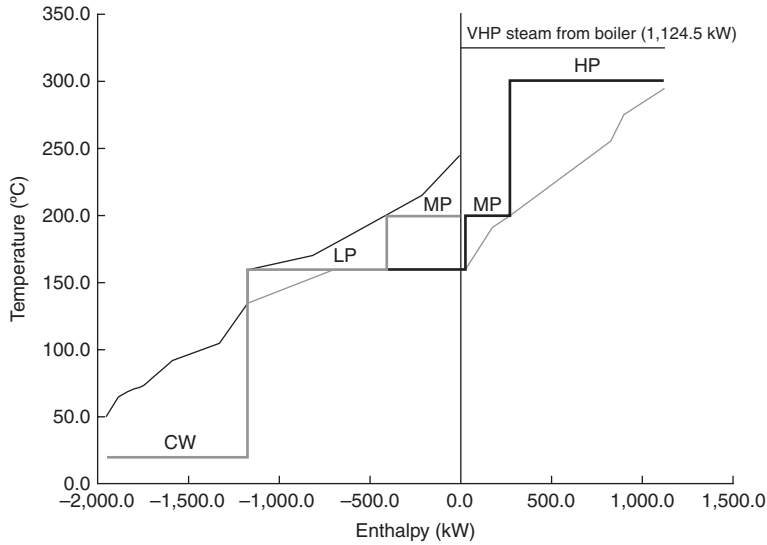

6.15 Total Site Composite Curves with minimum VHP demand from boilers and maximum heat recovery through the steam system.

If we now add back the Site Profiles to the construction, we produce the Total Site Composite Curves, representing the maximum heat recovery through the steam system, and the minimum amount of steam to be supplied by the site boilers (Fig. 6.15).

The number of steam levels (mains) used in the site utility system and their pressure, and consequently the saturated temperature of the steam levels, have a significant effect on the amount of heat recovery through the steam system and the amount of VHP steam that is needed from the site boilers. If we now consider the situation where the LP steam mains is no longer available for steam generation or use in the example we are considering, we will have the Total Site Profiles as shown in Fig. 6.16. In this case the site processes are being supplied with HP and MP steam only, and the heat sources in the site processes are only able to generate MP steam. The remaining heat sources have to be disposed of to cooling water. The amount of HP steam used by the site processes is 849 kW and the amount of MP steam used is 1,451 kW. The amount of MP steam generated is 405 kW. If we have no heat recovery, as depicted in Fig. 6.16, then the amount of steam that is required for the boiler is the same as the original situation, 2,299.5 kW.

If we now look at maximising the heat recovery in the Total Site, we will achieve heat recovery as shown by the Total Site Composite Curves as in Fig. 6.17. We are now only able to achieve 405.94 kW of heat recovery and the site boilers are required to supply 1,893.56 kW. This is an increase of 769.06 kW of steam heat that has to be supplied by the site boilers.

© Woodhead Publishing Limited, 2013

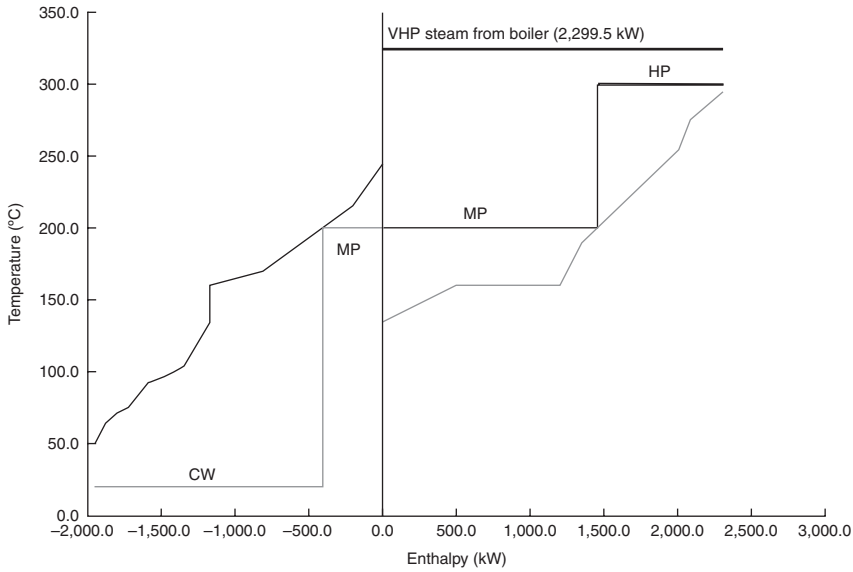

6.16 Total Site Profiles. No LP steam generation or use.

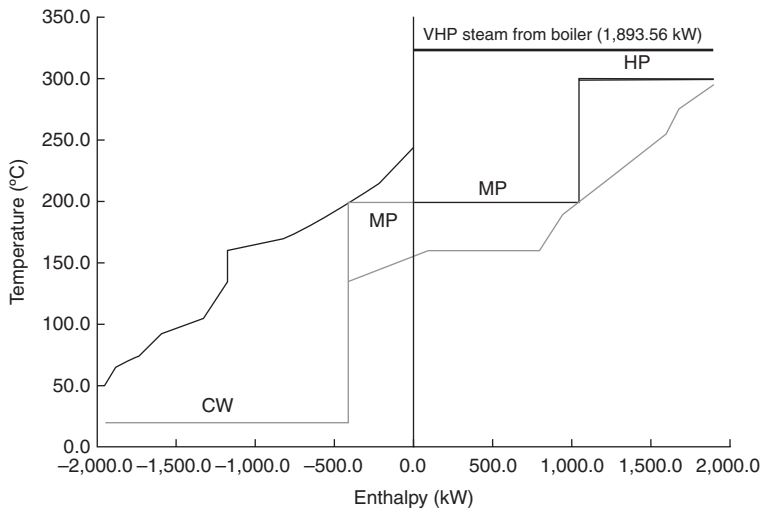

6.17 Total Site Composite Curves. No LP steam generation or use.

© Woodhead Publishing Limited, 2013

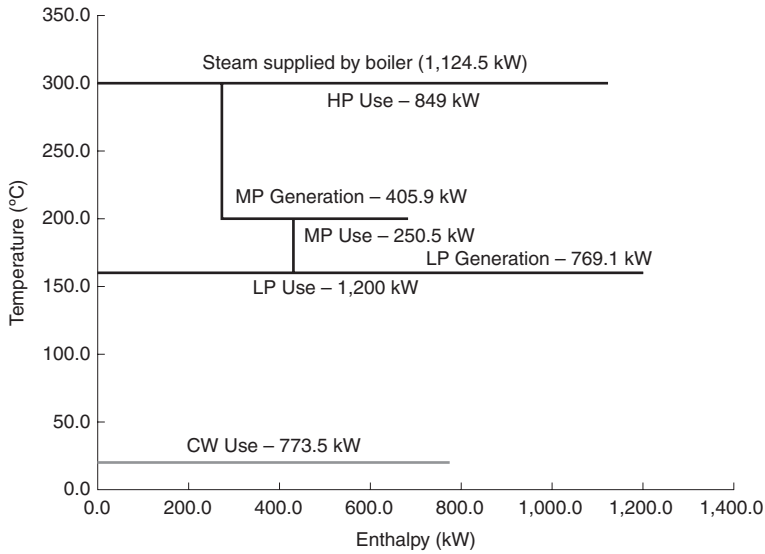

6.18 SUGCC with maximum heat recovery.

6.4 Site Utility Grand Composite Curve (SUGCC)

The final targeting tool that is available for Total Sites is the SUGCC, which represents the potential co-generation that is available in the site utility system due to the distribution of steam to the site process heat sinks and the generation of steam from site boilers and process heat sources. The SUGCC can be derived from the targeting information already obtained in the form of Total Site Profiles and Total Site Composite Curves.

Consider Fig. 6.18, which is the SUGCC for the situation described in Fig. 6.15 when we have maximum heat recovery through the steam system. The construction is carried out in the following way.

The amount of steam being supplied by the site boilers in this situation is 1,124.5 kW, which has been determined from the Total Site Composite Curves in Fig. 6.15. We are assuming here that the boilers are producing steam at a pressure of 86 bar and a saturated steam temperature of 300°C. This is at the same pressure and temperature as the HP steam being supplied to the site processes. In many cases it is likely that the steam produced by the site boilers will have a higher pressure and the steam will be expanded down to this lower pressure level, perhaps through steam turbines and consequently producing power. A horizontal line representing the steam at 300°C is then drawn from the 0 kW enthalpy value to the 1,124.5 kW enthalpy value. The amount of HP steam used by the site processes is 849 kW, and this amount is traced back along the original HP steam line, leaving the enthalpy coordinate at an enthalpy value of

© Woodhead Publishing Limited, 2013

275.5 kW. A vertical line is then dropped to this enthalpy value at the temperature of the MP steam, 200 °C. The amount of MP steam generated at the MP level is 405.9 kW, and a horizontal line is drawn from the current point on the graph to an enthalpy value of 681.4 kW. The amount of MP steam used by the site process heat sinks is 250.5 kW, and again the line is traced back to an enthalpy value of 430.9 kW. A vertical line is now dropped to the LP steam temperature level, 160°C. The amount of LP steam generated by the site processes is 769.1 kW, and a horizontal line is drawn from the dropped point at 430.9 kW to 1,200 kW. The amount of LP steam used by the site processes is 1,200 kW, and the horizontal line is traced back to the 0 kW enthalpy value.

We can see from the SUGCC in Fig. 6.18 that between the HP steam level and the LP steam level there is an enclosed area. This represents the amount of co-generation shaft work that could be produced if steam turbines were used to expand steam from a higher pressure level to a lower pressure level. We can see from Fig. 6.18 that of the 1,124.5 kW of steam supplied by the boilers, only 849 kW is being used by the site processes, which means that 275.5 kW of steam is being passed to the MP steam level. If this amount of steam is expanded in a steam turbine, then this will produce power that can be used on the site. At the MP steam level, 405.9 kW of MP steam is being generated by the site processes, and only 250.5 kW is required by the heat sinks of the site processes. This leaves 155.4 kW of MP steam that can be expanded to the LP steam level, in addition to the 275.5 kW of HP steam that has been supplied by the steam boilers. At the LP steam level there is a requirement for 1200 kW of steam by the heat sinks of the site processes. This is supplied by the excess HP steam, 275.5 kW, the excess MP steam, 155.4 kW, and the LP steam generated by the site process, 769.1 kW.

Raissi (1994) produced a simple model to relate the enclosed area in Fig. 6.18 to the production of co-generation shaft work. Several other authors have also looked at models to calculate the amount of co-generation power produced by the generation and use of steam by site processes, and the supply of boiler steam to make up the difference. These are briefly mentioned in the Sources of Further Information at the end of this chapter. However, the production of co-generation shaft work is more fully explored in the previous Chapter 5.

We have seen that the SUGCC represented in Fig. 6.18 is related to the situation where we have maximised heat recovery through the steam system and minimised the amount of VHP steam that is needed to be supplied by the site boilers. In producing the Total Site Composite Curves, which represent the situation of maximum heat recovery and minimal VHP supply, we started from the Total Site Profiles, which represent the situation of no heat recovery and maximum VHP supply from the site boilers. We also showed

© Woodhead Publishing Limited, 2013

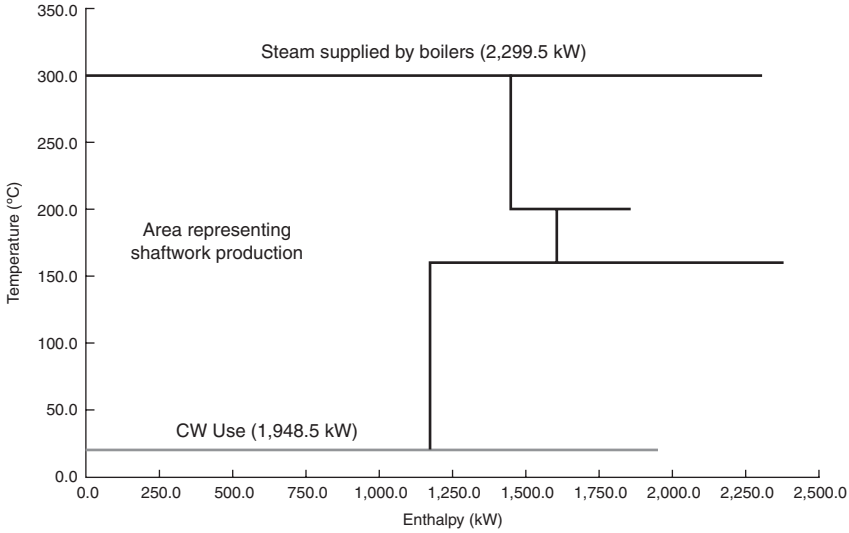

6.19 SUGCC with no heat recovery and maximum boiler steam supply.

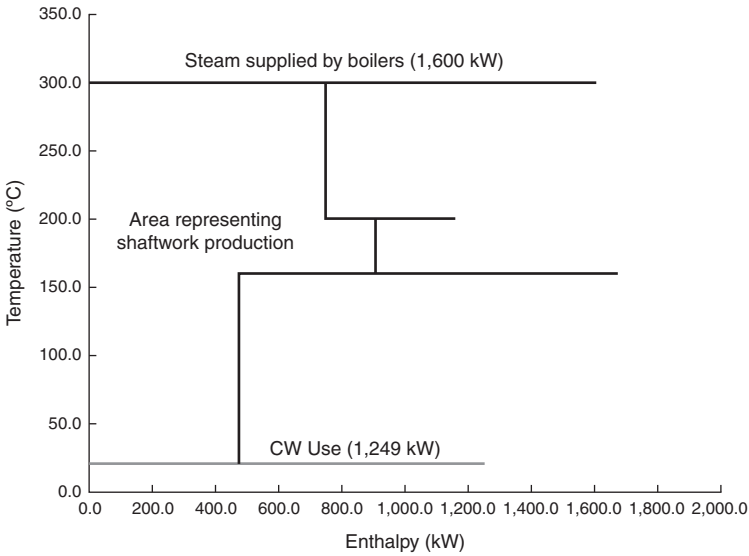

6.20 SUGCC with 699.5 kW of heat recovery and 1,600 kW boiler steam supply.

an intermediate step where the amount of VHP steam supply from the boilers was reduced from the maximum of 2,299.5 to 1,600 kW, before finally being minimised to a value of 1,124.5 kW. These three different operating scenarios can be represented by their SUGCCs. The scenario of maximum

© Woodhead Publishing Limited, 2013

overlap is shown in Fig. 6.18. In contrast, the SUGCC for no heat recovery and maximum steam supply from the steam boilers is shown in Fig. 6.19, and the intermediate scenario of 699.5 kW of heat recovery and 1,600 kW of boiler steam supply is shown in Fig. 6.20.

In Fig. 6.19 we see that we are required to supply 2,299.5 kW of steam from the steam boilers. Although this is 1,175 kW greater than the scenario of maximum heat recovery through the steam system, we can observe that the area representing the potential co-generation shaft work of the system is much greater. In other words we have traded off additional steam supply from the boiler for increased potential co-generation shaft work production. In Fig. 6.20, the intermediate scenario, we have reduced the amount of steam supplied by the boiler and also decreased the potential co-generation shaft work production. The most appropriate scenario is determined by a number of factors, which includes the number and pressure of the steam levels, and is consequently an optimisation problem, depending on the relative costs of fuel and the site requirements for power and the value of power. Again, further discussion is outside of the scope of this chapter, but there are some references to this work in Section 6.6.

6.5 Conclusion

This chapter has looked closely at the techniques available for analysing Total Sites from the point of view of process heat sources and heat sinks that can be met by heat recovery through the generation and use of steam, thereby minimising the amount of steam that has to be supplied by central site utility boilers.

The extraction of heat sources and sinks, after maximising process heat recovery, can be accomplished with the aid of the individual Grand Composite Curves and the results of the Problem Table Algorithm. The sources of heat from the individual site processes can be integrated to produce the Site Source Profile. Similarly the sinks of heat from the individual site processes can be integrated to produce the Site Sink Profile. Plotted together they make up the Site Profiles, showing the total amount of heat available from all the processes on the site in relation to temperature, and the amount of heat needed by all the site processes.

The heat sources can be related to the generation of steam from the individual processes at various selected pressures, and the heat sinks can be related to the use of steam at various pressures. The use and generation of steam at these predetermined pressures in relation to the heat sources and sinks can be shown in the Total Site Profiles. Without any heat recovery between the generation and use of steam, the Total Site Profiles can show

© Woodhead Publishing Limited, 2013

the amount of steam that has to be supplied by the central site utility boilers. However, the generation of steam from the process heat sources can be used to supply the process heat sinks, and consequently reduce the steam supply from the site utility boilers. The maximum amount of heat recovery from the site processes through the steam-distribution system can be shown in the Total Site Composite Curves.

The generation and use of steam related to the process heat sources and heat sinks, and accompanied by the supply of steam from the site utility boilers, can be shown on the SUGCC. This plot can also indicate the amount of potential co-generation shaft work that can accompany this steam generation and use at the various pressure levels chosen.

6.6 Sources of Further Information

Although Total Site Analysis and Targeting has been used extensively for a number of years, there remains considerable academic and industrial interest in the area. Consequently new journal and conference papers continue to be published in a number of research journals, although books are considerably less numerous.

Smith (2005), in his book in Chapter 23, examines the development of Total Sites and Total Site Targeting including Total Site Profiles, Total Site Composites and SUGCCs. He particularly pays attention to the use of the SUGCCs in relation to the co-generation shaft work and the methods used to calculate the co-generation shaft work.

Kemp (2007) also refers to Total Site Analysis in his chapter on Utilities, heat and power systems. He briefly examines the construction of the Site Source and Site Sink Profiles.

A number of authors have extended the Total Site Targeting methodology. Perry *et al.* (2008) made use of Total Site Targeting using processes with different $\Delta T_{\min}$ values to represent heat sources and sinks for the integration of small scale chemical processes with a hospital complex and domestic buildings and office complexes. The work also examined the possibility of integrating renewable energy sources to reduce carbon based emissions – for more details see Chapter 7.

All previous Total Site research up to 2010 was overviewed in the recent book of Klemeš *et al.* (2010).

This work was continued by Varbanov *et al.* (2012), where the methodology of data extraction for processes with different $\Delta T_{\min}$ values was more extensively examined. These authors examined the effect of varying Minimum Approach Temperatures on the potential heat recovery of the Total Site and found that the choice of $\Delta T_{\min}$ was critical for the efficiency of heat recovery.

© Woodhead Publishing Limited, 2013

Varbanov and Klemeš (2011) also examined the Total Site when there were varying supply and demands for heat. They examined cases where renewable energy sources could contribute to the supply of heat, but were not available at all times. They included the possibility of including heat storage and release in the construction and analysis of the Total Site.

Liew *et al.* (2012) looked at the Total Site from the point of view of plant shutdown and variations in heat supply and heat demand. They produced a number of new tools to examine the sensitivity of heat recovery in these situations.

Matsuda *et al.* (2009) applied Total Site analysis to the Kashima industrial area in Japan, which consists of 31 sites. They extracted data from the heaters and coolers from the Total Site in order to produce the Site Source and Site Sink Profiles.

Hackl *et al.* (2011) also applied Total Site Analysis to a cluster of five chemical companies producing a variety of products with varying supplies and demands for heating and cooling. They used the Total Site Profiles and Total Site Composite Curves to identify potential heat recovery and the identification for the need of a site-wide hot water circuit.

6.7 References

Dhole, V. R., Linnhoff, B. (1993). Total site targets for fuel, co-generation, emissions, and cooling. *Computers and Chemical Engineering*, **17**(supplement), S101–S109.

Hackl, R., Andersson, E., Harvey, S. (2011). Targeting for energy efficiency and improved energy collaboration between different companies using total site analysis (TSA). *Energy*, **36**, 4609–4615.

Kemp, I. C. (1982, last edition 1994). Pinch analysis and process integration. In: Linnhoff, B., Townsend, D. W., Boland, D., Hewitt, G. F., Thomas, B. E. A., Guy, A. R, Marsland, R. H. (eds), *User Guide on Process Integration for the Efficient Use of Energy.* IChemE, Rugby, Butterworth-Heinemann/IChemE Series, 2007, 396 pp..

Klemeš, J., Dhole, V. R., Raissi, K., Perry, S. J., Puigjaner, L. (1997). Targeting and design methodology for reduction of fuel, power and CO_2 on total sites. *Applied Thermal Engineering*, **7**, 993–1003.

Klemeš, J., Friedler, F., Bulatov, I., Varbanov, P. (2010). *Sustainability in the Process Industry: Integration and Optimization*, McGraw Hill Companies Inc, New York, USA.

Liew, P. Y., Wan Alwi, S., Varbanov, P. S., Abdul-Manan, Z., Klemeš, J. J. (2012). A numerical technique for Total Site sensitivity analysis. *Applied Thermal Engineering*, **40**, 397–408.

Matsuda, K., Hirochi, Y., Tatsumi, H., Shire, T. (2009). Applying heat integration total site based pinch technology to a large industrial area in Japan to further improve performance of highly efficient process plants. *Energy*, **34**, 1687–1692.

© Woodhead Publishing Limited, 2013

Perry, S., Klemeš, J., Bulatov, I. (2008). Integrating waste and renewable energy to reduce the carbon footprint of locally integrated energy sectors. *Energy*, **33**, 1489–1497.

Raissi, K. (1994). Total site integration. PhD thesis, UMIST, Manchester, UK.

Smith, R. (2005). *Chemical Process Design and Integration*. John Wiley & Sons, Chichester, UK.

STAR. (2012). Process Integration Software, Centre for Process Integration, CEAS, The , UK.

Varbanov, P. S., Klemeš, J. J. (2011). Integration and management of renewables into Total Sites with variable supply and demand. *Computers and Chemical Engineering*, **35**, 1815–1826.

Varbanov, P. S., Fodor, Z., Klemeš, J. J. (2012). Total Site targeting with process specific minimum temperature difference (ΔT_{min}). *Energy*, **44**, 20–28.

© Woodhead Publishing Limited, 2013

7

Extending Total Site Methodology to Address Varying Energy Supply and Demand

PETAR SABEV VARBANOV, University of Pannonia, Veszprém, Hungary

DOI: 10.1533/9780857097255.2.226

Abstract: Reducing CO_2 emissions could be achieved by maximising heat recovery and increasing the share of renewables in the primary energy mix. Process Integration (PI) can be used for facilitating this and maximising the efficiency of the resulting systems. One of the important developments in PI has been Total Site Heat Integration (see Chapter 6), in which the heating and cooling requirements of individual processes are combined, allowing better integration. This chapter describes the extension of the Total Site Methodology covering industrial, residential, service, business and agricultural energy users, and the incorporation of renewable energy sources (solar, wind, biomass and some types of waste), accounting for the often substantial variability on the supply and demand sides and for the use of non-isothermal utilities.

Key words: Total Site Integration, Energy Management, Integration of Renewables, Varying Energy Supply, Varying Energy Demand.

7.1 Introduction

Although commonly described using steady state models, in reality energy systems, including Total Sites, are subject to variations on both the supply and demand sides. These variations involve both regular changes in the rates and property of the energy carriers, referred to as patterns, as well as random, transient variations, referred to as fluctuations. Therefore, what energy system designers and planners face is a problem of satisfying energy demands of varying rate but of constant quality requirements, using energy sources of varying availability and quality. Another important feature of this problem is the multiplicity of energy sources (fossil fuels, nuclear, biomass, wind, solar, etc.) combined with the multiplicity of energy users (industrial, residential, large commercial complexes, hotels, hospitals).

There is an apparent trend of harvesting ever-increasing amounts of energy from renewable sources – such as wind and solar. Adopting renewable energy resources and maximising their utilisation acts simultaneously

© Woodhead Publishing Limited, 2013

to reduce CO_2 emissions and energy dependency. This necessitates the development of models and algorithms for designing and operating energy conversion and supply systems handling the variable availability of energy from such sources as well as the variability in the user demands.

Energy recovery and improved efficiency are most optimally and transparently achieved by applying PI, especially Total Site Heat Integration – reviewed in Friedler (2009), an extended version in Friedler (2010). Klemeš *et al*. (2010) also provide an extensive review of the fundamentals and several worked examples. A detailed overview of the historical developments is provided in Chapter 1.

The Total Site Integration of heat systems, based on the concept of the site heat source and Heat Sink Profiles, was introduced by Dhole and Linnhoff (1993). Klemeš *et al*. (1997) made further advances in the field by adding targets for power co-generation. The concept has been initially applied to industrial sites-refinery and petrochemical processes. The latter generally operate as parts of large sites or factories. The Heat Integration on such Total Sites is performed through a set of energy carriers – usually steam at several pressure levels, plus hot water and cooling water. The site processes are serviced by a centralised utility system providing the thermal energy carriers and power. Total Site Integration has been applied to a number of chemical industrial sites (Matsuda *et al*., 2009) and even to a heterogeneous Total Site involving a brewery and several commercial energy users. It has also been used as the targeting stage for the synthesis of utility systems, first in Shang and Kokossis (2004) and then elaborated for choosing steam header pressure levels by Varbanov *et al*. (2005). This topic is covered in detail in Chapters 5 and 11.

Renewable resources are usually available on a smaller scale distributed over a given area. Their availability (with the exception of biomass) is usually well below 100%. The resource availability varies significantly with time and location, because of changing weather and geographic conditions. The energy demands (heating, cooling and power) of industrial sites and other users vary significantly with time of day and season. The variations of the renewable supplies and the demands are partly predictable and some change in very regular time patterns – day and night for solar energy, for instance. However, the availability of other renewables, such as wind-generated energy, can be less predictable. Demand variability is treated later in the chapter.

As a result, optimising the design of energy systems serving variable customer demands and using renewable resources is a complex task compared to using just fossil fuels to satisfy a constant demand.

In seeking the optimal solution for such energy systems, one would like to provide adequate tools and ensure the necessary degrees of freedom,

© Woodhead Publishing Limited, 2013

so as to satisfy the demands with the available supplies at minimum cost or maximum profit (Varbanov *et al.*, 2005). The optimisation objectives can be purely economic or include the corresponding environmental aspects resulting in the criteria of eco-cost or eco-profit (Čuček *et al.*, 2012). Two tools are likely to play a significant role in this regard: energy storage on the demand side and establishment of a hierarchy for utilisation of the available energy sources concerning the supply. Installation of buffering vessels as part of the utility system can help in smoothing the fluctuations in supplies and demands and facilitate system control.

7.2 Characteristics of Energy Supply and Demand

To understand the problem better, a characterisation of supply and demand types is needed. Both supply and demand for energy can vary with time and location. Accounting for temporal variations introduces dynamic modelling elements and concepts very similar to those used for batch processes – including terms such as horizon and Time Slice (period).

7.2.1 Classification of Energy Supply Sources

The sources of energy for the considered users are in most part common:

- **Fossil fuels**. Currently dominate the energy markets. They can be used in all three site categories – residential, industrial sites and service building complexes.
- **Solar radiation**. Can be captured into thermal energy carriers (water, steam, antifreeze, etc.) or to generate electricity. A combination of both is a possibility as well but not very much developed so far.
- **Wind**. Mostly used for electricity generation, with future potential for generating H_2 for the hydrogen economy.
- **Waste biomass** and **Energy crop biomass**. They can be directly utilised on-site for larger consumers such as industrial sites, building complexes and farms, or in district heating plants.
- **Hydropower**. Harnessed for electricity generation. This, however, is performed mostly in centralised larger-scale power stations on dams. Micro-hydropower technologies are available, but they are mainly suitable for remote locations, with generally less requirement for Energy Integration.
- **Geothermal energy**. Harnessed at locations where it is available, or nearby.
- **Ground heat or cold**. Heat pumps are considered as renewable sources of energy in most classifications.

© Woodhead Publishing Limited, 2013

7.2.2 Classification of Energy Users

Energy demands vary with type of end user, as well as with the time schedules. Industrial sites mostly require:

- Heating in a wide range, from 100°C up to 400°C and even close to 1,000°C,
- Cooling in the range 20–50°C, and chilling in the range 0–10°C,
- Refrigeration to temperatures of −100°C and lower.

A special class of applications is farming and agriculture production. There are various examples of using the low potential waste and renewables heat for supplying greenhouse demands e.g. the work by Kondili and Kaldellis (2006).

Residential sites (residential dwellings and their complexes in the case of district heating) feature demands for:

- Moderate-temperature heating of space and hot water,
- Air conditioning,
- Direct electricity consumption for lighting, cooking, refrigerators and other household appliances,
- Electricity for heat pumps.

The energy demands for the service industry and for building complexes (hotels, hospitals, schools and universities, banks, entertainment premises, governmental complexes) are generally similar in structure to residential sites. Some specific features are:

- A part of the heating demand can be at a temperature in the range 90–150°C. For example, steam can be used in hotels for cooking, and in hospitals for sterilising bedding and other appliances.
- The share of air conditioning may be significantly higher compared with residential homes.
- The specific resource consumption per person in the service industry (as hotels and hospitals) is generally higher than in residential homes, because of the overheads of running additional services, infrastructures and facilities, such as restaurants, bars and entertainment facilities.

7.2.3 Variability of Demand

The time variations of energy demands have been subject to research in both industrial and residential contexts. An example is a study investigating

© Woodhead Publishing Limited, 2013

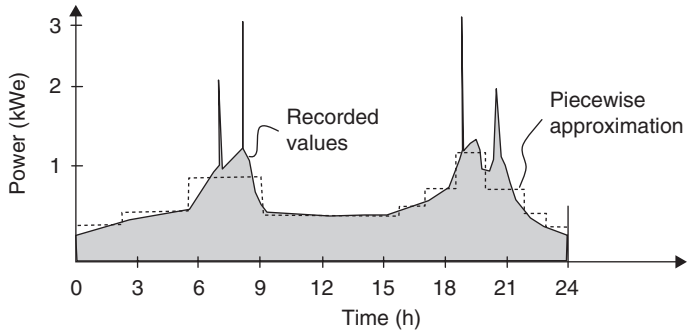

7.1 Typical residential electricity demands within a 24 h cycle (after Bance, 2008).

the variation of residential energy consumption for heating, electricity and hot water (Bance, 2008). The results show two types of trend: hourly variations during each day, and seasonal variations during the year. For the hourly variations in residential energy consumption there are nearly steady periods during usual office hours and two consumption peak intervals in the morning and in the evening. Figure 7.1 shows a typical trace for electricity consumption, but hot water consumption variation follows a close trend. The seasonal variations are relatively smooth, with more substantial space-heating demands from October until April.

Demand variations are mostly predictable and feature minor uncertainties—mainly in the timing of the consumption. The picture may differ among buildings, industrial sites and farms. A similar situation occurs in service buildings such as hotels and hospitals, where the demand levels will also depend on the occupancy rate and some less predictable features. Table 7.1 shows the types of temporal variations in energy demands typical for the various users.

7.2.4 Variability in Energy Supply from Renewable Resources

For their efficient exploitation, it is necessary to assess an overall availability of renewables and variability with time. Some of them are close to the performance of fossil fuels and can be well stored for continuous energy generation. An example is biomass, where the supply varies by year, season and by bio-waste availability. However, sufficient storage could be made available. The availability of other renewable sources, such as wind and solar varies more rapidly – in hours and even minutes.

Two examples of more detailed studies on variability of renewable energy sources can be given. One is a report for the International Energy Agency (IEA, 2005), which deals with the intermittency of wind-power generation,

© Woodhead Publishing Limited, 2013

Table 7.1 Demand variability types

	House/ dwelling	Industrial site	Service building complex	Farms/ agriculture
Electricity	Peak/off-peak	Main shift/other shifts, campaign/ off campaign	Day/night – sometimes less	Summer/ winter
Heating	Winter/ summer	Winter/summer – campaign/off campaign	Winter/ summer	Winter/ summer
Cooling	Summer/ winter	Winter/summer – campaign/off campaign	Summer/ winter	Summer/ winter
Air conditioning	Summer mainly	Summer mainly	Summer mainly sometimes less predictable	Not used too widely
Direct shaft power	Not used	Widespread, using steam or gas turbines	Not typical	Not typical

as well as that from other renewable energy sources. It provides an analysis of the time scales of variation of the availability of those sources, based on the natural cycles of variation. It can be seen that solar-energy availability may vary on a time scale from minutes to years. A second example is the chapter by Von Bremen (2010), which describes variations of wind and solar power availability, also providing visual examples in terms of plots. The chapter also discusses the implications of these variations and strategies for performing power balancing in order to keep the demand satisfied.

These types of variation present an integration challenge where the time horizons of the changes are diverse. From the given examples, for biomass, the Time Slices to model the problem would last on the order of months, and at the smallest – weeks. For wind and solar energy, the Time Slice durations will obviously be much shorter (Nemet *et al*., 2012a). This makes necessary the extension of the Total Site methodology, as initially conceived by Dhole and Linnhoff (1993) and elaborated for co-generation by Klemeš *et al*. (1997), to deal with the described variations.

7.2.5 Requirements for Energy System Design and Operation

From the above analysis, the need for several important requirements to energy system design and operation can be identified:

© Woodhead Publishing Limited, 2013

- It is necessary to cater for a diverse set of energy users. The most notable customers are large and small industrial plants, residential, commercial and service buildings, as well as potentially farm complexes.
- Integration of renewables is of strategic importance for reducing CO_2 emissions and for a great number of countries – also to lessen external energy dependence.
- It is vital to account for the variations in energy supplies and demands. A number of tools can be used, all centred around heat storage.
- A uniform framework for modelling the site heat sources and sinks, combined with heat storage and non-isothermal utilities is needed.

7.3 Thermal Energy Storage and Integrated Architecture

The variability of energy demand and supply, together with the potential benefits of exchanging heat at various temperature levels have prompted the development of strategies for accommodating them. Integrating several processes and energy users/suppliers through a common utility system is a good way of allowing for the efficient exchange. However, because the variations of both the demand and supply can be significant, storage consideration is added, to allow for the transfer of energy from time periods of energy excess to periods of energy deficit.

7.3.1 Thermal Energy Storage

The idea of using storage for smoothing variations in energy supply and demand, allowing delayed use of available heat, is not new. There are a number of ways to store heat, based on physical, chemical and physico-chemical principles. A simple but effective technique applied in industry is a stratified water tank used within a heat recovery loop. Atkins *et al*. (2010) have presented an evaluation of such an arrangement for a milk powder plant. A comprehensive review on the various forms of heat storage can be found in Huggins (2010). The source discusses several storage types, among which are sensible heat storage and latent heat storage. The latter is based on various Phase-Change Materials (salts, paraffin-based materials, glycol polymers). Heat storage based on reversible chemical reactions is also described, emphasising salt hydration/dehydration.

The use of energy storage for industrial Heat Integration has been researched previously – good examples are the research papers on Heat Integration of batch processes by Kemp and Deakin – the work establishing the basic concepts and targeting procedures (1989a), the advanced Heat Cascade analysis

© Woodhead Publishing Limited, 2013

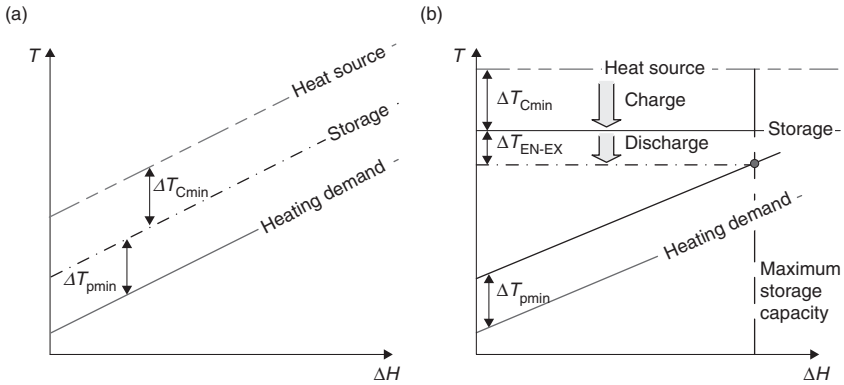

7.2 Storage types by temperature change (after Nemet *et al.,* 2012b). (a) Non-isothermal charge and discharge and (b) isothermal charge and discharge.

(1989b) and case study (1989c). A detailed report on the matter has been written by Klemeš *et al*. (1994) for an EU-funded research project. These sources focus on the context of a single process. They explore the Time Slice Model and the Time Average Model for heat-integrating batch processes and selecting the storage properties – temperature levels and capacity.

In turn, this philosophy has been extended and applied to Total Sites, first by Perry *et al*. (2008) who introduced other than industrial process types into the Total Site concept and, after that, by Varbanov and Klemeš (2011) who provided a fully-fledged framework for modelling and selecting the levels and capacities of heat storage facilities located in the utility system of a Total Site.

Despite the variety of heat storage methods and devices, for the purposes of Heat Integration they can be all classified into two types (Nemet *et al*., 2012b) – facilities with temperature change during charge/discharge, and facilities where each of the two operating modes takes place at virtually constant temperature (Fig. 7.2).

7.3.2 Integration Architecture

To account for variation of the demands, renewables availability and simultaneously maximising heat recovery, it is necessary to apply Total Site Integration and, when needed, to consider heat storage possibilities.

Traditional Total Sites (see details in Chapter 6) as introduced by Dhole and Linnhoff (1993) and developed further by Klemeš *et al*. (1997) include only industrial processes with their demands for heating, cooling and power, connected via the steam mains of the site utility system (Fig. 7.3). This model

© Woodhead Publishing Limited, 2013

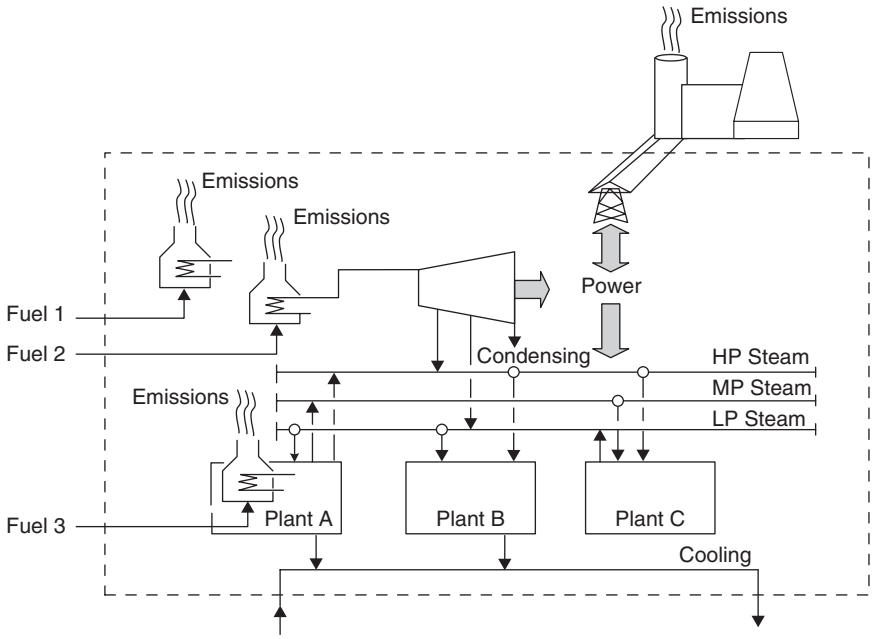

7.3 A typical industrial Total Site (after Klemeš *et al.*, 1997).

has served industry for a couple of decades and has proved its usefulness across a number of applications.

Perry *et al*. (2008) extended that notion by proposing the addition of residential and service buildings (hospitals, hotels, offices) as site processes, as well as alternative energy sources (biomass, wind, solar, ground heat) and conversion technologies (small-scale boilers, Stirling Engines, fuel cells, microturbines, solar thermal collectors, solar photovoltaic panels). They have coined the term ***Locally Integrated Energy Sector*** (LIES) (Fig. 7.4) to denote the resultant architecture.

This conceptual extension allows application of the Total Site Integration strategy to local communities involving a larger number of smaller-scale entities, and is referred to as the LIES. Adding the energy user and generator types and conversion technologies allows combining the temporal patterns of different user and generator types and potentially smoothing their inherent variations. Also, using distributed power and heat generation at or close to the locations of use enables direct trade-off between centralised and distributed generation. The latter is an important element allowing exploration of the most advantageous arrangement accounting for energy losses during transportation of fuel and the energy products (heat and power).

© Woodhead Publishing Limited, 2013

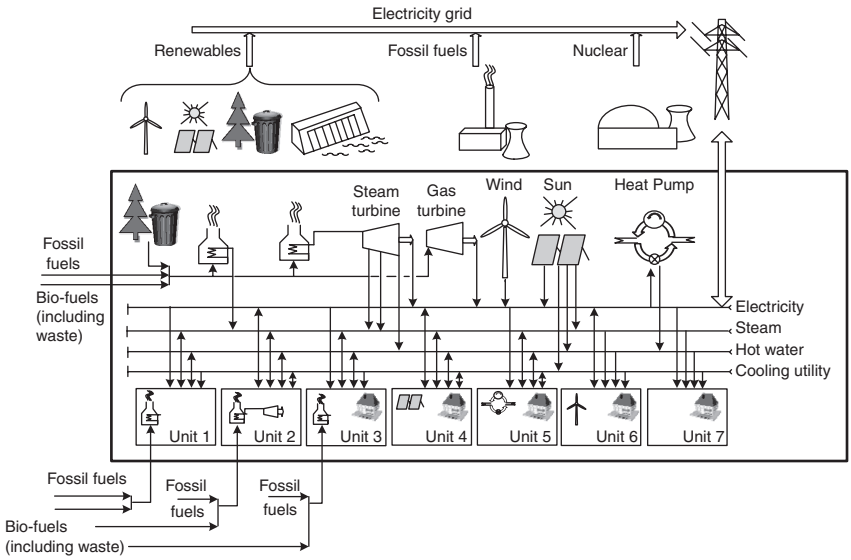

7.4 LIES (after Perry *et al.*, 2008).

7.4 Terminology for Process Streams and Utilities

From the Heat Integration basics (Klemeš *et al.*, 2010) it is known that hot utilities can be consumed for process heating and/or generated for process cooling. To establish an efficient procedure for dynamic energy targeting of Total Sites, the classification of the various heat sources and sinks on the site needs to be updated. The heating and cooling demands of individual processes, remaining after internal Heat Integration, are used to create the Heat Source Profile and the Heat Sink Profile for an industrial site (Chapter 6). Further, the available utilities are placed using the Site Composite Curves.

From the viewpoint of Heat Integration, steam, hot oil, flue gas, cooling water, etc., are clearly utilities. When integrating renewables and dealing with temporal variations in their availability as well as demand variations, it is necessary to decide how to treat the intermittent heat sources and sinks associated with the renewable energy supply and heat storage. Capturing renewable energy thermally always results in a heat source. On the other hand, the heat storage can be charged, acting as a heat sink, or discharged, acting as a heat source.

An important issue is how to treat these heat sources and sinks – as additional processes and process streams, or as utilities? The answer lies in analysing the role and meaning of process heating and cooling demands (Process Heat Sinks and Sources) on the one hand, and that of utilities on the other. Process heating and cooling demands are part

© Woodhead Publishing Limited, 2013

of the problem specification. As such, they have to be satisfied and cannot be varied or manipulated by the user. On the other hand, utilities are tools providing degrees of freedom to satisfy the heating and cooling demands with or without heat recovery. They may be used, but do not impose requirements.

Consider solar thermal energy capture. Solar irradiation falls on the capture area and as such cannot be controlled by the process operators and managers. Having a specification of the maximum potential capture area defines an upper limit on the solar-heat flow that can be captured. Within this limit, any capture rate is possible and this is a degree of freedom to be used. Similarly, heat storage also has a certain capacity and the storage may be charged or discharged according to this capacity also providing a degree of freedom to the system. If the balance of Process Heat Sources and Sinks does not require it, neither solar heat should be captured, nor is there a need for heat from storage to be used. As a result of the above, renewables and heat storage are classified as utilities.

7.5 Identification of Time Slices

In terms of energy management for demand/supply variations, a basic methodology has been developed previously for Heat Integration of batch processes: Time Slice (TS) and Time Average Composite Curves (TACC) (Kemp and Deakin, 1989a). They have been included in a more comprehensive report originating from an EC Project (Klemeš *et al*., 1994). This methodology has been recently revisited by Foo *et al*. (2008). TSs are defined as modelling time intervals, within which the rates of heat demand and supply streams can be modelled as constants. They are obtained by combining the starting and ending times of *process streams* (see Chapter 2). A key issue in applying this approach is the identification of the TSs. A procedure for identifying the number and durations of TSs for a problem featuring variable renewable energy supply has been formulated, and developed for solar-energy utilisation by Nemet *et al*. (2012a).

7.5.1 Time Slices for Variable Energy Sources

The variation in the renewables availability in time can be described as a series of continuous trends, where the switch points are usually created by weather changes. While the switch points are obvious candidates for TS boundaries, it is not so straightforward to identify TSs within a continuously varying energy flow profile. An example of this is shown in Fig. 7.5, where the availability of solar irradiation through a day is approximated by a parabolic curve, assuming that no clouds appear.

© Woodhead Publishing Limited, 2013

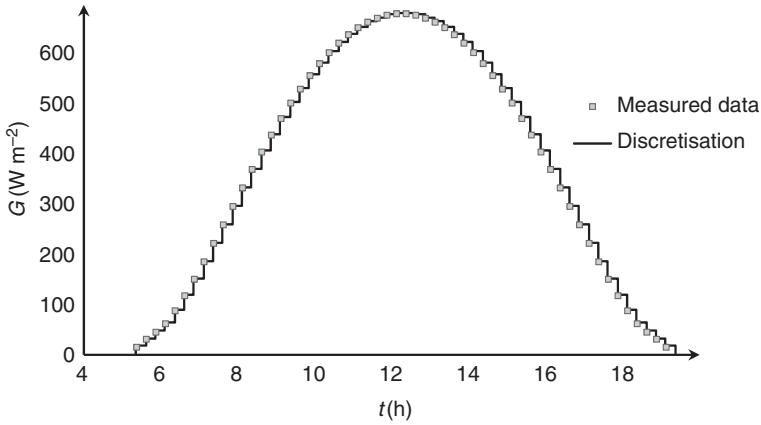

7.5 Approximation of solar irradiation availability during a day (after Nemet *et al.,* 2012a).

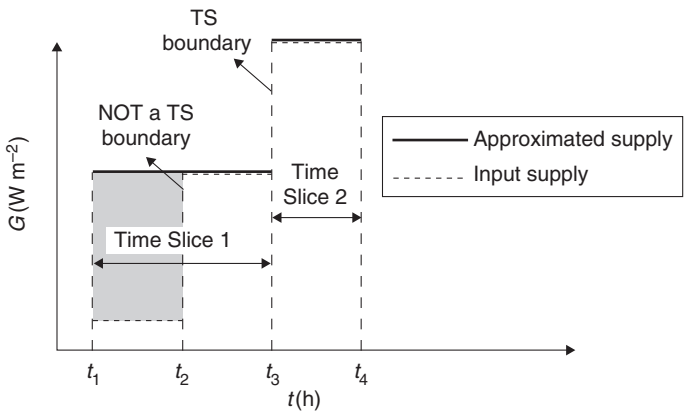

7.6 Acceptance/rejection of the candidate time period boundary as a TS boundary (after Nemet *et al.,* 2012a).

The profile is expressed as a series of sampling points connected with a piecewise-constant discretisation curve. The latter suggests all sampling points as potential TS boundaries. Considering these as a superset, an optimal subset of sampling points has to be selected which will represent the continuous solar profile in a sufficiently small number of TSs at minimum inaccuracy. This task is performed by solving an mixed-integer linear programming (MILP) problem (Nemet *et al.*, 2012a), where each candidate TS has a single level of the resource availability (Fig. 7.6) approximation, which is allowed to vary. These are accompanied by defining binary selection variables for each candidate for a TS boundary where, if the candidate boundary is selected,

© Woodhead Publishing Limited, 2013

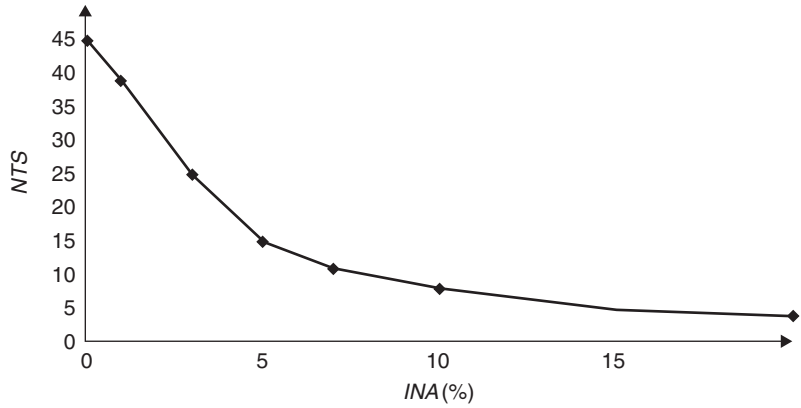

7.7 Dependence of Number of TSs (NTS) on the allowed tolerance (INA) value (after Nemet *et al.*, 2012a).

the availability level approximation for that interval is allowed to vary, while in the opposite case the level is set equal to that from the previous candidate slice.

The overall inaccuracy of the approximation using the selection of TSs can be minimised, subject to a number of constraints ensuring consistency of the formulation. The overall inaccuracy itself is defined as a summation of the absolute values (mathematical) of the differences between the levels of the sampling points and the approximation variables. Several options for solving this optimisation problem exist, and (Nemet *et al.*, 2012a) provides a discussion on their merits and weaknesses.

The optimal selection of TSs depends on the required accuracy. Figure 7.7 shows a typical trend of resulting numbers of TSs at various tolerances.

7.5.2 Time Slices for Different Energy Demands

For continuous industrial processes and for residential activities, the energy demands usually vary smoothly and change discontinuously when the operating mode changes. This pattern results in a similar set of continuous trends and switching points, as in the case of characterising the availability of renewable energy sources. Therefore, the procedure from Section 7.5.1 can be directly applied to this case too.

There is also the case of batch and semi-continuous processes in industry, which are characterised with transient operations – (Kemp and Deakin, 1989a), further developed in an EU project (Klemeš *et al.*, 1994). This results in energy demands with periods of changing activity and inactivity. Thus, each energy demand can usually be assigned clear starting and ending time points, which then become TS boundaries.

© Woodhead Publishing Limited, 2013

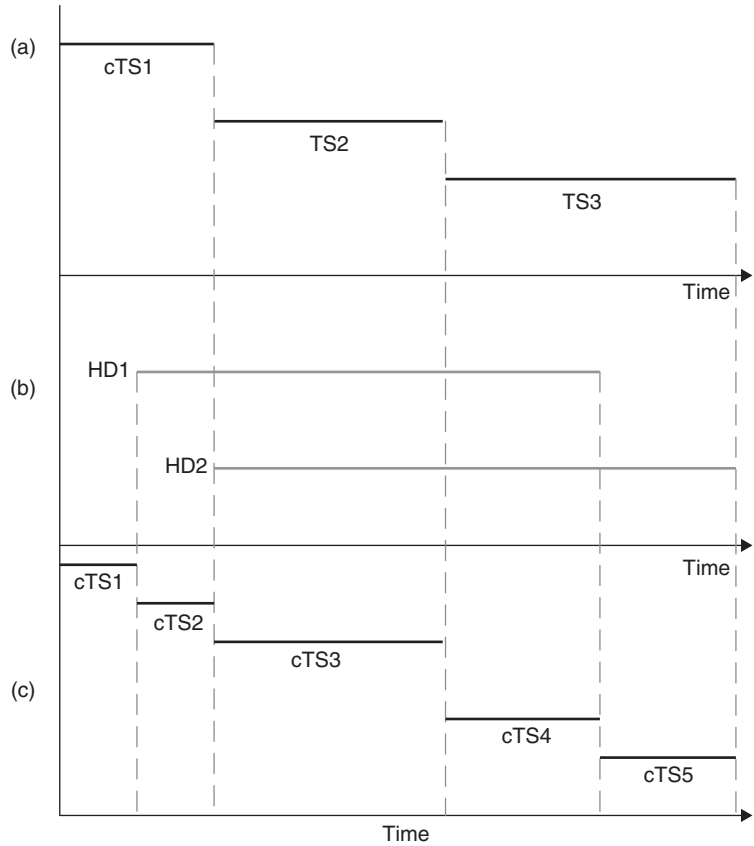

7.8 Merging TS boundaries for supply and demand for obtaining combined TS (after Nemet *et al.*, 2012a). (a) TS for solar thermal energy, (b) TS for the varying heat demand and (c) Combined TS. HD – heat demand.

7.5.3 Combining Time Slices

Having identified TSs for the supply and demand sides of the problem allows combining them, which is necessary for treating the system states uniformly. The combination can be performed by simply merging the TS boundaries for the supply and the demand sides as shown in Fig. 7.8.

7.6 Heat Cascades for the Evaluation of Total Site Targets When There Is Variation in Supply and Demand

Heat cascades have been developed previously for Total Sites, mainly for the purpose of identifying the specifications for Utility System Synthesis.

© Woodhead Publishing Limited, 2013

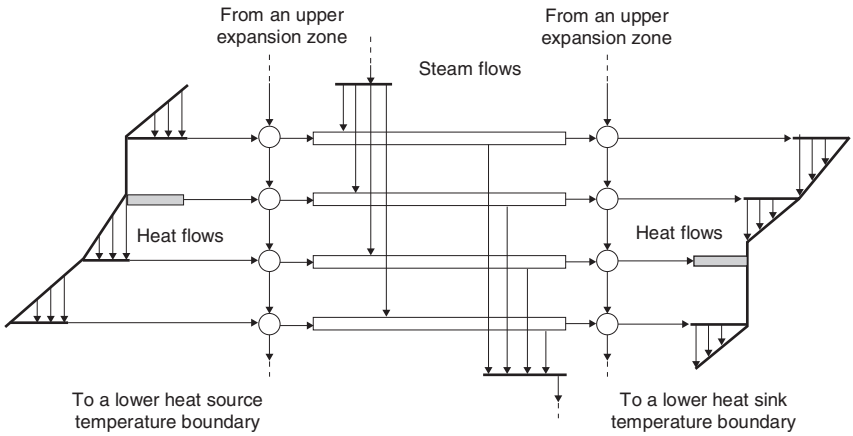

7.9 Total Site Heat Cascade for building steam network superstructure during synthesis (Varbanov *et al.*, 2005).

The first relevant version is by Shang and Kokossis (2004) for performing initial targeting, and the second version has been formulated by Varbanov *et al*. (2005) for choosing steam header pressure levels. These constructions (Fig. 7.9) generally consist of three parts for expressing utility (mostly steam) generation from Process Heat Sources, the utility (steam) cascading and distribution via steam mains, as well as utility use by Process Heat Sinks.

The same cascade type can be constructed for describing Total Site Targets numerically. A variation of this has been the work by Liew *et al*. (2012), which uses the same cascading principle expressed in a table form, termed the Total Site Problem Table.

For the purposes of evaluating Total Site Targets for varying energy supplies and demands, this technique has been revisited and adapted by Varbanov and Klemeš (2011) and is provided below.

7.6.1 Total Site Profiles and Cascading of Utilities

When utilities are placed against Targeting Profiles, it is necessary to account for the generation of each utility carrier from Process Heat Sources or its consumption by Process Heat Sinks. The potential for utility generation on a site is represented by the Site Source Composite Curve and that for consumption – by the Site Sink Composite Curve (Fig. 7.10a) (Klemeš *et al*., 2010).

If, for a given utility, the generation from processes is insufficient to cover the demands, the two curves are displaced and part of the demands for the current utility are left to be covered by a higher-temperature utility. For

© Woodhead Publishing Limited, 2013

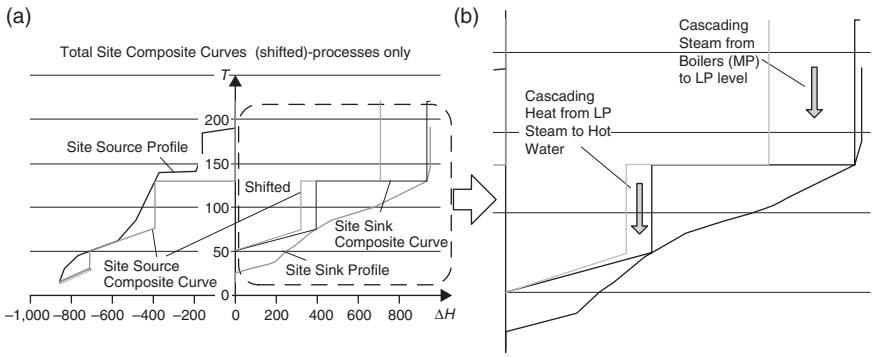

7.10 Mapping of the heat cascading flows on the Site Composite Curves (after Varbanov and Klemeš, 2011). (a) Total Site Profiles and Site Composite Curves and (b) cascading heat between utility levels.

the example in Fig. 7.10, the utility placement starts from hot water (the lowest-temperature utility), where the generation from processes is smaller than the process use of hot water. As a result, some of the generated Low Pressure (LP) steam should be used to cover the needs for hot water. Continuing up the temperature scale, the remaining unused LP steam from process generation is, in turn, insufficient to cover the LP steam demands and some Middle Pressure (MP) steam from the site boilers is used to satisfy the remaining need.

This kind of use of higher-temperature utilities for satisfying lower-temperature utility needs is referred to as utility cascading. It can be implemented in various ways, such as MP to LP steam let-down, or direct use of the MP steam instead of LP steam. Utility cascading is similar to cascading heat in Pinch Analysis using the Problem Table Algorithm (Linnhoff and Hindmarsh, 1983). For the purposes of Total Site Utility Targeting and placement for continuous processes and without heat storage, utility cascading is represented as in Fig. 7.11, where a part of the Site Source Profile is allocated for generating a utility (e.g. steam) and feeding it to a mains vessel. Another input to this vessel is the heat cascaded from a higher-temperature utility. There are also two outputs – the use of the current utility by transferring heat to a part of the Site Sink Profile and the heat cascading to a lower-temperature utility.

The flowsheet-style diagram of utility cascading from Fig. 7.11 needs a more compact representation in order to be used in more comprehensive diagrams providing views of complete systems. Such a representation is shown in Fig. 7.12a, which also refers to a key term: utility interval. This is an analogue from the process Heat Cascade (Linnhoff and Hindmarsh, 1983). An equivalent Sankey diagram (Sankey, 1896) in Fig. 7.12b illustrates

© Woodhead Publishing Limited, 2013

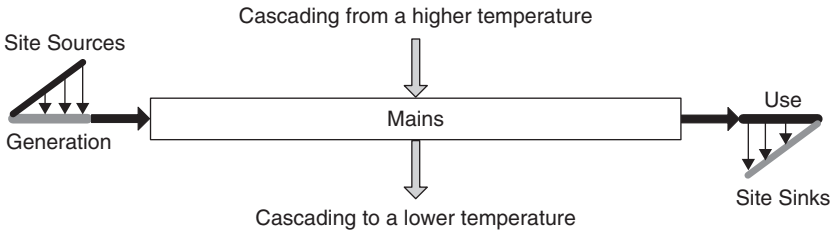

7.11 Utility cascading without storage (after Varbanov and Klemeš, 2011).

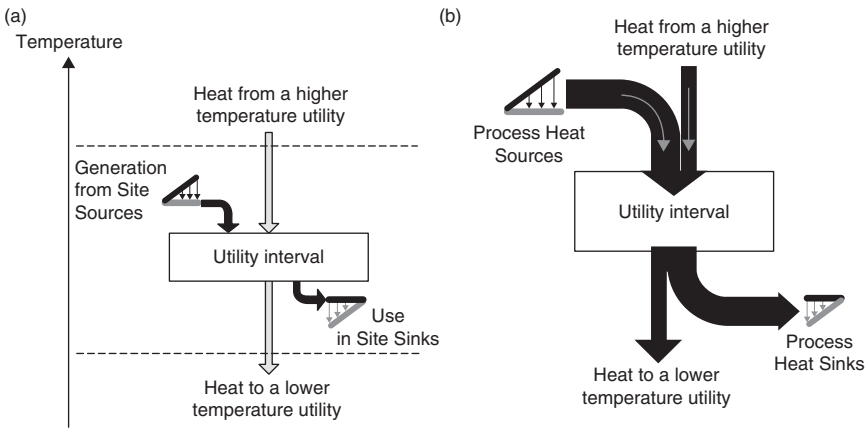

7.12 Heat Cascade Cell for a Total Site with continuous processes (after Varbanov and Klemeš, 2011). (a) Flows configuration and (b) Sankey Diagram.

the possible contributions of the heat inputs to the utility interval and the split between the outputs. This cascade representation is similar to the one by Shang and Kokossis (2004).

7.6.2 Accounting for Non-isothermal Heat Sources and Sinks

As indicated above, integrating renewables implies a new kind of Total Sites called LIESs (Perry *et al.*, 2008), involving entities and processes of different types – industrial, commercial (e.g. hotels), service (e.g. hospitals) and office buildings. The main reasons are the distributed availability of the renewables and the need to maximise the reuse of any available waste heat in a given area. These necessitate minimising the transportation of the captured energy and limiting the scale of the capture facilities. As a result, some of

© Woodhead Publishing Limited, 2013

the processes to be integrated feature lower-temperature heating demands, for which using hot water is sufficient. Hot water is a non-isothermal utility and it is important that the Total Site Targeting methodology supports its representation.

Non-isothermal utilities include hot water, cooling water, flue gas and hot oil, among others. The profile of a non-isothermal utility in a temperature–enthalpy plot is represented by one or more segments with slope, as can be seen in the lower-temperature range of Fig. 7.10. This is in contrast to representing isothermal utilities (such as steam) by horizontal segments, approximating their heat transfer flows with latent heat exchange only.

It is important to stress that the slopes of the non-isothermal utility segments in the Site Composite Curves are provisional at the time of constructing the curves. It is possible later to break the Site Composite Curves into non-continuous shapes to accommodate, for instance smaller CPs of utility generation by changing the shape of the utility use and the CP value in the corresponding Site Sink Composite Curve. The opposite situation is also possible – heat supply from process generation or solar-heat capture may suggest large CP, resulting in flatter segment slopes. This may be accompanied by an excess of the generated and/or captured heat compared with the process demand for the particular utility (e.g. hot water). In such cases it is possible to split the utility generation and/or solar-heat capture stream (the T-H diagram at the top of Fig. 7.13) and produce two or more segments with steeper slopes (smaller CP values), matching one of the segments with the utility use (Site Sink Composite Curve) and sending the remainder to heat storage. These techniques are demonstrated in the illustrative example in Section 7.7.

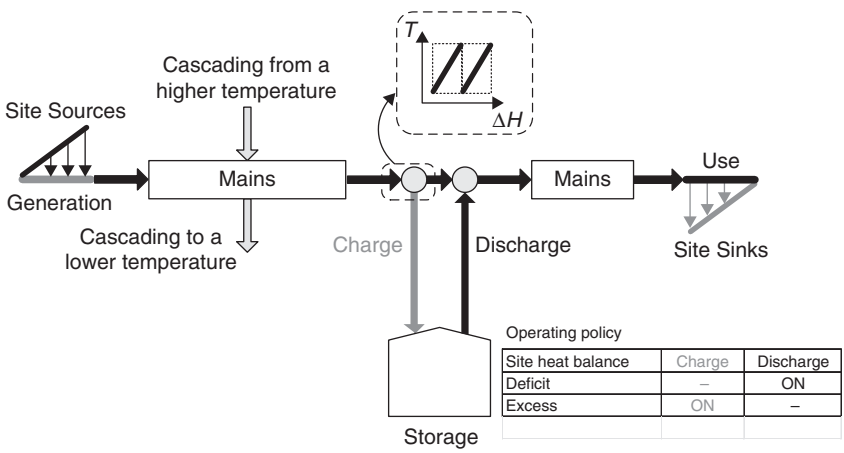

7.13 Utility cascading with storage (after Varbanov and Klemeš, 2011).

© Woodhead Publishing Limited, 2013

7.6.3 Handling the Variability

Demands are imposed on energy conversion systems, and do not belong to the degrees of freedom. However, in some cases shifting certain demands in time can be suggested and, if sufficiently supported by economic gains, even achieved. Short-term fluctuations are usually modelled using time-differential equations. For the longer interval variations, considered here, piecewise-constant approximations of the demands are used.

The piecewise representation of the demands can be embedded within a Total Site formulation to model the changes in the demand over longer periods. Typical examples are campaigns in the sugar industry, and first shift and the other shifts in the industrial plants, where the second and third shift could feature considerably lower energy consumption or might not be covered at all. Approximating winter and summer demands, especially for the residential buildings, is another example.

Heat Cascading for Intermittent Processes and Sites

The approach of representing the Site Integration parameters in a piecewise-constant form reveals the need for setting up a time horizon for the model and further partitioning it into a set of TSs (Kemp and Deakin, 1989a) – later this work was extended by Klemeš *et al*. (1994). The partitioning can be performed using the procedure described previously (Nemet *et al*., 2012a). The Total Site Targeting is then performed within each TS. An important feature of this type of problem is that some TSs may feature heat excess in one or several Temperature Intervals and heat can be transferred to later TSs within the same Temperature Intervals or to lower temperatures.

Such heat transfers from an earlier TS to a later one can be implemented using heat storage. This positions heat storage among the very important issues related to the optimal design of intermittent processes. If storage is available at required capacity with feasible cost, it can considerably increase the system heat recovery and efficiency.

Energy storage is a complicated and demanding issue, which is still waiting for a major breakthrough (Sharma *et al*., 2009). The Heat Integration methodology could contribute to this problem solution by providing targets that could be achieved.

The next step is to identify the possible degrees of freedom. Important ones are:

(i) Integration of several unit processes and/or consumers into Total Sites. There is an important effect from establishing Total Sites, where district heating systems are a special case (Gogenko *et al*., 2007). Integrating

© Woodhead Publishing Limited, 2013

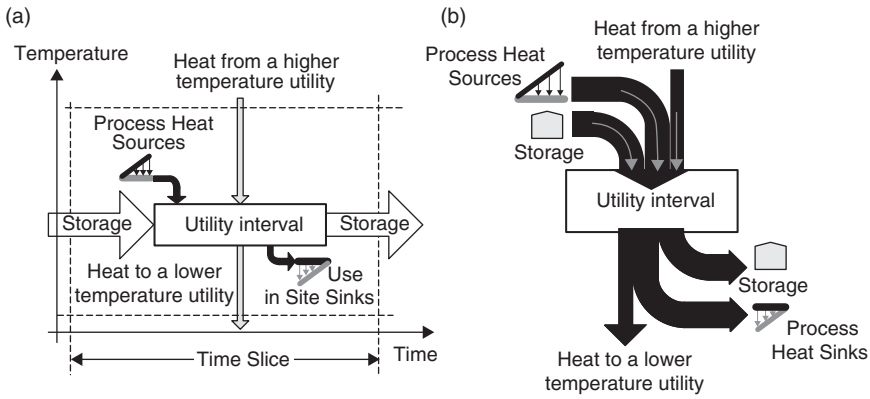

7.14 Heat Cascade Cell for a Total Site with intermittent processes (after Varbanov and Klemeš, 2011). (a) Flows configuration and (b) Sankey Diagram.

many users with different temporal energy consumption patterns provides the opportunity for more efficient utilisation of the primary resources as well as to exchange heat for better recovery.

(ii) Selection of the degree of utilisation of the available renewable resources – solar, wind, biomass (including waste), hydro power, geothermal, ground heat pumping.

(iii) Storing excess waste heat and its utilisation in a future TS.

To ensure the transfer of heat from one TS to another for a particular utility, it is necessary to use heat storage. One possibility is, starting from the utility use-generation pattern shown in Fig. 7.11, to separate the utility mains into two parts and to add the heat storage facility between them, as illustrated in Fig. 7.13. This arrangement allows for several storage operating policies to be applied, including storage charge, discharge or lack of heat transfer, depending on the situation at any given moment.

Switching the view from Process Flowsheet to Heat Cascade, as shown in Fig. 7.14a, allows displaying the time dimension of the problem explicitly. The diagram shows a Heat Cascade cell in two dimensions – temperature (vertical) and time (horizontal). An equivalent Sankey diagram (Sankey, 1896) in Fig. 7.14b illustrates the possible contributions of the cell heat inputs and the split between its outputs.

7.6.4 Heat Storage Model for Heat Integration

There is another important issue, which should be optimised: the size and location of heat storage facilities. There are three obvious options: centralised,

© Woodhead Publishing Limited, 2013

distributed and their combination. This optimisation has its own economic background and is related to specific features of heat storage. However, it is also closely interconnected with Total Site Heat Integration.

Storage Scope

For Total Site Targeting, a central heat storage facility for each utility is assumed to be available without predetermining the installation of local storage capacities for the processes. One heuristic for deciding on installation of a local storage can be to evaluate the variability of the heating and cooling demands of the site processes and, if they are clearly concentrated within one or two processes and not typical for the remaining ones, then installing local storages may be justified and should be evaluated in detail at the system design stage.

Heat Losses

From any kind of heat storage there are heat losses. They may be in the form of load loss, temperature loss, or both. The following cases illustrate some of the possible storage options:

- If steam is stored in a large drum or other vessel without heat replenishment, part of the steam would condense as a result of casing heat losses. Until there is some steam in the vessel the temperature would not deteriorate. Therefore, assuming reasonably short storage durations and/or sufficient insulation, heat loss from steam storage can be assumed to involve only load loss and no temperature loss.
- If cooling capacity is stored in the form of ice, it would have similar properties to steam storage, due to the fact that the main cooling effect comes from ice melting, i.e. there is again a phase change.
- In the case of sensible heat storage – for instance storing heat in the form of hot water or storing cooling capacity as cold/chilled water (storing 'cold'), the load loss is always accompanied by an equivalent loss of temperature potential – temperature reduction for hot water and temperature increase for cooling water storage.
- There is also the possibility that heat is stored in a device based on a chemical or physico-chemical reaction. Storing heat in a reactor using a hydration–dehydration (endothermic/exothermic) reaction is a popular choice presented by Masruroh *et al*. (2006) and later, in different form of the process, by Weber and Dorer (2008). In any case, charging the storage with heat takes place at higher temperature than the discharge operation. Therefore, there is always a temperature loss in addition to any load loss due to heat exchange with the ambience.

© Woodhead Publishing Limited, 2013

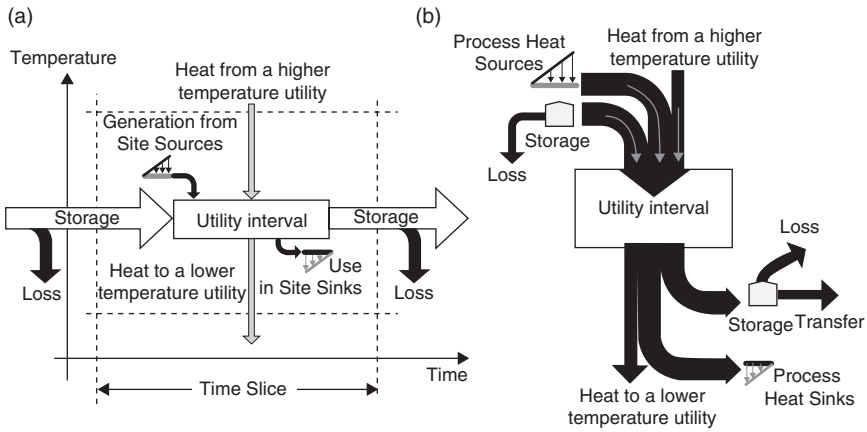

7.15 Accounting partially for heat deterioration (after Varbanov and Klemeš, 2011). (a) Flows configuration and (b) Sankey Diagram.

For energy targeting, the heat load losses can easily be accounted for. In a Heat Cascade (e.g. Fig. 7.14), the cascading flows between the TSs represent the heat storage. Adding another flow accounting for the load loss (Fig. 7.15) is straightforward.

However, accounting for the temperature deterioration is not as simple. To do so it is necessary to know specifics of the employed storage technology and to make additional decisions on the storage operating policy, which are in some cases beyond targeting, such as whether to simply accept the losses or to provide some auxiliary heating to the storage maintaining its load and temperature. At the current state of the art in terms of Total Site Targeting the heat losses during storage are generally neglected.

7.6.5 Heat Storage Operating Policy and Management

The energy storage may be used in three modes: charge, discharge and idle (dormant). For the purposes of targeting, if the storage exchanges heat, it is normally assumed that in a given TS it may operate only in one direction – either charge or discharge mode. Although it is technically possible to devise storage facilities, which can handle two-directional operation, this would tend to complicate the storage and increase its investment and operating costs at no added benefit for the site. Therefore, the storage is assumed to be exclusively in only one of its three operating modes during a given TS.

© Woodhead Publishing Limited, 2013

7.6.6 Utility Prioritisation

Both renewables and heat from storage have to be used before the constant-availability utilities (coming mainly from fuels) in order to maximise the energy efficiency and save fuel. The policy of unidirectional heat transfer from/to the energy storage has further implications on the priority with which the utilities are used. When both renewable heat and heat from the storage are available, precedence is given to the renewable heat, in order to guarantee that heat will be transferred only from the storage if the renewable source capacity is insufficient, or to the storage, if the sum of the renewable and stored heat exceeds the process needs for a given TS.

Therefore, the first priority for using utilities is to maximise the utilisation of the heat captured from renewables. As a second option, the heat from storage facilities is applied. The remaining demands are covered by other non-transient utilities (with constant availability).

7.6.7 Total Site Heat Cascade

After considering the main issues and establishing the targeting and cascading rules, the Total Site Heat Cascade can be defined. Figure 7.16 provides a generalised view of the Total Site Heat Cascade where the temperature intervals are allocated to specific utilities – MP steam, LP steam and Hot Water. The diagram shows the options for heat cascading. After evaluating a particular operating scenario for the Site, some of the flows shown may become zero and, in such cases, could be omitted from the diagram for enhancing the clarity. For instance, the heat storage transfer flows from the left of TS 1 will exist only in the case of cyclic operation and also the heat storage transfers for corresponding utilities from the last TS (No. 3 in Fig. 7.16) are positive.

Overall Procedure

The overall procedure for Targeting Total Sites with temporal variations and renewables is then defined as follows:

(i) Analyse the temporal variations in the heating and cooling demands of the site processes (plants, buildings, farms) and partition the modelling horizon into TSs.
(ii) Assume initially that no heat is stored before the first TS for all utility types.

© Woodhead Publishing Limited, 2013

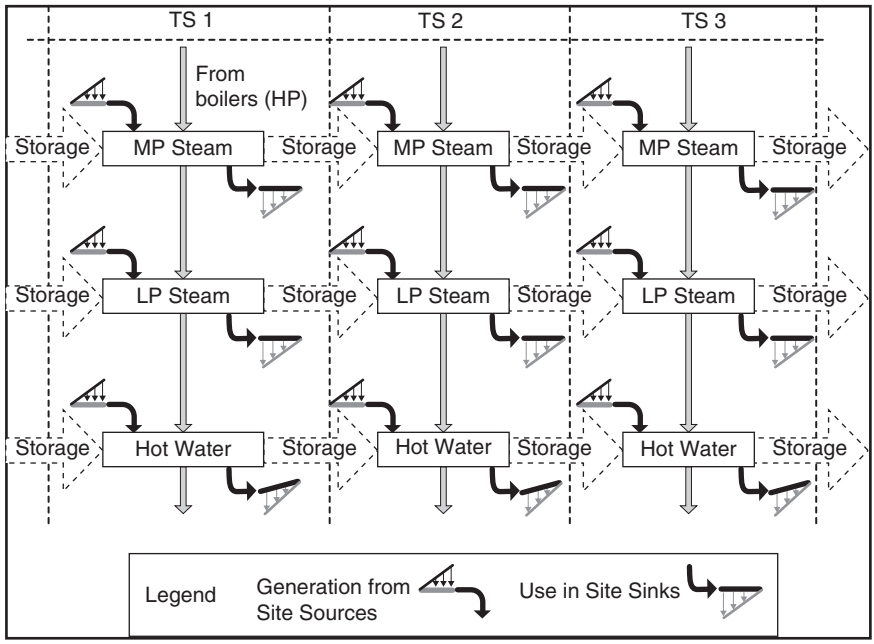

7.16 Total Site Heat Cascade with TSs (after Varbanov and Klemeš, 2011).

Steps (iii) to (iv) are performed for each TS.

(iii) Obtain the Heat Integration targets for each process unit.
(iv) Obtain the Total Site Utility Targets using the Total Site Heat Cascade, Total Site Profiles and Site Composite Curves. The targets calculation should follow the utility placement priorities identified in Section 7.6.6.
(v) For cyclic operation, the heat transfer flows from the last TS in the Total Site Heat Cascade should be fed/recycled to the first TS. At this point, a reiteration of step (iv) is needed until the values of the heat transfers to the first TS become equal to or sufficiently close to those of the heat transfers from the last TS.
(vi) Identify the target for energy storage capacity for each utility type using the heat transfer flows between the TSs in the Total Site Heat Cascade. For each utility type the heat storage capacity will be equal to the largest heat transfer flow between TSs.

© Woodhead Publishing Limited, 2013

7.7 Case Study: Integration of Solar Thermal Energy into a Locally Integrated Energy Sector (LIES)

The case study is based on a configuration first introduced by Perry *et al*. (2008) and adapted by Varbanov and Klemeš (2011), where four areas are integrated in a Total Site – two industrial plants, a hotel and a residential area (Fig. 7.17). Each of these areas is referred to as a process. Each process features a number of streams – hot and/or cold. It is possible to establish a connection to a District Heating plant.

The process streams with their main properties and periods of activity are given in Tables 7.2–7.5. The time intervals are expressed for a 24 h cycle. The Minimum Allowed Temperature Difference for all processes is $\Delta T_{min} = 10°C$. The residential area has a number of solar thermal collector cells for generating domestic hot water and space heating. The utilities available at the Total Site are listed in Table 7.6. An assumed storage facility uses hot water. The operating temperature of the storage facility is assumed to be 75°C and for the current example the heat losses are neglected.

After analysing the process streams data from Tables 7.2–7.5, three switching time points over the 24 h horizon have been identified: 6, 17 and 20 h. They define three TSs as listed in Table 7.7. In the residential area there are also solar thermal collectors, which capture solar heat. The available solar heat flows are shown in the last column of Table 7.7.

The energy targets have been evaluated for the described Total Site, applying the described procedure (Section 7.8).

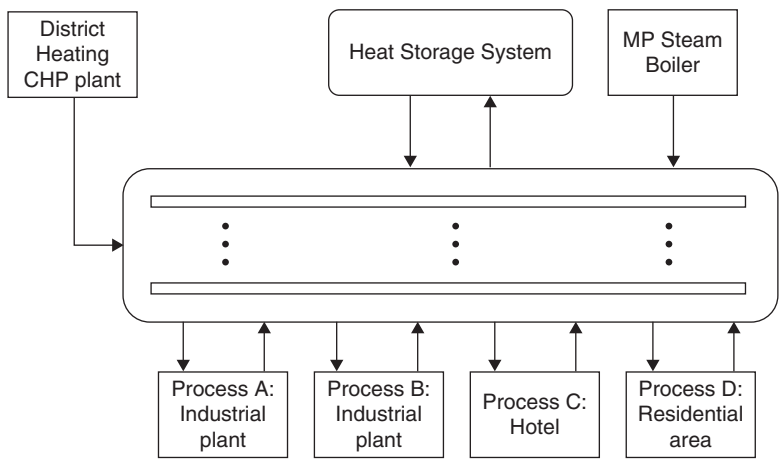

7.17 Configuration of the considered LIES (derived from Perry *et al.*, 2008).

© Woodhead Publishing Limited, 2013

Table 7.2 Heating and cooling demands for process A

No.	Stream	Temperature (°C)		ΔH (kW)	Type	CP (kW/°C)	Time interval (h)	
		Supply	Target				From	To
1	A2	170	80	120.0	Hot	1.333	0	24
2	A1	150	149	180.0	Hot	180.000	0	24
3	A5–1	50	135	104.4	Cold	1.228	0	24
4	A5–2	85	100	82.3	Cold	5.487	0	24
5	A6	62	100	130.0	Cold	3.421	0	24
6	A7	72	55	130.0	Hot	7.647	0	24

Table 7.3 Heating and cooling demands for process B

No.	Stream	Temperature (°C)		ΔH (kW)	Type	CP (kW/°C)	Time interval (h)	
		Supply	Target				From	To
1	B1	200	195	160.0	Hot	32.00	6	20
2	B2	20	54.7	10.0	Cold	0.288	6	20
3	B3	50.5	85	107.3	Cold	3.109	20	6
4	B4	100	120	130.0	Cold	6.500	6	20
5	B5	150	40	83.5	Hot	0.759	6	17
6	B6	80	95	48.0	Cold	3.200	6	20
7	B7	95	25	80.0	Hot	1.143	6	17

Table 7.4 Heating and cooling demands for process C

No.	Stream	Temperature (°C)		ΔH (kW)	Type	CP (kW/°C)	Time interval (h)	
		Supply	Target				From	To
1	Soapy Water	85	40	20.0	Hot	–0.444	6	17
2	Condensate	80	40	75.0	Hot	–1.875	6	17
3	Sanitary Water	25	55	17.3	Cold	0.576	20	6
4	Laundry	55	85	18.0	Cold	0.600	20	6
5	Boiler feed water (BFW)	33	60	12.0	Cold	0.446	0	24
6	Sanitary Water	25	60	15.0	Cold	0.429	6	17
7	Sterilisation	82	121	34.1	Cold	0.874	20	6
8	Swimming Pool Water	25	28	23.1	Cold	7.700	6	17
9	Cooking	80	100	32.0	Cold	1.600	6	17
10	Heating	18	25	41.1	Cold	5.864	0	24
11	Bedpan Washers	21	121	5.0	Cold	0.050	6	17

© Woodhead Publishing Limited, 2013

Table 7.5 Heating and cooling demands for process D

No.	Stream	Temperature (°C)		ΔH (kW)	Type	CP (kW/°C)	Time interval (h)	
		Supply	Target				From	To
1	Space heating	15	25	88.0	Cold	8.800	0	24
2	Hot water base	15	45	25.0	Cold	0.833	0	24
3	Hot water day	15	45	65.0	Cold	2.167	6	20

Table 7.6 Site utility specifications

Name	Type	Temperature level(s)
Cooling water	Cold	15–30°C
Solar hot water	Hot	80–50°C
District hot water	Hot	75–50°C
MP Steam	Hot	At 220°C
LP Steam	Hot	At 130°C

Table 7.7 Time Slices for the example

	From (h)	To (h)	Duration (h)	Share (%)	Solar capture (kW)
TS 1	6	17	11	46	112.9
TS 2	17	20	3	12	40
TS 3	20	6	10	42	0

For TS 1, the Total Site Profiles and Utility Composite Curves (Fig. 7.18) have been obtained. Several observations can be made:

- The generation of hot water by processes (shifted Site Source CC) can completely satisfy the Process Heat Sinks in its temperature interval and 11.0 kW of hot water (121.4 kWh for the whole slice duration) remain unused.
- The 112.9 kW (1,241.9 kWh) captured solar heat also cannot be immediately utilised.
- The site needs 113.2 kW (1,245.4 kWh) MP steam, of which 94.7 kW (1,042.2 kWh) is the MP steam cascaded to satisfy LP steam demands.
- The demand for cooling water is 139.8 kW (1,537.9 kWh).

As a result of the above, the excess heat available from solar hot water and the excess of process-generated hot water are directed to storage,

© Woodhead Publishing Limited, 2013

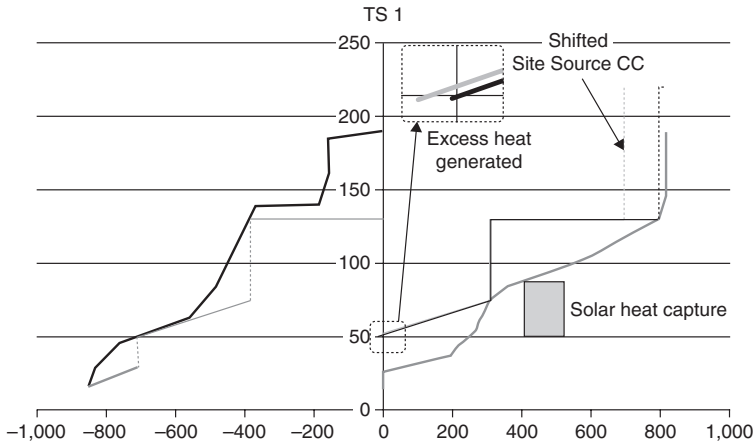

7.18 Total Site Targets for TS 1 (after Varbanov and Klemeš, 2011).

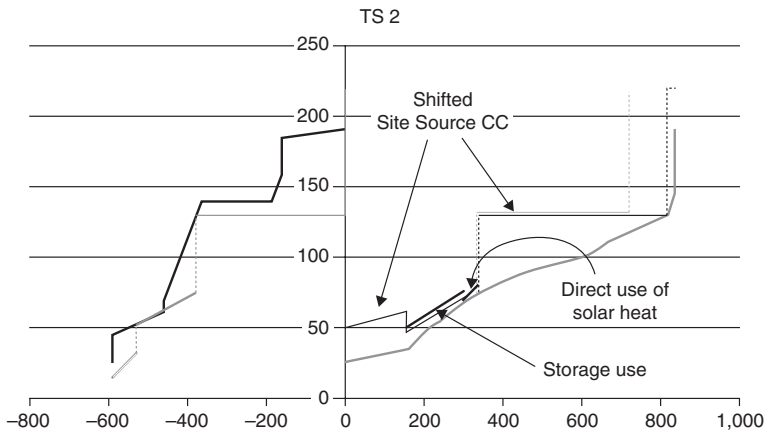

7.19 Total Site Targets for TS 2 (after Varbanov and Klemeš, 2011).

with the overall amount 1,363.3 kWh and are made available as utility for TS 2 at 75 °C.

For TS 2, the active process streams can be supplemented with the heat available from the storage with availability of 1,363.3 kWh. The targets for TS 2 are shown in Fig. 7.19. It can be seen that 145.2 kW (435.5 kWh) heat is drawn from the storage, leaving another 927.8 kWh remaining stored. Also, the full extent of the solar capture for this TS is used amounting to 40 kW (120 kWh). The remaining utility targets are 114.3 kW (342.8 kWh) MP steam and 56.2 kW (168.5 kWh) cooling water.

Finally, the targets for TS 3 are shown in Fig. 7.20. The remaining stored heat from TS 2, amounting to 927.8 kWh, is completely used. There is also

© Woodhead Publishing Limited, 2013

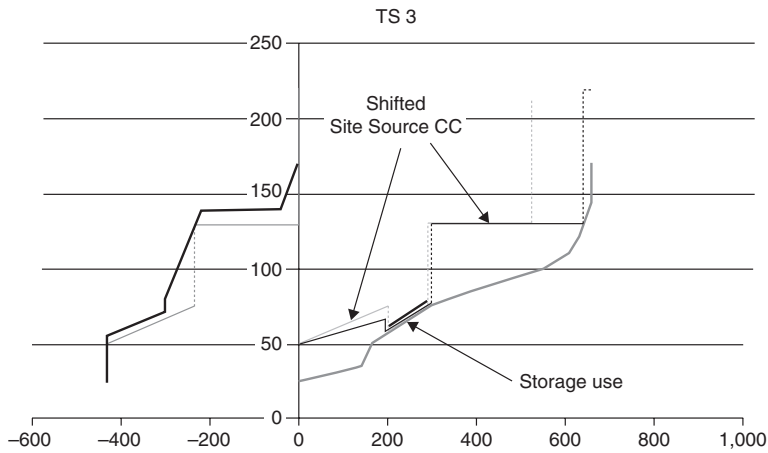

7.20 Total Site Targets for TS 3 (after Varbanov and Klemeš, 2011).

a need for 136.7 kW (1,366.7 kWh) MP steam and cooling water is not required. The fact that all the remaining stored heat is used in this TS means that, according to the procedure in the section 'Overall Procedure', recalculation of the targets is not needed.

The Total Site Heat Cascade for the whole case is shown in Fig. 7.21. Besides providing a single view of the analysis, two more important results can be inferred from the diagram. One is the total of the utility targets for the overall process cycle of 24 h: the MP steam target is 2,954.9 kWh and for cooling water is 1,706.3 kWh. The other important result is the storage capacity required. In the current example only storage for hot water is needed. It has to be taken as the largest heat transfer flow from the cascade between the TSs, which in this case is 1,363.3 kWh, representing 46% of the MP steam target.

It is important to mention that the overall MP steam target for the same stream data but without applying heat storage would be 4,438.2 kWh, meaning that the benefit from the heat storage is saving 1,483.3 kWh MP steam or 33 % of the no-storage case.

An important advantage of using the Total Site Heat Cascade is the ability to trace the routes for possible improvement of the site targets by rescheduling some of the heating or cooling demands. The benefits to look for in the rescheduling actions could involve reduction of the required storage capacity and also reduction in the final utility targets. For instance, in Fig. 7.21, it can be seen that the likely improvements in the utility and storage targets should be sought by rescheduling streams intersecting the interval of the hot water. Looking back into the process heating and cooling demands, stream

© Woodhead Publishing Limited, 2013

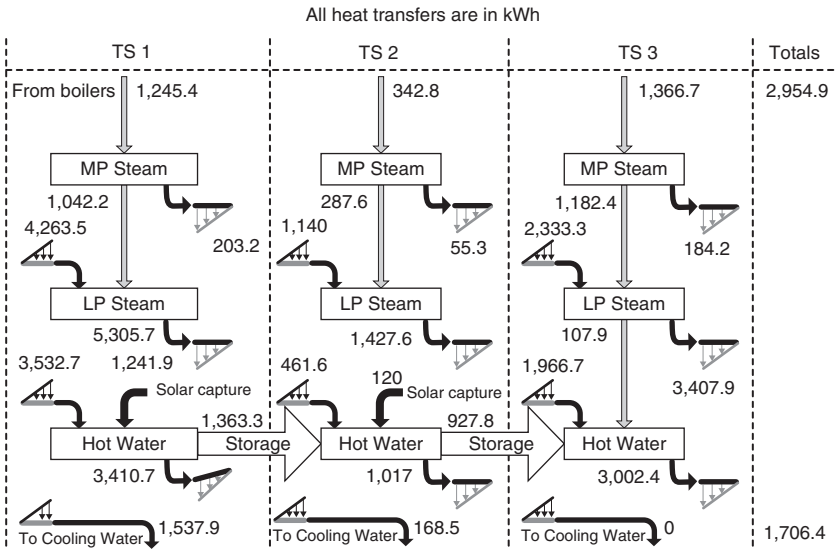

7.21 Total Site Heat Cascade for the initial case (after Varbanov and Klemeš, 2011).

B3 from Table 7.3 (Process B) as well as streams '3: Sanitary water' and '7: Sterilisation' from Table 7.4 (Process C) are present in the desired temperature range. The next step is to map the TSs during which these streams are active and in which TS there is most local excess of the required heat. All the identified streams are active during TS 3. Also, the most heat excess for the hot water utility is in TS 1. As a result, the targeting procedure has been performed, after moving the streams activity to TS 1 and keeping their total heating demands as amounts (kWh) the same. As a result, the cascade shown in Fig. 7.22 has been obtained. Here, the required storage capacity takes approximately 15% of the MP steam target.

The comparison of the diagrams from Figs 7.21 and 7.22 shows that moving the identified streams activity would be beneficial for reducing both the requirements for MP steam and for heat storage, but would slightly increase the need for cooling water. Any further analysis of these options requires deeper knowledge of the individual processes and is beyond the scope of the current paper. Some simple dependencies can be inferred, however. For example moving the streams '3: Sanitary water' and '7: Sterilisation' in Process C from the night shift to the day time may introduce the need to increase the inventory of sanitary materials, beddings, bed sheets, etc. As well as for various tools which are sterilised, in order to have such items available while the other items await their processing.

© Woodhead Publishing Limited, 2013

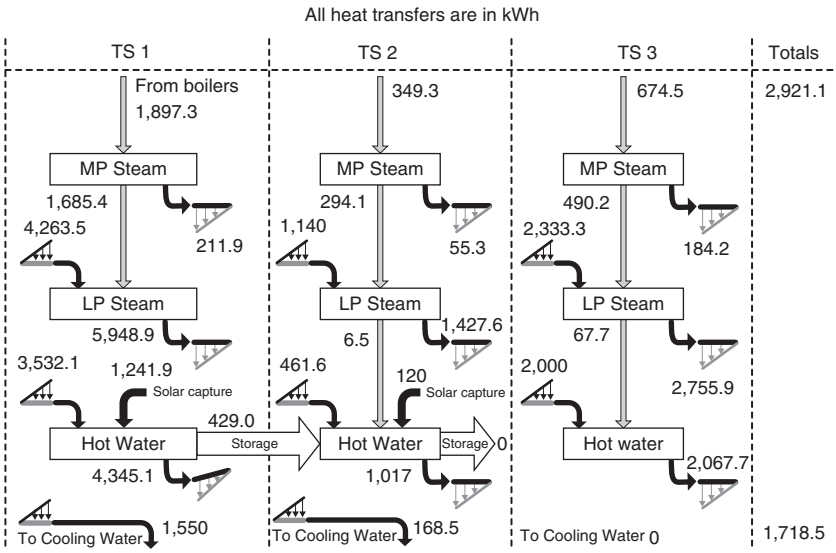

7.22 Total Site Heat Cascade for the modified case (after Varbanov and Klemeš, 2011).

7.8 Conclusion

As has been shown, applying Total Site Heat Integrated storage can significantly reduce the targets for fossil fuel as well as solar-based utilities, when applied to the integration of renewables with time varying availability. The methodology can be used for simultaneously obtaining several important targets for Total Sites integrating renewables. These are the maximum amounts (upper bound) of renewables capture, the minimum consumption (lower bound) of fossil fuels, and the maximum capacity (upper bound) of energy storage. The identified targets can be further used for more detailed system design.

The illustrated procedure shows the potential to employ the developed Total Site Heat Cascade as a tool for seeking energy efficiency improvement by demand-side management of the process energy demands and potential operation rescheduling.

7.9 Sources of Further Information

This section provides a concise collection of sources where to seek further information. It includes books, journals, conferences and key web resources. Since this is a fast developing area, most attention should be

© Woodhead Publishing Limited, 2013

paid to surveying research journals and web sources, in order to have most up to date picture.

This chapter deals with very recent research topics, which have been developing fast and every month some new works have been published. For this reason there are not too many books dealing with the integration of varying supplies with varying demands for energy on a *Total Site*. However, for a firm grasp of *PI*, the other chapters of the current book should be consulted as well as the sources recommended there. In addition, below are recommended a few previously published books to aid in this process.

Ian Kemp in 2007 published an updated and extended version (Kemp, 2007) of Linnhoff's 'User Guide' (Linnhoff *et al*., 1982, last extended edition 1994). A valuable part in it is dedicated to the *Heat Integration* of batch processes, where there is a description of the basic procedures of using TSs for Heat Integration of single processes. A more recent book is *Sustainability in the Process Industry: Integration and Optimization* (Klemeš *et al*. 2010), which extends the recent developments until 2010. *Energy Storage* (Huggins, 2010) is not specifically a Heat Integration related book; however, it can be useful for dealing with case studies where energy storage is used.

Some recent works have been developing the topic of this chapter in more detail, dealing with some more Total Site features originating from real life implementations:

- An example is a recent work dealing with the integration of solar thermal energy with processes having net heat demand, which provides more detailed insight into the problem (Nemet *et al*., 2012b).
- Recommended for further reading is the initial research on storage optimisation using Heat Integration (Nemet and Klemeš, 2011). This work uses Heat Integration tools and reasoning to arrive at the optimal temperature parameters of heat storage for a system capturing varying solar heat and delivering it to varying process demands.
- Another source recommended for further study is a real life case study 'The challenge of integrating non-continuous processes – milk powder plant case study' by Atkins *et al*. (2010). The authors provide a validated model from a pilot plant and optimise the system.
- Until recently Total Site Integration has been considering mainly steam and cooling water as energy carriers. An important step extending the scope is to include power in the form of electricity and/or direct mechanical shaft work. In this direction it is recommended to explore a recent work titled 'A Process Integration Targeting method for hybrid power systems' (Wan Alwi *et al*., 2012).

© Woodhead Publishing Limited, 2013

- One of the recent works dedicated to the integration of renewables is e.g. 'Integration and Management of Renewables into Total Sites with Variable Supply and Demand' (Varbanov and Klemeš, 2011).
- An important new development in Total Site methodology 'A numerical technique for Total Site Sensitivity Analysis' (Liew *et al*., 2012) has been recently published. It deals with the Total Sites where not only have the supply and demand been changing but also the unit's performance. It can be due to shut-downs or reduction of output due to potential accidents, planned and/or emergency maintenance, and issues stemming from varying product demand. More in this direction will be presented at coming conferences (PSE ASIA, 2013; PRES, 2013).
- A good example of a comprehensive survey of problems and measures to be taken is the report 'Variability of wind power and other renewables Management options and strategies' (IEA, 2005).

7.10 References

Atkins, M. J., Walmsley, M. R. W., Neale, J. R. (2010). The challenge of integrating non-continuous processes – milk powder plant case study. *Journal of Cleaner Production*, **18**, 927–934.

Bance, P. (2008). Residential-scale fuel cell CHP: a better match for domestic loads. *Cogeneration & On-Site Power Production*, **9**(3), <www.cospp.com/display_article/330132/122/CRTIS/none/none/1/Residential-scale-fuel-cell-CHP-a-better-match-for-domestic-loads> accessed on 04/07/2010.

Čuček, L., Varbanov, P. S., Klemeš, J. J., Kravanja, Z. (2012). Total footprints-based multi-criteria optimisation of regional biomass energy supply chains. *Energy*, **44**(1), 135–145. DOI: 10.1016/j.energy.2012.01.040.

Dhole, V. R., Linnhoff, B. (1993). Total site targets for fuel, co-generation, emissions, and cooling. *Computers and Chemical Engineering*, **17**(Supplement), S101–S109.

Foo, D. C. Y., Chew, Y. H., Lee, C. T. (2008). Minimum units targeting and network evolution for batch heat exchanger network. *Applied Thermal Engineering*, **28**(16), 2089–2099.

Friedler, F. (2009). Process integration, modelling and optimisation for energy saving and pollution reduction. *Chemical Engineering Transactions*, **18**, 1–26.

Friedler, F. (2010). Process integration, modelling and optimisation for energy saving and pollution reduction. *Applied Thermal Engineering*, **30**(16), 2270–2280.

Gogenko, A. L., Anipko, O. B., Arsenyeva O. P., Kapustenko P. O. (2007). Accounting for fouling in plate heat exchanger design. *Chemical Engineering Transactions*, **12**, 207–212.

Huggins, R. A. (2010). *Energy Storage*. Springer, New York, USA, ISBN: 978-1-4419-1023-3, DOI: 10.1007/978-1-4419-1024-0.

IEA. (2005). Variability of wind power and other renewables Management options and strategies. <www.uwig.org/IEA_Report_on_variability.pdf>, accessed 12/08/2012.

© Woodhead Publishing Limited, 2013

Kemp, I. C. (2007). *Pinch Analysis and Process Integration. A User Guide on Process Integration for Efficient Use of Energy* (authors of the first edition: Linnhoff, B., Townsend, D.W., Boland, D., Hewitt, G. F., Thomas, B. E. A., Guy, A. R., Marsland, R. H. (1982 and 1994). *A User Guide on Process Integration for the Efficient Use of Energy.*, IChemE, Rugby, UK). Elsevier, Amsterdam, The Netherlands.

Kemp, I. C., Deakin, A.W. (1989a). The cascade analysis for energy and process integration of batch processes. Part 1: Calculation of energy targets. *Chemical Engineering Research and Design*, **67**, 495–509.

Kemp, I. C., Deakin, A. W. (1989b). The cascade analysis for energy and process integration of batch processes. Part 3: Network design and process scheduling. *Chemical Engineering Research and Design*, **67**, 510–516.

Kemp, I. C., Deakin, A. W. (1989c). The cascade analysis for energy and process integration of batch processes. Part 3: A case study. *Chemical Engineering Research and Design*, **67**, 517–525.

Klemeš, J., Dhole, V. R., Raissi, K., Perry, S. J., Puigjaner, L. (1997). Targeting and design methodology for reduction of fuel, power and CO_2 on total sites. *Applied Thermal Engineering*, **7**, 993–1003.

Klemeš, J., Friedler, F., Bulatov, I., Varbanov, P. (2010). *Sustainability in the Process Industry: Integration and Optimization.* McGraw Hill Companies Inc., New York, USA.

Klemeš, J., Linnhoff, B., Kotjabasakis, E., Zhelev, T. K., Gremouti, I., Kaliventzeff, B., Heyen, G., Maréchal, F., Lebon, M., Puigjaner, L., Espuña, A., Graells, M., Santos, G., Prokopakis, G. J., Ashton, G. J., Murphy, N., Paor, de A. M., Kemp, I. C. (1994). Design and operation of energy efficient batch processes. Final Report, Commission of the European Communities. Brussels, Belgium.

Kondili, E., Kaldellis, J. K. (2006). Optimal design of geothermal–solar greenhouses for the minimisation of fossil fuel consumption. *Applied Thermal Engineering*, **26**(8–9), 905–915.

Linnhoff, B., Hindmarsh, E. (1983). The pinch design method for heat exchanger networks. *Chemical Engineering Science*, **38**(5), 745–763.

Linnhoff, B., Townsend, D. W., Boland, D., Hewitt, G. F., Thomas, B. E. A., Guy, A. R., Marsland, R. H. (1982). *A User Guide to Process Integration for the Efficient Use of Energy.* IChemE, Rugby, UK.

Liew, P. Y., Wan Alwi, S. R., Varbanov, P. S., Manan, Z. A., Klemeš, J. J. (2012). A numerical technique for Total Site sensitivity analysis. *Applied Thermal Engineering*, **40**, 397–408.

Masruroh, N. A., Li, B., Klemeš, J. (2006). Life cycle analysis of a solar thermal system with thermochemical storage process. *Renewable Energy*, **31**(4), 537–548.

Matsuda, K., Hirochi, Y., Tatsumi, H., Shire, T. (2009). Applying heat integration total site based pinch technology to a large industrial area in Japan to further improve performance of highly efficient process plants. *Energy*, **34**(10), 1687–1692.

Nemet, A., Klemeš, J. J. (2011). Optimising the temperature of heat storage to serve processes with varying supply and demand – captured solar energy curve. *Chemical Engineering Transactions*, **25**, 605–610, DOI:10.3303/CET1125101.

Nemet, A., Klemeš, J. J., Varbanov, P. S., Kravanja, Z. (2012a). Methodology for maximising the use of renewables with variable availability. *Energy*, **44** (1) 29–37.

© Woodhead Publishing Limited, 2013

Nemet, A., Kravanja, Z., Klemeš, J. J. (2012b). Integration of solar thermal energy into processes with heat demand. *Clean Technologies and Environmental Policy*, **14**(3), 453–463.

Perry, S., Klemeš, J., Bulatov, I. (2008). Integrating waste and renewable energy to reduce the carbon footprint of locally integrated energy sectors. *Energy*, **33**(10), 1489–1497.

PRES. (2013). <www.conferencepres.com>, accessed 21/08/2012.

PSE ASIA. (2013). <www.cheme.utm.my/pseasia2013>, accessed 21/08/2012.

Sankey, M. H. P. R. (1896). The thermal efficiency of steam-engines. *Minutes of Proceedings of the Institution of Civil Engineers*, **125**, 182–242, E-ISSN: 1753–7843.

Shang, Z., Kokossis, A. (2004). A transhipment model for the optimisation of steam levels of total site utility system for multiperiod operation. *Computers and Chemical Engineering*, **28**(9), 1673–1688.

Sharma, A., Tyagi, V. V., Chen, C. R., Buddhi, D. (2009). Review on thermal energy storage with phase change materials and applications. *Renewable and Sustainable Energy Reviews*, **13**, 318–345.

Varbanov, P., Perry, S., Klemeš, J., Smith, R. (2005). Synthesis of industrial utility systems: cost-effective de-carbonization. *Applied Thermal Engineering*, **25**(7), 985–1001.

Varbanov, P., Klemeš, J. (2011). Integration and management of renewables into total sites with variable supply and demand. *Computers and Chemical Engineering*, **35**(9), 1815–1826.

Von Bremen, L. (2010). Large-scale variability of weather dependent renewable energy sources. In: Troccoli, A. (ed.), Management of Weather and Climate Risk in the Energy Industry, Proceedings of the NATO Advanced Research Workshop on Weather/Climate Risk Management for the Energy Sector, Santa Maria di Leuca, Italy, 6–10 October 2008, Management of Weather and Climate Risk in the Energy Industry. Springer, Dordrecht, The Netherlands, ISBN 978–90–481–3690–2, pp. 189–206.

Wan Alwi, S. R., Erniza Mohammad Rozali, N. E., Manan, Z. A., Klemeš, J. J. (2012). A process integration targeting method for hybrid power systems. *Energy*, **44**(1), 6–10.

Weber, R., Dorer, V. (2008). Long-term heat storage with NaOH. *Vacuum*, **82**, 708–716.

7.11 Appendix: Nomenclature

A number of terms can be used in different contexts and in some cases their meaning changes depending on the context. Where this is the case, the context in which a term is defined is specified [**in bold**] within square brackets.

Acronyms

TS	Time Slice
LP (steam)	Low Pressure (steam)
MP (steam)	Medium Pressure (steam)

© Woodhead Publishing Limited, 2013

HP (steam)	High Pressure (steam)
CHP	'Combined Heat and Power', usually meaning 'Combined Heat and Power Generation' – see Chapter 2
LIES	Locally Integrated Energy Sector
CC	Composite Curve – see Chapter 2

Symbols

G	solar irradiation, W/m^2
t	time, h
NTS	number of TSs
INA	inaccuracy, %
T	temperature, °C
ΔH	enthalpy difference (enthalpy flow) – see Chapter 2
CP	heat capacity flowrate, kW/°C – see Chapter 2

© Woodhead Publishing Limited, 2013

8

Analysis and Design of Heat Recovery Systems for Grassroots and Retrofit Situations

TRULS GUNDERSEN, Norwegian University of Science and Technology, Trondheim, Norway

DOI: 10.1533/9780857097255.2.262

Abstract: This chapter builds on Chapters 2 and 4 and describes more advanced concepts, representations, procedures and graphical diagrams related to the analysis and design of heat recovery systems for both grassroots and retrofit situations. The grassroots case is extended to add more industrial realism, and to bring investment costs into the discussion. Key elements of the grassroots component are Multiple Utilities, Heat Transfer Area considerations, additional design tools beyond the Pinch Design Method, forbidden matches and an introduction to the use of optimisation for heat exchanger network design. Key elements of the retrofit part are procedures for Targeting, Design and Optimisation, where in all these stages focus is on maximum utilisation of existing equipment, making the task very different from the grassroots case. The Network Pinch concept will also be described, which as the name indicates is a feature of the Heat Exchanger Network (HEN), while the Heat Recovery Pinch is a feature of the stream data.

Key words: Extended Pinch Design Method, area targeting, cross-Pinch Analysis, retrofit design, forbidden matches, optimisation, design evolution.

8.1 Introduction

This section provides a brief introduction to, and motivation for this chapter, which consists of two main, rather different parts. In the first part, the procedures for Performance Targets, Network Design and Optimisation (or evolution) that were presented in Chapter 4 is considerably extended to add industrial realism to the Grassroots case. In the second part, corresponding, but quite different, procedures for Targeting, Design and Optimisation are introduced for the Retrofit case. Various retrofit actions, such as new units, modified heat exchangers, changes in piping and other Process Modifications, are also be discussed.

© Woodhead Publishing Limited, 2013

8.1.1 Improved Grassroots Methodologies

The main objective of Chapter 4 was to introduce the basic concepts, representations, procedures and graphical diagrams of Pinch Analysis, in order to convey understanding of, and insight into, the heat recovery problem and the new methodologies that were introduced in the late 1970s and early 1980s. Three important elements in basic Pinch Analysis are (a) Performance Targets ahead of design, (b) the Composite Curves representation that can be used whenever an 'amount' (such as heat) has a 'quality' (such as temperature), and (c) the fundamental Pinch Decomposition into a heat-deficit region and a heat-surplus region. Of course, the key to all this was the discovery of the Heat Recovery Pinch. In order to keep the discussion simple and thereby maximise understanding, the emphasis in Chapter 4 was on energy savings, while the industrial reality of course is focused on Total Annual Cost.

The references given for Chapter 4 are highly relevant also for Chapter 8; however, these are not be repeated except where they include more advanced topics relevant to this chapter, since Chapter 8 is meant to be an extension and a natural continuation of Chapter 4. Besides, Chapters 4 and 8 are both part of this *Handbook of Process Integration (PI)*.

In order to add industrial realism to the problem of designing heat recovery systems, this chapter discusses topics such as Multiple Utilities, Heat Transfer Area (considering differences in film Heat Transfer Coefficients, different materials of construction and different pressure ratings), more realistic heat exchanger types, heat exchanger shells versus units (for shell-and-tube exchangers) and restrictions in heat exchange matching (forbidden, required or restricted matches). Additional design tools to supplement the basic Pinch Design Method with emphasis on efficient use of heat transfer area (i.e. Driving Force Plot and Remaining Problem Analysis) will be described. The chapter will conclude with a brief presentation of the use of optimisation methods, such as Mathematical Programming, for analysing and designing Heat Exchanger Networks (HENs).

8.1.2 Improving Existing Facilities

Considerably more engineering time in the process industries is spent on improving existing production facilities (i.e. revamping, debottlenecking or retrofitting) than on designing new plants. Unfortunately, the powerful tools for grassroots design cannot be readily used for the retrofit case; however, the insight that was instrumental in developing the grassroots tools is equally important when retrofitting Heat Exchanger Networks (HENs). The three main reasons why retrofit design is considerably different from

© Woodhead Publishing Limited, 2013

grassroots design are (a) the need to focus on maximum utilisation of existing equipment that has been invested and installed, (b) the need to appreciate that plant downtime is required to implement a retrofit action, and that this can be critical for the economy of the project due to loss of production and thus loss of income, and (c) the need for more accurate modelling (or rating) of existing heat exchangers.

Projects for improving existing production facilities have different names according to their main objectives. For a major increase in production capacity, the word ***revamp*** is often used and signals major investments in new equipment throughout the plant. For a smaller increase in production capacity, the word ***debottlenecking*** is used and signals investments in a particular part of the plant that is limiting production. Sometimes this bottleneck is situated in the Plant Utility System, in which case additional heat recovery may be an economic alternative to making major investments in the Plant Utility System. Finally, the word ***retrofit*** is used for cases where increased energy efficiency is the main objective. Since the economic benefits from retrofit projects can be somewhat limited, these projects should be combined with other ***process modification*** projects, whenever possible. Then plant downtime will not affect the retrofit project since the plant has to be shut down for some period anyhow, and the incentive and payback for retrofit projects can be considerably improved. The availability of investment capital can also be enhanced in such cases.

8.2 Extended Procedures for Grassroots Analysis

While Chapter 4 described graphical diagrams and numerical procedures for obtaining Performance Targets for Minimum Energy Consumption and the Minimum Number of Units (heat exchangers), this section will introduce Targeting procedures for multiple utilities, heat transfer area, heat exchanger shells (for shell-and-tube exchangers) and total annual cost.

8.2.1 Multiple Utilities and Utility Pinches

The simplified presentation in Chapter 4 had only one hot utility (Steam – ST) and one cold utility (Cooling Water – CW); however, the process industries typically have a considerable number of available utilities, such as different steam levels (high, medium and low pressure steam – HP, MP, LP), fired heaters (furnaces), hot oil circuits, cooling water, chilled water, sea water and various refrigeration cycles. In processes where combustion takes place, air preheat is also utilised as a cold utility, thereby reducing the need for fuel.

© Woodhead Publishing Limited, 2013

Table 8.1 Stream and utility data for the illustrative example

ID	T_s (°C)	T_t (°C)	CP (kW/K)	ΔH (kW)
H1	270	160	18	1,980
H2	220	60	22	3,520
C1	50	210	20	3,200
C2	160	210	50	2,500
HP	250	250	n.a.	Variable
MP	200	200	n.a.	Variable
LP	150	150	n.a.	Variable
CW	15	20	n.a.	Variable

The simplifying assumption made in Chapter 4 was that utilities (such as ST and CW) are available at 'extreme' temperatures and thus can be introduced at the top (ST) and the bottom (CW) of the Heat Cascade. This also means that utility exchangers with steam and cooling water can be placed last to complete the HEN and to make sure the streams reach their Target Temperatures. With multiple hot and/or cold utilities, however, some of the utilities will have moderate temperatures and thus have to be treated as intermediate utilities.

With multiple utilities, both the targeting stage and the design stage will be affected, and maximum use of intermediate utilities (that are less expensive) to save more extreme utilities (that are more expensive) will introduce new Pinch points for the heat recovery problem, referred to as Utility Pinch points, with the same decomposing effect as a Process Pinch.

In order to illustrate the case with multiple utilities, consider the Stream and Utility Data presented in Table 8.1. In this illustrative example, there are two hot streams, two cold streams, three hot utilities (three steam levels) and one cold utility. The value for $\Delta T_{\min}$ is assumed to be 20°C.

As discussed in Chapter 4, the stream data can be used to set up a Heat Cascade with temperature intervals based on supply and target temperatures of the streams, and the heat flow of the Heat Cascade is the basis for the Grand Composite Curve (GCC). Figure 8.1 illustrates a simplified Heat Cascade (left) where the hot and cold streams are removed, focusing on the heat flow in the cascade with minimum external heating and cooling. The figure also shows (right) the corresponding GCC for the example in Table 8.1.

As indicated by the Heat Cascade in Fig. 8.1, the Process Pinch is at 180°C/160°C for hot/cold Process Streams. It is the Supply Temperature of cold stream C2 (160°C) that is causing the Pinch. Minimum hot and cold utility requirements are also indicated as $Q_{H,\min} = 1{,}000$ kW and $Q_{C,\min} = 800$ kW. With the hot and cold utilities listed in Table 8.1, it turns

© Woodhead Publishing Limited, 2013

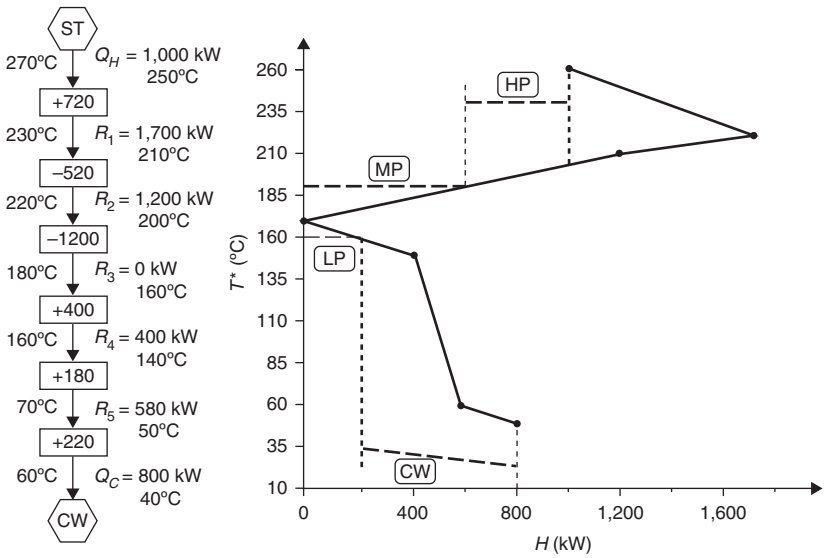

8.1 Simplified Heat Cascade and GCC for the illustrative example.

Table 8.2 Utility selection for the illustrative example

ID	Modified temperatures (°C)	Duty (kW)	Cost (USD/y)
HP	T^* = 250 – 10 = 240	400	80,000
MP	T^* = 200 – 10 = 190	600	102,000
LP	T^* = 150 + 10 = 160	200	–28,000
CW	T^* = 15/20 + 10 = 25/30	600	12,000

out that for this example, the Pinch temperature for hot streams (180°C) is higher than the temperature of LP steam (150°C), which means LP steam cannot be used as a hot utility in this case. However, LP steam could be used as a cold utility, since it can be generated using surplus heat from hot process streams below Pinch. Assuming there are nearby customers for this steam, this contributes to the total utility cost as income (credit).

Since the GCC uses modified temperatures (described in Chapter 4), utilities must also be drawn at modified temperatures, as indicated in Fig. 8.1 (right-hand part). Table 8.2 provides temperatures, duties and cost contributions for the utilities when placed in a way that maximises the use of cheaper utilities, as drawn in Fig. 8.1. The following utility prices are assumed, all in USD/kWy: HP steam @ 200, MP steam @ 170, LP steam @ 140 and CW @ 20. This is the 'optimal' solution when only Energy Cost (no Investment Cost) is included.

© Woodhead Publishing Limited, 2013

The annual utility cost with the mix of utilities indicated in Table 8.2 is 166,000 USD/y, while using HP steam and CW only would cost 216,000 USD/y. Using intermediate utilities would result in cost savings of 50,000 USD/y, i.e. 23.1%, which to a large extent is due to the production of LP steam and the corresponding credit.

With reference to Fig. 8.1, a graphical procedure for Targeting the utility mix is thus to start at the Process Pinch and place utilities one at a time, always selecting the cheapest utility and maximising its use. The maximum duty is found whenever the dotted utility lines in Fig. 8.1 touch either the GCC (as is the case for MP and LP steam) or a heat Pocket in the GCC (as is the case for HP steam). The dotted line for CW in Fig. 8.1 does not touch the GCC, since the temperature of cooling water is lower than any of the process stream temperatures.

The Heat Cascade can be used to develop numerical Targeting procedures for the case of multiple utilities, where linear interpolation is used to find the duties when the temperatures of the utilities are known. Even in grassroots cases, there are often existing production sites with established utility systems, so it would make sense to connect to the existing steam headers, which would mean the steam temperatures are known. A slightly more complex problem is where there is no existing Utility System and both the loads and levels of the utilities (steam types and refrigeration cycles) can be selected. For the GCC in Fig. 8.1, one could have reduced the number of utilities required by selecting one steam level where the heat Pocket ends. This modified temperature can be found by interpolation (enthalpy value is 1,000 kW) to be 203.3°C, which means a real steam temperature of 213.3°C to satisfy $\Delta T_{min} = 20$°C.

The next important observation when maximising intermediate utilities (such as LP and MP steam in this case) is that new Pinch points will appear, referred to as ***Utility Pinch*** points. When maximising the use of MP steam, there will be some hot streams that will be heated to 190°C in modified temperature by MP steam. The true temperatures are then 200°C for MP steam and 180°C for the hot process streams, i.e. $\Delta T = \Delta T_{min} = 20$°C. Utility Pinch points have the same decomposing property as Process Pinch points, in the sense that there has to be no heat transfer across these Utility Pinch points if the maximum use of intermediate (and cheaper) utilities is to be realised in the resulting HEN. Of course, there is an investment cost penalty involved, since driving forces will be reduced in the network and the heat transfer area will increase. It is important to notice that this reduction in driving forces will not only be experienced in the utility exchangers (using MP steam rather than HP steam), but also in many of the heat exchangers, since the shape of the Composite Curves will be changed. This is illustrated in Fig. 8.2, where so-called ***Balanced Composite Curves*** are drawn for two cases: (1) using only HP steam and CW – solid lines, and (2) using all four

© Woodhead Publishing Limited, 2013

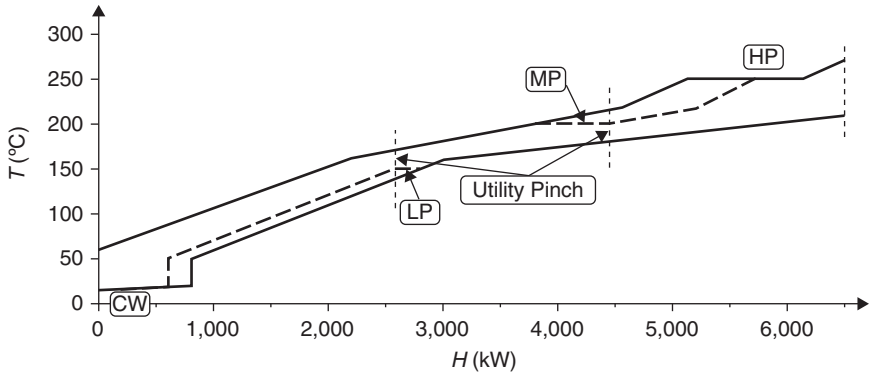

8.2 Balanced Composite Curves with two (solid lines) and four (dotted lines) utilities.

utilities – dotted lines. As suggested, the reduction in driving forces goes beyond the utility exchangers.

8.2.2 Three-Way Trade-Off in Heat Recovery Systems

There are three cost factors in HENs. Hot and cold utility consumption represents the energy (or operating) cost, while the capital (or investment) cost reflects the total heat transfer area in the network, and how this area is distributed into a number of heat exchangers (referred to as units). Obviously, there are trade-offs between these three factors – Energy, Area and Units. As mentioned in Chapter 4 as part of Design Evolution, this three-way trade-off is to a large extent affected by the selected value for ΔT_{min}. While Chapter 4 focused on the trade-off between energy and units, where network complexity and cost can be improved by removing small heat exchangers resulting from strict Pinch Decomposition as part of the Pinch Design Method, this chapter will address the full trade-off between Energy, Area and Units. In order to be able to do this, the chapter will present Targeting and Design methods related to heat transfer area.

8.2.3 Targets for Heat Transfer Area

Counter-current flow is a well-known and good engineering principle that maximises the use of available driving forces in heat transfer and mass transfer processes. This can be used to minimise the size of the equipment needed to transfer certain amounts of heat or mass, and correspondingly to maximise the amount of heat or mass transferred with given equipment sizes. The counter-current principle has been adopted in the composite

© Woodhead Publishing Limited, 2013

curves, where the cooling curve (hot streams to be cooled or condensed) is drawn counter-currently to the heating curve (cold streams to be heated or vaporised).

The closest one can come to pure counter-current heat transfer for multiple hot and cold streams is Vertical Heat Transfer between the Composite Curves. This insight was the basis for developing the so-called Bath Formula (Townsend and Linnhoff, 1984). The enthalpy axis of the Composite Curves is divided into enthalpy intervals to ensure vertical heat transfer. Next, all hot streams in a certain interval are allowed to match with all cold streams in the same interval, while making sure that the outlet temperatures for each match are the same as the interval temperatures. The resulting network will consist of a very large number of heat exchangers, stream splits and mixers, and is referred to as the Spaghetti Design. Of course, this is not a tractable design solution; it only serves as a model to be able to estimate total heat transfer area. The resulting Targeting formula (Bath Formula) for area is given by Equation [8.1].

$$A_{\min} = \sum_j \frac{1}{\Delta T_{LM,j}} \cdot \sum_k \frac{\Delta q_k}{h_k} \qquad [8.1]$$

In Equation [8.1], index j indicates the summation over enthalpy intervals, while index k indicates the summation over all process streams and utilities transferring heat in interval j. All elements in Equation [8.1] are available as soon as the Balanced Composite Curves (Fig. 8.2) are established:

- $\Delta T_{LM,j}$ is the log mean Temperature Difference of enthalpy interval j.
- Δq_k is the heat supplied/rejected for stream/utility k in enthalpy interval j.
- h_k is the film Heat Transfer Coefficient for stream/utility k in enthalpy interval j.

Consider the heat transfer equation in Equation [8.2], which has been made applicable to any type of heat exchanger by including the correction factor f_T for deviation from pure counter-current heat transfer. It is obvious that heat transfer area in *one* heat exchanger is minimised when f_T has its largest value. This is the case for pure counter-current heat exchangers where $f_T = 1.0$, and this assumption has been the basis for developing the formula in Equation [8.1].

$$A = \frac{Q}{U \cdot \Delta T_{LM} \cdot f_T} \qquad [8.2]$$

© Woodhead Publishing Limited, 2013

However, with multiple heat exchangers, as is the case for HENs, the value of the Heat Transfer Coefficient (U) depends on which pairs of hot (i) and cold (j) streams are matched, as indicated by the simplified formula in Equation [8.3], neglecting heat transfer resistance in the wall and geometrical effects, such as inner and outer diameter of tubes in heat exchangers. In fact, Equation [8.3] was used in the development of the Targeting formula in Equation [8.1].

$$\frac{1}{U_{ij}} = \frac{1}{h_i} + \frac{1}{h_j} \qquad [8.3]$$

The important implication is that, in order to minimise total heat transfer area, one should not focus on the optimal distribution of driving forces (ΔT). It is the product of Heat Transfer Coefficient and Temperature Difference ($U \cdot \Delta T$) that should be optimally distributed. This means that vertical heat transfer will not always minimise total heat transfer area, since a low U-value can be compensated by a large Δt-value and vice versa. For significant differences in film heat transfer coefficients, it may thus be optimal from an area point of view to have non-vertical ('criss-cross') heat transfer resulting from careful matching of hot and cold streams to optimise the distribution of ($U \cdot \Delta T$). In this respect, even the Process Pinch is no exception, and this affects the design procedure, as will be discussed in Section 8.3.

8.2.4 Total Annual Cost and Near-Optimal $\Delta T_{\min}$

With reference to the three-way trade-off discussed in Section 8.2.2 and Targeting procedures established for energy and units (Chapter 4) as well as area (Section 8.2.3), it is possible to estimate Total Annual Cost (TAC) for heat recovery systems ahead of design. The individual target values for energy (i.e. external heating and cooling), units and area, all depend on the value of $\Delta T_{\min}$. As a result, with cost data for utilities and heat exchangers, as well as some key economic parameters, it is possible to estimate TAC for different values of $\Delta T_{\min}$, and the resulting curve will obviously pass through a minimum, due to the economic trade-offs involved. This minimum then identifies a near-optimal value for $\Delta T_{\min}$ that can be used to develop the initial Maximum Energy Recovery (MER) design as described in Chapter 4.

Since estimating TAC takes place ahead of design, there are a number of issues involved that need to be addressed. Assume that target values for $Q_{H,\min}$ and $Q_{C,\min}$ are used to establish Operating Cost, and that target values for $U_{\min,\mathrm{MER}}$ and $A_{\min}$ are used to establish Investment Cost. Assume further that these targets are available for a given range of values for $\Delta T_{\min}$. The following sources of inaccuracy are present in the estimation of TAC:

© Woodhead Publishing Limited, 2013

- The targets for minimum number of units and minimum heat transfer area are not compatible, since minimum area requires a much larger number of units. This then represents an optimistic assumption reducing the estimate for TAC.
- The area distribution among the heat exchangers is not known ahead of design, and in lack of a better model, total area is equally divided among the units. With an economy of scale cost law for heat exchangers, equal area distribution is the most expensive solution and represents a conservative assumption increasing the estimate for TAC.
- The Targeting formula for minimum heat transfer area is based on the assumption of vertical heat transfer between the Composite Curves, while criss-cross heat transfer may reduce total heat transfer area due to a better distribution of $(U \cdot \Delta T)$. This then represents a conservative assumption increasing the estimate for TAC.

Interestingly, practitioners of these methods have claimed that the three sources of inaccuracy discussed above tend to cancel, thus making the estimate for TAC as a function of $\Delta T_{\min}$ accurate within 5–10% (relative to the cost of the designed HEN, using the same models as in the Targeting stage). It should be emphasised that the main objective of this exercise is not to get very accurate estimates for TAC, but to get a reasonable starting value for the Level of Heat Recovery as represented by the economic parameter $\Delta T_{\min}$.

The reason why a good initial estimate for $\Delta T_{\min}$ is critical is that its value affects the position of the Process Pinch. When designing the HEN, the location of the Pinch is crucial since it affects the Pinch Exchangers and the basic structure of the HEN. Since the optimisation stage primarily involves design evolution (keeping the basic network structure and making minor adjustments to improve network economy and reduce design complexity), the Pinch location is important. Supertargeting is the jargon often used for this pre-optimisation activity, since it combines individual targets with focus on TAC.

8.2.5 Heat Exchanger Details

In order to add even more industrial realism to the heat recovery problem, some practical aspects of heat exchanger equipment design should be included. For higher pressure levels, thicker materials has to be used in the heat exchangers, and this affects and shifts the trade-off between energy cost and investment cost towards lower levels of heat recovery. In the case of corrosive fluids, more expensive construction materials has to be used, and this also shifts the trade-off towards lower levels of heat recovery. The process streams as well as the utilities will have considerable differences in

© Woodhead Publishing Limited, 2013

film heat transfer coefficients due to phase condition, pressure level, velocity and temperature. For a detailed TAC estimation, all such factors has to be included and they affect the identified near-optimal value for ΔT_{min}.

Another equipment aspect that needs to be considered is the heat exchanger configuration. The pure counter-current model used in the simplified analysis of Chapter 4 is seldom found in industrial environments. In the chemical and petrochemical industry as well as in the oil and gas industry, shell and tube exchangers are commonly used. These units have two important features that affect the Targeting and Design stages: (a) they do not have pure counter-current flow, and (b) they are often divided into multiple shells. The departure from pure counter-current flow puts a limit on the amount of heat that can be transferred between a hot and a cold stream with given temperatures. The Tubular Exchanger Manufacturers Association (TEMA) has classified shell-and-tube exchangers and provided charts and procedures to establish the f_T factor (see Equation [8.2]) for a given exchanger and a given set of stream data. Industrial rules of thumb indicate that f_T should be at least 0.75, otherwise more shells should be added until f_T is satisfied for all shells of that unit. This indicates a simplified procedure for Targeting number of shells rather than units in heat recovery problems. Ahmad (1985) described procedures for Targeting both minimum number of shells and minimum heat transfer area for networks using 1–2 shell-and-tube exchangers, i.e. the 'work horse' in the process industries.

With more detailed focus on the heat exchangers as building blocks in heat recovery systems, procedures for estimating TAC will also need to be refined, as described by Hall *et al*. (1990). In addition to dealing with shells rather than units, they also considered mixed construction materials and different pressure ratings. Unfortunately, similar developments have not been made for plate exchangers, which are also commonly used in certain industries.

8.2.6 Stream Contributions to ΔT_{min}

The concept of individual stream contributions to ΔT_{min} was briefly discussed in Chapter 4 as part of the procedure for finding modified temperatures that could be used when hot and cold streams are represented by the same curve in the same diagram, i.e. the GCC. This is obviously more realistic in an industrial setting than using half of ΔT_{min} as contributions for all streams. When discussing a Performance Target for heat transfer area in Section 8.2.3, it was emphasised that it is the product of driving forces (ΔT) and heat transfer coefficients (U) that should be optimally distributed in a HEN, not only driving forces as the strict vertical heat transfer model is

© Woodhead Publishing Limited, 2013

aiming for. Since film heat transfer coefficients in the process industries often vary by one or two orders of magnitude, it is obviously wrong to use a single global value for ΔT_{min} in the entire HEN. This is not going to be optimal in grassroots design and certainly not in retrofit projects.

Townsend (1989) and later Ahmad *et al*. (1990) utilised results regarding optimal heat transfer systems by Nishimura (1980) to introduce the relation in Equation [8.4] as an approximate value for the individual stream contributions to ΔT_{min} as a function of the film heat transfer coefficients for the individual streams. The constant C is common for all streams and can be used to manipulate the level of heat recovery. In fact, these contributions were proven optimal in cases with one cold and several hot streams (as in crude oil preheat trains), or vice versa.

$$\Delta T_i = \frac{C}{\sqrt{h_i}} \qquad [8.4]$$

Both Hall *et al*. (1990) and Ahmad *et al*. (1990) discussed how the ΔT_{min} contributions could be manipulated by adding correction factors to the film heat transfer coefficients in order to account for differences in construction materials and different pressure ratings. Even though this will improve the accuracy of Capital Cost targets, there is a problem using this approach related to the pairing effect for streams requiring different materials or pressures.

8.3 Extended Procedures for Grassroots Design

In the same way as energy targets provided insight (i.e. Pinch Decomposition) about how to design energy optimal HENs, the development of an Area Target described in Section 8.2.3 yielded insight (i.e. vertical heat transfer) about designing of minimum or reduced total heat transfer area. As a result, procedures with focus on heat transfer area have been developed to complement the original Pinch Design Method, which focused primarily on (i) minimum external heating and cooling through Pinch Decomposition and application of the '*CP*' rules, and (ii) the fewest number of units by using the 'tick-off' rule (see Chapter 4). The next sections will describe graphical (Section 8.3.1) and numerical (Section 8.3.2) procedures to include area considerations in the design phase for HENs.

8.3.1 The Driving Force Plot (DFP)

The available driving forces for a heat recovery problem can be shown graphically by plotting the Temperature Difference between the Hot and

© Woodhead Publishing Limited, 2013

Cold Composite Curves as a function of, for example, cold stream temperatures (Linnhoff and Vredeveld, 1984). This curve, referred to as the Driving Force Plot (DFP), has a minimum at the Process Pinch where ΔT is equal to ΔT_{min}. A heat exchanger can be represented in this diagram as a trapezoid by plotting ΔT in the hot and cold end of the exchanger, as shown in Fig. 8.3. For optimal use of driving forces, the trapezoids of the heat exchangers should fit as closely as possible under the DFP.

If one heat exchanger uses too much Driving Force relative to what is available in the process for that particular temperature range, then another heat exchanger in the same temperature range will have less ΔT available. In such cases, the inverse relationship between driving forces and heat transfer area (see Equation [8.2]) results in an increase in total heat transfer area. A perfect match to the DFP would require a spaghetti design, as mentioned in Section 8.2.3, with a large number of stream splits, mixers and heat exchangers. Such a design is of course not tractable, since it has a very high investment cost, high complexity and low operability. The DFP has to be used with care in trying to get a reasonable but not perfect fit of the trapezoids.

Figure 8.3 shows an incomplete HEN (left) and a DFP (solid line) with the trapezoids (dotted lines) drawn (right) for three Pinch Exchangers (i.e. heat exchangers operating immediately adjacent to the Pinch) to illustrate two important applications of the DFP. Heat Exchanger 3 below Pinch has been designed using the 'tick-off' rule, and even though the profile was perfect in the beginning (i.e. from the Pinch to the first kink), the large duty of this exchanger results in a large overshoot of the DFP, using much more Driving Forces than are available in this temperature region. This means that other heat exchangers in this region (not included in the incomplete network to the left) will suffer from less Driving Force.

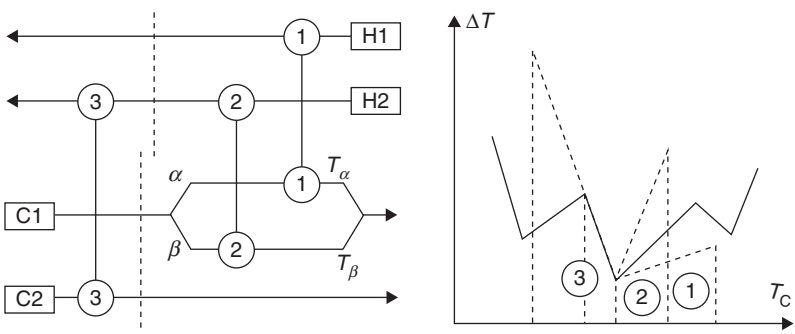

8.3 DFP (right) for an incomplete HEN (left).

© Woodhead Publishing Limited, 2013

Above Pinch, the split of cold stream C1 introduces a degree of freedom, in the sense that the flowrate through the two branches (α and β) can be adjusted. Assuming the duties of Heat Exchangers 1 and 2 are fixed, the cold outlet temperatures from the two units (T_α and T_β) can be manipulated by adjusting the split ratio (α and β). If the flowrate in the upper branch (α) is increased, the temperature (T_α) will be decreased and the Temperature Difference in the hot end of the exchanger will increase. This means that the trapezoid for Heat Exchanger 1 will increase in height and approach the DFP. At the same time, and as a consequence of increasing α, the flowrate in the lower branch (β) will decrease, the temperature (T_β) will increase, and the Temperature Difference in the hot end of the exchanger will decrease. This means that the trapezoid for Heat Exchanger 2 will decrease in height and approach the DFP.

In summary, it has been illustrated that the DFP can be used in a graphical manner to 'tame' the 'tick-off' rule (reduce the duty of Heat Exchanger 3), and to adjust stream split ratios in order to reduce total heat transfer. Reducing Heat Exchanger 3 will most likely introduce the need for one more unit; in fact, the general insight is that the number of units will increase when efforts are made to reduce heat transfer area (i.e. there is a trade-off). The true art is then to save some heat transfer area without approaching the spaghetti design. In fact, there are a number of limitations when using the DFP for area considerations in network design:

- It is difficult to know how much deviation from the DFP is acceptable.
- There is no link between the size of a trapezoid and the duty or Heat Transfer Area of the corresponding heat exchanger, since the DFP only uses temperature information.
- One cannot quantify how design changes to save area affect the number of units.
- While avoiding excessive or unnecessary large heat transfer area requirements is desirable, the bottom line is total investment cost, which is a function of the number of heat exchangers, total heat transfer area and area distribution among the units.

Finally, it should be mentioned that other versions of the DFP exist. Perhaps the most commonly used diagram in software packages and industrial practice plots cold temperature as the x-axis, while hot temperatures are plotted as the y-axes. The diagonal is then the limiting case of $\Delta T = 0$, and any feasible heat exchanger must be positioned above the diagonal. Heat exchangers are represented as straight lines in this version of the diagram. The DFP presented in Fig. 8.3, however, appears to have an advantage as a pedagogic tool.

© Woodhead Publishing Limited, 2013

8.3.2 The Remaining Problem Analysis (RPA)

While the DFP offers general insight into heat transfer area utilisation, it has a number of limitations, as described in Section 8.3.1. The RPA is a numerical tool that quantitatively measures the effect of each suggested design action on the total network. As the name suggests, this is done by analysing the remaining problem through Targeting procedures to estimate the effect of individual design decisions. The remaining problem is obtained by removing stream segments from the original stream data for those parts of hot and/or cold streams that are involved in heat exchangers that either are accepted (decided) or proposed. The RPA tool is designed for, and works perfectly well with, sequential design procedures such as the Pinch Design Method (PDM).

The steps of the RPA are as follows:

1. Obtain targets for energy ($Q_{H,\min}, Q_{C,\min}$), units ($U_{\min}$) and area ($A_{\min}$) for the original and overall problem from the available stream and utility data.
2. Initialise variables that are used to measure the accumulated effects of design decisions: $U_{\text{HEN}} = 0, A_{\text{HEN}} = 0, Q_{H,\text{HEN}} = 0, Q_{C,\text{HEN}} = 0$
3. Propose a new exchanger k to be added to the network

    a. If it is a process/process heat exchanger then:

    $$U_{\text{HEN}} = U_{\text{HEN}} + 1,\ A_{\text{HEN}} = A_{\text{HEN}} + A_k$$

    b. If it is a hot utility exchanger then:

    $$U_{\text{HEN}} = U_{\text{HEN}} + 1,\ A_{\text{HEN}} = A_{\text{HEN}} + A_k,\ Q_{H,\text{HEN}} = Q_{H,\text{HEN}} + Q_k$$

    c. If it is a cold utility exchanger then:

    $$U_{\text{HEN}} = U_{\text{HEN}} + 1,\ A_{\text{HEN}} = A_{\text{HEN}} + A_k,\ Q_{C,\text{HEN}} = Q_{C,\text{HEN}} + Q_k$$

    d. For all three cases (a, b and c), remove parts of the stream data (i.e. Stream segments for hot and/or cold streams) that are involved in exchanger k.

4. Estimate the total properties for the design under development by adding the targets for the remaining problem (RP) to the accumulated values for the accepted matches:

© Woodhead Publishing Limited, 2013

$$U_{\text{total}} = U_{\text{HEN}} + U_{\text{min,RP}}, A_{\text{total}} = A_{\text{HEN}} + A_{\text{min,RP}}$$
$$Q_{H,\text{total}} = Q_{H,\text{HEN}} + Q_{H,\text{min,RP}}, Q_{C,\text{total}} = Q_{C,\text{HEN}} + Q_{C,\text{min,RP}}$$

5. Compare estimated values for the overall network with original targets for the entire problem in order to accept or reject exchanger *k* proposed in step 3:

    a. If exchanger *k* is rejected then recalculate values for U, A, Q_H and Q_C by subtracting contributions from this unit, restore stream data by adding the segments that were removed in step 3.d, and return to step 3.
    b. If exchanger *k* is accepted, then check if all stream data have been removed. If there are no more stream data (i.e. network design is complete), then continue to step 6, otherwise return to step 3.

6. End of the RPA procedure, network design is complete.

The main advantage with the RPA compared to the DFP is of course that effects on heat transfer area by the individual design decisions are measured quantitatively by the RPA, while this can only be addressed qualitatively by the DFP. In addition, the RPA also considers number of units and external heating and cooling. Still, the remaining question is how much increase in heat transfer area and/or number of units is acceptable during network design. It is also possible that being too 'greedy' in the initial phase of the procedure will give penalties towards the end of the design.

A reasonable question is why there is a need to monitor hot and cold utility consumption, since minimum external heating and cooling is taken care of by Pinch Decomposition and the original and basic PDM. The answer is that, for more complicated industrial situations, there may be near Pinch situations in addition to the identified Process Pinch. These designs are difficult for manual and sequential procedures, thus there is a need for guidance also on how utility consumption develops as the network design is evolving.

8.3.3 Three Reasons for Splitting Streams

As described in Chapter 4, there are three different reasons why it is often beneficial and profitable to split streams into two or more branches:

- Reduce energy consumption
- Reduce total heat transfer area
- Reduce the number of units

© Woodhead Publishing Limited, 2013

In Chapter 4, the discussion about stream splitting was focused on energy consumption. The PDM uses *CP* rules and topology rules to ensure that Pinch Exchangers have sufficient driving forces. If these rules cannot be obeyed for the original set of streams, then one or more hot and/or cold streams must be split into two or more branches in order to obtain an MER design, i.e. a network with MER.

When discussing the DFP in Fig. 8.3, it was illustrated that stream splitting provides degrees of freedom in the sense that stream branch flowrates can be varied to reduce total heat transfer area. Consider the stream split of cold stream C1 in Fig. 8.3. If the duties of the heat exchangers between C1 and the two hot streams H1 and H2 are fixed, then there is a local optimisation problem related to finding the values of α and β that will minimise the sum of the cost of the two heat exchangers. The optimal values of the stream branch flowrates depend on a number of factors, such as:

- The duties of the two exchangers: Q_1 and Q_2
- The heat transfer coefficients for the units: U_1 and U_2
- Temperatures of the hot streams: T_{H1} and T_{H2}
- Possible differences in materials of construction and thus cost equations

Despite all the factors affecting the optimal split ratio for C1, the relation in Equation [8.5] provides a good initial estimate focusing on the best distribution of driving forces.

$$\frac{\alpha}{\beta} = \frac{CP_{H1}}{CP_{H2}} \qquad [8.5]$$

A more general relation indicating near-optimal *CP* ratios for a match between a hot stream *i* and a cold stream *j* is given by Equation [8.6]. The motivation behind this relation is to try to make individual heat exchangers mimic the profiles of the Composite Curves. Of course, the summation should only include hot and cold streams present in the same temperature region as streams *i* and *j*. Whenever considerable deviations from Equation [8.6] are experienced, one should consider stream splitting, while making sure the number of units remains reasonable.

$$\frac{CP_{Hi}}{CP_{Cj}} \cong \frac{\sum_i CP_{Hi}}{\sum_j CP_{Cj}} \qquad [8.6]$$

Finally, stream splitting can also be used to reduce the number of heat exchangers in the network. It is important to realise that the variable *N* in

© Woodhead Publishing Limited, 2013

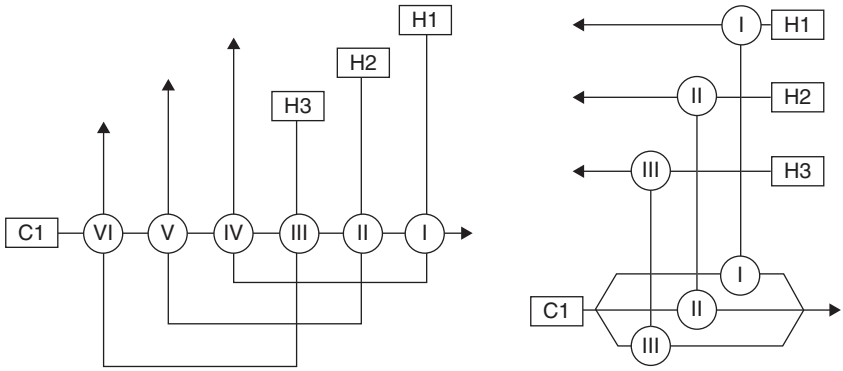

8.4 Serial and parallel heat exchange between one cold and three hot streams.

the so-called $(N-1)$ rule that was used in Chapter 4 to establish a target for the minimum number of units only refers to the original streams and different utility types. When splitting streams into branches, the value of N remains the same. This may seem counter-intuitive for some; however, it is easy to come up with examples where the number of units is reduced, not increased, by stream splitting.

Figure 8.4 shows a case where one large cold stream is heat integrated with three small hot streams, where 'large' and 'small' refer to the CP values of the streams. In the case of serial design, the heat exchangers will be limited by driving forces in the cold end due to the low CP values of the hot streams. This is why a cyclic arrangement is introduced (left in Fig. 8.4) in order to increase the heat recovery from the hot streams. An alternative design would be a split stream arrangement, where the hot streams provide heat to the cold stream in a parallel configuration, with a considerable reduction in the number of units (right in Fig. 8.4).

In fact, the situation described in Fig. 8.4 is not uncommon in the process industries. The best example is oil refineries, where the cold crude oil is preheated in a number of stages before the main fractionator. The various products from this large distillation tower, as well as pumparounds and other hot streams in the plant, are used in the so-called crude-preheat train. Most refineries in the world today have a complex stream split arrangement in order to maximise the amount of heat recovered while minimising the number of heat exchangers.

8.3.4 Limitations with the Pinch Design Method (PDM)

The PDM has been used frequently and successfully in a large number of industrial companies around the world since its birth in the early 1980s.

© Woodhead Publishing Limited, 2013

Simple design guidelines and rules allow engineers to develop HENs that are near-optimal from a cost perspective and feasible from a practical aspect, since the engineer is in complete control of every step of the design process. With additional tools, such as the DFP and the RPA, networks can be developed with a good balance (trade-off) between energy consumption, heat transfer area and number of heat exchange units.

Nevertheless, there are important limitations with the PDM:

- It is a sequential design procedure, where one design decision is made at a time, thus providing no guarantee on optimality for the complete design.
- The multiple trade-offs involved in HENs are very difficult to balance or optimise by manual procedures.
- For cases where the Composite Curves have regions of nearly parallel profiles or cases where there are several Pinch Points (combinations of Process Pinch, near Pinch Points and Utility Pinch points), the simple rules of the PDM become difficult to apply.
- The PDM only results in an initial design with MER which is subject to further evolution using Heat Load Loops and Paths in order to simplify the network and reduce TAC. This fine tuning cannot resolve situations where the basic network structure is wrong.
- In cases with considerable differences in film heat transfer coefficients, the matching of hot and cold streams becomes much more difficult since strict Pinch Decomposition is relaxed and non-vertical (criss-cross) heat transfer can be favourable.
- The strict Pinch Decomposition often prevents the engineer from identifying networks with reduced cost and reduced complexity (fewer units and fewer stream splits).
- PDM and Pinch Analysis in general are unable to properly address heat recovery situations where there are restrictions in the matching between hot and cold streams. This applies to cases with Forbidden Matches (due to safety, integrity, operability, product purity, etc.) as well as required (for start-up) and restricted matches.

It is the limitations explained in the bulleted list above that have motivated the use of other approaches to design HENs, such as the use of optimisation methods that will be discussed in Section 8.5. Some of these methods (such as the deterministic ones using Mathematical Programming) are based on insight from Pinch Analysis; however, they represent simultaneous approaches to the design problem with considerably better capabilities to handle the complex trade-offs and they can easily handle issues such as forbidden matches. The major limitation with these methods is numerical problems related to non-convexity (local optima) and computational complexity (combinatorial

© Woodhead Publishing Limited, 2013

explosion). Non-deterministic methods (such as stochastic search algorithms) overcome the numerical problems; however, they do not utilise insight from Pinch Analysis and do not guarantee an optimum solution.

8.4 Retrofit Analysis and Design

There are two fundamentally different situations where energy saving retrofit projects for HENs may be considered. In order to illustrate this, consider the Area–Energy Diagram in Fig. 8.5. By calculating area and energy targets for different values of $\Delta T_{\min}$, the limiting trade-off curve (solid line) in Fig. 8.5 can be obtained by plotting corresponding values for $A_{\min}$ and $E_{\min}$, where $E_{\min}$ (energy) typically can be hot utility consumption ($Q_{H,\min}$). No feasible designs exist below this curve, and designing very close to this line would require a large number of units (i.e. the spaghetti design) in order to achieve $A_{\min}$, which is why the curved dotted line is added to indicate an economic trade-off curve.

Two existing designs (B and C) have been plotted in the Area–Energy Diagram (Tjoe and Linnhoff, 1986) of Fig. 8.5 together with an optimal grassroots design (A). Design (B) is located on the economic trade-off curve, indicating that it is a good design; however, it was designed when energy was cheap and has a wrong trade-off (uses too much energy). Design (C) is far from the economic trade-off curve, which means it basically is a poor design irrespective of the trade-off situation between equipment cost and energy cost. For the invested heat transfer area (A^C_{exist}), it uses more energy than necessary ($\Delta E = E^C_{\text{exist}} - E^C_{\min}$), whereas, for the current energy consumption (E^c_{exist}), more Heat Transfer Area than necessary ($\Delta A = A^C_{\text{exist}} - A^C_{\min}$) has been installed.

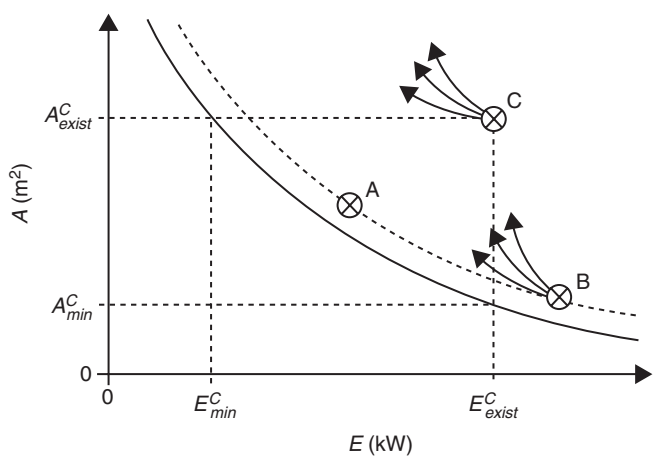

8.5 Area–Energy Diagrams for heat recovery problems.

© Woodhead Publishing Limited, 2013

From an economic point of view, the poor design (C) is a much easier retrofit candidate than the considerably better design (B). This may sound counter-intuitive, but is related to the fact that reduction in energy consumption can only result from making investment in equipment (new heat exchangers and/or additional heat transfer area to existing units). For design (B), the possible investment/saving curves (indicated by the set of curved arrows) will be steeper than the investment/saving curves for design (C). For a poor design (C), even rearranging the piping may result in savings, while a good design (B) does not have such 'low hanging fruit'. When process plants are designed without knowledge about Pinch Analysis, it is much more likely to end up with HENs of type (C) than of type (B). This is why a number of retrofit projects with considerable savings (tens of millions of US$) and short payback times (less than a year) were identified during the 1980s in the chemical and petrochemical, as well as the oil and gas, industries. These processes are often extremely complex and, without systematic tools, it is virtually impossible to design heat recovery networks that have close to Minimum Energy Consumption, low total heat transfer area and close to the Minimum Number of Units.

8.4.1 Special Challenges in Retrofit Design

As explained in Chapter 4 and Section 8.1.2, retrofit design of HENs is very different from the grassroots case, mostly because the invested equipment of the existing design needs to be maximally re-utilised in the modified and improved network. More specifically, the new or additional challenges in the retrofit case include:

- Since heat exchangers do not have a second-hand value, and most exchangers are tailor-made for the fluids and flowrates of their current operation, retrofit design is focused on the re-utilisation of existing units and making minor changes to the network, while keeping the basic structure of the design. Thus, an MER design produced by the PDM has no value in the retrofit case, not even as a starting point.
- In order to maximise the utilisation of existing exchangers, detailed modelling (also referred to as rating) is required. In grassroots design, making an error in modelling means there will be a minor error in cost. For retrofit cases a similar modelling error could result in the difference between identifying and not identifying the need for additional heat transfer area for an existing heat exchanger, thus giving a significant error in cost since there is a step change in the cost model when more area is needed.

© Woodhead Publishing Limited, 2013

- Retrofit projects for energy savings are normally limited by investment capital, which is another argument for keeping the basic network structure and trying to identify limited projects with considerable savings (the 'big apples' or the 'low hanging fruit').

Despite the differences between grassroots design and retrofit projects, the fundamental insight from Pinch Analysis is heavily utilised also in the retrofit case. Pinch Decomposition, for example, is used to identify the heat exchangers that are responsible for heat transfer Across the Pinch, and thus result in excess use of external heating and cooling. Retrofit design involves the same stages as the grassroots case, but with quite different content. Data Extraction was discussed in depth in Chapter 4 and will not be repeated here.

8.4.2 Retrofit Design Actions

For stand-alone retrofit projects focusing on increased energy efficiency by enhanced heat recovery, economical constraints (available capital and short payback times) normally limit the retrofit design actions to smaller investments that can be implemented in the plant without extensive down time, preferably projects that can be installed during planned maintenance stops. The retrofit actions fall into one of the following four main modification classes:

- Purchase new heat exchangers.
- Add heat transfer area to existing units:
  - purchase one or more additional shells for shell-and-tube exchangers,
  - purchase additional plates for plate exchangers.
- Heat Exchanger Enhancement, i.e. to change the internals of the units in order to:
  - increase available heat transfer area,
  - increase the Heat Transfer Coefficient.
- Make changes to the piping connecting streams and heat exchangers:
  - switch from serial to parallel heat exchange,
  - change fluids on the hot and/or cold side of heat exchangers.
- Increased heat recovery may result in the need for additional pumping and/or compression, the latter being a considerable investment.

Common to all these modifications to an existing heat recovery system is that changes in operating conditions, such as hot and cold stream temperatures, are be experienced in large parts of the network. In fact such

© Woodhead Publishing Limited, 2013

network interactions are utilised on purpose and in the best possible way to convert investment in equipment and network changes into savings in hot and cold utilities. By making strategic investments in new heat exchangers, Cross-Pinch heat transfer can be reduced, and maximum use of existing equipment can be realised.

8.4.3 Targeting the Level of Heat Recovery

While Energy Targeting in the grassroots case establishes values for minimum external heating and cooling as well as an optimal utility mix for cases with multiple utilities, the emphasis in retrofit energy targeting is on establishing an optimal level of heat recovery and thereby to identify the potential for energy savings that can be achieved through retrofit investments.

The level of heat recovery is indicated by the relative position of the Composite Curves, and can thus be directly related to the value of $\Delta T_{\min}$. However, this chapter will use another Driving Force related parameter that was introduced in the early 1980s as part of a double-temperature approach (Challand *et al*., 1981). These authors studied crude-preheat trains in oil refineries and observed a massive difference between the value of $\Delta T_{\min}$ representing the level of heat recovery (which could be as high as 50–60°C) and the smallest driving forces observed in the individual heat exchangers (which could be as low as 10–12°C). The Heat Recovery Approach Temperature (*HRAT*) points to the level of heat recovery, while the Exchanger Minimum Approach Temperature (*EMAT*) refers to the smallest allowed driving forces in the network. For obvious reasons, this means that $EMAT \leq HRAT$. When using stream individual contributions to $\Delta T_{\min}$, the application of *EMAT* is shown in Equation [8.7], while *HRAT* is only used as the smallest vertical distance between the Composite Curves.

$$\Delta T_i + \Delta T_j \geq EMAT \qquad [8.7]$$

Allowing $EMAT < HRAT$ opens up for non-vertical (criss-cross) heat transfer as discussed in Section 8.2.3 on Area Targeting. Using stream individual contributions to $\Delta T_{\min}$ allows for a better distribution of driving forces while considering differences in heat transfer coefficients.

As already stated in this section, the main objective of retrofit energy targeting is to establish a near-optimal value for *HRAT* reflecting the improved level of heat recovery in the plant after retrofit. Several methods have been proposed with different levels of sophistication to identify good values for *HRAT*. The simplest possible Targeting procedure is to plot the relationship between Minimum Energy Consumption (such as hot utility $Q_{H,\min}$) and *HRAT* (i.e. $\Delta T_{\min}$). Figure 8.6 shows an illustration of

© Woodhead Publishing Limited, 2013

an Energy-Target Plot, where the following can be observed: (i) there is an $HRAT_{\text{exist}}$ corresponding to the existing energy consumption in the plant ($Q_{H,\text{exist}}$), and (ii) the relationship between $Q_{H,\min}$ and $HRAT$ has kinks and regions of different slope (energy sensitivity) that are caused by kinks in the Composite Curves.

Figure 8.6 can be used for Retrofit Targeting by the following qualitative procedure:

- Start at the point corresponding to existing values of $HRAT$ and Q_H.
- Move along the Energy-Target Plot towards lower values of $HRAT$ and reduced values for minimum hot utility consumption, $Q_{H,\min}$.
- Steep segments of the Energy-Target Plot means significant energy savings with moderate reductions in $HRAT$ and moderate changes for the HEN.
- Flat segments have the opposite characteristics; considerable changes in $HRAT$ and the HEN with only moderate energy savings.
- Retrofit Targeting means to move as far down the Energy-Target Plot as economy allows; however, investment cost is only indirectly indicated through $HRAT$.

Moving too far down the Energy-Target Plot (Fig. 8.6) will result in a small value of $HRAT$ and considerable (and expensive) modifications to the HEN. Moving too little will not save much energy, so there is a balance here in trying to save as much energy as possible while staying within acceptable payback times. Based on the arguments above about steep and flat regions of the Energy-Target Plot, candidates for improved level of heat recovery are points (a), (b) and (c). Using purely qualitative considerations, one could

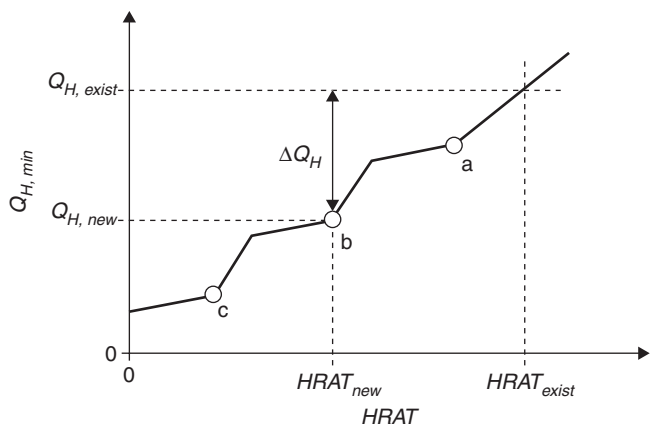

8.6 Simple Energy-Target Plot for the retrofit case.

© Woodhead Publishing Limited, 2013

argue that point (a) will not save enough energy to be an interesting retrofit project, point (c) will be too expensive, while point (b) appears to be the most promising candidate. The outcome of the Targeting procedure is thus $HRAT_{\text{new}}$ and $\Delta Q_H = Q_{H,\text{exist}} - Q_{H,\text{new}}$.

The most obvious limitation of the simple Targeting procedure described above is the lack of investment considerations beyond some qualitative arguments about the relation between the change in *HRAT* and the resulting need for modifications of the HEN and investment in new equipment. A more advanced retrofit Targeting procedure uses insight from the Area–Energy Diagram in Fig. 8.5 and some assumptions about trajectories of retrofit projects. Consider the set of curved arrows from design (B) or design (C) in Fig. 8.5 that are meant to indicate possible relationships between invested area and saved energy. The steeper the curves are, the more expensive the retrofit project are be for a given energy savings. In an attempt to suggest possible retrofit trajectories in the Area–Energy Diagram, Tjoe and Linnhoff (1986) introduced a new parameter α called ***Area Efficiency*** and is defined by Equation [8.8].

$$\alpha = \left(\frac{A_{\text{min}}}{A_{\text{exist}}} \right)_{E_{\text{exist}}} \qquad [8.8]$$

The Area Efficiency α measures, as the name indicates, how efficient area is installed (or used) in the existing design. More specifically, the current energy consumption (E_{exist}) corresponds to a value of *HRAT*, and it is this value of *HRAT* (or ΔT_{min}) that is used in the calculation of the area target (A_{min}) in Equation [8.8]. A conservative assumption is that new heat transfer area will be at least as efficient as the existing area, which means that α is assumed constant. This works well for processes with high α values, such as crude-preheat trains in oil refineries, where values of α typically are around 80%. For many chemical processes with low level of Heat Integration and thus low α values, however, the constant α method is too conservative, which is why an 'incremental α' method was proposed by Tjoe (1986). What is important to realise, whether α is constant or incremental, is that with information about α, one can obtain values for how much additional area is needed for a specified energy saving. This can then be used to calculate the investment cost required to obtain a certain reduction in energy cost.

By calculating corresponding values for investment cost and savings in energy cost for different values of *HRAT*, the energy savings vs investment curve in Fig. 8.7 can be obtained. Similar to the Energy-Target Plot in Fig. 8.6, the savings in energy as a function of investment cost will have kinks and segments with different slopes. This is again due to kinks in the Composite Curves. In addition, Fig. 8.7 indicates the general situation that increasing the scope of retrofit projects means moving towards diminishing return on

© Woodhead Publishing Limited, 2013

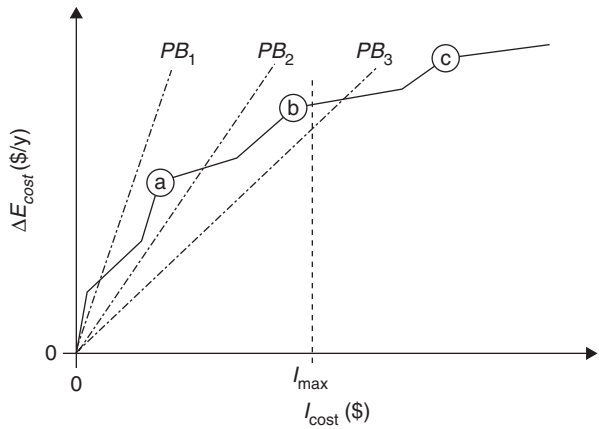

8.7 Energy savings vs investment for the retrofit case.

investment. The origin represents the existing HEN and a level of heat recovery that corresponds to $HRAT_{exist}$. With reduced values of $HRAT$, the retrofit project will move along the curve with increased investment and increased energy savings. Since simple payback time (PB) is defined by Equation [8.9], constant payback will give straight lines in Fig. 8.7. The steeper the gradient of the savings versus investment curve, the shorter the payback time is.

$$\mathrm{PB} = \frac{I_{\mathrm{cost}}}{\Delta E_{\mathrm{cost}}} \qquad [8.9]$$

Retrofit projects will normally be limited by two constraints: available investment capital and upper values for expected payback period. The more advanced retrofit Targeting approach then is to move from the origin along the curve in Fig. 8.7 until either maximum investment or maximum payback is reached, whichever comes first. In Fig. 8.7, three retrofit candidates (a, b and c) are indicated. These are all placed at favourable positions of the curve after regions of considerable savings with moderate investments. The logic is similar to the retrofit candidates indicated in Fig. 8.6; however, with the cost estimations in Fig. 8.7, there is no need to rely on such qualitative considerations. The maximum allowed investment is indicated by the dotted vertical line. The following situations can be anticipated with reference to Fig. 8.7:

- Case 1: $\mathrm{PB} \geq \mathrm{PB}_3$: maximum investment ($I_{\mathrm{max}}$) is limiting.
- Case 2: $\mathrm{PB} \leq \mathrm{PB}_3$: either payback or maximum investment are limiting.
- Case 3: $\mathrm{PB} \leq \mathrm{PB}_2$: payback is limiting.
- Case 4: $\mathrm{PB} \leq \mathrm{PB}_1$: payback is limiting.

© Woodhead Publishing Limited, 2013

Design (c) is not feasible in any of the cases, design (b) is feasible in Case 1 and possibly in Case 2, while design (a) is feasible in Cases 1 and 2, possibly in Case 3, but not in Case 4. The main outcome of this Targeting effort, however, is that the point on the savings versus investment curve that is found by either maximum investment or maximum payback corresponds to a value for HRAT that will be referred to as $HRAT_{new}$ in the remaining of Section 8.4.

8.4.4 Retrofit Design Methodology

Whether a simplified (only energy considerations) or advanced (including investment cost) method is used for retrofit Targeting, the main results are the following:

- A value for HRAT: $HRAT_{new}$
- A potential for energy savings: $\Delta Q_H = \Delta Q_C = Q_{H,exist} - Q_{H,min}(HRAT_{new})$
- Cross-Pinch heat transfer in the existing design: $Q_{XP} = \Delta Q_H = \Delta Q_C$

Heat transfer across the Pinch results in energy penalties in the sense that both external heating and external cooling are increased ('Double Penalty'). The amount of Cross-Pinch heat transfer (also called penalty heat flow, QP) is indicated above, since this is what needs to be reduced or eliminated through the retrofit project in order to reduce energy consumption. Cross-Pinch heat transfer can occur in three different ways in HENs:

- Process-to-process heat transfer across Pinch, QP_P
- Use of external heating below Pinch, QP_H
- Use of external cooling above Pinch, QP_C

The total penalty heat flow can now be calculated by Equation [8.10], which also indicates the obvious advantage of the methodology that double bookkeeping is available. The total sum of cross-Pinch heat transfer in the network must add up to the difference between the current energy consumption and the Minimum Energy Consumption for the identified value of $HRAT_{new}$.

$$QP = QP_P + QP_H + QP_C = Q_{XP} = \Delta Q_H = \Delta Q_C \quad [8.10]$$

The best way to identify cross-Pinch heat transfer in the existing design is to draw the network in a Grid Diagram where the Pinch Point is clearly marked for the established $HRAT_{new}$ from the Targeting stage. Each Heat Exchanger is placed according to the hot and cold inlet and outlet temperatures. Consider the HEN in Fig. 8.8 with corresponding stream data in Table

© Woodhead Publishing Limited, 2013

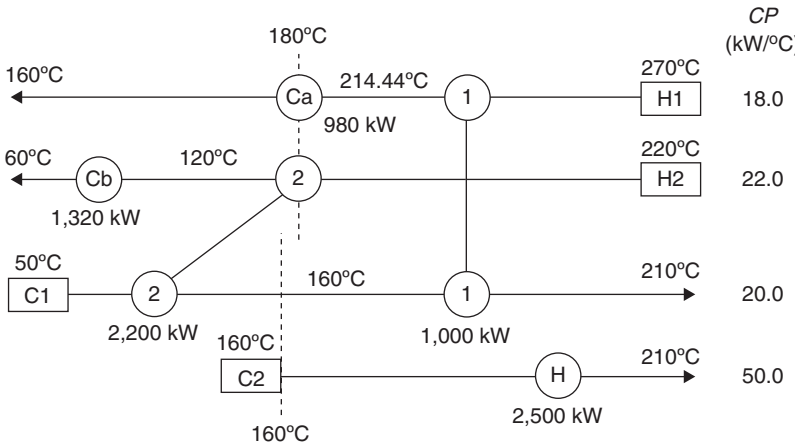

8.8 Existing HEN in a Grid Diagram.

8.1. As indicated in the Grid Diagram, the value of $HRAT_{\text{new}}$ is 20°C, which corresponds to $Q_{H,\min} = 1{,}000$ kW and $Q_{C,\min} = 800$ kW (see Fig. 8.1).

The following information can be established from the network in Fig. 8.8:

- External heating is 2,500 kW while external cooling is 980 + 1,320 = 2,300 kW.
- Excess use of energy in the form of hot and cold utilities is then:

$$\Delta Q_H = 2{,}500 - 1{,}000 = 1{,}500 \text{ kW and } \Delta Q_C = 2{,}300 - 800 = 1{,}500 \text{ kW}$$

- Cross-Pinch heat transfer in the network is located in Exchanger 2 and cooler Ca:

$$QP_P = Q_{XP,2} = 22.0 \cdot (220 - 180) = 880 \text{ kW}$$
$$QP_H = 0 \text{ kW}$$
$$QP_C = Q_{XP,Ca} = 18.0 \cdot (214.44 - 180) = 620 \text{ kW}$$
$$QP = Q_{XP} = 880 + 620 = 1{,}500 \text{ kW}$$

The amount of cross-Pinch heat transfer in the individual heat exchangers (including heaters and coolers) is easily obtained by comparing the amount of heat released from the hot stream above Pinch with the amount of heat received by the cold stream above Pinch. Notice that heat can also be transferred from below to above Pinch; however, this can only happen if ΔT in

© Woodhead Publishing Limited, 2013

one end of the exchanger is less than $HRAT_{new}$. For heaters, cross-Pinch heat transfer is the amount of heating of the cold stream that takes place below the Cold Pinch temperature, while cross-Pinch heat transfer for coolers is the amount of cooling of the hot stream that takes place above the Hot Pinch temperature.

Having established where in the existing network cross-Pinch heat transfer occurs, the next question is how to eliminate or reduce such 'heat leakage' across the Pinch. It is not a good idea to remove heat exchangers with cross-Pinch heat transfer, since this is equipment that is already paid for and installed in the plant. A considerably better approach is to change the operating conditions (temperatures) of the heat exchangers in such a way that cross-Pinch heat transfer is reduced or even eliminated. This method is referred to as 'shifting' and was proposed by Tjoe and Linnhoff (1986). Depending on the situation, this shifting of operating conditions means decreasing temperatures on the hot side or increasing temperatures on the cold side of the exchanger. Figure 8.9 shows how shifting can modify the network in Fig. 8.8. As indicated, the shifting of operating conditions in this case releases heat from hot streams above Pinch (small rectangles) that can be used to reduce hot utility consumption.

In Fig. 8.9, shifting has completely removed cross-Pinch heat transfer in the network and released 620 + 880 = 1,500 kW of heat that can be used to reduce the duty of the heater. The duties of the two coolers have already been reduced. The duty of Exchanger 2 has been kept unchanged after the shifting procedure and, since the temperature driving forces have been considerably reduced (reduced hot stream temperatures), additional heat transfer area will be required for this unit. The two coolers will have excess heat transfer area after the shifting.

In order to complete the retrofit design for the network in Fig. 8.8, which is modified in Fig. 8.9, two new heat exchangers has to be purchased and installed between the two hot streams and cold stream C2. These two new units will be Pinch Exchangers and have to obey the *CP* rules and the topology rules. Since two hot streams need to be cooled to Pinch Temperature, two cold streams (or stream branches) are required. This can be achieved by splitting cold stream C2, which has a *CP* value larger than the sum of the *CP* values of the two hot streams. The split ratio should be optimised, but this is not discussed here.

Figure 8.10 shows the resulting HEN after this retrofit project. Obviously, this is a very expensive solution, since two new heat exchangers are required in addition to additional heat transfer area in Exchanger 2 and investments related to piping and flow control (a valve is needed) for the splitting of stream C2. The savings in hot and cold utility are 1,500 kW, and the resulting energy consumption is equal to the minimum for $HRAT_{new} = 20°C$.

© Woodhead Publishing Limited, 2013

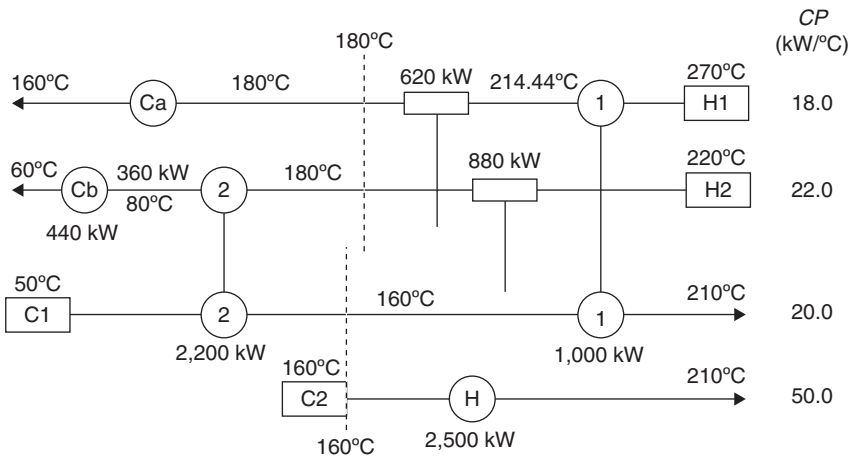

8.9 Shifting of operating conditions.

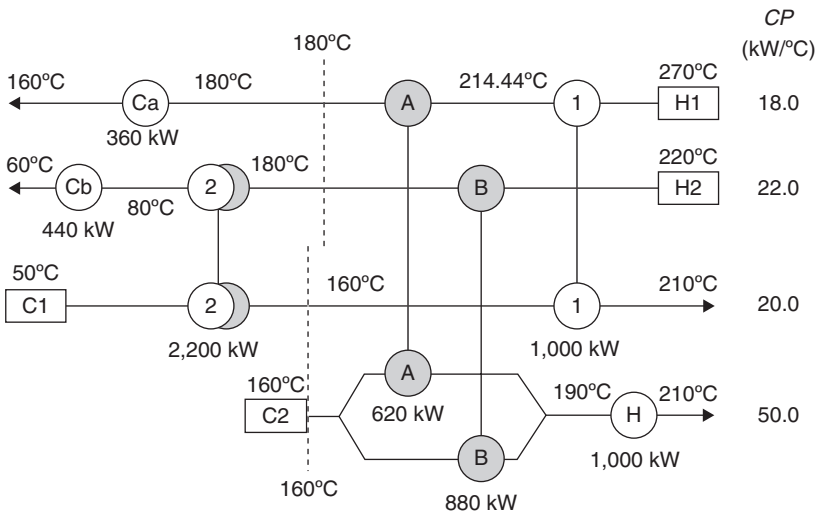

8.10 An expensive retrofit design.

As mentioned in Section 8.4.3, retrofit projects will normally be limited by the available investment capital and an upper limit on payback period. Without actually doing the cost calculations for the retrofit design in Fig. 8.10, one can qualitatively argue that this would be a rather expensive retrofit project and thus not economically feasible. Rather than removing all Cross-Pinch Heat Transfer, one should look for moderate changes in the network that will give significant energy savings. Considering the existing network

© Woodhead Publishing Limited, 2013

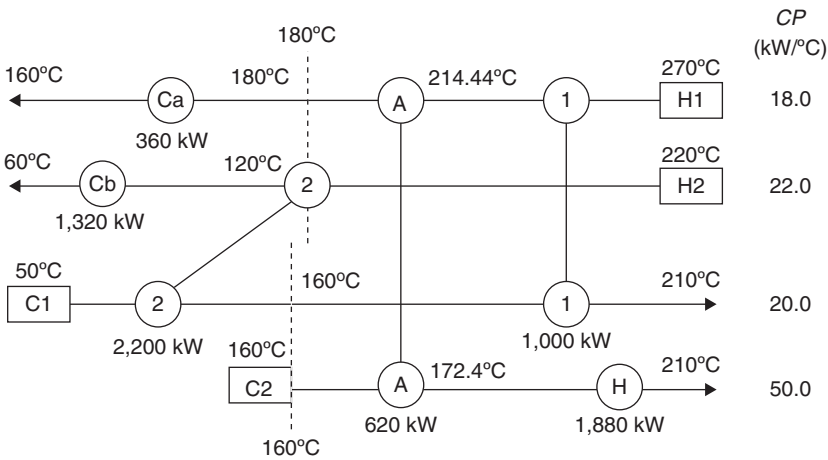

8.11 A cheaper retrofit design.

in Fig. 8.8, a much smaller retrofit project in terms of investment cost is to leave Heat Exchanger 2 as it is and focus only on the Cooler Ca. By shifting the inlet temperature of this cooler to below the hot Pinch temperature, 620 kW of heat from H1 will be released. A new heat exchanger can then be installed between H1 and C2, thus reducing the duty of Heater H. This simpler and much cheaper retrofit network is shown in Fig. 8.11. Notice that by introducing a new unit between H1 and C2, a Heat Load Path is formed from the heater through the new unit to the cooler. Manipulating this path can be regarded as a continuous optimisation problem trading off investment in the new heat exchanger with the resulting savings in hot and cold utilities. One possible solution is the one mentioned above, i.e. to select the shifted duty to be 620 kW, which removes cross-Pinch heat transfer in cooler Ca. However, both smaller and larger shifts in duty along this path can be considered. In the latter case, some heat will be transferred from below to above the Pinch, and ΔT in the cold end of the unit will be less than $HRAT_{\text{new}}$.

The considerably simpler retrofit design solution in Fig. 8.11 saves 620 kW of external heating and cooling, which is 41.3% of the identified potential of 1,500 kW. The only investment is this case is the new Heat Exchanger A between streams H1 and C2, making it a considerably simpler and cheaper retrofit project than the network in Fig. 8.10.

For larger and more complex retrofit situations, the shifting of operating conditions (i.e. duties and temperatures) of selected units will affect many other heat exchangers in the network. In order to analyse whether a heat exchanger will be able to operate in the new situation or if additional Heat

© Woodhead Publishing Limited, 2013

Transfer Area is required, a so-called *UA* analysis is done for the units that experience changes. The term (*UA* analysis) reflects that the heat transfer equation [8.2] can be reformulated as shown in Equation [8.11] when ignoring the correction factor f_T for deviation from pure counter-current heat transfer. The motivation for treating *UA* as a lumped parameter is that it can be measured very accurately for the existing exchanger from the duty and the inlet and outlet temperatures of the hot and cold streams. In the new operating condition, a reasonable assumption is that the Heat Transfer Coefficient *U* remains unchanged, thus a change in *UA* reflects a change in area *A*. *UA* analysis is then simply to calculate *UA* for all relevant exchangers in the existing design and for the new situation in the retrofitted network.

$$UA = \frac{Q}{\Delta T_{LM}} \qquad [8.11]$$

The assumption of constant *U* is reasonable when changing operating temperatures for a heat exchanger, but far more questionable when flowrates are modified (in the case of stream splitting) or when the heat exchanger is subject to re-piping (changing fluid on the hot and/or cold side of the exchanger). In such cases, the *UA* analysis has limited value and more sophisticated methods must be employed in order to estimate new values for *U*.

When comparing *UA* for the existing network with *UA* values for the retrofit design, three distinctively different situations can occur for each of the existing heat exchangers:

- $UA_{new} > UA_{exist}$: additional heat transfer area is required
- $UA_{new} \cong UA_{exist}$: the existing exchanger is fully utilised, and no additional area needed
- $UA_{new} < UA_{exist}$: the existing heat exchanger is not fully utilised in the retrofit design

Of course, the difference between the UA values for the existing and the new design must be significant (say more than 5–10%) before additional area is purchased or actions are taken to improve the utilisation of the existing heat exchanger in the retrofitted network.

Similar to grassroots design, Heat Load Loops and Paths can be used to evolve the network. While the objective in grassroots design is to remove small units, simplify the network and fine-tune the economic trade-offs involved, the objective in retrofit design is to maximise the use of existing heat exchangers, to minimise additional equipment or heat transfer area, and to fine-tune the trade-offs between investments in new equipment and savings in energy usage.

© Woodhead Publishing Limited, 2013

Combining cross-Pinch Analysis, shifting of operating conditions and *UA* analysis certainly provides a retrofit methodology that will identify energy saving projects in HENs. One of the drawbacks (Smith, 2000) is that the Process Pinch (which is only a characteristic of the stream data) relates to an ideal new design and not to the existing HEN. One of the possible methods to overcome this apparent drawback is the so-called ***Network Pinch*** proposed by Asante and Zhu (1996). Contrary to the Process Pinch, the Network Pinch is a characteristic of the existing HEN topology.

The concept of Network Pinch can be explained by considering the situation where Heat Load Paths in the design are utilised to reduce hot and cold utilities without considering heat transfer area. This shifting of duty will be limited by the situation when one of the units in the path reaches $\Delta T = 0°C$. This unit is then referred to as a pinching exchanger. Asante and Zhu (1996) discussed retrofit trajectories in the Area-Energy Diagram for 0, 1, 2, etc. modifications of the network topology. The advantage of few topology changes is low network complexity and few new units, while the disadvantage is that additional heat transfer area tends to increase rapidly. When a Network Pinch is removed by a topology change, the next Network Pinch can be identified, and the procedure continues as long as the project economy allows.

The disadvantage of this methodology is that quite a few existing HENs do not have a Network Pinch. Considering the existing design in Fig. 8.8, there is no Heat Load Path from the heater to any of the coolers, since the heater is the only unit on stream C2. In Fig. 8.11, however, a new unit has been placed between H1 and C2 as a cheap retrofit project. The duty of the new unit was set to 620 kW in order to remove all cross-Pinch heat transfer in the cooler Ca. When shifting more duty through this loop, the heater can be reduced further from 1,880 to 1,520 kW. Cooler Ca then is removed from the network, and the new Heat Exchanger A has a duty of 980 kW, however, $\Delta T = 0°C$ in the cold end of the unit. This is then the Pinching Exchanger, and additional topology changes are required in order to reduce energy consumption even further. One should notice that the minimum hot and cold utility targets for $HRAT = 0°C$ are 200 and 0 kW. This clearly illustrates the difference between the Process Pinch (only based on stream data) and the Network Pinch (a characteristic of the existing design topology). This also shows that there are inherent deficiencies in the existing design that will be extremely expensive to overcome.

8.4.5 A Brief Summary of the Retrofit Case

It should be obvious from what has been presented in Section 8.4, that the retrofit design case is vastly different from the grassroots case. Data Extraction

© Woodhead Publishing Limited, 2013

is quite different, and the stages of Targeting, Design and Optimisation (or design evolution) are very different. The main elements of a retrofit design methodology also indicating differences from grassroots design are:

- Much more detailed modelling (rating) is required.
- Retrofit projects are limited by investment capital and short payback times, thus a 'greedy' approach is used, looking for small projects with significant savings.
- Retrofit Targeting means to identify an optimal level of heat recovery.
- Assumptions has to be made during Targeting regarding the Area Efficiency for new heat exchangers or additional heat transfer area for existing units.
- Cross-Pinch Analysis is used to identify where in the network changes has to be done to reduce hot and cold utility consumption.
- Cross-Pinch heat transfer has three components: process-to-process heat transfer across Pinch, external heating below Pinch and external cooling above Pinch.
- An MER design is not a good initial network candidate for retrofit.
- Shifting of heat exchanger temperatures is used to reduce cross-Pinch heat transfer and to release heating resources above Pinch or cooling resources below Pinch.
- *UA* analysis is used to evaluate the implications of new investments and the utilisation of existing heat exchangers.
- Heat Load Loops and Paths are used to evolve and fine-tune the retrofit design with focus on minimum new investments and maximum reuse of existing equipment.
- The Network Pinch represents a different approach to retrofit design with its advantages and disadvantages. It certainly is a more complicated methodology than the simple procedures described here, and software and optimisation tools may be required. As shown, some existing designs do not have a Network Pinch.

8.5 Use of Optimisation for Heat Exchanger Network Synthesis

Methodologies for grassroots and retrofit design of HENs based on Pinch Analysis and the PDM have obvious limitations as mentioned in Section 8.3.4. These limitations relate to all three stages of Targeting, Design and Optimisation (or evolution). This section will briefly describe alternative approaches using numerical optimisation, more precisely Mathematical Programming, to address some of the challenges in analysis, design and optimisation of HENs.

© Woodhead Publishing Limited, 2013

8.5.1 Rigorous Targeting Methods

Despite the fact that Pinch Analysis and the PDM are firmly based on thermodynamics, there is also considerable use of heuristics or rules of thumb. The concept of Composite Curves, and the way it is used to identify the Process Pinch as well as minimum hot and cold utility requirements, is based on the principle that all hot and cold streams are heating and cooling resources at certain temperatures that can be used freely for Heat Integration purposes. As soon as restrictions such as forbidden, required or restricted matches are introduced, the concept of Composite Curves breaks down, and other methods are required for energy targeting. For the minimum number of units, it was clearly stated in Chapter 4 that the $(N-1)$ rule is a simplification of Euler's Rule from Graph Theory. Since the targets are required ahead of design, assumptions have to be made regarding loops and sub-graphs. Finally, and as discussed in Sections 8.2.3 and 8.2.4, the Bath Formula (Equation [8.1]) for Targeting total heat transfer area does not provide the true minimum, since it is based on vertical heat transfer and optimal distribution of driving forces, when it should have been based on optimal distribution of the product $(U \cdot \Delta T)$. The following paragraphs will show how Mathematical Programming can be used to obtain rigorous targets for energy, units and area. It should be emphasised, however, that these models use insight from Pinch Analysis extensively.

Rigorous Energy Targeting

Methods were developed in the early 1980s for calculating minimum hot and cold utility requirements using linear programming (LP) based on both transshipment (Papoulias and Grossmann, 1983) and transportation models (Cerda and Westerberg, 1983). Since the Heat Cascade used in Chapter 4 is a special case of a transshipment model from Operations Research, the approach by Papoulias and Grossmann (1983) is described here. It also provides a more compact formulation of the minimum utility problem. Consider Fig. 8.12 that shows one of the temperature intervals in a Heat Cascade (or transshipment model).

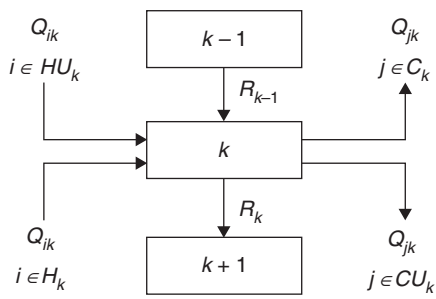

8.12 Temperature intervals in a Heat Cascade.

© Woodhead Publishing Limited, 2013

An LP formulation for minimum utility cost in the case of multiple utilities can now be formulated as shown in model [8.12], where the objective function minimises total utility cost and the equality constraints are the heat balances for each temperature interval k. The residuals (R_k) must be non-negative as a result of simple thermodynamics.

$$\min\left[\sum_{k\in TI}\left(\sum_{i\in HU_k} c_i\cdot Q_{ik}+\sum_{j\in CU_k} c_i\cdot Q_{jk}\right)\right]$$
$$\text{subject to :} \qquad [8.12]$$
$$R_k - R_{k-1} + \sum_{j\in CU_k} Q_{jk} - \sum_{i\in HU_k} Q_{ik} = \sum_{i\in H_k} Q_{ik} - \sum_{j\in C_k} Q_{ik} \quad \text{for} \quad k = 1,2,\ldots,K$$
$$R_k \geq 0 \quad \text{for} \quad k = 1,2,\ldots,K-1, R_0 = R_K = 0$$

In model [8.12] and in Fig. 8.12, the following sets and variables are defined:

- Set of temperature intervals: TI where $\dim(TI) = K$
- Set of hot and cold utilities in interval k: HU_k and CU_k
- Set of hot and cold process streams in interval k: H_k and C_k
- Heat supplied from hot process stream or utility i to interval k: Q_{ik}
- Heat supplied to cold process stream or utility j from interval k: Q_{jk}
- Residual heat flow leaving interval k: R_k
- Prices for hot and cold utilities: c_i and c_j

Heat flows from hot process streams to the cascade and from the cascade to the cold streams are available from stream data and the interval temperatures, and therefore enters model [8.12] as known or fixed variables. By convention, these are put on the right-hand side of the equations (equalities). Model [8.12] only contains linear relationships, and the corresponding optimisation model is therefore an LP model that can be easily solved.

Model [8.12] does not contain anything new compared with the Heat Cascade based Targeting methods described in Chapter 4. However, model [8.12] can be easily extended to handle situations where heat exchange is restricted, such as the case of forbidden matches. If a stream is not allowed to exchange heat with any other streams, then that stream can simply be removed from the stream data and Composite Curves can be developed for the remaining streams. A considerably more challenging problem is when pairing specific forbidden matches exist. These can be due to safety, integrity, operability, distance, product contamination, etc. In this case, the concept of Composite Curves breaks down, since hot and cold streams are no longer resources that can be used with no limit for heat recovery purposes. It turns

© Woodhead Publishing Limited, 2013

out that this is a very trivial problem to handle when using Mathematical Programming and extending Equation [8.12].

With forbidden matches, there is a need to keep track of where heat from certain hot streams is flowing, in order to prevent this heat from entering into a forbidden match. In Equation [8.12], all residual heat is lumped into one variable (R_k), and thus the identity of the heat is lost. An extended model can be developed based on Fig. 8.13, where residual heat flows are assigned for each hot process stream and utility. Such individual residuals are introduced at the first (counting from the top) interval where the process stream or utility is adding heat. From this point on, and to the end of the cascade, individual residuals must be included since there is a possibility that this heat will reach even the last interval. New sets have to be defined for hot process streams and utilities, H_k' and HU_k' which refer to hot streams and utilities that are present (delivers heat) in interval k or have delivered heat in any of the earlier intervals (higher temperatures). Since heat exchange between the hot and cold streams has to be 'monitored' to avoid heat exchange between streams in forbidden matches, new variables Q_{ijk} has to be introduced for heat exchange between hot stream or utility i and cold stream or utility j in temperature interval k. The heat balances for the intervals must be expanded into heat balances for the individual process streams and utilities, which means the model will increase considerably in size. This is, however, not a problem, since very large LP problems can be solved efficiently.

$$
\begin{gathered}
\min\left[\sum_{k\in TI}\left(\sum_{i\in HU_k} c_i\cdot Q_{ik}+\sum_{j\in CU_k} c_j\cdot Q_{jk}\right)\right] \\
\text{subject to for all } k\in TI: \\
R_{i,k}-R_{i,k-1}+\sum_{j\in C_k,CU_k} Q_{ijk}=Q_{ik} \quad \text{for } i\in H_k' \\
R_{i,k}-R_{i,k-1}+\sum_{j\in C_k} Q_{ijk}-Q_{ik}=0 \quad \text{for } i\in HU_k' \\
\sum_{i\in H_k',HU_k'} Q_{ijk}=Q_{jk} \quad \text{for } j\in C_k \\
\sum_{i\in H_k'} Q_{ijk}-Q_{jk}=0 \quad \text{for } j\in CU_k \\
R_{i,k}\geq 0 \quad \text{for} \quad k=1,2,\ldots,K-1, \quad R_{i,0}=R_{i,K}=0 \quad \text{for } i\in H,HU \\
Q_{ijk}\geq 0 \quad \text{for} \quad i\in H,HU, \quad j\in C,CU \quad \text{and} \quad k\in TI \\
Q_{ijk}=0 \quad \text{for} \quad (i,j)\in P
\end{gathered}
\qquad [8.13]
$$

The extended model that handles forbidden matches is shown in model [8.13], where set P contains the pairs of hot and cold streams that are not allowed to exchange heat. Thus, forbidden matches are modelled simply by forcing the corresponding variable Q_{ijk} to zero. In model [8.13], total sets for process streams and utilities (H, HU, C, CU) are introduced for simplicity.

© Woodhead Publishing Limited, 2013

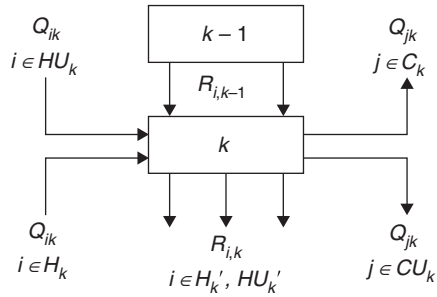

8.13 Temperature intervals in an extended Heat Cascade.

Rigorous Units Targeting

Since a unit is required whenever heat is transferred from a hot stream to a cold stream, model [8.13] with its variables Q_{ijk} can actually also be used to address the minimum number of units problem in a rigorous way. The major limitation with the $(N - 1)$ rule, beyond the assumptions about loops and sub-graphs mentioned in Chapter 4, is the fact that neither heat (duty) nor temperature is accounted for. Since model [8.13] is based on the Heat Cascade, the load and level of heat is fully accounted for, which is why the model can be used for rigorous Targeting of the minimum number of units. In fact, only two modifications are required. It should also be mentioned that Units Targeting is done after energy targeting, thus heat duties for hot and cold utilities are known, and these duties are moved to the right-hand side of the equalities.

The two modifications needed to convert model [8.13] into a units targeting model are:

1. The objective function has to be changed from focus on energy to focus on units.
2. A link has to be created between the variables Q_{ijk} and required heat exchangers.

In both cases, there is a need for new binary variables defining the existence or not of a heat exchanger between pairs of hot and cold process streams and utilities as shown in Equation [8.14].

$$y_{ij} = \begin{cases} 1 \text{ if there is a match between hot stream/utility } i \text{ and cold stream/utility } j \\ 0 \text{ otherwise} \end{cases} \quad [8.14]$$

The objective function is obviously to minimise the number of units, which is equivalent to minimising the number of binary variables that have the

© Woodhead Publishing Limited, 2013

value 1. The link between a non-negative Q_{ijk} and the existence of a heat exchanger can now be made through the binary variable y_{ij}. This can be done through a logical constraint, as shown in model [8.15]. The logical constraint contains an upper limit U_{ij} which is the largest duty that can be exchanged between hot stream/utility i and cold stream/utility j. The value of U_{ij} can be calculated ahead of running the optimisation Model [8.15], only based on stream and utility data. If the variable Q_{ijk} is zero for all temperature intervals k then the binary variable y_{ij} is free to take any value (0 or 1); however, the objective function will then force this variable to 0 during optimisation. If at least one of the Q_{ijk} for the pair (i, j) is positive, then the logical constraint will force the binary variable y_{ij} to 1 (a heat exchanger exists). The rest of model [8.15] is a copy of model [8.13].

$$
\begin{gathered}
\min \sum_{i\in H,HU} \sum_{j\in C,CU} y_{ij} \\
\text{subject to all } k \in TI: \\
R_{i,k} - R_{i,k-1} + \sum_{j\in C_k,CU_k} Q_{ijk} = Q_{ik} \quad \text{for } i \in H_k{}' \\
R_{i,k} - R_{i,k-1} + \sum_{j\in C_k} Q_{ijk} = Q_{ik} \quad \text{for } i \in HU_k{}' \\
\sum_{i\in H_k{}',HU_k{}'} Q_{ijk} = Q_{jk} \quad \text{for } j \in C_k \\
\sum_{i\in H_k{}'} Q_{ijk} = Q_{jk} \quad \text{for } j \in CU_k \\
\sum_{k\in TI} Q_{ijk} - U_{ij} \cdot y_{ij} \le 0 \\
R_{i,k} \ge 0 \quad \text{for} \quad k = 1,2,\ldots,K-1, \quad R_{i,0} = R_{i,K} = 0 \quad \text{for } i \in H,HU \\
Q_{ijk} \ge 0 \quad \text{for} \quad i \in H,HU, \quad j \in C,CU \quad \text{and} \quad k \in TI \\
Q_{ijk} = 0 \quad \text{for} \quad (i,j) \in P
\end{gathered}
\qquad [8.15]
$$

The introduction of binary variables y_{ij} converts the LP model [8.13] into a Mixed Integer Linear Programming (MILP) model [8.15], which significantly increases the computational complexity of the problem. Optimisation problems with binary (or integer) variables are solved as a sequence of LP problems using a Branch and Bound type algorithm in a search tree that grows exponentially with the number of binary variables. According to Anantharaman *et al.* (2010), optimised versions of model [8.15] can typically be solved in less than 50 s when the number of binary variables is less than 150. When the number of binary variables is more than 5,000, however, the model does not solve in 12 h. The number of binary variables is the product of the number of hot streams/utilities and the number of cold streams/utilities. The combinatorial complexity depends on the actual stream data; however, experience shows that problems with more than 30 streams are hard to solve.

© Woodhead Publishing Limited, 2013

Rigorous Heat Transfer Area Targeting

As explained several times already (Sections 8.2.3 and 8.2.4 and the beginning of this section), the Bath Formula for Minimum Area [8.1] does not provide the true minimum, since it is based on vertical heat transfer without any consideration of differences in heat transfer coefficients. Saboo *et al*. (1986) formulated the Minimum Area Targeting problem using an LP model, where the size of temperature intervals is gradually decreased until the calculated Area Target converges. This 'brute force' method was later improved by Colberg and Morari (1990) who used non-linear programming (NLP). Yee *et al*. (1990) also used an NLP model to establish Minimum Heat Transfer area Targets. However, as indicated in Section 8.2.4, the main use of an Area Target is to estimate TAC in order to pre-optimise the value for ΔT_{min}. This is why even a reasonable Area Target is good enough, and details of various other methods, such as those using Mathematical Programming as mentioned above, are omitted here.

8.5.2 Automated Network Design and Optimisation

Of course, rigorous targets for energy, total area and number of units are convenient to have been available; however, the real issue in Heat Exchanger Network Synthesis (HENS) is network design. In addition to being able to rigorously address the different trade-offs in HEN, Mathematical Programming also offers a potential framework for automated network design. The models used in Mathematical Programming approaches to process synthesis and integration are typically based on some kind of Superstructure, which is a representation where multiple flowsheets are drawn together, and where binary variables make the selection of one specific flowsheet topology. In the area of HENs, a considerable number of such superstructures have been proposed.

The first really successful superstructure used for network generation and optimisation is the clever stream superstructure of Floudas *et al*. (1986). The HENs problem was solved in three consecutive stages:

1. Minimum utility requirements as an LP problem using the transshipment model.
2. Minimum number of units as an MILP problem, also using the transshipment model.
3. Network generation and optimisation as an NLP problem minimising total cost.

As pointed out by Gundersen and Grossmann (1990), the second stage has multiple solutions, where each solution is referred to as a heat load

© Woodhead Publishing Limited, 2013

distribution (HLD) with information on the pairs of streams (i, j) that are matched and the corresponding heat duty Q_{ij}. These HLDs tend to have very different properties when it comes to total area and cost of the networks that can be developed. Gundersen and Grossmann (1990) used insights from Pinch Analysis, i.e. vertical heat transfer reduces total area, to improve the selection of HLDs in the MILP stage. Since strict vertical heat transfer does not guarantee minimum area, the MILP model was further developed in order to account for differences in film heat transfer coefficients.

At the same time, completely simultaneous optimisation models were formulated to overcome the limitations of the sequential approach. These Mixed Integer Non-Linear Programming (MINLP) models that were proposed by Yee and Grossmann (1990) and Ciric and Floudas (1991) are extremely hard to solve for two reasons:

1. The binary variables cause a combinatorial explosion and prohibitive computer times for large industrial problems.
2. The non-linear relations in the model (both physical and economical) are non-convex, which means there is a tendency to end up in local rather than global optima.

Efforts have been made to overcome these problems, in particular the non-convexity issue. The problem can be reformulated using so-called convex estimators; unfortunately, the experience seems to be that the size of the model grows in a way that industrial size problems cannot be solved. This is one reason why there has been an increasing interest in using stochastic search algorithms that avoid gradient information and recover from local optima.

An alternative approach is to break down the MINLP problem and solve the HENs problem using a ***Sequential Framework*** (Anantharaman and Gundersen, 2007), where the three-way trade-off between energy, units and heat transfer area, is addressed by adjusting key decision variables in a system of nested loops, as shown in Fig. 8.14. The framework is based on ideas of a decomposed approach to HENS as suggested by Floudas *et al*. (1986) and modified vertical matching between the Composite Curves to minimise heat transfer area, where differences in film heat transfer coefficients are fully accounted for.

Contrary to what would be expected with four nested loops, the framework identifies optimal solutions within 3–7 inner loop iterations for each value of HRAT. Pre-optimisation (or supertargeting), as described in Section 8.2.4, is used to find a near-optimal starting value for $\Delta T_{\min}$ (or *HRAT*) by combining targets for Energy, Area and Units into an estimate for TAC for various values of HRAT. The core engines of the sequential framework are the vertical MILP model for matching streams and providing heat load

© Woodhead Publishing Limited, 2013

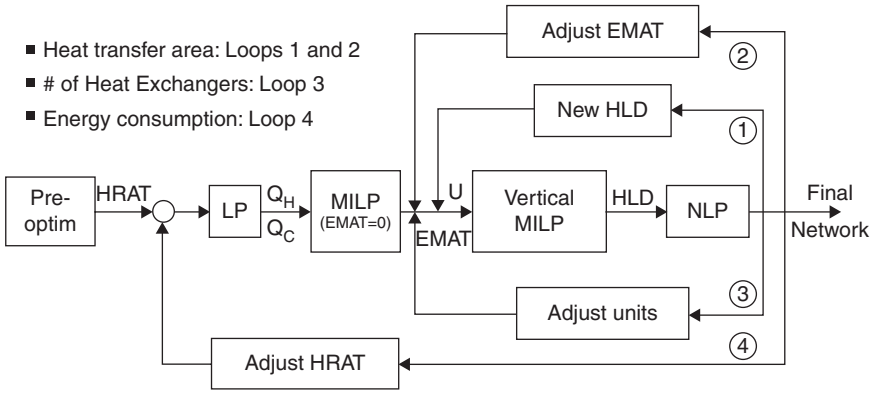

8.14 Sequential framework for HEN Synthesis.

distributions (HLD), and the NLP model for generating and optimising the network. The framework allows considerable user interaction, and practical aspects such as complexity and operability can be addressed together with TAC to select the best HEN.

While this brief presentation on the use of optimisation methods in Heat Integration has focused entirely on the grassroots case, it should be emphasised that similar methods have been developed and used also for the retrofit of existing HENs. Since there are more constraints in retrofit than the grassroots case, the advantages of using Mathematical Programming are even larger for retrofit design.

8.6 Conclusion

In this chapter, the main concepts, representations and graphical diagrams of retrofit HEN analysis and design have been presented and used for illustrative purposes in small and simple examples. The grassroots case has been significantly expanded from the rather basic description in Chapter 4 with new features related to both Targeting and design. Reflecting a strong trend today, the chapter also has a brief introduction to the use of optimisation methods such as Mathematical Programming in analysis and design of HENS. The most important topics covered in this chapter are:

- Multiple utilities, utility placement and Utility Pinches
- Balanced Composite Curves with utilities included
- Target for minimum heat transfer area
- Pre-optimisation of ΔT_{min} using TAC estimates
- Driving Force Plot for area
- Remaining Problem Analysis for energy, units and area

© Woodhead Publishing Limited, 2013

- Area–Energy Diagram
- Retrofit Targeting for level of heat recovery
- Cross-Pinch Analysis
- Heat exchanger 'shifting' of operating conditions
- '*UA* analysis'
- Network Pinch
- Rigorous Targeting for Energy, Units and Area using optimisation
- Automated network design using Mathematical Programming

8.7 Sources of Further Information

The majority of the methods described in this chapter were developed in the 1980s and early 1990s. Of course, there have been numerous publications on HENS both for grassroots and retrofit design during the last 20 plus years. It would be beyond the scope even of this handbook to go into all these details. In addition, it is probably fair to say that no major breakthroughs have been made when it comes to solving the classical heat recovery problem. Rather, there have been some developments adding industrial realism to the problem definition, and there is a lot of literature available combining the design of heat recovery systems with other sections of processing plants.

The various chapters of this handbook provide insight into other application areas of Process Integration. A critical review with an annotated bibliography for the literature on HENS up to year 2000 was published by Furman and Sahinidis (2002), while Anantharaman (2011) presented a HENS bibliography for the following period up to year 2010.

More realistic ***problem definitions*** for HENs, in particular for approaches using optimisation, have been published in areas such as non-constant *CP* values, including phase changes (Ponce-Ortega *et al*., 2008, and later Hasan *et al*., 2010). Within Pinch Analysis, the issue of Pressure Drop in heat exchange equipment introduces an interesting trade-off between mechanical and thermal energy, since increased heat transfer coefficients are related to additional Pressure Drop. In addition, Pressure Drop considerations in heat recovery systems (Polley *et al*., 1990) are important in cases where feed pumps become the bottlenecking elements of process plants, which is a typical situation in crude-preheat trains. A later work on Pressure Drop was presented by Nie and Zhu (1999), who also discussed heat exchange enhancements.

In fact, the use of heat exchanger enhancements provides a cost-effective alternative to the purchase of new heat exchangers and/or investment in piping in ***retrofit design*** of heat recovery systems, as discussed by Wang *et al*. (2012). Key elements are low investment cost and avoiding fundamental

© Woodhead Publishing Limited, 2013

structural modifications to the network. Bulatov (2005) has presented a retrofit optimisation framework for compact heat exchangers. Varbanov and Klemeš (2000) used the concept of Heat Load Paths for the debottlenecking of HENs. A review of the recent developments in retrofit methodologies for HENs is provided by Smith *et al*. (2010).

New ***graphical diagrams*** referred to as advanced Composite Curves have been developed at Chalmers University of Technology with special applications to retrofit design of HENS including the use of heat pumps – firstly introduced by Wallin (1996) and later by Nordman and Berntsson (2001). The most recent work is by Nordman and Berntsson (2009). The main objectives addressed by the use of these alternative temperature–enthalpy diagrams are (1) to identify heat recovery projects that reduce the problem size and are economically feasible, and (2) to identify temperature levels where usable excess heat can be extracted and used by other processes.

In optimisation-based approaches to HENs, the main emphasis has been on developing new and better ***superstructures*** and improved solution algorithms that are able to deal with the non-convexities and local optima issues inherent in these types of design problems. The most commonly used of these superstructures is the stage-wise model proposed by Yee and Grossmann (1990). The main limitations of this superstructure are:

(i) The isothermal mixing assumption whenever there are stream splits, and
(ii) The fact that only one heat exchanger can be placed on each stream branch.

The first assumption makes the model linear except for the objective function. The second assumption is related to the layout of the superstructure and the use of binary variables representing heat exchangers. Bjørk and Westerlund (2002) removed the isothermal mixing assumption and were still able to develop global optimisation models.

New superstructures are also needed for the design of ***sub-ambient*** HENs. In such processes, standard two-stream heat exchangers are replaced by multi-stream exchangers, and the close relation between the HEN and the refrigeration systems makes it necessary to include unit operations for compression and expansion in the superstructure. Such an extended superstructure was developed by Wechsung *et al*. (2011), and an MINLP model based on this superstructure was used to design an offshore LNG process using liquid CO_2 and liquid nitrogen as refrigerants. Often in sub-ambient design, process streams are compressed and/or expanded in order to temporarily act as part of the utility (refrigeration) system.

With the inherent numerical challenges in the use of Mathematical Programming to design and optimise HENS (combinatorial explosion caused

© Woodhead Publishing Limited, 2013

by the binary variables in the models and non-convexities caused by the non-linearities in the models), a considerable amount of research has been addressing the use of gradient-free ***stochastic search algorithms*** for optimisation. A large number of such algorithms have been applied to HENs, including Simulated Annealing – see e.g. Dolan *et al*. (1990) and Athier *et al*. (1997), and Genetic Algorithms – see e.g. Ravagnani *et al*. (2005) and Dipama *et al*. (2008). Other stochastic (also referred to as meta-heuristic) approaches include tabu search, ant colony and harmony search. It is again beyond the scope of this chapter to provide references to all these methods.

One topic that has not been discussed at all in this chapter is ***operability*** of HENs. Here, operability includes flexibility, controllability, start-up and shutdown. There is considerable prejudice against Heat Integration, since such efficiency measures in processing plants often comes at the expense of reduced operability. While the arrogant answer to these concerns is that most plants in the process industries are heavily integrated, and that the real issue is correct rather than maximum level of Heat Integration, it should be mentioned that several researchers have tried to tackle operability in a systematic manner. An introduction to this field is given by Floudas and Grossmann (1987) and later by Mathisen *et al*. (1992) and by Papalexandri and Pistikopoulos (1994).

Finally, it should be mentioned that HEN Synthesis is quite often combined with other engineering design issues such as water networks, separation systems, etc. Again, it is beyond the scope of this chapter to dive deeply into these subjects.

8.8 References

Ahmad, S. (1985). Heat exchanger networks: cost trade-offs in energy and capital. PhD thesis, UMIST, Manchester, UK.

Ahmad, S., Linnhoff, B., Smith, R. (1990). Cost optimum heat exchanger networks – 2. Targets and design for detailed capital cost models. *Computers & Chemical Engineering*, **14**, 751–767.

Anantharaman, R. (2011). Energy efficiency in process plants with emphasis on heat exchanger networks – optimization, thermodynamics and insight. PhD thesis, Norwegian University of Science and Technology, Trondheim, Norway.

Anantharaman, R., Gundersen, T. (2007). The sequential framework for heat exchanger network synthesis – network generation and optimization. *Chemical Engineering Transactions*, **12**, 19–24.

Anantharaman, R., Nastad, I., Nygreen, B., Gundersen, T. (2010). The sequential framework for heat exchanger network synthesis – the minimum number of units sub-problem. *Computers & Chemical Engineering*, **34**, 1822–1830.

Asante, N. D. K., Zhu, X. X. (1996). An automated approach for heat exchanger network retrofit featuring minimal topology modifications. *Computers & Chemical Engineering*, **20**, s7–s12.

© Woodhead Publishing Limited, 2013

Athier, G., Floquet, P., Piboleau, L., Domenech, S. (1997). Synthesis of heat exchanger networks by simulated annealing and NLP procedures. *AIChE Journal*, **43**, 3007–3020.

Bjцrk, K.-M., Westerlund, T. (2002). Global optimization of heat exchanger network synthesis problems with and without the isothermal mixing assumption. *Computers & Chemical Engineering*, **26**, 1581–1593.

Bulatov, I. (2005). Retrofit optimization framework for compact heat exchangers. *Heat Transfer Engineering*, **26**, 4–14.

Cerda, J., Westerberg, A. W. (1983). Synthesizing heat exchanger networks having restricted stream/stream match using transportation problem formulations. *Chemical Engineering Science*, **38**, 1723–1740.

Challand, T. B., Colbert, R. W., Venkatesh, C. K. (1981). Computerized heat exchanger networks. *Chemical Engineering Progress*, **77**, 65–71.

Ciric, A. R., Floudas, C. A. (1991). Heat exchanger networks synthesis without decomposition. *Computers & Chemical Engineering*, **15**, 385–396.

Colberg, R. D., Morari, M. (1990). Area and capital cost targets for heat exchanger network synthesis with constrained matches and unequal heat transfer coefficients. *Computers & Chemical Engineering*, **14**, 1–22.

Dipama, J., Teyssedou, A., Sorin, M. (2008). Synthesis of heat exchanger networks using genetic algorithms. *Applied Thermal Engineering*, **28**, 1763–1773.

Dolan, W. B., Cummings, P. T., Le Van, M. D. (1990). Algorithmic efficiency of simulated annealing for heat exchanger network design. *Computers & Chemical Engineering*, **14**, 1039–1050.

Floudas, C. A., Ciric, A. R., Grossmann, I. E. (1986). Automatic synthesis of optimum heat exchanger network configurations. *AIChE Journal*, **32**, 276–290.

Floudas, C. A., Grossmann, I. E. (1987). Synthesis of flexible heat exchanger networks with uncertain flowrates and temperatures. *Computers & Chemical Engineering*, **11**, 319–336.

Furman, K. C., Sahinidis, N. V. (2002). A critical review and annotated bibliography for heat exchanger network synthesis in the 20th century. *Industrial & Engineering Chemistry Research*, **41**, 2335–2370.

Gundersen, T., Grossmann, I. E. (1990). Improved optimization strategies for automated heat exchanger network synthesis through physical insights. *Computers & Chemical Engineering*, **14**, 925–944.

Hall, S. G., Ahmad, S., Smith, R. (1990). Capital cost targets for heat exchanger networks comprising mixed materials of construction, pressure ratings and exchanger types. *Computers & Chemical Engineering*, **14**, 319–335.

Hasan, M. M. F., Jayaraman, G., Karimi, I. A., Alfadala, H. E. (2010). Synthesis of heat exchanger networks with non-isothermal phase changes. *AIChE Journal*, **56**, 930–945.

Linnhoff, B., Vredeveld, D. R. (1984). Pinch technology has come of age. *Chemical Engineering Progress*, **80**, 33–40.

Mathisen, K. W., Skogestad, S., Wolff, E. A. (1992). Bypass selection for control of heat exchanger networks. *Computers & Chemical Engineering*, **16**, 263–272.

Nie, X. R., Zhu, X. X. (1999). Heat exchanger network retrofit considering pressure drop and heat transfer enhancement. *AIChE Journal*, **45**, 1239–1254.

Nishimura, H. (1980). A theory for the optimal synthesis of heat exchanger systems. *Journal of Optimization Theory and Applications*, **30**, 323–450.

© Woodhead Publishing Limited, 2013

Nordman, R., Berntsson, T. (2001). New pinch technology based HEN analysis methodologies for cost-efficient retrofitting. *Canadian Journal of Chemical Engineering*, **79**, 655–662.

Nordman, R., Berntsson, T. (2009). Use of advanced composite curves for assessing cost-effective HEN retrofit – I. Theory and concepts. *Applied Thermal Engineering*, **29**, 275–281.

Papalexandri, K. P., Pistikopoulos, E. N. (1994). Synthesis and retrofit design of operable heat exchanger networks – 1. Flexibility and structural controllability aspects. *Industrial & Engineering Chemistry Research*, **33**, 1718–1737.

Papoulias, S. A., Grossmann, I. E. (1983). A structural optimization approach in process synthesis – II. Heat recovery networks. *Computers & Chemical Engineering*, **7**, 707–721.

Polley, G. T., Panjeh Shahi, M. H., Jegede, F. O. (1990). Pressure drop considerations in the retrofit of heat exchanger networks. *Chemical Engineering Research and Design*, **68**, 211–220.

Ponce-Ortega, J. M., Jimйnez-Gutiйrrez, A., Grossmann, I. E. (2008). Optimal synthesis of heat exchanger networks involving isothermal process streams. *Computers & Chemical Engineering*, **22**, 1918–1942.

Ravagnani, M. A. S. S., Silva, A. P., Arroyo, P. A., Constantino, A. A. (2005). Heat exchanger network synthesis and optimization using genetic algorithm. *Applied Thermal Engineering*, **25**, 1003–1017.

Saboo, A. K., Morari, M., Colberg, R. D. (1986) Reshex: an interactive software package for the synthesis and analysis of resilient heat exchanger networks – II. Discussion of area targeting and networks synthesis algorithms. *Computers & Chemical Engineering*, **10**, 591–599.

Smith, R. (2000). State of the art in process integration. *Applied Thermal Engineering*, **20**, 1337–1345.

Smith, R., Jobson, M., Chen, L. (2010). Recent developments in the retrofit of heat exchanger networks. *Applied Thermal Engineering*, **30**, 2281–2289.

TEMA, Tubular Exchanger Manufacturers Association, Inc., <www.tema.org> accessed 23.09.2012.

Tjoe, T. N. (1986). Retrofit of heat exchanger networks. PhD thesis, UMIST, Manchester, UK.

Tjoe, T. N., Linnhoff, B. (1986). Using pinch technology for process retrofit. *Chemical Engineering*, **93**, 47–60.

Townsend, D. W. (1989). Surface area and capital cost targets for heat exchanger networks. PhD thesis, UMIST, Manchester, UK.

Townsend, D. W., Linnhoff, B. (1984). Surface area targets for heat exchanger networks. *IChemE Annl. Res. Mtg.*, Bath, UK. Lecture 6A.

Varbanov, P. S., Klemeš, J. (2000). Rules for paths construction for HENs debottlenecking. *Applied Thermal Engineering*, **20**, 1409–1420.

Wallin, E. (1996). Process integration of industrial heat pumps in grassroot and retrofit situations. PhD thesis, Chalmers University of Technology, Gothenburg, Sweden.

Wang, Y., Pan, M., Bulatov, I., Smith, R., Kim, J.-K. (2012). Application of intensified heat transfer for the retrofit of heat exchanger networks. *Applied Energy*, **89**, 45–59.

Wechsung, A., Aspelund, A., Gundersen, T., Barton, P. I. (2011). Synthesis of heat exchanger networks at subambient conditions with compression and expansion of process streams. *AIChE Journal*, **57**, 2090–2108.

© Woodhead Publishing Limited, 2013

Yee, T. F., Grossmann, I. E., Kravanja, Z. (1990). Simultaneous optimization models for heat integration – I. Area and energy targeting and modeling of multi-stream exchangers, *Computers & Chemical Engineering*, **14**, 1151–1164.

Yee, T. F., Grossmann, I. E. (1990). Simultaneous optimization models for heat integration – II. Heat exchanger networks synthesis. *Computers & Chemical Engineering*, **14**, 1165–1184.

© Woodhead Publishing Limited, 2013

9

Heat Integration in Batch Processes

THOKOZANI MAJOZI, University of Pretoria, South Africa and Council for Scientific and Industrial Research, South Africa

DOI: 10.1533/9780857097255.2.310

Abstract: This chapter addresses Heat Integration in multipurpose batch plants in situations where the schedule is known a priori, as well as cases that are characterised by unknown prior production schedules. In most published literature, Heat Integration of batch facilities is treated as a secondary objective to production scheduling, which implies that the starting and ending times of tasks are fixed a priori. However, suppression of time as a variable in the overall optimisation framework has proven to result in suboptimal results. True optimum is achieved when time is treated as a variable. The chapter presents a promising graphical technique that could be used in setting targets for heat recovery and design of the corresponding utility system. As in all graphical techniques, time is treated as a parameter rather than as a variable. This is followed by a mathematical model that allows time to be treated as a variable in setting energy targets and storage design. The performance of this model is demonstrated through a case study.

Key words: batch, heat, Integration, design, utility.

9.1 Introduction

The use of Process Integration in general, and Pinch Analysis in particular, within the batch-processing environment is relatively new (Obeng and Ashton, 1988; Kemp and Deakin, 1989 a,b,c). Most of the work conducted in this area has focused on continuous processes. This is due to the fact that it was initially thought that the application of Pinch Analysis-based techniques in batch processes would have very limited benefits, due to the intrinsic time constraints. Moreover, the incorporation of Process Integration in batch processes was perceived to culminate in reduced flexibility, which is the main feature of batch processes. Pinch Analysis was also regarded as only an energy optimisation technique of not having much significance, since energy usually constitutes a small component of batch operating costs. Steep increases in energy costs, and enhanced focus on emissions reduction in recent years, have changed this attitude among researchers and engineers. Early contributions on energy optimisation in

© Woodhead Publishing Limited, 2013

batch processes include the work of Obeng and Ashton (1988), Kemp and Deakin (1989a,b,c), and Wang and Smith (1995). The latter contribution is presented in detail in this chapter.

Obeng and Ashton (1988) drew the comparison between the Time–Temperature Cascade and the Overall Plant Bottleneck (OPB) approaches. The cascade approach generated a time-dependent analysis of energy flows with respect to time and temperature. This was achieved by setting up the Problem Table analogously to that in the analysis of continuous processes (Linnhoff and Hindmarsh, 1983), but allowing heat to be cascaded with respect to time and temperature. Other than setting the energy targets, this approach also allowed the heat storage opportunities to be identified. In setting energy targets, the OPB approach first removed the time constraint by using the concept of the Time Average Model (TAM). In this model the heat loads were averaged over a chosen period, followed by the construction of the Hot and Cold Stream Composite Curves as in the continuous process (Linnhoff and Hindmarsh, 1983). The Time Slice Model (TSM) was then used to set targets based on a chosen schedule. The Time Slices were constructed by plotting each of the process duration times on a time plane. The target was then set by calculating the energy demand in each of the time intervals. This target was then optimised by increasing the direct heat transfer opportunities between hot and cold streams by schedule modification. The schedule modification was achieved by allowing some processes to start earlier, end later, and/or finish earlier than prescribed in the initial schedule. Attention was drawn to the fact that these process changes could have an impact on plant capacity, flexibility, and process yields, as well as energy consumption.

It was then concluded that the TAM target could be achieved by modifying the initial schedule using the time slice diagram. The cascade approach also yielded the same energy target as the TAM when applied to repeated batch operations. The cascade analysis was, therefore, found to be rigorous with respect to the energy target, but not with respect to the heat storage capacity, since this is highly dependent on the initial assumptions made. The implication was that the TAM could be used as a shortcut in setting the targets. This was, however, later criticised by Kemp and Deakin (1989). Neither of these techniques included cost factors.

Kemp and Deakin (1989a,b,c,) produced a series of three papers on Cascade analysis. In their first paper, the application of cascade analysis in setting energy targets was revisited. This was compared with the OPB approach presented by Obeng and Ashton (1988). Rather than confining the targeting procedure to simple scheduling diagrams, the thermodynamic capability of hot and cold streams to exchange heat was explored in sufficient detail. The shortcomings of using the TAM in dealing with batch processes was highlighted by using a simple batch-process flowsheet with one

© Woodhead Publishing Limited, 2013

inlet and one outlet stream. Each of the streams was fully specified with respect to thermodynamic properties. The conclusion was that an analytical method that does not allow for variations with time, like the TAM, is inadequate for even the simplest batch processes (Kemp and Deakin, 1989). This paper also introduced the use of a three-dimensional cascade plot to aid visualization of heat flows and the mathematical formulation of the technique for computer programming.

In the second paper of the series, the application of cascade analysis in the design of maximum heat exchanger (MHX) networks was presented. Attention was drawn to the fact that, unlike continuous processes, batch processes do allow the transfer of heat across the overall Pinch without compromising the maximum efficiency of the network. The implication is that the Pinch violation rules, which apply to continuous processes for Heat Integration (Linnhoff and Hindmarsh, 1983) as well as Mass Integration (El-Halwagi, 1997) do not apply to batch processes. Rescheduling opportunities were also divided into four broad classes, and their effect in the overall targeting procedure was assessed.

The third paper of the series presented a case study in the application of Pinch analysis in a system of batch operations from a speciality chemicals plant. The problem formulation had eight cold streams and five hot streams, with their supply and target temperatures, start and finish times, and heat capacity flowrates specified. The study showed that the application of cascade analysis to this problem could lead to 28% and 12.2% savings in energy consumption using heat storage and direct heat exchange, respectively.

Extensive work has also been conducted in the development of mathematical models that allow time to be treated as a variable (see Vaselenak *et al*., 1986; Ivanov *et al*., 1993; Papageorgiou *et al*., 1994; Vaklieva-Bancheva *et al*., 1996; Chen and Chang, 2009; Halim and Srinivasan, 2009). Each of these techniques relies heavily on mathematical modelling in order to cater for the inherent multiple dimensionality of the batch scheduling problem.

Vaselenak *et al*. (1986) explored heat exchange between hot and cold vessels requiring cooling and heating, respectively, in order to reduce utility consumption. Heuristics were used when temperatures were not limiting, and an MILP formulation when temperatures were limiting. Ivanov *et al*. (1993) addressed the problem of designing a minimum-total-cost Heat Exchanger Network for given pairwise matches of batch vessels. An implicit, predefined schedule was also assumed.

Vaklieva-Bancheva *et al.* (1996) improved the work of Ivanov *et al*. (1993) by embedding the Heat Integration framework within an overall scheduling framework. However, the authors only addressed a special case in which the plant is assumed to operate in a zero-wait overlapping mode, where each product must pass through a subset of the equipment stages, and production is organised in a series of long campaigns. The non-linear objective function

© Woodhead Publishing Limited, 2013

was linearised with additional variables and constraints, and the resulting overall formulation was an MILP problem that was solved to global optimality. Zero-wait fixed the relative timing of all stages, and the method was suitable for existing plants with a fixed set of processing equipment. Only specific pairs of units were allowed to undergo Heat Integration.

Papageorgiou *et al*. (1994) embedded a Heat Integration model within the scheduling formulation founded on discrete time representation. Opportunities for both direct and indirect Heat Integration were considered, as well as possible heat losses from the heat storage tank. Differential equations were integrated numerically over the discrete time horizon; however, discretisation of the time horizon always leads to an explosive binary dimension. The resulting model was a non-convex MINLP problem, for which a global optimum could not be guaranteed. The operating policy, in terms of heat integrated or standalone, was also predefined for tasks.

Halim and Srinivasan (2009) discussed a sequential method using direct Heat Integration. A number of optimal schedules with minimum makespan were found and Heat Integration analysis was performed on each. The schedule with the minimum utility requirement was chosen as the best. It was argued that sequential procedures could lead to a higher number of practicably implementable networks with an optimal schedule, and were also more suitable for complex problems.

Chen and Chang (2009) extended the work of Majozi (2006) to periodic scheduling, based on the Resource Task Network (RTN). The resultant direct Heat Integration formulation was an MILP problem. The state sequence network (SSN) formulation of Majozi (2009) used fewer binary variables than the RTN approach for the heat integrated short-term scheduling case, while achieving the same objective value. However, for the periodic case, all heat sources and sinks operated in integrated mode, making the process more economical.

In this chapter a recently published batch-process Heat Integration technique by Stamp and Majozi (2011) is presented in detail.

9.2 Graphical Technique for Heat Integration in Batch Process

As aforementioned, most of the graphical techniques in published literature rely on predetermined schedule, i.e. time is fixed *a priori*. This ultimately allows the analysis to be confined in a 2-dimensional space with relative ease, albeit at the expense of accuracy. Time is intrinsic in batch operations. Consequently, it has to form part of the analysis for the results to be of any practical value. Figure 9.1 depicts the essence of the foregoing statement. The temperature and time scales show that streams B and D are

© Woodhead Publishing Limited, 2013

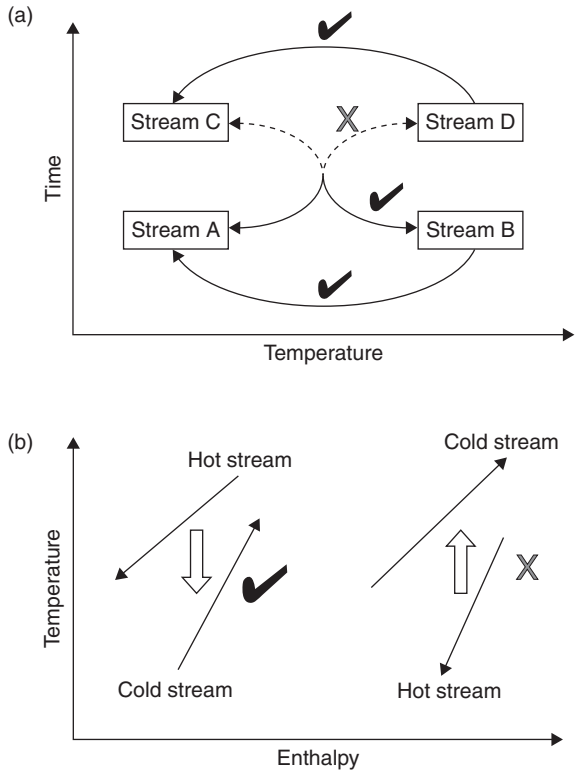

9.1 (a) Time as an intrinsic constraint; (b) Interpretation of driving forces, i.e. temperature.

hotter than streams A and C. Moreover, streams C and D are only available later than streams A and B. In Fig. 9.1a, since stream B is hotter and available earlier than stream C, there exists an opportunity for Heat Integration between the two streams. The discrepancy in time, however, suggests that this can only be achieved via heat storage. In a situation where hot and cold streams appear simultaneously, as for streams C and D as well as streams A and B, direct Heat Integration is possible if the driving forces allow (Fig. 9.1b). On the other hand, although stream D is hotter than stream A, it is only available later in the process, thereby nullifying opportunities for Heat Integration.

This section of the chapter presents in sufficient detail one of the graphical techniques that has been published in literature with promising results (Wang and Smith, 1995). The advantage of this technique is its ability to place emphasis on minimum degradation of heat and assessment of heat storage in utility system design.

© Woodhead Publishing Limited, 2013

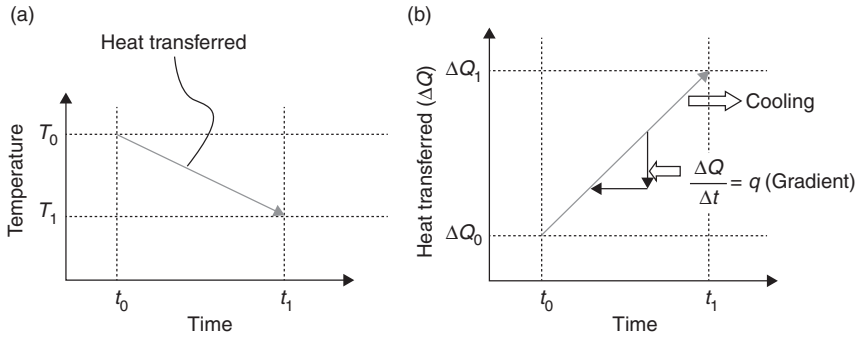

9.2 (a) Quantity of heat; (b) Representation of heat flow.

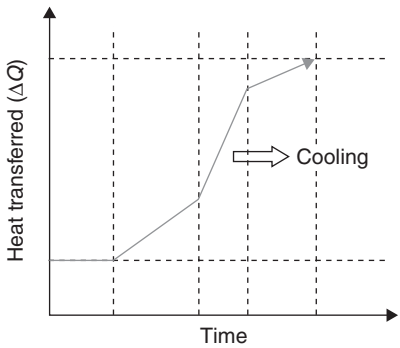

9.3 Hot Stream Composite Curve.

Shown in Fig. 9.2a is the representation of the quantity of heat from a hot stream that is cooling from temperature T_0 to temperature T_1, over time interval $[t_0,t_1]$. This quantity of heat can be described as follows.

$$\Delta Q = mc_p(T_0 - T_1)(t_0 - t_1) \qquad [9.1]$$

In Equation [9.1], m is the average mass flowrate of the batch stream, while c_p is the specific heat capacity of the batch stream. Equation [9.1] can also be written in the following form, where q is the heat flow and also the gradient of the ΔQ-time diagram as shown in Fig. 9.2b. In the presence of several hot streams within a common time interval, heat flows can be summed to yield a Hot Stream Composite Curve as shown in Fig. 9.3.

$$\Delta Q = q(t_0 - t_1) \qquad [9.2]$$

© Woodhead Publishing Limited, 2013

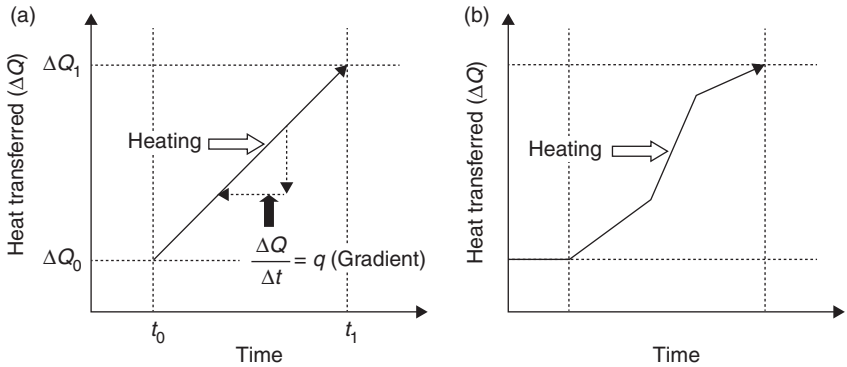

9.4 (a) Representation of heat flow; (b) Cold Stream Composite Curve.

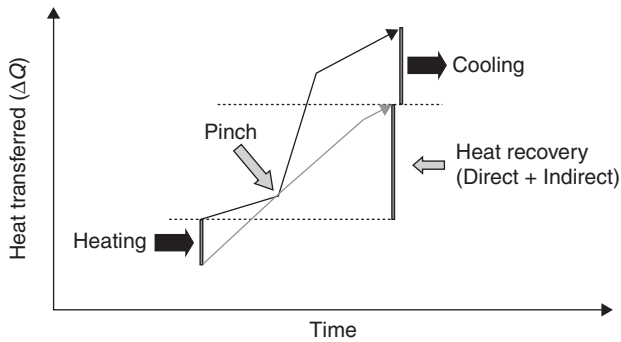

9.5 Targeting for hot and cold external utilities.

A curve similar to Fig. 9.3 can also be developed for cold streams by following the same procedure as shown in Fig. 9.4. Consequently, a plot of both Hot and Cold Stream Composite Curves on the same ΔQ-time axis, followed by a vertical shift so that both curves touch at the Pinch Point as shown in Fig. 9.5, yields the extent of possible heat recovery through process–process heat exchange, as well as targets for external hot and cold utilities. Worthy of mention, however, is that Fig. 9.5 only sets the targets, but does not show the temperature levels at which utilities have to be supplied.

In order to get an indication of the temperature levels at which external utilities have to be supplied, a Grand Composite Curve (GCC) is constructed, as shown in Fig. 9.6. In principle, the GCC has the same purpose as encountered in continuous processes where it has proven to be a powerful tool for the placement of utilities (Linnhoff *et al.*, 1982). The 'shaded pockets' in Fig. 9.6 show opportunities for indirect Heat Integration from

© Woodhead Publishing Limited, 2013

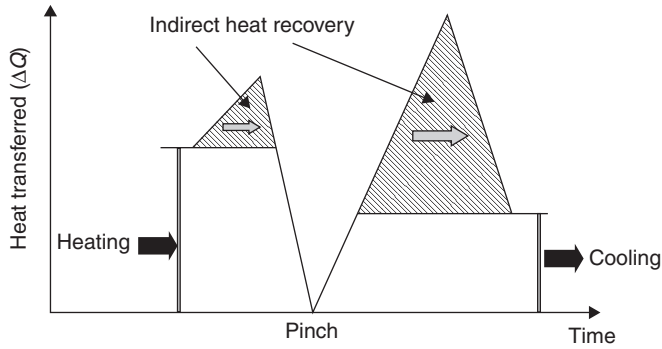

9.6 GCC for batch processes.

one time interval to another. A positive gradient in Fig. 9.6 signifies heat surplus, while the negative gradient signifies heat deficit, hence the direction of heat recovery. Also shown in Fig. 9.6 are the targets for external hot and cold utilities. The construction of the GCC follows a four-step procedure as summarised below.

9.2.1 Construction of the GCC for Batch Processes

(i) Step 1: demarcate the entire problem into temperature intervals by shifting the hot streams downward by $\Delta T_{min}/2$ and shifting the cold streams upward by the same amount. ΔT_{min} is the predefined Minimum Temperature Difference for the problem.
(ii) Step 2: identify streams present in each temperature interval.
(iii) Step 3: conduct heat balance in each time period within the temperature interval. When there is a heat deficit in a time period, the slope of the line on the GCC will be negative, and when there is a heat surplus in a time period, the slope of the line on the GCC will be positive. This allows Heat Integration opportunities to be exhausted fully within a particular time period before cascading to subsequent temperature intervals. Consequently, time is treated as a primary constraint, while temperature is treated as a secondary constraint.
(iv) Step 4: targets are then set by heat that cannot be supplied or removed by the existing streams due to temperature and time constraints.

To illustrate the use of the GCC, a simple example is considered with data shown in Table 9.1 (Wang and Smith, 1995). The Minimum Temperature Difference for the problem was chosen to be 20°C.

© Woodhead Publishing Limited, 2013

Table 9.1 Data for the literature example

Streams		Temperature (°C)		CP (kW/°C)	Time (h)	
No.	Type	T_0	T_1		t_0	t_1
1	H	400	300	2	0	1
2	C	0	100	2	1	2
3	C	280	380	2	2	3
4	H	120	20	2	2	3

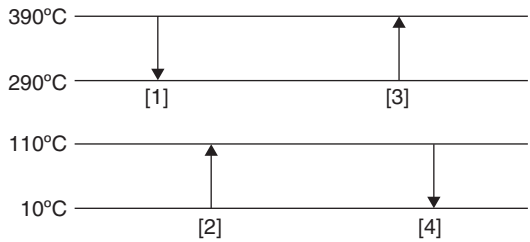

9.7 Temperature intervals.

Figure 9.7 shows the temperature interval diagram after shifting hot and cold streams by $\Delta T_{min}/2$. Streams 1 and 3 exist in the [290°C, 390°C] temperature interval, while streams 2 and 4 exist in the [10°C, 110°C] temperature interval. None of the streams in the given data is in the [110°C, 290°C] temperature interval. Exploration of Heat Integration opportunities for streams within each temperature interval is shown in Fig. 9.8. Stream 1 is active during the [0 h, 1 h] time interval and generates 200 kWh of heat, which is stored during the [1 h, 2 h] time interval for later use by stream 3 during the [2 h, 3 h] time interval, as appears in Fig. 9.8a. This ultimately exhausts all the Heat Integration options in the [290°C, 390°C] temperature interval. Similar consideration of streams in the [10°C, 110°C] yields Fig. 9.8b. In this interval there exists no opportunity for heat recovery, since the cold stream (stream 2) is active before the hot stream (stream 4). Consequently, external hot and cold utilities, of 200 kWh each, have to be used as indicated in the diagram.

The advantage of the GCC as used in this context is that both time and temperature are handled within a unified framework, so that targets are achieved without violating either of these two constraints. On the other hand, the composite curves could have been used, albeit without the possibility of minimising energy degradation. Figure 9.9 shows the targets set by the application of the composite curves. It is evident from Fig. 9.9 that, while

© Woodhead Publishing Limited, 2013

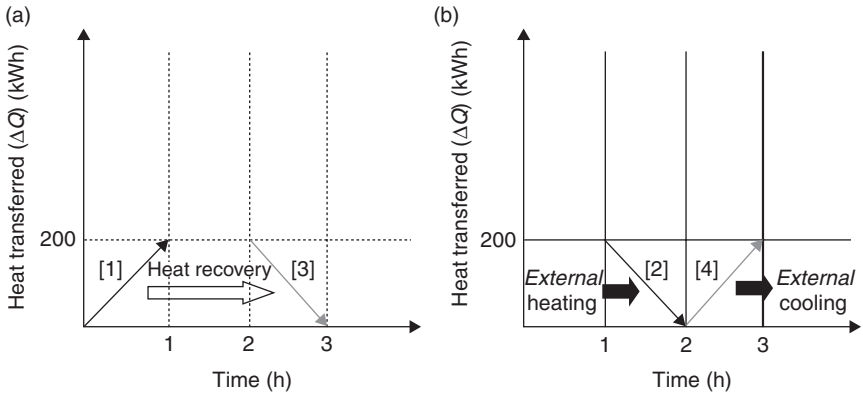

9.8 Targeting (a) In the [290°C, 30°C]; and (b) In the [10°C, 110°C] temperature intervals.

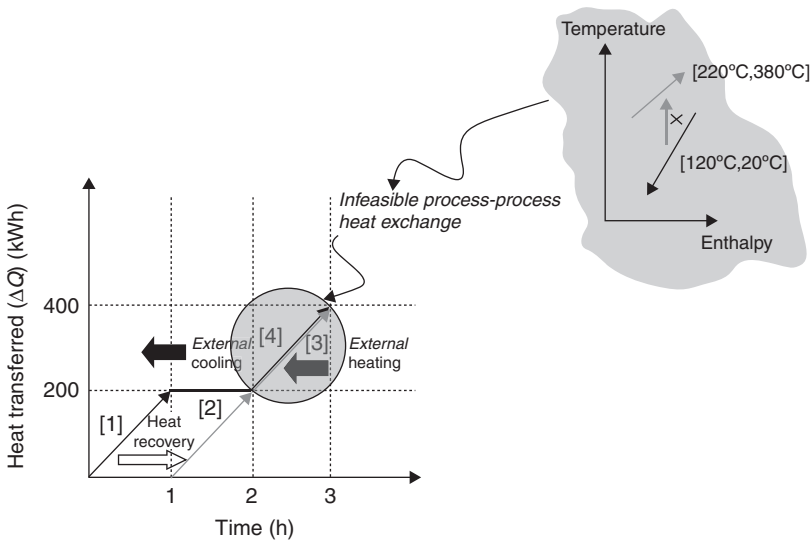

9.9 Targeting using the Composite Curves instead of GCC.

the quantity of external hot and cold utilities remains 200 kWh each, the hot utility has to be supplied at a much higher temperature of 420°C, instead of merely 120°C as suggested by the GCC.

The setting of energy targets has to be followed by the design of appropriately sized utility systems. While the design of such systems is well established for continuous operations, the inherent time dimension in batch processes renders the optimum design of a utility system a very challenging

© Woodhead Publishing Limited, 2013

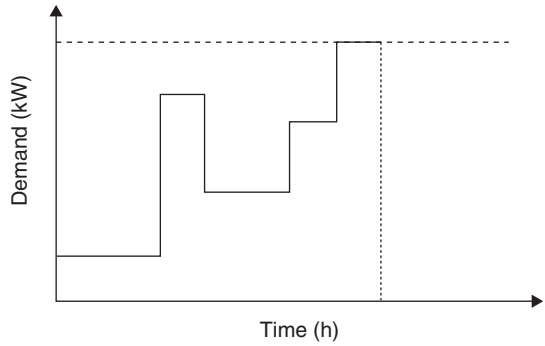

9.10 Utility demand pattern in a batch facility.

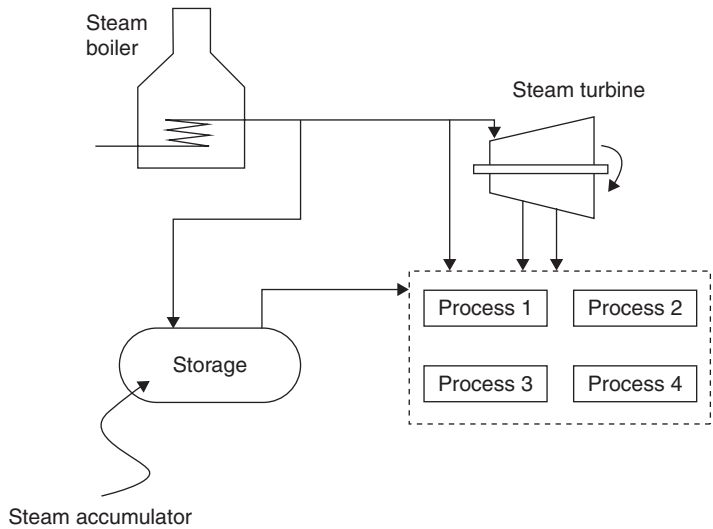

9.11 Utility system for a batch facility with the accumulator.

task. In most instances, utility systems for batch facilities overdesigned in order to guarantee satisfaction of demand. Figure 9.10 demonstrates a typical utility demand pattern in a batch facility. In general, the utility stream will be designed to the capacity of maximum demand, although this period might be very short compared to the overall time horizon of interest, hence the overdesign. The method of Wang and Smith (1995) is based on optimum design, or sizing of the accumulator for heat storage so as to minimise overdesign in the utility system, Fig. 9.11.

Figure 9.12 shows the ΔQ-time diagram that is used as the basis for the design of optimum capacity for heat storage. As illustrated earlier in this

© Woodhead Publishing Limited, 2013

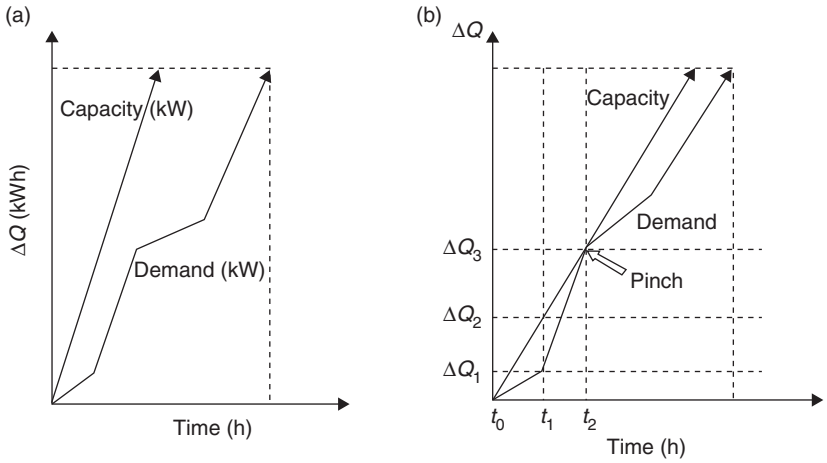

9.12 *Q*-Time diagram for optimum sizing of the accumulator.

chapter, the gradient of Fig. 9.12 is the heat flow or power. Consequently, the gradient of the capacity curve would be equal to the steepest gradient in the Demand Curve for the utility system to meet all its demands, Fig. 9.12a. Through shifting either the Capacity Curve or the Demand Curve until the formation of the Pinch Point, as shown in Fig. 9.12b, one can determine the appropriate size of heat storage that would allow heat recovery across different time periods. Worthy of note is the fact that shifting the Demand Curve towards the Capacity Curve is associated with the increase in gradient, which is equivalent to an increase in demand. Conversely, shifting the Capacity Curve towards the Demand Curve is equivalent to designing a smaller utility system, as signified by the decrease in gradient. As seen in Fig. 9.12b, the heat demand in the $[t_0,t_1]$ time interval is ΔQ_1, whereas the available heat in the same time interval is ΔQ_2. This corresponds to a heat surplus of $(\Delta Q_2 - \Delta Q_1)$. On the other hand, $[t_1,t_2]$ time interval has a heat demand of $(\Delta Q_3 - \Delta Q_1)$ and heat capacity of $(\Delta Q_3 - \Delta Q_2)$, which implies a heat deficit of $(\Delta Q_2 - \Delta Q_1)$. Therefore, an accumulator of $(\Delta Q_2 - \Delta Q_1)$ capacity is required to store heat from $[t_0,t_1]$ time interval to $[t_1,t_2]$ time interval. For the diagram shown in Fig. 9.12, this suffices to fix the capacity of the accumulator, as the demand Above Pinch is less than or equal to the installed capacity, judging by the gradient of the Demand Curve Above Pinch.

In order to illustrate the application of the method, a simple example from literature (Wang and Smith, 1995) is used. The utility demand pattern for the batch process in the example is shown in Fig. 9.13. The batch facility is supplied by two boilers, of 6 and 4 MW capacities. The 6 MW boiler is

© Woodhead Publishing Limited, 2013

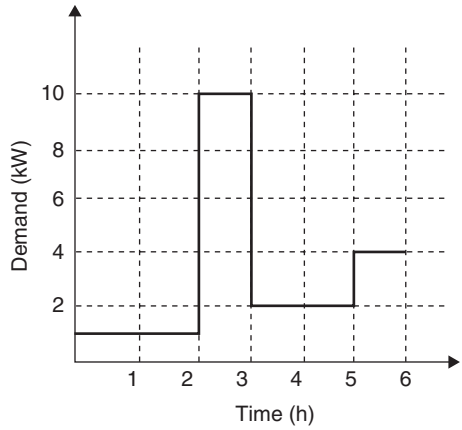

9.13 Utility demand pattern for the literature example.

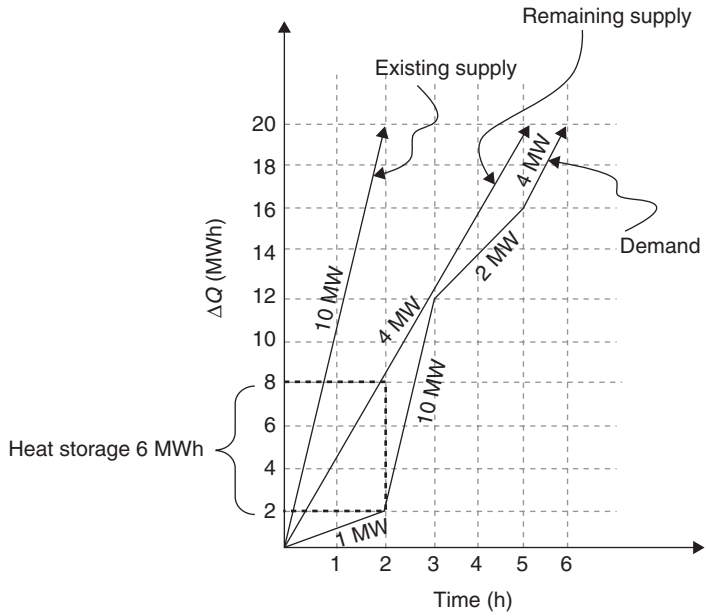

9.14 Targeting for the optimum accumulator size.

coming to the end of its life and the decision has to be made as to whether to replace it or install an accumulator with the 4 MW boiler. Figure 9.14 shows the ΔQ-Time diagram with capacity and demand curves. It is evident from Fig. 9.14 that the 4 MW boiler is capable of satisfying the demand as long as heat recovery via the accumulator is allowed. In order to determine

© Woodhead Publishing Limited, 2013

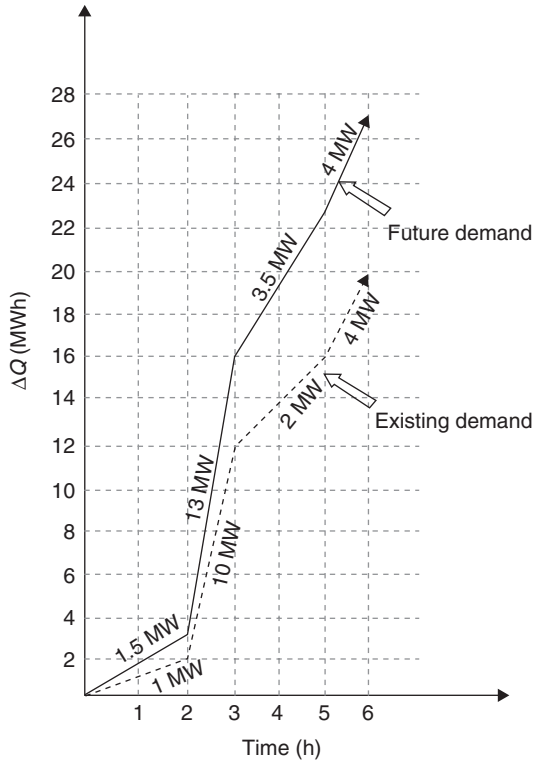

9.15 Demand Curve corresponding to 30% increase in the literature example.

the optimum size of the accumulator, it is observed that the amount of heat required in the [1 h, 2 h] time interval is only 2 MWh, whereas 8 MWh is available. Therefore, there exists a heat surplus of 6 MWh in the [1 h, 2 h] time interval. However, in the [2 h, 3 h] time interval there is a heat demand of 10 MWh, whereas only 4 MWh is available. This implies a heat deficit of 6 MWh. It is then apparent from the foregoing observation that the optimum size of the accumulator will be 6 MWh.

Another interesting assessment of the batch facility used in the example pertains to a situation where demand is increased by about 30%, due to increase in plant throughput as shown in Fig. 9.15. Typical questions could be: how much additional boiler capacity is required, and what would be the corresponding size of the accumulator? Figure 9.16 provides answers to both questions. The additional boiler capacity would be 1.3 MW, which corresponds to an overall capacity of 5.3 MW, and the minimum accumulator capacity would be 9 MWh.

© Woodhead Publishing Limited, 2013

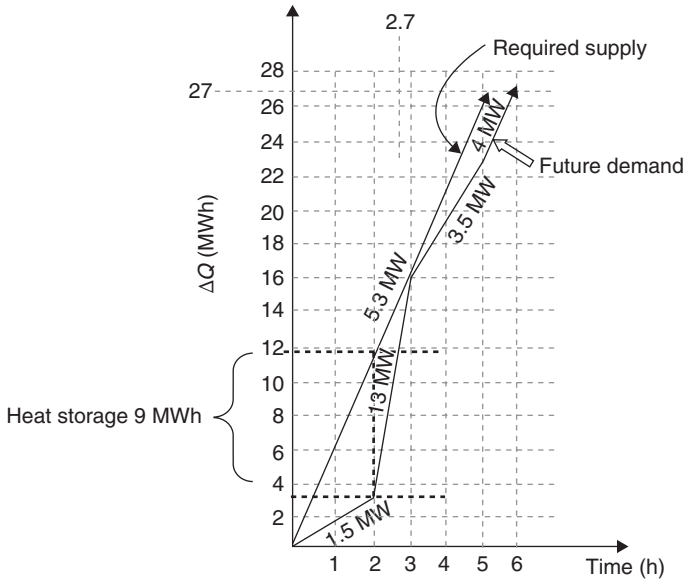

9.16 Targeting the minimum size of boiler capacity and size of accumulator.

9.3 Mathematical Technique for Heat Integration of Batch Plants

In this section a mathematical formulation that treats time as a variable is presented in sufficient detail to allow verification and repetition of results by the reader. The formulation is based on uneven discretisation of the time horizon so as to limit the number of binary variables that usually lead to lengthy CPU times.

9.3.1 Problem Statement and Objectives

The problem addressed in Heat Integration of batch plants can be stated as follows.

Given:

(i) Production scheduling data, including equipment capacities, durations of tasks, time horizon of interest, product recipes, cost of starting materials and selling price of final products,
(ii) Hot duties for tasks requiring heating and cold duties for tasks that require cooling,
(iii) Costs of hot and cold utilities,

© Woodhead Publishing Limited, 2013

(iv) Operating temperatures of heat sources and heat sinks,
(v) Minimum allowable temperature differences, and
(vi) Design limits on heat storage.

Determine:

(i) An optimal production schedule where the objective is to maximise profit, defined as the difference between revenue and the cost of hot and cold utilities, and
(ii) The optimal size of heat storage available, as well as the initial temperature of heat storage.

9.3.2 Mathematical Model

The SSN recipe representation, and an uneven discretisation of the time horizon, are used to model the process (Seid and Majozi, 2012). This has proven to result in fewer binary variables, which ultimately allows a problem to be solved in relatively short CPU times.

The model is based on the superstructure in Fig. 9.17. The symbols are as defined thereafter. Each task may operate using either direct or indirect Heat Integration. Tasks may also operate in standalone mode, using only external utilities. This may be required for control reasons, or when thermal driving forces or time do not allow for Heat Integration. If either direct or indirect Heat Integration is not sufficient to satisfy the required duty, external utilities may make up for any deficit.

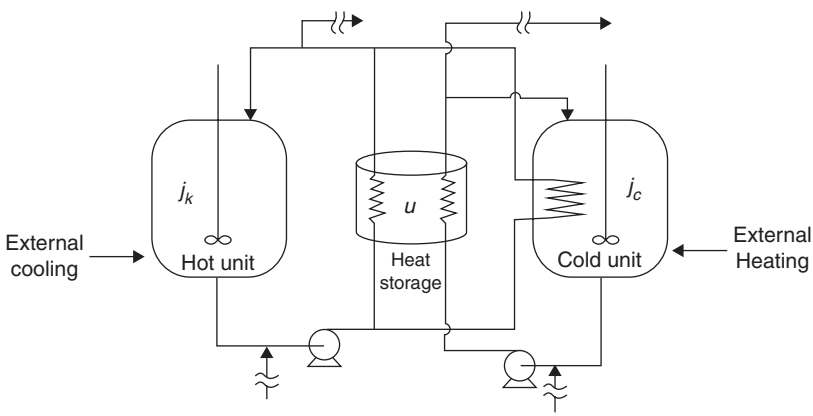

9.17 Superstructure for mathematical model (Majozi, 2009).

© Woodhead Publishing Limited, 2013

The mathematical model comprises the following sets, variables, parameters and constraints.

Sets

$J = \{j|j \text{ is a processing unit}\}$
$J_c = \{j_c|j_c \text{ is a processing unit which may conduct tasks requiring heating}\} \subset J$
$J_h = \{j_h|j_h \text{ is a processing unit which may conduct tasks requiring cooling}\} \subset J$
$P = \{p|p \text{ is a time point}\}$
$S = \{s|s \text{ is any state}\}$
$S_{\text{in},j} = \{\text{s}_{\text{in},j}|\text{s}_{\text{in},j} \text{ is an input stream to a processing unit}\} \subset S$
$U = \{u|u \text{ is a heat storage unit}\}$

Continuous Variables

$A_1(u)$ = area for convective heat transfer from heat transfer medium
$A_3(u)$ = area for convective heat transfer to environment
$cw(s_{\text{in},j}, p)$ = external cooling required by unit j_h conducting the task corresponding to state $s_{\text{in},jh}$ at time point p
$L(u)$ = height of heat storage vessel
$Q(s_{\text{in},j}, u, p)$ = heat exchanged with heat storage unit u at time point p
$Q_{\text{loss}}(u, p)$ = heat lost from idle heat storage unit
$R_{\text{conv}}(u)$ = convective resistance of heat transfer medium
$R_{\text{conv}_3}(u)$ = convective resistance of ambient air
$R_{\text{ins}}(u)$ = conductive resistance of insulation
$R_{\text{ves}}(u)$ = conductive resistance of heat storage vessel
$R_{\text{tot}}(u)$ = thermal resistance for heat storage unit
$\text{st}(s_{\text{in},jc}, p)$ = external heating required by unit j_c conducting the task corresponding to state $s_{\text{in},jc}$ at time point p
$\Delta T(u, p)$ = temperature drop in heat storage unit u due to heat losses
$T_{\text{co}_{\text{in}}}(u, p)$ = steady-state temperature equal to the final temperature in the heat storage vessel, $T_f(u, p)$
$T_0(u, p)$ = initial temperature in heat storage unit u at time point p
$T_f(u, p)$ = final temperature in heat storage unit u at time point p
$\Delta t(p)$ = time interval over which heat loss takes place
$t_0(s_{\text{in},j}, u, p)$ = time at which heat storage unit commences activity
$t_f(s_{\text{in},j}, u, p)$ = time at which heat storage unit ends activity
$t_u(s_{\text{in},j}, p)$ = time at which a stream enters unit j
$V(u)$ = volume of heat storage unit u
$W(u)$ = capacity of heat storage unit u

© Woodhead Publishing Limited, 2013

$\Gamma(s_{\text{in},j}, u, p)$ = Glover Transformation variable
$\Psi(s_{\text{in},j}, u, p)$ = Reformulation–Linearisation variable

Binary Variables

$$x(s_{\text{in},j_c}, s_{\text{in},j_k}, p) = \begin{cases} 1 \leftarrow \text{if unit } j_c \text{ conducting task corresponding to state } s_{\text{in},j_c} \\ \quad \text{is integrated with unit } j_h \text{ conducting the task} \\ \quad \text{corresponding to state } s_{\text{in},j_c} \text{ at time point } p \\ 0 \leftarrow \text{otherwise} \end{cases}$$

$$y(s_{in,j}, p) = \begin{cases} 1 \leftarrow \text{if state } s \text{ is used in unit } j \text{ at time point } p \\ 0 \leftarrow \text{otherwise} \end{cases}$$

$$z(s_{\text{in},j}, u, p) = \begin{cases} 1 \leftarrow \text{if unit } j \text{ conducting the task corresponding to state } s_{\text{in},j} \text{ is} \\ \quad \text{integrated with storage unit } u \text{ at time point } p \\ 0 \leftarrow \text{otherwise} \end{cases}$$

Parameters

c_p = specific heat capacity of heat storage fluid
$E(s_{\text{in},j})$ = amount of heat required by or removed from unit j conducting the task corresponding to state $s_{\text{in},j}$
h_1 = convective heat transfer coefficient for free convection of liquids
h_3 = convective heat transfer coefficient for free convection of gases
k_{ins} = thermal conductivity of insulation
k_{ves} = thermal conductivity of heat storage vessel
M = any large number
r_1 = inside radius of heat storage vessel
r_2 = outside radius of heat storage vessel
r_3 = outside radius of insulation
$T(s_{\text{in},j})$ = operating temperature for processing unit j conducting the task corresponding to state $s_{\text{in},j}$
T^L = lower bound for heat storage temperature
T^U = upper bound for heat storage temperature
$\Delta T^{\min}$ = minimum allowable thermal driving force
$T_{\infty_{\text{out}}}$ = steady-state ambient temperature
$\tau(s_{\text{in},j})$ = duration of the task corresponding to state $s_{\text{in},j}$ conducted in unit j
W^L = lower bound for heat storage capacity
W^U = upper bound for heat storage capacity

© Woodhead Publishing Limited, 2013

Constraints

In addition to the necessary short-term scheduling constraints (Seid and Majozi, 2012), Constraints [9.3]–[9.24] constitute the Heat Integration model, useful for multipurpose batch processes with fixed batch sizes. Both direct and indirect Heat Integration are considered. The formulation is based on previous models in the literature that catered for direct Heat Integration (Majozi, 2006) and indirect Heat Integration (Majozi, 2009). These models could not adequately address multipurpose facilities, but were ideal for multiproduct cases.

Constraints [9.3] and [9.4] are active simultaneously and ensure that one hot unit will be integrated with one cold unit when direct Heat Integration takes place, in order to simplify operation of the process. Also, if two units are to be heat integrated at a given time point, they must both be active at that time point. However, if a unit is active, it may operate in either integrated or standalone mode.

$$\sum_{s_{\text{in}jc}} x(s_{\text{in},j_c}, s_{\text{in},j_h}, p) \le y(s_{\text{in},j_h}, p), \qquad \forall p \in P, s_{\text{in},j_h} \in S_{\text{in},j} \tag{9.3}$$

$$\sum_{s_{\text{in}jh}} x(s_{\text{in},j_c}, s_{\text{in},j_h}, p) \le y(s_{\text{in},j_c}, p), \qquad \forall p \in P, s_{\text{in},j_c} \in S_{\text{in},j} \tag{9.4}$$

Constraint [9.5] ensures that only one hot or cold unit is heat integrated with one heat storage unit at any point in time.

$$\sum_{s_{\text{in},jc}} z(s_{\text{in},j_c}, u, p) + \sum_{s_{\text{in},jh}} z(s_{\text{in},j_h}, u, p) \le 1, \qquad \forall p \in P, u \in U \tag{9.5}$$

Constraints [9.6] and [9.7] ensure that a unit cannot simultaneously undergo direct and indirect Heat Integration. This condition simplifies the operation of the process.

$$\sum_{s_{\text{in},j_c}} x(s_{\text{in},j_c}, s_{\text{in},j_h}, p) + z(s_{\text{in},j_h}, u, p) \le 1, \qquad \forall p \in P, s_{\text{in},j_h} \in S_{\text{in},j}, u \in U \tag{9.6}$$

$$\sum_{s_{\text{in},j_c}} x(s_{\text{in},j_c}, s_{\text{in},j_h}, p) + z(s_{\text{in},j_h}, u, p) \le 1, \qquad \forall p \in P, s_{\text{in},j_h} \in S_{\text{in},j_h} \in S_{\text{in},j}, u \in U \tag{9.7}$$

Constraints [9.8] and [9.9] quantify the amount of heat received from or transferred to the heat storage unit. There will be no heat received or

© Woodhead Publishing Limited, 2013

transferred if the binary variable signifying use of the heat storage vessel, $z(s_{\text{in},j}, u, p)$, is zero. These constraints are active over the entire time horizon, where p is the current time point and $p - 1$ is the previous time point.

$$Q(s_{\text{in},j_c}, u, p-1) = W(u)c_p(T_0(u,p-1) - T_f(u,p))z(s_{\text{in},j_c}, u, p-1) \\ \in \forall p \in P, p > p0, s_{\text{in},j_c} \in S_{\text{in},j}, u \in U \qquad [9.8]$$

$$Q(s_{\text{in},j_h}, u, p-1) = W(u)c_p(T_f(u,p) - T_0(u,p-1))z(s_{\text{in},j_h}, u, p-1) \\ \forall p \in P, p > p0, s_{\text{in},j_h} \in S_{\text{in},j}, u \in U \qquad [9.9]$$

Constraint [9.10] quantifies the heat transferred to the heat storage vessel at the beginning of the time horizon. The initial temperature of the heat storage fluid is $T_0(u, p0)$

$$Q(s_{\text{in},j_h}, u, p0) = W(u)c_p(T_f(u,p1) - T_0(u,p0))z(s_{\text{in},j_h}, u, p0) \\ \forall s_{\text{in},j_h} \in S_{\text{in},j}, u \in U \qquad [9.10]$$

Constraint [9.11] ensures that the final temperature of the heat storage fluid at any time point becomes the initial temperature of the heat storage fluid at the next time point. This condition will hold regardless of whether or not there was Heat Integration at the previous time point.

$$T_0(u,p) = T_f(u,p-1), \qquad \forall p \in P, u \in U \qquad [9.11]$$

Constraints [9.12] and [9.13] ensure that the temperature of heat storage does not change if there is no Heat Integration with the heat storage unit, unless there is heat loss from the heat storage unit. M is any large number, thereby resulting in an overall 'Big M' formulation. If either $z(s_{\text{in},j_c}, u, p-1)$ or $z(s_{\text{in},j_h}, u, p-1)$ is equal to one, Constraints [9.12] and [9.13] are be redundant. However, if these two binary variables are both zero, the initial temperature at the previous time point are be equal to the final temperature at the current time point if heat losses are ignored. If heat losses are considered, the temperature drops over the interval for which the vessel remains idle.

$$T_0(u,p-1) \le T_f(u,p) + \Delta T(u,p-1)\Delta t(p) + M\left(\sum_{s_{\text{in},j_c}} z(s_{\text{in},j_c}, u, p-1) + \sum_{s_{\text{in},jh}} z(s_{\text{in},j_h}, u, p-1)\right) \\ \forall p \in P, p > p0, u \in U \qquad [9.12]$$

© Woodhead Publishing Limited, 2013

$$T_0(u,p-1) \geq T_f(u,p) + \Delta T(u,p-1)\Delta t(p) - M\left(\sum_{s_{\text{in},j_c}} z(s_{\text{in},j_c},u,p-1) + \sum_{s_{\text{in},j_h}} z(s_{\text{in},j_h},u,p-1)\right), \quad \forall p \in P, p > p0, u \in U \qquad [9.13]$$

Constraint [9.14] ensures that Minimum Thermal Driving Forces are obeyed when there is direct Heat Integration between a hot and a cold unit.

$$T(s_{\text{in},j_h}) - T(s_{\text{in},j_c}) \geq \Delta T^{\min} - M(1 - x(s_{\text{in},j_c}, s_{\text{in},j_h}, p-1)), \quad \in \forall p \in P, \boldsymbol{p} > p0, s_{\text{in},j_c}, s_{\text{in},j_h} \in S_{\text{in},j} \qquad [9.14]$$

Constraints [9.15] and [9.16] ensure that Minimum Thermal Driving Forces are obeyed when there is Heat Integration with the heat storage unit. Constraint [9.13] applies for Heat Integration between heat storage and a heat sink, while constraint [9.14] applies for Heat Integration between heat storage and a heat source.

$$T_f(u,p) - T(s_{\text{in},j_c}) \geq \Delta T^{\min} - M(1 - z(s_{\text{in},j_c},u,p-1)), \quad \forall p \in P, p > p0, s_{\text{in},j_c} \in S_{\text{in},j}, u \in U \qquad [9.15]$$

$$T(s_{\text{in},j_h}) - T_f(u,p) \geq \Delta T^{\min} - M(1 - z(s_{\text{in},j_h},u,p-1)), \quad \forall p \in P, p > p0, s_{\text{in},j_h} \in S_{\text{in},j}, u \in U \qquad [9.16]$$

Constraint [9.17] states that the cooling of a heat source will be satisfied by either direct or indirect Heat Integration as well as external utility if required.

$$E(s_{\text{in},j_h})y(s_{\text{in},j_h},p) = Q(s_{\text{in},j_h},u,p) + cw(s_{\text{in},j_h},p) + \sum_{s_{\text{in},j_c}} \min_{s_{\text{in},i_c}, s_{\text{in},ih}} \left\{E\left(s_{\text{in},j_c}\right), E\left(s_{\text{in},j_h}\right)\right\} x\left(s_{\text{in},j_c}, s_{\text{in},j_h}, p\right), \quad \forall p \in P, s_{\text{in},j_h} \in S_{\text{in},j}, u \in U \qquad [9.17]$$

Constraint [9.18] ensures that the heating of a heat sink will be satisfied by either direct or indirect Heat Integration as well as external utility if required.

$$E(s_{\text{in},j_c})y(s_{\text{in},j_c},p) = Q(s_{\text{in},j_c},u,p) + st(s_{\text{in},j_c},p) + \sum_{s_{\text{in},i_h}} \min_{s_{\text{in},i_c}, s_{\text{in},ih}} \left\{E\left(s_{\text{in},j_c}\right), E\left(s_{\text{in},j_h}\right)\right\} x\left(s_{\text{in},j_c}, s_{\text{in},j_h}, p\right), \quad \forall p \in P, s_{\text{in},j_c} \in S_{\text{in},j}, u \in U \qquad [9.18]$$

© Woodhead Publishing Limited, 2013

Constraints [9.19] and [9.20] ensure that the times at which units are active are synchronised when direct Heat Integration takes place. Starting times for the tasks in the integrated units are the same. This constraint may be relaxed for operations requiring preheating or precooling and is dependent on the process.

$$t_u(s_{\text{in},j_h},p) \geq t_u(s_{\text{in},j_c},p) - M(1-x(s_{\text{in},j_c},s_{\text{in},j_h},p)) \quad \forall p \in P, s_{\text{in},j_c}, s_{\text{in},j_h} \in S_{\text{in},j} \qquad [9.19]$$

$$t_u(s_{\text{in},j_h},p) \leq t_u(s_{\text{in},j_c},p) + M(1-x(s_{\text{in},j_c},s_{\text{in},j_h},p)) \quad \forall p \in P, s_{\text{in},j_c}, s_{\text{in},j_h} \in S_{\text{in},j} \qquad [9.20]$$

Constraints [9.21] and [9.22] ensure that if indirect Heat Integration takes place, the time at which a unit is active will be equal to the time a heat storage unit starts either to transfer or receive heat.

$$t_u(s_{\text{in},j},p) \geq t_0(s_{\text{in},j},u,p) - M(y(s_{\text{in},j},p) - z(s_{\text{in},j},u,p)) \quad \forall p \in P, u \in U, s_{\text{in},j} \in S_{\text{in},j} \qquad [9.21]$$

$$t_u(s_{\text{in},j},p) \leq t_0(s_{\text{in},j},u,p) + M(y(s_{\text{in},j},p) - z(s_{\text{in},j},u,p)) \quad \forall p \in P, u \in U, s_{\text{in},j} \in S_{\text{in},j} \qquad [9.22]$$

Constraints [9.23] and [9.24] state that the time when heat transfer to or from a heat storage unit is finished will coincide with the time the task transferring or receiving heat has finished processing.

$$t_u(s_{\text{in},j},p-1) + \tau(s_{\text{in},j})y(s_{\text{in},j},p-1) \geq t_f(s_{\text{in},j},u,p) - M(y(s_{\text{in},j},p-1) - z(s_{\text{in},j},u,p-1)), \quad \forall p \in P, p > p0, u \in U, s_{\text{in},j} \in S_{\text{in},j} \qquad [9.23]$$

$$t_u(s_{\text{in},j},p-1) + \tau(s_{\text{in},j})y(s_{\text{in},j},p-1) \leq t_f(s_{\text{in},j},u,p) + M(y(s_{\text{in},j},p-1) - z(s_{\text{in},j},u,p-1)), \quad \forall p \in P, p > p0, u \in U, s_{\text{in},j} \in S_{\text{in},j} \qquad [9.24]$$

Constraints [9.8], [9.9] and [9.10] have trilinear terms resulting in a non-convex MINLP formulation. The bilinearity resulting from the multiplication of a continuous variable with a binary variable may be handled effectively with the Glover transformation (Glover, 1975). This is an exact linearisation technique and, as such, will not compromise the accuracy of

© Woodhead Publishing Limited, 2013

the model. The procedure is demonstrated for Constraint [9.9] in Appendix A, and leads to Constraint [9.25].

$$Q(s_{\text{in},j_h},u,p-1) = W(u)c_p(\Gamma_1(s_{\text{in},j_h},u,p) - \Gamma_2(s_{\text{in},j_h},u,p-1)), \quad \forall p \in P, p > p0, s_{\text{in},j_h} \in S_{\text{in},j}, u \in U \qquad [9.25]$$

The heat storage capacity, $W(u)$, is also a continuous variable and is multiplied with the continuous Glover transformation variable. This results in another type of bilinearity, which results in a non-convex model. A method to handle this is a Reformulation–Linearisation technique (Sherali and Alameddine, 1992) as discussed by Quesada and Grossmann (1995). This is demonstrated for Constraint [9.25], resulting in Constraints [9.26]–[9.32].

Let

$$W(u)\Gamma_1(s_{\text{in},j_h},u,p) = \Psi_1(s_{\text{in},j_h},u,p) \qquad [9.26]$$

With lower and upper heat storage capacity and temperature bounds known

$$W^L \le W(u) \le W^U \qquad [9.27]$$

$$T^L \le \Gamma_1(s_{\text{in},j_h},u,p) \le T^U \qquad [9.28]$$

Then

$$\Psi(s_{\text{in},j_h},u,p) \ge W^L\Gamma_1(s_{\text{in},j_h},u,p) + T^L W(u) - W^L T^L \qquad [9.29]$$

$$\Psi_1(s_{\text{in},j_h},u,p) \ge W^U\Gamma_1(s_{\text{in},j_h},u,p) + T^U W(u) - W^U T^U \qquad [9.30]$$

$$\Psi_1(s_{\text{in},j_h},u,p) \ge W^U\Gamma_1(s_{\text{in},j_h},u,p) + T^L W(u) - W^U T^L \qquad [9.31]$$

$$\Psi_1(s_{\text{in},j_h},u,p) \ge W^L\Gamma_1(s_{\text{in},j_h},u,p) + T^U W(u) - W^L T^U \qquad [9.32]$$

This is an inexact linearisation technique and increases the size of the model by an additional type of continuous variable and four types of continuous constraints.

The final completely linearised form of Constraint [9.9] can be seen in Constraint [9.33].

© Woodhead Publishing Limited, 2013

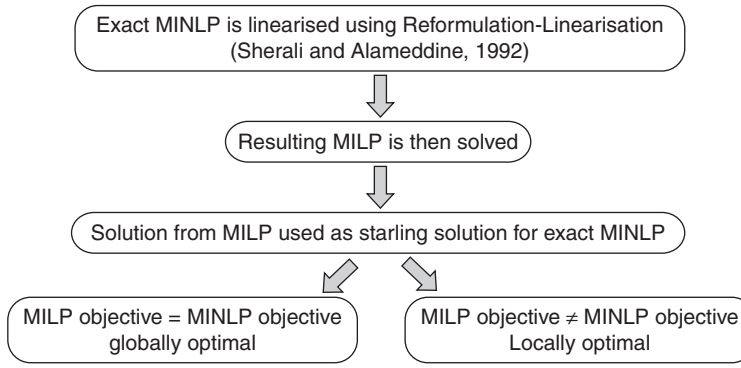

9.18 Solution algorithm for Reformulation–Linearisation technique.

$$Q(s_{\text{in},j_h}, u, p-1) = c_p(\Psi_1(s_{\text{in},j_h}, u, p) - \Psi(s_{\text{in},j_h}, u, p-1)) \\ \in \forall p \in p, p > p0, s_{\text{in},j_h} \in S_{\text{in},j}, u \in U \quad [9.33]$$

The full linearisation procedure is carried out for each of the trilinear terms resulting from Constraints [9.8], [9.9] and [9.10]. Bounds on the heat storage capacity will be determined by the available space in the plant, as batch plants usually operate in limited space.

The linearised model is solved as an MILP, the solution of which is then used as a starting point for the exact MINLP model. If the solutions from the two models are equal, the solution is globally optimal, as global optimality can be proven for MILP problems. If the solutions differ, the MINLP solution is locally optimal. The possibility also exists that no feasible starting point is found. The solution algorithm is shown graphically in Fig. 9.18.

Heat Loss considerations

Constraint [9.34], which is used in Constraints [9.12] and [9.13], accounts for heat loss from an idle heat storage vessel. As the temperature drop of heat storage due to heat loss will be minimal, it is assumed the temperature of the fluid has reached steady state and the rate of heat transfer in the time interval is constant. The heat storage vessel may be represented as in Fig. 9.19.

$$\Delta T(u,p) = \frac{Q_{\text{loss}}(u,p)}{W(u)c_p} \quad \forall p \in P, p > p0, u \in U \quad [9.34]$$

© Woodhead Publishing Limited, 2013

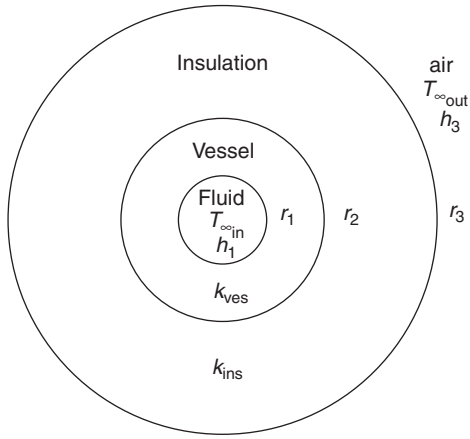

9.19 Insulated heat storage vessel.

The idle time for the heat storage vessel, when heat is neither stored nor released, is defined by Constraint [9.35].

$$\Delta t(p) = t_0(s_{\text{in},j}, u, p) - t_f(s_{\text{in},j}, u, p-1) \quad \forall p \in P, p > p0, s_{\text{in},j_h} \in S_{\text{in},j}, \boldsymbol{u} \in U \tag{9.35}$$

The amount of heat lost to the environment is quantified in Constraint [9.36].

$$Q_{\text{loss}}(u,p) = \frac{T\infty_{\text{in}}(u,p) - T\infty_{\text{out}}}{R_{\text{tot}}(u)} \quad \forall p \in P, p > p0, u \in U \tag{9.36}$$

$T_{\infty_{\text{in}}}$ is equal to the final temperature in the heat storage vessel, $T_f(u,p)$ and $T_{\infty_{\text{out}}}$ is the steady-state ambient temperature. The total thermal resistance due to convection and conduction is given by Constraint [9.37] with each term defined in Constraint [9.38].

$$R_{\text{tot}}(u) = R_{\text{conv}_1}(u) + R_{\text{ves}}(u) + R_{\text{ins}}(u) + R_{\text{conv}_3}(u) \quad \forall u \in U \tag{9.37}$$

$$R_{\text{tot}}(u) = \frac{1}{h_1 A_1(u)} + \frac{\ln(r_2/r_1)}{2\pi L(u) k_{\text{ves}}} + \frac{\ln(r_3/r_2)}{2\pi L(u) k_{\text{ins}}} + \frac{1}{h_3 A_3(u)} \quad \forall u \in U \tag{9.38}$$

The internal area for heat loss by convection from the heat transfer medium is given by Constraint [9.39] and the area for convective heat transfer losses to the environment is given in Constraint [9.40].

© Woodhead Publishing Limited, 2013

$$A_1(u) = 2\pi r_1 L(u) \qquad \forall u \in U \qquad [9.39]$$

$$A_3(u) = 2\pi r_3 L(u) \qquad \forall u \in U \qquad [9.40]$$

If the density of the heat transfer fluid is assumed to be 1,000 kg/m^3, the volume in m^3 will be numerically equal to the mass of the storage requirement in t. This volume is given by Constraint [9.41].

$$W(u) = V(u) = \pi r_1^2 L(u) \quad \forall u \in U \qquad [9.41]$$

The radius of the tank is assumed to be fixed, with the height of the tank allowed to vary.

9.4 Case Study of a Multipurpose Batch Facility

A scheduling problem was taken from literature and modified to include heating and cooling tasks for the reactions taking place in the process (Sundaramoorthy and Karimi, 2005). In this way, opportunities for Heat Integration were explored. The state task network for the process is shown in Fig. 9.20 and the SSN is shown in Fig. 9.21. The process requires sharing of equipment and multiple tasks and states.

Scheduling data are shown in Tables 9.2 and 9.3 (Sundaramoorthy and Karimi, 2005), while Heat Integration data are shown in Table 9.4. A heat storage fluid with a high heat capacity will provide good temperature control and facilitate easy heat recovery. Heating and cooling requirements for tasks are shown in Table 9.5.

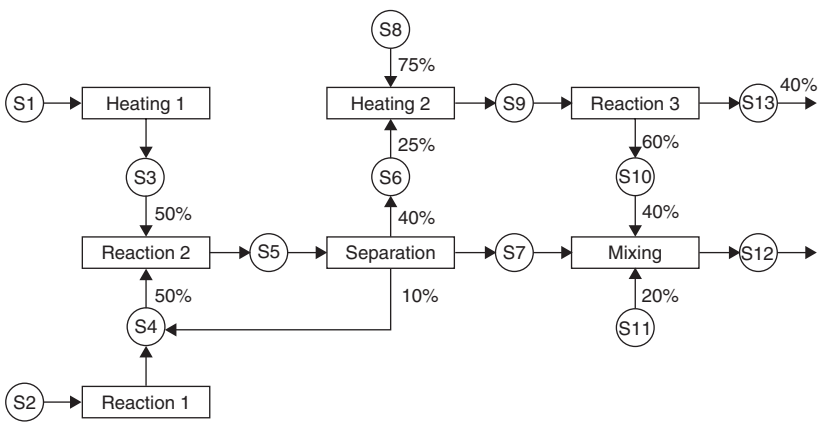

9.20 State task network of multipurpose batch facility.

© Woodhead Publishing Limited, 2013

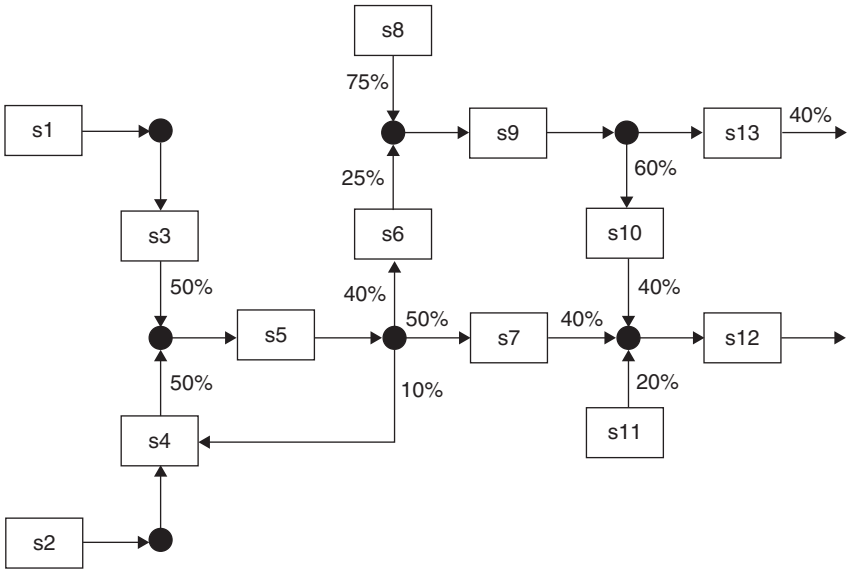

9.21 SSN of multipurpose batch facility.

Table 9.2 Scheduling data for literature example

Unit	Capacity	Suitability	Mean processing time (h)
Heater	100	H1, H2	1, 1.5
Reactor 1	100	RX1, RX2, RX3	2, 1, 2
Reactor 2	150	RX1, RX2, RX3	2, 1, 2
Separator	300	Separation	3
Mixer 1	200	Mixing	2
Mixer 2	200	Mixing	2

Parameters for heat loss considerations may be found in Table 9.6.

The batch sizes for all units were fixed at 80% of design capacity. The resulting optimal schedule for the literature example is shown in Fig. 9.22. Heat Integration is indicated with arrows and one heat storage unit was used.

The variation in temperature of the heat storage vessel may be seen in Fig. 9.23.

The results for the literature example are summarised in Table 9.7. Heat from the first exothermic reaction was stored and used for heating the second reaction. As seen from the results, there were no opportunities for direct Heat Integration and using indirect Heat Integration eliminated the requirement for external utilities. The solution procedure as described

© Woodhead Publishing Limited, 2013

Table 9.3 Scheduling data for literature example

State	Description	Storage capacity (t)	Initial amount (t)	Revenue (cu/t)
s1	Feed 1	Unlimited	Unlimited	0
s2	Feed 2	Unlimited	Unlimited	0
s3	Intermediate 1	100	0	0
s4	Intermediate 2	100	0	0
s5	Intermediate 3	300	0	0
s6	Intermediate 4	150	50	0
s7	Intermediate 5	150	50	0
s8	Feed 3	Unlimited	Unlimited	0
s9	Intermediate 6	150	0	0
s10	Intermediate 7	150	0	0
s11	Feed 4	Unlimited	Unlimited	0
s12	Product 1	Unlimited	0	5
s13	Product 2	Unlimited	0	5

Table 9.4 Heat Integration data for literature example

Parameter	Value
Specific heat capacity, c_p (kJ/kg °C)	4.2
Product selling price (cu/t)	1,000
Steam cost (cu/kWh)	10
Cooling Water Cost (cu/kWh)	2
ΔT^{min} (°C)	10
T^L (°C)	20
T^U (°C)	180
W^L (t)	1
W^U (t)	3

Table 9.5 Heating/cooling requirements for literature example

Reaction	Type	Heating/cooling requirement (kWh)	Operating temperature (°C)
RX1	Exothermic	60 (cooling)	100
RX2	Endothermic	80 (heating)	60
RX3	Exothermic	70 (cooling)	140

previously in Fig. 9.18 was used in solving the MINLP problem for the case including heat storage. The result obtained from the linearised model was the same as for the exact model, therefore, the result obtained was globally optimal. CPLEX 9.1.2 was used to solve the linearised model. DICOPT2 was used in the solution of the MINLP problem with CPLEX 9.1.2 as the

© Woodhead Publishing Limited, 2013

Table 9.6 Data for literature example with heat losses

Parameter	Value
Tank wall thickness (mm)	5
Insulation thickness (mm)	30
r_1 (m)	0.5
r_2 (m)	0.505
r_3 (m)	0.535
h_1 (kW/m²°C)	0.1
h_3 (kW/m²°C)	0.02
k_{ves} (kW/m°C)	0.015
k_{ins} (kW/m°C)	0.00005
$T_{\infty_{out}}$ (°C)	20

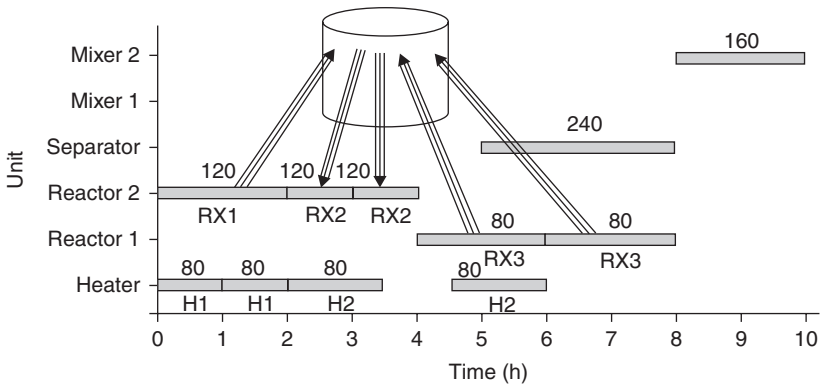

9.22 Optimal schedule for literature example with heat losses.

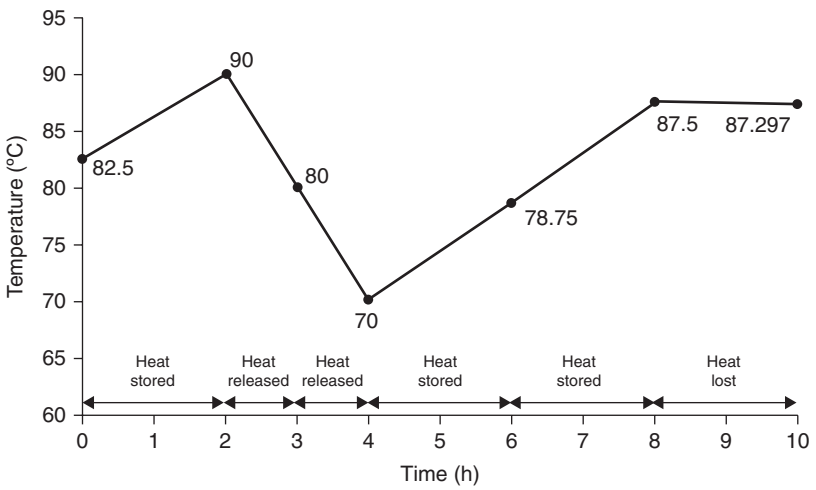

9.23 Variation in heat storage vessel temperature for literature example.

© Woodhead Publishing Limited, 2013

Table 9.7 Results for literature example

	No Heat Integration	Direct Heat Integration only	Direct and indirect Heat Integration – optimal heat storage capacity and initial temperature
Performance index (cost units)[a]	222,000	222,840	224,000
External cold duty (kWh)	200	130	0
External hot duty (kWh)	160	90	0
Heat Storage capacity (ton)			1.905
Initial heat storage temperature (°C)			82.5
CPU time (s)			68
Binary variables			156
Time points			7

[a] Performance Index = Revenue – Utility Costs.

MIP solver and MINOS as the NLP solver in GAMS 22.0. The problem was solved on a Pentium 4, 3.2 GHz processor with 512 MB RAM. Both the size of the heat storage vessel as well as the initial temperature did not change when heat losses were considered compared to the case where heat losses were disregarded, as the heat storage vessel was only idle at the end of the time horizon.

9.5 Industrial Case Study

The flowsheet for the process is shown in Fig. 9.24.

The STN for the process is shown in Fig. 9.25 and the SSN is shown in Fig. 9.26. The scheduling data may be obtained from Tables 9.8, 9.9 and 9.10 (Majozi and Zhu, 2001). The plant consumes 55% of the steam utility in an agrochemical facility. Each of the units processes a fixed batch size of eight tons, 80% of design capacity. The process requires three consecutive chemical reactions, which take place in four available reactors. Reaction 1 takes place in either Reactor 1 or Reactor 2 and takes two hours. The intermediate from Reaction 1 is then transferred either to Reactor 3 or Reactor 4, where two consecutive reactions take place. Reaction 2 takes 3 h and Reaction 3, takes 1 h. Reaction 2 is highly exothermic and requires almost 9 t of cooling water (equivalent to 100 kWh). For operational purposes, these two consecutive reactions take place in a single reactor. Some of the intermediate from the first of these two reactions can be stored in an intermediate buffer tank prior to the final reaction to improve throughput. Both the second

© Woodhead Publishing Limited, 2013

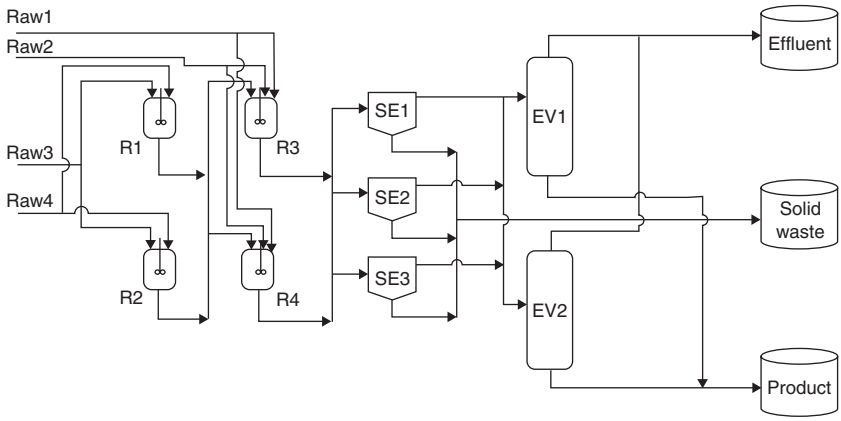

9.24 Flowsheet for the industrial case study.

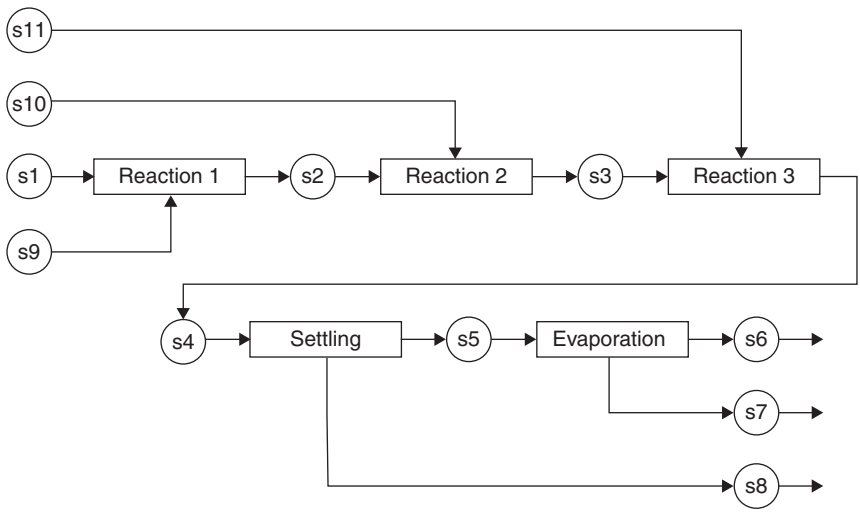

9.25 State task network of industrial case study.

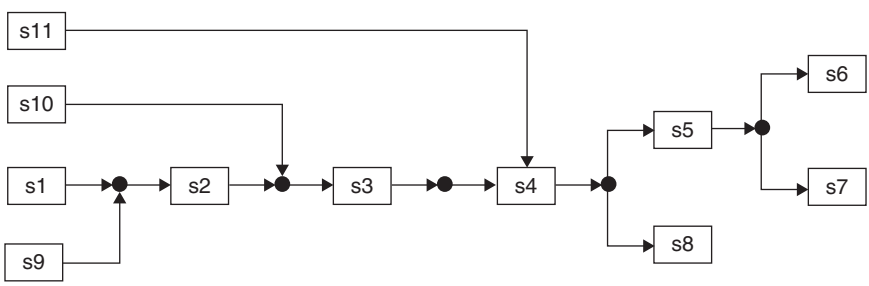

9.26 SSN of industrial case study.

© Woodhead Publishing Limited, 2013

Table 9.8 Scheduling data for industrial case study

Unit	Capacity	Suitability	Mean processing time (h)
R1	10	RX1	2
R2	10	RX1	2
R3	10	RX2, RX3	3, 1
R4	10	RX2, RX3	3, 1
SE1	10	Settling	1
SE2	10	Settling	1
SE3	10	Settling	1
EV1	10	Evaporation	3
EV2	10	Evaporation	3

Table 9.9 Scheduling data for industrial case study

State	Storage capacity (t)	Initial amount (t)	Revenue (cu/t)
s1	Unlimited	Unlimited	0
s2	Unlimited	Unlimited	0
s3	100	0	0
s4	100	0	0
s5	300	0	0
s6	150	50	0
s7	150	50	0
s8	Unlimited	Unlimited	0
s9	150	0	0
s10	150	0	0
s11	Unlimited	Unlimited	0

Table 9.10 Stoichiometric data for industrial case study

State	t/t output	t/t product
s1	0.20	
s9	0.25	
s10	0.35	
s11	0.20	
s7		0.7
s8		1

and third reactions form sodium chloride as a by-product. The intermediate from Reaction 3 is transferred to one of the three Settlers, to separate the sodium chloride from the aqueous solution containing the active ingredient. This process takes one hour. This salt-free solution is then transferred to one of the two Evaporators, where steam (equivalent to 110 kWh) is used

© Woodhead Publishing Limited, 2013

Table 9.11 Heat Integration data for industrial case study

Parameter	Value
Specific heat capacity, c_p (kJ/kg°C)	4.2
Product selling price (cu/t)	10,000
Steam cost (cu/kWh)	20
Cooling Water Cost (cu/kWh)	8
ΔT^{min} (°C)	5
T^L (°C)	20
T^U (°C)	180
W^L (t)	0.2
W^U (t)	1

Table 9.12 Heating/cooling requirements for industrial case study

Reaction	Type	Heating/cooling requirement (kWh)	Operating temperature (°C)
RX2	Exothermic	100 (cooling)	150
Evaporation	Endothermic	110 (heating)	90

to remove excess water from the product, which takes 3 h. This water is discarded as effluent. The final product is collected in storage tanks before final formulation, packaging and transportation to customers.

The temperatures for the exothermic second reaction (150°C) and endothermic evaporation stage (90°C) allow for possible Heat Integration.

Necessary Heat Integration data for the industrial case study may be found in Table 9.11, with heating and cooling requirements summarised in Table 9.12.

Heat Integration in Fig. 9.27 is indicated with arrows. One heat storage unit was used and initially heat losses were not included. Heat is transferred throughout the duration of a task. The heat storage capacity and initial heat storage temperature were optimised. It can be seen from the results that it is possible to reuse energy which was stored previously in the process.

For non-optimal values for the heat storage capacity and initial heat storage temperature, heat was stored, but not reused over the time horizon (Majozi, 2009). The results for different scenarios are summarised in Table 9.13.

The variation in temperature of the heat storage vessel, disregarding heat losses is shown in Fig. 9.28.

The solution procedure as described previously in Fig. 9.18 was used in solving the MINLP problem for the case including heat storage. The result obtained from the linearised model was the same as for the exact model,

© Woodhead Publishing Limited, 2013

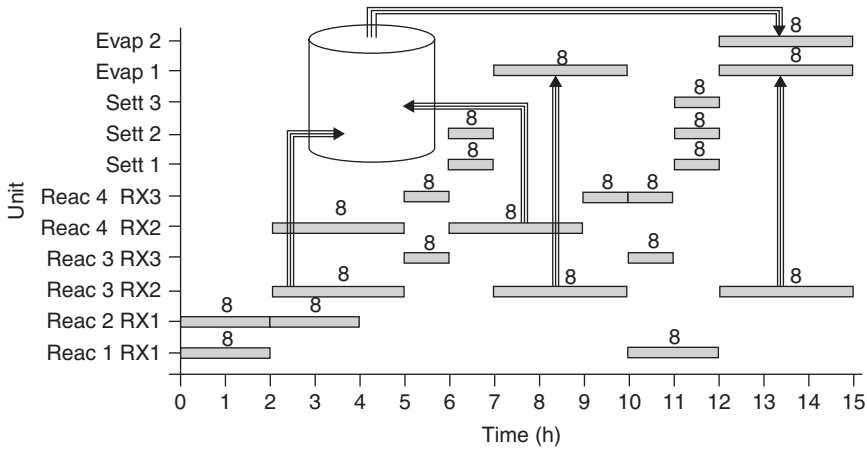

9.27 Schedule shows improvement in energy usage (no heat losses).

Table 9.13 Results for industrial case study (no heat losses)

	No Heat Integration	Direct Heat Integration only	Direct and Indirect Heat Integration (Majozi, 2009)	Direct and Indirect Heat Integration – optimal heat storage capacity
Performance index (cost units)[a]	131,376.471	138,176.471	139,776.471	139,976.471
External cold duty (kWh)	400	300	100	100
External hot duty (kWh)	330	30	30	20
Heat storage capacity (ton)	–	–	2	0.524
Initial heat storage temperature (°C)	–	–	80	54.091
CPU time (s)	–	–	2,805.2	95,396
Binary variables	–	–	–	194
Time points	–	–	–	11

[a] Performance index = Revenue – Utility costs.

meaning the result obtained was globally optimal. CPLEX 9.1.2 was used to solve the linearised model, while DICOPT2 was used in the solution of the MINLP problem with CPLEX 9.1.2 as the MIP solver and CONOPT as the NLP solver in GAMS 22.0. The problem was solved on a Pentium 4, 3.2 GHz processor with 512 MB RAM.

© Woodhead Publishing Limited, 2013

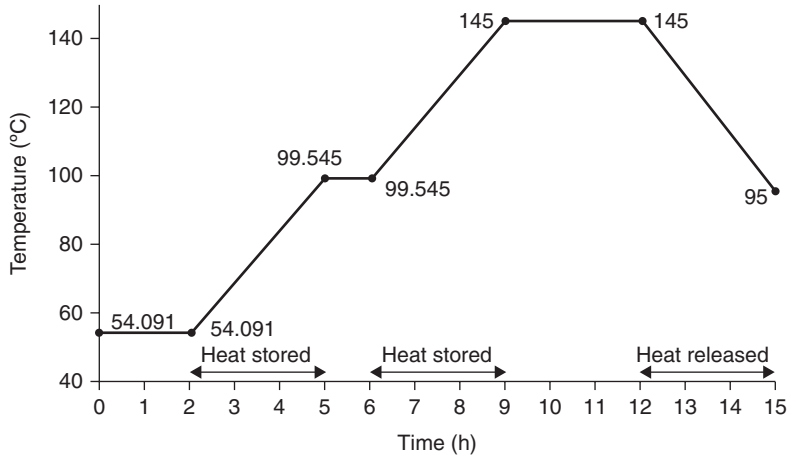

9.28 Temperature variation in heat storage vessel (no heat losses).

Table 9.14 Data for industrial case study with heat losses accounted for

Parameter	Value
Tank wall thickness (mm)	5
Insulation thickness (mm)	30
r_1 (m)	0.5
r_2 (m)	0.505
r_3 (m)	0.535
h_1 (kW/m²°C)	0.1
h_3 (kW/m²°C)	0.02
k_{ves} (kW/m°C)	0.015
k_{ins} (kW/m°C)	0.00005
$T_{\infty_{out}}$ (°C)	20

9.5.1 Heat Loss Considerations

Heat losses from the idle heat storage tank for the industrial case study were included with the parameters in Table 9.14. The time horizon of interest was decreased to 10 h in order to reduce the solution time.

The results may be obtained from Table 9.15.

The Gantt chart for the case where heat losses from the heat storage vessel were considered can be seen in Fig. 9.29.

As can be seen from the results in Table 9.14, the shorter time horizon requires a higher starting temperature when compared to the horizon of 15 h. This is due to the heat storage vessel being unable to receive heat from

© Woodhead Publishing Limited, 2013

Table 9.15 Results for industrial case study with heat losses taken into account

	No heat loss	Heat loss
Performance index (cost units)	46,258.824	46,258.824
External cold duty (kWh)	100	100
External hot duty (kWh)	0	0
Heat storage capacity (t)	0.524	0.530
Height of heat storage vessel (m)	0.667	0.675
Initial Heat Storage temperature (°C)	99.545	100.298

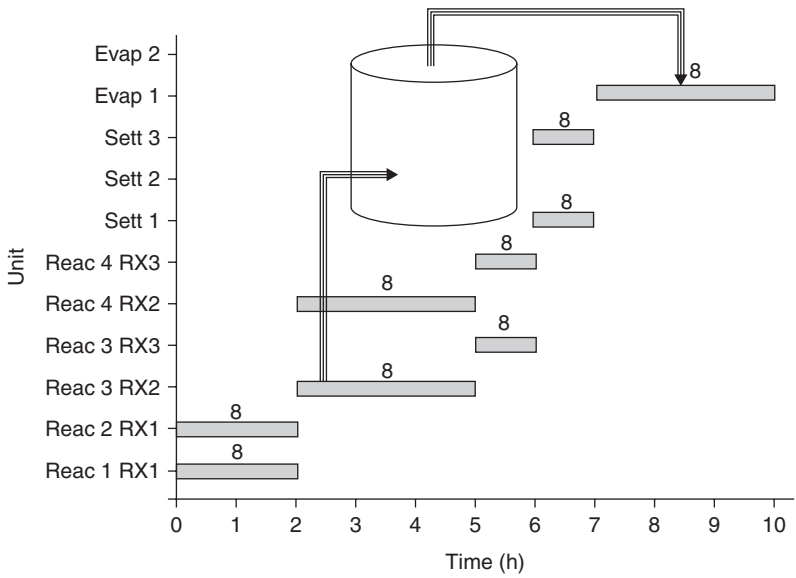

9.29 Optimal schedule over shorter time horizon.

the exothermic reaction twice. However, heat is still able to be transferred to the endothermic evaporation stage. The variation in the temperature of the heat storage vessel with heat losses can be seen in Fig. 9.30.

The heat losses from the heat storage vessel depend on both the initial temperature in the vessel as well as the time over which the vessel is idle. As can be seen from Fig. 9.30, the temperature gradient is steeper from 5–7 h {(145 – 144.438)/2 = 0.281} when compared to 0–2 h, {(100.298 – 100.057)/2 = 0.121} due to the higher initial temperature in the heat storage vessel. The capacity of the heat storage tank as well as the initial temperature were increased when heat losses were considered. The objective function and external hot and cold utility requirements were, however, unaffected.

© Woodhead Publishing Limited, 2013

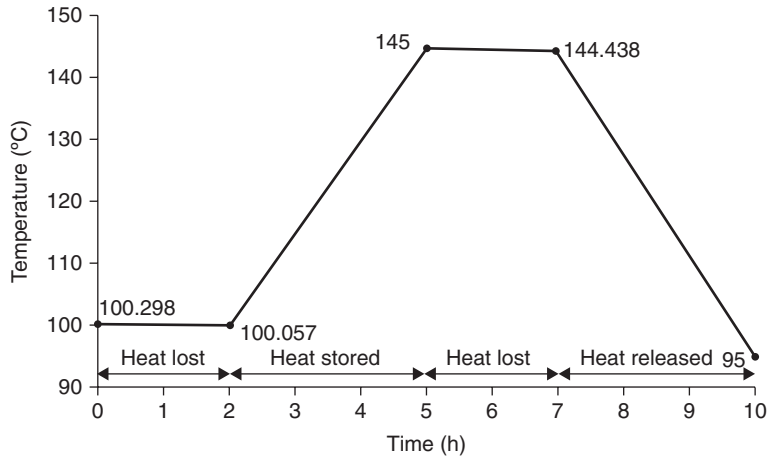

9.30 Temperature variation in Heat Storage vessel with heat losses considered.

The temperature drop due to heat losses may be considered negligible for a well-insulated heat storage vessel over short time horizons if temperatures are low.

9.6 Conclusion

The chapter presents techniques for Heat Integration in batch plants in situations where time is fixed beforehand and situations where time is treated as a variable. Using both direct Heat Integration and indirect Heat Integration, via heat storage, significantly reduces utility needs in a batch-processing Plant. Optimising the size of the heat storage vessel as well as the initial temperature of the heat storage fluid decreased the requirement for external hot utility for an industrial case study by 33% compared to using suboptimal parameters. Also considered in this chapter is stored energy degradation due to heat losses to the environment. The temperature drop of heat storage due to heat losses depends on the temperature in the heat storage vessel due to Newton's law of cooling – a gradient of 0.281 for an initial temperature of 145°C compared to a gradient of 0.121 for an initial temperature of 100.298°C. Heat losses may be considered negligible for a well-insulated vessel over short time horizons if temperatures within storage are low.

9.7 Sources of Further Information

For a detailed background on Process Integration and its application to complex process systems the reader is referred to Smith (2005) and Kemp

© Woodhead Publishing Limited, 2013

(2007). Although these sources are mainly focused on continuous processes, they also cover applications of Process Integration in batch chemical processes and highlight the significance of the time dimension in these operations. Worthy of mention, however, is that these sources focus on graphical analysis, where time is fixed *a priori*, rather than mathematical modelling, where time can be treated as variable.

The only graphical technique that treats time as a variable is that of Adonyi *et al*. (2003) that considers incorporation of Heat Integration in batch-process scheduling using a graph-theoretic framework called the S-graph.

The challenge of integrating non-continuous processes was highlighted by Atkins *et al*. (2010) through a milk powder plant case study.

Other pertinent references that have demonstrated practical applications of Process Integration in batch processes include the works of:

(a) Mignon and Hermia (1993), who used the batch-processing software, so called batches, for modeling and optimizing the brewhouses of an industrial brewery.
(b) Boyadjiev *et al*. (1996) who presented optimal Energy Integration in batch antibiotics manufacture.
(c) De Boer *et al*. (2006) who addressed the aspect of heat storage systems as encountered in an industrial batch processes.
(d) Fritzson, and Berntsson (2006) who presenetd efficient energy use in a slaughter and meat processing plant through exploitation of opportunities for process integration.
(e) Waheed *et al*. (2008) who presented energetic analysis of fruit juice processing operations in Nigeria.
(f) Fadare *et al*. (2010) who presented energy and exergy analysis of malt drink production in Nigeria.
(g) Rašković *et al*. (2010) who presented Process Integration in bioprocess industry and focused on waste heat recovery in yeast and ethyl alcohol plant as well as,
(h) Tokos *et al.* (2010) who explored energy saving opportunities in heat integrated beverage plant retrofit.

9.8 References

Adonyi, R., Romero, J., Puigjaner, L., Friedler, F. (2003). *Applied Thermal Engineering Journal.*

Atkins, M. J., Walmsley, M. R. W., Neale, J. R. (2010). *Journal of Cleaner Production*.

Boyadjiev, C. H. R., Ivanov, B., Vaklieva-Bancheva, N., Pantelides, C. C., Shah, N. (1996). *Computers and Chemical Engineering*.

Chen C. L., Chang C. Y. (2009). A resource-task network approach for optimal short-term/periodic scheduling and heat integration in multipurpose batch plants. *Applied Thermal Engineering*, **29**, 1195–208.

© Woodhead Publishing Limited, 2013

De Boer, R., Smeding, S. F., Bach, P. W. (2006). The Tenth International Conference on Thermal Energy Storage, ECOSTOCK (2006).

El-Halwagi, M. M. (1997). *Pollution Prevention Through Process Integration.* Academic Press, California, USA.

Fadare, D. A., Nkpubre, D. O., Oni, A. O., Falana, A., Waheed, M. A., Bamiro, O. A. (2010). *Energy.*

Fritzson, A., Berntsson, T. (2006). *Journal of Food Engineering*.

Glover, F. (1975). Improved linear integer programming formulations of nonlinear integer problems. *Man Sci*, **22**(4). 455–460.

Halim, I., Srinivasan, R. (2009). Sequential methodology for scheduling of heat-integrated batch plants. *Industrial & Engineering Chemistry Research*, **48**(18), 8551–8565.

Ivanov, B., Peneva, K., Bancheva, N. (1993). Heat integration in batch reactors operating in different time intervals Part 1. A hot-cold reactor system with two storage tanks. *Hungarian Journal of Industrial Chemistry*, **21**, 201–207.

Kemp, I. C. (2007). *Pinch Analysis and Process Integration, Second Edition: A User Guide on Process Integration for the Efficient Use of Energy.* IChemE, UK.

Kemp, I. C., Deakin, A. W. (1989a). The cascade analysis for energy and process integration of batch processes, Part 1. *Chemical Engineering Research and Design*, **67**, 495–509.

Kemp, I. C., Deakin, A. W. (1989b). The cascade analysis for energy and process integration of batch processes, Part 2. *Chemical Engineering Research and Design*, **67**, 510–516.

Kemp, I. C., Deakin, A. W. (1989c). The cascade analysis for energy and process integration of batch processes, Part 3. *Chemical Engineering Research and Design*, **67**, 517–525.

Linhoff, B., Hindmarsh, E. (1983). The Pinch design method for heat exchanger networks. *Chemical Engineering Science*, **38**(5), 745–763.

Linnhoff, B., Townsend, D. W., Boland, D. (1982). *A User Guide to Process Integration for the Efficient Use of Energy.* IChemE, UK.

Majozi, T. (2006). Heat integration of multipurpose batch plants using a continuous-time framework. *Applied Thermal Engineering*, **26**, 1369–1377.

Majozi, T. (2009). Minimization of energy use in multipurpose batch plants using heat storage: an aspect of cleaner production. *Journal of Cleaner Production*, **17**, 945–950.

Mignon, D. and Hermia, J. (1993). *Computers and Chemical Engineering.*

Obeng, E. D. A., Ashton, G. J. (1988). On Pinch Technology based procedures for the design of batch processes. *Chemical Engineering Research and Design*, **66**, 255–259.

Papageorgiou, L. G., Shah, N., Pantelides, C. C. (1994). Optimal scheduling of heat-integrated multipurpose plants. *Industrial & Engineering Chemistry Research*, **33**(12). 3168–3186.

Quesada, I., Grossmann, I. E. (1995). Global optimization of bilinear process networks with multicomponent flows. *Computers & Chemical Engineering*, **19**(12), 1219–1242.

Rašković, P., Anastasovski, A., Markovska, L. J., Meško, V. (2010). *Energy*.

Seid, R., Majozi, T. (2012). A robust mathematical formulation for multipurpose batch plants. *Chemical Engineering Science*, **68**(1), 36–53.

Sherali, H. D., Alameddine, A. (1992). A new reformulation-linearization technique for bilinear programming problems. *Journal of Global Optimization*, **2**(4), 379–410.

Smith, R. (2005). *Chemical Process: Design and Integration*, Wiley.

© Woodhead Publishing Limited, 2013

Sundaramoorthy, A., Karimi, I. A. (2005). A simpler better slot-based continuous-time formulation for short-term scheduling in multipurpose batch plants. *Chemical Engineering Science*, **60**, 2679–2702.
Tokos, H., Pintarič, Z. N., Glavič, P. (2010). *Applied Thermal Engineering*.
Vaklieva-Bancheva, N., Ivanov, B. B., Shah, N., Pantelides, C. C. (1996). Heat exchanger network design for multipurpose batch plants. *Computers & Chemical Engineering*, **20**(8), 989–1001.
Vaselenak, J. A., Grossmann, I. E., Westerberg, A. W. (1986). Heat integration in batch processing. *Industrial & Engineering Chemistry Process Design and Development*, **25**(2), 357–366.
Waheed, M. A., Jekayinfa, S. O., Ojediran, J. O., Imeokparia, O. E. (2008). *Energy*.
Wang, Y. P., Smith, R. (1995). Time Pinch analysis. *Transactions of IChemE*, **73a**, 905–914.

9.9 Appendix: Glover Transformation (Glover, 1975)

From Constraint [9.9],Let

$$T_f(u,p)z(s_{\text{in},j_h},u,p-1) = \Gamma_1(s_{\text{in},j_h},u,p) \qquad [9.A1]$$

With lower and upper temperature bounds known

$$T^L \le T_f(u,p) \le T^U \qquad [9.A2]$$

Then

$$\Gamma_1(s_{\text{in},j_h},u,p) \ge T_f(s_{\text{in},j_h},u,p) - T^U(1-z(s_{\text{in},j_h},u,p-1)) \qquad [9.A3]$$

$$\Gamma_1(s_{\text{in},j_h},u,p) \le T_f(s_{\text{in},j_h},u,p) + T^L(1-z(s_{\text{in},j_h},u,p-1)) \qquad [9.A4]$$

$$\Gamma_1(s_{\text{in},j_h},u,p) \ge z(s_{\text{in},j_h},u,p-1)T^L \qquad [9.A5]$$

$$\Gamma_1(s_{\text{in},j_h},u,p) \le z(s_{\text{in},j_h},u,p-1)T^U \qquad [9.A6]$$

The result from the Glover transformation for Constraint [9.7] is seen in Constraint [9.A7] and includes the addition of one new continuous variable and four new continuous constraints.

$$Q(s_{\text{in},j_h},u,p-1) = W(u)c_p(\Gamma_1(s_{\text{in},j_h},u,p) - \Gamma_2(s_{\text{in},j_h},u,p-1)), \quad \forall p \in P, p > p0, s_{\text{in},j_h} \in S_{\text{in},j}, u \in U \qquad [9.A7]$$

© Woodhead Publishing Limited, 2013

10

Water Pinch Analysis for Water Management and Minimisation: An Introduction

SHARIFAH RAFIDAH WAN ALWI and ZAINUDDIN ABDUL MANAN, Process Systems Engineering Centre (PROSPECT), Faculty of Chemical Engineering, Universiti Teknologi Malaysia, Johor Bahru, Malaysia

DOI: 10.1533/9780857097255.3.353

Abstract: This chapter describes approaches for water management and minimisation based on the Water Pinch Analysis (WPA) concept. The chapter presents the step-wise procedure for implementing WPA. The significance of WPA and its applications in the industrial sector are also discussed.

Key words: Water Pinch Analysis, targeting, network design, water minimisation, water management.

10.1 Approaches for Water Management and Minimisation

Water is a vital resource in industry. It is used for numerous purposes, such as product formulation (as raw material), cleaning, heating and cooling, mass separating agents (MSA), and general plant services (e.g. fire-fighting). Stricter environmental regulations, increases in water tariff and wastewater treatment costs, and shortages of clean water resources have encouraged efforts for water management and minimisation in industry.

Wan Alwi and Manan (2006) introduced the Water Management Hierarchy (WMH) shown in Fig. 10.1 as a guide for holistic water minimisation. The WMH consists of five levels that are arranged from the most preferred option at the top of the hierarchy (level 1) to the least preferred at the bottom (level 5).

Source elimination at the top of the hierarchy is concerned with the complete avoidance of fresh water usage. Sometimes it is possible to eliminate water rather than to reduce, reuse or recycle water. Examples include using alternative cooling media, such as air, instead of water. Even though source elimination is the ultimate goal, often it is not possible to eliminate water completely. An attempt should be made to reduce the amount of water being

© Woodhead Publishing Limited, 2013

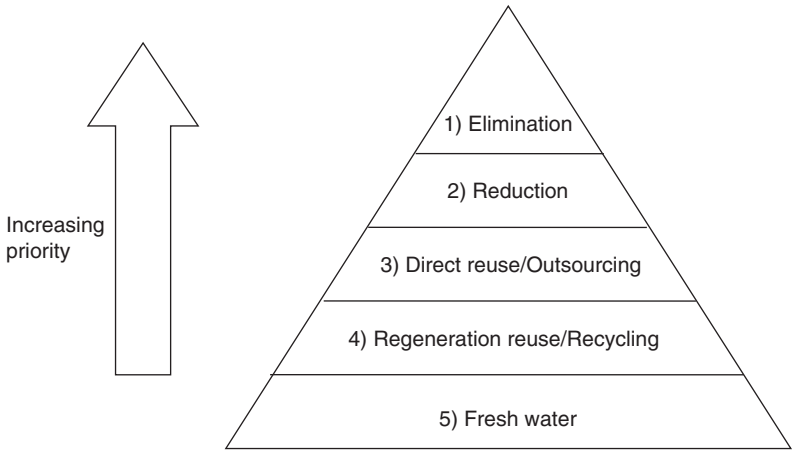

10.1 The WMH (Wan Alwi and Manan, 2006).

used at the source of water usage, e.g., certain equipment or processes. Such a measure is referred to as *source reduction*, and is the second-best option in the WMH (level 2).

When it is not possible to eliminate or reduce fresh water at source, wastewater recycling should be considered. Levels 3 and 4 in the WMH represent two different modes of Water Recycling – *direct reuse/outsourcing* (level 3) and *regeneration reuse/recycling* (level 4). Direct reuse may involve using spent process water directly within the process system subject to its quality being acceptable to operations. Outsourcing involves the use of available external water source e.g. rainwater or river water. Through direct reuse/outsourcing (level 3), spent water or external water source is utilised to perform tasks which can accept lower quality water.

However, in most industrial applications, regeneration (level 4) may be necessary prior to recycling. Regeneration refers to partial treatment of wastewater or even external water source to match the quality of water required for further use. There are two possible cases of regeneration. Regeneration–recycling involves reuse of treated water in the same equipment or process after treatment. Regeneration–reuse involves reuse of treated water in other equipment after treatment. All this can be illustrated in Fig. 10.2.

Fresh water usage (level 5) should only be considered when wastewater cannot be recycled or when wastewater needs to be diluted to obtain a desired purity. Note that wastewater has to undergo *end-of-pipe* treatment before discharge to meet the environmental guidelines. Use of fresh water is the least desirable option from the water minimisation point of view and is

© Woodhead Publishing Limited, 2013

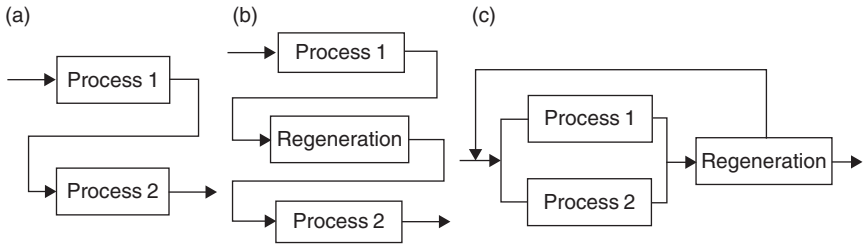

10.2 Categorisation of water reuse/recycling strategies (Wang and Smith, 1994a). (a) reuse, (b) regeneration–reuse and (c) regeneration–recycling.

to be avoided whenever possible. Through the WMH, the use of fresh water may not be eliminated, but it will become economically legitimate.

10.2 Water Integration and Water Pinch Analysis

WPA can be defined as a systematic technique of implementing water minimisation strategy through integration of processes for maximum water efficiency (Manan *et al.*, 2004). In production terms, the 'Pinch' refers to limits on productivity, or 'bottlenecks'. In terms of mass recovery, Pinch occurs at the smallest driving force that limits mass recovery (i.e. the bottleneck for mass recovery).

The fundamental principle of WPA was introduced by Wang and Smith (1994a, 1994b) which was developed based on the general approach of Mass Exchange Network synthesis technique established by El-Halwagi and Manousiouthakis (1989). Water is assumed as a Mass Separating Agent (lean stream) that functions to remove impurities from the rich stream (also known as *fixed flowrate* problem). These include processes such as absorption, solvent extraction and vessel cleaning. In 1996, Dhole *et al.* (1996) introduced a new version of WPA which caters for other water usages, such as water consumed and generated in a reactor, and water losses (also known as the *fixed load* problem). The new version of WPA separates the water sources and demand during data extraction. Since then, WPA techniques have gone through various improvements and extensions from these two angles.

WPA proposes for wastewater to be reused in a process that requires less pure water, instead of being discharged into wastewater treatment. The basic message of WPA is as follows (Tainsh and Rudman, 1999):

> Don't solve an end-of-pipe problem with an end-of-pipe solution. Unless you have explored the in-process solutions, your end-of-pipe solution could be the worst solution of your problem.

© Woodhead Publishing Limited, 2013

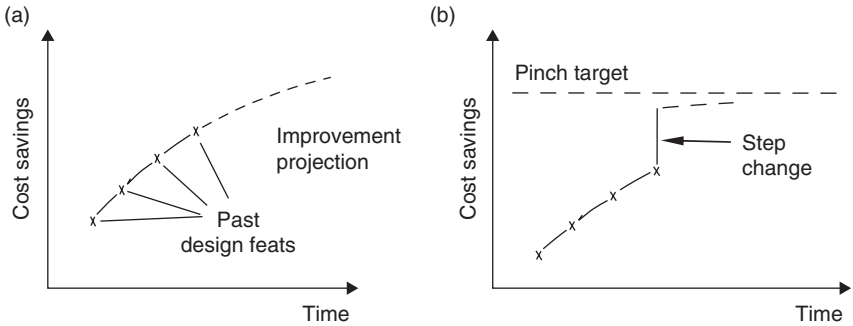

10.3 Pinch Analysis critical success factor – the design targets (Linnhoff, 1986). (a) Design/retrofit based on past performance and (b) design/retrofit based on Pinch targets.

10.2.1 Significance of Water Pinch Analysis

It is generally easy to identify potential design improvements on existing plants and utility systems that can yield good investment paybacks. However, it is difficult to be sure if the proposed schemes are the best for a given process. Quite often a technologist working on an improvement retrofit project is left with the nagging doubt – 'Can I do better?'. Even until today, progress made in-process design has largely been based upon the learning curve as shown in Fig. 10.3a (adapted from Linnhoff, 1996).

A technologist would typically use a previous achievement (e.g. the specific water consumption of a similar plant elsewhere) as a benchmark for improvement. Such a benchmark can be referred to as an *apparent target*, since any improvement is only relative to a previous design achievement. A *true minimum target* should be based on the specific structure, operating conditions and thermodynamics of the plant undergoing retrofit, instead of on the performance of a similar plant built elsewhere. This is where Pinch Analysis has a key advantage. It has been proven useful in representing the overall systems water quality and quantity, and in generating the true water targets and in assessing network inefficiencies.

With the notion of true minimum design targets made available through Pinch Analysis, a technologist would be less likely to settle for a marginal improvement and would strive to achieve the true minimum, hence a step-change in improvement (see Fig. 10.3b (adapted from Linnhoff, 1996)). Promising projects can be conveniently screened from the marginal ones and worthwhile improvements can be quickly assessed simply by comparing the performance gap between an existing design and the one meeting the true minimum target. Knowing the targets and the maximum potential

© Woodhead Publishing Limited, 2013

Table 10.1 Applications of WPA

Company	Process/industry	Location	Flow reduction, %
Confidential	Chemical and fibres	Germany	25
Cerestar	Corn processing	UK	25
Gulf Oil	Oil refining	UK	30
Monsanto	Chemicals	UK	40
Parenco	Paper mill	Netherlands	20
Sasol	Coal chemicals	South Africa	50
Polymers (batch)	UK	60	
US Air Force	Military base	USA	40
Confidential	Oil refining	Netherlands	40
Confidential	Chemicals	USA	40
Confidential	Chemicals and fibres	USA	25
Confidential	Semiconductor	Malaysia	72
Confidential	Chloralkali	Malaysia	7
Confidential	Paper mill	Malaysia	13
Confidential	Beet sugar	Slovenia	69
Confidential	Citrus	Argentina	30

Source: Tainish and Rudman (1999).

savings ahead of design would be vital in steering technologists toward the best achievable network design.

10.2.2 Applications of Water Pinch Analysis

WPA has been proven to give beneficial water savings. Table 10.1 shows some of the savings from WPA applications in industry reported by Tainsh and Rudman (1999) – corn processing, paper mill, coal chemicals, polymers, military base, oil refining, chemicals and fibres, Thevendiraraj *et al*. (2003) – citrus, Zbontar Zverand and Glavič (2005) – beet sugar, Manan *et al*. (2007) – paper mill, Wan Alwi and Manan (2008a) – semiconductor and Handani *et al*. (2010) – chloralkali.

10.3 Water Pinch Analysis Steps

WPA involves five key steps as follows:

(i) Analysis of water network
The first step is to analyse the existing or the base case water network through plant auditing.

(ii) Data extraction
The second step is to identify water sources and water sinks having potential for reuse and recycling and to extract the limiting water flowrate and limiting concentration data. Non-limiting concentrations in

© Woodhead Publishing Limited, 2013

the water system are situated at a concentration below their maximum limits and do not affect the water sink for that operation.

(iii) Setting the minimum utility targets
The third step is to establish the minimum possible quantity of fresh water requirement and wastewater generation, or the minimum water targets using a targeting method.

(iv) Water network design/retrofit
The fourth step is to design a water recovery network to realise the minimum water targets.

(v) Economic evaluation
The final step is to evaluate the economics of the water network.

A detailed explanation of each of the steps is described next.

10.3.1 Step 1: Analysis of Water Network

Good candidates for implementing water-saving projects include process units making high-value products, process units that are large water users, units generating high toxicity waste, plant sites with poor water availability or rising water costs, plant sites undergoing expansion, process units or plant sites with disposal problems, sites with tightening environmental regulations and plants with capacity constraints in their wastewater treatment facilities (Liu *et al.*, 2004).

In implementing WPA for a plant, the overall water network of the plant should first be obtained from process flow diagrams (PFD) and process and instrumentation diagrams (P&ID). A water mass balance is conducted for all the water streams. The mass balance data can be obtained from existing material balances, computer monitoring, routine measurement, previous plant studies and laboratory reports (Liu *et al.*, 2004). Note that in general, water-using operations can be classified into two main categories, i.e., mass-transfer-based (MTB) and non-mass-transfer-based (NMTB) operations as follows (Manan *et al.*, 2004):

Mass-Transfer-Based Operations

An MTB water-using operation is characterised by the preferential transfer of species from a rich stream to water which is being utilised as a lean stream or an MSA (Manan *et al.*, 2004). This can be clearly illustrated by using a mass exchanger block diagram as in Fig. 10.4.

Two major examples of MTB water-using operations are cleaning and absorption processes. Cleaning involves the preferential transfer of species (contaminants) from a 'rich stream' (in this case, the equipment being

© Woodhead Publishing Limited, 2013

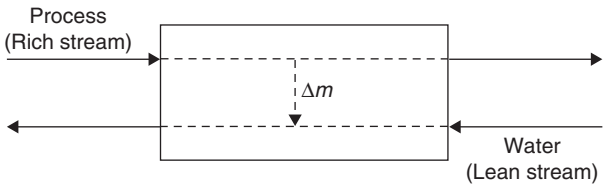

10.4 Transfer of species from a rich to lean stream in a mass exchanger.

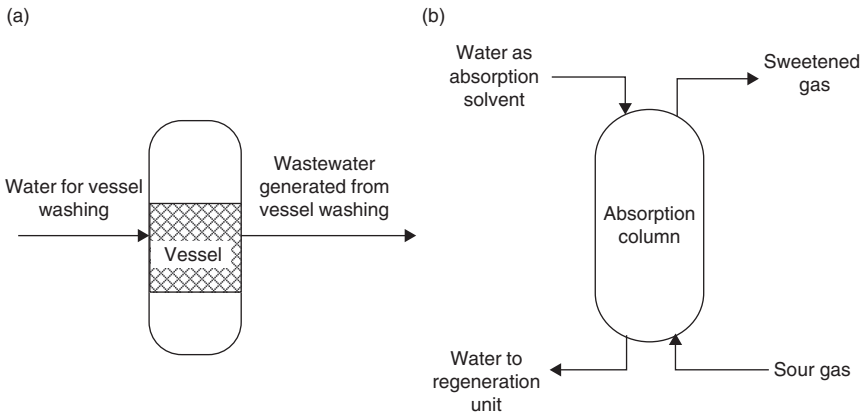

10.5 MTB water-using operations: (a) vessel washing and (b) sour gas absorption where water sink and water source exist (Manan *et al.*, 2004).

washed) to a lean stream or MSA (in this case, water) – Manan *et al.*, 2004. Figure 10.5a shows the water used for the cleaning process (as a sink) and the wastewater generated (as a source). For an absorption process, water is the MSA and is used to remove contaminants such as H_2S and SO_2 from a sour gas stream – see Fig. 10.5b. Note that the input and output flowrates of a mass-transfer process are assumed to be the same. Hence, this type of operation is also known as a fixed flowrate problem.

Non-Mass-Transfer-Based Operations

An NMTB water-using operation covers functions of water other than as an MSA (Manan *et al.*, 2004). An example of such an operation is water being utilised as a heating or cooling medium where there is no mass transfer involved. For such operations, sometimes only water sinks or water sources exist, as shown in Fig. 10.6. Water goes into the system but is lost as it evaporates in Fig. 10.6a. In Fig. 10.6b, water is generated from the

© Woodhead Publishing Limited, 2013

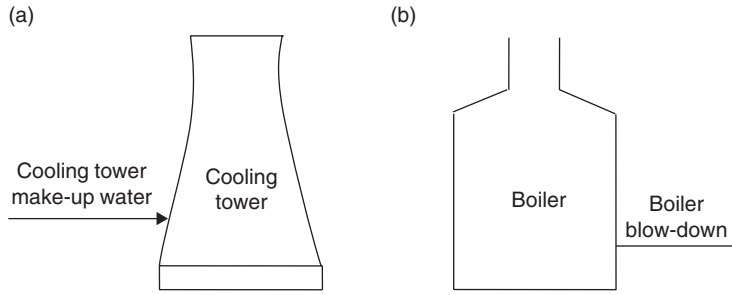

10.6 Two other common types of the NMTB water-using operations: (a) cooling tower make-up and (b) boiler blow-down (Manan *et al.*, 2004).

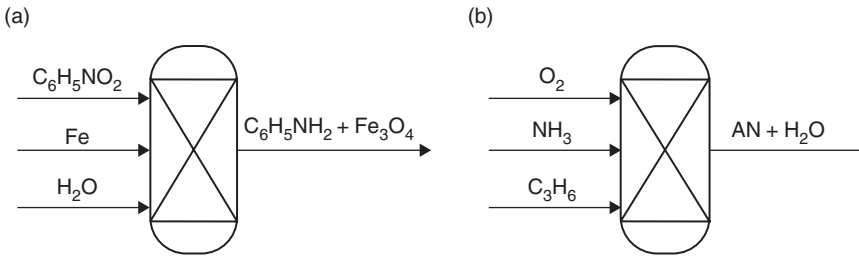

10.7 NMTB water-using operations: (a) a reactor that consumes water in aniline production and (b) a reactor that produces water as a by-product in acrylonitrile (AN) production (Manan *et al.*, 2004).

condensation of steam. Another example is in cases where water is being fed in as a raw material, or being withdrawn as a product or a by-product of a chemical reaction (see Fig. 10.7). Water as a heating/cooling medium and as a raw material fed into a reactor is not intended to preferentially transfer species (contaminants) between streams, hence it clearly represents non-mass-transfer operation. Note that water flowrate is more important than the amount of contaminant accumulated for NMTB water-using operations. For this reason, an NMTB process can have different inlet and outlet flowrates. The NMTB operation is also known as a fixed contaminant load problem.

Next, those water sources and sink streams having the potential to be reused need to be identified. The key contaminants, such as chemical oxygen demand (COD), biological oxygen demand (BOD), total suspended solid (TSS), total organic content (TOC) and total dissolved solid (TDS), that prevent direct reuse in the water systems with its limits into a process and within wastewater effluent has to be identified. The three most important key contaminants are normally chosen.

© Woodhead Publishing Limited, 2013

According to Savelski and Bagajewicz (2000), several measures exist to assess the quality of discharged water. For example, TOC, BOD and COD measurements indicate the organic matter content. Oil and grease (O&G) and total petroleum hydrocarbon (TPH) give a measure of the presence of oil, grease and other hydrocarbons. Several physical characteristics of wastewater include the TSS, pH, temperature, colour and odour (Bagajewicz, 2000).

10.3.2 Step 2: Data Extraction

After analysing the water network, the water processes are grouped into plant sections. Processes chosen are preferably close geographically, and are also chemically related. The main contaminants that prevent direct reuse in the water system are chosen. The system can be modelled either as a single contaminant or a multiple contaminant approach, based on the water quality requirements of the plant processes. However, the problem of multiple contaminants involves complex modelling procedures, and relies on mathematical modelling and optimisation techniques. An alternative is the use of aggregated contaminants, such as suspended solids and TDS, that allow multiple quality factors to be modelled in a single-contaminant approach (The Institution of Chemical Engineers, 2000). The modelling of aggregated contaminants as a single contaminant is known as a pseudo-single contaminant system. The proposed network then needs to be reassessed by checking that all other contaminant concentrations not considered are still within allowable limits before implementation.

The entire water sources and sinks flowrates and quality requirements for each water-using process are extracted. The water sources data are obtained by identifying the maximum concentration limit and the minimum flowrate limit of the wastewater source from each process. The water sinks data are usually obtained from historical variations, emergency water substitution, estimates from engineers, vendors and operators, and description in equipment list (Liu *et al.*, 2004).

10.3.3 Step 3: Setting the Minimum Utility Targets

After extracting the relevant data, water targeting can now be performed. Methods that have been proposed for minimum water targeting are as follows:

(i) Limiting Composite Curves (LCC) by Wang and Smith (1994) – Water-using processes are plotted on a Concentration vs Flowrate diagram. Only applicable for the fixed flowrate problem.

© Woodhead Publishing Limited, 2013

(ii) Water Surplus Diagram (Hallale, 2002) – Water sources and sinks are plotted, separately and on a Concentration vs Flowrate diagram to determine the water surplus and deficit. The water surplus and deficit are then summed to form the Water Surplus Diagram (WSD). The fresh water targets are then predicted by using a trial-and-error method until all the WSD lies on the right-hand side of the y-axis. This method is applicable to both fixed flowrate and fixed load problems.

(iii) Source/Sink Composite Curves (El-Halwagi *et al.*, 2003; Prakash and Shenoy, 2005a) – Water sources and sinks are plotted on a Contaminant mass load vs Flowrate diagram. It was first introduced by El-Halwagi *et al.* (2003) for material recycle/reuse. But later Prakash and Shenoy (2005a) introduced an almost similar method for water systems, which they later claimed had been published earlier in their students' thesis. The Source/Sink Composite Curves overcome the limitation of WSD, which requires two graphs and an iterative process. Applicable for both fixed flowrate and fixed load problem.

(iv) Water Cascade Analysis (WCA) (Manan *et al.*, 2004) – A numerical version of WSD by Hallale (2002) that eliminates the iterative process and provides a more accurate result.

(v) Algebraic Targeting Approach (Al-Mutlaq *et al.*, 2005) – A numerical version of Source/Sink Composite Curves. It uses the load interval diagram.

(vi) Source Composite Curves (Bandyopadhyay, 2006) – A hybrid of the numerical and graphical approaches. They use a cascading approach almost similar to WCA but only requiring single instead of double cascading. The result of the numerical step is then used to plot Source Composite Curves, a plot of Concentration vs Mass load. The plot consists of a Source Composite Curve and a wastewater line. The advantage of this method is that it can predict the average outlet wastewater concentration.

In this chapter, the three most widely used graphical approaches, i.e., LCC, Source/Sink Composite Curves and the numerical approach, WCA, will be described in detail.

Limiting Composite Curve

The LCC was introduced by Wang and Smith (1994a) and is only applicable for MTB operations (or fixed flowrate problem). The LCC is a plot of Contaminant concentrations vs Contaminant mass load. Each water-using process is assumed to have fixed flowrate. There is a transfer of mass load from Process Stream 1 to Process Stream 2, as shown in Fig. 10.4. In the LCC, each process stream that has an inlet contaminant (C_{in}) and outlet

© Woodhead Publishing Limited, 2013

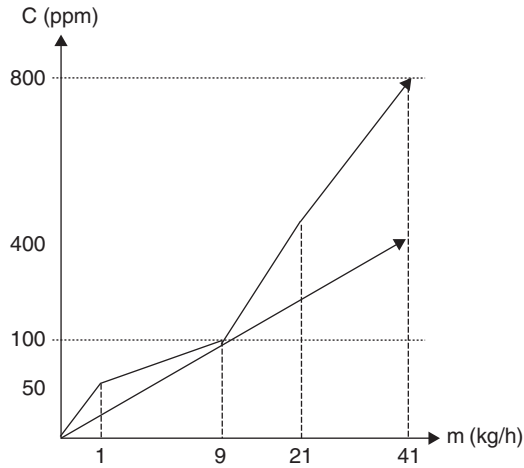

10.8 LCCs (Wang and Smith, 1994a).

contaminant concentration (C_{out}) is plotted on the LCC. The streams are then composited according to the concentration intervals. A limiting Fresh Water Supply Line is drawn starting from zero concentration and mass load with a slope that just touches the Composite Curves at one point (the Water Supply Line has to be located below the Composite Curve). This gives the minimum flowrate target for the system. The point where the supply line and Composite Curve touch is termed the Pinch Point. Figure 10.8 shows the LCC by Wang and Smith (1994a).

Water Cascade Analysis Technique

WCA is a numerical targeting method, with the aim of establishing the minimum water targets, i.e., the overall fresh water requirement and wastewater generation, for a process after looking at the possibility of using available water sources within a process to meet its water sinks. To achieve this objective, the net water flowrate, water surplus and deficit at different water purity levels within the process under study have to be established. Manan *et al.* (2004) introduces the Water Cascade Table (WCT) for this purpose.

A conceptual illustration of how water cascading can minimise fresh water needs and wastewater generation is represented by Fig. 10.9 (Manan *et al.*, 2004). In Fig. 10.9a, 100 kg/s of wastewater is produced by a water source at the purity level of 0.999900 (100 ppm) and 50 kg/s water is needed by a water sink at the purity level of 0.999800 (200 ppm). Without considering water reuse, 100 kg/s of wastewater would be generated while 50 kg/s of fresh water would be required. However, as shown in Fig. 10.9b, by making use of 100 kg/s of the water source at the purity level of 0.999900 (100 ppm)

© Woodhead Publishing Limited, 2013

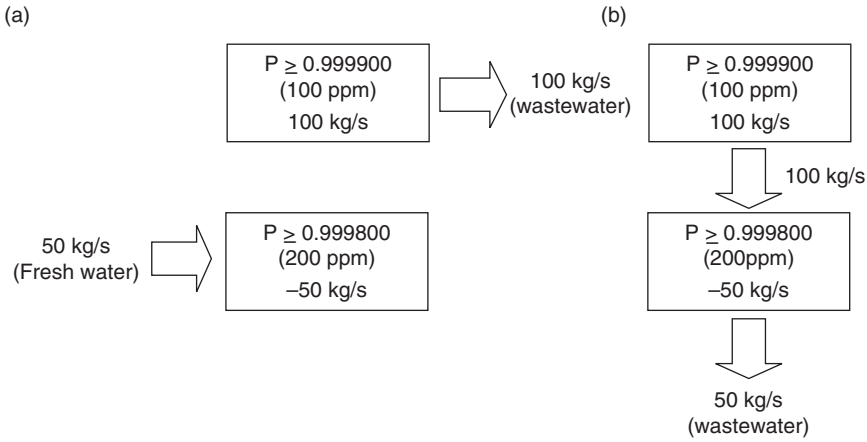

10.9 The principle of water cascading (Manan *et al.,* 2004).

Table 10.2 General structure of a WCT

C	P	ΔP	ΣF_{SKi}	ΣF_{SRj}	$\Sigma F_{SKi} + \Sigma F_{SRj}$	ΣF	$\Delta P \times \Sigma F$	Cumulative $(\Delta P \times \Sigma F)$
			–1.2			$F_{FW} = 2.0571$		
0	10.99999			0.855.9	–0.4			
	0.999986	0.00001	–5.8			1.6571	0.00001657	
10	0.999975				–58			0.00001657
	0.999966	0.000004		1.4		–4.1429	–0.00001657	
14					5			0 (PINCH)
		0.000011				0.8571	0.00000943	
25					5.9			0.00000943
		0.000009				6.7571	0.00006081	
34					1.4			0.00007024
		0.999966				$F_{WW} = 8.1571$	8.15686551	
								8.15693576

Source: Manan *et al.* (2004).

to satisfy the water sink of 50 kg/s at the purity level of 0.999800 (200 ppm), it is possible to avoid sending part of the water source directly to effluent (at $P = 0.999900$). Doing so not only reduces wastewater generation, but also fresh water consumption, in both cases by 50 kg/s.

A general structure of WCT is shown in Table 10.2.

(1) The first step in setting up the WCT is to list all the contaminant concentration (C) of the water-using processes. Remove duplicates (if any) and set up the contaminant concentration intervals in an ascending order, as illustrated in the first column of Table 10.2.
(2) Next, the purity (P) of each contaminant concentration (column 2) is calculated. As the concentration of pure water is one million ppm, the water purity of contaminated stream is defined as:

© Woodhead Publishing Limited, 2013

$$\text{Purity, } P = \frac{1{,}000{,}000 - C}{1{,}000{,}000} \quad [10.1]$$

where:

C = contaminant concentration in ppm.

(3) In the third step, the purity difference (ΔP) is calculated using equation

$$\Delta P = P_n - P_{n+1} \quad [10.2]$$

(4) The flowrate of the all water sinks (F_{SK}) and sources (F_{SR}) are summed at each purity level in the column $\left(\sum_j F_{SK,j}\right)$ and $\left(\sum_j F_{SK,j}\right)$, respectively (for simplicity, all Σ_i will be presented by Σ in the following text). Note that water sinks are written as negative values, while the sources are positive.

(5) Water sinks and sources are summed up in the sixth column ($\Sigma F_{SK,i} + \Sigma F_{SR,j}$) for each different purity level. A positive value in this column signify a net surplus of water present at the respective purity level, while a negative value signify a net deficit of water. Any water sources at higher purity can be used as a source for water sinks with lower purity.

(6) In the column cumulative flowrate (ΣF), water in the sixth column is cascaded. The first row in this column represents the estimated flowrate of fresh water required for the water-using processes (F_{FW}). The estimated fresh water flowrate value will be added to the value in the second row in column ($\Sigma F_{SK,i} + \Sigma F_{SR,j}$) to get the cumulative water flow at its purity level. This cascade process is continued until the last value in column ($\Sigma F_{SK,i} + \Sigma F_{SR,j}$) is added. The total cumulative water flowrate value in the final column represents the total wastewater generated in the process (F_{WW}).

(7) In the next column, the product of the purity difference and cumulative flowrate ($\Delta P \times \Sigma F$) are calculated at every purity level. These values represent the pure water surplus or deficit in each region.

(8) Lastly, the sum of ($\Sigma F \times \Delta P$) down each purity level is obtained. This represents the situation in the WSD. With the assumed fresh water flowrate, a negative value means that there will not be sufficient water purity in the networks. Thus, more fresh water needs to be added until there is no negative value in this column. The minimum fresh water target will be the flowrate that results in zero cumulative water surplus in this column.

(9) In order to ensure that there is sufficient fresh water at all points in the network, a fresh water flowrate (F_{FW}) of exactly the same magnitude as the absolute value of the largest negative $F_{FW,k}$ should be supplied at the highest purity level of a *feasible* water cascade. The zero value that appears is the Pinch Point.

© Woodhead Publishing Limited, 2013

The Water Cascade Diagram is similar to the interval heat balance table for the PTA in Heat Integration (Linnhoff *et al.*, 1982) and the table of exchangeable loads for CIT in Mass Integration (Castro *et al.*, 1999).

Source/Sink Composite Curve

The Source/Sink Composite Curve is used to target the minimum usage of fresh resources for material recycle/reuse network. There are five key steps to constructing the curve in terms of the water system:

1. Rank the sinks in ascending order of maximum allowable contaminant concentration.
2. Rank the sources in ascending order of maximum allowable contaminant concentration.
3. Plot the maximum Mass load of each sink vs its flowrate. Create a Sink Composite Curve by superimposing the sink arrows in ascending order.
4. Plot the Mass Load of each source vs its flowrate. Create a Source Composite Curve by superimposing the sources in ascending order. This is as shown in Fig. 10.10a.
5. Shift the source composite stream until it touches the sink composite stream, with the Source Composite Curve located below the Sink Composite Curve in the overlapped region. The Pinch is where the two Composite Curves touch. The minimum fresh water target is that flowrate of sinks below which there are no sources on the left-hand side. The minimum wastewater generation target is the flowrate of sources above which there are no sinks on the right-hand side. This is illustrated in Fig. 10.10b.

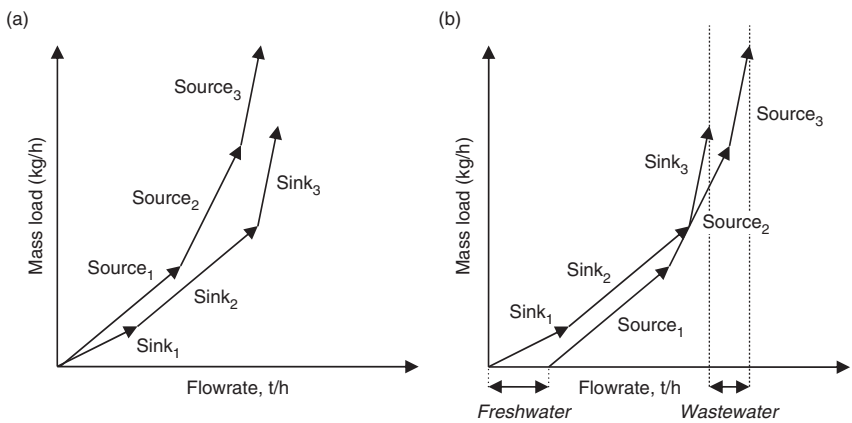

10.10 Source/sink Composite Curve. (a) Before shifting source composite and (b) after shifting source composite (El-Halwagi *et al.*, 2003).

© Woodhead Publishing Limited, 2013

After targeting, the next step is to consider process modifications. Process modifications are changes made to the individual water-using operations to modify either the flowrates or concentrations of water sources or sinks (Hallale, 2002). The appropriate steps to modify a process depend on the location of the water sources and sinks relative to the Pinch Point of the system. The process modification heuristics are as follows:

(a) Above the Pinch – Beneficial changes can be achieved by either increasing the flowrate or water purity of a source or by decreasing the flowrate or water purity requirements of a sink. These changes will have the effect of increasing the water surplus Above the Pinch, and thus the amount of fresh water required will be reduced.
(b) Below the Pinch – There is already a surplus of water Below the Pinch; hence, any flowrate changes made there will not affect the target. An exception to this rule of thumb is for the case where source purity is increased so that it moves to the region Above the Pinch, as in the case of regeneration.
(c) At the Pinch Point – Increasing the flowrate of the source at the Pinch concentration will not reduce the targets.

To date, only two possible scopes for process modifications to further reduce the water targets, and hence, water consumption, have been explored. These are water regeneration and equipment (hardware) modifications (El-Halwagi, 1997; Hallale, 2002). El-Halwagi (1997) proposes a targeting technique involving water elimination, segregation, recycle, interception and sink/source manipulation. Hallale (2002) introduced guidelines for reduction and regeneration based on WPA. The following are further explanations on equipment (hardware) modifications and regeneration:

(a) Equipment (hardware) modifications
Equipment is usually modified in order to eliminate or reduce water-using operations. Water elimination may involve eliminating one of the water sinks, for example using alternative cooling media, such as air instead of water. Water reduction involves changing the process equipment into one that uses less water, for example a water-saving toilet flushing system. These will reduce the water sink flowrate.
(b) Water regeneration
Water regeneration involves the partial or total upgrading of water purity using purification techniques such as filtration, gravity settling, activated carbon, membranes and biological treatment. Regenerated water source will have a higher water quality. Regeneration techniques can be used in isolation or combination, for example filtration might be essential before a membrane to prevent membrane fouling. To increase

© Woodhead Publishing Limited, 2013

water availability, Hallale (2002) proposed the use of Water Composite Curves and the Pinch purity to guide the regeneration of water sources as follows:

1. *Regeneration Above the Pinch*: water source(s) in the region Above the Pinch are partially treated to upgrade water purity.
2. *Regeneration Across the Pinch*: water source(s) in the region Below the Pinch are partially treated to achieve purity higher than the Pinch purity.
3. *Regeneration Below the Pinch*: water source(s) in the region Below the Pinch are partially treated to upgrade purity. However, the resulting water source is still maintained Below the Pinch.

Note that, regeneration above and across the Pinch will reduce fresh water consumption and wastewater generation, while regeneration Below the Pinch will only reduce wastewater generation.

Wan Alwi and Manan (2008a) developed a method known as Cost Effective Minimum Water Network (CEMWN) to systematically and cost effectively apply WPA within the context of the WMH (Fig. 10.1). This method uses a screening technique known as Systematic Hierarchical Approach for Process Screening (SHARPS) to screen various process options to meet a desired payback period.

10.3.4 Step 4: Water Network Design/Retrofit

For water recovery network, there are three important heuristics:

- **Heuristic 1:** Do not feed water sources Above the Pinch (including fresh water) to sinks Below the Pinch and vice versa (Hallale, 2002).

  It has to be noted that in order to achieve fresh water and wastewater flowrate targets, it is necessary to observe the Pinch division. The water sources Above the Pinch (including fresh water) may not feed sinks Below the Pinch and may not mix with sources that are Below the Pinch concentration and vice versa.
- **Heuristic 2:** Start the source–sink matching process with the sink at the lowest contaminant concentration (Polley and Polley, 2000).

  After all the sinks and sources have been separated according to the Pinch Division (Above and Below Pinch Concentration), the source–sink matching process is carried out. All the sinks and sources in the water utilisation network will be mixed according to their contaminant constraints. This means that the sink with the lowest contaminant concentration is first matched with the source with the lowest contaminant concentration. The quantity of water from the contaminated source that will be required to provide the contamination load

© Woodhead Publishing Limited, 2013

associated with the sinks is determined by mass load contamination, Δm, for each sink. Contamination load for an operation, i can be calculated as follows:

$$F(t/h) = \frac{\Delta m_i\,(\text{kg/h})}{\Delta C_i\,(\text{ppm})} \times 1{,}000 \qquad [10.3]$$

- **Heuristic 3:** Map the available sources one after the other, and add fresh water as required, to each sink according to heuristic 2 until all sinks have been satisfied in terms of both quality (contaminant load) and quantity (flowrate) (see Manan *et al.* (2005)).

Polley and Polley (2000) proposed a design principle regarding the systematic mixing of source streams with each other and, where necessary, with fresh water to produce streams to just meet the targets of the individual sinks in terms of both quantity and quality. The quantity of water from the contaminated source is determined by calculating the contaminant load associated with the sink. The result takes one of the following forms:

(a) If this quantity is equal to the required value, then no fresh water needs to be supplied.
(b) If the quantity is less than the sink, then some fresh water is required.
(c) If the quantity required from the source exceeds the sink, then part of the sink's contaminant load should be satisfied using a source having a higher contaminant concentration.

Constraints for network design between water sources i and sink j are given as follows (Halale, 2002):

(a) Sinks
  (i) Flowrate

$$\sum_i F_{i,j} = F_{\text{SK},j} \qquad [10.4]$$

where F_i is the total flowrate available from source i to Sink j.
Where $F_{\text{SK},j}$ is the flowrate required by sink j.

  (ii) Concentration

$$\frac{\sum_i F_{\text{SR}i,\text{SK}j} C_i}{\sum_i F_{\text{SR}i,\text{SK}j} C_i} \le C_{\max,\text{SK}j} \qquad [10.5]$$

© Woodhead Publishing Limited, 2013

where C_{SKj} is the contaminant concentration of source i and $C_{max,SKj}$ is the maximum acceptable contaminant concentration of sink j. The constraints can be written in terms of water purity, in which case the inequality sign would be reversed.

(b) Sources

(i) Flowrate

$$\sum_i F_{SRi,SKj} \leq F_{SRi} \qquad [10.6]$$

Based on these guidelines, a water network can be constructed using the Source–Sink Mapping Diagram method introduced by Polley and Polley (2000) or Source and Sink Allocation Curves by El-Halwagi *et al*. (2003).

(i) Source–Sink Mapping Diagram

All the water sinks are aligned horizontally at the top while all water sources are lined up vertically on the left-hand side (as in Fig. 10.11). Both are arranged according to increasing contaminant concentration.

Figure 10.11 shows one possible network design generated by the source–sink mapping. It is emphasized that this is only one of many possible solutions that can achieve the targets. The designers can influence the solution by imposing other constraints, such as forbidden or forced connection, for safety or economic reasons. However, these additional constraints may sometimes result in a water penalty.

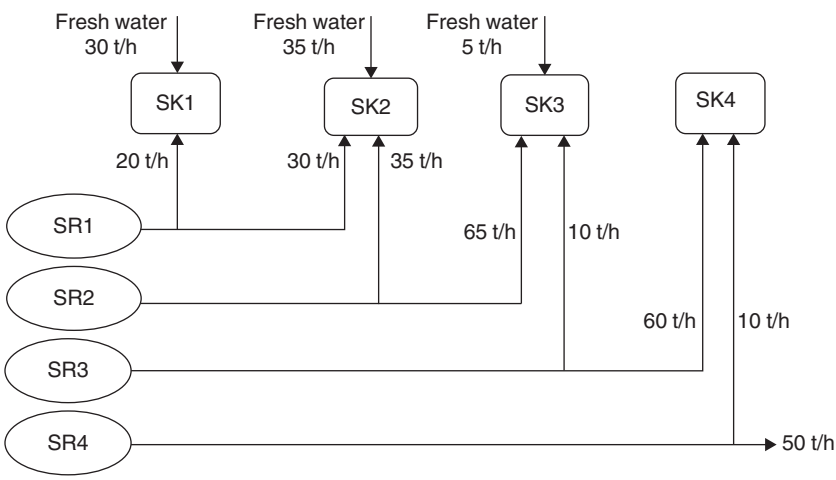

10.11 Network design by source-sink mapping diagram (Polley and Polley, 2000).

© Woodhead Publishing Limited, 2013

(ii) Source and Sink Allocation Composite Curves

Source and Sink Allocation Composite Curves can be used to show the water network allocation or design between the source and sink. In constructing a Source and Sink Allocation Composite Curve, El-Halwagi *et al.* (2003) proposed the following steps where the authors assumed fresh water has zero mass load:

(1) Satisfy a sink using the water sources. If the sink mass load is met but not the flowrate, add fresh water. For example, in Fig. 10.12, Sink 1 (SK_1) Flowrate can be satisfied by part of Source 1 ($F_{SR1,SK1}$) and also by Freshwater Flowrate of $F_{FW,SK1}$. The mass load is fulfilled by $m_{SR1,SK1}$ and $m_{FW,SK1}$. Sink 2 (SK_2) Flowrate is satisfied by the remainder of Source 1 ($F_{SR1,SK2}$), part of Source 2 ($F_{SR2,SK2}$) and fresh water ($F_{FW,SK2}$).
(2) The procedure is repeated until all sinks have been satisfied by the available sources and fresh water. The mass load allocation for each sink is as shown on the y-axis of the graph, and the flowrate allocation is represented on the x-axis.

The source–sink allocation method by El-Halwagi *et al.* (2003) uses a concept similar to Polley and Polley (2000), who proposed that the cleanest source be

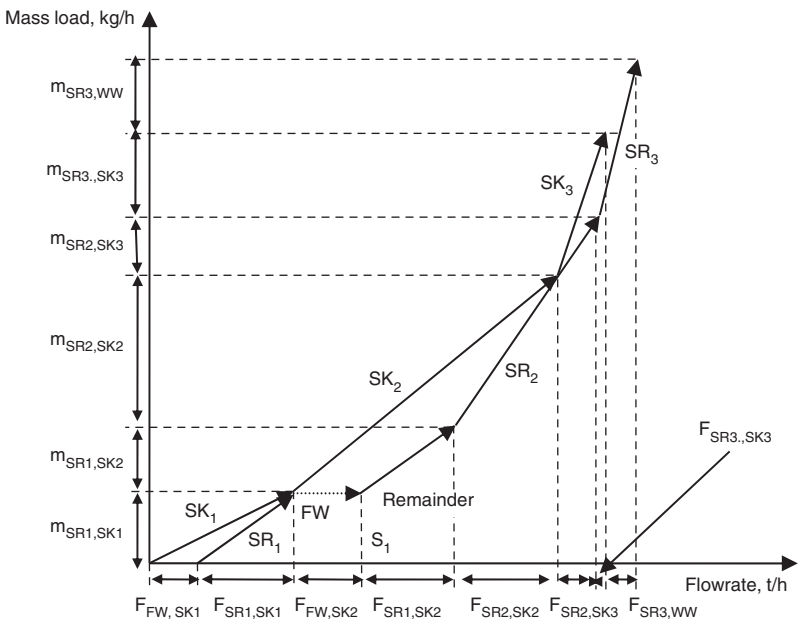

10.12 Source and sink allocation using composite curves by El-Halwagi *et al.* (2003) for freshwater with zero mass load.

© Woodhead Publishing Limited, 2013

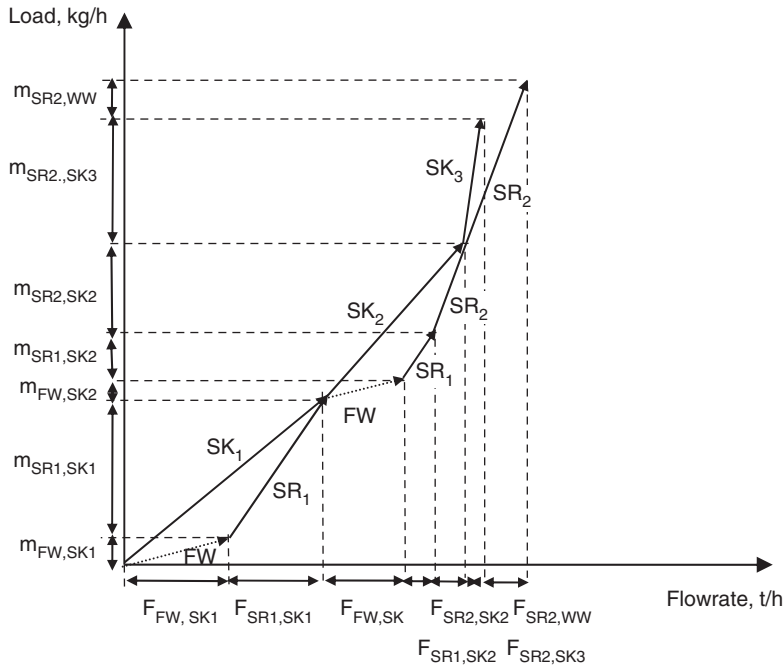

10.13 Source-sink allocation using Composite Curve by Kazantzi and El-Halwagi (2005) for freshwater with non-zero mass load and superior than other streams.

reused first to satisfy the cleanest sink. If the quality of the sink has not yet been met, but the quantity has, fresh water is added. The same illustration was shown by Kazantzi and El-Halwagi (2005) for fresh water with non-zero mass load and superior to other streams as shown in Fig. 10.13.

The cleanest-to-cleanest matching rule used by Polley and Polley (2000), El-Halwagi *et al*. (2003) and Kazantzi and El-Halwagi (2005) was later found by Wan Alwi and Manan (2008b) to only cater for the '*flowrate deficit case*', i.e., the case where the mass load of a sink is satisfied but not its flowrate as shown in Fig. 10.14a. There is another important case which is the '*mass load deficit case*', where the source(s) meet(s) only the flowrate of a sink but not the mass load (see Fig. 10.14b). The cumulative water sources below and between Pinch regions have to exactly have the same flowrate and mass load as the cumulative sink. Note that using the cleanest source that does not meet the mass load of a sink results in an excess mass load of source and ultimately an unsatisfied flowrate for subsequent sinks. Hence, Wan Alwi and Manan (2008a) have introduced another rule for the '*mass load deficit case*', which is to satisfy the mass load and flowrate of a sink using the cleanest as well as the dirtiest sources in the Pinch region and making

© Woodhead Publishing Limited, 2013

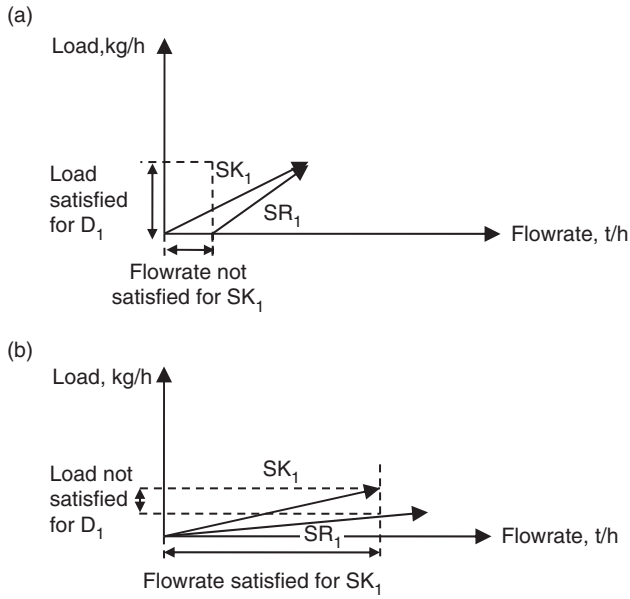

10.14 Satisfying the cleanest sink with cleanest water source using source-sink allocation Composite Curve (a) flowrate deficit case and (b) mass load deficit case (Wan Alwi and Manan, 2008b).

sure the Pinch Point and the utility targets are satisfied. The authors also introduced the Network Allocation Diagram (NAD), which translates the Source and Sink Allocation Composite Curves into a network mapping diagram for easy visualisation, as shown in Fig. 10.15.

10.3.5 Step 5: Economic Evaluation

Most authors resort to complex mathematical modelling in order to calculate the network cost, going into detailed piping routing, geographical constraints, and associated fixed and variable costs. For preliminary economic calculations, the payback period is widely used as a criterion to assess the feasibility of a proposed network solution. The payback period is calculated using the Equation [10.7]. Net capital investment is the investment needed for pipe rerouting, pumping, storage tanks for intermittent processes, and control systems. The net annual savings is the amount of savings that results from fresh water reductions.

$$\text{Playback period (years)} = \frac{\text{Net Capital Investment}(\$)}{\text{Net Annual Savings}(\$/\text{y})} \qquad [10.7]$$

© Woodhead Publishing Limited, 2013

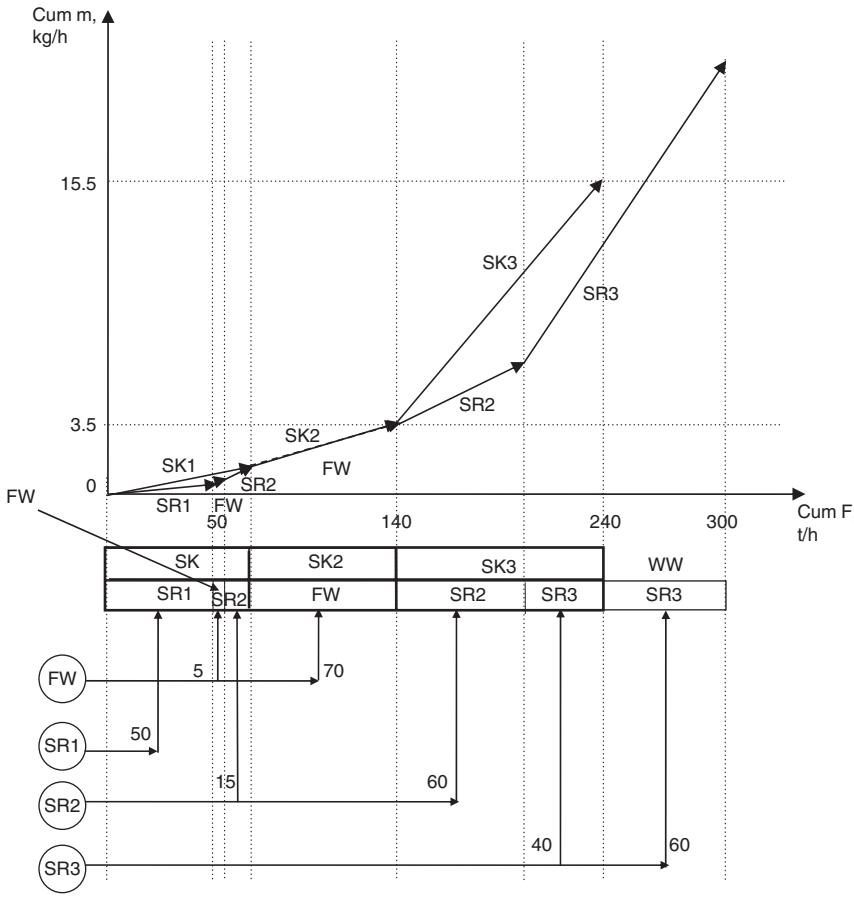

10.15 NAD (Wan Alwi and Manan, 2008b).

10.4 Examples of Successful Case Studies

WPA has been implemented in various industries which consume a high amount of fresh water and produce wastewater, such as semiconductor, chloralkali, paper mill, palm oil, refinery and food industries. An example of an application of WPA on a tyre-to-fuel case study, described by Noureldin and El-Halwagi (1999), is illustrated next.

10.4.1 Case study: Tyre-to-Fuel Process

Figure 10.16 shows a tyre-to-fuel process (Noureldin and El-Halwagi, 1999). Scrap tyres are converted into gaseous and liquid fuel via a pyrolysis

© Woodhead Publishing Limited, 2013

© Woodhead Publishing Limited, 2013

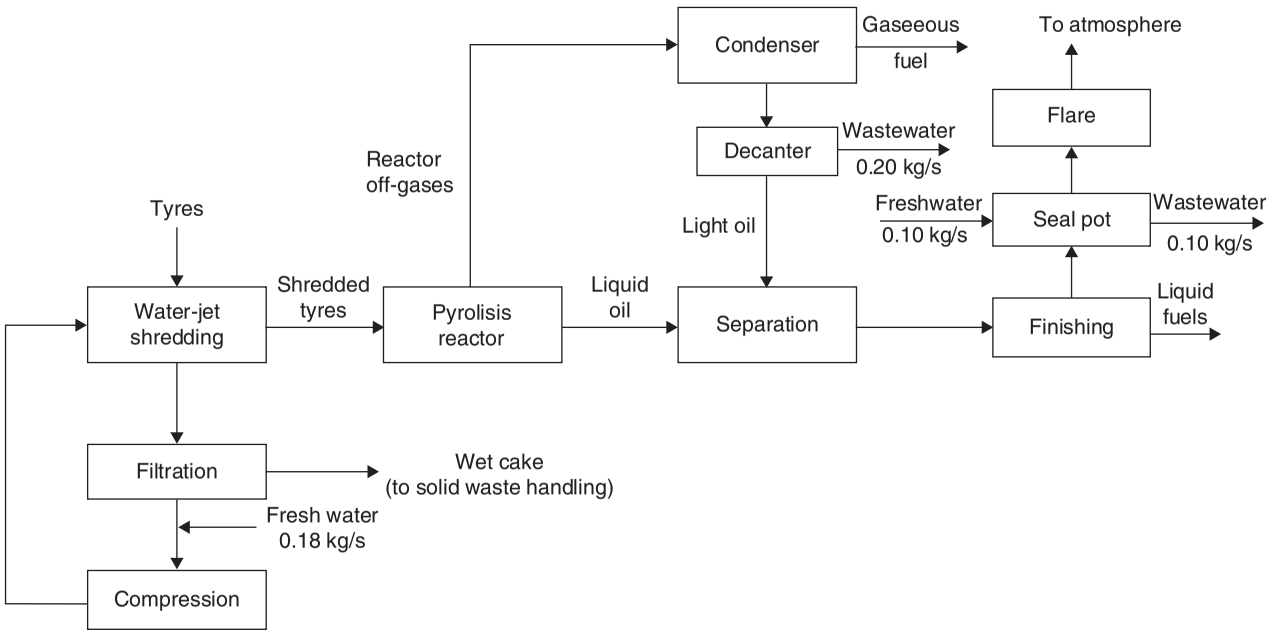

10.16 Tyre-to-fuel process (Noureldin and El-Halwagi, 1999).

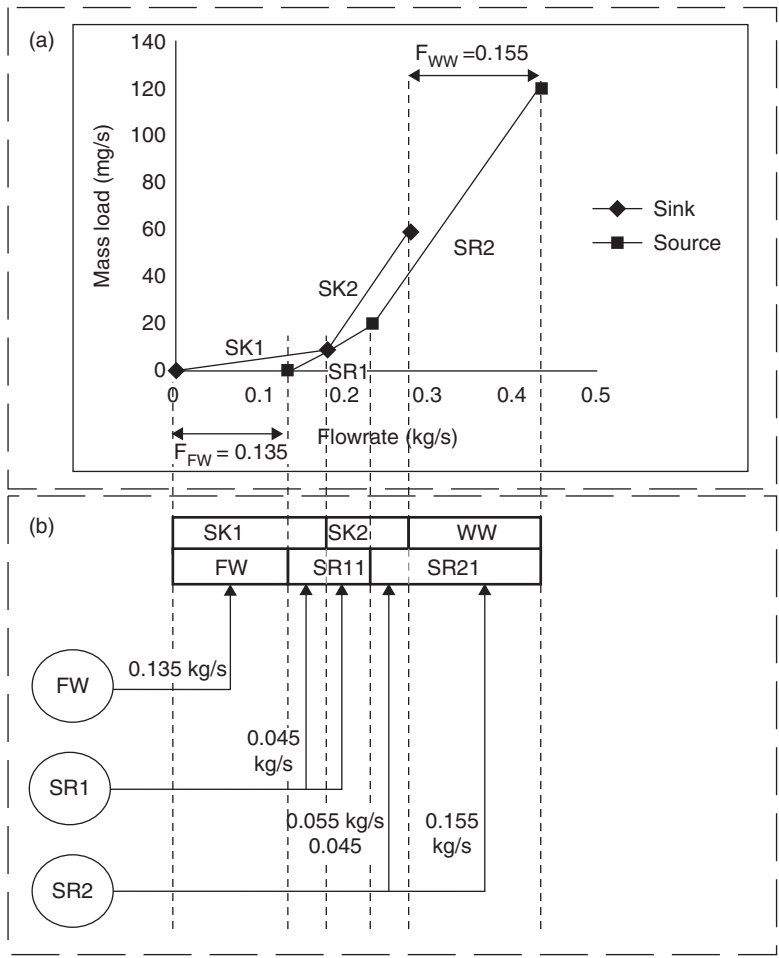

10.17 (a) Source/sink allocation curve and (b) NAD.

Table 10.3 Limiting water data for tyre-to-fuel case study

SK_j	Sinks	F_{SKj} (kg/s)	C_{SKj} (ppm)	m (mg/h)
SK1	Water-jet make-up	0.18	50	9
SK2	Seal-pot feed water	0.1	500	50
SR_i	Sources	F_{SRi} (kg/s)	C_{SRi} (ppm)	m (mg/h)
SR1	Seal-pot wastewater	0.1	200	20
SR2	Decanter wastewater	0.2	500	100

Source: Klemes *et al*. (2010).

© Woodhead Publishing Limited, 2013

© Woodhead Publishing Limited, 2013

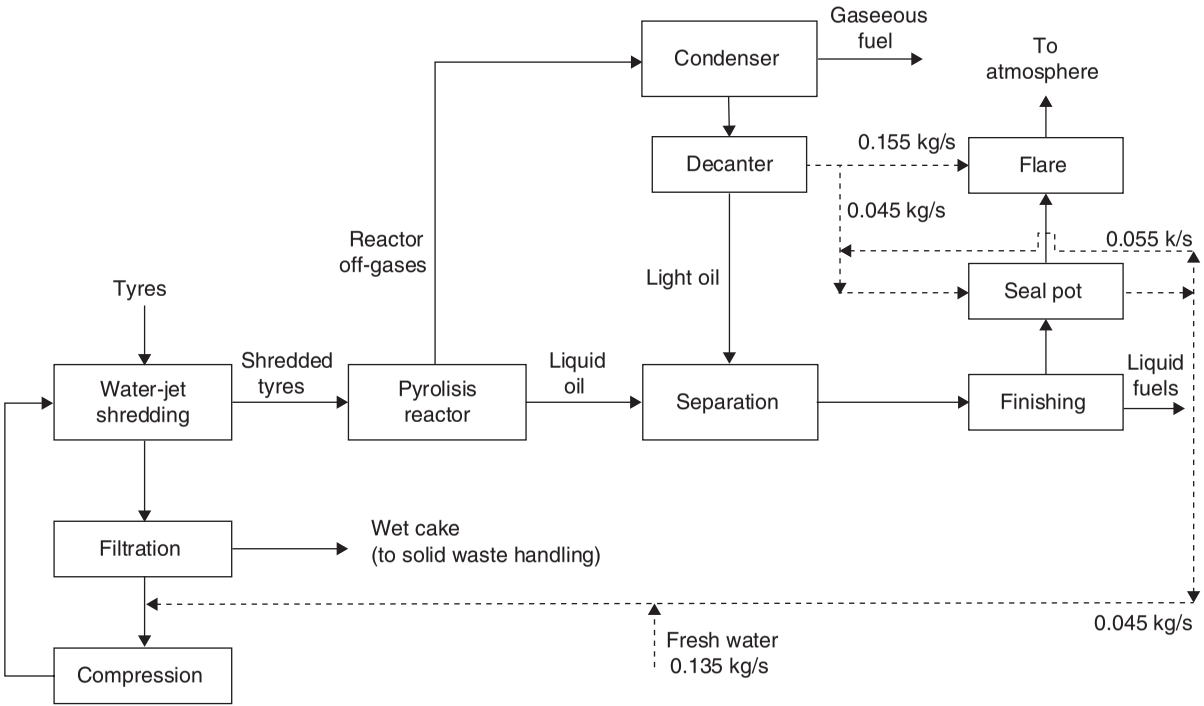

10.18 Tyre-to-fuel process after water recovery.

reaction. From the process, it can be observed that there are two wastewater streams with potential as water sources, i.e., effluent from decanter and seal pot, and two water sinks, i.e., seal pot and water-jet compression station. Heavy organic content was identified as the main contaminant concentration for this process. The following flowrate and contaminant concentration constraints were identified for the water sinks:

(i) Seal pot:
$0.10 \leq$ Flowrate of feed water (kg/s) ≤ 0.20
$0 \leq$ Impurity concentration of feed water (ppm) ≤ 500
(ii) Make-up to water-jet compression station:
$0.18 \leq$ Flowrate of feed water (kg/s) ≤ 0.20
$0 \leq$ Impurity concentration of make-up water (ppm) ≤ 50

On the other hand, the water sources have the following operating condition:

(i) Decanter:
Wastewater flowrate = 0.20 kg/s
Impurity concentration = 500 ppm
(ii) Seal pot:
Wastewater flowrate = flowrate of its water sink
Impurity concentration = 200 ppm

As described in Section 10.3.2, the maximum contaminant concentration and the minimum flowrate should be selected for the limiting water data. The limiting water data for this process are summarised in Table 10.3. Figure 10.17a shows the Source–Sink Composite Curve which gives the minimum Fresh Water flowrate (F_{FW}) of 0.135 kg/s and minimum Wastewater flowrate (F_{WW}) of 0.155 kg/s. This represents a significant flow reduction of 51.8% and 48.3% for fresh water and wastewater. Since this is a very simple problem, the same Fig. 10.17a also represents the Source/Sink Allocation Curve. The picture below the curve (Fig. 10.17b) shows the NAD for the process. The final network is illustrated in Fig. 10.18.

10.5 Sources of Further Information and Advice

The following is a list of suggested books which provide good reviews on the fundamentals of WPA:

El-Halwagi, M. M. (1997). *Pollution Prevention through Process Integration: Systematic Design Tools*. Academic Press, San Diego, USA.

© Woodhead Publishing Limited, 2013

Klemeš, J., Smith, R., Kim, J.-K. (eds) (2008). *Handbook of Water and Energy Management in Food Processing*. Woodhead Publishing Limited, Cambridge, England, **195** (4): 1029. ISBN 1 84569.

Klemeš, J., Varbanov, P., Lam, H. L. (2009). Water footprint, water recycling and food industry supply chain. In: Waldron, K. (ed), *Waste Management and Co-product Recovery in Food Processing*. Vol 2, Woodhead Publishing Limited, Cambridge, **391**(6): 134–168. ISBN: 978-1-84569.

Klemeš, J., Friedler, F., Bulatov, I., Varbanov, P. (2010). *Sustainability in the Process Industry: Integration and Optimization*. McGraw-Hill Professional, New York USA.

Klemeš, J., Lam, H. L., Foo, D. C. Y. (2010). Water recycling and recovery in food and drink industry. In: Waldron, K., Moates, G. K., Faulds, C. B. (eds), *Total Food, Sustainability of the Agri-Foot Chain*. Royal Society of Chemistry, Cambridge, 186–195.

Klemeš. J., Perry, S. J. (2007). Process optimisation to minimise water use and wastage. In: Waldron, K. (ed), *Waste Management and Co-product Recovery in Food Processing*. Woodhead Publishing Limited, Cambridge, 90–118.

Linnhoff, B., Towsend, D. W., Boland, D., Hewitt, G. F., Thomas, B. E. A., Guy, A. R., Marsland, R. H. (1994). *A User Guide on Process Integration for the Efficient Use of Energy*. The Institution of Chemical Engineers, Rugby, UK.

Smith, R. (2005). *Chemical Process Design and Integration*. John Wiley & Sons, Ltd., UK.

For more information on the history of WPA development, the following references are highly recommended:

Foo, D. C. Y. (2009). State-of-the-art review of pinch analysis techniques for water network synthesis. *Industrial and Engineering Chemistry Research* **48** (11), 5125–5159.

Jeżowski, J. (2010). Review of water network design methods with literature annotations. *Industrial and Engineering Chemistry Research* **49** (10), 4475–4516.

Klemeš, J. J. (2012). Industrial water recycle/reuse. *Current Opinion in Chemical Engineering* **1** (3): 238–245.

10.6 References

Alva-Argáez, A., Vallianatos, A., Kokossis, A. (1999). A multi-contaminant transhipment model for mass exchange networks and wastewater minimisation problems. *Computers and Chemical Engineering*, **23**, 1439–1453. DOI: 10.1016/S0098–1354(99)00303–8.

Almutlaq, A. M., Kazantzi, V., El-Halwagi, M. M. (2005). An algebraic approach to targeting waste discharge and impure fresh usage via material recycle/reuse networks. *Cleaner Technology and Environmental Policy*, **7** (4), 294–305.

Bagajewicz, M. J., Rivas, M., Savelski, M. J. (2000). A robust method to obtain optimal and sub-optimal design and retrofit solutions of water utilization systems with multiple contaminants in process plants. *Computers and Chemical Engineering*, **24**, 1461–1466.

Bandyopadhyay, S. (2006). Source composite curve for waste reduction. *Chemical Engineering Journal*, **125** (2), 99–110.

© Woodhead Publishing Limited, 2013

Dhole, V. R., Ramchandani, N., Tainsh, R. A., Wasilewski, M. (1996). Make your process water pay for itself. *Chemical Engineering*, **103**, 100–103.

El-Halwagi, M. M. (1992). Synthesis of reverse osmosis networks for waste minimisation. *AIChE Journal*, **38** (8), 1185–1198. DOI: 10.1002/aic.690380806.

El-Halwagi, M. M. (1997). *Pollution Prevention Through Process Integration: Systematic Design Tools*, San Diego, California, USA: Academic Press.

El-Halwagi, M. M., Manousiouthakis, V. (1989). Synthesis of mass-exchange networks. *AIChE Journal*, **35** (8), 1233–1244. DOI: 10.1002/aic.690350802.

El-Halwagi, M. M., Gabriel, F., Harell, D. (2003). Rigorous graphical targeting for resource conservation via material recycle/reuse networks. *Ind. Eng. Chem. Res*., **42**: 4319–4328. DOI: 10.1021/ie030318a.

Hallale, N. (2002). A new graphical targeting method for water minimization. *Advances in Environmental Research*, **6** (3), 377–390. DOI: 10.1016/S1093-0191(01)00116-2.

Kazantzi, V., El-Halwagi, M. M. (2005). Targeting material reuse via property integration. *Chemical Engineering Progress*, **101** (8), 28–37.

Klemeš, J., Dhole, V. R., Raissi, K., Perry, S. J., Puigjaner, L. (1997). Targeting and design methodology for reduction of fuel. Power and CO_2 on total sites. *Applied Thermal Engineering*, **17** (8–10), 993–1003. DOI: 10.1016/S1359-4311(96)00087-7.

Klemeš, J., Lam, H. L., Foo, D.C.Y. (2010). Water recycling and recovery in food and drink industry. In: Waldron, K., Moates, G.K., Faulds, C.B. (eds), *Total Food, Sustainability of the Agri-Foot Chain*. Royal Society of Chemistry, Cambridge, 186–195.

Liu, Y. A., Lucas, B., Mann, J. (2004). Up-to-date tools for water-system optimization. *Chemical Engineering Magazine*, January, 30–41.

Linnhoff (1986). MSc Process Integration Lectures, UMIST, Manchester, UK.

Manan, Z. A. (2004). Maximizing energy efficiency and minimizing environmental emissions in the process industry using thermal pinch analysis. *ASEAN Journal of Chemical Engineering (AJChE)*, **4** (2), 32–39.

Manan, Z. A., Tan, Y. L., Foo, D. C. Y. (2004). Targeting the minimum water flowrate using water cascade analysis technique. *AIChE Journal*, **50** (12), 3169–3183. DOI: 10.1002/aic.10235.

Manan, Z. A., Wan Alwi, S. R., Ujang, Z. (2005). Systematic design of a maximum water recovery network for an urban system based on pinch analysis. *IEM Journal*, **1** (67), 57–64.

Manan, Z. A., Tan, Y. L., Foo, D. C. Y., Tea, S. Y. (2007). Application of water cascade analysis technique for water minimisation in a paper mill plant. *International Journal of Pollution Prevention*, **29** (1–3), 90–103.

Noureldin, M. B., El-Halwagi, M. M. (1999). Interval-based targeting for pollution prevention via mass integration. *Computers and Chemical Engineering*, **23**, 1527–1543.

Polley, G. T., Polley, H. L. (2000). Design better water networks. *Chemical Engineering Progress*, **96** (2), 47–52.

Prakash, R., Shenoy, U. V. (2005a). Targeting and design of water networks for fixed flowrate and fixed contaminant load operations. *Chemical Engineering Science*, **60** (1), 255–268. DOI: 10.1016/j.ces.2004.08.005.

Prakash, R., Shenoy, U. V. (2005b). Design and evolution of water networks by source shifts. *Chemical Engineering Science*, **60**, 2089–2093. DOI: 10.1016/j.ces.2004.11.042.

© Woodhead Publishing Limited, 2013

Savelski, M. J., Bagajewicz, M. J. (2000). On the optimality conditions of water utilization systems in process plants with single contaminants. *Chemical Engineering Science*, **55**, 5035–5048.

Tainsh, R.A., Rudman A. R. (1999). Practical techniques and methods to develop an efficient water management strategy. Linnhoff March International, Paper presented at: IQPC conference 'Water Recycling and Effluent Re-Use'. In: KBC Advanced Technologies PLC. <dev-kbcat.contentactive.com/default/documents/technical papers/IQPC_Water_Paper.pdf>, Accessed 22 March 2012.

Thevendiraraj, S., Klemeš, J., Paz, D., Aso, G., Cardenas, J. (2003). Water and wastewater minimisation study of a citrus plant. *Resources, Conservation and Recycling*, **37**, 227–250.

The Institution of Chemical Engineers (2000). Guide to Industrial Water Conservation. Part 1. Water Re-use in Single Contaminant Systems, ESDU 0020, Rugby, UK.

Wan Alwi, S. R., Manan, Z. A. (2006). SHARPS – A new cost-screening technique to attain cost-effective minimum water utilisation network. *AIChe Journal*, **11** (52), 3981–3988. DOI: 10.1002/aic.10986.

Wan Alwi, S. R., Manan, Z. A. (2008a). A holistic framework for design of cost-effective minimum water utilisation network. *Journal of Environmental Management*, **88**, 219–252. DOI: 10.1016/j.jenvman.2007.02.011.

Wan Alwi, S. R., Manan, Z. A. (2008b). Generic graphical technique for simultaneous targeting and design of water networks. *Industrial and Engineering Chemistry Research*, **47** (8), 2762–2777. DOI: 10.1021/ie071487o.

Wang, Y. P., Smith, R. (1994a). Wastewater minimisation. *Chemical Engineering Science*, **49** (7), 981–1006. DOI: 10.1016/0009–2509(94)80006–5.

Wang, Y. P., Smith, R. (1994b). Design of distributed effluent treatment systems. *Chemical Engineering Science*, **49**, 3127–3145. DOI: 10.1016/0009–2509(94) E0126-B.

Zbontar Zver, L., Glavic, P. (2005). Water minimization in process industries: Case study in beet sugar plant. *Resources, Conservation and Recycling*, **43** (2), 133–145.

10.7 Appendix: Nomenclature

C	Contaminant concentration, ppm
CEMWN	Cost Effective Minimum Water Network
C_i	Contaminant concentration of Source *i*
C_{in}	Contaminant concentration inlet, ppm
C_j	Contaminant concentration of Sink *j*
$C_{\text{max},j}$	Maximum acceptable contaminant concentration of Sink *j*
C_{out}	Contaminant concentration outlet, ppm
SK	Water sinks
F	Flowrate
F_{FW}	Fresh water flowrate
$F_{\text{SR}i}$	Total flowrate available from Source *i*
$F_{\text{SK}j}$	Total flowrate required by Sink *j*

© Woodhead Publishing Limited, 2013

F_{SK}	Water sinks flowrate
F_{SR}	Water sources flowrate
F_{WW}	Wastewater flowrate
LCC	Limiting Composite Curve
m	Contaminant mass load
NAD	Network Allocation Diagram
P	Purity
SR	Water sources
SHARPS	Systematically Hierarchical Approach for Process Screening
WCA	Water Cascade Analysis
WCT	Water Cascade Table
WSD	Water Surplus Diagram
WMH	Water Management Hierarchy
WPA	Water Pinch Analysis

© Woodhead Publishing Limited, 2013

11

Using Systematic Design Methods to Minimise Water Use in Process Industries

JIN-KUK KIM, Hanyang University, Seoul, South Korea

DOI: 10.1533/9780857097255.3.383

Abstract: Water, an essential utility in the process industry, serves in a wide range of unit operations as either a mass separation agent or a heat transfer medium. This chapter highlights how water is utilised from the viewpoint of Total Site, as well as how water can be used effectively with the aid of water reuse methods in a holistic manner to the benefit of the whole plant. The site-wide investigation and implementation in practice of water reuse for water minimisation is envisaged through the strategic application of Process Integration tools, including Water Pinch Analysis and superstructure-based optimisation techniques.

Key words: water minimisation, water reuse, Process Integration, Total Site, process design.

11.1 Introduction

Water is widely used in the process industries as a raw material, mass separation agent, energy carrier and washing medium. Efficient use of water is important in the process industries, not only to reduce the cost of the supply, distribution and discharge of freshwater associated with the process, but also to minimise environmental emissions associated with the use and discharge of water. Significant efforts have been made to improve water efficiency in the process industries over a few decades, because accessing clean water resources near industrial plants has become more difficult, and stricter environmental regulations have been introduced to control water resources and protect ecosystems (European Commission, 2012; EPA, 2012).

A wide range of design options and methods are available for reducing water consumption and environmental burden (Envirowise, 2005). These options can be broadly categorised in two groups as follows:

1. Stand-alone design options: The water requirements for water-using unit operations can be reduced by changing the characteristics of water use and discharge for equipment on an individual basis or by replacing

© Woodhead Publishing Limited, 2013

water-using equipment with new pieces that have better water efficiency. For example, a simple distributor in the washing operation can be changed to spray ball type distributor. The number of stages in a steam stripping column can be increased, which reduces demand for steam as a stripping agent. The introduction of a controller to regulate the water stream can eliminate unnecessary water use. Collection of steam condensate from utility systems can reduce the amount of boiler feedwater required.

2. Integrated design options: All the water-using operations can be simultaneously considered within a single design framework, with which the most appropriate way of reusing water between water-using operations can be sought. Reusability of water within the plant can be further improved with the aid of regeneration and recycling of wastewater before discharge to the environment. A system-wide approach is applied to systematically investigate the potential of water saving throughout the plant, and to propose an integrated water network design with much reduced water use. This option does not simply involve considering the possibility of water minimisation for individual equipment, but screens possible integrated design features for water use and provides a holistic solution for an industrial water network.

An ideal approach would be to consider the individual design options as well as an integrated one. A water-saving project based on individual design options would be more or less straightforward, while in practice the application of an integrated design needs considerable care and attention, due to design interactions and engineering complexities associated with the introduction of integrated features into the water systems.

Each water-using operation has its own mechanism, making it difficult to generalise the nature of mass transfer for various water streams. Wang and Smith (1994) identified a break-through in the development of an integrated design methodology for water systems, by proposing a Limiting Water Profile that represents how water removes contaminants from water-using operations. This Limiting Water Profile works by conceptualising the mass load of contaminants transferred from process stream to water stream in a graphical format, based on limiting the flowrate and concentrations of inlet and outlet water streams. The 'limited' information represents the maximum allowable operating conditions for the mass transfer to occur in water-using operations, thereby indicating the design boundary for feasible operations below the limiting conditions.

The key to reducing water consumption for the plant is to improve the reusability of water between water-using operations. Significant

© Woodhead Publishing Limited, 2013

water savings can be achieved through the implementation of water reuse between water-using operations, such that contaminated water after its use in the particular unit is either partially mixed with freshwater or fed on to another operation. The Limiting Water Profile provides a design basis for evaluating the feasibility of such water reuse between operations, by checking the levels of water contaminants against limiting conditions.

Using the Limiting Water Profile for a water-system design does have a limitation, as complex interactions between the water stream and the process stream within the operation are often not fully reflected. However, the benefits of the Limiting Water Profile have been well recognised in the academic and industrial community, because design complexities in the synthesis of water networks can be greatly simplified when considering limiting water conditions, while not requiring any process stream information during the synthesis. This allows the evaluation of various water-using operations in a common design basis and, consequently, deals with industrial water systems problems effectively and confidently that might otherwise develop from the wide range of water-using operations and behaviour. Another benefit of using a Limiting Water Profile is to provide visualised information on how water is used collectively within the whole water system. This graphical representation of limiting water information helps engineers to gain a conceptual understanding of water network synthesis and to identify the maximum potential for water saving and the bottleneck point for limiting water minimisation within the network.

Another approach for demonstrating how water streams behave in the water-using operations represents those that are fed into water-using operations as water sinks, and those that are discharged from water-using operations as water sources. The level of contaminants for inlet and outlet water streams is typically fixed to that of water sources and sinks, from which feasible water reuse between the sources and sinks is then identified (Dhole *et al*., 1996).

Process industries have adopted a wide range of successful industrial applications for reducing water consumption and wastewater generation, and this chapter aims to review how the water is used in these process industries and to discuss what should be taken into account for improving the efficiency of water use in terms of Process Integration. Process Integration is a well-established design method which effectively considers complex system interactions in a holistic manner to identify the optimal network configuration for design problems in process industries (Smith, 2005). Another focus of this chapter is the concept of Total Site, whereby the overall manufacturing processes of a plant are collectively investigated as a whole and, consequently, an optimal design and operating strategy can be devised with

© Woodhead Publishing Limited, 2013

consideration of the economic and environmental trade-off of the whole system (Klemeš *et al.*, 2010).

11.2 Water Use in Process Industries

Water used in process industries is typically supplied either from local water sources, e.g. river, sea, borehole water, etc., or from external water companies. water-using operations require a certain level of purity for the water to regulate the product quality, or to reduce any potential maintenance activities. Industrial water is used as a raw material in manufacturing, and as a Mass Separating Agent for separation or washing, but the majority of water consumption in process industries is related to cooling water systems and utility systems.

11.2.1 Cooling Water Systems

When recovering low-grade heat is not economically viable, or the temperature of a hot stream is too low to facilitate heat recovery, it is common to discharge low-grade heat into the environment with the aid of cooling water. Air cooling can be used as an alternative to water cooling, but the effectiveness of heat transfer via cooling water is far better than that of air. Process industries therefore favour the use of cooling water, unless there is a water scarcity near the plant.

If water is readily available and the supply of freshwater is relatively cheap, water is pumped to the cooler and then discharged after removing the heat from the process stream. This once-through use of cooling water may not be seen as a sustainable practice, as a large quantity of water needs to be extracted from water sources. Alternatively, process industries may decide to reuse water repeatedly within the plant and reproduce cold water through a re-circulating cooling tower system, which minimises the intake of freshwater from the environment, and one that is widely used in process industries. However, the repeated use of water can cause build-ups of undesired materials and increase corrosion problems, which then make it necessary to take a blowdown of circulated water from the circuit. Also, a certain amount of water is lost during tower operation, or is leaked from various parts of the cooling water systems. To compensate for the blowdown and water loss, the makeup of the water must therefore be addressed. Dealing with this composition is one of the major elements of the water systems used in process industries.

Although re-circulating cooling water systems are employed, the amount of water used for cooling water makeup is large, and it becomes more important to minimise the amount of water required in cooling water systems.

© Woodhead Publishing Limited, 2013

11.2.2 Water Use in Energy Production Systems

Along with cooling water, one of the largest water requirements in process industries is the water necessary for producing steam and consumed in relevant energy production systems. Energy is a key utility in manufacturing industries, as heating utility is used for providing heat to the chemical or physical conversion, the heating process streams and the driving rotational equipment (e.g. pumps, compressors), amongst other areas. The most common utility in process industries is steam, which is widely used as a heating medium in downstream processes and is also expended through steam turbines to produce shaft power or electricity. Steam is typically produced in the central utility systems in which boiler feedwater is converted to steam with the heat generated from combustion. The distribution of steam throughout a plant is relatively well-established in process industries, and the effectiveness of heat transfer through steam is high, due to the relatively high latent heat content in steam compared to other potential fluids. Therefore, steam at ambient pressure and 350°C is widely used for providing energy input to various unit operations.

Typically, steam is produced from either a boiler or a Heat Recovery Steam Generator (HRSG), in which water is supplied after the treatment. The treatment of freshwater in utility systems is required to remove suspended solids, dissolved salts, dissolved solids and dissolved gases of water. First, raw water is typically treated by filtration to remove any suspended solids. A softening process is then applied to remove scale-forming ions. If high-pressure steam is to be produced from a boiler, ion exchange or reverse osmosis is employed to remove inorganic salts to create deionised water (Kemmer, 1988). Boiler feedwater is then treated in the deaerator to remove dissolved gases (mainly oxygen and carbon dioxide) as these dissolved gases would otherwise cause corrosion in the boiler systems, and a final chemical treatment agent is applied to further remove oxygen after the deaeration (BETZ, 1991).

11.2.3 Effluent Treatment Systems

Effluent generated in process industries needs to be treated before discharge. Lumped indicators that represent the intensity of contamination in wastewater, such as biological oxygen demand (BOD) or chemical oxygen demand (COD), may be used when environmental regulations are concerned with the quality of effluent. Besides these lumped parameters, the level of individual contaminants (e.g. mg/L) or total amount of contaminant (e.g. kg/d) for specific contaminants (phenol, benzene, heavy metals, halogenated compounds, phosphates, nitrates, etc.) may be used for imposing regulation (Smith, 2005).

© Woodhead Publishing Limited, 2013

Wastewater treatment may be classified into physical unit operations, chemical unit operations and biological unit operations, depending on the nature of the separation principles. Physical unit operations mainly exploit the differences in density between the two phases when effluent stream contains heterogeneous contaminant(s). This phase separation can be enhanced by gravity, centrifugal force, pressure gradient or a magnetic field. Physical treatment units include: sedimentation, flotation, gravity separation, centrifugal separation, and filtration. Chemical unit operations involve the following (Seader and Henley, 1986):

1. Addition of chemical treatment agents to change the physical or chemical state of dissolved or suspended solids and to accelerate their removal (e.g. chemical precipitation, wet oxidation, chemical oxidation, pH adjustment, etc.).
2. Selective destruction of disease-causing organisms, using chemical disinfectants (i.e. chemical disinfection).
3. Separation of homogenous mixture using external Mass Separating Agents (e.g. absorption, stripping, extraction, etc.).
4. Application of a force field or gradient to influence the transport of certain species (e.g. ion exchange, membrane, etc.).

Biological unit operations are used to break organic contaminants into stabilised wastes and to coagulate and remove the unsettleable colloidal solids with the aid of microorganisms. Three main types of biological processes include (Tchobanoglous and Burton, 1991):

1. Aerobic processes, in which organic components (e.g. carbon, oxygen, hydrogen, nitrogen, etc.) react with oxygen and nutrients and are mainly converted to water, carbon dioxide and ammonia.
2. Anaerobic processes, in which reactions occur without oxygen, and where organic components are mainly converted to carbon dioxide and methane.
3. Anoxic processes, which follow different aerobic pathways to anaerobic processes although reactions also occur without the presence of oxygen, which are used for denitrification when converting nitrate to nitrogen.

11.3 Process Integration for Water Systems

Various design methodologies based on the concept of Process Integration have been introduced for effectively managing water resources and treating wastewater in process industry. Key developments made in the last three decades for water systems will be presented in this section.

© Woodhead Publishing Limited, 2013

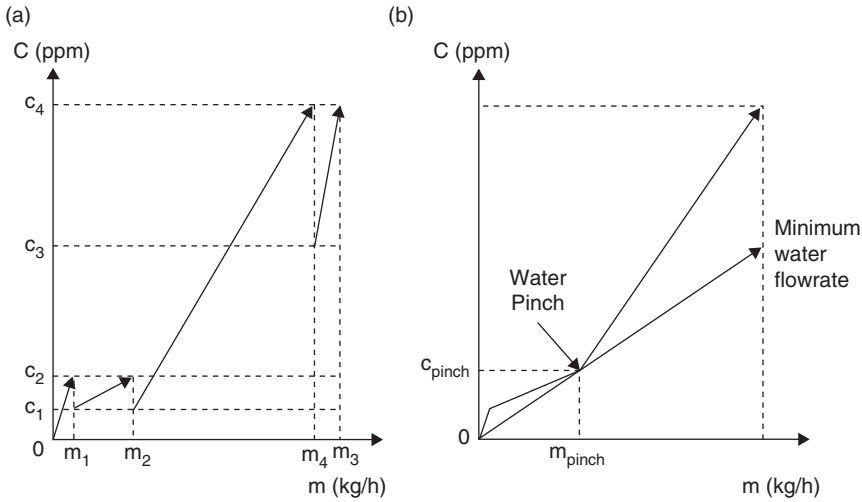

11.1 Targeting minimum water flowrate (I) (Wang and Smith, 1994). (a) Limiting water profile and (b) water Composite Curve.

11.3.1 Water Pinch Analysis for Water and Wastewater Minimisation

Pinch Analysis used for energy minimisation within heat recovery systems has also been adopted in the area of water minimisation. Early development of design methodology for water minimisation was largely based on the use of graphical profiles for water-using operations. Two major graphical profiles for quantifying contamination level and flowrate of water are the Limiting Water Profiles proposed by Wang and Smith (1994) and water demand and source composites suggested by Hallale (2002).

Using Limiting Water Profiles, the Water Composite Curve can be constructed by combining all the segments of Limiting Water Profiles for each contaminant interval and redraw the collective mass load change with a single segment for each interval, as shown in Fig. 11.1. The constructed curve represents the overall relationship between mass load of contaminants and concentration for the whole water-using systems. Minimum freshwater requirements can be targeted by plotting the feedwater profile against the Water Composite Curve and finding a point with the Minimum Driving Force for mass transfer. This point is known as 'Water Pinch', which provides a basis for the design of water networks. The design of a water network is made by following a design procedure known as a 'water main method' developed by Kuo and Smith (1998), with which mass balances are solved around water mains, and stream matching between water sources and water sinks are identified. When there are combinatorial

© Woodhead Publishing Limited, 2013

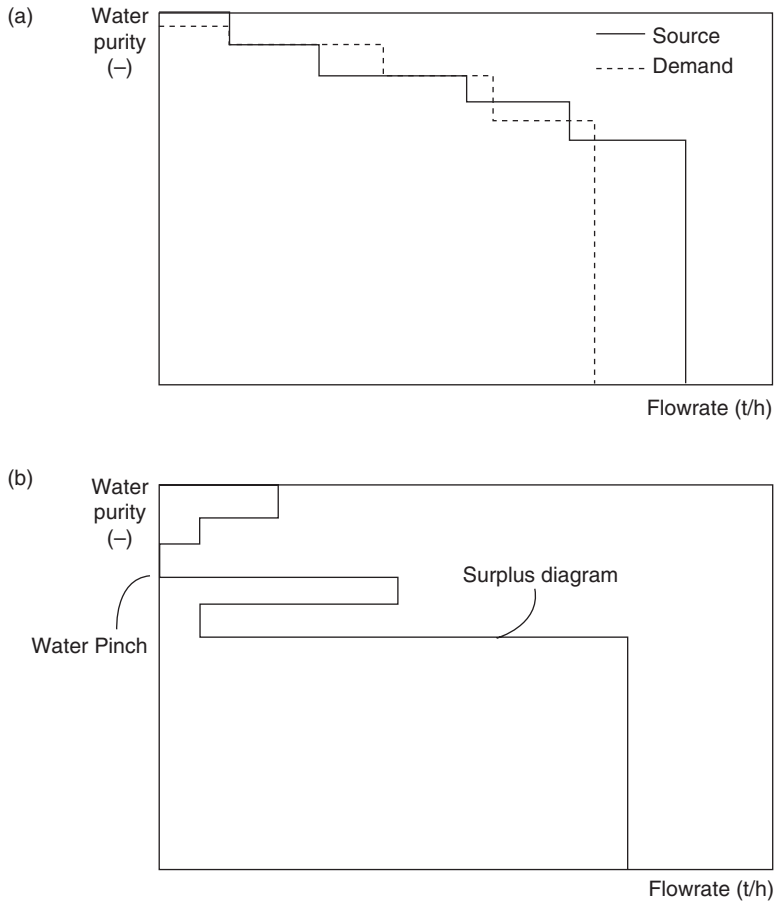

11.2 Targeting minimum water flowrate (II) (Hallale, 2002). (a) Source and demand Composite Curves and (b) surplus diagram.

choices for selecting matches between sources and sinks, users choose the most appropriate connection, subject to engineering constraints or economic evaluation.

A different targeting approach proposed by Hallale (2002) is based on the creation of Source-Demand Composite Profiles based on fixed inlet and outlet conditions of water-using processes. Compared to Wang and Smith's method (1994), these Source-Demand Composite Curves do not include mass transfer operations, and the potential change of water flowrate and inlet and outlet concentrations during the design of the water network cannot be made. Therefore, the design problem for the water network is to identify how water is distributed from sources to sinks. However, Hallale's approach is more convenient to model water-using operations in which

© Woodhead Publishing Limited, 2013

several streams enter and leave at different concentrations, or the water flowrate changes due to water losses and gains. As shown in Fig. 11.2, the water purity of a contaminated stream is defined as calculated from the contaminant concentration of water. The surplus deficit concept for analysing industrial hydrogen systems in refineries by Alves (1999) was adopted to test the feasibility of the water network characterised by Source-Demand Composite Profiles, and to target the minimum water requirement such that sufficient pure water at all points in the network is available and no part of the surplus diagram is negative.

11.3.2 Distributed Effluent Treatment Systems

Conventional effluent treatment systems are typically based on a series of water treatment facilities in which all the wastewater collected from water-using operations are combined and treated as a single effluent stream. This centralised approach treats wastewater collectively in sequence. For example, the combined effluent is first treated by a primary treatment unit, which is then dealt with by a secondary treatment unit. Biological processes may be taken further after the secondary units. The design of such centralised treatment facilities is mainly focused on the sizing of units and design of individual treatment units.

With a centralised treatment scheme, the resulting wastewater stream is likely to be diluted and have a large volumetric flowrate leading to high operating costs and capital investment, because individual wastewater generated from water-using operations are all mixed up before being fed to the effluent treatment system. A different approach can be taken in order to fully take advantage of the high concentration and low volume of wastewater in the design of treatment systems, by strategically splitting and mixing individual effluents before sending them to treatment units. As each effluent has different contaminants with different levels of contamination, unnecessary mixing between effluent streams results in the increase of flowrate and the decrease of concentration. The capital cost for wastewater treatment facilities, in general, is proportional to the capacity of the unit, which is mainly dependent on the effluent flowrate treated through the unit. Also, a large driving force for effluent treatment is favoured due to the relative easiness of the removal of contaminants from wastewater, compared to operations with a small driving force. Therefore, dilution through mixing should be carefully considered, as this can result in difficulty in separation.

This distribution concept has been proposed to avoid any unnecessary mixing between effluent streams, and to correctly distribute effluent streams to treatment units, which then minimises the cost for effluent treatment (Kuo and Smith, 1997). How much wastewater is split or mixed

© Woodhead Publishing Limited, 2013

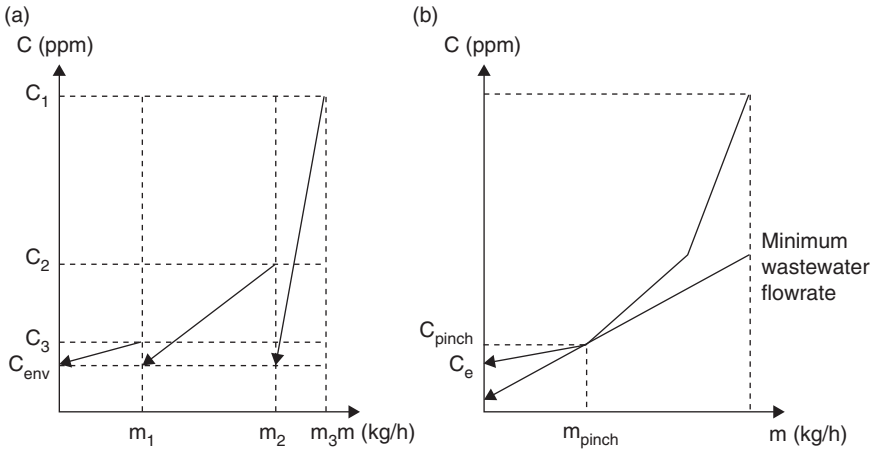

11.3 Effluent Composite Curve (Kuo and Smith, 1997). (a) Individual Effluent Profile and (b) Targeting of minimum effluent flowrate.

for the distribution of wastewater to treatment units is identified from an Effluent Composite Curve and a treatment profile. Similar to a graphical representation of water use in the water-using operations, the requirement of mass load removal for wastewater streams can be represented with a wastewater profile, which can be combined to create an Effluent Composite Curve as shown in Fig. 11.3. The targeting is carried out to create a Pinch Point between the Effluent Composite Curve and a treatment profile. The removal of contaminant from the wastewater during treatment can be represented with a treatment profile, which is based on either the fixed outlet concentration or the removal ratio of contaminant. The target determines how much wastewater should be treated or bypassed by the treatment, from which a network of wastewater effluent systems can be obtained (as shown in Fig. 11.4).

11.3.3 Optimisation of Total Water Systems

The design of water networks in process industries is complex when the number of water-using operations to be considered for water minimisation study is large. The design complexity is further increased if water regeneration and recycling is considered within the water wetwork. Graphical methods using graphical profiles of water-using and water-treating operations are very useful ways of representing overall characteristics of water systems and providing conceptual insights to the users. However, these graphical methods are not capable of dealing with larger design problem for water systems and the simultaneous consideration of water reuse, regeneration and recycling.

© Woodhead Publishing Limited, 2013

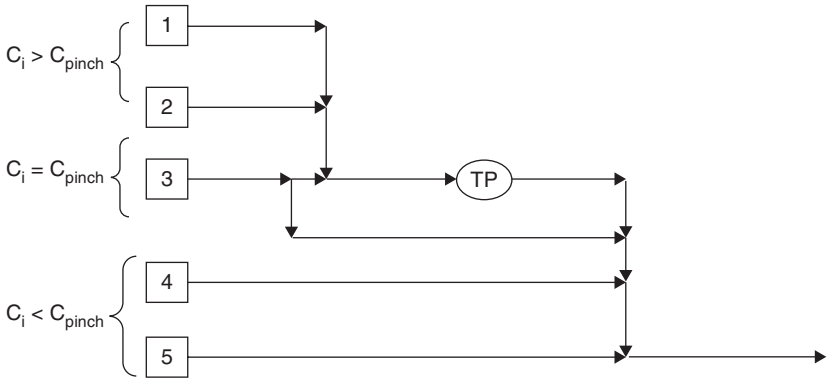

11.4 Distributed effluent treatment systems (Kuo and Smith, 1997). C_i - concentration of waste water source, C_{pinch} - Pinch concentration.

Mathematical optimisation is an effective method for screening a large number of design options and to identify the most appropriate network configuration in a holistic manner. In order to assess structural design options, a superstructure method is widely used in the area of process systems engineering. This includes all the possible network options, and selects only the necessary features in the optimisation. If a large number of options are necessary, a mathematical formulation for system behaviour (e.g. mass balances, etc.) and performance indicators (e.g. cost functions.) becomes highly non-linear, with a large number of equations to be solved simultaneously. Also, if users wish to include logical constraints or binary decisions in the network design, solving the resulting optimisation model is not straightforward and considerable computational resources are often required.

Figure 11.5 shows an example of the superstructure for a water network which includes two water-using operations and one treatment unit, showing also how water reuse, regeneration and recycling are embedded within the structure. Typically, binary variables are introduced to control whether the particular connection in the superstructure is activated in the optimised network or not. Continuous variables are determined from a set of mathematical equations which governs mass balances before, within and after the units. The optimisation framework may include engineering constraints, for example: regulating the total number of streams fed to the same operation, the minimum water flowrate, etc. A simple objective function, such as minimising the freshwater requirement for the network, can be considered in the optimisation, while economic trade-off can be performed by adding appropriate cost functions for operating cost and capital investment required in the construction of water networks. The optimisation is solved with either deterministic solvers or stochastic solvers (Klemeš *et al.*, 2010).

© Woodhead Publishing Limited, 2013

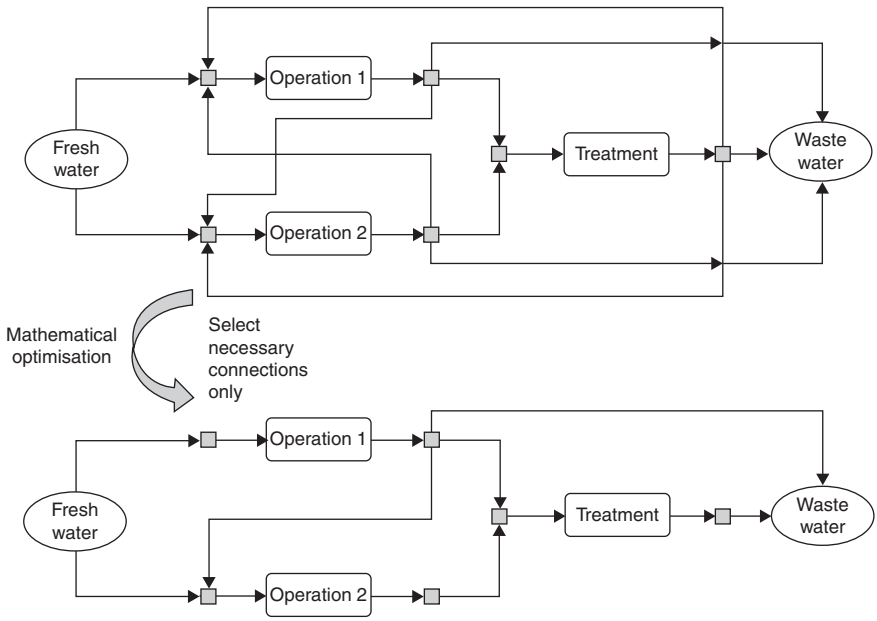

11.5 Superstructure approach for the design of water networks. Top figure: superstructure; bottom figure: optimized structure.

11.3.4 Retrofit of Cooling Water Networks

It is common in process industries for cooling water to be used in a parallel configuration, in which cooling water produced from the cooling tower removes heat from the process streams and returns it to the tower to prevent interaction with other cooling water streams. A water reuse concept developed for the water network was adopted in the design of a cooling water network, with the reuse of cooling water providing a new initiative for achieving efficient use of the cooling tower, especially in retrofit scenarios (Kim and Smith, 2001).

If the intensity of cooling water reuse between coolers is increased, the overall cooling water flowrate returned to the tower is relatively reduced, but the overall cooling water return temperature is increased, compared to the conventional cooling water network, in which a parallel water network is employed. Cooling tower operations can benefit from cooling water reuse, because a smaller cooling water flowrate with a high return temperature (rather than a larger flowrate with a lower return temperature) is more effective for removing heat from the returned hot cooling water (Kim and Smith, 2001). For retrofit scenarios in cooling tower operations, the operating capacity of the cooling tower is limited and, consequently, the produced cooling water temperature becomes higher than the desired temperature needed for

© Woodhead Publishing Limited, 2013

cooling purposes. Changing the configuration of the cooling water network by cooling water reuse allows the tower to manage the same cooling load under new operating conditions (i.e. the overall cooling water flowrate is reduced at the expense of an increased return temperature).

Within a water minimisation study, a graphic-based targeting method is available for cooling water network designs by using the cooling water limiting profile, which is a concept similar to the Limiting Water Profile, but is applied for the heat transfer operation of cooling water use in the cooler. The Cooling Water Composite Curve is constructed in a similar fashion to the water minimisation study. When water reuse is exploited in the water network, water reuse between operations is maximised to reduce operating costs. However, minimising cooling water flowrate in the cooling water systems may not be optimal, because it should be considered how the return cooling water conditions will influence the performance of the cooling tower, as shown in Fig. 11.6. Therefore, the targeting of cooling water flowrate is not based simply on the consideration of cooling water use in the cooler network, but an iterative procedure between consideration of cooling tower performance and cooling water reuse in the cooler network.

The identified cooling water flowrate determined from a targeting procedure is often different from the minimum cooling water flowrate, which results in the gap between the cooling water Composite Curve and the target line without having a Pinch Point. In order to design a cooling water network, modification of the Cooling Water Composite Curve is introduced to create the imaginary Pinch Point with the target line, with which the conventional water network design method devised by Kuo and Smith (1997) can be adopted to complete the cooling water network. A design method using mathematical optimisation has been also developed by Kim and Smith (2003) to enable automatic identification of cooling water reuse between coolers with the consideration of pressure drop and other engineering constraints.

11.3.5 Simultaneous Water and Energy Minimisation

The temperature of water is often adjusted to meet the temperature requirement of unit operations. It is common for the water stream to gain or lose heat during operations. Therefore, the recovery of available heat between the water streams provides an opportunity to reduce energy costs in water systems. Energy minimisation in water systems can be carefully exploited through the combined use of design methods for water minimisation and those for energy minimisation. Simultaneous consideration of both design techniques to a single design problem is quite challenging, as evaluating design complexity associated with the recovery of energy in the context of water reuse is much harder than doing a stand-alone study.

© Woodhead Publishing Limited, 2013

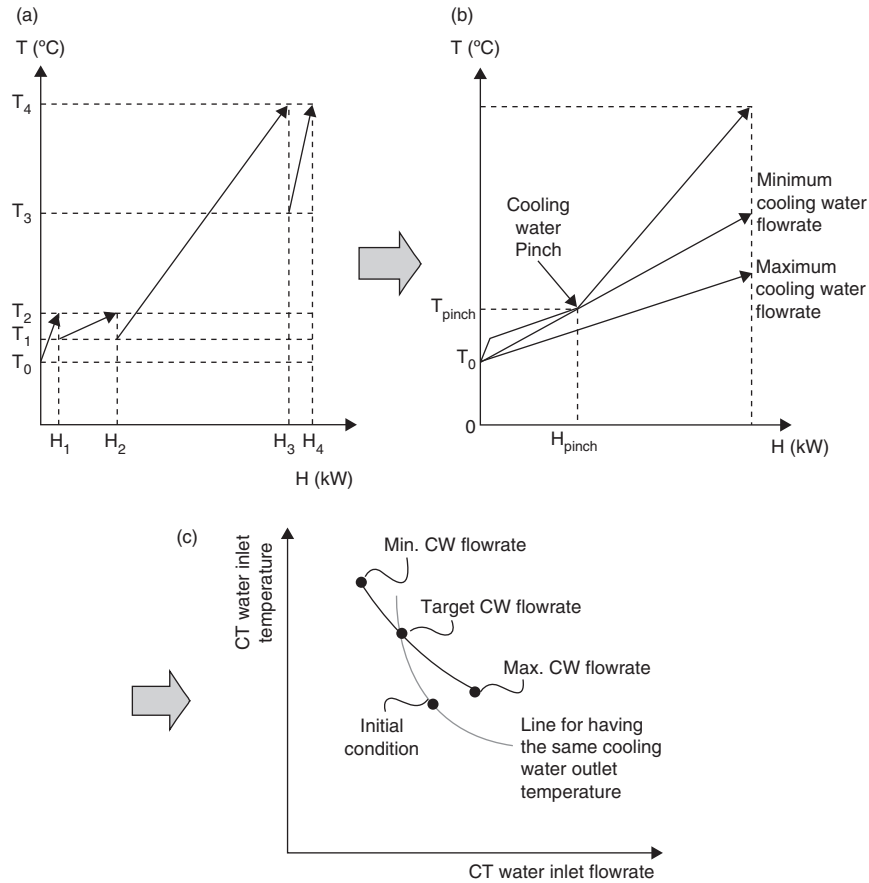

11.6 Targeting of cooling water flowrate (Kim and Smith, 2001). (a) Limiting cooling water profiles; (b) construction of cooling water Composite Curve; (c) identification of target. CT - cooling tower, CW - cooling water.

The design method proposed by Savulescu *et al*. (2005a, 2005b) presented various design options available for energy recovery in the water networks (Fig. 11.7), and a systematic design procedure to facilitate the efficient combination of water and energy networks. If a graphical design approach is used, the design of water networks should be carried out first, followed by the design of energy recovery systems with the resulting water network. This sequential method is inevitable because conceptual design methodology for energy recovery using a Pinch Concept is based on the manipulation of the fixed stream data and, therefore, it would be practically impossible to consider heat recovery options before the water network is confirmed.

However, the approach to Process Integration – to investigate design interactions between subsystems and to reflect them in an integrated manner

© Woodhead Publishing Limited, 2013

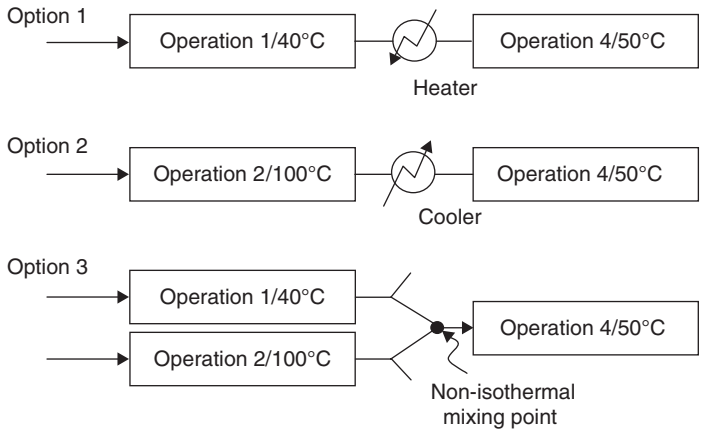

11.7 Energy recovery for water networks (Savulescu *et al.*, 2005a).

for gaining synergetic benefits for the whole system – can be applied to this design problem and a combined benefit, i.e. a simultaneous reduction in water and energy consumption for all systems, can be achieved with systematic selection of mixing or splitting between water streams, providing better heat recovery without compromising water requirements for the process. A distinctive feature in the design of heat recovery for water networks is to separate systems in which heat exchangers are employed in series, and where the withdrawal and supply of water is arranged in sequences as shown in Fig. 11.8 (Leewontanawit and Kim, 2009).

11.4 Conclusions and Future Trends

This chapter briefly reviews how the water is consumed in process industries, and how the water use can be minimised with the aid of a systematic design method. Most design methodologies developed so far have focused on particular design issues in the design, operation and management of water systems, and have simplified a wide range of water-using mechanisms for the sake of network synthesis. The design of water systems cannot be addressed without considering interactions between water systems and other subsystems, and therefore, a site-wide study considering the various water-system components and their interacts systematically should be made for the design of water systems. For the design and optimisation of industrial energy systems, there is a well-established method called Total Site analysis based on Site Composite Curves and Site Steam Profiles, etc. (Klemeš *et al.*, 2010). This kind of plant-wide investigation can be further exploited in water-systems design, which can provide a much better understanding of how water is used in process industries, and support our efforts for achieving sustainable management of water in practices.

© Woodhead Publishing Limited, 2013

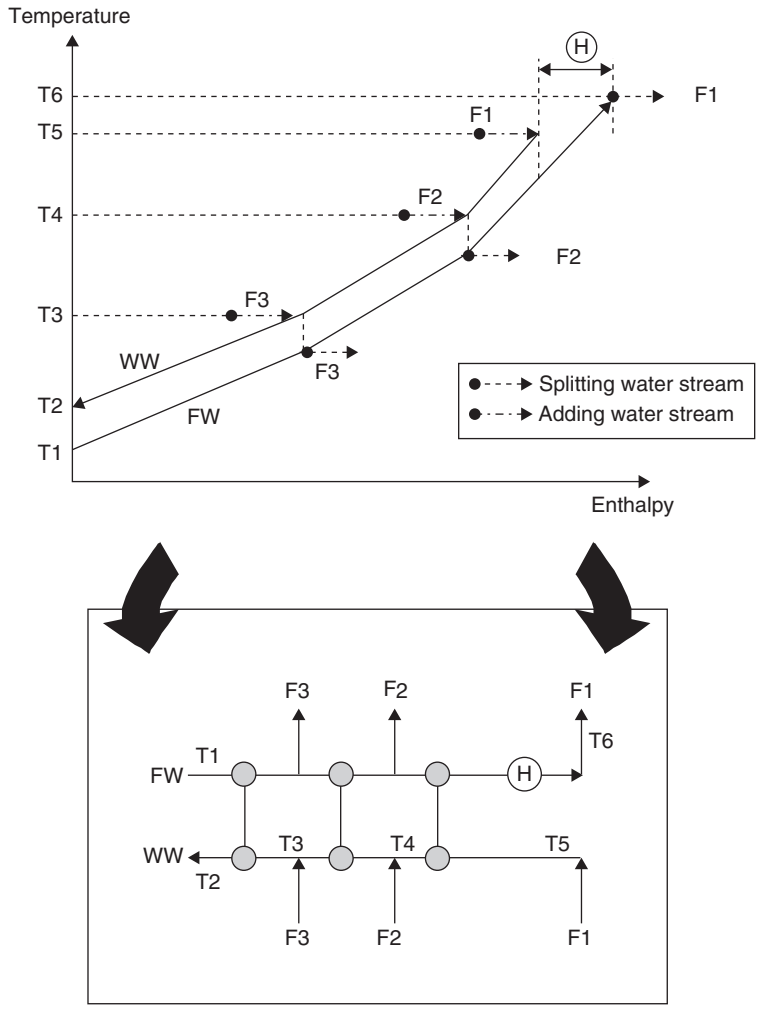

11.8 Separate systems for combined water and energy savings (Leewontanawit and Kim, 2009). FW - fresh water, WW - waste water, T - temperature, F - flowrate, H - heater.

11.5 Sources of Further Information

References are listed below that may be useful in the area of sustainable water use and its management. The concept and methodological details of Process Integration for water minimisation has been well-documented by Smith (2005), in which Water Pinch Analysis is explained for targeting for maximum water reuse and design of a water network using water main methods. Smith's book (2005) also addresses network design for water systems with regeneration and recycling, effluent treatment systems and cooling

© Woodhead Publishing Limited, 2013

water systems. Klemeš *et al*. (2010) outline how the automated design using mathematical optimisation can be effectively used in the design of water networks, and also explains case studies and industrial applications, which helps readers to avoid typical pitfalls faced in the application of Process Integration techniques in practice. Best Available Techniques for minimising water in the food industry are described in Klemeš *et al*. (2008), which covers not only general guidance on water minimisation based on conventional methods (e.g. process changes, water auditing, etc.), but also Process Integration techniques for systematically implementing water reuse in the plant. Further reading for water minimisation and its associated Process Integration methods includes Rossiter (1995), Mann and Liu (1999), and the most recent book of Foo *et al*. (2012).

11.6 References

Alves, J.J. (1999). Design and Analysis of Refinery Hydrogen Distribution Systems, PhD Thesis, UMIST, Manchester, UK.

BETZ (1991). *Handbook of Industrial Water Conditioning*, 9th ed., BETZ, New Jersey, US.

Dhole, V.R., Ramchandi, N., Tainsh, R.A., Wasilewski, M. (1996). Make your process water pay for itself, *Chemical Engineering*, **103**(1), 100–103.

Envirowise (2005). *Cost-effective Water Saving Devices and Practices – for Industrial Sites*, Envirowise, Didcot, UK.

European Commission (cordis.europa.eu/eesd/ka1/home.html) accessed on 18 October 2012.

European Environment Agency (www.eea.europa.eu/themes/water) accessed on 18 October 2012.

EPA (www.epa.gov/OW-OWM.html/water-efficiency) accessed on 18 October 2012.

Foo, D.C.Y., El-Halwagi, M.M., Tan, R.R. (2012). *Recent Advances in Sustainable Process Design and Optimization*, World Scientific Publishing Co., London, UK.

Foundation for Water Research (FWR) (www.fwr.org) accessed on 18 October 2012.

Hallale, N. (2002). A new graphical targeting method for water minimisation. *Advances in Environmental Research*, **6**(3), 377–390.

Kemmer, F.N. (1988). *The Nalco Water Handbook*, 2nd ed., McGraw-Hill, New York, US.

Kemp, I. (2007). *Pinch Analysis and Process Integration, Second Edition: A User Guide on Process Integration for the Efficient Use of Energy*, Elsevier, Oxford, UK.

Kim, J.K., Smith, R. (2001). Cooling water system design. *Chemical Engineering Science*, **56**(12), 3641–3658.

Kim, J.K., Smith, R. (2003). Automated retrofit design of cooling water systems. *AIChE Journal*, **49**(7), 1712–1730.

Kim, J.K., Smith, R. (2004). Cooling system design for water and wastewater minimization. *Industrial and Engineering Chemistry Research*, **43**(2), 608–613.

Klemeš, J., Smith, R., Kim, J.K. (2008) *Handbook of Water and Energy Management in Food Processing*, Woodhead Publishing, Cambridge, UK.

© Woodhead Publishing Limited, 2013

Klemeš, J., Dhole, V.R., Raissi, K., Perry, S.J., Puigjaner, L. (1997) Targeting and design methodology for reduction of fuel, power and CO_2 on total sites. *Applied Thermal Engineering*, **17**, 993–1003.

Klemeš, J., Friedler, F., Bulatov, I., Varbanov, P. (2010). *Sustainability in the Process Industry*, McGraw-Hill, New York, US.

Kuo, W.C.J., Smith, R. (1997). Effluent treatment system design. *Chemical Engineering Science*, **52**(23), 4273–4290.

Kuo, W.C.J., Smith, R. (1998). Designing for the interactions between water-use and effluent treatment. *Chemical Engineering Research and Design*, **76**(3), 287–301.

Leewontanawit, B., Kim, J.K. (2009) Improving energy recovery for water minimisation. *Energy*, **34**, 880–893.

Mann, J.G., Liu, Y.A. (1999). *Industrial Water Reuse and Wastewater Minimisation*, McGraw-Hill, New York, US.

PES2012 International Symposium on Process Systems Engineering (www.pse2012.sg).

PRES: Process Integration, Modelling, and Optimisation for Energy Saving and Pollution Reduction (www.conferencepres.com) accessed 10.07.2013.

Rossiter, A. P. (1995). *Waste Minimization Through Process Design*, McGraw-Hill, New York, US.

Savulescu, L., Kim, J.K., Smith, R. (2005a). Studies on simultaneous energy and water minimisation – Part I: Systems with no water re-use. *Chemical Engineering Science*, **60**(12), 3279–3290.

Savulescu L, Kim JK, Smith R (2005b) Studies on simultaneous energy and water minimisation – Part II: Systems with maximum re-use of water. *Chemical Engineering Science*, **60**(12), 3291–3308.

Seader, J.D., Henley, J.E. (1998). *Separation Process Principles*, Wiley, New York, US.

Smith, R. (2005). *Chemical Process Design and Integration*, Wiley, Chichester, UK.

Tchobanoglous, G., Burton, F.L. (1991). *Metcalf & Eddy Wastewater Engineering: Treatment, Disposal and Reuse*, 3rd ed., McGraw-Hill, New York, US.

The European Commission's research and development information service-Sustainable management and water quality (ec.europa.eu/environment/water/index_En.htm) accessed on 8 April 2013.

UK DEFRA Department for Environment, Food and Rural Affairs www.defra.gov.uk/environment/index.htm) accessed on 18 October 2012.

UK Environment Agency (www.environment-agency.gov.uk) accessed on 18 October 2012.

UK Envirowise (www.envirowise.gov.uk) accessed on 18 October 2012.

US EPA (Environmental Protection Agency) Office of Water (water.epa.gov/) accessed on 8 April 2013.

Wang, Y.P., Smith, R. (1994). Wastewater minimisation. *Chemical Engineering Science*, **49**(7), 981–1006.

© Woodhead Publishing Limited, 2013

12

Synthesis of Water Networks with Water Loss and Gain via an Extended Pinch Analysis Technique

XIAO FENG and CHUN DENG, China University of Petroleum, Beijing, China

DOI: 10.1533/9780857097255.3.401

Abstract: In this chapter, a new Process-based Graphical Approach (PGA) is presented for the simultaneous targeting and design of water networks. The PGA is extended from the Limiting Water Profile and conventional Water Pinch Analysis technique, which were developed for flowrate targeting of a water network. With the PGA procedure, in addition to locating the minimum freshwater and wastewater flowrate targets, the water network that corresponds to the minimum flowrate targets is also simultaneously identified. The revised Limiting Water Profile is introduced for the flowrate targeting of a water-using process with water loss/gain. The PGA procedure is illustrated by solving an example from the literature. In addition, the generalised procedure for the PGA presented is summarised in a diagram. Finally, comparison is made between this approach and others in the literature.

Key words: water network synthesis, wastewater minimisation, Pinch Analysis, direct reuse, water loss/gain.

12.1 Introduction

In recent years, water scarcity and stringent environmental protection legislation have led to increases in the cost of freshwater, as well as for the treatment of wastewater. This has motivated researchers and the process industries to develop wastewater minimisation techniques for their daily operations. To date, the Water Integration technique and Water Pinch Analysis have been commonly accepted as promising tools for the synthesis of water networks in the process industries. These have been developed by a number of authors. Water Pinch Analysis began with the pioneering work of Wang and Smith (1994). The concept of the Limiting Composite Curve, which could be considered as the basis of Water Pinch Analysis, was proposed, and this is the common graphical approach. Later, Castro *et al*. (1999) proposed the Mass Problem Table for accurate targeting of water networks,

© Woodhead Publishing Limited, 2013

which is considered as the typical tabular Water Pinch Analysis approach. Improvements to the Limiting Composite Curve and Mass Problem Table approaches have been presented by the authors of this chapter to locate targets for water networks for regeneration recycling (Feng *et al*., 2007) and regeneration reuse (Bai *et al*., 2007).

The basic characteristic of a water-using operation is that the model is mass-transfer-based, and water loss/gain is neglected. Water-using operations (e.g., washing, scrubbing and extraction) are mass-transfer based operations, whereby a fixed amount of contaminant is transferred from a contaminant-rich stream to water, which acts as a Mass Separating Agent. They are so-called Fixed Contaminant (FC) mass load operations or quality controlled operations. In addition, Wang and Smith (1995) explored techniques to target the water network with fixed flowrate constraints and water loss via the Limiting Composite Curve. Water-using operations, such as boilers, cooling towers and reactors, on the other hand, are characterised as water sinks/sources that consume/generate a fixed amount of water. They are termed Fixed Flowrate (FF) operations or quantity controlled operations. Dhole *et al*. (1996) first established that the water-using operations should be classified into two types of operation (mass-transfer-based and non-mass-transfer-based). Water Source and Water Sink Composite Curves (Dhole *et al*., 1996) are generated to target the water networks with FF operations. Moreover, many other Water Pinch Analyses (graphical or tabular/algorithmic) for the synthesis of water networks with FF operations have been developed subsequently, such as: the Water Surplus Diagram (Hallale, 2002); the Material Recovery Pinch Diagram, developed separately by two groups – dynamic programming for the derivation of optimality conditions (El-Halwagi *et al*., 2003), and the Nearest Neighbours Algorithm for network design (Prakash and Shenoy, 2005); Water Cascade Analysis – tabular approach; direct reuse (Manan *et al*., 2004) and regeneration reuse/recycle (Foo *et al*., 2006); Source Composite Curve: direct reuse with treatment unit (Bandyopadhyay *et al*., 2006); regeneration reuse/recycle with treatment unit (Bandyopadhyay and Cormos, 2008); and Composite Table Algorithm – tabular approach: basic development (Agrawal and Shenoy, 2006) and improvement for mutiple water resources and Property Integration (Deng and Feng, 2011). For further reading on Water Pinch Analysis, consult the thorough review conducted by Foo (2009).

In industrial practice, there may be water loss in certain water-using processes. For instance, make-up to cooling towers is necessary (water loss by evaporation and leakage from cooling towers is typically fixed flowrate). Water may also leave a factory with a product, another example of water loss. On the other hand, water gain may take place in some water-using processes. For example, the dewatering process may generate a certain amount of water. Obviously, the lost water cannot be reused by other water-using

© Woodhead Publishing Limited, 2013

processes, whereas the gained water can be considered as a new water source and probably reutilised by other processes. However, the original Water Pinch approach, such as Limiting Composite Curve (Wang and Smith, 1994) – see Chapter 2 for the definition and some further information elsewhere (Wang and Smith, 1994; and more recently Smith, 2005) – was developed for water networks omitting water loss/gain. In order to reflect water networks with water loss/gain, the conventional graphical Water Pinch approach based on the Limiting Composite Curve may be adjusted. Up-to-date graphical approaches concerning the synthesis of water networks with loss/gain are reviewed and analysed as follows.

The originally developed Water Pinch technique, including Limiting Composite Curve (Wang and Smith, 1994), cannot be directly utilised to target a water network with water loss/gain. To overcome this limitation, Wang and Smith (1995) firstly introduced the targeting procedure for a water network with water loss. The Limiting Composite Curve and Water Supply Line without considering water loss are constructed, and the Pinch Point is located first. Next, water loss at a certain concentration (lower than the Pinch concentration) is taken into account. Due to the water loss below the Pinch, the water supply may be insufficient and infeasibility may occur. Graphically viewed, the Water Supply Line would be above the Limiting Composite Curve. Thus, the freshwater flowrate has to be increased to eliminate such infeasibility and the Water Supply Line will lie below the Limiting Composite Curve. One example is utilised to illustrate the strategy for treating simultaneously the fixed flowrate constraint, multiple external water sources and water loss. The Water Supply Line is altered to take into account water loss, and additional external water sources and the flowrate targets are located. The corresponding water network is designed to fulfil the flowrate targets. In addition, the water network of a specialised chemical plant is synthesised to show the applicability of the proposed procedure for the water network with water loss/gain. The procedure can be summarised as follows:

(1) Data extraction and modification;
(2) Construction of Limiting Composite Curve and Water Supply Line without considering water loss/gain;
(3) Adjustment of Water Supply Line and determination of freshwater flowrate targets with the consideration of water loss/gain;
(4) Water network design and evolution to achieve the targets considering water loss/gain.

However, the procedure for the determination of freshwater flowrate targets is vague. Based on the earlier approach developed by Wang and Smith (1995), Mann and Liu (1999) later presented a synthesis procedure for a

© Woodhead Publishing Limited, 2013

water network with water loss/gain in certain detail. In addition, Foo (2009) reviewed the targeting procedure for water networks with loss/gain. In the work of Mann and Liu (1999), first, without considering water loss/gain, the Limiting Composite Curve and 'apparent' Water Supply Line are constructed and the located Pinch is defined as 'apparent' Freshwater Pinch. Generally, any water loss that happens below the apparent Freshwater Pinch would lead to increase of freshwater consumption. The additional freshwater is required to compensate for water loss. The equation that relates additional freshwater flowrate and water loss flowrate is derived. Similarly, water gain below the apparent Freshwater Pinch would lead to the reduction of freshwater consumption. The corresponding relationship between reduced freshwater flowrate and water gain flowrate is explored. The two equations could be used to determine the freshwater flowrate target once the apparent Freshwater Pinch stays constant. In addition, other special cases (i.e. a large amount of water loss above the apparent Freshwater Pinch and a large amount of water gain below the apparent Freshwater Pinch) would cause infeasibility in driving force, and the Freshwater Pinch may shift to a new position. In this case, the two derived equations should be reapplied to determine the freshwater flowrate targets based on the new apparent Freshwater Pinch. Next, the mass-content diagram is utilised to design the water network according to the freshwater flowrate targets that have been determined. The water network of a specialised chemical plant adopted from earlier literature (Wang and Smith, 1995) is synthesised according to the proposed procedure. As is in the literature (Wang and Smith, 1995), each water-using process with loss/gain is separated into two parts: one with constant flowrate and the other representing water loss/gain. Without considering water loss/gain, the concentration interval table is generated. The apparent Freshwater Pinch is located and the apparent minimum freshwater flowrate is determined. According to the data in the concentration interval table, the Limiting Composite Curve and Water Supply Line without considering water loss/gain are constructed. Once water loss/gain is taken into account, the derived equations are used to determine practical freshwater targets. The Water Supply Line considering water loss/gain is constructed to show whether it is feasible or not. However, if driving force infeasibility exists, the Freshwater Pinch would shift to a new position, and the derived equations thus would need to be solved again to determine the true practical freshwater targets.

In this chapter, the Water Pinch approach for synthesis of a water network with loss/gain is explored further. It aims to guide the targeting and design of the water network with loss/gain. Firstly, the significant methodologies for graphical analysis of the water network involving loss/gain are summarised and analysed. The drawbacks of former methodologies are pointed out. To overcome those drawbacks, several problems arise, which need to

© Woodhead Publishing Limited, 2013

be solved. The revised Limiting Water Profile is introduced in the following section. After that, a new PGA for simultaneous targeting and design of a direct reuse water network is presented. The generalised procedure for the presented PGA is illustrated via a diagram. Finally, a summary is made, comparing the different approaches.

12.2 Targeting a Single Water-Using Process

Typically, water-using processes can be broadly classified into four categories (Deng *et al.*, 2011), i.e. processes without water loss/gain, processes with water loss, processes with water gain and processes with fixed flowrate constraints. The graphical techniques for targeting processes without water loss/gain and processes with fixed flowrate constraints are adopted directly from the literature (Wang and Smith, 1995). The basic equation for determining the water flowrate and related descriptions are presented first.

For a water-using process, the contaminant to be removed by the water is denoted as contaminant mass load (Δm_i). In addition, the limiting inlet and outlet concentrations ($C_{i,\text{in}}^{\max}$ and $C_{i,\text{out}}^{\max}$) of a water-using process are specified according to several possible considerations (Wang and Smith, 1994) – see Chapter 2. The limiting water flowrate ($F_{i,\text{in}}^{\lim}$) can be determined via Equation [12.1].

$$\Delta m_i = F_{i,\text{in}}^{\lim}\left(C_{i,\text{out}}^{\max} - C_{i,\text{in}}^{\max}\right) \qquad [12.1]$$

Any Water Supply Line that is located below the Limiting Water Profile (with inlet concentration, $C_{i,\text{in}} < C_{i,\text{in}}^{\max}$ and outlet concentration, $C_{i,\text{out}} < C_{i,\text{out}}^{\max}$) can be used to remove the given Δm_i. Based on Equation [12.1], it is noted that for a given Δm_i, the water flowrate (with inlet concentration of $C_{\text{i,in}}$) can be minimised by maximising its outlet concentration ($C_{\text{i,out}}$) to the limiting value $C_{i,\text{out}}^{\max}$.

As is discussed in the last section, the graphical technique based on the conventional Limiting Composite Curve has to be altered or revised to target the water network with water loss/gain. The corresponding basic equation for contaminant mass load has to be redefined accordingly. For the practical water-using process with water loss/gain, the net mass load difference between outlet and inlet of the process can be determined via Equation [12.2].

$$\Delta m_i^{\text{net}} = F_{i,\text{out}}^{\lim} C_{i,\text{out}}^{\max} - F_{i,\text{in}}^{\lim} C_{i,\text{in}}^{\max} \qquad [12.2]$$

where $F_{i,\text{out}}^{\lim}$ denotes limiting outlet water flowrate of process *i*. Δm_i^{net} represents the net mass load difference for water-using process *i*.

© Woodhead Publishing Limited, 2013

Once water loss/gain is ignored, the mass load difference between the inlet and outlet of the process can be defined as pseudo-mass load, which can be determined by Equation [12.1].

Next, the graphical techniques for targeting a single process with water loss/gain or multiple feeds are introduced.

12.2.1 Process with Water Loss

Figure 12.1a shows a generic model for a water-using process with water loss, i.e. cooling towers with water evaporation or leakage. The make-up water is necessary to supplement the loss. The loss flowrate (F_i^{loss}) is defined as the difference between the inlet ($F_{i,\text{in}}^{\text{lim}}$) and outlet ($F_{i,\text{out}}^{\text{lim}}$) flowrates of the process, i.e.:

$$F_i^{\text{loss}} = F_{i,\text{in}}^{\text{lim}} - F_{i,\text{out}}^{\text{lim}} \quad [12.3]$$

Considering water loss, the mass load difference (Δm_i^{loss}) between the pseudo-mass load and the net mass load of the process can be determined by Equation [12.4]:

$$\Delta m_i^{\text{loss}} = \left|\Delta m_i - \Delta m_i^{\text{net}}\right| = F_i^{\text{loss}} C_{i,\text{out}}^{\max} \quad [12.4]$$

To plot a revised Limiting Water Profile for the process with water loss, a Limiting Inlet Profile is first constructed within the concentration intervals of $C_{i,\text{in}}^{\max}$ and $C_{i,\text{out}}^{\max}$ in the concentration vs mass load diagram (CMD), as shown in Fig. 12.1b. The horizontal projection of the Limiting Inlet Profile is Δm_i, which can be determined via Equation [12.1]. Note also that water loss is not considered at this stage. The inverse slope of the Limiting Inlet Profile thus corresponds to the limiting inlet flowrate of the process. Next, the Water Loss Profile is plotted in the diagram, with its arrow head connected to that of the Limiting Inlet Profile, and its inverse slope corresponding to F_i^{loss}. In this case, the horizontal distance of the Water Loss Profile indicates the mass load difference for process with water loss, Δm_i^{loss} (calculated using Equation [12.4]). The Limiting Outlet Profile is constructed in the same concentration interval of the Limiting Inlet Profile, with its inverse slope corresponding to the limiting outlet flowrate ($F_{i,\text{out}}^{\text{lim}}$) calculated using Equation [12.3].

After the limiting profiles of the water-using process have been constructed, the Water Supply Line is located in the CMD. For a water source of concentration $C_{\text{i,in}}$ (lower than $C_{i,\text{in}}^{\max}$), the Water Supply Line is first placed as a straight line between intervals $C_{\text{i,in}}$ and $C_{i,\text{out}}^{\max}$, as shown in Fig. 12.1c. It is then observed in Fig. 12.1c that the Water Supply Line intersects the $C_{i,\text{in}}^{\max}$ interval line at point A. To determine the practical Water Supply Line that considers

© Woodhead Publishing Limited, 2013

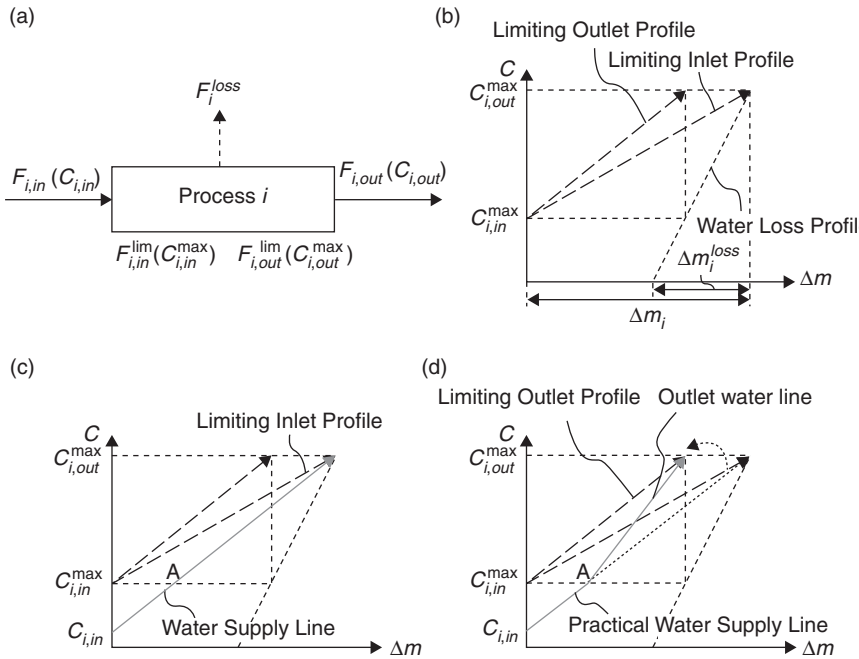

12.1 Graphical representation of water-using process with water loss. (a) Process model with water loss; (b) Water Loss Profile; (c) determine the inlet flowrate; (d) determine the outlet flowrate. (Source: Adapted with permission from John Wiley and Sons. http://onlinelibrary.wiley.com/doi/10.1002/aic.12508/full)

water loss in the process, the Water Supply Line is rotated anti-clockwise at point A until it touches the Limiting Outlet Profile, as shown in Fig. 12.1d. Note that two individual segments are then formed in the practical Water Supply Line. The portion below point A is referred to as the inlet segment. The inverse slope of the inlet segment determines the inlet flowrate, which can be calculated via solving Equation [12.1] with $C_{i,\text{in}}^{\max}$ replaced by $C_{\text{i,in}}$. The segment between the $C_{i,\text{in}}^{\max}$ and $C_{i,\text{out}}^{\max}$ interval is the *outlet segment* of the water-using process. The inverse slope of the outlet segment determines the outlet flowrate, which can be calculated via solving Equation [12.3].

12.2.2 Process with Water Gain

Figure 12.2a shows the general model for a process with water gain. A good example for this process is water generation as a by-product in the reactor. The water gain flowrate (F_i^{gain}) can be calculated by the difference between the inlet and outlet flowrates, as shown in Equation [12.5].

$$F_i^{\text{gain}} = F_{i,\text{out}}^{\text{lim}} - F_{i,\text{in}}^{\text{lim}} \qquad [12.5]$$

© Woodhead Publishing Limited, 2013

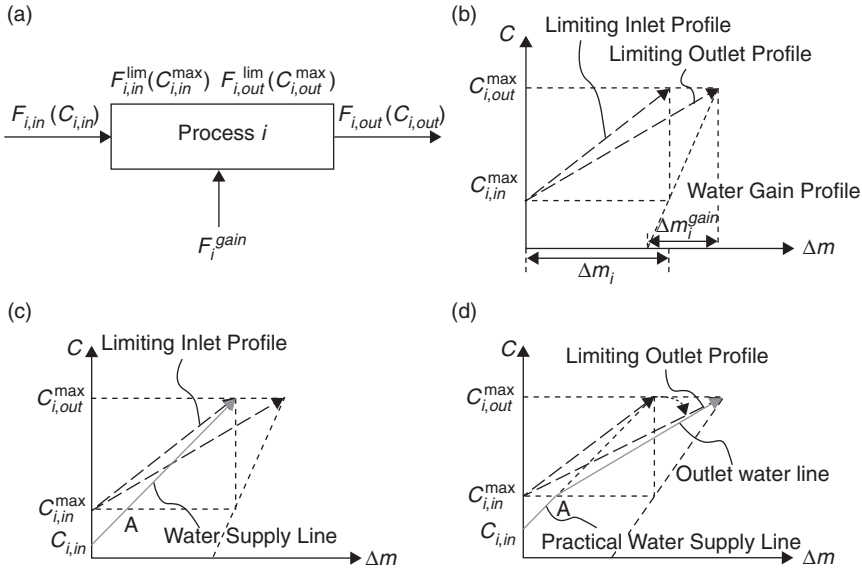

12.2 Graphical representation of water-using process with water gain. (a) Process model with water gain; (b) Water Gain Profile; (c) determine the inlet flowrate; (d) determine the outlet flowrate. (Source: Adapted with permission from John Wiley and Sons. http://onlinelibrary.wiley.com/doi/10.1002/aic.12508/full)

Considering water gain, the mass load difference (Δm_i^{gain}) between the pseudo-mass load and the net mass load of the process is determined by Equation [12.6]:

$$\Delta m_i^{\text{gain}} = \left|\Delta m_i - \Delta m_i^{\text{net}}\right| = F_i^{\text{gain}} C_{i,\text{out}}^{\max} \qquad [12.6]$$

In the CMD, the Limiting Inlet and Outlet Profiles of the process are first constructed in the $C_{i,\text{in}}^{\max}$ and $C_{i,\text{out}}^{\max}$ intervals (Fig. 12.2b), with their inverse slopes corresponding to their limiting inlet ($F_{i,\text{in}}^{\text{lim}}$) and outlet ($F_{i,\text{out}}^{\text{lim}}$) flowrates, respectively. Next, the Water Gain Profile is added in the diagram, with its arrow head connected to that of the Limiting Outlet Profile, and located within the concentration interval from zero to $C_{i,\text{out}}^{\max}$. The inverse slope of the Water Gain Profile hence corresponds to gained flowrate, F_i^{gain}, while its horizontal distance indicates the mass load difference for the process with water gain, Δm_i^{gain} (as shown in Fig. 12.2b) which can be determined by Equation [12.6].

For a given water source with inlet concentration of $C_{\text{i,in}}$ ($\leq C_{i,\text{in}}^{\max}$), the inlet segment of the practical Water Supply Line is initiated at $C_{\text{i,in}}$ and touches the Limiting Inlet Profile at $C_{i,\text{out}}^{\max}$ (see Fig. 12.2c), with its inverse slope corresponding to the supply flowrate. It can then be seen in Fig. 12.2c that the

© Woodhead Publishing Limited, 2013

Water Supply Line intersects the $C_{i,\text{in}}^{\max}$ interval line at point A. To determine the practical Water Supply Line that considers water gain in the process, the Water Supply Line is rotated clockwise at point A until it touches the Limiting Outlet Profile, as shown in Fig. 12.2d. Note that two individual segments are then formed as the practical Water Supply Line. The portion below point A is referred to as the inlet segment. The inverse slope of the inlet segment represents the inlet flowrate, which can be determined from Equation [12.1] with $C_{i,\text{in}}^{\max}$ replaced by $C_{\text{i,in}}$. Also, the portion between the $C_{i,\text{in}}^{\max}$ and $C_{i,\text{out}}^{\max}$ interval is the outlet segment of the water-using process. Similarly, the inverse slope of the outlet segment denotes the outlet flowrate, which can be calculated from Equation [12.5].

12.2.3 Process with Multiple Feeds

For water-using processes with a single water source, the supplied water flowrate can be targeted as per the procedure in the literature (Wang and Smith, 1994) – see Chapter 2. However, such a procedure does not apply where multiple water sources are utilised. Hence, a revised procedure for targeting processes with multiple feeds is now introduced.

In a water network, there are effluents of different contaminant concentrations generated from processes (known as internal water sources). Those internal water sources should be prioritised for reuse/recycle before an external water source is considered, because the external water source usually needs additional cost. Therefore, it is possible that a water-using process is fed by multiple sources (internal water sources and/or external water sources). As shown in Fig. 12.3a, three sources are available for use in process i, i.e. SR1, SR2 and SR3, each with respective flowrates (F_1, F_2 and F_3) and concentrations (C_1, C_2 and C_3, where $C_1 < C_2 < C_3$). Furthermore, we assume that C_2 has the same value as $C_{i,\text{in}}^{\max}$, while C_3 is lower than $C_{i,\text{out}}^{\max}$. In order to minimise the cleanest water source (SR1, which is most often an external water source), the reuse of SR2 and SR3 are to be maximised prior to SR1. In this case, SR2 should be fully recovered since $C_2 = C_{i,\text{in}}^{\max}$. When the flowrate of SR2 is sufficient for the process ($F_2 \geq F_{i,\text{in}}^{\lim}$), the entire inlet flowrate of process i ($F_{i,\text{in}}^{\lim}$) is supplied by SR2. When SR2 has insufficient flowrate ($F_2 \geq F_{i,\text{in}}^{\lim}$), the entire flowrate of SR2 is utilised first. Part of the contaminant mass load of process i is removed by SR2, and the removed mass load Δm_2 can be calculated by Equation [12.1]. However, the residual mass load ($\Delta m_i - \Delta m_2$) needs to be removed. The internal water source SR3 with lower quality (higher contaminant concentration) is considered to be utilised prior to SR1, which has higher quality. Since $C_3 > C_{i,\text{in}}^{\max}$, SR3 needs to be 'diluted' with SR1, with lower concentration, in order to meet the inlet concentration limit ($C_{i,\text{in}}^{\max}$). To determine the mixing ratio of SR1 and SR3,

© Woodhead Publishing Limited, 2013

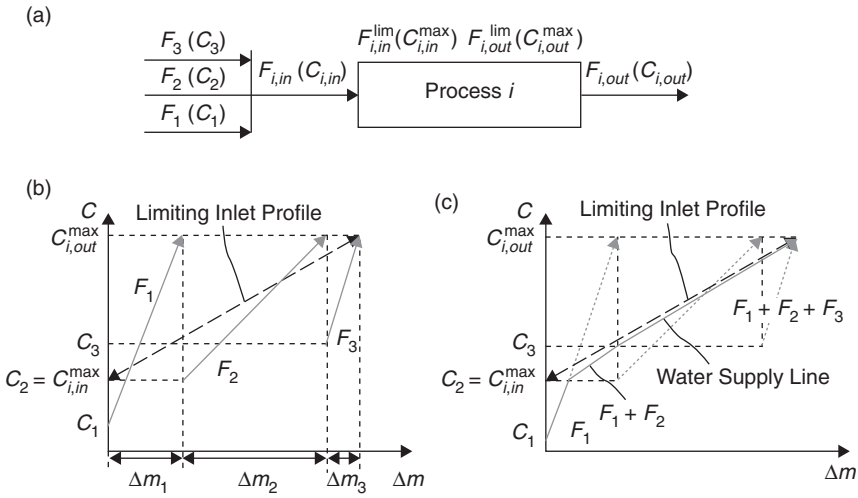

12.3 Targeting for water-using process with multiple feeds. (a) Process model with multiple feeds; (b) determine the separate flowrates from each sources; (c) determine the inlet flowrate. (Source: Adapted with permission from John Wiley and Sons. http://onlinelibrary.wiley.com/doi/10.1002/aic.12508/full)

the mass and flowrate balance Equations [12.7] and [12.8] have to be solved, respectively. Note that the mass load removed by SR2 as well as its supplied flowrate are to be subtracted from the total requirements of process *i*.

$$\Delta m_1 + \Delta m_3 = \Delta m_i - \Delta m_2 \qquad [12.7]$$

$$F_1 + F_3 = F_{i,\text{in}}^{\text{lim}} - F_2 \qquad [12.8]$$

where Δm_1 and Δm_3 correspond to the partial mass loads of process *i* removed by SR1 and SR3.

As shown in Fig. 12.3b, the water profiles of all the sources are constructed within their respective concentration intervals; for example, concentration interval of SR1 is located between C_1 and $C_{i,\text{out}}^{\text{max}}$. The horizontal projection of those water profiles corresponds to their removed mass loads, as determined by Equations [12.1], [12.7] and [12.8]. The individual water profiles can then be combined in respective concentration intervals to form the Water Supply Line, as shown in Fig. 12.3c.

In the concentration interval between the origin and $C_{i,\text{in}}^{\text{max}}$ (C_2), only a single water source, SR1, is found (with flowrate F_1). Within concentration interval of C_2 and C_3, the accumulated flowrate of F_1 and F_2 is allocated to process *i*. In the concentration interval between C_3 and $C_{i,\text{out}}^{\text{max}}$, the flowrates of SR1, SR2 and SR3 accumulate to the value of $F_{i,\text{in}}^{\text{lim}}$. Note that the Water

© Woodhead Publishing Limited, 2013

Supply Line is identical to Limiting Inlet Profile in the concentration interval above C_3. Also note that the average inlet concentration ($C_{i,\text{in}}$) and inlet flowrate are equal to the maximum inlet concentration ($C_{i,\text{in}}^{\max}$) and limiting inlet flowrate ($F_{i,\text{in}}^{\lim}$), respectively.

A special case for the reuse of SR3 (where $C_3 < C_{i,\text{out}}^{\max}$) is worthy of mention. When C_3 is equal to the maximum outlet concentration ($C_3 = C_{i,\text{out}}^{\max}$), its corresponding mass load removal (Δm_3) will remain zero, whatever its reutilised flowrate is. However, the usage of the water source with $C_3 = C_{i,\text{out}}^{\max}$ has the advantage of compensating the water flowrate deficit for processes with water loss. The compensating flowrate (F_3) can be determined by $F_{i,\text{in}}^{\lim} - F_1 - F_2$. Here, the average inlet concentration ($C_{i,\text{in}}$, after source mixing) will then be equal to the maximum inlet concentration ($C_{i,\text{in}}^{\max}$).

12.3 Process-based Graphical Approach (PGA) for Synthesis of Direct Reuse Water Networks

Based on the revised Limiting Water Profile, the procedures for determining the flowrate allocation for individual process with water loss/gain are proposed. In addition, the flowrate allocation for processes with multiple feeds can be determined via the procedure presented. Based on the flowrate allocation procedure for an individual process, a new PGA is proposed for simultaneous targeting and design of a water network. This approach can be considered as an extension of the Limiting Composite Curve technique (Wang and Smith, 1994) – see Chapter 2. The synthesis of reuse/recycle network from an example in the literature is presented to illustrate the proposed PGA in detail.

12.3.1 Preliminary Analysis

The limiting data adopted from the literature (Wang and Smith, 1995) is shown in Table 12.1. It is assumed that a single pure freshwater supply ($0\ \mu g \cdot g^{-1}$) is available in service. The first step of the PGA procedure involves preliminary analysis of the problem. Note that both the reactor and cooling system streams involve water loss, and the filtration stream involves water gain. The overall flowrate loss/gain (ΔF_p) of the entire water network is determined by Equation [12.9].

$$\Delta F_P = \sum_{i}^{N_P} \left(F_{i,\text{out}}^{\lim} - F_{i,\text{in}}^{\lim} \right) \qquad [12.9]$$

A positive value of ΔF_p indicates water surplus within the water-using system, while a negative value implies a water deficit. Based on the limiting data in

© Woodhead Publishing Limited, 2013

Table 12.1 Limiting data

Operation	Δm_i (g·h^{-1})	$F_{i,\text{in}}^{\text{lim}}$ (t·h^{-1})	$F_{i,\text{out}}^{\text{lim}}$ (t·h^{-1})	$C_{i,\text{in}}^{\text{max}}$ (μg·g^{-1})	$C_{i,\text{out}}^{\text{max}}$ (μg·g^{-1})	Process Sequence, Pi
Reactor	72,000	80	20	100	1,000	5
Cyclone	25,000	50	50	200	700	4
Filtration	1,000	10	40	0	100	2
Steam system	100	10	10	0	10	1
Cooling system	1,350	15	5	10	100	3
Total	–	165	125	–	–	–

Adapted from John Wiley and Sons, http://onlinelibrary.wiley.com/doi/10.1002/aic.12508/full.

Table 12.1, ΔF_p of this example is determined as – 40 t·h^{-1} (= [125 – 165] t·h^{-1}). This indicates that the overall water network experiences a water flowrate deficit. Hence, a minimum freshwater supply of 40 t·h^{-1} is required to supplement the network.

In order to minimise freshwater consumption, water recovery should be maximised for the internal water sources. In order to achieve rational reuse of internal water sources, the water-using processes are arranged in an ascending order based on their outlet concentrations. For cases where the water-using processes have the same outlet concentrations, such processes are arranged based on their inlet concentrations. Following this step, the sequence of processes in Example 1 is listed in the last column of Table 12.1. Note that the outlet concentrations of filtration (P2) and cooling system (P3) are given as 100 μg·g^{-1}; hence, these processes are arranged based on their inlet concentrations.

For processes without water loss/gain (i.e. stem system (P1), cyclone (P4)), the mass loads are given as shown in the second column of Table 12.1. However, for processes with water loss/gain (i.e. filtration (P2), cooling system (P3), reactor (P5)), the values shown in the second column of Table 12.1 are the pseudo-mass loads and Equation [12.1] relates those values to the corresponding limiting inlet flowrates.

12.3.2 Targeting and Design

For water processes without water loss/gain, the Limiting Water Profiles are constructed based on the procedure proposed by Wang and Smith (1994) – see Chapter 2. However, the Limiting Water Profiles for processes with water loss/gain are constructed based on the newly proposed revised procedure (Figs 12.1 and 12.2). Figure 12.4 shows all the Limiting Water Profiles for all processes. Note that the processes are arranged based on the sequence as

© Woodhead Publishing Limited, 2013

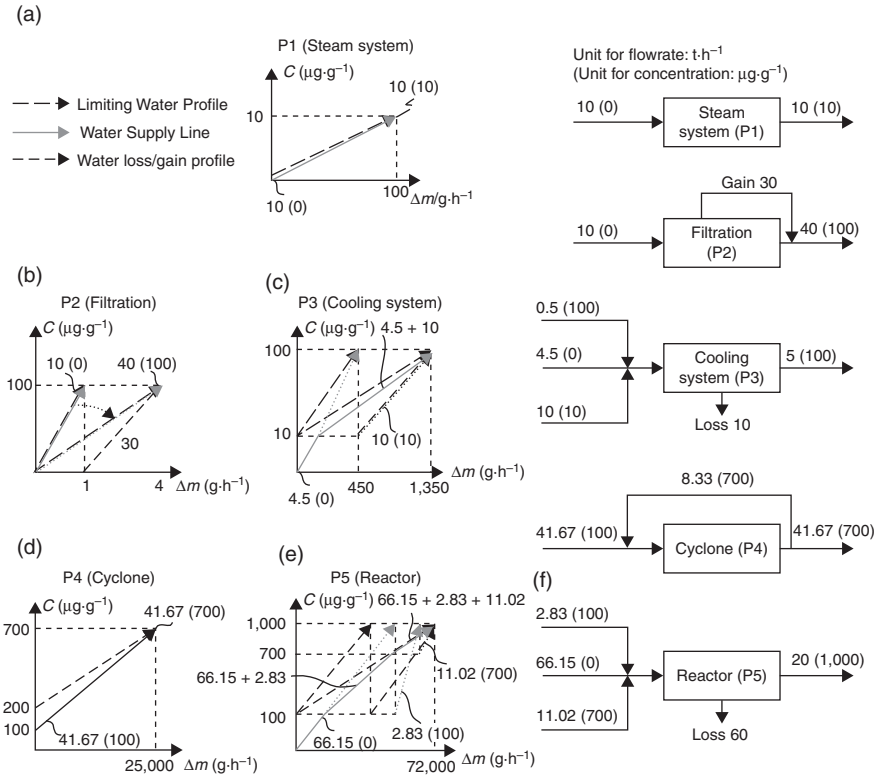

12.4 (a)–(e)Targeting for water-using processes P1–P5; (f) Water sources allocation for each water-using process involving flowrate constraints (unit for the flowrate is t·h^{-1} and unit for contaminant concentration is μg·g^{-1} in parenthesis). (Source: Adapted with permission from John Wiley and Sons. http://onlinelibrary.wiley.com/doi/10.1002/aic.12508/full)

determined in Section 12.3.1 (see Table 12.1). Filtration (P2) is considered as a process with water gain, while cooling system (P3) and reactor (P5) are processes with water loss. Their Limiting Water Profiles are plotted as shown in Figures 12.4b, 12.4c and 12.4e.

Since the Limiting Inlet Concentrations of steam system (P1) and filtration (P2) are given as 0 μg·g^{-1} (Table 12.1), only freshwater can be used to fulfil the requirement of these processes. By solving Equation [12.1], the minimum freshwater flowrates for P1 and P2 ($F_{FW,1}$ and $F_{FW,2}$) are both determined to be 10 t·h^{-1}. As P1 does not involve water loss/gain, the effluent of P1 is determined as 10 t·h^{-1} with the concentration of 10 μg·g^{-1} (see Limiting Water Profile in Fig. 12.4a). Due to 30 t·h^{-1} of water gain in P2, the outlet flowrate of effluent is determined as 40 t·h^{-1} at 100 μg·g^{-1}. The revised Limiting Water Profile for P2 is shown in Fig. 12.4b. Effluents from both processes are then taken as internal water sources for other processes, before freshwater is considered.

© Woodhead Publishing Limited, 2013

As shown in Table 12.1, the Limiting Inlet Concentration of cooling system (P3) is given as 10 $\mu g \cdot g^{-1}$. Hence, 10 $t \cdot h^{-1}$ of internal water source from P1 (10 $\mu g \cdot g^{-1}$) can be directly reused in P3. Solving Equation [12.1], a mass load of 900 $g \cdot h^{-1}$ is removed by internal water source from P1. Next, freshwater and an internal water source at 100 $\mu g \cdot g^{-1}$ are available for use. However, as mentioned in Section 12.2.3, since the internal water source has a concentration equal to the Limiting Outlet Concentration of P3, i.e. 100 $\mu g \cdot g^{-1}$, this water source will not remove any mass load and can only be used for meeting the fixed flowrate constraint of P3. Thus, the remainder of the 1,350 $g \cdot h^{-1}$ mass load of P3, i.e. 450 $g \cdot h^{-1}$ (= 1,350 – 900 $g \cdot h^{-1}$) is to be removed by freshwater. Based on Equation [12.1], the freshwater flowrate is determined as 4.5 $t \cdot h^{-1}$. To construct the Water Supply Line in the CMD (Fig. 12.4c), the internal water source segment is first constructed in the concentration interval between 10 and 100 $\mu g \cdot g^{-1}$, and touches at the arrowhead of the inlet profile. After that, 4.5 $t \cdot h^{-1}$ of freshwater is constructed in the concentration interval between 0 and 100 $\mu g \cdot g^{-1}$ to the left of the internal water source segment (see Fig. 12.4c). As shown in Fig. 12.4c, the Water Supply Line in concentration interval between 10 and 100 $\mu g \cdot g^{-1}$ is constructed by combining Water Supply Lines for two sources. Since the cooling system is considered as a fixed flowrate process, where 15 $t \cdot h^{-1}$ of fixed water flowrate is required, an additional water flowrate of 0.5 $t \cdot h^{-1}$ (= 15 – 10 – 4.5 $t \cdot h^{-1}$) for this process may be supplied either from the internal source from P2 (available at 40 $t \cdot h^{-1}$, 100 $\mu g \cdot g^{-1}$) or the effluent from P3 via the local recycling scheme (Wang and Smith, 1995). The former scheme is recommended, to avoid the build-up of unexpected contaminants within P3 via local recycling. Hence, the remaining internal water source from P2 at 100 $\mu g \cdot g^{-1}$ is reduced from 40 to 39.5 $t \cdot h^{-1}$. The water allocation of P3 is shown in Fig. 12.4f. Note that the three water sources are supplied to P3 with an average inlet concentration of 10 $\mu g \cdot g^{-1}$. Due to 10 $t \cdot h^{-1}$ of water loss in this process, the effluent of P3 with 100 $\mu g \cdot g^{-1}$ is reduced from 15 to 5 $t \cdot h^{-1}$. Combining the effluent of P3 with the effluent from P2, the internal water source of 100 $\mu g \cdot g^{-1}$ is increased from 39.5 to 44.5 $t \cdot h^{-1}$.

The water allocation for cyclone (P4) is then analysed. Since a total of 44.5 $t \cdot h^{-1}$ of 100 $\mu g \cdot g^{-1}$ internal water source is available, this internal water source should be reused for P4, before the freshwater source is considered. In order to fulfil the requirements of P4, the flowrate of this internal water source is determined as 41.67 $t \cdot h^{-1}$ using Equation [12.1]. Since there is no water gain or loss in P4, the effluent from P4 has the same flowrate as its inlet stream (i.e. 41.67 $t \cdot h^{-1}$), with an outlet concentration of 700 $\mu g \cdot g^{-1}$ (see Fig. 12.4d). To maintain the flowrate requirement for P4 (50 $t \cdot h^{-1}$), a local recycling scheme (Wang and Smith, 1995) is implemented. As shown in Fig. 12.4f, 8.33 $t \cdot h^{-1}$ (= 50 – 41.67 $t \cdot h^{-1}$) of effluent from P4 is being recycled, apart from the reuse of 41.67 $t \cdot h^{-1}$ of internal water source at 100 $\mu g \cdot g^{-1}$. The

© Woodhead Publishing Limited, 2013

average inlet concentration is calculated as 200 $\mu g \cdot g^{-1}$, which matches the Limiting Inlet Concentration of P4.

After water allocation is completed for P4, two internal water sources are available for the reactor (P5), i.e. effluents from P3 (2.83 $t \cdot h^{-1}$ = 44.5 – 41.67 $t \cdot h^{-1}$, 100 $\mu g \cdot g^{-1}$) and P4 (41.67 $t \cdot h^{-1}$, 700 $\mu g \cdot g^{-1}$). Since the inlet concentration of P5 is given as 100 $\mu g \cdot g^{-1}$, the internal water source of 100 $\mu g \cdot g^{-1}$ can be completely reused in P5. As mentioned in Section 12.2.3, if the internal water source at 700 $\mu g \cdot g^{-1}$ is reused, freshwater is required for dilution. Solving the mass and flowrate balance Equations [12.7] and [12.8], 11.02 $t \cdot h^{-1}$ of internal water source at 700 $\mu g \cdot g^{-1}$ and 66.15 $t \cdot h^{-1}$ of freshwater are required to fulfil the process requirement. As shown in Fig. 12.4e, 11.02 $t \cdot h^{-1}$ of internal water source at 700 $\mu g \cdot g^{-1}$ is first constructed in the concentration interval between 700 and 1,000 $\mu g \cdot g^{-1}$. Next, 2.83 $t \cdot h^{-1}$ of the 100 $\mu g \cdot g^{-1}$ internal water source is constructed in the concentration interval between 100 and 1,000 $\mu g \cdot g^{-1}$ to the left of the 700 $\mu g \cdot g^{-1}$ internal water source. Finally, 66.15 $t \cdot h^{-1}$ of freshwater is plotted in the concentration interval between 0 and 1,000 $\mu g \cdot g^{-1}$ to the left of the 100 $\mu g \cdot g^{-1}$ internal water source (see Fig. 12.4e). The average inlet concentration and total flowrate are determined as 100 $\mu g \cdot g^{-1}$ and 80 $t \cdot h^{-1}$, which are equal to the Limiting Inlet Concentration and limiting inlet flowrate of P5 (see Table 12.1). However, due to 60 $t \cdot h^{-1}$ of water loss, the flowrate of P5 effluent is reduced to 20 $t \cdot h^{-1}$.

Based on the detailed allocation of freshwater and internal water sources as shown in Fig. 12.4f, an overall minimum freshwater flowrate is determined as 90.65 $t \cdot h^{-1}$ (10, 10, 4.5 and 66.15 $t \cdot h^{-1}$ for P1, P2, P3 and P5), while the overall wastewater flowrate is determined as 50.65 $t \cdot h^{-1}$ (30.65 $t \cdot h^{-1}$ WW1 at 700 $\mu g \cdot g^{-1}$, and 20 $t \cdot h^{-1}$ WW2 at 1,000 $\mu g \cdot g^{-1}$). Both freshwater and wastewater flowrate targets are identical with the earlier reported results (Wang and Smith, 1995; Mann and Liu, 1999). In the work of Wang and Smith (1995), the targets are located by adjusting the Water Supply Line until it is feasible, when the water losses and gains are considered. However, in the work of Mann and Liu (1999), the freshwater and wastewater flowrate targets are determined by introducing the 'apparent' Water Pinch and deducing the corresponding equations.

It is also worth noting that the individual Limiting Water Profiles in Fig. 12.4 can be plotted in one figure (see Fig. 12.5a) in order to construct the Limiting Composite Curve. A revised Limiting Composite Curve (Fig. 12.5b) that considers water loss/gain can then be constructed by combining all individual Limiting Water Profiles in Fig. 12.5a. For the processes with water loss (P3 – cooling system and P5 – reactor), their Limiting Outlet Profiles are combined in the Limiting Composite Curve. The underlying principle is that the water loss is assumed to occur in the inlet of the process. In contrast, for the process with water gain (P2 – filtration), its Limiting Outlet Profile

© Woodhead Publishing Limited, 2013

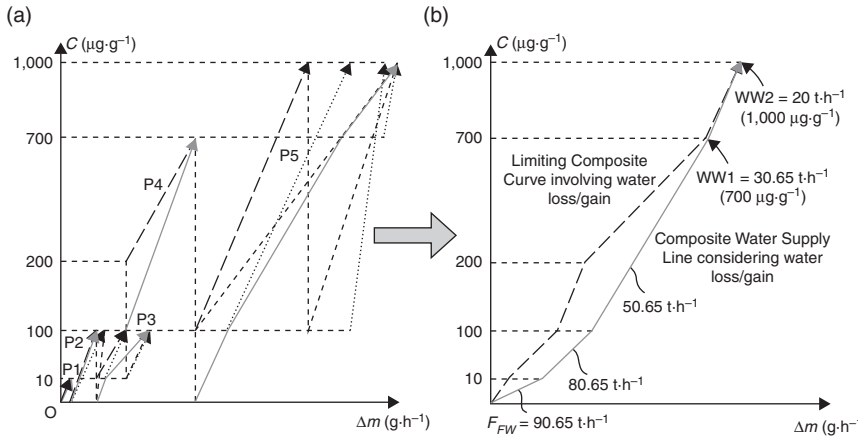

12.5 (a) Optimal Water Supply Lines for water-using processes; (b) Composite Water Supply Line for water network with reuse/recycling. (Source: Adapted with permission from John Wiley and Sons. http://onlinelibrary.wiley.com/doi/10.1002/aic.12508/full)

is excluded in the construction of the Limiting Composite Curve (only its Limiting Inlet Profile is included). In other words, the model assumes that water gain occurs at the outlet of the process.

In addition, the corresponding composite Water Supply Line can be determined by combining the Water Supply Lines for all processes within the respective concentration intervals, similar to the construction of the Limiting Composite Curve. This Composite Water Supply Line takes into account the water loss/gain of the individual process. As shown in Fig. 12.5b, the total flowrates found between 0 and 10 $\mu g \cdot g^{-1}$ corresponds to the overall freshwater flowrate (F_{FW}) of 90.65 $t \cdot h^{-1}$.

The summation of the flowrates in the next concentration interval (10–100 $\mu g \cdot g^{-1}$) gives 90.65 $t \cdot h^{-1}$. However, due to 10 $t \cdot h^{-1}$ of water loss (in cooling system) at 10 $\mu g \cdot g^{-1}$, the flowrate of water supply is reduced to 80.65 $t \cdot h^{-1}$.

The slope of the composite water supply curve in the concentration interval between 10 and 100 $\mu g \cdot g^{-1}$ increases slightly compared to previous concentration interval. For the concentration interval between 100 and 700 $\mu g \cdot g^{-1}$, the total flowrate is calculated as 110.65 $t \cdot h^{-1}$ (= 41.67 + 66.15 + 2.83 $t \cdot h^{-1}$).

At this concentration interval, 30 $t \cdot h^{-1}$ of water gain (filtration) occurs at 100 $\mu g \cdot g^{-1}$, which increases the water supply flowrate from 80.65 to 110.65 $t \cdot h^{-1}$.

On the other hand, 60 $t \cdot h^{-1}$ of water loss (reactor) also occurs, thus the practical water supply flowrate reduces to 50.65 $t \cdot h^{-1}$ (= [110.65 – 60] $t \cdot h^{-1}$). The summation of water supply flowrates in the final concentration interval ([700–1000] $\mu g \cdot g^{-1}$) gives 80 $t \cdot h^{-1}$ (= [66.15 + 2.83 + 11.02] $t \cdot h^{-1}$).

© Woodhead Publishing Limited, 2013

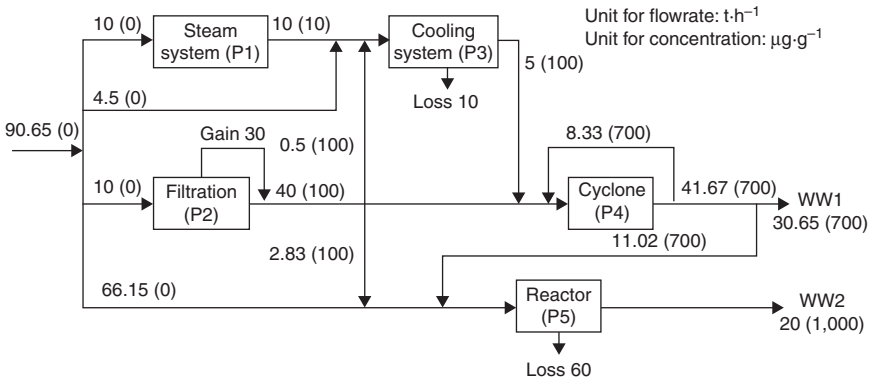

12.6 An optimal water network with reuse/recycling. (Source: Adapted with permission from John Wiley and Sons. http://onlinelibrary.wiley.com/doi/10.1002/aic.12508/full)

Because of 60 $t \cdot h^{-1}$ of water loss in the reactor, the practical water supply flowrate in this interval is reduced to 20 $t \cdot h^{-1}$ (= [80 – 60] $t \cdot h^{-1}$). Since 50.65 $t \cdot h^{-1}$ of internal water source is generated from the previous concentration interval at 700 $\mu g \cdot g^{-1}$, a surplus of 30.65 $t \cdot h^{-1}$ (= [50.65 – 20] $t \cdot h^{-1}$) of internal water source is discharged as wastewater (denoted as WW1).

Also, 20 $t \cdot h^{-1}$ of wastewater (WW2) is generated at 1,000 $\mu g \cdot g^{-1}$, from the last concentration interval. The corresponding flowrate of each concentration interval can also be determined based on the inverse slope of each segment of the composite Water Supply Line in the respective concentration interval (Fig. 12.5b).

Combining all the individual matches in Fig. 12.4f, a final water network design for direct reuse/recycle scheme is constructed, as shown in Fig. 12.6. The network design in Fig. 12.6 has a quite similar structure to those reported in the literature (Wang and Smith, 1995; Mann and Liu, 1999). However, there are slight differences between those figures. The local recycle stream of cyclone (P4) in Fig. 12.6 has a lower flowrate (8.33 $t \cdot h^{-1}$). Also, a higher flowrate of freshwater (66.15 $t \cdot h^{-1}$) is being allocated to reactor (P5) in Fig. 12.6. Both of these flowrate allocations reduce the build-up of unexpected contaminant within P4 and P5. On the other hand, the blowdown of cooling system (P3) may be contaminated with treatment chemicals; hence, it is not advisable to reuse the blowdown to the reactor, which would be sensitive to the contamination. As shown in Fig. 12.6, effluent from the cooling system (P3) is not reused in reactor (P5).

The presented PGA can be generalised in a flow chart, as shown in Fig. 12.7. Based on the given limiting data, the sequence of processes is first determined. Next, the Limiting Water Profiles are plotted for the processes. For each process, the appropriate water sources are determined. If a fixed

© Woodhead Publishing Limited, 2013

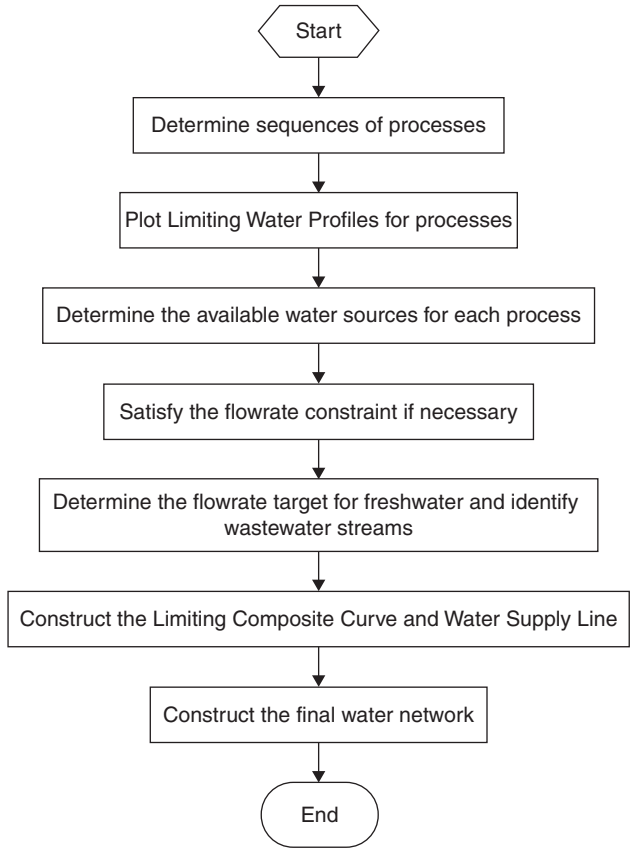

12.7 The procedures of PGA for the synthesis of water network with reuse/recycling.

flowrate process is involved, the fixed flowrate constraint is satisfied. Until this stage, the flowrate targets and allocations for the individual processes have been determined simultaneously. After that, the freshwater flowrate target for the whole water network is located by summing the freshwater flowrate targets for the individual processes. The wastewater streams are also identified. The Limiting Composite Curve and Water Supply Line considering water loss/gain are constructed accordingly by combining the Limiting Water Profiles and Water Supply Line for the individual processes. Finally, all the flowrate allocations for the individual processes are combined to synthesise the water network. Note that the flowrate targeting and network design for individual processes are performed simultaneously, which is the novel feature of the PGA presented here.

© Woodhead Publishing Limited, 2013

12.4 Conclusion

As presented in Section 12.2, how to determine the flowrate targets with water loss in the work of Wang and Smith (1995) is not clear. The targeting procedure for the water network with water loss/gain in the work of Mann and Liu (1999) may be trial-and-error. In addition, the targeting stage and design stage for the synthesis of a water network with loss/gain in the literature (Wang and Smith, 1995; Mann and Liu, 1999) are performed separately. However, the PGA can target and design water networks simultaneously. In addition, the flowrate targeting and water source allocation for individual water-using processes with water loss/gain can be dealt through the revised Limiting Water Profiles presented. The targeting procedure for a water-using process with multiple feeds is also proposed. The synthesis of a water network with a direct reuse scheme is illustrated to show the applicability of the proposed PGA.

12.5 Sources of Further Information and Advice

The PGA that has been presented can be used to synthesise water networks involving regeneration and waste treatment (total water network) with multiple freshwater sources. A recently published article (Deng *et al*., 2011) can be referred to for further reading. Moreover, several important reviews and books, such as the review of Water Pinch Analysis (Foo, 2009), the comprehensive review of water network design with literature annotations (Jezowski, 2010), current opinion on industrial water recycle/reuse (Klemeš, 2012), the water system design chapter in Smith (2005), the edited book including recent advances on material resource conservation and waste reduction (Foo *et al*., 2012), and the recently released book on Process Integration for resource conservation (Foo, 2012) are all recommended for a deeper understanding of the synthesis of water networks. Once the single-contaminant concentration can be replaced by a certain property (i.e. COD, pH and colour), PGA can be applied for the synthesis of property-based water networks, which belongs to the framework of Property Integration. The book authored by El-Halwagi (2006) is recommended for further reading.

12.6 Acknowledgements

Financial support provided by the National Basic Research Program of China (No. 2012CB720500) and National Natural Science Foundation of China united with China National Petroleum Corporation (No. U1162121) are gratefully acknowledged.

© Woodhead Publishing Limited, 2013

12.7 References

Agrawal, V., Shenoy, U. V. (2006). Unified conceptual approach to targeting and design of water and hydrogen networks. *AIChE Journal*, **52**, 1071–1082.

Bai, J., Feng, X., Deng, C. (2007). Graphically based optimisation of single-contaminant regeneration reuse water systems. *Chemical Engineering Research and Design*, **85**, 1178–1187.

Bandyopadhyay, S., Cormos, C. C. (2008). Water management in process industries incorporating regeneration and recycle through a single treatment unit. *Industrial and Engineering Chemistry Research*, **47**, 1111–1119.

Bandyopadhyay, S., Ghanekar, M. D., Pillai, H. K. (2006). Process water management. *Industrial and Engineering Chemistry Research*, **45**, 5287–5297.

Castro, P., Matos, H., Fernandes, M. C., Nunes, C. P. (1999). Improvements for mass-exchange networks design. *Chemical Engineering Science*, **54**, 1649–1665.

Deng, C., Feng, X. (2011). Targeting for conventional and property-based water network with multiple resources. *Industrial and Engineering Chemistry Research*, **50**, 3722–3737.

Deng, C., Feng, X., Ng, D. K. S., Foo, D. C. Y. (2011). Process-based graphical approach for simultaneous targeting and design of water network. *AIChE Journal*, **57**, 3085–3104.

Dhole, V. R., Ramchandani, N., Tainsh, R. A., Wasilewski, M. (1996). Make your process water pay for itself. *Chemical Engineering*, **103**, 100–103.

El-Halwagi, M. M. (2006). *Process Integration*. Academic Press, San Diego, USA.

El-Halwagi, M. M., Gabriel, F., Harell, D. (2003). Rigorous graphical targeting for resource conservation via material recycle/reuse networks. *Industrial and Engineering Chemistry Research*, **42**, 4319–4328.

Feng, X., Bai, J., Zheng, X. S. (2007). On the use of graphical method to determine the targets of single-contaminant regeneration recycling water systems. *Chemical Engineering Science*, **62**, 2127–2138.

Foo, D. C. Y. (2009). State-of-the-art review of pinch analysis techniques for water network synthesis. *Industrial and Engineering Chemistry Research*, **48**, 5125–5159.

Foo, D. C. Y. (2012). *Process Integration for Resource Conservation*. CRC Press, Boca Raton, USA.

Foo, D. C. Y., El-Halwagi, M. M., Tan, R. R. (2012). *Recent Advances in Sustainable Process Design and Optimisation*. World Scientific Publishing Company, Singapore.

Foo, D. C. Y., Manan, Z. A., Tan, Y. L. (2006). Use cascade analysis to optimize water networks. *Chemical Engineering Progress*, **102**, 45–52.

Hallale, N. (2002). A new graphical targeting method for water minimisation. *Advances in Environmental Research*, **6**, 377–390.

Jezowski, J. (2010). Review of water network design methods with literature annotations. *Industrial and Engineering Chemistry Research*, **49**, 4475–4516.

Klemeš, J. J. (2012). Industrial water recycle/reuse. *Current Opinion in Chemical Engineering*, **1**, 238–245.

Manan, Z. A., Tan, Y. L., Foo, D. C. Y. (2004). Targeting the minimum water flow rate using water cascade analysis technique. *AIChE J.*, **50**, 3169–3183.

Mann, J. G., Liu, Y. A. (1999). *Industrial Water Reuse and Wastewater Minimisation*. McGraw-Hill Professional, New York, USA.

© Woodhead Publishing Limited, 2013

Prakash, R., Shenoy, U. V. (2005). Targeting and design of water networks for fixed flowrate and fixed contaminant load operations. *Chemical Engineering Science*, **60**, 255–268.

Smith, R. (2005). *Chemical Process Design and Integration*, 2nd ed.. John Wiley & Sons Ltd, Chichester, UK.

Wang, Y. P., Smith, R. (1994). Wastewater minimisation. *Chemical Engineering Science*, **49**, 981–1006.

Wang, Y. P., Smith, R. (1995). Wastewater minimisation with flowrate constraints. *Chemical Engineering Research and Design*, **73**, 889–904.

12.8 Appendix: Nomenclature

$C_{i,\text{in}}^{\max}$	limiting inlet concentration of process *i,* $\mu g \cdot g^{-1}$
$C_{i,\text{out}}^{\max}$	limiting outlet concentration of process *i,* $\mu g \cdot g^{-1}$
$F_{i,\text{in}}^{\lim}$	limiting inlet water flowrate of process *i,* $t \cdot h^{-1}$
$F_{i,\text{out}}^{\lim}$	limiting outlet water flowrate of process *i,* $t \cdot h^{-1}$
$F_{i,\text{in}}$	optimal water supply flowrate of process *i,* $t \cdot h^{-1}$
$F_{i,\text{out}}$	the outlet water flowrate of process *i,* $t \cdot h^{-1}$
F_i^{loss}	water loss flowrate for process *i,* $t \cdot h^{-1}$
F_i^{gain}	water gain flowrate from process *i,* $t \cdot h^{-1}$
ΔF_p	overall flowrate difference for all the water-using processes, $t \cdot h^{-1}$
i	index of the water-using processes
Δm_i	the pseudo-mass load difference for water-using process *i,* $g \cdot h^{-1}$
Δm_i^{net}	the net mass load difference for water-using process *i,* $g \cdot h^{-1}$
Δm_i^{gain}	the mass load difference for water-using process *i* with or without considering water gain, $g \cdot h^{-1}$
Δm_i^{loss}	the mass load difference for water-using process *i* with or without considering water loss, $g \cdot h^{-1}$
N_P	total number for the water-using processes
PGA	process-based graphical approach
CMD	concentration vs mass load diagram
WW	wastewater stream

© Woodhead Publishing Limited, 2013

13

Conserving Material Resources through Process Integration: Material Conservation Networks

MAHMOUD M. EL-HALWAGI, Texas A&M University, USA

DOI: 10.1533/9780857097255.3.422

Abstract: This chapter provides an overview of key problems and tools in the area of conserving material resources. The introduction discusses the primary classes and strategies of material conservation problems. Next, overall mass targeting techniques are presented to determine performance benchmarks independent of technologies and cost. Then, various techniques are discussed to attain these targets in a cost-effective manner. Examples of low/no-cost strategies are given (e.g., Water Pinch, Hydrogen Pinch, Material Recycle Pinch diagram). Targeting and synthesis techniques for medium-cost strategies are also given with a description of the basic Mass Exchange Network problem. Finally, Property Integration is discussed and a sample tool (Property-Based Material Recycle Pinch diagram) is described along with applications.

Key words: Mass Integration, Property Integration, material recycle, water recycle, hydrogen recycle, Mass Pinch, Property Pinch.

13.1 Introduction

The process industries are characterised by tremendous use of natural resources in the form of energy and materials. Process Integration provides an attractive framework for the design of resource-conservation networks that integrate process streams and units to garner savings in energy and material usage. The focus of this chapter is on material conservation networks (MCNs), which may be defined as integrated systems of streams and units aimed at the enhancement of the effectiveness of mass utilisation and productivity in industrial facilities as well as the protection of natural material resources. Examples include:

- Reducing the usage of fresh raw materials.
- Decreasing the usage of material utilities (e.g., solvents, water, hydrogen).

© Woodhead Publishing Limited, 2013

- Enhancing the yield of the desired products and by-products.
- Reducing the discharge of process wastes (especially those that can potentially harm natural resources and the environment).

Because of the holistic nature of Process Integration, it is uniquely suited to generating comprehensive material conservation strategies such as:

- In-plant modification: which involves changes in the design and operation of the process to reach the desired objectives.
- Recycle/reuse: which is based on allocation of process and terminal streams back to the process to reduce the usage of fresh resources and the discharge of waste materials.
- Treatment and regeneration: which includes the addition of units for adjusting the composition and characteristics of the utilised streams to enable recycle/reuse or acceptable discharge.

Based on the targeted domain, Process Integration may be categorised into the following three classes:

- **Energy Integration**: which has been covered in Part 2 of this book.
- **Mass Integration**: which is a 'systematic methodology that provides a fundamental understanding of the global flow of mass within the process and employs this understanding in identifying performance targets and optimising the generation and routing of species throughout the process' (El-Halwagi, 1997).
- **Property Integration:** which is a 'functionality-based, holistic approach to the allocation and manipulation of streams and processing units, which is based on the tracking, adjustment, assignment, and matching of functionalities throughout the process' (El-Halwagi *et al.*, 2004).

Reviews of the basic principles and applications of Mass and Property Integration are available in literature (e.g., Smith, 2005; El-Halwagi, 2006, 2012; Kemp, 2007; Foo, 2009, 2012; Majozi, 2010; Klemeš *et al.*, 2011; Noureldin, 2011).

This chapter provides an overview of key tools and application of Mass and Energy Integration in the area of resource conservation. Emphasis is given to the graphical tools providing insights. A discussion of algebraic and optimisation tools will be briefly offered. The topics are discussed under the following headings:

- Overall targeting of MCNs
- Mass Exchange Networks
- Water-Pinch Analysis and extensions

© Woodhead Publishing Limited, 2013

- Material Recovery Pinch diagram
- Property Based Material Recovery Pinch diagram

13.2 Overall Targeting of Material Conservation Networks

One of the hallmarks of Process Integration is its ability to benchmark the performance of a system ahead of detailed design. This benchmarking is referred to as targeting. Before specific strategies are considered for conserving materials, it is beneficial to benchmark the mass utilisation performance of the process when there are no limitations of the strategies, technologies, or capital expenditures. This is referred to as overall mass targeting. Systematic techniques for overall mass targeting (for minimising waste discharges, minimising fresh usage of raw materials, and maximising process yield) are reviewed by El-Halwagi (2006, 2012). Here, an example is given in the area of minimising the usage of fresh raw materials and material utilities with now constraints on strategies or economics. Consider a process which uses a certain load of a specific fresh-resource chemical (F). Within the process, the net generation of this chemical compound due to chemical reaction is termed Net_G (when the value is negative, Net_G becomes net depletion). The load of the targeted chemical in streams leaving the process is designated T. A superscript BMI is used to represent the values before Mass Integration. Therefore, for the generic process shown by Fig. 13.1., the overall component material balance for the targeted chemical is given by:

$$F^{\mathrm{BMI}} = T^{\mathrm{BMI}} - \mathrm{Net_G}^{\mathrm{BMI}} \qquad [13.1]$$

In order to minimise fresh usage, Equation [13.1] indicates that the terminal discharges should be minimised and the net generation should be maximised. The general approach to targeting this problem is derived and described by Noureldin and El-Halwagi (1999). Nonetheless, there are approaches based on simplifying assumptions, such as the procedure shown by Fig. 13.2 (El-Halwagi, 2006). The key steps start with extracting

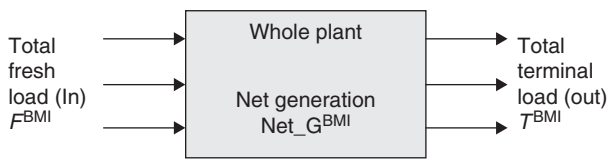

13.1 Overall material balance for the targeted species before Mass Integration (El-Halwagi, 2006).

© Woodhead Publishing Limited, 2013

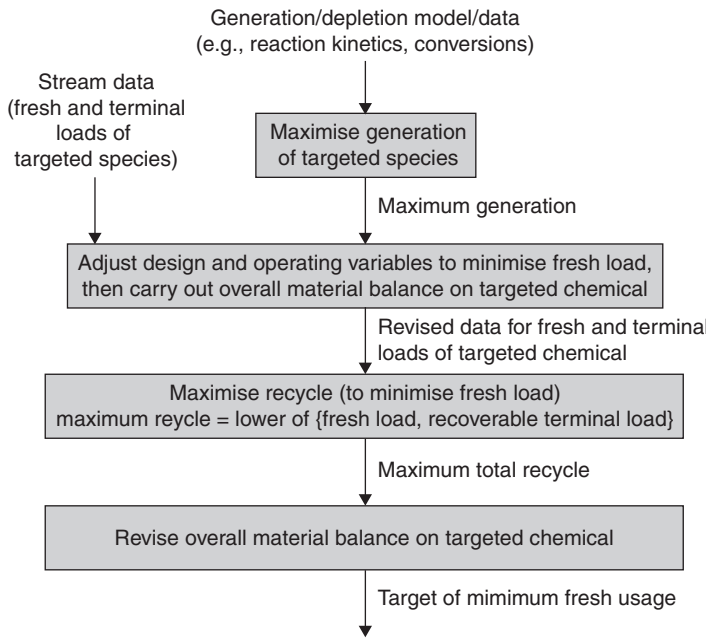

13.2 Procedure for identifying minimum fresh usage.

data on the generation and depletion of the targeted chemical along with stream data for fresh usage and waste discharge. Next, the generation of the targeted chemical is carried out by functionally relating the net generation of the chemical to the design and operating degrees of freedom and maximising this function. Then, fresh usage of the chemical is reduced by adjusting design and operating variables impacting on the usage of the fresh chemicals. Recycle is next used to its maximum extent by allowing a recovery network (the details of which are irrelevant at the targeting stage) to be used to render the terminal stream in a condition needed to replace the equivalent amount of the fresh chemical. Hence, the maximum extent of recycle corresponds to the lower of the two loads: the fresh usage and the terminal discharge. Finally, the overall balance for the targeted chemical is adjusted based on the changes associated with the aforementioned steps. The calculated fresh usage is the overall mass target for the chemical of interest regardless of the available technologies, strategies, and cost.

Now that the overall mass target has been identified, it is necessary to determine the specific steps that will lead to the cost-effective implementation of the target. One way of classifying these implementations is based on cost, impact (the contributions to reaching the target), and acceptability (the likelihood of adopting the proposed implementation). Figure 13.3

© Woodhead Publishing Limited, 2013

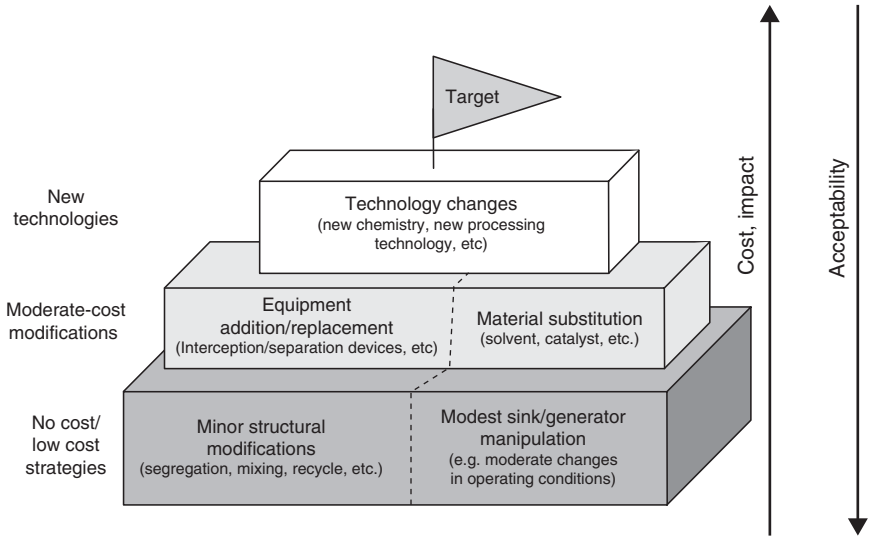

13.3 Hierarchy of Mass Integration strategies to reach overall mass targets (El-Halwagi, 1999).

schematically illustrates the hierarchy of these strategies (El-Halwagi, 1999), which include:

- No/low-cost strategies (such as minor changes in design and operating variables or direct recycle of process streams without adding new equipment)
- Medium-cost strategies (such as addition or substitution of separation units and/or Mass Separating Agents)
- New technologies (involving substantial changes in process technology and/or chemical pathways)

The following sections give examples of these implementation strategies. Water and Hydrogen Pinch, as well as Material Recovery Pinch diagrams for direct recycle, fall in the category of no/low-cost strategies, while Mass Exchange Networks belong to the medium-cost strategies since they typically involve the addition and/or substitution of new equipment and/or material utilities.

13.3 Mass Exchange Networks

A mass exchanger is any direct-contact mass transfer operation that is used to remove some components from a stream that is rich in these components to a stream that is lean in these components – a Mass Separating Agent (MSA). The problem of targeting and synthesising Mass Exchange Networks

© Woodhead Publishing Limited, 2013

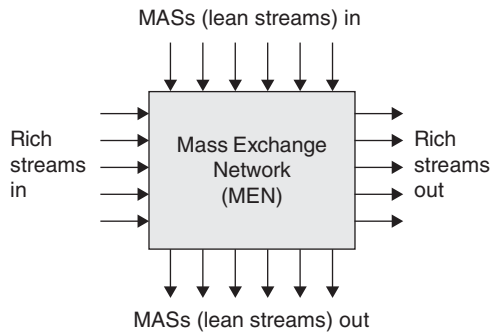

13.4 Schematic representation of the MEN synthesis problem (El-Halwagi and Manousiouthakis, 1989).

(MEN) was introduced by El-Halwagi and Manousiouthakis (1989), and served as the basis for numerous contributions in Mass Integration. In its basic form (Fig. 13.4), the problem of synthesising MENs deals with the transfer of certain components for a set of rich streams to a set of lean streams. The design questions entail the selection of mass transfer technologies, the selection of type and flow of the MSAs, and the matching among the rich and the lean streams. When the plant possesses process MSAs, effort is made to maximise the usage of the process resources in order to minimise the use of external MSAs. But even when all the candidate MSAs are external to the process, they should be screened and selected along with their flowrates based on thermodynamic and economic criteria.

Instead of attempting to make individual decisions for matching pairs of streams, a holistic approach is adopted by developing composite representation of all rich streams (the rich composite stream) and all process MSAs (the lean composite stream). These composites represent the cumulative mass to be exchanged versus the composition. In order to insure thermodynamic feasibility of mass exchange, thermodynamic equilibrium minus a minimum allowable mass transfer driving force (ε_j) is used for each lean stream (j) to create a one-to-one correspondence among the composition scales for which mass transfer is feasible. Mass transfer is practically feasible when the lean composite stream lies to the left of the rich composite stream. The point at which the two Composite Curves touch is referred to as the mass exchange Pinch Point (Fig. 13.5). Three targets can be determined from this Pinch diagram: maximum integrated mass exchange, minimum load to be removed by the external MSAs, and excess capacity of the process MSAs.

On the Pinch diagram, the vertical overlap between the two composite streams represents the maximum amount of the transferrable component that can be transferred from the rich streams to the process MSAs. It is

© Woodhead Publishing Limited, 2013

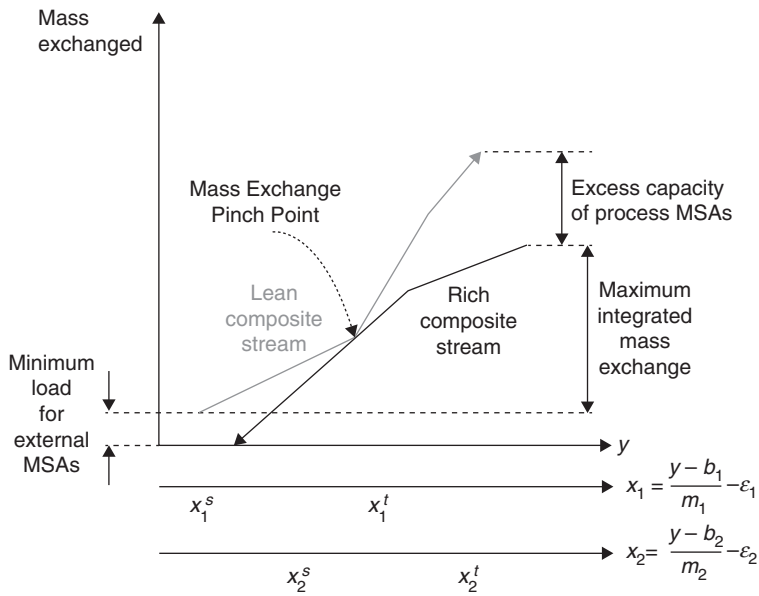

13.5 The Mass Exchange Pinch diagram (El-Halwagi and Manousiouthakis, 1989).

referred to as the 'integrated mass exchange'. The vertical distance of the lean composite stream that lies above the upper end of the rich composite stream is referred to as 'excess process MSAs'. It corresponds to that capacity of the process MSAs to remove mass that cannot be used because of thermodynamic infeasibility. According to the designer's preference or to the specific circumstances of the process, such excess can be eliminated from service by lowering the flowrate and/or the outlet composition of one or more of the process MSAs. Finally, the vertical distance of the rich composite stream that lies below the lower end of the lean composite stream corresponds to the mass to be removed by external MSAs. For these targets to be attained, three design rules must be observed:

- No mass should be passed through the Pinch (i.e. the two composites must touch).
- No excess capacity should be removed from MSAs Below the Pinch.
- No external MSAs should be used Above the Pinch.

The Mass Exchange Pinch diagram is analogous to the Heat Exchange Pinch diagram discussed in Part II of this book. The direct-contact nature of mass transfer, the presence of multiple components, and the need to include

© Woodhead Publishing Limited, 2013

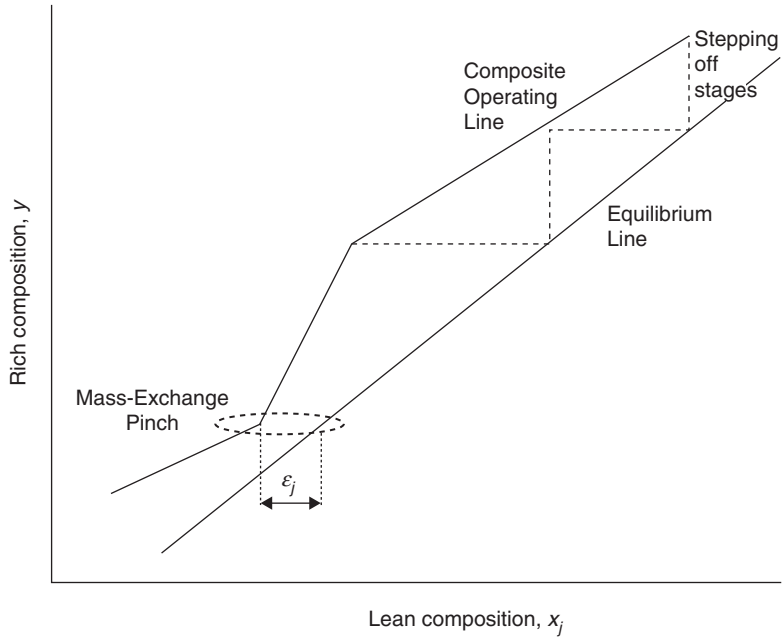

13.6 Supertargeting of MENs (Hallale and Fraser, 2000).

mass transfer equilibrium functions pose additional complications for the synthesis of MENs.

In addition to operating cost and material conservation targets, capital cost targets may be identified through Supertargeting (Hallale and Fraser, 2000). The key idea is to develop the Composite Curves on a rich composition versus lean composition representation (Fig. 13.6). Composite Operating Lines as well as the Equilibrium Line are plotted. This enables the 'stepping off' of mass exchange stages and the indirect determination of capital cost. Design rules can then be used to minimise the overall number of stages by adhering closely to the Composite Operating Line.

13.4 Water-Pinch Analysis

A particularly useful class of Mass Integration problems deals with water reuse. Wang and Smith (1994) developed Water-Pinch Analysis to identify targets for minimum fresh-water usage and wastewater discharge. First, a limiting water profile is determined for each unit based on the allowable concentration of contaminant versus the contaminant mass load. Next, the Limiting Composite Curve for all water users is plotted on composition-vs-load diagram. As shown by Fig. 13.7, a maximum-slope line is passed by the Limiting Composite Curve while lying completely below it to determine the

© Woodhead Publishing Limited, 2013

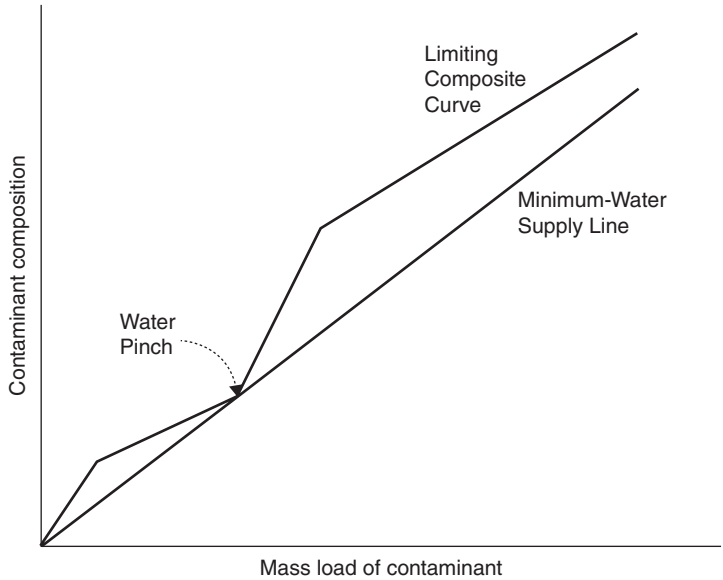

13.7 Water-Pinch diagram (Wang and Smith, 1994).

minimum flowrate of fresh water that is utilised successively in the water-using operations.

An important and analogous problem to water minimisation is hydrogen minimisation. Alves and Towler (2002) introduced a Hydrogen Pinch Analysis based on the concept of hydrogen surplus that tracks the cumulative usage and availability of hydrogen in a plant and incorporates the purity of available hydrogen in assigning the sources of hydrogen to the users.

Significant developments have been made in the field of water minimisation. For a recent review of the subject, the reader is referred to Foo (2009). Algebraic methods have been developed using cascade analysis (Foo *et al.*, 2006). Mathematical programming has also been used as a basis for targeting and synthesising water networks (e.g., Savelski and Bagajewicz, 2001; Gabriel and El-Halwagi, 2005). Also, combined water- and heat-recovery networks have been synthesised using optimisation approaches (Savulescu *et al.*, 2005). Graphical techniques offer the advantage of providing clear insights through visualisation. These insights are remarkably powerful and enable the designer to see the 'big picture' of the process and to make insightful decisions. Algebraic approaches provide an effective computation framework. Mathematical programming enables the tackling of complex problems and the relaxation of most assumptions associated with graphical and algebraic procedures. Ultimately, there is not a single definitive approach to be employed

© Woodhead Publishing Limited, 2013

and the user should select the approach based on the specific needs and circumstances of the problem.

13.5 Direct Recycle and Material Recycle Pinch Diagram

Direct recycle refers to the allocation of process and waste streams (referred to as sources) to process units that can utilise these streams (referred to as sinks) without the addition of new pieces of equipment (e.g., mass exchangers). The objective is to maximise the use of the process sources through recycle and to minimise the usage of fresh resources and the discharge of waste streams. A particularly useful tool is the Material Recycle Pinch diagram developed by El-Halwagi *et al.* (2003). First, data are extracted for the flows and compositions of the process sources and constraints on process sinks in the form of required flowrates and maximum allowable compositions of impurities. Next, the sources and the sinks are arranged in

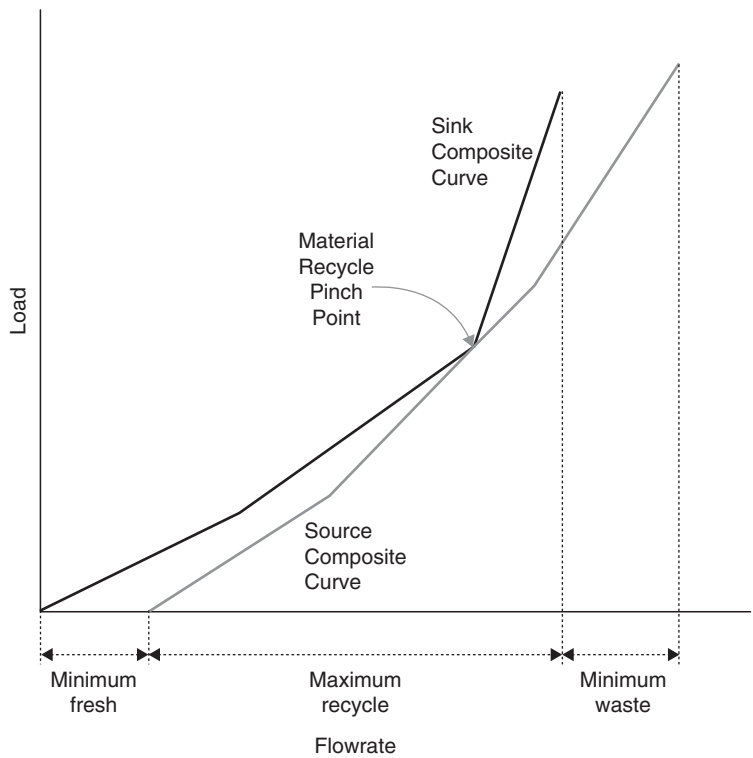

13.8 Identifying targets for minimum fresh usage, maximum direct recycle, and minimum waste discharge (El-Halwagi *et al.*, 2003).

© Woodhead Publishing Limited, 2013

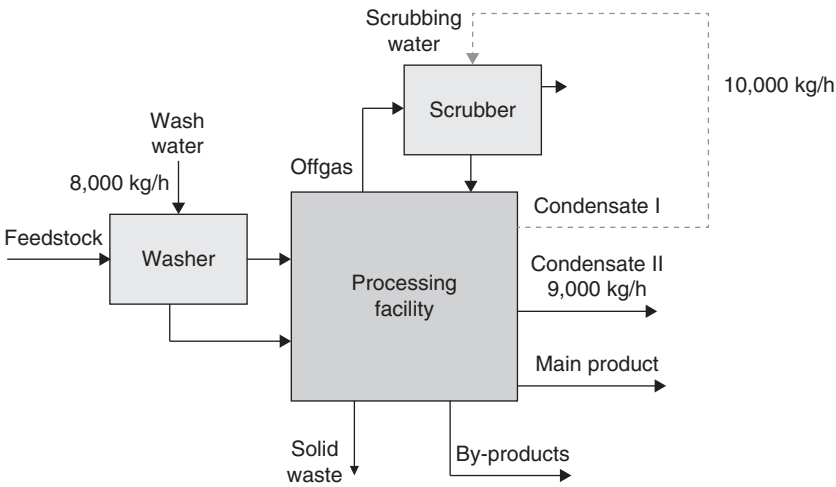

13.9 Food-processing plant (El-Halwagi, 2006).

ascending order of compositions of impurities. Sink- and Source-Composite Curves are constructed by plotting load of impurities vs flowrate (Fig. 13.8). By maintaining the source composite below the sink composite at all flowrates, feasibility of recycle is insured because of the satisfaction of the constraints for maximum admissible loads of impurities to the sinks. The point where the two composites touch is referred to as the Material Recycle Pinch Point. Three rigorous targets are determined from the Pinch diagram: maximum recycle of process sources, minimum usage of fresh materials, and minimum discharge of waste. To attain these targets, three design rules must be observed:

- No flowrate should be passed through the Pinch (i.e. the two composites must touch).
- No waste should be discharged from sources Below the Pinch.
- No fresh should be used in any sink Above the Pinch.

The Material Recycle Pinch diagram and the associated design rules are not only useful for designing and targeting new systems, they are also beneficial in assessing existing designs. Consider the food process plant (Fig. 13.9) described by El-Halwagi (2006). There are two recyclable process water sources and two process sinks that require water. One of the process sources (Condensate I) is recycled to the Scrubber, because it provides the necessary flowrate and contains impurities less than the maximum admissible composition to the unit. At first glance, this recycle arrangement appears

© Woodhead Publishing Limited, 2013

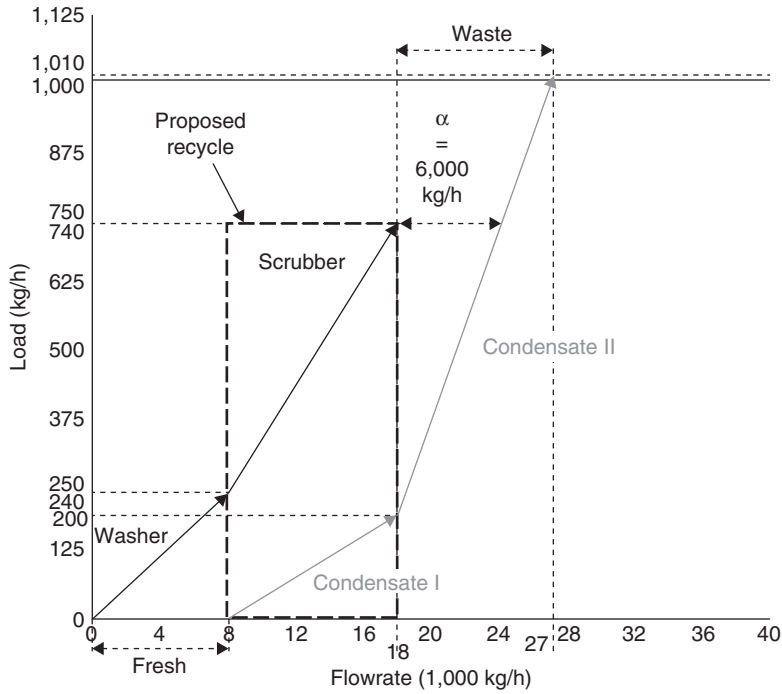

13.10 Representation of proposed recycle on Pinch diagram which results in passing 6,000 kg/h through the Pinch (El-Halwagi, 2006).

attractive because it fully utilises Condensate I and completely eliminates the use of fresh water in the Scrubber. Nonetheless, in constructing the Material Recycle Pinch diagram (Fig. 13.10), a design flaw is detected. Mass (6,000 kg/h of water) is passed through the Pinch, resulting in an equivalent increase in the fresh consumption of water and discharge of wastewater.

13.6 Property-Based Material Recycle Pinch Diagram

Mass Integration techniques are based on tracking chemical constituents. This 'chemo-centric' approach is valuable when the identity of the tracked chemicals is important. Nonetheless, there are material conservation problems that are largely dependent on the properties of the streams and units and not necessarily the chemical compositions. Examples include environmental regulations that are based on properties (e.g., pH, toxicity, color), desired stream characteristics (e.g., physical and thermodynamic properties), and systems involving numerous components (e.g., fossil fuels and forestry products). El-Halwagi and co-workers (e.g., Shelley and El-Halwagi, 2000; El-Halwagi *et al.*, 2004) introduced framework of *Property Integration*, which

© Woodhead Publishing Limited, 2013

is a functionality-based, holistic approach to the allocation and manipulation of streams and processing units based on the tracking, adjustment, assignment, and matching of functionalities throughout the process (El-Halwagi *et al.*, 2004). As a sample of Property-Integration problems and approaches, the Property-Based Material Recycle Pinch diagram is described. More details on the problem and its solution technique can be found in Kazantzi and El-Halwagi (2005). The concepts of sources and sinks are similar to those described in the previous section. An important distinction is that the constraints imposed on acceptable recycle for each sink are given in terms of properties, that is

$$p_j^{\min} \le p_j^{in} \le p_j^{\max} \qquad \text{where } j = 1,2,\ldots,N_{\text{sinks}} \qquad [13.2]$$

where $p_j^{\min}$ and $p_j^{\max}$ are the specified lower and upper bounds on admissible property to sink j. One complication, compared to heat and Mass Integration where both heat and mass are conserved, is that properties are not conserved. Therefore, property-mixing rules are used in the following form:

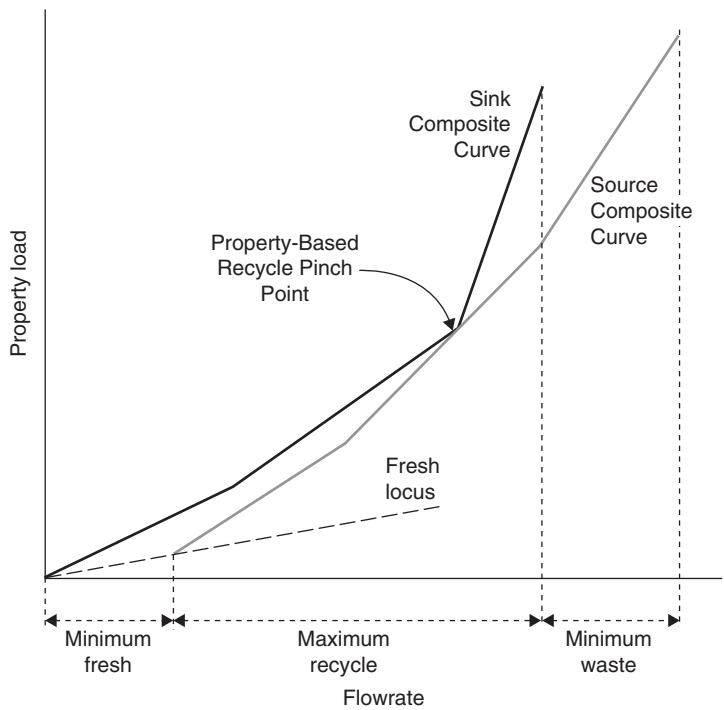

13.11 Property-Based Material Reuse Pinch diagram (Kazantzi and El-Halwagi, 2005).

© Woodhead Publishing Limited, 2013

$$\bar{F} * \psi\left(\bar{p}\right) = \sum_i F_i * \psi\left(p_i\right) \quad [13.3]$$

where $\psi(p_i)$ is the property-mixing operator and $\bar{F}$ is the total flowrate of the mixture which is given by:

$$\bar{F} = \sum_i F_i \quad [13.4]$$

Defining the flowrate times the property operator as property load, an analogy is established with the composition-based recycle problem, and an analogous tool referred to as the Property-Based Material Reuse Pinch diagram (Kazantzi and El-Halwagi, 2005) is developed (Fig. 13.11). Again, three rigorous targets are determined: maximum recycle, minimum fresh, and minimum waste.

For an illustration, consider the metal degreasing process (Kazantzi and El-Halwagi, 2005) shown by Fig. 13.12. Recycle is to be used to reduce the consumption of a fresh organic solvent used in the degreaser and the

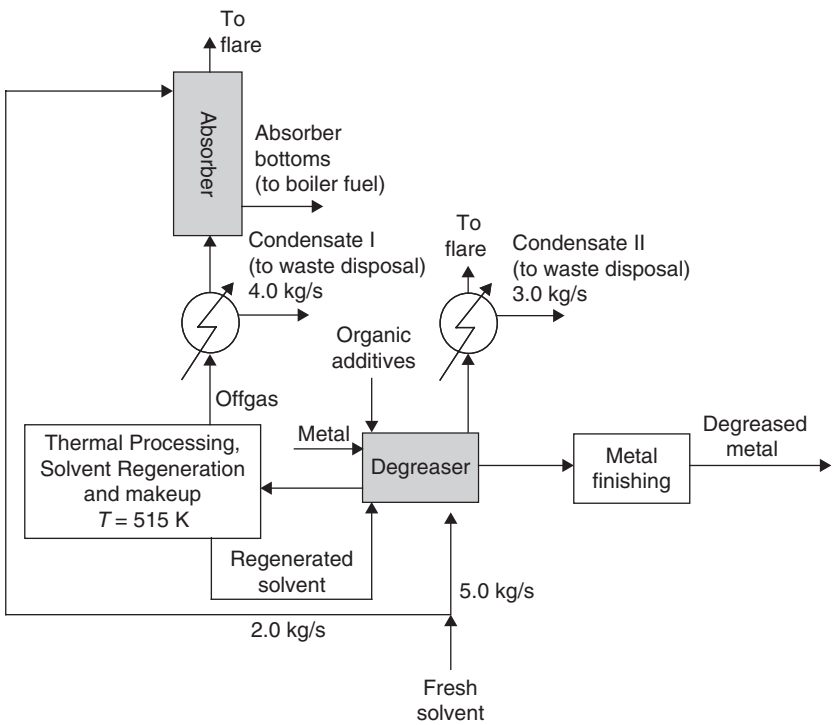

13.12 A degreasing plant (Kazantzi and El-Halwagi, 2005).

© Woodhead Publishing Limited, 2013

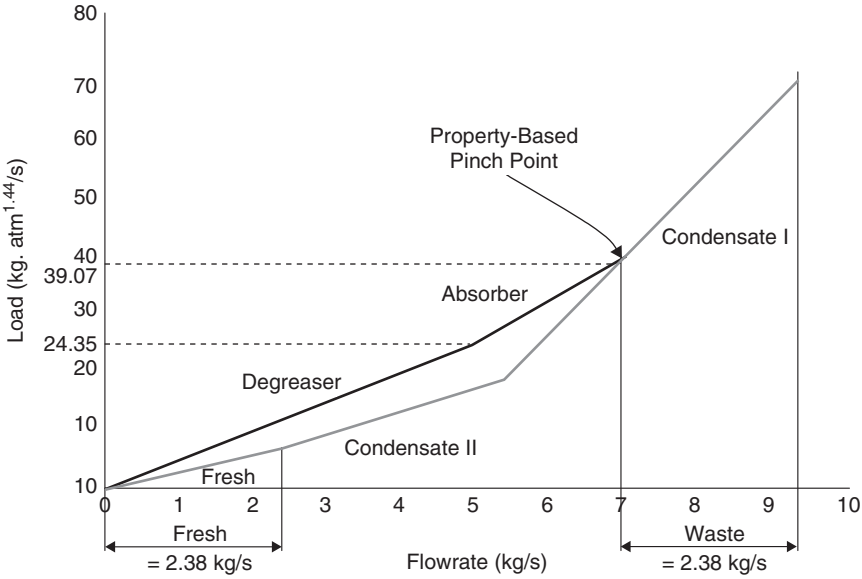

13.13 Property-Based Pinch diagram for the degreasing case study (Kazantzi and El-Halwagi, 2005).

absorber. The constraints for the feed to these units are given in terms of Reid Vapour Pressure (RVP), which is used to account for the volatility, makeup, and regeneration of the solvent.

The mixing rule for RVP is given by the following expression:

$$\overline{\mathrm{RVP}}^{1.44} = \sum_{i=1}^{N_s} x_i \mathrm{RVP}_i^{1.44} \qquad [13.5]$$

The Property-Based Pinch diagram, along with the three material targets, is shown by Fig. 13.13.

Graphical representation can be used for up to three targeted properties. This may be accomplished through the clustering technique developed by Shelley and El-Halwagi (2000). Property clusters are constructed through special transformations to enable the conserved tracking of properties. Specifically, these clusters are conserved within a stream (they add up to one) and are conserved via mixing (they follow level-arm rules). In the aforementioned degreasing case study, if density and sulfur content are considered in addition to RVP, the ternary-clustering diagram may be constructed to determine minimum fresh usage, maximum recycle, and minimum waste discharge (Fig. 13.14).

© Woodhead Publishing Limited, 2013

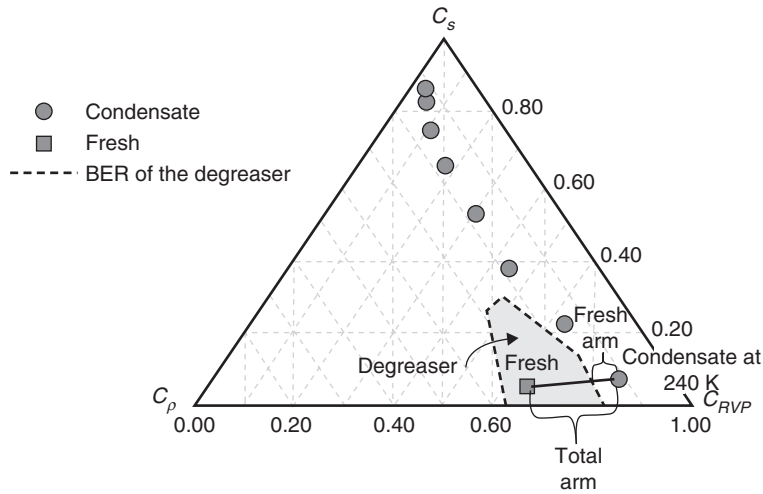

13.14 Determining the fresh usage target via the ternary property-cluster diagram for the degreaser (Shelley and El-Halwagi, 2000).

Targets for property-based recycle may be determined algebraically (e.g., Qin *et al*., 2004; Foo *et al*., 2006; Ng *et al*., 2010) and through mathematical programming (e.g., Ponce-Ortega *et al*., 2009, 2010). Property-based clusters have also been used as interfaces between process design and molecular design (Eljack *et al*., 2007, 2005; Kazantzi *et al*., 2007). This enables the designer to synthesise and select molecular structures and process configurations for material conservation.

13.7 References

Alves, J. J., Towler, G. P. (2002). Analysis of refinery hydrogen distribution systems. *Industrial and Engineering Chemistry Research*, **41**, 5759–5769.

El-Halwagi, M. M. (2012). *Sustainable Design through Process Integration: Fundamentals and Applications to Industrial Pollution Prevention, Resource Conservation, and Profitability Enhancement*. Butterworth-Heinemann/ Elsevier, Oxford, UK.

El-Halwagi, M. M. (2006). *Process Integration.* Elsevier, Amsterdam, The Netherlands.

El-Halwagi, M. M. (1997). *Pollution Prevention through Process Integration: Systematic Design Tools.* Academic Press, San Diego, CA, USA.

El-Halwagi, M. M. (1999). Sustainable pollution prevention through mass integration. In: Sikdar, S., Diwekar U. (eds), *Tools and Methods for Pollution Prevention.* Kluwer Publishing, Norwell, USA, 233–275.

© Woodhead Publishing Limited, 2013

El-Halwagi, M. M., Gabriel, F., Harell, D. (2003). Rigorous graphical targeting for resource conservation via material recycle/reuse networks. *Industrial and Engineering Chemistry Research*, **42**, 4319–4328.

El-Halwagi, M. M., Glasgow, I. M., Eden, M. R., Qin, X. (2004). Property integration: componentless design techniques and visualization tools. *AIChE Journal*, **50**(8), 1854–1869.

El-Halwagi, M., Manousiouthakis, V. (1989). Synthesis of mass exchange networks. *AIChE Journal*, **35**(8), 1233–1244.

Eljack, F. M., Eden, M. R., Kazantzi, V., Qin, X., El-Halwagi, M. M. (2007). Simultaneous process and molecular design – a property based approach. *AIChE Journal*, **35**(5), 1232–1239.

Foo, D. C. Y. (2012). *Process Integration for Resource Conservation*. CRC Press/ Taylor and Francis, Boca Raton, USA.

Foo, D. C. Y. (2009). State-of-the-art review of pinch analysis techniques for water network synthesis. *Industrial and Engineering Chemistry Research*, **48**, 5125–5159.

Foo, D. C. Y., Manan, Z. A., Tan, Y. L. (2006). Use cascade analysis to optimize water networks. *Chemical Engineering Progress*, **102**(7), 45–52.

Foo, D. C. Y., Kazantzi, V., El-Halwagi, M. M., Manan, Z. A. (2006). Surplus diagram and cascade analysis technique for targeting property-based material reuse network. *Chemical Engineering Science*, **61**, 2626–2642.

Gabriel, F., El-Halwagi, M. M. (July 2005). Simultaneous synthesis of waste interception and material reuse networks: Problem reformulation for global optimization. *Environmental Progress*, **24**(2), 171–180.

Hallale, N., Fraser, D. M. (2000). Capital and total cost targets for mass exchange networks. Part 1: Simple capital cost models. *Computers and Chemical Engineering*, **23**, 1661–1679.

Kazantzi, V., El-Halwagi, M. M. (2005). Targeting material reuse via property integration. *Chemical Engineering Progress*, **101**(8), 28–37.

Kazantzi, V., Qin, X., El-Halwagi, M. M., Eljack, F., Eden, M. (2007). Simultaneous process and molecular design through property clustering – a visualization tool. *Industrial and Engineering Chemistry Research*, **46**, 3400–3409.

Kemp, I. (2009). *Pinch Analysis and Process Integration – A User Guide on Process Integration for the Efficient Use of Energy*, 2nd ed. Butterworth-Heinemann, Oxford, UK.

Klemeš, J., Friedler, F., Bulatov, I., Varbanov, P. (2011). *Sustainability in the Process Industry: Integration and Optimization*. McGraw Hill, New York, USA.

Majozi, T. (2010). *Batch Chemical Process Integration: Analysis, Synthesis, and Optimization.* Springer, Heidelberg, Germany.

Ng, D. K. S., Foo, D. C. Y., Tan, R. R., El-Halwagi, M. M. (2010). Automated targeting techniques for concentration- and property-based total resource conservation networks. *Computers and Chemical Engineering*, **34**(5), 825–845.

Noureldin, M. B. (2011). *Pinch Technology and Beyond: New Vistas on Energy Efficiency Optimisation*, Nova Science Publishers, Happauge, USA.

Noureldin, M. B., El-Halwagi, M. M. (1999). Interval-based targeting for pollution prevention via mass integration. *Computers and Chemical Engineering*, **23**, 1527–1543.

Ponce-Ortega, J. M., El-Halwagi, M. M., Jimйnez-Gutiйrrez, A. (2010). Global optimization for the synthesis of property-based recycle and reuse networks

© Woodhead Publishing Limited, 2013

including environmental constraints. *Computers and Chemical Engineering*, **34**(3), 318–330.

Ponce-Ortega, J. M., Hortua, A. C., El-Halwagi, M. M., Jimйnez-Gutiйrrez, A. (2009). A property-based optimization of direct-recycle networks and wastewater treatment processes, *AIChE Journal*, **55**(9), 2329–2344.

Qin, X., Gabriel, F., Harell, D., El-Halwagi, M. M. (2004). Algebraic techniques for property integration via componentless design. *Industrial and Engineering Chemistry Research*, **43**, 3792–3798.

Savelski, M. J., Bagajewicz, M. J. (2001). Algorithmic procedure to design water utilization systems featuring a single contaminant in process plants. *Chemical Engineering Science*, **56**, 1897–1911.

Savulescu, L., Kim, J., Smith, R. (2005). Studies on simultaneous energy and water minimisation – Part I: Systems with no water re-use. *Chemical Engineering Science*, **60**(12), 3279–3290.

Shelley, M. D., El-Halwagi, M. M. (2000). Component-less design of recovery and allocation systems: a functionality-based clustering approach. *Computers and Chemical Engineering*, **24**, 2081–2091.

Smith, R. (2005). *Chemical Process Design and Integration*. Wiley, New York, USA.

Wang, Y. P., Smith, R. (1994). Wastewater minimisation. *Chemical Engineering Science*, **49**(7), 981–10 06.

13.8 Appendix: Nomenclature

C	property cluster
F	flowrate, t/h
F^{BMI}	fresh load before Mass Integration, t/h
i	index for rich streams or a process source
j	index for a lean stream or a process sink
MEN	Mass Exchange Network
max	maximum value
min	minimum value
MSA	Mass Separating Agent
Net_G^{BMI}	net generation of targeted component before Mass Integration, t/h
p_i	property of source i
RVP	Reid Vapour Pressure
T^{BMI}	terminal load before Mass Integration, t/h
x_j	concentration in the jth lean stream, ppm
y	concentration in the rich phase, ppm

© Woodhead Publishing Limited, 2013

14

Process Integration for Cleaner Process Design

DOMINIC C. Y. FOO and DENNY K. S. NG,
University of Nottingham Malaysia, Selangor, Malaysia

DOI: 10.1533/9780857097255.4.443

Abstract: This chapter discusses the use of Process Integration (PI) for overall process design. In the past three decades, various models/techniques have been proposed for better process design to achieve sustainable development goals. More recently, PI techniques have also been developed for design of resource conservation and its associated treatment system that ensures maximum recovery of useful resources in the process plants. By making use of PI, we can now design cleaner processes that feature the minimum use of resources and waste discharge. In other words, PI enhances plant efficiency and makes processes cleaner and more sustainable.

Key words: process design, Process Integration, total material network, material recovery.

14.1 Introduction

As described in Chapter 2, Process Integration (PI) is a family of methodologies for combining operations within a process or several processes to reduce consumption of resources and/or harmful emissions. With PI, both raw material consumption (and its associated treatment) as well as the quantity of generated waste are reduced significantly. Thus, cleaner and more economical process design can be achieved.

14.2 A Revised 'Onion Diagram'

The *Onion Diagram* is one of the most well-accepted representations for chemical process design, first reported in Linnhoff *et al*. (1982). Throughout the past three decades, several variants of the Onion Diagram have been proposed, and one version reported by Klemeš *et al*. (2010) is given in Fig. 14.1. The use of the Onion Diagram for process design is now explained.

As shown in Fig. 14.1, process design begins from the centre of the onion, i.e. the reactor. The reactor design influences the separation structures at

© Woodhead Publishing Limited, 2013

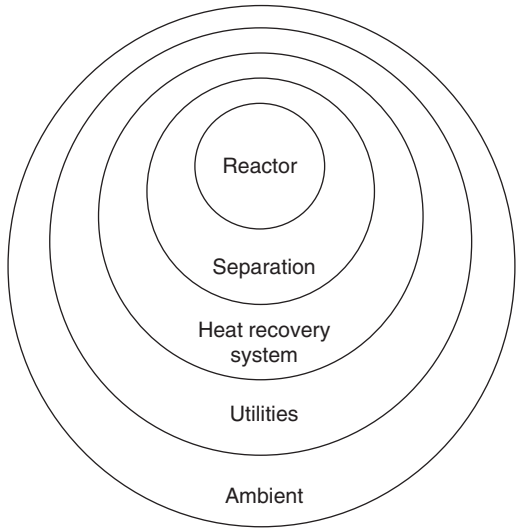

14.1 The conventional Onion Diagram (Klemeš *et al.,* 2010).

the second layer of the onion. Moving to the third layer, we observe that the reactor and separator structures dictate the overall heat-recovery problem. Hence, the heat-recovery system is designed next. The process energy utility system at the fourth layer is then being designed, to provide additional heating and cooling requirements that cannot be satisfied through the heat-recovery system. At the final layer, the ambient system is designed, to handle the various emissions/effluents emitted from the process prior to final environmental discharge.

With the latest development of PI techniques for a resource conservation system, the Onion Diagram can now take a revised form, such as that shown in Fig. 14.2. As shown, a new layer of the material-recovery system has been added. This new layer includes the recycle system of the raw material, as well as the recovery of various other useful materials in the process, e.g. utility waste, etc. Additionally, in the final layer, instead of having the waste-treatment system, the pre- and post-treatment of the processes are both included. The former refers to the purification system for the raw material or utility feedstock.

In the context of PI, the layer of the material-recovery system is very much established. Various methods are discussed in Chapters 4–13 of this handbook for the design of water, utility gases and property networks. Typically, it involves the various material-recovery strategies, such as *direct reuse/recycle*, as well as material *regeneration* (Chapters 13 and 26). According to Wang and Smith (1994), *reuse* means that the effluent from a resource-consuming unit is sent to other operations and does not re-enter operations from where

© Woodhead Publishing Limited, 2013

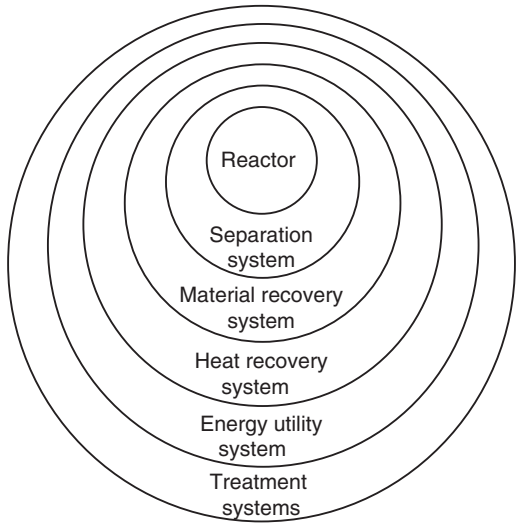

14.2 The extended Onion Diagram.

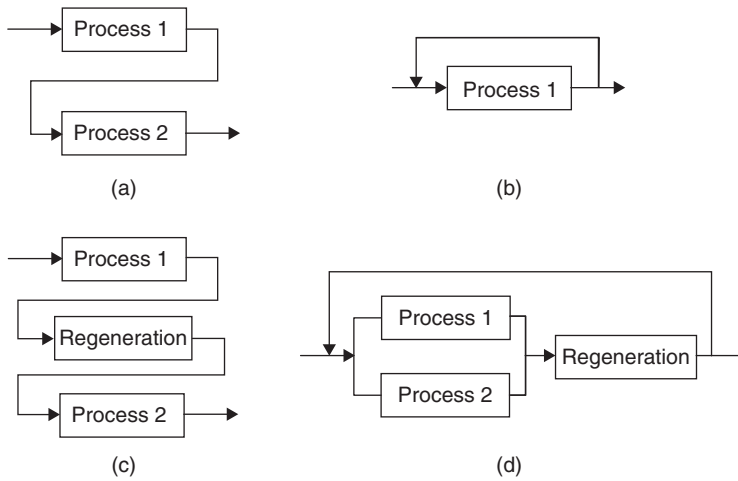

14.3 Various schemes for material recovery (a) reuse, (b) recycle, (c) regeneration-reuse, and (d) regeneration-recycling.

it was emitted (Fig. 14.3a). On the other hand, the *recycle* scheme permits the effluent to re-enter the operations wherein it was generated (Fig. 14.3b). In *regeneration* schemes, effluent is partially treated by purification unit (e.g. filtration, adsorption, stripping, etc.) before reuse (Fig. 14.3c) or recycle (Fig. 14.3d) takes place (Wang and Smith, 1995).

© Woodhead Publishing Limited, 2013

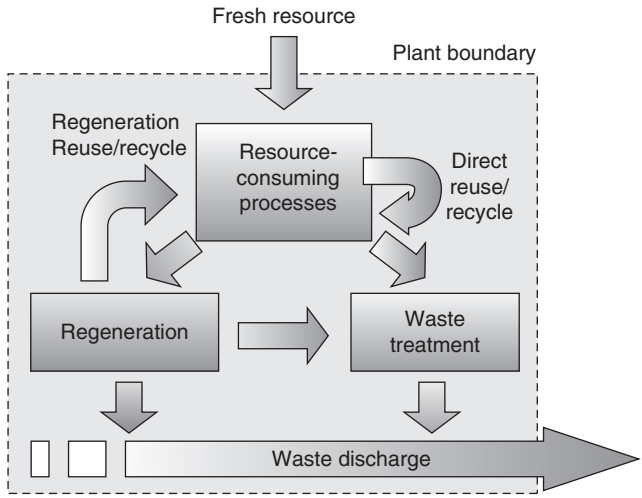

14.4 The overall framework of a TMN (Foo, 2012).

One recent development of PI is the establishment of *Total Material Network* (TMN). TMN is *an overall framework that explores the interactions between the various material-recovery elements with the waste-treatment section*. A representation for such a framework is given by Fig. 14.4. Note that the original version of this framework was proposed by Kuo and Smith (1998a) for water minimisation problem. It was then extended to all types of material-recovery networks, e.g. water, hydrogen and property networks (Foo, 2012). As shown in Fig. 14.4, the TMN consists of three individual elements, i.e. direct reuse/recycle, regeneration and waste treatment. Since there are interactions among these individual elements, they are analysed as an overall framework. After material-recovery potential is maximised with direct reuse/recycle scheme, fresh resource and waste flowrates can be further reduced by employing interception unit for regeneration of process sources. Waste treatment is finally employed to treat the effluent prior to environmental discharge.

14.3 Different Models for Total Material Network (TMN)

In recent years, different variants of models have been proposed for the design of a TMN. In general, the design models for TMN can be divided into two categories, i.e. fixed-load and fixed-flowrate problems. The fixed-load problem, which is commonly referred to the mass-transfer–based process operation, is characterised by the preferential transfer of species from a rich stream to a lean stream (e.g., water), or a mass-separating agent – MSA

© Woodhead Publishing Limited, 2013

(Manan *et al.*, 2004). Meanwhile, fixed-flowrate problem refers to process operation which is characterised by the inlet and outlet flowrates of the processes (Foo, 2009). In the following section, design models for both types of problems are discussed.

Figure 14.5 shows the flowchart for designing a fixed-load TMN first proposed by Kuo and Smith (1998a) specifically cater for water minimisation problems. As shown, direct reuse flowrate is first located via the Limiting Composite Curve (Wang and Smith, 1994). Next, in order to further reduce the fresh material (water) consumption, regeneration-reuse and recycle can be considered. Following the procedure proposed by Kuo and Smith (1998b), the minimum regeneration flowrate can be determined. In addition, the minimum number of effluent treatment units can also be determined. In cases where more than one treatment unit is required, reduction of the treatment unit is considered (Kuo and Smith, 1998a). Based on the minimum fresh water and regeneration targets, as well as the number of

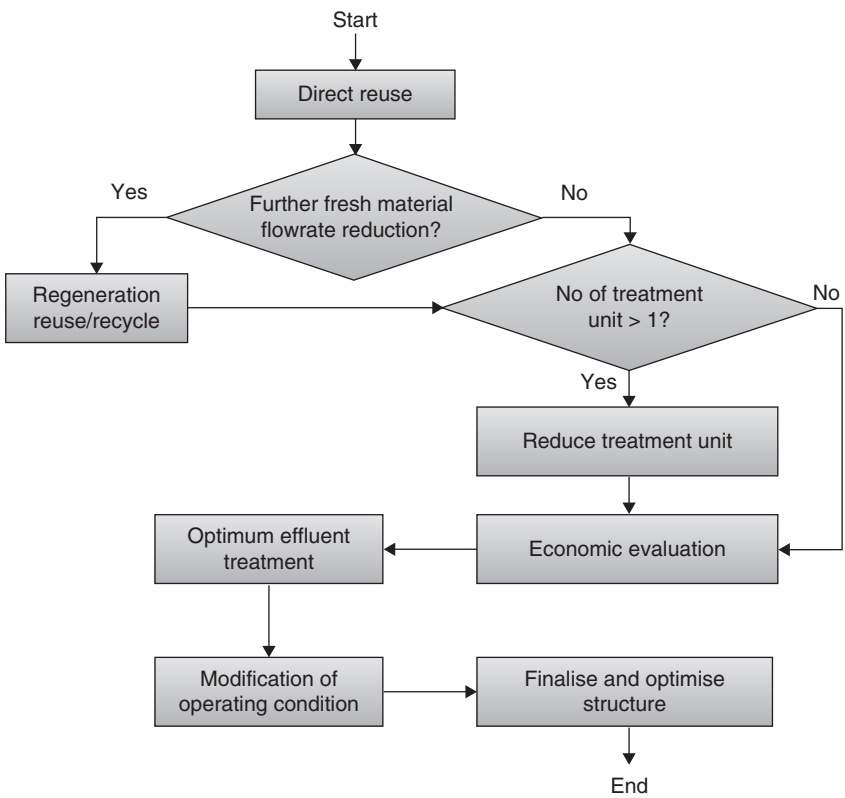

14.5 Targeting procedure for a fixed-load TMN with insight-based approach (Kuo and Smith, 1998a).

© Woodhead Publishing Limited, 2013

treatment units, preliminary economic evaluation can be performed. Appropriate changes to the process conditions in the operations can be made without suffering an increase in fresh water consumption and effluent treatment. A TMN results following the above procedure.

Note, however, that the procedure of Kuo and Smith (1998a) is limited to water minimisation problems that consist of only fixed-load operations (e.g. absorption, extraction etc.). In order to address the fixed-flowrate problems (which also includes hydrogen and property networks), a revised TMN procedure has been proposed by Ng and co-workers, who introduced waste-stream identification (Ng *et al.*, 2007a) and waste-treatment targeting and its interactions with water-system elements (Ng *et al.*, 2007b). Note that this new TMN procedure makes use of various targeting techniques developed for the fixed-flowrate problems, e.g. Material Cascade Analysis (Manan *et al.*, 2004) and Material-Recovery Pinch diagram (developed independently by El-Halwagi (2003) and Prakash and Shenoy (2005)). Figure 14.6 shows the detailed procedure reported by Foo (2012). As shown, the fresh material and waste flowrate targets are first identified for the direct reuse/recycle network. Next, the waste stream can be identified either via targeting approach, e.g. Ng *et al.* (2007c), or via a detailed network design (e.g. Prakash and Shenoy, 2005). To further reduce the fresh material requirement, the interception system can be considered for source regeneration. After the regeneration process, the

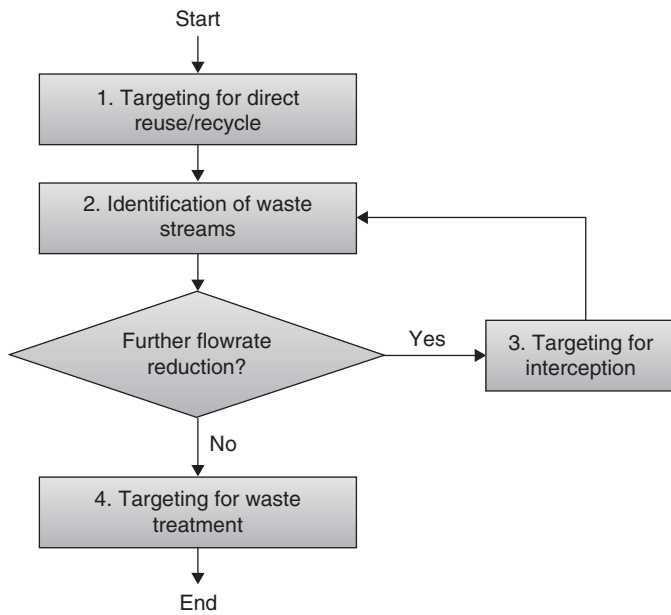

14.6 Targeting procedure for a fixed-flowrate TMN with insight-based approach (Foo, 2012).

© Woodhead Publishing Limited, 2013

waste stream needs to be re-identified. Based on the identified waste stream, the minimum treatment flowrate and the number of units can be targeted via the Wastewater Composite Curve (Ng *et al.*, 2007b). Following the above procedure, a TMN for the fixed-flowrate problem can be synthesised.

On the other hand, Deng *et al.* (2011) also presented an alternative approach for TMN synthesis based on the Process-Based Graphical Approach (PGA), which can be used for simultaneous TMN targeting and design (see Fig. 14.7). According to Deng *et al.* (2011), preliminary analysis is conducted to determine the sequence of the processes. Next, targeting and design of the reuse/recycle network is first performed via the revised Limiting Composite Curve, which takes account of water loss/gain (Deng *et al.*, 2011). Based on the revised limiting water profile, the flowrate allocation for the individual process based on the available sources and the associated network design can be determined (Deng *et al.*, 2011). In the case where flowrate constraint is taken into consideration, mixing of sources to fulfil the process requirement is performed. Next, the minimum regeneration flowrate and load are targeted, and the waste streams for regeneration

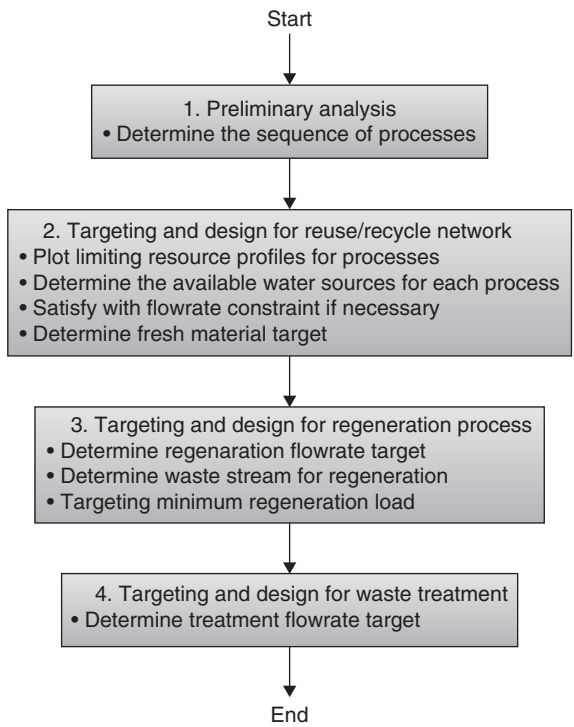

14.7 Targeting procedure for a TMN with insight-based approach of Deng *et al.* (2011).

© Woodhead Publishing Limited, 2013

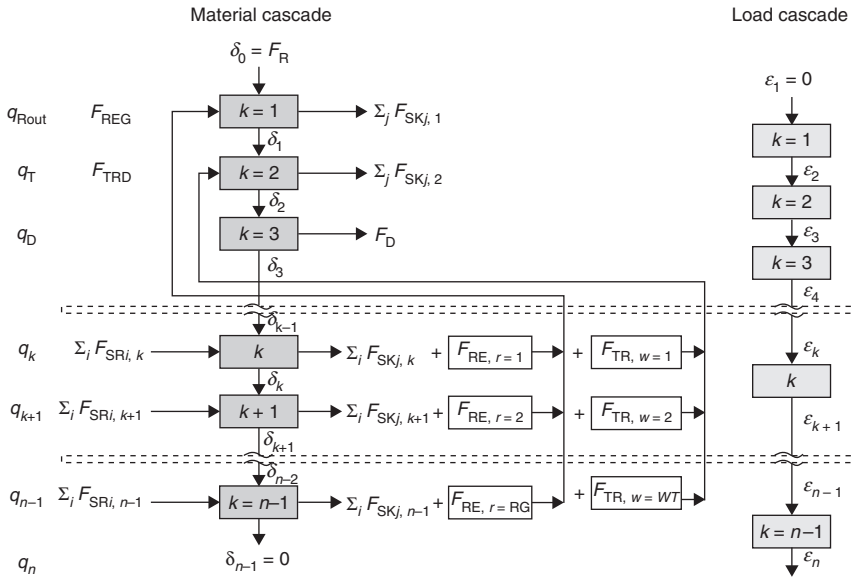

14.8 Targeting procedure for a TMN with ATM (Ng *et al.,* 2010).

are identified. After all flowrates targets have been established, the waste stream for final treatment can then be determined. Finally, the minimum treatment flowrate is located and a TMN can be synthesised.

Other than the insight-based approaches, Ng *et al.* (2010) also presented an optimisation-based *Automated Targeting Model* (ATM) to determine the minimum resource consumption/target(s) for a single-impurity TMN. This optimisation-based targeting technique provides the same benefits as insight-based Pinch Analysis, discussed earlier, in yielding various targets for a TMN prior to detailed design. In addition, flexibility in setting the objective function (for cost minimisation) is the major advantage of the ATM over Conventional Pinch Analysis (Ng *et al.*, 2010). Following the proposed approach (Ng *et al.*, 2010), the first step of the ATM is to construct a Resource Conservation Cascade Diagram (RCCD), as shown in Fig. 14.8. The objective of the proposed approach is to locate the minimum network targets prior to the detailed design of a TMN. Depending on the problem, the objective function in some cases may be set to determine the minimum resource flowrate(s) of the network, while in others, set to minimise operating/total cost.

In the following section, the TMN for a case study on water minimisation in wafer fabrication plant is solved following the model presented in Fig. 14.6.

© Woodhead Publishing Limited, 2013

14.4 Case Study: Water Minimisation in a Water Fabrication Plant

Figure 14.9 shows a semi-conductor plant, where a large amount of fresh water is consumed (Ng *et al*., 2009). Apart from being utilised for the utility section, i.e. general cleaning, cooling tower makeup and scrubber feed water, a large amount of fresh water is consumed to produce ultrapure water (UPW) for use in the wafer fabrication section (FAB). As shown Fig. 14.9, there are four UPW-consuming processes in the FAB, i.e. wet processing section (Wet), lithography, combined chemical and mechanical processing (CMP), and miscellaneous operations (MisOp). Note that the UPW fed to these processes may be viewed as process feedstock, while those for general cleaning purposes are treated as utility water. Upon usage, some processes produce wastewater streams.

In order to reduce the UPW, and hence fresh water usage, the wastewater is evaluated for the possibility of direct reuse/recycle to the UPW-using processes. The most significant water quality factor in considering water recovery is *resistivity* (R), which is an index that reflects the total ionic content in aqueous streams. To determine the resistivity value of the mixture, a linearised mixing rule is used:

$$\frac{1}{R_{\mathrm{M}}} = \sum_{l} \frac{x_l}{R_l} \qquad [14.1]$$

The limiting data of the case study is first identified and summarised in Table 14.1. As shown, the resistivity values of the UPW sinks and sources are now converted to their corresponding *operator values* (ψ). Note that the lower bounds of the resistivity values of the sinks are taken as limiting data (see discussion in Foo, 2012). Note also that the reject streams of the pretreatment system are not considered for recovery.

We can then carry out the flowrate targeting step to identify the minimum UPW flowrate, using any of the graphical or algebraic targeting techniques discussed in Chapters 2 and 10. Table 14.2 shows the results from the algebraic targeting technique of *Material Cascade Analysis*. As shown, the minimum UPW (F_{UPW}) and wastewater (F_{WW}) flowrates are identified as 1,516.47 and 626.47 t/h. Note that this corresponds to Step 1 of the TMN procedure outlined in Fig. 14.6.

The UPW recovery scheme can then be designed using the *Nearest Neighbour Algorithm* (NNA) (see Prakash and Shenoy (2005) for detailed steps), given as in Fig. 14.10.

The recovery scheme corresponds to the second layer of the Onion Diagram, as it involves the recovery of process feedstock (UPW) as

© Woodhead Publishing Limited, 2013

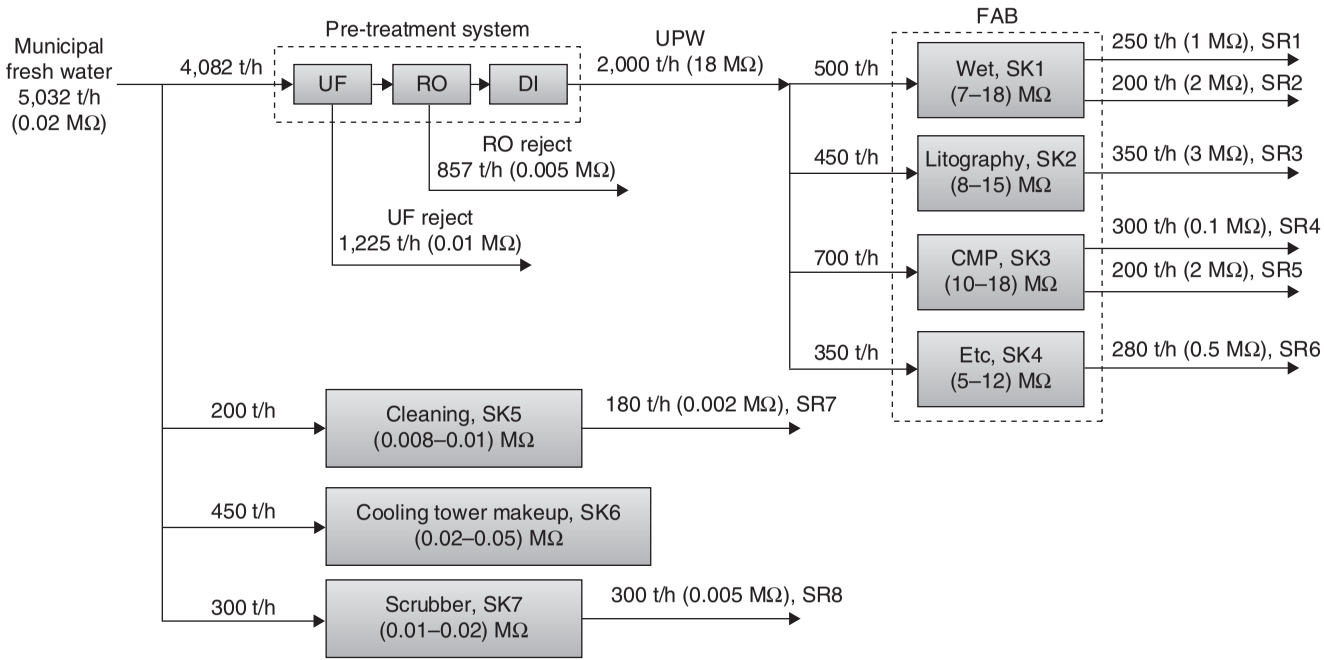

14.9 A semi-conductor plant (Ng *et al.*, 2009).

© Woodhead Publishing Limited, 2013

Table 14.1 Limiting data for water minimisation study

j	Sinks, SK_j	F_{SKj} (t/h)	ψ_{SKj} $(M\Omega.m)^{-1}$	i	Sources, SR_i	F_{SRi} (t/h)	ψ_{SRi} $(M\Omega.m)^{-1}$
1	Wet	500	0.143	1	Wet I	250	1
2	Lithography	450	0.125	2	Wet II	200	0.5
3	CMP	700	0.1	3	Lithography	350	0.333
4	MisOp	350	0.2	4	CMP I	300	10
5	Cleaning	200	125	5	CMP II	200	0.5
6	Cooling tower makeup	450	50	6	Etc.	280	2
7	Scrubber	300	100	7	Cleaning	180	500
				8	Scrubber	300	200

Table 14.2 Material cascade analysis for flowrate targeting of UPW

C_k (ppm)	$\Sigma_j F_{SKj}$ (t/h)	$\Sigma_i F_{SRi}$ (t/h)	$\Sigma_i F_{SRi} - \Sigma_j F_{SKj}$ (t/h)	$F_{c,k}$ (t/h)	Δm_k (kg/h)	Cum. Δm_k (kg/h)
				F_{UPW} = 1,516.47		
0.056				1,516.47	67.40	
0.100	700		−700	816.47	20.41	67.40
0.125	450		−450	366.47	6.54	87.81
0.143	500		−500	−133.53	−7.63	94.35
0.200	350		−350	−483.53	−64.47	86.72
0.333		350	350	−133.53	−22.25	22.25
0.500		400	400	266.47	133.24	0.00 (PINCH)
1.000		250	250	516.47	516.47	133.24
2.000		280	280	796.47	6,371.79	649.71
10.000		300	300	1,096.47	43,858.93	7,021.50
50.000	450		−450	646.47	32,323.66	50,880.42
100.000	300		−300	346.47	8,661.83	83,204.08
125.000	200		−200	146.47	10,985.49	91,865.92
200.000		300	0	446.47	133,941.96	102,851.41
500.000		180	180	F_{WW} = 626.47	313,236.61	236,793.37
1,000.000						550,029.98

© Woodhead Publishing Limited, 2013

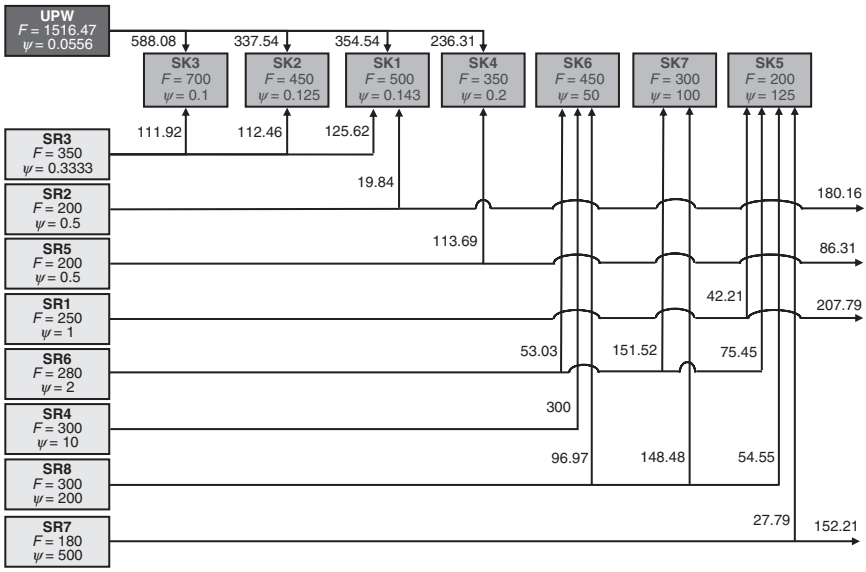

14.10 Network design with NNA for UPW recovery scheme (flowrates in t/h; operators in $(M\Omega.m)^{-1}$).

Table 14.3 Data for wastewater streams

y	Waste	F_{WWy} (t/h)	C_{WWy} (ppm)
1	Wet I	207.79	5
2	Wet II	180.16	4.5
3	CMP II	86.31	4.5
4	Cleaning	152.21	15
5	UF reject	928.45	1.5
6	RO reject	649.92	10

well as utility wastewater. Next, we move to the final layer, where pre- and post-treatment systems are considered in the overall framework of the TMN.

In the pre-treatment system, the ultrafiltration (UF) and reverse osmosis (RO) units both produce wastewater streams, with 30% of their treatment flowrates. In other words, 30% of the inlet flowrate to these units will end up as effluent streams. Since it has been determined that the UPW has a flowrate of 1,516.47 t/h, we can then calculate the effluent from RO and UF units as 649.92 t/h (= 1,516.47 t/h/0.7 × 0.3) and 928.45 t/h (= 649.92 t/h/0.7).

© Woodhead Publishing Limited, 2013

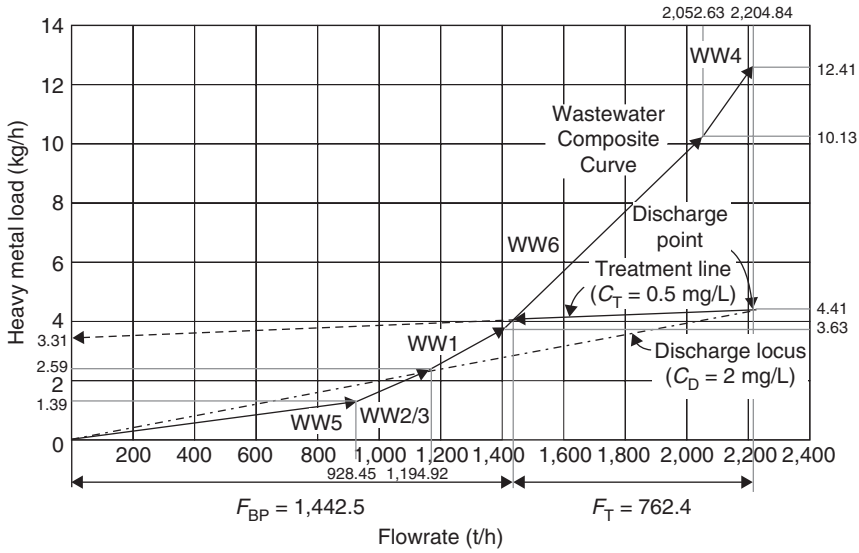

14.11 Minimum flowrate targeting for wastewater treatment.

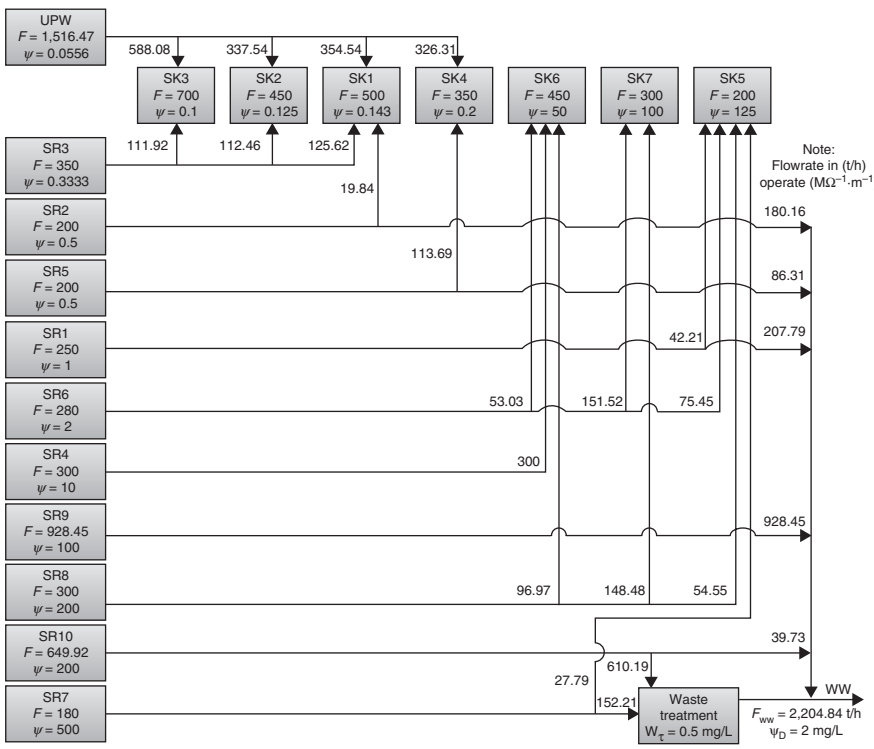

14.12 Total water network for semi-conductor plant.

© Woodhead Publishing Limited, 2013

© Woodhead Publishing Limited, 2013

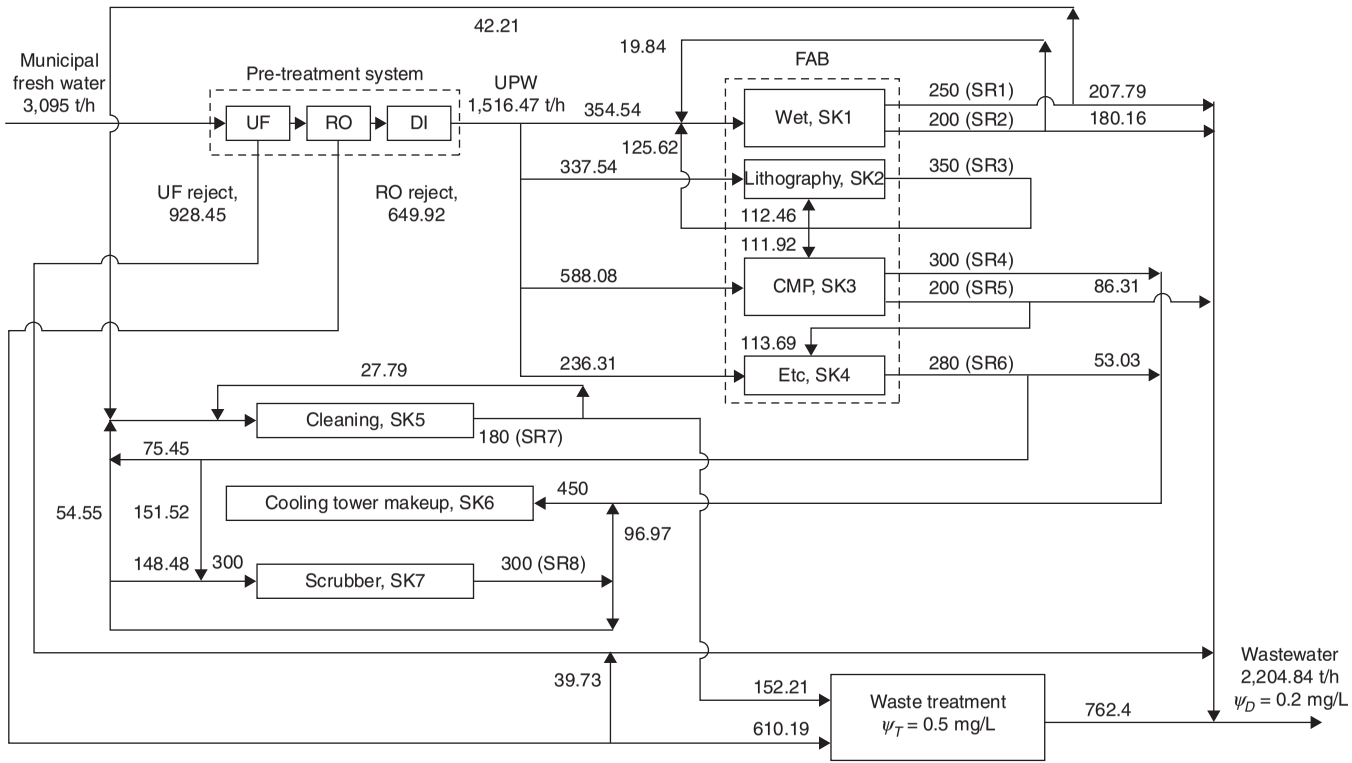

14.13 Total water network for semi-conductor plant.

We next proceed to analyse the post-treatment system of the process. For this case, the wastewater streams are to be treated before they are discharged into the environment. The critical parameter in concern is the heavy metal content of these streams, with their data given in Table 14.3. This corresponds to Step 2 of the TMN procedure outlined in Fig. 14.6. The environmental discharge limit is set to 2 mg/L; while the water treatment facility can produce an outlet stream of 0.5 mg/L.

Flowrate targeting for waste treatment may be handled by the Waste-Treatment Pinch Diagram (Ng *et al.*, 2007b), as given in Fig. 14.11. As shown, the minimum treatment (F_T) and bypass (F_{BP}) flowrates for this case are targeted as 762.4 and 1,442.5 t/h. This corresponds to Step 4 of the TMN procedure outlined in Fig. 14.6.

We can then incorporate the waste-treatment system with the overall design of the UPW recovery scheme to form the total water network, as given in Fig. 14.12. Figure 14.13 shows the PFD of the total water network for semi-conductor plant. Finally, note that Step 3 of the TMN procedure in Fig. 14.6 has not been considered here. Readers may refer to the work of Ng *et al*. (2010) for reference, where the ATM is used for flowrate targeting.

14.5 Conclusion

In the past decade, the synthesis of a TMN for various fixed-flowrate problems based on PI is fairly well established. In this chapter, it is demonstrated that the established techniques may be combined with the revised Onion Diagram in designing cleaner processes. In particular, the revised Onion Diagram incorporates a new layer of the material-recovery system, which also includes pre- and post-treatment processes. A case study of water minimisation in a wafer fabrication plant is used to elucidate the concept.

14.6 Sources of Further Information

As mentioned in Section 14.3 of this chapter, there exist several insight-based approaches for the synthesis of the TMN, including those for fixed-load (Kuo and Smith, 1998a) and fixed-flowrate type problems with Ng *et al*. Part I and Part II (2007a, 2007b) for sequential targeting and design, and Deng *et al*. (2011) for simultaneous targeting and design for the TMN. Among these techniques, the work of Deng *et al*. (2011) focuses on the simultaneous targeting and design of the TMN. In other words, the structure of the TMN is identified when the minimum resources are targeted. On the other hand, the optimisation-based ATM of Ng *et al*. (2010) may also be used for the TMN synthesis. The main advantage of this technique is its ability to determine cost targets, apart from minimum resources and waste generation.

© Woodhead Publishing Limited, 2013

14.7 References

Deng, C., Feng, X., Ng, D. K. S., Foo, D. C. Y. (2011). Process-based graphical approach for simultaneous targeting and design of water network, *AIChE Journal*, **57**(11): 3085–3104.

El-Halwagi, M. M. (1997). *Pollution Prevention through Process Integration: Systematic Design Tools*, Academic Press, San Diego, CA, USA.

El-Halwagi, M.M., Gabriel, F., Harell, D. (2003). Rigorous graphical targeting for resource conservation via material recycle/reuse networks, *Industrial and Engineering Chemistry Research*, **42**: 4319–4328.

Foo, D. C. Y. (2009). A state-of-the-art review of pinch analysis techniques for water network synthesis, *Industrial and Engineering Chemistry Research*, **48**(11): 5125–5159.

Foo, D. C. Y. (2012). *Process Integration for Resource Conservation*, CRC Press, Boca Raton, Florida, USA.

Klemeš, J., Friedler, F., Bulatov, I. and Varbanov, P. (2010). *Sustainability in the Process Industry: Integration and Optimization*, McGraw-Hill, New York, USA.

Kuo, W. C. J., Smith, R. (1998a). Designing for the interactions between water-use and effluent treatment, *Chemical Engineering Research and Design*, **76**: 287–301.

Kuo, W. C. J., Smith, R. (1998b). Design of water-using systems involving regeneration, *Process Safety and Environment Protection*, **76**: 94–114.

Linnhoff, B., Townsend, D. W., Boland, D., Hewitt, G. F., Thomas, B. E. A., Guy, A. R., Marshall, R. H. (1982). *A User Guide on Process Integration for the Efficient Use of Energy*, IChemE, Rugby, UK.

Manan, Z. A., Tan, Y. L., Foo, D. C. Y. (2004). Targeting the minimum water flow rate using water cascade analysis technique, *AIChE Journal*, **50**(12): 3169–3183.

Ng, D. K. S., Foo, D. C. Y., Tan, R. R. (2007a). Targeting for total water network – Part 1: Waste stream identification, *Industrial and Engineering Chemistry Research*, **46**: 9107–9113.

Ng, D. K. S., Foo, D. C. Y., Tan, R. R. (2007b). Targeting for total water network – Part 2: Waste treatment targeting and interactions with water system elements, *Industrial and Engineering Chemistry Research*, **46**: 9114–9125.

Ng, D. K. S., Foo, D. C. Y., Tan, R. R., Tan, Y. L. (2007c). Ultimate flowrate targeting with regeneration placement, *Chemical Engineering Research and Design*, **85**(A9): 1253–1267.

Ng, D. K. S., Foo, D. C. Y., Tan, R. R., Tan, Y. L. (2008). Extension of targeting procedure for "Ultimate Flowrate Targeting with Regeneration Placement" by Ng *et al*., *Chemical Engineering Research and Design*, 85(A9): 1253–1267 and *Chemical Engineering Research and Design*, **86**(10): 1182–1186.

Ng, D. K. S., Foo, D. C. Y., Tan, R. R., Pau, C. H., Tan, Y. L., (2009). Automated targeting for conventional and bilateral property-based resource conservation network, *Chemical Engineering Journal*, **149**: 87–101.

Ng, D. K. S., Foo, D. C. Y., Tan, R. R., El-Halwagi, M. M. (2010). Automated targeting technique for concentration- and property-based total resource conservation network, *Computers and Chemical Engineering*, **34**(5): 825–845.

Prakash, R., Shenoy, U. V. (2005). Targeting and design of water networks for fixed flowrate and fixed contaminant load operations, *Chemical Engineering Science*, **60**(1): 255–268.

© Woodhead Publishing Limited, 2013

Tan, R. R., Ng, D. K. S., Foo, D. C. Y. (2010). Graphical approach to minimum flowrate targeting for partitioning water pretreatment unit, *Chemical Engineering Research and Design*, **88**(4): 393–402.

Wang, Y. P., Smith, R. (1994). Wastewater minimisation. *Chemical Engineering Science*, **49**: 981–1006.

Wang, Y. P., Smith, R. (1995). Wastewater minimisation with flowrate constraints. *Chemical Engineering Research and Design*, **73**: 889–904.

14.8 Appendix: Nomenclature

ATM	Automated Targeting Model
CMP	combined chemical and mechanical processing
DI	deionised water system
Etc.	miscellaneous operations
FAB	wafer fabrication plant
MSA	mass-separating agent
NNA	Nearest Neighbour Algorithm
PFD	process flow diagram
PGA	Process Graphical Approach
PI	Process Integration
RCCD	Resource Conservation Cascade Diagram
RO	reverse osmosis
TMN	Total Material Network
UF	ultrafiltration
UPW	ultrapure water
Wet	wet processing section
i	index of source
j	index of sink
k	index of quality level
l	index of stream
r	index of regeneration unit
w	index of waste treatment
y	index of waste stream
C_{D}	concentration of discharge stream
C_k	concentration level k
C_{T}	outlet concentration of treatment unit
Cum. Δm_k	cumulative mass load of level k
$C_{\mathrm{WW}y}$	concentration of wastewater stream y
F_{BP}	flowrate of bypass
$F_{C,k}$	cumulative flowrate at level k
F	total flowrate of discharge
F_{R}	flowrate of fresh resource
F_{REG}	total flowrate of regenerated source

© Woodhead Publishing Limited, 2013

$F_{RE,r}$	flowrate of regeneration unit r
F_{SRi}	flowrate of source i
F_{SKj}	flowrate of sink j
F_T	flowrate of treatment
F_{TRD}	total flowrate of waste treatment
$F_{TR,w}$	flowrate of waste treatment w
F_{WW}	flowrate of wastewater
F_{WWy}	flowrate of wastewater stream y
n	number of quality level
q	quality level
R	resistivity
R_i	resistivity of source i
R_M	mean value of resistivity
x_l	fraction of stream l
δ	net material flowrate
ε	residual impurity/property load
Δm_k	mass load of level k
ψ	operator values
ψ_{SKj}	operator value of sink j
ψ_{SRi}	operator value of source i

© Woodhead Publishing Limited, 2013

15

Process Integration Concepts for Combined Energy and Water Integration

LUCIANA ELENA SAVULESCU, Natural Resources Canada – Varennes, Canada and ALBERTO ALVA-ARGAEZ, Process Ecology Inc., Canada

DOI: 10.1533/9780857097255.4.461

Abstract: All sectors of the process industries depend on water and energy resources to transform raw materials into a large number of products demanded by society. The sustainability issue is an essential consideration in process design, which drives significant efforts to improve both water and energy efficiency. Most of these processes display strong interactions between water and energy use such that any changes to the energy network often impact the water network, although this impact is seldom followed in any systematic way by process-design engineers. Due to a number of market externalities, the economic balance between energy and water is heavily inclined towards energy. However, with water shortages becoming more frequent throughout the world, it is likely that the balance will change in the near future. Other environmental aspects associated with chemical process design include energy-related issues such as greenhouse gas and other air emissions as well as water quality. This chapter reviews several useful Process Integration (PI)-based concepts recently developed across a number of worldwide research teams, in support of process-design applications dealing with problems characterised by strong energy and water interactions.

Key words: Combined Energy and Water Integration, Simultaneous Energy and Water Minimisation, Water–Energy Network, water management, energy savings non-isothermal mixing separate systems, energy-efficient water utilisation, systems targeting and design approaches.

15.1 Introduction

Water and energy are two critical resources required by all industrial processes and their demand is continually increasing against limited supplies. Water is an integral part of most industrial energy production and distribution networks. Also, liquid–liquid extraction and washing operations are among numerous processes where water is intensively utilised.

Industrial processes with strong energy–water interactions, such as pulp and paper production and food and drink manufacturing, are continuously

© Woodhead Publishing Limited, 2013

seeking opportunities for reducing operating cost and, increasingly, to reduce their environmental footprint (Alva-Argaez and Savulescu, 2009). PI has been shown to provide excellent opportunities to achieve these goals in a systematic manner. Since the energy system is highly intertwined with the water system, the identification of opportunities for water and energy efficiency improvement and the multiple cross-effects due to the energy/water system interactions need to be systematically and globally addressed.

Reusing water between water-using operations can contribute to both improved efficiency of water utilisation and increased heat recovery potential as a water stream is also an energy carrier. A warm/hot process water source available for reuse will contribute to the energy required by the process, leading to energy savings in the utility system. The energy of wastewater

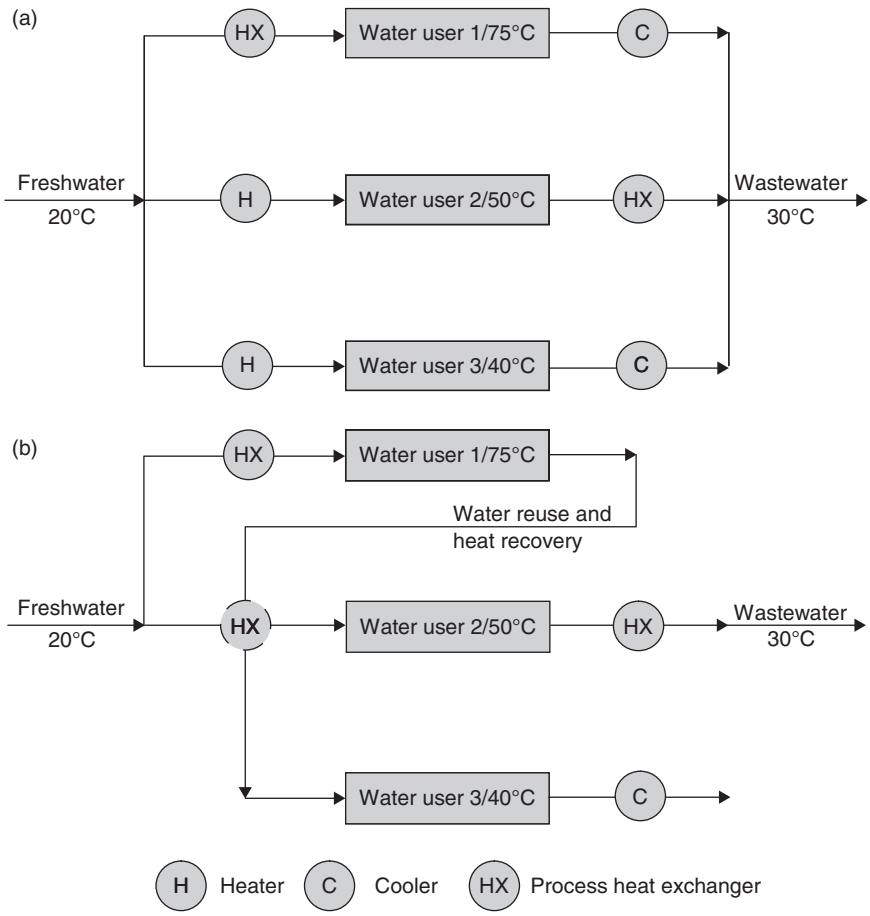

15.1 Combined Energy and Water Integration/WEN: (a) no water reuse network and (b) network with water reuse and heat recovery.

© Woodhead Publishing Limited, 2013

streams can also be recovered directly if the contaminant concentrations allow the reuse, and/or indirectly through Heat Exchanger Networks (HEN) between the water streams as shown in Fig. 15.1. Therefore, water and energy are inextricably linked and consequently, they should be considered together when searching for sustainable solutions. Water and energy systems are each complex, and therefore even more challenging when their interrelation is added to the identification and evaluation of improved process design.

This chapter provides an overview of the methodologies and approaches recently developed and applied to improve energy and water efficiency through PI in a combined/simultaneous manner. These novel conceptual methodologies apply different visualisation tools and heuristics to select relevant data for energy and water, to represent the combined systems towards water reuse and energy targets, and to guide the overall resource integration through promising energy and water efficiency improvement projects. The specific features of several representative research results in the area of Energy–Water Integration will be highlighted together with a proposed state-of-the-art integrated approach. A discussion on sequential versus simultaneous Water/Energy Integration will also be included.

15.2 Water–Energy Specifics and Challenges

An in-depth understanding of the specific process requirements for water and energy, as well as of the associated interactions between these systems, should be the foundation of any water and energy analysis, as indicated by El-Halwagi (1997) and highlighted later in the context of their integrated combined analysis by Koufos and Retsina (2001). To describe the key elements of the design problem it is convenient to consider the hierarchy of process-design stages and their sequence, as described by the well-known Onion Diagram (Douglas, 1988). The layers of this representation can be used to define a decomposition design strategy. Figure 15.2 illustrates these layers as different features of water use: mass separation agent, being utilities such as cooling water and steam production, within the water treatment system and inside the design of the HEN itself, highlighting the complex interactions between them.

When dealing with water and energy interactions, there are several stances that process designers may take, as commented by Grossmann and Martin (2010). A simplification to approach this problem as independent systems was proposed by Polley (2010). However, research from Savulescu (1999) points out the important fact that saving water has a definite effect on energy demands and, consequently, such separate approaches could result in the unintended consequence of limiting the water and/or energy savings potential. Therefore, specific insights on water/energy interactions,

© Woodhead Publishing Limited, 2013

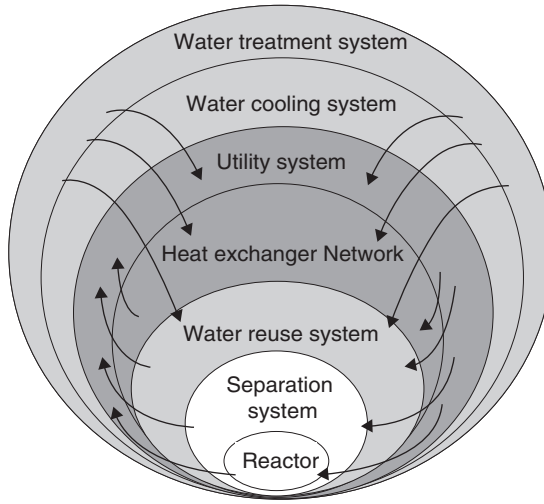

15.2 Water interactions within the layers of the Onion Diagram.

as generated through the systematic combined water and energy approach developed by Alva-Argaez, Savulescu and Cripps (2008), have to be accounted for while checking on the consequences of one system action on the other as an important step of a global analysis. The positive or negative impact of the energy–water design options has to be identified and controlled through a rigorous and systematic cross-effect analysis. Moreover, the sequence in which the analysis should be performed also has to be considered. The energy/water interactions have to be identified and depending on the problem boundaries and the overall objective, their relative importance may vary (Leewongtanawit, 2005). Therefore, it is important at first to correctly define the specific context of the problematic.

The main components of a Water–Energy Network (WEN) design problem, clearly described by Dong (2008), are illustrated schematically in Fig. 15.3 where a given water source(s) is distributed to the process and utility systems. The freshwater intake streams are heated/cooled to process/utility system temperature conditions through various paths, which may involve heat exchangers and direct heat-transfer design features, such as storage tanks and other mixing points. Such stream distribution is driven by the process water demands (process-water type) and by the energy system demand for cooling (cooling-water type) subject to operating conditions/constraints (temperatures, flowrates and contaminant concentration levels).

The main assumptions typically adopted for the WEN design have been summarised by Klemeš *et al*. (2008):

© Woodhead Publishing Limited, 2013

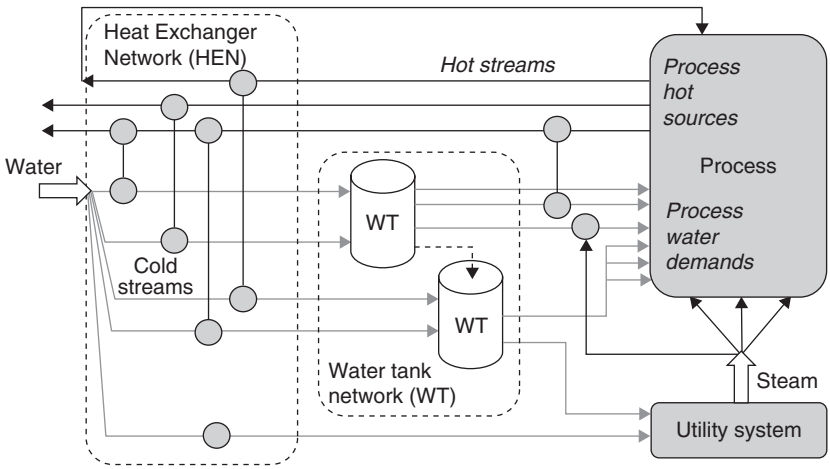

15.3 WEN – general problematic.

- Maximum inlet concentration as a key parameter for each water-using operation.
- Fixed mass of contaminant transferred in each operation.
- Constant source/sink operating temperature or isothermal operation.
- Only reuse of water is considered (no water regeneration).
- No water/heat losses.
- Other hot/cold process streams are excluded for simplification.
- For the same water quality non-isothermal mixing (NIM) is considered.
- When the concentration resulting from stream mixing is lower than the water-demand requirements the NIM is also considered.

It is then clear that the multitude of system interactions between these layers should be monitored, quantified and accounted for in the decision making steps at each stage of process design. Direct and indirect energy transfer, the associated plant-water sources and sinks, and the utility steam and cooling systems are the key components involved in the Energy/Water Integration assessment (Fig. 15.4).

A characteristic challenge of WEN design derives from the additional degrees of freedom related to the stream population or, in other words, the network considerations. In the context of the energy problem, the stream population is well defined; however, in the combined WEN problem, the water streams are yet to be established as connections between operations such that the stream population for the energy analysis is not available at the onset (Klemeš *et al.*, 2008). This feature provides significant advantage for HEN Design, as the energy streams within a water network can be selected

© Woodhead Publishing Limited, 2013

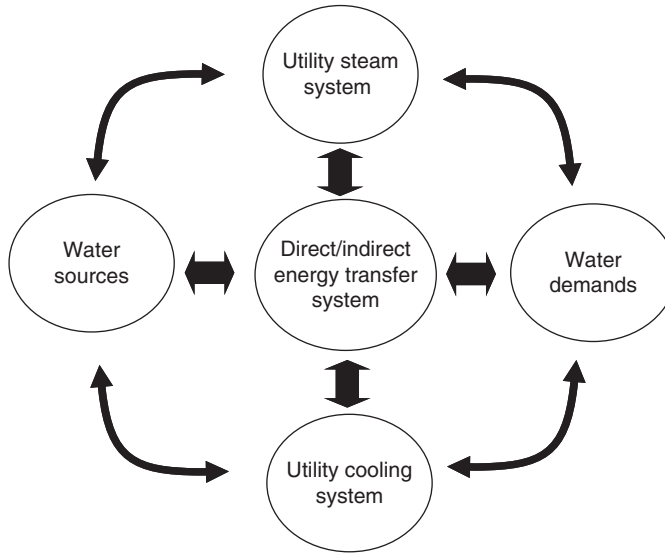

15.4 Energy–water system interactions.

to lower the number of indirect exchangers to a minimum while balancing the energy network for a minimum temperature variation through splitting, mixing and the use of 'Separate Systems' exchangers as proposed in the work of Savulescu *et al*. (2005a). Although the separate systems approach deals with a single contaminant problem, the evaluation using graphical tools is expected to provide relevant insights for multi-contaminant extensions.

15.3 Water Path Concept

The concept of a 'water path' to assess and track the evolution of WENs has been explored by several researchers. Ng and Foo (2006) use the path concept for the water minimisation stand-alone problem to reduce the number of connections by providing the possibility to manipulate the water loads along the paths. Feng *et al*. (2009) defined water network sub-streams (paths) as fixed flowrate connections from water intake to point of discharge. These water paths (FW→WU1→WU3→WW, Fig. 15.5) are used to systematically evaluate and explain why the energy consumption varies between different water-allocation networks as the temperature profile of each network path is observed through its fluctuations of peaks/valleys. Their aim is to minimise the heat capacity along the path as well as temperature fluctuations. Savulescu and Alva-Argaez (2008) considered the water path in the context of retrofit through a graphical representation of the temperature profile in the process to track the energy transformations along the path,

© Woodhead Publishing Limited, 2013

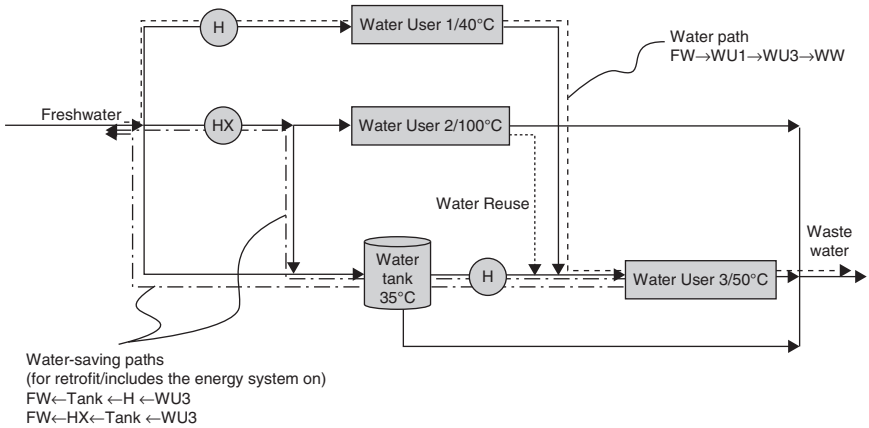

15.5 Water paths/water-saving paths. H and HX in the figure denote the heater and Process Heat Exchanger.

exploring how temperature varies across heat exchanges and water tanks before reaching the water-using operation.

In order to identify the best plant modifications, a systematic retrofit approach has been proposed for the pulp and paper sector (Alva-Argaez and Savulescu, 2009) that identifies and evaluates the water and energy interrelations to ensure that any intervention to improve the efficiency of the water system will not result in overall mill energy penalties. This approach looks at the water-saving retrofit path starting from the point of water reuse (as water-use operation, see Fig. 15.5) and going backwards to the initial freshwater source to ensure that the retrofit savings could be achieved. Two water-saving paths are illustrated in Fig. 15.5, FW←Tank←Heater←WU2 and FW←HX←Tank←WU3, associated with the reduction of the freshwater demand at the inlet of WU3, as a result of water-reuse opportunity from water user 2 (WU2) to water user 3 (WU3). Beside the graphical representation of water–energy-based paths/curves, a matrix approach is used to represent and to evolve the design step. Practical considerations are embedded to enhance the navigation along the paths and their selection towards the retrofit process changes for Simultaneous Energy and Water Minimisation.

Therefore, the definition of 'water path' varies in relation to the purpose of the design analysis; paths extending from the freshwater source to the discharge point as wastewater have been considered for new design, while fresh water to process paths are applied for retrofit scenarios.

In practice the water streams lose their identity, since their characteristic parameters of flow, composition and temperature are varying. Therefore, the water path concept proves to be a powerful tool to capture and characterise an Energy/Water Network and to keep track of the modifications that

© Woodhead Publishing Limited, 2013

can be implemented on the WEN, as well as to follow-up on the impacts of design changes to both water usage and energy demands.

15.4 State-of-the-Art Methodology for Combined Energy and Water Integration

Successful PI graphical tools (summarised by Kemp, 2007) have been further developed and adapted to address the complexity of the WEN, while considering water reuse together with heat recovery. It has been observed that the context of the Energy and Water Network is often characterised from the thermodynamic point of view as a 'threshold' problem (Polley, 2010). Therefore, in such a context, the water minimisation target can be identified first and then the energy targets are easily derived from this information and the temperature data on the raw water and wastewater discharge. However, several examples of Water–Energy Pinched problems have been reported in the literature, such as the work by Sorin and Savulescu (2004) in the context of a pulp and paper mill case study. Similarly, Leewongtanawit and Kim (2008) extended the examples from Savulescu (1999) to demonstrate their automated procedure; Martinez-Patino *et al*. (2011) adapted an example from Wang and Smith (1994) to illustrate their proposed method, and all these cases resulted in Pinched problems. It is therefore misleading to just assume that energy targets are simply a consequence of total freshwater usage, but rather an in-depth approach should be followed to define specifically the type of energy problem (Fig. 15.6). These Pinched cases are particularly influenced by the degree of water reuse and the contribution of the resulting hot/cold water reuse streams to the overall Energy Composite Curves. Another aspect that may influence the energy type of the water problem is the type of water (process/utility water – depending on the role of water usage) that is incorporated in the analysis (process, steam generation/cooling utility, auxiliary water). Furthermore, in the case of retrofit, when the analysis of the energy network includes more than just the WEN streams, one should expect the energy problem to be a Pinched problem. Process modification and operational changes may be introduced once the problem is identified as Pinched, to try to simplify to such theoretical global target corresponding to a threshold problem.

The most well-known approach is the two-step energy–water methodology proposed by Savulescu (1999) and later presented in detail by Savulescu *et al*. (2005a) for studies with no water reuse, and in part II of this paper (Savulescu *et al*., 2005b) the problematic of water reuse is considered. In the first step, the water limiting contaminant concentrations, flowrates and temperature data are plotted to establish the water and energy theoretical targets. In the second step, a Combined Water-and-Energy Integration

© Woodhead Publishing Limited, 2013

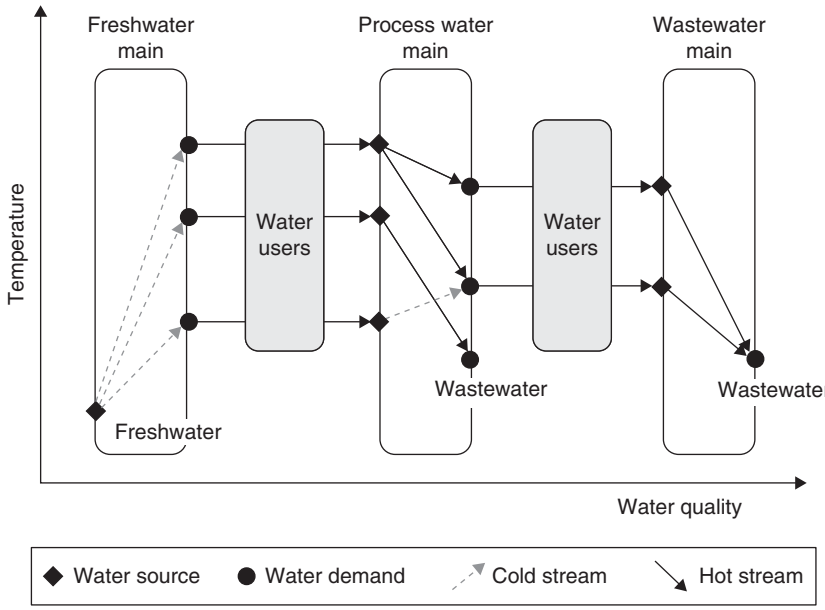

15.6 Temperature vs water type usages.

network is designed through the implementation of a Two-Dimensional Grid Diagram (Fig. 15.6). This temperature vs quality representation provides insights for the selection of alternative water paths based on their energy profiles and on specific design guidelines by Klemeš *et al.* (2008). Water mains of constant quality are considered, and within them distinctive rules have been developed to guide the population of hot/cold water streams as water network source–sink connections (Fig. 15.6). Once these streams are defined for minimum energy use, the energy network design is built based on the Composite Curves profile through their adjustment towards generation of Separate Systems (Fig. 15.7). This network construction distinguishes between the direct heat transfer (through NIM) and the indirect energy network of separate systems by modifying the Cold Composite Curve.

More recently, Wan Alwi *et al.* (2011) have enriched the targeting step through the introduction of a Superimposed Mass-and-Energy representation that simultaneously assesses water and heat reduction (Fig. 15.8). This enhanced representation is a functional visualisation to examine the implications of water and energy reduction and provides a link between the targeting and design steps. The realisation of the minimum utility requirement is then guided following the steps introduced by Mannan *et al.* (2009) through the Source/Demand Water Allocation Curves represented together with the Heat Surplus Diagram on a flowrate versus mass load/temperature

© Woodhead Publishing Limited, 2013

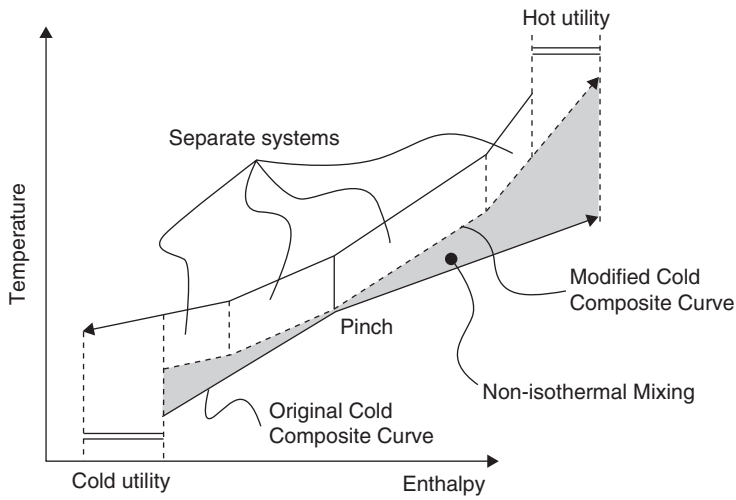

15.7 Composite Curves with separate system for WEN.

Table 15.1 Single contaminant water-using system data

Water Users	C_{IN} (ppm)	C_{OUT} (ppm)	Temperature (°C)	Limiting water flow (kg/s)	Mass load (g/s)
Water User 1	0	100	40	20	2
Water User 2	50	100	100	100	5
Water User 3	50	800	75	40	30
Water User 4	400	800	50	10	4

Fresh water temperature = 20°C
Wastewater discharge temperature = 30°C

graph. The Superimposed Mass/Energy Curves are briefly described for a single contaminant water-using system as listed in Table 15.1. This tabulated data is converted into a source/demand data table to complete the representation of Water Source/Demand Curves (Wan Alwi *et al.*, 2011). The cumulative load of water demands is plotted versus cumulative flowrate. By superimposing on the same graph the Energy Match Diagram (EMD), a tool is obtained to perform step-by-step changes to these curves. Similarly, the water source profile is generated and Pinched to the water-demand profile to identify the minimum fresh water and effluent targets (Fig. 15.8). The temperature effect is represented through the EMD on the same plot. Following specific heuristic rules leads to the identification of water targets as well as designs based on low energy usage. The combined graphs facilitate simultaneous targeting and design.

© Woodhead Publishing Limited, 2013

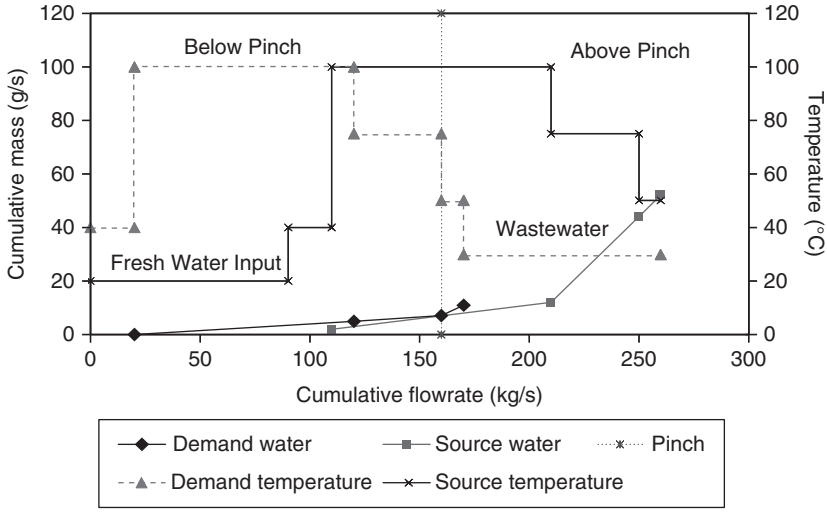

15.8 Superimposed Mass-and-Energy Curves – to be reviewed.

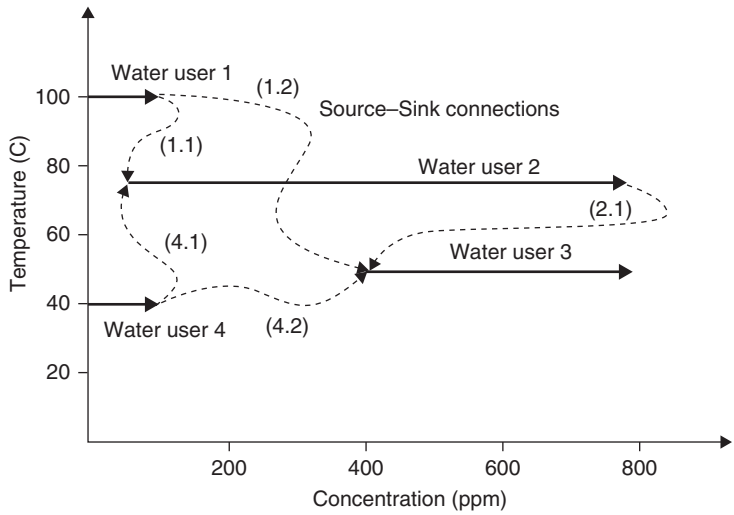

15.9 Temperature vs concentration diagram (Martínez-Patiño, 2011).

Another contribution with similar aims has been the 'Temperature-Concentration Diagrams' (Martinez-Patino, 2011), which have been introduced to visualise and to guide the user towards the selection of the minimum energy–water paths required to develop improved designs (Fig. 15.9). The complexity of the WEN design has been addressed in this approach

© Woodhead Publishing Limited, 2013

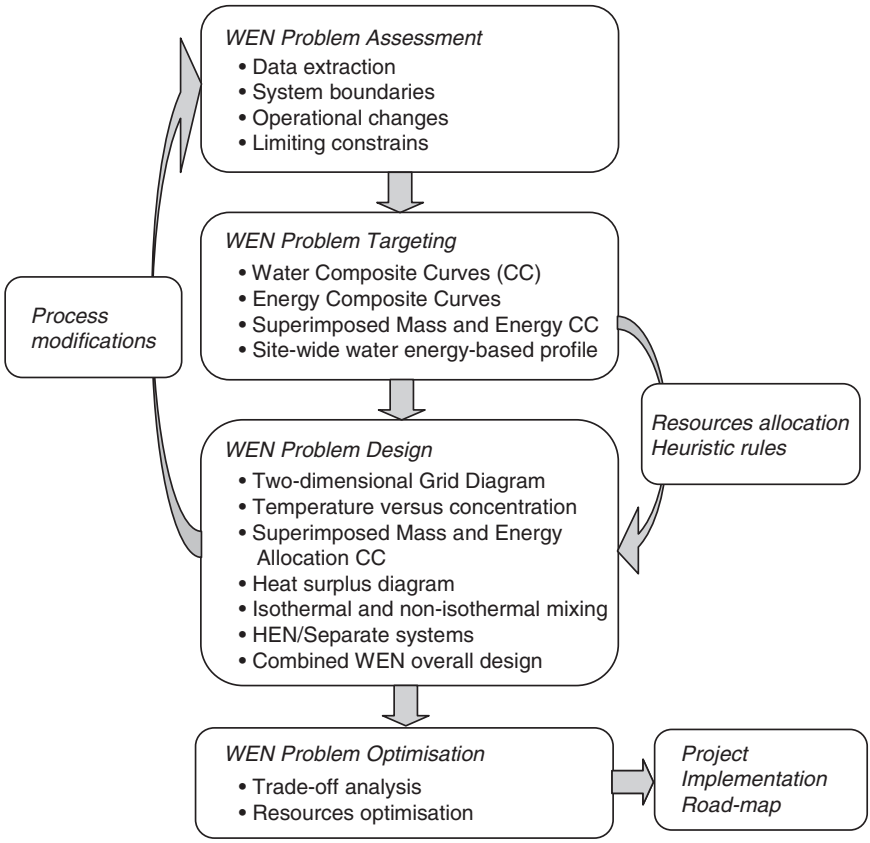

15.10 Combined energy and water state-of-the-art methodology.

through a distinct segregation of the overall problem into two main sections. It has been suggested to consider primarily the energy/water interactions at the level of the simultaneous heat-and-mass transfer sub-network. This sub-network includes only the water thermal flows and their distribution between water sources and sinks according to contaminant concentration constraints. The other sub-network is orientated to both direct and indirect heat recovery aspects and it looks after the management of the water flows and heat recovery.

The next section aims at summarising the key contributions to date and presenting these proposals in a common conceptual framework that defines an improved methodology for WEN design. As discussed earlier each contribution fits well within an overall methodology that includes the following steps (Fig. 15.10).

© Woodhead Publishing Limited, 2013

Step 1 – WEN Problem Assessment

In the first step, the WEN problematic has to be defined as system boundaries and operating conditions. All water sources and demands/users should be characterised in terms of flowrates, contaminants and their minimum and maximum levels, temperatures and other process constraints. Selection of WEN system boundaries, data extraction and identification of key interactions should be performed to formulate the problem. In the case of retrofit, the case-study process-flow diagram and resource balance should be evaluated towards a deep understanding of the process requirements and to obtain key knowledge about the process context to support the problem formulation. Furthermore, detailed WEN audits may also be performed early in the analysis, as suggested by Klemeš *et al*. (2008), where a review of the local operating aspects and individual equipment efficiencies can result in low cost, immediate modifications reducing the water and energy demands. It is important to consider any operational changes that may influence the water/energy systems to maximise the saving potential (Martinez-Patino, 2009).

Step 2 – WEN Problem Targeting

Once the WEN data is available, several Resource Utilisation Profiles are constructed to inspect the global demands for water and energy. The concentration-based Water Composite Curves reviewed and illustrated through examples by Smith (2005) are considered for Water Pinch Analysis to obtain the minimum freshwater targets. Wan Alwi *et al*. (2011) incorporate the two components water and energy within a novel representation that superimpose the mass-and-energy curves. In this context, the water Source–Demand Curves are overlapped together with the EMD. Such a representation is used to expand the scoping evaluation towards a simultaneous energy and water outcome. A conventional energy targeting for a specific water network configuration (Energy Composite Curves) can still be considered when a sequential/decomposition approach is used to iterate between targeting and design.

Step 3 – WEN Problem Design

The design step has two main elements: water-allocation network, and direct and indirect heat-transfer network (Fig. 15.10). As previously mentioned, it is recommended to develop the possible water–energy paths through the use of the 'water mains' concept and temperature levels provided by the Two-Dimensional Grid Diagram (TDGD) – conceptually illustrated in Fig. 15.7 as described in the work of Savulescu *et al*. (2005b), the water–energy

© Woodhead Publishing Limited, 2013

balance diagram (Leewongtanawit, 2008) and temperature-concentration diagrams (Martinez-Patino, 2011). A set of heuristic rules provides guidance to the designer when selecting the most appropriate water paths (i.e. network connections).

Once the water network analysis has been completed, a Composite Curves-based approach for isothermal and NIM is applied to obtain the energy characteristics of the network as well as network simplification by reducing the number of heat exchanges through the generation of separate systems. This analysis can also be enhanced by applying the EMD following the water allocation and performing the HEN design using the Grid Diagram approach and reducing the number of exchangers through Loop Breaking techniques (Wan Alwi and Manan, 2011). The design of the water-allocation network contributes to the number, and also to the type, of streams that should be accounted for in the energy network and that are subject to the HEN analysis.

Overview of Design Rules

There are several rules formulated to design the optimal water-allocation networks with lower energy consumption:

- **Rule 1** – Relates to the availability of water sources and their conditions and states that any clean water demand has to be first satisfied using the zero contaminant water sources (Kuo, 1998). Within the context of the Two-Dimensional Grid Diagram, water has to be allocated to each 'Water Main' characterised by the same quality level (in terms of contaminant concentration), starting with the fresh water as a clean source (Savulescu *et al*., 2005b).
- **Rule 2** – The minimum water consumption is defined mainly by the demands located Below the Mass Pinch region; consequently, all the water demands Below the Pinch have to be satisfied by freshwater or mixtures with freshwater – in other words, no effluent streams for reuse are available Below the Pinch. The 'Water Main' concept (Kuo, 1998) is used to characterise the concentration level for the allocation of water between sources and demands and provides information on the flowrate of water entering the main, the amount consumed by the main and the flowrate of waste effluent.
- **Rule 3 –** Match the temperature of the water sources with the demands by reusing the water source to the nearest temperature demand while accounting for the mass and flowrate constraints. The water main characterised by the temperature profile facilitates the implementation of this rule (Savulescu *et al*., 2005b) and consequently following-up the thermal aspects of any water source-demand connection. Also, the

© Woodhead Publishing Limited, 2013

temperature-concentration graph (Martinez-Patino, 2011) supports the implementation of this rule.

- **Rule 4 –** Taking into consideration the global requirement to reduce the effluent temperature, it is imperative to start consuming the hottest water source (Savulescu *et al.*, 2005b). This will ensure higher heat recovery potential by designing a network with hot-water reuse streams rather than cold ones. The aim is to avoid unnecessary energy exchange in the heat-transfer network.
- **Rule 5** – Above the Mass Pinch region the demand concentration will be satisfied if the source concentration is lower than the demand concentration, and temperature-based stream mixing rules should be applied – for details see Wan Alwi and Manan (2008)
- **Rule 6** – Implement NIM points when the temperatures of the demands are intermediate to the source operations.

In the case of retrofit design, the characterisation of the water-saving paths and the constraints associated with each of them are captured in the WEN matrix (Alva-Argaez and Savulescu, 2009). This characterisation is then used to navigate through the water-saving path alternatives and select the options with simultaneous savings in water and energy.

Step 4 – WEN Optimisation

Once network designs are obtained through the application of the above methodology, it is always recommended to fine-tune the trade-off analysis through optimisation, seeking to reduce the total cost (operating cost, equipment cost, piping and pumping costs), evaluate design flexibility and operating schedules, which are some of the elements that the mathematical programming can help to screen and refine between the design alternatives and process modifications.

Step 5 – WEN Project Implementation Road Map

The sequence and grouping of water and energy projects is crucial for the practical implementation of the simultaneous energy and water savings in retrofit scenarios. It is likely that competing and mutually exclusive projects will be identified; similarly, a set of projects may be recommended but their implementation could exceed available resources. A project road map can be prepared with the support of the graphical tools presented earlier, such that competing projects can be evaluated and screened and the implications of accepting or rejecting them can be assessed in terms of water and energy savings. More specific decision-support practical

© Woodhead Publishing Limited, 2013

guidelines for pulp and paper industrial sector are described by Alva-Argaez *et al*. (2007).

The methodology described above summarises the key contributions to the field in a general step-by-step framework; as is always the case in process design, the sequential nature of the approach calls for iterations and is never a simple linear process. Following the conceptual background built under the PI field, the specification of problem boundaries and parameters followed by a targeting step ahead of design presents also some flexibility in the actual tools to be applied. It must be noted that the various contributions to the area discussed here complement each other, and it is highly recommended that the various graphical tools are applied during a combined water-and-energy study.

15.5 Sequential, Simultaneous, Mathematical Programming

There has been significant debate in the academic literature with respect to the most appropriate strategy to be applied when assessing industrial design problems characterised by strong energy and water interactions. As noted in the previous section, the origins of Combined Water and Energy Analysis are based on graphical tools (Savulescu, 1999), wherein the Water Pinch concept was extended to consider temperature constraints, and systematic/heuristic design guidelines were derived from this analysis. Later on, mathematical programming techniques were introduced to deal with the high complexity of such problematics. Papalexandri and Pistikopoulos (1994) presented an optimisation framework to deal with the more general problem of Heat-and-Mass Exchange Networks; in this early work, the authors considered changes in both temperature and composition according to a set of discrete values. A multiperiod mixed integer non-linear programming (MINLP) mass-and-heat exchange hyperstructure formulation was proposed and they applied the Generalised Benders Decomposition to find a solution to this highly non-linear problem. For the specific case of water networks, Bagajewicz *et al*. (2002) presented a targeting approach for energy-efficient water networks that combine the classical transshipment problem for energy optimisation with the water network as an linear programming (LP) formulation (single contaminant); their observation of the necessary conditions of optimality for water networks enabled the targeting step to remain a linear problem. The solution of the LP targeting stage was used to set up an mixed integer linear programming (MILP) model whose solution provided structural information to design the network that would achieve those targets; it is noted that a merging procedure was also suggested to evolve the design and reduce the number of heat exchangers.

Leewongtanawit and Kim (2004) presented a methodology that combined the conceptual elements from Savulescu (1999) with a superstructure

© Woodhead Publishing Limited, 2013

approach, to attempt a simultaneous approach, that is with no decomposition in targeting and design stages. As has been usually the case, heat exchange is allowed only between water streams, and hot and cold process streams are not considered in the superstructure representation. The model includes NIM options and incorporates heat exchanger capital cost in the objective function. The resulting MINLP model is solved in a two-step approach whereby a relaxed MILP problem is initially solved (also based on the optimality conditions) and the result used as an initial point for the MINLP solver. Dong *et al*. (2008) generalised the optimisation approach by describing the combined heat and water network problem using a state-space approach; the resulting MINLP problem formulation includes all water-allocation options, water treatment options, and heat exchange (direct and indirect heat transfer). To deal with the complexity of the solution, these authors proposed the use of random generation of initial points to be submitted to the MINLP solver; by performing stochastic perturbations on the initial guesses, a set of bounds could be identified and the likelihood of finding a globally optimal solution increased. In a final step the HEN is further improved by heat-load shifting and breaking heat-load loops. Feng *et al*. (2008) discussed the energy performance of alternative water-allocation networks, and concluded that reducing the number of temperature fluctuations in sub-streams was beneficial for the energy performance of the network. Their proposed problem formulation added the minimisation of 'peak' or 'valley' temperatures as well as 'unnecessary' water flows as a procedure to guide the solver toward an energy-efficient design. Xiao *et al*. (2009) described what they called 'Holistic Mathematical Programming' whereby a complete superstructure including water use and heat transfer is developed; the authors claim a more general representation of the problem; however, it is not very clear what the extensions are compared to the model presented by Dong and co-authors. The solution strategy for the large MINLP requires the generation of initial points based on a sequential approach, whereby the water network is generated followed by a HEN. They also include random perturbations in the variables to explore the solution space and improve the quality of the solutions.

Grossman and Martin (2010) discussed a sequential approach for the combined water and energy problem in the context of biofuel plants where in the first stage energy consumption is minimised via a superstructure that embeds HENs and alternative separation technologies (e.g., simple distillation versus multiple effect columns). In the second stage the water network is optimised via a water network superstructure as proposed by Ahmetovic and Grossman (2011). The water network superstructure incorporates all possible interconnections between water users, treatment units and water sources. Ahmetovic and Grossman also incorporated tighter bounds for decision variables, as well as the cut proposed by Karuppiah and Grossman

© Woodhead Publishing Limited, 2013

whereby the addition of overall contaminant mass balances was found to enhance the efficiency of the solution.

The WEN problematic calls for an MINLP formulation that is complex and difficult to converge. As noted above, some researchers, considered the relaxed MINLP formulations. However, in many cases it has been well established that the quality of the solution and the numerical iteration process in solving an MINLP problem is highly dependent on the initial guesses (decision variables selected are the binary variables on the split ratios of all the splitters) and may converge to a local optimum.

When it comes to practical application of these methods, there should be a judgement call with respect to the simplifying assumptions required to reduce the complexity and enable the algorithms to find solutions. This includes the extent to which the problem may be decomposed for a sequential approach that benefits from the application of existing engineering concepts. Translating the available conceptual engineering insights into mathematical programming language to accelerate the search for solutions also relies on de-coupling the problem to convert from large MINLP formulations to a sequence of LP/MILP problems that can identify promising network structures and typically followed by non-linear programming (NLP). Many of the mathematical algorithms have incorporated some of the early stage concepts into their formulation.

It is now widely recognised that an approach that benefits from the engineering insights of conceptual methods, and is coupled with the power of mathematical programming or other optimisation tools, will result in an inclusive approach that will enable the identification of practical and economical energy and water efficient designs.

The conceptual design methods may reach their limitations when dealing with a large number of water-using operations, or where there are many contaminants involved. Also, in practice a wide range of constraints need to be considered in water network design, such as minimum or maximum flowrates, Forbidden Matches because of long pipe-runs and compulsory or Forbidden Matches for operability or safety concerns.

15.6 Conclusion

Although Combined Energy and Water Integration is a recent area of research in the PI field, a significant amount of research material has already been published in journals and synthesised in books. The selection of WEN data, targeting calculations through graphical tools, is well detailed and illustrated through multiple examples and case studies in journal publications. González Cortés *et al*. (2011) highlights the benefits of simultaneous energy and water retrofitting in a sugar plant as 87% water savings together with 65% energy reduction.

© Woodhead Publishing Limited, 2013

In most PI applications, a key success factor is the synergy between detailed process knowledge and a good understanding of the design methods. The methodologies described in this chapter have applications in a large number of industrial sectors, and it is imperative that process considerations are well understood throughout the application of the methods. Data extraction for a water-and-energy analysis requires significant effort and it is likely to be the most time-consuming step of the approach; there are not many references that discuss the pitfalls in data extraction but a good summary is presented through a pulp and paper Kraft mill example by Savulescu and Alva-Argaez (2008).

A previously published industrial case study (Leewongtanawit and Kim, 2008) showed 18% additional reduction in annualised cost resulting from a combined water-and-energy approach, and as compared with water-only minimisation using Water Pinch Analysis. This case study and other published results provide extensive support for the application of PI methods with expanded boundaries, such as combining water and energy simultaneously.

With the wide availability of computer software, design engineers should not restrict themselves to the recommendations of a particular author, but should explore the use of many alternative graphical representations. The targeting stage provides the insights to better understanding of these complex systems and their interactions; graphical representations of the data, such as those described here, need to be exploited fully ahead of the design stage. The amount of information and understanding of what a simple set of Composite Curves can provide cannot be over emphasised. Based on the experience gained by the authors of this chapter, it is recommended to master the interpretation of the visualisation tools before attempting a full-blown mathematical optimisation exercise. Clearly, the benefits of complementing graphical representations with powerful numerical optimisation techniques are much greater than the use of each approach separately.

15.7 Sources of Further Information

The area of simultaneous water and energy optimisation continues to gather interest from the academic and industrial communities, with a number of recent publications expanding on the boundaries of the design problem, introducing new concepts, and reporting on applications to industrial case studies. There is a clear trend toward the use of numerical optimisation methods, which is explained by the large number of interactions between the various elements of the system that are difficult to capture with purely conceptual methods. Boix *et al*. (2012) presented an approach for the combined water and energy problem where they propose a two-stage method where an MILP problem is solved in the first step as a multi-objective optimisation problem that considers freshwater use, energy consumption and complexity

© Woodhead Publishing Limited, 2013

constraints (number of heat exchangers and number of interconnecting pipes). In the second step, the most promising designs are further refined via MINLP optimisation; applications to the pulp and paper industry demonstrate potential energy savings of 20% compared to previous results.

Yiquing *et al*. (2012) studied in more detail the impact of various NIM strategies on the energy consumption of water networks and presented guidelines to identify design features of the water network that could lead to utility penalties and suggested minimising the temperature approach in NIM points to alleviate the energy penalties while simultaneously taking advantage of mixing to simplify the structure of HENs. Hung and Kim (2012) extended the problem definition by taking into account pressure-drop considerations and pumping arrangements in the design of the water network; these authors also relied on the application of MINLP optimisation methods. The paper recently published by Chew *et al*. (2013) reports on the application of mathematical programming tools to the brown-stock washing system in pulp and paper mills; the results indicate significant opportunities for water and energy savings. Also, in the context of the multi-objective optimisation, water and energy as foot print indexes are incorporated with the sustainability assessment as described by Čuček *et al*. (2012).

15.8 References

Ahmetović, E., Martin, M., Grossmann, I. E. (2010). Optimization of energy and water consumption in corn-based ethanol plants. *Industrial & Engineering Chemistry Research*, **49**(17), 7972–7982.

Ahmetović, E., Grossmann, I. E. (2010). Global superstructure optimization for the design of integrated process water networks. *AIChE Journal,* **57**(2), 434–457.

Alva-Argaez, A., Savulescu, L., Poulin, B. (2007). A process integration-based decision support system for the identification of water and energy efficiency improvements in the pulp and paper industry. PAPTAC 93rd Annual Meeting Conference Proceedings, Montreal, C23–C26.

Alva-Argaez, A., Savulescu, L., Cripps, H. R. (2008). Water-based energy assessment. A conceptual approach to retrofit systems with strong energy-water interactions. 11th PRES Conference 24–28 August 2008, Prague – Czech Republic, J6.1 (1192).

Alva-Argaez, A., Savulescu, L. (2009). Water Reuse Project Selection: A retrofit path to water and energy savings. *Chemical Engineering Transactions,* **18**, 403–408, DOI: 10.3303/CET 0918065.

Bagajewicz, M. J., Rodera, H., Savelski, M. (2002). Energy-efficient water utilisation systems in process plants. *Computers and Chemical Engineering*, **26**(1), 59–79.

Bogataj, M., Bagajewicz, M. J. (2008). Synthesis of non-isothermal heat integrated water networks in chemical processes. *Computers and Chemical Engineering*, **32**(12), 3130–3142.

© Woodhead Publishing Limited, 2013

Bandyopadhyay, S., Sahu, G. C. (2011). Energy targeting in heat integrated water networks with isothermal mixing. *Computer Aided Chemical Engineering*, **29**, 1989–1993.

Boix, M., Pibouleau, L., Montastruc, L., Azzaro-Pantel, C., Domenech, S. (2012). Minimising water and energy consumption in water and heat exchange networks. *Applied Thermal Engineering*, **36**, 442–455.

Chew, I. M. L., Foo, D. C. Y., Bonhivers, J.-C., Stuart, P., Alva-Argaez, A., Savulescu, L. E. (2013). A model-based approach for simultaneous water and energy reduction in a pulp and paper mill. *Applied Thermal Engineering*, **51**, 393–400.

Čuček, L., Varbanov, P. S., Klemeš, J., Kravanja, Z. (2012). Total footprints-based multi-criteria optimisation of regional biomass energy supply chains. *Energy*, **44**(1), 135–145.

Dong, H. G., Lin, C. Y., Chang, C. T. (2008). Simultaneous optimization approach for integrated water-allocation and heat-exchange networks. *Chemical Engineering Science*, **63**(14), 3664–3678.

Douglas, J. M. (1988). *Conceptual Design of Chemical Processes.* McGraw-Hill, New York, USA.

Du, J., Meng, X., Du, H., Yu, H., Fan, X., Yao, P. (2004). Optimal design of water network with energy integration in process industries. *Chinese Journal of Chemical Engineering*, **12**, 247–255.

El-Halwagi, M. M. (1997). *Pollution Prevention through Process Integration: Systematic Design Tools.* Academic Press, San Diego, CA, USA.

Feng, X., Li, Y., Shen, R. (2009). A new approach to design energy efficient water allocation networks. *Applied Thermal Engineering,* **29**, 2302–2307.

Feng, X., Li, Y., Yu, X. (2008). Improving energy performance of water allocation networks through appropriate stream merging. *Chinese Journal of Chemical Engineering*, **16**, 480–484.

González Cortés, M., Verelst, H., Pedraja, R. E., Suárez, E. G. (2011). Simultaneous energy and water minimisation applied to sugar process production. *Chemical Engineering Transactions,* **25**, 177–182, DOI:10.3303/CET1125030.

Grossmann, I. G., Martín, M. (2010). Energy and water optimisation in biofuel plants. Plenary Lecture in the 2nd Symposium on Sustainable Chemical Product and Process Engineering, Zhejiang University of Technology, Hangzhou, China. *Chinese Journal of Chemical Engineering*, **18**(6), 914–922.

Hung, S. W., Kim, J.-K. (2012). Optimisation of water systems with the consideration of pressure drop and piping. *Industrial & Engineering Chemistry Research*, **51**(2), 848–859.

Isafiade, A., Fraser, D. (2007). Optimization of combined heat and mass exchanger networks using pinch technology, *Asia Pacific Journal of Chemical Engineering*, **2**(6), 554–565.

Jian, D. U., Hongmei, Y. U., Xishan, F. A. N., Ping, J. (2003). Integration of mass and energy in water network design, *Computer Aided Chemical Engineering*, **15**, 796–801.

Karuppiah, R., Grossmann, I. E. (2006). Global optimization for synthesis of integrated water systems in chemical processes. *Computers and Chemical Engineering*, **30**, 650–673.

Kim, I. Y., Kim, J. K., Kim, J. H., Yoo, C. K., Moon, I. (2009). A simultaneous optimization approach for the design of wastewater and heat exchange networks based on cost estimation. *Journal of Cleaner Production*, **77**, 162–171.

© Woodhead Publishing Limited, 2013

Klemeš, J. J., Varbanov, P. S., Pierucci, S. (2010). Process integration for energy and water saving, increasing efficiency and reducing environmental impact. *Applied Thermal Engineering,* **30**, 2265–2269.

Kok Sum, Ng. D., Foo, D. C. Y. (2006) Evolution of water network using improved source shift algorithm and water path analysis. *Industrial & Engineering Chemistry Research*, **45**(24), 8095–8104.

Koufos, D., Retsina, T. (2001). Practical energy and water management through pinch analysis for the pulp and paper industry. *Water Science Technology,* **43**(2), 327–332.

Kuo, W. J., Smith, R. (1998). Designing for the interactions between water-use and effluent treatment. *Transaction of IChemE,* **76**(Part A), 287–301.

Klemeš, J., Smith, R., Kim, J. K. (2008). *Handbook of Water and Energy Management in Food Processing.* Woodhead Publishing, Cambridge, UK.

Leewongtanawit, B. (2005). Heat-integrated water system design. PhD Thesis, The , UK.

Leewangtanwit, B., Kim, J. K. (2008). Synthesis and optimisation of heat-integrated multi-contaminant water systems. *Chemical Engineering and Processing*, **27**, 670–694.

Manan, Z. A., Tea, Y. S., Wan Alwi, S. R. (2009). A new technique for simultaneous water and energy minimisation in process plant. *Chemical Engineering Research and Design*, **87**, 1509–1519.

Martínez-Patiño, J., Picón-Núñez, M., Serra, L. M., Verda, V. (2009). Exploiting inherent process flexibility for the reduction of water and energy consumption. Application to the pulp and paper industry. *Chemical Engineering Transactions*, **18**, 923–929, DOI: 10.3303/CET 0918151.

Martínez-Patiño, J., Picón-Núñez, M., Serra, L. M., Verda, V. (2009). Integrated optimisation of water and energy consumption. Part II: Systematic approach for the synthesis of integrated water and energy networks. *Energy*, **36**, 3888–3896.

Martínez-Patiño, J., Picón-Núñez, M., Serra, L. M., Verda, V. (2011). Design of water and energy networks using temperature concentration diagrams. *Energy*, **36**, 3888–3896.

Norman, R., Berntsson, T. (2006). Design of Kraft pulp mill hot and warm water systems – A new method that maximizes excess heat. *Applied Thermal Engineering*, **26**, 363–373.

Papalexadri, P. K., Pistikopoulos, E. N. (1994). A multi-period MINLP model for the synthesis of flexible heat and mass exchange network. *Computers and Chemical Engineering*, **18**, 1125–1139.

Polley, G. T., Picón-Núñez, M., López-Maciel, J. J. (2010). Design of water and heat recovery networks for the simultaneous minimization of water and energy consumption. *Applied Thermal Engineering*, **30**, 2290–2299.

Savulescu, L. (1999). Simultaneous energy and water minimisation. PhD Thesis, Department of Process Integration, UMIST, Manchester, UK.

Savulescu, L., Alva-Argaez, A. (2008). Direct heat transfer considerations for improving energy efficiency in pulp and paper Kraft mills. *Energy,* **33**, 1562–1571.

Savulescu, L., Kim, J. K., Smith, R. (2005a). Studies on simultaneous energy and water minimisation. Part I: Systems with no water reuse. *Chemical Engineering Science*, **60**, 3279–3290.

© Woodhead Publishing Limited, 2013

Savulescu, L., Kim, J. K., Smith, R. (2005b). Studies on simultaneous energy and water minimisation. Part II: Systems with maximum reuse of water. *Chemical Engineering Science,* **60**, 3291–3308.

Savulescu, L., Sorin, M., Smith, R. (2002). Direct and indirect heat transfer in water network systems. *Applied Thermal Engineering*, **22**, 981–988.

Sorin, M., Savulescu, L. (2004). On minimization of the number of heat exchangers in water networks. *Heat Transfer Engineering*, **25**(5), 30–38.

Sahu, G. C., Bandyopadhyay, S. (2012). Energy optimisation in heat integrated water allocation networks. *Chemical Engineering Science*, **69**, 352–364.

Wan Alwi, S. R., Ismail, A., Manan, Z. A., Handani, Z. B. (2011). A new graphical approach for simultaneous mass and energy minimisation. *Applied Thermal Engineering*, **31**, 1021–1030.

Wan Alwi, S. R., Manan, Z. A. (2008). Generic graphical technique for simultaneous targeting and design of water networks. *Industrial Engineering Chemical Research*, **47**, 2762–2777.

Wang, Y., Smith, R. (1994), Wastewater minimization. *Chemical Engineering Science,* **49**(7), 981–1006.

Xiao, W., Zhou, R., Dong, H. G., Meng, N., Lin, C. Y. (2009). Simultaneous optimal integration of water utilization and heat exchange networks using holistic mathematical programming. *Korean Journal of Chemical Engineering*, **26**(5), 1161–1174. DOI: 10.2478/s11814–009–0196–5

Yiqung, L., Tingbi, M., Sucai, L., Xigang, Y. (2012). Studies on the effect of non-isothermal mixing on water-using energy performance. *Computers and Chemical Engineering,* **36**, 140–148.

Zheng, X. S., Feng, X., Cao, D. L. (2003). Design water allocation with minimum freshwater and energy consumption. *Computer Aided Chemical Engineering*, **15**, 388–393.

Zhelev, T. K. (2005). Water conservation through energy management. *Journal of Cleaner Production*, **13**, 1395–1404.

© Woodhead Publishing Limited, 2013

16

Process Integration Techniques for Cogeneration and Trigeneration Systems

MARTÍN PICÓN-NÚÑEZ, University of Guanajuato, México and JOSÉ MARTÍN MEDINA-FLORES, Polytechnic University of Guanajuato, México

DOI: 10.1533/9780857097255.4.484

Abstract: The production of various energy outputs and other useful secondary by-products from one or more energy inputs is known as polygeneration. The application of polygeneration schemes implies a high degree of Process Integration. This is particularly the case when various utility services are provided from a single source; for instance, when using a waste stream as fuel, energy can be extracted via combustion; then steam can be raised and used for process heating, power production and even process cooling. When only heating and power are produced for use within the site, the system is referred to as cogeneration; when cooling is additionally produced, the system is referred to as trigeneration. This chapter focuses on trigeneration systems, describes their main components, establishes the criteria for its appropriate selection and looks at the use of Process Integration techniques for the design of such systems in the context of background processes. The design of trigeneration systems requires the development of simple and reliable thermodynamic models for evaluating the thermal performance of prime movers at full and part load. Such models are necessary to evaluate operation in situations where plant throughput changes due to seasonal marked demands.

Key words: polygeneration, Combined Heat and Power, trigeneration, Heat Integration.

16.1 Introduction

Polygeneration is defined, according to Esdaile-Bouquet (2007), as the use of multiple primary energy inputs to create multiple energy outputs, with energy outputs being the different forms of energy which are useful in an activity. The technical report on polygeneration (POLYSMART, 2008) defines polygeneration as an integrated process which has three or more outputs that include energy outputs and that are produced from one or more natural resources. The term polygeneration implies a high degree of Process

© Woodhead Publishing Limited, 2013

Integration; this is particularly true when utility services are provided from a single source. Typical polygeneration schemes are:

a. Gasification of coal or heavy oil. This operation produces a syngas, which in turn can be used to produce heat, power and cold; the solid residue finds application as a raw material for other industrial applications.
b. Biogas production from biomass. A biogas is produced, which in turn is used to produce heat and power. The solid residue finds application as a fertilizer.
c. Bioethanol production. Starting from the use grains or agricultural residues, bioethanol is produced, which in turn is used for heat and power production; solid residues can be used for either heat production after burning or as a feedstock for other processes.

A particular type of polygeneration system, in which heat, power and cold are simultaneously produced for use within a site from the combustion of a single fuel input, is referred to as trigeneration. This technique was introduced in the early 1980s and its first applications were for municipal heating and cooling (Maidment and Tozer, 2002); however, due to the frequent need of these three utilities in the chemical and petrochemical industries, this technology has found wider application in processing plants (Dharmadhikari, 1997). The optimum design of trigeneration systems involves the analysis of a range of parameters, such as: energy tariffs, the type of application and the mode of operation (Kavvadias *et al.*, 2010). Figure 16.1 shows a general diagram of a trigeneration plant.

When cooling is required at near ambient temperature, a refrigeration system is used. The most common type of refrigeration systems in process plants are those operated by means of an intermediate fluid or refrigerant. Typical refrigeration systems are vapour compression and vapour absorption refrigeration.

16.2 Combined Heat and Power

When compared with the stand-alone production of utility services, the heating, cooling and power needs of a process are best, and more efficiently supplied by means of an integrated system or a Combined Heat and Power (CHP) system. Figure 16.2 shows a performance comparison between a CHP and the conventional mode of process energy supply. Using average thermal efficiencies for the sake of simplicity, we see that the total primary energy input required to supply the power (35 units) and thermal (53 units) needs of the process is 162.25 units in the case of a stand-alone boiler and power station. In order to supply the same process duties, the CHP system consumes only 125.71 units; this represents a reduction of 36.54 units, or a

© Woodhead Publishing Limited, 2013

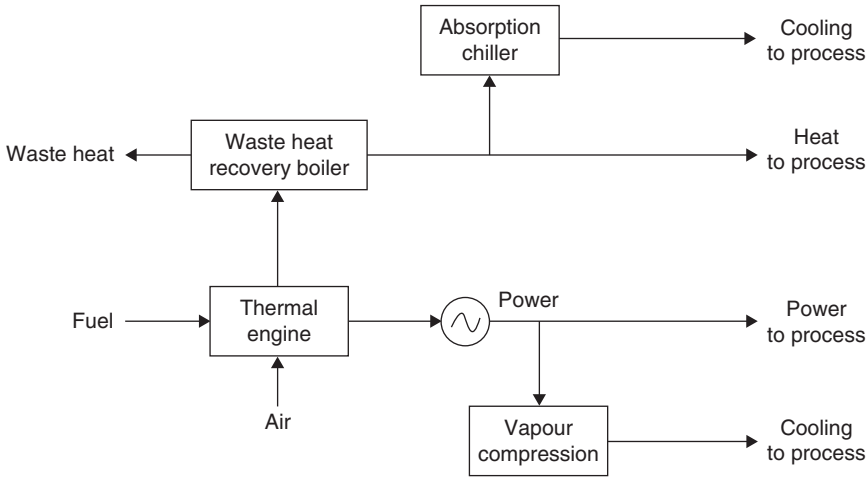

16.1 General diagram of a trigeneration system.

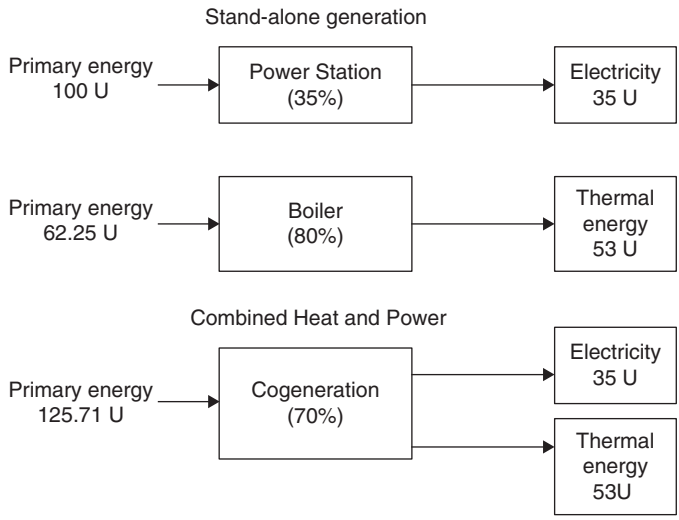

16.2 Overall benefit of a CHP against a conventional system.

saving of 22.5%, in the consumption of primary energy (Hernández and Sánchez, 2003).

The energy balance of Fig. 16.2 depends on the type of heat engine employed. There are three basic types of heat engines available for use in CHP systems, namely: internal combustion engines (diesel engines), gas turbines and steam turbines. Each of these technologies operates with a certain thermal efficiency, and produces a certain amount of power and thermal

© Woodhead Publishing Limited, 2013

energy. For instance, a diesel engine finds its highest efficiency (41%) at a rate production of heat to power of 1; a gas turbine operates more efficiently (35%) at a heat to power ratio of 3. In the case of a back-pressure steam turbine, its highest efficiency (23%) is found at around a heat to power ratio of 9. The thermal energy contained in flue gases from the internal engine or the gas turbine can be used for heating purposes, either directly or through the production of steam. A heat recovery system for steam production has an efficiency of around 67% (Eastop and Croft, 1995).

The use of a CHP is best suited for situations where the energy balance of the process remains constant and the heat/power ratio is near optimum for the type of heat engine being used. The economics of a CHP system are affected by operational factors, for instance: maintenance costs, the price of fuel, and the energy policies of the region with regard to economic incentives and energy export schemes for surplus power production (Lozano *et al*., 2010). In order to further illustrate the benefits of the implementation of a CHP for energy supply in a Processing Plant, an example taken from a real case study is presented. Table 16.1 shows the energy needs of an existing specialty batch chemical plant. Given the nature of the processes involved and the variations on plant throughput round the year, the heat/power ratio of the site fluctuates between 3.6 and 5.5. The type of prime mover that is most suitable for the production of power at this rate is a gas turbine. Considering the local costs of energy, an overall saving of 35.8% during the year is achieved (Table 16.2). However, despite the evident benefits of the use of CHP systems, there are reasons that make it difficult to provide an accurate financial appraisal and discourage companies from their implementation, some of them being:

Table 16.1 Heat/power needs of an existing specialty chemical batch plant

Month	Thermal energy		Electricity		Heat/power ratio
	Consumption (kWh)	Cost (USD/kWh)	Consumption (kWh)	Cost (USD/kWh)	
January	6,219,875.3	0.0131	1,219,168	0.0372	5.1
February	5,299,350.3	0.0095	1,114,454	0.0371	4.8
March	4,620,355.3	0.0060	1,121,030	0.0350	4.1
April	4,176,722.1	0.0065	1,151,320	0.0328	3.6
May	6,476,191.3	0.0073	1,380,732	0.0275	4.7
Jun	6,754,897.9	0.0080	1,501,791	0.0314	4.5
July	6,753,258.9	0.0076	1,451,661	0.0321	4.6
August	6,592,925.9	0.0076	1,543,398	0.0341	4.3
September	6,228,385.6	0.0086	1,530,016	0.0340	4.1
October	5,800,346.6	0.0104	1,415,374	0.0361	4.1
November	7,023,722.0	0.0111	1,599,282	0.0396	4.4
December	8,036,111.1	0.0080	1,468,788	0.0413	5.5

© Woodhead Publishing Limited, 2013

Table 16.2 Total energy costs for the operation with and without a CHP for the case of the specialty chemical site

Month	Total cost without cogeneration	Total cost with cogeneration	Savings
	USD/month	USD/month	USD/month
January	127,126.02	62,168.19	64,957.83
February	91,848.80	61,484.40	30,400.40
March	67,127.41	59,787.59	7,439.8
April	65,164.72	59,719.79	5,444.92
May	85,839.20	65,279.25	20,559.95
June	101,339.43	68,17.21	32,622.22
July	97,934.57	67,875.86	30,058.71
August	102,954.08	69,472.39	33,481.69
September	105,639.26	67,591.33	38,047.93
October	111,657.70	67,160.60	44,497.09
November	141,453.49	71,465.47	69,988.01
December	131,912.55	68,179.73	63,732.81
	Total annual savings:	441,231.44	
	% savings:	35.8%	

1. The continuous changes in energy demand of a plant, as a consequence of changes in production rate or the introduction of new processes,
2. The continuous change in fuel prices with time, and
3. The capital cost investment of a CHP installation, which makes the payback period too long.

As a consequence, companies might decide that it is safer to produce steam from the site boilers and purchase electricity from the local utility company. In the case shown in Tables 16.1 and 16.2, the total investment cost of the CHP was around 4 MUSD, giving a payback period of 9 years.

Trigeneration can be considered as a special case of the application of cogeneration systems, where a fraction of the shaft work or residual heat is used for running a refrigeration system (Teopa *et al*., 2005). Due to the important economic and environmental benefits of the application of trigeneration systems, a wide range of applications have been reported (Bassols, 2002). The application of trigeneration systems has also been extended to consider renewable energy (Tora and El-Halwagi, 2011). Trigeneration systems will be considered in more detail in the following sections.

16.3 Heat Integration of Trigeneration Systems

There are various possible combinations of thermal engines and refrigeration systems for a trigeneration scheme. The selection of the

© Woodhead Publishing Limited, 2013

most appropriate combination requires understanding of the basic principles of operation of each of the components. From the trigeneration diagram shown in Fig. 16.1, it follows that once a thermal engine has been chosen, refrigeration can be produced either through the use of an absorption system or by an electrically driven compression system. As mentioned earlier, the choice of the appropriate trigeneration arrangement depends on the process heat/power-ratio needs and on the temperature operating conditions.

Process Integration graphical tools provide a quick and easy means of sizing and selecting the utility systems for maximum overall fuel efficiency (Polley and Sarabchi, 2000). Pinch Analysis techniques are used in this chapter to thermally integrate trigeneration systems into background processes. Among these tools is the Grand Composite Curve (see Chapter 2). In the following section, a simple methodology for the selection of trigeneration systems using the Grand Composite Curve is presented.

16.3.1 Gas Turbine-Vapour Compression Systems

The efficiency of a gas turbine reaches a maximum value at around a heat/power ratio of 3. The temperature of the exhaust gases is around 500°C, which makes the system suitable for heat recovery. The maximum amount of energy that can be recovered can be limited by either the Acid Dew Point of the flue gas or the shape of the Grand Composite Curve. Figure 16.3 shows these possible limiting conditions.

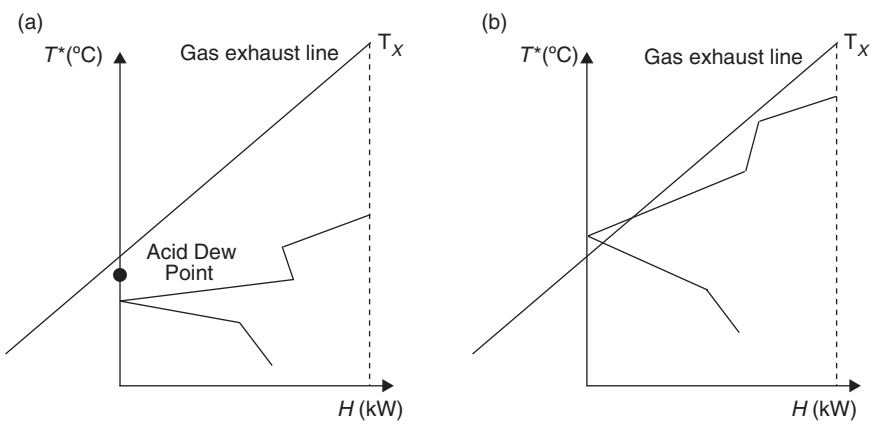

16.3 Energy recovery from hot exhaust gases. Energy recovery limited by: (a) flue gas Acid Dew Point; (b) shape of the Grand Composite Curve.

© Woodhead Publishing Limited, 2013

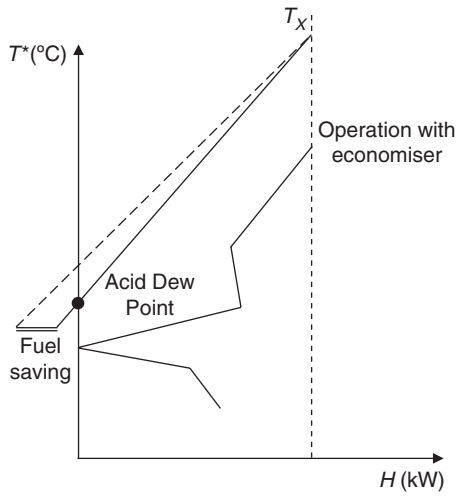

16.4 Operation of a gas turbine with an economiser.

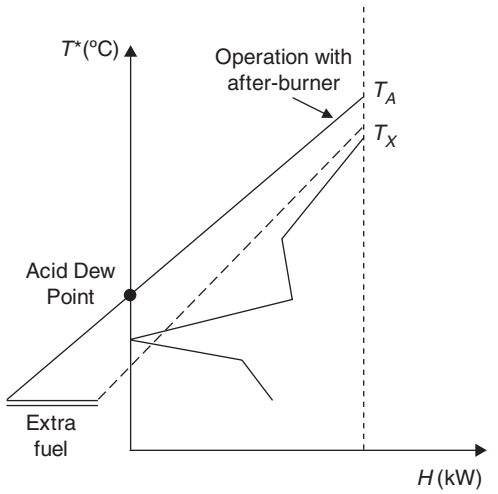

16.5 Operation of a gas turbine with an after-burner.

The temperature profile of the gas exhaust line depends on the size and the operating load of the gas turbine. Two schemes of operation of a gas turbine that result in a modified flue gas temperature profile are:

1. The incorporation of heat recovery through the use of an economiser (Fig. 16.4), and
2. Operation with an after-burner, shown in Fig. 16.5.

© Woodhead Publishing Limited, 2013

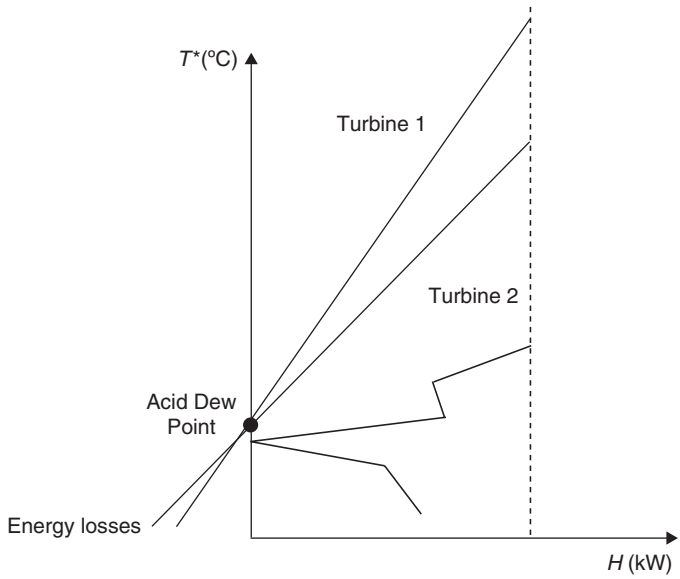

16.6 Comparison of temperature profiles of different gas turbines.

In a practical application, a gas turbine is selected so that either the process power needs or the heating requirements are met. In consequence, one of the two utilities will either fall short or be in excess. This situation reduces the efficiency of the system if no further use of the energy flow that is in surplus is found. A situation like this may lead to part load operation.

The choice of the commercial gas turbine that best matches the background process can be accomplished by comparing the gas exhaust temperature profile on the process Grand Composite Curve as shown in Fig. 16.6. A basic principle is that the turbine that minimises the energy losses to ambient renders the highest thermal efficiency.

The energy content of the hot flue gas can be recovered to supply the thermal demands of the process by direct use or indirectly through the production of steam. Of the two, the production of steam is the most practical way of supplying heat to a process.

The overall First Law efficiency for a trigeneration system composed of a gas turbine and a compression refrigeration system can be expressed as:

$$\eta_{\mathrm{TR}} = \frac{W_e + Q_{h\min} + W_{\mathrm{er}}}{F} \qquad [16.1]$$

where W_e is the process power requirement; $Q_{h\min}$ is the process heating load; W_{er} is the electrical power required by the compressor of the refrigeration

© Woodhead Publishing Limited, 2013

system and F is the fuel consumption of the turbine. The mechanical power required by the compressor is calculated from:

$$W_{\text{er}} = \frac{W_{\text{ad}}}{\eta_{\text{ad}}} = \frac{m\left(H_{v'1} - H_{v_2}\right)}{\eta_{\text{ad}}} \quad [16.2]$$

where W_{ad} is the adiabatic compression work; η_{ad} is the compressor adiabatic efficiency; m is the mass flow rate of refrigerant; $H_{v'1}$ is the adiabatic outlet enthalpy and H_{v2} is the inlet enthalpy. The specific net power (W_n) generated by a gas turbine can be determined from:

$$W_n = C_p * T_1 * \left[\eta_T \left(\frac{T_3}{T_1} \right) \left(1 - \frac{1}{\gamma_T^{\frac{k-1}{k}}} \right) - \frac{1}{\eta_c} \left(\gamma_c^{\frac{k-1}{k}} - 1 \right) \right] \quad [16.3]$$

where C_p is the specific heat capacity of the gas; T_1 is compressor air inlet temperature; T_3 is the turbine gas inlet temperature; η_T is the turbine efficiency; η_c is the turbine compressor efficiency; k is the ratio between the heat capacity of the gas at constant pressure and heat capacity of the gas at constant volume; r_c is the air compression ratio and r_T is the turbine inlet/outlet pressure ratio. The hot gas outlet temperature (T_4) can be obtained from:

$$T_4 = T_3 - \eta_T \left(T_3 - T_{4s} \right) \quad [16.4]$$

where T_{4s} is the adiabatic gas outlet temperature, which can be determined from:

$$T_{4s} = T_3 * \left(\frac{1}{r_T^{\frac{k-1}{k}}} \right) \quad [16.5]$$

For an ideal system, the First Law efficiency of a heat engine can be calculated from:

$$\eta_{\text{HEideal}} = 1 - \frac{T_{\text{SK}}}{T_{\text{SR}}} \quad [16.6]$$

where T_{SK} is the heat-engine sink temperature and T_{SR} is the heat-engine source temperature. The selection of a trigeneration system proceeds after the determination of the heating, cooling and power needs of the process.

© Woodhead Publishing Limited, 2013

Table 16.3 Stream data for a gas recompression station

Stream	CP (kW/°C)	T_S (°C)	T_T (°C)	ΔH (kW)
1H	75	160	15	10,875.0
2H	320	50	30	6,400.0
3H	200	75	10	13,000.0
4C	35	25	140	–4,025.0
5C	398	25	79	–21,492.0
6C	165	80	150	–11,550.0

A number of commercial gas turbines will be available for the particular application, and selection of the appropriate one requires analysis of the performance of the units under ambient conditions away from the standard ones, also referred to as ISO conditions. So, a thermodynamic model is used to reproduce the performance parameters of any selected turbine given its ISO rating, such as power production at 100% load, exhaust gas temperature and flow rate. Such analysis also gives operating parameters such as compressor efficiency and generator efficiency.

As discussed earlier, a CHP system seldom satisfies exactly both the heat and power needs of a process. In cases where the surplus production of any of these is not suitable for sale, then operation of the turbine at a partial load will give the exact amount of heat or power. It is convenient to assess the viability of this scenario, seeking to determine the operating load at which the ambient losses are minimised and thus maximising fuel consumption.

To illustrate the concepts outlined above, a natural-gas recompression station is analysed (Teopa *et al.*, 2005). The process information is given in Table 16.3. Considering a $\Delta T_{\min}$ of 10°C, the heating and cooling duties of the process are $Q_{h,\min}$ = 17,283 kW and $Q_{c,\min}$ = 10,543 kW, with a power requirement of 9800 kW. Refrigeration is required, since the target temperature of stream 3H is below ambient. An ammonia refrigeration cycle is chosen to provide brine at 5°C as an intermediate cooling medium. The power requirement for the operation of the refrigeration system is 2,355 kW. So, the total power consumption of the process is 12,155 kW.

Table 16.4 shows the ISO performance of three commercial gas turbines (Gas Turbine World, 2001). The performances of these turbines for the site conditions (air temperature of 23°C and an above-sea-level altitude of 1,721 m), and assuming a minimum temperature on the gas stream for heat recovery of 150°C, are presented in Table 16.5. The gas turbines are analysed for the operation at a part load that exactly meets the 12,155 kW of compression power required by the process.

From the results shown in Table 16.5, it is seen that the three turbines can provide the required power at part load. Additionally, apart from turbine 3, turbines 1 and 2 are also able to supply the process heating requirements.

© Woodhead Publishing Limited, 2013

Table 16.4 Technical specifications of some commercial gas turbines

Turbine	ISO rating (kW)	Compression ratio	Air flow rate (kg/s)	$T_{exhaust}$ (°C)	Heat rate (kJ/kWh)
1	17,000	12.0	92.39	375	10,046.7
2	14,700	14.7	52.21	545	10,044.8
3	13,958	21.5	46.76	487	89,804

Table 16.5 Performance of various commercial gas turbines for full load and part load operation

Turbine	Load (%)	W_{eT} (kW)	T_{hot} gases (°C)	Fuel (kg/s)	Q (kW)	Q_{loss} (kW)	$W_{surplus}$ (kW)	η_T (%)	Gas exhaust (kg/s)	$T_{exhaust}$ (°C)
1	100	15,977	893	1.143	23,278	12,622	3,822	55.9	93.5	376.2
1	76	12,155	804.6	0.947	18,176	12,722	0	67.4	93.3	327.0
2	100	14,017	1,218	0.970	23,144	6,871	1,862	65.8	53.2	545.6
2	87	12,155	1,143.1	0.877	20,702	6,952	0	72.9	53.1	504.5
3	100	13,278	1,230	0.821	17,701	6,227	1,123	77.8	47.6	488.2
3	92	12,155	1,183.9	0.77	16,462	6,266	0	83.0	47.5	464.8

From the on-going analysis it can be concluded that, for given heat and power duties, one of the turbine energy outputs is limiting whereas the other is in excess. In the cases of turbines 1 and 2, power is the limiting energy output, whereas the heat flow is for turbine 3. In terms of the overall fuel efficiency, the higher trigeneration efficiencies are obtained when turbines operate at part load. Turbine 3 has lower heat losses to the ambient and higher overall fuel efficiency at full load, which makes this turbine the ideal candidate for the application. Figure 16.7 shows the comparison of performance on the Grand Composite Curve.

16.3.2 Steam Turbine-Absorption Systems

This section presents a thermodynamic analysis for the design of trigeneration systems where a back-pressure steam turbine produces the required power and cooling is produced through the operation of a LiBr–H_2O refrigeration system. As in the previous section, three commercial steam turbines are analysed.

When the scenario is such that any power surplus produced by a CHP plant can readily be sold to the utility company, then the turbine that meets the thermal requirements of the process and produces the larger amount of power becomes the most attractive option. However, if selling is not a viable option, then the turbine selection is based on total minimum costs.

© Woodhead Publishing Limited, 2013

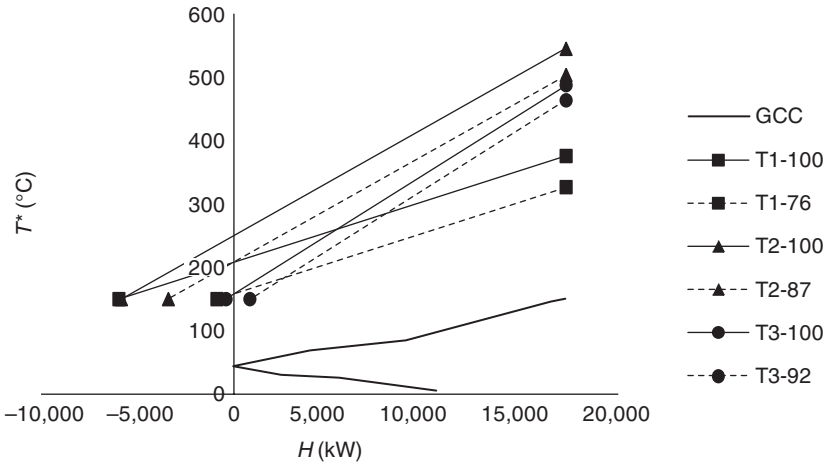

16.7 Comparison of performance of three gas turbines at full load and part load.

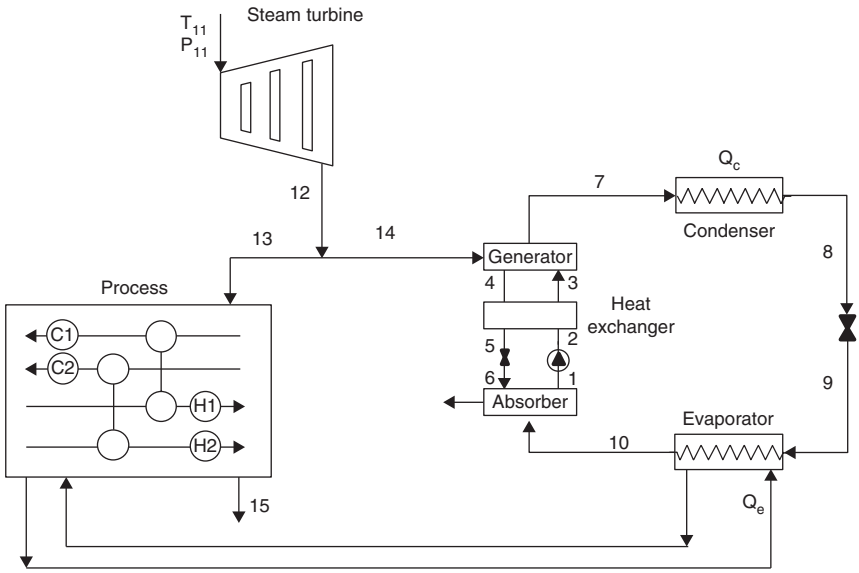

16.8 Trigeneration system: back-pressure steam turbine and an absorption refrigeration system.

Again, a key issue in the appropriate selection of a trigeneration system starts with selection of the right steam turbine. Figure 16.8 shows a schematic of a trigeneration system operated with a back-pressure steam turbine and an absorption refrigeration system.

© Woodhead Publishing Limited, 2013

The net power production of a steam turbine can be calculated from:

$$W_T = M_{12}(H_{11} - H_{12}) \quad [16.7]$$

where M_{12} is the mass flow rate of the steam that flows through the turbine; H_{11} and H_{12} are the specific enthalpies at the turbine inlet and outlet conditions. The enthalpy change ($H_{11} - H_{12}$) can be computed using the expression of the isentropic efficiency (η_{iso}) given by:

$$\eta_{iso} = \frac{H_{11} - H_{12}}{H_{11} - H_{12\,iso}} \quad [16.8]$$

where $H_{12\,iso}$ is the isentropic specific enthalpy of the steam evaluated at the turbine outlet conditions. The relationship between the sectional area of the admission valve, the pressure drop and the mass flow rate flowing through a turbine is given by (Cotton, 1993):

$$\frac{M_{12}}{A} = \sqrt{2\frac{k}{k-1}}\sqrt{\frac{P_{11}}{v_1}}\sqrt{\left(\frac{P_{12}}{P_{11}}\right)^{\frac{2}{k}} - \left(\frac{P_{12}}{P_{11}}\right)^{\frac{k+1}{K}}} \quad [16.9]$$

where A is the sectional area of the turbine nozzle; M_{12} is the steam flow rate; k is the isentropic constant of the gas; P_{11} and P_{12} are the pressure at the inlet and outlet conditions.

The large amount of mechanical power that is needed to compress a gas from a low to a high pressure in a mechanical compression system is drastically reduced in the case of an absorption refrigeration system. This is achieved by replacing the compressor with a pump, and the gas with a solution (Herold *et al.*, 1996). In this manner, the energy required to increase the pressure within the system is substantially reduced, since the compression of a liquid is accomplished with low expenditure of power. In the absorption system, the vapour coming from the evaporator is dissolved in a liquid; this liquid is then compressed and later heated to release the vapour at a high pressure, which is then sent to the condenser. The absorption of vapour takes place in a tank called absorber, and the heating and desorption of the vapour in another tank called generator. Systems such as NH_3–H_2O and LiBr–H_2O are industrially used in cooling absorption systems (Colonna and Gabrielli, 2003). In some designs, a heat exchanger is used to recover heat between the streams flowing from the generator to the absorber (see Fig. 16.8). The type of compression system determines the type of energy source that is used for the production of cooling; for instance, a mechanical

© Woodhead Publishing Limited, 2013

compression system is run using electrical power whereas an absorption system uses electrical power for the operation of a pump and thermal energy to release the vapour at high pressure. Absorption cycles are convenient in cases where there is a surplus of low grade thermal energy in the process.

The refrigeration load given by the evaporator duty is represented by Q_e. Apart from the electrical energy required to compress the liquid solution, the main energy input to the system is the heat load of the generator (Q_g). In the system, the mass flow rate of the refrigerant can be obtained from:

$$m = \frac{Q_e}{h_5 - h_4} \quad [16.10]$$

where m is the mass flow rate of the refrigerant and h is the specific enthalpy of the refrigerant at the corresponding position within the cycle (see Fig. 16.8). From a mass balance around the absorber we get:

$$\begin{aligned} mx_1 &= m_3 x_3 \\ m_1 &= m + m_3 \end{aligned} \quad [16.11]$$

Combining these equations we find that:

$$m_3 = \frac{x_1}{x_3 - x_1} m \quad [16.12]$$

$$m_1 = \frac{x_3}{x_3 - x_1} m \quad [16.13]$$

From an energy balance around the generator, the absorber and the condenser we get:

$$Q_g = h_3 m_3 + h_2 m - h_1 m_1 \quad [16.14]$$

$$Q_a = h_5 m + h_3 m_3 - h_1 m_1 \quad [16.15]$$

$$Q_c = m(h_2 - h_4) \quad [16.16]$$

In the equations above, x is the concentration of the refrigerant. For a specified refrigeration load (Q_e), the energy required to run the system is given by Q_g.

© Woodhead Publishing Limited, 2013

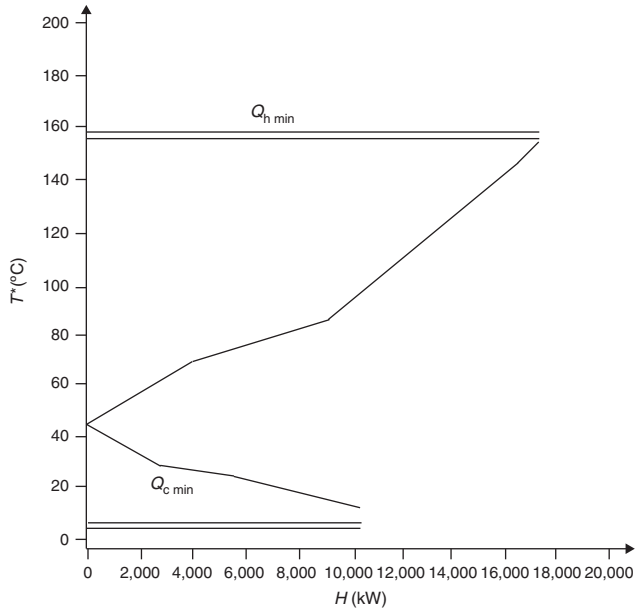

16.9 Grand Composite Curve for a ΔT_{min} of 10°C.

To illustrate the Heat Integration of trigeneration systems composed of a steam turbine and an absorption system, the case study presented in Table 16.4 is used. The electrical, heating and cooling requirements of the process are: 9,500 kW, $Q_{h,min}$ = 17,283 kW and $Q_{c,min}$ = 10,543 kW. The Grand Composite Curve of the process for a ΔT_{min} of 10°C is shown in Fig. 16.9.

The design of the trigeneration system starts from the calculation of the heat load required by the absorption system. The results of a detailed study of the operation of a LiBr–H_2O absorption system are shown in Table 16.6. The operation of the cycle includes an electrically driven pump that consumes 0.14 kW of power; the heat required by the generator to supply 10,530 kW of cooling is 13,652 kW. Therefore, the total process power requirement is 9500.14 and the total heating needs are 30,935 kW. Once this is known, the next step consists in the appropriate selection of the commercial steam turbine. Table 16.7 shows the operating data at ISO conditions of three commercial steam turbines.

The steam turbines are analysed at full load (Table 16.8) and at part load (Table 16.9). Considering the highest cold stream target temperature and a minimum temperature approach of 10°C, it can be seen that the minimum temperature of steam for heating purposes in the process is 170°C if a single extraction turbine is to be used. Multiple extraction turbines can also be considered (Medina and Picón, 2010), which leads to the possibility of

© Woodhead Publishing Limited, 2013

Table 16.6 Performance data of the absorption system

Stage	P (kPa)	T (°C)	H (kJ/kg)	m (kg/s)	X (%LiBr)
1	1.0	32.9	73.6	22.6	53.3
2	9.0	32.9	73.6	22.6	53.3
3	9.0	86.8	187.7	22.6	53.3
4	9.0	104.8	270.1	18.1	66.7
5	9.0	50.9	175.7	18.1	66.7
6	1.0	59.4	175.7	18.1	66.7
7	9.0	200.0	2,879.0	4.52	0.0
8	9.0	43.7	183.2	4.52	0.0
9	1.0	6.9	183.2	4.52	0.0
10	1.0	6.9	2,513.0	4.52	0.0
COP = 0.7713		P_{low} = 1 kPa		$Q_{generator}$ = 13,652 kW	
ε = 0.75		$Q_{absorber}$ =12,870 kW		$Q_{evaporator}$ = 10,530 kW	
P_{high}= 9 kPa		$Q_{condenser}$ =12,182 kW		W_{pump} = 0.14 kW	

Table 16.7 Operating data for three commercial steam turbines

	Turbine 1[a]	Turbine 2[b]	Turbine 3[c]
Inlet temperature (°C)	520	538	540
Inlet pressure (kPa)	8,500	11,300	15,000
Back pressure (kPa)	1,600	1,270	6,000
Steam mass flow rate (kg/s)	30	54.7	167.9
Power output (kW)	11,000	25,000	40,000

[a] www.tgmturbinas.com.br
[b] www.toshiba.co.jp
[c] www.gepower.com

Table 16.8 Turbine performance parameters for 100% load

	Turbine 1	Turbine 2	Turbine 3
Q (kW)	66,507.34	119,779.15	330,758.0
A (m^2)	1.35	236	3.08
T_{12} (°C)	318.53	280.29	402.50
$T_{12\ sat}$ (°C)	201.39	190.55	275.60
P_{12} (kPa)	1,600	1,270	6,000
M_{11} (kg/s)	30.0	54.74	167.9
η (%)	76.36	76.11	85.01
W_T (kW)	11,000	25,000	40,000

using lower steam extraction pressures. Going back to the turbine selection process, the three chosen turbines are able to satisfy the heating needs of the process operating at part load; however, only turbine 3 provides the full power duty, and is therefore the best candidate for this application.

© Woodhead Publishing Limited, 2013

Table 16.9 Steam turbine performance at part load

Parameter	Turbine 1	Turbine 2	Turbine 3
$P_{extraction}$ (kPa)	500	300	650
$T_{extraction}$ (°C)	220	170	170
% admission valve aperture	85.5	55.5	22.8
Steam flow rate (kg/s)	13.72	13.82	14.79
Steam flow rate to process (kg/s)	7.67	7.73	8.27
Steam to absorption system (kg/s)	6.05	6.09	6.52
Heating load (kW)	30,974	30,974	30,974
Thermal efficiency	75.4	75.0	83.6
W_T (kW)	7,478	9,034	9,501
% load	68	36	24

16.4 Conclusions

The use of trigeneration systems represents an attractive option for improved overall plant energy efficiency. Two important elements for the design and selection of trigeneration systems are the use of Process Integration techniques and a thermodynamic model for assessing the performance of its various components. Out of the possible options for the conformation of trigeneration systems, in this chapter we have looked at the use of gas turbines and steam turbines for the production of power on the one hand, and on the other, vapour compression and absorption systems for the production of below ambient cooling.

In the exposition of the subject, the importance of reconciling real turbine performance with process needs for their appropriate selection has been shown; this implies the assessment of the performance of turbines at site conditions and part load operation. A situation that influences the implementation of trigeneration systems is that related to the possibility of exporting surplus power to the grid. Here, different scenarios may exist; for instance, the case where exporting surplus power is desirable and economically attractive, and the opposite situation where selling surplus power is not an economic option as a consequence of rigid country energy policies.

Another important consideration for the appropriate selection of trigeneration systems is the heat/power ratio of the process, which, in principle, must be coupled to the optimum heat/power ratio of the thermal engine. Overall, internal combustion engines exhibit higher efficiency at a ratio of 1; gas turbines at around 3 and steam turbines in the neighbourhood of 9. These values indicate that refrigeration using compression cycles is more suitable for use with internal combustion engines and gas turbines, whereas for the case of absorption refrigeration systems, where cooling is produced from the consumption of heat, steam turbines are a more suitable option. However, the process needs will dictate the choice of the appropriate system.

© Woodhead Publishing Limited, 2013

16.5 Sources of Further Information

This chapter focuses mainly on the application and the Heat Integration of trigeneration systems in industrial sites. In this section, further reading to consider other aspects of the application of Process Integration tools, analysis and modelling of trigeneration systems is presented. For instance, alternative tools for the Heat Integration of trigeneration systems in process plants based on the use of the Grand Composite Curve and Exergy Grand Composite Curve are presented by Marinova *et al*. (2007). The stand-alone efficiency of trigeneration systems is analysed by Havelsky (1999). Emho (2003) shows the application of trigeneration systems with improved efficiencies in district heating. The economic aspects of the use of this technology are explored by Sevilgen and Sancar (2011), whereas techniques for cost optimisation are described by Lozano *et al*. (2010). Performance comparison studies of various trigeneration configurations are presented by Fahad *et al*. (2011). Other type of trigeneration systems that produce power, heat and other products such as water are described by Horitsugi *et al*. (2011). Detailed thermodynamic models for the performance analysis of cooling systems based on the use of LiBr–H_2O absorption systems are presented by Mehrabian and Shahbeik (2005).

16.6 References

Al-Sulaiman, F. A., Hamdullahpur, F., Dincer, I. (2011). Performance comparison of three trigeneration systems using organic Rankine cycles. *Energy*, **36**(9), 5741–5754.

Bassols, J., Kuckelkorn, B., Langreck, J., Schneider, R., Veelken, H. (2002). Trigeneration in the food industry. *Applied Thermal Engineering*, **22**, 595–603.

Colonna, P., Gabrielli, S. (2003). Industrial trigeneration using ammonia – water absorption refrigeration systems (AAR). *Applied Thermal Engineering*, **23**, 381–396.

Cotton, K. C. (1993). *Evaluating and Improving Steam Turbine Performance*. Cotton Fact Inc., Burnt Hills, NY, USA.

Dharmadhikari, S. (1997). Consider trigeneration techniques for process plants. *Hydrocarbon Processing*, **76**(7), 91–100.

Dijkema, G. P. J., Luteijn, C. P. (1998). Design of trigeneration systems-process integrated applications of energy conversion devices in chemical plants. *Chemical Engineering Communications*, **168**, 111–125.

Eastop, T. D., Croft, D. R. (1995). *Energy Efficiency*. Longman Group, Ltd, Essex, UK.

Emho, L. (2003). District energy efficiency improvement with trigeneration: basic considerations and case studies. *Energy Engineering: Journal of the Association of Energy Engineering*, **100**(2), 66–80.

Esdaile-Bouquet, T. (2007). Optimum integration of polygeneration in the food industry-quantifying the technical potential in the food transformation

© Woodhead Publishing Limited, 2013

industry. 1st European Conference on Polygeneration, Tarragona (Spain), 16–17 October, 313–331.
Farmer, R. (ed.) (1992). *Gas Turbine World 2001–2002 Handbook.* Vol. 22, Pequot Publishing Inc., Fairfield, CT, USA.
Haberle, A., Warmuth, W. (2008). POLYSMART, Polygeneration in Europe – A technical report: Contract/Proposal No. 019988, 31 July 2008.
Havelsky, V. (1999). Energetic efficiency of cogeneration systems for combined heat, cold and power production. *International Journal of Refrigeration*, **22**, 479–485.
Hernández-Santoyo, J., Sánchez-Cifuentes, A. (2003). Trigeneration: an alternative for energy savings. *Applied Energy*, **76**, 219–227.
Herold, K. E., Radermacher, R., Klein, S. A. (1996). *Absorption Chillers and Heat Pumps*, First edition. CRC Press, Boca Raton, FL, USA.
Horitsugi, M., Kuba, S., Hatamiya, S. (2011), Trigeneration gas turbine system (electricity, heat, and water purification). *Power Systems*, **60**(7), 377–381.
Kavvadias, K. C., Tosios, A. P., Maroulis, Z. B. (2010). Design of a combined heating, cooling and power system: sizing, operation strategy selection and parametric analysis. *Energy Conversion and Management*, **51**, 833–845.
Lozano, M. A., Carvalho, M., Ramos, J. C., Serra, L. M. (2009). Thermoeconomic analysis of simple trigeneration systems. *International Journal of Thermodynamics*, **12**(3), 147–153.
Lozano, M. A., Ramos, J. C., Serra, L. M. (2010). Cost optimization of the design of CHCP (combined heat, cooling and power) systems under legal constraints. *Energy*, **35**, 794–805.
Maidment, G. G., Tozer, R. M. (2002). Combined cooling heat and power in supermarket. *Applied Thermal Engineering*, **22**, 653–665.
Marinova, M., Espejel, E. M., Bakhtiari, B., Paris, J. (2007). A new methodology for the implementation of trigeneration in industry: application to the kraft process. 1st European Conference on Polygeneration, Tarragona (Spain), 16–17 October 2007, 333–351.
Medina-Flores, J. M., Picón-Núñez, M. (2010). Modelling the power production of single and multiple extraction steam turbines. *Chemical Engineering Science*, 65, 2811–2820.
Mehrabian, M. A., Shahbeik, A. E. (2005). Thermodynamic modelling of a single – effect LiBr – H_2O absorption refrigeration cycle. *Journal Process Mechanical Engineering, Part E*, **219**, 261–273.
Polley, G. T., Sarabchi, K. (2000). Maximize fuel efficiency of cogeneration systems. *Chemical Engineering Progress*, **96**(5), 69–74.
Sevilgen, S. H., Sancar, O. (2011). Economical analysis of trigeneration systems. *International Journal of the Physical Sciences*, **6**(5), 1068–1073.
Teopa-Calva, E., Picón-Núñez, M., Rodríguez-Toral, M. A. (2005). Thermal integration of trigeneration systems. *Applied Thermal Engineering*, **25**, 973–984.
Tora, E. A., El-Halwagi, M. M. (2011). Integrated conceptual design of solar-assisted trigeneration systems. *Computers and Chemical Engineering*, **35**, 1807–1814.

16.7 Appendix: Nomenclature

A	sectional area of turbine nozzle, m^2
C_p	specific heat capacity at constant pressure, J/(kg °C)

© Woodhead Publishing Limited, 2013

C_v	specific heat capacity at constant volume, J/(kg °C)
CHP	Combined Heat and Power
CP	heat capacity mass flow rate, kW/°C
F	fuel consumption [Trigeneration], kW
h	refrigerant specific enthalpy, kJ/kg
H	specific enthalpy, kJ/kg
Hv_1	adiabatic compressor outlet stream enthalpy, kJ/kg
Hv_2	compressor inlet stream enthalpy, kJ/kg
H_{11}	steam specific enthalpy at inlet conditions, kJ/kg
H_{12}	steam specific enthalpy at outlet conditions, kJ/kg
$H_{12\,\mathrm{iso}}$	isentropic specific enthalpy of steam at turbine outlet conditions, kJ/kg
k	ratio of C_p/C_v
M	steam mass flow rate [steam turbine], kg/s
m	refrigerant mass flow rate, [refrigeration system], kg/s
P	pressure, kPa
P_{11}	pressure of steam at inlet conditions, kPa
P_{12}	pressure of steam at outlet conditions, kPa
Q	heat load available from turbine exhaust gases, kW
Q_a	absorber heat load [absorption system], kW
Q_c	condenser heat load, kW
$Q_{c,\mathrm{min}}$	minimum process external cooling, kW
Q_e	evaporator heat load, kW
Q_g	generator heat load [Absorption system], kW
$Q_{h,\mathrm{min}}$	minimum process external heating, kW
Q_{SK}	heat delivered to the sink in a heat engine, kW
Q_{SR}	heat available from the source of a heat engine, kW
Q_{loss}	heat lost to ambient, kW
r_C	air compression ratio
r_T	turbine inlet/outlet pressure ratio
S	entropy, kW/K
T	temperature, °C or K
T_{4s}	adiabatic turbine gas outlet temperature, °C or K
T_S	stream supply temperature, °C or K
T_{SK}	temperature of sink [thermal engine], K
T_{SR}	temperature of source [thermal engine], K
T_T	stream target temperature, °C or K
V	specific volume, m^3/kg
W_{pump}	pump power consumption, kW
W_{ad}	adiabatic compression work, kW
W_c	compressor power consumption, kW
W_e	process power requirement, kW
W_{er}	compression system power consumption, kW
W_{eT}	turbine power production, kW

© Woodhead Publishing Limited, 2013

W_n	specific net power, kW
W_p	pump power consumption, kW
W_{surplus}	power surplus, kW
W_T	power output, kW
X	concentration of refrigerant, %
ΔH	enthalpy change, kW
ΔT_{min}	minimum temperature approach, °C

Greek Symbols

ε	exchanger thermal effectiveness
η_{ad}	compressor adiabatic efficiency
η_c	turbine air compressor efficiency
η_{Carnot}	Carnot efficiency
η_{HE}	thermal efficiency of a thermal engine
$\eta_{\text{HE ideal}}$	thermal efficiency of an ideal engine
η_{TR}	thermal efficiency of a trigeneration system
η_T	turbine efficiency

© Woodhead Publishing Limited, 2013

17

Pinch Analysis for Sustainable Energy Planning Using Diverse Quality Measures

RAYMOND R. TAN, De La Salle University, Manila, Philippines and
DOMINIC C. Y. FOO, University of Nottingham, Selangor, Malaysia

DOI: 10.1533/9780857097255.4.505

Abstract: This chapter presents the generalised Pinch principles for energy planning involving the optimal matching of sources and sinks (or demands) using diverse measures of energy quality such as Carbon Footprint, Agricultural-Land Footprint, Water Footprint, emergy and inoperability. These indices provide numerical measures of the quality of energy streams allocated between sources and sinks under different contexts. Nevertheless, there are common principles that apply to all such systems, which allow the use of a two-phase insight-based Pinch Analysis approach comprising targeting (benchmarking with first principle), followed by the determination of the optimal energy allocation network. Five different examples are solved here to illustrate the application of such Energy Planning Composite Curves (EPCC).

Key words: sustainable energy planning, Pinch Analysis, source–sink matching, energy quality, Energy Planning Composite Curves.

17.1 Introduction

Recent trends have led to new opportunities for the use of Pinch Analysis in non-traditional applications. A recent paper in *Nature* identified climate change, land use and water resource depletion among the most critical global environmental issues (Rockstrom *et al.*, 2009). This paper implies complex linkages and feedback loops that are closely connected with sustainable energy planning. For example, it is well-understood that CO_2 emissions from energy use are a major cause of anthropogenic climate change; thus, increased use of low-carbon energy is an essential measure to mitigate climate change. On the other hand, the potential availability of some low-carbon technologies, particularly bioenergy, is heavily constrained by limited water and land resources. The problem is further compounded by the potential change in long-term regional water resource profiles brought about by climate change. It should be noted that other forms of renewable energy (e.g., hydroelectricity) are also vulnerable to such long-term trends (Atkins *et al.*, 2010).

© Woodhead Publishing Limited, 2013

An early extension of Pinch Analysis to incorporate emissions aspects in Total Sites was developed by Dhole and Linnhoff (1993). Subsequently, the use of Pinch Analysis for energy-planning problems using Carbon Footprint as the main quality index was proposed by Tan and Foo (2007). This technique was adapted by other researchers, notably for electricity-production planning with CO_2 emission constraints in Ireland (Crilly and Zhelev, 2008a) and New Zealand (Atkins *et al*., 2010). The use of this approach within a larger energy-planning framework was further explored by Crilly and Zhelev (2010) in their subsequent work. Recently, a number of new variants and applications have also been reported by researchers in developing countries, such as China (Shi *et al*., 2009) and India (Shenoy, 2010) using alternative graphical or algebraic approaches. Applications in China for eco-industrial parks indicating potential Carbon Footprint reductions of 10% (Jia, 2009) and 30% (Jia *et al*., 2010) have also been demonstrated. More recently, urban planning uses have also been proposed (Liang and Zhang, 2011).

Furthermore, in addition to the original graphical approach, an algebraic variant based on cascade analysis has been reported (Foo *et al*., 2008). This latter work also proposed an analogous energy-planning problem, involving the allocation of crops for the regional production of biofuels under land-availability constraints. Later work led to graphical approaches to account for biomass surplus or deficit in multiple regions (Lam *et al*., 2010, 2011).

In addition to agricultural-land constraints, the concept of virtual water embedded in agricultural crops (Allan, 1998) led to the emergence of the Water Footprint index. The latter was used as a quality measure in biomass allocation by Tan *et al*. (2009).

On the other hand, the concept of emergy was proposed as a unified index of the cumulative amount of natural resource, typically measured in terms of solar energy equivalents (Odum, 1996). This basis is justified since majority of natural ecosystem cycles are driven by solar energy; Odum (1996) thus proposed the unit of *solar emjoule* (sej) to indicate one joule of solar energy required in total to generate a given output through various natural pathways such as photosynthesis or precipitation.

The use of emergy in the context of Pinch Analysis has been explored in more recent work. Applications of emergy as a quality index have been reported for process design applications (Zhelev and Ridolfi, 2006) as well as more general energy planning at the sectoral level (Crilly and Zhelev, 2008b). Bandyopadhyay *et al*. (2010) then demonstrated the similarity of emergy-based planning to general resource conservation problems. Finally, historical disasters (for example, the loss of nuclear power plants at Chernobyl in 1986 and Fukushima in 2011) and grid-wide power failures (Anderson

© Woodhead Publishing Limited, 2013

et al., 2007) have demonstrated the vulnerability of energy infrastructure to natural calamities or human error.

Future low-carbon energy systems should be designed for robustness to ensure sustainability in the face of seismic events, malicious attacks, or the gradual onset of climate change. The relevant quality index in this case is *inoperability*, a dimensionless index proposed by Haimes and Jiang (2001) as an indicator of the degree of failure of public infrastructure. Notable applications of this concept have been reported for the case of power failures (Anderson *et al*., 2007) and loss of oil supply (Khanna and Bakshi, 2009). Recently, Tan (2011) proposed the use of inoperability for planning energy allocation using a mixed integer linear programming (MILP) source–sink model.

The consideration of multiple footprints for sustainability assessment has been discussed in recent work by De Benedetto and Klemeš (2009) and more recently in a comprehensive review by Čuček *et al*. (2012).

Geldermann *et al*. (2006a, 2006b) proposed an approach known as Multi-Objective Pinch Analysis (MOPA), which consists of determining different optimal production networks derived from Pinch Analysis using diverse quality measures; this step is followed by the application of an appropriate multiple attribute decision-making (MADM) tool, such as PROMETHEE (Brans *et al*., 1986), to find a compromise among the different solutions. Some recent work has been published that underscores the presence of general principles underlying seemingly diverse resource allocation problems. For example, Bandyopadhyay *et al*. (2010) developed a segregated targeting approach for multi-zone problems in water and energy allocation with various quality constraints, while Shenoy (2011) proposed a unified algorithm for targeting on diverse problems exhibiting a common source–sink structure. A comprehensive treatment of many graphical and algebraic Pinch techniques can also be found in a recent book by Foo (2012).

It is evident from the broad scope of Process Integration literature that Pinch principles are readily extendable to various problem domains, provided that these applications exhibit a common underlying structure. An overview of the quality indices used in this chapter is given in Table 17.1.

This chapter presents a unified approach for a special class of such problems that involves allocation of energy sources to corresponding energy sinks or demands. These allocation problems are a fundamental component of sustainable energy planning, where quality issues arise because energy streams are not fully interchangeable. Hence, because of the essential role that quality measures play in these planning problems, time-tested Pinch principles can be applied to aid in optimal planning and decision support. A generalised formal problem statement for such problems is first defined in

© Woodhead Publishing Limited, 2013

Table 17.1 Quality indices for energy streams in case studies

Quality index	Brief definition and sustainability implications
Carbon Footprint	CO_2 emissions intensity per unit of energy is essential to address climate change mitigation through effective energy allocation (De Benedetto and Klemeš, 2009)
Agricultural-Land Footprint	Agricultural land use intensity is essential for planning of large-scale bioenergy production, in order to minimise conflicts with traditional uses of land (e.g., for food production) (Čuček *et al.*, 2012)
Water Footprint	Local water resource use intensity is also essential for planning the production of biofuels, which may divert resources from other important uses; in addition, water stress (i.e., local water scarcity) may be induced in some geographic regions as a result of climate change (Allan, 1998)
Emergy transformity	Emergy transformity provides a quantitative index of the efficiency at which solar energy is converted into various downstream forms of energy; thus, the emergy content of any natural resource provides an index of its scarcity or its value by quantifying the cumulative amount of solar energy needed to form the natural resource (Odum, 1996)
Inoperability	Inoperability provides a quantitative index of loss of physical output as a result of natural calamities such as drought, earthquakes and storms (Haimes and Jiang, 2001)

the next section. Then, a motivating example on carbon-constrained energy planning is given; this example serves to illustrate the step-by-step application of the methodology that follows. Next, a Graphical Pinch Analysis approach for targeting is described in the context of the motivating example. The unified approach is then applied to four other different energy-planning case studies, each using a unique index of energy quality. Finally, conclusions and prospects for future work are given at the end of the chapter.

17.2 Generalised Problem Statement

The problem statement for the general quality-constrained energy-planning problem is as follows:

- Energy streams within the given system are quantified in energy or power units.
- Energy streams within the system are also characterised by a quality index. This index conforms to a linear mixing rule and follows an inverse scale (i.e., zero corresponds to the highest quality, while larger positive numerical values indicate lower quality levels).

© Woodhead Publishing Limited, 2013

- The given system contains m internal sources. Each source i ($i = 1, 2, \ldots, m$) is able to supply an energy stream of quantity S_i at quality level Q_i.
- The given system also contains n sinks or demands. Each sink j ($j = 1, 2, \ldots, n$) requires energy to be supplied at a quantity D_j and within a limiting quality level $Q_j^{\max}$.
- Energy may also be supplied to the system from an external resource whose supply is unlimited. This resource is available at a quality level Q^{ext}. The external resource is considered to be of superior quality compared to the internal sources (i.e., $Q^{\text{ext}} < Q_i$). It is also assumed that it is desirable to make use of this external resource sparingly.
- The main problem is to target the minimum quantity of external energy resource needed to satisfy both energy quantity and quality requirements of the system sinks; note that this condition is also equivalent to maximizing the use of the available internal energy sources. The secondary problem is to determine the appropriate allocation of energy streams by matching energy sources and sinks such that the determined target is satisfied.

17.2.1 Motivating Example

Consider a problem in which Carbon Footprint is used as the quality index to plan the allocation of three primary energy sources (coal, oil and natural gas) across three geographic regions. The data for energy sources and sinks, based on Tan and Foo (2007), are shown in Table 17.2. It is also assumed that there is a fourth energy resource with a negligible Carbon Footprint relative to these three fossil fuels. This energy resource is taken as the external resource, with the approximation that $Q^{\text{ext}} = 0$. It is assumed that the use of this resource is to be minimised during energy planning; for instance, this zero-carbon resource may represent nuclear energy, which, while generating a relatively small Carbon Footprint, may nevertheless need to be used sparingly due to social acceptability problems. The primary problem, corresponding to the targeting step in conventional Pinch applications, is to determine the minimum amount of this zero-carbon resource that is required in order to meet the Carbon Footprint limits specified within the

Table 17.2 Source and sink data for motivating example

Source	S_i (TJ)	Q_i ($t\,CO_2$/TJ)	Sink	D_j (TJ)	$Q_j^{\max}$ ($t\,CO_2$/TJ)
Natural Gas	200,000	55	Region I	1,000,000	20
Oil	800,000	75	Region II	400, 000	50
Coal	600,000	105	Region III	600,000	100

© Woodhead Publishing Limited, 2013

system. Subsequently it will also be necessary to determine the allocation that satisfies the target determined.

17.3 Graphical Targeting Procedure

The graphical approach based on the Material Recovery Pinch Diagram (MRPD) which was developed independently by researchers in the US (El-Halwagi *et al.*, 2003) and in India (Prakash and Shenoy, 2005) and which became the basis for the subsequent Carbon Emissions Pinch Diagram (Tan and Foo, 2007), is used here for targeting.

However, various alternative graphical or algebraic techniques may also be used to achieve the same results; most of these variants are described in detail in a review paper by Foo (2009). Note that each approach presents its own unique advantages and disadvantages. Generally, graphical techniques provide intuitive insights to aid the decision-maker in proper energy planning, while algebraic techniques lend themselves to automation (e.g., using spreadsheets) to achieve more precise calculations in less time.

Here, we refer to the graphical approach as the EPCCs. The steps involved in the targeting procedure are as follows:

- The sources are first arranged in order of ascending values of Q_i (i.e., in order of decreasing quality). In the case of the motivating example, this step has already been accomplished as shown in Table 17.2.
- For each source, its Quality Load is calculated by multiplying the quantity (S_i) by the corresponding quality (Q_i). The result is shown in Table 17.3.
- The Source Composite Curve is plotted with cumulative energy quantity as the horizontal axis, and cumulative quality load as the vertical axis. Starting at the origin, each source is plotted in sequence to form a segment of the Composite Curve; the effect is similar to the graphical addition of two-dimensional vectors. Note that the mapping used results in the slope of each segment being equivalent to the stream quality (Q_i). Since the sources have previously been arranged in order of ascending values of Q_i, the resulting Composite Curve curls upwards (i.e., each

Table 17.3 Quality loads of sources in motivating example

Source	S_i (TJ)	Q_i ($t\ CO_2$/TJ)	S_iQ_i (t/CO_2)
Natural Gas	200,000	55	11,000,000
Oil	800,000	75	60,000,000
Coal	600,000	105	63,000,000

Source: Tan and Foo (2007).

© Woodhead Publishing Limited, 2013

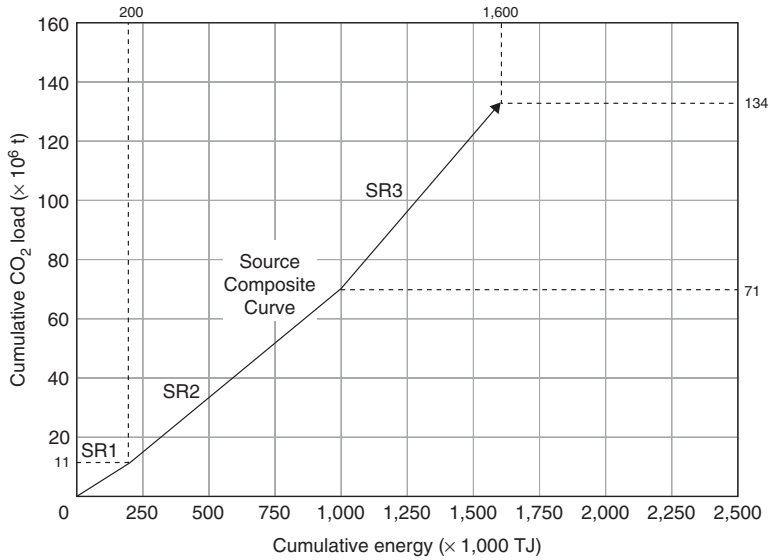

17.1 Source Composite Curve for motivating example (Tan and Foo, 2007).

segment is steeper than the previous one). The resulting Composite Curve is shown in Fig. 17.1.

- Next, the Sink Composite Curve is plotted following exactly the same procedure as was used for the Source Composite Curve. The detailed steps need not be shown here and are left for the reader as an exercise.
- The relative positions of the two Composite Curves indicate the state of the current solution. A feasible solution is indicated when the Source Composite Curve is always below and to the right of the Sink Composite Curve. This geometric condition indicates that all quality limits of the sinks are satisfied. If this condition is met immediately, then the target requirement of external energy resource is zero. In the case of our example, this condition is not met, as can be seen in Fig. 17.2.
- Thus, the Source Composite Curve must be shifted along a locus with slope Q^{ext}, until it lies just below and tangent to the Sink Composite Curve. The Shifted Composite Curves are shown in Fig. 17.3.

The horizontal distance of the Source Composite Curve from its original position is equivalent to the external energy resource target, which in this example is found to be 813,333 TJ. Note that this is the same as the result in Tan and Foo (2007). The point where the two Composite Curves are tangential to each other is the Pinch Point (note that there may be Multiple

© Woodhead Publishing Limited, 2013

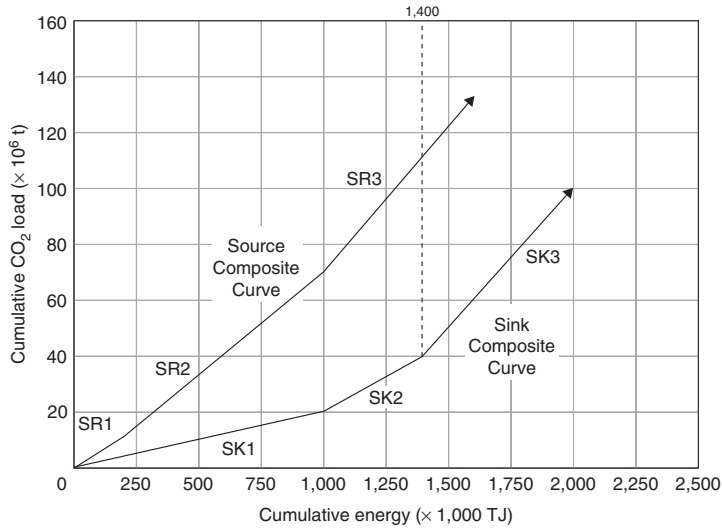

17.2 EPCC showing initial infeasible solution for motivating example (Tan and Foo, 2007).

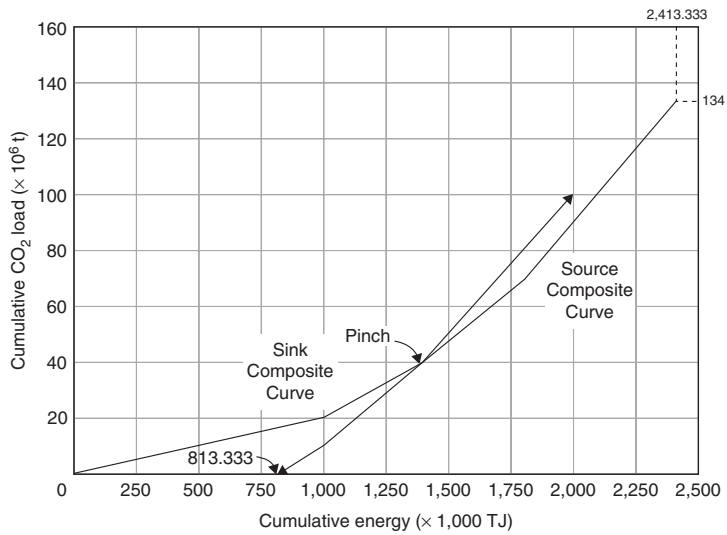

17.3 EPCC showing optimal solution for motivating example (Tan and Foo, 2007).

Pinch Points in some cases). As in the case of all Pinch-based strategies, the target and the Pinch Point location already provide valuable clues for subsequent identification of an optimal energy allocation scheme, following the so-called 'Golden Rule' of Pinch. In this case, the external energy resource

© Woodhead Publishing Limited, 2013

Table 17.4 Optimal energy allocation for motivating example (in TJ)

Source	Region I	Region II	Region III	Unutilised
Zero-carbon resource	680,000	133,333	0	0
Coal	0	0	500,000	100,000
Oil	120,000	266,667	100,000	313,333
Natural gas	200,000	0	0	0

Source: Tan and Foo (2007).

should only be used in the region comprised of demands below (and to the left) the Pinch. The high- and low-quality regions (i.e., Below and Above the Pinch Point) may be analysed separately, and Cross-Pinch Transfer of energy should be avoided. The only exception here is for the energy source that lies at the Pinch Point itself; this source must be split to supply the requirements of both regions. Note that, in cases where the external energy resource has a non-zero quality index, the Composite Curve is shifted along a locus of slope Q^{ext}.

- Detailed network design may then be achieved through inspection in the case of simple problems, or using systematic approaches such as the Nearest Neighbour Algorithm (NNA) developed by Prakash and Shenoy (2005), and later extended to energy-planning problems (Shenoy, 2010). For this example, the optimal allocation is shown in Table 17.4, which matches the result reported by Tan and Foo (2007). It should be noted that multiple solutions may exist (i.e., different allocation schemes may exist for the same target), which may be found using source shifting.

The general approach described here is illustrated in the next section using four additional case studies, each emphasising a separate quality index relevant to sustainable energy planning. These cases may be solved using the same general procedure, by merely replacing Carbon Footprint by the appropriate index.

17.4 Case Studies

17.4.1 Case 1: Energy Planning Based on Agricultural-Land Footprint

This case study, which was originally solved algebraically by Foo *et al.* (2008), involves planning the production of ethanol from sugarcane and corn to meet the requirements of three distinct geographic regions. It is assumed that geographic limitations prevent substantial trade of ethanol

© Woodhead Publishing Limited, 2013

Table 17.5 Source and sink data for Case 1

Source	S_i (ML)	Q_i (ha/ML)	Sink	D_j (ML)	Q_j^{max} (ha/ML)
Sugarcane ethanol	499.8	238	Region I	422	177.7
Corn ethanol	27.5	1,429	Region II	105	214.3
			Region III	117.6	516.2

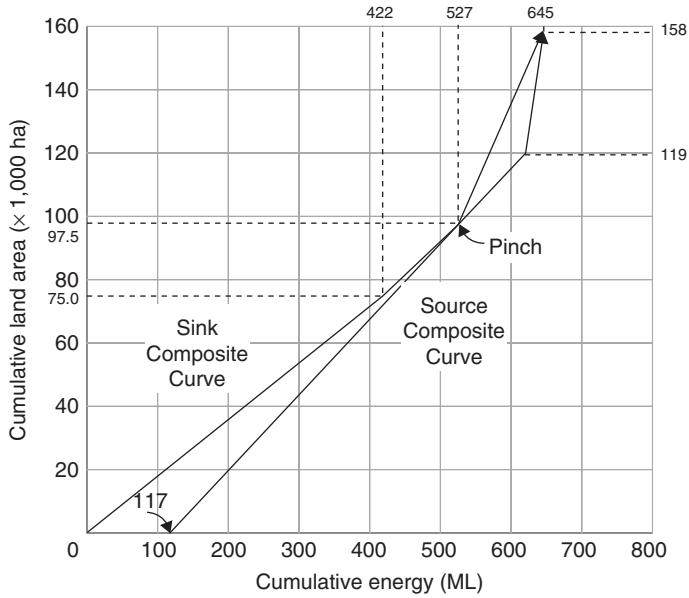

17.4 EPCC showing optimal solution for Case 1.

among these regions. Production is also limited by the available agricultural land; thus, the agricultural-land footprint (i.e., the inverse of energy crop yield) becomes the relevant energy quality index. Note that the production of each feedstock is expressed in terms of millions of litres (ML) of ethanol equivalent. Deficits are to be met through the importation of ethanol from an external supplier, which thus generates no land footprint in any of the three regions, so that $Q^{ext} = 0$. The data for sources and sinks are given in Table 17.5.

Again, the Composite Curves can be drawn and shifted horizontally (since $Q^{ext} = 0$) to give the EPCC in Fig. 17.4, where the target is identified to be 117.4 ML of imported ethanol. This external stream is utilised in Regions I and II which lie Below the Pinch Point. Using NNA, the optimal allocation of ethanol across three regions can be determined, as shown in Table 17.6.

© Woodhead Publishing Limited, 2013

Table 17.6 Optimal energy allocation for Case 1 (in ML)

Source	Region I	Region II	Region III	Unutilised
Imported ethanol	106.9	10.5	0	0
Sugarcane ethanol	315.1	94.5	90.1	0
Corn ethanol	0	0	27.5	0

Table 17.7 Source and sink data for Case 2

Source	S_i (ML)	Q_i (t/L)	Sink	D_j (ML)	Q_j^{max} (t/L)
Sugarcane ethanol	300	2.4	Region I	422	1.8
Corn ethanol	250	3.3	Region II	105	2.1
			Region III	117.6	5.2

17.4.2 Case 2: Energy Planning Based on Water Footprint

This case study is adapted from Tan *et al*. (2009) and, as in the previous example, involves planning the production of ethanol from sugarcane and corn to meet the requirements of three geographic regions. Other assumptions regarding trade between regions are the same. However, in this case, production is constrained by locally available water resource, which is a function of precipitation levels and land mass. Water Footprint is hence the appropriate quality index to use for this scenario. Again, since imported ethanol does not consume local water resource, we assume $Q^{ext} = 0$. The data for sources and sinks are given in Table 17.7.

The shifted EPCC can be drawn to show the optimal solution as in Fig. 17.5. The target minimal requirement for imported ethanol is found to be 148.2 ML, which is once again to be used only in the regions Below the Pinch Point (Regions I and II). Using NNA, the optimal allocation of ethanol across three regions can be determined as shown in Table 17.8.

17.4.3 Case 3: Energy Planning Based on Emergy

Emergy-Based Pinch Analysis was first proposed by Crilly and Zhelev (2008), and later extended to the context of source–sink allocation problems by Bandyopadhyay *et al*. (2010). This case study is adapted from the latter work, where emergy quantifies the cumulative solar radiation needed for naturally occurring processes to generate usable energy sources such as biomass or fossil fuels. Thus, emergy (measured in *solar emjoules* or sej) assumes the role of quality load, while the ratio of emergy content to calorific value, which is known as transformity, is the quality index. Note that transformity is always greater than unity, and lower values indicate that

© Woodhead Publishing Limited, 2013

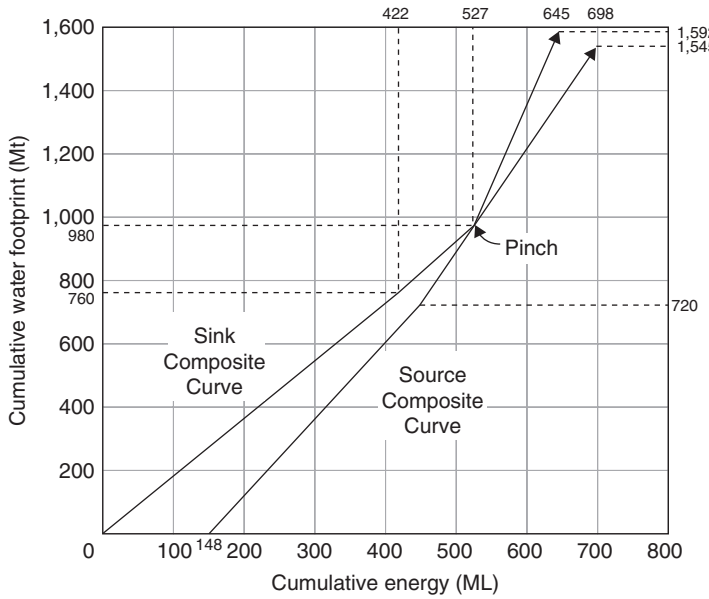

17.5 EPCC showing optimal solution for Case 2.

Table 17.8 Optimal energy allocation for Case 2 (in ML)

Source	Region I	Region II	Region III	Unutilised
Imported ethanol	110	38.2	0	0
Sugarcane ethanol	300	0	0	0
Corn ethanol	12	66.8	117.6	53.6

a given resource is easier to generate through natural processes and thus requires less solar inputs to form. Source and sink data for this example are given in Table 17.9, which shows that the problem involves allocating energy to two different industrial sectors. The external resource is this case is wood biomass, with a transformity of Q^{ext} =7,000 sej/J (i.e., the cumulative requirement of solar energy to generate enough wood to give 1 J of chemical energy is 7,000 J).

Since $Q^{ext} \neq 0$, it is necessary to shift the EPCC along a diagonal locus whose slope corresponds to the transformity of wood (7,000 sej/J), thus giving the optimal solution shown in Fig. 17.6. The target minimal requirement for wood is 0.25 EJ. Since the Pinch Point separates two sectors, the high-quality resource is used only for Sector A, which lies Below the Pinch. NNA can once again be used to determine the allocation which satisfies this target, which is shown in Table 17.10. Note that none of the oil is used in the system.

© Woodhead Publishing Limited, 2013

Table 17.9 Source and sink data for Case 3

Source	S_i (EJ)	Q_i (sej/J)	Sink	D_j (EJ)	Q_j^{max} (sej/J)
Coal	0.5	40,000	Sector A	0.8	30,000
Natural gas	0.4	48,000	Sector B	0.3	60,000
Oil	0.8	54,000			

Table 17.10 Optimal energy allocation for Case 3 (in EJ)

Source	Sector A	Sector B	Unutilised
Wood	0.25	0	0
Coal	0.5	0	0
Natural gas	0.05	0.30	0.05
Oil	0	0	0.8

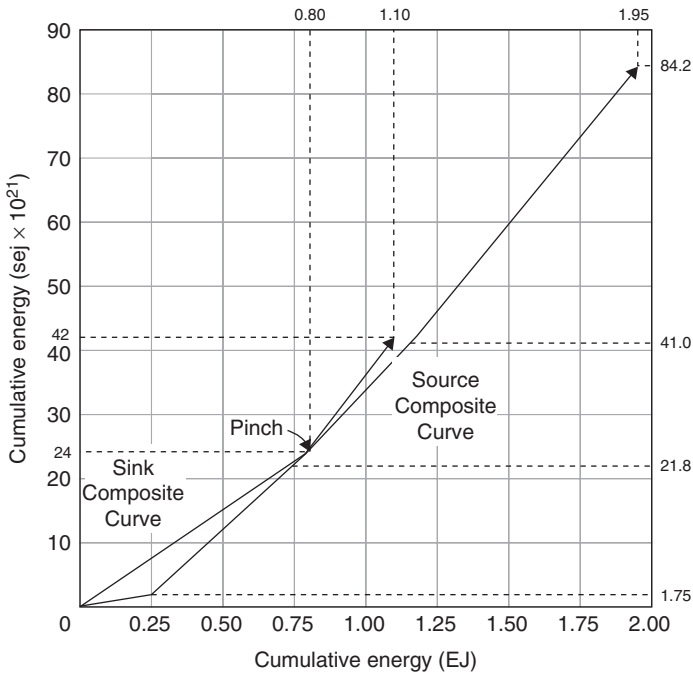

17.6 EPCC showing optimal solution for Case 3.

17.4.4 Case 4: Energy Planning Based on Inoperability

The use of inoperability in energy planning is essential due to the vulnerability of modern energy infrastructure to catastrophes such as seismic events

© Woodhead Publishing Limited, 2013

Table 17.11 Source and sink data for Case 4

Source	S_i (EJ)	Q_i	Sink	D_j (EJ)	Q_j^{max}
A	3	0.03	Region I	5	0.02
B	2	0.1	Region II	3	0.15
C	2	0.2			

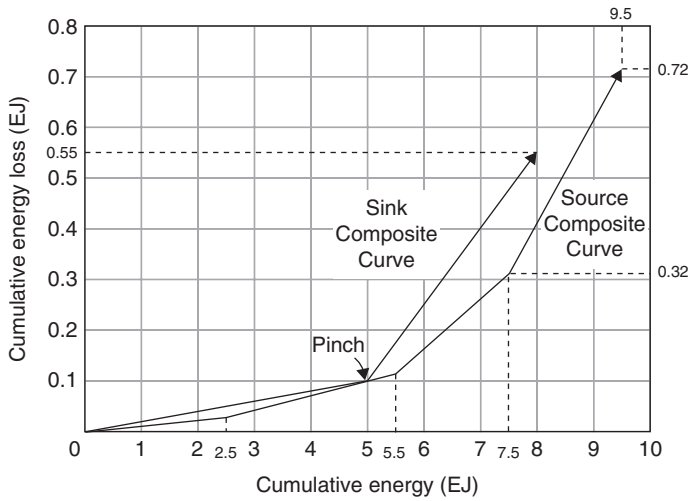

17.7 EPCC showing optimal solution for Case 4.

or unfavourable weather conditions (Tan, 2011a). The use of inoperability as a Pinch Analysis quality index was recently proposed (Tan, 2011b) and is illustrated here with a case study. Source and sink data for this example are given in Table 17.11. The problem is to allocate energy sources between two regions given inoperability characteristics. For the sources, the inoperability values indicate the potential loss of supply relative to the expected level; thus, it measures how reliable the supply will be in the face of an adverse event. For the sinks, the inoperability limit measures the sensitivity of the region to disruptions in energy supply; the higher the limit, the more robust the region is. Note that inoperability is a dimensionless quantity in the interval [0, 1], and that a high-quality external energy resource denoted as S with inoperability of $Q^{ext} = 0.01$ is available to the system.

As in the previous example, the Source Composite Curve has to be shifted diagonally along a locus with slope $Q^{ext} = 0.01$ to get the optimal EPCC as in Fig. 17.7. The target minimal requirement for energy source S is 2.5 EJ. The Pinch Point separates two regions, such that S is used only for Region I. The complete energy allocation table found using ANN is shown in Table 17.12.

© Woodhead Publishing Limited, 2013

Table 17.12 Optimal energy allocation for Case 4 (in EJ)

Source	Region I	Region II	Unutilised
S	2.5	0	0
A	2.5	0.5	0
B	0	2	0
C	0	0.5	1.5

17.5 Conclusion

Pinch Analysis provides an effective insight-based strategy for energy allocation problems under quality constraints. Energy quality measures that are relevant to contemporary sustainability issues include Carbon Footprint, agricultural-land footprint, Water Footprint, emergy transformity and inoperability. The problem may be expressed in generalised form and solved using the graphical *EPCC,* provided that the energy system has a single quality index that conforms to a linear mixing rule and follows an inverse scale. Alternatively, such problems may also be solved using various graphical or algebraic Pinch strategies available in the literature. Once the target external energy resource requirement and Pinch Point are identified, subsequent analysis may be facilitated using time-tested Pinch principles. Detailed energy allocation may also be determined using suitable approaches such as the *NNA*. However, as the Pinch-based approach remains restricted to problems with a single energy index, the development of a Pinch Analysis technique for solving problems with multiple quality indices remains a significant research challenge for the Process Integration community.

17.6 Sources of Further Information

The inherently multi-dimensional aspect of sustainable energy planning is reflected in the case studies of this chapter. A recent article by Čuček *et al*. (2012) gives a comprehensive discussion of various sustainability or footprint metrics. The reader may also refer to the book of Odum (1996) for a detailed treatment of the theory underlying the concept of emergy. Likewise, the seminal paper on inoperability input–output analysis (Haimes and Jiang, 2001) provides an excellent discussion of this linearised measure of risk.

The graphical procedure used in this chapter was originally developed for Targeting in Resource Conservation Networks, simultaneously by El-Halwagi *et al*. (2003) and by Prakash and Shenoy(2005). A mathematical proof of optimality using dynamic programming is also given by El-Halwagi *et al*. (2003). Meanwhile, the systematic Network Design Procedure known as the NNA was proposed by Prakash and Shenoy (2005). As previously

© Woodhead Publishing Limited, 2013

noted, the literature contains various alternative procedures that will yield equivalent results through either graphical or algebraic methods. Many of these are described in the review paper of Foo (2009). More detailed treatment of key approaches for targeting and network design can also be found in a recent textbook by Foo (2012).

17.7 References

Allan, A. J. (1998). Watersheds and problemsheds: explaining the absence of Armed Conflict over water in the Middle East. *Middle East Review of International Affairs,* **2**, Article 7.

Anderson, C. W., Santos, J. R., Haimes, Y. Y. (2007). A risk-based input–output methodology for measuring the effects of the August 2003 Northeast Blackout. *Economic Systems Research*, **19**, 183–204.

Atkins, M. J., Morrison, A. S., Walmsley, M. R. W. (2010). Carbon emissions pinch analysis (CEPA) for emissions reduction in the New Zealand electricity sector. *Applied Energy*, **87**, 982–987.

Bandyopadhyay, S., Sahu, G. C., Foo, D. C. Y., Tan, R. R. (2010). Segregated targeting for multiple resource networks using decomposition algorithm. *AIChE Journal*, **56**, 1235–1248.

Brans, J. P., Vincke, Ph., Mareschal, B. (1986). How to select and how to rank projects: The Promethee method. *European Journal of Operational Research*, **24**, 228–238.

Crilly, D., Zhelev, T. (2008a). Emissions targeting and planning: An application of CO_2 emissions pinch analysis (CEPA) to the Irish electricity generation sector. *Energy*, **33**, 1498–1507.

Crilly, D., Zhelev, T. (2008b). An emergy-based targeting technique for treatment and utilisation of greenhouse gas emissions. Presented in the 18th International Congress of Chemical and Process Engineering (CHISA)/PRES 2008 Paper No. K 2.1 Czech Republic.

Crilly, D., Zhelev, T. (2010). Further emissions and energy targeting: an application of CO_2 emissions pinch analysis to the Irish electricity generation sector. *Clean Technologies and Environmental Policy*, **12**, 177–189.

Čuček, L., Klemeš, J. J., Kravanja, Z. (2012). A review of footprint analysis tools for monitoring impacts on sustainability. *Journal of Cleaner Production,* **34**, 9–20, DOI: 10.1016/j.jclepro.2012.02.036.

De Benedetto, L., Klemeš, J. J. (2009). The Environmental Performance Strategy Map: an integrated LCA approach to support the strategic decision-making process. *Journal of Cleaner Production*, **17**, 900–906.

Dhole, V. R., Linnhoff, B. (1993). Total site targets for fuel, co-generation, emissions, and cooling. *Computers & Chemical Engineering*, **17**, S101–S109.

El-Halwagi, M. M., Gabriel, F., Harell, D. (2003). Rigorous graphical targeting for resource conservation via material reuse/recycle networks. *Industrial & Engineering Chemistry Research*, **42**, 4319–4328.

Foo, D. C. Y. (2009). A state-of-the-art review of pinch analysis techniques for water network synthesis. *Industrial & Engineering Chemistry Research*, **48**(11), 5125–5159.

© Woodhead Publishing Limited, 2013

Foo, D. C. Y. (2012). *Process Integration for Resource Conservation.* CRC Press, Boca Raton, Florida, USA.

Foo, D. C. Y., Tan, R. R., Ng, D. K. S. (2008). Carbon and footprint-constrained energy sector planning using cascade analysis technique. *Energy*, **33**, 1480–1488.

Geldermann, J., Treitz, M., Rentz, O. (2006a). Integrated technique assessment based on the pinch analysis approach for the design of production networks. *European Journal of Operational Research*, **171**, 1020–1032.

Geldermann, J., Treitz, M., Schollenberger, H., Rentz, O. (2006b). Evaluation of VOC recovery strategies: multi-objective pinch analysis (MOPA) for the evaluation of VOC recovery strategies. *OR Spectrum*, **28**, 3–20.

Haimes, Y. Y., Jiang, P. (2001). Leontief-based model of risk in complex interconnected infrastructures. *Journal of Infrastructure Systems*, **7**, 1–12.

Jia, X. P., Liu, H. C., Qian, Y. (2009). Carbon emission pinch analysis for energy planning in chemical industrial park. *Modern Chemical Industry*, **29**, 81–85.

Jia, X. P., Liu, H. C., Qian, Y. (2010). Carbon emission reduction using pinch analysis. Presented at the 4th International Conference on Bioinformatics and Biomedical Engineering, ICBBE 2010, Chengdu, 2010 article no. 5516600.

Khanna, V., Bakshi, V. R. (2009). Modeling the risks to complex industrial networks due to loss of natural capital. IEEE International Symposium on Sustainable Systems and Technology, ISSST 09 in Cooperation with 2009 IEEE International Symposium on Technology and Society, ISTAS, art. no. 515677.

Lam, H. L., Varbanov, P. S., Klemeš, J. J. (2011). Minimising carbon footprint of regional biomass supply chains. *Resources, Conservation and Recycling*, **54**, 303–309.

Lam, H. L., Varbanov, P. S., Klemeš, J. J. (2010). Regional renewable energy and resource planning. *Applied Energy*, **88**, 545–550.

Liang, S., Zhang, T. (2011). Managing urban energy system: a case of Suzhou in China. *Energy Policy*, 39, 2910–2918.

Odum, H. T. (1995). *Environmental Accounting: Emergy and Environmental Decision-Making*. Wiley, New York.

Prakash, R., Shenoy, U. V. (2005). Targeting and design of water networks for fixed flowrate and fixed contaminant load operations. *Chemical Engineering Science*, **60**, 255–268.

Rockstrom, J., Steffen, W., Noone, K., Persson, A., Chapin, F. S., Lambin, E. F., Lenton, T. M., Scheffer, M., Folke, C., Schellnhuber, H. J., Niykvist, B., De Wit, C. A., Hughes, T., Van der Leeuw, S., Rodhe, H., Sorlin, S., Snyder, P. K., Constanza, R., Svedin, U., Falkenmark, M., Karlberg, L., Corell, R. W., Fabry, V. J., Hansen, J., Walker, B., Liverman, D., Richardson, K., Crutzen, P., Foley, J. A. (2009). A safe operating space for humanity. *Nature*, **461**, 472–475.

Shenoy, U. V. (2010). Targeting and design of energy allocation networks for carbon emission reduction. *Chemical Engineering Science*, **65**, 6155–6168.

Shenoy, U. V. (2011). Unified targeting algorithm for diverse process integration problems of resource conservation networks. *Chemical Engineering Research and Design*, **89**, 2686–2705.

Shi, X., Liao, Z., Wang, J., Jiang, B., Yang, Y. (2009). Graphical optimization approach to carbon-constrained energy sector planning. *Huagong Xuebao/CIESC Journal*, **60**, 1237–1244.

Tan, R. R., Foo, D. C. Y. (2007). Pinch analysis approach to carbon-constrained energy sector planning. *Energy*, **32**, 1422–1429.

© Woodhead Publishing Limited, 2013

Tan, R. R., Foo, D. C. Y., Aviso, K. B., Ng, D. K. S. (2009). The use of graphical pinch analysis for visualizing water footprint constraints in biofuel production. *Applied Energy*, **86**, 605–609.

Tan, R. R. (2011). A general source-sink model with inoperability constraints for robust energy sector planning. *Applied Energy*, **88**, 3759–3764.

Zhelev, T. K., Ridolfi, R. (2006). Energy recovery and environmental concerns addressed through emergy-pinch analysis. *Energy*, **31**, 2150–2162.

17.8 Appendix

Indices

i	source index
j	sink index
k	quality index

Parameters

D_j	energy requirement of sink j
Q^{ext}	quality index of external resource
Q_i	quality index of internal source i
$Q_j^{\max}$	quality index limit of sink j
Q_k^{ext}	kth quality index of external resource
Q_{ik}	kth quality index of internal source i
$Q_{jk}^{\max}$	kth quality index limit of sink j
S_i	energy available from internal source i

Variables

F_j	external energy resource allocated to sink j
R_{ij}	energy allocation from internal source i to sink j

The generalised quality-constrained energy allocation problem may be expressed as an equivalent linear programming (LP) problem using any dimensionally consistent set of physical units. This equivalency was first reported for Resource Conservation networks by El-Halwagi *et al*. (2003), and subsequently for the case of energy planning by Tan and Foo (2007):

$$\text{minimise } \Sigma_j F_j \qquad [17.1]$$

subject to:

$$\Sigma_j R_{ij} \leq S_i \; \forall i \qquad [17.2]$$

$$F_j + \Sigma_i R_{ij} = D_j \; \forall j \qquad [17.3]$$

© Woodhead Publishing Limited, 2013

$$Q^{\text{ext}}F_j + \Sigma_i\, Q_i R_{ij} \leq Q_j^{\max} D_j \;\forall j \quad [17.4]$$

$$F_j \geq 0 \;\forall j \quad [17.5]$$

$$R_{ij} \geq 0 \;\forall i, j \quad [17.6]$$

The objective function is to minimise the external energy resource requirement (Equation [17.1]). The energy source balance is given by Equation [17.2], the energy demand balance is given by Equation [17.3] and the quality load balance at the sinks is given by Equation [17.4]. All system variables are non-negative (Equations [17.5] and [17.6]). Furthermore, the LP formulation can be expanded to the general case with multiple quality indices. Note that this variant in general cannot be solved using Pinch Analysis. The LP approach simply involves specifying a separate quality load balance constraint for each quality index k; Equation [17.4] is thus modified to give:

$$Q_k^{\text{ext}}F_j + \Sigma_i\, Q_{ik} R_{ij} \leq Q_{jk}^{\max} D_j \;\forall j, k \quad [17.7]$$

© Woodhead Publishing Limited, 2013

18

A Unified Targeting Algorithm for Diverse Process Integration Problems

UDAY V. SHENOY, Synew Technologies, India

DOI: 10.1533/9780857097255.4.524

Abstract: This chapter demonstrates how a single algorithm suffices to establish the complete minimum-resource targets for diverse Process Integration problems from heat/mass exchange to allocation networks for water, hydrogen, carbon emission and material reuse. It discusses the basis and the systematic calculation steps for the Unified Targeting Algorithm (UTA), along with the graphical representation of the tabular UTA data in terms of the Grand Composite Curve (GCC) or the Limiting Composite Curve (LCC) depicting net load deficit/surplus at various levels. The chapter includes nine practical case studies from diverse domains to illustrate the wide applicability of the unified algorithm.

Key words: Pinch Analysis targets, Heat Exchanger Networks, water allocation networks, refinery hydrogen management, carbon emission reduction.

18.1 Introduction to Targeting Algorithms

The Problem Table Algorithm (PTA), proposed by Linnhoff and Flower (1978), has long been established as a reliable and convenient tool to algebraically calculate energy targets in Heat Exchanger Networks (HENs). Its related graphical representation, the GCC, provides an effective means of visualising heat-load requirements at different temperature levels and targeting utilities based on an explicit decomposition of the system at the Pinch (Linnhoff *et al*., 1982).

The Composition Interval Table (CIT) algorithm, proposed by El-Halwagi and Manousiouthakis (1989), is the analogue of the PTA for algebraically computing targets for external mass separating agents (MSAs) in Mass Exchange Networks (MENs). The associated graphical representation, the MEN GCC, displays mass loads at different composition levels along with the Pinch division for Targeting MSAs (Fraser *et al*., 2005).

The Composite Table Algorithm (CTA), proposed by Agrawal and Shenoy (2006), is a versatile tool to algebraically calculate minimum

© Woodhead Publishing Limited, 2013

freshwater and makeup hydrogen targets in water and hydrogen networks, respectively. Its related graphical representation, the LCC, provides a powerful visual means of identifying loads at different concentration/purity levels and locating the Pinch. The LCC was first developed by Wang and Smith (1994) for water networks of the fixed contaminant-load type. Recently, the CTA and LCC have been extended to carbon emission networks (CEN) by Shenoy (2010) and to carbon capture and storage (CCS) by Shenoy and Shenoy (2012).

This chapter discusses a single algorithm, referred to as the UTA hereafter, to target diverse resource optimisation problems of Process Integration. The UTA provides a simple algebraic method to determine minimum utility/resource targets for (heat/mass) exchange networks as well as (water, hydrogen, carbon emission and material reuse) allocation networks. The UTA is implemented in a convenient tabular form, and the tabular data can then be readily plotted to appropriately obtain their graphical representation in terms of either the GCC or the LCC. The UTA lends itself admirably to spreadsheet implementation, as well as to manual calculation. The presentation of the UTA that follows is inspired by, and draws largely from, the original work of Shenoy (2011); however, an attempt is made to improve the UTA approach wherever possible, primarily through simplification of certain steps and sign conventions.

18.2 Unified Approach to Diverse Resource Optimisation Problems

In this chapter, resource optimisation problems in Process Integration are classified into two broad categories: exchange networks (where one stream gains and another loses) and allocation networks (where sources are mixed to satisfy demands). Two primary types of exchange networks are HENs and MENs. Similarly, two primary types of allocation networks are fixed load (FL) networks and fixed flow (FF) networks. Water networks with fixed contaminant-load (FC) processes, and cooling-water networks with fixed heat-load operations are examples of FL networks. Water networks with fixed flowrate processes, hydrogen networks, CENs and material reuse networks are examples of FF networks.

For an exchange process transferring heat/component from a hot/rich stream to a cold/lean stream, the basic equations for the heat/mass load are:

$$Q = MC_{p,h}\,(T_{\text{in},h} - T_{\text{out},h}) = MC_{p,c}\,(T_{\text{out},c} - T_{\text{in},c}) \quad \text{for heat exchange process} \qquad [18.1]$$

$$m = G\,(y_{\text{in}} - y_{\text{out}}) = L\,(x_{\text{out}} - x_{\text{in}}) \text{ for mass exchange process} \qquad [18.2]$$

© Woodhead Publishing Limited, 2013

For an FC water process, the basic equation for the mass load of contaminant is:

$$m = F\,(C_{out} - C_{in}) \text{ for FC process} \quad [18.3]$$

The above equation applies to water-using processes that may be modelled as mass transfer units (Wang and Smith, 1994), such as absorption, extraction, scrubbing and washing (Hallale and Fraser, 1998). Here, water is used as the only MSA that picks up a fixed mass load m of contaminant from the process stream (Polley and Polley, 2000). Each operation has the maximum allowable contaminant concentration at the outlet (C_{out}) and inlet (C_{in}) specified, based on process constraints. Because the flowrate F of water entering and leaving each process unit is the same (assuming no water loss/gain), the wastewater flowrate for the network equals the freshwater flowrate.

For an FF process, the basic equation for the load at the inlet ($m_{in} = F_{in}\,C_{in}$) and outlet ($m_{out} = F_{out}\,C_{out}$) is of the form:

$$m = FC \text{ for FF process} \quad [18.4]$$

The above equation is applicable to a FF water process when m is the mass load of contaminant, F is the water flowrate and C is the concentration level of contaminant in the water stream (Prakash and Shenoy, 2005a). Note that FF water networks comprise operations such as boilers, cooling towers and reactors not involving mass transfer where the main concern is the flowrate and not the amount of contaminant picked up (Wang and Smith, 1995). Equation [18.4] also applies to a hydrogen-consuming process if m is the hydrogen load, F is the hydrogen flowrate and $C \equiv 1 - y$ (where y is the percentage hydrogen purity) is the equivalent contaminant concentration (Agrawal and Shenoy, 2006). Further, the equation is applicable to a carbon-constrained energy planning process in a CEN, provided m is the emission load, F is the energy and C is the emission factor (Shenoy, 2010). In general, FF units have inlet flowrate F_{in} and outlet flowrate F_{out} specified, which may not necessarily be equal and therefore losses or gains can be accounted for. Consequently, the flowrate entering the network does not necessarily equal the flowrate leaving. As before, the maximum allowable outlet concentration level C_{out} and inlet concentration level C_{in} are specified.

The overall objective in the above Process Integration problems is to optimally exchange/allocate resources (e.g., heat, mass, water, hydrogen, energy and material) that necessarily have both a quantity (load) and a quality (level). A unified approach to these apparently diverse resource optimisation problems is possible provided analogous variables are identified as in Table 18.1.

© Woodhead Publishing Limited, 2013

Table 18.1 Analogues for application of UTA to diverse Process Integration problems

(a) Exchange networks

	HENs	MENs
Level or quality variable *C*	Temperature in °C	Composition as mass ratio
Flow variable *F*	Heat capacity flowrate in kW/°C	Mass flowrate in kg/s
Load or quantity variable *m*	Heat load in kW	Mass load in kg/s
High level resource/utility *R*	Hot utility	Process MSAs excess
Low level resource/utility *E*	Cold utility	External MSAs

(b) Allocation networks

	Water networks	Hydrogen networks	CENs
Level or quality variable *C*	Contaminant concentration in ppm	1 – hydrogen purity as fraction	Emission factor in t CO_2/TJ
Flow variable *F*	Water flowrate in t/h	Hydrogen flowrate in MMscfd or mol/s	Energy in TJ
Load or quantity variable *m*	Contaminant load in kg/h	Hydrogen load in MMscfd or mol/s	Emission load or Carbon Footprint in t CO_2
High-quality resource *R*	Freshwater	Makeup hydrogen utility	Zero-carbon or low-carbon resource
Low-quality waste/excess *E*	Wastewater	Hydrogen purge	Unused or excess energy

18.3 Basis for Unification

This section discusses the basis for unification, whereby a stream is converted to an equivalent demand–source pair (or inlet–outlet pair).

18.3.1 Unification of Fixed Flow and Fixed Load Processes

The basic conceptual difference between FF and FC network processes is that FF networks consist of demands (sinks) and sources as in Fig. 18.1a, whereas FC networks are made up of streams. However, in an FC process (Dhole *et al.*, 1996), an inlet may be regarded as a demand (to a unit) and

© Woodhead Publishing Limited, 2013

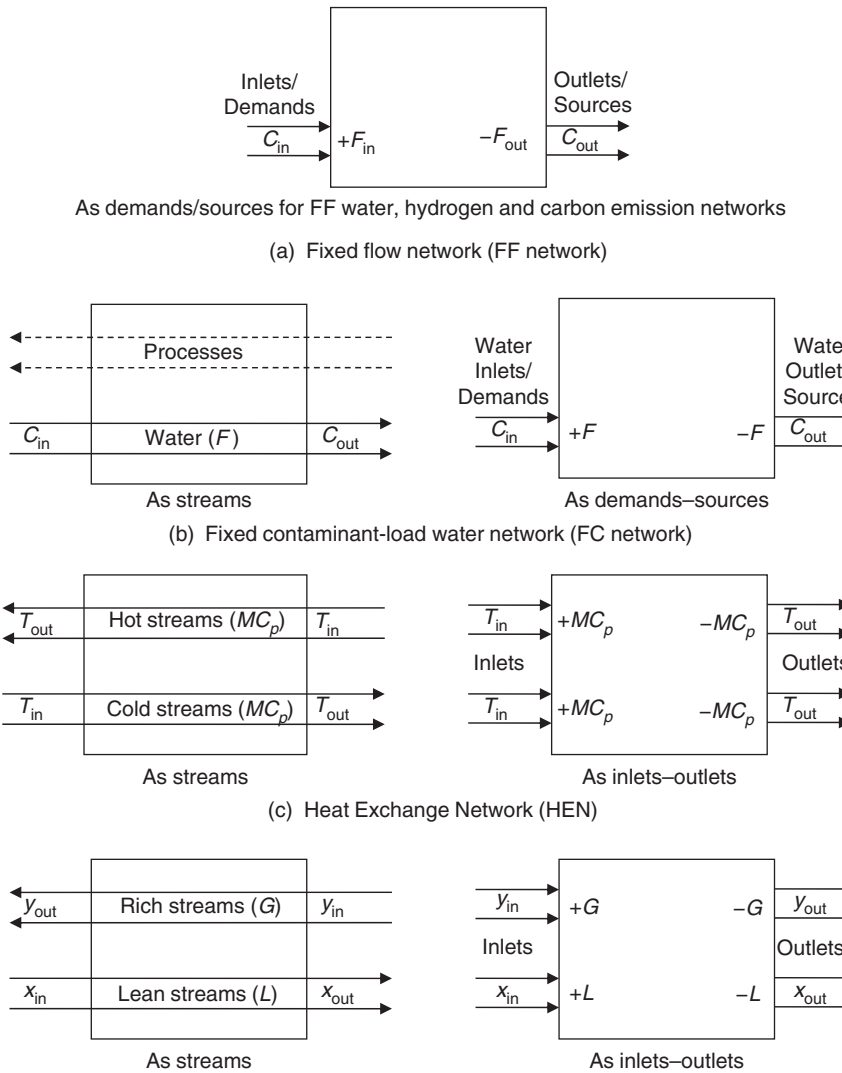

18.1 Conceptual representation of diverse network processes (Shenoy, 2011).

an outlet may be regarded as a source (to other units). This allows inlet and outlet streams (even for the same unit) to be treated independently (Prakash and Shenoy, 2005a). Furthermore, units having multiple inlet streams and multiple outlet streams can be modelled. Thus, all inlet streams may be treated as demands, and all outlet streams as sources (Agrawal and

© Woodhead Publishing Limited, 2013

Shenoy, 2006), in an FC network as in Fig. 18.1b. Importantly, the FC allocation process (Equation [18.3]) may be considered a special case of the FF allocation process (Equation [18.4]) where inlet and outlet flows are equal ($F_{in} = F_{out}$).

18.3.2 Unification of Allocation and Exchange Processes

For allocation processes where two or more sources S are mixed to satisfy demand D, the following conservation balance equations and linear mixing rules fundamentally hold for flow and load:

$$\sum F_S = F_D \text{ flow balance for allocation process} \quad [18.5]$$

$$\sum F_S\, C_S = F_D\, C_D \text{ load balance for allocation process} \quad [18.6]$$

To observe the same form for heat/mass exchange processes, Equations [18.1] and [18.2] may be rearranged in the following form:

$$MC_{p,h}\, T_{out,h} + MC_{p,c}\, T_{out,c} = MC_{p,h}\, T_{in,h} + MC_{p,c}\, T_{in,c} \text{ for heat exchange process} \quad [18.7]$$

$$G\, y_{out} + L\, x_{out} = G\, y_{in} + L\, x_{in} \text{ for mass exchange process} \quad [18.8]$$

The above equations provide the basis for the equivalence in Fig. 18.1c and 18.1d of representing streams in terms of inlet–outlet pairs. Recognising the analogues for the flow variable F (as MC_p, G or L) and the level variable C (as T, y or x) in the unified approach, Equations [18.7] and [18.8] may be written in the following general form:

$$\sum F_{out}\, C_{out} = \sum F_{in}\, C_{in} \quad [18.9]$$

Equation [18.9] has the same form as Equation [18.6], and shows the unification of heat/mass exchange processes with allocation processes by conversion of streams into equivalent inlet–outlet pairs as in Fig. 18.1. On treating inlets as demands and outlets as sources as discussed in Section 18.3.1, Equation [18.9] is importantly applicable to both exchange and allocation processes.

Equation [18.9] may be further rearranged into the following two equivalent forms:

$$\sum F_{in}\, C_{in} + \sum(-F_{out})\, C_{out} = 0 \quad [18.10]$$

$$\sum(-F_{in})\, C_{in} + \sum F_{out}\, C_{out} = 0 \quad [18.11]$$

© Woodhead Publishing Limited, 2013

Equation [18.10] follows the positive inlets sign convention, where inlet flows are positive and outlet flows are negative. In contrast, Equation [18.11] follows the negative inlets sign convention, where inlet flows are negative and outlet flows are positive. The same targeting results are obtained irrespective of the sign convention used in the UTA. Equations [18.10] and [18.11] may be further unified with a built-in sign convention as follows:

$$\sum F_{\text{in}}\, C_{\text{in}} + \sum F_{\text{out}}\, C_{\text{out}} = 0 \qquad [18.12]$$

where F_{in} and F_{out} necessarily have opposite signs. Equations are presented henceforward in the form of an algebraic sum as in Equation [18.12] with the understanding that inlet flows and outlet flows must be opposite in sign.

Based on the discussion thus far, Fig. 18.1c and 18.1d show the stream representation of a HEN and a MEN in terms of equivalent inlet–outlet pairs. Note that N_h hot/rich streams and N_c cold/lean streams in a HEN/MEN (for a PTA/CIT calculation) may be represented as $N_h + N_c$ inlets with positive values of the flow variable (i.e., MC_p, G or L) and $N_h + N_c$ outlets with negative values of the flow variable (for a UTA calculation). Extending the argument from the previous section further, the heat/mass exchange processes (Equations [18.7] and [18.8]) may also be considered as special cases of the FF process (Equation [18.4]) where inlet and outlet flows (i.e., MC_p, G or L) are equal, and suitable analogues are identified for load (i.e., Q or m) and level (i.e., T, y or x). Thus, for the overall unification, Equation [18.4] may be written in the following elegant form:

$$\text{load} = \text{flow} \times \text{level for UTA} \qquad [18.13]$$

where the load m, flow F and level C variables are appropriately defined as in Table 18.1 for the diverse problems. Notably, the FF process provides the most general model for the purposes of the UTA.

Equation [18.12] as presented applies to a single heat/mass exchanger. It may be extended to a network by accounting for the system deficit/surplus through external resources/utilities. In general, overall balances for the flow and load over the total network system (Agrawal and Shenoy, 2006) yield:

$$F_R - F_E = \Delta_1 \text{ where } \Delta_1 \equiv \sum F_d + \sum F_s \qquad [18.14]$$

$$F_R\, C_R - F_E\, C_E = \Delta_2 \text{ where } \Delta_2 \equiv \sum F_d\, C_d + \sum F_s\, C_s \qquad [18.15]$$

$$m_R - m_E = -\Delta_3 \text{ where } \Delta_3 \equiv \sum F_{\text{in}}\, C_{\text{in}} + \sum F_{\text{out}}\, C_{\text{out}} \qquad [18.16]$$

where subscripts R and E denote the high-quality resource and the low-quality resource/excess. For allocation networks, the net system flow deficit

© Woodhead Publishing Limited, 2013

(Δ_1) and the net system load deficit (Δ_2) are obtained from Equations [18.14] and [18.15] by adding the appropriate quantities for all demands (denoted by subscript *d*) and all sources (denoted by subscript *s*). For exchange networks, the net system flow deficit is necessarily zero ($\Delta_1 = 0$) and the net system load deficit ($-\Delta_3$) is obtained from Equation [18.16] by adding the appropriate quantities for all inlets (denoted by subscript *in*) and all outlets (denoted by subscript *out*). Equations [18.14]–[18.16] are valid for the positive inlets/demands sign convention (with positive flows F_{in}/F_d and negative flows F_{out}/F_s). For the negative inlets/demands sign convention (with negative flows F_{in}/F_d and positive flows F_{out}/F_s), the sign on the right-hand side of Equations [18.14]–[18.16] is reversed. Importantly, Δ_1, Δ_2 and Δ_3 are constant for a given problem. Defining such net system quantities (Δ) that are constant is useful (Bandyopadhyay *et al.*, 1999, 2004) in Process Integration problems.

18.3.3 Conversion of Stream to Equivalent Inlet–Outlet Pair

The CTA, originally developed for allocation networks, can be fruitfully utilised for exchange networks, provided analogous variables are identified as in Table 18.1. The unified approach to targeting depends on a generalisation of the CTA so as to effectively include the PTA and the CIT algorithm. The PTA for HENs and the CIT for MENs both use streams as their primary representation. In the PTA, each stream is shown by a line segment extending between its inlet and outlet levels. On the other hand, the CTA for allocation networks depends on demands (inlets) and sources (outlets) for its primary representation. In the CTA, each demand or source is shown by a line segment starting at its specified level; however, all line segments end at the same (arbitrarily-chosen) reference level. Therefore, it is meaningful to convert a stream (in a HEN or MEN) to an equivalent inlet–outlet pair, and then use this new representation in the UTA.

Consider for concreteness the PTA for HENs (noting that analogous arguments exist in the CIT for MENs), where a hot stream (with $T_{in} > T_{out}$ and a positive MC_p) is represented by a line segment between levels T_{in} and T_{out} as in Fig. 18.2a (Shenoy, 2011). The CTA representation, wherein a stream is the equivalent composite of an inlet–outlet pair, is shown as two line segments: one for the inlet starting from T_{in} and another for the outlet starting from T_{out}. The equivalence is established by appropriately adding the Heat capacity flowrate values in the two intervals: combining gives the Heat capacity flowrate value as $+MC_p$ for $T_{out} \le T \le T_{in}$, and the value as $(+MC_p) + (-MC_p) = 0$ for $T < T_{out}$. Likewise, Fig. 18.2b (Shenoy, 2011) shows that a cold stream (with $T_{in} < T_{out}$ and a negative MC_p) represented by a

© Woodhead Publishing Limited, 2013

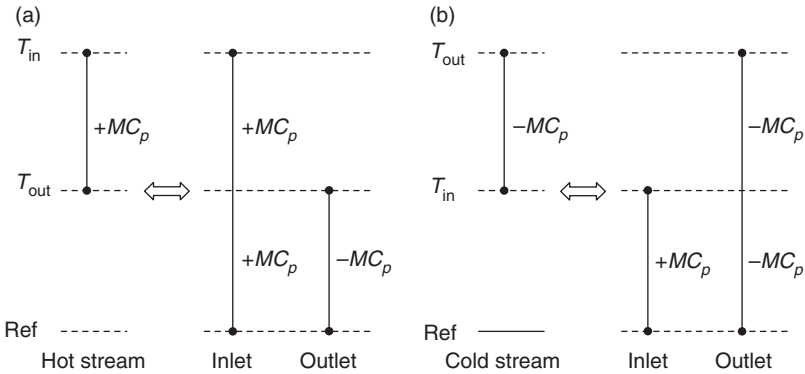

18.2 Representation of stream as equivalent inlet–outlet pair for UTA (Shenoy, 2011). (a) hot stream equivalence and (b) cold stream equivalence.

single line segment can be decomposed into its equivalent inlet–outlet pair with two line segments. The equivalence is again confirmed by adding the Heat capacity flowrate values in the two intervals: combining gives the value as $-MC_p$ for $T_{in} \leq T \leq T_{out}$, and as $(+MC_p) + (-MC_p) = 0$ for $T < T_{in}$.

The equivalence proven above for a hot/cold stream in a HEN clearly holds for a rich/lean stream in a MEN, so long as analogous variables from Table 18.1a are used. The noteworthy implication of the above equivalence, which is central to the UTA, is that any stream (hot/cold in a HEN, or rich/lean in a MEN) can be represented distinctly by an inlet (with a positive value of the flow variable, i.e., MC_p, G or L) and an outlet (with a negative value of the same flow variable).

18.4 Unified Targeting Algorithm (UTA)

Before implementing the main steps in the UTA, it is convenient to perform a pre-processing step in order to obtain the data in the form of (shifted) levels and (signed) flows for inlets/demands and outlets/sources. For the case of HENs/MENs, pre-processing converts the original stream data to inlet–outlet data with level shifting. The levels of streams are shifted to ensure that there is an adequate driving force, when a minimum is specified as in the case of heat/mass transfer. Typically, half the Minimum Driving Force is subtracted from levels of hot/rich streams and the remaining half is added to levels of cold/lean streams. Rather than shift by a uniform amount (namely, half the Minimum Driving Force), levels may be shifted by different individual stream-dependent contributions (for instance, when stream heat/mass transfer coefficients differ significantly) as this is permissible in the algorithm.

© Woodhead Publishing Limited, 2013

In the pre-processed data table, the (shifted) levels are tabulated along with the flows for inlets/demands and outlets/sources with opposite signs. For the positive inlets/demands sign convention (adopted throughout this chapter), flows of inlets/demands are positive and flows of outlets/sources are negative. For the negative inlets/demands sign convention, the signs are reversed. For HENs/MENs, the flow values for inlet and outlet are equal in magnitude but opposite in sign for each stream. The pre-processing step may not be required for allocation networks where the data are in the form of demands and sources with zero level shifting necessary. The calculated values of Δ_1 and Δ_2 for allocation networks, or $-\Delta_3$ for exchange networks based on the definitions in Equations [18.14]–[18.16] may be recorded at the bottom of the pre-processed data table for ready reference.

18.4.1 Main Steps in the UTA

The main steps in the UTA, where calculations are conveniently done through a compact table (as in Table 18.3 for Case Study 1), are succinctly given below. More details are given by Shenoy (2011).

1. Arrange in the first column all levels C (after shifting, if necessary) for inlets/demands and outlets/sources in decreasing or increasing order. Exchange networks use decreasing order, whereas allocation networks use increasing order when level is specified as impurity/contaminant concentration, or decreasing order when level is specified as purity. Do not repeat a value even if the level occurs more than once. These levels define the limits of the various intervals (e.g., the first interval goes from the first level to the second level).
2. Tabulate in the second column the algebraic sum of the corresponding flows of inlets/demands and outlets/sources present at each level l using:

$$F_l = \sum F_{\text{in},l} + \sum F_{\text{out},l} \text{ or } F_l = \sum F_{d,l} + \sum F_{s,l} \quad [18.17]$$

3. Tabulate in the third column the cumulative flows based on the previous (second) column. This yields the net flow deficit/surplus for each interval by summing the flows up to the previous level in accordance with:

$$F_{\text{net},l} = \sum F_l = F_{\text{net},l-1} + F_{l-1} \quad [18.18]$$

where $F_{\text{net},1} = 0$ and the summation goes from 1 to $(l-1)$. The net flow in an interval corresponds to the reciprocal of the slope of the associated segment on the GCC or LCC.

© Woodhead Publishing Limited, 2013

4. Tabulate in the fourth column the net load for each interval by multiplying the net flow (from the previous step) and the absolute value of the level difference (from the first column) for that interval according to the following equation:

$$m_{\text{net},l} = F_{\text{net},l} \mid C_l - C_{l-1} \mid \qquad [18.19]$$

where $m_{\text{net},1} = 0$. These values signify the net load deficit/surplus in each interval, after complete exchange/allocation within the interval.

5. Tabulate in the fifth column the cumulative load by summing the net loads (from the previous column) up to that level according to:

$$m_{\text{cum},l} = \sum m_{\text{net},l} = m_{\text{cum},l-1} + m_{\text{net},l} \qquad [18.20]$$

where $m_{\text{cum},1} = 0$ and the summation goes from 1 to l. The resulting load cascade in the fifth column is infeasible if a negative value exists and is revised in the next step.

6. Tabulate in the sixth column the revised feasible cascade by subtracting the most negative m_{cum} in the fifth column from each value in that column. Thus,

$$m_l = m_{\text{cum},l} - \min(m_{\text{cum}}) \text{ if } \min(m_{\text{cum}}) < 0 \qquad [18.21]$$

No revision is actually required if all the values in the fifth column are non-negative (which is typically the case for many allocation networks and threshold problems in exchange networks). For HENs/MENs, the minimum utility load targets are given by the first and last values in this revised cascade and may be validated using $m_R - m_E = -\Delta_3$. Further, the level in the first column that corresponds to zero revised load in the sixth column defines the (Process) Pinch.

7. If the target is required in terms of minimum-resource flow (rather than load), then tabulate in the seventh column possible target flows for different (m_l, C_l) value-pairs using the following equation:

$$F_{p,l} = \frac{m_l - m_1}{C_l - C_R} \qquad [18.22]$$

where m_l is the revised load (sixth column), m_1 is the first entry in the sixth column, C_l is the level (first column) and C_R is the (shifted) level of the utility or (contaminant) level of the high-quality resource R. The highest value in this seventh column specifies the minimum flow target F_R for the resource, and the level in the first column corresponding to

© Woodhead Publishing Limited, 2013

it defines the (Utility) Pinch. This column is useful when targets are to be set for the minimum flow (which is usually the case for allocation networks and variable-level non-point utilities in exchange networks). For allocation networks, Equations [18.14] and [18.15] may be then used to determine the targets for the low-quality resource/excess in terms of flow (from $F_E = F_R - \Delta_1$) and level (from $C_E = (F_R\, C_R - \Delta_2)/F_E$). Further, the distribution target for the Pinch-causing source (i.e., the source at the Pinch level) in an allocation network is obtained as follows: the difference between the net flow (third column) at the Pinch level and the minimum fresh resource target F_R is the Below Pinch portion, whereas the remainder is the Above Pinch portion.

18.4.2 Further Details Regarding UTA

Some noteworthy aspects of the UTA are listed below.

1. In spreadsheet software, Equation [18.17] may be readily implemented using the SUMIF function. Further, Equations [18.18] and [18.20] are similar in form, with the summation forms being suitable for easy implementation in a spreadsheet.
2. For manual calculations, the second form of Equation [18.18] may be used to obtain the net flow in an interval by adding the net flow in the previous interval and the flow at the previous level (from the second column). Similarly, the second form of Equation [18.20] may be utilised to obtain the cumulative load in an interval by adding the cumulative load in the previous interval and the net load at the present level (from the fourth column).
3. Two checks may be performed to ensure the correctness of the UTA calculations. The first check is provided by the last entry in the third column as per Equation [18.18], which must equal the net system flow deficit/surplus (Δ_1) because the last net flow calculation includes all the inlets/demands and outlets/sources in the problem. For exchange networks, Δ_1 is necessarily zero and therefore the last entry may not be tabulated but simply used as a mental check. The second check is provided by the last entry in the fifth column as per Equation [18.20], which must equal $\pm\Delta_3$ (for exchange networks) or $\pm(\Delta_2 - \Delta_1 C_{\text{last}})$ for allocation networks.
4. For allocation networks, it is prudent to include a demand/source with zero flow at an arbitrarily-chosen level such that an extra level entry appears at the bottom of the first column after sorting. The arbitrary entry (Agrawal and Shenoy, 2006) provides an endpoint and facilitates

© Woodhead Publishing Limited, 2013

the plotting of the last segment of the LCC, whose slope and initial point are well-defined. The last segment is not needed if its slope is negative.

5. Step 5 results in a load cascade across intervals, where cascading essentially involves transfer from an interval to the next lower interval (starting with the highest interval). In addition to complete exchange/allocation within an interval in Step 4, transfers can occur from higher intervals to lower ones satisfying some deficits in the lower intervals. However, the cascade is infeasible if a negative value exists in the fifth column.
6. The infeasible cascade with the negative transfer is a consequence of the load from a higher interval being inadequate to satisfy the requirements of lower intervals. This may be rectified in Step 6 using Equation [18.21] by supplying just enough load to ensure non-negative transfer at every interval resulting in the conversion of the infeasible cascade to a feasible cascade.
7. Equation [18.22], in the given form, is based on a load balance over the Below Pinch region for increasing-level sort order and the Above Pinch region for decreasing-level sort order.
8. Equation [18.20] follows the positive inlets/demands sign convention, which is adopted in this chapter without any loss of generality. The alternative form of Equation [18.20] based on the negative inlets/demands sign convention (Shenoy, 2011) is

$$m_{\mathrm{cum},l} = -\sum m_{\mathrm{net},l} = m_{\mathrm{cum},l-1} - m_{\mathrm{net},l}.$$

9. Four possibilities for the UTA implementation exist as discussed in detail by Shenoy (2011) based on the level sort order (decreasing or increasing) and the sign convention for inlets/demands (positive or negative). The original PTA (Linnhoff and Flower, 1978) is consistent with the decreasing-level sort order and negative inlets sign convention. When the inlets sign convention is changed from negative to positive, the values for F, F_{net} and m_{net} in the second, third and fourth columns change sign; however, the entries for m_{cum} and m in the fifth and sixth columns remain unchanged. When the level sort order is reversed from decreasing to increasing, the columns on the whole are vertically flipped; although the values for C and m in the first and sixth columns are identical (specifically, for HEN and MEN problems where $\Delta_1 = 0$), the entries in the other columns are changed (especially in the fifth column for m_{cum}). Importantly, the targets are unique, being independent of the level sort order and the inlets/demands sign convention used in the UTA because the first and last columns are sacrosanct in a sense. Without loss of generality, the positive inlets/demands sign convention will be used in this chapter.

© Woodhead Publishing Limited, 2013

18.4.3 Grand Composite Curve (GCC) and Limiting Composite Curve (LCC)

Two important graphical representations in Process Integration, the GCC (for exchange networks) and the LCC (for allocation networks) are directly obtained from the UTA table when the level C (first column) is plotted against the revised load m (sixth column). The GCC and LCC depict the net load deficit/surplus at various levels and thus help visualise the minimum-resource targets.

In exchange networks, the level at which the GCC touches the vertical axis specifies the Process Pinch on a shifted scale. In HENs, the top and bottom heat-load gaps of the GCC (see Figs 18.3 and 18.5) specify the hot and cold utility targets. In MENs, the top and bottom mass load gaps of the GCC (see Fig. 18.6) specify the excess process MSA and external MSA targets.

In allocation networks, the resource targets are in terms of flowrate (and not load as in the case of exchange networks). Targeting may be done graphically on the LCC (see Figs 18.7–18.11) by rotating a horizontal line with an appropriate pivot until it just touches the LCC. The reciprocal of the slope of this rotated target line (which can never be above the LCC) gives the minimum-resource flowrate requirement. The point where the target line touches the LCC defines the Pinch, which is a Utility Pinch and not a classical Process Pinch. This graphical procedure (Agrawal and Shenoy, 2006) is identical in principle to that suggested by Wang and Smith (1994) for the determination of the minimum freshwater target in water networks. The mathematical alternative is to use Equation [18.22] and tabulate the possible flowrates $F_{p,I}$ (since the Pinch Point is not known *a priori*) for different (m, C) value-pairs in the seventh column of the UTA table. The possible flowrate corresponds to the reciprocal of the slope of a line originating from the pivot (m_1, C_R) to a point on the LCC. Since the target lines can never be above the LCC, the minimum slope is required; so, the maximum value in the seventh column gives the minimum-resource target.

18.4.4 Illustrative Four-Stream HEN Case Study

To illustrate the UTA, a utility minimisation problem of a HEN from Shenoy (1995) is considered as a motivating example. The flowsheet (not reproduced here for brevity) shows a simplified portion of a petrochemical process involving an exothermic reaction followed by separation using distillation. Table 18.2a shows the data extracted for two hot and two cold process streams in terms of inlet/outlet temperatures in °C and heat loads in kW for Case Study 1. The remaining values for Heat capacity flowrate

© Woodhead Publishing Limited, 2013

Table 18.2 Data for four-stream HEN problem (Case Study 1)

(a) Original stream data

Stream	Inlet temperature T_{in} (°C)	Outlet temperature T_{out} (°C)	Heat capacity flowrate MC_p (kW/°C)	Heat load Q (kW)
H1 (reactor effluent)	175	45	(10)	1,300
H2 (bottoms product)	125	65	(40)	2,400
C3 (reactor feed)	20	155	(20)	2,700
C4 (top product)	40	112	(15)	1,080

(b) Pre-processed inlet–outlet data with level shifting (ΔT_{min} = 13°C) for UTA

Stream	Shifted level for inlet $C_{T_{in}}$ (°C)	Shifted level for outlet $C_{T_{out}}$ (°C)	Flow for inlet F_{MC_p} (kW/°C)	Flow for outlet F_{MC_p} (kW/°C)
H1	168.5	38.5	10	–10
H2	118.5	58.5	40	–40
C3	26.5	161.5	20	–20
C4	46.5	118.5	15	–15

$\sum F_{in}\ C_{in}$ = 7,652.5; $\sum F_{out}\ C_{out}$ = –7,732.5; $-\Delta_3$ = 80 kW.

(kW/°C in parenthesis) are easily calculated using Equation [18.1]. The net system parameter for the constant difference between hot and cold utility requirements is first calculated from Equation [18.16] as $Q_{\text{hot utility}} - Q_{\text{cold utility}} = -\Delta_3 = 80$ kW.

Given the Minimum Temperature Driving Force ΔT_{min} (as 13°C), $\Delta T_{min}/2$ (i.e., 6.5°C) is subtracted from hot stream temperatures and $\Delta T_{min}/2$ is added to cold stream temperatures to obtain the two columns for shifted levels in Table 18.2b. The flows (in this case, the Heat capacity flowrate MC_p values with opposite signs) for inlets and outlets are also tabulated in the last two columns of Table 18.2b.

To target the minimum resources (i.e., hot and cold utility in a HEN), the steps for the UTA in Section 18.4.1 are performed as shown in Table 18.3. The shifted level of 118.5°C corresponds to the inlet of stream H2 (40 kW/°C) and the outlet of stream C4 (15 kW/°C). In Step 1, the 118.5°C level is, however, not repeated in the first column. In Step 2, the flow at the 118.5°C level is F = 40 + (–15) = 25 kW/°C. The remaining entries in the second column correspond to either a single inlet or a single outlet. The last entries in the second and third column add to zero, as expected from the first check. In Step 4, the first two intervals yield $m_{net,2}$ = 10 (168.5 – 161.5) = 70 kW and $m_{net,3}$ = –10 (161.5 – 118.5) = –430 kW in the fourth column. The last entry in the fifth column is –80 kW, which tallies with Δ_3 as required by the second check. In

© Woodhead Publishing Limited, 2013

Table 18.3 UTA for four-stream HEN (Case Study 1) at ΔT_{min} = 13°C

Shifted level C (°C)	Flow at level F (kW/°C)	Net flow F_{net} (kW/°C)	Net load m_{net} (kW)	Cumulative load m_{cum} (kW)	Revised load m (kW)	Target flow MC_p (kW/°C)
168.5	10	0	0	0	360	0
161.5	–20	10	70	70	430	–0.854
118.5	25	–10	–430	–360	0	2.88
58.5	–40	15	900	540	900	
46.5	15	–25	–300	240	600	
38.5	–10	–10	–80	160	520	
26.5	20	–20	–240	–80	280	

Targets: hot utility = 360 kW; cold utility = 280 kW; Pinch at 125/112°C; minimum hot-oil flow = 2.88 kW/°C.

Step 6, 360 kW is simply added to every entry in the fifth column (since –360 is the most negative value) to obtain the sixth column. Now, for ΔT_{min} = 13°C, the targets for minimum hot and cold utility loads are 360 and 280 kW (first and last values in the sixth column), which agree with $-\Delta_3 = 360 - 280 = 80$ kW. The level in the first column corresponding to the zero in the sixth column defines the (Process) Pinch at a Shifted Temperature level of 118.5°C (i.e., 125°C for hot streams and 112°C for cold streams). These energy targets from the UTA are identical to those reported by Shenoy (1995) through the PTA.

Consider the use of a hot-oil circuit (as an example of a non-point recirculating utility) with a supply temperature of 250°C to meet the heating demand. Using m_1 = 360 kW (first entry in the sixth column of the UTA table) and C_R = 243.5°C (i.e., 250°C – 6.5°C, the shifted supply temperature) in Equation [18.22], the first three entries in the seventh column of Table 18.3 for the Above Pinch region are obtained as $F_{p,1} = MC_{p,1} = (360 - 360)/(168.5 - 243.5) = 0$, $F_{p,2} = MC_{p,2} = (430 - 360)/(161.5 - 243.5) = -0.854$ and $F_{p,3} = MC_{p,3} = (0 - 360)/(118.5 - 243.5) = 2.88$. The highest of these values specifies the minimum flowrate target for the hot-oil utility with C_p = 2.1 kJ/(kg·°C) as $M = 2.88/2.1 = 1.37$ kg/s. The Process Pinch at 118.5°C continues to limit the hot-oil flowrate and consequently its minimum return temperature to 125°C (i.e., 118.5° + 6.5°).

Plotting the data from Table 18.3 (first column C vs sixth column m), the GCC for Case Study 1 is shown in Fig. 18.3 with the minimum hot utility (as the top horizontal gap of 360 kW), minimum cold utility (as the bottom horizontal gap of 280 kW), and Pinch (level where GCC touches vertical axis at 118.5°C) labelled. The hot oil is also shown in Fig. 18.3 as a dashed sloping line from its supply to target temperature (Pinch, in this case), and provides

© Woodhead Publishing Limited, 2013

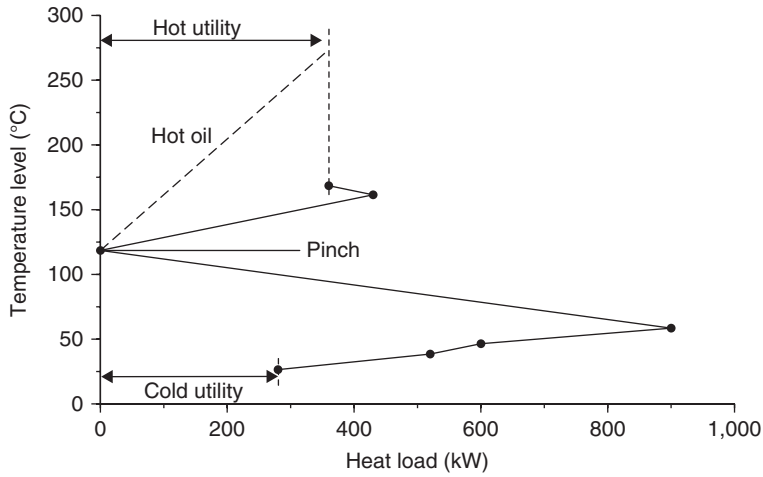

18.3 GCC for four-stream HEN problem (Case Study 1).

an example of a variable-temperature recirculating hot utility matching the Above Pinch portion of the GCC.

18.4.5 Comparison of UTA with Other Targeting Approaches (PTA, CTA)

Figure 18.4 shows the representations used in the various algorithms. The PTA represents each stream by an arrow starting from the inlet level to the outlet level, as in Fig. 18.4a. The CTA represents all inlets (demands) and outlets (sources) as line segments starting from the specified levels to the same (arbitrary) reference level as in Fig. 18.4b. Both the PTA and CTA then calculate the net flow based on the stream population in each interval. One of the main advantages of the UTA is that it does not require drawing of arrows and line segments to determine the stream populations in various intervals, making its representation in terms of inlets–outlets (and demands–sources) at appropriate levels with their corresponding flows a truly tabular approach (Fig. 18.4c). Without loss of generality, the data in Table 18.2 for Case Study 1 are used for concreteness in Fig. 18.4. Since all line segments in Fig. 18.4b end at the same reference level, the net flow in each interval is simply given by the cumulative flow, permitting a straightforward tabular implementation of this calculation (Step 3 in Section 18.4.1) in the UTA. The net flow values in Fig. 18.4 and Table 18.3 (third column) are identical proving the correctness and equivalence (with the PTA/CTA) of the UTA approach. Such a tabular implementation for the flow calculation has been earlier used by Bandyopadhyay and Sahu (2010).

© Woodhead Publishing Limited, 2013

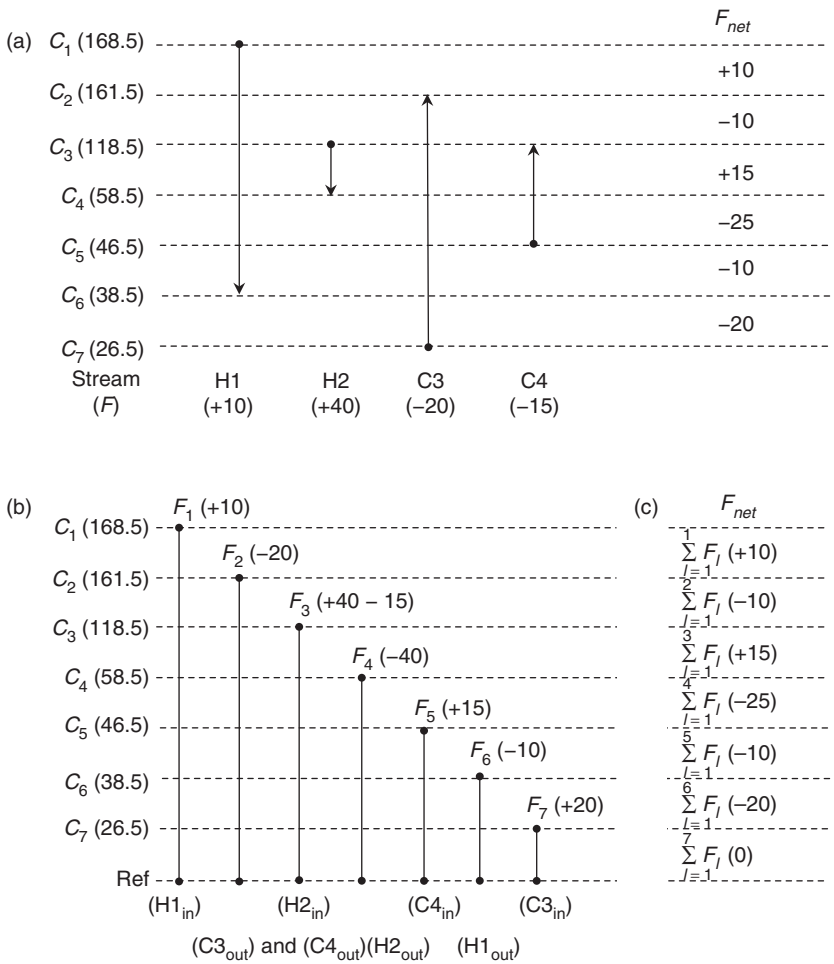

18.4 Comparison of PTA, CTA and UTA for calculation of net flow. (a) Stream arrows in PTA, (b) inlet–outlet (demand–source) line segments in CTA in UTA and (c) tabular representation.

18.5 Heat Exchange Networks (HENs) and Mass Exchange Networks (MENs)

This section illustrates the application of the UTA to exchange networks through first a HEN case study and then a MEN case study.

18.5.1 Organics Distillation Plant Case Study

A utility minimisation problem for an organics distillation plant (Kemp, 2007) is discussed below. The flowsheet (not reproduced here) provided by Kemp (2007) shows details of a cold crude fed to an atmospheric pressure

© Woodhead Publishing Limited, 2013

distillation column and split into three fractions (light oil, middle oil and residue). There are three hot and two cold process streams associated with the HEN of the atmospheric distillation unit (ADU). The residue from the ADU is reheated to become the feed to a vacuum distillation unit (VDU), where heavy oil is drawn part way up the column and cooled. Thus, there is just one hot (H4) and one cold (C3) process stream associated with the HEN of the VDU. Shenoy (2011) has demonstrated the UTA to establish targets for the ADU taken separately. Here, the UTA is illustrated for the combined atmospheric and vacuum units comprising four hot and three cold process streams as given in Table 18.4a for Case Study 2. Streams H3 (hot overheads) and C1 (cold crude feed), whose heat capacity flowrates MC_p are significantly temperature-dependent, are divided into segments (in this case, two segments each). Using Equation [18.16], $Q_{\text{hot utility}} - Q_{\text{cold utility}} = -\Delta_3 = 4{,}090$ kW.

Table 18.4 Data for organics distillation HEN problem (Case Study 2)

(a) original stream data

Stream	Inlet temperature T_{in} (°C)	Outlet temperature T_{out} (°C)	Heat capacity flowrate MC_p (kW/°C)	Heat load Q (kW)
H1 (bottoms)	261	158	(10)	1,030
H2 (middle oil)	199	70	(10)	1,290
H3A (overheads)	123	112	(80)	880
H3B (overheads)	112	52	(30)	1,800
H4 (vacuum crude)	151	67	(12.5)	1,050
C1A (crude feed)	20	103	(23.072)	1,915
C1B (crude feed)	103	180	(27.078)	2,085
C2 (dehydrate)	152	302	(30)	4,500
C3 (heavy oil draw)	155	319	(10)	1,640

(b) pre-processed inlet–outlet data with level shifting ($\Delta T_{\text{min}} = 20$°C) for UTA

Stream	Shifted level for inlet $C_{T_{\text{in}}}$ (°C)	Shifted level for outlet $C_{T_{\text{out}}}$ (°C)	Flow for inlet F_{MC_p} (kW/°C)	Flow for outlet F_{MC_p} (kW/°C)
H1	251	148	10	–10
H2	189	60	10	–10
H3A	113	102	80	–80
H3B	102	42	30	–30
H4	141	57	12.5	–12.5
C1A	30	113	23.072	–23.072
C1B	113	190	27.078	–27.078
C2	162	312	30	–30
C3	165	329	10	–10

$\sum F_{\text{in}}\, C_{\text{in}} = 28{,}524.474$; $\sum F_{\text{out}}\, C_{\text{out}} = -32{,}614.474$; $-\Delta_3 = 4{,}090$ kW.

© Woodhead Publishing Limited, 2013

The stream data in Table 18.4a are pre-processed and converted to inlet–outlet data in Table 18.4b. With the Minimum Temperature Driving Force specified as ΔT_{min} = 20°C, the Shifted Temperature levels are obtained by subtracting $\Delta T_{min}/2$ (i.e., 10°C) from all hot stream temperatures and adding $\Delta T_{min}/2$ to all cold stream temperatures. The MC_p values are tabulated with positive values for inlets and negative for outlets.

On implementing the steps for the UTA described in Section 18.4.1 (in decreasing-level sort order), Table 18.5 yields the energy targets at ΔT_{min} = 20°C to be 6,085 kW for minimum hot utility and 1,995 kW for minimum cold utility (in accordance with $-\Delta_3$ = 6,085 – 1,995 = 4,090 kW), with the Process Pinch at a Shifted Temperature level of 113°C (i.e., 123°C for hot streams and 103°C for cold streams). The targets agree with those obtained by Kemp (2007) through the PTA.

Now, consider the use of a Combined Heat and Power (CHP) system to generate power while simultaneously providing the hot utility through a typical gas turbine exhaust (as an example of a non-point once-through utility) with an exhaust gas temperature of 500°C. Using m_1 = 6,085 kW (first entry in the sixth column of the UTA table) and C_R = 460°C (i.e., 500°C – 40°C, the shifted exhaust temperature based on a higher ΔT_{min} of 50°C for a gas stream match) in Equation [18.22], the first three entries in the seventh column of Table 18.5 for the Above Pinch region are obtained as $F_{p,1} = MC_{p,1}$ = (6,085 – 6,085)/(329 – 460) = 0, $F_{p,2} = MC_{p,2}$ = (5,915 – 6,085)/(312 – 460) = 1.149 and

Table 18.5 UTA for organics distillation HEN (Case Study 2) at ΔT_{min} = 20°C

Shifted level C (°C)	Flow at level F (kW/°C)	Net flow F_{net} (kW/°C)	Net load m_{net} (kW)	Cumulative load m_{cum} (kW)	Revised load m (kW)	Target flow MC_p (kW/°C)
329	–10	0	0	0	6,085	0
312	–30	–10	–170	–170	5,915	1.149
251	10	–40	–2440	–2,610	3,475	12.488
190	–27.078	–30	–1830	–4,440	1,645	16.444
189	10	–57.078	–57.078	–4,497.078	1,587.922	16.594
165	10	–47.078	–1,129.870	–5,626.948	458.052	19.074
162	30	–37.078	–111.234	–5,738.182	346.818	19.256
148	–10	–7.078	–99.091	–5,837.273	247.727	18.709
141	12.5	–17.078	–119.545	–5,956.818	128.182	18.673
113	84.006	–4.578	–128.182	–6,085	0	17.536
102	–50	79.428	873.705	–5,211.295	873.705	
60	–10	29.428	1,235.964	–3,975.331	2,109.669	
57	–12.5	19.428	58.283	–3,917.048	2,167.952	
42	–30	6.928	103.916	–3,813.133	2,271.867	
30	23.072	–23.072	–276.867	–4,090	1,995	

Targets: hot utility = 6,085 kW; cold utility = 1,995 kW; Pinch at 123/103°C; minimum MC_P of exhaust gases from gas turbine = 19.256 kW/°C.

© Woodhead Publishing Limited, 2013

$F_{p,3} = MC_{p,3}$ = (3,475 – 6,085)/(251 – 460) = 12.488. The highest value ($F_{p,7} = MC_{p,7}$ = (346.818 – 6,085)/(162 – 460) = 19.256 kW/°C) in the last column specifies the minimum flowrate target for the exhaust gas with C_p = 1.1 kJ/(kg·°C) as M = 19.256/1.1 = 17.5 kg/s. The level in the first column corresponding to the highest value of 19.256 kW/°C specifies a new Utility Pinch at 162°C. The heat released by the exhaust gas over the temperature range 500°C – 20°C is 9,242.7 kW (i.e., 19.256 (500°C – 20°C)), which consists of 6,085 kW of useful heat (from 500°C to 184°C) and 3,157.7 kW of waste heat (from 184°C to 20°C). Taking an average performance (30% power-generation efficiency and 4% heat losses assumed) of a typical gas turbine for initial sizing purposes (Kemp, 2007), the heat released is 66% of the fuel used. Thus, the total heat input is 14,004.1 kW (i.e., 9,242.7/0.66) comprising 4,201.2 kW of power (30%), 6,085 kW of useful heat, 3,157.7 kW of waste heat and 5,60.2 kW of heat losses (4%).

On plotting the first column for C against the sixth column for m from Table 18.5, the GCC in Fig. 18.5 is obtained with the minimum hot utility (as the top horizontal gap of 6,085 kW), minimum cold utility (as the bottom horizontal gap of 1,995 kW) and Process Pinch (level where GCC touches vertical axis at 113°C). The gas turbine exhaust is also shown in Fig. 18.5 as a dashed sloping line from the exhaust to ambient temperature, and provides an example of a variable-temperature once-through hot utility matching the Above Pinch portion of the GCC. The minimum gas flow for a given exhaust temperature is obtained when the gas turbine exhaust profile just touches the GCC at or above the Process Pinch. In this case, the shape of the GCC

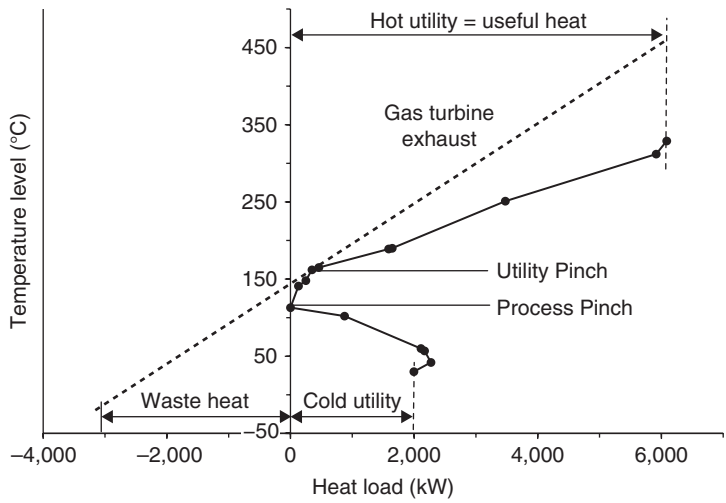

18.5 GCC for organics distillation HEN problem (Case Study 2).

© Woodhead Publishing Limited, 2013

causes the exhaust profile to touch it above the Process Pinch and creates a new Utility Pinch at 162°C, which limits the gas flowrate.

18.5.2 Transformation of MEN Problem into Equivalent HEN Problem

A MEN problem can be transformed into an equivalent HEN problem along the lines originally suggested by Shenoy (1995) as discussed below. Equation [18.2] is the Operating Line equation for mass exchange. The aim is to reduce the rich stream composition from y_{in} to y_{out}, and maximise the lean stream composition (x_{out} if x_{in} is specified, and vice versa) by varying L/G. The maximum is theoretically achieved when the Operating Line touches the Equilibrium Line, which requires an infinitely large exchanger. Consequently, a minimum composition difference (ε based on the lean phase or Δy_{min} based on the rich phase) is necessary between the Operating and Equilibrium Lines in practice. If a linear equilibrium relationship (say, $y = K\,x + b$) for the distribution of the key component among the various streams holds over the operating range or its subintervals, then the minimum allowable composition difference may be mathematically expressed as:

$$y - \Delta y_{min} = K(x + \varepsilon) + b \qquad [18.23]$$

Letting $T_y = y$ and $T_x = K(x + \varepsilon) + b - \varepsilon$ yields $T_y - \Delta y_{min} = T_x + \varepsilon$. This equation has the form $T_{hot} - \Delta T_{h,min} = T_{cold} + \Delta T_{c,min}$ as in HENs (where the equilibrium relationship is $T_{hot} = T_{cold}$, and the driving force is $\Delta T_{min} = \Delta T_{h,min} + \Delta T_{c,min}$ in terms of the individual hot and cold stream ΔT contributions). Equation [18.2] may be now rewritten as:

$$G\,(T_{in,y} - T_{out,y}) = (L/K)\,(T_{out,x} - T_{in,x}) \qquad [18.24]$$

Next, letting $MC_{p,G} = G$ and $MC_{p,L} = L/K$ yields an equation identical in form to the heat-load balance in a HEN problem given by Equation [18.1]. In essence, the given MEN problem is transformed into an equivalent HEN problem when the inlet/outlet compositions and flowrates of all lean process streams/MSAs are transformed using the following:

$$T_x = K(x + \varepsilon) + b - \varepsilon \qquad [18.25]$$

$$MC_{P,L} = \frac{L}{K} \qquad [18.26]$$

© Woodhead Publishing Limited, 2013

The calculations can be performed for two distinct cases: specified Δy_{min} or specified ε. The minimum composition differences based on the rich phase (Δy_{min}) and lean phase (ε) are related to each other as follows (Hallale, 1998):

$$\Delta y_{min} = K\,\varepsilon \qquad [18.27]$$

Now, the values of K vary for the different lean streams/MSAs. So, if Δy_{min} has a specified value, then each lean stream/MSA effectively has a different value of ε. Conversely, if ε has a specified value, then each lean stream/MSA has a different value of Δy_{min}.

18.5.3 Coke Oven Gas (COG) Sweetening Case Study

A problem of targeting MSAs in a MEN based on the COG sweetening process presented by El-Halwagi and Manousiouthakis (1989) is used as Case Study 3 here. The aim of the process is to remove hydrogen sulphide from two rich streams (the sour COG stream R1 and the tail gases stream R2 from a Claus unit) using a lean process stream (the aqueous ammonia stream S1, which is the process MSA available from within the process) and an external MSA (the chilled methanol stream S2 purchased from outside). Mass transfer of hydrogen sulphide is governed by the following equilibrium solubility relations: $y = 1.45\,x_1$ (in aqueous ammonia S1) and $y = 0.26\,x_2$ (in chilled methanol S2). The data for the two rich process streams and the two MSAs are given in Table 18.6a. Using Equation [18.16], the constant difference between process MSA excess and external MSA is given by $m_{\text{process MSA excess}} - m_{\text{external MSA}} = -\Delta_3 = 0.0021$ kg/s.

As in HENs, the stream data in Table 18.6a is pre-processed to obtain the inlet–outlet data in Table 18.6b for the specified ε of 0.0001. First, lean stream data are transformed using Equations [18.25] and [18.26], whereas rich stream data are left untransformed. To obtain shifted levels in Table 18.6b, $\varepsilon/2$ (or $\Delta y_{min}/2$) is subtracted from rich stream compositions and $\varepsilon/2$ (or $\Delta y_{min}/2$) is added to lean stream transformed compositions. Then, the flow values (for G and L/K) are tabulated with positive sign for inlets and negative sign for outlets.

The steps for the UTA in Section 18.4.1 are next implemented in decreasing-level sort order to obtain Table 18.7. For $\varepsilon = 0.0001$, the targets are 0.002835 kg/s for excess capacity of process MSA and 0.000735 kg/s for minimum mass load requirement of external MSA (first and last entries in the sixth column), which agree with $-\Delta_3 = 0.002\,835 - 0.000\,735 = 0.0021$ kg/s. The level in the first column corresponding to the zero in the sixth column defines the Pinch at a shifted composition level of 0.000965 (i.e., 0.001015

© Woodhead Publishing Limited, 2013

Table 18.6 Data for COG sweetening MEN problem (Case Study 3)

(a) Original stream data

Stream	Inlet composition	Outlet composition	Mass flowrate
Rich stream	y_{in} (mass ratio)	y_{out} (mass ratio)	G (kg/s)
R1 (sour COG)	0.0700	0.0003	0.9
R2 (tail gases)	0.0510	0.0001	0.1
Lean stream	x_{in} (mass ratio)	x_{out} (mass ratio)	L (kg/s)
S1 (aqueous ammonia)	0.0006	0.0310	2.3
S2 (chilled methanol)	0.0002	0.0035	∞

Equilibrium function $y = K\,x + b$: $K = 1.45$ and $b = 0$ (for S1); $K = 0.26$ and $b = 0$ (for S2).

(b) Pre-processed inlet–outlet data with level shifting ($\varepsilon = 0.0001$) for UTA

	Shifted level for inlet $C_{yin\ or\ xin}$	Shifted level for outlet $C_{yout\ or\ xout}$	Flow for inlet $F_{G\ or\ L}$ (kg/s)	Flow for outlet $F_{G\ or\ L}$ (kg/s)
R1	0.06995	0.00025	0.9	–0.9
R2	0.05095	0.00005	0.1	–0.1
S1	0.000965	0.045045	1.5862	–1.5862

$\sum F_{in}\ C_{in} = 0.06958$; $\sum F_{out}\ C_{out} = -0.07168$; $-\Delta_3 = 0.0021$ kg/s.

Table 18.7 UTA for COG sweetening MEN (Case Study 3) at $\varepsilon = 0.0001$

Shifted level C	Flow at level F (kg/s)	Net flow F_{net} (kg/s)	Net load m_{net} (kg/s)	Cumulative load m_{cum} (kg/s)	Revised load m (kg/s)
0.06995	0.9	0	0	0	0.002835
0.05095	0.1	0.9	0.0171	0.0171	0.019935
0.045045	–1.5862	1	0.005905	0.023005	0.02584
0.000965	1.5862	–0.5862	–0.02584	–0.002835	0
0.00025	–0.9	1	0.000715	–0.00212	0.000715
0.00005	–0.1	0.1	0.00002	–0.0021	0.000735

Targets: process MSA excess = 0.002835 kg/s; external MSA = 0.000735 kg/s; Pinch at 0.000965.

for rich streams, and 0.0006 for S1 after inverse transformation for the lean stream). Thus, the minimum flowrate of the external MSA S2 required is 0.2227 kg/s (i.e., 0.000735/(0.0035 – 0.0002)) using the specified inlet and outlet compositions of S2. Further, the reduced flowrate of the process MSA S1 compatible with the minimum S2 flowrate is 2.2067 kg/s (i.e., 2.3 – 0.002835/(0.031 – 0.0006)) using the specified inlet and outlet compositions

© Woodhead Publishing Limited, 2013

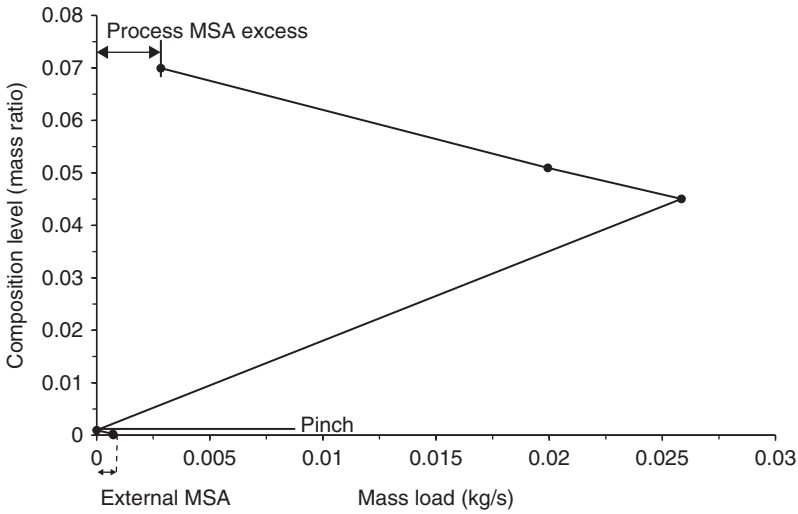

18.6 GCC for COG sweetening MEN problem (Case Study 3).

of S1. Note that the seventh column for the target flow is not necessary in this case because the outlet compositions of the MSAs are specified. These targets from the UTA agree with those obtained through the CIT by El-Halwagi and Manousiouthakis (1989). On plotting the first column for C against the sixth column for m from the UTA table, the GCC (Fig. 18.6) is obtained. A MEN case study on the dephenolisation of aqueous wastes that uses a minimum composition difference $\Delta y_{\min}$ based on the rich phase (rather than ε based on the lean phase) is discussed by Shenoy (2011).

18.6 Water Networks: Case Study of a Specialty Chemical Plant

The problem of minimising freshwater consumption and wastewater discharge in a practical water system for a specialty chemical plant (Wang and Smith, 1995) is explained below. The limiting data for five water-using processes are given in Table 18.8 for Case Study 4. The reactor (P1) and Cooling System (P5) show water losses, whereas the filtration process (P3) shows a water gain. The system involves a single contaminant, where FF and FC problems are equivalent (Foo, 2009). The data in Table 18.8 are consistent with $m = F_{\text{in}}\,(C_{\text{out}} - C_{\text{in}})$, which is a form of Equation [18.3], as well as $F_{\text{out}} = F_{\text{in}} \pm F_{gain/loss}$, which assumes the water gain/loss to totally occur at the outlet of each process (Deng and Feng, 2009). Using Equation [18.14] with the data in Table 18.8, the constant difference between the freshwater and wastewater flows is given by $F_R - F_E = F_{\text{freshwater}} - F_{\text{wastewater}} = \Delta_1 = 40$ t/h (which

© Woodhead Publishing Limited, 2013

Table 18.8 Data for specialty chemical plant water network (Case Study 4)

Water-using process	Inlet concentration C_{in} (ppm)	Outlet concentration C_{out} (ppm)	Inlet flowrate F_{in} (t/h)	Outlet flowrate F_{out} (t/h)	Mass load m (kg/h)
P1 (reactor)	100	1000	80	(–)20	72
P2 (cyclone)	200	700	50	(–)50	25
P3 (filtration)	0	100	10	(–)40	1
P4 (steam system)	0	10	10	(–)10	0.1
P5 (Cooling System)	10	100	15	(–)5	1.35

$\sum F_{in} = 165$; $\sum F_{out} = (-)125$; $\Delta_1 = 40$ t/h.
$\sum F_{in}\, C_{in} = 18.15$; $\sum F_{out}\, C_{out} = (-)59.6$; $\Delta_2 = -41.45$ kg/h.

Table 18.9 UTA for specialty chemical plant water network (Case Study 4)

Level C (ppm)	Flow at level F (t/h)	Net flow F_{net} (t/h)	Net load m_{net} (kg/h)	Cumulative load m_{cum} (kg/h)	Revised load m (kg/h)	Target flow (t/h)
0	20	0	0	0	0	–
10	5	20	0.2	0.2	0.2	20
100	35	25	2.25	2.45	2.45	24.5
200	50	60	6	8.45	8.45	42.25
700	–50	110	55	63.45	63.45	90.643
1000	–20	60	18	81.45	81.45	81.45
(1100)	0	40	(4)	(85.45)	(85.45)	(77.682)

Targets: freshwater = 90.643 t/h (at 0 ppm); wastewater = 50.643 t/h (at 818.48 ppm); Pinch at 700 ppm.

is the total system water flow deficit). Using Equation [18.15], $(FC)_{freshwater} - (FC)_{wastewater} = \Delta_2 = -41.45$ kg/h.

Water networks require neither pre-processing (as the data are already in the inlet–outlet form in Table 18.8) nor level shifting (as the limiting water data already incorporate the necessary driving forces in case of mass transfer). Therefore, the steps for the UTA described in Section 18.4.1 may be directly implemented in increasing-level sort order to obtain Table 18.9. The highest value in the last column specifies the freshwater target as $F_R = F_{freshwater} = 90.643$ t/h and the corresponding contaminant concentration determines the Pinch (700 ppm). Since $F_R = F_{freshwater} = 90.643$ t/h and $C_R = C_{freshwater} = 0$, Equations [18.14] and [18.15] give $F_E = F_{wastewater} = 90.643 - 40 = 50.643$ t/h and $C_E = C_{wastewater} = -(-41.45/50.643) \times 10^3 = 818.48$ ppm. The Pinch at 700 ppm identifies the outlet from the cyclone (P2) to be the Pinch-causing source (as per Table 18.8) with its distribution target in the allocation network being 19.357 t/h (i.e., 110 – 90.643) for the Below Pinch portion

© Woodhead Publishing Limited, 2013

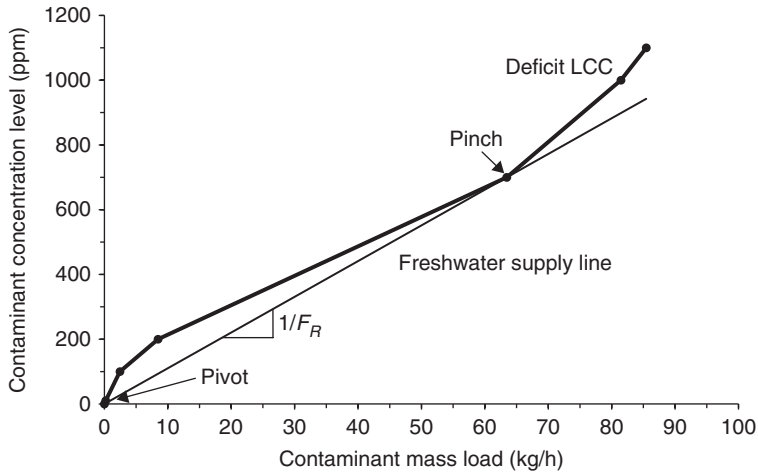

18.7 LCC for specialty chemical plant water network (Case Study 4).

and the remainder of 30.643 t/h (i.e., 50 – 19.357) for the Above Pinch portion. The Below Pinch portion is obtained as the difference between 110 t/h (i.e., the net flow at the 700 ppm Pinch level from the third column in Table 18.9) and 90.463 t/h (the minimum freshwater target F_R).

Plotting the first column for C against the sixth column for m in the UTA Table gives the LCC. Specifically, the Deficit LCC in Fig. 18.7 (obtained from the UTA Table in increasing-level sort order) allows targeting of the minimum freshwater (by rotating a horizontal line with the pivot at the origin for freshwater at 0 ppm). In general, the Deficit LCC can be used to target regeneration–reuse, regeneration–recycle and zero discharge systems (Agrawal and Shenoy, 2006; Deng *et al.*, 2008). Shenoy (2011) illustrates the application of the UTA for an alumina plant (Deng and Feng, 2009), which is a hybrid water system with both FF and FC processes, all suffering water losses.

18.7 Hydrogen and Other Gas Networks

This section applies the UTA to networks involving various gases such as hydrogen, nitrogen, oxygen and carbon emissions.

18.7.1 Refinery Hydrogen Network Case Study

Hydrogen, an expensive and essential resource (Hallale *et al.*, 2002) in crude oil refining and petrochemicals processing, is used in processes such as reforming, hydrocracking and hydrotreating. It is utilised to hydrogenate

© Woodhead Publishing Limited, 2013

aromatics and olefins, upgrade heavy hydrocarbons to lighter ones, and reduce sulphur content in fuels. This subsection discusses the problem of minimising hydrogen consumption (Hallale and Liu, 2001). Every hydrogen-consuming process typically has a makeup, recycle and purge. From a Process Integration perspective, each hydrogen demand (inlet to process) consists of a makeup and recycle taken together, whereas each hydrogen source (outlet from process) comprises the purge and recycle in total. The makeup hydrogen supply from a hydrogen plant or import is the high-quality resource R, while the purge streams (analogous to wastewater sent to effluent treatment) often sent to a fuel system where they are burned for their heating value or flared are the low-quality waste/excess E. Hydrogen and water are both allocation networks with similar overall data representations (Agrawal and Shenoy, 2006) in terms of demands and sources; so, the procedure in the previous section is adapted with the hydrogen purity fraction (y) treated in terms of equivalent contaminant concentration (C) using $C \equiv 1 - y$. Note that the water supply is often freshwater with 0 ppm contaminant concentration (i.e., $C_R = 0$), whereas the fresh makeup hydrogen supply is not available at 100% purity (i.e., $C_R = 1 - y_R \neq 0$). Pre-processing may be done to convert the hydrogen purity (y) data to equivalent contaminant concentration (C) data; then, the UTA may be applied with increasing-level sort order to target and obtain the Deficit LCC (Shenoy, 2011). Here, the UTA is applied in decreasing-level sort order directly on the hydrogen purity (y) data without pre-processing or conversion to equivalent contaminant concentration (C) data to target and obtain the Deficit LCC.

The process data (Alves and Towler, 2002) for a refinery are given in Table 18.10. Case Study 5 consists of four internal demands and four internal sources of hydrogen related to various processes: hydrocracking unit (HCU), straight-run naphtha hydrotreater (NHT), diesel hydrotreater (DHT) and cracked naphtha hydrotreater (CNHT). Two more internal sources, whose

Table 18.10 Data for refinery hydrogen network (Case Study 5)

Hydrogen-using process	Demand purity y_d (fraction)	Source purity y_s (fraction)	Demand flowrate F_d (mol/s)	Source flowrate F_s (mol/s)
–, S1 (SRU)		0.93		(–)623.8
–, S2 (CRU)		0.80		(–)415.8
D1, S3 (HCU)	0.8061	0.75	2495	(–)1,801.9
D2, S4 (NHT)	0.7885	0.75	180.2	(–)138.6
D3, S5 (DHT)	0.7757	0.73	554.4	(–)346.5
D4, S6 (CNHT)	0.7514	0.70	720.7	(–)457.4

$\sum F_d = 3{,}950.3$; $\sum F_s = (–)3{,}784$; $\Delta_1 = 166.3$ mol/s.
$\sum F_d\, y_d = 3{,}124.88926$; $\sum F_s\, y_s = (–)2{,}941.274$; $\Delta_2 = 183.615$ mol/s.
$\Delta_{2y} = \Delta_1 - \Delta_{2C} = 166.3 - (–17.315) = 183.615$ mol/s.

© Woodhead Publishing Limited, 2013

Table 18.11 UTA for refinery hydrogen network (Case Study 5)

Level y (fraction)	Flow at level F (mol/s)	Net flow F_{net} (mol/s)	Net load m_{net} (mol/s)	Cumulative load m_{cum} (mol/s)	Revised load m (mol/s)	Target flow (mol/s)
0.93	–623.8	0	0	0	77.2888	0
0.8061	2,495	–623.8	–77.2888	–77.2888	0	–537.101
0.80	–415.8	1,871.2	11.4143	–65.8745	11.4143	–439.163
0.7885	180.2	1,455.4	16.7371	–49.1374	28.1514	–304.256
0.7757	554.4	1,635.6	20.9357	–28.2017	49.0871	–161.8
0.7514	720.7	2,190	53.217	25.0153	102.3041	125.958
0.75	–1,940.5	2,910.7	4.0750	29.0903	106.3791	145.451
0.73	–346.5	970.2	19.404	48.4943	125.7831	220.428
0.70	–457.4	623.7	18.711	67.2053	144.4941	268.821
(0.65)	0	166.3	(8.315)	(75.5203)	(152.8091)	(251.734)

Targets: hydrogen makeup = 268.821 t/h (at 95% purity); hydrogen to fuel = 102.521 t/h (at 70% purity); Pinch at 70% purity.

use has to be maximised before purchasing fresh makeup hydrogen supply (at a purity of 95% or $y_R = 0.95$), are the hydrogen-producing facilities associated with the steam reforming unit (SRU) and the catalytic reforming unit (CRU).

Since the data for hydrogen networks are in the demand–source form, the UTA may be directly implemented on the hydrogen purity (y) data without pre-processing (i.e., without conversion to equivalent contaminant concentration (C) data and without level shifting) to obtain Table 18.11. Note that the level data in the first column of the UTA must be in decreasing order if hydrogen purity (y) is used or increasing order if contaminant concentration (C) is used. The makeup hydrogen target is $F_R = F_{\text{makeup}} = 268.821$ mol/s (highest value in the last column of Table 18.11) and the corresponding level specifies the Pinch at a hydrogen purity of 70% (i.e., $y_P = 0.7$). Using Equations [18.14] and [18.15] with the data in Table 18.10, $F_R - F_E = F_{\text{makeup}} - F_{\text{fuel}} = \Delta_1 = 166.3$ mol/s and $F_R\, y_R - F_E\, y_E = (Fy)_{\text{makeup}} - (Fy)_{\text{fuel}} = \Delta_2 = 183.615$ mol/s (in terms of hydrogen purity y). Since $F_R = F_{\text{makeup}} = 268.821$ mol/s and $y_R = y_{\text{makeup}} = 0.95$, Equations [18.14] and [18.15] yield $F_E = F_{\text{fuel}} = 268.821 - 166.3 = 102.521$ mol/s and $y_E = y_{\text{fuel}} = (268.821 \times 0.95 - 183.615)/102.521 = 0.7$.

The Pinch at 70% hydrogen purity identifies S6 (the CNHT outlet) to be the Pinch-causing source (as per Table 18.10). The distribution target for S6 in the allocation network is 354.879 mol/s (i.e., 623.7 – 268.821) for the Below Pinch portion and the remainder of 102.521 mol/s (i.e., 457.4 – 354.879) for the Above Pinch portion.

Although the UTA uses hydrogen purity y, the LCC (obtained using y vs m data from Table 18.11) in Fig. 18.8 plots $C \equiv 1 - y$ vs m to make it

© Woodhead Publishing Limited, 2013

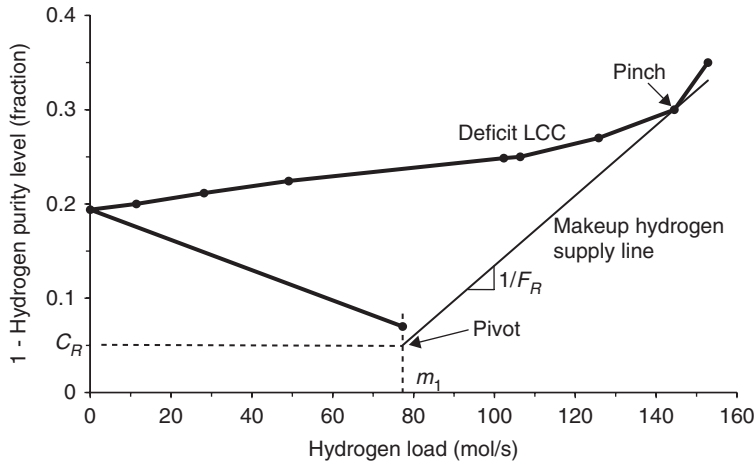

18.8 LCC for refinery hydrogen network (Case Study 5).

analogous to the LCC for water in Fig. 18.7. This Deficit LCC allows graphic visualisation and targeting of the minimum makeup hydrogen supply to be imported. Note the pivot location in Fig. 18.8 is unusual because it is neither on the vertical/horizontal axis nor at the origin. The reciprocal of the slope of the rotated target line gives the hydrogen makeup target, and the point where the target profile touches the LCC defines the hydrogen Utility Pinch Point. Shenoy (2011) has solved the same case study in terms of contaminant concentration C (rather than hydrogen purity y as done here) and shown how the Surplus LCC (not shown here) allows targeting of the hydrogen sent to fuel.

18.7.2 Nitrogen Network Case Study

The minimum utility flowrate targeting (through maximum reuse/recycle) of a nitrogen gas network for a magnetic tape manufacturing plant (El-Halwagi, 1997) is presented in this subsection. The Process Flow Diagram (not reproduced here for conciseness) provided by El-Halwagi (1997) shows two demands where nitrogen gas is used to evaporate an organic solvent during coating on a base film and drying of the coated film. The two sources are the exhaust gas stream after drying and the retentate stream leaving the membrane unit. The limiting data (Foo and Manan, 2006) in terms of flowrate F (kg/s) and organic solvent concentration C (wt/wt %) for Case Study 6 are given in Table 18.12. Using Equations [18.14] and [18.15] with the data in Table 18.12, $F_R - F_E = F_{\text{makeup}} - F_{\text{discharge}} = \Delta_1 = 0$ and $F_R\, C_R - F_E\, C_E = (FC)_{\text{makeup}} - (FC)_{\text{discharge}} = \Delta_2 = -6.75 \times 10^{-2}$ kg/s.

© Woodhead Publishing Limited, 2013

Table 18.12 Data for magnetic tape plant nitrogen network (Case Study 6)

Nitrogen-using process	Demand concentration C_d (wt/wt %)	Source concentration C_s (wt/wt %)	Demand flowrate F_d (kg/s)	Source flowrate F_s (kg/s)
D1, S1 (drying)	0.1	0.4	5.5	(–)5.5
D2, S2 (coating/ membrane)	0.2	1.9	3	(–)3

$\sum F_d = 8.5$; $\sum F_s = (-)8.5$; $\Delta_1 = 0$.

$\sum F_d\, C_d = 1.15$; $\sum F_s\, C_s = (-)7.9$; $\Delta_2 = -6.75 \times 10^{-2}$ kg/s.

Table 18.13 UTA for magnetic tape plant nitrogen network (Case Study 6)

Level C (wt/wt %)	Flow at level F (kg/s)	Net flow F_{net} (kg/s)	Net load m_{net} (10^{-2} kg/s)	Cumulative load m_{cum} (10^{-2} kg/s)	Revised load m (10^{-2} kg/s)	Target flow (kg/s)
0.1	5.5	0	0	0	0	0
0.2	3	5.5	0.55	0.55	0.55	2.75
0.4	–5.5	8.5	1.7	2.25	2.25	5.625
1.9	–3	3	4.5	6.75	6.75	3.553
(2)	0	0	0	6.75	6.75	(3.375)

Targets: nitrogen makeup = 5.625 kg/s; nitrogen discharge = 5.625 t/h (at 1.2 wt/wt %); Pinch at 0.4 wt/wt %.

Since the data are in the demand–source form, the UTA may be directly implemented (without pre-processing) in increasing-level sort order for solvent concentration C to obtain Table 18.13. The minimum flowrate target for fresh makeup nitrogen gas (solvent-free with $C_R = 0$) is $F_R = F_{\text{makeup}} =$ 5.625 kg/s (highest value in the last column of Table 18.13) and the corresponding level specifies the Pinch at a solvent concentration of 0.4%. Equations [18.14] and [18.15] now yield $F_E = F_{\text{discharge}} = 5.625$ kg/s and $C_E = C_{\text{discharge}} = -(-6.75)/5.625 = 1.2$ wt/wt %. The Pinch at 0.4 wt/wt % identifies S1 (the drying outlet) to be the Pinch-causing source (as per Table 18.12). The distribution target for S1 in the allocation network is 2.875 kg/s (i.e., 8.5 – 5.625) for the Below Pinch portion and the remainder of 2.625 kg/s (i.e., 5.5 – 2.875) for the Above Pinch portion. The LCC (obtained using C vs m data from Table 18.13) in Fig. 18.9 shows graphical targeting of the minimum makeup nitrogen supply (as the reciprocal of the slope of the rotated target line using the origin as pivot) and the Pinch Point (where the target profile touches the LCC). As observed by Shenoy (2011), the LCC is unique (i.e., the Deficit LCC and Surplus LCC are identical in principle) and the UTA does not really depend on the level sort order used (increasing or decreasing) because $\Delta_1 = 0$ for this problem.

© Woodhead Publishing Limited, 2013

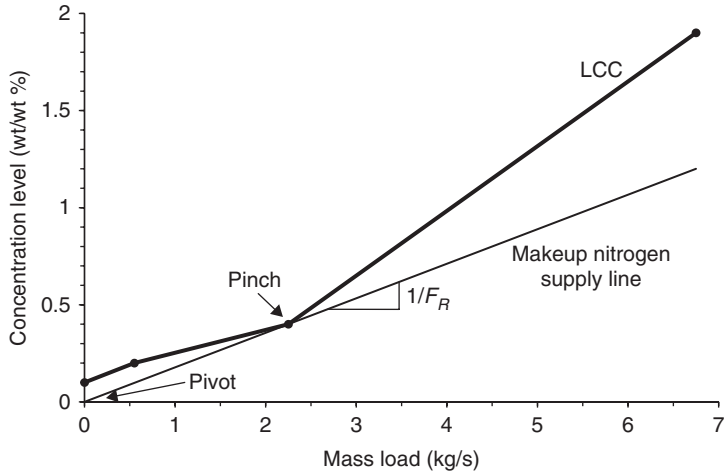

18.9 LCC for magnetic tape plant nitrogen network (Case Study 6).

18.7.3 Oxygen Network Case Study

The minimum utility flowrate targeting (through maximum reuse/recycle) of an oxygen gas network for possible site-wide integration between process and utility sections (Foo and Manan, 2006) is briefly dealt with in this subsection. The Process Flow Diagram (not shown) provided by Foo and Manan (2006) shows four demands (two oxidation processes, the combustion system, and the aerobic section of the wastewater treatment plant) and two sources (two oxidation processes). The limiting data in terms of flowrate F (kg/s) and impurity concentration C (wt/wt %) for Case Study 7 are given in Table 18.14. Using Equations [18.14] and [18.15] with this data, $F_R - F_E = F_{\text{makeup}} - F_{\text{discharge}} = \Delta_1 = 26$ kg/s and $F_R\, C_R - F_E\, C_E = (FC)_{\text{makeup}} - (FC)_{\text{discharge}} = \Delta_2 = 90 \times 10^{-2}$ kg/s.

As in the nitrogen network problem, the data are in the demand–source form and the UTA may be directly implemented (without pre-processing) in increasing-level sort order for impurity concentration C to obtain Table 18.15. The minimum flowrate target for fresh makeup oxygen gas (with 5% impurity or $C_R = 5\%$) is $F_R = F_{\text{makeup}} = 30$ kg/s (highest value in the last column of Table 18.15) and the corresponding level specifies the Pinch at an impurity concentration of 40%. Equations [18.14] and [18.15] now yield $F_E = F_{\text{discharge}} = 4$ kg/s and $C_E = C_{\text{discharge}} = (30 \times 5 - 90)/4 = 15$ wt/wt %. The Pinch at 40 wt/wt % identifies S1 (the outlet of oxidation process 1) to be the Pinch-causing source (as per Table 18.14). The distribution target for S1 in the allocation network is 5 kg/s (i.e., 35 – 30) for the Below Pinch portion and the remainder of 5 kg/s (i.e., 10 – 5) for the Above Pinch portion. The

© Woodhead Publishing Limited, 2013

Table 18.14 Data for oxygen network (Case Study 7)

Oxygen-using process	Demand concentration C_d (wt/wt %)	Source concentration C_s (wt/wt %)	Demand flowrate F_d (kg/s)	Source flowrate F_s (kg/s)
D1, S1 (oxidation process 1)	10	40	25	(–)10
D2, S2 (oxidation process 2)	10	50	10	(–)5
D3 (combustion)	65		4	
D4 (wastewater treatment)	65		2	

$\sum F_d = 41$; $\sum F_s = (-)15$; $\Delta_1 = 26$ kg/s.
$\sum F_d C_d = 740$; $\sum F_s C_s = (-)650$; $\Delta_2 = 90 \times 10^{-2}$ kg/s.

Table 18.15 UTA for oxygen network (Case Study 7)

Level C (wt/wt %)	Flow at level F (kg/s)	Net flow F_{net} (kg/s)	Net load m_{net} (10^{-2} kg/s)	Cumulative load m_{cum} (10^{-2} kg/s)	Revised load m (10^{-2} kg/s)	Target flow (kg/s)
10	35	0	0	0	0	0
40	–10	35	1,050	1,050	1,050	30
50	–5	25	250	1,300	1,300	28.89
65	6	20	300	1,600	1,600	26.67
(70)	0	26	130	1,730	1,730	(26.62)

Targets: oxygen makeup = 30 kg/s (at 5 wt/wt %); oxygen discharge = 4 t/h (at 15 wt/wt %); Pinch at 40 wt/wt %.

LCC (not shown, but obtainable using C vs m data from Table 18.15) is similar to Fig. 18.9 (except that the pivot is on the vertical axis at $C_R = 5\%$).

18.7.4 Energy Planning Case Study into Carbon Emission Networks (CENs)

Rising concerns about climate change, along with more stringent environmental protection norms for sustainable development, are the stimulus for optimal energy planning to reduce emissions of greenhouse gases such as carbon dioxide (CO_2), methane (CH_4) and nitrous oxide (N_2O) that contribute to global warming.

This section presents the targeting of minimum clean energy resources (zero-carbon and/or low-carbon) in energy-allocation networks (Shenoy, 2010) under carbon emission constraints (Tan and Foo, 2007). The data (Lee *et al.*, 2009) for a carbon-constrained energy sector planning problem

© Woodhead Publishing Limited, 2013

Table 18.16 Data for carbon emission network in energy sector planning (Case Study 8)

Energy demands and energy sources	Demand emission factor C_d (t CO_2/TJ)	Source emission factor C_s (t CO_2/TJ)	Demand energy F_d (10^4 TJ)	Source energy F_s (10^4 TJ)	Emission load m_d/m_s (10^6 t CO_2)
D1 (Region I)	(30)		40		12
D2 (Region II)	(40)		72		28.8
D3 (Region III)	(50)		72		36
S1 (Natural Gas)		55		(–)80	(44)
S2 (Oil)		75		(–)100	(75)
S3 (Coal)		105		(–)500	(525)

$\sum F_d = 184$; $\sum F_s = (-)680$; $\Delta_1 = -496 \times 10^4$ TJ.
$\sum F_d\, C_d = 76.8 \times 10^6$; $\sum F_s\, C_s = (-)644 \times 10^6$; $\Delta_2 = -567.2 \times 10^6$ t CO_2.

are given in Table 18.16 for Case Study 8. There are three demands (three regions of the transportation sector with their expected energy requirements F_d in TJ and emission load limits m_d in t CO_2) and three common fossil fuel sources (natural gas, oil and coal with their emission factors C_s in t CO_2/TJ and energy availabilities F_s in TJ). The values for C_d in t CO_2/TJ and m_s in t CO_2 (in parentheses) in Table 18.16 are calculated using Equation [18.13]. The clean-carbon resource to be minimised is biodiesel with an emission factor of 16.5 t CO_2/TJ ($C_R = 16.5$). Using Equation [18.14], the constant difference between the clean-carbon resource and excess (or unused) energy is given by $F_R - F_E = \Delta_1 = -496 \times 10^4$ TJ. Using Equation [18.15], $F_R\, C_R - F_E\, C_E = \Delta_2 = -567.2 \times 10^6$ t CO_2.

Since no pre-processing and no level shifting is necessary for CENs (because the data are already in the demand–source form for an allocation network problem), the steps for the UTA are directly implemented in increasing-level sort order to obtain Table 18.17. The maximum value in the last column gives the minimum-resource target for biodiesel as $F_R = 772,650$ TJ and the corresponding emission factor level specifies the Pinch as 75 t CO_2/TJ. Equations [18.14] and [18.15] now give $F_E = 772,650 - (-4,960,000) = 5,732,650$ TJ and $C_E = (772,650 \times 16.5 + 5,67.2 \times 10^6)/5,732,650 = 101.166$ t CO_2/TJ (which is the minimum possible value when demands are at maximum emission load limit). The Pinch at 75 t CO_2/TJ identifies S2 (oil) to be the Pinch-causing source (as per Table 18.16). The distribution target for S2 in the energy-allocation network is 267,350 TJ (i.e., 1,040,000 – 772,650) for the Below-Pinch portion and the remainder of 732 650 TJ (i.e., 1,000, 000 – 267,350) for the Above Pinch portion.

The LCC in Fig. 18.10 (obtained by plotting C vs m from Table 18.17) allows graphical visualisation of the minimum target as the reciprocal of the

© Woodhead Publishing Limited, 2013

Table 18.17 UTA for carbon emission network in energy sector planning (Case Study 8)

Level C (t CO_2/TJ)	Flow at level F (10^4TJ)	Net flow F_{net} (10^4TJ)	Net load m_{net} (10^6 t CO_2)	Cumulative load m_{cum} (10^6 t CO_2)	Revised load m (10^6 t CO_2)	Target flow (10^4TJ)
30	40	0	0	0	0	0
40	72	40	4	4	4	17.0213
50	72	112	11.2	15.2	15.2	45.3731
55	–80	184	9.2	24.4	24.4	63.3766
75	–100	104	20.8	45.2	45.2	77.2650
105	–500	4	1.2	46.4	46.4	52.4294
(110)	0	–496	(–24.8)	(21.6)	(21.6)	(23.1016)

Targets: clean-carbon resource = 772,650 TJ (at 16.5 t CO_2/TJ); excess energy = 5,732,650 (at 101.166 t CO_2/TJ); Pinch at 75 t CO_2/TJ.

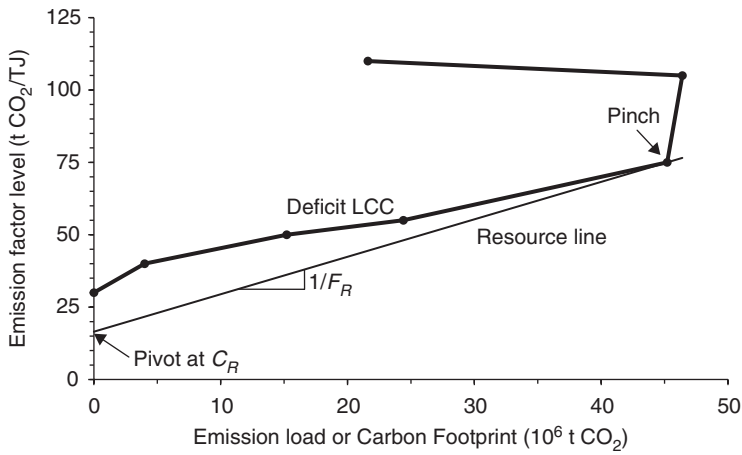

18.10 LCC for carbon emission network (Case Study 8).

slope of the rotated clean resource line with the pivot at C_R on the vertical axis and the Pinch as the point where the resource line touches the LCC.

18.8 Property-Based Material Reuse Networks

This section discusses the problem of minimising resources in Property-Based Material Reuse networks (Shelley and El-Halwagi, 2000). In addition to concentration, purity and emission factor, other properties such as density, reflectivity, solubility, vapour pressure, viscosity, volatility and pH can be considered (Eden *et al.*, 2004). Although these properties are not directly conserved (Eljack *et al.*, 2005), they follow certain blending or mixing rules

© Woodhead Publishing Limited, 2013

and an appropriately defined quality (level) based on the mixing rule is conserved (Qin *et al.*, 2005) as illustrated below.

18.8.1 Papermaking Process Case Study

The data for Case Study 9 are given in Table 18.18a for a material reuse problem of a papermaking process, whose Process Flow Diagram (not reproduced here) is provided by El-Halwagi *et al.* (2004). The primary property of the produced paper considered here is its reflectivity R_∞ (Kazantzi and El-Halwagi, 2005), which is defined as the reflectance of an infinitely thick material with respect to an absolute standard (i.e., magnesium oxide) and is therefore dimensionless. Although reflectivity R_∞ itself is not conserved, it follows the blending rule: $\sum F_S\ (R_{\infty,S})^{5.92} = F_D\ (R_{\infty,D})^{5.92}$ where F is the mass flowrate (in t/h). There are two demands (paper machines I and II) and two sources (process fibre and broke). Fresh fibre feed with reflectivity of 0.95 ($y_R = 0.95^{5.92} = 0.7381$) is the resource to be minimised, where the

Table 18.18 Data for papermaking process material reuse network (Case Study 9)

(a) Original data in terms of primary property (paper reflectivity)

Demands and sources	Demand property $R_{\infty,d}$	Source property $R_{\infty,s}$	Demand flowrate F_d (t/h)	Source flowrate F_s (t/h)
D1 (paper machine I)	0.85		100	
D2 (paper machine II)	0.9		40	
S1 (process fibre)		0.88		90
S2 (broke)		0.75		60

(b) Pre-processed demand–source data in terms of level (quality)

Demands and sources	Level for demand y_d	Level for source y_s	Flow for demand F_d (t/h)	Flow for source F_s (t/h)
D1	0.3821		100	
D2	0.5359		40	
S1		0.4692		–90
S2		0.1821		–60

$\sum F_d = 140$; $\sum F_s = -150$; $\Delta_1 = -10$ t/h.
$\sum F_d\ y_d = 59.646$; $\sum F_s\ y_s = -53.154$; $\Delta_2 = 6.4928$ t/h.
$\Delta_{2y} = \Delta_1 - \Delta_{2C} = -10 - (-16.4928) = 6.4928$ t/h.

© Woodhead Publishing Limited, 2013

Table 18.19 UTA for papermaking process material reuse network (Case Study 9)

Level y	Flow at level F (t/h)	Net flow F_{net} (t/h)	Net load m_{net} (t/h)	Cumulative load m_{cum} (t/h)	Revised load m (t/h)	Target flow (t/h)
0.5359	40	0	0	0	1.6842	0
0.4692	–90	40	2.6705	2.6705	4.3546	9.9297
0.3821	100	–50	–4.3546	–1.6842	0	–4.7304
0.1821	–60	50	9.9981	8.3140	9.9981	14.9534
(0.1)	0	–10	(–0.8212)	(7.4928)	(9.1769)	(11.7424)

Targets: fresh fibre feed = 14.9534 t/h (at 0.95 reflectivity or $y = 0.7381$); waste discharge = 24.9534 t/h (at 0.75 reflectivity or $y = 0.1821$); Pinch at 0.75 reflectivity or $y = 0.1821$.

level (quality) variable is defined as $y = 1 - C = (R_\infty)^{5.92}$ analogous to the case of hydrogen networks in Section 18.7.1. For this material reuse network, the data in demand–source form require no level shifting (as in the case of the hydrogen problem). However, pre-processing is done to convert the R_∞ data in Table 18.18a to equivalent level (quality $y = R_\infty^{5.92}$) data in Table 18.18b. Using Equations [18.14] and [18.15] with the data in Table 18.18b, $F_R - F_E = F_{fresh} - F_{discharge} = \Delta_1 = -10$ t/h and $F_R\, y_R - F_E\, y_E = (Fy)_{fresh} - (Fy)_{discharge} = \Delta_2 = 6.4928$ t/h (in terms of y).

The steps for the UTA are now implemented with decreasing y (or increasing C) in the first column to obtain Table 18.19. The minimum-resource target for fresh fibre feed is $F_R = 14.9534$ t/h and the corresponding level (quality) specifies the Pinch at 0.75 reflectivity ($y = 0.1821$). Since $F_R = 14.9534$ t/h and $y_R = 0.7381$, Equations [18.14] and [18.15] yield $F_E = 14.9534 - (-10) = 24.9534$ kg/s (discharge flowrate target) and $C_E = (14.9534 \times 0.7381 - 6.4928)/24.9534 = 0.1821$ (discharge level target of 0.75 reflectivity). The Pinch at 0.75 reflectivity identifies S2 (broke) to be the Pinch-causing source (as per Table 18.18a). The distribution target for S2 in the allocation network is 35.0466 t/h (i.e., 50 – 14.9534) for the below-Pinch portion and the remainder of 24.9534 t/h (i.e., 60 – 35.0466) for the Above Pinch portion. These targets agree with those reported by Foo *et al.* (2006).

Although the UTA uses y, the LCC (obtained using y vs m data from Table 18.19) in Fig. 18.11 plots $C \equiv 1 - y$ vs m to make it analogous to the LCC for water (Fig. 18.7) and hydrogen (Fig. 18.8). This Deficit LCC allows graphic visualisation and targeting of the minimum fresh resource by rotating a horizontal line with the pivot at (m_1, C_R) as in Fig. 18.8 until it just touches the LCC to define the Pinch Point. The reciprocal of the slope of the rotated line gives the fresh resource target.

© Woodhead Publishing Limited, 2013

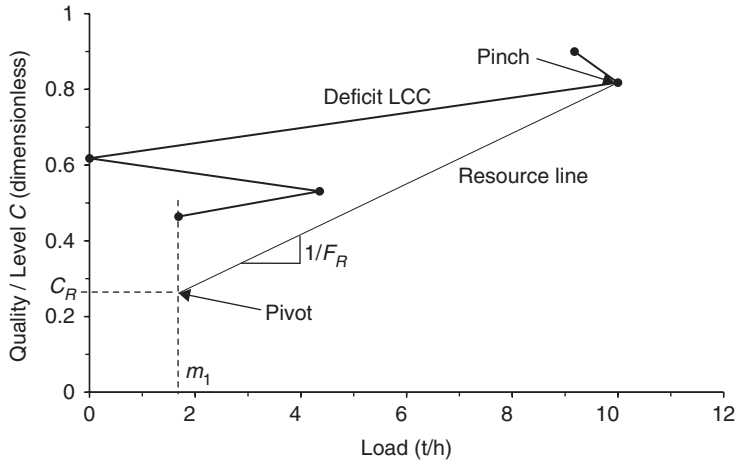

18.11 LCC for papermaking process material reuse network (Case Study 9).

Shenoy (2011) has shown the application of the UTA to solve a material reuse problem of a metal degreasing process (Kazantzi and El-Halwagi, 2005), where the Reid vapour pressure (RVP) in atm. is the primary property that characterises the solvent volatility for its reuse and recycle (Das *et al.*, 2009).

18.9 Alternative Approaches to Targeting

This section provides a brief survey of some approaches (other than PTA, CTA, UTA and GCC) for targeting exchange and allocation networks. The survey is limited to techniques based on Pinch Analysis and excludes methods based on mathematical programming.

18.9.1 Alternative Targeting Approaches for Exchange Networks

For HENs, one of the first and foremost targeting approaches is based on the composite curves (Whistler, 1948), which provide a comprehensive picture of the heat availability (hot streams) and heat requirement (cold streams) on a temperature–enthalpy diagram (Hohmann, 1971). The top-right enthalpy gap (overshoot of the cold composite) is the hot utility target, the bottom-left enthalpy gap (overshoot of the hot composite) is the cold utility target, and the point where the composite curves have the smallest vertical temperature gap ($\Delta T_{\min}$) is the Pinch (Hohmann and Lockhart,

© Woodhead Publishing Limited, 2013

1976). Varying ΔT_{min} requires horizontal translation of the Composite Curve making the graphical procedure cumbersome. However, the composite curves form the basis for area targeting in HENs based on the vertical heat transfer model (Linnhoff and Ahmad, 1990) using the Uniform Bath Formula (Townsend and Linnhoff, 1984). The pre-design optimisation of ΔT_{min} for total cost minimisation is called Supertargeting (Linnhoff and Ahmad, 1989, 1990). The GCC as in Figs 18.3 and 18.5 is useful for Multiple Utility Targeting (Linnhoff *et al.*, 1982) considering the minimisation of only utility (operating) costs. The targeting of the optimum loads for multiple utilities considering the cost trade-offs in utility as well as capital uses the optimum load distribution (OLD) plot based on the cheapest utility principle (CUP) proposed by Shenoy *et al.* (1998). The application of the CUP on a fluidised catalytic cracking unit (FCCU) for downstream gas processing and its comparison with the conventional GCC approach of setting targets for multiple utility loads is described by Shethna *et al.* (1999). The targeting of furnace systems with air preheat using separate process and utility GCCs has been developed by Hall and Linnhoff (1994), whereas the targeting for Energy Integration of fired heaters has been addressed by Varghese and Bandyopadhyay (2007, 2009). The basic methodology for retrofit targeting (Tjoe and Linnhoff, 1986) uses the Area–Energy Plot and the investment–savings plot as two important graphical representations along with the concept of Area Efficiency. In contrast to total cost minimisation based on the classical capital–energy trade-off in grassroots designs, the typical aim of retrofitting is energy savings maximisation subject to a minimum payback period or a maximum investment ceiling.

For MENs, El-Halwagi and Manousiouthakis (1989) made the first effort to develop Pinch targets based on the CIT. The analogy of a MEN with a HEN is not complete because, in contrast to the two temperature scales (one cold and one hot) in a HEN, there are $N_{ls} + 1$ composition scales (N_{ls} lean and one rich) in a MEN. Hallale and Fraser (2000a, 2000b) presented methods for MENs to target the minimum capital cost and optimise the total cost (Supertargeting) by varying the minimum composition difference for a single MSA, non-overlapping MSAs and overlapping MSAs with stagewise and continuous contactors. Fraser and Hallale (2000) extended the retrofit targeting methodology of Tjoe and Linnhoff (1986) to MENs using the COG sweetening process (discussed in Section 18.5.3) as an example.

18.9.2 Alternative Targeting Approaches for Allocation Networks

For water networks, several targeting techniques have been developed and are well-summarised in the reviews of Bagajewicz (2000), Foo (2009) and

© Woodhead Publishing Limited, 2013

Jezowski (2010). Note that the Deficit LCC (in Fig. 18.7, obtained from the UTA Table in increasing-level sort order) allows targeting of the minimum freshwater. On the other hand, the Surplus LCC (not shown here, but obtained from the UTA Table in decreasing-level sort order) allows targeting of the minimum wastewater (Shenoy, 2011). The Surplus LCC is a mirror-reflection in the vertical axis (horizontal flip) of the Source Composite Curve (Bandyopadhyay *et al*., 2006), which can be used to simultaneously target the minimum freshwater requirement and the distributed effluent treatment system. Thus, the UTA includes the Waste Targeting Algorithm (Bandyopadhyay, 2006) for generation of the Source Composite Curve. Note that a different sign convention (Shenoy and Bandyopadhyay, 2007) in Equation [18.20] would cause a horizontal flip (mirror-reflection in the vertical axis) of the LCC as outlined by Shenoy (2011).

A non-iterative graphical targeting method was proposed by El-Halwagi *et al*. (2003) based on the material recovery Pinch diagram, where separate source and demand composites are plotted with cumulative flow as the horizontal axis and cumulative load as the vertical axis (Prakash and Shenoy, 2005a). Here, the slopes of the individual segments correspond to contaminant concentrations arranged in increasing order. Targeting involves horizontal translation of the source composite to the right until it is just below the demand composite. The point where the composites touch is the Pinch, the bottom-left gap (overshoot of the demand composite), is the freshwater flowrate target, and the top-right gap (overshoot of the source composite) is the wastewater flowrate target.

The CTA (Agrawal and Shenoy, 2006) is similar to the Mass Problem Table method (Castro *et al*., 1999), which is applicable to FC problems. The vertical line segments representing demands/sources all terminate at the same reference concentration in the CTA, whereas such line segments terminate at different concentrations for FC problems in the Mass Problem Table. The CTA is conceptually similar to, but simpler than, the Water Cascade table technique (Manan *et al*., 2004), which requires the Water Cascade and the pure water surplus cascade diagrams to be integrated with the interval water balance table. Further, unlike the Water Cascade table, the CTA and UTA directly provide the LCC representation.

For hydrogen (and other utility gas) networks, the concept of the surplus diagram (Alves and Towler, 2002) provides a graphical approach. However, like the water surplus diagram (Hallale, 2002), the method based on the hydrogen-surplus diagram requires transferring of data from one plot to another and involves trial and error, because it needs an initial guess at the hydrogen target. The material recovery Pinch diagram (El-Halwagi *et al*., 2003) provides a non-iterative graphical alternative.

For CENs, Tan and Foo (2007) in their seminal work used a method based on the material recovery Pinch diagram (El-Halwagi *et al*., 2003; Prakash and

© Woodhead Publishing Limited, 2013

Shenoy, 2005a) and obtained approximate targets graphically. Lee *et al*. (2009) extended the method to low-carbon resources, but the graphical approach is not straightforward because it requires diagonal shifting (El-Halwagi *et al*., 2003) of a curve (Source Composite Curve) along a locus whose slope corresponds to the emission factor of the low-carbon resource. Exact targets may be obtained by an elaborate three-stage cascade analysis approach (Foo *et al*., 2008) for CEN problems including multiple resources; however, the CTA (Shenoy, 2010) as well as the UTA provides a simple accurate alternative.

For Property-Based Material Reuse networks, the property surplus diagram and the property cascade analysis technique (Foo *et al*., 2006) provide extensions of the graphical and algebraic techniques developed for water and hydrogen networks.

Summing up, the UTA along with fundamental balances as in Equations [18.14] and [18.15] provides several definite advantages for targeting minimum resources: a unified conceptual approach applicable to large complicated problems; a simple numerical tabular method capable of yielding accurate targets without graphical plotting and horizontal/diagonal shifting, and an associated graphical representation to form the targeting basis for multiple resources and regeneration problems.

18.10 Conclusion

This chapter has presented a UTA for targeting minimum resources in diverse Process Integration problems. From a pedagogical viewpoint, a single targeting algorithm prevents confusion and reduces errors frequently encountered during the implementation of several different algorithms. Moreover, a unified approach helps in better appreciation of the basic Process Integration concepts and the similarities/differences in diverse resource optimisation networks.

The key basis for the unified approach is the conversion of streams to equivalent demand–source (inlet–outlet) pairs. The UTA includes as special cases various earlier algorithms such as the PTA for HENs, the CIT Algorithm for MENs, as well as the Waste Targeting Algorithm (WTA) and the CTA for water, hydrogen, carbon emission and material reuse allocation networks. The UTA eliminates the necessity in these earlier algorithms to draw line segments to determine the stream populations in various level intervals. The UTA calculations being truly tabular lend themselves admirably to both manual and computer (in a simple spreadsheet without macros) implementations. The data from the UTA table may be plotted if desired (although not a necessity) to obtain graphical representations (GCC and LCC) that provide a means of visualising load deficits/surpluses at different levels, identifying the Pinch and targeting minimum-resource requirements. Although graphical representations are valuable in providing visual insights, graphical targeting

© Woodhead Publishing Limited, 2013

methodologies can be unwieldy at times. A purely numerical/algebraic algorithm such as the UTA offers several advantages including ease of application to real-world problems with large data sets, high accuracy and non-iterative straightforward computation with rapid what-if analysis.

In this chapter, the UTA is illustrated in nine case studies from diverse domains closely related to real-world process systems. The UTA table establishes the targets for the minimum-resource/utility and Pinch level for exchange and allocation networks. Equations [18.14] and [18.15] are fundamental system balances that may then be used to calculate the flow and level targets for the low-quality waste/excess in the case of allocation networks. The UTA and the LCC are also suitable (Agrawal and Shenoy, 2006) to target multiple fresh resources and regeneration problems (including zero discharge) for allocation networks. Network designs to meet the targets can be synthesized (not shown here) by the Pinch Design Method (Linnhoff and Hindmarsh, 1983) for exchange networks and by the Nearest Neighbours Algorithm (Prakash and Shenoy, 2005a) for allocation networks. These minimum-resource networks may then be evolved by loop-breaking and path-relaxation (Linnhoff *et al*., 1982), as well as by source shifts (Prakash and Shenoy, 2005b) for exchange networks (Shenoy, 1995) and allocation networks (Das *et al*., 2009).

18.11 Sources of Further Information

Recently, Deng *et al*. (2011) have proposed a process-based graphical approach for the simultaneous targeting and design of water networks. Saw *et al*. (2011) have introduced the Material Surplus Composite Curve as a graphical targeting tool to avoid the repetitive computations in the surplus diagram methods. Shenoy and Shenoy (2012) have developed the methodology for targeting and design of CENs with CCS, where the LCC may be obtained by a single computation of the CTA/UTA including only non-CCS sources. Shenoy (2012) has enhanced the Nearest Neighbours Algorithm, earlier applicable to fixed flowrate processes, to FL processes by giving priority to local-recycle matches and then eliminating them to yield superior practical designs. It is possible to extend the UTA to aggregate production planning in supply chain management (Singhvi and Shenoy, 2002; Singhvi *et al*., 2004). Most recently, Shenoy and Shenoy (2013) have extended the applicability of the UTA to cooling-water networks as examples of fixed heat-load operations.

18.12 References

Agrawal, V., Shenoy, U. V. (2006). Unified conceptual approach to targeting and design of water and hydrogen networks. *AIChE Journal*, **52**(3), 1071–1082.

© Woodhead Publishing Limited, 2013

Alves, J. J., Towler, G. P. (2002). Analysis of refinery hydrogen distribution systems. *Industrial and Engineering Chemistry Research*, **41**(23), 5759–5769.

Bagajewicz, M. (2000). A review of recent design procedures for water networks in refineries and process plants. *Computers & Chemical Engineering*, **24**, 2093–2113.

Bandyopadhyay, S. (2006). Source composite curve for waste reduction. *Chemical Engineering Journal*, **125**, 99.

Bandyopadhyay, S., Ghanekar, M. D., Pillai, H. K. (2006). Process water management. *Industrial and Engineering Chemistry Research*, **45**, 5287.

Bandyopadhyay, S., Malik, R. K., Shenoy, U. V. (1999). Invariant rectifying-stripping curves for targeting minimum energy and feed location in distillation. *Computers & Chemical Engineering*, **23**, 1109–1124.

Bandyopadhyay, S., Mishra, M., Shenoy, U. V. (2004). Energy-based targets for multiple-feed distillation columns. *AIChE Journal*, **50**, 1837–1853.

Bandyopadhyay, S., Sahu, G. C. (2010). Modified problem table algorithm for energy targeting. *Industrial and Engineering Chemistry Research*, **49**, 11557–11563.

Castro, P., Matos, H., Fernandes, M. C., Pedro Nunes, C. (1999). Improvements for mass-exchange networks design. *Chemical Engineering Science*, **54**, 1649–1665.

Das, A. K., Shenoy, U. V., Bandyopadhyay, S. (2009). Evolution of resource allocation networks. *Industrial and Engineering Chemistry Research*, **48**(15), 7152–7167.

Deng, C., Feng, X. (2009). Optimal water network with zero wastewater discharge in an alumina plant. *WSEAS Transactions on Environment and Development*, **2**(5), 146–156.

Deng, C., Feng, X., Bai, J. (2008). Graphically based analysis for water system with zero liquid discharge. *Chemical Engineering Research and Design*, **86**(2), 165–171.

Deng, C., Feng, X., Ng, D. K. S., Foo, D. C. Y. (2011). Process-based graphical approach for simultaneous targeting and design of water network. *AIChE Journal*, **57**(11), 3085–3104.

Dhole, V. R., Ramchandani, N., Tainsh, R. A., Wasilewski, M. (1996). Make your process water pay for itself. *Chemical Engineering*, **103**, 100–103.

Eden, M. R., Jørgensen, S. B., Gani, R., El-Halwagi, M. M. (2004). A novel framework for simultaneous separation process and product design. *Chemical Engineering Processing*, **43**(5), 595–608.

El-Halwagi, M. M. (1997). *Pollution Prevention through Process Integration: Systematic Design Tools.* Academic Press, San Diego, USA.

El-Halwagi, M. M., Gabriel, F., Harell, D. (2003). Rigorous graphical targeting for resource conservation via material recycle/reuse networks. *Industrial and Engineering Chemistry Research*, **42**(19), 4319–4328.

El-Halwagi, M. M., Glasgow, I. M., Qin, X., Eden, M. R. (2004). Property integration: componentless design techniques and visualization tools. *AIChE Journal*, **50**(8), 1854–1869.

El-Halwagi, M. M., Manousiouthakis, V. (1989). Synthesis of mass exchange networks. *AIChE Journal*, **35**(8), 1233–1244.

Eljack, F. T., Abdelhady, A. F., Eden, M. R., Gabriel, F. B., Qin, X., El-Halwagi, M. M. (2005). Targeting optimum resource allocation using reverse problem formulations and property clustering techniques. *Computers & Chemical Engineering*, **29**(11–12), 2304–2317.

© Woodhead Publishing Limited, 2013

Foo, D. C. Y. (2009). State- of-the-art review of pinch analysis techniques for water network synthesis. *Industrial and Engineering Chemistry Research*, **48**(11), 5125–5159.

Foo, D. C. Y., Kazantzi, V., El-Halwagi, M. M., Manan, Z. A. (2006). Surplus diagram and cascade analysis technique for targeting property-based material reuse network. *Chemical Engineering Science*, **61**, 2626–2642.

Foo, D. C. Y., Manan, Z. A. (2006). Setting the minimum utility gas flowrate targets using cascade analysis technique. *Industrial and Engineering Chemistry Research*, **45**, 5986–5995.

Foo, D. C. Y., Tan, R. R., Ng, D. K. S. (2008). Carbon and footprint-constrained energy planning using cascade analysis technique. *Energy*, **33**, 1480–1488.

Fraser, D. M., Hallale, N. (2000), Retrofit of mass exchange networks using pinch technology. *AIChE Journal*, **46**(10), 2112–2117.

Fraser, D. M., Howe, M., Hugo, A., Shenoy, U. V. (2005). Determination of mass separating agent flows using the mass exchange grand composite curve. *Chemical Engineering Research and Design*, **83**, 1381–1390.

Hall, S. G., Linnhoff, B. (1994). Targeting for furnace systems using pinch analysis. *Industrial and Engineering Chemistry Research*, **33**, 3187–3195.

Hallale, N. (1998). Capital cost targets for the optimum synthesis of mass exchange networks. PhD thesis, Department of Chemical Engineering, University of Cape Town, South Africa.

Hallale, N. (2002). A new graphical targeting method for water minimisation. *Advances in Environmental Research*, **6**(3), 377–390.

Hallale, N., Fraser, D. M. (1998). Capital cost targets for mass exchange networks. A special case: water minimisation, *Chemical Engineering Science*, **53**(2), 293–313.

Hallale, N., Fraser, D. M. (2000a). Capital and total cost targets for mass exchange networks. *Computers & Chemical Engineering*, **23**(11–12), 1661–1699.

Hallale, N., Fraser, D. M. (2000b). Supertargeting for mass exchange networks. *Chemical Engineering Research and Design*, **78**(2), 202–216.

Hallale, N., Liu, F. (2001). Refinery hydrogen management for clean fuels production. *Advances in Environmental Research*, **6**, 81–98.

Hallale, N., Moore, I., Vauk, D. (2002). Hydrogen: liability or asset? *Chemical Engineering Progress*, **Sept**, 66–75.

Hohmann, E. C. (1971). Optimum networks for heat exchanger. PhD thesis, University of Southern California, USA.

Hohmann, E. C., Lockhart, F. J. (1976). Optimum heat exchanger network synthesis. *AIChE 82nd National Meeting*, Atlantic City, NJ, USA, Paper No 22a.

Jezowski, J. M. (2010). Review of water network design methods with literature annotations. *Industrial and Engineering Chemistry Research*, **49**(10), 4475–4516.

Kazantzi, V., El-Halwagi, M. M. (2005). Targeting material use via property integration. *Chemical Engineering Progress*, **101**(8), 28–37.

Kemp, I. C. (2007). *Pinch Analysis and Process Integration: A User Guide on Process Integration for the Efficient Use of Energy* (a second edition of Linnhoff, B., Townsend, D. W., Boland, D., Hewitt, G. F., Thomas, B. E. A., Guy, A. R., Marsland, R. H. (1982)). *A User Guide on Process Integration for the Efficient Use of Energy*. Institution of Chemical Engineers, Rugby, Oxford, UK, Butterworth-Heinemann.

© Woodhead Publishing Limited, 2013

Lee, S. C., Ng, D. K. S., Foo, D. C. Y., Tan, R. R. (2009). Extended pinch targeting techniques for carbon-constrained energy sector planning. *Appl Energy*, **86**, 60–67.

Linnhoff, B., Ahmad, S. (1989). Supertargeting: optimum synthesis of energy management systems. *ASME Journal of Energy Resources Technology*, **111**(3), 121–130.

Linnhoff, B., Ahmad, S. (1990). Cost optimum heat exchanger networks – I. Minimum energy and capital using simple models for capital cost. *Computers & Chemical Engineering*, **14**(7), 729–750.

Linnhoff, B., Flower, J. R. (1978). Synthesis of heat exchanger networks. I. Systematic generation of energy optimal networks, *AIChE Journal*, **24**, 633–642.

Linnhoff, B., Hindmarsh, E. (1983). The pinch design method for heat exchanger networks. *Chemical Engineering Science*, **38**, 745–763.

Linnhoff, B., Townsend, D. W., Boland, D., Hewitt, G. F., Thomas, B. E. A., Guy, A. R., Marsland, R. H. (1982). *A User Guide on Process Integration for the Efficient Use of Energy*. Institution of Chemical Engineers, Rugby, UK.

Manan, Z. A., Tan, Y. L., Foo, D. C. Y. (2004). Targeting the minimum water flow rate using water cascade analysis technique. *AIChE Journal*, **50**, 3169–3183.

Polley, G. T., Polley, H. L. (2000). Design better water networks. *Chemical Engineering Progress*, **96**(2), 47–52.

Prakash, R., Shenoy, U. V. (2005a). Targeting and design of water networks for fixed flowrate and fixed contaminant load operations. *Chemical Engineering Science*, **60**(1), 255–268.

Prakash, R., Shenoy, U. V. (2005b). Design and evolution of water networks by source shifts. *Chemical Engineering Science*, **60**, 2089–2093.

Qin, X., Gabriel, F., Harell, D., El-Halwagi, M. M. (2005). Algebraic techniques for property integration via componentless design. *Industrial and Engineering Chemistry Research*, **43**, 3792–3798.

Saw, S. Y., Lee, L., Lim, M. H., Foo, D. C. Y., Chew, I. M. L., Tan, R. R., Klemeš, J. J. (2011). An extended graphical targeting technique for direct reuse/recycle in concentration and property-based resource conservation networks. *Clean Technologies* and *Environmental Policy*, **13**, 347–357.

Shelley, M. D., El-Halwagi, M. M. (2000). Componentless design of recovery and allocation systems: a functionality-based clustering approach. *Computers & Chemical Engineering*, **24**, 2081–2091.

Shenoy, A. U., Shenoy, U. V. (2012). Targeting and design of energy allocation networks with carbon capture and storage. *Chemical Engineering Science*, **68**(1), 313–327.

Shenoy, A. U., Shenoy, U. V. (2013). Targeting and design of CWNs (cooling water networks). *Energy*, doi:10.1016/j.energy.2013.03.095.

Shenoy, U. V. (1995). *Heat Exchanger Network Synthesis: Process Optimisation by Energy and Resource Analysis*. Gulf Publishing, Houston, USA.

Shenoy, U. V. (2010). Targeting and design of energy allocation networks for carbon emission reduction. *Chemical Engineering Science*, **65**(23), 6155–6168.

Shenoy, U. V. (2011). Unified targeting algorithm for diverse process integration problems of resource conservation networks. *Chemical Engineering Research and Design*, **89**(12), 2686–2705.

Shenoy, U. V. (2012). Enhanced nearest neighbours algorithm for design of water networks. *Chemical Engineering Science*, **84**, 197–206.

© Woodhead Publishing Limited, 2013

Shenoy, U. V., Bandyopadhyay, S. (2007). Targeting for multiple resources. *Industrial and Engineering Chemistry Research*, **46**(11), 3698–3708.
Shenoy, U. V., Sinha, A., Bandyopadhyay, S. (1998). Multiple utilities targeting for heat exchanger networks. *Chemical Engineering Research and Design*, **76**, 259–272.
Shethna, H. K., Singh, H., Makwana, Y., Castillo, F. J. L., Shenoy, U. V. (1999). Multiple utilities optimisation to improve process economics. *Petroleum Technology Quarterly*, **Autumn**, 133–139.
Singhvi, A., Madhavan, K. P., Shenoy, U. V. (2004). Pinch analysis for aggregate production planning in supply chains. *Computers & Chemical Engineering*, **28**, 993–999.
Singhvi, A., Shenoy, U. V. (2002). Aggregate planning in supply chains by pinch analysis. *Chemical Engineering Research and Design*, **80**, 597–605.
Tan, R. R., Foo, D. C. Y. (2007). Pinch analysis approach to carbon-constrained energy sector planning. *Energy*, **32**, 1422–1429.
Tjoe, T. N., Linnhoff, B. (1986). Using pinch technology for process retrofit. *Chemical Engineering*, **28 April**, 47–60.
Townsend, D. W., Linnhoff, B. (1984). Surface area targets for heat exchanger networks. *IChemE 11th Annual Res Meeting*, April, Bath, UK.
Varghese, J., Bandyopadhyay, S. (2007). Targeting for energy integration of multiple fired heaters. *Industrial and Engineering Chemistry Research*, **46**(17), 5631–5644.
Varghese, J., Bandyopadhyay, S. (2009). Energy integration of fired heaters into overall processes. *International Journal of Environment and Sustainable Development*, **8**(1), 36–59.
Wang, Y. P., Smith, R. (1994). Wastewater minimisation. *Chemical Engineering Science*, **49**(7), 981–1006.
Wang, Y. P., Smith, R. (1995). Wastewater minimisation with flowrate constraints. *Transactions IChemE – Part A*, **73**, 889–904.
Whistler, A. M. (1948). Heat exchangers as money makers. *Petroleum Refinery*, **27**(1), 83–86.

18.13 Appendix: Nomenclature

b	constant in linear equilibrium relationship (in MEN)
C	level variable
CEN	carbon emission network
CIT	Composition Interval Table (in MEN)
CTA	Composite Table Algorithm (in allocation networks)
D	demand
FC	fixed contaminant-load (water network)
FF	fixed flow
FL	fixed load
F	flow variable
G	flowrate of rich steam (in MEN)
GCC	Grand Composite Curve (in HEN or MEN)

© Woodhead Publishing Limited, 2013

HEN	Heat Exchange Network
K	coefficient in linear equilibrium relationship (in MEN)
LCC	Limiting Composite Curve (in allocation networks)
L	flowrate of lean stream/MSA (in MEN)
MEN	Mass Exchange Network
MSA	Mass Separating Agent (in MEN)
m	load variable
MC_p	Heat capacity flowrate (in HEN)
N	Number of streams
PTA	Problem Table Algorithm (in HEN)
Q	heat load (in HEN)
S	source
T	temperature (in HEN)
UTA	Unified Targeting Algorithm
x	composition in lean stream (in MEN)
y	purity level or composition in rich stream (in MEN)
Δ_1	overall system flow loss/gain in allocation networks
Δ_2, Δ_3	overall system load loss/gain in allocation/exchange networks
ΔT_{min}	minimum approach temperature (in HEN)
Δy_{min}	minimum composition difference in rich stream (in MEN)
ε	minimum composition difference in lean stream (in MEN)

Subscripts

c	cold (stream)
cum	cumulative
d, D	demand
E	low-quality waste/excess
h	hot (stream)
in	inlet
l	level (index for row in UTA)
net	net (after taking algebraic sum of demands/inlets and sources/outlets)
out	outlet
R	high-quality resource/utility
s, S	source

© Woodhead Publishing Limited, 2013

19

A Process Integration Approach for Supply Chain Development

HON LOONG LAM and W. P. Q. NG,
The University of Nottingham, Malaysia, Selangor, Malaysia

DOI: 10.1533/9780857097255.4.571

Abstract: This chapter extends the application of the Process Integration (PI) approach to supply chains, especially developing further the analogy between Pinch Analysis and the field of operational research. The first part of this chapter introduces supply chains and supply chain performance measurement. In the following parts, the chapter provides clear insight into how the PI concept brings a significant contribution to the development of supply chain design. This novel approach, Pinch Analysis for the supply chain, will be presented. After an overview of the approach, case studies are outlined for purposes of demonstration.

Key words: supply chain, Process Integration, Pinch Analysis.

19.1 Introduction

Conventionally, supply chain design or supply chain management is carried out with the aim of minimising total supply chain cost to meet a pre-set and known demand (Shapiro, 2001).

However, concerns about CO_2 emissions are introducing a new dimension. According to the Energy Information Agency of United States (EIA, 2011), the transportation and industrial sectors appear to be those with the largest CO_2 emissions. Over the years, supply chain design has been investigated and improved to incorporate social sustainability to some extent.

The Pinch Analysis process, which, together with the provides clear insights can contribute significantly to the development of supply chain design. Supply chain design with PI provides a simpler analysis pathway, and better displays the outcomes of the analysis than traditional supply chain design methods. Furthermore, the combination of the two techniques enables the design of an optimal supply network in which the trade-offs between cost and environmental impact, required in order to reduce carbon emissions, can be achieved.

The main objective of this chapter is to introduce the benefits of the combination of supply chain design and PI. The chapter opens with an

© Woodhead Publishing Limited, 2013

introduction to supply chains and their performance measurement, followed by a description of the advantages that PI brings to supply chains, in terms of social, economic and environmental impacts, and resource utilisation. Then the incorporation of PI into supply chain design, which optimises the supply chain model, will be discussed. Several case studies are included to boost readers' conceptual understanding of a supply chain with PI. Finally, future developments in supply chain analysis with PI are expressed.

19.2 Supply Chain Characteristics and Performance Measurement

The concept of supply chain has been developed for business and operational management since long time ago. This section will review the development of conventional supply chain methods and the extension of supply chain with PI approach.

19.2.1 Introduction to Supply Chains and Supply Chain Design

The APICS dictionary defines the 'supply chain' as: 'The processes from initial raw materials to the ultimate consumption of the finished products linking across supplier-user companies', and 'The functions inside and outside a company that enable the value chain to make products and provide services to the customer' (Cox and Blackstone, 1998). According to Beamon (1998), there are two basic integrated supply chain processes: (1) the production planning and inventory control process; (2) the distribution and logistics process. The first process embraces the product manufacturing process while the latter controls the final products transportation and delivery, as referred in Fig. 19.1.

The incorporation of optimisation methods into business planning has been made possible by the advancement of information technology. Since then, integrated planning has been available to managers as a decision-making tool. A supply chain that performs well ensures a high-quality logistics service, punctual delivery and minimal transportation-cost incurrence. Research into supply chain design continues apace. A classic work is Clark and Scarf (1960), on which most conventional research on supply chains is based. The development of supply chains with PI has been carried out by various groups of researchers, as described in Section 19.3.

19.2.2 Measuring Supply Chain Performance

The performance of a supply chain design, in general, corresponds to the effectiveness of a firm's operation and management. In this context, two parties of measures for the performance of supply chain are introduced:

© Woodhead Publishing Limited, 2013

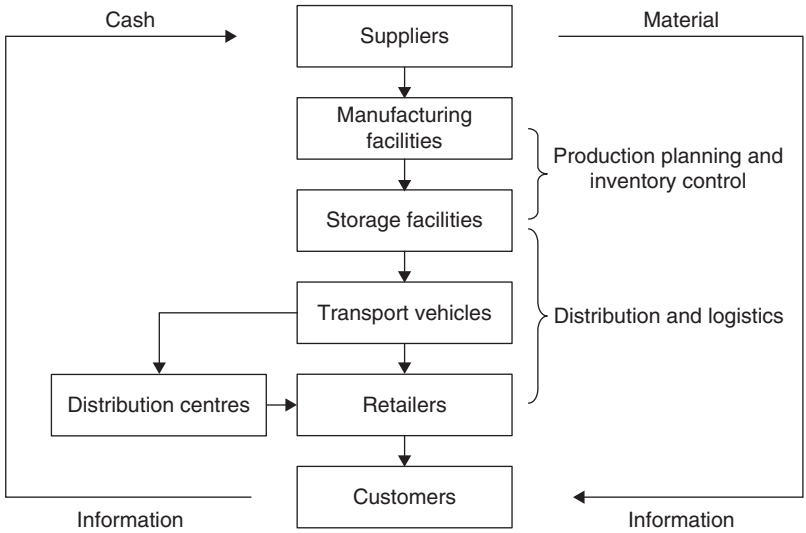

19.1 Supply chain processes. (After Beamon, 1998).

the first is presented by Beamon (1998), and the second by Krajewski *et al.* (2010). Beamon (1998) categorised the performance measures into qualitative measures and quantitative measures. Interested readers are referred to Beamon (1998) for a comprehensive description of these measures. On the other hand, Krajewski *et al.* (2010) classifies the performance measures of supply chain into inventory measures and financial measures. The inventory measures are evaluated according to the three following basic approaches:

- *Average Aggregate Inventory Value*

As the total average value of all inventory items, the average aggregate inventory value represents the amount of assets being held up in inventory. The more efficient a supply chain, the lower the average aggregate inventory value.

- *Weeks of Supply*

Weeks of supply is the ratio of average aggregate inventory value to weekly cost of goods sold.

- *Inventory Turnover*

Inventory turnover is the ratio of cost of annual sales to the average aggregate inventory value. The performance of a supply chain is directly proportional to its inventory turnover.

© Woodhead Publishing Limited, 2013

A supply chain requires inventory, which involves huge funding on the part of an organisation or management. According to Krajewski *et al.* (2010), the financial measures of a supply chain, which are contributed on the whole by inventory units, include these main items:

- *Total Revenue*

An efficient supply chain ensures on-time delivery. This will increase the total revenue, as customers will return for the services and products supplied (Krajewski *et al.*, 2010).

- *Cost of Goods Sold*

A competent supply chain results in a high contribution margin, the difference between the price and the variable costs to produce a product. This improves the cost of goods sold, and thus the net income of the organisation.

- *Operating Costs*

A supply chain with a low capital investment reduces the capital depreciation. The supply chain design with infrastructure selection affects the overhead. The depreciation charges and the overhead as fixed charges are operating costs, which affect the supply chain performance.

- *Cash Flow*

A well-designed supply chain increases the cash flow by reducing lead times and order backlogs.

- *Working Capital*

Working capital is the funding required to ensure a firm's on-going operation. The reduction in inventory investment, lead time and backlogs reduces the working capital (Krajewski *et al.*, 2010). This is the result of the shorter weeks of supply or the higher inventory turnover. The reduction in working capital decreases the amount of total asset, which affects the Return on Assets.

- *Return on Assets (ROA)*

ROA is the net income over total assets. A proficient supply chain has a high ROA. The reduction in total assets, e.g. warehouses or aggregate inventory investment, increases the ROA (Krajewski *et al.*, 2010).

© Woodhead Publishing Limited, 2013

19.2.3 Effects of PI on Supply Chains

Generally, a supply chain system engages production facilities, warehouses, distributors, suppliers, retailers and customers. Among the players, one of them will act as a 'bottleneck' or Pinch, which will impose a limitation on the system capacity. PI of the supply network provides an alternative graphical solution of 'quality' versus 'quantity', which is not attainable by most of the other models. The graphical plot through Pinch Methodology allows the identification of the Pinch location. In other words, the application of PI to the supply chain allows the identification of 'bottleneck' which then allows 'debottlenecking'. The 'debottlenecking' process removes the system restriction which may lead to an improvement in the supply chain system's performance.

The PI method is flexible. It can be easily modified to suite other applications, which include supply chain analysis, as long as directional cumulative magnitudes are available. The applications of PI are illustrated in Fig. 19.2: (a) for a heat recovery system, the quality is stream temperature while the quantity is heat load (Linnhoff and Hindmarsh, 1983); (b) for mass transfer system, the quality is concentration while the quantity is mass load (Wang and Smith, 1994); (c) for supply chain system, the quality is time while the quantity is material load (Singhvi *et al*., 2004); (d) Lam *et al*. (2010) modifies the Composite Curve to relate regional land use with resource planning with 'quality', being cumulative area, and 'quantity', being cumulative energy balance. Figures 19.2a and 19.2b refer to the original Pinch Methodology, whereas Figs 19.2c and 19.2d demonstrate the extended Pinch Methodology. The Composite Curves, which present a Cumulative Supply vs Cumulative Demand Curve, compare both the supply and demand on one platform. This allows direct comparison of the material availability constraints as well as analysis of any supply deficit or surplus.

Apart from the optimisation of resource utilisation, e.g. minimum utility consumption through the heat recovery system, minimum material requirement through the mass transfer system, etc., the economic performance of the supply chain can be taken into consideration when designing the supply network through PI. For example, a supply network can be selected through the minimisation of cost functions (logistic cost, managerial cost, production cost, etc.).

Regarding environmental impact, the carbon emissions along the supply network can be investigated. The environmental impact factor can be integrated into the supply network design for the generation of a green supply chain system. The detailed method of supply chain analysis with PI will be presented in Section 19.3, and several case studies will be demonstrated in Section 19.4.

© Woodhead Publishing Limited, 2013

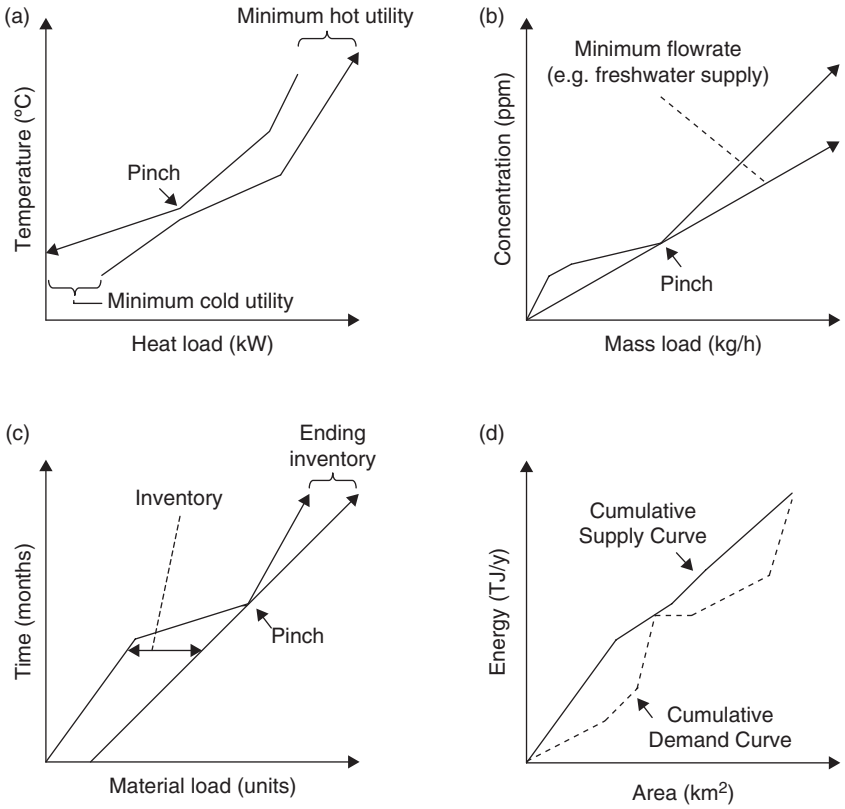

19.2 The comparison of 'quality' vs 'quantity' for four PI applications. (a) Heat recovery system, (b) Mass transfer system, (c) Supply chain system and (d) Resource planning system. ((a) after Linnhoff and Ahmad, 1990; (b) after Wang and Smith, 1993; (c) after Singhvi *et al.*, 2004; (d) after Lam *et al.*, 2010.)

19.3 Supply Chain Development with Process Integration

This section covers the integration of Pinch Analysis into supply chains, which optimises supply chain management. The first research work to apply Pinch Analysis to a supply chain problem was presented by the group of Shenoy (Singhvi and Shenoy, 2002); later, Foo *et al.* (2008) extended the scope with supply chain cascade analysis. Further work has been carried out by Lam *et al.* (2010) with the extension to biomass supply chain clustering synthesis. The details of those approaches are summarised in the following subsections.

© Woodhead Publishing Limited, 2013

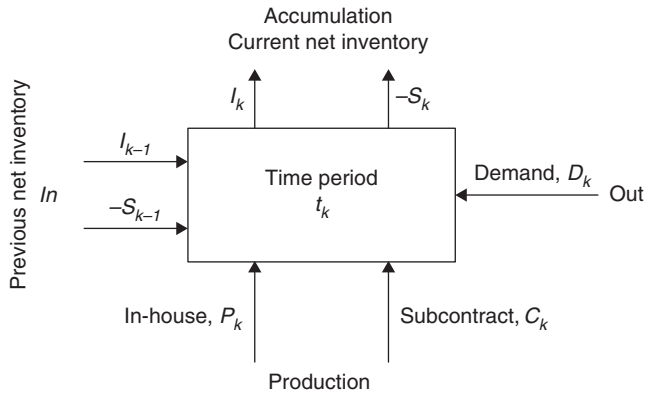

19.3 Schematic diagram for aggregate planning in supply chain. (After Singhvi and Shenoy, 2002).

19.3.1 Supply Chain with Pinch Analysis

Singhvi and Shenoy (2002) presented a novel extension of the targeting methods from Pinch Analysis to aggregate planning in supply chains. This method is then further enhanced with larger case study by Singhvi *et al.* (2004). Aggregate planning aims at meeting demand over a specified time horizon in a way that maximises profit through optimal levels of production, capacity, subcontracting, inventory and stock-outs.

A schematic diagram for aggregate planning in a supply chain is shown in Fig. 19.3. D_k represents the demand forecast for each period t_k in a planning horizon that extends over T time periods, maximising the profit over the specified time horizon. Other symbols shown in Fig. 19.3 are: production rate, P_k, number of units produced in-house in time period t_k; subcontract, C_k, number of units subcontracted (outsourced) in time period t_k; inventory, I_k, inventory at the end of time period t_k; and, stock-out, S_k, number of units stocked out (backlogged) at the end of time period t_k.

These variables are plotted in demand and production composites (Fig. 19.4) on a time vs material quantity plot (Singhvi and Shenoy, 2002). A simple balance of the flow of materials at time t_k in a particular stage of the supply chain with I_0 as the initial inventory can be written as:

$$I_0 + P_k + C_k = D_k + I_k \qquad [19.1]$$

As shown in Fig. 19.4, the Demand Composite Curve $D(t_k)$ is simply a plot of the cumulative demand and needs to be matched by a supply Composite Curve $P(t_k)$. Based on the fundamental principle of material balance, the demand has to be met by products supplied either by in-house production or outsourcing.

© Woodhead Publishing Limited, 2013

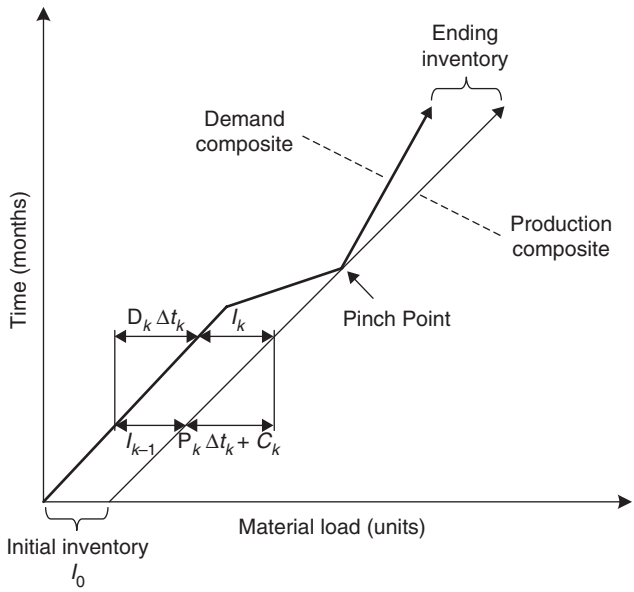

19.4 Demand and Production Composite Curves by Pinch Analysis. (After Singhvi *et al.*, 2004.)

Singhvi *et al.* (2004) noted that the vertical difference between the demand and supply composites is the lead time, which is the time interval between producing an order and servicing the demand. The point where $P(t_k - T) = D(t_k)$ is the Pinch. The minimum lead time separates the two composite curves. Compared to the original Heat Pinch Graph, minimum lead time is analogous to the Minimum Temperature Driving Force (ΔT_{min}) in a heat recovery system. When $T = 0$, the Pinch will be the point where $P(t_k) = D(t_k)$. The horizontal distance between the two Composite Curves at any given time gives the total inventory in the system. The Pinch is defined as the point of minimum inventory. The area between the two Composite Curves gives the measure of inventory in the system, which when multiplied by the inventory holding cost factor provides the actual inventory cost.

This work is then extended by Foo *et al.* (2008). The concept of supply chain cascade analysis is illustrated in Fig. 19.5.

19.3.2 Regional Energy Surplus–Deficit Curves (RESDC) for Biomass Network

Generating a biomass transfer network is an optimisation task, which involves determining the links and the biomass flows from the available

© Woodhead Publishing Limited, 2013

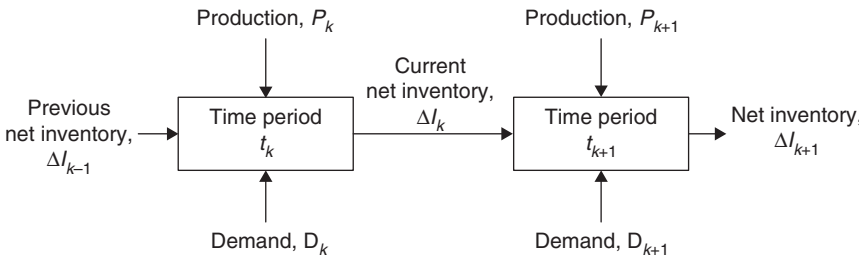

19.5 The concept of supply chain analysis. (After Foo *et al.*, 2008.)

energy source points to the target sink points. This is followed by a step that groups the zones into suitable clusters.

The RESDCs are a pair of Cumulative Curves representing cumulative energy surplus and deficit profiles. They indicate the size of each cluster and the total energy involved in the supply chain within the cluster. Below are the problem-solving steps:

(i) Tabulate the energy source and demand data. The table should contain the quantity of the potential energy sources, the bioenergy demand and the locations of the collection points. The biomass resources surpluses and deficits should be obtained from the local sources and demand analysis inside each zone. The distribution centroid is specified by a 2-D Cartesian coordinate system and the centroid point for Zone 1 is marked as reference point.

(ii) Obtain an optimised targeting result for the biomass transfer network/link using Linear Programming. The objective is to minimise the total CFP within the boundary of the given region. For biomass transfer from Zone i (source) to Zone j (sink) varying $i = 1 \ldots N_{\text{zones}}; j = 1 \ldots N_{\text{zones}}; i \neq j$, the following objective function is defined:

$$\text{Min CFP} = \sum_{ij} \text{CFP}_{i,j} \qquad [19.2]$$

$$\text{CFP}_{i,j} = \text{FC}_{i,j} \times \text{Dist}_{i,j} \times \frac{B_{i,j}}{C} \times \text{CEF} \qquad [19.3]$$

where, $\text{CFP}_{i,j}$ is the Carbon Foot Print, $\text{FC}_{i,j}$ is Fuel Consumption, $\text{Dist}_{i,j}$ is 2-way distance, $B_{i,j}$ is Biomass load, C is the truck capacity and CEF is the Carbon Emission Factor for diesel trucks.

© Woodhead Publishing Limited, 2013

The following constraints are necessary:

(a) The total amount of biomass transported out from Zone_i to other zones may not exceed the available surplus AB_i (Equation [19.3]), and flows for transferring biomass to the same zone are forbidden (Equation [19.4]).

$$\sum_j B_{i,j} \leq AB_i \ \forall i \qquad [19.4]$$

$$B_{i,j} \|_{i=j} = 0 \qquad [19.5]$$

(b) The total bioenergy delivered to $Zone_j$ may not exceed the deficit in that zone:

$$\sum_i TE_{i,j} \leq D_j \ \forall j \qquad [19.6]$$

$$TE_{i,j} = HV_i \times B_{i,j} \qquad [19.7]$$

where HV_i is the heating value for the particular biomass from $Zone_i$ and D_j is the total deficit in $Zone_j$.

(c) The biomass load in the system must be non-negative

$$B_{i,j} \geq 0 \ \forall i, j \qquad [19.8]$$

(iii) Clusters are formed based on the priority that the residual bioenergy imbalance within the newly formed clusters is minimised (preferably zero) by using Mixed Integer Linear Programming (MILP).

(iv) To plot the RESDC

(a) Arrange the zones within each cluster in descending order according to their energy balance, starting with the largest surplus.

(b) Illustrate the clustering result with a pair of monotonic Cumulative Curves. Plot the energy supply cumulative curve (Fig. 19.6) with the cumulative area as x-axis, and the accumulated energy balance on the y-axis. The cluster with the smallest imbalance will be the first cluster.

(c) Plot the energy Demand Cumulative Curve (Fig. 19.6) in the same manner as step (b).

© Woodhead Publishing Limited, 2013

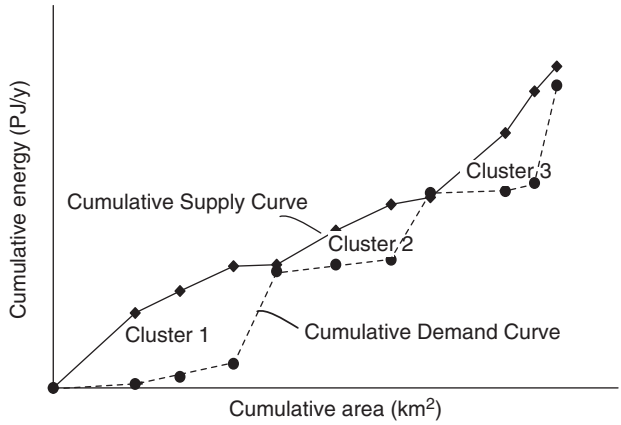

19.6 Regional Energy Supply–Demand Curves. (Source: After Lam *et al.*, 2010.)

19.3.3 Resource Management Curve (RMC)

The RMC (Lam *et al.*, 2010) has been developed to graphically represent the relationship between land use and the generation and consumption of energy. The RMC is a graphical tool that can be used to support the decision-making process in regional resource management, as shown in the following sections. The principle idea of a Grand Composite Curve (Townsend and Linnhoff, 1983) has been exploited and translated to the problem of regional resource management. For regional resource management, the x-axis represents the energy supply/demand profile (TJ/y), and the y-axis represents the cumulative land area for the studied region. The pockets represent the supply–demand among the zones. A demonstration case study for the application of RMC was demonstrated by Lam *et al.* (2011).

The procedure for construction of the RMC is:

1. Construct a Regional Energy Cascade Analysis for biomass transfer between zones.

   (i) Order the clusters by descending imbalance. Start with the zone with the largest energy surplus.
   (ii) Calculate the energy–land use rate, L, for each zone.

$$L_i = \frac{A_i}{S_i - D_i} \qquad [19.9]$$

   where A_i is the Area for Zone i, S_i and D_i are the bioenergy supply and demand from *Zone i*.

© Woodhead Publishing Limited, 2013

(iii) Sequence the zones within the cluster by descending value of L_i.
(iv) Cascade the surplus or deficit value of each zone by using bottom-up or top-down direction. Each zone size becomes a cumulative area interval for the plot. The cascade is just a cumulative tool and it does not reflect the individual links between the clusters.

2. Plot the RMC with the cumulative area (km^2) as y-axis, and the accumulated energy balance (TJ/y) on the x-axis. The coordinates for the points in the RMC represent the accumulated area and the surplus/deficit value from cascade interval. Figure 19.7 shows two options for presenting the RMC. The energy cascading can be performed from the bottom-up (a), or from the top-down (b). In Lam *et al.* (2011), bottom-up cascading is used.

The RMC puts together the information about energy surpluses/deficits as well as land use, allowing for a direct assessment of the trade-off between them. The curve from Point A to E in Fig. 19.7 represents Cluster 1. From the left-hand turning Point E, to Point H the curve represents Cluster 2. The intra-cluster energy transfer (supply–demand relationships) is represented by the shaded areas or Pockets B-C-D-E, F-G-H.

For the bottom-top cascaded RMC, as shown in Fig. 19.7a, the zones with positive slope supply biomass to the demand zones with negative slope. Since the zone areas are fixed, a steeper positive slope means less net energy is available from a zone. A steeper negative slope means the net energy demand for the zone is smaller. The parts of the RMC plotted on the right-hand side of the y-axis represent the activities within the studied region. The parts plotted on the left-hand side represent the import–export activities at the energy market.

Based on the RMC, several options are possible to tackle the problem of resource management in a region. They are mainly based on energy surplus and deficit, and land-use management.

There are five basic rules to be applied while manipulating regional resources such as land and the surplus energy. These rules give a clear overview picture and useful hints to the planner on how to manage regional resources with a single graph.

Rule 1: If m TJ/y of surplus energy is being planned for export from Zone i, the curve of Zone i and all of the curves after that are shifted together to the left horizontally by m TJ/y.
Rule 2: If extra land of n km^2 from Zone 1 is being used for purposes other than energy production, the segment given by n km^2 is cutting out and shifting the curves on the section above it to the left.

© Woodhead Publishing Limited, 2013

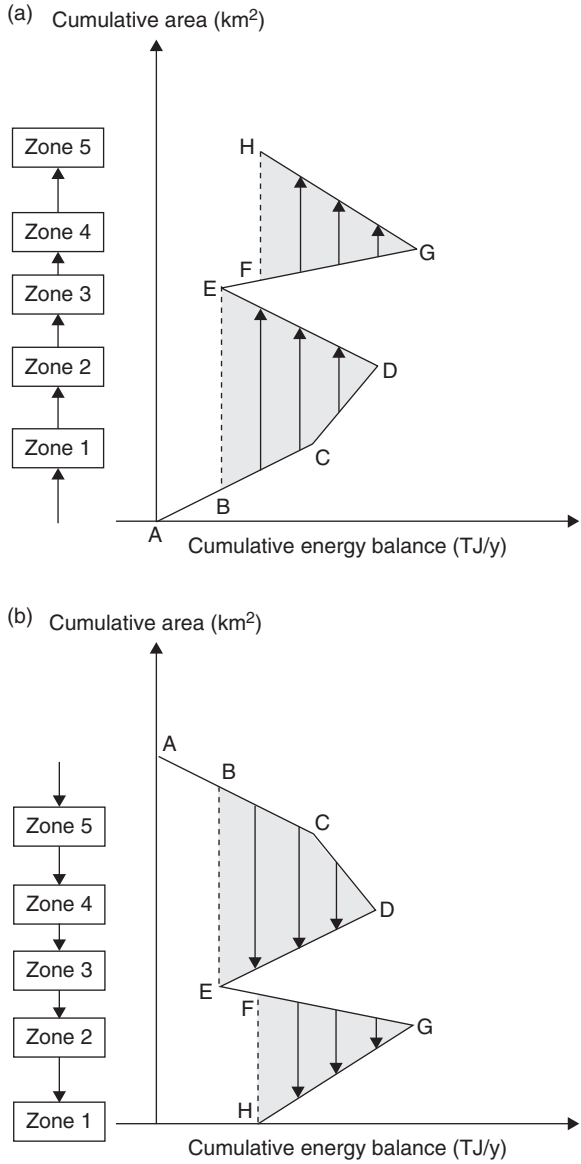

19.7 Constuction of the RMC. (a) bottom-up cascaded RMC; (b) top-down cascaded RMC. (After Lam *et al.*, 2011.)

Rule 3: If p TJ/y of external energy is planned to be imported to Zone i, the curve of Zone i and all of the subsequent curves are shifted together to the right horizontally by p TJ/y.

© Woodhead Publishing Limited, 2013

Rule 4: If the production rate for energy crops in Zone *i* is increasing, or the energy demand is decreasing, the slope of the curve is decreased.

Rule 5: If the production rate for energy crops in Zone *i* is decreasing or the energy demand is increasing, the slope of the curve is increased.

19.4 Case Studies

This section demonstrates two case studies, with the aim of boosting readers' understanding of supply chain PI. The first case study shows the application of Composite Curves for Regional Energy Clustering (Lam *et al.*, 2010), and the second case study demonstrates the implementation of the Grand Composite Curve analogy to address the regional resources management issue.

19.4.1 Case Study 1: Regional Energy Clustering (REC)

This study focuses on the biomass transportation network and supply chain clustering. The steps that were discussed in Section 19.3.2 are illustrated by using a set of data collected from a generalised rural region.

Step 1. Specification of the energy sources and demands. The information needed as an input to the REC procedure is shown in Table 19.1. It contains the relevant regional data – potential biomass sources, energy demands, and the area and location of the collection point for each particular zone.

The assumptions for the major parameters are:

(i) Carbon Emission Factor, CEF = 2.69 (kg CO_2)/L (IEA, 2005).
(ii) Fuel Consumption by a 20 t truck = 0.3 L/km.
(iii) Ratio of energy lost during the energy conversion from the raw materials to the final energy carriers such as heat and energy, $L_f = 0.5$.

Taking the balance between the supply and demand inside each zone, the source and sink sets of the linear programming problem, as described in Section 19.3.2, are formed. Zones 1, 2, 3, 5, 8 and 9 become Source Zones (i) and Zone 4, 6, 7 and 10 become Sink Zones (j).

Step 2. Optimise biomass exchange flows between zones. Using the obtained source and sink zones with their specified parameters, an LP optimisation problem as described in Section 19.3.2 is formulated. The LP problem is solved by GAMS and the optimal biomass exchange flows, $BE_{i,j}$ obtained in the solution is listed in Table 19.2.

The optimal biomass exchange flows are further illustrated in Fig. 19.8, where they are combined with the locations of the zone centroids (represented by the '●' symbol). The biomass exchanged is represented by the corresponding flow magnitudes, and also arrows indicating the directions.

© Woodhead Publishing Limited, 2013

Table 19.1 Regional data for demonstration case study

Zone	Area (km^2)	Location (km, km)	Biomass Potential (t/y)	Heating value (MJ/kg)	Energy Supply (TJ/y)	Energy Demand (TJ/y)
1	11.60	(0, 0)	2,700	18.0	24.0	1.7
2	6.12	(4.4, 2.5)	1,100	18.5	10.2	4.5
3	9.58	(5.3, 2.4)	1,760	17.3	15.3	11.8
4	6.35	(4.1, 0.2)	940	6.4	3.0	33.0
5	8.38	(7.9, 5.1)	1,380	15.5	10.7	2.1
6	5.57	(6.4, 5.5)	420	10.5	2.2	22.0
7	10.63	(2.4, 6.8)	2,220	18.2	20.2	0.5
8	7.83	(9.4, 5.5)	980	16.8	8.2	1.5
9	4.12	(3.2, 6.6)	1,510	17.3	13.1	2.6
10	3.15	(2.3, 7.3)	1,140	13.7	7.8	30.6

Table 19.2 Optimised bioenergy exchange flows

Variable	Value (TJ/y)	Variable	Value (TJ/y)
BE_{1-4}	22.3	BE_{7-10}	19.7
BE_{2-4}	2.4	BE_{8-6}	6.7
BE_{2-6}	2.1	BE_{9-6}	1.4
BE_{3-4}	2.7	BE_{9-10}	3.1
BE_{5-6}	8.6		

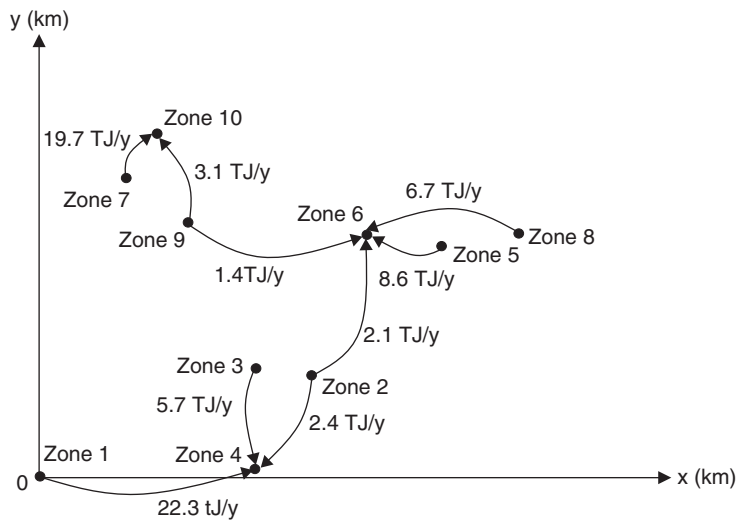

19.8 Optimal biomass exchange flows resulting from the LP optimisation.

© Woodhead Publishing Limited, 2013

Table 19.3 Cluster properties

Cluster	Zone	Area (km^2)	Supply (TJ/y)	Demand (TJ/y)	Energy balance (TJ/y)	Imbalance within the cluster (TJ/y)
1	1	11.6	24.0	1.7	22.3	1.5
	2	6.12	10.2	4.5	5.7	
	3	9.58	15.3	11.8	3.5	
	4	6.35	3.0	33.0	–30.0	
2	5	8.38	10.7	2.1	8.6	–4.5
	8	7.83	8.2	1.5	6.7	
	6	5.57	2.2	22.0	–19.8	
3	7	10.63	20.2	0.5	19.7	7.4
	9	4.12	13.1	2.6	10.5	
	10	3.15	7.8	30.6	–22.8	

Step 3. Cluster formation. The clusters formed are presented in Table 19.3. It can be seen that the region is partitioned into three clusters. Zones 1, 2, 3 and 4 form Cluster 1. Zones 5, 6 and 8 are grouped into Cluster 2, and Zones 7, 9 and 10 into Cluster 3. Table 19.3 contains also columns (Zone, Area, Supply, Demand and Energy balance) needed for the following cluster visualisation. The composite behaviour of the clusters is further illustrated in the RESDC (Fig. 19.9). The solid line is the Cumulative Supply Curve, and the dashed line represents the cumulative demand. Figure 19.9 indicates the size of each cluster and the total energy involved in the supply chain within the cluster. Since each cluster is a group of entities with relatively stronger links, this provides an opportunity to develop efficient energy planning and management strategies within a simpler supply chain, confined within the cluster, rather than comprising the whole region.

19.4.2 Case Study 2: Resource Management Curve (RMC)

The data for construction of the RMC is tabulated in Table 19.4. The data is arranged according to the procedure described in Section 19.2.3. This data is then plotted in a RMC (Fig. 19.10). The RMC displays the information about energy surpluses/deficits as well as land use, allowing for the trade-off assessment between them directly.

The first interval has a surplus of 1.0 TJ/y, which is cascaded to the next interval. This cascaded result is reflected as point L on the RMC on the right-hand side. The second interval and the third interval have also 1.50 and 2.00 TJ/y, which accumulate to 4.50 TJ/y (Point N) to be cascaded further. In the fourth interval, the zone has a deficit of 3.75 TJ/y, which leaves 0.75 TJ/y (Point O) to be cascaded to the next interval, and so on. The RMC also shows that the region is divided into two clusters. Each left-hand turning

© Woodhead Publishing Limited, 2013

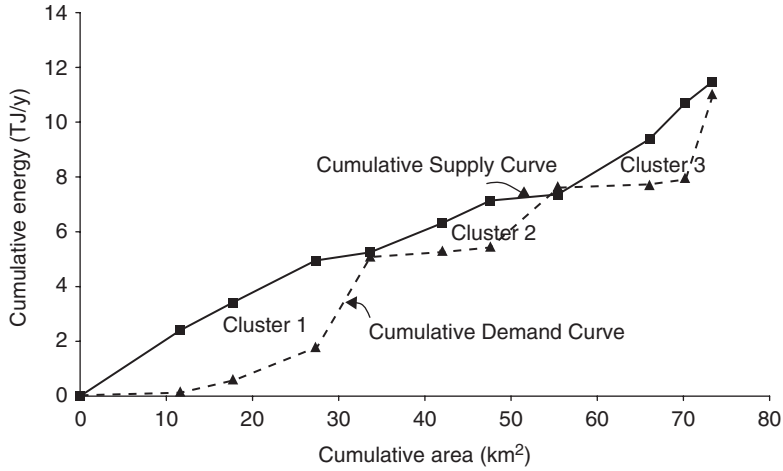

19.9 RESDC for the case study.

Table 19.4 Data for RMC construction

Cluster	Zone, *Z*	Area (km²)	Surplus/ Deficit (TJ/y)	L_i (km²/TJ/y)
1	1	30	1.00	30.00
	3	20	1.50	13.33
	4	25	2.00	12.50
	2	20	−3.75	−5.33
2	6	15	1.00	15.00
	7	25	2.25	11.11
	5	30	−4.50	−6.67

point (which could be also called a Cluster Pinch) indicates the start of a new cluster. The cluster will have surplus of biomass energy if the last point is plotted to the right of the starting point; otherwise, the cluster will have energy deficit. The energy balance for the whole region shows a deficit of 0.50 TJ/y, represented by Point S that is plotted on the left of y-axis. Figure 19.10 also indicates the size of each cluster and the total energy involved in the supply chain within the cluster.

There are several possible options to tackle the energy–land trade-off problem. The segment between points J and K in Fig. 19.10 represents the surplus in Cluster 1. Three options can be considered to deal with this surplus:

(i) Export 0.75 TJ/y of energy from Zone 1 to energy market. Figure 19.11 shows that the whole composite profile is moved to the left by 0.75 TJ/y (Rule 1). The point J' is plotted on the left of y-axis. This means that 0.75 TJ/y is transported to the energy market.

© Woodhead Publishing Limited, 2013

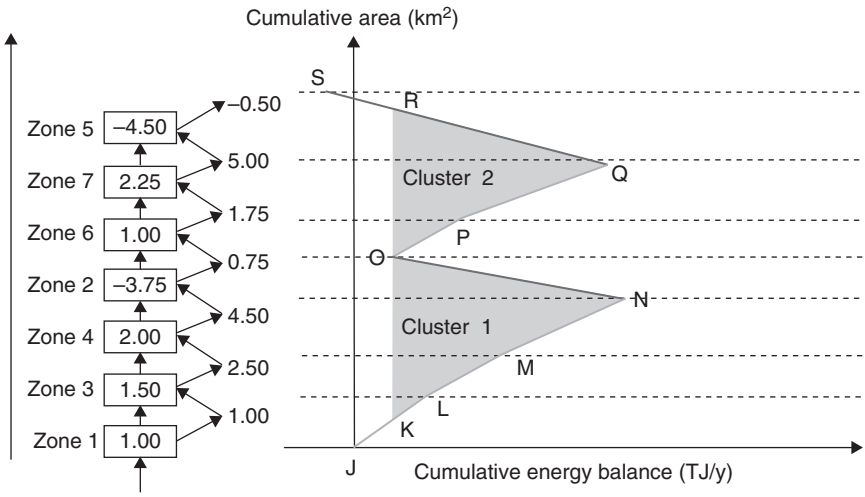

19.10 Energy and land use management with RMC.

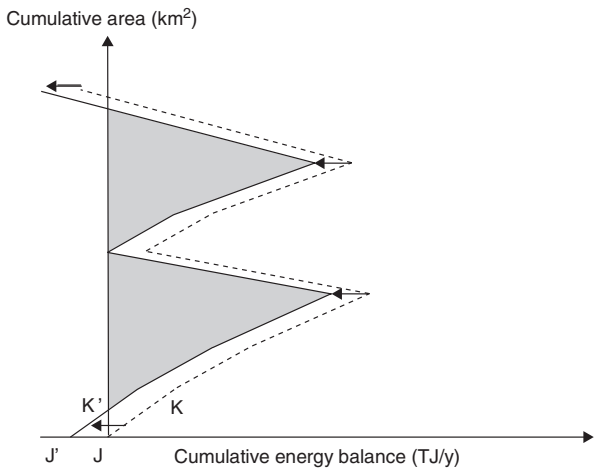

19.11 Modification of the RMC if the surplus in Cluster 1 is exported to energy market.

(ii) Use the extra land of 22.5 km^2 from Zone 1 for other purposes instead of energy production. As shown in Fig. 19.12, the new point K' is created by cutting out the segment 22.5 km^2 and shifting the remaining part of the RMC 0.75 TJ/y to the left (Rule 2).
Another option is to use 16.67 km^2 of area from Zone 4. As illustrated in Fig. 19.13, point T is shifted by 0.75 TJ/y to T'. A gap of 16.67 km^2 area appears on the resulting RMC.

© Woodhead Publishing Limited, 2013

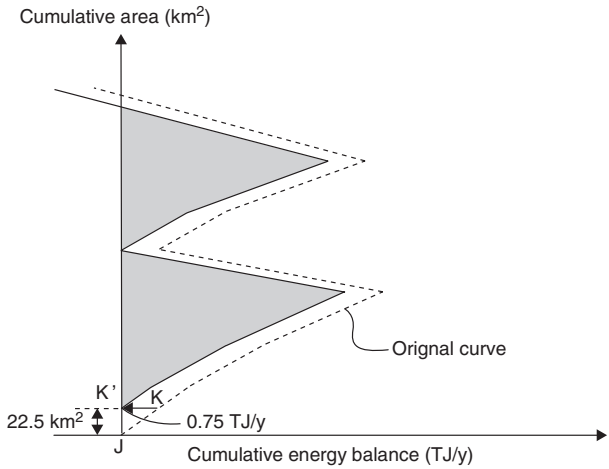

19.12 Modification of the RMC if a certain area in Zone 1 is used for other purposes.

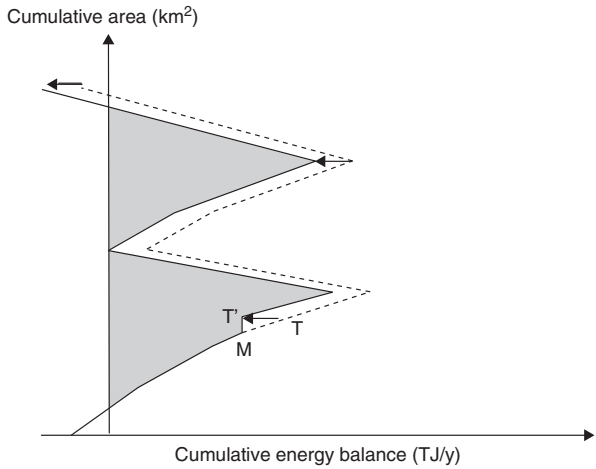

19.13 Modification of the RMC if a certain area in Zone 4 is used for other purposes.

(iii) Transfer 0.75 TJ/y of energy to Cluster 2. This situation is presented by Fig. 19.14. Firstly, the original RMC in Fig. 19.10 moved to the left. The intermediate step is resulted as in Fig. 19.10. The exported energy (Segment J'K') is transferred to Cluster 2 (as shown by the arrow). As a result, the segment of 22.5 km^2 land is cut out (Rule 2) and the point after *O* is horizontally moved 0.75 TJ/y to the right (Rule 3).

© Woodhead Publishing Limited, 2013

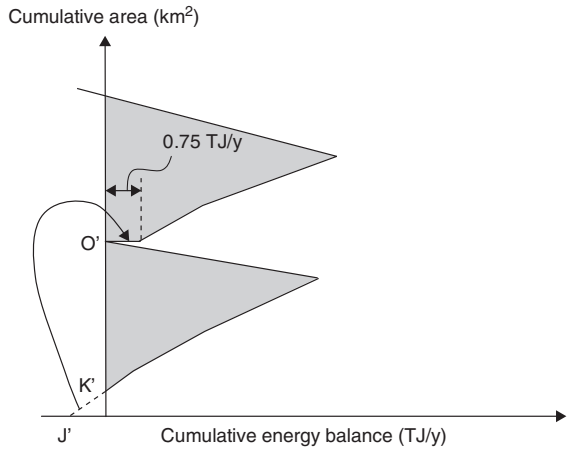

19.14 Modification of the RMC if the surplus in Cluster 1 is transferred to Cluster 2.

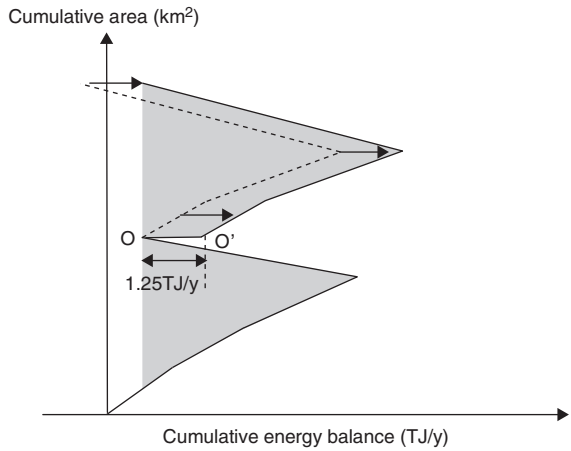

19.15 Modification of the RMC if a certain amount of energy is imported to fulfil the demand in Cluster 2.

For the deficit case in Fig. 19.10, the energy demand can be satisfied by

(i) Importing 1.25 TJ/y from the energy market. Figure 19.15 shows that after having received the import, the Pocket for Cluster 2 has been expanded by moving 1.25 TJ/y to the right after Point O (Rule 2).
(ii) Increasing the biomass production rate in the Cluster 2 (Rule 4), e.g.:
  – Convert certain areas of land from other applications to energy crops.

© Woodhead Publishing Limited, 2013

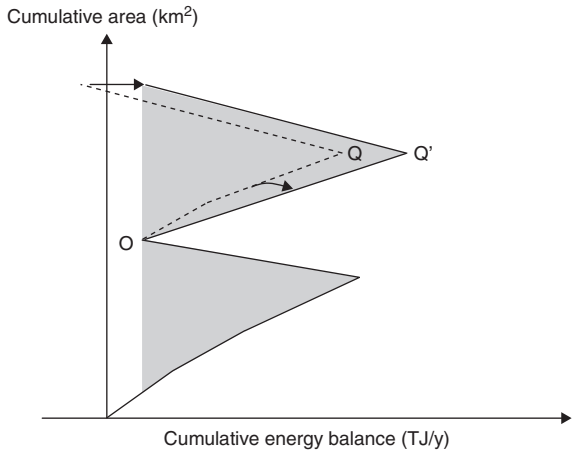

19.16 Modification of the RMC if the biomass production rate in the Cluster 2 is increased.

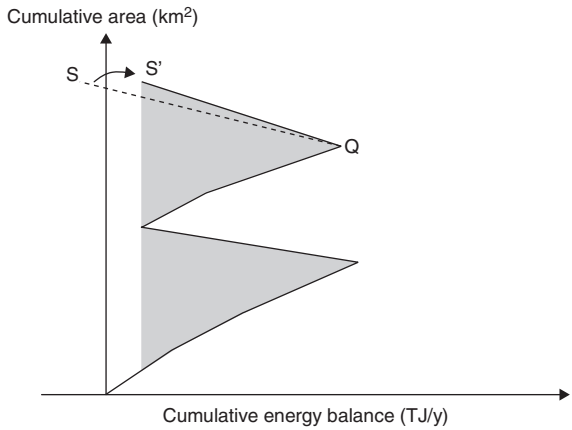

19.17 Modification of the RMC if the energy demand in the Cluster 2 is reduced.

- Grow other types of energy crops with higher yield.
- Increase the share of agriculture residues into energy sources; for example, use straw for energy production instead of using it for animal feed.

The effect of these changes decreases the slope of OQ' as shown in Fig. 19.16.

(iii) Reducing the energy demand in Cluster 2 by improving the efficiency of energy-conversion technologies (Rule 5). The slope of QS' is increased as shown in Fig. 19.17.

© Woodhead Publishing Limited, 2013

19.5 Future Trends

The analysis of supply chains with PI can be developed further by incorporating other elements, such as life cycle assessment. The life cycle of a supply chain is first quantified into an LCA index, which is able to replace one of the axes in the Pinch diagram. Through Pinch Analysis, the bottlenecks in systems with constrained environmental impacts can be investigated through life cycle assessment. Another potential element which may extend supply chain PI is the engagement of the industrial symbiosis approach in network design. The potential co-operation among industries is first identified and quantified, then the quantified factor can be used to explore the optimal symbiosis approach. For example, we can replace the concept of 'hot stream' and 'cold stream' for the source and sink flow in the original Pinch Analysis with 'discharged waste flow' and 'wanted material flow'. This makes available an assessment plan to the management level and allows favourable choices to be made.

19.6 Sources of Further Information

The references below provide further details about supply chains and supply chain design or management:

Useful Books

1. *Decision-Making for Supply Chain Integration*, H. K. Chan, F. Lettice, O.A. Durowoju (Ed), 2012, Springer, USA.
2. *Global Integrated Supply Chain*, Y-C. Lan and B. Unhelkar, 2006, Idea Group Publishing, USA.

Related Websites

1. Surviving Supply Chain Integration: Strategies for Small Manufacturers <www.nap.edu/openbook.php?record_id=6369&page=R1>
2. The Premier Online Community for Global Supply Chain Professionals <www.ebnonline.com>
3. The Green Supply Chain <www.thegreensupplychain.com>
4. Green Supply Chain case study <greeneconomypost.com/green-supply-chain-studies-7580.htm>

Publications on Integrated Supply Chains

1. PI – Industrial Symbiosis Approach:
Ng, W. P. Q., Ng, T. L., Lam, H. L., Kamal, M., Ng, E. H., Ng, D. K. S. (2012). Biomass corridor synthesis for Malaysia green energy supply chain. *Chemical Engineering Transactions*, **29**, 703–708.

© Woodhead Publishing Limited, 2013

2. PI – Industry Clustering Approach:
   Ng, W. P. Q., Tokos, H., Lam, H. L., Yang, Y. (2012). Process heat exchanger network integration and decomposition via clustering approach. *Computer Aided Chemical Engineering*, **31**, 1562–1566.

19.7 References

Beamon, B. M. (1998). Supply chain design and analysis: models and methods. *International Journal of Production Economics*, **55**, 281–294.

Clark, A. J., Scarf, H. (1960). Optimal policies for a multi-echelon inventory problem. *Management Science*, **6**(4), 475–490.

Cox, J. F., Blackstone, J. H. (ed.) (1998). *APICS Dictionary*, 9th ed. APICS, p. 93.

EIA. (2011). *Annual Energy Review 2010: Report No. DOE/EIA-0384(2010).* Energy Information Administration, Washington, USA.

Foo, D. C. Y., Ooi, M. B. L., Tan, R. R., Tan J. S. (2008). A heuristic-based algebraic targeting technique for aggregate planning in supply chains. *Computers & Chemical Engineering*, **32**, 2217–2232.

Krajewski, L. J., Ritzman, L. P., Malhotra, M. K. (2010). *Operations Management: Processes and Supply Chains*, 9th ed. Pearson Education, New Jersey, USA.

Lam, H. L., Varbanov, P. S., Klemeš, J. J. (2010). Optimisation of regional energy supply chains utilising renewables: P-graph approach. *Computers & Chemical Engineering*, **34**, 782–792.

Lam, H. L., Varbanov, P. S., Klemeš, J. J. (2011). Regional renewable energy and resource planning. *Applied Energy*, **88**, 545–550.

Linnhoff, B., Ahmad, S. (1990). Cost optimum heat exchanger networks – I. Minimum energy and capital using simple models for capital cost. *Computers & Chemical Engineering*, **14**(7), 729–750.

Linnhoff, B., Hindmarsh, E. (1983). The pinch design method for heat exchanger networks. *Chemical Engineering Science*, **38**(5), 745–763.

Shapiro, J. F. (2001). *Modeling the Supply Chain*. Duxbury Press, California, USA.

Singhvi, A., Madhavan, K. P., Shenoy, U. V. (2004). Pinch analysis for aggregate production planning in supply chains. *Computers & Chemical Engineering*, **28**, 993–999.

Singhvi, A., Shenoy, U. V. (2002). Aggregate planning in supply chains by pinch analysis. *Trans IChem*, **80**, Part A, 597–605.

Townsend, D. W., Linnhoff B. (1983). Heat and power networks in process design. Part II: design procedure for equipment selection and process matching. *AIChE Journal*, **29**(5), 748–771.

Wang, Y. P., Smith, R. (1994). Wastewater minimisation. *Chemical Engineering Science*, **49**, 981–1006.

© Woodhead Publishing Limited, 2013

20

Application of Heat Recovery Loops to Semi-continuous Processes for Process Integration

MICHAEL R. W. WALMSLEY, MARTIN JOHN ATKINS
and TIMOTHY G. WALMSLEY
University of Waikato, New Zealand

DOI: 10.1533/9780857097255.4.594

Abstract: Heat recovery loop (HRL) systems are shown to enhance indirect Heat Integration of large multi-plant sites containing semi-continuous processes. Process Integration (PI) methodologies developed for batch processes are applied to semi-continuous processes and to multi-plant sites containing numerous semi-continuous processes. A design methodology for liquid heat recovery loop systems based on traditional Pinch Targeting methods is presented, and the method is demonstrated using two illustrative examples and an industry case study.

Key words: heat recovery loops, indirect Heat Integration, semi-continuous processes, multi-plant integration.

20.1 Introduction

Effectively applying traditional Pinch Analysis techniques to semi-continuous processes, either within a single plant or across a large multi-plant site, is a significant challenge due to the time dependency of the process streams. As a result, in sectors such as food and beverage, pharmaceuticals and speciality chemicals, where processes are often batch or semi-continuous, PI has had less impact. In these industries, plants are designed to operate in a non-continuous manner to accommodate process scheduling conditions, regular cleaning of the equipment for hygiene purposes, changes in product grade or production rate, and seasonal fluctuations in raw material supply and quality. Stream variability and stream availability are therefore additional issues that need to be accounted for when applying PI to these processes.

When semi-continuous processes are clustered into one large site, the opportunity exists across plant indirect Heat Integration. Excess heat from one plant can be transferred to other plants with the aid of an intermediate fluid and thermal storage acting as an HRL system (Rodera and Bagajewicz,

© Woodhead Publishing Limited, 2013

1999). The intermediate fluid is not consumed in the process but acts as a heat transfer medium that is stored and recirculated as needed. Multiple HRL systems may be feasible depending on the temperatures of the streams available for cross-plant heat transfer, and the capital and operating costs of each HRL needs to be economically justified by the savings in utilities achieved.

In general, three types of processes are commonly found in the processing industry: (1) continuous processes, (2) batch processes, and (3) semi-continuous processes. Continuous processes operate without interruption, 24 h per day 7 days per week, and are generally large scale. Materials simultaneously enter and leave the process, there is little flexibility in how the process operates or what products are made, and maintenance shut-downs occur once or twice per year. Batch processes, in contrast, are generally smaller in scale, operate with discrete units of material being processed stage by stage over a prescribed cycle time and materials do not continually leave and enter the process. Instead, there are numerous start-ups and shut-downs and stream variables regularly change in a prescribed manner. Semi-continuous processes, on the other hand, have characteristics of both. When the process is running it behaves like a continuous process and traditional PI techniques apply. However, when the process regularly shuts for equipment cleaning, either planned or unplanned, the process behaves more like a Batch Process, and Heat Integration strategies developed for batch processes can be incorporated into the overall PI strategy. Like batch processes, thermal storage is a useful strategy for increasing integration opportunities of semi-continuous processes.

Numerous studies have been conducted into the development of PI techniques for targeting and designing indirect heat exchange and thermal-storage systems for batch processes (Fernández *et al.*, 2012). Much less has been reported for semi-continuous processes (Atkins *et al.*, 2010) and multi-plant semi-continuous processes, even though similar time related issues exist (Atkins *et al.*, 2012). In this chapter, PI methodologies developed for batch processes will be applied to semi-continuous processes and to multi-plant sites containing numerous semi-continuous processes. A design methodology for liquid HRL systems based on traditional Pinch Targeting methods will be presented. The method will be demonstrated using two illustrative examples and an industry case study.

20.2 Indirect Heat Recovery Systems

Indirect heat recovery systems involve the use of an intermediate heat transfer medium, Heat Storage Tanks (HSTs) or units and a flow circuit to absorb heat from hot streams and to release the heat to cold streams (Fig. 20.1). Storage relaxes the limitation of heat interchange between time-dependent

© Woodhead Publishing Limited, 2013

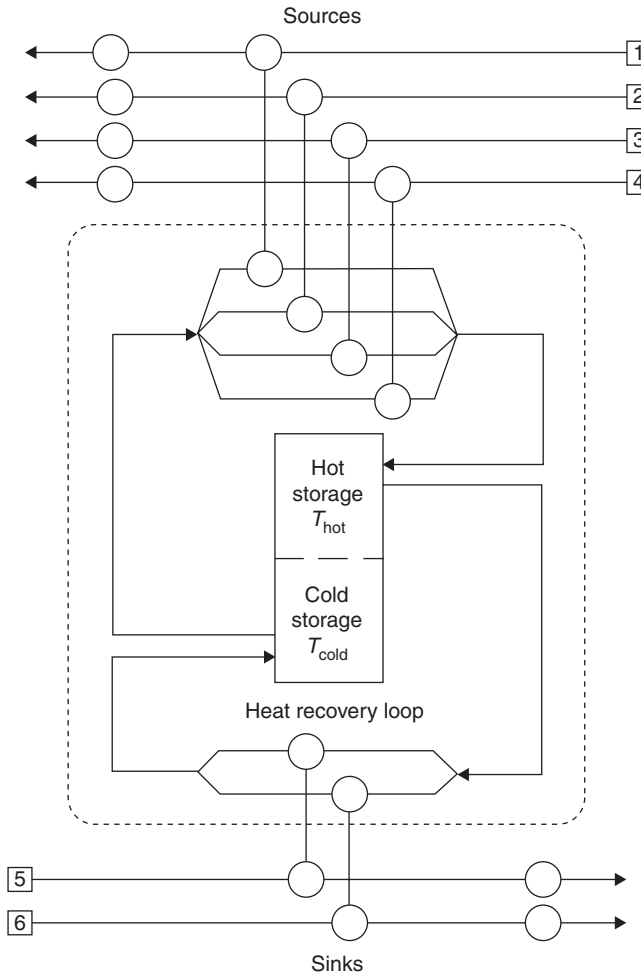

20.1 Indirect Heat Integration system with storage (From Atkins *et al.* (2010)).

streams and provides operating flexibility to the system. High-heat capacity liquids such as water are the most suitable heat transfer medium for processing sites with low Pinch Temperatures (<100°C). However, oil can be used for applications above 100°C. The HST may be multiple tanks or a single stratified tank (Dinçer and Rosen, 2010).

20.2.1 Targeting and Design Methods

Methods for designing indirect heat recovery schemes have been proposed by numerous researchers (Stamp and Majozi, 2011). The methods

© Woodhead Publishing Limited, 2013

apply almost exclusively to batch processes (Chen and Ciou, 2008), but the principles also apply to semi-continuous processes (Atkins *et al.*, 2011), especially when integrating across multiple plants on the same site.

The Time Slice Model (TSM) approach developed by Kemp and MacDonald (1987, 1988) and later expanded by Kemp and Deacon (1989) has been applied to the Heat Integration of Batch Process. Various programming techniques, such as Mixed Integer Linear Programming (MILP), have also been applied to improve the integration of batch processes by attempting to optimise the scheduling (Papageorgiou *et al.*, 1994; Lee and Reklaitis, 1995), pairing of batch vessels (Vaselenak *et al.*, 1986) and Heat Exchanger Network (HEN) design (Foo *et al.*, 2008). The basis for integrating batch processes is that the process is operated in a cyclic fashion, and the scheduling of the operations is interdependent and constrained. Rescheduling of the operations may be permitted, depending on the constraints of the process and final product.

Stoltze (1995) proposed a combinatorial approach called the Permutation Method, where a search is performed among a set of feasible operating temperatures of HSTs and a sub-set of process streams to be integrated, to find the most cost-effective configuration of process stream – tank matches. The storage tanks were assumed to be fixed-temperature/variable-mass systems and the feasible operating temperatures of the tanks based on the supply and target temperatures of the process streams. The heuristic rules restricted the solution domain to enable an exhaustive search. The method was further developed by Mikkelsen (1998), using a post-optimisation stage for fine tuning the system variables, but the method has been difficult to apply in practice.

A graphical Pinch Methodology for indirect heat recovery using constant-temperature heat storage and variable mass storage was proposed by Krummenacher and Favrat (1995) and Sadra-Kazemiand and Polley (1996). Both independently made the link between the stream schedules and the possible number of HSTs. Krummenacher and Favrat (2001) further developed the method using the Time Average Model (TAM) and Composite Curve (CC) diagram to identify tank temperatures and hot and cold utility targets. Variable temperature and variable mass storage have been investigated by Chen and Ciou (2009) for batch systems. The constraint of fixed-temperature heat storage was shown to reduce heat recovery for the same size storage tanks. MILP was used to find the optimal storage volumes for minimal external utility and total annual cost for the overall heat recovery system.

Total Site Analysis (refer to Chapters 6 and 7) was also developed to integrate entire processing sites (Goršek *et al.*, 2006) or groups of sites (Ahmad and Hui, 1991) that are serviced by a centralised utility system (Dhole and Linnhoff). Insight-based techniques (e.g. Pinch Analysis)

© Woodhead Publishing Limited, 2013

(Rodera and Bagajewicz, 1999) and optimisation-based techniques (e.g. mathematical programming) (Bagajewicz and Rodera, 2000) have been developed and applied to the problem of Total Site Integration directly using process streams or indirectly using intermediate fluids (Bagajewicz and Rodera, 2002). Both approaches have their relative merits and weaknesses and can be employed iteratively or simultaneously (Kralj *et al.*, 2005; Sieniutycz and Jeżowski, 2009). Methods have also been developed to apply and extend traditional Pinch Analysis to heat recovery in a cheese factory with non-continuous process operations (Becker et al., 2011) and between four existing petrochemical plants (Kralj *et al.*, 2002). In addition, a modified Pinch Analysis approach has been applied to heat recovery In addition, targeting of a large multi-plant dairy processing site with a HRL for different operating states throughout the year (Atkins *et al.*, 2010).

20.2.2 Selection of Intermediate Fluid and Heat Storage Tanks

In low-temperature (<100°C) HRL applications, liquid water is used as the intermediate fluid due to its high volumetric thermal capacity, 4.17 MJ/m^3K. For higher temperature applications (>100°C), high boiling point liquids such as oil, 1.64 MJ/m^3K, can be used (Dinçer and Rosen, 2010). In theory, a pressurised vapour–liquid refrigerant fluid could also be used; however, the thermal-storage system will be more complicated and the overall cost of the system is likely to be well above an equivalent system using water.

Thermal storage is an important part of the HRL system. In general there are three storage systems: (1) single tanks, (2) thermally stratified tanks, and (3) phase-change storage tanks. Single tanks can either be constant-temperature variable-storage systems, or variable-temperature constant-storage, or variable-temperature and variable-storage. To be economical, tanks must be simple and cheap in construction, and the operation must be simple, reliable and low in maintenance. HRL system controls are also required to maintain the tanks at constant temperature, if that is what is required, or at minimum levels to maintain some buffer capacity.

Thermally stratified tanks exploit the density difference of the HRL intermediate fluid due to a difference in temperature thus creating natural stratification within the tank (Dinçer and Rosen, 2010). Housing the hot and cold intermediate fluids in a single tank effectively doubles the storage capacity compared to using two separate tanks. Operational issues and analysis of stratified tanks are well established in the literature (Atkins *et al.*, 2010) Maldistribution (Walmsley *et al.*, 2009). Stratified tanks have been applied to dairy factories in New Zealand, with significant energy savings being realised.

© Woodhead Publishing Limited, 2013

Phase-change storage takes advantage of the high energy density associated with latent heat. This type of storage is most applicable to processes that require large amounts of storage with relatively small space and large enthalpy change over a small temperature difference. A main disadvantage of phase-change systems is an additional ΔT_{min} that occurs due to heat being transferred from a process stream to an intermediate fluid, $\Delta T_{min,1}$, and then to the phase-change storage, $\Delta T_{min,2}$. Storage systems using phase-change materials are an emerging technology.

The amount of storage required is dependent on the frequency and amplitude of the variability of the process streams, the intermediate fluid flow rate and the storage material. For example, streams with high frequency variation in the range of minutes require much less storage volume than low frequency changes that result in sustained heat-cooling imbalances over a few hours. For retrofit studies, actual logged stream data can be sourced and a simple algorithm, such as the model developed by Atkins *et al*. (2012), can be used to track the storage tank levels over time and to select correctly sized storage tank(s). Storage tank volumes which give a fluid mean resident time of at least a couple of hours are recommended.

20.2.3 Sizing Heat Exchangers

Sizing the HRL system heat exchangers is an important part of the design process and has a direct impact on the HRL economics. The stream design heat capacity flow rate (CP) should be used when sizing heat exchangers, rather than the daily average values that are used during the targeting stage (see Section 20.3.1). Daily averages give more meaningful average heat recovery targets but, due to the semi-continuous nature of the streams the peak or design values, should be used for sizing heat exchangers so that the maximum amount of heat can be recovered. The daily average is lower than the design point or peak flow value (Section 20.3.1) and using it for design will under-predict the size of the heat exchanger needed to recover heat when the plant is running at full capacity. For extreme cases, where a plant only runs a few hours a day, installing a large exchanger to recover the peak may not be economically justified and a smaller heat exchanger may be the economic optimum. These types of decisions need to be made on a case-by-case basis.

20.2.4 Heat Recovery Loop Costing

Costing of HRL systems involves estimation of four main capital components: (1) heat exchangers, (2) storage tanks, (3) piping, and (4) instrumentation and control systems. The distribution of the capital between

© Woodhead Publishing Limited, 2013

these areas is largely process and site dependent. For example, in the New Zealand dairy industry where plate heat exchangers are common practice and sites are very large, the cost of stainless-steel piping becomes increasingly significant. In many cases oversizing heat exchangers can provide additional heating or cooling loads at critical times that may reduce the need for large amounts of thermal storage. Therefore, there is a design trade-off between the size of the storage and the oversizing of the heat exchangers.

20.2.5 Operational Considerations

Stream variability in the form of flow rate changes often gives rise to load imbalance on the loop. When the flow rate of a process stream changes, the loop temperature control systems either increase or decrease to ensure that loop temperature stays constant. The dynamics of the other streams on the loop similarly affect the loop flow rate and the quantity of liquid produced at each storage temperature. The storage tanks have buffer capacity to allow the system to be out of balance for a period of time, typically a few hours. Load imbalance causes excess liquid at one tank temperature to become in-excess while the other on the loop becomes in-deficit. Once a tank, or tanks, becomes either full or empty the tank-level control system has to drop off streams from the loop to restore the level in the tank to an acceptable value (Atkins *et al.*, 2011). Another method of balancing the load is to transfer fluid from one storage tank to another and use the heating or cooling utility to change the temperature of the intermediate fluid (Krummenacher and Favrat, 2001).

20.3 Application of Heat Recovery Loops to Semi-continuous Plants

Liquid HRL systems can be used in batch and semi-continuous processes to enhance the heat recovery potential of time-dependent processes. Similar Pinch Analysis methodologies can be used for both situations. In this section, a graphical PI method for targeting heat recovery systems for multiple semi-continuous plants will be presented using a similar method proposed by Krummenacher and Favrat (2001) for batch processes. The method will be extended to the design of HRL systems for large multi-plant sites. A key stage in the method is the determination of the number and the temperatures of HSTs (also termed heat storage units), which have a major effect on the amount of heat recovery possible and the design of the HEN (Sadr Kazemi and Polly, 1996). The method is also applied to the variable-temperature/variable-volume HST.

© Woodhead Publishing Limited, 2013

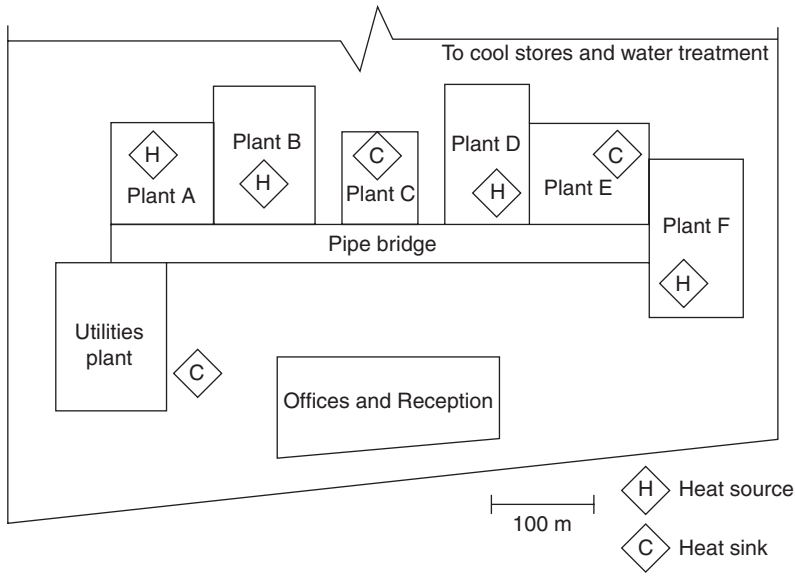

20.2 Illustration of a large multi-plant site.

20.3.1 Targeting for Multi-plant Sites

Consider a large multi-plant site made up of six semi-continuous operating plants serviced by a common utilities plant. A schematic of the plant is presented in Fig. 20.2. For steady-state targeting, daily average CP values are used for the streams to be integrated. The daily average CP is calculated over the full period (weeks or months) the plant is producing product. A comparison between the average CP and the peak or design CP is illustrated in Fig. 20.3.

The data in Table 20.1 will be used to demonstrate a graphical method for targeting an indirect HR system for the Total Site, including the number of constant-temperature thermal-storage tanks, intermediate fluid temperature ranges and operating flow rates. The site operates with two production states: 60% of the year in state A and 40% of the year in state B. Stream characteristics stay the same for both production states.

For production state A stream data from Table 20.1 are shown as a series of Hot and Cold CCs ranging from no heat recovery (I) to maximum heat recovery for a two-tank system (VI) in Fig. 20.4. The starting point of each stream is indicated in I by a small circle on the CC. This becomes important for determining the limiting temperatures of the HST. Shifted temperatures are used, where hot-stream temperatures are shifted by subtracting a full ΔT_{min} and cold-stream temperatures are shifted by adding a full ΔT_{min} to

© Woodhead Publishing Limited, 2013

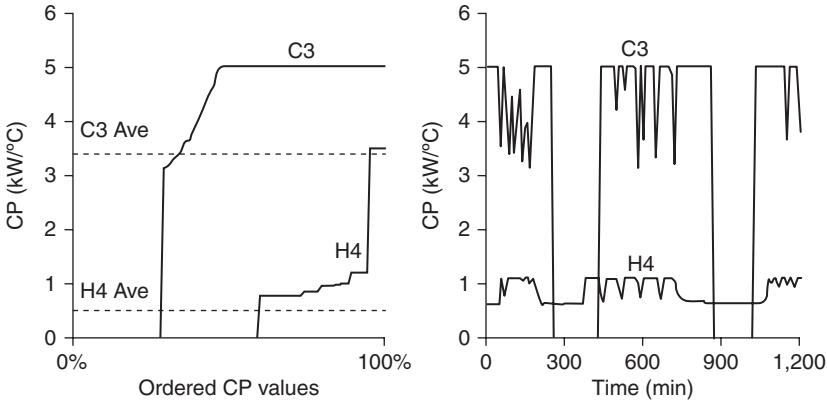

20.3 Comparisons between the time-averaged and design point heat flow rates.

Table 20.1 Sink and source data for the HRL system

Stream	TS (°C)	TT (°C)	Time average CP (kW/°C)	Design CP (kW/°C)	Time average ΔH (kW)	Production state
C1	25	100	0.850	1.0	63.75	A
C2	130	180	1.800	3.0	90.00	A, B
C3	80	105	3.375	5.0	84.38	A
H1	135	15	0.853	1.1	102.36	A
H2	100	95	9.000	20.0	45.00	A, B
H3	165	125	0.263	3.5	10.52	A, B
H4	165	125	0.525	3.5	21.00	A, B

Source: Adapted from Krummenacher and Favrat (2001).

account for the heat transfer between the process streams and the intermediate fluid. In this case the $\Delta T_{\min}$ used is 5°C. The temperatures of the HST are real temperatures and can therefore touch the CC and still remain feasible.

As the Cold CC is shifted to the left (Fig. 20.4 II), the amount of heat recovery (Q_R) increases, and the HST and intermediate fluid can be used to indirectly transfer heat from the hot streams to the cold streams. Graphically, a two-tank HRL can be represented by a single sloping line on the CC diagram, the slope of the line indicating the average intermediate fluid CP. In Fig. 20.4 II, 24 kW can be recovered with two HSTs, and the cold-storage temperature (HST1) can be anywhere between point B (30°C) and point A (112°C). Hence, the hot storage temperature can range anywhere between points C to D. Points A, B, C and D all represent Storage Pinch Points that

© Woodhead Publishing Limited, 2013

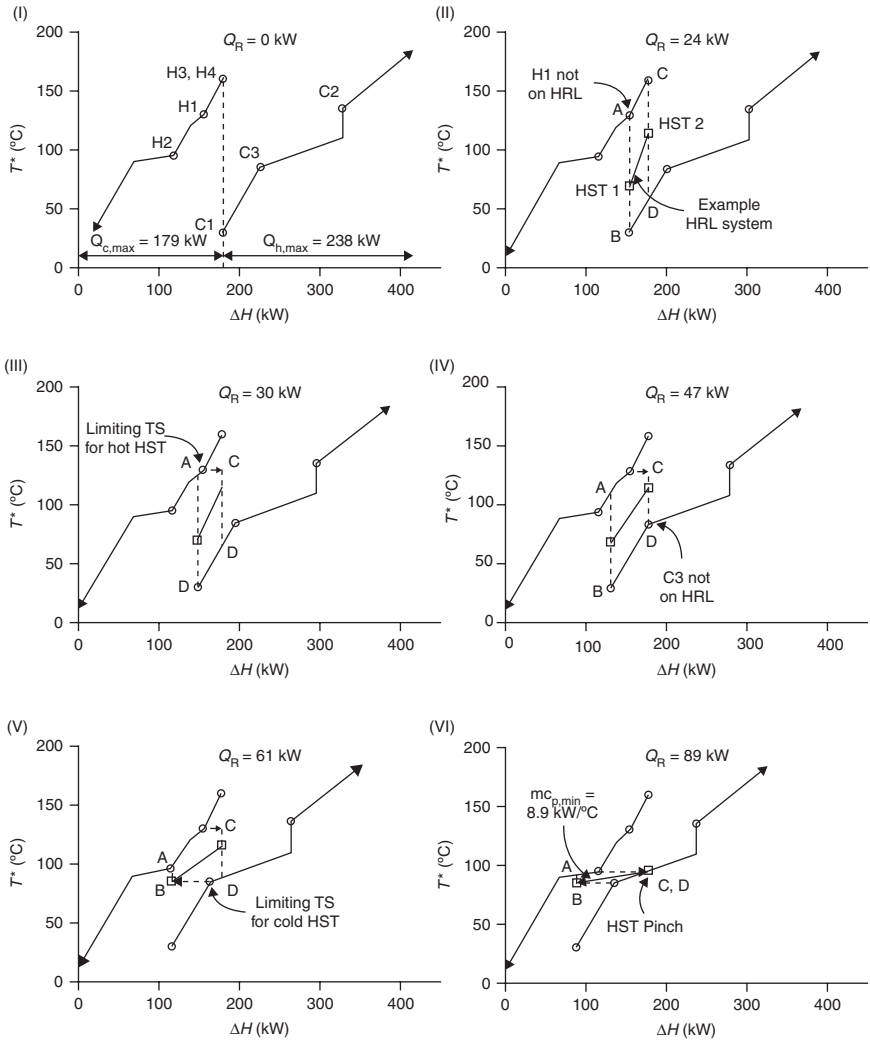

20.4 Hot and Cold CC for two HSTs ranging from no heat recovery to maximum heat recovery for two tanks. Stream data from Table 20.1, production state A.

define the limits of feasible heat transfer for this amount of heat recovery. However, for counter-current heat transfer the cold-storage temperature should always be lower than the hot-storage temperature. On the Cold CC side, only one stream (C1) is included in the two-tank HRL system. On the Hot CC side, two streams are included (H3, H4).

The maximum and minimum temperatures of the hot and cold HSTs as a function of heat recovery are illustrated in Fig. 20.5, and the streams

© Woodhead Publishing Limited, 2013

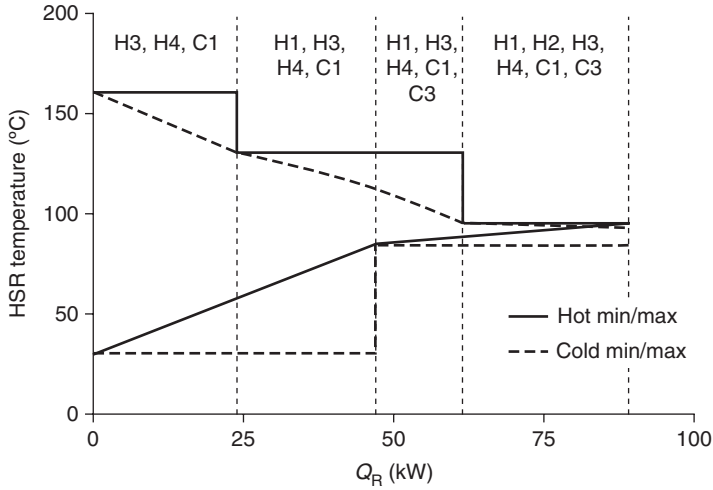

20.5 Maximum and minimum hot and cold HST temperatures as a function of heat recovery for a two-tank system, production state A.

included are indicated above the various regions. There are four distinct regions where certain streams are constraints for the temperatures of the HST, and the constraining streams are shown in bold in the figure. As heat recovery is increased other streams become included in the HRL and the constraint on the HST temperatures can shift. This is shown in Fig. 20.4 IV, where the stream H1 limits the maximum temperature of the hot HST. The supply temperature of stream H1 (135°C) limits the hot storage temperature (HST 2) to a maximum of 130°C, point C. If a temperature above 130°C is chosen, stream H1 would no longer be able to be utilised as a source, the heat recovery targets shown would not be feasible, and the CC would need recalculating to exclude H1. Cold streams may also become constraints on the HST temperatures, as illustrated in Fig. 20.4 V.

If the CC is shifted to the maximum $Q_{R,}$ as in Fig. 20.4 VI, there is a smaller ΔT_{HST}, which requires a larger intermediate fluid flow rate between storage units. At some point the temperature range reduces to a single temperature on either the hot- or cold-storage sides, causing a Storage Pinch. In this case, points C and D for the hot storage temperature converge to 95°C. The cold-storage temperature is limited to a small range of 85–92.2°C. This is the point of maximum heat recovery for a two-tank system, and bringing the CCs closer results in an infeasible system.

Increasing the number of tanks from two to three opens the way to increase the maximum Q_R as illustrated in Fig. 20.6. In Fig. 20.6 I, Streams H2 and C3 starting at 95°C (Hot CC) and 85°C (Cold CC), limit the middle

© Woodhead Publishing Limited, 2013

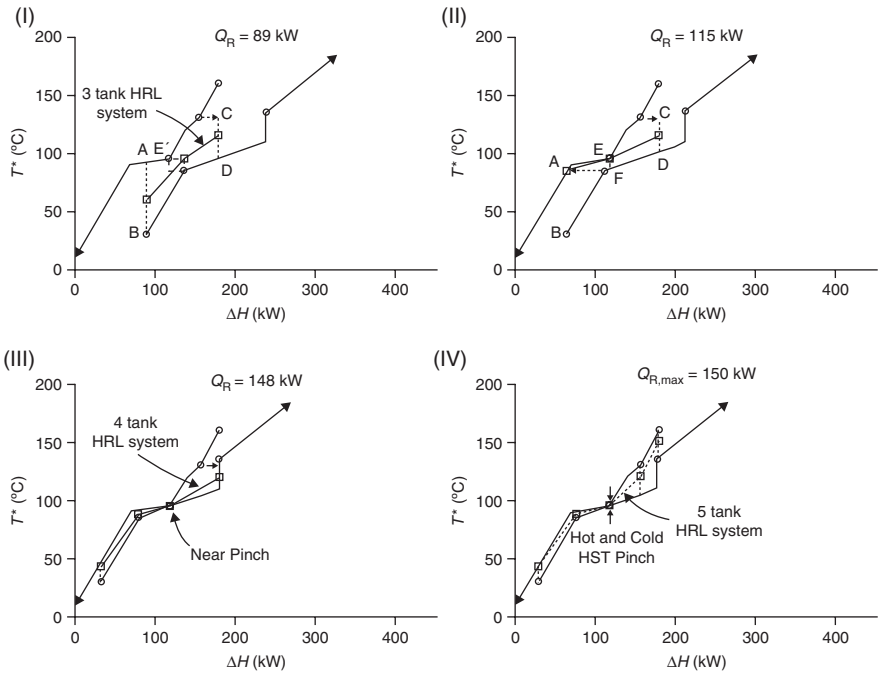

20.6 Hot CC and Cold CC with cross-plant heat recovery for three-tank HRL systems, production state A, with (I) same HR as two-tank maximum, (II) practical three-tank system with large differences between tank temperatures, (III) maximum four-tank HRL, and (IV) maximum five tank HR.

tank temperature. The high-temperature storage has to fall between C and D as before. The low-temperature storage must lie between A and B. Any point within box E' provides a feasible temperature for the middle HST, and gives the heat target that must be transferred between the three tanks to balance the network. Moving the Cold CC further left (Fig. 20.6 II) reduces the freedom of selecting the balance of the heat transfer between each storage tank and, as happened in the two-tank case, reduces the range of feasible temperatures at the hot (high) and cold (low) tanks. The maximum heat recovery with three HSTs is 115 kW; however, the increase in Q_R is at the expense of running an HRL at a significantly higher flow rate.

Using the same procedure, the maximum heat recovery for four tanks (Fig. 20.6 III) and five tanks (Fig. 20.6 IV) can be determined. A storage tank must be placed at some point along each of the dotted lines or the CC Pinch Point. With each additional tank, the average temperature driving force is reduced and the number of heat exchangers are increased. For a $\Delta T_{\min} = 5°C$ between the process streams and the heat storage medium, a minimum of

© Woodhead Publishing Limited, 2013

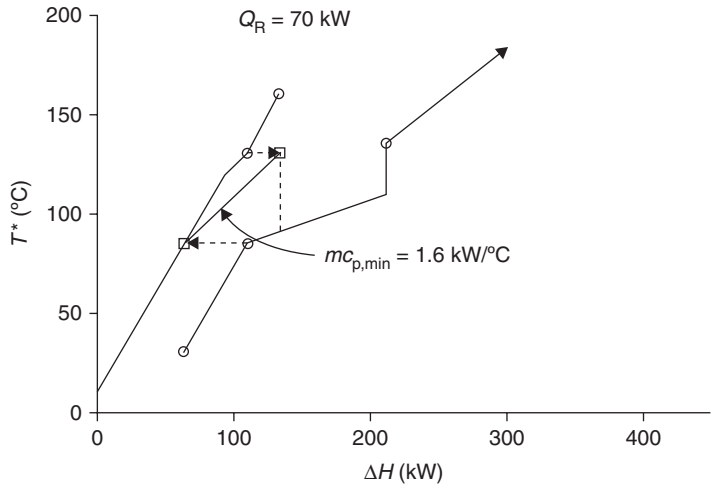

20.7 Two-tank HRL system with H2 stream removed, production state A.

five tanks is needed to ensure that the maximum amount of indirect heat recovery occurs.

On occasions the CCs contain streams that limit the temperature range of the storage tanks, which in turn can limit the indirect heat recovery potential. Rather than increase the number of tanks to increase heat recovery, a more cost-effective option may be to stay with two tanks but to remove the limiting stream from the HRL system. This in turn will allow the temperature of the second HST to be increased, and is partly demonstrated by removing stream H2 from Fig. 20.4 to give a new CC and a new feasible two-tank system with a higher tank HST2 temperature, including a much lower loop heat flow rate for only a modest reduction in Q_R (Fig. 20.7). In other situations, an increase in Q_R can occur, as demonstrated in case study (Section 20.5). The benefits of excluding a stream from the HRL system are not always obvious but, with experience, the designer can incorporate this type of analysis at the targeting stage.

Targeting is then repeated for each of the other production states to determine the yearly average heat recovery target for the site. For production state B, the stream data in Table 20.1 can be drawn as CCs (Fig. 20.8) and, for the two-tank case with HST1 at 135°C and HST2 at 150°C, a heat recovery of 20 kW is possible. Applying the heat recovery targets for each production state (e.g. A and B), the weighted yearly average $\bar{Q}_R$ is 74 kW. For 'n' production states the generalised equation is

$$\bar{Q}_R = \sum_i^n Q_{R_i} F_i \qquad [20.1]$$

© Woodhead Publishing Limited, 2013

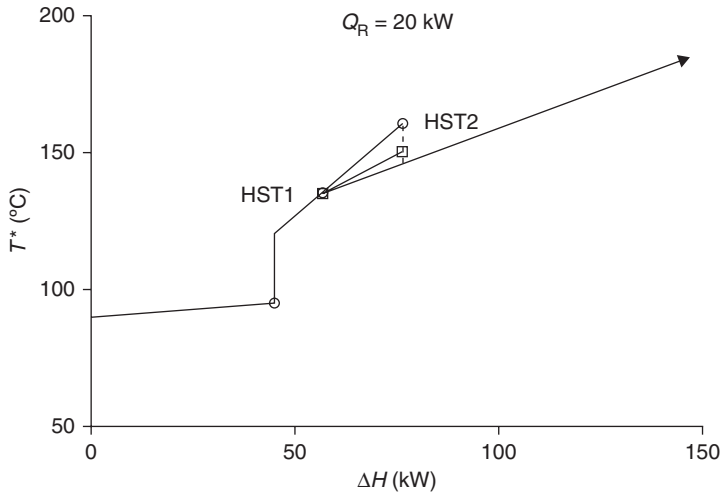

20.8 Two-tank HRL system for production state B.

where F_i is the fraction of the year production state '*i*' is operational and Q_{R_i} is the heat recovery target of production state '*i*' when running.

20.3.2 Heat Exchanger Network Design

Once the number of storage tanks and their associated temperatures are selected, the CC indicates the heat recovery target between each tank for a balanced network design. This is illustrated for production state A with the three-tank–two-loop example in Fig. 20.9, with storage tank temperatures of 60°C, 90°C and 120°C. The heat transfer between the 60°C tank and the 90°C tank is 47 kW and between the 90°C tank and the 120°C tank is 61 kW, for a total heat recovery of 108 kW. Heat recovery is limited by the sources, due to the Storage Pinch occurring at 85°C (HST1) on the hot CC.

A feasible HEN Design achieving 108 kW of indirect heat recovery can be developed with vertical heat transfer within the overlapped region (Fig. 20.9a). Portions of the source streams exchange heat to the storage fluid, which in turn supplies heat to the sink streams. The remaining parts of the stream reach their target temperatures by utility. The individual average heat exchanger duties and areas are given, and some of the main HEN parameters are summarised, in Fig. 20.9. Areas are sized according to the design CP values given in Table 20.1, which would result in the peak exchanger duties. Heat transfer from streams outside the overlapped regions on the non-limiting CC is also possible provided there is no $\Delta T_{\min}$ violation. This flexibility on the Sink Curve can be used to reduce the number of heat exchangers in the network and to allow for the installation of smaller tank sizes.

© Woodhead Publishing Limited, 2013

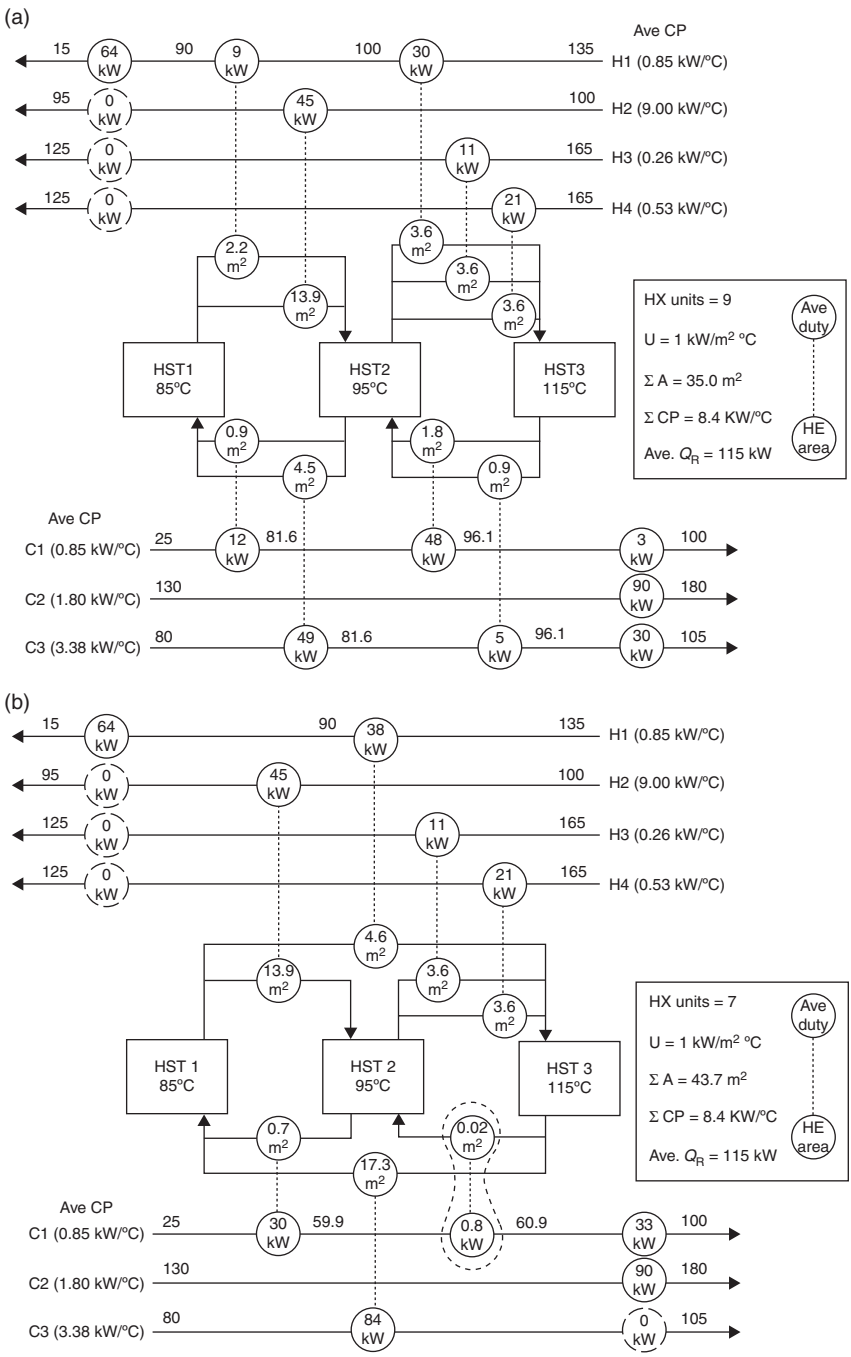

20.9 Three-tank HRL system Grid Diagram for production state A. (a) Vertical heat transfer, (b) Simplified and improved network.

© Woodhead Publishing Limited, 2013

Practical design improvements can be made to the HEN Design in Fig. 20.9a to reduce the number of heat exchangers, and thereby probably lowering the overall cost. On the source side, the two exchangers on stream H1 can be combined into a single unit that takes fluid at 85°C and heats it directly to 115°C, effectively bypassing HST2. On the sink side a similar combining can happen on stream C3, with fluid being cooled from HST3 to HST1. Attempting also to combine the exchangers on C1 leads to a mass-flow imbalance between the tanks, hence two exchangers are necessary for stream C1. However, duty from both exchangers on C1 can be shifted to the exchanger on C3 until stream C3 reaches its target temperature. When streams bypass an intermediate HST, it is important to verify that at steady state both the heat and mass flows balance.

The HEN Design and storage tank temperatures for production state B can also be determined (Fig. 20.10), and the overall network derived, by combining the HENs for each production state (Fig. 20.11). On streams H3 and H4, larger area heat exchangers are needed to meet the target for production state B compared to production state A, and an additional heat exchanger is needed on stream C2. The final exchanger area used for the overall network is an economic trade-off between the costs of the extra area required for production state B vs the value of the extra heat recovery achieved for both production states A and B. For this example the larger exchangers calculated for state B are not economically justifiable, and the areas calculated for state A have been used for the overall network. The exchanger on sink stream C2 has also been downsized to balance the load

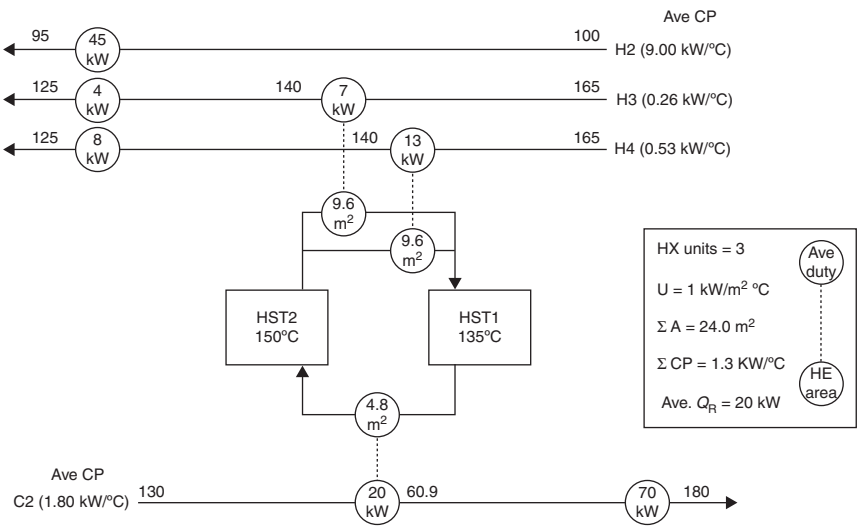

20.10 Two-tank HRL system Grid Diagram for production state B.

© Woodhead Publishing Limited, 2013

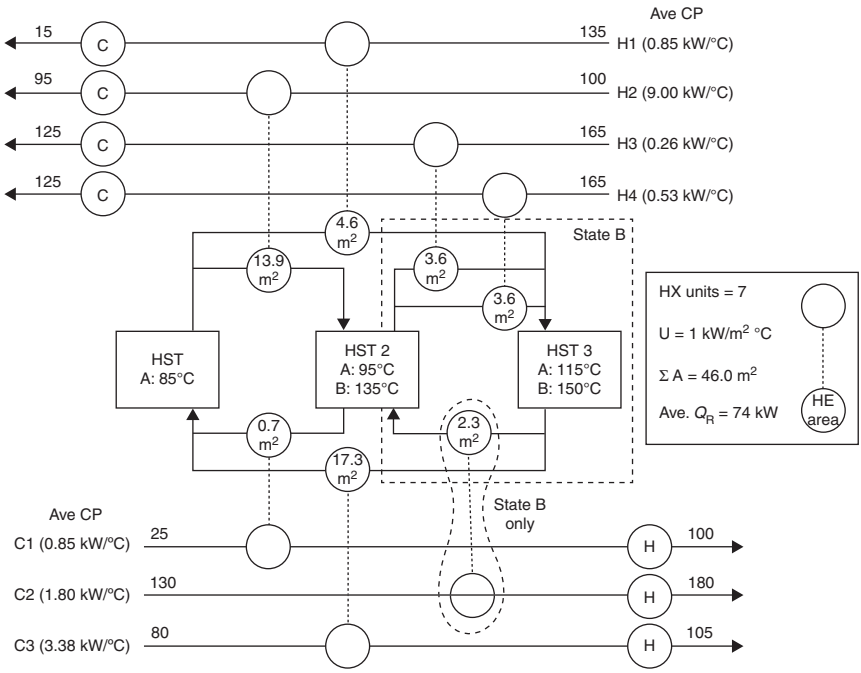

20.11 Combined HRL system Grid Diagram for production states A and B.

with the smaller exchangers on H3 and H4. The yearly average heat recovery target covering both states A and B is, therefore, 74 kW.

20.3.3 Sizing the Heat Storage Tanks

A dynamic spread-sheet model was developed, using the method of Atkins *et al.* (2012), to determine the optimum tanks, sizes for the overall network (Fig. 20.11). Using stream history, the storage tank levels and actual heat recovered can be modelled over time for a range of tank volumes. The semi-continuous nature of the process is observed in the fluctuating tank levels illustrated in Fig. 20.12a and with the increasing heat recovery that is possible with increasing tank volume (Fig. 20.12b). Larger storage tanks reduce the periods when the HRL flow rate between two storage tanks has to be slowed to balance the load around one of the tanks and to prevent the tanks becoming full or empty. An optimum tank volume of 25 m^3 for all three tanks that minimises total cost can then be determined (Fig. 20.13).

© Woodhead Publishing Limited, 2013

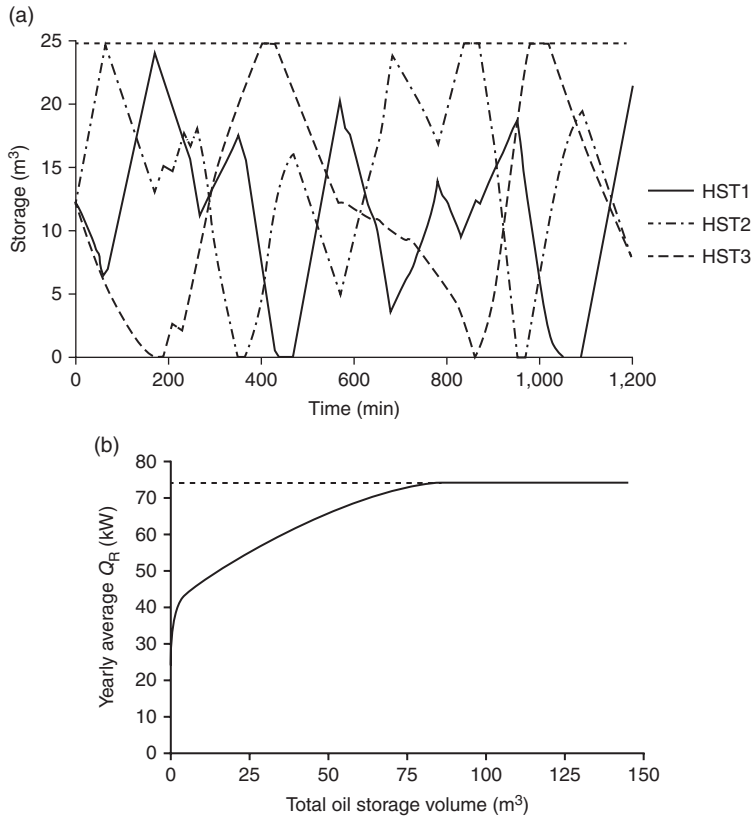

20.12 HST modelling with oil as the intermediate fluid, (a) storage levels for three 25 m^3 tanks during state A, (b) yearly average heat recovery for a range of total storage tank sizes.

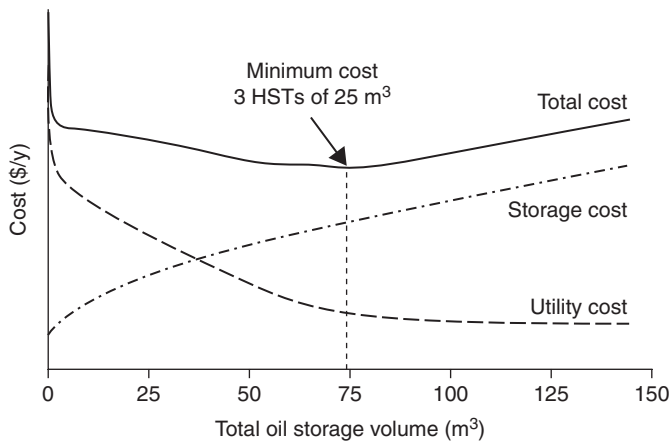

20.13 Cost optimisation of the storage tank size.

© Woodhead Publishing Limited, 2013

20.3.4 Variable-Temperature Heat Storage System

It is possible to set up an HRL that operates with variable-temperature tanks rather than fixed-storage temperature tanks (Chen and Ciou, 2009). For this situation, the intermediate fluid exchanges heat with the streams on the loop to within ΔT_{min} of the supply temperature of the stream, rather than to a specific storage temperature. The intermediate fluid streams as a consequence are heated or cooled to variable temperatures. The hot intermediate fluid streams after heating are mixed in the storage tank, and the cold streams are similarly mixed together. As the flow rate of process streams on the loop fluctuates, and heat imbalances occur, the tank levels and temperatures also vary. Streams that previously had to drop out due to an insufficient supply temperature can now be considered for heat exchange, and the possibility exists for a greater heat recovery target. If this concept is applied to state A with the same ΔT_{min}, and the unsteady nature of the process streams is modelled, a maximum heat recovery of 125 kW is feasible for two tanks of 37.5 m^3 (Fig. 20.14). The tank size is comparable to the total storage volume of the three-tank constant-temperature system (Figs 20.9 and 20.13), which was able to recover 113 kW. The increase in heat recovery for the variable-temperature case, however, requires twice the total heat exchanger area, due to the much lower temperature driving forces present in the heat exchangers. Further research is required in this area to more clearly evaluate the merits of this approach to semi-continuous processes.

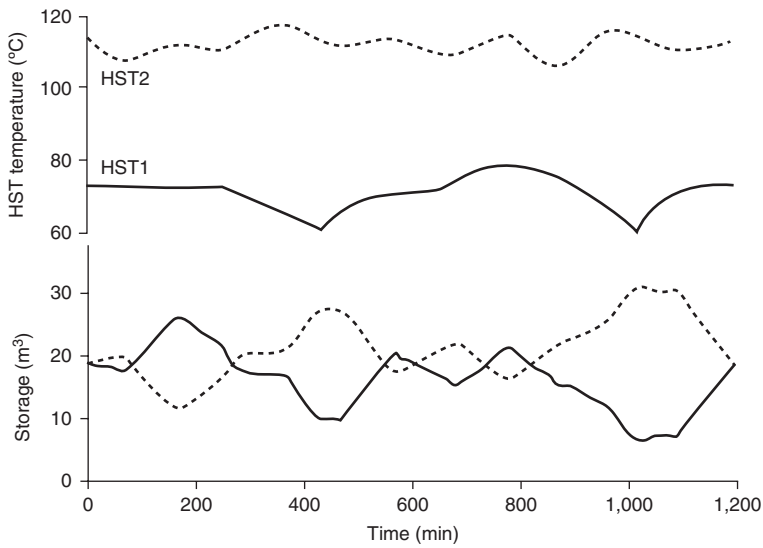

20.14 Variable-temperature HST modelling for state A.

© Woodhead Publishing Limited, 2013

20.4 A More Complex Example of a Heat Recovery Loop (HRL)

This section uses a more complex example, involving a total of 78 streams, to demonstrate the graphical method for designing HRL. Some aspects of the method that were not previously gone into with much depth are highlighted in this case. The method is presented in a step-by-step manner following the decision-flow diagram presented in Fig. 20.15.

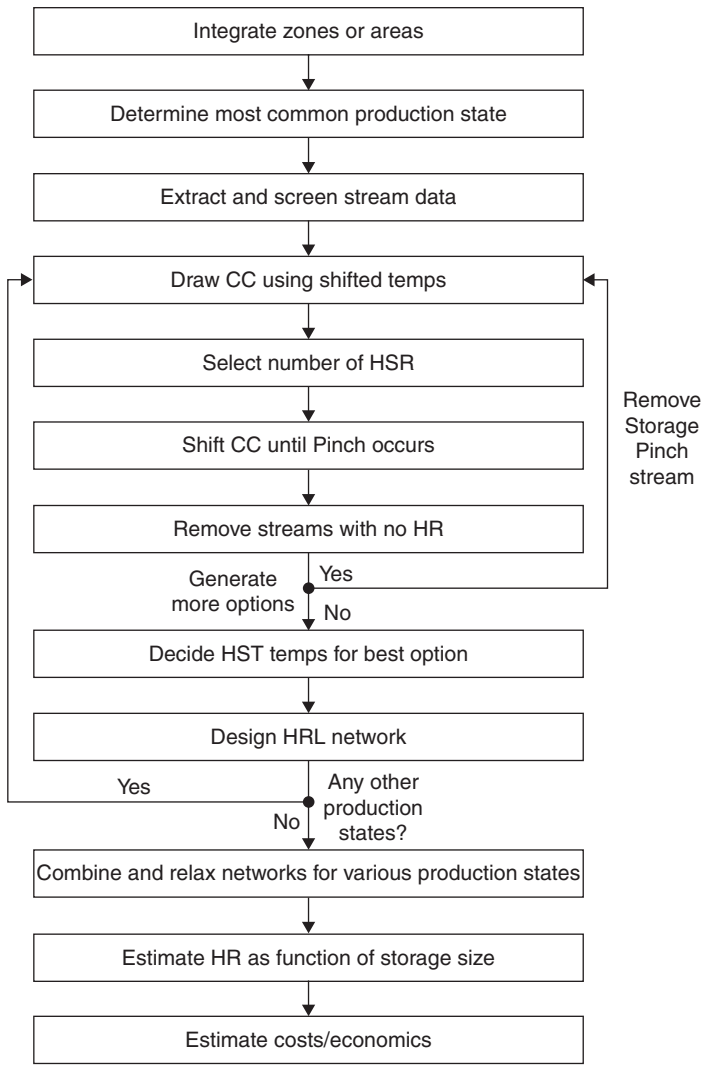

20.15 Semi-continuous multi-plant integration method.

© Woodhead Publishing Limited, 2013

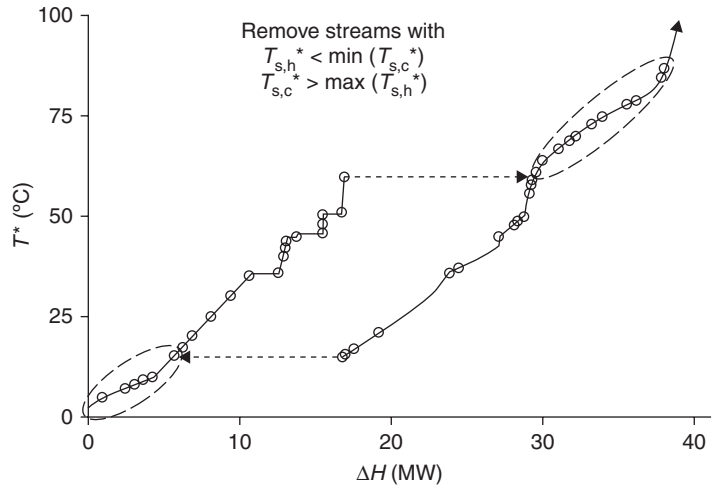

20.16 CCs of streams left over after intra-plant integration.

A large industrial site with seven individual plants/processes is considered in this example. Individual plants were first integrated and candidate streams for the HRL included any stream that is not integrated within its base plant and uses utility. The site has a number of different production states and the first targeting analysis should focus on the dominant production state. The time average CP across the production state is used in the targeting procedure. The TS and TT of the streams remain fairly constant throughout the production state.

There are 78 streams that are potential candidate streams once the initial zone integration is performed. The Hot and Cold CCs for all 78 streams are illustrated in Fig. 20.16 using shifted temperatures. Streams that are either too hot or too cold for any integration in an HRL are removed (streams within the indicated region in Fig. 20.16). In the example, the number of streams reduces from 78 to 42.

Further screening or assessment of the streams can occur based on any number of criteria, such as heat recovery potential, economics, stream matching constraints, physical distance to the location of the HRL, or product quality concerns. In this case, screening was conducted based an economic criteria where the maximum savings for each individual stream was calculated and streams that fell below an economic threshold were excluded, as shown in Fig. 20.17. This further reduced the number of streams from 42 to 28. The stream data for these streams are given in Table 20.2.

The Hot and Cold CCs for the remaining streams are plotted in Fig. 20.18 I. Only the analysis for one production state and an HRL with two HSTs will be presented here, although the analysis could be repeated for additional

© Woodhead Publishing Limited, 2013

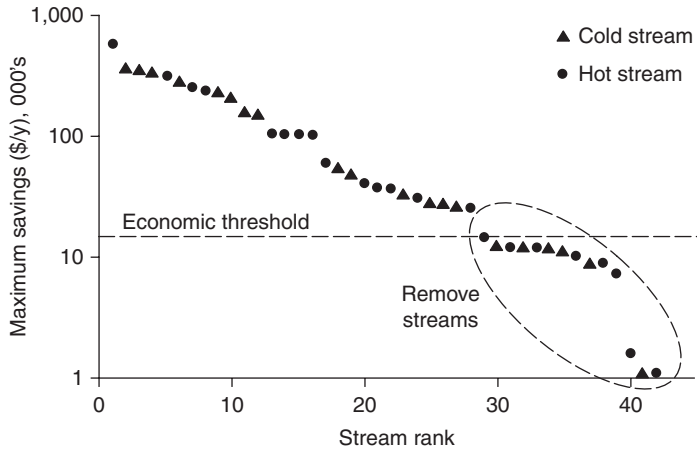

20.17 Maximum savings of HRL stream candidates.

Table 20.2 Stream data after preliminary screening

Plant	Stream	Type	TS (°C)	TT (°C)	CP (kW/°)	ΔH (kW)
A	X1	Hot	65.0	35.0	6.5	–
A	X2	Hot	47.0	9.0	21.0	–
A	X3	Hot	45.0	25.0	10.7	–
B	Y1	Cold	32.0	65.0	6.5	–
B	Y2	Cold	31.0	38.0	260.7	–
B	Y3	Cold	31.0	36.0	220.7	–
B	Y4	Cold	12.0	55.0	3.4	–
C	X4	Hot	55.0	10.0	4.6	–
C	Y5	Cold	53.0	65.0	68.0	–
D	Y6	Cold	40.0	45.0	307.2	–
D	Y7	Cold	10.0	26.0	118.6	–
D	Y8	Cold	10.0	15.0	51.0	–
D	Y9	Cold	10.0	22.0	68.0	–
E	X5	Hot	56.0	(56.0)	–	1,250
E	X6	Hot	51.0	(51.0)	–	1,680
E	X7	Hot	51.0	20.0	17.4	–
E	X8	Hot	50.0	(50.0)	–	552
E	X9	Hot	49.0	20.0	4.7	–
F	X10	Hot	50.0	25.0	8.0	–
F	X11	Hot	41.0	(41.0)	–	549
F	X12	Hot	41.0	(41.0)	–	1,362
F	X13	Hot	40.0	10.0	153.1	–
F	X14	Hot	40.0	10.0	16.1	–
G	Y10	Cold	44.0	58.0	26.1	–
G	Y11	Cold	16.0	35.0	44.1	–
G	Y12	Cold	12.0	32.0	97.4	–
G	Y13	Cold	10.0	30.0	61.8	–
G	Y14	Cold	10.5	13.0	70.0	–

© Woodhead Publishing Limited, 2013

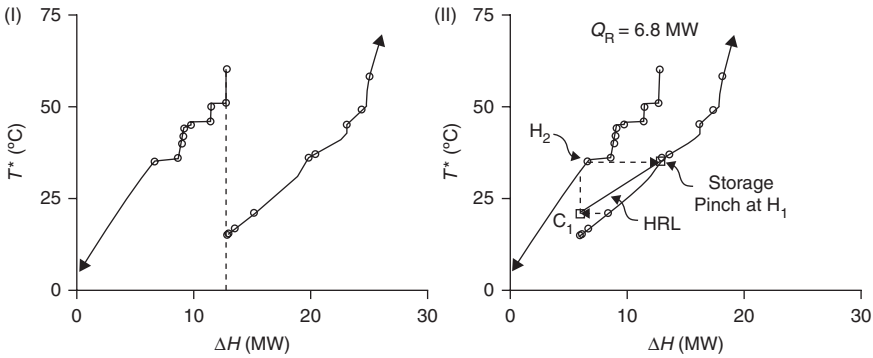

20.18 CC for streams in Table 20.4 (I) with Storage Pinch at 35°C and Q_R = 6.8 MW (II).

production states and numbers of HSTs. The CCs are shifted together until a Storage Pinch occurs, being caused by the start of hot streams X13 and X14. The temperature of the hot HST is constrained to 35°C and the cold HST temperature can range from 21°C to 32°C, with a total amount of heat recovery of 6.8 MW being achievable.

Now that the Storage Pinch is found with the CCs pushed as close together as possible, streams that start outside the HRL overlap region become obsolete and can be removed (Fig. 20.19 I). In the example, cold streams above 35°C (on the T^* scale) are removed and the CCs are redrawn. At present the streams causing the Storage Pinch (X13, X14) are limiting how close the CCs can be moved together and therefore limit the amount of heat recovery. Removing these two streams allows an additional 0.2 MW to be recovered and the Storage Pinch shifts to 36°C (Fig. 20.19 II). This step should be repeated a few times, as is shown by sequential options II–IV in Fig. 20.19. Near Pinch streams can also be removed to generate additional options and the relative merits of each option can be assessed. Several options need to be generated to ensure that the best HRL is targeted and designed.

In this case Option II has the greatest heat recovery potential, 7.0 MW and the ΔT_{HST} of 15°C is acceptable (Fig. 20.19 II). The ΔT_{HST} is important because it dictates the HRL flow rate. High HRL high flows can be detrimental, because it can result in excessive pressure drops and the requirement for large amounts of storage to achieve the heat recovery target. The heat recovery and CP of the different options are summarised in Fig. 20.20.

It is recommended that the first network design be based on vertical heat transfer (Fig. 20.21). The unknown outlet temperatures (28.2°C for hot streams and 31°C for cold streams) of the heat exchangers are taken from the CCs. The next step is to size the individual heat exchangers, based on the peak or design CP values.

© Woodhead Publishing Limited, 2013

© Woodhead Publishing Limited, 2013

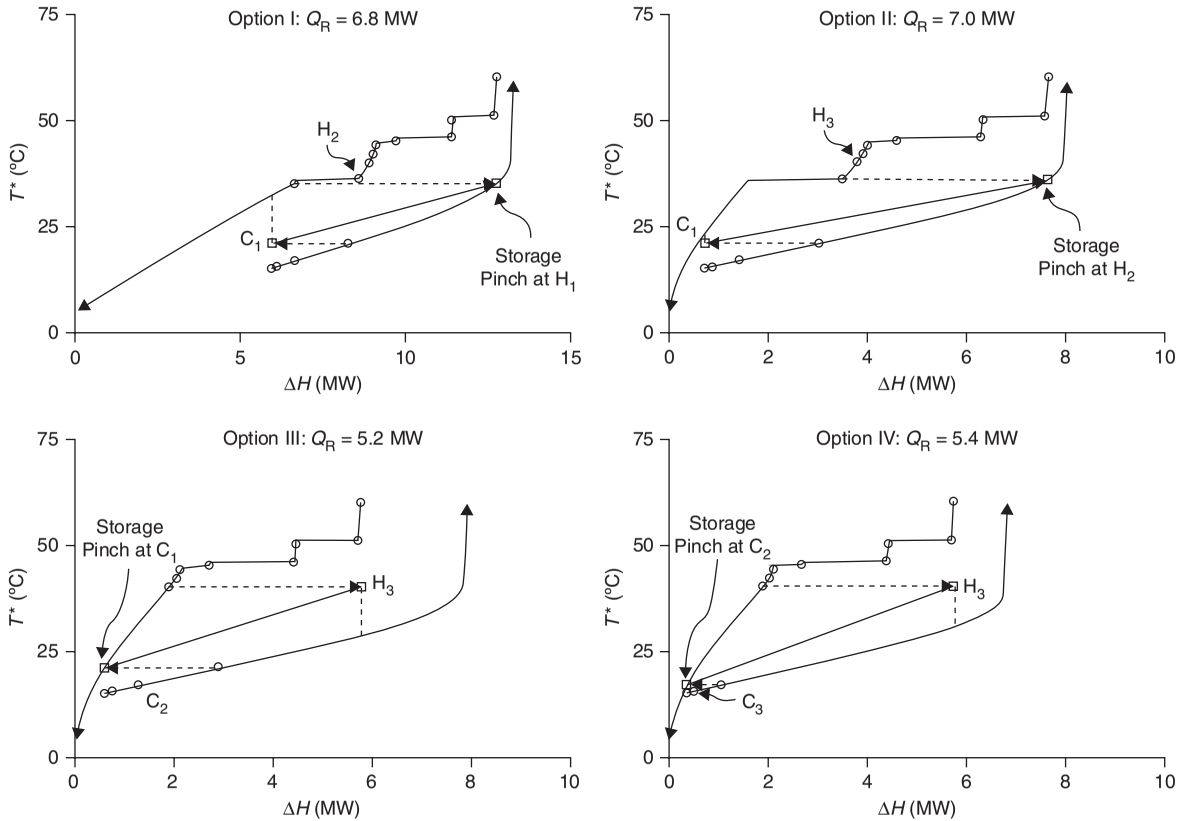

20.19 HRL options generated from removing the stream causing a Storage Pinch.

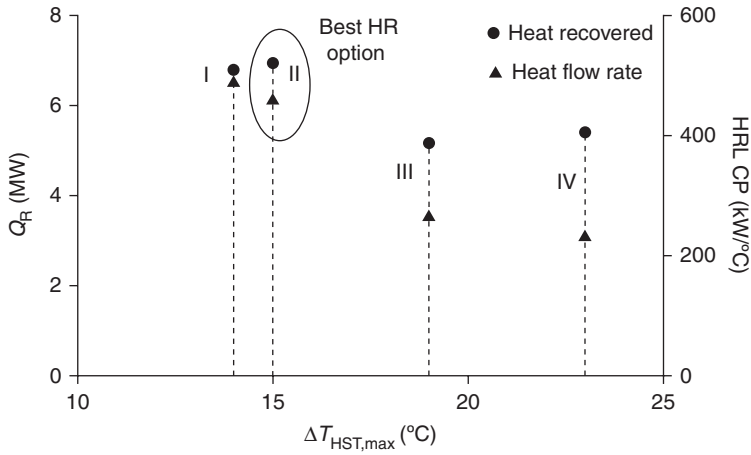

20.20 Summary of two-tank HRL options.

In the example, the cold streams are limiting heat recovery as evidenced by the Storage Pinch on the Cold CC and network relaxation must come from the hot streams. The smallest hot-stream duty is 95 kW from stream X9. This duty can be shifted to several other hot streams without violating ΔT_{min} and the exchanger on stream X9 removed (network not shown).

Once the network is designed the targeting procedure can be repeated for other production states followed by HEN Design and examining the effect of storage size on total heat recovery. Dynamic modelling of HRL performance and HST levels or temperatures can be modelled using historical stream data for a retrofit situation or projected stream data for a new plant. This can be useful for designing the control system for the HRL and also for economic assessment.

20.5 Case Study: Semi-continuous Multi-plant Dairy Factory

The dairy factory case study of Atkins *et al.* (2010, 2012) is one of the few industry examples presented in the literature on semi-continuous multi-plant PI using an HRL. In the case study the dairy factory processes around 8 ML/d of milk at peak production and produces about 250,000 t of milk powder and 85,000 t of cream products annually. There are six separate plants on site: milk treatment, three milk-powder plants, Anhydrous Milk Fat (AMF)/butter and cream product (Fig. 20.22).

© Woodhead Publishing Limited, 2013

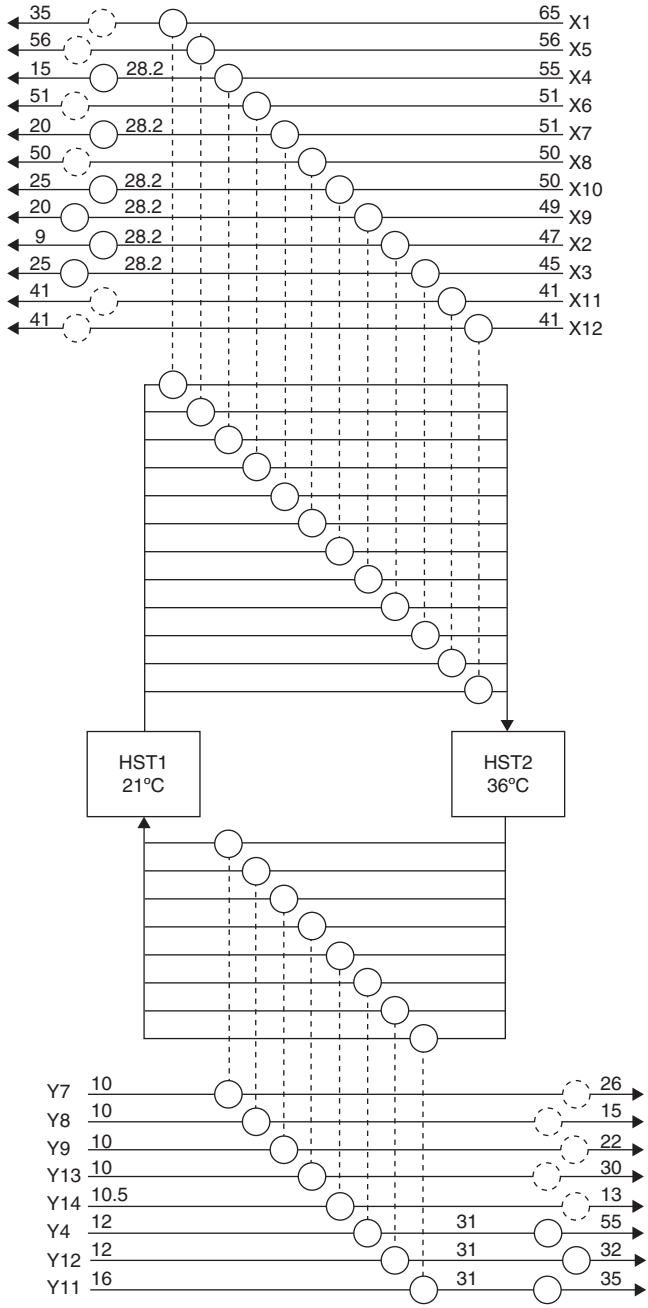

20.21 HRL network for vertical integration.

© Woodhead Publishing Limited, 2013

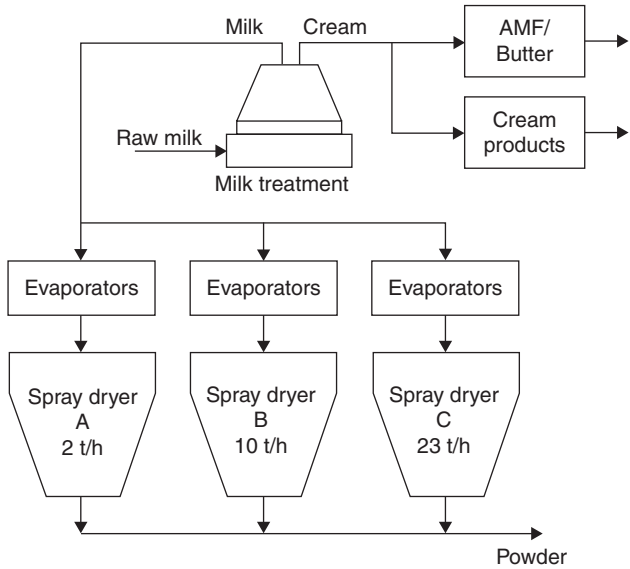

20.22 Schematic of the dairy factory with the six separate plants.

The production capacity of the site varies throughout the year, as a result of the changing milk supply. Variable raw material supply is accommodated through a variable site production schedule (Fig. 20.23a). Within the scheduled production periods, plants operate in a semi-continuous manner, because the process equipment must be cleaned regularly to ensure an acceptable quality. For example, the milk-powder dryers can be either on product, offline, cleaning cycle (CIP), warm running (hot air is fed to the dryer, but no feed is added), or water running (water is sprayed into the dryer instead of milk concentrate). The different operating states for a two week period for Dryer B are shown in Fig. 20.23b.

The individual plants at this site were previously integrated and the stream candidates for inclusion on an HRL are given in Table 20.3. Heat flow rate data are presented as time average values while a plant is in scheduled production and as a design value, which represents the maximum CP required during production. Initial analysis focuses on looking at the most common production state D (Fig. 20.23a). Each of the streams shown in Table 20.3 also has some variability in flow rate due to their changing operating states and process fluctuations. The total available heat flow rate for the sources and sinks is shown in Fig. 20.24 for a 30 h period.

Using the information in Table 20.3, the Time-Average CCs provide insight into the level of HR possible for four different scenarios (Fig. 20.25) for production state D. The CC temperatures are shifted by a $\Delta T_{min} = 5°C$,

© Woodhead Publishing Limited, 2013

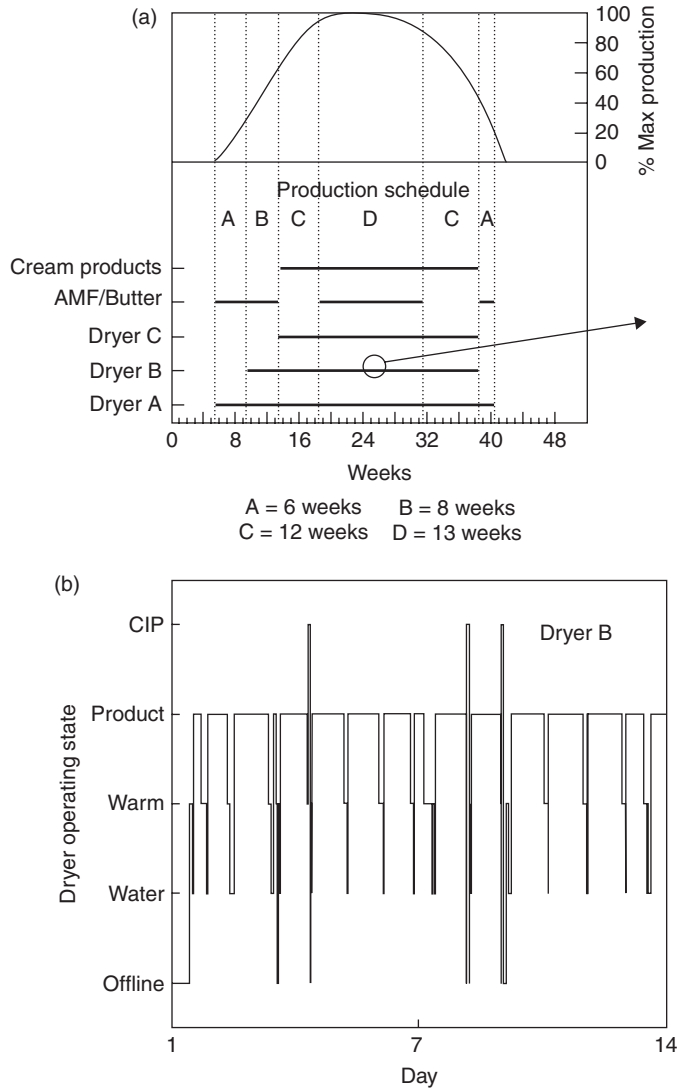

20.23 A representative operating schedule for (a) the dairy factory showing the milk production during the year and (b) a typical production cycle over 2 weeks for Dryer B showing the five operating states.

which is standard for liquid streams in dairy processing, and the supply temperatures are circled.

In Fig. 20.25a, the Cold CC has been shifted until a Storage Pinch occurs and maximum average heat recovery is identified for the four hot and three

© Woodhead Publishing Limited, 2013

Table 20.3 Stream data for potential streams on the HRL

Stream name	Plant	Stream type	TS (°C)	TT (°C)	Time average CP (kW/°C)	Design CP (kW/°C)	Schedule
Cow Water A	Dryer A	Hot	52.0	10.0	17.2	19.2	A,B,C,D
Cow Water B	Dryer B	Hot	50.0	10.0	78.4	96.0	B,C,D
Cow Water C	Dryer C	Hot	55.0	10.0	208.3	223.8	C,D
AMF	AMF	Hot	60.0	12.0	15.2	18.6	A,B,D
Site hot water	Site	Cold	10.0	65.0	150.8	156.8	A,B,C,D
Product heating	Cream	Cold	10.0	50.0	22.3	27.2	C,D
Cleaning	Milk treatment	Cold	10.0	60.0	20.9	20.9	A,B,C,D

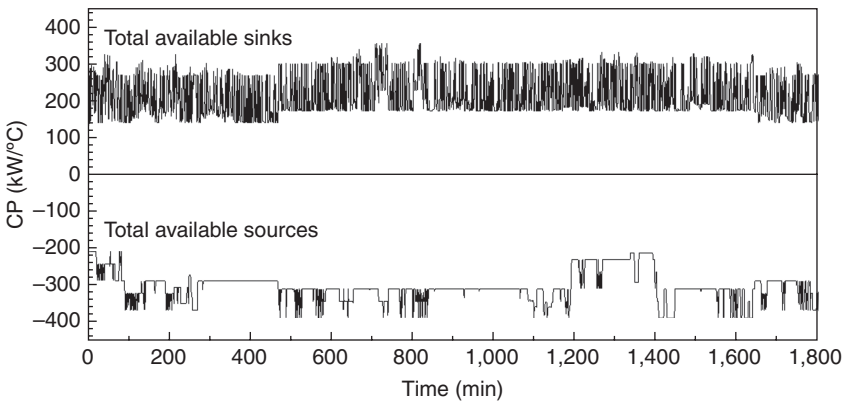

20.24 Instantaneous total available heat flow rate (CP) of the heat sources and sinks.

cold streams considered. Heat recovery and the hot-storage temperature are limited and set by the temperature of the lowest hot stream at 45°C, and the cold-storage temperature can range between 15°C and 31°C. As limiting streams, Cow water A and then Cow water B, are removed from consideration, HR increases from 5.8 to 6.2 MW (Fig. 20.25b) to a maximum of 6.8 MW (Fig. 20.25c). As each limiting stream is removed, the temperature of the hot storage tank is able to be increased from 45°C to 47°C to 50°C. If Cow water C, which is the limiting supply temperature on the hot-storage, is also removed, insufficient heat sources are now available and HR drops to 0.6 MW (Fig. 20.25d).

© Woodhead Publishing Limited, 2013

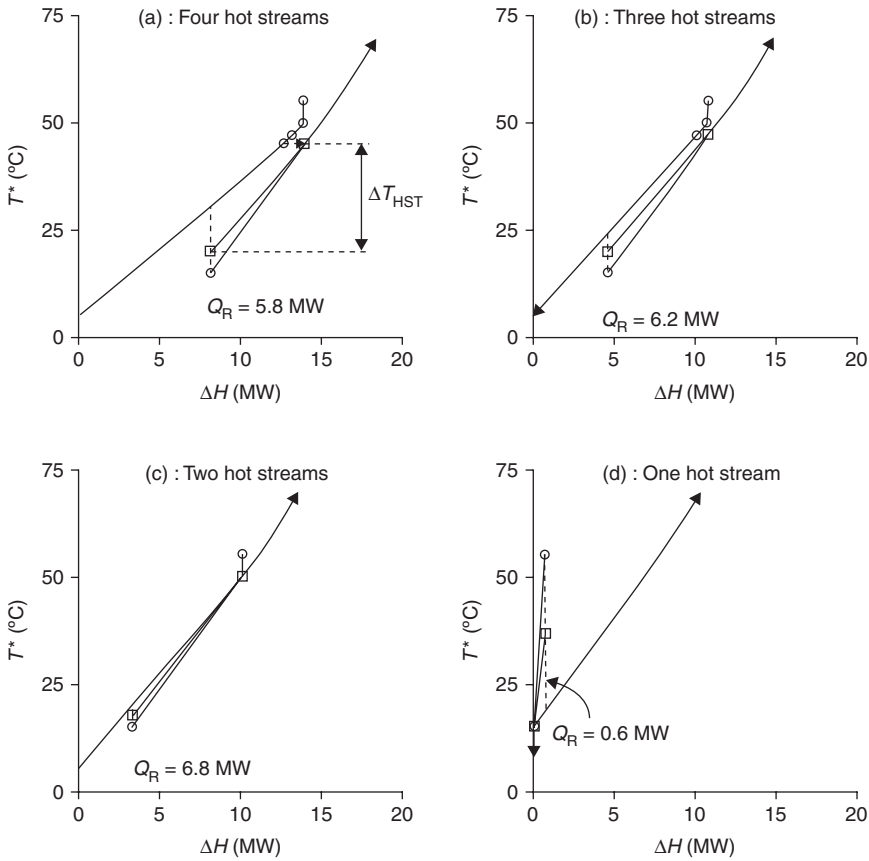

20.25 Heat recovery opportunities for production state D.

Clearly option C with two hot streams provides the largest HR opportunity. The four HR targets in Fig. 20.25 represent the average HR if sufficient storage is available.

The same targeting procedure used for production state D was applied to the other three states, A, B and C. For each production state a range of ΔT_{HST} were examined by holding the cold-storage temperature constant at 15°C and varying the hot-storage temperature (Fig. 20.26). Due to the significant difference in stream availability during the four production states, the maximum average heat recovery target was shown to change considerably with hot-storage temperature. Clearly there is merit for the factory to change the temperature of the hot-storage tank of the HRL at different times of the year. During production states C and D 50°C is best, and for production states A and B 45°C is best. The current site HRL is operating at

© Woodhead Publishing Limited, 2013

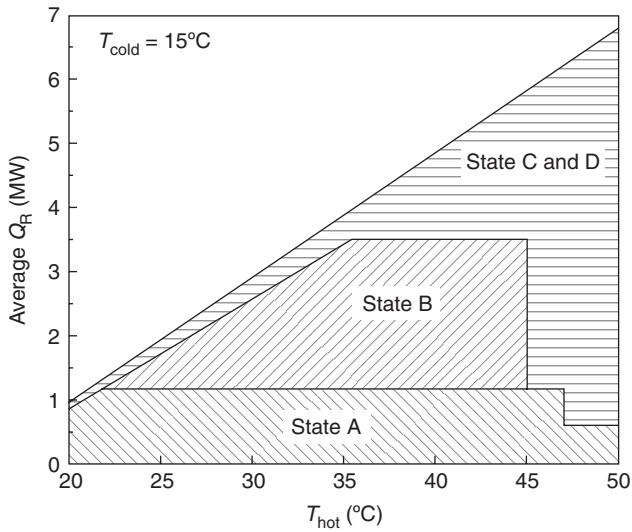

20.26 Effect of T_{hot} on average heat recovery for the several operating conditions.

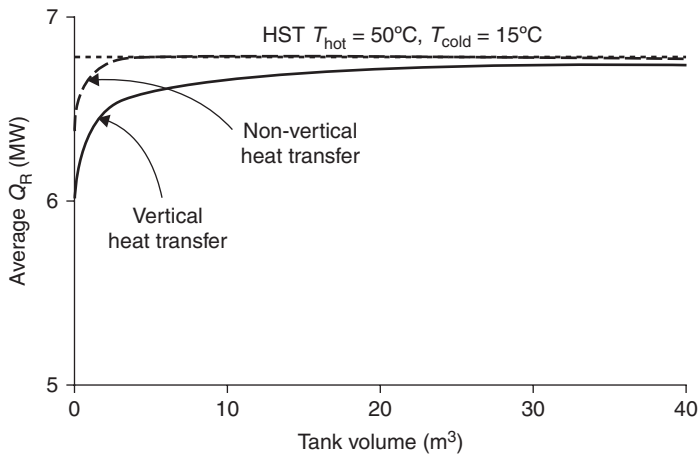

20.27 Impact of storage volume on average heat recovery for state D.

a hot-storage temperature below 50°C and therefore the system has potential for increased indirect heat recovery.

At the site, the two storage temperatures are catered for in a single, large, stratified tank. Simulations of the real-time operation of various capacity tanks were modelled by Atkins *et al.* (2012) for the most common production state D. The HRL average duty for a single stratified tank of up to 40 m^3 is shown in Fig. 20.27. Results suggest that the increase in heat recovery from

© Woodhead Publishing Limited, 2013

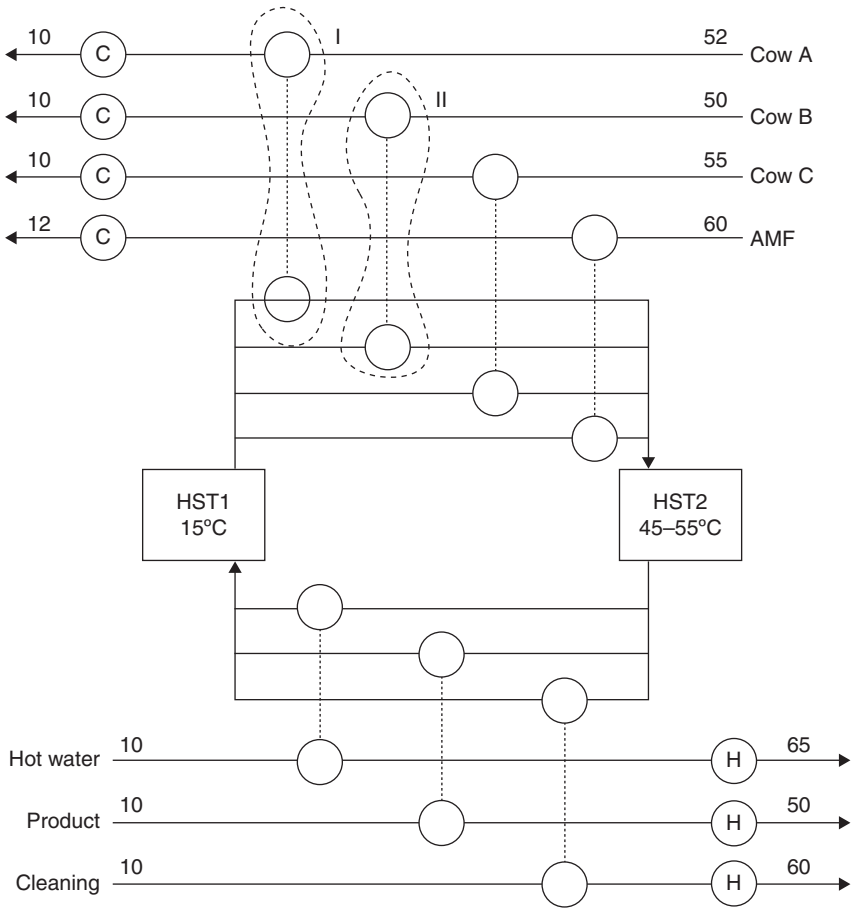

20.28 HRL and HEN Design.

adjusting the storage temperatures to 50°C can be accommodated for by the current tank capacity.

Each production state has a best network design and storage temperature to achieve the most heat recovery. Combining the networks for the four production states results in heat exchangers being placed on all process streams (Fig. 20.28). However, because state D does not require exchangers I and II to achieve maximum heat recovery, the decision to include these exchangers depends on their profitability. One method to determine the usefulness of exchangers I and II is to look at the added benefit to cost. Table 20.4 summarises the benefit to the site of including exchangers I and II over a whole year. If the benefits outweigh the marginal cost of including the exchanger, then it should be included in the retrofit final design.

© Woodhead Publishing Limited, 2013

Table 20.4 Summary of network design options

Production state	Operating hours (h)	Average Q_R (MW)			
		D	D + I	D + II	D + I/II
A	1,008	0.61	0.61	1.16	1.16
B	1,344	0.61	2.96	1.16	3.51
C	2,016	6.79	6.79	6.79	6.79
D	2,184	6.79	6.79	6.79	6.79
	Heat recovery (MWh/y)	29,945	33,104	31,236	34,396
	Annual savings ($/y)	$1,497,000	$1,655,000	$1,562,000	$1,720,000

20.6 Conclusions and Future Trends

A PI methodology for designing heat recovery systems for semi-continuous multi-plant site has been presented. A CC approach enables the maximum average indirect heat recovery target for an HRL to be identified for a site production state. The feasible temperature ranges of each storage tank can be determined directly on the CC diagrams, provided the supply temperatures of the hot and cold streams which limit the storage temperature ranges are adequately accounted for. Selecting tank temperatures that balance the temperature driving force between the hot streams and the intermediate fluid, and the intermediate fluid and the cold streams, is important for minimising the total heat exchanger area of the HRL system. A large temperature difference between storage tanks is helpful to minimise intermediate fluid flow rate and pumping costs, and to maximise thermal-storage capacity, but possibly at the expense of heat recovery. Increasing the number of storage tanks can increase the total heat recovery but this must be weighed against a lower temperature driving number, driving force, increased heat exchanger number, total area and greater number of tanks. In some cases, it may be worthwhile removing streams that limit the temperature range of storage tanks, in order to reduce the number of tanks or improve heat recovery. Using variable-storage tank temperatures on the HRL is also an option, but any increase in heat recovery is likely to occur with the increase in heat exchanger area. The optimum HRL system is therefore a complex compromise between many of these factors.

Future application of HRL to industry will be driven by increasing energy prices and the desire to minimise energy costs. The technology has significant potential to improve the levels of indirect heat recovery of low Pinch Temperature industries, such as food and beverage, and large multi-plant sites that use large amounts of hot water and operate semi-continuously.

© Woodhead Publishing Limited, 2013

20.7 Sources of Further Information

The reliable design and application of HRLs to industrial sites may be aided by further understanding of related topics on batch processing, thermal energy storage, pumping and pipe system design, and process instrumentation and control. Excellent sources of information on batch processing and batch PI include books by Majozi (2010) and Korovessi and Linninger (2005). Practical Batch Process management with emphasis on best practice automation and control issues is also covered by Barker and Rawtani (2005).

General information on energy optimisation and PI including HEN Synthesis, numerical optimisation of thermal energy recovery and storage, and review of optimisation methods is linked together in the book by Sieniutycz and Jeżowski (2009). The new edition of Thermal Energy Storage Systems by Dincer and Rosen (2011) offers up-to-date coverage of the fundamental principles and practical applications of thermal energy storage technology. Numerous handbooks and manuals are available on pumping and pipe system design, such as texts by Silowash (2009) and Karassik *et al*. (2008). Further aspects of HRL area targeting and storage temperature selection are also presented in the recent paper by Walmsley *et al*. (2012).

20.8 References

Ahmad, S., Hui, D. (1991). Heat recovery between areas of integrity. *Computers & Chemical Engineering*, **15**, 809–832.

Atkins, M. J., Walmsley, M. R. W., Neale, J. R. (2010). The challenge of integrating non-continuous processes – milk powder plant case study. *Journal of Cleaner Production*, **18**, 927–934.

Atkins, M. J., Walmsley, M. R. W., Neale, J. R. (2011). Application of heat recovery loops for improved process integration between individual plants at a large dairy factory. *Chemical Engineering*, **25**, 183.

Atkins, M. J., Walmsley, M. R. W., Neale, J. R. (2012). Process integration between individual plants at a large dairy factory by the application of heat recovery loops and transient stream analysis. *Journal of Cleaner Production*, **34**, 21–28, DOI: 10.1016/j.jclepro.2012.01.026.

Bagajewicz, M., Rodera, H. (2000). Energy savings in the total site heat integration across many plants. *Computers & Chemical Engineering*, **24**, 1237–1242.

Bagajewicz, M., Rodera, H. (2002). Multiple plant heat integration in a total site. *AIChE Journal*, **48**, 2255–2270.

Barker, M., Rawtani, J. (2005). *Practical Batch Process Management*. Elsevier, Oxford, UK.

Becker, H., Vuillermoz, A., Maréchal, F. (2011). Heat pump integration in a cheese factory. *Chemical Engineering*, **25**, 195.

Chen, C.-L., Ciou, Y.-J. (2008). Design and optimisation of indirect energy storage systems for batch process plants. *Industrial & Engineering Chemistry Research*, **47**, 4817–4829.

© Woodhead Publishing Limited, 2013

Chen, C.-L., Ciou, Y.-J. (2009). Design of indirect heat recovery systems with variable-temperature storage for batch plants. *Industrial & Engineering Chemistry Research*, **48**, 4375–4387.

Dhole, V. R., Linnhoff, B. (1993). Total site targets for fuel, co-generation, emissions, and cooling. *Computers & Chemical Engineering*, **17**, S101–S109.

Dinçer, I., Rosen, M. (2010). *Thermal Energy Storage: Systems and Applications*. John Wiley and Sons, UK.

Fernández, I., Renedo, C. J., Pérez, S. F., Ortiz, A., Mañana, M. (2012). A review: Energy recovery in batch processes. *Journal of Renewable and Sustainable Energy Reviews*, **16**, 2260–2277.

Foo, D. C. Y., Chew, Y. H., Lee, C. T. (2008). Minimum units targeting and network evolution for batch heat exchanger network. *Applied Thermal Engineering*, **28**, 2089–2099.

Goršek, A., Glavič, P., Bogataj, M. (2006). Design of the optimal total site heat recovery system using SSSP approach. *Chemical Engineering and Processing: Process Intensification*, **45**, 372–382.

Karassik, I. J., Messina, J. P., Cooper, P., Heald, C.C. (2008). *Pump Handbook*, 4th Ed. McGraw Hill, New York, US.

Kemp, I. C. (2007). *Pinch Analysis and Process Integration: A User Guide on Process Integration for the Efficient Use of Energy.* Butterworth-Heinemann, Oxford, UK.

Kemp, I. C., Deakin, A. W. (1989). Cascade analysis for energy and process integration of batch processes. Part 1. Calculation of energy targets. *Chemical Engineering Research and Design*, **67**, 495–509.

Kemp, I. C., MacDonald, E. K. (1987). Energy and process integration in continuous and batch processes. *IChemE Symposium Series*, **105**, 185–200.

Kemp, I. C., MacDonald, E. (1988). Application of pinch technology to separation, reaction and batch processes. *IChemE Symposium Series*, **109**, 239–257.

Klemeš, J., Friedler, F., Bulatov, I., Varbanov, P. (2010). *Sustainability in the Process Industry – Integration and Optimisation*. McGraw-Hill, New York, USA.

Korovess, E., Linninger, A. A. (2005). *Batch Processes*. CRC Taylor & Francis, Oxon, UK.

Kralj, A. K., Glavič, P., Kravanja, Z. (2002). Waste heat integration between processes. *Applied Thermal Engineering*, **22**, 1259–1269.

Kralj, A. K., Glavič, P., Kravanja, Z. (2005). Heat integration between processes: Integrated structure and MINLP model. *Computers & Chemical Engineering*, **29**, 1699–1711.

Krummenacher, P. (2002). Contribution to the heat integration of batch processes (with or without heat storage). PhD Thesis, Ecole Polytechnique Federale de Lausanne (EPFL), Switzerland.

Krummenacher, P., Favrat, D. (1995). Intégration énergétique de procédés industriels par la méthode du pincement étendue aux procédés discontinus (Energy integration of industrial processes using an extended pinch method for batch processes). Final report contract OFEN EF-PROC(92)037, EPFL-DGM-LENI, CH-1015 Lausanne, Switzerland (in French).

Krummenacher, P., Favrat, D. (2001). Indirect and mixed direct-indirect heat integration of batch processes based on Pinch Analysis. *International Journal of Thermodynamics*, **4**, 135–143.

© Woodhead Publishing Limited, 2013

Lee, B., Reklaitis, G. V. (1995). Optimal scheduling of cyclic batch processes for heat integration-I. Basic formulation. *Computers & Chemical Engineering*, **19**, 883–905.

Majozi, T. (2010). *Batch Chemical Process Integration: Analysis, Synthesis and Optimisation*. Springer, New York, US.

Mikkelsen, J. B. (1998). Thermal-energy storage systems in batch processing. PhD Thesis, Department of Energy Engineering, Technical University of Denmark, Copenhagen.

Papageorgiou, L. G., Shah, N., Pantelides, C. C. (1994). Optimal scheduling of heat-integrated multipurpose plants. *Industrial & Engineering Chemistry Research*, **33**, 3168–3186.

Rodera, H., Bagajewicz, M. J. (1999). Targeting procedures for energy savings by heat integration across plants. *AIChE Journal*, **45**, 1721–1742.

Sadr-Kazemi, N., Polley, G. (1996). Design of energy storage systems for batch process plants. *Chemical Engineering Research & Design*, **74**, 584–596.

Sieniutycz, S., Jeżowski, J. (2009). *Energy Optimisation in Process Systems*. Elsevier Science, Dordrecht, Netherlands; Oxford, UK.

Silowash, B. (2009). *Piping Systems Manual*. McGraw Hill, New York, US.

Stamp, J., Majozi, T. (2011). Optimum heat storage design for heat integrated multipurpose batch plants. *Journal of Energy*, **36**, 5119–5131.

Stoltze, S., Mikkelsen, J., Lorentzen, B., Peterson, P., Qvale, B. (1995). Waste-heat recovery in batch process using heat storage. *Journal of Energy Resources Technology*, **117**, 142.

Vaselenak, J. A., Grossmann, I. E., Westerberg, A. W. (1986). Heat integration in batch processing. *Industrial & Engineering Chemistry Process Design and Development*, **25**, 357–366.

Walmsley, M. R. W., Atkins, M. J., Riley, J. (2009). Thermocline management of stratified tanks for heat storage. *Chemical Engineering Transactions*, **18**, 231–236.

Walmsley, M. R. W., Walmsley, T. G., Atkins, M. J., Neale, J. R. (2012). Area targeting and storage temperature selection for heat recovery loops. *Chemical Engineering Transactions*, **29**, 1219–1224.

© Woodhead Publishing Limited, 2013

21

Applications of Energy and Water Process Integration Methodologies in Oil Refineries and Petrochemical Complexes

M. HASSAN PANJESHAHI, University of Tehran, Iran

DOI: 10.1533/9780857097255.5.633

Abstract: In this chapter, energy- and water-consuming systems in oil refining and petrochemical complexes are classified into three groups: heat and power systems, water and wastewater networks, and effluent treatment systems. In the first section, Heat and Power Integration methods for optimum design and retrofit in oil and petrochemical plants are demonstrated. The second section focuses on methods for water and wastewater minimisation. In the third section, the application of Process Integration in the design of energy-efficient effluent treatment systems for grass-roots and retrofit situations is presented. Applications of the proposed methods are demonstrated through real-life case studies.

Key words: oil refinery, petrochemical plant, heat and power system, water and wastewater network, effluent treatment system.

21.1 Introduction

Process plants typically comprise several interconnected process units and a central utility system. Oil industry refining and petrochemical complexes are the main energy-intensive sectors of process industries. The global energy crisis, and continuous increase in energy demand, particularly in the oil and petrochemical industries, has created a challenging situation for process engineers to design energy-efficient and cost-effective plants. In this respect, Process Integration (PI) techniques provide a rational framework to identify opportunities for energy and material conservation and efficient use of resources in process industries. PI techniques are considered as system-oriented and integral methods, which are introduced based on Pinch Analysis. Since the establishment of PI based on Pinch Analysis, the application of energy conservation techniques has been widely industrialised in the context of process design.

The main perspective of research on the PI subject area has been getting more interest due to the extensive application in process industries. PI

© Woodhead Publishing Limited, 2013

techniques in large-scale oil and petrochemical industries have been extensively developed and have proven to be successful in reducing energy costs. The aim of this chapter is to illustrate the role and applicability of Process Integration in the oil refining and petrochemical industry using recent developments in PI tools. As PI techniques aim at the conservation of water and energy sources in plant components, in this chapter we have classified the water- and energy-consuming component of the Total Site into three main sections: site heat and power system, site water and wastewater network, and effluent treatment system. Therefore, in the first section, Heat and Power Integration methods for optimum design and retrofit of energy sectors of process industries are demonstrated. The second section of the proposed chapter focuses on methods for water and wastewater minimisation in oil and petrochemical plants. In the third section of this chapter, the application of PI in the design of energy-efficient effluent treatment systems is presented for grass-roots and retrofit situations. Applications of the proposed tools are demonstrated through implementation in industrial case studies.

21.2 Heat and Power Integration

Integration of heat and power in process plant provides opportunity for both heat and power conservation by allowing energy–capital trade-offs into design. Procedures for Heat and Power Integration have been widely used in industry. However, for a sustainable integration, depending on the type of process unit, operational issues related to the type of process plant required are to be addressed.

In this section, we present recent strategies for the integration of heat and power in process plants while satisfying the heating and power demands of the process units. Moreover, methods for the design of efficient Heat Exchanger Networks (HENs) have been presented to include the power cycles of utility systems.

21.2.1 Retrofit of Crude Preheat Train in an Oil Refinery

Process Description

Several researches have been addressed retrofit of process units in oil refinery plants (Polley *et al*., 1990). The crude preheat train is one of the most important features of the crude distillation unit (CDU) in every refinery plant, as it accounts for a large fraction of the energy used in oil refining. In practice, refinery plant overall economy revolves around the performance of the crude preheat train. Therefore, increasing the energy efficiency of the preheat train can result in improving the economic performance of the refinery (Panjeshahi, 1992).

© Woodhead Publishing Limited, 2013

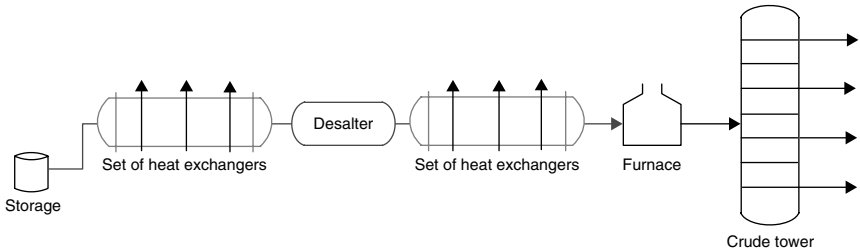

21.1 Typical flow sheet of a crude oil preheat train.

Table 21.1 Process stream data

Process unit	Stream	T_{Supply} (°C)	T_{Target} (°C)	Flowrate (kW/°C)
Crude oil preheat HEN	Hot 1	172.5	67.6	1,169.51
	Hot 2	260.0	189.8	751.04
	Hot 3	309.0	269.5	951.38
	Hot 4	333.4	189.4	149.1
	Hot 5	116.8	49.7	722.42
	Hot 6	272.0	210	3,037.11
	Hot 7	210.0	79.8	588.00
	Hot 8	146.0	18.2	1,449.2
	Hot 9	50.5	18.2	1,526.87
	Hot 10	189.0	26.1	696.61
	Cold 11	26.0	261.7	2,218.87
	Cold 12	261.7	356.5	4,301.91
	Cold 13	338.2	409.8	2,571.47
	Cold 14	26.0	96.1	1,362.83

The crude preheat train utilises CDU products, and pumps waste heat around the streams for partially preheating the crude oil fed to the column. Figure 21.1 illustrates a typical crude preheat train. Any improvement in the heat recovery within the HEN will reduce the amount of external utility requirement for the process units, and increases energy efficiency of the system.

Project Objectives

In this project, a mathematical approach is implemented for retrofitting of the crude preheat train of an oil refinery plant (Caltex Oil Refinery), with the objective of increasing the energy efficiency of system. Figure 21.2 represents the Grid Diagram for the existing HEN. Process stream data of the crude preheat train are shown in Table 21.1. The implemented approach allows the existing configuration of the system HEN to be planned, constraining the

© Woodhead Publishing Limited, 2013

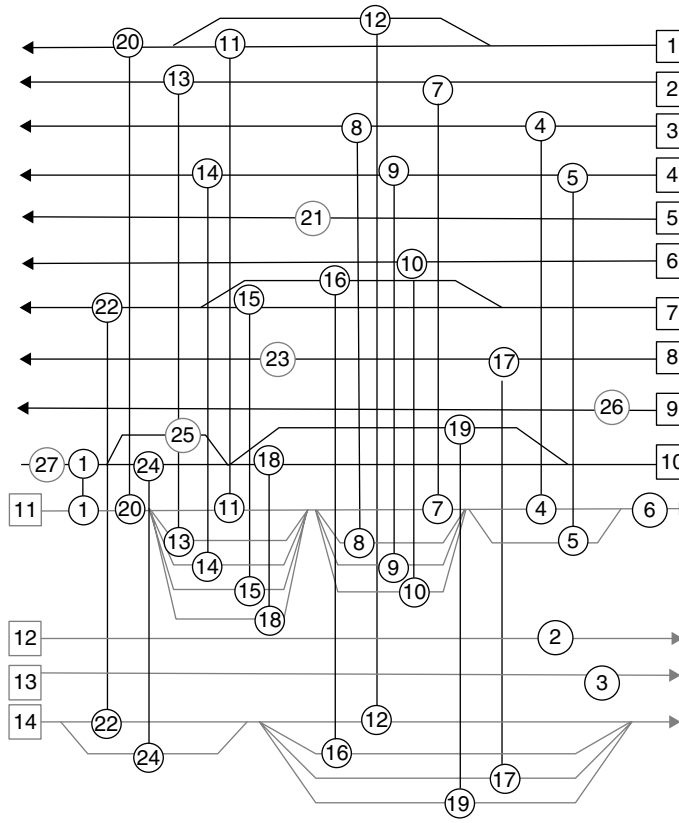

21.2 HEN Grid Diagram of crude oil preheat train.

number of modifications in the revamp procedure (Smith *et al*., 2010). The presented procedure is based on a modified Network Pinch approach, which combines structural modifications and cost optimisation in computation, to avoid missing cost-effective design solutions.

Design Approach

To carry out the retrofit of a HEN in the crude preheat train, the concept of Network Pinch approach (Asante and Zhu, 1997) has been implemented in an automated way in SPRINT® software (version 2.5.1) – see also Chapter 34. This method is able to search for the most cost-effective structural changes in the HEN. The model is based on a rigorous optimisation and allows the capital–energy trade-off through a Simulated Annealing (SA) technique in computational procedure. The optimisation model can optimise both continuous variables and structural options existing for the retrofit of

© Woodhead Publishing Limited, 2013

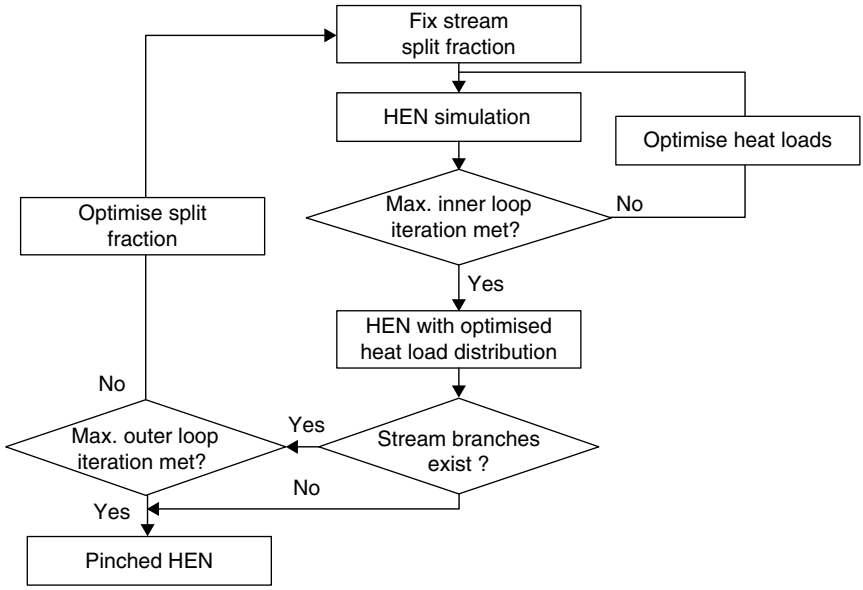

21.3 Computational procedure for finding Network Pinch (Smith *et al.*, 2010).

the HEN. The HEN modification options include structural changes (i.e. discrete options) and adding area to existing heat exchangers (i.e. continuous options). Discrete options consist of any modification that changes the network configuration. The computational procedure is performed in two steps (Gharaie *et al.*, 2011).

Step I: The first step of the computational procedure identifies the Network Pinch by redistributing the heat transfer loads between the existing heat exchangers through changing the split fraction to maximise the heat recovery between the process–process matches. Adjusting the heat loads and stream split fraction is done to ensure that the Network Pinch is not caused by the heat transfer area limit but by the existing configuration of the HEN (Gharaie *et al.*, 2011). Figure 21.3 shows the computational procedure of adjusting heat loads and stream split fraction for the existing configuration of the HEN.

Step II: After adjusting the heat load and stream split fraction, structural modifications are suggested and applied to overcome the Network Pinch. These structural modifications include installation of a new heat exchanger, introduction of additional stream splitting to the existing network, repiping and resequencing of existing matches, or a combination of these options (Gharaie *et al.*, 2012). Figure 21.4 shows the retrofit direction of the modified Network Pinch strategy.

© Woodhead Publishing Limited, 2013

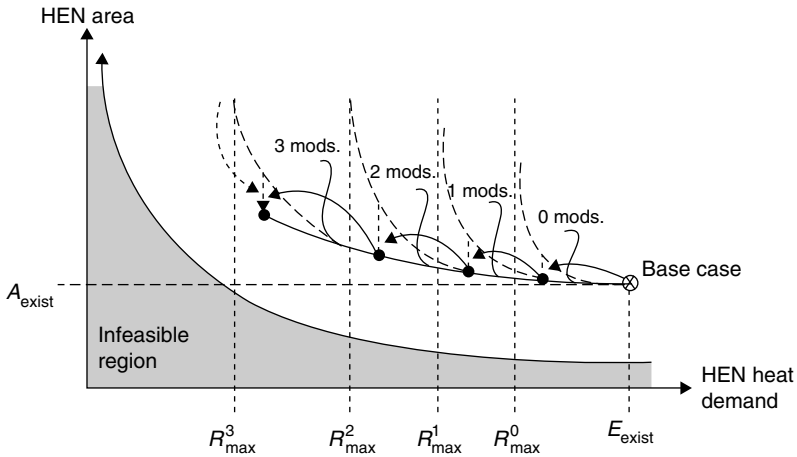

21.4 Retrofit direction of modified Network Pinch strategy (Asante and Zhu, 1997).

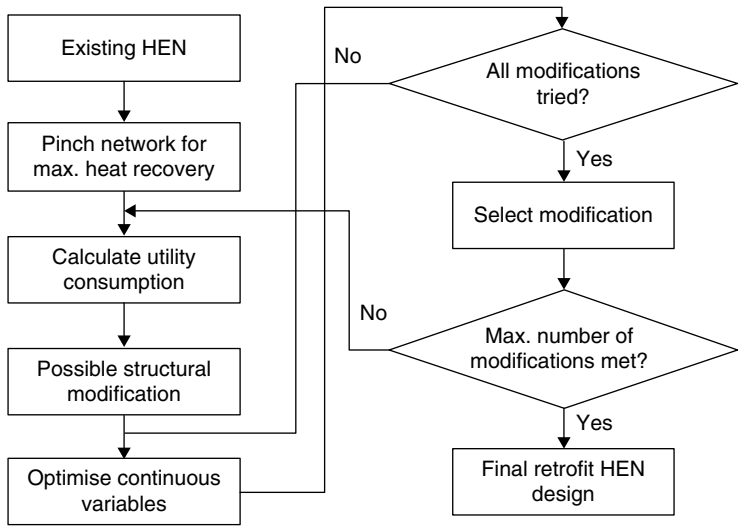

21.5 Optimisation procedure for retrofit of HEN (Smith *et al.*, 2010).

Various retrofit options, having different degrees of heat recovery, are generated and their performance, in terms of energy saving and additional capital investment required, are computed; then an SA solver finds cost-effective retrofit options for the network, subject to economic parameters and configurational constraints set by the users. Figure 21.5 shows the overall optimisation procedure for retrofit of the HEN.

© Woodhead Publishing Limited, 2013

Results and Discussion

Table 21.2 shows the existing heat transfer areas for exchanger units of the crude oil preheat unit. For retrofit study, as the extent of energy savings increases, the capital investment required for saving energy for the plant increases correspondingly. The energy-saving cost is calculated using the unit costs of utilities and the energy saving of each utility. The utility costs are calculated using the unit cost of energy. The unit cost of the hot utility, which is supplied by a local furnace, is mainly associated with fuel cost. The unit cost of utilities, and correlations to calculate heat exchanger capital cost, are taken from Smith *et al*. (2010). The unit cost of utilities is given in Table 21.2 (Gharaie *et al*., 2012).

Table 21.2 Existing heat exchanger data

Unit	Heat exchanger ID	Existing heat exchange area (m^2)	Heat load (kW)
Crude oil preheat HEN	1	226.09	1,605.00
	2hu	6,322.58	407,799.00
	3hu	8,219.24	184,117.00
	4	3,467.24	35,212.00
	5	856.07	9,154.28
	6hu	60.35	5,584.00
	7	2,696.22	37,552.00
	8	130.016	2,367.04
	9	841.405	9,243.74
	10	12,469.70	188,301.00
	11	3,685.86	65,141.70
	12	0.22	3.25759
	13	449.72	15,171.00
	14	139.39	3,071.31
	15	2,673.15	54,801.6
	16	0.17	2.74
	17	4,333.59	46,043.2
	18	2,048.33	38,238.5
	19	807.86	12,059.3
	20	3,235.44	57,537.00
	21cu	1,658.92	48,477.5
	22	2,004.89	21,754.9
	23cu	7,621.21	139,165.00
	24	1,980.85	15,666.3
	25cu	1,029.24	30,516.7
	26cu	5,536.74	49,315.4
	27cu	1,301.70	15,391.4

Note: Exchanger additional area capital cost ($) = 9,665 $(\text{area})^{0.68}$.
New exchanger unit capital cost ($) = 94,093 + 1,127 $(\text{area})^{0.98}$.
Hot utility cost ($/kWy) = 234.66.
Cold utility cost ($/kWy) = 5.25.

© Woodhead Publishing Limited, 2013

Table 21.3 Some retrofit modification options of crude oil preheat unit

Retrofit ID	Modification type	Total new area (m^2)	Investment cost (MM$)	Energy-saving cost (M$/y)	Payback Time (y)
1	Add. area	2,530	2.79	1.34	2.08
2	Add. area	15,584	8.91	4.13	2.16
3	Add. area New match	20,346	15.54	6.97	2.22
4	Add. area New match	29,139	23.48	8.99	2.60
5	Add. area New match Resequencing	35,134	28.69	10.44	2.74
6	Add. area New match Resequencing	40,549	34.48	11.62	2.96

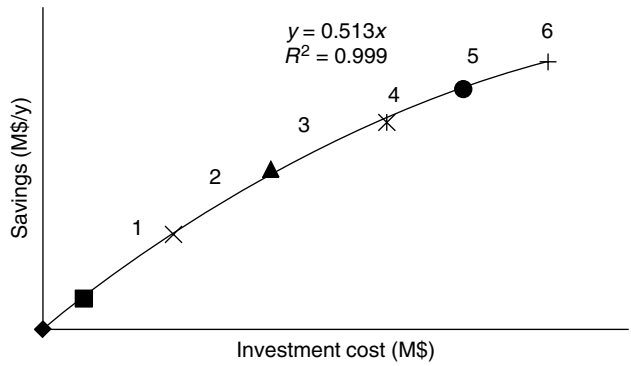

21.6 Retrofit payback plot of the crude preheat train.

Having set the energy-saving level for the existing HEN, the solver searches to find the most cost-effective modification option. Table 21.3 shows some of the retrofit modification options.

The final decision as to the best solution depends on the available investment cost and Payback Time of the retrofit scenario. Figure 21.6 shows the retrofit payback plot of the crude preheat train. In general, the retrofit option with quickest return on expenses is preferred by the plant manager. Therefore, based on the economic potential for each retrofit option, the payback period can help in identifying the most attractive retrofit scenario.

© Woodhead Publishing Limited, 2013

Table 21.4 Process stream data

Stream	T_{Supply} (°C)	T_{Target} (°C)	Heat load (MW)
Hot 1	327	50	31.51
Hot 2	495	307	29.30
Hot 3	220	59	30.47
Hot 4	222	67	12.33
Cold 5	102	327	25.81
Cold 6	35	164	10.47
Cold 7	140	500	54.74
Cold 8	80	123	3.84
Cold 9	59	169	7.91
Cold 10	85	125	4.77
Cold 11	480	500	37.80

21.2.2 Retrofit of Heat Exchanger Network in an Aromatics Plant

Process Description

Pinch Analysis provides a rational framework to identify energy conservation potential and efficient heat recovery in HENs. Over the last decades, several studies have contributed to improving and automating the Pinch method, especially in the context of the process industries, including petrochemical complexes (Panjeshahi and Nouzari, 2001). Retrofit of aromatic plants, as one of the large energy-consuming classes of petrochemical complexes, can provide great energy-saving opportunities. In this project, an aromatic plant is examined to improve the energy efficiency of the plant HEN. Figure 21.7 shows a simplified flowsheet of the aromatic plant. As shown in Fig. 21.7, feed from the desulphurisation reactor is separated into aromatic hydrocarbons through a combination of solvent extraction, distillation extraction method, and reforming processes. Process stream data for the HEN are given in Table 21.4. Figure 21.8 shows the plant's associated Grid Diagram.

Project Objectives

The objective of this project is retrofitting of an aromatics plant to increase energy efficiency of HEN. In this project it is tried to achieve better understanding of some fundamental features of HEN retrofit aiming at identifying a near-optimal retrofit strategy through a conceptual approach. The retrofit procedure implemented in this project is a heuristic approach, which is based on a combination of Pinch and Exergy Analysis. While Pinch Analysis adopted in this approach employs Driving Force Plot (DFP) for evaluation of heat transfer verticality, the exergy destruction factor provides

© Woodhead Publishing Limited, 2013

© Woodhead Publishing Limited, 2013

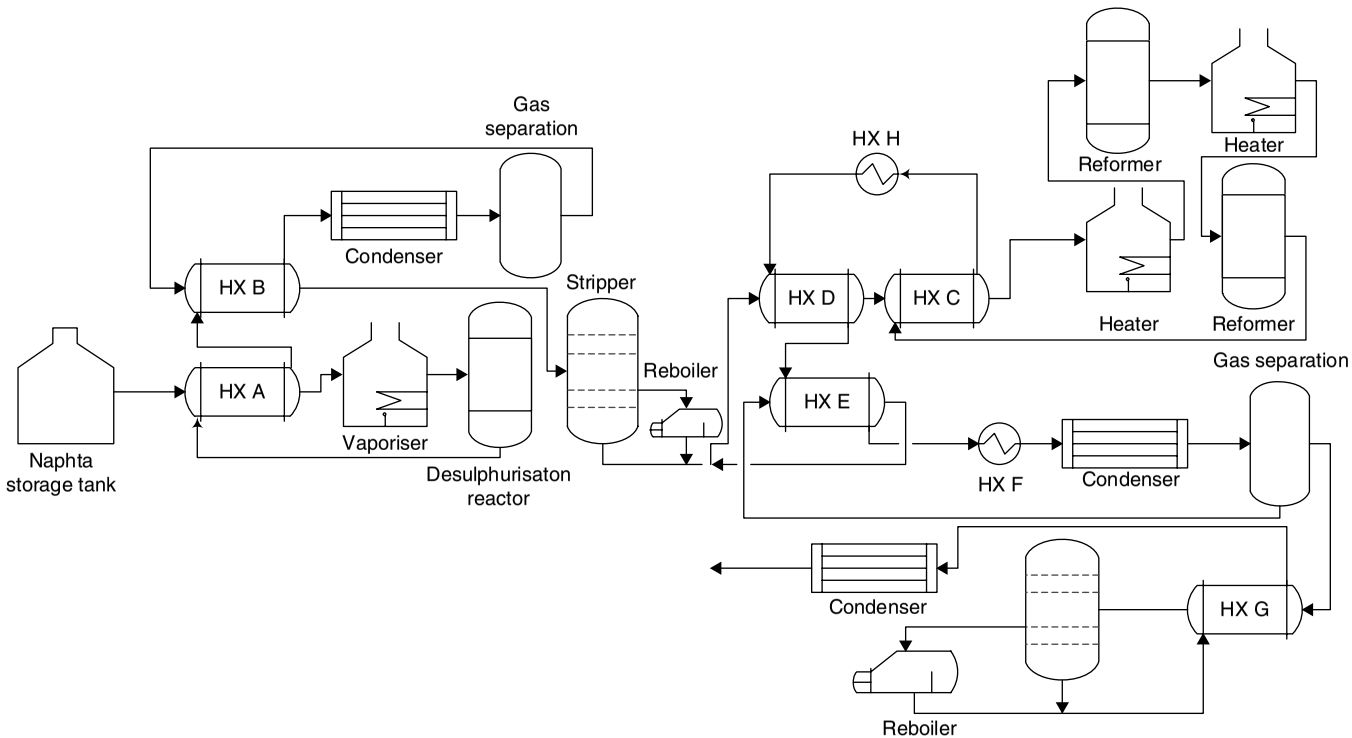

21.7 Schematic of the aromatics plant.

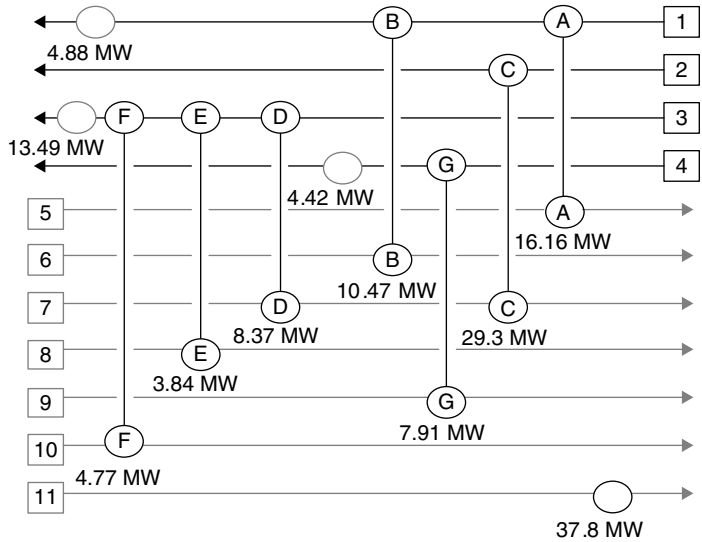

21.8 Existing HEN Grid Diagram.

quantitative analysis of the potential energy saving associated with any heat exchanger in the network.

Design Approach

In general, each HEN has some scope for improvement, as it includes sub-optimal use of the heat transfer driving force. The implemented retrofit method allows utilisation of the existing driving force within the network to be considered through the DFP concept. The multi-approach retrofit employed is carried out in five steps (Piacentino, 2011).

Step 1: The first step is to identify the inefficient use of the available driving force through the DFP. The DFP is graphically represented on a plot of temperature difference between the Hot and Cold Composite Curves vs the temperature of either hot or cold streams.

Step 2: The second step is to identify the improvement direction of the HEN by exploring the inefficiency distribution of the heat load within the HEN through exergy analysis. Having fixed the supply and target temperatures of the process streams, any changes in the utility consumption are associated with an equal change in exergy destruction through the HEN. This case study mainly focuses on the effect of irreversible heat transfer on network exergy destruction. In this respect, for counter-current type of heat exchangers, temperature profiles within the exchanger can be categorised into three groups. Figure 21.9 shows the temperature profile of counter-current heat exchange profiles. As shown in this figure, the presented categories of temperature profiles are associated with different classes of stream heat

© Woodhead Publishing Limited, 2013

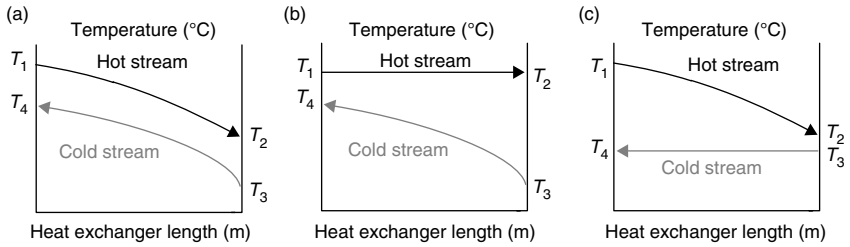

21.9 Temperature profiles of counter-current heat exchanger.

capacities. Figure 21.9a refers to finite heat capacity of both the hot and cold streams. For a specified heat exchange area, temperature of hot stream along the heat exchanger reduces from T_1 to T_2 while the temperature of cold stream increases from T_3 to T_4; Fig. 21.9b refers to infinite heat capacity for the hot stream; and Fig. 21.9c is related to the infinite heat capacity for the cold stream (Piacentino, 2011). As shown in Fig. 21.9b and 21.9c, stream temperature profiles for infinite heat capacity, remains constant along the heat exchanger. [16].

To identify the thermodynamic inefficiency of heat exchangers, the exergy destruction factor is introduced. Based on the exergy destruction factor and temperature profiles of each heat exchanger, the improvement direction of the existing HEN is identified.

Step 3: The third step is structural modification of the HEN. Structural modifications include resequencing and repiping existing heat exchangers, adding new matches and stream splitting. It is clear that the retrofit modification of existing HEN is not unique. In this case study, topology change is performed through a conceptual analysis based on in-depth understanding of the problem by applying Driving Force Analysis.

Step 4: The forth step is maximising the energy saving for each structural modification option proposed from the previous step.

Step 5: The final step is cost evaluation of the retrofit scenario by relaxation of maximum energy saving. Relaxation of maximum energy saving is done aiming at modifying a maximum energy saving with high cost or high-complexity design into a more feasible network. This will eventually be characterised by a less-than-maximum energy saving but lower cost and/or complexity.

Results and Discussion

Having followed the step-wise retrofit procedure, the DFP of the individual heat exchanger is presented in Fig. 21.10. The DFP in this figure indicates an inefficient utilisation of the available driving force through most of the heat exchangers in network.

Figure 21.11 reflects the heat recovery within the existing HEN, based on the actual network configuration (Piacentino, 2011). As shown in Fig. 21.11,

© Woodhead Publishing Limited, 2013

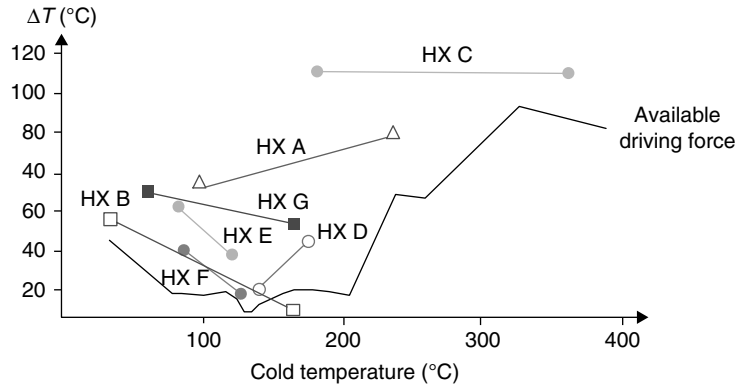

21.10 DFP of existing HEN.

assuming constant heat capacity with temperature variation between T_i and T_o, each stream identifies through a rectangle whose area represents the heat load on the stream.

Having investigated the clues achieved from the DFP and exergy analyses, seven structural modification retrofit scenarios are introduced. For each suggested scenario, the energy saving is then maximised by maximising the capacity of each heat exchange with respect to ΔT_{min}. Figure 21.12 shows a representation of the suggested retrofit scenarios.

To modify retrofit scenarios for minimum cost, relaxation of maximum energy saving is carried out. The relaxation results are presented in Fig. 21.13 in terms of the heat transfer area vs energy consumption. It is noted that the 'R' symbol in this figure represents the relaxed condition of maximum energy saving for the shown scenarios.

The cost of retrofit scenarios is plotted in Fig. 21.14. As shown in Fig. 21.14, relaxation of maximum energy saving has allowed relevant reductions in retrofit cost. As shown in this figure, scenario 4 results in €230 saving per unit of energy penalty (kW). Retrofit scenario 4 is highlighted in this figure.

Figure 21.15 shows the Payback Time of each proposed retrofit scenario. As presented in this figure, economic viabilities of the modification solutions are rather different. Decision making on the optimal scenario will be made based on the available expenses and Payback Time.

21.2.3 Optimum Design of Multi-Stream Heat Exchangers in Petrochemical Industries

Process Description

Over the last decade, continuous demand of low-cost equipment, particularly in petrochemical plants, has created a challenging situation for process engineers to design efficient and cost-effective plants (Xiangkun *et al.*,

© Woodhead Publishing Limited, 2013

© Woodhead Publishing Limited, 2013

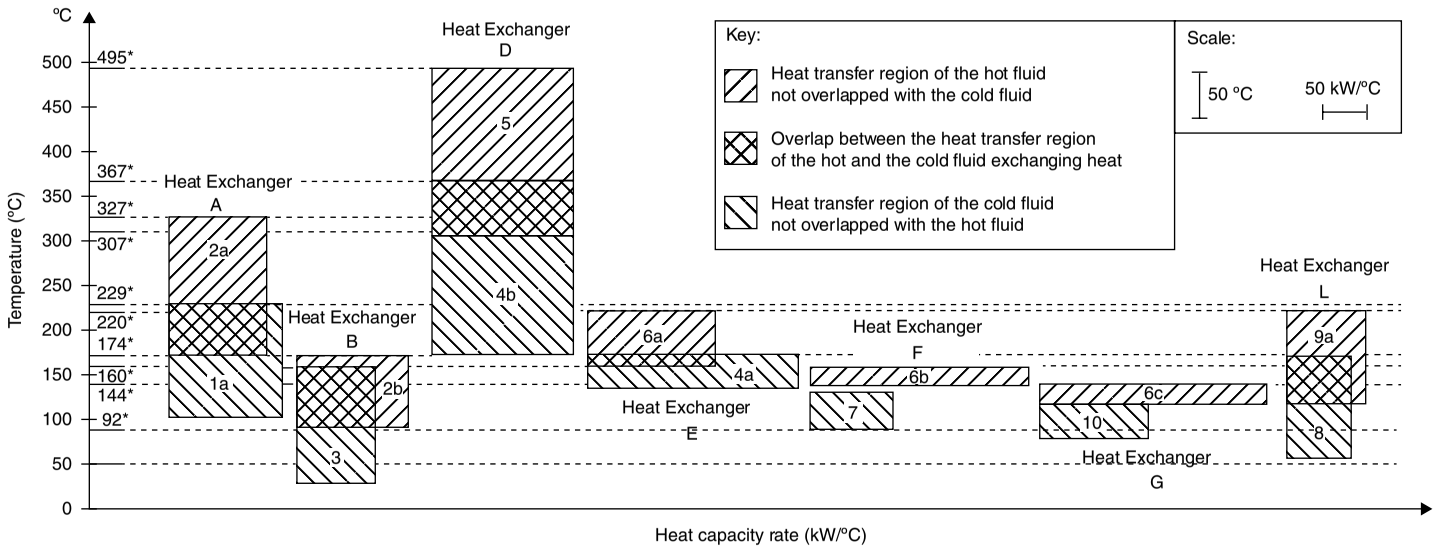

21.11 Heat load distribution with the existing HEN.

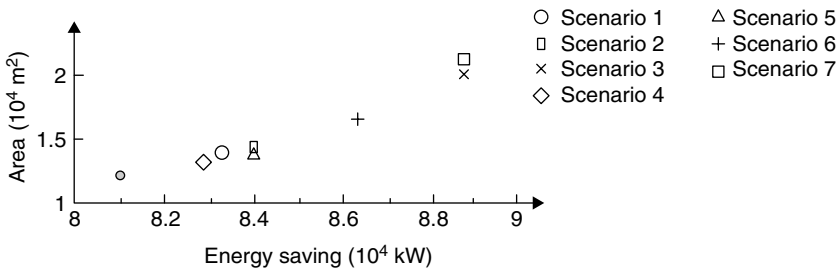

21.12 Maximised energy-saving retrofit scenarios.

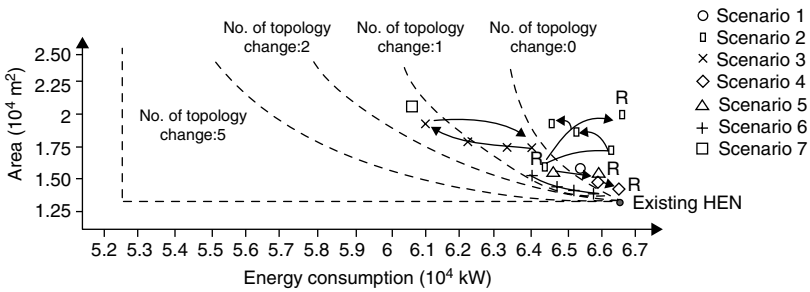

21.13 Relaxation of maximum energy saving.

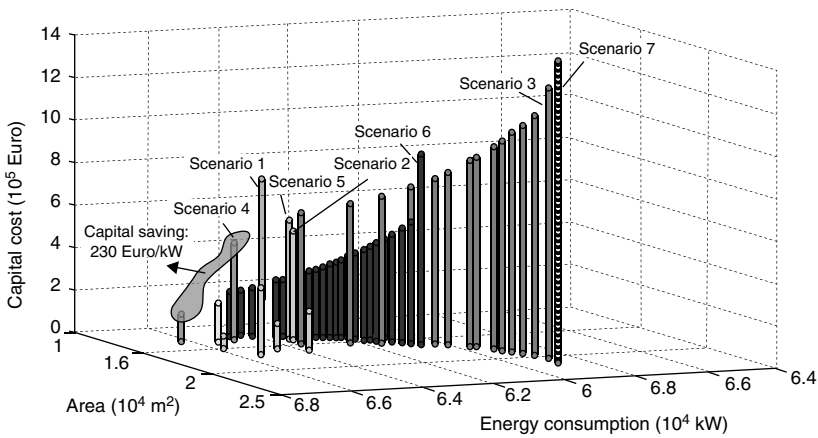

21.14 Cost evaluation of retrofit scenarios.

2008). In this respect, recent developments in the design of Multi-Stream Heat Exchangers (MSHEs) have established a demanding market scope. Compared to conventional heat exchangers, the compact structure of MSHEs provides lower capital cost as well as operational cost (Prasad, 1996). The MSHE is a single process unit, in which simultaneous heat

© Woodhead Publishing Limited, 2013

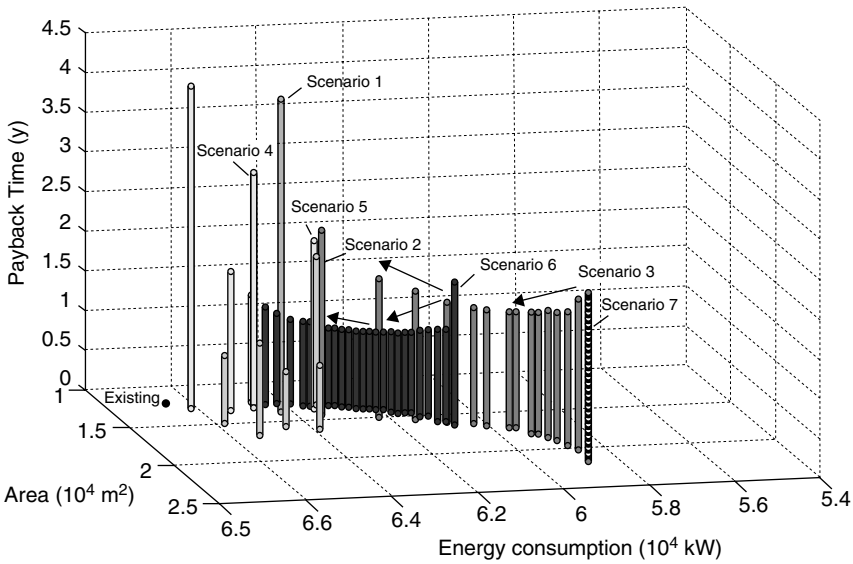

21.15 Payback Time of proposed retrofit scenarios.

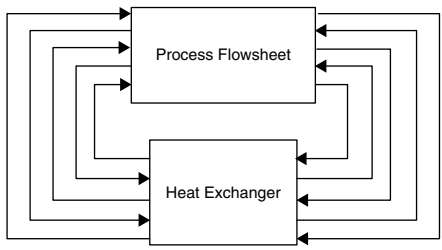

21.16 Schematic of stream flow through the MSHE.

exchange occurs through multiple hot and cold streams. Figure 21.16 shows a schematic representation of an MSHE.

In general, heat transfer modelling in the HEN is graphically presented through Composite Curve on the temperature–enthalpy diagram. The Hot and Cold Composite Curves are the cumulative heat content of all the hot and cold streams. When both curves are superimposed, the overlap between them indicates the amount of heat that can be recovered within the process (Fig. 21.17). The entry port of each heat exchange interval is positioned so that the temperature difference between the incoming stream and the opposing stream is a finite value (Panjeshahi *et al.*, 2010c).

In a heat transfer problem of the process HEN, hot and cold streams often have different temperatures before the process. Therefore, these streams should enter the exchanger at different points along the length so that they enter and leave the unit without disrupting the temperature profile. Hence, the MSHE often has intermediate entry and exit points along its length.

© Woodhead Publishing Limited, 2013

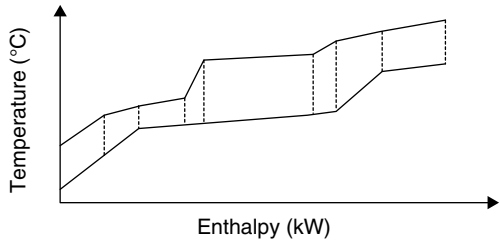

21.17 Representation of Hot and Cold Composite Curves.

Table 21.5 Process stream data

Stream	T_{Supply} (°C)	T_{Target} (°C)	Mass (kg/s)	Pr	C_p (J/kg K)	ρ (kg/m^3)	μ (kg/ms)	ΔP (Pa)
Hot 1	88	38	29.17	4	3,800	1,050	0.0004	25,000
Hot 2	76	40	96.25	3	4,180	990	0.0005	70,000
Hot 3	76	40	137.58	3	4,180	990	0.0005	80,000
Cold 4	0	45	43.73	7	4,180	990	0.001	40,000
Cold 5	45	70	60.23	3	4,180	990	0.0005	50,000
Cold 6	0	60	62.15	5	4,180	990	0.0008	60,000
Cold 7	60	70	76.45	3	4,180	990	0.0004	60,000
Cold 8	70	90	38.50	2	4,180	990	0.0004	30,000

Early approaches of MSHE modelling are not capable of taking all the complexities into consideration. A new and easy-to-use approach is proposed and implemented on a petrochemical process unit to cope with the technical issues in MSHE design. Stream process data and physical properties of the petrochemical process unit are presented in Table 21.5.

Project Objectives

In this project, a conceptual method is applied to finding the optimum MSHE design for heat recovery in a petrochemical plant. The proposed method is based on thermodynamics, and allows for pressure drop consideration in the design.

Design Approach

The design approach proposed and implemented here is carried out in two steps (Joda *et al.*, 2011):

Step I: Obtaining the flow length of MSHE. The design procedure in each section is obtained by selecting the fin type for all streams. Heat transfer coefficients and friction factor are corrected based on the Reynolds number (Picon-Nunez *et al.*, 2002). The Reynolds number is a function of the mass velocity of stream and the hydraulic diameter (Kays and London, 1984). The calculation procedure of flow length is presented in Fig. 21.18.

© Woodhead Publishing Limited, 2013

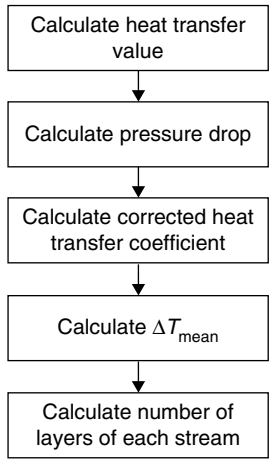

21.18 Calculation procedure of flow length (Panjeshahi *et al.,* 2010c).

Step II: Pressure drop maximisation. The MSHE design procedure proceeds with determining the heat exchanger geometry for each section. The MSHE network design problem involves issues at heat exchanger level and network level. At the exchanger level, the flow length of different streams must match within a reasonable limit in each section. Therefore, the stream with flow length larger than others is selected as a reference stream (Joda *et al.*, 2011). The fin type of other streams has to be changed until the flow lengths of them are adjusted to the flow length of the reference stream.

At the network level, MSHE in different sections has to have the same height and width, due to the manufacturing constraints and easy distribution. Here, the MSHE width is set to 1 m with respect to industrial requirements, but MSHE height is calculated from the number of layers of streams. After initial design of an MSHE in each section, the height of the different sections may not be the same, so the procedure has to be iterated through changing the number of layers, and consequently the Reynolds number, of streams in different sections. This iteration continues until the MSHE height is achieved, at a height equal to the largest section height. Since the flow length is sensitive to any changes in the Reynolds number, it is important that the process design at the exchanger level and network level is simultaneously performed. Also, maximum stream pressure drop is considered to be the design objective (Panjeshahi *et al.*, 2010c).

Results and Discussion

Having followed the design procedure, first, the Composite Curve is constructed at a minimum temperature approach of 5°C (Fig. 21.19) (Panjeshahi *et al.*, 2010c).

© Woodhead Publishing Limited, 2013

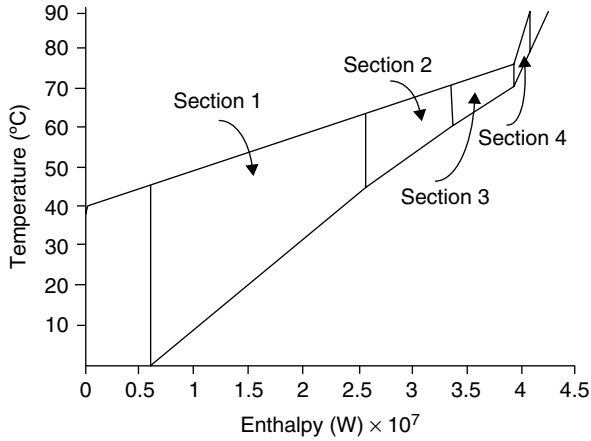

21.19 Composite Curve of the case study.

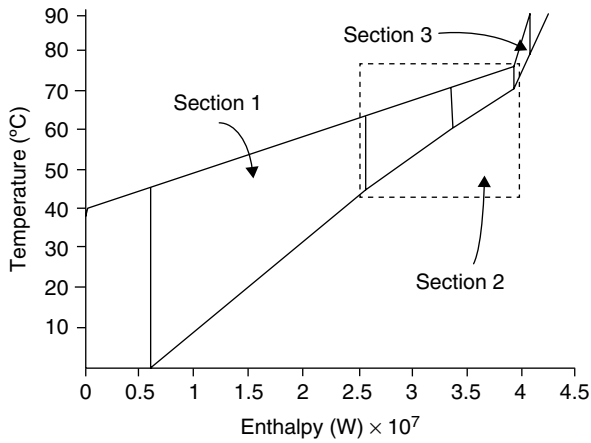

21.20 The number of sections corresponding to the proposed design method (Panjeshahi *et al.*, 2010c).

Using the conventional approach, the problem is divided into four sections, in which the design method is implemented for each section separately. However, by applying the proposed optimum design method, the number of sections is reduced to three, in which two intermediate sections are considered as one section. Therefore, in this section, cold streams enter the MSHE at different temperatures (Fig. 21.20). The entrance temperature of stream 6 is 60°C, while stream 8 enters this section at 45°C. Table 21.6 shows the dimensions obtained through the proposed optimum design method. It is assumed that the allowable pressure drop is linearly distributed through the network. Table 21.7 presents a comparison of the pressure drop between the conventional method and the optimum design approach (Panjeshahi *et al.*, 2010c).

© Woodhead Publishing Limited, 2013

Table 21.6 MSHE dimension

Section	Width (m)	Height (m)	Length (m)
1	1	0.74	0.26
2	1	0.74	0.98
3	1	0.76	0.42

Table 21.7 Pressure drop comparison between the conventional method and optimum design approach

Stream	Pressure drop (Pa)	
	Conventional method	Optimum design method
Hot 1	21,020.19	21,021.67
Hot 2	17,912.28	10,460.50
Hot 3	15,737.52	8,304.90
Cold 4	2,547.77	24,386.95
Cold 5	4,886.81	39,054.48
Cold 6	5,036.19	42,016.21
Cold 7	2,820.00	16,486.50
Cold 8	188.03	137.53

Table 21.8 Comparison between total area and TAC obtained from optimum design method and conventional method

Method	Area (m^2)	TAC (M$/y)
Conventional method	2,116.07	1.64
Optimum design method	1,905.68	1.48

Table 21.8 shows a comparison of total area and Total Annual Cost (TAC) between the conventional design method and the proposed optimum design approach (Joda *et al.*, 2011).

As presented in Table 21.8, the TAC obtained through the implemented design method is lower than with the conventional approach. In conclusion, the proposed approach enables the designer to find the optimum entrance point of the MSHE. Implementation of the new method is quite straightforward, and can be used in any process-related industry.

21.2.4 Retrofit of Ammonia Plant for Improving Energy Efficiency

Process Description

Retrofit of energy-efficient process plants requires tools that enhance engineering understanding of the complex interactions between process plants

© Woodhead Publishing Limited, 2013

and the utility system. Over the last decade, considerable research has been focused on the subject of PI technologies, through the use of graphical diagrams, mathematical modelling and subsequent optimisation techniques. These techniques facilitate improvement of the overall utility consumption, and setting process and utility system configuration prior to final detailed simulation and optimisation (Panjeshahi *et al.*, 2008).

Ammonia production is an energy-intensive process. The main sections of the ammonia plant under study, which is located in the south of Iran, include natural gas purification, a reforming process unit, CO conversion and CO_2 absorption unit, and a methanation and refrigeration unit (Panjeshahi *et al.*, 2008). In terms of the energy consumption, the overall ammonia plant can be divided into two sections: the hot-end section and the cold-end section. Increasing the energy efficiency of the process via heat recovery techniques could result in sizable energy savings through the overall plant. The highly energy-consuming nature of the process is the key driving force for improving the energy efficiency of the process technology and reducing the overall cost of manufacturing. Hence, any energy conservation in the process goes a long way in many aspects. Optimisation of the ammonia process HEN for increasing energy recovery enables the engineer to address multiple and complex trade-offs, which is not possible manually. In this project, a mathematical optimisation model for the retrofit of industrial energy-intensive plants is presented, and is implemented in part of the ammonia plant (Silva *et al.*, 2009). Table 21.9 shows the process stream data. Figure 21.21 shows the existing configuration of HEN. Hot and cold utility costs are 23 and 1.52 $/kW/y (Silva *et al.*, 2009).

Project Objectives

In this project, a mathematical optimisation approach for retrofit of the HEN is implemented in an ammonia plant. The optimisation approach is to maximise heat recovery through the HEN while minimising the cost of any new heat exchanger in the network. The optimisation model used in the proposed approach is based on the Particle Swarm Optimisation (PSO)

Table 21.9 Process stream data

Stream	T_{Supply} (°C)	T_{Target} (°C)	Heat capacity (kW/°C)
Hot 1	393.2	45	21.8206
Hot 2	105.9	40	95.5842
Hot 3	242	73.7	324.224
Hot 4	73.5	40	490.949
Cold 5	45	371.1	21.2919
Cold 6	45	200	8.92258
Cold 7	54.6	215	340.1933
Cold 8	56.9	90	9.81873

© Woodhead Publishing Limited, 2013

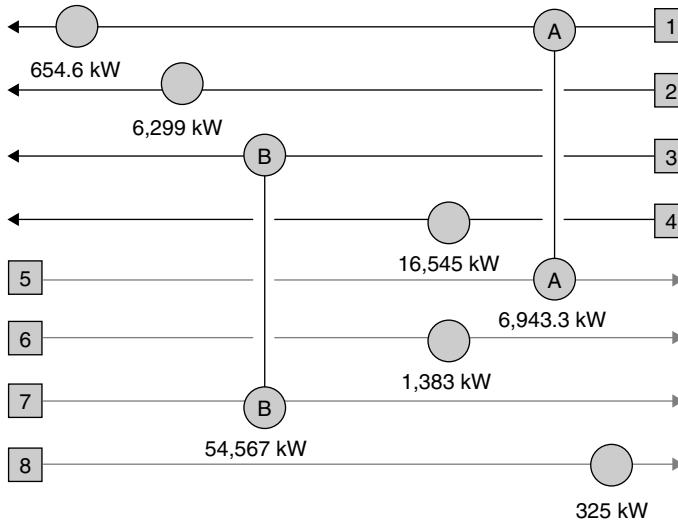

21.21 Existing configuration of HEN.

method (Silva *et al.*, 2009). The PSO method is capable of solving highly non-linear problems while avoiding local optima.

Design Approach

The method is based on construction of the superstructure (Yee and Grossmann, 1991). The retrofit approach tries, obligatorily, to retain the existing heat exchangers The optimisation model allows the placement of matches to be reconfigured to increase energy efficiency while minimising the additional cost. The problem considers a set of hot and cold streams with known inlet and outlet temperatures and flowrates. The existing HEN is identified through its heat transfer areas. The objective function of the optimisation problem takes the utility costs used in the generated HEN associated with the cost involving the introduced new heat exchangers (Equations [21.1] and [21.2]). The constraints are the thermodynamic restrictions in the heat matches (Silva *et al.*, 2009).

$$\text{Obj Func: Min}\left(\text{Cost}_{\text{area}} + \text{Cost}_{\text{Utility}}\right) \qquad [21.1]$$

$$\begin{aligned}\text{Subject to}: \left(\text{T}_{\text{hot}}^{\text{in}}\right)_{\text{i}} &> \left(\text{T}_{\text{cold}}^{\text{out}}\right)_{\text{i}} \\ \left(\text{T}_{\text{hot}}^{\text{out}}\right)_{\text{i}} &> \left(\text{T}_{\text{cold}}^{\text{in}}\right)_{\text{i}}\end{aligned} \qquad [21.2]$$

The proposed problem is solved with the PSO. The PSO is a stochastic optimisation technique (Kennedy and Eberhart, 2001). As an optimisation tool

© Woodhead Publishing Limited, 2013

Table 21.10 HEN specifications

Case	Heat load (kW)	Area (m^2)	Additional cost ($)
Base case	6,110	2,686	–
Base case	54,567	23,909	–
Optimised	325	115	24,656
Optimised	1,383	288	43,412

Table 21.11 Comparison of the utility consumption and the corresponding cost

Utility type	Case			
	Base case		Optimised	
	Consumption (kW)	Cost ($/y)	Consumption (kW)	Cost ($/y)
Hot utility	1,708	39,284	832	19,136
Cold utility	23,498	35,717	22,623	34,387
Total	–	75,001	–	53,523

it provides a population-based search procedure in which individuals, called particles, change their position (state) with time. In a PSO system, particles fly around a multidimensional search space. During flight, each particle adjusts its position according to its own experience, and according to the experience of a neighbouring particle, making use of the best position encountered by itself and its neighbour (Silva *et al.*, 2009).

Results and Discussion

Following the proposed procedure, Table 21.10 shows the specifications of the HEN for the base case and for the optimised retrofitted case.

The additional investment cost of the modified HEN is $ 68,068. Optimising the existing HEN, the energy saving achieved through the utilities is 21,478 $/y.

Table 21.11 shows the utility consumption and corresponding utility cost for the base case and the optimised retrofitted HEN. Figure 21.22 shows the optimised configuration of HEN. The highlighted heat exchangers are the new matches introduced into the network. The payback period of the retrofit project is 3.2 y.

21.2.5 Heat Recovery Improvement in Aniline Production Unit

Process Description

The concept of Pinch Technology has been under publication over the last 40 years. Early research on the application of Pinch Technology has been,

© Woodhead Publishing Limited, 2013

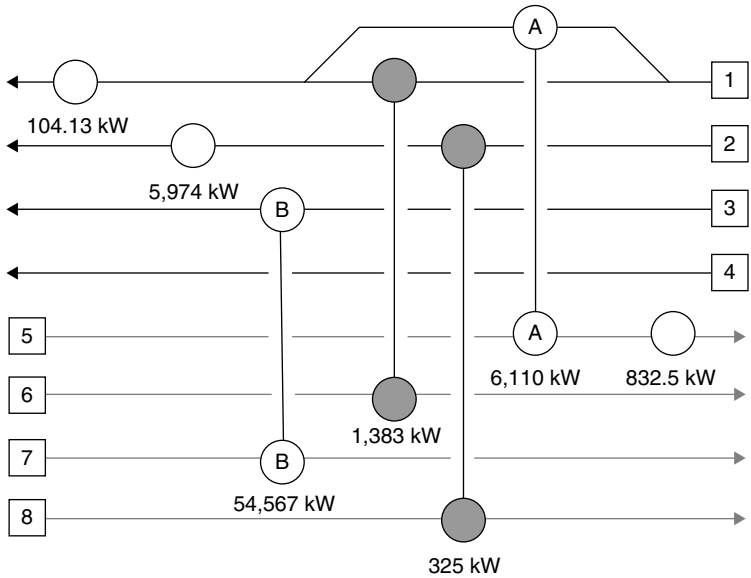

21.22 Configuration of retrofitted HEN.

mainly, focused on individual process units. Some pioneering works have addressed issues of Total Site heat recovery to improve the energy efficiency of a site (Dhole and Linnhoff, 1992). However, the productivity and performance of a petrochemical complex is affected by the interactions within the inter-process units and utility system. In this respect, proper elucidation of the site boundaries for Heat Integration can provide guidelines to address the interactions in heat recovery improvement of the system. In this project, the aniline production unit is investigated to improve energy efficiency through a retrofit procedure allowing the interactions between the aniline plant and the other subsystems within the petrochemical complex to be considered systematically (Feng *et al.*, 2011).

The aniline production unit includes four sections: the nitrobenzene unit, the aniline unit, the natural gas unit and the waste acid treatment unit. Figure 21.23 shows a schematic of the aniline production plant. In the nitrobenzene unit, benzene and nitric acid react to generate nitrobenzene. The nitric acid is regenerated from the waste acid treatment unit. In the waste acid treatment unit, the waste acid and acid benzene are separated. The wastewater is then treated to ensure compliance with environmental regulations before discharge. In the aniline unit, the nitrobenzene reacts with hydrogen to produce aniline. The reaction mixture undergoes purification to produce an aniline product stream. The hydrogen is produced and purified in a natural gas unit (Feng *et al.*, 1982).

Process stream data of the aniline plant are presented in Table 21.12. Figure 21.24 shows a representation of the plant HEN structure.

© Woodhead Publishing Limited, 2013

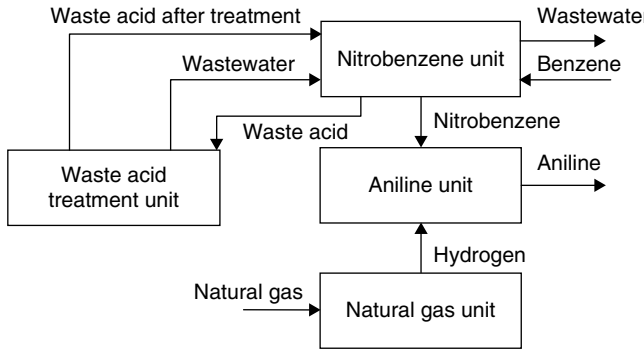

21.23 Schematic of overall aniline production plant (Feng *et al.*, 2011).

Project Objectives

In this project, a retrofit procedure is implemented in an aniline production unit (Feng *et al.*, 2011) to improve the energy efficiency of the plant. To accomplish effective Heat Integration, the proposed retrofit procedure allows the interactions within the plant subsystems to be considered by defining system boundaries.

Design Approach

The objective of the retrofit approach is to provide significant energy savings without having to make major network structural changes. The retrofit procedure is implemented in three steps (Feng *et al.*, 2011).

Step I: Identification of energy savings potential in the Total Site and subsystems. The energy-saving potential of the HEN is the actual heating utility consumption minus the minimum heat utility. The minimum heat utility is targeted using Pinch Analysis.

Step II: Defining Heat Integration boundaries. The boundary for Heat Integration in a petrochemical complex can be the Total Site or each individual subsystem within the site. The boundary will be determined based on the obtained energy-saving potentials. If the energy-saving potential of the whole system is close to the total energy-saving potential of its subsystems, each subsystem will be defined as the boundary for Heat Integration. On the other hand, if there is a noticeable difference between the energy-saving potential of the whole system and the total energy-saving potential of its subsystems, the Total Site will be defined as the boundary for Heat Integration, so that the energy-saving potential can be maximised.

Step III: Implementation of the Heat Integration strategy. Based on the defined boundaries for Heat Integration, retrofit of the plant will be carried out either through matching streams within each subsystem, or by exploring opportunities for inter-process transfer. The overall retrofit procedure is presented in Fig. 21.25.

© Woodhead Publishing Limited, 2013

Table 21.12 Aniline plant process stream data

Unit	No.	Stream	T_{Supply} (°C)	T_{Target} (°C)	Heat load (kW)
Nitrobenzene unit	Hot 1	Waste acid	70	39	1,685.16
	Hot 2	Mixed acid	37	20	498.48
	Hot 3	Azeotrope from cooler	100.1	99.1	1,214.48
	Hot 4	Benzene from distillation column	92.8	22.9	434.91
	Hot 5	Nitrobenzene from 1st distillation	116	28.3	4478.2
	Hot 6	Nitrobenzene	17	16	227.58
	Hot 7	Nitrobenzene	51.6	43.9	509.61
	Hot 8	Waste acid from cooler	74	62	567.31
	Cold 9	Wastewater from cooler	10	32	498.48
	Cold 10	Wastewater from reboiler	57	65	1,428.17
	Cold 11	Nitrobenzene from preheater	36.1	121.7	809.28
	Cold 12	Liquid from reboiler	151.9	157.35	718.83
	Cold 13	Liquid from distillation	141.8	142.8	1,683.09
Aniline unit	Hot 1	Hydrogen	197.6	160	183.1
	Hot 2	Reacted gas I	216	116.5	835.58
	Hot 3	Nitrobenzene from condenser	116.6	64.7	812.12
	Hot 4	Reacted gas II	29.1	27.1	107.22
	Hot 5	Heat medium	31.2	18	155.65
	Hot 6	Wastewater	93.6	64.2	305.84
	Hot 7	Aniline from top of distillation column	88.5	47.1	188.91
	Hot 8	Aniline water	154.1	40	536.32
	Hot 9	Aniline from cooler	48.9	20.3	115.51
	Hot 10	Aniline from condenser	109.8	49.9	5,230.28
	Cold 11	Nitrobenzene from heater	149.0	154.7	44.67
	Cold 12	Mixed gas	149.0	194.5	659.02
	Cold 13	Circulating hydrogen	61.9	197.5	835.58
	Cold 14	Aniline water from preheater	20.9	38.7	305.40
	Cold 15	Aniline water from reboiler	96.0	99.6	188,566.00
	Cold 16	Impure aniline from preheater	31.8	113.1	812.01
	Cold 17	Aniline from reboiler	178.8	179.1	1,019.66
	Cold 18	Aniline from distillation column	109.0	135.4	2,046.60
	Cold 19	Pure nitrobenzene	154.7	160.0	1,664.19
Natural gas unit	Hot 1	Transformed gas	793.0	365.0	3,366.37
	Hot 2	Middle transformed gas	370.0	21.0	5,869.98
	Hot 3	Flue gas	855.4	129.4	8,683.25
	Hot 4	Gas after de-carbonisation	60.0	23.0	245.24
	Hot 5	Waste liquid from cooler	60.0	35.0	435.97
	Hot 6	Carbon dioxide	48.0	30.0	550.08
	Cold 7	Desalinating water	11.0	84.0	1,226.42
	Cold 8	Natural gas to transformer	70.0	268.4	1,061.16
	Cold 9	Raw material gas to transformer	212.1	600.3	3,634.35
	Cold 10	Stream to transformer	216.4	220.2	1,810.45
	Cold 11	Air to transformer	25.0	278.3	2,177.29
	Cold 12	Saturation water	207.0	208	3,366.37
	Cold 13	Water from preheater	86.0	207	3,803.80

© Woodhead Publishing Limited, 2013

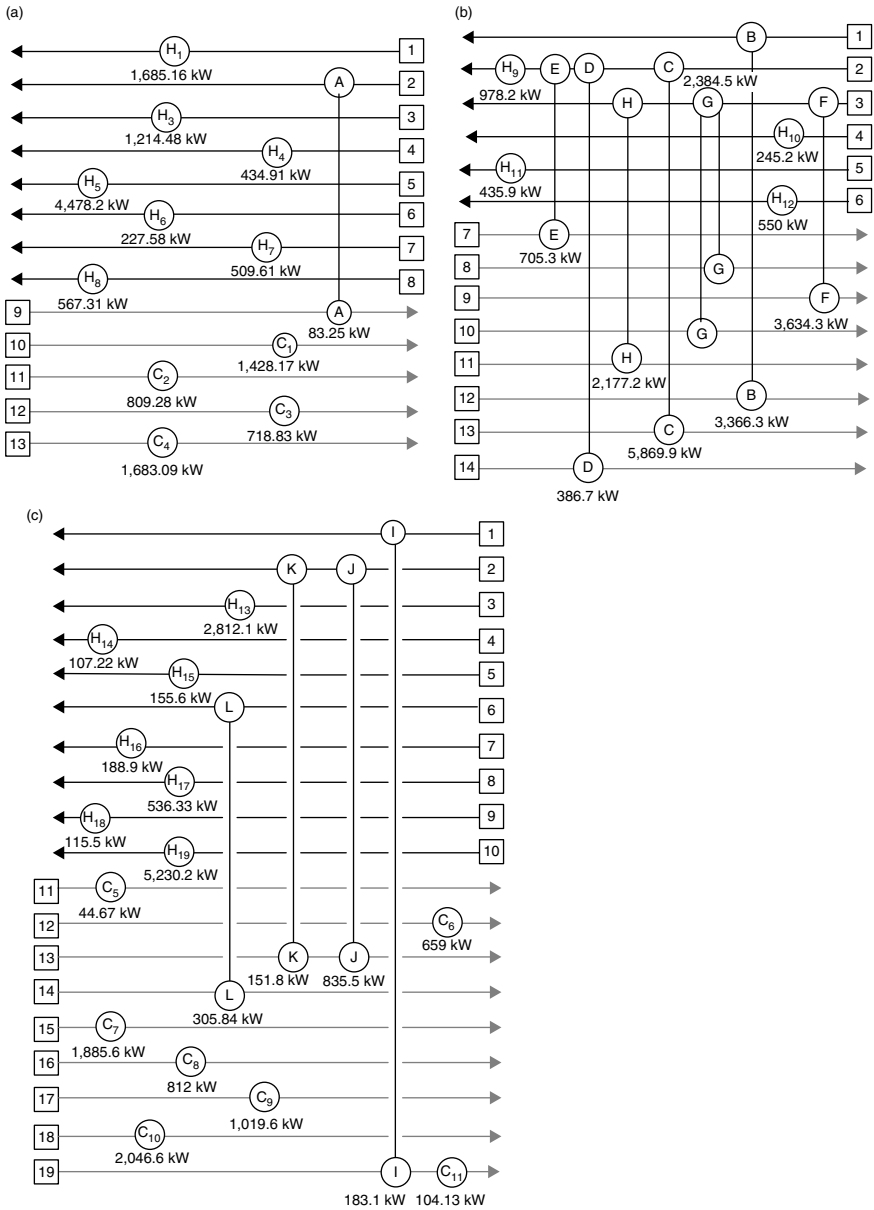

21.24 Representation of HEN structure (a: Nitrobenzene unit, b: Natural gas unit, c: Aniline unit).

Results and Discussion

Applying the retrofit procedure on the aniline plant, the energy-saving potentials of the total system and each subsystem are presented in Table 21.13 (Feng *et al.*, 2011).

© Woodhead Publishing Limited, 2013

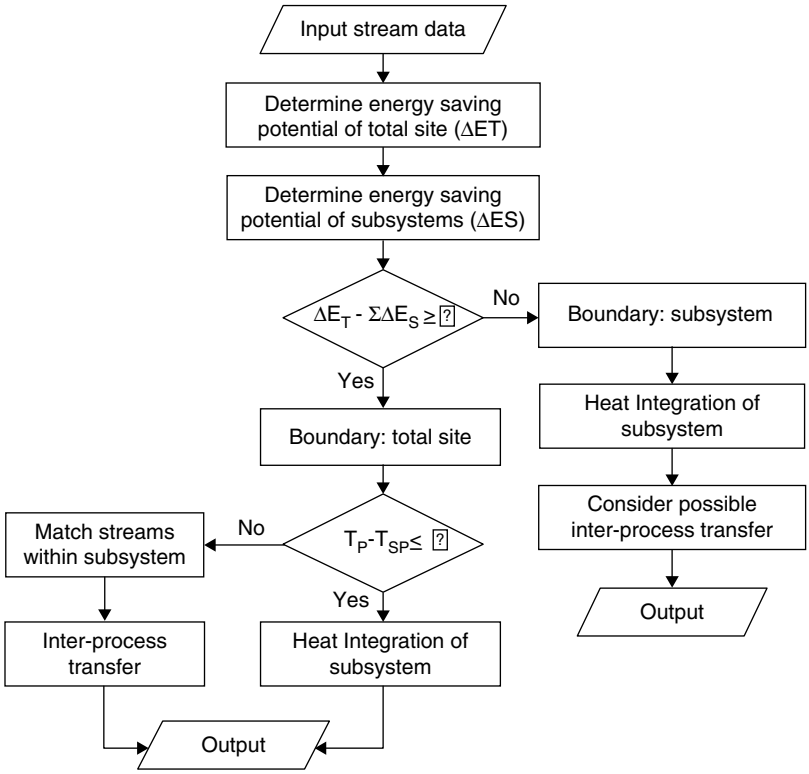

21.25 Overall retrofit procedure (Feng *et al.*, 2011).

Table 21.13 Energy-saving potential

Unit	Minimum hot utility (kW)	Minimum cold utility (kW)	Energy saving (kW)	Energy saving (%)
Nitrobenzene unit	4,639.37	9,117.25	1,900	40.9
Aniline unit	7,073.75	8,271.48	874.9	11
Natural gas unit	0	NA	–	–
Total Site	9,148.35	16,367.91	3,439.72	27.32

Based on the results obtained from the energy-saving analysis, it is clear that the energy-saving potentials of the two schemes are quite close to each other. Therefore, each subsystem is selected as the boundary for Heat Integration.

It is noted that the natural gas unit HEN is a Threshold Problem that only consumes cooling utility and no heating is used. Inter-process transfer is an option to reduce the cooling load of the unit. Therefore, when considering

© Woodhead Publishing Limited, 2013

Table 21.14 Unreasonable Heat Exchange Matches of the aniline plant

Unit	Heat exchanger ID	Linked stream	Reason
Nitrobenzene unit	C_2	Cold 10	Hot utility Below the Pinch
	C_1	Cold 9	Hot utility Below the Pinch
Aniline unit	K	Hot 2-cold 13	Heat transfer across the Pinch
	H_{17}	Hot 8-cooling water	Cold utility Above the Pinch
	C_8	Cold 16-steam	Hot utility Below the Pinch

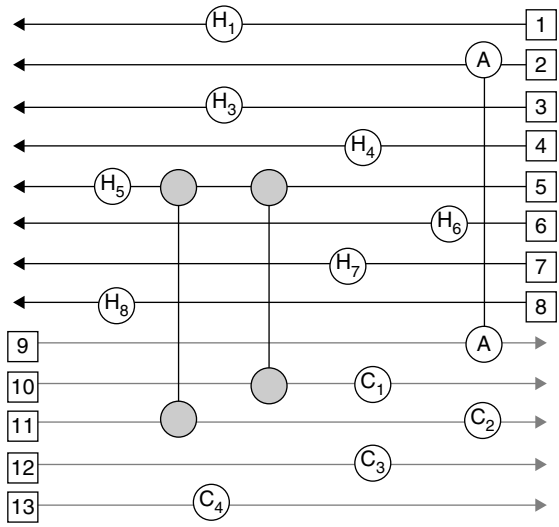

21.26 Final retrofitted configuration of nitrobenzene unit HEN.

inter-process transfer opportunities for the subsystems, a key concept is to use the hot streams of the natural gas unit to heat the cold streams in the nitrobenzene unit or the aniline unit. However, due to the operational difficulties related to matching the hot stream in the natural gas unit with other streams, Heat Integration is carried out for each individual unit without including any inter-process heat transfer. Having explored the possible matches, Table 21.14 presents the unreasonable Heat Exchanger Matches of the aniline plant. The final retrofit schemes are presented based on removing these unreasonable Heat Exchange Matches as follows.

The final retrofitted HENs of the nitrobenzene and aniline units, including the newly added heat exchangers, are shown in Figs 21.26 and 21.27, respectively. Table 21.4 shows the new heat exchangers added to the aniline plant. Retrofitting the aniline plant, 2621 kW of energy savings were achieved through heat recovery, equivalent to 20.8 % of the existing energy consumption of the system.

© Woodhead Publishing Limited, 2013

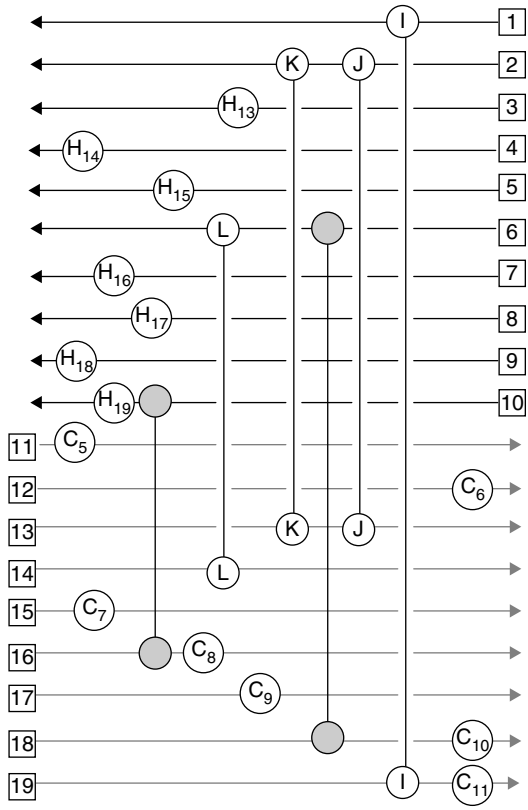

21.27 Final retrofitted configuration of aniline unit HEN.

21.2.6 Optimum Design of Low-Temperature Gas Separation Processes

Process Description

In the chemical process industry, many processes, such as natural gas liquefaction, gas separation and ethylene production, operate partially or totally below ambient temperature. They require heat removal through refrigeration systems, which must be integrated with the process streams on the site, with HENs, or with external utilities to remove the heat extracted from separation processes to available heat sinks. For large-scale systems, multiple levels of refrigeration, cascaded systems and mixed refrigerants are used. This, coupled with a high degree of Heat Integration, makes the design of such systems enormously complicated, due to the complex interactions that arise (Smith, 2005).

Ethane extracted from associated gas (i.e., gas produced with crude oil) and non-associated gas (i.e., gas produced without oil or condensate) is the

© Woodhead Publishing Limited, 2013

Table 21.15 Problem data for a natural gas stream originated from non-associated gas

i	Component	Composition (mol %)	Product	Product specification
1	Methane	0.3019	A	99% recovery of ethane
2	Ethane	0.2587		
3	Propane	0.2648	B	98% purity of propane
4	Butane	0.1198	C	98% purity of butane
5	Pentane	0.0358	D	97% purity of pentane
6	Hexane	0.0190	E	99% recovery of hexane
Feedflowrate		4,313 kmol/h, saturated liquid at 20 bar		

Source: Smith (2005).

Table 21.16 Specification of the available hot and cold utilities

Type	Temperature (°C)	Unit cost (GBP/kW.y)
Hot utility	–	–
Hot water	45–90	25.0
Low pressure steam	150	27.8
Medium pressure steam	200	55.6
High pressure steam	250	83.3
Cold utility	–	–
Cooling water	25–35	33.3
Electric power	–	330

Source: Tahouni *et al*. (2010).

cheapest method of producing ethylene. Table 21.15 shows the composition of the natural gas stream achieved from non-associated gas after the demethaniser. The ethane should be extracted from natural gas and used as cracker feedstock to produce ethylene. The main technique to extract ethane from natural gas is low-temperature separation, that is, cooling of the gas stream until a liquid fraction containing the bulk of the ethane and other liquefied gas components are condensed (Farry, 1998).

Table 21.16 shows the available utilities satisfying the external heating and/or cooling requirements of the processes. The available refrigerants are methane, ethylene and propylene, which provide cooling at temperatures as low as –161°C, between –104°C and –47°C, and between 47°C and ambient temperature.

Project Objectives

The objective of this project is to implement a simultaneous design procedure in a plant of producing ethylene, for optimum design of a separation system including Heat Integration within and between the systems of

© Woodhead Publishing Limited, 2013

separation columns, refrigeration cycles, and the associated HEN, which can achieve minimum utility cost.

Synthesis and Optimisation Procedure

Figure 21.28 illustrates the optimisation procedure for the design of low-temperature separation processes. The basic stages consist of construction of a superstructure including different separation sequences, selection of refrigerants and definition of desired product specifications. First, the Genetic Algorithm (GA) or SA generates a random solution in the search space. At this stage, separation sequencing, task representation for each separator, operating pressure and feed conditions for each separator are considered to be the design parameters. Then, a feasible point, which is randomly found by the optimiser, is passed to simulation stage (Wang and Smith, 2005).

All calculations are carried out by COLOM software version 2.1, 2007 – for more details see Chapter 34, a program for analysing a variety of separation problems. The full shortcut models for various separation options used in software have already been verified and reported in the literature (Bausa and Watzdorg, 1996).

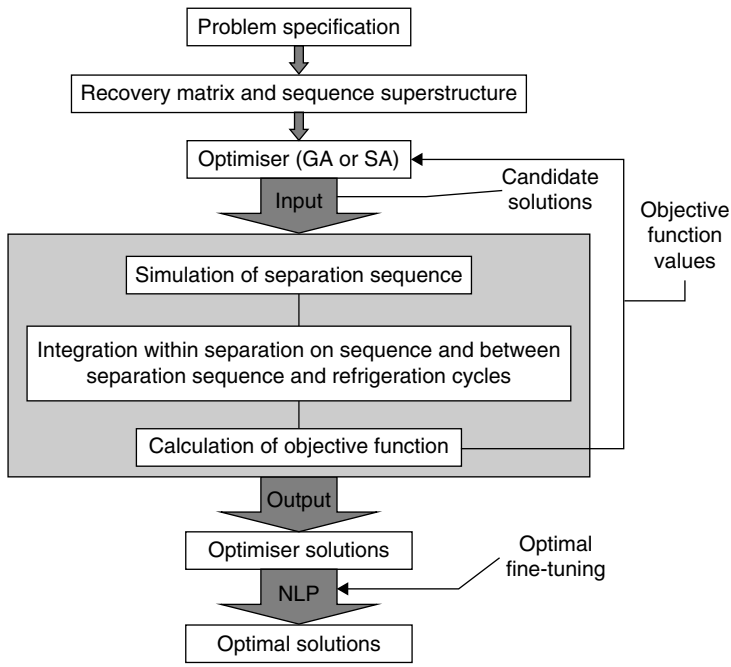

21.28 Schematic diagram of synthesis and optimisation of low-temperature gas separation processes (Tahouni *et al.*, 2010).

© Woodhead Publishing Limited, 2013

The Peng–Robinson equation of state is applied to calculate the thermodynamic properties. Simulation provides the required cooling and heating duties, which is the basis for Heat Integration with refrigeration systems and external utilities. After achieving an integrated separation scheme, the calculated objective function is returned to the optimiser for calculating the fitness values. Afterwards, values for crossover and mutation (used in the GA method) are varied within a cycle to produce another feasible solution. Similarly, for the SA method, annealing temperature is reduced, and the associated Markov Chain length is located in order to find another solution (Calrberg and Westerberg, 1989).

For the problem, two stochastic methods, the GA and SA, are implemented to design an optimum sequence that recovers desired products from a given feed, optimising all synthesis issues simultaneously. Both techniques should be parameterised to avoid premature convergence before the best solution is found (Tahouni *et al.*, 2011)

Results and Discussion

Figure 21.29 compares the optimisation results of low temperature of ethylene plant, achieved by GA and SA with a different set of key parameters. Two important points can be seen. First, if we choose a wrong set of parameters, the optimiser may lead to local optima whether we use the Genetic Algorithm or SA optimisers. Second, in this separation system, SA is more powerful than the GA to converge to a lower utility cost (Tahouni *et al.*, 2010).

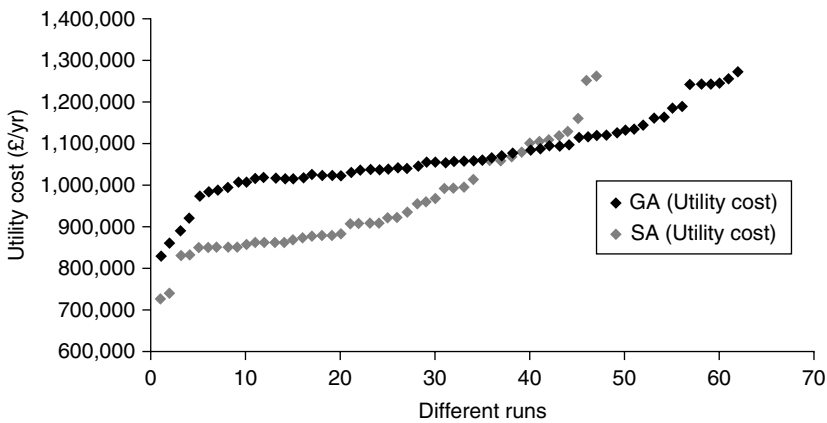

21.29 Comparison of optimisation results for the ethylene case study by GA and SA for different sets of parameters (Tahouni *et al.,* 2010).

© Woodhead Publishing Limited, 2013

Design I

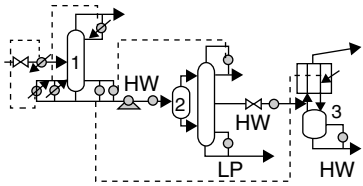

	Separation	Press (bar)	Condenser temp/duty (°C/MW)	Reboiler temp/duty (°C/MW)
1	A/BCDE	4.5	–56.43/2.23	4.07/17.53
2	B/CD/E	8.8	11.07/6.50	121.56/3.73
3	C/D	6.4	44.80/5.53	60.12/3.38

Heat integrated with refrigeration system
Directly heat exchanger

1: Simple column; 2: Pre-fractionator; 3: Dephlegmator–stripper

Design II

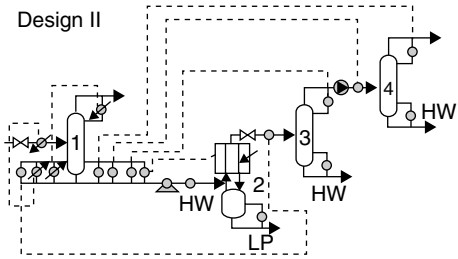

	Separation	Press (bar)	Condenser temp/duty (°C/MW)	Reboiler temp/duty (°C/MW)
1	A/BCDE	5.2	–51.28/2.39	9.89/17.64
2	B/CD/E	9.6	40.48/4.03	125.86/1.59
3	BC/D	8.7	27.48/2.80	73.44/5.94
4	BC	9.7	21.94/2.28	62.48/2.06

1, 3, 4: Simple column; 2: Dephlegmator–stripper

Design III

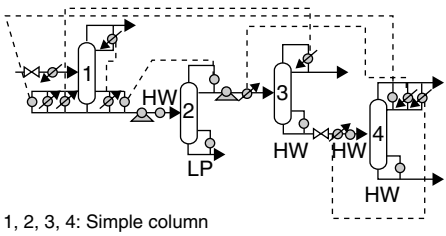

	Separation	Press (bar)	Condenser temp/duty (°C/MW)	Reboiler temp/duty (°C/MW)
1	A/BCDE	4.8	–53.63/2.30	6.60/17.58
2	BCD/E	8.3	18.68/5.41	118.30/1.51
3	B/CD	9.3	13.45/4.11	67.95/4.59
4	C/D	4.0	28.79/3.36	42.24/3.06

1, 2, 3, 4: Simple column

21.30 Three selected designs for the ethylene case study by SA optimiser (Tahouni *et al.,* 2011).

Figure 21.30 illustrates the three best results obtained for designing the ethylene case study by SA. The best separation sequence is presented in Design I. Here, the separation tasks of A/BCDE, B/CD/E and C/D are carried out in a simple column, a pre-fractionator and a dephlegmator–stripper, respectively.

Applying the integration method proposed in Fig. 21.28, an integrated refrigeration process is illustrated in Fig. 21.30. A HE with a crossed arrow, which is linked by a dashed line to another heat exchanger, indicates the Heat Integration between a heat sink and a heat source via a refrigeration

© Woodhead Publishing Limited, 2013

cycle. In Design I, there are two cascade refrigeration cycles of ethylene/propylene and a simple cycle of propylene. In addition, HEs without arrows indicate either direct heat transfer between two process streams if there is a dashed line between two exchangers, or direct heat transfer to an external utility if there is no dashed line (Tahouni *et al*., 2010).

The results show the separation system optimisation, Heat Integration in the process context and also the selection of different refrigerants that should simultaneously be considered in order to attain a minimum cost design. Although reducing the costs will generally increase the design complexity, the designer would be able to explore the trade-offs between the two and make the final decision. Sometimes, avoiding the cheapest design and thinking of simpler solutions is the best decision (Tahouni *et al*., 2011).

21.2.7 Concluding Remarks

By performing the Heat and Power Integration in process plant HEN and utility system, external energy requirement of process units have been reduced. Pinch-based conceptual methods help better understanding of the process capacity for energy conservation potential. However, mathematical methods can also offer excellent solution options to the problem. While individual integration of heat or power in process plant provides energy savings, Combined Heat and Power Integration has also resulted in further reduction of energy consumption by allowing Heat Integration between the power system and the heat recovery network of the process. Effective design procedures for energy saving in grass-roots and retrofit situations are presented. Results have shown that recent developments in the energy system HEN Design are more energy-efficient and provide better economies.

21.3 Water and Wastewater Minimisation

21.3.1 Introduction

Water is used for a wide variety of purposes in the chemical and petroleum industries. In the past, water had been assumed to be a limitless and low-cost commodity. However, increased water awareness, scarcity of water resources and ever-increasing water costs, have encouraged efficient water system design. Moreover, environmental regulations for increasing the ecological protection and rising cost of wastewater treatment have resulted in focusing on wastewater minimisation problems (Kim and Smith, 2002).

Research on water and wastewater minimisation has focused on the individual components of water system. However, to maximise water conservation

© Woodhead Publishing Limited, 2013

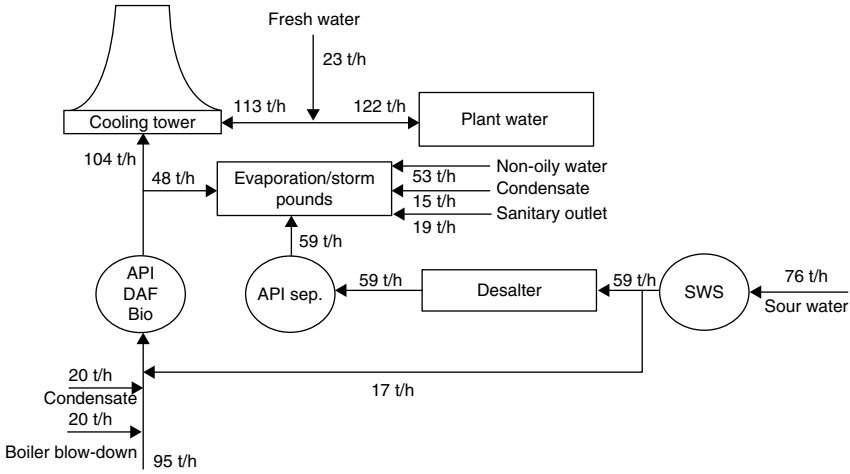

21.31 Water and wastewater system of petroleum refinery.

potential in process site water system, simultaneous consideration of interactions between the water-consuming operations is needed.

21.3.2 Water and Wastewater Minimisation in a Refinery

Process Description

An oil refinery plant includes several water-consuming operations. Figure 21.31 shows a schematic of water-using operations and wastewater system in a petroleum refinery plant. As shown in this figure, the main component of the water and wastewater system includes the water network and the cooling tower. The existing performance parameters of the base case for the water network side and the cooling cycle side (cooling tower) are presented in Table 21.17.

Project Objectives

In this project, a new strategy is implemented for minimisation of water and wastewater in a petroleum refinery complex. The implemented solution strategy is capable of minimising the water requirement by using an advanced Water Pinch method, taking advantage of the most recent technologies for improving the quality of recycling water and increasing the water reuse flowrate (Panjeshahi *et al.*, 2009). The proposed solution strategy sets performance targets prior to design. Although the solution strategy is focused on solving the problem of a petroleum refinery, it is capable of being applied to any process requiring water in a number of operations.

© Woodhead Publishing Limited, 2013

Table 21.17 Performance parameters of base case

Water network side	Performance parameter	Unit	Quantity
	Fresh water consumption	m^3/h	505
	Fresh water inlet temperature	°C	25
	Wastewater evaporator flowrate	m^3/h	160
	Wastewater treated in API Sep.	m^3/h	59
	Wastewater treated in sanitary	m^3/h	19
	Wastewater treated in biological/API/DAF	m^3/h	152
	Wastewater treated in warm lime softener	m^3/h	0
	Regenerated wastewater in SWS	m^3/h	76
	Total operating cost of wastewater treatment and regeneration units	$/h	289.2
Cooling cycle side	Water flowrate	m^3/h	22,600
	Cycle of concentration	–	5.85
	Temperature difference (range)	°C	20
	Evaporation flowrate	m^3/h	175
	Blow-down flowrate	m^3/h	37
	Drift flowrate	m^3/h	5
	Make-up flowrate	m^3/h	217
	Cooling capacity	MW	524.82
	Fan power	hp	1,319.8
	Pumping power	hp	1,194

Targeting

Consider a water-using operation in a refinery process. In order to minimise the water consumption and to maximise the water reuse from other operations to this operation, first, the water with the highest inlet concentration should be specified. Then, by specifying the maximum possible outlet concentration, the water will be minimised at the maximum inlet concentration (Fig. 21.32) (Smith, 2005). It is noted that this profile (limiting profile) is a representation of a limiting case and will not necessarily be used in the final design. Therefore, any Water Supply Line below the limiting profile will meet the requirements of process and operational feasibility (Wang and Smith, 1994). Table 21.18 presents the limiting process water data in the water and wastewater system of the refinery.

Step 1: The first step in targeting the minimum water flowrate is the construction of the Limiting Composite Curve (Figs 21.33a and 21.33b) (Panjeshahi *et al.*, 2010a). As shown in this figure, the inlet and outlet concentrations of the processes define the concentration intervals. The Limiting Composite Curve is obtained by combining operations within the concentration intervals.

Step 2: The second step is to define the feasible Cooling Water Supply Line from Composite Curve and the parallel supply line (Fig. 21.34) (Panjeshahi *et al.*, 2010a).

© Woodhead Publishing Limited, 2013

Table 21.18 Limiting process water data

ID	Stream description	Flowrate (m^3/h)	T (°C)	SS (ppm)	Oil (ppm)	COD (ppm)	BOD (ppm)	TH (ppm)	PO_4 (ppm)	NH_3 (ppm)	H_2S (ppm)
1	Sanitary outlet	19	25	1	0	70	70	200	0	0	0
2	Oily water	95	25	5	250	375	300	310	0	0	0
3	Cooling tower blow-down	37	49	4	4	100	70	1,250	0	0	0
4	Boiler blow-down	20	66	4	0	0	0	0	30	0	0
5	SWS outlet	76	35	13	0	0	0	12	0	50	7
6	Desalter outlet	59	25	20	100	0	0	160	0	0	0
7	DM unit blow-down	16	25	16	4	0	0	840	0	0	0
8	Condensate water	45	80	1	0	0	0	0	0	0	0
9	Fresh water	Unlimited	25	1	0	0	0	150	0	0	0

© Woodhead Publishing Limited, 2013

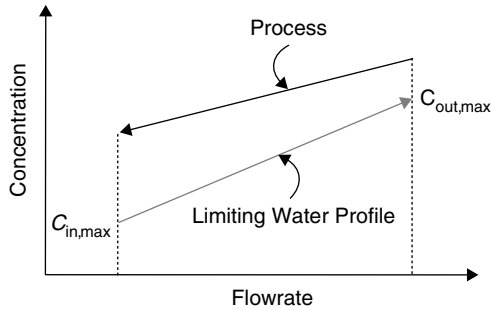

21.32 Limiting profile of a single process (Smith, 2005).

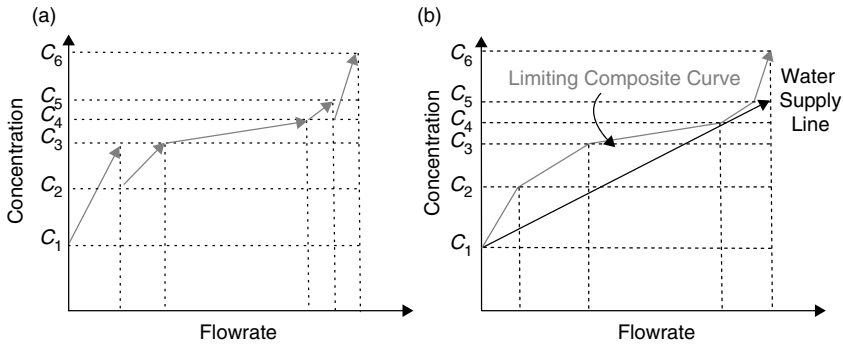

21.33 Construction of Limiting Composite Curve (Panjeshahi *et al.*, 2009).

Step 3: The third step is to target the cooling tower supply conditions from the cooling system model and the feasible Cooling Water Supply Line. Details of the targeting procedure are given by Panjeshahi *et al.* (2010a).

Design

In this stage, the objective is to design a water network for targeted conditions (flowrate and concentrations) using Pinch Migration through the temperature shifting concept and water main method. Following the water main method often allows more than one Network design to achieve the target (Kim and Smith, 2001). In the design of a water system, certain design features are essential. Also, it is necessary for the cooling water to be reused in the design to achieve the target. The design procedure is then followed with strategies for further decrease of external fresh water requirement to reduce the operational cost of the water and wastewater system.

© Woodhead Publishing Limited, 2013

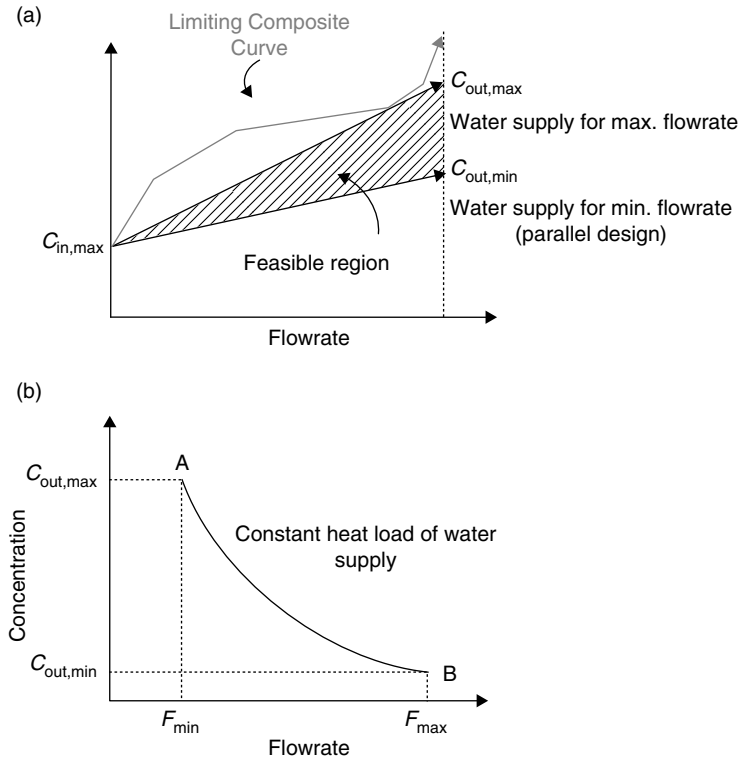

21.34 Feasible Water Supply Line (Panjeshahi *et al.*, 2010a).

Increasing the cycle of concentration in the cooling system provides the opportunity to reduce fresh make-up water by improving the quality of the recycling water in cooling tower. In the proposed solution strategy, integration of the ozone water treatment with cooling system is considered as a safe, non-chemical and eco-friendly treatment method for the use of make-up water (Ataei *et al.*, 2010). Integration of the ozone treatment unit also improves the energy efficiency of cooling cycle, as it removes the bio-film accumulated on the sides of the cooling system components, impeding the heat transfer. Figure 21.35 shows a schematic of the ozone treatment system integrated with the cooling system. As shown in this figure, first ambient air is compressed, dried and ionised in the ozone treatment unit to produce ozone. The ozone produced is then added to the circulating water in the cooling tower to inactivate infectious bacteria, algae and viruses. Installation of the water ozone treatment unit will necessitate capital as well as Operating cost (pumping cost) on the system. However, the operational cost reduction can compensate for the cost penalties of integration and make the payback period short. It is clear that the payback period can vary

© Woodhead Publishing Limited, 2013

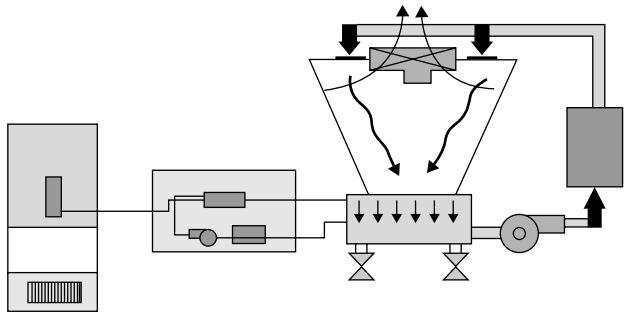

21.35 Schematic of cooling system integrated ozone water treatment (Panjeshahi *et al.*, 2009).

from project to project and depends on the capacity and existing performance of cooling system.

On the cooling cycle side of the system, if the temperature of the hot return cooling water decreases, the heat duty of the cooling tower will decrease. This can help in reducing evaporation loss from cooling tower as it reduces the tower temperature range (Panjeshahi *et al.*, 2010, 2010b). To decrease the water return temperature, an air-cooler can be installed between the cooling tower and the water network. This keeps the water flowrate of the return hot cooling water constant while reducing the temperature. Because the air-cooler influences only the temperature of the hot return cooling water, there is no change in the cycles of concentration. In the presented solution strategy, installation of an air-cooler between the cooling water network and the cooling tower is proposed as an extra design feature to reduce the cooling duty of cooling tower. Design of the air-cooler is performed in Aspen B-Jac® software.

Results and Discussion

Following the targeting procedure on the case study (petroleum refinery complex), the results of targeting stages are presented in Table 21.19.

The specifications of the water network at Pinch Point are presented in Table 21.20.

It was attempted, in the design stage, to achieve design features that met the targeted values. Having applied the design procedure, Table 21.21 shows a comparison between the performance parameters at targeting and final design stages.

Figure 21.36 shows the final modified configuration of the water and wastewater system. Applying the proposed solution strategy resulted in 31.3% (158 m^3/h) fresh water conservation and 93.9 kW energy savings in

© Woodhead Publishing Limited, 2013

Table 21.19 Targeting result of water and wastewater system

Performance parameter	Unit	Targeted value
Fresh water consumption	m^3/h	77
Wastewater evaporator flowrate	m^3/h	50
Wastewater treated in API Sep.	m^3/h	59
Wastewater treated in sanitary	m^3/h	19
Wastewater treated in biological/API/DAF	m^3/h	116
Wastewater treated in warm lime softener	m^3/h	28
Regenerated wastewater in SWS	m^3/h	76
Air-cooler heat transfer area	m^2	55,000

Table 21.20 Pinch Point water specification

Location	T (°C)	SS (ppm)	Oil (ppm)	COD (ppm)	BOD (ppm)	TH (ppm)	PO_4 (ppm)	NH_3 (ppm)	H_2S (ppm)
Pinch Point	30	4	4	4	4	20	4	4	4

Table 21.21 Comparison between the targeting and design values of the proposed strategy

Performance parameter	Unit	Targeting stage	Design stage	Error (%)
Upstream air-cooler heat duty	MW	41.986	41.986	0
Air-cooler heat transfer areas	m^2	55,000	57,005	3.6
Air-cooler inlet water temperature	°C	49	49	0
Air-cooler exist water temperature	°C	47.4	47.4	0
Air-cooler maximum inlet water flowrate	m^3/h	22,600	22,600	0
Cycle of concentration	–	15	15	0
Recycle ratio	%	6.67	6.67	0
Water ozone treatment capacity	m^3/h	178	200	12.3
Cooling tower inlet water temperature	°C	47.7	47.7	0
Cooling tower exit water temperature	°C	29	29	0
Cooling tower fan pressure	In H_2O	0.5	0.5	0
Cooling tower temperature Difference (range)	°C	18.4	18.4	0
Drift flowrate	m^3/h	5	5	0
Evaporation flowrate	m^3/h	161	161	0
Blow-down flowrate	m^3/h	12	12	0
Make-up water flowrate	m^3/h	178	178	0
Cooling tower cooling duty	MW	482.83	482.83	0

© Woodhead Publishing Limited, 2013

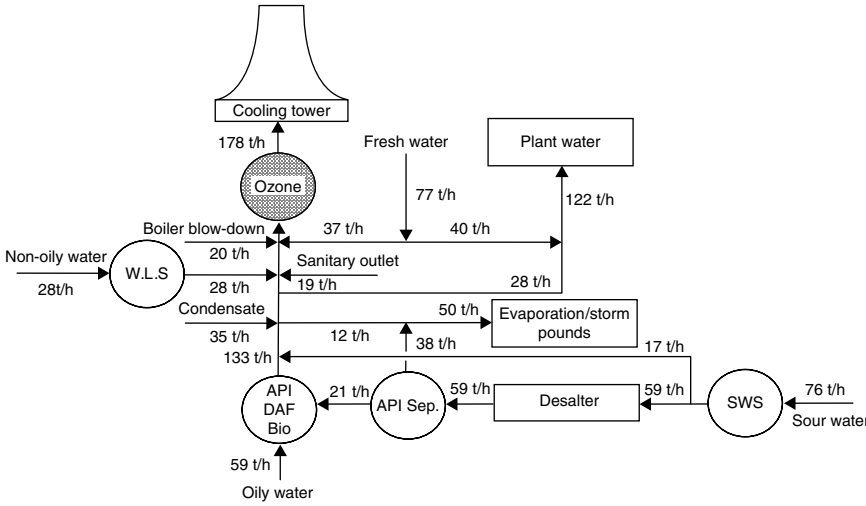

21.36 Optimum configuration of water and wastewater system.

Table 21.22 Economical evaluation of the solution strategy

Economical parameter	Unit	Value
Total operating cost	$/h	252.8
Annual operating cost saving	$/y	313,040
Annual energy-saving cost	$/y	32,302
Annual water conservation cost	$/y	135,880
Total annual saving	$/y	481,222
Air-cooler capital and installation cost	$	1,542,108
Water ozone treatment capital and installation cost	$	63,800
Total project capital cost	$	1,605,908
Project Payback Time	y	3.3

the water and wastewater system of the refinery plant. Table 21.22 shows the economical evaluation achieved from the solution strategy.

21.3.3 Optimum Design of Cooling Water Systems for Energy and Water Conservation in Oil Industry

Process Description

Recirculating Cooling Water (RCW) systems are by far the most common type of cooling water systems in process industries, refinery units and petrochemical plants. The main components of RCW systems include the

© Woodhead Publishing Limited, 2013

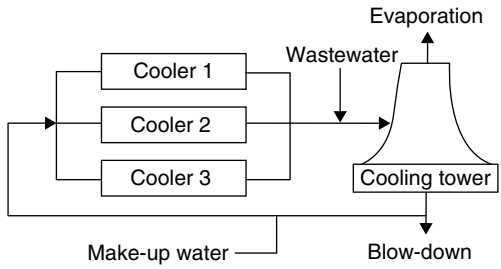

21.37 Conventional design of cooling water systems in a typical oil refinery (Panjeshahi *et al.*, 2009).

cooling tower and the HEN. Conventional design of cooling water networks utilises parallel configuration (Fig. 21.37) (Kim and Smith, 2001). In parallel configuration, fresh cooling water is supplied to individual process unit HENs. The hot cooling water from the individual process unit gathers and returns to the cooling tower afterwards. In the cooling tower, blow-down is necessary to avoid the build-up of undesirable materials in the recirculating water as a result of evaporation. The flowrate loss caused by evaporation and blow-down is then compensated by make-up water. Mixing water from individual process units reduces the driving force, and consequently provides poor cooling performance (Smith, 2005).

Usually, in industrial sites, not all cooling duties require cooling water at cooling water supply temperature. This can provide an opportunity for reusing water by changing the conventional configuration of cooling system from parallel to series arrangement. While a series arrangement can provide water and energy conservation, including features of the water quality requirements of the water-using operations into the design, if applicable, can provide further improvement on the cooling system, in terms of water and energy requirements (Panjeshahi *et al.*, 2009). For example, in a typical plant, the quality of the cooling tower make-up water is not generally as high as the water-using processes. Therefore, the cooling tower make-up water can be replaced by the reused water, provided that the quality of the reused water is relatively high.

Project Objectives

In this project, a new systematic design tool has been implemented on an oil refinery plant to design the RCW system for minimum total cost. The proposed design method is based on a combination of Pinch Technology and mathematical optimisation, which takes advantage of some patterns from the regeneration–recycling concept to improve water and energy conservation in the RCW system design.

© Woodhead Publishing Limited, 2013

Table 21.23 Hot process stream data

Heat exchanger	$T_{in,hot}$ (°C)	$T_{out,hot}$ (°C)	Heat capacity (kW/°C)	Total heat load (kW)
HX 1	50	40	40	400
HX 2	55	45	100	1,000
HX 3	70	45	50	1,250
HX 4	70	65	100	500
HX 5	75	70	50	250

Table 21.24 Cold process stream data

Heat exchanger	$T_{in,cold}$ (°C)	$T_{out,cold}$ (°C)	Heat capacity (kW/°C)	Total heat load (kW)
HX 1	30	40	40	400
HX 2	35	45	100	1,000
HX 3	35	60	50	1,250
HX 4	55	60	100	500
HX 5	60	65	50	250

Table 21.25 Design parameters

Performance parameter	Unit	Quantity
Air wet bulb temperature	°C	15
Ambient air temperature	°C	25
Minimum approach temperature	°C	5
Pump efficiency	%	60
Pumping head	m	10.67
Interest rate	%	15
Plant life time	y	10
Cooling tower temperature limit	°C	57
Cost of electricity	$/kWh	0.1
Cost of fresh water	$/t	0.26
Cost of chemical treatment	$/t	0.13
Cost of blow-down treatment	$/t	0.13

Targeting

Consider some hot process stream data of an oil refinery plant (Table 21.23). Table 21.24 shows the cooling water data extracted from the hot process stream data. The design parameters used for the case study are presented in Table 21.25.

The procedure presented is based on setting targets prior to design. The targeting phase of the proposed method is carried out in two steps.

Step 1: The first step is to target the optimum cooling water supply conditions (flowrate and temperature). In targeting the optimum water supply,

© Woodhead Publishing Limited, 2013

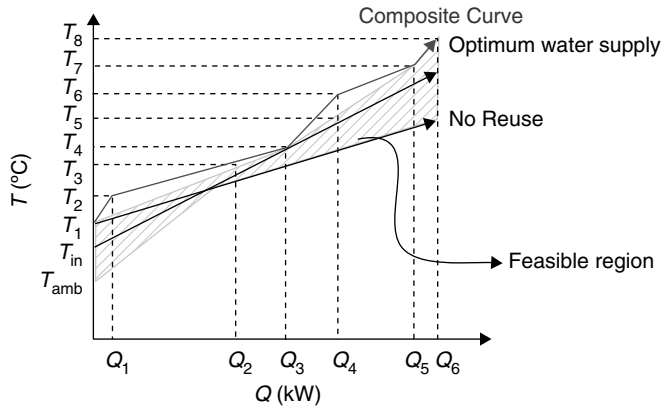

21.38 Cooling water feasible region (Panjeshahi *et al.,* 2009).

first the Cooling Water Composite Curve is plotted. Then the feasible region is defined by introducing the system constraints and boundaries (minimum and maximum water supply flowrate). Figure 21.38 shows the Cooling Water Composite Curve and the feasible region highlighted with system boundaries. Finally, having investigated the feasible region for minimum total cost, the optimum cooling supply line is targeted (Ataei *et al.*, 2009e). Calculations of the optimisation procedure are performed through programming in MATLAB® software version 7.3.

Step 2: By adopting patterns from the regeneration–recycling concept (Wang and Smith, 1994), local regeneration of the cooling system is performed. In this step, installation of air-cooler in the water system is used as an option to reduce the cooling tower design capacity by shifting some of the tower cooling duty to the air-cooler. This reduces the fresh water requirement of the cooling tower and decreases the blow-down accordingly. It is clear that installation of an air-cooler requires extra capital as well as operational cost.

Design

After targeting the water supply condition and air-cooler performance, the HEN is designed using the water main method. To achieve the targeted minimum cooling water flowrate in design, the problem is decomposed into design regions. The minimum cooling water flowrate requirements in each design region is then determined by a line drawn across the Pocket (Kim and Smith, 2001). The strategy of using the cooling water is then translated into a cooling water design grid by setting water mains. The next step is to connect operations with water mains. After merging operations that cross the mains, the HEN Design is then achieved by removing the intermediate (Pinch) water mains (Ataei *et al.*, 2010).

© Woodhead Publishing Limited, 2013

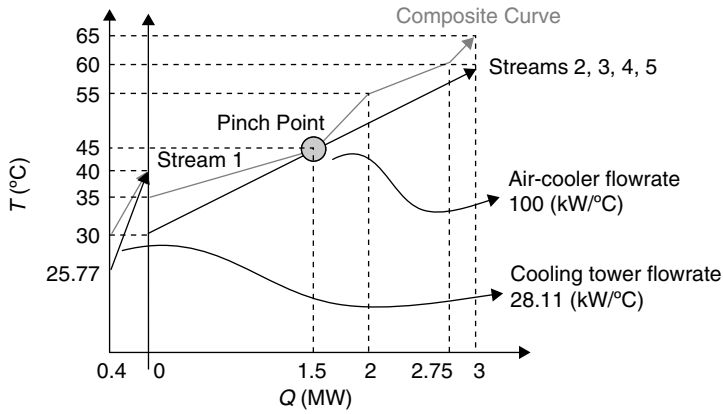

21.39 Targeting the water supply condition (Panjeshahi *et al.*, 2009).

Table 21.26 Performance parameters of water supply

Design method	Inlet water temperature (°C)	Outlet water temperature (°C)	Water flowrate (t/h)
Conventional method	49.75	30	148.25
Proposed method	60	25.77	24.21

Next, having considered the arrangement of heat exchangers in the network and their cooling duties, the placement of the air-cooler is determined. In this project the air-cooler water outlet temperature is set as 30°C. Air-cooler design is performed in Aspen B-Jac® software.

Results and Discussion

By applying the steps of the targeting phase on the oil refinery (case study), the cooling water supply conditions and air-cooler performance are achieved. Figure 21.39 shows the targeting of the Water Supply Line and air-cooler water flowrate.

Table 21.26 shows a comparison between the performance parameters of the water supply for a conventional design and the proposed methodology. Table 21.27 shows a comparison between the cooling tower design parameters for the conventional and the presented methodology.

Following the water main method in the design phase, Fig. 21.40 shows the final design of the HEN with placement of an air-cooler. It is noted that the only HE requiring water at the cooling tower exit condition is HX1.

Table 21.28 shows economic comparison of the conventional design and proposed design procedure.

© Woodhead Publishing Limited, 2013

Table 21.27 Cooling tower design parameters with conventional method and proposed procedure

Design method	Heat rejection (kW)	Evaporation loss (t/h)	Cross-section area (m^2)	Tower height (m)
Conventional method	3400	4.48	15.25	4.50
Proposed method	400	1.20	4.23	1.24

Table 21.28 Economic comparison of conventional method with the proposed design procedure

Design method	Capital cost (k$/y)	Operating cost (k$/y)	Total cost (k$/y)
Conventional method	6.56	34.47	41.03
Proposed method	24.04	6.80	30.87

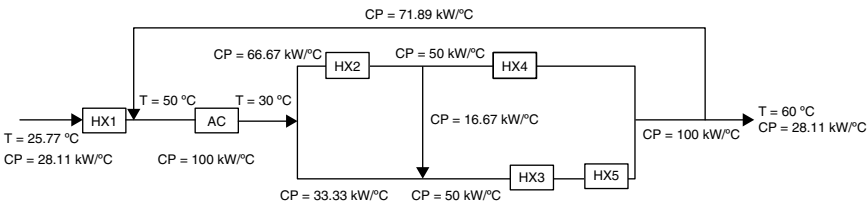

21.40 Optimum design configuration of cooling water system.

Implementing the proposed design method resulted in 84% fresh water conservation and 24% energy savings in the system relative to the conventional design method.

21.3.4 Simultaneous Energy and Water Minimisation in Multiple Contaminant Systems in a Petrochemical Plant

Process Description

Over the last decade, large-scale utilisation of water and energy resources by industries has exacerbated the imbalance between economic growth and environmental protection. Process industries and petrochemical plants, as major consumers of water and energy resources, have urged sustainable resource management strategies to minimise overexploitation and pollution. While cost-effective strategies are favoured by industries, increasing

© Woodhead Publishing Limited, 2013

environmental concerns have stimulated a strong challenge on chemical and petrochemical plants to meet environmental legislation.

In a petrochemical plant, energy is widely used to heat/cool several processes. Water streams need to be heated up or cooled down to satisfy the temperature requirements of the operations (Smith, 2005). Figure 21.41 shows a combined water and energy balance in a typical industrial plant. The energy embedded in the water system creates an inextricable interaction between the water and the energy resources in the plant. Efficient use of energy and water can improve the economic performance of system.

Having considered the interactions between the water and energy flow in the system, a methodology is implemented for simultaneous minimisation of energy and water in a petrochemical plant. Figure 21.42 shows a schematic of a plant water system. Table 21.29 shows specifications of some of the stream in water network.

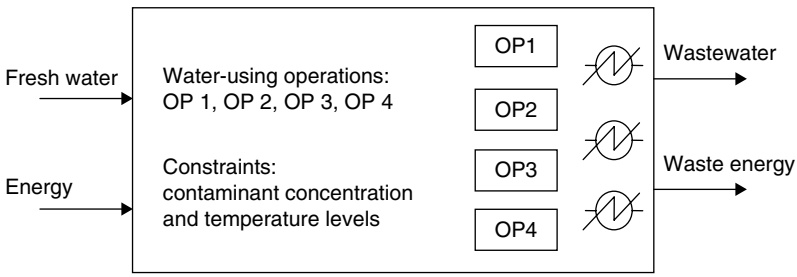

21.41 Combined water and energy balance in a typical industrial plant (Ataei *et al.*, 2009a).

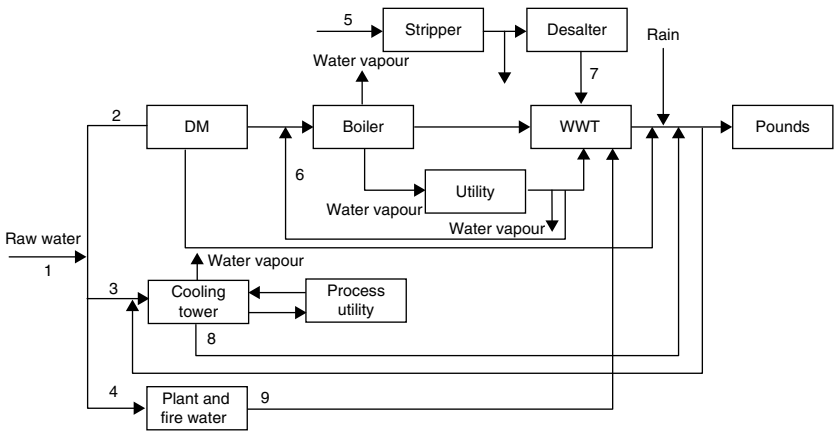

21.42 Schematic of water and wastewater system in the petrochemical plant.

© Woodhead Publishing Limited, 2013

Table 21.29 Water system specifications

ID	Flowrate (m^3/h)	PH	T. Conduct. ($\mu s/cm$)	T.H. (ppm)	M-ALK (ppm)	SiO_2 (ppm)	SS (ppm)	TSS (ppm)	T.Fe (ppm)	Cl (ppm)
1	550	7.9	360	150	140	9.3	1	2.15	<0.05	<0.05
2	224	7.9	360	150	140	9.3	1	2.15	<0.05	<0.05
3	113	7.9	360	150	140	9.3	1	2.15	<0.05	<0.05
4	168	7.9	360	150	140	9.3	1	2.15	<0.05	<0.05
5	78	9.5	14,960	10	44	6.5	348	850	<0.12	<0.05
6	59	6.5	1,600	160	40	1.4	20	25	3.12	<0.05
7	37	7.1	4,350	1,250	30	48.9	1	2.95	0.35	2.5
8	160	7.3	930	241	23	22	0	0	0	0
9	432	9.1	2.3	0	0	0	1	2	<0.05	<0.05

Table 21.30 Performance parameters of treatment unit

Treatment process	Maximum flowrate (m^3/h)	Contaminant	Removal ratio	Maximum concentration (ppm)
API AB	280	COD	0.28	350
API C		BOD	0.22	256
	76.2	Oil	0.92	1,000
		SS	0.98	500
Biological	280	Oil	0.92	12.5
		BOD	0.93	288
		COD	0.61	260
		SS	0.80	25
DAF	280	BOD	0.09	Unlimited
		COD	0.02	Unlimited
		SS	0.87	100
		Oil	0.87	100
Warm lime softener	170	TH	0.93	Unlimited
SWS	78	H_2S	0.99	7,030
		NH_3	0.98	3,374
Sanitary, Bio	16	BOD	0.95	Unlimited
		COD	0.95	Unlimited
		SS	0.95	Unlimited

As part of the water and wastewater system of the plant, Table 21.30 shows the performance parameters of the existing treatment unit.

Project Objectives

In this project, a systematic strategy is implemented on the water system of a petrochemical plant for simultaneous energy and water conservation. The proposed solution strategy comprises aspects of non-isothermal mixing point identification and separate system generation through modification of

© Woodhead Publishing Limited, 2013

the water system and the HEN accordingly (Ataei *et al.*, 2009a). Depending on the type of problem, the presented strategy can be applied to existing industrial plants to provide economic performance improvement through simultaneous energy and water conservation; it can also be used in grass-roots situations for the design of water and wastewater system, comprising multiple contaminant in water streams, to maximise energy and water conservation while minimising the total system cost. It is clear that, in retrofit situations, there can be a set of modification scenarios resulting in water and energy conservation. The final decision will then be made based on Payback Time.

Targeting

The proposed strategy is a sequential approach based on setting performance targets followed by the design phase. Targeting is performed in two steps:

Step 1: Identification of non-isothermal mixing point and setting energy targets. Non-isothermal mixing enables direct heat recovery between water streams, and therefore allows reduction of the number of heat transfer units. However, non-isothermal mixing can cause degradation of temperature driving forces and reduces the number of indirect heat transfer matches between hot and cold streams. Thus, non-isothermal mixing in a water network should be identified, ensuring that no energy penalty occurs. In this project, an NLP model is formulated to identify feasible non-isothermal mixing points, which satisfies inlet requirements of operations (temperature and contaminant concentration levels) while achieving minimum freshwater and utility requirements, creating an overall water network with less heat exchanger units (Ataei *et al.*, 2009d). Figure 21.43 shows an illustration for the identification of non-isothermal mixing points used in the model. (Ataei *et al.*, 2009a)

Step 2: Generation of separate system. This is carried out through a two stage strategy. First, the minimum water supply is targeted by plotting Composite Curve. In the second stage, the minimum number of separate

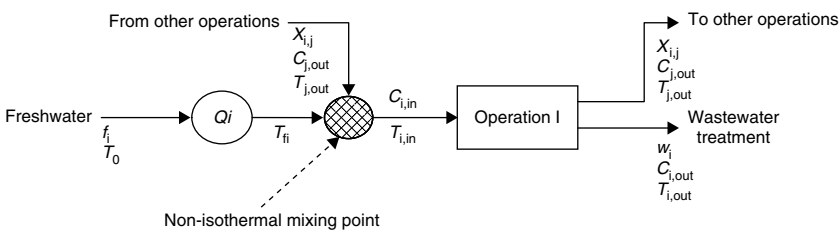

21.43 Illustration for identification of non-isothermal mixing point (Ataei *et al.*, 2009a).

© Woodhead Publishing Limited, 2013

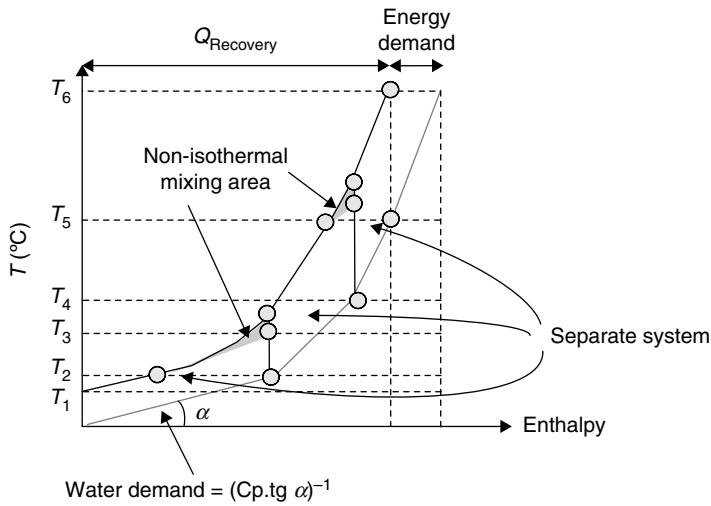

21.44 Non-isothermal mixing area and separate systems in Composite Curve.

systems is targeted by following the kink point on the Composite Curve. Figure 21.44 shows the non-isothermal mixing area and separation system.

Details of the procedure given by the author are available in Ataei *et al*. (2009a). Calculations of the targeting procedure are performed in Water and Wastewater Targeting© engineering software developed by author (Panjeshahi and Ataei, 2008).

Figure 21.45 shows a snapshot of software environment.

Design

The design phase of the proposed strategy includes determination of the water distribution between the separate systems and operations, and optimisation of the heat transfer area in the HEN. The design of the water distribution involving non-isothermal mixing of wastewater streams is carried out by balancing water and energy in the system through solving a series of mass and heat balance equations. Then the optimum heat transfer area in each separate system is achieved for minimum cost by exploring the trade-off between the capital cost of the heat exchanger and the cost penalty associated with compensation for pressure drops in the tube side and shell side in the HEN (Ataei *et al*., 2009b).

Results and Discussion

Following the solution strategy, a set of modification scenarios is suggested, to increase water and energy conservation in the petrochemical plant

© Woodhead Publishing Limited, 2013

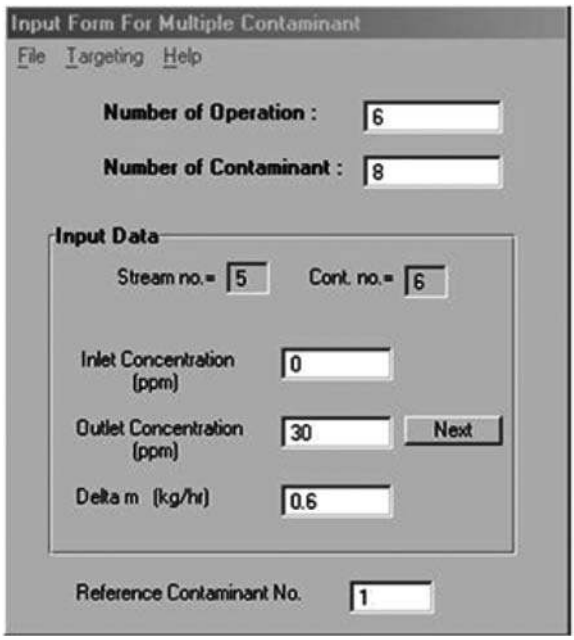

21.45 Snapshot of Water and Wastewater Targeting software (Panjeshahi and Ataei, 2008).

Table 21.31 Cost evaluation of suggested modification scenarios

Modification scenario	Water saving (%)	Total water saving (k$/y)	Capital cost (k$)	Total saving (k$/y)	Payback Time (y)
I	37.82	284.06	55	620.0	0.08
II	38.21	285.17	160	702.0	0.23
III	37.82	284.1	55	124.0	0.44
IV	38.21	285.2	160	124.0	1.29
V	37.82	108.7	55	526.4	0.1
VI	37.82	284.1	55	721.0	0.07
VII	38.21	285.2	160	721.0	0.22
VIII	37.82	284.1	55	142.0	0.38
IX	38.21	285.2	160	143.0	1.12
X	37.82	108.7	55	437.0	0.12

simultaneously. Based on the limitations of the existing system i.e. capacity of piping, treatment units and the allowable exit concentration, the potential for rearranging the network configuration is studied. Table 21.31 shows the economic evaluation of some suggested scenarios. As shown in this table, scenario VI can achieve 37.82% water conservation and 721 k$/y saving in total operating cost, which results from water and energy saving in water

© Woodhead Publishing Limited, 2013

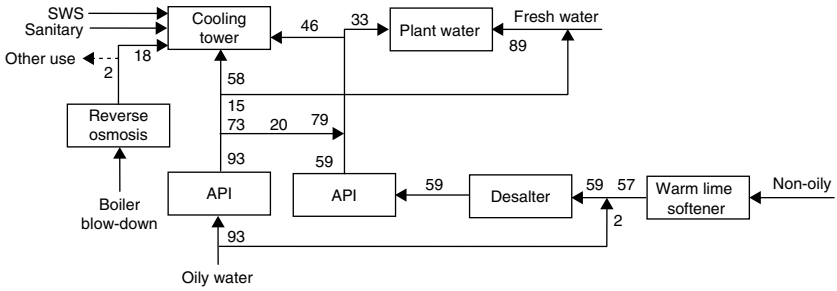

21.46 Modified configuration of water and wastewater network of the petrochemical plant.

system. Figure 21.46 shows the final modified configuration of water and wastewater system configuration (Scenario IV).

21.3.5 Concluding Remarks

PI techniques have been developed and implemented in the water system to minimise water consumption in the process plant. Moreover, technologies to increase the quality of recycling water in the system have been employed for maximisation of water reuse. In addition, a systematic design approach for the simultaneous conservation of water and energy in a process plant water system has been developed, which takes the heat loss in process units into the design method.

Having investigated water and wastewater minimisation in a process plant, the second main water-consuming component of process plants is effluent treatment networks. To achieve higher levels of water conservation potential, the effluent treatment systems needs to be designed based on water saving techniques. Therefore, in the following section, we will discuss methodologies to achieve minimum water consumption in an effluent treatment network.

21.4 Effluent Treatment and Regeneration

21.4.1 Introduction

Treatment of wastewater is required to solve effluent contamination problems to meet operational and environmental criteria. The assessment of effluent quality includes issues related to concentration of pollutants in effluent stream, chemical properties of effluent, discharge flowrate and temperature of the effluents. When solving issues of effluent thermal treatment, introduction of the cooling system is therefore necessary for effluent

© Woodhead Publishing Limited, 2013

temperature reduction. Process plant effluent systems are, generally, interconnected with wastewater producing processes and cooling system, which has both energy and water implications.

Over the last decade, PI technology has been widely expanded to address water conservation in process plants. In this regard, much attention has been put on the design of the water systems. However, little attention has been paid to the issues of design and retrofit of effluent treatment and regeneration networks. Here we present strategies for the optimum design of effluent treatment systems in grass-roots and retrofit situations, taking the operational and environmental issues of the system into account.

21.4.2 Optimum Design of Distributed Cooling Systems for Effluent Thermal Treatment in a Typical Oil Industry

Process Description

Oil industries usually produce large quantities of aqueous waste, which must be permanently removed to maintain standard operating parameters. Therefore, thermal treatment of wastewater is required to solve effluent temperature problems in order to meet environmental criteria.

In conventional, centralised thermal-treatment systems, effluent streams generated from the various processes are collected in a common sewer before being transported to the thermal-treatment unit. After collecting all effluent streams and combining them into a single effluent, the effluent stream generated is likely to have a lower energy level (Kim *et al.*, 2001). Therefore, central cooling system need to remove the heat from the effluent streams with a lower temperature and a higher flowrate relative to the cooling system have placed on the higher temperature effluents before mixing. Because a centralised cooling policy cannot avoid the degradation caused by mixing effluents with low temperatures, a distributed cooling policy for cooling system is proposed and implemented in this project (Ataei *et al.*, 2009d).

Consider the water-using operation in an oil refinery. Several processes streams are contacted with water to reduce temperature and the level of a contaminant in the process streams. The water in turn becomes contaminated with particles and heat. The contaminated water, for instance, could be the wastewater from petroleum refinery unit operations or from the utility system. This is a common example of a wastewater system in a refinery complex. Table 21.32 shows some of the selected data from a typical refinery effluent system. The wastewater is first treated to remove the chemical contaminant. We will not address the chemical treatment for single or multiple contaminant problems until later. The second stage is the thermal treatment of effluents.

© Woodhead Publishing Limited, 2013

Table 21.32 Effluent stream data

Effluent	Flowrate (kg/s)	Temperature (°C)
1	83.33	60
2	83.33	45
3	111.11	32

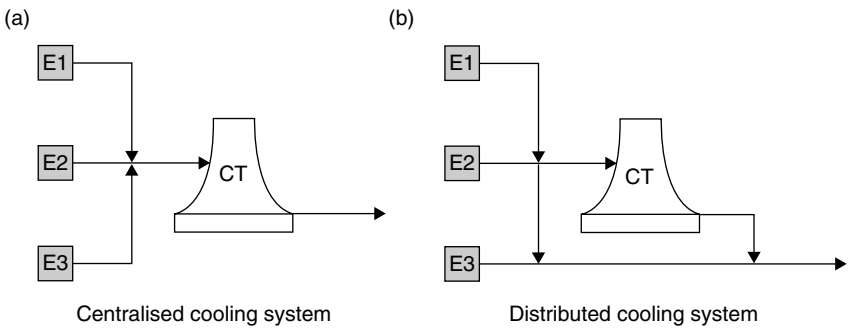

21.47 Schematic of effluent cooling system (Ataei *et al.*, 2009d)

Figures 21.47a and 21.47b shows schematics of centralised and distributed effluent cooling system. As shown in Fig. 21.47a, in centralised cooling system effluent streams are totally combined to be transported to cooling tower. In distributed cooling systems, effluent stream are segregated and combined if appropriate, prior to treatment (Fig. 21.47b).

Project Objectives

The objective of this project is to implement a systematic design procedure in an oil refinery, for optimum design of an effluent cooling system to achieve minimum total cost.

Targeting

The methodology, Optimum Design of Effluent Cooling System (ODEC) which is applied in this work is based on targeting ahead of design. The targeting stage of this project includes three steps:

Step 1: Construction of the Effluent Composite Curve. The disposable heat to be removed by cooling each effluent stream is calculated by specifying the environmental discharge temperature (Ataei *et al.*, 2009d). The individual profiles are plotted on a graph of temperature vs disposable heat, as shown in Fig. 21.48a. The Composite Curve is constructed by combining all

© Woodhead Publishing Limited, 2013

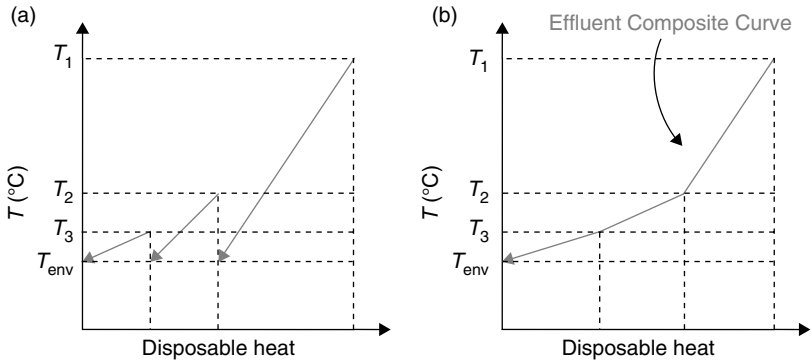

21.48 Construction of the Effluent Profile Composite Curve (Ataei *et al.*, 2009d).

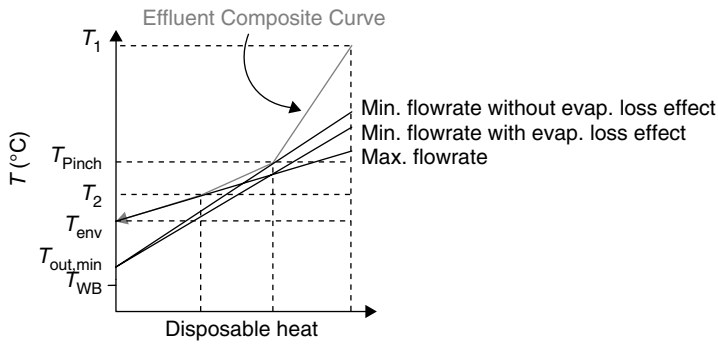

21.49 Feasible boundaries for the distributed cooling system (Ataei *et al.*, 2009d).

the individual profiles into a single curve within the temperature intervals (Fig. 21.48b).

Step 2: Generation of feasible region. To generate the feasible region, the upper and lower limits of the inlet effluent flowrates and temperatures to the cooling tower are specified (Fig. 21.49).

Step 3: In the third step, the optimum inlet effluent flowrate to the cooling tower is targeted by exploring the feasible region for minimum total cost. For targeting the minimum effluent flowrate, the evaporation-loss effect of the cooling tower is examined (Ataei *et al.*, 2009b).

Design

The design stage includes the final design of the effluent cooling network and the design of the cooling tower for minimum cost. The final design of

© Woodhead Publishing Limited, 2013

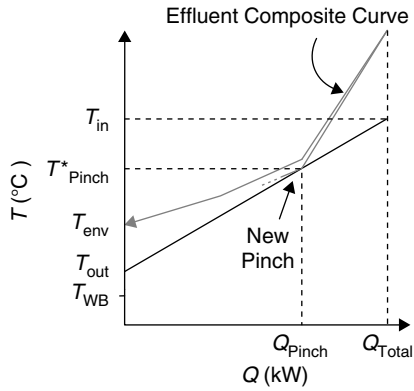

21.50 Creating a Migrated Pinch Point (Ataei *et al.*, 2009b).

the effluent cooling network is carried out based on design grouping rules to achieve the targets. Having considered the minimum effluent flowrate, because the effluent supply line does not create a Pinch Point with the The Effluent Composite Curve needs to be modified. To create a new Pinch Point with the targeted effluent supply line, the concept of Pinch Migration is applied (Figure 21.50).

After finding the new Pinch Point, the segregation of the effluent streams is then performed based on the modified design grouping rules. The effluent streams with starting temperature located above the Migrated Pinch (Group I) pass through the thermal-treatment process totally. The effluent streams located at the Migrated Pinch (Group II) are partially treated. The effluent streams located below the Migrated Pinch (Group III) totally bypass the thermal-treatment process (Ataei *et al.*, 2009c).

To achieve the optimum cooling tower design, an iterative calculation is performed. The computation procedure is presented in Fig. 21.51 (Ataei *et al.*, 2009c).

Results and Discussion

Following the targeting steps, the optimum cooling tower supply line is achieved by exploring the feasible region (Table 21.33). Figure 21.52 shows the final design of the optimum effluent thermal-treatment network.

Figure 21.53 illustrates the effect of the water flowrate on the capital and operation costs of the distributed cooling system. The results reveal that an increase in the water flowrate reduces the cooling tower capital costs, whereas the operating costs increase. Therefore, a trade-off between the capital costs and the energy costs has been introduced.

© Woodhead Publishing Limited, 2013

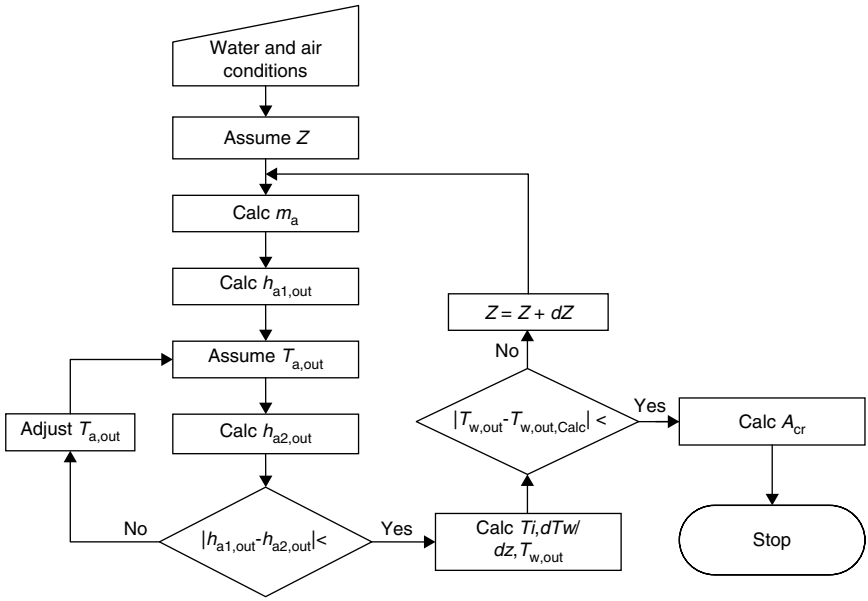

21.51 Flowchart of optimum cooling tower design (Ataei *et al.*, 2009c).

Table 21.33 Feasible boundary water supply conditions

Effluent condition	Flowrate (kg/s)	Inlet temperature (°C)	Outlet temperature (°C)
Minimum flowrate	137.61	53.74	25
Maximum flowrate	277.77	44.31	30

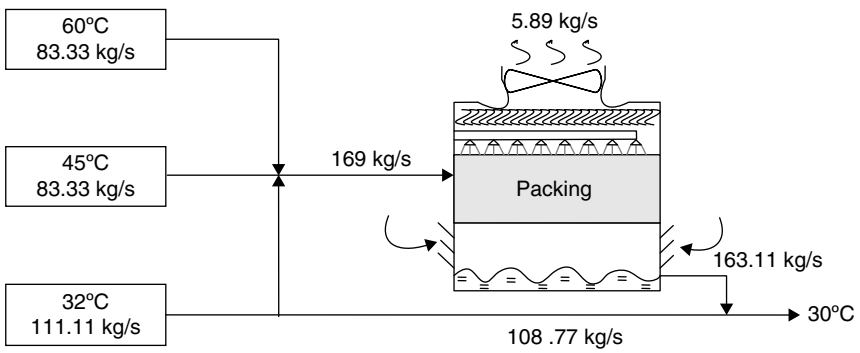

21.52 Optimum effluent network of the ODEC.

© Woodhead Publishing Limited, 2013

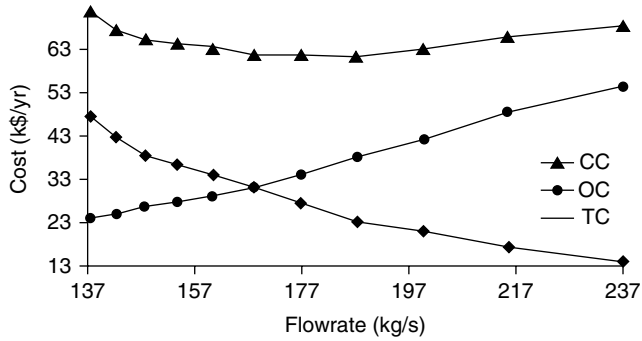

21.53 Overall cost of the distributed cooling system.

Table 21.34 Water supply conditions with conventional and ODEC design methods

Design method	Flowrate (kg/s)	Inlet temperature (°C)	Outlet temperature (°C)
Conventional	277.77	44.31	30
ODEC	169.00	51.07	27.55

Table 21.35 Cost comparison of conventional design method and ODEC

Design method	Operating cost (k$/y)	Capital cost (k$/y)	Total cost (k$/y)
Conventional	45.52	41.79	87.31
ODEC	31.51	30.31	61.82

The optimum water flowrate is achieved by exploiting this trade-off. The optimum cooling line, which is located between the maximum and minimum flowrates, achieves the minimum total costs. Table 21.34 shows a comparison of the water supply conditions of the proposed procedure and the conventional design method (centralised cooling system).

The cost comparison for the cooling tower design between the conventional and the proposed method indicates 30% improvement in the total costs (Table 21.35).

The cooling tower design parameters for the proposed design method and the conventional design (centralised cooling system) method are given in Table 21.36.

Applying the proposed design procedure, the evaporative loss is reduced by the distributed design for the effluent network. This provides greater

© Woodhead Publishing Limited, 2013

Table 21.36 Cooling tower design parameters for the ODEC and the conventional design method

Design method	Q_{rej} (KW)	W (m)	Z (m)	A_{cr} (m^2)
Conventional	17,150	10.82	5.61	60.7
ODEC	17,150	9.7	4.65	45.11

Table 21.37 Water conservation opportunity with the ODEC

Design method	Evaporative loss (kg/s)	Water saving (%)
Conventional	7.79	–
ODEC	5.89	24

opportunities for water conservation compared with those of the conventional design method. Table 21.37 shows the water conservation opportunity achieved though the proposed design approach.

21.4.3 Debottlenecking of an Effluent Thermal-Treatment System in a Petrochemical Plant

Process Description

While chemical, physical or biological treatment processes can be used for controlling the chemical pollution problems of effluents, a thermal-treatment system is required for effluent temperature reduction problems where the temperature of the effluent streams is too high to be discharged directly into the receiving water.

A typical effluent system in a petrochemical plant incorporates wastewater producing processes and a cooling system, which interact with each other through water and energy flow. Consider some of the possible changes to an existing effluent system. For example, a new wastewater stream might be introduced into an existing system, or the heat duty of the wastewater stream changed, or a process change might change the operating conditions (Kim *et al*., 2001). These process changes influence the thermal-treatment performance and consequently affect the conditions of the discharge stream into the environment. In such situations, to overcome the bottlenecked effluent cooling system, a combined water and energy analysis procedure is required (Panjeshahi *et al*., 2010b).

Here we will present a systematic solution implemented for debottlenecking the effluent thermal-treatment system in a typical petrochemical complex. In this project a new Effluent Collection Point (ECP) is introduced

© Woodhead Publishing Limited, 2013

Table 21.38 Effluent stream data

ECP	Description	Flowrate (kg/s)	Temperature (°C)
ECP 1	Existing	83.33	60
ECP 2	Existing	83.33	45
ECP 3	Existing	111.11	32
ECP 4	New	58.33	47.5

Table 21.39 Performance conditions of effluent cooling system

Case	Inlet water temperature (°C)	Inlet water flowrate (kg/s)	Heat load (MW)
System with three ECPs	44.2	277.7	16.47
Base case (including new ECP)	44.7	336.1	20.8
Change percentage (%)	1.1	20.9	26.3

into the existing effluent cooling system, which bottlenecks the thermal-treatment process. Table 21.38 shows some of the ECP data, including the new wastewater stream. The environmental temperature discharge limit is 30°C. The operating performance conditions of the effluent cooling system with the new ECP are given in Table 21.39. As shown in Table 21.39, the discharge effluent temperature is hotter than the desired environmental temperature limit. This means additional cooling equipment needs to be installed to cool the effluent to meet environmental criteria. Then the heat load of the treatment network (20.8 MW) is bigger than the heat removal of the tower (16.47 MW), which also means 4.33 MW of heat load needs to be dissipated by additional cooling. Figure 21.54 shows the base case configuration of effluent thermal treatment in a typical petrochemical plant.

Project Objectives

In this project, a methodological solution strategy to overcoming the bottlenecks in the effluent cooling system of a petrochemical plant is implemented. An attempt is made to solve the problem through feasibility analysis of the cooling system with respect to the effluent network while keeping the costs of debottlenecking as low as possible.

Targeting

The proposed solution strategy is based on targeting prior to design. The overall computational procedure of the proposed procedure is outlined in Fig. 21.55. As shown in this figure, the targeting procedure applied to this project is carried out in three main steps (Panjeshahi *et al.*, 2010b).

© Woodhead Publishing Limited, 2013

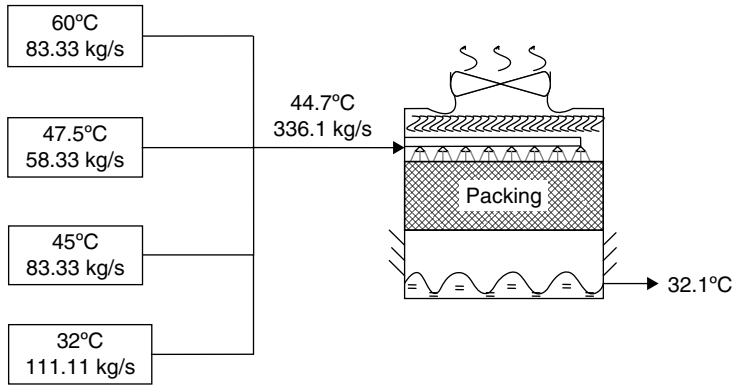

21.54 Base case of effluent thermal-treatment network.

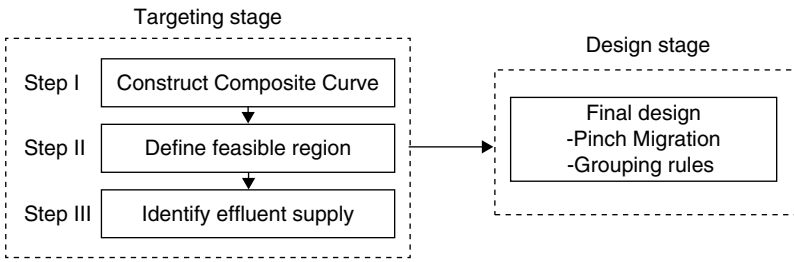

21.55 Overall solution strategy flow chart.

Step 1: Construction of the Effluent Composite Curve. To construct the Effluent Composite Curve, the disposable heat to be removed by cooling for each effluent stream is first calculated (Panjeshahi *et al.*, 2010b). The heat load requirement of each individual stream is graphically represented on a plot of temperature vs disposable heat as shown in Fig. 21.56a. All the individual profiles are then combined into single Composite Curve by summing the individual heat loads within the same temperature intervals (Fig. 21.56b) (Panjeshahi *et al.*, 2010b).

Step 2: To define the feasible region of the effluent network by highlighting the system boundaries. The effluent network configuration and performance can be changed within the feasible region. The feasible region is bounded by the maximum flowrate (B) and the minimum flowrate (A) of the effluent supply to the cooling tower (Figs 21.57a and 21.57b). The heat load of the Cooling Water Supply Line needs to be removed through the effluent cooling system (Figs 21.57a). The heat removal of cooling system increases as the configuration changes from full centralised to maximum distributed (Min. flowrate 5 b).The targeting procedure of the debottlenecking procedure incorporates the evaporation effect. In Fig. 21.57b, the

© Woodhead Publishing Limited, 2013

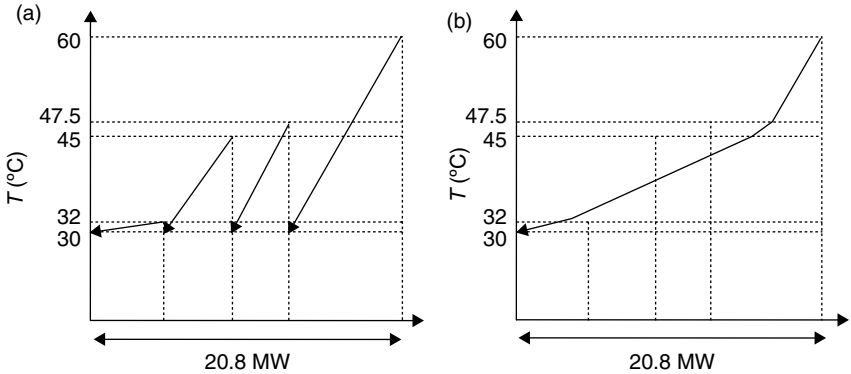

21.56 Construction of the Effluent Profile Composite Curve (Panjeshahi *et al.*, 2010b).

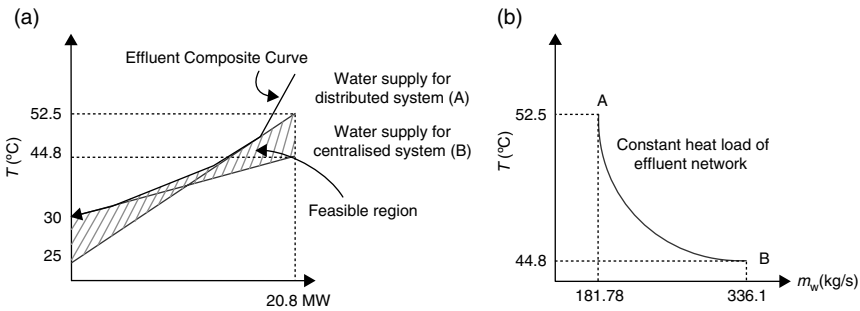

21.57 Feasible region for Feasible Water Supply Line (Panjeshahi *et al.*, 2010b).

line AB represents the attainable conditions from the cooling tower model by changing the effluent network configurations from centralised to distributed arrangement. It has been noted that the inlet conditions to the cooling tower affect the cooling performance (Panjeshahi *et al.*, 2010b).

Step 3: Targeting the cooling tower supply. The feasible Cooling Water Supply Line can move from C to D (Fig. 21.58). The target conditions, which satisfy the desired discharge temperature, are found by changing the cooling water supply conditions from C to D. Calculation of the cooling tower performance is carried out through a simulation model (Ataei *et al.*, 2009c).

The heat removal of the cooling system is the same as the heat load of the effluent streams entering the tower, where the discharge limit temperature of effluent network is satisfied. Target conditions are achieved from the intersection between the feasible Water Supply Line and the cooling tower line.

© Woodhead Publishing Limited, 2013

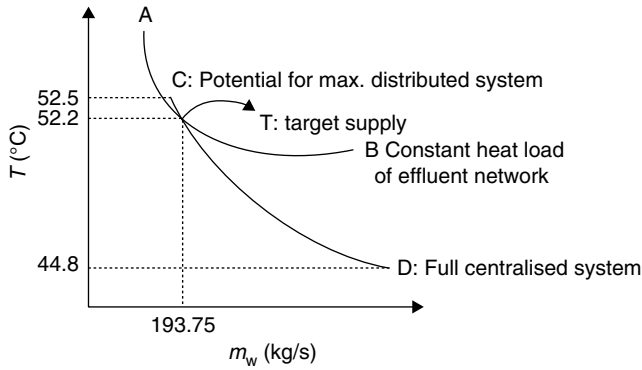

21.58 Targeting cooling tower inlet supply condition (Panjeshahi *et al.*, 2010b).

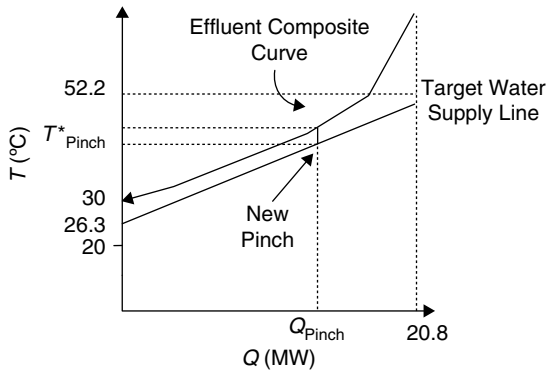

21.59 New Pinch Point of Target Water Supply Line (Panjeshahi *et al.*, 2010b).

Design

The aim of the design stage of the proposed solution is to modify the existing configuration of the effluent system through the Pinch Migration concept and applying the design grouping rules. The grouping rule is based on the concept of the Pinch Technology, and cannot be applied to problems without Pinch. It has been noted that any cooling water line at or below the Composite Curve profile is considered to be a feasible design. As shown in Fig. 21.59, because the new Water Supply Line creates no Pinch with the Effluent Composite Curve. The Effluent Composite Curve should be modified to make the Pinch Point with the targeted Water Supply Line within the feasible region. To modify the Composite Curve, Pinch Migration is applied on the basis of temperature shifting (Fig. 21.60) (Panjeshahi *et al.*, 2010b).

© Woodhead Publishing Limited, 2013

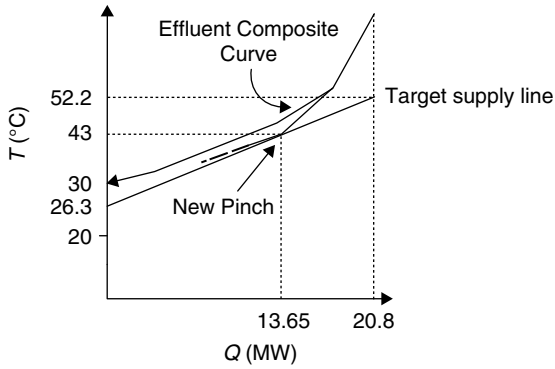

21.60 Effluent Composite Curve modification (Panjeshahi *et al.*, 2010b).

The new Pinch Point can be calculated through Equation [21.3] (Panjeshahi *et al.*, 2010b). Figure 21.60 shows the new Pinch Point.

$$T^{*}_{\text{Pinch}} = \left[\frac{(T_{\text{in}} - T_{\text{out}})}{Q_{\text{Total}}} \times Q_{\text{Pinch}}\right] + T_{\text{out}} \qquad [21.3]$$

The final stage of design is to modify the configuration of the existing effluent cooling system based on the design grouping rules (Panjeshahi *et al.*, 2010b).

Results and Discussion

Having applied the aforementioned targeting steps, the feasible new water supply to cooling system is achieved (Table 21.40). The final design of the debottlenecked effluent cooling system is presented in Fig. 21.61.

Table 21.41 shows the economic comparison between the implemented solution strategy and the base case. It was revealed that if the centralised design were adopted for the thermal treatment (base case), the additional cooling cost (including both capital and operational costs) would be 21.24 k$/y. While the proposed design strategy requires additional pipes, with their associated piping cost (Alva-Argaez, 1999) for splitting the effluent streams, this resulted in a 61% cost reduction compared to the base case.

Concluding Remarks

In this section, having considered the water and energy implications of the effluent treatment network on a water system, two design approaches were

© Woodhead Publishing Limited, 2013

Table 21.40 Targeted water supply of cooling tower

State	T_{in} (°C)	T_{out} (°C)	m_w (kg/s)	Q (MW)
Feasible water supply	52.2	26.3	193.75	20.8

Table 21.41 Economic comparison of the base case and proposed strategy

Solution strategy	Total cost (k$/y)	Cost reduction
Base case	21.24	–
Proposed strategy	8.3	61%

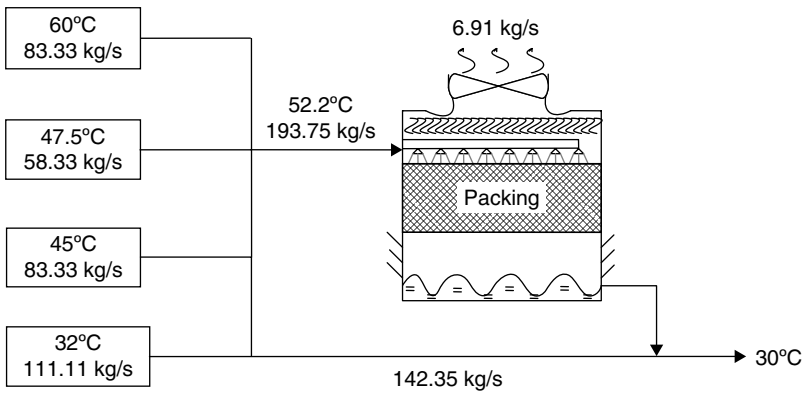

21.61 Final design of effluent cooling system.

introduced. The first approach helps grass-roots design of effluent treatment system for minimum water and energy consumption. The second approach provides a debottlenecking solution strategy for existing effluent networks in case of changes in operational conditions. The proposed methods have been applied to real-life case studies, and the results have proven the effective and successful application of both approaches.

21.5 Conclusion

In this chapter, we have discussed the rationale for the application of PI in oil refining and petrochemical industries. A number of recently developed methodologies in PI have been applied to some industrial case studies to demonstrate the applicability of the developed techniques for energy

© Woodhead Publishing Limited, 2013

and water conservation in process plants. Some of the major outcomes are summarised as follows:

- Conceptual methods of PI, based on Pinch Technology, help to develop insight.
- While mathematical methods provide optimal solutions for energy conservation, combined exergy and Pinch Analysis helps obtaining near-optimal solutions for Heat Integration in HENs with better, and in-depth, understanding of the problem.
- Applying the presented design method of MSHE provides a 10% total costs saving compared to the conventional methods.
- Integration of ozone treatment technology into refinery water and wastewater system, together with the application of Water Pinch techniques, could bring about 30% savings in fresh water consumption and a considerable amount of energy savings in the water and wastewater system of the refinery plant.
- Employing the water system optimum design procedure may provide up to 25% total costs reduction compared to the current conventional design methods.
- Following the retrofit procedure for simultaneous water and energy conservation in the petrochemical plant water system provides a set of modification options that obtain approximately 40% water conservations, while the payback period of the retrofit modification project is around 1 year.
- Having compared the conventional effluent system design method through the proposed optimum effluent system design of a typical oil refinery, one can conclude that 30% total costs reduction and 25% water savings are achievable goals.
- When debottlenecking an effluent thermal-treatment system, it is important to manage the retrofit modification strategy to avoid unnecessary expenses. Application of the proposed method for debottlenecking the effluent thermal-treatment system results in a 60% reduction in system cost.

Although classical, conventional approaches to energy and water conservation usually focus on improving the energy efficiency of the individual process units, the aforementioned results, obtained through applying the proposed approaches of PI, show that the optimal integration of water and energy flow with respect to interactions between site components results in more efficient plants. Moreover, the outcomes have demonstrated that the proposed Water and Energy Integration methodologies are cost-effective, easy-to-apply and efficient in providing water and energy conservation.

© Woodhead Publishing Limited, 2013

21.6 Sources of Further Information

Since the advent of Process Integration, several methodologies and tools have been presented and implemented in process industries to achieve conservation of energy and material consumption and increase process productivity. Although in this chapter we have presented some of these tools, several applicable methods have been developed by other researchers to increase process energy efficiency and profitability. Some of these recently developed design methods, for the presented categories in this chapter, are as below.

Heat and Power Integration

1. Beith, R. (ed.) (2011). *Small and Micro Combined Heat and Power (CHP) Systems, Advanced Design, Performance, Materials and Applications.* Woodhead Publishing Limited, Cambridge, UK.
2. Klemeš, J. J., Friedler F, Bulatov I., Varbanov P. (2010). *Sustainability in the Process Industry – Integration and Optimization.* McGraw-Hill, New York, USA.
3. Klemeš, J. J., Perry, S. (2008). Energy efficiency and carbon footprint reduction. In: Pistikopoulos, E., Georgiadis, M. and Kikkinides, E. S. (eds), *Process Systems Engineering*, Vol. 5, Energy Systems Engineering. Wiley-VCH Verlag GmbH & Co. KGaA, Weinheim, Germany.
4. Milosevic, Z., Eastwood, A. (2010). *Heat Integration and Pinch Analysis in Managing CO Emissions in the Chemical Industry.* Wiley-VCH Verlag GmbH & Co. KGaA, Weinheim, Germany.
5. Klemeš, J. J., Varbanov, P., Lam, H. L. (2009). Water footprint, water recycling and food industry supply chain. In: Waldron, K. (ed.), *Waste Management and Co-product Recovery in Food Processing.* Woodhead Publishing Limited, Cambridge, UK.
6. Klemeš, J., Smith, R., Kim, J.-K. (eds) (2008). *Handbook of Water and Energy Management in Food Processing.* Woodhead Publishing Limited, Cambridge, UK.
7. Klemeš, J., Perry S. J. (2008). Methods to minimise energy use in food processing. In: Klemeš, J., Smith, R.and Kim, J.K. (eds), *Handbook of Water and Energy Management in Food Processing.* Woodhead Publishing Limited, Cambridge, UK.
8. Lin, S., Lee, C. (2007). *Water and Wastewater Calculations Manual*, 2nd ed. Mc-Graw Hill, New York, USA.
9. Urbaniec, K., Klemeš, J. (2008). Water and energy management in the sugar industry. In: Klemeš, J., Smith, R. and Kim, J. K. (eds), *Handbook of Water and Energy Management in Food Processing.* Woodhead Publishing Limited, Cambridge, UK.

© Woodhead Publishing Limited, 2013

Effluent Treatment and Regeneration

10. Man, J., Liu, Y. A. (1999). *Industrial Water Reuse and Wastewater Minimization.* McGraw-Hill Professional, New York USA.
11. Klemeš, J. J., Bulatov, I. (2010). Editorial special issue, *Clean Technologies and Environmental Policy*, **12**, 585–586.
12. Klemeš, J. J., Stehlík, P., Worrell, E. (2010). Waste treatment to improve recycling and minimise environmental impact. *Resources, Conservation and Recycling*, **54**, 267–270.
13. Tchobanoglous, G., Burton, F. L., Stensel, H. D. (2002). *Wastewater Engineering, Treatment and Reuse.* Mc-Graw Hill, New York, USA.

21.7 References

Alva-Argaez, A. (1999). Integrated design of water systems. PhD Thesis, UMIST, Manchester, UK.

Asante, N. D. K., Zhu, X. X. (1997). An automated and interactive approach for heat exchanger network retrofit. *Chemical Engineering Research and Design*, **75**, 349–360.

ASPEN BJac Software, version 10.2. (2006).

Ataei, A., Gharaie, M., Parand, R., Panjeshahi, E. (2010). Application of ozone treatment and pinch technology in cooling water systems design for water and energy conservation. *International Journal of Energy Research*, **34**, 494–506.

Ataei, A., Panjeshahi, M. H., Gharaie, M. (2009a). New method for industrial water reuse and energy minimization. *International Journal of Environmental Research*, **3**, 289–300.

Ataei, A., Panjeshahi, M. H., Gharaie, M., Tahouni, N. (2009b). New method for designing an optimum distributed cooling system for effluent thermal treatment. *International Journal of Environmental Research*, **3**, 155–166.

Ataei, A., Panjeshahi, M. H., Gharaie, M. (2009c). A new algorithm for optimum design of mechanical draft wet cooling towers. *Journal of Applied Science*, **9**, 561–566.

Ataei, A., Panjeshahi, M. H., Karbassian, S. (2009d). Simultanuous energy and water minimization – approach for systems with optimum regeneration of wastewater. *Research Journal of Environmental Sciences*, **3**, 604–618.

Ataei, A., Panjeshahi, M. H., Parand, R., Tahouni, N. (2009e). Application of an optimum design of cooling water system by regeneration concept and pinch technology for water and energy conservation. *Journal of Applied Science*, **9**, 1847–1858.

Bausa, J., Watzdorf, R. V. (1996). Minimum energy demands for non-ideal multi-component distillations in complex columns. *Computers & Chemical Engineering*, **20**, S55–S60.

Calrberg, N. A., Westerberg, A. W. (1989). Temperature heat diagrams for complex columns 2, underwood's method for side strippers and enriches. *Industrial & Engineering Chemistry Research*, **28**, 1379–1386.

COLOM Software, Version 2.1 (2007). Department of Process Integration, The , Manchester, UK.

© Woodhead Publishing Limited, 2013

Dhole, V. R., Linnhoff, B. (1992). Total site targets for fuel, co-generation, emissions and cooling. *Computers & Chemical Engineering*, **17**, 101–109.

Farry, M. (1998). Ethane from associated gas still the most economical. *Oil & Gas Journal*, **96**, 23.

Feng, X., Pu, J., Yang, J., Chu, K. H. (2011). Energy recovery in petrochemical complexes through heat integration retrofit analysis. *Applied Energy*, **88**, 1965–1982.

Gharaie, M., Jobson, M., Panjeshahi, M. H., Zhang, N. (2012). Energy management strategies for process site co_2 emissions reduction. Proceedings of the 22nd European Symposium on Computer Aided Process Engineering (ESCAPE), London, UK, pp. 352–356.

Gharaie, M., Kim, J. K., Panjeshahi, M. H., Smith, R. (2011). Retrofit design method for CO_2 emission reduction. Proceedings of the IASTED International Conference Environmental Management and Engineering (EME), Calgary, Canada, pp. 133–138.

Joda, F., Polley, G. T., Tahouni, N., Panjeshahi, M. H. (2011). Improving multi-stream heat exchanger design by reducing the number of sections. Proceedings of the 4th International Conference on Modelling, Simulation and Applied Optimization (ICMSAO), IEEE, Malaysia, Kuala Lumpur, pp. 1–5.

Kays, W. M., London, A. L. (1984). *Compact Heat Exchangers*, 3rd ed.. Mc-Graw Hill, New York, USA.

Kennedy, J., Eberhart, R. (2001). *Swarm Intelligence.* Academic Press, London, UK.

Kim, J. K., Savulescu, L., Smith, R. (2001). Design of cooling systems for effluent temperature reduction. *Chemical Engineering Science*, **56**, 1811–1830.

Kim, J. K., Smith, R. (2001). Cooling water system design. *Chemical Engineering Science*, **56**, 3641–3658.

Kim, J. K., Smith, R. (2002). Process integration for aqueous emissions reduction. *Theo. Appl. Chem. Eng.*, **8**, 10–13.

Panjeshahi, M. H. (1992). Pressure drop consideration in process integration. PhD thesis, UMIST, Manchester, UK.

Panjeshahi, M. H., Ataei, A. (2008). Water and wastewater targeting software. Tehran, Iran.

Panjeshahi, M. H., Ataei, A., Gharaie, M. (2010a). A comprehensive approach to an optimum design and simulation model of a mechanical draft wet cooling tower. *Iranian Journal of Chemical Engineering*, **29**, 21–32.

Panjeshahi, M. H., Ataei, A., Gharaie, M., Parand, R. (2009). Optimum design of cooling water systems for energy and water conservation. *Chemical Engineering Research and Design*, **87**, 200–209.

Panjeshahi, M. H., Gharaie, M. Ataei, A. (2010b). Debottlenecking procedure of effluent thermal treatment system. *Energy*, **35**, 5202–5208.

Panjeshahi, M. H., Ghasemian Langeroudi, E., Tahouni, N. (2008). Retrofit of ammonia plant for improving energy efficiency. *Energy*, **33**, 46–64.

Panjeshahi, M. H., Joda, F., Tahouni, N. (2010c). Pressure drop optimization in multi-stream heat exchanger networks using genetic algorithm. *Chemical Engineering Transactions*, **21**, 247–252.

Panjeshahi, M. H., Nouzari, M. M. (2001). Retrofit of heat exchanger networks considering existing structure, a new targeting procedure. *Iranian Journal of Chemical Engineering*, **20**, 44–52.

© Woodhead Publishing Limited, 2013

Piacentino, A. (2011). Thermal analysis and new insights to support decision making in retrofit and relaxation of heat exchanger networks. *Applied Thermal Engineering*, 31, 3479–3499.

Picon-Nunez, M., Polley, G. T., Medina-Flores, M. (2002). Thermal design of multistream heat exchangers. *Applied Thermal Engineering*, **22**, 1643–1660.

Polley, G. T., Panjeshahi, M. H., Jegede, F. O. (1990). Pressure drop considerations in the retrofit of heat exchanger networks. *Transactions of IChemE*, **68A**, 211–220.

Prasad, B. S. V. (1996). The sizing and passage arrangement of multi-stream plate-fin heat exchangers. *Heat Transfer Engineering*, **17**, 35–43.

Silva, A. P., Ravangnani, M. A. S. S., Jr E. C. B. (2009). Particle swarm optimization applied in retrofit of heat exchanger networks. *Computer Aided Chemical Engineering*, **27**, 1035–1040.

Smith, R. (2005). *Chemical Process Design and Integration.* John Wiley & Sons Ltd, West Sussex, UK.

Smith, R., Jobson, M., Chen, L. (2010). Recent development in the retrofit of heat exchanger networks. *Applied Thermal Engineering*, **30**, 2281–2289.

SPRINT Software, Version 2.5.1 (2011). Centre for Process Integration, The , Manchester, UK.

Tahouni, N., Panjeshahi, M. H., Ataei, A. (2011). Comparison of sequential and simultaneous design and optimization in low-temperature liquefaction and gas separation processes. *Journal of the Franklin Institute.*, **348**, 1456–1469.

Tahouni, N., Smith, R., Panjeshahi, M. H. (2010). Comparison of stochastic methods with respect to performance and reliability in low temperature gas separation processes. *Canadian Journal of Chemical Engineering*, **88**, 256–267.

Wang, J., Smith, R. (2005). Synthesis and optimization of low temperature gas separation processes. *Industrial & Engineering Chemistry Research*, **44**, 2856–2870.

Wang, Y. P., Smith, R. (1994). Wastewater minimisation. *Chemical Engineering Science*, **49**, 981–1006.

Xiangkun, M., Pingjing, Y., Xing, L., Roetzel, W. (2008). Synthesis of multi-stream heat exchanger network for multi-period operation with genetic/simulated annealing algorithms. *Applied Thermal Engineering*, **28**, 809–823.

Yee, T. F., Grossmann, I. E. (1991). A screening and optimization approach for the retrofit of heat-exchanger networks. *Industrial & Engineering Chemistry Research*, **30**, 146–162.

© Woodhead Publishing Limited, 2013

22

Process Integration of an Oil Refinery Hydrogen Network

NAN ZHANG, Process Integration Limited Manchester, UK

DOI: 10.1533/9780857097255.5.705

Abstract: This chapter discusses the development and applications of Process Integration technologies for refinery hydrogen management since the late 1990s. Both targeting and design methods are reviewed. A case study is used to illustrate the importance of incorporating targeting with detailed mathematical programming for effective industrial applications.

Key words: refinery hydrogen management, Process Integration, targeting, mathematical programming, case study.

22.1 Introduction

Hydrogen is an important resource in oil refineries. It is required not only for removing contaminants, such as sulphur and nitrogen, in various hydrotreating operations, but also for breaking down large hydrocarbon molecules to form lighter and more valuable molecules in gasoline and diesel ranges. Three global trends are happening to the oil refining industry (Swain, 1998): crude oil processed in oil refineries is becoming heavier; demand for light fuels, such as gasoline, diesel and jet fuel, is increasing; and environmental concerns are leading to tighter fuel specifications. These trends have resulted in a significantly increased demand for hydrogen, while the supply of hydrogen is under pressure. Therefore, hydrogen supply becomes one of the focal points in the oil refining industry, leading to wide interest and investigation in technologies for refinery hydrogen management.

Refinery hydrogen management is a typical network problem, in which hydrogen suppliers (hydrogen sources) need to be matched with hydrogen users (hydrogen sinks). A typical hydrogen network is illustrated in Fig. 22.1. Each block in the flow diagram represents a complex process unit, either producing hydrogen or consuming hydrogen, or doing both at the same time.

A typical hydrogen consumer, including a hydrotreating reactor and a separator, can be simplified as shown in Fig. 22.2. Hydrogen is used to react with liquid hydrocarbon. The partial pressure in the reactor is a very

© Woodhead Publishing Limited, 2013

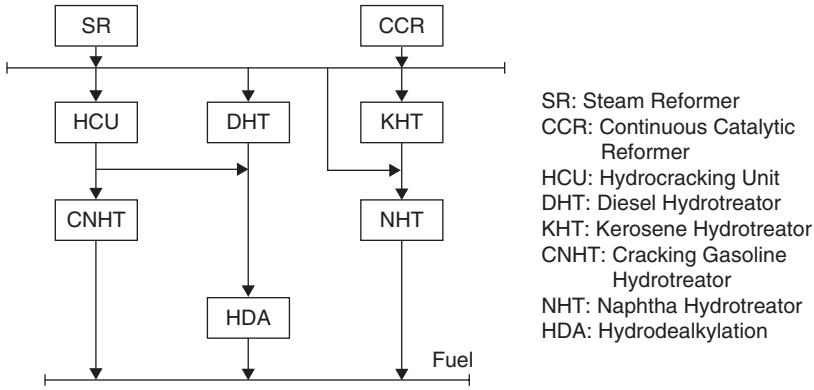

22.1 A refinery hydrogen network.

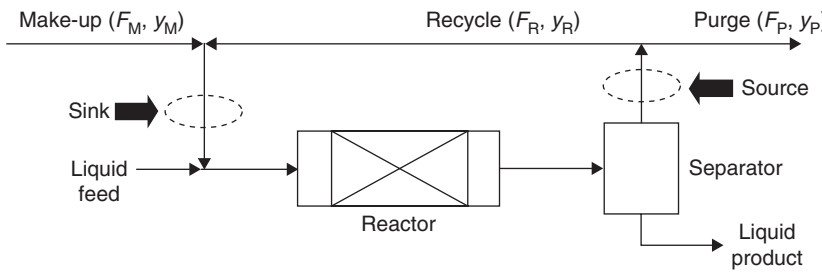

22.2 Simplified diagram of a hydrogen consumer with source and sink locations (Alves, 1999).

important parameter in the reaction. In typical hydrogen management exercises, the partial pressure of hydrogen is assumed to be constant, as well as other parameters such as operating temperature, reactor feedstock, products, etc. Under these assumptions, a constant flowrate and hydrogen purity is imposed on the reactor gas inlet stream. Therefore, if the operating conditions do not change, the inlet of the reactor and the outlet of the separator will be fixed. Thus, as pointed out by Alves (1999), the mixture of the makeup hydrogen and the recycle is defined as the sink, and the mixture of the purge and the recycle is defined as the source (Fig. 22.2).

Similar to problems of Energy Integration and water management, this problem naturally fits into the technical area of Process Integration.

22.2 Technology Review

Since the late 1990s, extensive research activity on refinery hydrogen management has been published in the academic world. The developed

© Woodhead Publishing Limited, 2013

technologies can be distinguished in two main categories, which will be discussed in detail in the subsequent sections:

- Targeting for minimum hydrogen utility;
- Mathematical programming for detailed design and retrofit.

22.2.1 Targeting for Minimum Hydrogen Utility

Targeting methods are typically represented by the approach of Hydrogen Pinch Analysis, a graphical approach first proposed by Alves in 1999. It is a simple yet very effective approach for deciding the minimum hydrogen utility before design or retrofit. Therefore, it is worth going through the basics of this Hydrogen Pinch Analysis.

The mass balance of each sink and source in a hydrogen distribution network can be conveniently represented in two-dimensional plots, with the flowrate of total gas on the horizontal axis and the purity of hydrogen on the vertical axis, called hydrogen demand and supply profiles. These purity profiles contain the hydrogen sinks and sources ordered by decreasing purity. Then, putting the hydrogen demand profile and the hydrogen supply profile together gives the Hydrogen Composite Curves (Fig. 22.3).

The Hydrogen Composite Curves can be divided into different regions with alternating surplus and deficit of hydrogen. Calculating these surpluses and deficits (area) of hydrogen, and plotting them against the purity level constructs the Hydrogen Surplus Diagram, as illustrated in Fig. 22.4.

One of the necessary conditions for a feasible network is that there is no negative hydrogen surplus anywhere in the Hydrogen Surplus Diagram, because if this is the case, the sources cannot provide enough hydrogen to the sinks. For an existing network, when the hydrogen utility is reduced, the surplus diagram moves towards the vertical axis until a vertical segment between the purity of the sink and the source touches the zero axes (Fig. 22.5). The

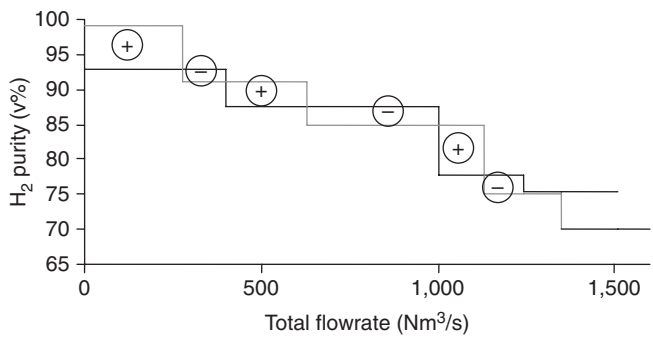

22.3 Hydrogen Composite Curve.

© Woodhead Publishing Limited, 2013

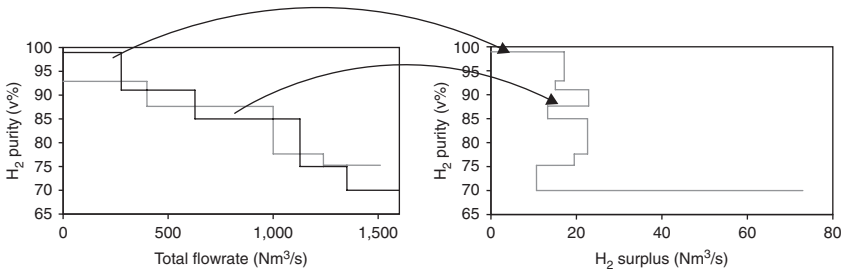

22.4 From hydrogen Composite Curve to Hydrogen Surplus Diagram.

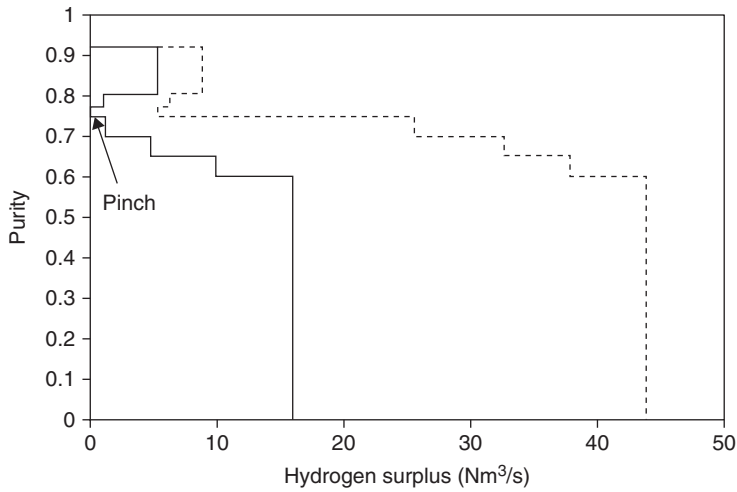

22.5 Hydrogen Pinch in Hydrogen Surplus Diagram.

purity at which this occurs is defined as the 'Hydrogen Pinch', which is the theoretical target of the minimum hydrogen to be used from the sources to the sinks. Detailed discussions of the concept can be found in both Alves, 1999.

The benefits of carrying out Hydrogen Pinch Analysis are as follows:

- With limited data, the hydrogen saving targets can be easily obtained before design and retrofit.
- Purity trade-offs. One aspect is to reduce the hydrogen utility flowrate by increasing the purity of one or more sources. It takes advantage of the fact that if two streams have the same hydrogen flowrate, the one with higher purity will provide the hydrogen system with more hydrogen surplus.
- Identification of purification locations. The installation of a hydrogen purification unit is equivalent to adding one sink and two sources to a

© Woodhead Publishing Limited, 2013

hydrogen distribution system. The sink is the feedstock to purification. The sources are the purified product stream and the residue stream. The introduction of a new purification unit usually affects the entire hydrogen system, even if the unit is captive to an individual consumer process. It is found that the beneficial option is for purification across the Pinch to reduce the requirement of the utility and at the same time, since the hydrogen loss happens Below the Pinch, the utility flowrate will not be affected.

Due to the above features of Hydrogen Pinch Analysis, it leads to widely reported applications across the global refining industry. More targeting approaches were further proposed by Foo and Manan (2006) for setting H_2 utility targets using gas cascade analysis, and by Ding *et al*. (2011) for taking pressure constraints into consideration using the concept of average pressure profiles in combination of the Hydrogen Surplus Diagram. However, such a two-dimensional approach has a limited coverage of practical constraints and actual physical processes. Therefore, more detailed description and analysis are required for detailed design and retrofit, leading to the development of detailed mathematical programming methods.

22.2.2 Mathematical Programming Methods for Design and Retrofit

Similar to solving other design and retrofit problems, such as Heat Integration and water management using mathematical programming, the basic elements are common: decision variables, the objective function, and a set of constraints including unit models, flowsheet configurations, and practical restrictions, etc. The objective function is typically minimum total annualised cost, which covers both capital cost and operating Cost. Unit models represent the detailed mass and energy flows in all the necessary processing elements, such as hydrogen producers, hydrogen consumers, purification units, compressors and pipeworks, etc. Flowsheet configurations are typically based on a network superstructure, which in theory should contain all potentially viable options. Practical constraints relate to the throughput limits, quality requirement and connection restrictions, etc.

Following the introduction of Hydrogen Pinch Analysis, Alves (1999) also introduced a superstructure-based mathematical approach for designing a detailed hydrogen network using linear programming (LP). Then Liu (2002) has further extended the superstructure-based approach to take into account detailed practical constraints such as pressure, compression and piping. He further extended his work to cover the issues of selection of purification processes for hydrogen recovery (Liu and Zhang, 2004), and integration of

© Woodhead Publishing Limited, 2013

hydrogen plants in hydrogen networks. To achieve these objectives, he has extended the mathematical approach from LP to non-linear programming (NLP), and then mixed integer non-linear programming (MINLP).

Since then, more mathematical programming based methods have been introduced. Jeong and Han (2010) discussed detailed pipework modelling and optimisation in refinery hydrogen networks. Liao *et al*. (2011) proposed using the targeting approach more effectively to simplify the mathematical model for optimisation. Zhang *et al*. (2008) proposed an approach to take into account impurities such as light hydrocarbons and H_2S in the design and optimisation of hydrogen networks, by building an iterative procedure between rigorous simulation and simplified optimisation. This method was further improved by Jia and Zhang (2011) by incorporating the vapour–liquid-equilibrium (VLE) calculations into the optimisation model. Ahmad *et al*. (2010) extended Liu's work to consider the design of hydrogen networks for multi-period operation.

To overcome the difficulty of solving MINLP problems, Khajehpour *et al*. (2009) used the Genetic Algorithm to solve a reduced superstructure of hydrogen networks. Kumar *et al*. (2010) interestingly compared different modelling techniques using LP, NLP and MILP (mixed integer linear programming)/MINLP for refinery hydrogen network optimisation. They concluded that MINLP methods are superior, when it comes to the representation of complexity and practicality of such problems. The research conducted by Jiao and Su in 2010 also indicated that MINLP methods are more appropriate for tackling such problems, while Liao *et al*. (2010) demonstrated how the MINLP approach could be effectively applied to an industrial retrofit case study.

Most of the developed techniques focus on reducing the hydrogen utility consumption. However, an equally if not more important question for oil refiners is how hydrogen can be used more effectively to enhance the productivity and profitability of their operations. To address this issue, Sun (2004) investigated the interactions between a Hydrocracking process and a Hydrogen network. Then Wu (2010) further developed an integrated optimisation framework for integrating hydroprocessors with hydrogen networks. Both investigations show significant economic potential if refiners can consider their hydrogen usage in a much wider context.

The advances in mathematical programming technology for refinery hydrogen management have greatly enhanced the capability of tackling practical industrial problems. However, one should not forget the targeting method using Hydrogen Pinch Analysis, because such a simple approach can provide very valuable physical insights into practical problems, and help to reduce the complexity of industrial investigations and justify recommended solutions. Therefore, it is always advisable to apply both targeting and mathematical programming methods in conjunction with each other in practice.

© Woodhead Publishing Limited, 2013

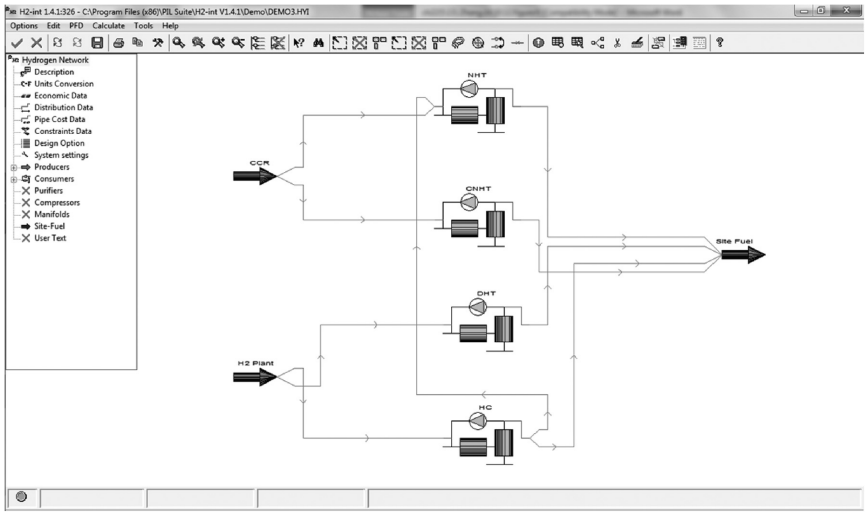

22.6 H2-*int* software.

22.2.3 Software Development

General software development activities in Process Integration have been discussed in detail in Chapter 35, including those developed for refinery hydrogen management. Many companies have developed their in-house software packages for refinery hydrogen management. For instance, Technip developed HyNDT, a software tool with LP hydrogen management (Pagano, 2009). On the other hand, Process Integration Limited has developed a dedicated commercial software package called **H2-*int*** (2012) – see also Chapter 35. H2-*int* has a Windows drag-and-drop interface, as shown in Fig. 22.6. Users can conveniently build up a hydrogen network and define detailed unit parameters and constraints. It has both targeting and mathematical optimisation functionality. The practical design issues of hydrogen network connections with compression and piping, hydrogen plant integration, purification selection and design, and effects of impurities, etc., can be quantitatively modelled and investigated.

H2-*int* software is a typical example of how basic thermodynamic analysis can be effectively combined with advanced mathematical programming in Process Integration. The following case study will demonstrate the significant economic benefit in industrial applications when it is systematically executed.

22.3 An Industrial Case Study

This project was to optimise a hydrogen network in Sinopec M Refinery, which consists of a refinery and a petrochemical complex. It was jointly

© Woodhead Publishing Limited, 2013

executed by Luoyang Petrochemical Engineering Co. in China and Process Integration Limited in the UK, using H2-*int* software for simulation and optimisation of hydrogen networks. Initially, the refinery has the capacity to process 13.5 Mt/y of crude oil, and the ethylene production is 1 Mt/y. There are two stages in the project: operational optimisation of the existing network, and retrofit study for increased refinery throughput.

22.3.1 Operational Optimisation

The existing hydrogen network is shown in Fig. 22.7.

The Hydrogen Surplus Diagram for the base case is shown in Fig. 22.8. On the surface, the hydrogen supply is very close to the minimum target based on the current hydrogen purifying strategy, which seems to indicate little potential for saving hydrogen. However, it is also shown in this diagram that there is a large amount of hydrogen (over 8,000 Nm^3/h pure hydrogen) purged to the fuel gas system at purities Below the Pinch. With purities Below the Pinch purity, these streams have lower hydrogen concentration, and cannot be reused directly. Therefore, hydrogen recovery through additional hydrogen purification could be an economically attractive option, which should be investigated further.

One obvious option to consider is that the refinery has installed a membrane process to recover hydrogen from the feedstock of a steam reformer (hydrogen

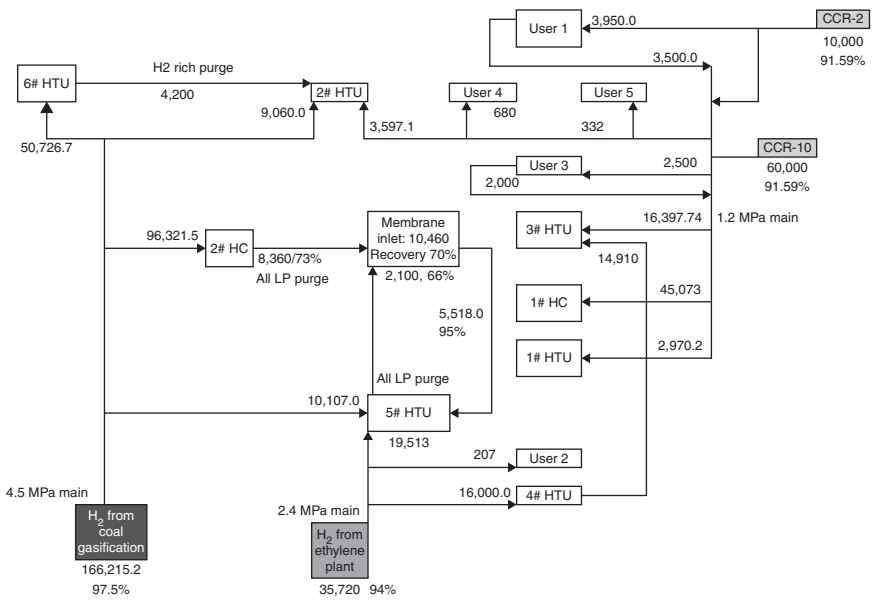

22.7 Base case – hydrogen network. (Numbers in Nm^3/h.)

© Woodhead Publishing Limited, 2013

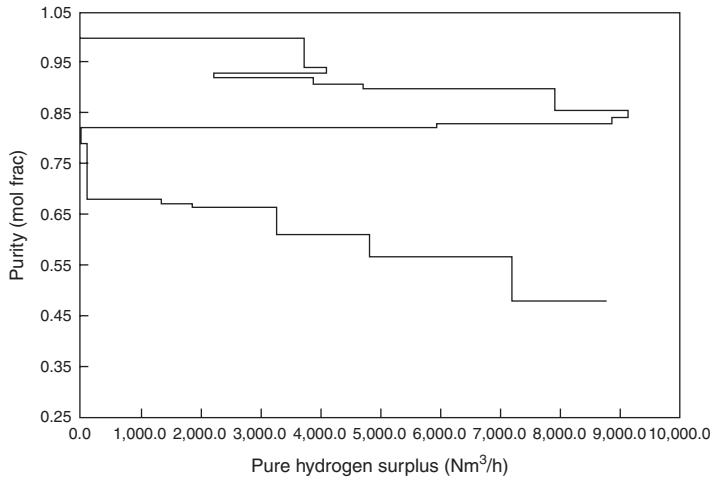

22.8 Hydrogen Surplus Diagram.

plant), which is not currently in use. According to the design conditions, the feedstock of the membrane unit has a flowrate of around 10,200 Nm^3/h and a purity of about 62.62 v%. Product hydrogen has a flowrate of about 4,782 Nm^3/h and a purity of about 94.84 v%. The overall recovery is over 71%. Membrane inlet and outlet pressures are 3.4 and 1.2 MPa(G).

Another issue with the current option is that one of the hydrotreating units adopts a once-through hydrogen flow instead of hydrogen recycle, in order to reduce the power consumption of the recycle compressor. The purged hydrogen is then sent to the 1.2 MPa hydrogen main. Even though it seems that the purged hydrogen is not wasted, it does dilute the hydrogen purity in the hydrogen main, which affects all the hydrogen consumers linked with this main.

The objective for the hydrogen network optimisation is to minimise the total operating Cost:

- Total operating cost = H_2 generation cost + Total compression cost – Fuel gas value
- Fuel gas flowrate = Total supply from all H_2 providers – Net H_2 consumption in all H_2 consumers
- H_2 concentration in fuel gas = Pure H_2 supply from all providers – (Net H_2 consumption in all H_2 consumers)/Fuel gas flowrate

The net H_2 consumption in each H_2 consumer is assumed to be fixed. The impurities are lumped as methane, so the net heating value of fuel gas can be calculated based on H_2 concentration and fuel gas flowrate.

© Woodhead Publishing Limited, 2013

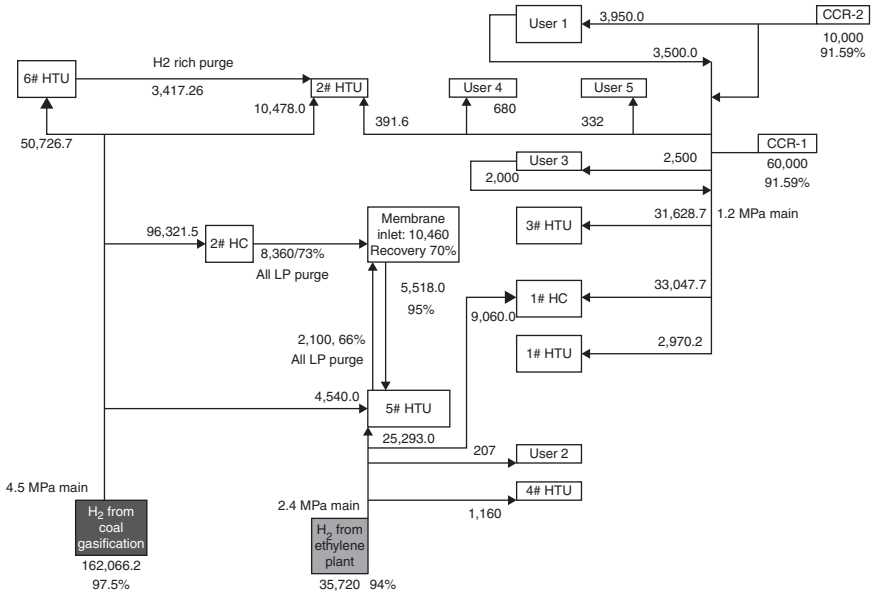

22.9 Operational optimisation of the existing hydrogen network. (Numbers in Nm^3/h.)

Through optimisation, it is shown that using the membrane unit at the right place, and changing the once-through arrangement to recycle, are indeed beneficial in improving hydrogen utilisation efficiency. To accommodate these changes, there are some other connection adjustments to be made, which can be achieved through operational adjustment on the existing pipelines, as shown in Fig. 22.9.

Table 22.1 shows the comparison between the base case and the optimised case. With the recommended options implemented, the overall cost of the hydrogen network is reduced by 11.9 MRMB/y (RMB: Chinese currency unit), equivalent to around 1.89 MUSD/y, without capital investment.

An interesting and very important issue in this study is that when hydrogen mains are included in optimisation, any changes of their purity levels will affect the operation of hydrogen-consuming units taking hydrogen from them. It then probably results in changes of reaction conditions within these units. Therefore, it is important to maintain the required hydrogen flow and purity to various units in optimisation. In this case study, a conservative condition is chosen, which is not to allow reaction conditions to deteriorate, as shown in Table 22.2. Even though such a strict condition is imposed on the problem, the result still shows significant savings to be achieved. On the other hand, if the reactor inlet conditions are not allowed to change in any direction, this solution would not be reached under such a rigid constraint.

© Woodhead Publishing Limited, 2013

Table 22.1 Comparison between the base case and the optimised case

Item	Base case	Optimisation
Total pure H_2 supply, Nm^3/h	143,484	141,069
Total H_2 consumption, Nm^3/h	132,406	132,406
Net H_2 loss, Nm^3/h	11,078	8,663
Effective H_2 usage, %	92.28	93.86
Membrane inlet, Nm^3/h	0	2,107
Membrane outlet, Nm^3/h	0	973.4
Fuel gas flow, Nm^3/h	11,078	8,663
H_2 concentration in fuel gas, v%	26.9	6.5
Fuel gas value: MRMB/y	124.5	113.9
Total compression duty for make-up H_2 compression, kW	21,112	21,196
Total compression duty in recycle compressors, kW	12,517	12,872
Total compression cost: MRMB/y	169.5	171.7
Total cost: MRMB/y	1,412.2	1,400.3
Savings: MRMB/y	–	11.9

Table 22.2 Optimisation – reactor inlet conditions for major hydrogen consumers

	H_2 concentration (V%)		Flowrate (Nm^3/h)		Pure H_2 flow (Nm^3/h)	
	Base case	Optimised	Base case	Optimised	Base case	Optimised
1# HC	82.13	82.36	213,000	212,394	174,937	174,928
1# HTU	86.61	86.90	11,662	11,623	10,100	10,100
2# HTU	86.07	86.21	92,000	91,851	79,184	79,185
3# HTU	84.13	84.40	118,350	117,969	99,568	99,565
4# HTU	94.00	92.20	16,000	16,313	15,040	15,041
5# HTU	80.40	82.10	150,810	152,500	125,202	125,203
6# HTU	92.97	92.97	256,000	256,000	238,003	238,003
User 3	90.27	91.50	300	296	271	271
2# HC	90.00	90.00	2,500	2,500	2,250	2,250
User 1	90.00	90.00	3,950	3,950	3,555	3,555
User 2	94.00	94.00	207	207	195	195

22.3.2 Revamping optimisation

In order to increase the crude oil processing capacity to 18 Mt/y, many new processes will be installed, including a crude distillation unit (CDU), fluid catalytic cracker (FCC), hydrocracker (HC), sulphur recovery, etc. The required hydrogen supply is therefore significantly increased. As estimated in the feasibility study, the overall hydrogen usage would reach 270,000 Nm^3/h. Meanwhile, the hydrogen production is facing new limitations. According to local environmental legislation, heavy fuel oil is no longer allowed to be used as fuel in furnaces and fired heaters, and desulphurised fuel gas is

© Woodhead Publishing Limited, 2013

considered as the substitution. Therefore, there will be a shortage of fuel gas to be used as raw material for hydrogen production. Moreover, the local natural gas and naphtha prices are high, so that hydrogen production based on them would be uneconomical.

After many investigations, Sinopec decided to install a coal-gasification based hydrogen plant, with a design capacity of 200,000 Nm^3/h. The existing hydrogen plant based on fuel gas will be used as a stand-by. The hydrogen pressure from the new hydrogen plant is 4.5 MPa(G). Hence, there will be three hydrogen mains – new 4.5, and existing 2.4 and 1.2 MPa(G) in the refinery. This introduces new complexity to the design of the hydrogen network. Therefore, this project is to improve the hydrogen utilisation efficiency and economics under the new refining configuration.

A basic hydrogen network design has been produced at the feasibility study stage for the debottlenecking project, which is used as the base case for optimisation design, as shown in Fig. 22.10.

The Hydrogen Surplus Diagram for the base case is shown in Fig. 22.11. Similar to the situation of the existing network, the hydrogen supply is very close to the minimum target based on the current hydrogen purifying strategy. However, it is also shown that there is large amount of hydrogen (over 25,000 Nm^3/h pure hydrogen) purged to the fuel gas system at purities Below the Pinch. Therefore, hydrogen recovery through additional hydrogen purification could be an economical attractive option.

After optimisation, a new PSA process is introduced into the hydrogen network, and the exiting membrane unit is still used. The new PSA process also contains a product hydrogen compressor and a tail gas compressor. The optimised capacity for the PSA unit is 10,000 Nm^3/h. The new PSA process makes it possible to recover hydrogen from low pressure purge gases from various consumers and the membrane residue stream. The total hydrogen supply can be reduced by 14,500 Nm^3/h comparing with the base case.

Figure 22.12 shows the optimised hydrogen distribution system. The corresponding Hydrogen Surplus Diagram is shown in Fig. 22.13. The reactor inlet conditions for major hydrogen consumers are listed in Table 22.3. The same as the operational optimisation, reactor inlet conditions are allowed to improve only if changes have to be made to the hydrogen mains.

Table 22.4 shows the comparison between the base case and the optimised case. With the recommended options implemented, the overall cost of the hydrogen network is reduced by 66.2 MRMB/y, equivalent to around 10.5 MUS$/y, with Payback Time of just under half a year. The optimised network design shows great improvement with relatively small capital investment.

© Woodhead Publishing Limited, 2013

© Woodhead Publishing Limited, 2013

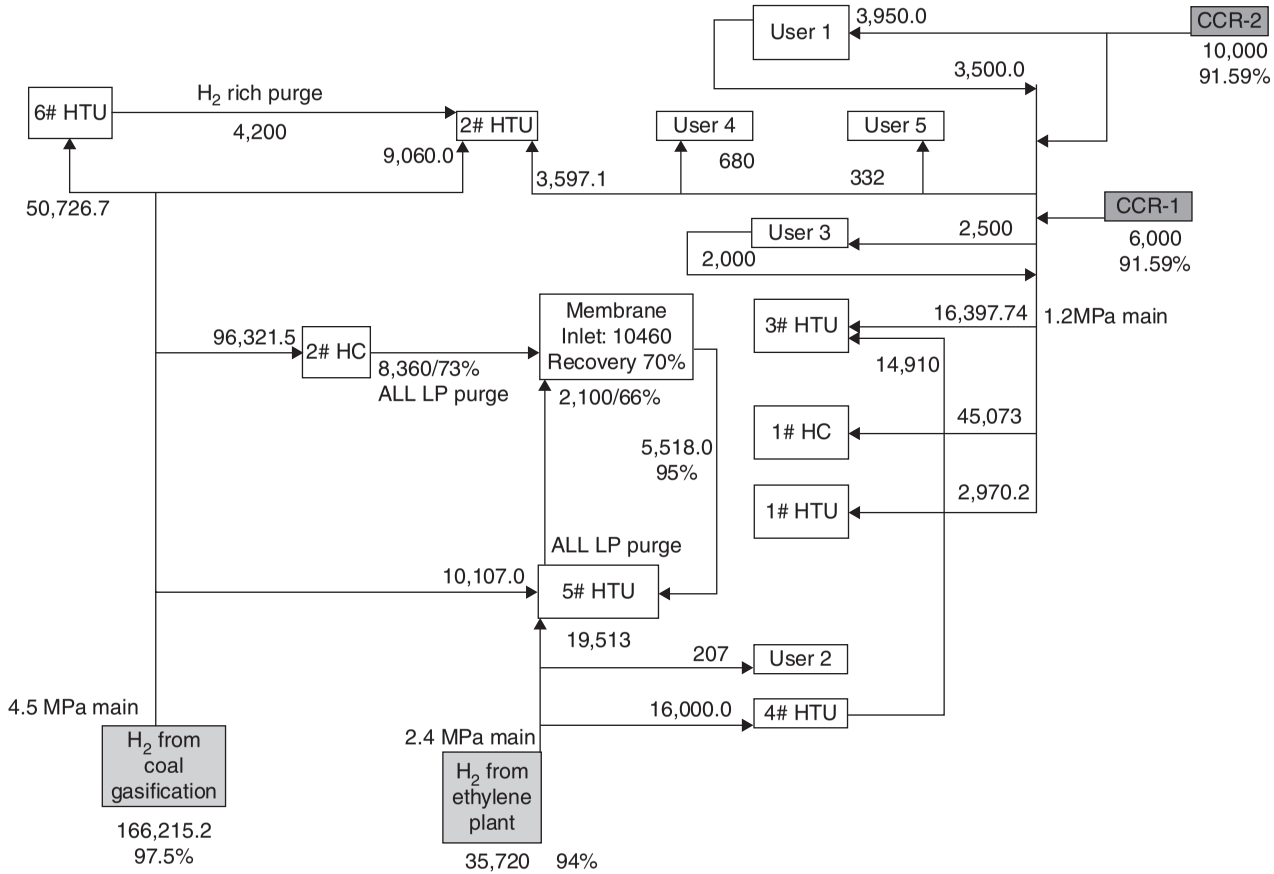

22.10 Base case – revamping design. (Numbers in Nm^3/h.)

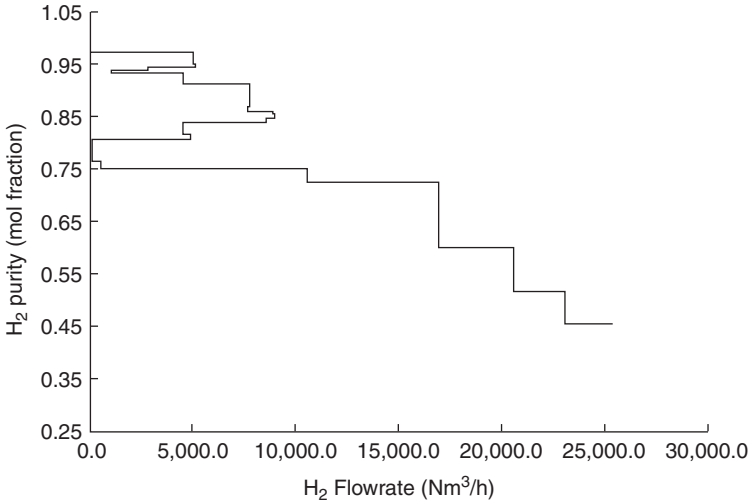

22.11 Base case – Hydrogen Surplus Diagram.

22.4 Hydrogen Management in the Wider Context of Process Integration: Future Trends

Hydrogen Pinch Analysis, developed for refinery hydrogen networks, aims at saving hydrogen while maintaining the process requirement of hydrogen quality and quantity. As effective as it is demonstrated in the case study, one must be aware of the scope covered by such a technology, and its limitations. There are three areas relating to refinery hydrogen management that will require more research and development of comprehensive and practical Process Integration technology:

- Exploiting interactions between hydrogen recovery and light-ends recovery;
- Exploiting interactions between hydrogen networks and energy systems; and
- From saving hydrogen to utilising hydrogen more effectively.

22.4.1 Exploiting Interactions between Hydrogen Recovery and Light-Ends Recovery

Hydrogen losses through purging off-gas to refinery fuel gas often combine with significant light-ends loss (C3+ hydrocarbons). The same as hydrogen, light ends are much more valuable than methane, and their use as fuel gas should be minimised for economic reasons.

For off-gases containing a reasonable amount of hydrogen and C3+ hydrocarbons, the interaction between hydrogen recovery and light-ends recovery

© Woodhead Publishing Limited, 2013

© Woodhead Publishing Limited, 2013

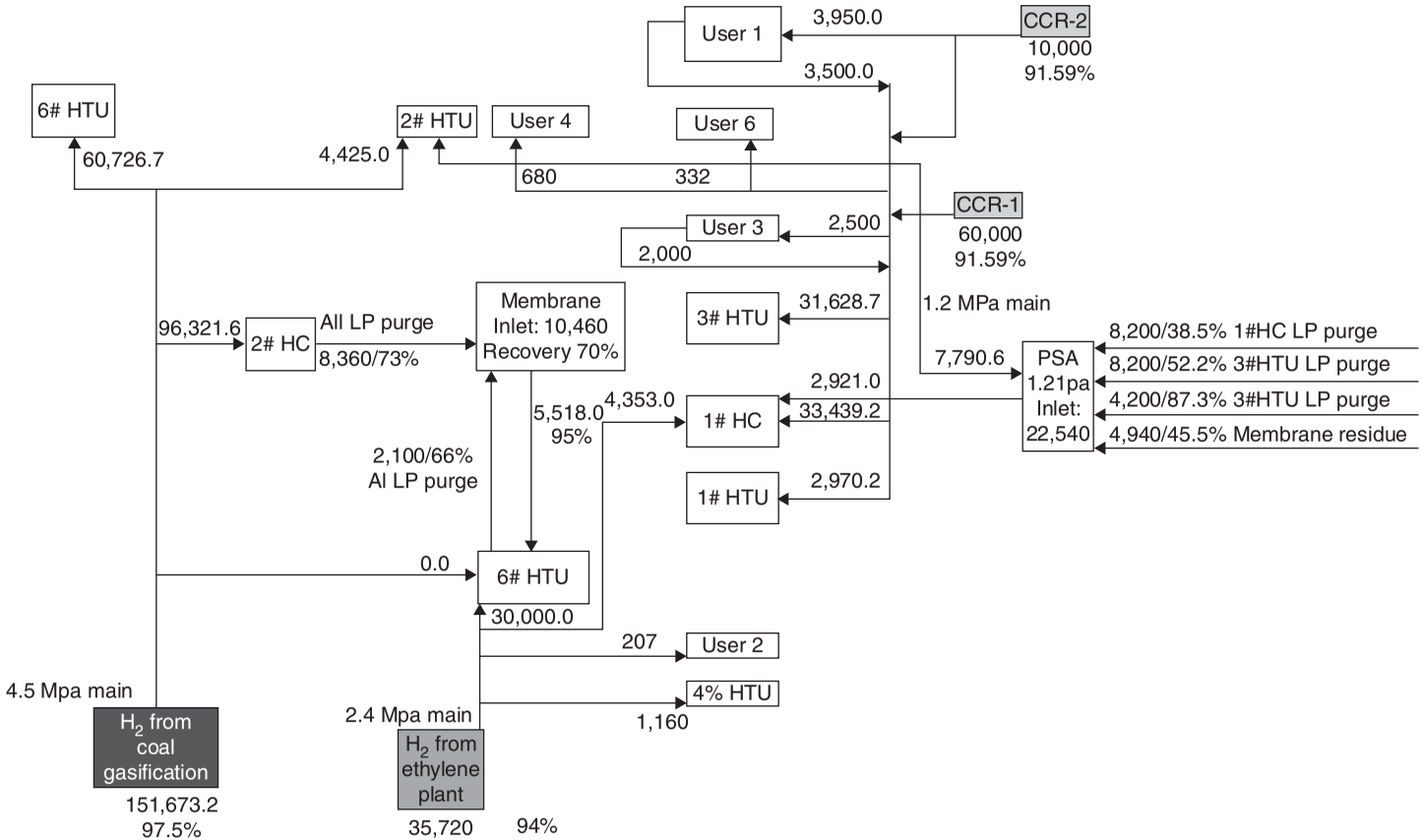

22.12 Optimised hydrogen network. (Numbers in Nm^3/h.)

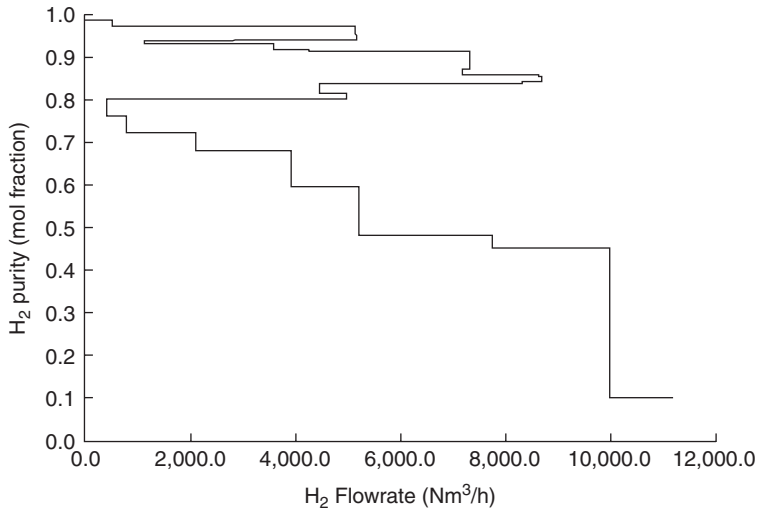

22.13 Hydrogen Surplus Diagram.

is obvious: removing either hydrogen or light ends will make the remaining one more concentrated and easier to upgrade. Therefore, it is logical to consider both aspects simultaneously, in order to maximise the economic return of investment. This is a natural territory for Process Integration applications, where various separation technologies, such as membrane, pressure swing adsorption, cryogenic distillation, physical absorption, etc., should be considered and integrated in a similar way to that described by Liu and Zhang (2004) for hydrogen recovery. It is a more complex Process Integration problem in comparison with hydrogen recovery only. Hence, more research effort is required to develop a more effective modelling and optimisation framework.

22.4.2 Exploiting Interactions between Hydrogen Networks and Energy Systems

Recovery of hydrogen and light ends from refinery off-gases will lead to a reduced amount of fuel gas generation. Careful trade-offs need to be carried out between fuel balance and level of hydrogen and light-ends recovery. For example, if a refinery is very restricted by its fuel gas supply and has to supplement its fuel gas with expensive LPG to meet the heating demand, it is normally not sensible to recover any light ends or even hydrogen. On the other hand, if a refinery has a sufficient supply of natural gas, recovering hydrogen and light ends together could produce a significant economic return of investment.

If a refinery is highly constrained by its fuel gas supply, its restriction on hydrogen and light-ends recovery can be overcome by shifting energy

© Woodhead Publishing Limited, 2013

Table 22.3 Reactor inlet conditions for major hydrogen consumers

	H_2 concentration (V%)		Flowrate (Nm^3/h)		Pure H_2 flow (Nm^3/h)	
	Base case	Optimised	Base case	Optimised	Base case	Optimised
1# HC	84.22	84.28	165,346	165,233	139,254	139,254
1# HTU	87.03	87.03	11,733	11,732	10,211	10,210
2# HTU	87.02	87.27	123,102	122,749	107,123	107,125
3# HTU	84.46	84.54	128,094	126,875	108,188	107,261
4# HTU	92.00	92.10	16,000	16,000	14,720	14,736
5# HTU	80.39	80.40	158,979	158,967	127,803	127,808
6# HTU	94.19	93.91	409,977	409,977	386,157	384,998
User 3	91.00	91.59	2,484	2,500	2,260	2,290
2# HC	94.89	94.45	503,921	503,921	478,171	475,956
User 1	91.59	91.59	3,950	3,950	3,618	3,618
User 2	94.00	94.00	207	207	195	195

Table 22.4 Results comparison

Item	Base case	Optimised design
Coal gasification H_2, Nm^3/h	166,215	151,673
Total H_2 supply, Nm^3/h	271,935	257,393
Total pure H_2 supply, Nm^3/h	259,749	245,571
Total H_2 consumption, Nm^3/h	234,502	234,502
Net H_2 loss, Nm^3/h	25,247	11,069
Effective H_2 usage, %	90.23	95.49
H_2 generation cost: MRMB/y	2,489.7	2,354.8
Membrane inlet, Nm^3/h	10,460	10 460
Membrane outlet, Nm^3/h	5,518	5,518
PSA inlet, Nm^3/h	0	22,541.9
PSA outlet, Nm^3/h	0	10,711
Fuel gas flow, Nm^3/h	37,433	22,891
H_2 concentration in fuel gas, v%	67.40%	48.40%
Fuel gas value: MRMB/y	265.5	201.3
Total compression duty for make-up H_2 compression, kW	38,627	39,205
Total compression duty in recycle compressors, kW	17,647	18,005
Total compression cost: MRMB/y	270.1	274.6
Total operating cost: MRMB/y	2,494.3	2,428.1
(H_2 generation cost + Total compression cost–Fuel gas value)	Base	Base-66.2
Capital investment: MRMB/y		32
Payback Time: y		0.48

savings through Energy Integration modifications to hydrogen and light-ends recovery. In this way, more room is created for hydrogen and light-ends recovery, and low cost energy can be transformed to high-value hydrogen and light hydrocarbon. Therefore, for oil refineries, it is worth

© Woodhead Publishing Limited, 2013

bringing Energy Integration and Hydrogen Integration into the same context. However, the technical challenges to cover such a big scope should not be underestimated.

22.4.3 From Saving Hydrogen to Utilising Hydrogen More Effectively

The existing Hydrogen Integration techniques have been developed on the basis of maintaining constant hydrogen partial pressure (hydrogen purity at reactor inlet) and hydrogen-to-oil ratio (quantity of hydrogen flow), which leaves a big question mark as to the efficiency of hydrogen utilisation in each hydroprocessor. Therefore, a significant area to exploit further hydrogen saving opportunities is ignored. Furthermore, one can also argue that it is possible to use more hydrogen in certain processes to improve the overall economics of refining operation.

However, exploiting such opportunities will require Hydrogen Integration to be combined with detailed process modelling and integration. Further research is required to develop practical and effective approaches for overall integration of refining processes and the hydrogen network.

22.5 Conclusion

Process Integration technology of refinery hydrogen management has been actively investigated and developed over the last decade. Both thermodynamic analysis for targeting, and mathematical programming for design, have been developed and tested. As demonstrated in the case study, effective applications will require an integrated approach with both methods.

With more mature technology, commercial software tools are available now to assist industry in practical applications. With increasing computing power, and more efficient optimisation algorithms being developed, the Process Integration technology for refinery hydrogen management is moving more towards a level of integrating detailed unit models with hydrogen networks, for more efficient use of hydrogen, rather than simply trying to save hydrogen.

22.6 Sources of Further Information

Process Integration for refinery hydrogen management is a relatively new area. Therefore, not many references are available, and many of them have already been mentioned in the previous discussion in this chapter. However, some general knowledge of Process Integration will be very useful in understanding the principles and development of Process Integration techniques for refinery hydrogen management. In this regard, there are three useful

© Woodhead Publishing Limited, 2013

references to understand the principles of Pinch Technology. One is from Robin Smith, 2005, in his book '*Chemical Process: Design and Integration*', which covers both Pinch Analysis and mathematical programming aspects in Process Integration. Another is from Ian Kemp, who in 2007 published an updated and extended 2nd version (Kemp, 2007) of '*User Guide on Process Integration*'. A more recent book is '*Sustainability in the Process Industry: Integration and Optimisation*' (Klemeš *et al*., 2010), which extends the recent developments in Process Integration until 2010. Even though these three books do not address the refinery hydrogen management problem directly, readers can find detailed discussions of many relevant techniques and theories in Process Integration that have been extended into the technology development for refinery hydrogen management.

22.7 References

Ahmad, M. I., Zhang, N., Jobson, M. (2010). Modelling and optimisation for design of hydrogen networks for multi-period operation. *Journal of Cleaner Production*, **18**, 889–899.

Alves, J. J. (1999). Analysis and design of refinery hydrogen distribution systems. PhD thesis, UMIST, Manchester, UK.

Alves, J. J., Towler, G. P. (2002). Analysis of refinery hydrogen distribution systems. *Industrial and Engineering Chemistry Research*, **41**, 5759–5769.

Ding, Y., Feng, X., Chu, K. H. (2011). Optimization of hydrogen distribution systems with pressure constraints. *Journal of Cleaner Production*, **19**, 204–211.

Foo, D. C. Y., Manan, Z. A. (2006). Setting the minimum utility gas flowrate targets using cascade analysis technique. *Industrial & Engineering Chemistry Research*, **45**, 5986–5995.

H2-int, Process Integration Ltd, Manchester, UK, www.processint.com/soft/h2_int.html, accessed 25/10/2012.

Jeong, C., Han, C. (2011). Byproduct hydrogen network design using pressure swing adsorption and recycling unit for the petrochemical complex. *Industrial & Engineering Chemistry Research*, **50**, 3304–3311.

Jia, N., Zhang, N. (2011). Multi-component optimisation for refinery hydrogen networks. *Energy*, **36**, 4663–4670.

Kemp, I. C. (2007). *Pinch Analysis and Process Integration*, 2nd ed. Butterworth-Heinemann (Elsevier), Oxford, UK (authors of the first edition: Linnhoff, B., Townsend, D. W., Boland, D., Hewitt, G. F., Thomas, B. E. A., Guy, A. R., Marsland, R. H. (1982 and 1994). *A User Guide on Process Integration for the Efficient Use of Energy*. IChemE, Rugby, UK).

Khajehpour, M., Farhadi, F., Pishvaie, M. R. (2009). Reduced superstructure solution of MINLP problem in refinery hydrogen management. *International Journal of Hydrogen Energy*, **34**, 9233–9238.

Klemeš, J., Friedler F., Bulatov I., Varbanov P. (2010). *Sustainability in the Process Industry: Integration and Optimization.* McGraw-Hill, New York, USA.

Kumar, A., Gautami, G., Khanam, S. (2010). Hydrogen distribution in the refinery using mathematical modeling. *Energy*, **35**, 3763–3772.

© Woodhead Publishing Limited, 2013

Liao, Z., Rong, G., Wang, J., Yang, Y. (2011). Rigorous algorithmic targeting methods for hydrogen networks – Part I: systems with no hydrogen purification. *Chemical Engineering Science*, **66**, 813–820.

Liao, Z., Wang, J., Yang, Y., Rong, G. (2010). Integrating purifiers in refinery hydrogen networks: a retrofit case study. *Journal of Cleaner Production*, **18**, 233–241.

Liu, F. (2002). Hydrogen integration in oil refineries. PhD thesis, UMIST, Manchester, UK.

Liu, F., Zhang, N. (2004). Strategy of purifier selection and integration in hydrogen networks. *Chemical Engineering Research and Design*, **82**, 1315–1330.

Pagano, M. (2009). Hydrogen Management Console (HyN.DT™), ERTC – 09–11 November 2009.

Smith, R. (2005). *Chemical Process Design and Integration*. John Wiley & Sons Ltd, Chichester, West Sussex, UK.

Sun, J. (2004). Molecular modelling and integration analysis of hydroprocessors. PhD theŠfiš, , Manchešter, UK.

Swain, E. J. (1998). US refining crude slates continue towards heavier feeds, higher sulfur contents. *Oil & Gas Journal*, **96**(40), 43–47.

Wu, Y. (2010). Refinery optimisation based on molecular management. PhD thesis, The , Manchešter, UK.

Zhang, N., Singh, B. B., Liu, F. (2008). A systematic approach for refinery hydrogen network management. PRES 2008, August 2008, Prague, Czech Republic. Lecture J8.3 [1296].

© Woodhead Publishing Limited, 2013

23

Retrofit Mass Integration of Acid Gas Removal Systems in Petrochemical Plants

DUNCAN MCKENZIE FRASER, University of Cape Town, South Africa

DOI: 10.1533/9780857097255.5.725

Abstract: Acid gas removal systems are common in refineries as well as in gas treatment facilities. They are generally designed to be optimum as individual units by suppliers, but not optimised as a whole system. This chapter examines the retrofit of two industrial Mass Exchange Networks for the removal of hydrogen sulphide from process streams, in order to reduce the sulphur emissions from the plants. By optimising each of these networks as a system, it was possible to improve on the individual unit designs. The approach to retrofitting of each of these two very different systems is presented in detail. One system used conventional counter-current absorbers, whereas the other used cross-flow of the absorbent and gas through three venturi scrubbers with co-current flow in each of the scrubbers.

Key words: retrofit, hydrogen sulphide removal, Mass Exchange Networks, cross-flow system, optimisation.

23.1 Introduction

Acid gas removal systems are common in refineries as well as in gas treatment facilities. In refineries the emphasis is usually on the removal of H_2S, whereas in gas treatment facilities it may be on CO_2 removal. Often these acid gas removal systems are designed by the suppliers of the solvents, which are frequently of a proprietary nature. There are two problems with this: the equilibria for acid gases in proprietary solvents are not generally available, and individual treatment units are optimised (rather than a whole removal system, if there are multiple treatment units). Both these problems are covered in the two case studies presented in this chapter.

Mass Integration/Mass Exchanger Network Synthesis (MENS), described in Chapter 3, has developed over the past 24 years, following the pioneering work of El-Hawagi and Manouthiousakis (1989). MENs are systems in which particular components (often pollutants) are removed from rich process streams using lean process streams or external mass separating agents (MSAs) in units such as absorbers, strippers, ion exchange columns, adsorbers and mixer–settlers.

© Woodhead Publishing Limited, 2013

El-Halwagi and Manouthiousakis introduced methods for targeting the minimum amount of MSA required, and hence the minimum operating cost for such systems. More recently Hallale and Fraser introduced methods for also targeting the size of mass exchange units, and hence the capital cost for MENs: this was first shown for water minimisation (Hallale and Fraser, 1998), and then for more general MENs, using both simple capital cost models (Hallale and Fraser, 2000a) and detailed capital cost models (Hallale and Fraser, 2000b). They then also demonstrated how this opened up the optimisation of MENs using Supertargeting (i.e. trading off Operating and Capital Costs before design, Hallale and Fraser, 2000c, 2000d).

These techniques were developed for grass-roots designs, but have also been applied to the retrofit of existing systems, either to simply reduce operating cost (Fraser and Hallale, 2000a), or to reduce pollution (Fraser and Hallale, 2000b).

This handbook has largely focused on Heat Integration (which is the most fully developed field in Process Integration), together with particular applications of Mass Integration, such as Water Pinch (the best developed application in Mass Integration), Hydrogen Pinch and Oxygen Pinch. Chapter 3 in particular briefly introduced MENs, and then dealt with Water Pinch, Material Recovery Pinch and Property-Based Material Recovery Pinch in some detail. This chapter will focus on the more general development of Mass Integration and apply it to two particular systems, both involving the removal of acid gases from streams in petrochemical plants. Both were retrofit studies aimed at improving the performance of existing systems, and thus illustrating the importance of Mass Integration to improve process efficiency and to reduce environmental impact, as compared to conventional design approaches.

All the mass transfer systems studied before this involved counter-current flow of the rich and lean streams in the contacting units (as in the first system presented here), whether tray columns, packed columns, or a series of mixer–settlers. The second system presented is an industrial MEN system, which involved cross-flow of the rich and lean streams in three successive venturi scrubbers in which the internal flows of the rich and lean streams were co-current. It was therefore necessary to develop a methodology for handling this sort of system. This methodology (which has only previously been published in conference proceedings) is presented in Section 23.4.1 of this chapter.

Process Synthesis/Integration can be approached in three different ways: heuristics, physical and thermodynamic insight, and mathematical programming. Hybrid methods, where two or all of the synthesis methods are combined, have also been used, taking advantage of the combined strengths of the individual techniques. Grossmann and Daichendt (1996) highlighted as

© Woodhead Publishing Limited, 2013

one of the important challenges to be solved the question of how the optimisation and targeting approaches, and heuristics for that matter, can be combined in such a way that, on one hand, the integration is conceptually consistent and rigorous and, on the other hand, it exploits the strengths of each approach. In this study we have therefore developed a new method of synthesis for MENs such that the techniques of Pinch Technology, developed by El-Halwagi and Mathousiouthakis (1989) for establishing MSA targets, and Hallale (1998), for determining mass exchanger size and cost targets, were combined with the Mixed Integer Non-Linear Programming (MINLP) hyperstructure approach proposed by Papalexandri *et al*. (1994). In Section 23.4.2 of this chapter I will describe how we addressed this challenge.

This chapter will first present a general overview of the field of MENS, insofar as it has not been covered in this handbook, plus how retrofit of existing mass exchange systems has been approached. This will be followed by an overview of the two systems that have been studied, in order to describe the developments that were needed to solve them. The overview leads into the specific developments undertaken to solve the problems at hand. Next, the fits to the equilibrium absorption data for the two systems studied are presented, as these were needed in order to be able to work with them. Finally, the results of this study are given, followed by conclusions as to how to approach similar problems.

23.2 Review of Previous Work on Mass Exchanger Network Synthesis (MENS) and Retrofit of Existing Systems

The basis for the work covered in this chapter is what has been done in the area of Mass Exchange Network Synthesis, coupled with previous work on retrofit of existing mass exchange systems. These topics are described in this section.

23.2.1 Mass Exchange Network Synthesis

Given the well-known analogy between heat and mass transfer, it was not too long before the Pinch Technology approach was applied to MENs (El-Halwagi and Manousiouthakis, 1989). Typical unit operations with mass exchangers are:

- absorption and stripping (gas–liquid),
- liquid extraction (liquid–liquid),
- ion exchange (liquid–solid), and
- adsorption (gas–solid).

© Woodhead Publishing Limited, 2013

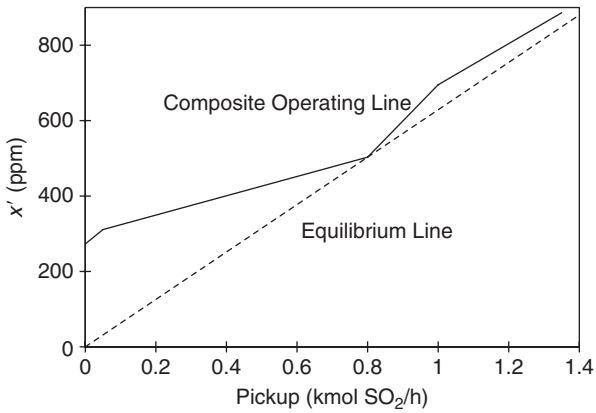

23.1 Concentration–Pickup diagram.

Note the wide variety of physical systems, needing different kinds of contacting devices. In these units an MSA, such as water, MEA, LIX, ion exchange resin, or activated carbon, is used to remove undesirable components from the process streams.

The first target for MENS was the utility (MSA) target. This is obtained by using a minimum composition difference in the lean phase, ε, and a Composition–Pickup diagram (Fig. 23.1). In Fig. 23.1, the concentration $x' = x - \varepsilon$. The line of maximum slope just touching the process line represents the minimum MSA target. Note that this construction is similar to that used for Water Integration.

It took another ten years before the steps for formulating size targets for MENS were established. This was because in the design of mass exchangers, the driving force is not simply the equivalent of the difference in temperature in heat exchangers, but is determined by the equilibrium concentration in the lean phase.

The key to this was the development of the y–x Composite Curve plot shown in Fig. 23.2. This makes use of a Composite Operating Line and an Equilibrium Line, targeting the size of the system of mass exchangers by stepping off the number of stages as on a McCabe–Thiele diagram, for stagewise contactors (Hallale and Fraser, 1998).

This development opened up the way to perform Supertargeting for MENs (Hallale and Fraser, 2000b). Similarly to HENs, this is done by varying the minimum composition difference and determining the annual operating and annualised capital cost targets, leading to a diagram like Fig. 23.3.

Methods have also been developed for the sizing of continuous contact systems, as well as systems involving multiple MSAs. In the latter case, a y–y* Composite Curve plot is used so that all the MSAs are brought onto a common basis by using the equilibrium concentration in the lean phase (see Fig. 23.4).

© Woodhead Publishing Limited, 2013

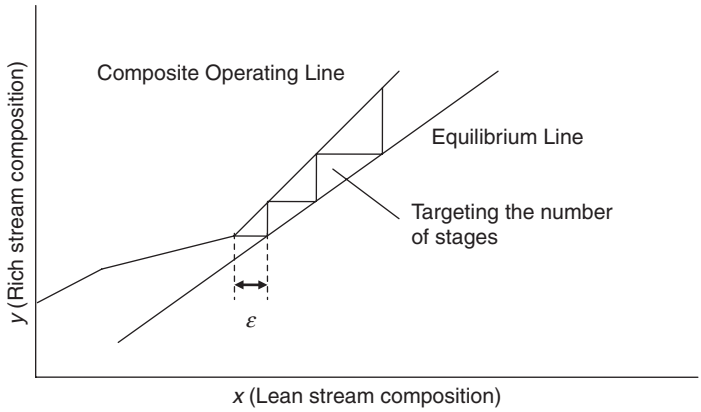

23.2 *y–x* Composite Curves for MENS.

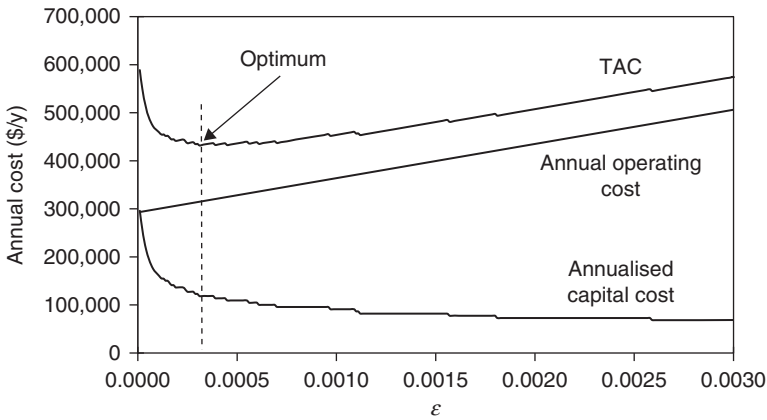

23.3 Supertargeting for MENS (Hallale and Fraser, 2000c).

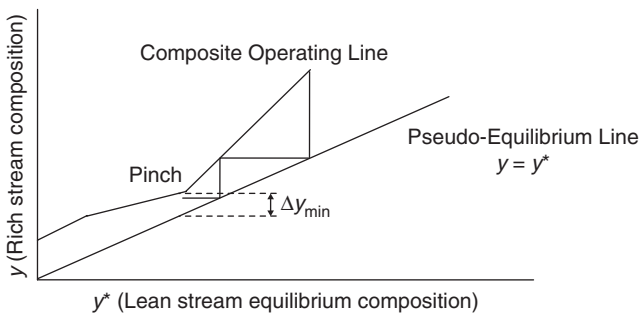

23.4 The *y–y** Composite Curve plot for problems with overlapping MSAs.

© Woodhead Publishing Limited, 2013

This also involves using a minimum composition difference in the rich phase, Δy_{min} (Hallale and Fraser, 2000a).

The design of MENs follows similar principles to the design of HENs. These are:

- Do not violate the minimum composition difference;
- Do not transfer mass across the Pinch;
- Match the available driving force profile; and
- Try to minimise the number of exchange units.

Experience has shown that, in mass exchange matching, the driving forces are more important than minimising the number of exchange units. The reason for this is shown in Fig. 23.5, which is the equivalent of the Driving Force Plot (DFP) for HENS. Poor matches either use too much driving force, or too little driving force. A match using too much driving force leads to one which will have to use too little driving force. In a MENS, too little driving force means a dramatic increase in size, because the Operating Line approaches the Equilibrium Line (Hallale and Fraser, 1998a).

As far as mathematical approaches to optimisation of synthesis problems is concerned, Papoulias and Grossmann (1983) and Cerda, *et al*. (1983) used the transhipment and transportation models respectively to target the minimum energy and Minimum Number of Units in HENS. The MEN analogue of the transhipment model for minimum MSA and number-of-units targets was presented by El-Halwagi and Manousiouthakis (1990). The simplified stagewise superstructure (SWS), which is a simultaneous method for HENS, was first presented by Yee *et al*. (1990). The SWS model does not partition the network at the Pinch and it trades off operating and capital cost by minimising the Total Annual Cost (TAC). Heat can be exchanged within each stage of the SWS, and the amount of heat exchanged in each of the stages defines the temperature of the next stage boundary.

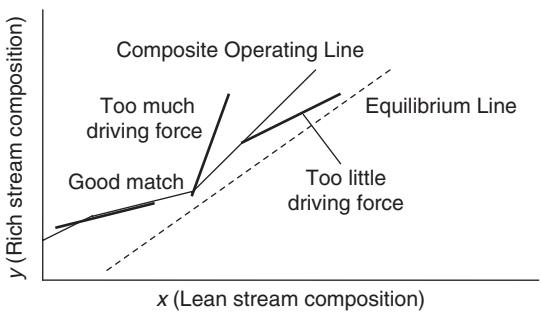

23.5 DFP for MENS.

© Woodhead Publishing Limited, 2013

Papalexandri *et al.* (1994) were the first to develop an MINLP model in MENS for simultaneous generation of a network and determination of the TAC without resorting to any Pinch decomposition concepts.

The concept upon which the SWS for HENS is based has equally found application in MENS. This includes the mass exchange SWS of Chen and Hung (2005a), which includes non-linear mass balances for each exchange unit, and the fairly linear SWS model presented by Szitkai *et al.* (2006), which does not include non-linear mass balances for exchangers. It should be noted that these two SWS methods for MENS can handle multicomponent problems. Chen and Hung extended their mass exchange SWS model to handle both MENS retrofit (2005b) and multi-period MENS problems (2007). Isafiade and Fraser presented a different MINLP model, called the Interval Based MINLP Superstructure (IBMS), which they applied to the following types of problems: standard and multiple utility HENS, as well as HENS with regeneration (2008a); standard and multiple utility MENS, as well as MENS with regeneration (2008b); combined heat and mass exchange (2009a); multi-period MENS operations (2009b); and multi-period HENS operations (2010).

23.2.2 Retrofit of Existing Systems

A full description of the procedures used in general for retrofit targeting and design will be found in Fraser and Hallale (2000a). They applied the approach used by Tjoe and Linnhoff (1986) for retrofit of HENs to MENs, and demonstrated that the same retrofit path ideas applied in HENS could be successfully used in MENS. They also showed that the retrofit targets developed in this way were meaningful, in that they could be achieved, or at worst closely approached, in retrofit designs.

A Size–Load plot replaces the Area–Energy Plot (see Fig. 23.6, in which Size is represented by Volume). A Savings–Investment Diagram can also be developed, as shown in Fig. 23.7 (Fraser and Hallale, 2000a). The Savings–Investment Diagram features a region of diminishing return on investment, as well as a maximum savings (which is limited by the thermodynamics of the system being investigated). Figure 23.8 shows a retrofit design for the problem used in Figs 23.6 and 23.7.

A full treatment of retrofit for effluent reduction may be found in Fraser and Hallale (2000b). The same retrofit path was used as before. For the chosen retrofit path, you can then relate the reduction in environmental impact to the investment required. In this case this leads to an effluent reduction–investment diagram which has been termed the Impact Diagram, shown in Fig. 23.9. Note how, similarly to the Savings–Investment Diagram, the Impact Diagram also features a region of diminishing return

© Woodhead Publishing Limited, 2013

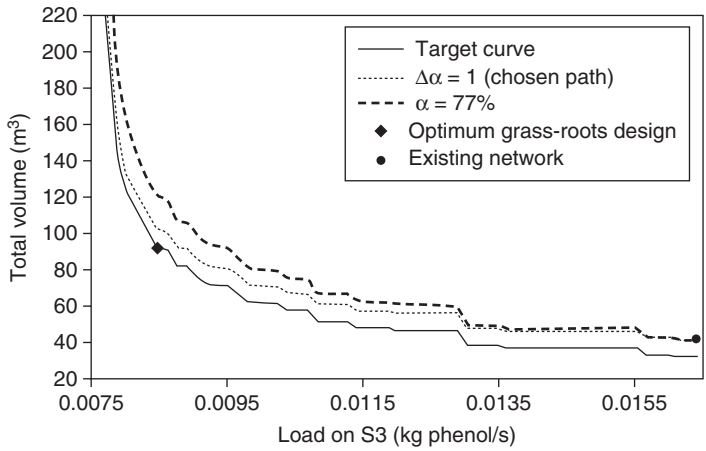

23.6 Retrofit path for MENS.

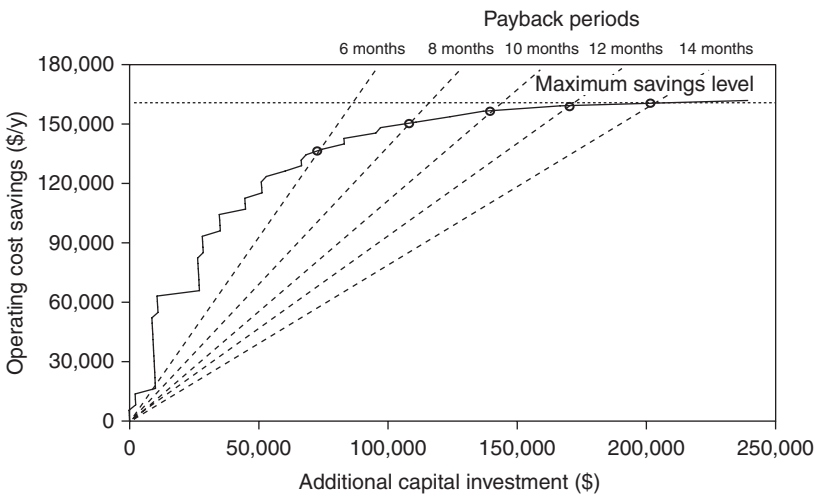

23.7 Savings–Investment Diagram for MENS.

on investment, as well as a maximum effluent reduction (which, as before, is limited by the thermodynamics of the system being considered) (Fraser and Hallale, 2000b). In this case it was also demonstrated that the effluent reduction and investment targets could be realised or closely approached in actual retrofit designs.

The Impact Diagram is a very powerful tool, which can be utilised to determine the maximum reduction in environmental impact using a particular technology. It can also be used to compare alternative technologies, both for retrofit and grass-roots designs. A three-way trade-off plot has also been

© Woodhead Publishing Limited, 2013

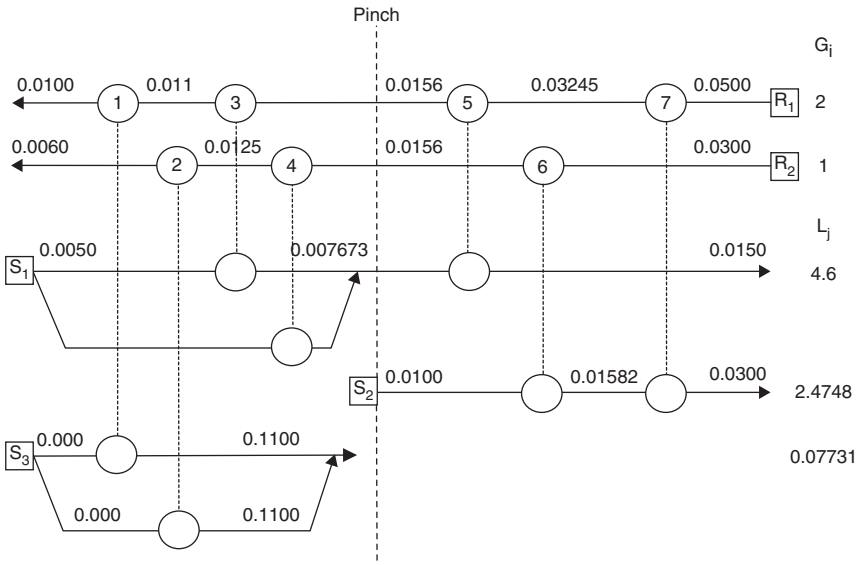

23.8 Retrofit design for the phenol problem.

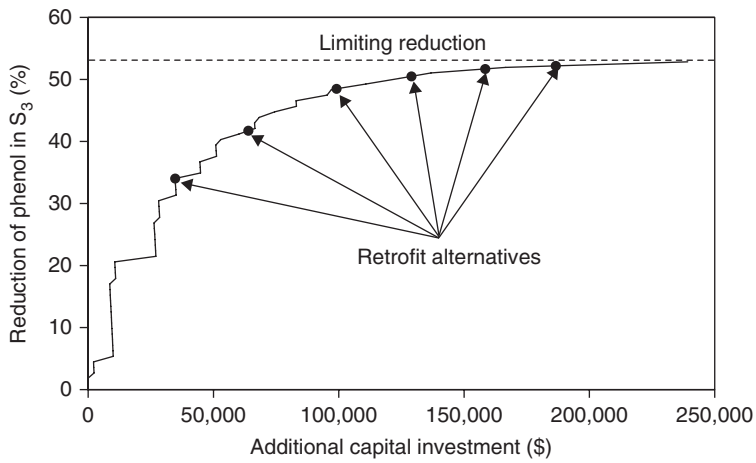

23.9 Impact diagram for MENS retrofit.

suggested for examining the trade-offs between operating cost reduction, reduction in environmental impact and capital investment.

The significance of this work is that it may be applied to retrofit situations to evaluate what could possibly be achieved by process changes. This is especially important, in so far as effluent reduction in existing processes is concerned, with the Impact Diagram and the thermodynamic limit being

© Woodhead Publishing Limited, 2013

particularly significant. It is envisaged that these techniques could be used to compare alternative technologies for effluent reduction, such as use of a different MSA in the same hardware, or use of a completely different system. Given the evidence so far that the targets can be achieved in actual designs, one need only compare alternatives on the basis of the targets, without having to perform designs for any of them.

23.3 Systems Studied: Venturi Scrubber System and Ethanolamine Absorber System

Two completely different systems are covered in this section. The venturi scrubber system (which has an unusual cross-flow configuration) will be dealt with first, followed by the more common ethanolamine absorber system.

23.3.1 Venturi Scrubber System

In the system under consideration, shown in Fig. 23.10, gas streams from seven different sources were combined and then split into four scrubbing units in which the hydrogen sulphide was removed before the combined gas stream from the four scrubbers was sent to incineration and then disposed of up a stack. Another stream also containing hydrogen sulphide (Stream 8) joined the combined exit stream from the four units (Stream 9) before the incinerator. This stream contained phenol and could not be treated in the four units.

Note that all these streams contain a high proportion of carbon dioxide (between 89% and 98%). The hydrogen sulphide absorbed in the four units is converted to sulphur and the solvent regenerated and returned to the scrubbers (note that Fig. 23.10 only shows the gas streams). Note also that the maximum flow to each of the units is 18.33% of stream 10, so that 22.46% of the combined stream bypasses the four units, as shown in Fig. 23.10.

Each of the four scrubbing units consisted of three venturi scrubbers, with the gas flowing through them in series and the liquid in parallel, as shown in

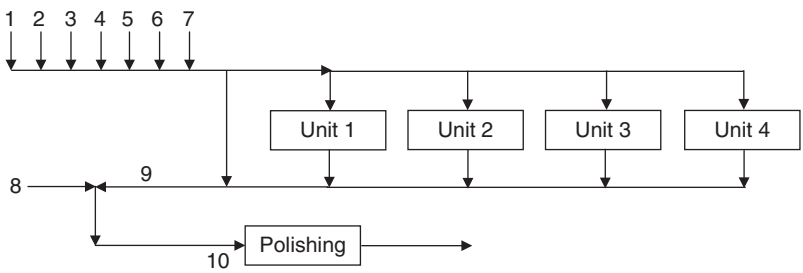

23.10 Sulphur recovery system.

© Woodhead Publishing Limited, 2013

Table 23.1 Stream flows and compositions

Stream	1	2	3	4	5	6	7	8	9	10
Flow (% of 10)	24.48	25.78	17.85	11.38	8.53	1.71	1.04	5.43	94.57	100.0
H_2S (%)	1.11	1.32	1.52	1.76	2.05	10.74	5.16	2.37	0.62	0.72

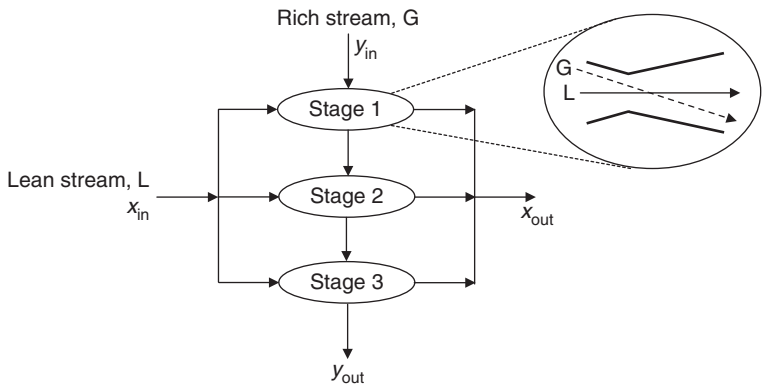

23.11 Arrangement of the three venturi scrubbers in each unit.

Fig. 23.11. The overall flow of gas and liquid though each unit is thus clearly cross-flow, while within each scrubber the gas and liquid flow together in a co-current manner (see Fig. 23.11 inset).

Nominal flows and hydrogen sulphide compositions for the eight feed streams are given in Table 23.1, together with the outlet composition of the scrubbing units (Stream 9) and the overall stream to the incinerator (Stream 10).

The objective of this study was to reduce the sulphur emission up the stack. Plant personnel were already investigating increasing the contact time in the scrubbers, as well as increasing the gas flow through the scrubbers, which was limited by the capacity of the exit cyclones. We decided to compare what could be achieved by segregation of the streams (instead of the current arrangement where they are all mixed together before going to the scrubbing units), and also to quantify the extent of reduction in sulphur emissions for increased gas flow.

The only data available for this study were the flows and compositions of all the feed streams to the process and the outlet compositions from the scrubbing units, the maximum flow to each of the units, and a relationship between unit throughput and absorption in it. Unfortunately, the solvent used in this system was a proprietary mixture, so equilibrium data for the system was not available.

© Woodhead Publishing Limited, 2013

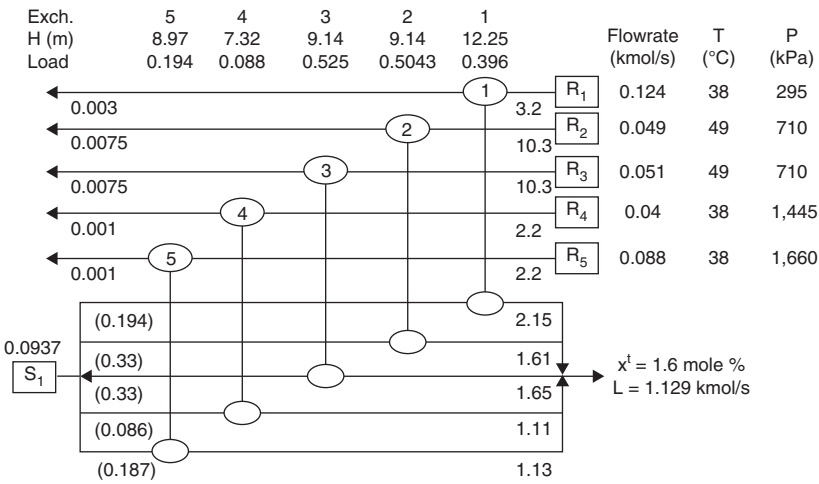

23.12 Original MEA system configuration.

23.3.2 Ethanolamine Absorber System

The second system chosen was an oil-refinery acid gas removal system. This consisted of two independent systems, one using mono-ethanolamine (MEA) and the other using di-ethanolamine (DEA). The one using MEA treated three gaseous streams and two liquid streams, and the one using DEA treated a fourth gaseous stream. In both systems, H_2S was the main acid gas being removed, but CO_2 was also present in two of the gaseous streams in the MEA system. Because the CO_2 was present in fairly low concentrations, it was assumed for the purposes of this study that H_2S was the dominant species being transferred, and that the CO_2 did not affect the H_2S equilibrium. Each system also included a regenerator for stripping off the acid gases, which were then sent to a Klaus unit for the recovery of sulphur.

Figure 23.12 shows the original MEA system configuration, and Fig. 23.13 shows the original DEA system configuration. These two figures contain all the specifications for these systems as well.

The challenge in setting up this problem was that each contactor was at a different temperature and pressure. This meant that there was a different equilibrium function for each contactor. Section 23.6.2 describes in detail how this problem was overcome in this study.

23.4 Pinch Approach

This section describes how the Pinch approach was applied to each of the two systems studied. In particular, the Pinch approach for the cross-flow system needed to be developed, and so this is dealt with first in some detail.

© Woodhead Publishing Limited, 2013

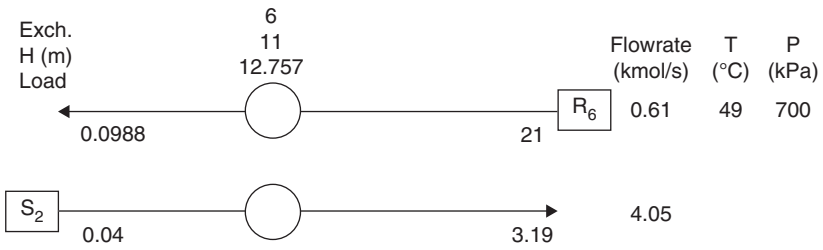

23.13 Original DEA system configuration.

23.4.1 Venturi Scrubber System

The approach we took to solving this problem was first of all to develop a model for the combined cross and co-current flows in each of the four scrubbing units. This model was then used to estimate a pseudo-equilibrium for the system, by fitting it to the plant's current operation (assuming the equilibrium to be linear). In doing this an efficiency was assumed for each of the venturi scrubbers, with a view to possibly estimating the effect of increased contact time. Where the flow to a unit exceeded the maximum specified, the balance was assumed to bypass it (as happens in the existing system). When the results obtained in this way were compared to the relationship between throughput and absorption, a discrepancy was found, which was accounted for by adjusting the relationship to fit the plant data (Fraser *et al.*, 2001a).

Analysis of Combined Cross and Co-current Flow System

In a co-current flow scrubber, standard analysis shows that the Operating Line has a slope of (–L/G) (Treybal, 1981). The system under consideration has three co-current flow scrubbers, with the gas flowing in series between them, and fresh regenerated liquid entering each scrubber (so the liquid is in cross-flow).

One approach to the analysis of co-current flow systems is presented in Fig. 23.14 (Fraser *et al.*, 2001b). Here a particular Minimum Driving Force has been assumed, which leads to a Pinch Line that is a fixed distance away from the Equilibrium Line, assumed to be a linear function. Figure 23.14 show how three stages with equal (low) flowrates may be used to achieve the same removal of a species as a single stage with a much higher flowrate. Note that the Operating Lines for the second and third scrubbers start at the unknown exit gas composition, y, of the preceding scrubber (Treybal, 1981).

The liquid flowing to each of the scrubbers had been optimised on the plant, and it had been found that the best arrangement was for the flow to the first scrubber to be twice the flow to the second and third scrubbers. The slope of the Operating Line for the first scrubber is therefore twice that of the other

© Woodhead Publishing Limited, 2013

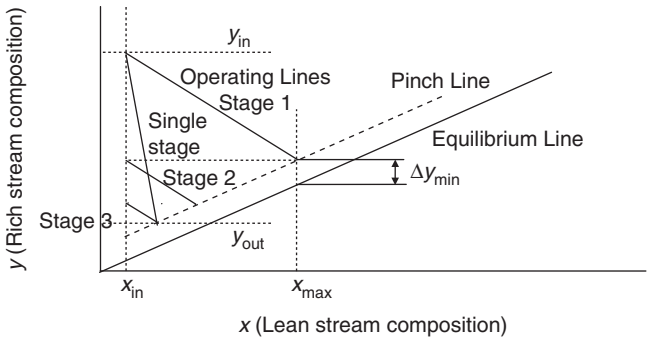

23.14 Co-current system with fixed minimum composition difference.

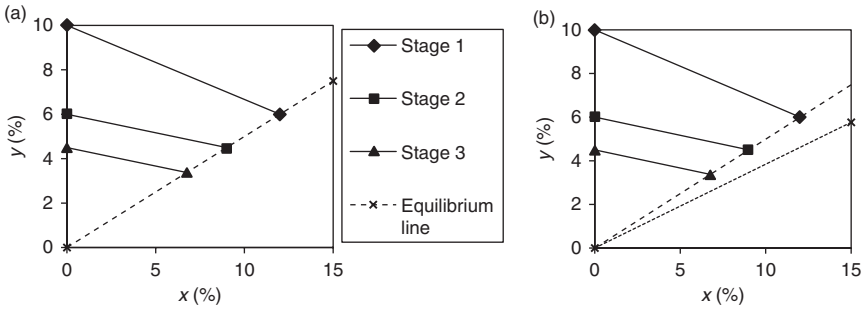

23.15 y–x diagram showing construction of Operating Lines: (a) 100% efficiency; (b) 80% efficiency.

two scrubbers. Figure 23.15a shows this system with each scrubber assumed to operate at 100% efficiency (i.e. the minimum composition difference is effectively zero). Knowing the inlet and outlet compositions from the unit as a whole, and the liquid and gas flows to each scrubber, one can postulate a linear Equilibrium Line, and then solve for the slope of the Equilibrium Line which intersects each of the three Operating Lines, as shown in Fig. 23.15a. This approach precluded investigating increase in contact time.

It is, however, more likely, given the short contact time in each scrubber, that they do not operate at equilibrium. Figure 23.15b shows the solution for this system if it is assumed that each stage operates at 80% efficiency, where it has been assumed that this means the final outlet composition from each stage may be obtained as 80% of the change that would have occurred if it had been at equilibrium. The results obtained were checked to see to what extent they were affected by the approach to equilibrium assumed, and it was found that they were independent of it. This is because the fitted Equilibrium Line simply shifts to accommodate the different efficiencies, as may be seen by comparing Fig. 23.15a with Fig. 23.15b, in which the only

© Woodhead Publishing Limited, 2013

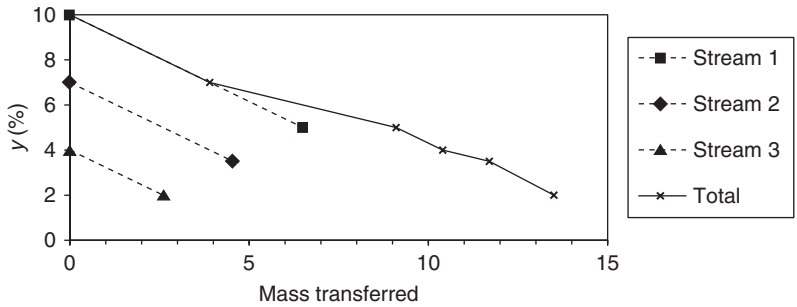

23.16 Mass Transfer Composite Curve for cross-flow system.

difference is that the slope of the Equilibrium Line in (b) is 80% of the slope in (a).

We are also given a relationship between % approach to equilibrium (A) and gas flowrate (Q), which we used with a correction factor (k) to check this analysis. This relationship was:

$$A = 100 \times k \times \left[1.03 - \exp\left(\frac{-1,925.61}{Q^{0.6014}} \right) \right]$$

where Q is in Nm^3/h and $k = 0.957$. In this way, we were able to match the result of the analysis, which led to an Equilibrium Line with a slope of 0.0113 and an approach to equilibrium of 63%, with the equation above.

Mass Transfer Composite Curve

A helpful way of comparing different options was developed by analogy with the Mass Transfer Composite Curve introduced by Hallale and Fraser (1998a) for counter-current flow systems. A typical Mass Transfer Composite Curve for cross-flow is shown in Fig. 23.16, for a system with three units, with each unit having a feed of different composition, and each one removing 50% of the transferred species. This figure plots rich stream composition against mass transferred, and is derived by vector addition of the individual mass transfer lines.

This Composite Curve was used as follows. The streams entering the four units were segregated and then different combinations were put together, so that each scrubber unit had a different feed. This was aimed at maximising mass transfer driving force, while maintaining a minimum flow close to the maximum flow though each of the four units. Any combined flow greater than the maximum was bypassed around the unit.

Fifteen different combinations of streams were tried. The best option out of the fifteen tried (i.e. the option with the highest increase in sulphur recovery)

© Woodhead Publishing Limited, 2013

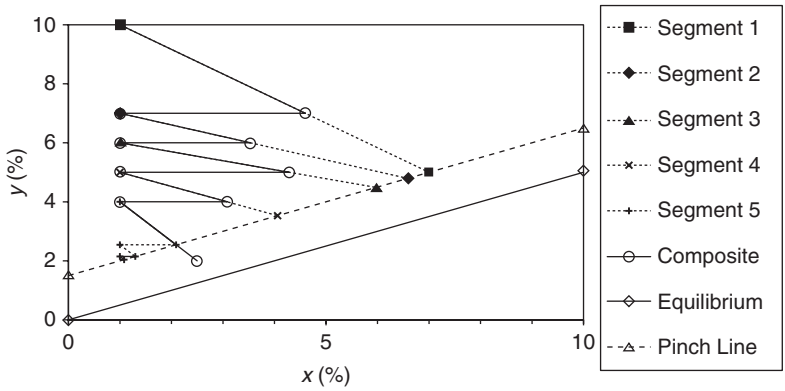

23.17 Stages targeting for co-current systems.

was then selected for further analysis. The first variation tried was changing the split ratio between the stages from 2:1:1 to 1:1:1, 3:1:1 and 1:2:2. The second variation was to include Stream 8 with two other streams to a unit that was below its capacity in the best option. This was to test whether it would be worthwhile to explore removing the phenol from this stream. The last variation was to increase the maximum flow through each unit by 15%, to see what incentive there might be to debottleneck the cyclones on the scrubbers.

This method requires some programming to produce the Mass Transfer Composite Curves, but it does provide a clear way of seeing which option will transfer the most mass. Figure 23.17 shows how the Mass Transfer Composite Curve for a co-current system can be used for determining the number of stages for a system that uses a particular minimum composition difference (Fraser *et al.*, 2001b). In Fig. 23.17 Segments 1 to 4 each represent a fraction of a stage, whereas Segment 5 crosses the Pinch Line and therefore requires multiple stages in order to achieve the required outlet concentration.

23.4.2 Ethanolamine Absorber System

The Pinch approach taken for this system was to first do a standard Pinch Analysis of the system, which led to the Supertargeting Curves for each of the two systems in use. This was followed by developing the Load–Height Diagram for each of the systems, which enabled us to identify the best retrofit path for each of the systems. This then led to the development of the Impact Diagram for each system, which showed the trade-off between additional capital investment and reduced operating cost (Fraser and Hallale, 2000a), and also the trade-off between capital investment and environmental impact (Fraser and Hallale, 2000b).

© Woodhead Publishing Limited, 2013

23.5 Hybrid Approach

This section deals with the hybrid approach that was used for the ethanolamine system, combining the Pinch approach with mathematical programming.

23.5.1 Rationale for Using the Hybrid Approach

The philosophy behind the integration is to combine the strengths of the Pinch Technology and Mathematical Programming approaches and by so doing hopefully avoid their weaknesses.

The Pinch Technology approach for MENs is given in Table 23.2, and the advantages and disadvantages of this approach are given in Table 23.3. Table 23.4 gives the Mathematical Programming approach, and Table 23.5 gives its strengths and weaknesses.

On the basis of the strengths and weaknesses of these two approaches given in Tables 23.3 and 23.5, the hybrid approach sought to maximise the strengths and minimise the weaknesses of both approaches, as shown in Table 23.6. Figure 23.18 shows how this was achieved. The problem of MINLP getting trapped in local optima was overcome by comparing the solution to the targets established by Pinch Technology. If the MINLP solution did not meet the criterion of a close approach to these targets,

Table 23.2 Pinch Technology approach

Establish targets	Find MSA target, and hence annual operating cost target
	Find network capital cost target, and hence annual capital cost target
	Find optimum minimum composition difference at the lowest TAC (Supertargeting)
Design to meet targets	Design Above and Below Pinch separately to ensure MSA target is met, working away from the Pinch in both cases
	Apply heuristics to achieve minimum number of exchange units and approach capital cost target
	Evolve network to trade-off decreased capital cost and increased operating cost

Table 23.3 Pinch Technology advantages and disadvantages

Strengths	Easy to understand and implement
	Designer remains in control
	Can readily take advantage of insights
Weaknesses	Difficult to handle large systems if not supported by proper software tools (however similar problem for mathematical programming occurs)
	Multicomponent systems not readily handled (especially if species interact)

© Woodhead Publishing Limited, 2013

Table 23.4 Mathematical programming approach

Set up a superstructure	This must contain all possible options
	Set up the optimisation procedure
Initialise the network	Start from a feasible solution
Run the optimisation (MINLP)	MILP master program for structure
	NLP primal problem for operating and sizing parameters
Check that the solution is not trapped in a local optimum	This may be done by starting from different initial points

Table 23.5 Strengths and weaknesses of mathematical programming approach

Strengths	Simultaneous optimisation and design
	Handling of multicomponent problems
	Handling of large problems
Weaknesses	Getting trapped in local optima
	Handling of discontinuities
	Handling of Integral numbers of stages
	Time and expertise needed to set up problems

Table 23.6 The hybrid approach

Avoid problems	Pinch approach	Difficult to handle large problems
	Mathematical programming	Getting trapped in local optima
Best of both worlds	Pinch approach	Targets DFP
	Mathematical programming	Ability to handle large problems if supported by powerful software tools

then the DFP was used to re-initialise the model. The details of this are discussed below.

23.5.2 Detailed Steps Involved

In following the algorithm set out in Fig. 23.18, the following steps were undertaken:

1. Determine the Pinch Targets

This was done using the standard Pinch methods developed by El-Halwagi and Manouthiosakis (1989) for MSA Targeting and Hallale and Fraser (2000b) for capital cost targeting.

© Woodhead Publishing Limited, 2013

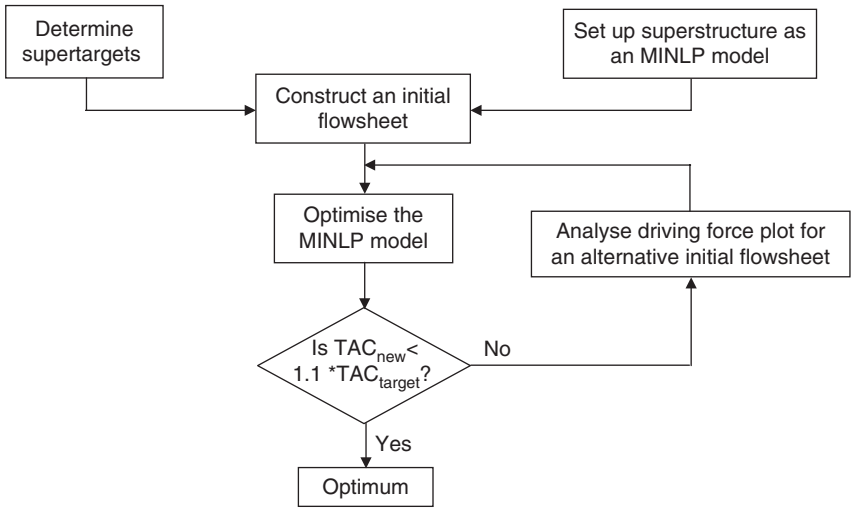

23.18 The philosophy of the hybrid synthesis method.

2. Perform Supertargeting to find the optimum minimum composition difference

The minimum composition difference was varied over an appropriate range, and for each value the TAC was calculated and then plotted against the minimum composition difference. The optimum minimum composition difference was then the value at the minimum TAC (Hallale and Fraser, 2000c).

3. Set Up MINLP Superstructure

The superstructure was set up in GAMS as an MINLP that was optimised using the TAC as the objective function. The basis for the superstructure was the hyperstructure of Papalexandri *et al.* (1994).

4. Construct Initial Flowsheet

The initial structure is generated in two different ways:

- A network in which the mass exchange duty is effected by external MSAs alone (this approach is analogous to a HEN where the heating and cooling duties are completed by utilities such as steam or cooling water), or
- A Pinch-based solution found using the approach listed in Table 23.2.

© Woodhead Publishing Limited, 2013

5. Optimise MINLP Model

Once an initial solution is incorporated into the MINLP model, the model is solved via the DICOPT solver employing the Outer Approximation algorithm for Equality Relaxation and Augmented Penalty (OA/ER/AP).

6. Check Optimum TAC against Target

If the optimum is close enough to the target, the solution is stopped. The following rationale was used to determine how to define 'close enough'. Most MINLP-models are non-convex and their solutions are not guaranteed to be global; therefore, total cost can be used to measure the optimality of MENs generated by MINLP. The installed cost of process units is commonly estimated from cost charts and cost indices, which estimate the costs within 20–30%. These costs are then annualised by factors in the range 20–40%, before being added to annual operating cost to give TACs. This means that a 10% approach of the TAC targets can be regarded as being optimal. In the hyperstructure model of Papalexandri *et al*. (1994) we incorporated physically meaningful structures to initialise the MINLP solver.

7. Use DFP to Generate a New Initial Flowsheet and Return to Step 5

If the optimum is not close enough to the target we use the DFP to generate an alternative flowsheet and returned to Step 5. If the resulting solution does not meet the 10% TAC margin, an alternative initial flowsheet is presented to the MINLP solver. A Driving Force Diagram is used to help the designer identify the regions in the reported network that do not make appropriate use of the available driving force. The model is then solved with the new initial flowsheet and if the solution is within the target margin, it is accepted as an optimal solution.

23.6 Solution Equilibria

Solution equilibria were needed to solve both systems studied. This section covers how these were established, focusing mainly on the ethanolamine system which required the greatest effort.

23.6.1 Fitting Actual Data for Scrubber System

The solvent used in the venturi scrubbers was a proprietary mixture, so there was no equilibrium data available. The approach taken was to fit the scrubber actual performance to an assumed linear equilibrium relationship. The way this was done is closely linked to the modelling of this system, which is described in detail in the section 'Analysis of combined cross and co-current flow system' above. In this way we were able to obtain an equilibrium relationship that was a good representation of the solvent being used.

© Woodhead Publishing Limited, 2013

23.6.2 Equilibrium Relationships for MEA and DEA Solutions

The challenge in finding appropriate relationships for the H_2S equilibria in the MEA and DEA solutions being used was that each of the absorbers operated at a different temperature and pressure, apart from the two absorbers treating the liquid streams, which operated under the same conditions. It should be noted that this system is not pure physical absorption, but absorption with chemical reaction. We also needed to find relationships for both MEA and DEA for all the operating conditions so that alternative configurations could be investigated.

We accordingly used a thermodynamic model for the prediction of partial pressures of acid gases over different alkanolamine solutions developed by Deshmuk and Mather (1981). This model is based on the Debye–Huckel theory of electrolyte solutions, and takes into account the fugacity and activity coefficients of the reacting species. In order to develop the required relationships, the following steps were followed:

1. Operating conditions were specified, including the ethanolamine solution concentrations.
2. The activity and fugacity coefficients were determined from equations of state and the interaction parameters of the dominant species from the Debye–Huckel Law.
3. The molalities of the species were obtained by solving the mass balances and chemical equilibria for the reacting species.
4. The molalities of the acid gases were converted to liquid mole fractions.
5. The partial pressures of the acid gases in the gas phase were converted to gas mole fractions.
6. Convex power functions were fitted to the sets of data generated in this way, for both H_2S and CO_2 in both MEA and DEA, under all the required operating conditions.

Table 23.7 shows the equilibrium functions generated in this way for H_2S in both MEA and DEA for the specific operating conditions of each of the absorbers. The coefficient in these expressions is a function of pressure and the exponent is a function of temperature. We assumed in the analysis that follows that the CO_2 absorption did not affect the H_2S absorption, and could therefore be ignored. Note that the temperatures and pressures are those at the top of each absorber where the fresh regenerated ethanolamine solution contacts the process stream leaving the absorber. The process streams generally entered the absorbers at temperatures higher than the ethanolamine solution and cooled down to the solution temperature in the absorber.

© Woodhead Publishing Limited, 2013

Table 23.7 Equilibrium functions for H_2S for each of the streams

Stream	Type	T(K)	P(kPa)	H_2S-MEA	H_2S-DEA
R1	Gas	311	295	$y = 0.1773\ x^{1.8039}$	$y = 2.6341\ x^{2.1487}$
R2 and R3	Liquid	322	710	$y = 0.1038\ x^{2.412}$	$y = 1.035\ x^{2.0584}$
R4	Gas	311	1,445	$y = 0.0362\ x^{1.8039}$	$y = 0.5378\ x^{2.1487}$
R5	Gas	311	1,660	$y = 0.0315\ x^{1.8039}$	$y = 0.4681\ x^{2.1487}$
R6	Gas	322	4,760	$y = 0.01549\ x^{2.412}$	$y = 0.1545\ x^{2.0584}$

23.7 Results and Discussion

In this section, the results of the approaches taken to retrofitting the two systems studied are discussed.

23.7.1 Venturi Scrubber System

The methods described above were used to determine the reduction in sulphur emissions (in the form of sulphur dioxide) due to enhanced sulphur recovery, for different retrofit possibilities.

It was found that segregation of the streams before scrubbing (rather than mixing them all together) gave a definite increase in sulphur recovery. The best option found was Option 7, in which Stream 1 went on its own to Unit 1, Streams 2 and 7 went together to Unit 2, Streams 3 and 6 went to Unit 3, and finally Streams 4 and 5 went to Unit 4. In each unit the gas flow exceeded the capacity of the units, and the extra gas flow was bypassed around the units. This configuration gave a 10.5% increase in sulphur recovery. Figure 23.19 compares the Mass Transfer Composite Curve for the original configuration with that for Option 7. This shows clearly the improved sulphur recovery of 10.5% for Option 7 compared to the original configuration.

Using this option, the liquid split to the three stages in each unit was varied. This indicated that the present 2:1:1 split could be improved, and that, in fact, for the best segregation option, a split of 1:1:1 gave a further 2.4% increase in sulphur recovery.

Another possibility that was examined was the effect of including Stream 8 (the one containing phenol) in the scrubbing system (presuming that the phenol could be removed and therefore that it had been removed). This indicated that a maximum sulphur recovery increase of 8.8% was possible. This is less than the best option without including this stream, so there does not appear to be any incentive to remove the phenol so that Stream 8 can be sent to the scrubbing units.

The final possibility considered was debottlenecking the cyclones to allow a larger gas flow through the scrubbing units. It was found that a 15%

© Woodhead Publishing Limited, 2013

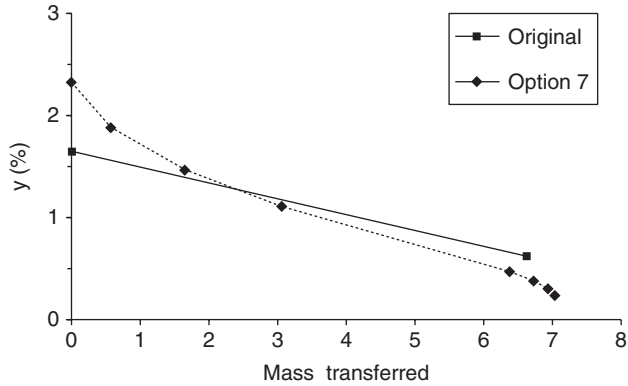

23.19 Mass Transfer Composite Curve for Option 7.

increase in throughput (for the best segregation option) would result in an additional 11.6% increase in sulphur recovery. There is therefore a good incentive to increase the cyclone capacity.

23.7.2 Ethanolamine Absorber System

The Pinch approach for this system did not yield any helpful results, so none are presented here. We will focus instead on the results of the hybrid approach. In analysing this system we examined the range of options shown in Table 23.8. Each of the alternatives was solved in the manner described in Section 23.5.2.

Table 23.9 shows the results of optimising each of the options studied. As may be seen from these results, the DEA system is operating close to the optimum, whereas the flowrate of the MEA can be reduced considerably, with a concomitant reduction in operating cost that would easily justify the capital cost required. The three options of using only MEA, only DEA and swopping them around do not seem to have yielded viable solutions. The best option seems to be allowing only one of the ethanolamines to be used, in which case only MEA is used and the operating cost is reduced very significantly, with a lower capital cost requirement than for optimisation of the separate systems. The optimum design for Option 5 is shown in Fig. 23.20.

The two options selected would need to be checked out more carefully to see if what has been identified in this study will actually prove viable. Issues to be resolved are how the reduced solvent flowrates would affect the performance of the columns, and whether one could only operate one of the regeneration columns. Other issues that arose during this study were the level of regenerated DEA, and the impact of plant layout on the designs.

© Woodhead Publishing Limited, 2013

Table 23.8 Options studied using hybrid approach

Option	Configuration
0	Present system without any changes
1	Optimisation of separate systems, including flowrates and column sizes
2	Optimisation of system using only MEA
3	Optimisation of system using only DEA
4	Optimisation with swopping MEA and DEA systems
5	Optimisation allowing either MEA or DEA in all contactors

Table 23.9 Results of the optimisation

Option	Capital cost ($)	Operating cost ($/y)	MEA usage (m^3/h)	DEA usage (m^3/h)
0 Original	–	2,656,000	83,900	29,800
1 Separate systems	644,000	1,364,000	24,100	28,900
2 Only MEA	352,000	2,412,000	111,800	0
3 Only DEA	638,000	2,995,000	0	104,800
4 Swop	661,000	2,751,000	27,900	75,000
5 Either	530,000	776,000	35,400	0

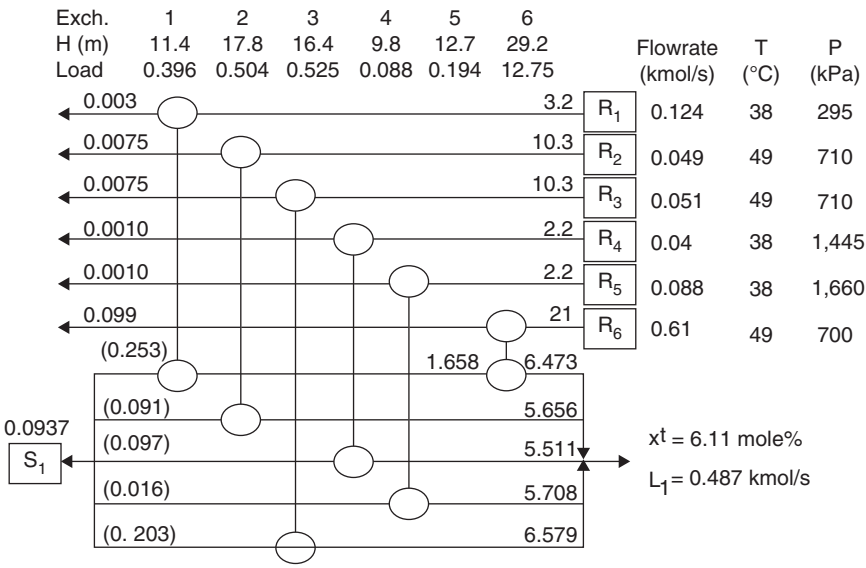

23.20 Optimal system configuration using only MEA (Option 5).

© Woodhead Publishing Limited, 2013

23.8 Conclusions and Sources of Further Information

Two diagrams are presented for the modelling and analysis of the combined cross and co-current flow venturi scrubber unit examined in this case study: one is the y–x diagram for a combined cross and co-current flow system, and the other is the Mass Transfer Composite Curve for such a system. These diagrams enabled us to examine a range of retrofit options to improve the sulphur recovery in these units.

This approach of using the y–x diagram and the Mass Transfer Composite Curve is recommended for design and analysis of similar cross and co-current flow absorption systems. I would also recommend that in general, whenever streams of different compositions are to be treated for removal of acid gas or other pollutants, they should not be mixed before treatment, but rather treated separately to take advantage of better driving forces.

This chapter has presented and tested a design philosophy for the synthesis of MENs whereby an MINLP approach is integrated with Pinch Analysis tools. At the heart of the integration is the use of Pinch-based total cost targets to evaluate the optimality of MINLP solutions and Driving Force Diagrams to identify different initial solution structures.

I would recommend that an acid gas treatment system, such as one in a refinery with multiple streams requiring acid gas removal, should be optimised as whole system, and not just as a set of individual units. This will probably require a systems approach using mathematical programming, possibly in conjunction with Pinch Analysis, as demonstrated in the hybrid approach used in this case study.

Where equilibrium relationships are not available for the modelling and optimisation of such systems (particularly where proprietary solvents are being used), these need to be approximated as done in these case studies in order to be able to perform system-wide optimisation.

For more information on the specific ways to solve particular problems, the reader is referred to the references given in Sections 23.2, 23.3 and 23.4.

23.9 Acknowledgements

The work reported in this chapter was largely done by students under the author's supervision. The author would particularly like to acknowledge the sterling work done by Natasha Harding and Carol Matthews on the Pinch Studies and by Andrew Msiza on the hybrid approach.

The author also wishes to acknowledge the collaboration and support of Caltex (now Chevron) and Sasol Technology staff in this study, particularly Mr Bradford Plaatjes and Mr Matthew Marx of Chevron and Mr Vian Smith and Mr Daan le Roux of Sasol.

© Woodhead Publishing Limited, 2013

23.10 References

Brooke, A., Kendric, D., Meeraus, A. (1988). *GAMS, A User's Guide.* The Scientific Press, San Fransisco, USA.

Cerda, J., Westerberg, A. W., Mason, D., Linnhoff, B. (1983). Minimum utility usage in heat exchanger network synthesis-a transportation problem. *Chemical Engineering Science*, **38**, 373–387.

Chen, C.-L., Hung, P.-S. (2007). Synthesis of flexible heat-exchange networks and mass exchange networks. *Computers & Chemical Engineering*, **31**, 1619–1632.

Chen, C.-L., Hung, P.-S. (2005a). Simultaneous synthesis of mass exchange networks for waste minimisation. *Computers & Chemical Engineering*, **29**, 1561–1576.

Chen, C.-L., Hung, P.-S. (2005b). Retrofit of mass exchange networks with superstructure-based MINLP formulation. *Industrial & Engineering Chemistry Research*, **44**, 7189–7199.

El-Halwagi, M. M. (1997). *Pollution Prevention Through Process Integration*. Academic Press, San Diego, USA.

El-Halwagi, M. M., Manousiouthakis, V. (1989). Synthesis of mass exchanger networks. *AIChE Journal*, **35**(8), 1233–1244.

El-Halwagi, M. M., Manousiouthakis, V. (1990), Automatic synthesis of mass exchange networks with single component targets. *Chemical Engineering Science*, **45**(9), 2813–2831.

Fraser, D. M., Hallale, N. (2000a). Retrofit of mass exchange networks using pinch technology. *AIChE Journal*, **46**(10), 2112–2117.

Fraser, D. M., Hallale, N. (2000b). Determination of effluent reduction and capital cost targets through pinch technology. *Environmental Science & Technology*, **34**(19), 4146–4151.

Grossmann, I., Daichendt, M.M. (1996). New trends in optimization-based approaches to process synthesis. *Computers & Chemical Engineering*, **20**(6–7), 665–683.

Hallale, N. (1998). Capital cost targets for the optimum synthesis of mass exchange networks. PhD thesis, University of Cape Town, South Africa.

Hallale, N., Fraser, D. M. (1998). Capital cost targets for mass exchange networks. A special case: water minimisation. *Chemical Engineering Science*, **53**(2), 293–313.

Hallale, N., Fraser, D. M. (2000a). Capital and total cost targets for mass exchange networks, Part 1: simple capital cost models. *Computers & Chemical Engineering*, **23**(11–12), 1661–1679.

Hallale, N., Fraser, D. M. (2000b). Capital and total cost targets for mass exchange networks, Part 2: detailed capital cost models. *Computers & Chemical Engineering*, **23**(11–12), 1681–1699.

Hallale, N., Fraser, D. M. (2000c). Supertargeting for mass exchange networks: Part I – targeting and design techniques. *Transactions of IChemE* (Part A), **78**(Mar), 202–207.

Hallale, N., Fraser, D.M. (2000d). Supertargeting for mass exchange networks, Part II: applications. *Transactions of IChemE*, **78**, Part A, 208–216.

Harding N., Matthews C. (1999). Retrofit design of mass exchange networks. Undergraduate Project, Department of Chemical Engineering, University of Cape Town, South Africa.

Isafiade, A. J., Fraser, D. M. (2008a). Interval based MINLP superstructure synthesis of heat exchange networks. *Chemical Engineering Research and Design*, **86**(3), 245–257.

Isafiade, A. J., Fraser, D. M. (2008b). Interval based MINLP superstructure synthesis of mass exchange networks. *Chemical Engineering Research and Design*, **86**(8), 909–924.

© Woodhead Publishing Limited, 2013

Isafiade, A. J., Fraser, D. M. (2009a). Interval based MINLP superstructure synthesis of combined heat and mass exchanger networks. Chemical Engineering Research and Design, **87**(11), 1536–1542.

Isafiade, A. J., Fraser, D. M. (2009b). Interval based MINLP superstructure synthesis of multi-period mass exchanger network. Chemical Product and Process Modeling, **4**(5), Article 14. DOI: 10.2202/1934–2659.1405 <www.bepress.com/cppm/vol4/iss5/14> accessed 16 February 2012.

Isafiade, A. J., Fraser, D. M. (2010). Interval based MINLP superstructure synthesis of heat exchanger networks for multi-period operations. *Chemical Engineering Research and Design*, **88**(10), 1329–1341.

Kravanja, Z., Glavic, P. (1997). Cost targeting for HEN through simultaneous optimization: a unified pinch technology and mathematical programming design of large HEN. *Computers & Chemical Engineering*, **21**(8), 833–853.

Msiza, A. K. (2002). Hybrid synthesis method for mass exchange networks. MSc Dissertation, University of Cape Town, South Africa.

Papalexandri, K. P., Pistikopoulos, E. N., Floudas, C. A. (1994). Mass exchange networks for waste minimisation: a simultaneous approach. *Transactions of IChemE* (Part A), **72**, 279–294.

Papoulias, S. A., Grossmann, I. E. (1983). A structural optimization approach to process synthesis-II. Heat recovery networks. *Computers & Chemical Engineering*, **7**, 707–721.

Szitkai, Z., Farkas, T., Lelkes, Z., Fonyo, Z., Kravanja, Z. (2006). Fairly linear mixed integer nonlinear programming model for the synthesis of mass exchange networks. *Industrial & Engineering Chemistry Research*, **45**, 236–244.

Tjoe, T. N., Linnhoff, B. (1986). Using pinch technology for process retrofit. *Chemical Engineering,* April 28, 47–60.

Treybal, R. E. (1981). *Mass Transfer Operations*, 3rd ed. McGraw-Hill, Singapore.

Wang, Y., Smith, R. (1994). Wastewater minimisation. *Chemical Engineering Science*, **49**, 981–1006.

Yee, T. F., Grossmann, I. E. (1990). Simultaneous optimization models for heat integration-II. Heat exchanger network synthesis. *Computers & Chemical Engineering*, **14**(10), 1165–1184.

23.11 Appendix: Nomenclature

A	approach to equilibrium (%)
Composition–Pickup Diagram	diagram in which the composition of the Composite Operating Line, corrected for the minimum composition difference, is plotted against the amount of mass picked up by the lean stream. The Equilibrium Line of the material being transferred to the lean stream is also plotted on this diagram. The Pinch Point is where these two lines touch.
k	correction factor (-)
Q	gas flowrate (Nm^3/h)
x'	composition with minimum driving force subtracted ($= x - \varepsilon$)

© Woodhead Publishing Limited, 2013

24

Applications of Pinch Technology to Total Sites: A Heavy Chemical Industrial Complex and a Steel Plant

KAZUO MATSUDA, Chiyoda Corporation, Japan

DOI: 10.1533/9780857097255.5.752

Abstract: This chapter discusses an energy-saving study based on a Total Site approach, as applied to one of the biggest heavy chemical complexes in Japan and to a large-scale steel plant. The study is based on Pinch Technology using Total Site Profile (TSP) analysis and R-curve analysis. It became apparent that the available Pinch Technology tools and techniques lend themselves very well in the analysis of large-size complexes and steel plants, and it also became clear that there is still a potential for huge energy savings by adopting this approach even though the process systems and plants under study are already extremely efficient. This chapter also describes the practical area-wide energy-saving projects that have resulted from this approach.

Key words: Total Site approach, Total Site Profile analysis, R-curve analysis, heavy chemical complex, steel industry.

24.1 Introduction

The history and the development of Process Integration have been described in detail in Part I (Chapter 1) and Part II (Chapters 4–8). Just as a brief reminder of the history of the development: Linnhoff *et al.* (1982) introduced the concept of 'target before design' in the 1980s, using Pinch Technology for the design of individual processes, and Linnhoff and Hindmarsh (1983) developed Pinch Technology for Heat Exchanger Network (HEN) design. Linnhoff and Ahmad (1990) and Ahmad *et al.* (1990) then evolved the methodologies to incorporate total cost targeting and block-decomposition-based HEN synthesis. Later, a HEN retrofit framework was established based on the 'Process Pinch' (Tjoe and Linnhoff, 1986) and 'Network Pinch' (Asante and Zhu, 1996) concepts. Over time, Pinch Technology has been applied to increasingly large and complex sites. To facilitate this, a variety of tools and techniques have been developed to enhance the methodology and simplify the analysis. This Total Site study, which uses TSP (Klemeš *et al.,* 1997) analysis and R-curve analysis (Kimura and Zhu, 2000), considers the

© Woodhead Publishing Limited, 2013

largest energy-consuming areas, such as a heavy chemical complex and a steel plant. The above-mentioned developments provide background to the successful application of Pinch Technology to these areas.

24.2 Case Study of a Heavy Chemical Complex

The Total Site study demonstrates that, despite the very high energy efficiency of the individual sites in the complexes, there is a huge amount of energy-saving potential through energy-sharing projects across various sites. Such a Total Site study is based on Matsuda *et al.* (2009) and is described within this section.

24.2.1 Study Basis

The heavy chemical complex under study in Japan has 17 sites, consisting of process industries including petrochemicals, a refinery, a power company, and others. There is a joint thermal power plant supplying heat and power to all the sites and, therefore, the individual sites do not have any boilers or gas turbines. Data were collected on the utility systems and on 532 heat exchangers, including 170 heaters (heat duty; 2,650 GJ/h) and 362 coolers (7,275 GJ/h).

24.2.2 Total Site Profile (TSP) Analysis

The utility system consisting of a number of process plants has to be understood and optimised in the context of the Total Site. A graphical method, so-called Site Profiles, was first introduced by Dhole and Linnhoff (1993) and Raissi (1994). This methodology was considerably extended to site-wide applications by Klemeš *et al.* (1997). Heat recovery data for individual processes are first converted to Grand Composite Curves (GCC) and the GCCs are combined to form a Site Heat Source Profile and a Site Sink Profile. These two profiles form a TSP, analogous to the Composite Curves for the individual processes and showing the energy and heat utilisation profile of the whole plant. TSP analysis can identify the opportunities for Inter-Process Integration via the utility system and the preparation of the appropriate integration strategy.

24.2.3 R-curve Analysis

A method for analysing and optimising energy systems was developed by Kimura (1998). This method builds on the concepts of the R-curve by Kenney (1984) and Top-Level Analysis by Makwana *et al.* (1998). Kimura and Zhu (2000) further developed the R-curve analysis method to determine the most economic modifications that could be made to existing utility

© Woodhead Publishing Limited, 2013

systems. The R-curve provides a target for the efficiency of a utility system by converting fuel energy into power (*W)* and heat (Q_{heat}). The integrated energy efficiency (Equation [24.1]), which is the fuel utilisation efficiency, is defined as a ratio of the useful part of energy and the integrated energy consumption (Q_{fuel}). The shape of the R-curve is determined by the fact that the production of shaft power from fuel energy requires a heat sink. In an integrated site the process plant acts as the heat sink for power generation. The larger the heat demand relative to power demand, the more efficient the overall generation becomes. This is represented by the R-ratio – the ratio of power-to-heat demand from the process (Equation [24.2]) at the operating condition of the site.

$$\text{Integrated energy efficiency} = \frac{W + Q_{heat}}{Q_{fuel}} \quad [24.1]$$

$$\text{R-ratio (power-to-heat ratio)} = \frac{W}{Q_{heat}} \quad [24.2]$$

24.2.4 Results

TSP Analysis

Figure 24.1 shows the result of TSP analysis, which reveals that unutilised exhaust heat exists in the region between 100°C and 150°C. Two kinds of energy-saving potential are identified on the left side of Fig. 24.1: (1) recovery of low pressure steam at 0.3 MPaG, equivalent to 1.5×10^6 GJ/y, and (2) recovery of a combination of very low pressure steam at 0.1 MPaG and hot water, which is equivalent to 1.0×10^6 GJ/y. In total, a combined 2.5×10^6 GJ/y of energy-saving potential can be achieved by the recovery of such heat.

R-curve Analysis

The existing utility system in this complex comprises boilers and steam turbines, but no gas turbines, and all heat and power are provided by the utility plants within the complex. Figure 24.2 shows the result of R-curve analysis for the existing utility consumption, in which it can be seen that the efficiency of the utilities at the current point is close to the theoretical curve for a B (boiler) + BPT (back pressure turbine) + CT (condensing turbine) system. This suggests that the use and generation of steam is quite efficient. However, the lack of gas turbines in the utility plant results in an efficiency gap, as the B + BPT + CT line is substantially below the upper line that can be achieved in gas turbine (GT) combined systems. The introduction

© Woodhead Publishing Limited, 2013

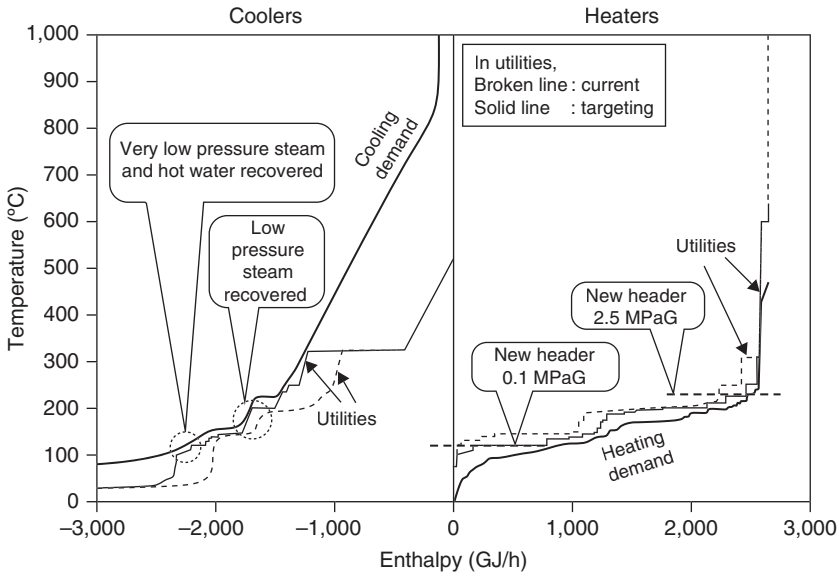

24.1 TSP analysis for a heavy chemical complex.

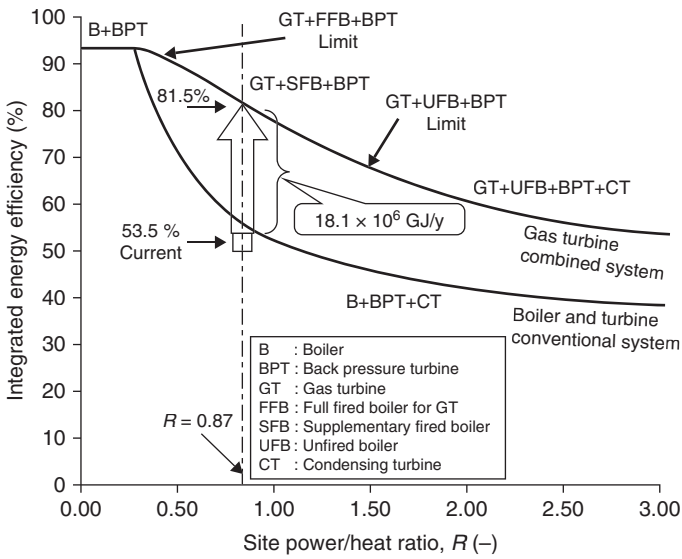

24.2 R-curve analysis for a heavy chemical complex.

of the ideal 'GT combined system' is able to increase the integrated energy efficiency from 53.5% to 81.5% while the present heat and power demands remain constant. This saving potential is equivalent to 18.1×10^6 GJ/y. The parameters for the R-curve analysis are shown in Table 24.1. The R-curve

© Woodhead Publishing Limited, 2013

Table 24.1 Parameters for R-curve analysis for a heavy chemical complex

W, kW	453,673
Q_{heat}, GJ/h	1,878
Q_{fuel}, GJ/h	6,569
Integrated energy efficiency, %	53.5
Site power/heat ratio (R)	0.87

Table 24.2 Result of energy-saving studies for a heavy chemical complex

	× 10^6 GJ/y
Number of sites	17 sites
Integrated energy consumption (Q_{fuel})	52.6
Energy-saving potential by TSP analysis	2.5
Energy-saving potential by R-curve analysis	18.1

target is based on a newly installed GT combined system generating 4 MPaG steam matching existing middle pressure steam (MPS) conditions. This is because not much supplementary firing would be needed at the R-ratio in question, so the exhaust temperature may not always be at a sufficiently high level for the generation of high-pressure steam (HPS) of 12 MPaG.

Amount of Theoretical Energy-Saving Potential

It became clear as a result of the TSP and R-curve analyses that there is a huge amount of energy-saving potential, as summarised in Table 24.2. The theoretical energy-saving potential is 2.5 × 10^6 GJ/y by TSP analysis and 18.1 × 10^6 GJ/y by R-curve analysis, and the sum of potentials is equivalent to 39% of the integrated energy consumption. This suggests that a huge amount of energy-saving potential exists in highly efficient process plants and that installing new headers, such as 2.5 MPaG and 0.1 MPaG as shown on the right side of Fig. 24.1, can theoretically yield 44.2 MW of power generation. This power generation has not been included in the total area-wide potential, because it does not result in less energy consumption but only in more effective conversion of fuel into power.

24.2.5 Energy-Saving Projects

Integration across Two Sites

A number of ideas for area-wide integration project have been identified as a result of this study. For example, adjacent sites X and Y have air fin coolers

© Woodhead Publishing Limited, 2013

on the hot process streams and new steam generators have been installed. The recovered low pressure steam at 0.2 MPaG is collected and sent to a new condensing turbine at site X, where it will be used to generate 3.5 MW of electricity to be shared by the two sites in proportion to the amount of steam generated by each site.

Achieving Theoretical Energy Saving

A 300 MW GT combined system would achieve the theoretical energy saving proposed by R-curve analysis by providing 18.1×10^6 GJ/y of energy saving.

24.3 Case Study of a Steel Plant

A steel plant consumes a huge amount of energy. Studies have been undertaken for many years on energy saving, and a great deal of equipment has also been introduced to significantly improve energy efficiency. Bisio and Rubatto (2000) studied the energy saving in coke-oven plants. Chan *et al*. (2010) found the huge energy-saving potential in the Taiwanese iron-and-steel industry. The renewable energy would be a significant reduction in CO_2 emission from the steel industry (Xu and Cang, 2010). These approaches concentrated on the study of individual process systems (Worrell *et al*., 2001) but a Total Site approach has not previously been considered by cited works. Pinch Technology needs and makes use of the data obtained from the heat exchangers in the pressurised system of a heavy chemical complex. However, most process systems in a steel plant are operated under atmospheric pressure, and the concept of using heat exchangers for heat recovery in a steel plant is barely recognised, despite improved heat recovery systems. Pinch Technology is based on using data obtained from heat exchangers. In order to analyse the heat recovery systems in a steel plant when applying Total Site approach, data equivalent to that obtained from heat exchangers are a basic requirement. It was, therefore, necessary to establish a procedure for the retrieval of such data in a steel plant and it is important that the procedure should be able to analyse and understand how the heat is utilised in each process system. A Total Site approach study for a steel plant, based on the study (Matsuda *et al*., 2012), is described in this section.

24.3.1 Study Basis

The study was undertaken on a large steel plant with an annual production capacity of 8,000,000 t of crude steel. An adjacent thermal power plant receives fuel gas as a by-product of the steel plant and supplies generated electricity and heat back to the steel plant. Most of the process systems in

© Woodhead Publishing Limited, 2013

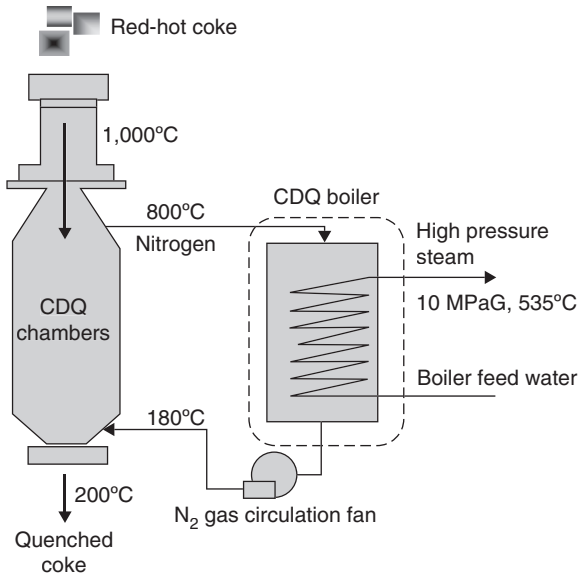

24.3 CDQ unit.

a steel plant are operated under atmospheric pressure and heat exchangers are not much used despite improved heat recovery systems. The heat in each process is utilised as follows. Figure 24.3 shows a coke dry quench (CDQ) unit, one of the most effective heat recovery systems, which is equipped with a coke-oven process (one of the major processes in a steel plant). This unit cools the red-hot coke from the coke oven while recovering its heat. The red-hot coke (1,000°C) in the recovery system is initially charged into the CDQ chambers (sealed vessels) and the heat is recovered by an inert gas (nitrogen), which is heated to about 800°C. The hot nitrogen is then introduced into the CDQ boiler (waste heat boiler) to produce HPS. Finally the very high temperature coke produces HPS through the nitrogen. There are two heat exchanging systems in the CDQ unit, the CDQ chamber and the CDQ boiler. The CDQ chamber treats the heat of the red-hot coke and the nitrogen, and the CDQ boiler treats the heat of the nitrogen and the steam. TSP analysis uses the data of the utility/process fluids in the heat exchangers. In the first exchanger (CDQ chamber), it appears that the nitrogen is a utility fluid, but its operating condition is fixed like that of a process fluid. The first heat exchanger treated a process/process fluid and the data from such exchanger was considered not to be suitable for TSP analysis. It was eventually decided to use the data of the second exchanger (CDQ boiler). In this way, all the heat exchanging systems in the steel plant have been checked. The input data of the heat exchangers (heaters and coolers) were chosen for TSP analysis. Five utility conditions are used for heaters and three used

© Woodhead Publishing Limited, 2013

Table 24.3 Utility conditions for a steel plant

A	Utilities for heaters	Current (GJ/h)	Targeting (GJ/h)
FG-H (1,900–850°C)	Flue gas at steel material heating	734.4	0.0
FG-L (1,400–230°C)	Flue gas at Blast Furnace	1,431.9	2,070.7
IPS (235°C)	Intermediate pressure steam (3 MPaG)	0.0	42.4
MPS (180°C)	Middle pressure steam (1 MPaG)	71.2	11.6
LPS (151°C)	Low pressure steam (0.5 MPaG)	49.4	162.2
STC (140°C)	Steam condensate	27.6	27.6
	Total	2,314.5	2,314.5
B	Utilities for coolers	Current (GJ/h)	Targeting (GJ/h)
VHPS Gen (100–535°C)	Very high-pressure steam (12 MPaG)	0.0	1,041.5
HPS Gen (100–535°C)	High-pressure steam (10 MPaG)	630.1	0.0
IPS Gen (80–235°C)	Intermediate pressure steam (3 MPaG)	0.0	31.6
MPS Gen (90–180°C)	Middle pressure steam (1 MPaG)	350.9	0.0
LPS Gen (80–151°C)	Low pressure steam (0.5 MPaG)	0.0	0.0
HW Gen (76–98°C)	Hot water	92.1	0.0
	Total	1,073.1	1,073.1

for coolers. Utilities for heaters are two kinds of flue gas (FG-H and FG-L), two pressure levels of steam, and a steam condensate. FG-H and FG-L are the flue gases at the heating unit and furnaces, which are combusted gases of the by-product gases from the steel plant. The utilities for coolers are two pressure levels of generated steam and hot water.

24.3.2 Result of TSP Analysis

The 'current' column in Table 24.3 summarises the utility conditions of heaters and coolers for the current operation case ('current case') after determination of the appropriate data from the heat exchangers for TSP analysis. There are five utilities for heaters (Table 24.3A) and three utilities for coolers (Table 24.3B). The data zero for intermediate pressure steam (IPS) indicates that IPS is not used. In Table 24.3B, the terms 'HPS Gen' and 'MPS Gen' are used to differentiate them from mere high and middle pressure

© Woodhead Publishing Limited, 2013

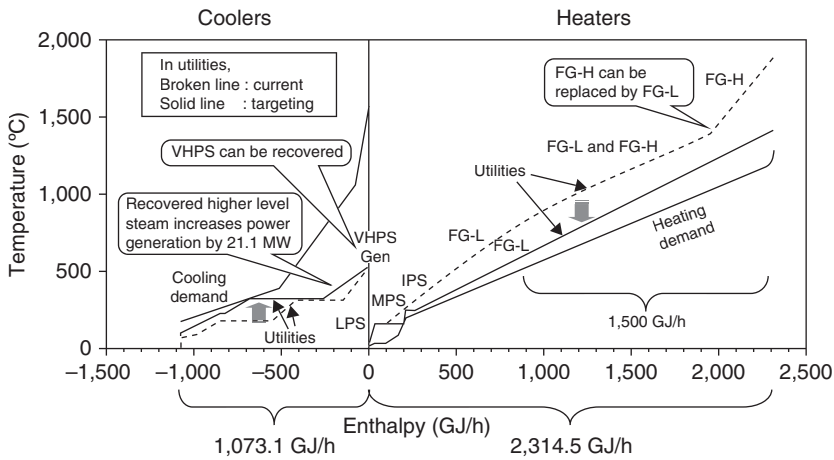

24.4 TSP analysis for a steel plant.

steam conditions. For example, HPS Gen means the range from supplied cold boiler feed water (100°C) up to superheated high-pressure steam (10 MPaG, 535°C).

Current Case

Figure 24.4 shows the TSP chart, which is based on the current data for heaters and coolers as shown in Table 24.3. The right side of Fig. 24.4 shows the information for the heaters and the left side shows that for the coolers. It is acknowledged that the heaters' duty (2,314.5 GJ/h) is almost twice as large as that of the coolers (1,073.1 GJ/h). A large-scale steel plant consumes a huge amount of energy but only half the consumed heat is recovered, which means that despite the very high efficiency of the individual processes in the plant, there is a huge energy-saving potential. The difference between the heater duty and the cooler duty is considered as unrecovered heat. When heat recovery technology is significantly improved, the amount of the unrecovered heat will be greatly reduced. There is also a large gap between two Composite Curves for heaters, such as the heating demand and the utilities (current) as shown on the right side of Fig. 24.4, which suggests that the lower temperature utility can be used instead of the utilities (current). Simultaneously, the higher temperature utility for coolers can be used due to the large gap between two Composite Curves as shown on the left side of Fig. 24.4.

Targeting Case

The targeting case for energy saving is studied by changing the utility conditions for heating and cooling as shown by the broken and solid lines of

© Woodhead Publishing Limited, 2013

Fig. 24.4. The current FG-H (1,900–850°C) for heaters can be replaced by FG-L (1,400–230°C) because the heating demand level is adequately satisfied by the lower level utility, FG-L. On the other hand, the current HPS Gen condition for coolers causes the large gap from the cooling demand. It is therefore possible to produce a new utility such as very high-pressure steam (VHPS) Gen. The result of the targeting case study is summarised in the 'Targeting' column of Table 24.3.

24.3.3 Energy-Saving Projects

Heater Side

It can be seen in Table 24.3A that FG-H can be totally replaced by FG-L. This suggests that the original fuel gas of FG-H would not need to be used to heat the steel, but would be able to be sent to an adjacent thermal power plant for power generation (Modesto and Nabra, 2006; Wang *et al.*, 2011). A steel plant uses very high temperature heat in large quantities, and the heating demand of more than 500°C (approximately 1,500 GJ/h on the right side of Fig. 24.4) occupies 70% of the total demand (2,314.5 GJ/h). The lower level utilities (targeting) can be used in Fig. 24.4. Newly installed IPS can be used for a lower part of current FG-L user and LPS can be used for a part of current MPS user.

Cooler Side

The left side of Fig. 24.4 and the 'Targeting' column in Table 24.3 suggest that new VHPS Gen can be generated in the cooler side, as shown in Table 24.3B, instead of the present HPS Gen and MPS Gen. The generated VHPS Gen shifted from MPS Gen will be able to produce power generation of 21.1 MW because the suction steam pressure for the steam turbine generator increases and the thermal pressure drop increases. However, the VHPS Gen shifted from HPS Gen will generate little power increase because their operating conditions are close to each other. The current HW Gen will be a preheating part of the IPS Gen.

24.4 Conclusion

It was generally believed that there was no further potential for energy saving in heavy chemical complexes and steel plants, because it was considered that almost all possible energy-saving measures had already been introduced and developed. However, it became clear that the concept of energy-saving studies had been limited to only the individual process systems in the plant. The Total Site approach, based on Pinch Technology, is able to identify

© Woodhead Publishing Limited, 2013

a large energy-saving potential, which could be realised in practical energy-saving projects.

24.5 Sources of Further Information

For further understanding the Total Site approach related in this chapter, the following articles are recommended for reading from recently published ones. Zhang *et al.* (2013) integrates the operation of distillation and heat recovery in a crude oil distillation unit. Varbanov *et al.* (2012) deals with the modified Total Site Targeting procedure, which allows obtaining more realistic heat recovery targets for Total Sites. Varbanov and Klemeš (2010) analyse some of the most common heat transfer applications at Total Sites. Sikos and Klemeš (2010) propose a new methodology to use comprehensive up-to-date commercial software tools for HEN reliability modelling and optimisation. Lam *et al.* (2011) provides an overview of software tools in the areas of Process Integration, modelling and optimisation. Wan Alwi *et al.* (2012) proposes Power Pinch Analysis (PoPA) tools to determine the minimum target for outsourced electricity and the amount of excess electricity for storage during start up and normal operations. Liew *et al.* (2012) analyses a site's overall sensitivity to plant maintenance shutdown and production changes. Klemeš and Varbanov (2012) demonstrate that Heat Integration (HI) in Process Integration has some potential pitfalls and needs proper expertise to be successfully implemented.

24.6 Acknowledgements

Total Site study for a heavy chemical complex described herein is based on the study by Matsuda *et al.* (2009). The study for the steel plant is based on the study by Matsuda *et al.* (2012), which was conducted in the program of Environmentally Harmonized Steelmaking Process Technology Development (COURSE50), Japan.

24.7 References

Ahmad, S., Linnhoff, B., Smith, R. (1990). Targets and design for detailed capital cost models. *Computers and Chemical Engineering*, **14**(7), 751–767.

Asante, N. D. K., Zhu, X. X. (1996). An automated approach for heat exchanger retrofit featuring minimal topology modifications. *Computers Chemical Engineering,* **20**(Suppl.), s7–s12.

Bisio, G., Rubatto, G. (2000). Energy saving and some environment improvements in coke-oven plants. *Energy*, **25**(3), 247–265.

Chan, D. Y. L., Yang, K. H., Lee, J. D., Hong, G. B. (2010). The case study of furnace use and energy conservation in iron and steel industry. *Energy*, **35**(4), 1665–1670.

Dhole, V. R., Linnhoff, B. (1993). Total site targets for fuel, co-generation, emissions, and cooling. *Computers Chemical Engineering,* **17**(Suppl.), s101–s109.

© Woodhead Publishing Limited, 2013

Kenney, W. F. (1984). *Energy Conservation in the Process Industries*. Academic Press, Orlando, USA.

Kimura, H. (1998). R-curve concepts for analysis and optimization of cogeneration systems. MSc Dissertation, UMIST, Manchester, UK.

Kimura, H., Zhu, X. X. (2000). R-curve concept and its application for industrial energy management. *Industrial and Engineering Chemistry Research*, **39**(7), 2315–2335.

Klemeš, J., Dhole, V. R., Raissi, K., Perry, S. J., Puigjaner, L. (1997). Targeting and design methodology for reduction of fuel, power and CO_2 on total sites. *Applied Thermal Engineering*, **7**, 993–1003.

Klemeš, J., Varbanov, P. (2012). Heat integration and renewables – recent developments and achievements. *Global Journal of Technology and Optimization, Transaction on Energy, Protection and Planning*, ISSN: 2229–8711 Online Publication <www.pcoglobal.com/gjto.htm> IR-S18 /GJTO, Vol. 3, June.

Lam, H. L., Klemeš, J., Kravanja, Z., Varbanov, P. (2011). Software tools overview: process integration, modelling and optimization for energy saving and pollution reduction. *Asia-Pacific Journal of Chemical Engineering*, **6**(5), 696–712, DOI:10.1002/apj.469.

Liew, P. Y., Wan Alwi, S. R., Varbanov, P., Manan, Z. A., Klemeš, J. (2012). A numerical technique for total site sensitivity analysis. *Applied Thermal Engineering*, **40**, 397–408, DOI: 10.1016/j.applthermaleng.2012.02.026.

Linnhoff, B., Ahmad, S. (1990). Cost optimum heat exchanger networks-1. Minimum energy and capital using simple models for capital cost. *Computers Chemical Engineering*, **14**(7), 729S–750S.

Linnhoff, B., Hindmarsh, E. (1983). The pinch design method of heat exchanger networks. *Chemical Engineering Science*, **38**(5), 745–763.

Linhoff, B., Townsend, D. W., Boland, D., Hewitt, G. F., Thomas, B. E. A., Guy, A. R., Marsland, R. H. (1982). *User Guide on Process Integration for the Efficient Use of Energy*, 1st ed. Institution of Chemical Engineers, Rugby, UK.

Makwana, Y., Smith, R., Zhu, X. X. (1998), A novel approach for retrofit and operation management of existing total sites. *Computer Chemical Engineering,* **22**(Suppl.), s793–s796.

Matsuda, K., Hirochi, Y., Tatsumi, H., Shire, T. (2009). Applying heat integration total site based pinch technology to a large industrial area in Japan to further improve performance of highly efficient process plant. *Energy*, **34**, 1687–1692.

Matsuda, K., Tanaka, S., Endou, M., Iiyoshi, T. (2012). Energy saving study on a large steel plant by total site based pinch technology. *Applied Thermal Engineering,* **43**, 14–19.

Modesto, M., Nebra, S. A. (2006). Analysis of a repowering proposal to the power generation system of a steel mill plant through the exergetic cost method. *Energy*, **31**(15), 3261–3277.

Raisi, K. (1994). Total site integration. PhD thesis, UMIST, UK.

Sikos, L., Klemeš, J. (2010). Reliability, availability and maintenance optimization of heat exchanger networks. *Applied Thermal Engineering*, **30**, 63–69.

Tjoe, T. N., Linnhoff, B. (1986). Using pinch technology for process retrofit. *Chemical Engineering*, **28**, 47–60.

Varbanov, P., Fodor, Z., Klemeš, J. (2012).Total site targeting with process specific minimum temperature difference (ΔT_{min}). *Energy*, **44**(1), 20–28.

© Woodhead Publishing Limited, 2013

Varbanov, P., Klemeš, J. (2010). Total sites integrating renewables with extended heat transfer and recovery. *Heat Transfer Engineering,* **31**(9), 733–741.

Wan Alwi, S. R., Mohammad, R. N. E., Abdul-Manan, Z., Klemeš, J. (2012). A process integration targeting method for hybrid power systems. *Energy*, **44**(1), 6–10.

Wang, C., Sandberg, J., Larsson, M. (2011). Analysis of oxygen enrichment and its potential influences on the energy system in an integrated steel plant using a new solution space based optimization approach. *Chemical Engineering Transactions*, **25**, 87–92, DOI: 10.3303/CET1125015.

Worrell, E., Price, L., Martin, N. (2001). Energy efficiency and carbon dioxide emissions reduction opportunities in the YS and steel sector. *Energy*, **26**, 513–536.

Xu, C., Cang, D. Q. (2010). A brief overview of low CO_2 emission technologies for iron and steel making. *Journal of Iron and Steel Research International*, **17**(3), 1–7.

Zhang, N., Smith, R., Bulatov, I., Klemeš, J. (2013). Sustaining high energy efficiency in existing processes with advanced process integration technology. *Applied Energy*, **101**, 26–32, DOI: 10.1016/j.apenergy.2012.02.037.

© Woodhead Publishing Limited, 2013

25

Applications of Process Integration Methodologies in the Pulp and Paper Industry

JEAN-CHRISTOPHE BONHIVERS and PAUL. R. STUART, École Polytechnique – Montreal, Canada

DOI: 10.1533/9780857097255.5.765

Abstract: This chapter describes the mass and energy requirements of pulp and paper processes in general, and specifically the Kraft process, which is the dominant pulping process as well as the most intensive steam user. The strong interactions between water and heat networks in pulp and paper mills are discussed. Water in pulp and paper processes is used for dilution, washing, cooling and heating, and is the main heat transporter and dissipator in pulp and paper processes. Approaches to increasing energy efficiency in existing mills are presented. Results show that there is a heat-savings potential of approximately 15–30% in typical existing mills. Finally, trends in Process Integration techniques in the pulp and paper industry are presented.

Key words: Kraft pulp process, Pinch Analysis, water network, Heat Exchanger Network retrofit, Combined Heat and Power.

25.1 Introduction

The pulp and paper sector is energy intensive by many measures. The pulp and paper sector accounts for about 15% of industry usage in International Energy Agency member countries (IEA report, 2007). In Canada, the pulp and paper industry accounts for 25% of total industrial energy consumption. Energy accounts for up to 30% of the total manufacturing cost for thermo-mechanical pulping.

Table 25.1 presents world pulp production in 2010. Global pulp and paper production is increasing annually by approximately 2%. Table 25.2 shows typical energy demands for different pulp processes per air-dried t (adt). The Kraft pulping process is the dominant manufacturing process by which wood chips are transformed into pulp, the intermediate material from which a very broad spectrum of finished or semi-finished paper products are made. Among pulping processes, the Kraft process is also the greatest user of steam and is described in the next section. The second most widely used pulp process is thermo-mechanical pulping. Its principle is the separation of the fibres

© Woodhead Publishing Limited, 2013

Table 25.1 World pulp production by category (2010)

Pulp category	Production in Mt
Chemical	149
Kraft	133
Sulfite	8
Semichemical	8
Mechanical	43
Non-wood	20
Total virgin fibres	213
Recovered fibres	167
Total pulp	380

Table 25.2 Typical steam and power demands for pulp processes

Type of pulp	Steam demand (GJ/adt)	Electricity demand (kWh/adt)
Kraft, softwood, bleached dried	11.5–18.0	660–800
Kraft, hardwood, bleached dried	11.0–17.5	630–760
Neutral sulfite semi-mechanical	3.8	400
Chemo-thermo-mechanical pulp	0	2,000
Thermo-mechanical pulp	–3.0	2,100–2,900
Mechanical pulp, groundwood	0–1	1,400–1,700
Recycled pulp, de-inked	1.0	310
Recycled pulp, not de-inked	0.0	50

in wood chips through friction between plates in refiners. Refiners consume a large quantity of electricity, which is degraded as heat: friction in the refiners heats the pulp and produces steam, from which heat can be recovered. Water is required mainly for adjustment of pulp consistency. This process provides an excess of thermal energy. Paper processes involve pretreatment of the fibres using screeners, cleaners or refiners, before formation of the sheet by filtration of the fibres suspended in water, followed by pressing and drying. Fillers, additives, or other specific treatments can be added to improve paper properties. Paper production requires heat and power (Table 25.3). Electricity is required mainly for pulp pretreatment, while heat is required for pulp drying and water heating. Integrated pulp and paper mills consume more heat and power than pulp mills because the paper-making process uses more energy than a pulp drying machine (2.5–4 GJ/adt, 100 kWh).

The chapter is organised as follows. First, the Kraft pulping process and its energy aspects are presented. Second, the interactions between the Heat Exchanger Network and the water network in pulp and paper mills are discussed. Then, the main approaches to improving energy efficiency in existing

© Woodhead Publishing Limited, 2013

Table 25.3 Typical steam and power demands for paper processes

Type of paper	Steam demand (GJ/adt)	Electricity demand (kWh/adt)
Newsprint	4–6	550–585
Tissue paper	6–8	1,010
Kraft liner	5–6	530
Bleached Kraft, board	7–8	600–780
Sack paper	6–7	1,000
Other Kraft paper and Kraft board	7.5	700

mills are described. Finally, trends in the evolution of pulp and paper mills are presented.

25.2 Energy Demands and Sources in the Kraft Pulping Process

The Kraft pulp is the most important intermediate material from which paper products are made. This section describes first the Kraft pulping process, and then the heat and power demands in the main departments.

25.2.1 Process Description

A simplified schematic of the Kraft process is given in Fig. 25.1. The core of the process is a chemical delignification step performed in a digester where the individual cellulosic fibres are separated to yield pulp. The delignification agent (white liquor) is a mixture of sodium hydroxide and sodium sulphide. After delignification, the fibres are washed and chemically bleached; a common bleaching agent is ClO_2, produced on-site. Finally, the fibres are drained, pressed and thermally dried. A key characteristic of the process is that the spent delignification liquor (called 'black liquor') separated from the fibres in the washing step is concentrated in evaporators, and then burned in the recovery boiler to produce steam and recover spent inorganic chemicals. The spent inorganic chemicals form a smelt composed of sodium carbonate and sodium sulphide, which is collected at the bottom of the recovery boiler. The smelt is dissolved (to form 'green liquor'), and then recausticised with quicklime produced on-site in a lime kiln to regenerate the pulping liquor (called 'white liquor').

25.2.2 Heat and Power Demands by Main Department

Wood Yard

The power demand for log handling, conveying, slashing, debarking, chipping, chip screening, chip storage, bark handling, etc., is approximately

© Woodhead Publishing Limited, 2013

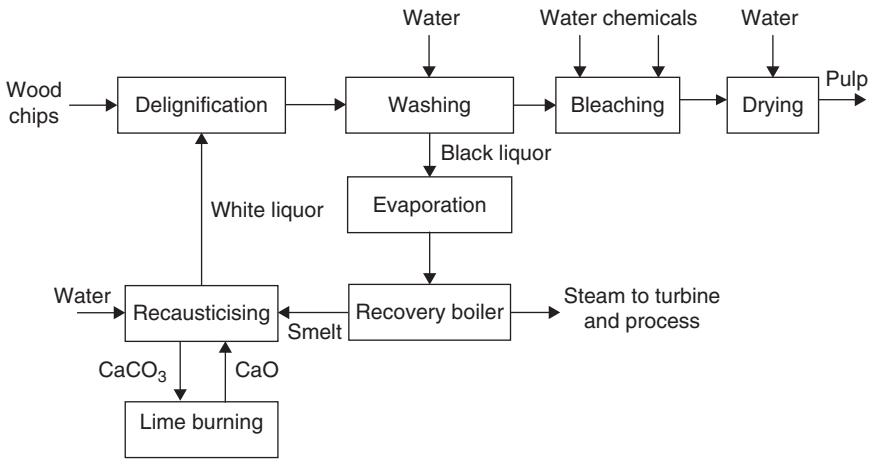

25.1 Simplified diagram of the Kraft pulp process.

25 kWh/adt. Heat demand depends on the need for log de-icing. If this is necessary, the heat demand is approximately 0.5 GJ/adt (Gullichsen, 2000).

Pulp Cooking, Washing and Screening

Chips are mixed with white liquor containing sodium hydroxide and sodium sulphide and heated to 160°C for several hours to achieve certain chemical reactions, i.e., hydrolysis of the lignin and a part of the hemicellulose. At the digester outlet, the pulp is separated from the cooking liquor using a set of washers, and is sent to bleaching. The separated cooking liquor, called black liquor, is sent to the evaporators for recuperation.

For continuous-flow cooking and displacement batch cooking, power and heat demands are 40–70 kWh/adt and 1.7–2.5 GJ/adt. These demands can be higher in an older pulping plant with inadequate heat recovery. The power consumption of washing, knot separation and screening is 90–130 kWh/adt. Softwood consumes a little more heat and power than hardwood does.

Bleaching

The pulp chromophores of the remaining lignin, i.e., the conjugate multiple bonds between atoms, are oxidised to suppress light absorption, through a set of steps involving chemical reaction and dissolved solids extraction by washers. The first step is usually oxygen delignification. The subsequent reactors use other oxidants such as ozone, elemental chlorine and chlorine dioxide.

The low-pressure steam consumption of the oxygen delignification stage is approximately 0.4–0.5 GJ/adt, and its power consumption is approximately

© Woodhead Publishing Limited, 2013

40–50 kWh/adt. The steam consumption of elemental chlorine-free (ECF) bleaching is approximately 0.5 GJ/adt, and its power consumption is 80–120 KWh/adt.

Bleached-Stock Cleaning and Pulp Drying

The power consumption for bleached-stock cleaning depends strongly on the method selected, e.g., centricleaning or slotted pressure screens. Consumption can range from 25 to 150 kWh/adt. The steam consumption of an air-borne drying machine is approximately 2.5–3.0 GJ/adt. The web dryness after the press section is approximately 45%, and the dryness of the final pulp is 90%; consequently, roughly one ton of water has to be evaporated. A shoe press enables an increase to 52% dryness, leading to savings of 0.5 GJ/adt.

Evaporation of Black Liquor

Black liquor is evaporated from 15–18% to 60–85% solids content through a series of five to seven evaporators with multiple effects. The first evaporator effect is fed by low- or medium-pressure steam. Vapour from the final evaporator is condensed in a surface condenser by fresh water, producing warm water. The dirty condensates are then stripped with low-pressure steam and eventually sent back to the washers in the fibre line or to the recausticising area. The heat consumption for evaporation depends on number of effects, the temperature of the incoming black liquor (usually about 90°C) and the dry solids content of the incoming (15–18%) and outgoing (65–80%) strong black liquor. The amount of dry solids in black liquor is 1.6–1.9 t/adt. Softwood black liquor dry solids content is approximately 10% higher than that of hardwood. Typical heat and power demands are 4–5 GJ/adt and 20–30 kWh/adt.

Recovery Boiler

Strong black liquor coming from evaporation is combusted with air. The heat of combustion is used to produce high-pressure steam (6–9 MPa), which is usually sent to a turbine to produce power and steam for the process. Smelt at the bottom of the boiler contains mainly sodium carbonate, which is a product of combustion, and sodium sulphide, which is regenerated by reduction in the recovery boiler of sodium sulphate produced in cooking. Steam is used for soot-blowing, primary and secondary air preheating, liquor pre-heating, and in smaller amounts for smelt shattering. Soot-blowing steam can be extracted from high pressure (HP) steam leaving the first superheater and then reduced to a suitable pressure of 2–3 MPa or extracted from the steam turbine. Soot-blowing steam demand is 2.5–4% of

© Woodhead Publishing Limited, 2013

HP steam generated. In older boilers, soot-blowing requirements can reach 10% of generated steam. Primary and secondary air is preheated from 30°C to 150°C using low-pressure steam and then medium-pressure steam. Air demand is 3–4 m^3N/kg dry solids (5–7 t/adt). Total power demand for the recovery boiler, including fans, electrostatic precipitator, pumps, agitators and feed-water pumps, is 55–70 kWh/adt.

Causticising and Lime Kiln

Smelt is cooled and dissolved in water. Hydroxide sodium is regenerated from sodium carbonate reacting with calcium hydroxide in causticisers. The calcium carbonate produced is regenerated in the lime kiln by heating. Regenerated white liquor, containing sodium hydroxide and sodium sulphide, is then sent back to chip cooking.

Low-pressure steam demand for causticising is approximately 20 MJ/adt. Medium pressure (MP) steam demand for lime-kiln oil burners (atomizing steam) is approximately 20 MJ/adt. Kiln fuel demand (heavy fuel oil, natural gas or bio-gas produced in a gasification plant using waste wood and bark) is approximately 2.0–2.8 GJ/adt. Total power demand, including clarifier, filters and the electrostatic precipitator for lime kiln, is approximately 40 kWh/adt.

Other Departments

Power demand for raw water pumping, chemical treatment and distribution and effluent treatment is approximately 50–70 kWh/adt. Power demand for mill and instrument air, lighting, workshops and offices is approximately 45 kWh/adt.

Stream Data Extracted from an Average Scandinavian Kraft Mill

Stream data for an average Scandinavian Kraft pulp mill (Future Resource-Adapted Mill programme) are presented in Table 25.4. The process requires mainly low-pressure steam. The medium-pressure steam process requirement is 2.8 GJ/adt, mainly in the cooking stage to heat chips and white liquor to 160–170°C and in certain bleaching reactors.

25.2.3 Overall Heat and Power Balance

Table 25.5 shows the energy demand of a Kraft pulp mill. The practical yield of the Kraft pulping process, i.e., the ratio between the weights of pulp fibres and wood chips, is 40–50%. Most of the remainder of the chips is burned in the recovery boiler, making it possible to produce steam and electricity. A

© Woodhead Publishing Limited, 2013

Table 25.4 Extracted data for an average Scandinavian Kraft pulp mill

Heat sources	T_c (°C)	T_h (°C)	Load (MJ/adt)
General cooling	35	40	773
Chemical preparation	47	48	103
Surface condenser	60	61	4,467
Stripper condenser	100	100	378
Steam smelt dissolver	100	100	275
BL flash steam 1	127	128	1,108
BL flash steam 2	107	109	1,065
Black liquor	93	105	421
Digester bottom	89	90	69
D1-stage effluent	39	66	1,022
D0-stage effluent	68	75	180
EOP-stage effluent	39	85	816
D0-stage effluent	39	75	627
D1-stage effluent	66	69	154
Pulp dryer effluent	39	60	154
Heat sinks	**T_c (°C)**	**T_h (°C)**	**Load (MJ/adt)**
Water 50	18	50	2,792
Water 75	50	75	1,984
Water 85	75	85	472
Make-up boiler water	18	75	481
Building heating (LP)	21	22	94
Wood yard (LP)	18	30	137
Wood chips (flash steam + LP)	7	120	1,795
Air heating (LP)	95	120	318
Circulating air (LP)	95	124	2,405
LP to stripper	150	151	550
LP to evap	150	151	4,467
LP to rest	150	151	567
White liquor – digester (MP)	85	165	1,031
Digester circulation (MP)	165	170	163
Hi-Heat digester (MP)	128	160	670
MP to oxygen stage	200	201	198
MP to bleach plant	200	201	515
MP to rest	200	201	189

modern Kraft pulp mill produces more heat and power than is necessary for the process. This is due to low heat and power consumption, high dry solids content of black liquor from the evaporation plant, and effective burning in the recovery and bio-fuel boilers (Gullichsen, 2000).

The heat and power balance of the mill depends on parameters such as:

- Amount of wood received as chips (barked or unbarked roundwood).
- Process heat and power consumption.
- Integration of the paper mill into the pulp mill.
- Pulp yields (depends on wood type and pulp type).

© Woodhead Publishing Limited, 2013

Table 25.5 Energy demands in Kraft pulp mills

Process area	Heat consumption State-of-the-art mill (GJ/adt)	Heat consumption Typical existing mill (GJ/adt)
Cooking	2.0	2.5–4.0
Bleaching	0.5	0.7–2.0
Evaporation	4.5	4.5–5.0
Drying machine	2.5	2.8–4.0
Stripper	0.5	0.6
Hot water production	–	0.5
Others	–	1.0
Total steam for process	10.0	12.6–17.1
Steam for soot-blowing	0.5 GJ/adt	0.5–1.8 GJ/adt
Heat to power generation	5 GJ/adt or 1,388 kWh/adt	2.2 GJ/adt or 555 kWh/adt
Power consumption	770 kWh/adt	880 kWh/adt
Fuel for Lime kiln	1.8 GJ/adt	1.8–2.8 GJ/adt

Combustion of Black Liquor in the Recovery Boiler

The high heating value of black liquor is 13.5–15.0 GJ per t dry solids (tds). Hardwood black liquor contains 1.6–1.7 tds and softwood black liquor contains 1.8–1.9 tds per air-dried t of pulp. Combustion heat enables the production of high-pressure steam. The remaining part of the heat is transferred to the smelt through an endothermic reaction involving the regeneration of sodium sulphide, salt fusion and heating to 800°C or exits the boiler with the flue gases or through radiation and convection losses. The higher the solids content of the inlet black liquor, the lower will be the heat loss in the flue gases. Table 25.6 presents a summary of data for black liquor combustion.

Power Boiler

Bark and wood waste are normally burned in a power boiler designed for such fuel. Steam generation using bark and wood fines depends on the amount of wood received as unbarked roundwood and sawmill chips. Bark and wood fines from the pulp mill can also be transported to a paper mill when the distance is reasonable. In the paper mill, this bio-fuel can then provide back-pressure power generation. With a boiler efficiency of 87%, this bio-fuel can generate 2.4–5.8 GJ/adt of steam.

Electricity Production Using Steam Turbines

In a Kraft mill, the steam turbine can be of the extraction back-pressure type or the multiple-extraction condensing type. High-pressure steam ranges from 6 MPa and 450°C to 9 MPa and 500°C depending on the

© Woodhead Publishing Limited, 2013

Table 25.6 Heat balance for combustion of black liquor in recovery boiler

	Units	Hardwood	Softwood
Black liquor dry solids	tds/adt	1.6–1.7	1.8–1.9
Dry solids high heating value (HHV)	GJ/tds	13.5–14.5	14.0–15.0
Black liquor solid concentration	%	70–85	70–85
Heat of combustion	GJ/adt	21.6–24.7	25.2–28.5
Heat transferred to steam	GJ/adt	15–17	17–19
Heat transferred to smelt	%	14	14
Heat loss	%	13–17	12–18

system. Medium-pressure steam is extracted at 1.0–1.3 MPa and low-pressure steam at 0.3–0.4 MPa. Electricity production can range from 500 to 1400 kWh/adt.

The following actions can increase the amount of power generated:

- Extracting soot-blowing steam from the turbine at approximately 2.5–3.0 MPa instead of removing it after the recovery boiler primary superheater.
- Increasing the amount of condensate return.
- Using make-up (demineralised water) water preheated with mill excess warm or hot water.
- Using controlled extraction (low-pressure steam at 0.6–0.8 MPa) for evaporation plant concentrators and recovery boiler air heaters following 0.3 MPa steam air heaters. Using controlled extraction for higher MP and lower MP steam.
- Increasing black liquor dissolved solids concentration at the recovery boiler inlet.
- Decreasing process heat demand.

25.3 Relations between the Heat Exchanger and Water Networks

The interactions between the heat and water networks are especially strong in the Kraft pulping process. Non-isothermal mixings decrease the energy quality, and water outlets often correspond to heat outlets and losses.

25.3.1 Degradation of Energy Quality

The Pinch Points reflect the first and second laws of thermodynamics in industrial processes. The energy quality is degraded: (1) from sinks to sources by the process, and (2) from sources to sinks by the Heat Exchanger Network. First, heat is required to increase the temperature of sinks above

© Woodhead Publishing Limited, 2013

that of the environment. Because of the increase in entropy, sources are available at lower temperature than sinks. This leads to a heat deficit at high temperatures and to a heat excess at lower temperatures. The existence of Pinch Points limiting these areas is the natural consequence of the increase in entropy. Second, heat can be transferred from sources only to sinks at lower temperature, leading to exergy loss. Consequently, saving energy in the Heat Exchanger Network requires managing the exergy losses due to transfers. In summary, the principles of energy conservation and quality degradation lead to a situation with exergy loss due to the process, i.e., source exergy is lower than sink exergy, and with an exergy loss for transferring heat between sources and sinks (Fig. 25.2).

In the Kraft pulping process, steam consumption is higher than the enthalpy change of reactions in the cooking or bleaching reactors. Steam is used mainly to concentrate the black liquor, as a source of activation energy for chemical delignification in cooking and bleaching reactors, for pulp drying, and to heat up water. The quality of heat in these sinks is then degraded to that of the heat sources. Heat from live steam to heat sinks degrades the quality of the energy, contained mainly in the liquid effluents. Water is the main heat transporter in a pulp and paper mill. It is used for dilution, washing, steam production and cooling. The energy efficiency of the Kraft process is strongly related to the proper management of water and steam. Reducing water consumption decreases heat degradation and dissipation, and either steam consumption or the required exchange area (Fig. 25.3).

25.3.2 Process Water Network

Process water is required in pulp and paper mills for washing the pulp after the cooking and bleaching reactors, for dissolving the smelt from the recovery boiler to produce white liquor, and for diluting the pulp before bleaching reactors, cleaners, screeners, refiners, and the pulp or paper machine. Depending on the Kraft pulp mill, process water consumption can vary from 10 to 60 m^3/adt. It is essential to compile the balance sheet for water producers and consumers. When this balance is known, warm and hot water production can be optimised. Typical flow rates for main process water are shown in Fig. 25.4. The usual process water reuses which are considered in mills are the following: condensate from evaporators to brown-stock washing and to recausticising, white water from the pulp machine to bleaching. The main process effluent from a Kraft mill comes from bleach plant washer filtrates, which have a dissolved solids content that limits their direct reuse in the process. Bleaching filtrate is usually sent to water treatment. Some mills reuse some alkaline bleaching filtrate for washing after oxygen delignification and brown-stock washing. Water closure around the bleach plant using

© Woodhead Publishing Limited, 2013

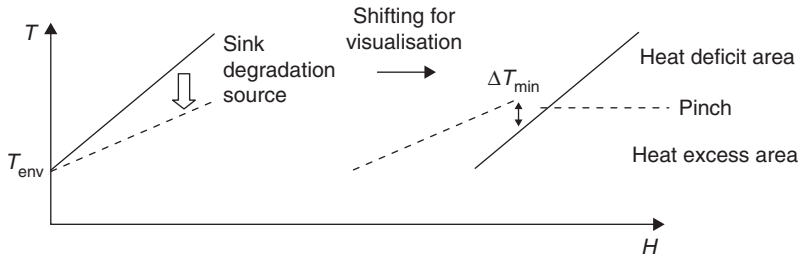

25.2 Sources come from sinks after heat degradation by process; this leads to an excess heat area.

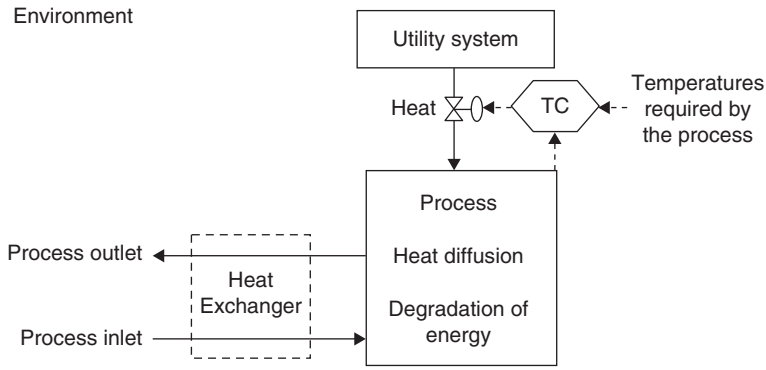

25.3 Reducing the process water consumption decreases the heat degradation and the steam consumption or heat exchanger area.

a treatment such as filtrate evaporation or membrane filtration requires investment and energy costs and is still in the research stage. Reducing process water consumption increases the dissolved solids concentration in the process. For any pulp and paper process, problems of contaminant build-up from wood or process chemicals limit the extent of water closure that can be achieved.

The proper management of water tanks, including white water, clean water, warm water and hot water, has a positive impact on steam and electricity consumption. This includes accounting for specific process dynamics such as those of batch cooking or paper sheet breaks to improve control of water inventories. Non-isothermal mixings in water tanks and between pulp and water are sources of heat quality degradation. Practical methodologies such as Combined Energy Water and Optimisation (Alva-Argaez, 2007) have been developed to track such exergy losses to improve both water and HEN in pulp and paper mills.

© Woodhead Publishing Limited, 2013

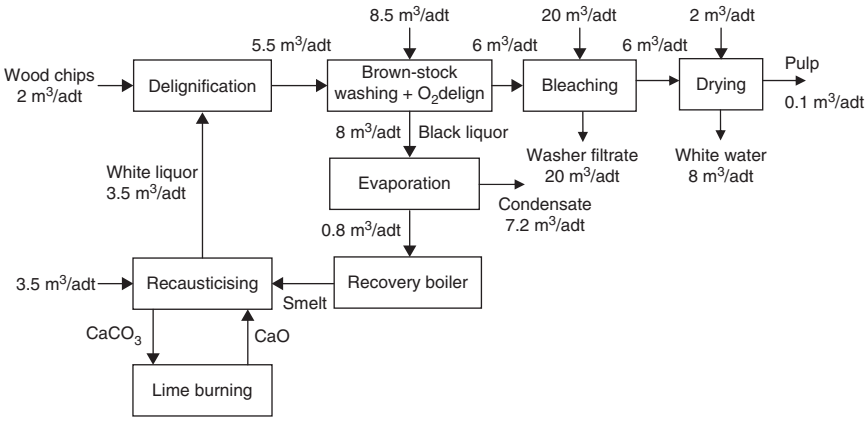

25.4 Typical flow rates of process water.

An excess of warm water is usually produced at the surface condenser of the evaporation area and from other sources in a modern pulp mill. The main way to decrease the flow of warm water from the surface condenser is to increase the number of evaporation stages (to a maximum of seven stages). The excess warm water from the evaporation surface condenser is eventually conveyed to a cooling tower and back to the condenser. In a modern closed pulp mill, hot water from the cooking plant can normally satisfy the mill's hot water demand. If additional hot water has to be produced, the usual heat sources are alkaline bleaching effluent or the stripping condenser.

Hot and warm water are, or can be, produced using the following heat sources:

- Surface condenser of the multiple-stage evaporators, where mainly warm water is produced. A lower water inlet temperature decreases the amount of warm water produced. Hot water could also be produced with a part of the steam from the last three effects.
- Continuous cooking area: primary and secondary black liquor condensers, black liquor cooler, turpentine cooler, condensate flash condenser.
- Conventional batch cooking area: blow heat accumulator, primary and secondary condensers, condensate flash condenser.
- Displacement batch cooking area: black liquor cooler, wash filtrate cooler, relief gas cooler.
- Alkaline bleaching effluent.
- Stripping condenser.
- Recovery boiler flue-gas scrubber.
- Flue-gas scrubber in the lime kiln.
- Air outlet from the drying machine.

© Woodhead Publishing Limited, 2013

25.4 Increasing Energy Efficiency in Existing Mills

Energy analysis has been performed for most pulp and paper mills. The heat consumption can be reduced by checking key points, or by applying a global methodology which is hereafter described. The effects of process dynamics on the heat consumption are also discussed.

25.4.1 Checking Key Points

Daily surveillance makes it possible to detect operation-related anomalies and to take immediate corrective action. Operating statistics, including energy consumption and heat, power, and water balances, should be maintained up to date for routine daily surveillance. The control system is important for all operations. Improvements in the control system have positive impacts on steam and water consumption. Process dynamics require appropriate control, including discontinuous operations, such as batch cooking and its subsequent hot water production and storage or paper breaks on the paper machine. Key points for Kraft mill energy conservation are described hereafter (Schroderus, 2010).

Wood Handling

The quality of hog fuel is important for achieving the highest possible energy conversion efficiency in the power boiler. Both dryness and particle size distribution are critically important parameters.

Cooking

Common reasons for increased heat consumption in a batch digester cooking plant are heat exchanger leakage and poor condensate return. The cooking operation is also an important source of hot water for bleach plant operation. For this hot water to be valuable, its temperature should be between 75°C and 85°C, the higher the better. Furthermore, the hot water should always be produced from warm water at 45–50°C to help meet the demand for hot water.

Brown-Stock Washing

This operation has an impact on heat consumption in the evaporators. If using more water is necessary to achieve acceptable dissolved solids removal in washing, the brown-stock washing operation should be studied to determine improvements, e.g., operating modifications or even an additional washer.

© Woodhead Publishing Limited, 2013

Bleaching

The important items to examine in the bleach plant are water consumption and bleaching conditions. If the consumption of hot water can be reduced by recycling washer filtrates, it is normally possible to increase the temperature of the water, which would reduce the steam consumption even further. The filtrate tanks must provide efficient air removal; otherwise, the operation of the washer, which receives the recycled filtrate, will suffer. Alkaline effluents are a convenient source of heat at 80°C, which can be used to produce hot water using an indirect-contact heat exchanger or to pre-heat chlorine dioxide solution to 45°C.

Pulp Drying Machine

The heat consumption in pulp drying depends mainly on the amount of water that needs to be evaporated in the dryer section, which depends essentially on pulp dryness after the press. It is important to study the entire water system because excessive water consumption tends to lower the temperature in the headbox, which impacts dewatering in the wire and press sections and results in reduced dryness after the press. Hot humid air at the dryer outlet can be used as a heat source to produce warm or hot water.

Black Liquor Evaporation

The amount of water to evaporate depends on the brown-stock washing operation. An energy-related item that affects other departments is the temperature of warm water from the surface condenser. The segregated clean condensates from evaporators and the foul condensates cleaned in an integrated stripper are key sources of hot water for brown-stock washing and recausticising.

Recovery Boiler

Most of the steam used in a Kraft mill is supplied by burning black liquor in the recovery boiler. The efficiency of the boiler operation is related to the quality of the fuel, its heating value, and its organic solids concentration. The concentration depends on the operation of the existing evaporation plant and can be increased, at a major capital cost. The heating value of the solids depends on the wood species used and, to some extent, on the cooking process.

Recausticising

The main source of hot water for recausticising should be evaporator condensates. Fuel consumption in the kiln depends on the moisture content

© Woodhead Publishing Limited, 2013

of the lime mud, the properties of the fuel and the kiln design. The key points for obtaining high mud dryness are the loading on the filter area, the vacuum pump capacity, high water temperature and continuous filter cleaning. Other ways to improve fuel consumption include installation of insulating refractory and use of a refractory dam, which are normal features in modern mills.

Overall Mill

Process heat consumption is strongly correlated with fresh-water temperature and production rate. By collecting and reusing clean excess warm and hot cooling water and adding it to the mill's water supply, it is possible to reduce process heat consumption during the cold season. However, it is necessary to provide a cooling tower to prevent the water temperature from getting too high under summer conditions, unless the temperature is controlled by sending excess warm water to sewer.

25.4.2 Overall Methodology

This methodology is a combination of various techniques that are used to improve the energy efficiency of pulp and paper mills in retrofit: analysis of the utility system; Heat and Water Pinch technologies; and exergy analysis. The objective is the development of energy enhancement measures that take into account the interactions of the utility and process systems and the economic and technical constraints. This development process consists of five stages, as shown in Fig. 25.5 (Mateos-Espejel, 2011).

The first stage is the base-case definition. A four-step procedure is used to define the base-case nominal conditions: data gathering; construction of a master diagram; analysis of utility systems; and computer-based simulation. The master diagram is constructed from the process and instrumentation diagrams and consists of three parts: the pulp and paper processes in the mill and the water and steam utility systems. From the master diagram, the steam and water utility systems can be analysed. Heat and power production and consumption are then analysed, including boiler efficiency, fuel consumption, steam pressures, turbines, direct or indirect heating of the process, percentage of condensate recovery, and make-up fresh-water utilisation without pre-heating. The water system analysis includes screened water for cooling, vent gas scrubbing and house-keeping, screened and demineralised water for steam production and use in sections where it is in direct contact with the pulp, and water balances in summer and winter.

The second stage involves benchmarking the base case to identify process inefficiencies and to establish guidelines for developing effective enhancement measures. At the end of this stage, it will be possible to estimate

© Woodhead Publishing Limited, 2013

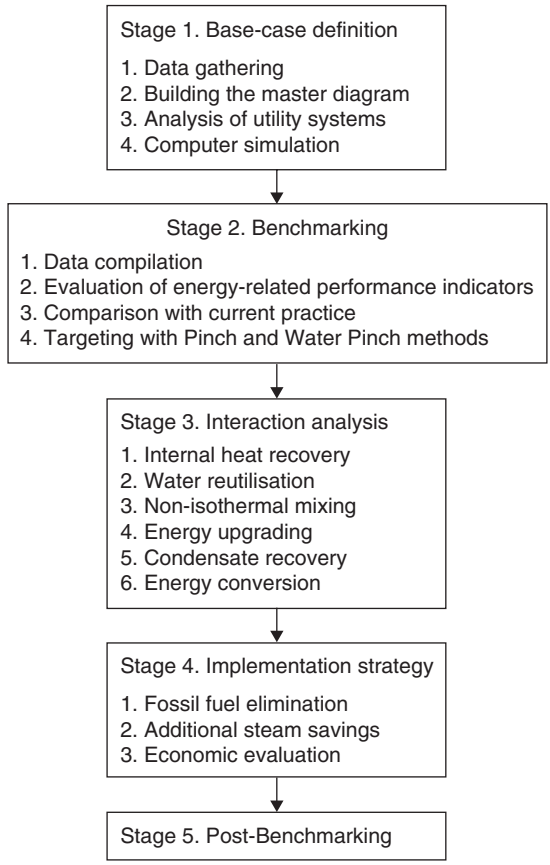

25.5 Overall methodology to increase energy efficiency in existing mills.

the savings that can be obtained, but the means by which they might be achieved will not yet have been identified; this will be done in the next stage. The steps in benchmarking are data compilation, comparison with current practice, computation of performance indicators, and target identification using thermal and Water Pinch Analysis. Data compilation involves determination of the initial and target temperatures and the heat loads of streams involved in the thermal analysis, the concentration of contaminants in the water sources and the concentration of contaminants allowed by the water sinks in the water analysis. Inefficient process sections are identified by comparison with current industrial practice. Exergy is used as an indicator of process inefficiencies. Performance indicators also include the energy and exergy contents of effluent and flue gases. Sankey diagrams of the exergy balances are constructed to quantify the exergy destroyed and

© Woodhead Publishing Limited, 2013

lost in the production and utilisation of steam. The fourth step is the identification of targets for steam and water consumption. The Heat and Water Composite Curves are constructed to determine the minimum water and energy requirements as well as the maximum potential for internal heat recovery and water reutilisation. A Minimum Temperature Difference of 10°C between the Composite Curves is often chosen for heat target identification in pulp and paper mills.

The third stage is interaction analysis, which incorporates six energy-enhancing techniques: increasing water reutilisation; suppressing non-isothermal mixing; increasing internal heat recovery; eventually upgrading thermal energy with a heat pump; increasing condensate recovery; and adapting energy conversion at the turbine level. Water Pinch Analysis is used to identify measures for water system closure. Non-isothermal mixing involves mainly water streams; their effects are evaluated using exergy losses and process analysis. Heat transfers crossing the Pinch are identified in the internal heat recovery step. Energy upgrading by installing a heat pump is costly and is analysed only after these first three steps.

The two last stages involve determination of the implementation strategy and a post-benchmarking analysis. For the economic evaluation, the investment cost is computed by the usual pre-engineering method based on the cost of a bare module and multiplying factors. A post-benchmarking analysis at the end makes it possible to quantify the improvement achieved in energy efficiency.

The following are examples of common energy-enhancing projects: replacement of steam injection by a heat exchanger for white-water heating; condensate recovery; reuse of the effluents of the black liquor evaporation section in pulp washing or recausticising; reuse of white water in the bleaching section; increased reuse of filtrate within the bleaching section; reuse of seal water from vacuum pumps; and pre-heating of fresh water before the deaerator.

25.4.3 Results of Heat Integration

Heat Pinch Analysis

Pinch Analysis has been performed for most pulp and paper mills at one time or another. The results show that reducing process water consumption usually leads to heat savings, leading in turn to a reduction in heat exchanger surface area or an increase in the temperature of the excess heat, i.e., the heat Below the Pinch. Depending on the water network and the data extraction technique used, the Pinch Temperature in a pulp and paper mill can range from 60°C to 120°C. The Minimum Temperature Difference chosen for targeting is usually between 10°C and 20°C. The

© Woodhead Publishing Limited, 2013

actual heat consumption is typically 15–30% greater than the targeted minimum energy requirement. The Payback Time for investment in steam-saving projects can be short if energy-use reduction projects lead to fossil-fuel savings. Typical Pinch violations include the heating of chips and white liquor in the cooking area and the production of hot and warm water. The heat of the live steam transferred to chips and white liquor in the cooking area is degraded to black liquor flash steam, which is typically used to produce hot water from warm water. Hot water can be produced from other heat sources, but this would require investment for modifications. This would make it possible to use the heat from black liquor flash steam for chip steaming and for heating white liquor before the digester. Live steam is also used on the pulp machine to maintain the temperature in the white-water network at approximately 55°C or to produce hot water, even though other heat sources could be used. Table 25.7 shows typical Cross-Pinch Transfers in average Scandinavian Kraft pulp mills (Axelsson, 2006). The average Scandinavian Kraft pulp mill uses 17.4 GJ/adt of steam. The amount of Cross-Pinch Transfers is 2.6 GJ/adt, of which 1.6 GJ/adt can be eliminated in practice.

Seasonal Effects

Depending on the season, the physical properties of wood and the outdoor conditions such as water and air temperature vary. Steam consumption tends to increase in winter compared to summer, particularly if process water consumption is high. Although ambient water temperature is Below the Pinch temperature year-round, a part of the available heat Below the Pinch is not recovered in some mills because this would require a supplementary investment for an indirect-contact heat exchanger to cool some of the effluent. In mills where water consumption is high, steam consumption can increase by 10% in winter.

Table 25.7 Typical Pinch violations in existing Kraft pulp mills

Area	Cold stream	Hot stream	Transferred heat (GJ/adt)
Cooking	Chips	LP steam	0.2
	White liquor and chips	MP steam	0.6
	Warm water	Gas from black liquor	1.0
Pulp machine	White water	LP steam	0.3
Hot water production	Warm-hot water	LP steam	0.5
Total			2.6

© Woodhead Publishing Limited, 2013

Influence of Short-Term Variations on Energy Opportunities

Studies indicate that short-term process variations, i.e., with ten-minute or less average period, contribute to a decrease in the energy-saving opportunities available under steady-state conditions (Persson, 2010). However, these variations do not seem to have serious implications for the results from the original steady-state analysis. These results indicate that the opportunities for energy savings will decrease by approximately 10% when short-term variations are taken into account. In other words, almost 90% of the steady-state opportunities remain.

25.5 Methodological Developments for Heat Integration in Existing Mills

Some difficulties are still encountered for Heat Integration in existing pulp and paper mills, where the interactions between the heat and water networks are strong. This part presents recent methodological developments to improve the energy analysis.

25.5.1 Advanced Composite Curves

The traditional Hot Cold and Grand Composite Curves are based on stream data only. They do not include data about the existing HEN, although such information is important for Heat Exchanger Network (HEN) retrofit. The major difference between the traditional and advanced curves is that information about the existing network is included in the latter.

The Advanced Composite Curves developed by Nordman and Berntsson (2008a, 2008b) and Nordman (2005) (see also Chapter 5, presented in many publications) provide the following supplementary information:

- Estimated heat-saving potential of economically feasible projects before detailed design calculations.
- Temperature levels at which usable excess heat, that is, heat Below the Pinch, can be extracted and used, for example, for Process Integrated evaporation of black liquor, a bioprocess based on wood residues, eco-cyclic industrial parks, district heating or cooling, or heat upgrading using a heat pump.

The Advanced Composite Curves are plotted at real temperatures. They provide in a single illustration, the actual situation as well as the potential savings that would result from a reduced temperature difference, the actual locations of heaters and coolers in the network before retrofit, the

© Woodhead Publishing Limited, 2013

theoretical upper and lower temperatures of each, and the excess heat, both directly available and potential.

The method uses four Composite Curves Above the Pinch and four Below (Nordman, 2005). Only the construction of the curves Above the Pinch is explained; the curves Below the Pinch are constructed in the same way. The four curves Above the Pinch are called the Hot Utility Curve (HUC), the Theoretical Heat Load Curve (THLC), the Actual Heat Load Curve (AHLC) and the Extreme Heat Load Curve (EHLC). The corresponding curves Below the Pinch are the Cold Utility Curve (CUC), the Theoretical Cooling Load Curve (TCLC), the Actual Cooling Load Curve (ACLC) and the Extreme Cooling Load Curve (ECLC). The HUC is a Composite Curve of the utility streams in the existing heaters plotted at real temperatures. Correspondingly, the AHLC is a Composite Curve of those parts of the process streams that run in the existing heaters. The EHLC shows the temperatures at which heat would be supplied if the heat exchange were carried out so that all the external heat were supplied at the highest possible temperature and with the same heat requirement as the AHLC. This corresponds to the overshooting part of the Cold Composite Curve. The THLC can then be evaluated as follows. Hot and Cold Composite Curves are moved such that the minimum energy requirement equals the actual energy consumption; this leads to Pinch Temperatures corresponding to the actual energy consumption and the Heat Recovery Minimum Approach Temperature Difference (HRATD). The parts of the curves above these Pinch Temperatures are separated from the parts below. Above the Pinch, the heat sources are shifted down by a chosen Exchanger Minimum Approach Temperature Difference (EMATD), e.g., 5 K. Then a Heat Cascade is evaluated Above the Pinch. This identifies the lowest possible temperatures at which heaters can be placed. The THLC shows the lowest possible temperatures at which heat would be supplied if all thermodynamically possible measures for energy conservation had been used with a given EMATD. Correspondingly, the TCLC shows the highest possible temperatures at which heat would be extracted if all thermodynamically possible measures for energy conservation had been used with a given EMATD. Consequently, a certain amount of cooling demand in the TCLC can be matched with a certain amount of heat demand in the THLC. This amount of transfer corresponds to the heat savings resulting from reducing the minimum temperature between the Composite Curves from HRATD to EMATD.

In summary, the curves show the loads and temperature levels of the utilities in heaters (HUC) and coolers (CUC), the process streams in the actual heaters (AHLC), the lowest (THLC) and highest (EHLC) possible temperature levels of process streams for heaters, the process streams in the actual coolers (ACLC), and the lowest (ECLC) and highest (TCLC) possible temperature levels of process streams for coolers.

© Woodhead Publishing Limited, 2013

Using the Advanced Composite Curves (ACC) to Identify HEN Retrofitting Opportunities

There are two ways that the ACC can be effectively employed in practice, as follows:

1. Releasing heaters placed low in temperature and coolers placed high in temperature is usually easier and less expensive than releasing other heaters or coolers, because fewer heat exchanger modifications and less exchange area are required (Figs 25.6 and 25.7). Consequently, the number of modifications and the required heat exchanger area of a HEN retrofit ought to be smaller when the AHLC is close to the THLC than when it lies close to the EHLC and should increase as the AHLC moves closer to the EHLC (Fig. 25.8). Symmetrically, the number of modifications and the required heat exchanger area of a HEN retrofit ought to be smaller when the ACLC is close to the TCLC than when it lies close to the ECLC. This principle is illustrated in Fig. 25.9a and 25.9b, which show ACCs Above the Pinch and Below the Pinch.
2. The ACCs show the excess heat at real temperature, both directly available excess heat and possible excess heat after network modifications. Excess heat directly available is represented by the ACLC; the potential excess heat, which is available after some modifications in the HEN, is represented by the TCLC (Fig. 25.9b). Studies have shown that 1–2 GJ/adt excess heat above 80°C can be made available in an average Scandinavian mill after modification of the hot-water production system. The quantity and temperature of excess heat increase as the process water consumption decreases.

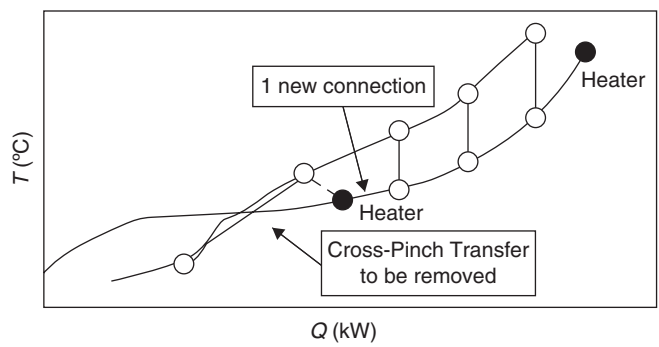

25.6 Few modifications are necessary to release heaters placed low in temperature.

© Woodhead Publishing Limited, 2013

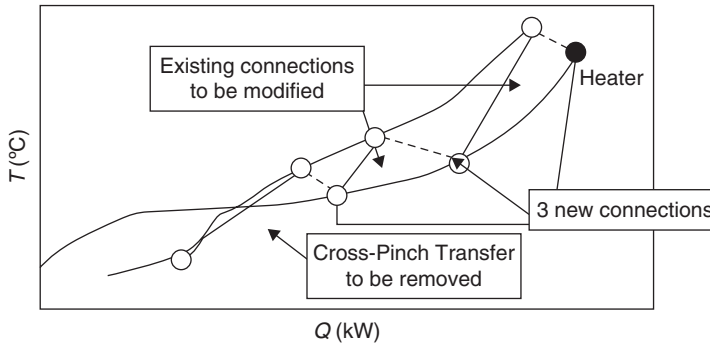

25.7 More modifications are required to release heaters placed high in temperature.

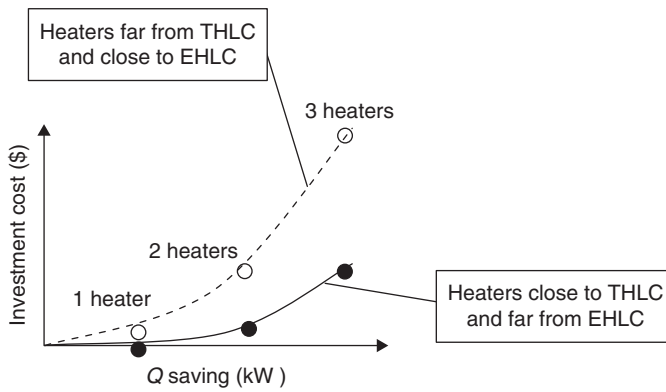

25.8 Removing heaters close to THLC and far from EHLC is usually cheaper than removing other heaters.

25.5.2 Bridge Analysis for HEN Retrofit

The principles of this analysis and an example involving a Kraft pulp mill are presented following.

Principles

'Integration' etymologically infers reducing the exchanges between the process and the environment. The main concepts of bridge analysis are (1) a network table that organises data from the existing network and shows possible modifications, and (2) a bridge structure consisting of a set of matches that enables the elimination of process heat outlets and inlets.

In the terminology used here, a Match is a heat exchange between a source segment and a sink segment: from a heat supplier to a receptor in an internal

© Woodhead Publishing Limited, 2013

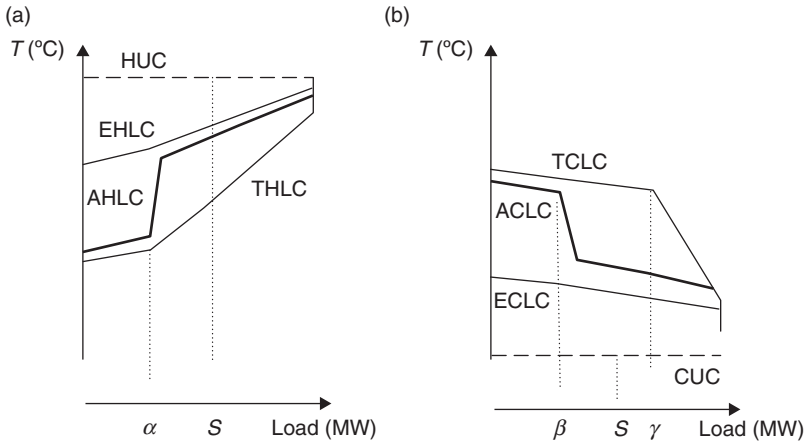

25.9 ACCs. S is the total heat saving resulting from reducing ΔT_{min} from HRATD to EMATD. (a) Curves Above the Pinch, showing α MW more easily accessible in heaters. (b) Curves Below the Pinch, showing β MW more easily accessible in coolers and γ MW of excess heat available after network modification.

heat exchanger; from a hot utility to a hot utility user in a heater; or from a heat outlet to a cold utility or to the environment. The first concept involves organising the HEN data into a network table to identify modifications that will save energy and reduce investment cost. In network Table D1, streams are decomposed according to their source and sink segments in the initial network. This table enables a visual representation of the network, and the identification of possible modifications. Each row corresponds to a source segment: a heat outlet, heat supplier, or hot utility; each column corresponds to a sink segment: a cold utility, heat receptor, or hot utility user. In network Table D2, streams are further decomposed according to the thermodynamic transferability criterion. Network Table D2 is more detailed and enables the evaluation of heat flows, the identification of necessary heat exchanger configurations, and the evaluation of investment cost. The second concept is the heat bridge, which is a set of matches that enables heat transfer from heat outlets to hot utility users through the network. For a given set of streams, only bridges can lead to heat savings. Bridge structures are the fundamental set of matches which enable energy savings. Heat from a source segment in a cooler is transferred to a sink segment in a heater through a set of matches.

Each retrofit energy programme is made up of (1) one bridge structure for achieving energy use reduction, and (eventually) of (2) a network rearrangement for other design objectives to reduce investment cost. The bridge analysis procedure includes three main steps: data extraction and analysis;

© Woodhead Publishing Limited, 2013

identification of bridge structures; and evaluation and selection of a solution. The first step includes analysis of the utility system, data extraction, setting practical connection constraints and drawing the heat transfer diagram. The heat transfer diagram is used rather than Composite Curves for graphic analysis. Its principle is the following: transferred heat (kW) in the existing network is evaluated as a function of temperature; heat transfer curves as a function of temperature correspond to total heat transfer, internal heat exchangers, heaters and coolers. Information available from the heat transfer diagram includes heat bridges; exergy losses; exchangers to be modified; maximum heat saving without practical constraints; available excess heat; placement of multiple utilities; and opportunities to insert a new process unit or a heat pump. The second step is the identification of bridge structures, which involves identifying useful matches, identifying bridge structures, and evaluating their characteristics: heat savings, new connections between streams and units to be removed. The heat savings achieved by bridge structures can be evaluated using network Table D2 and linear programming; an Excel-type solver is sufficient. Bridge structures are successively identified as the number of matches increases. Matches are added only to useful structures; a structure is useful if it leads to more energy savings than any of its sub-structures. In bridge structures, new matches represent the addition or modification of exchangers. This information enables the selection of the most promising structures for the third step, which will involve identification of the heat exchanger configuration using network Table D2 and the evaluation of profitability.

The main advantages of this approach are the following: modifications are visualised by means of a table and described in detail, and connection feasibility constraints are made explicit. Setting explicit connection constraints offers a number of advantages: Data extraction is easier, evaluation of savings potential is more precise, and all types of heat exchanges can be treated simultaneously, including direct- and indirect-contact heat exchanges. In pulp and paper mills, direct-contact heat exchanges are numerous and involve pulp, water, steam and gas. The following modifications entail direct-contact heat exchanges: pulp dilution, water reuse, elimination of water-tank overflows, mixing streams at different temperatures and recovering steam condensate. Water-reuse projects usually modify the Composite Curves. In bridge analysis, a water-reuse project is a heat exchange in which the Minimum Temperature Difference is equal to zero and in which the source can be cooled to ambient temperature.

Case Study: A Kraft Pulp Mill

The analysis performed in this example employs data from Carlsson *et al*. (1993). The Grid Diagram is shown in Fig. 25.10. Table 25.8 shows network

© Woodhead Publishing Limited, 2013

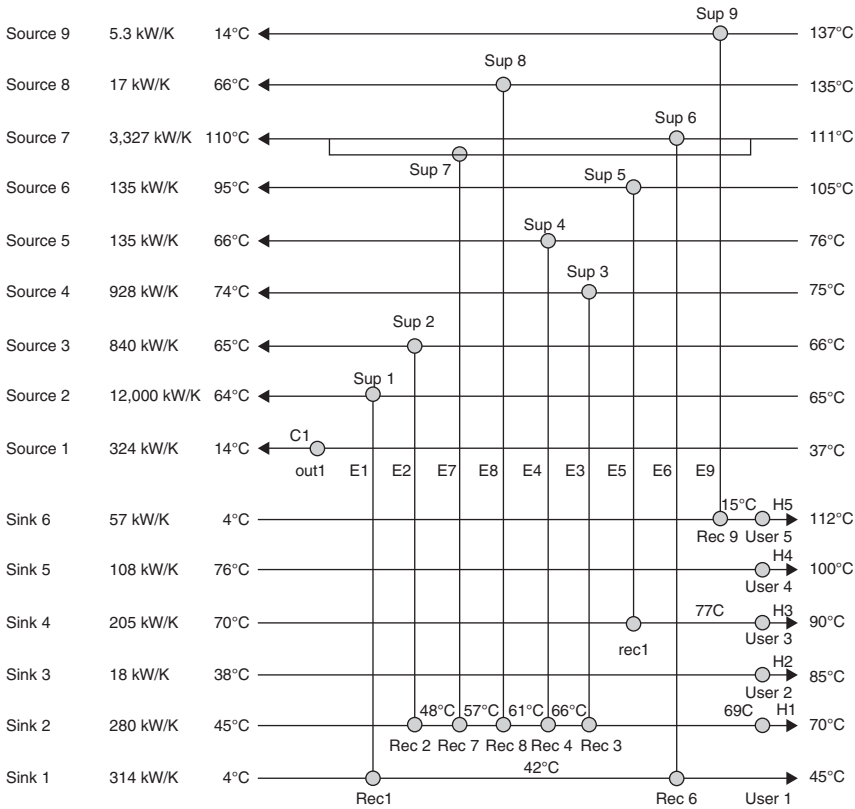

25.10 Grid diagram for example Kraft pulp mill.

Table D1, including the heat exchange capacities of useful new matches, with a reasonable Minimum Temperature Difference of 10°C. The useful matches meet the following criteria: practical feasibility, i.e., the connection requires a fixed investment cost lower than $170,000; exchange capacity greater than 300 kW; ability to be included in a bridge structure with a maximum of three new matches. Table 25.9 shows all the bridge structures with number of matches less than or equal to three. The heat savings potential of any bridge structure is equal to the upper bound as evaluated from match capacities.

25.6 Evolution of Pulp and Paper Mills

This section describes the recent improvements in process departments and a possible future of the industry where bioprocesses would be integrated in pulp and paper mills.

© Woodhead Publishing Limited, 2013

Table 25.8 Network Table D1 with exchange capacities in kW of useful matches

hu		saving										280	865		2,665	2,594		5,490
source 9	sup 9		j										498				651	594
source 8	sup 8		i															
source 7	sup 7		h				2,520								2,520	2,520		
	sup 6		g		942										942	942		
source 6	sup 5		f															
source 5	sup 4		e															
source 4	sup 3		d															
source 3	sup 2		c			840							423					840
source 2	sup 1		b	12,000	942	840	1,960						405				651	2,264
source 1	out 1	7,452	a	7,222														
				1	2	3	4	5	6	7	8	9	10	11	12	13	14	
				rec 1	rec 6	rec 2	rec 7	rec 8	rec 4	rec 3	user 1	user 2	rec 5	user 3	user 4	rec 9	user 5	
		cu		sink1				sink2				sink3		sink4	sink5	sink6		

sup: heat supplier; hu: hot utility; cu: cold utility; rec: heat receptor.
Source: Bonhivers *et al.*, 2013.

© Woodhead Publishing Limited, 2013

Table 25.9 Bridge structures

m	Bridge structure	Savings (kW)	New streams connections	Removed exchangers
2	{a1, b9}	405	2	0
2	{a1, b14}	2,264	2	0
3	{a1, b3, c9}	423	3	0
3	{a1, b3, c14}	840	3	1
3	{a1, b2, g11}	942	2	1
3	{a1, b2, g12}	942	2	1
3	{a1, b4, h11}	1,960	3	0
3	{a1, b4, h12}	1,960	3	0
3	{a1,b13, j9}	498	3	0
3	{a1, b13, j14}	594	2	0
3	{a1, b9, b14}	2,669	3	0

25.6.1 Recent Improvements in Process Departments in Modern Mills

Improvements in the heat economy of continuous and batch cooking reactors have been largely based on the use of hot black liquor displaced from cooking to heat the incoming white liquor and chips. Consequently, less heat is available for making hot water. In the most recent continuous digesters, the extracted black liquor is not used for heating water. Instead, the liquor is sent under pressure to the evaporator plant, where it is flashed and the flash vapour added to the evaporators for improved overall heat economy. The heat consumption in bleaching in a modern bleach plant including oxygen delignification has been reduced by half. This results in the reduction of water consumption by approximately one-half or more of the consumption of a typical bleach plant in the early 1980s. A major reason that such low water consumptions have been achieved is the introduction of new types of washers, such as press and drum displacement washers.

Modern evaporators are capable of reaching 75–80+% dry solids, which provides benefits in the recovery boiler operation: increased generation of steam, improved cleanability on the flue-gas side and reduced emissions of sulphur-containing gases. In addition, stripping of foul condensates is typically integrated into the evaporator set, where both the stripped foul condensates and the non-stripped evaporator condensates are an important source of hot water for brown-stock washing and recausticising.

The improvement in heat consumption in pulp drying is mainly due to the higher pulp dryness achieved from the press section, which results in less need for evaporation in the dryer. Another reason is reduced water consumption, which contributes to higher wet-end temperature.

© Woodhead Publishing Limited, 2013

In modern Kraft mills, the specific power consumption has been reduced due to larger mill size, reduced pumping in fibre-line operations, the use of variable-speed drives in specific applications and other energy-saving concepts that are now part of mill design. Modern softwood Kraft mills produce excess of electrical power which can be sold to the grid. The generation of electrical power is maximised by use of low-pressure steam in preference to medium-pressure steam. The power-generation turbine in the modern mill is typically a double-extraction condensing type. Today, the typical steam pressures for new Kraft mills are slightly over 8 MPa.

A significant development in power-boiler technology has been the introduction of the bubbling-bed type fluidised-bed boiler. The quality of hog fuel for the power boiler has also been improved. Dry debarking and efficient dewatering of bark and primary sludge by pressing are required to maximise the effective heating value of the fuel. Several new Kraft mills have now opted for burning the bio-sludge in the recovery boiler; the sludge is mixed with black liquor, and the two are evaporated and burned together.

25.6.2 Increasing Heat Integration

Best available technologies typically enable a reduction of 30–35% in energy consumption compared with average mills today. The potential for energy savings is 20–25% in existing mills using Process Integration.

Generic Tool for Easy Screening of Energy Savings Potential in Existing Mills

A tool called Heat Load Model for Pulp and Paper (HLMPP), using intelligent data collection, flowsheet simulation and energy targeting by Pinch Analysis has been recently developed by VTT, the Technical Research Centre of Finland (Hakala, 2008). It provides fast evaluation of the potential for energy improvements in a mill with sufficient data accuracy, before going into detailed calculations. HLMPP is a simplified representation of the process from the energy point of view and reveals the theoretical potential for savings by providing the minimum hot and cold utility consumptions for the given mill parameters. If the true utility consumptions (steam, fuel, cooling tower needs, river cooling, etc.) are considerably higher than what the energy target identification in HLMPP gives as a minimum, this is an indication that there is potential to improve the HEN.

The mill-specific parameters are fed into a Microsoft Excel worksheet in a format familiar to mill personnel. Flowsheet simulation is used to calculate certain flows, e.g., steam needed for drying, thermo-mechanical pulping (TMP) process steam generation, and moist exhaust air flow from the dryers, which would be otherwise difficult to obtain. The Balas steady-state software is used for this purpose. If process-specific parameters are available, the

© Woodhead Publishing Limited, 2013

tool can be expected to yield results within a few hours (Hakala, 2008). The HLMPP model includes a groundwood pulping line, a thermo-mechanical pulp line, a recycled-fibre pulping line and several types of paper machines. A model for a Kraft pulp line is under development.

Other Opportunities for Heat Savings

Excess heat is here defined as thermal energy Below the Pinch and above 80°C. If process water consumption is lower than 25 m^3/adt, Pinch Temperatures can be above 100°C. Approximately 1–2 GJ/adt of excess heat can be made available in a modern Kraft pulp mill after reorganisation of the HEN around the warm and hot water system. Investment in exchangers with small Minimum Temperature Difference, such as 5–7°C, is required. As hot-water consumption decreases, the quantity and quality of available excess heat increases. Excess heat could be used for heat pumping, district heating, an eco-cyclic industrial park, process-integrated evaporation, or another bioprocess.

The main steam user in the Kraft process is the evaporation area. Process-integrated evaporation using excess heat could decrease this steam demand by up to 66% (Algehed, 2002). By rebuilding the evaporation plant, the excess heat can be used in the evaporator effects that work with the corresponding temperatures. Excess heat from the process, such as flash steam at 100°C, is fed to an effect in the middle of the evaporation train. Effects are added at the end of the evaporation train, which is possible if the temperature of the surface condenser is decreased to 40°C (Fig. 25.11).

It is estimated that the following modifications to a typical Scandinavian Kraft pulp mill would lead to steam savings:

- Resolving Pinch violations in the cooking area and the hot-water production system would lead to savings of 1.5 GJ/adt.
- Replacing the evaporation plant with a typical 5.5-effect steam economy by a new seven-effect evaporator with integrated stripper, in which the head of the stripper is used as a heat source for the evaporation area, would make it possible to increase the dry solids content of the heavy black liquor from 73% to 80%, resulting in more high-pressure steam. Overall, this would provide savings of 2.4 GJ/adt.
- A new press section with a shoe press that provides 52% dryness instead of 45% would make it possible to save 0.5 GJ/adt steam at the dryer.

25.6.3 Integrating Bioprocesses in Pulp and Paper Mills

Biomass is chemically rich and can be an important base to produce compounds useful for society. High-value-added chemicals and material can be produced from bioprocesses that will be integrated in pulp and paper mills (Fig. 25.12).

© Woodhead Publishing Limited, 2013

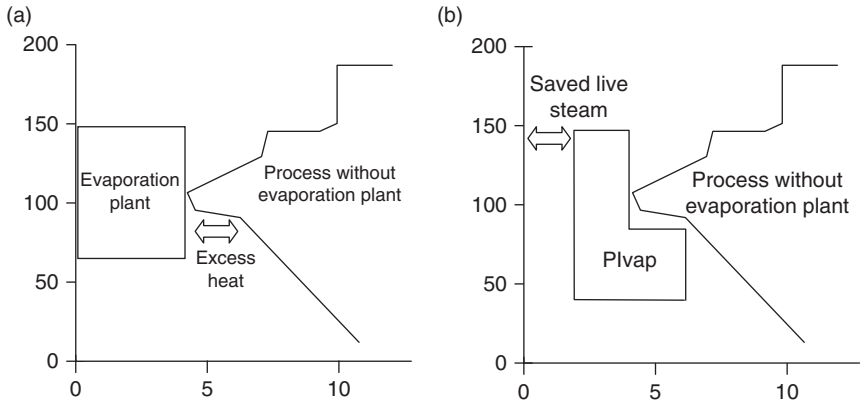

25.11 Concept of process-integrated evaporation. (a) Background/Foreground Curve in which the foreground represents a conventional evaporation plant, while the background represents the rest of the process. The amount of excess heat suitable for PIvap is indicated by an arrow. (b) By rebuilding the evaporation plant, the excess heat can be used for evaporation. Consequently, live steam is saved.

The main components of wood, i.e., lignin, hemicellulose, and cellulose, are possible sources for bio-products. Examples of lignin-based products are carbon fibre, fillers and plastic extenders, biopolymers, glues and binders. Hemicellulose can yield furfural, furfuryl alcohol, xylitol, mannitol, adhesives and thickeners. Cellulose can yield butanol, higher alcohols, keto-acids, polylactic acid, nanofibres, new viscose fibres and innovative paper products.

The main steps in a bioprocess are feedstock preparation, transformation and purification. The transformation step may involve thermal processes such as gasification or pyrolysis, or biochemical or chemical processes. The purification step may involve distillation, use of membranes, pervaporation, or hybrid systems. Energy, mass, and infrastructure integration is of crucial importance for the success of bioprocess additions to pulp and paper mills. Other important factors are the choice of technology and process flexibility. The resulting eco-cyclic system has been called an 'integrated forest biorefinery' (Chambost, 2008) and is presently the object of intensive study by many research and technology groups around the world.

25.7 Conclusion

The Kraft pulping process is the dominant manufacturing process by which wood chips are transformed into pulp, the intermediate material from which a very broad spectrum of finished or semi-finished paper products are made. This process is also the most intensive steam user among pulping processes.

© Woodhead Publishing Limited, 2013

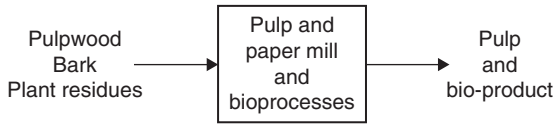

25.12 Integration of bioprocesses in P&P mills.

The water network has an important impact on heat consumption in pulp and paper mills. Water is the main heat transporter and dissipator. Non-isothermal mixing is an important source of heat degradation. Problems of build-up of contaminants from wood or process chemicals limit the extent of water closure achievable.

A first approach to improving the energy efficiency in existing pulp and paper mills should involve checking a list of key process-related strategies that are available to mills, including improved process control. More advanced energy analysis methodologies combine different integration techniques: analysis of the utility system, Heat and Water Pinch Technologies, and exergy analysis. Generally, energy analysis consists of five stages: definition of base case, benchmarking, analysis of interactions, definition of implementation strategy and post-benchmarking.

A modern Kraft pulp mill produces more heat and power than necessary for the process. In existing mills, improved Process Integration typically enables reduction of heat consumption by 15–30%. Over time, specific energy consumption can be decreased in existing mills thanks to Process Integration studies. Much of the Cross-Pinch energy-use reduction opportunity involves the hot- and warm-water production systems.

Recent methodological developments for HEN retrofit include ACCs by Berntsson and colleagues at Chalmers Institute of Technology. The major difference between traditional and advanced curves is that information about the existing network is included in the latter. Advanced curves provide the following supplementary information: the estimated heat savings potential of economically feasible projects before detailed design calculation, and the temperature levels at which usable excess heat, i.e., heat Below the Pinch, can be extracted and used. Excess heat can be used in Heat Integration projects: process-integrated evaporation of black liquor; heat upgrading with a heat pump; industrial parks including bioprocesses; district heating or cooling; etc.

The so-called Bridge Analysis method has recently been developed for HEN retrofit by Stuart and colleagues at École Polytechnique of the University of Montréal. Its main concepts are the network table, which organises data about the existing HEN, and the bridge structure, which is a set of matches that links heat outlets to hot utility users. The advantages of this approach are that detailed solutions for retrofit are visualised in a

© Woodhead Publishing Limited, 2013

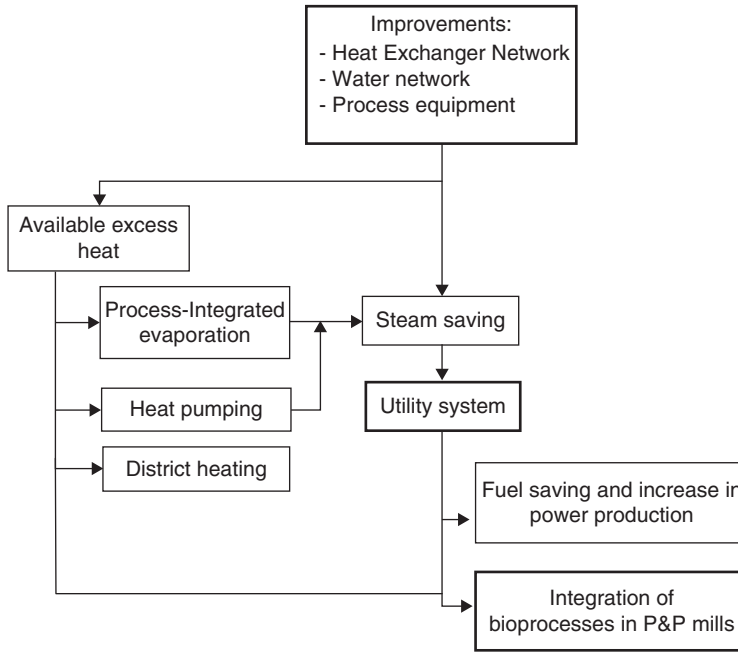

25.13 Evolution of P&P mills.

table and that connection-specific constraints are explicitly considered. The method is fundamental, and can consider indirect heat exchange as well as stream mixing, greenfield energy design as well as in retrofit, and is particularly well-suited for energy planning including for the range of biorefinery transformational projects that forest companies may be considering.

Integrating bioprocesses producing high-value-added chemicals and materials into pulp and paper mills is presently the object of intensive development in the forestry sector. Energy, mass and infrastructure integration is crucial for the success of such eco-cyclic systems, also called 'integrated forest biorefineries' in the literature. Optimisation techniques are also increasingly used for this purpose. Process Integration in the pulp and paper industry classically leads to fossil-fuel savings, increase in power production, and reduction of effluents and greenhouse gas emissions. Beyond these results, Process Integration is also a key factor in the success for ecological industrial systems around the mills of the future (Fig. 25.13).

25.8 Sources of Further Information

An energy benchmarking perspective and study to reduce the energy costs in the pulp and paper industry in Canada is presented by Francis *et al.* (2002).

© Woodhead Publishing Limited, 2013

Francis and Browne (2007) also outline an overall methodology for measuring, recording and reporting energy use in the various unit operations commonly used to make pulp and paper products. Best Available Techniques (BATs) in the Pulp and Paper Industry are described in the document from IPPC (2001), whose update is expected in the near-term. This document covers the processes involved in the production of pulp and paper in integrated pulp and paper mills as well as for non-integrated pulp mills (market pulp) and non-integrated paper mills using purchased pulp for paper production. The main operations covered are: chemical pulping, Kraft (sulphate) pulping, sulphite pulping, mechanical and chemo-mechanical pulping, recovered paper processing with and without de-inking, and paper-making and related processes. As a general reference on pulp and paper processes, the book authored by Gullichsen (2000) is excellent. Information on overall biorefinery design including energy design can be found in the book co-edited by Stuart and El-Halwagi (2012).

25.9 References

Algehed, J. (2002). Energy-efficient evaporation in future Kraft pulp mills. PhD thesis, Chalmers University of Technology, Gцteborg, Sweden.

Alva-Argaez, A., Savulescu, L., Poulin, B. (2007). A process integration-based decision support system for the identification of water and energy efficiency improvements in the pulp and paper industry. Preprints, PAPTAC 93rd Annual Meeting, Montreal, Canada.

Axelsson, E., Olsson, M. R., Berntsson, T. (2006). Heat integration opportunities in average Scandinavian Kraft pulp mills: Pinch analyses of model mills. *Nordic Pulp and Paper Research Journal*, **21**(4), 466–475.

Carlsson, A., Franck, P., Berntsson, T. (1993). Design better heat exchanger network retrofits. *Chemical Engineering Progress*, **89**(3), 87–96.

Chambost, V., McNutt, J., Stuart, P. R. (2008). Guided tour: implementing the forest biorefinery (FBR) at existing pulp and paper mills. *Pulp & Paper Canada*, **109**, 7.

Francis, D. W., Towers, M. T., Browne, T. C. (2002). Energy cost reduction in the pulp and paper industry – an energy benchmarking perspective. Pulp and Paper Research Institute of Canada (Paprican). Document available from <oee.nrcan.gc.ca> accessed 03/11/2012.

Francis, D. W., Browne, T. C. (2007). Reporting guidelines for energy use in pulp and paper operations. FPInnovations – Paprican. Document available from <iea-industry.org> accessed 03/11/2012.

Gullichsen, J., Fogelholm, C. J. (2000). *Chemical Pulping*. Book 6, Papermaking Science and Technology Series, TAPPI, ISBN 952-5216-06-03.

Hakala, J., Manninen, J., Ruohonen, P. (2008). *Generic Tool for Screening Energy Saving Potential in Pulp and Paper Industry*. VTT, Helsinki, Finland.

International Energy Agency Report. (2007). www.iea.org/publications/freepublications/publication/tracking_emissions.pdf> accessed 03/11/2012.

IPPC, Integrated Pollution Prevention and Control (2001). Reference Document on Best Available Techniques in the Pulp and Paper Industry, European Commission, Brussels, Belgium.

© Woodhead Publishing Limited, 2013

Mateos-Espejel, E., Savulescu, L., Marechal, F., Paris, J. (2011). Unified methodology for thermal energy efficiency improvement: application to Kraft process. *Chemical Engineering Science*, **66**, 135–151.

Nordman, R. (2005). New process integration methods for heat-saving retrofit projects in industrial systems. PhD thesis, Chalmers University of Technology, Gцteborg, Sweden.

Nordman, R., Berntsson, T. (2008a). Use of advanced composite curves for assessing cost-effective HEN retrofit I. Theory and concepts. *Applied Thermal Engineering*, **29**(2–3), 275–281.

Nordman, R., Berntsson, T. (2008b). Use of advanced composite curves for assessing cost-effective HEN retrofit II. Case studies. *Applied Thermal Engineering*, **29**(2–3), 282–289.

Persson, J., Berntsson, T. (2010). Influence of short-term variations on energy-savings opportunities in a pulp mill. *Journal of Cleaner Production*, **18**, 935–943.

Schroderus, S. K., Davidovsky, M. (2010). Energy consumption in Kraft pulp mills. Preprints, 96th PAPTAC Annual Meeting, Montreal, Canada.

Stuart, P. R., El-Halwagi, M. (2012). *Integrated Biorefineries: Design, Analysis, Optimization.* CRC Press/Taylor & Francis, Boca Raton, Florida, USA.

© Woodhead Publishing Limited, 2013

26

Application of Process Integration Methodologies to the Thermal Processing of Waste

PETR STEHLÍK, Brno University of Technology, Czech Republic

DOI: 10.1533/9780857097255.5.799

Abstract: The thermal processing of waste (incineration) often involves not only waste disposal, including reduction in volume, but also a waste-to-energy (WTE) process, with the majority of modern municipal solid waste (MSW) incinerators now able to deliver this technology. This chapter discusses a complex approach to the use of this technology, beginning with a brief introduction to incineration and incineration plants, followed by discussion of energy efficiency analysis and the effectiveness of energy utilisation, with specific reference to one type of MSW incinerator. The aim of the analysis was to determine the performance of the plant in terms of energy utilisation and to identify potential energy savings within the plant. Simulations were carried out based on industrial data acquired from the monitoring systems of a modern MSW incinerator, with the results showing that potential energy savings are available in the area of low-potential heat. Finally, the chapter outlines the potential for the use of Heat Integration to achieve improvements in energy efficiency, although this is somewhat limited in practical application.

Key words: Process Integration, waste-to-energy, municipal solid waste, hazardous waste, incineration.

26.1 Introduction

Thermal treatment of waste is a feasible combination of energy production and waste treatment and also an important part of waste treatment hierarchy and waste management systems in Europe.

26.1.1 Thermal Processing of Waste

The thermal treatment of municipal, hazardous and biological waste is an integral part of integrated waste management throughout Europe, as it is a safe and clean technology that is compatible with high levels of recycling

© Woodhead Publishing Limited, 2013

and offers a number of advantages over landfill. Using municipal solid waste (MSW) to produce energy is known as the waste-to-energy (WTE) process, and is not only an important waste treatment option but also reduces fossil fuel usage and can hence help to meet renewable energy targets. Thermal treatment processes recover energy from MSW incineration plants and convert it into heat and power (in the form of electricity, steam, gas, and so on); the thermal processing of MSW can therefore be considered as a method of recycling energy. The various potential uses of this recycled energy should be investigated and analysed to ensure maximum efficiency.

We will focus on a modern MSW incinerator with WTE capability. The energy released during the thermal oxidation of waste is used firstly to generate high pressure process steam and subsequently for co-generation. The modern incineration plant TERMIZO (Fig. 26.1) processes 100,000 t of MSW/y. It has one processing line with a capacity of 12 t/h, which produces 2.5 MW of electricity and 24 MW/h of thermal energy. One important feature of the plant is its Combined Heat and Power (CHP) or co-generation system, which is connected to a heating plant that produces steam for district heating. The incineration plant supplies the heating plant with steam and electricity, while the heating plant provides the incineration plant with demineralised (DEMI) water and returns condensate from the steam. A simplified flowsheet of the incineration plant is shown in Fig. 26.2.

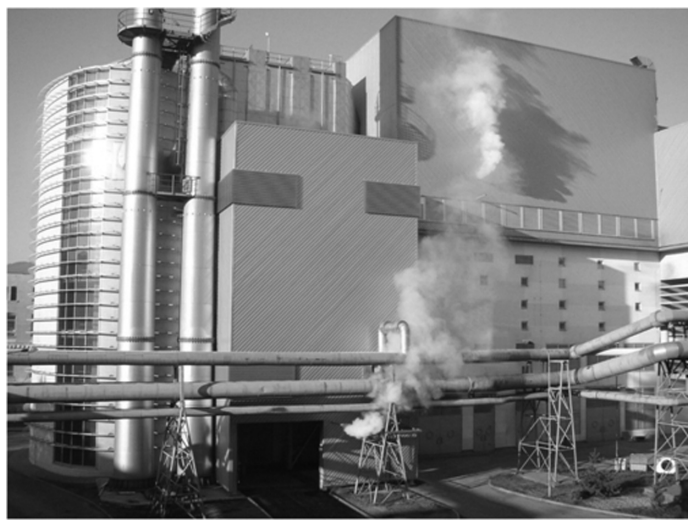

26.1 Overall view of MSW incinerator with capacity of 100 kt/y (Termizo, 2012).

© Woodhead Publishing Limited, 2013

© Woodhead Publishing Limited, 2013

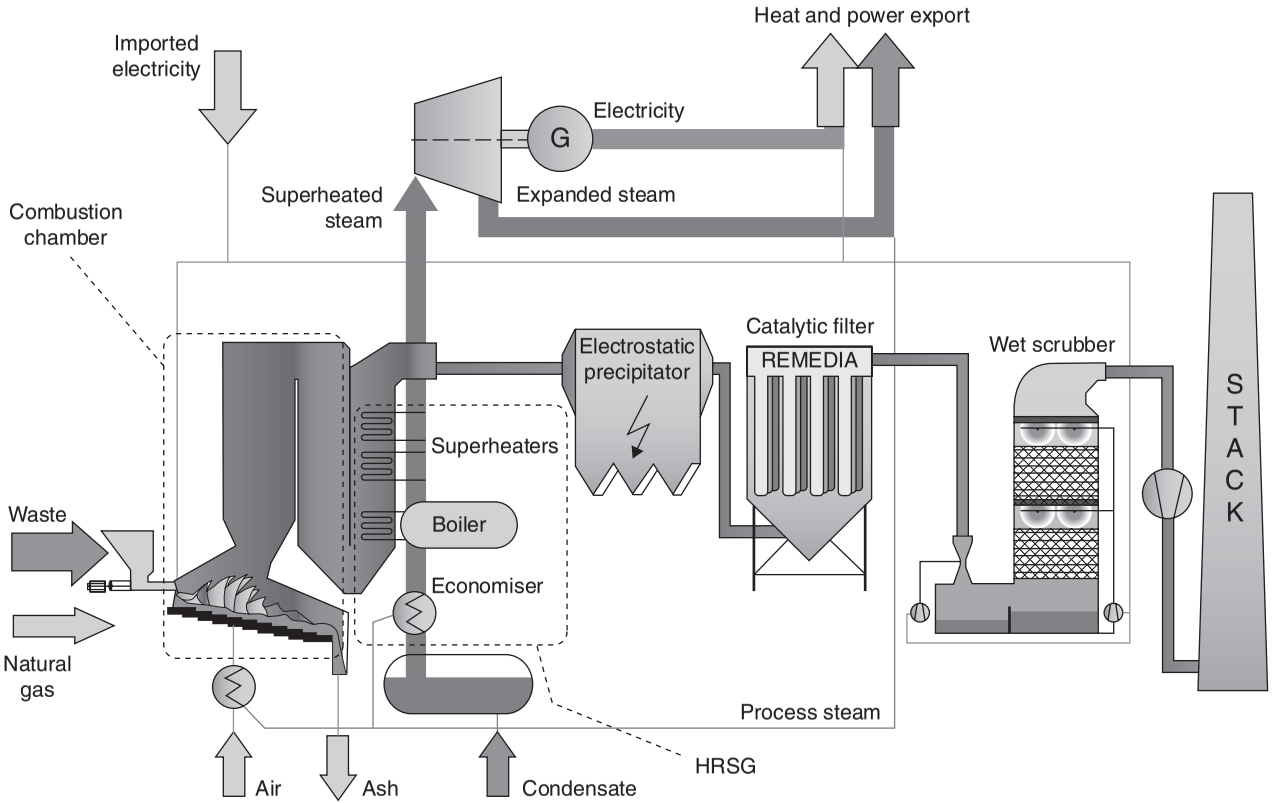

26.2 Simplified Process Flowsheet.

26.1.2 Scope for Process Integration

There is very little research devoted to Process Integration in the thermal processing of waste. El-Halwagi *et al*. (2008) present a systematic methodology for the targeting of the power co-generation potential of combustible waste. However, WTE systems constitute a very specific type of technology, without wide scope for process and/or Heat Integration. Heat recovery is a very important subsystem of WTE technology, but the energy generated is utilised for the primary purpose of waste processing. Moreover, environmental regulations are very strict in this area, creating restrictions that must be taken into account when any computational tool is used. Nearly all the technology, processes and facilities are designed for their specific purposes, making it impossible to apply general rules to all plants. This chapter will demonstrate how Heat Integration can be used to support improvements to WTE systems.

26.2 Types of Waste Thermal Processing Plants

Municipal solid waste incineration is widely used for energy recovery from waste. Industrial and hazardous waste combustion is used primarily for waste treatment – energy production is not energy recovery in this case. Pyrolysis or gasification is also possible.

26.2.1 Municipal Solid Waste (MSW) Incineration Plants

Waste incineration in MSW plants takes place in a combustion chamber, usually using moving grates. The primary air is drawn from the waste pit, and is preheated and injected through the grate, with the waste layer injected into the combustion chamber. The generated flue gas (70,000 Nm^3/h) flows from the chamber to the heat recovery steam generator (HRSG), where the heat content of the flue gas is used to produce superheated steam. The HRSG can be divided into three parts: economiser, boiler (evaporator) and superheaters. The flue gas leaves the HRSG at a temperature of around 200°C and is run through the electrostatic precipitator to remove solid particles. Some of the flue gas (around a seventh of the total amount generated) is consequently recycled and returned to the combustion chamber. The rest moves on to the flue gas cleaning unit, which consists of a dioxin filter and a wet scrubber. Once the content of compounds such as solid particles, dioxins, acid gases and heavy metals has been reduced to the level required by the relevant regulations, the cleaned flue gas is released into the atmosphere.

Superheated steam is generated in the HRSG at a rate of 35 t/h; this is moved into the backpressure turbine, which is used for electric power generation. Part of the electricity generated is supplied to all the internal

© Woodhead Publishing Limited, 2013

installations of the plant, with the surplus fed into the heating station. After the steam has left the turbine, boiler feed water (BFW) is injected into the steam to control the temperature. The majority of the steam is then exported (at a rate of 31 t/h), with the rest used in the incineration plant. The main use for steam in the incineration plant is for the preheating of primary air and heating of BFW, which is made up of the condensate from the incineration plant, DEMI water and returned condensate from the heating station.

26.2.2 Industrial and Hazardous Waste (IHW) Incinerators

According to EU legislation, waste is classed as hazardous if it exhibits one or more of the hazardous characteristics stated in Appendix III of the 2008/98/EC Directive. Hazardous waste must be processed thermally – using landfill to dispose this type of material is not possible. Units for the incineration of IHW are widely used; they are usually able to treat both solid and liquid wastes and are designed for a wide range of waste throughputs.

The set-up of IHW incinerator technology is very similar to that described in Section 26.2.1 for MSW incineration plants, although some differences can be found in the thermal block. Rotary kiln furnaces (Fig. 26.3) and two-stage combustion are commonly used to increase the quality of incineration processes. The incineration temperature in the furnace is affected by the ash melting point of 900–1,000°C. High temperatures are required in the thermal section of the unit, which is connected with the incineration of large amounts of auxiliary fuel such as natural gas.

26.3 Overall view of rotary kiln for thermal treatment of 12 kt IHW annually.

© Woodhead Publishing Limited, 2013

IHW incinerators (Fig. 26.3) can also produce heat and power, but the primary purpose of these plants is the treatment of waste. The production of power and heat in the majority of cases only reduces the external energy consumption and the cost of treating of this problematic material.

26.3 Analysis of Energy Efficiency in the TERMIZO Plant

The energy efficiency analyses discussed here are based on calculations using industrial data from the monitoring system of an incineration plant. The first step in the process was the identification of individual process streams, heat flows and utilities. The extracted data were used to create a mathematical model, using newly developed W2E software (Touš, 2009) designed for the simulation of WTE systems.

W2E software is a very efficient in-house computational tool for system design and assessment (in economic and environmental terms) in the WTE field, helping to achieve maximum heat recovery and energy utilisation from biomass and wastes. The core of the system consists of balance nodes of basic operations (such as mixing of streams, combustion of gaseous fuels, combustion of solid matter, heat exchange, and so on) supplemented by simple thermodynamic models of heat engines (such as a steam turbine or gas turbine). This means that the addition of new units is relatively simple, as are potential changes in the computational algorithm (such as recycle streams, investigation of parametric sensitivity and other partial changes). The whole system can therefore be used to build up balance models of common as well as non-traditional devices. An example of the output from the simulation is shown in Fig. 26.4.

26.3.1 Effectiveness of Energy Utilisation

The effectiveness of the energy utilisation in the incineration plant investigated was evaluated by a set of criteria that were proposed for the categorisation of equipment on the basis of the energy recovered from waste and the processing of waste. The criteria were drawn up with the aim of establishing a relationship between the extent of the energy output (produced or exported power) and the energy input.

The first of the criteria is energy efficiency (based on the R1 formula), and is particularly important as it allows the use of the term ‘energy recovery’ according to The Waste Framework Directive 2008/98/EC. This criterion takes into account the potential production of heat and power. The next criterion is the plant efficiency factor, which defines the ratio between the energy produced by incinerating the waste and the energy consumed by the process itself. Waste treatment in waste incineration plants can be referred

© Woodhead Publishing Limited, 2013

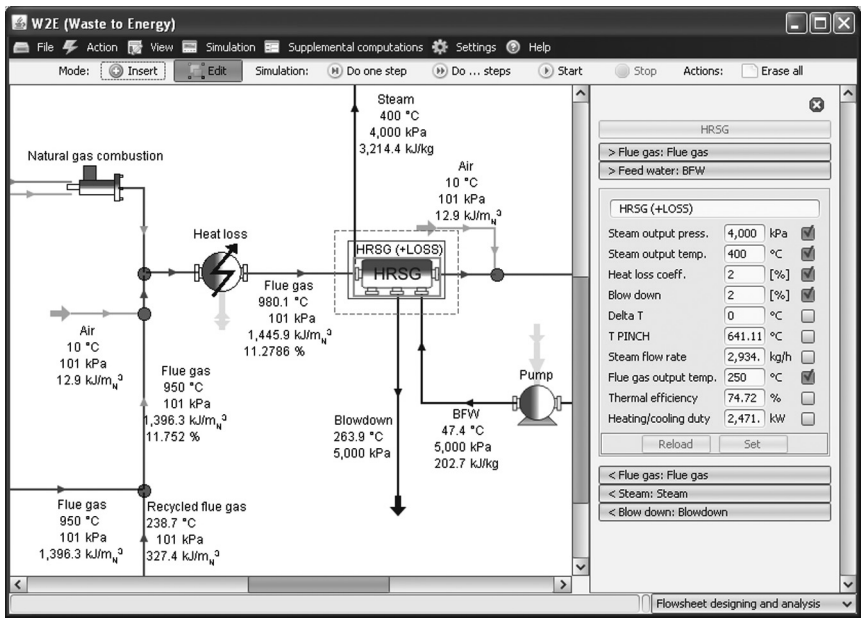

26.4 Part of model scheme in W2E software.

to as energy recovery if the plant energy efficiency factor allows energy to be delivered to third parties, i.e. when the energy produced by energy incineration outstrips the plant's own demand. Finally, a universal approach to evaluation is provided by the Primary Energy Savings criteria (PES) – PES refers to the absolute value, and pes to the specific value. These criteria offer a true picture of the savings that can be made in primary energy resources in CHP plants. Table 26.1 defines the factors involved and the required values for WTE plants are presented in Table 26.1. The value 0.97 in Equation [26.1] is a factor for energy losses caused by bottom ash and radiation.

The following symbols are used in Fig. 26.5 ('th' means thermal; 'el' means electrical):

E_f	Energy imported into the combustion process (e.g. supplementary fuel)
E_W	Energy released by waste combustion processes
I_{circ}	Circulated energy (thermal and electrical) required for the process (for example, to drive fans and pumps and to preheat combustion air and feed water)
I_{imp}	Imported energy not used for heat production
Q_{exp}	Total amount of exported energy (thermal and electrical)
Q_{prod}	Total amount of produced energy (thermal and electrical)

© Woodhead Publishing Limited, 2013

Table 26.1 Criteria for evaluation of WTE units (used nomenclature is in accordance with energy flows in the Fig. 26.5)

Reference	Criteria	WTE	Formula	
Directive 2008/98/EC	Energy efficiency (R1 factor)	$\eta_e > 0.6$ $\eta_e > 0.65$[a]	$\eta_e = \dfrac{Q_{\text{prod}} - \left(E_f + I_{\text{imp}}\right)}{0.97 \cdot \left(E_w + E_f\right)}$	[26.1]
European IPPC Bureau (2006)	Plant efficiency factor	$Pl_{\text{ef}} > 1$	$Pl_{\text{ef}} = \dfrac{Q_{\text{prod}} - \left(E_f + I_{\text{imp}}\right)}{E_f + E_{\text{imp}} + E_{\text{circ}}}$	[26.2]
Directive 2004/8/EC; Pavlas *et al.* (2010)	PES	–	$\text{PES} = \left(Q_{\text{exp}}\right) - \left(E_f + I_{\text{imp}}\right)$	[26.3]
	Specific primary energy savings (pes)	pes > 0 pes > 0.6[b]	$\text{pes} = \dfrac{Q_{\text{exp}} - \left(E_f + I_{\text{imp}}\right)}{\left(E_w + E_f + E_{\text{imp}}\right)}$	[26.4]

[a] For equipment put into operation after 12 December 2008.
[b] 0.6 value for highly efficient process.

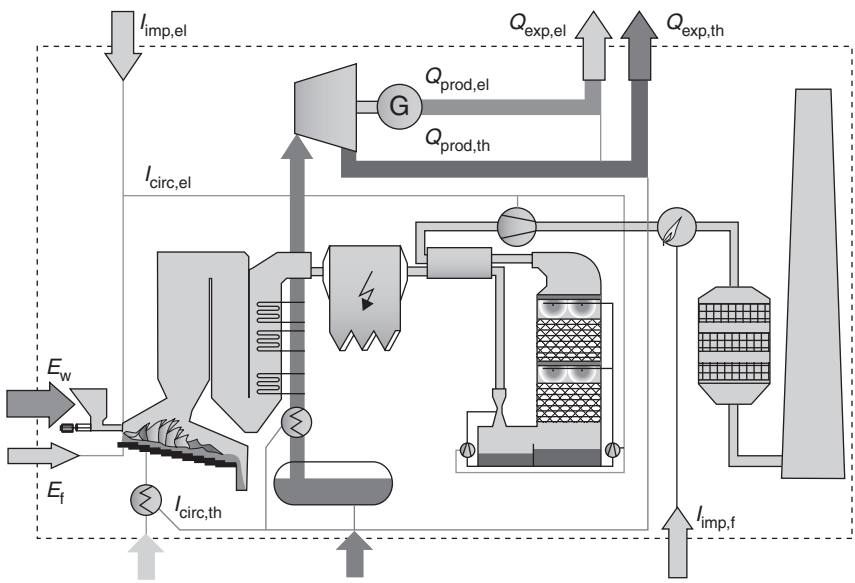

26.5 Energy streams in a MSW incineration plant.

© Woodhead Publishing Limited, 2013

Due to the complexity of the balanced system, slightly different technology was selected in the WTE plant: the flue gas was needed to be preheated to the required temperature before entering the reactor with the catalyst (known as DeNOx/DeDiox technology, and illustrated in Fig. 26.5).

All the above factors should be equivalent when substituted into the relation of the criteria. This means that individual forms of energy must be taken into account and a comparison of different units of measurements (MWh, MWh_{el}, MWh_{th}) is required. Conversion factors are therefore required, assuming an overall European average conversion efficiency for electricity generation $\eta_{el}^{Ref} = 38\%$ and conversion efficiency for heat generation $\eta_{th}^{Ref} = 91\%$ (European IPPC Bureau, 2006). These conversion factors are evaluated using the following equations:

$$\text{Electricity generation conversion factor} = \frac{100}{\eta_{el}^{Ref}} = \frac{100}{38} = 2.6 \quad [26.5]$$

$$\text{Heat generation conversion factor} = \frac{100}{\eta_{th}^{Ref}} = \frac{100}{91} = 1.1 \quad [26.6]$$

This is the only means by which different types of energy can be evaluated and adequately summarised with reference to a comparable energy mix. There are therefore two columns with figures in Table 26.2, which shows both the applied data and the results of the evaluation. The first column shows the values obtained from the annual statement of the plant, while the second shows the values after multiplying by the conversion factors for the specific energy type. The latter figures were used for the evaluation of the criteria.

The amount of imported energy is small (I_{imp} and E_f are negligible), demonstrating that this plant is almost independent and relies little on external energy supplies. Auxiliary energy is consumed only under non-standard conditions such as regular shut-down or short-term breakdown. The values determined for the criteria discussed above (energy efficiency, plant efficiency factor and specific pes) are significantly above the minimum value expected for WTE plants (see Table 26.2). The operational parameters of the plant, in terms of both production and energy recovery, result in high values for these criteria; the plant investigated can therefore be characterised as a very effective WTE plant.

26.3.2 Effectiveness of the Heat Recovery System

Using the model created with the W2E software (illustrated in Fig. 26.4), an analysis of the effect of the layout of the heat recovery system was carried

© Woodhead Publishing Limited, 2013

Table 26.2 Balance data per ton of treated MSW and evaluated criteria

Parameter	Unit	Actual value	Conversion factor	Converted values
Energy supplied by waste (E_w)	GJ/t	10.500	–	10.500
Imported energy:				
- power	GJ/t	0.061	2.6	0.159
- heat	GJ/t	0.053	1.1	0.058
- total (I_{imp})	GJ/t	0.114	–	0.216
Imported energy by supplementary fuel (E_f)	GJ/t	0.055	–	0.055
Produced energy:				
- power	GJ/t	0.636	2.6	1.654
- heat	GJ/t	8.627	1.1	9.490
- total (Q_{prod})	GJ/t	9.264	–	11.144
Exported energy:				
- power	GJ/t	0.252	2.6	0.654
- heat	GJ/t	7.048	1.1	7.753
- total (Q_{exp})	GJ/t	7.300	–	8.408
Energy circulated:				
- power	GJ/t	0.384	2.6	0.999
- heat	GJ/t	1.579	1.1	1.737
- total (I_{circ})	GJ/t	1.964	–	2.737
Energy efficiency (R1 factor)	–	1.06	–	–
Plant efficiency factor (Pl_{ef})	–	3.61	–	–
PES	GJ/t	8.14	–	–
Specific primary energy savings (pes)	–	0.76	–	–

out. The influence exerted by the principle parameters (e.g. steam pressure at outlet) was also investigated.

A number of different simulations were carried out using the W2E software. Small modifications were made to the original model and the effect of these modifications on the level of PES (expressed by factor Pl_{ef}) obtained was examined. The modification tested was the replacement of the backpressure turbine with a condensing turbine with a single extraction. An analysis was then carried out to determine any change in the amount of bleeding. The other modification was a change in the pressure at the outlet of the backpressure turbine. The results are presented in Fig. 26.6.

The x-axis shows the power-to-heat ratio, i.e. the ratio between electricity and heat energy: the value of both was calculated as the difference between the exported and imported values. Point N represents the results obtained from the simulation of the current plant status. The dashed line (N-A) shows results from simulations using a condensing turbine. As the flowrate of the bleeding rises, the Pl_{ef} factor decreases. The dotted line (N-B-C) demonstrates the effect of increasing the outlet pressure. As the heat drop over

© Woodhead Publishing Limited, 2013

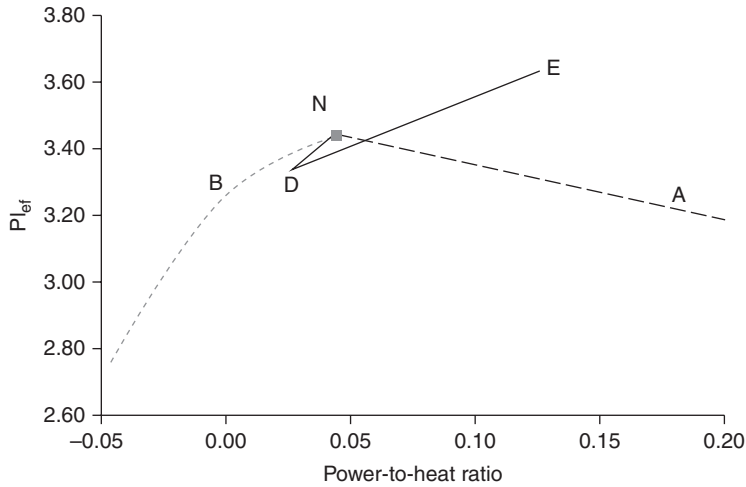

26.6 Influence of studied modifications on factor PI_{ef}.

the turbine falls, the power output also falls. Point B represents the state where no electricity is exported: the whole amount generated is consumed on-site. When the outlet pressure is increased, electricity has to be imported to cover on-site demand. Point C represents the state where no electricity is generated and the system generates only thermal energy.

The full line (N-D-E) shows the influence of reducing the pressure at the outlet from the backpressure turbine. As some of the steam generated is used to cover the demand of on-site consumers, this amount has to be fed through the by-pass of the turbine (in order to retain higher steam parameters). This line therefore shows an initial decrease to point D. But from this point the effect of increased power production as a result of increased heat drop on the turbine dominates and the PI_{ef} factor increases.

On the basis of the simulations carried out and the results obtained, general recommendations can be made for the achievement of maximum heat utilisation in MSW incinerators. The set-ups and modifications discussed above could serve as a type of user manual, to be consulted both in the design process for new modern plants and in retrofitting existing WTE plants.

A specific energy utilisation strategy can be determined for each unit. From the plant owner's point of view the best strategy is that which ensures maximum profit, while from a global perspective the best strategy leads to PES. The majority of the suggested options fulfil both requirements, meaning that they have a positive influence on the economy of the plant while simultaneously contributing to environment protection. However, in some cases and under certain circumstances (such as unexpected changes

© Woodhead Publishing Limited, 2013

in energy prices) they could be misleading. The fundamental rule to follow to achieve an effective plant with a high level of heat utilisation arises from the principle of process self-sufficiency and can be formulated as follows: minimise the amount of imported energy and maximise the amount of exported energy.

Specific methods for achieving this are described below:

1. Process optimisation and selection of the appropriate technology with the aim of reducing or completely eliminating the consumption of imported energy in the form of fossil fuels. It is difficult to substitute this type of energy with the energy produced in a heat recovery system only, due to low parameters of steam and so on. This type of energy is predominantly made up of supplementary fuel (E_f), which is consumed in a secondary chamber, and used for heating to very high temperatures.
2. Identification of the measures that lead to energy reductions in the process itself. The energy consumed by the process is made up of circulated energy (I_{circ}) and in some cases also by imported energy (I_{imp}). One way to reduce this energy consumption is the effective recovery of waste heat and low-potential heat. Heat Integration (discussed in Chapter 8) is a widely used and, thanks to its simplicity, also popular tool that allows energy flows within the processes to be studied and methods for maximal waste heat recovery to be identified by Klemeš *et al.* (1997), later overviewed also by Smith (2005) and most recently by Klemeš *et al.* (2010). The technique is based on the Pinch Analysis (Linnhoff and Hindmarsh, 1983).
3. Selection of suitable parameters for the heat recovery system that ensure the requirements of on-site consumption, and simultaneously allow for maximum energy export.
4. Use of backpressure turbine: the highest level of heat utilisation is achieved when the co-generation principle is applied, i.e. with combined heat and electricity generation. Co-generation in WTE plants is usually based on a steam turbine; the best results are achieved when a backpressure turbine is used. However, this arrangement only works if external customers require year-round heat.
5. Use of a condensing turbine with one or more extractions: if there is no year-round demand for heat, a more flexible solution is required. One option is the use of a condensing turbine with one or more extractions. The turbine then works in 'backpressure' or 'condensing' mode according to the requirements of heat export.
6. Low-pressure turbine expansion: provided that the requirements of the heat consumers allow it, it is profitable to perform the expansion on the turbine as the lowest pressure possible and similarly to export steam at the lowest possible parameters, or even to export hot water. Low steam

© Woodhead Publishing Limited, 2013

parameters enable an increase in the enthalpy drop over the turbine and thereby enable higher power output to be achieved.

7. Checking of steam parameters: if the on-site thermal energy consumption is also covered by steam from the turbine extraction, it is necessary to check the parameters of the low-pressure steam with respect to the heating of on-site streams (e.g. the heating of primary air). If the required parameters for on-site consumers are higher than the required parameters for export, the use of a turbine with several extractions may be profitable. Using a turbine by-pass for this purpose can negatively affect heat utilisation.
8. Improvement in electricity generation efficiency: if there is no consumer of heat, only electricity is required, and heat from the condenser is wasted. The efficiency of electricity generation is relatively low and can be increased by a number of different measures, such as regeneration and staged expansion with steam reheating.

The feasibility of applying any of these methods in real terms depends on numerous factors, including the properties of the incinerated waste, the technology used, local conditions, current energy prices and, last but not least, the financial resources of the investors, since modern environmentally-friendly solutions are usually connected with higher investment costs. A compromise between costs and environmentally-friendly technology is therefore likely to be required in order to arrive at an appropriate solution

26.4 Application of Heat Integration Technology

Chapter 4 outlined an alternative approach based on Heat Integration technology, using SPRINT software for Heat Integration (2007). This is an efficient methodology for Process Integration, based on thermodynamic and economic principles (for and overview see Smith (2005) and more recently Klemeš *et al*., (2010)) and the concept has also been extended to Total Site Integration (Klemeš *et al*., 1997).

The first task required in an analysis of this approach was data extraction. Data obtained from the previous calculations of the mass and heat balances of the processes within the plant were used as initial sources. The data extraction stage is extremely important: if too much data are extracted, the flowsheet obtained is likely to be the same as the original. It is also in some cases very difficult to decide precisely which data to extract. Data extraction relates to the extraction of information required for the Heat Integration analysis from a given process heat and mass balance. This involves the identification of the points at which process heating and cooling takes place. In the new simplified flowsheet the heating

© Woodhead Publishing Limited, 2013

Table 26.3 Characteristics of cold and hot streams in the MSW incinerator

Name	Description	T_s (°C)	T_t (°C)	m (kg/s)	cp (kJ/kg/K)	CP (kW/K)	DH (kW)
Hot streams							
H1	Flue gas	1,245	210	25.1	1.2	30.1	31,174
H2	Regulation of steam temperature	260	230	10	2.3	22.8	684
H3	Losses in furnace	80	20			3.2	192
H4	Blow down	263	95	0.65	4.5	2.9	486
H5	Solid residues	100	20	0.92	0.7	0.6	52
H6	Waste water	65	20	0.83	4.2	3.5	157
Hu1	Saturated steam	263	263	0.14	1646	230	230
	from boiler	263	95	0.14	4.4	0.6	104
Hu2	Superheated	230	184	1.67	2.5	4.1	190
	steam from	184	184	1.67	1,998	3,337	3,337
	turbine	184	95	1.67	4.3	7.2	638
Cold streams							
C1	Primary air	20	160	11.12	1.0	11.1	1,557
C2	Secondary air	20	100	3.22	1.0	3.2	258
C3	Condensate from incineration plant	95	119	1.39	4.2	5.8	140
C4	DEMI water	30	119	9.17	4.2	38.7	3,444
C5	Atmospheric air infiltration	20	172	0.72	1.0	0.7	109
C6	BFW	119	263	10	4.5	44.9	6,466
		263	263	10	1646	16,460	16,460
		263	385	10	3.0	30.3	3,697
Cu	Cooling water	16	18	2.70	4.2	11.3	23

and cooling demands are highlighted without any reference to the existing exchangers.

The results are displayed in Table 26.3, which shows the basic characteristics of the individual hot and cold streams that are required as input data into SPRINT. Net enthalpy was evaluated using the following equations:

$$\mathrm{CP} = m \times cp \qquad [26.7]$$

$$\mathrm{DH} = \mathrm{CP} \times (Ts - Tt) \qquad [26.8]$$

The stream data were processed by SPRINT, and a Problem Table and Composite Curves were created.

The Problem Table (Fig. 26.7) allows the Pinch Point to be identified (Linnhoff and Hindmarsh, 1983), and the minimum values of external

© Woodhead Publishing Limited, 2013

(c)CPI V:2.1.003 Sprint Lic : CPI 19 Jun 2007 16 : 53
Filename - liberec.net (M)

Proble table

*DTmin = 10.0000 [C]
Minimum hot utility = 0.00000 MW]
Minimum cold utility = 0.454063 [MW]

	Interval temperature [C]	Enthalpy [MW]	
1	1,240.0000	0.0000000	Pinch
2	390.00000	25.602000	
3	268.10000	25.580100	
4	268.00000	9.1230700	
5	258.00000	8.9752700	
6	255.00000	8.9396100	
7	225.00000	9.2669800	
8	205.00000	9.0292300	
9	177.00000	7.8530200	
10	165.00000	7.3274000	
11	124.00000	5.0756200	
12	105.00000	4.0393200	
13	100.00000	3.7504800	
14	95.000000	3.4907600	
15	90.000000	3.2342600	
16	75.000000	2.4213800	
17	60.000000	1.6565000	
18	35.000000	0.46885300	
19	25.000000	0.38076300	
20	15.000000	0.45406300	

26.7 Problem table.

heating and cooling requirements to be calculated. Figure 26.7 shows that the processes in an incineration plant are different from those in common chemical plants. Based on the large amount of steam that is generated, hot utilities are not required.

Figure 26.8 presents the Composite Curves of the whole process, and clearly shows that the utilisation of the heat content of individual streams is very good. There is also a significant temperature difference between the hot and cold streams, which leads to a strong driving force for the heat exchange. As the temperature axis is on a large scale, a magnified section of the Composite Curves from Fig. 26.8 (in the low temperature field) is given in Fig. 26.9. For ease of understanding, each section of the curves is labelled with the name of the stream to which it belongs. Some parts of the streams and their temperatures in the Hot Composite Curve can still not be seen clearly; Fig. 26.10 therefore shows a further magnified section of a narrower temperature range, with individual temperatures labelled. Both of the magnified figures indicate that the largest possible energy saving could be made

© Woodhead Publishing Limited, 2013

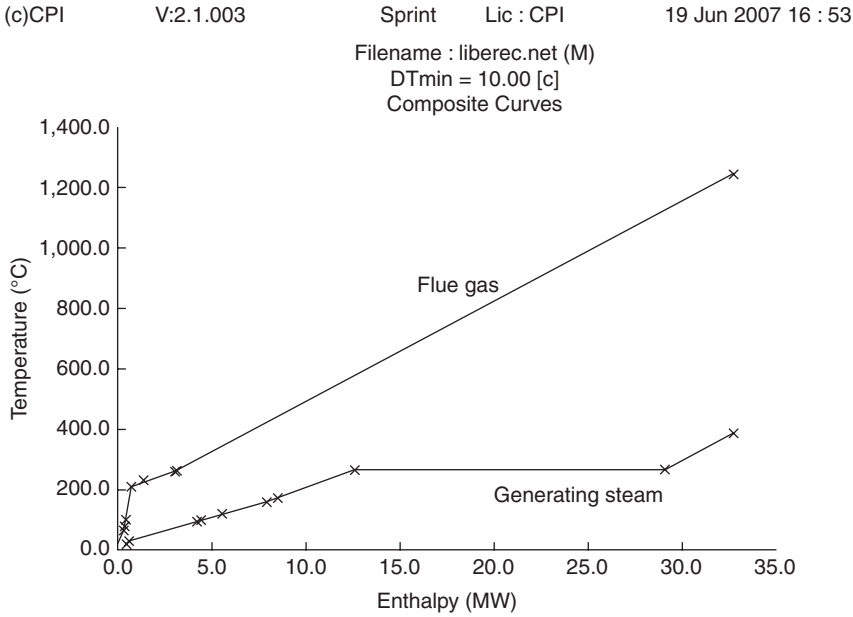

26.8 Composite Curves.

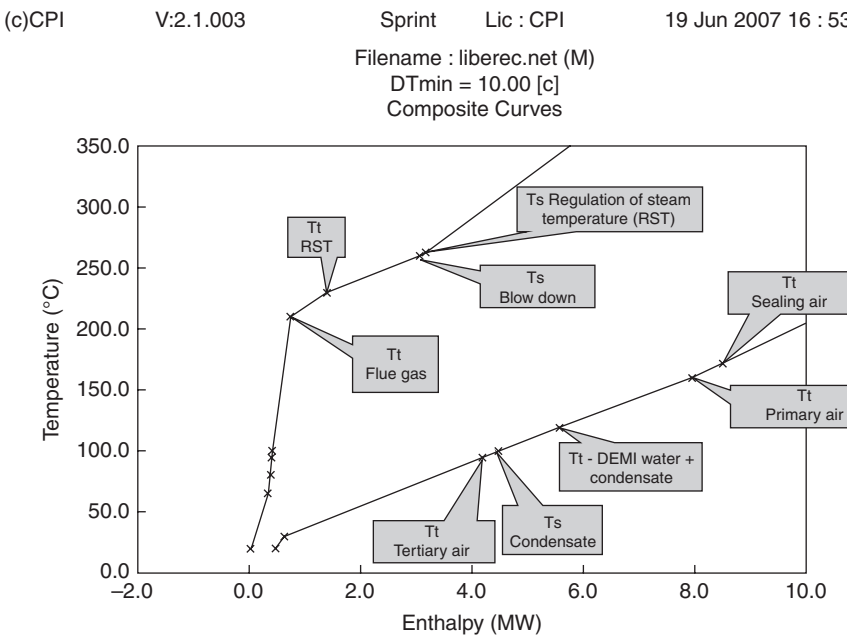

26.9 Lower temperatures of Composite Curves – a zoomed part.

© Woodhead Publishing Limited, 2013

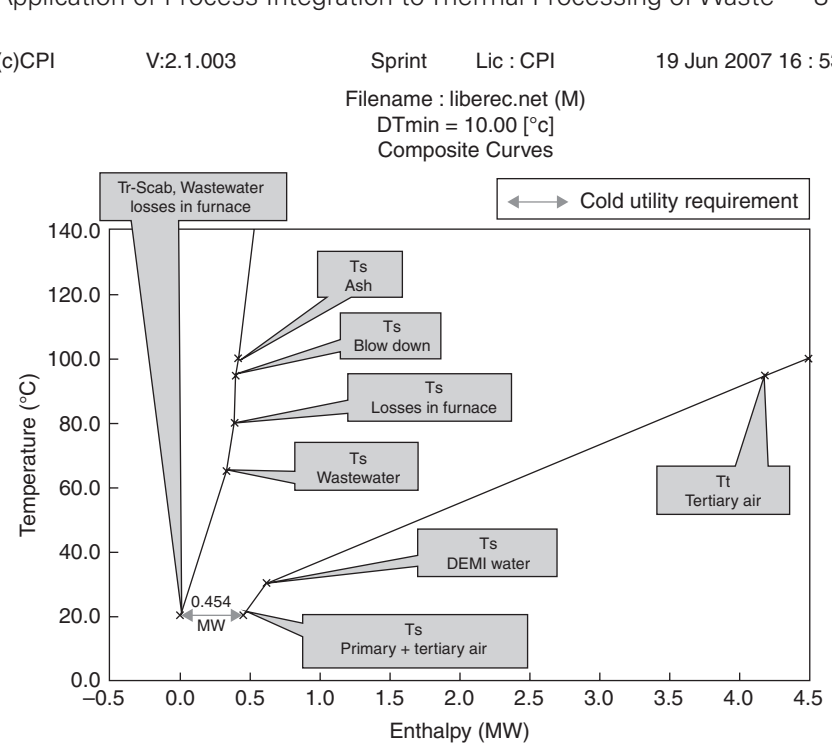

26.10 Lowest temperatures of Composite Curves – a zoomed part.

in the area of low-potential heat: this raises some problems in the identification of an appropriate use for this energy.

The following losses were identified at the plant:

- solid residues (e.g. ash, iron),
- filtration cake (from fly ash cleaning and from wastewater cleaning),
- wastewater,
- flue gas (60,000 Nm^3/h, $T = 60°C$, $p = 95$ kPa),
- heat losses from the combustion chamber,
- heat losses from the absorption column,
- waste steam from the water seal for the ash from the furnace,
- losses in the small cooling tower.

The following areas were identified as having the potential to offer energy savings:

- heating of DEMI water and condensate from the heating plant,
- heating of primary air,
- heating of BFW.

© Woodhead Publishing Limited, 2013

The main aim should be to reduce the consumption of steam inside the plant, thereby increasing the amount of steam that can be exported and sold to the heating station, and improving the overall economics of the plant. It was discovered that waste steam is generated in the water seal for the ash from the furnace, which has not yet been utilised. Similarly, the heat content of the blow down from the boiler is not currently used. The blow down could be extended to include the steam pressure at the turbine outlet, and both steam and hot water could be used to heat the returning condensate from the incineration plant. Another possibility is the use of the waste steam to heat some of the DEMI water from the heating station up to a temperature of 30°C.

26.5 Conclusion

The aim of this chapter was to analyse energy utilisation in incineration plants, specifically those using WTE technology. An example of a modern MSW incinerator with a capacity of 12 t/h was used to illustrate the methods and approaches that can be adopted in this regard. Modern incinerator plants are solely for the purpose of waste disposal only, but also produce renewable energy, which can in part replace conventional energy sources such as the combustion of fossil fuels. The effectiveness of energy utilisation in an incineration plant was evaluated on the basis of the plant efficiency and energy efficiency criteria, but also using the recently introduced PES criteria, which provides a real picture for balancing WTE systems. The industrial data from the incineration plant monitoring system were used in the calculations. The values obtained are high above the recommended values for WTE plants and indicate that the plant examined is extremely efficient. However, another analysis was also carried out using a model created with WTE software to study the influence of different factors on these criteria. From the results of this simulation, several general recommendations were drawn up for achieving maximum heat utilisation in the MSW incinerator. These results were further investigated by applying the principle of Heat Integration using the SPRINT software tool SPRINT (2007). Some further possible energy savings in the area of low-potential heat have been identified and require further research.

26.6 Sources of Further Information and Advice

As mentioned above there are a limited number of studies in this area. All those available are listed in the References. We should also mention the forthcoming monograph by Klemeš and Stehlík, *Waste to Energy* (Wiley-VCH). This monograph describes that in order to identify an efficient method of utilising Heat Integration in WTE technologies, complete familiarity with

© Woodhead Publishing Limited, 2013

the process is required, along with an understanding of the practical possibilities of low-potential energy utilisation in particular. In this regard, the following approach is advisable:

- Identification of the optimum placement of MSW incinerators (in the case of grassroots design), taking into account waste availability and price (for processing) at the 'plant gate', demand for heat, export of electricity to the network, potential future competitiveness, and so on. A new and original method based on stochastic programming is currently being developed by the Institute of Process and Environmental Engineering at Brno University of Technology.
- Selection of BAT for the incineration plant (European IPPC Bureau, 2006). However, a tailor made design is required, and practical experience should be used as much as possible, taking specific limitations into account.
- Design of key pieces of equipment with the aim of meeting the primary purpose of waste disposal and of utilising as much of the energy contained in flue gas as possible.
- Complex analysis of heat availability and demand for potential Heat Integration. It must then be decided whether the principles and methods of Process Integration would be suitable and beneficial for this specific process. If so, the approach outlined above can be followed.

26.7 References

Directive 2004/8/EC of the European Parliament and of the Council of 11 February 2004 on the promotion of cogeneration based on a useful heat demand in the internal energy market. *Official Journal of the European Communities*, Brussels, Belgium 21.2.2004, L52, 50–60.

Directive 2008/98/EC of the European Parliament and of the Council of 19 November 2008 on waste and repealing certain Directives, *Official Journal of the European Communities*, Brussels, Belgium, 22.11.2008, L 312, 3–30.

El-Halwagi, M., Harell, D., Spriggs H. D. (2008). Targeting cogeneration and waste utilization through Process Integration, *Appl Energy*, **86**(6), 880–887.

European IPPC Bureau (2006). *Reference Document of the Best Available Techniques for Waste Incineration*, Brussels, Belgium, <eippcb.jrc.es/reference/wi.html> accessed 30 January 2012.

Klemeš, J. J., Friedler, F., Bulatov, I. S., Varbanov, P. S. (2010). *Sustainability in the Process Industry: Integration and Optimization,* New York, McGraw Hill, USA.

Klemeš, J., Dhole, V. R., Raissi, K., Perry, S. J., Puigjaner, L. (1997). Targeting and design methodology for reduction of fuel, power and CO_2 on total sites, *Appl Therm Eng*, **17**(8–10), 993–1003.

Klemeš, J., Bulatov, I., Cockeril, T. (2007). Techno-economic modelling and cost functions of CO_2 capture processes, *Comput Chem Eng*, **31**(5–6), 445–455.

Klemeš, J. and Stehlík, P. (2013). *Waste to Energy*, Wiley-VCH Verlag GmbH & Co. KGaA Weinheim, Germany.

© Woodhead Publishing Limited, 2013

Linnhoff, B., Hindmarsh, E. (1983). The pinch design method of heat exchanger networks, *Chem Eng Sci*, **38**(5), 745–763.
Pavlas, M., Touš, M., Bébar, L., Stehlík, P. (2010). Waste-to-energy – an evaluation of the environmental impact, *Appl Ther Eng*, **30**, 2326–2332.
Smith, R. (2005). *Chemical Process Design and Integration*, John Wiley & Sons, Chichester. ISBN 0–471–48681–7.
SPRINT (2007). *Process Integration Software*, Centre for Process Integration – CEAS, The , UK.
Taal, M., Bulatov, I., Klemeš, J., Stehlík, P. (2003). Cost estimation and energy price forecast for economic evaluation of retrofit projects, *Appl Therm Eng*, **23**, 1819–1835.
Termizo, A. S. (2012). Liberec Incineration Plant, <www.termizo.cz>, accessed 30 January 2012.
Touš, M., Houdková, L., Pavlas, M., Stehlík P. (2009). Waste-to-Energy (W2E) Software – a support tool for decision making process, *Chem Eng Trans*, **18**, 971–976.
Wu, C. (2004). *Thermodynamic Cycles: Computer-aided Design and Optimization*, Marcel Dekker, New York, USA. ISBN 0824742982.

26.8 Appendix: Nomenclature

BFW	boiler feed water
Ci	*i*-th cold stream
CHP	Combined Heat and Power – co-generation
CP	heat capacity (kW/K)
Cui	*i*-th cold utility
cp	specific heat capacity (kJ/kg/K)
DEMI water	demineralised water
DH	net enthalpy (kW)
E_f	imported energy to the combustion process (e.g. supplementary fuel), (GJ/t)
E_W	energy released by waste combustion processes, (GJ/t)
Hi	*i*-th hot stream
HRSG	heat recovery steam generator
Hui	*i*-th hot utility
IHW	industrial and hazardous waste
I_{circ}	energy circulated (thermal and electrical), which is necessary for the process (energy for driving fans and pumps, for preheating of combustion air, preheating of feed water, etc.) (GJ/t)
I_{imp}	imported energy not used for heat production (GJ/t)
m	mass flow (kg/s)
MSW	municipal solid waste
p	pressure (kPa)
PES	primary energy savings (GJ/t)

© Woodhead Publishing Limited, 2013

pes	specific primary energy savings (–)
Plef	plant efficiency factor (–)
Qexp	total amount of exported energy (thermal and electrical) (GJ/t)
Qprod	total amount of produced energy (thermal and electrical) (GJ/t)
T	temperature (°C)
Ts	supply temperature (°C)
Tt	target temperature (°C)
W2E	WTE software
WTE	waste-to-energy
ηe	energy efficiency (R1 factor) (–)
η_{th}^{Ref}	average European conversion efficiency for electrical generation (–)
η_{th}^{Ref}	average European conversion efficiency for heat generation (–)

© Woodhead Publishing Limited, 2013

27

Application of Process Integration Methodologies in the Brewing Industry

FRANÇOIS MARECHAL, ANURAG KUMAR SACHAN and LEANDRO SALGUEIRO, Ecole Polytechnique Fédérale de Lausanne (EPFL), Switzerland

DOI: 10.1533/9780857097255.5.820

Abstract: This chapter presents the application of Process Integration techniques to increasing the energy efficiency of a typical brewery process. The example has been chosen to illustrate the application of Process Integration methodology and also to demonstrate the steps towards the implementation of Process Integration analysis. The chapter starts with a discussion on the definition of the process requirements, and of the system boundaries of the study. The Heat Cascade is then used to calculate the maximum heat recovery in the process. The integration of the refrigeration cycles and of the energy conversion technologies will then be studied to finally analyse the possible integration of heat pumping technologies as well as the integration of waste conversion units. It has been discussed how the targeting energy consumptions of the process can then be reached in a real industrial process implementation. The data used for the study are based on a flowsheeting model, and can therefore be considered as generic.

Key words: Process Integration, energy efficiency, Pinch Analysis, brewery process, cogeneration, heat pump, thermo-economic optimisation.

27.1 Introduction

Any industrial process is a system (Fig. 27.1) in which raw materials are converted into products and by-products. In most cases, the conversion is realised in a set of process unit operations or processing steps that require a production support such as water or solvent. The driving force of the conversion step is energy, which enters the system as energy resource flows being converted into a useful energy form such as heat, cold or work, in order to realise the required processing steps. As the conversion of the raw materials, as well as of the energy resources, is not perfect, part of the mass and the energy entering the system leaves the process as waste in the form of solid, liquid or gaseous, or as waste heat, which

© Woodhead Publishing Limited, 2013

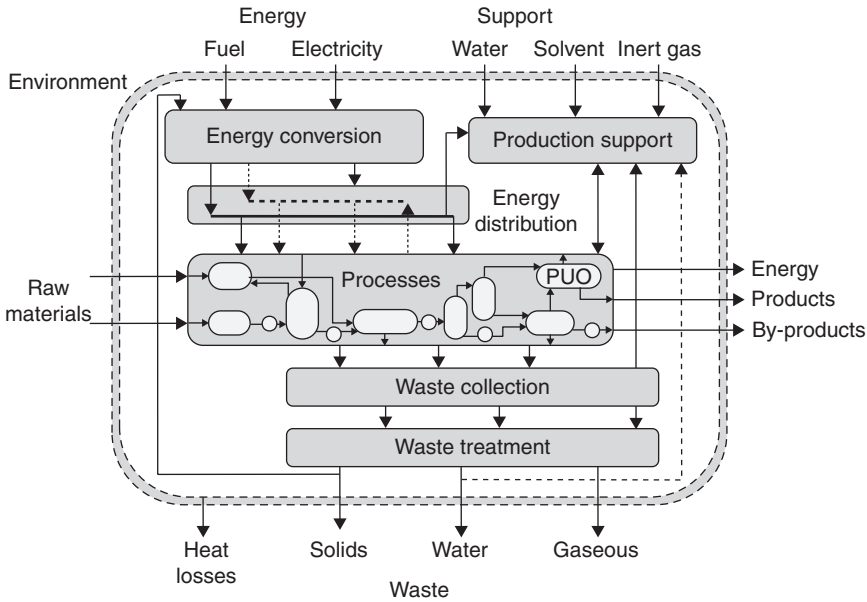

27.1 The industrial production system.

has to be treated and conditioned before leaving the system and released into the environment. When considering Process Integration, the goal is to optimise the overall efficiency of the process, thereby maximising the horizontal flows while minimising the vertical ones. Considering the system boundaries, Process Integration will address not only the processing steps, maximising the process throughput, but also the support streams management, maximising the recycling and the reuse of materials as well as the waste management and treatment and the energy conversion. This results sometimes in the addition of new products in the form of by-products or energy services.

The process used in this chapter is a beer-production process. The block flow diagram describing the major processing steps is sketched on Fig. 27.2. The beer production follows a recipe that converts a mixture of corn, water and hops (raw materials) into bottled beer (product) by means of a set of cooking, filtering and fermentation steps (processing steps). The process uses water as the production support, both for the process itself and for the equipment and conditioning washing. The conversion process requires energy in the form of heat for the cooking, and cold during the fermentation and conditioning. Waste resulting from the process is more or less humid, leaving the system as solid or liquid. In addition, the evaporation of a part of the water during the process also produces vapour, which is typically vented from the roof.

© Woodhead Publishing Limited, 2013

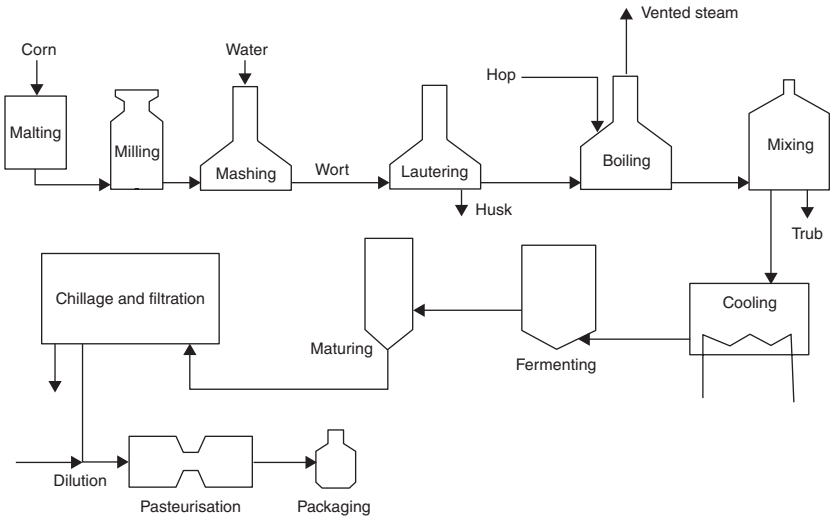

27.2 The brewery process block flow diagram.

In the brewery, beer is produced from a mixture of water and malted corn. By volume, water is the main raw material. The different operations are now described in more detail, in order to characterise the use of energy in the beer processing.

Malting: In this process, the barley grains are prepared for brewing by releasing the starches in the barley. In a three-step approach, the grain is added to a vat with water and allowed to soak for approximately 40 h during steeping. Then, in germination, the grain is spread out on the floor for around five days and, finally, the green malt goes through very high temperature drying in the kilning step.

Milling: In the process of milling, the grains are cracked so that they can absorb the water. The water, as a result of this mixing, extracts sugar from the malt.

Mashing: The milled barley grains and supplementary grains (corn, sorghum, rye and wheat) are mixed with water and then heated to 65°C in a vessel for approximately 2 h in the process of mashing. During the mashing, the process of saccharification takes place with the mash, resulting into a sugar rich liquid, 'Wort'.

Lautering: This wort is filtered from the mash, in the 'lautering' process.

The remaining solid particles of the malt (brewing dregs) may be used as animal feedstock or biomethanised.

Boiling: The wort is then boiled at 105°C (under atmospheric pressure) for 1 h in a tank. During boiling, hops are added to control the bitterness, flavour and aroma; finally the mixture is sterilised. Approximately 10% by

© Woodhead Publishing Limited, 2013

mass of the wort evaporates during the boiling, representing most of the total mass of wort that is evaporated in the brewing process.

Mixing–Whirlpool: The wort is then stirred and settles in a large tank, before being purified of all solid protein particles (trub). Approximately 0.2% by mass of the wort is settled and removed in the form of trub.

Cooling: This is the last step of the hot part of the brewing process. The purified wort is cooled to 10°C to prepare it for the process of fermentation.

Fermentation: Fermentation is the conversion of sugars to alcohols and carbon dioxide or organic acids, using yeasts or bacteria under anaerobic conditions. For this purpose the wort is stored in fermentation tanks, and maintained at a constant temperature of 10°C for 14 days. These chemical reactions are exothermic and, thus, cooling is necessary during fermentation.

Maturing: The wort is then maintained at 6°C for a period of 10 days for maturing. In this period, the CO_2 concentration is controlled and kept constant.

Chillage and Filtration: The wort is finally rapidly chilled to 1°C, and the yeast is eliminated by filtration. At this point a concentrated beer is obtained.

Dilution: The degasified cold water is mixed with the concentrated beer to achieve the desired alcohol content in the beer. In our case, it is diluted by adding 25% water by mass to the concentrated beer.

Pasteurisation: The beer is pasteurised by heating up to 70°C and, after a stay, cooling the beer to 5°C; it is then stored in the insulated tanks to be decanted into bottles or kegs.

Bottling: After pasteurisation, the beer is bottled. This step requires the bottle or kegs to be washed, and the packaging material to be prepared.

27.2 Process Flowsheet Analysis

For defining the global system requirements, it is important to develop a systematic methodology that guarantees that all the needs and the boundaries of the system are well characterised. Using the brewery case as reference, in the next sections this methodology is described in detail.

27.2.1 Block Flow Process Analysis

The Flowsheet of Fig. 27.3 shows the flow of various streams within the brewing plant with constraints of temperature and pressure as per the recipe of the beer. The conventional plants do not have direct process/process heat recovery and thus heat exchangers exist only between process streams and the utility streams, including the hot water system.

© Woodhead Publishing Limited, 2013

© Woodhead Publishing Limited, 2013

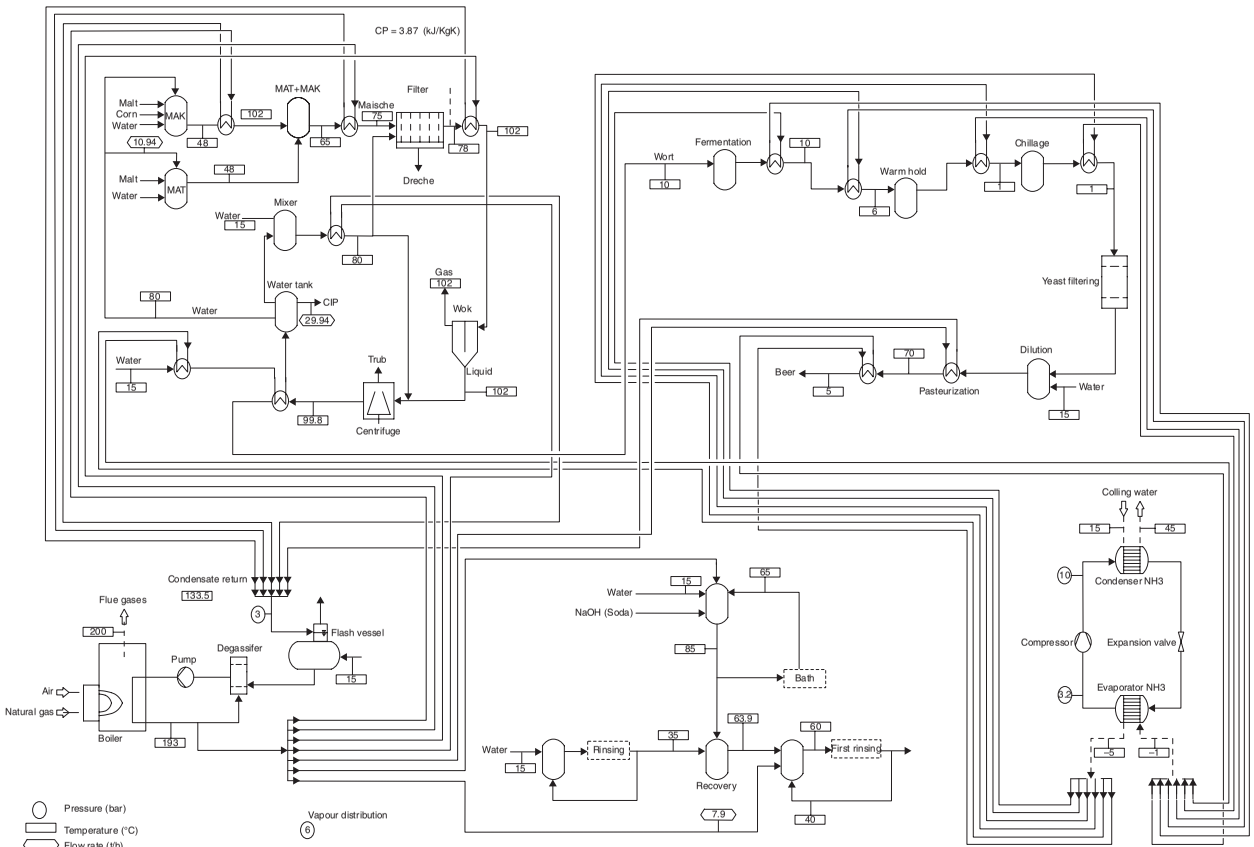

27.3 The Process Flowsheet.

The Process Flowsheet is divided into different sub-systems that are then allocated to process and utility sub-systems. The process subsystem refers to process units that are strictly related to process unit operations. The units in this system define therefore the requirements of the process. The utility system includes the units that are related to the supply of the energy (heating and cooling) services needed by the process. The utility subsystem includes the flows that we would like to optimise in order to minimise the energy bill.

The process subsystem is defined into three major sub-systems:

Hot section: The hot part (Fig. 27.4) corresponds to the cooking part of the brewing process. The malt is first mixed with water in a large tank (MAT) and heated to a temperature of 48°C with the addition of hot water. The malt is especially made of sprouted barley. When malt is heated, the enzymes decompose the starch into sugar. Later, this sugar will be transformed into alcohol during fermentation. Another tank (MAK) filled with malt, corn and water is also preheated to 48°C; the resulting flow is then heated to a temperature of 102°C, before being mixed with the MAT tank content and reheated to 75°C. At this point, the mixture is called mash. This mash passes through a pressing filter, which requires an additional amount

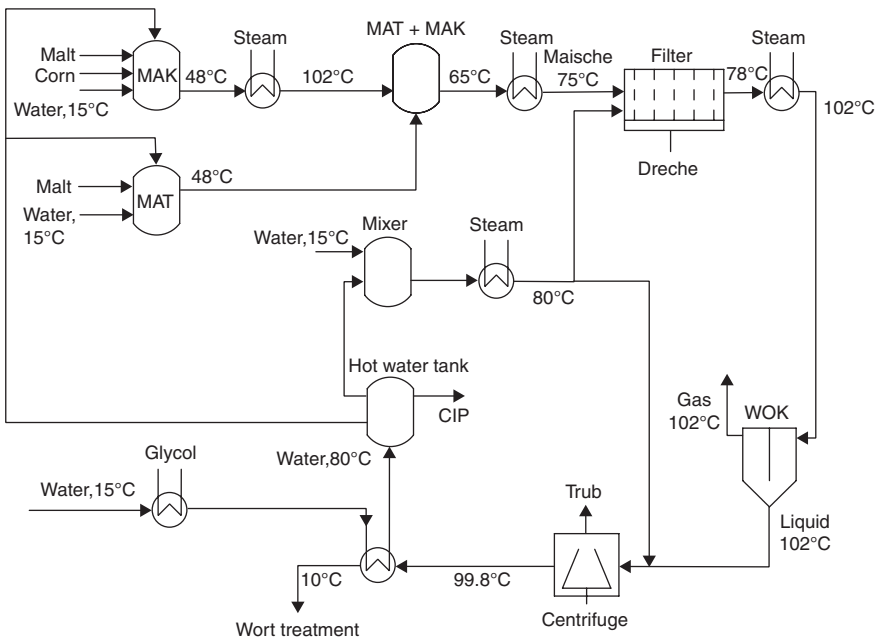

27.4 Brewing process: Hot section.

© Woodhead Publishing Limited, 2013

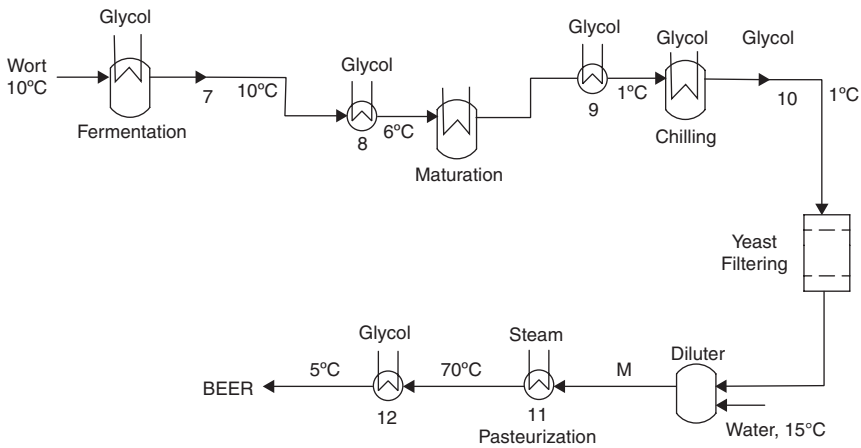

27.5 Brewing process: Cold section.

of hot water at 80°C. The wastage is essentially compressed malt that can be considered as dry and called dreche. After being filtered, the liquid is mixed with hops and heated in the WOK to a temperature of 102°C for approximately one hour. It is assumed that during this time about 10% of the liquid mass flow is evaporated. While the vapour is vented, the outgoing liquid (wort) is mixed with an additional amount of hot water before being filtered by a centrifugal device to separate the 0.2% of cooked proteins (trub). The wort is then cooled down to 10°C in a heat exchanger to reach the cold section of the process. The heat recovered is sent to the hot water tank to feed the hot water needs of the next operation.

Cold section: The cold section (Fig. 27.5) concerns mainly the fermentation and the subsequent beer-conditioning operations. The wort is first fermented at a temperature of 10°C. The fermentation reaction is exothermic; the observed heat of fermentation is 37.14 kJ/L_{wort}, and it includes heat gains from the ambience. Glycol–water is circulated in the fermentation tanks to maintain the temperature at 10°C for a fermentation period of 14 days. The wort is then cooled and maintained to a temperature of 6°C, to eliminate diacetyl residues that give the beer an unwanted taste of butter. This maturation period is usually 10 days, depending on the alcohol content required in the beer. The specific cooling requirement of the maturation is 29.55 kJ/L_{wort}. After the maturation process, the fresh beer is cooled down to 1°C, in order to precipitate the yeast that is filtered in the Chillage step. The specific heat for this step is 29.70 kJ/L_{beer}. The CO_2 concentration maintained during the maturation period is between 2.2 and 2.4 kg_{CO2} /hL_{wort}. At the end of the process, the alcohol concentration is controlled by diluting the beer mixture with water at 15°C. The beer is finally pasteurised, by heating up the mixture to 70°C and cooling it again to 5°C rapidly. This beer is now ready for packaging.

© Woodhead Publishing Limited, 2013

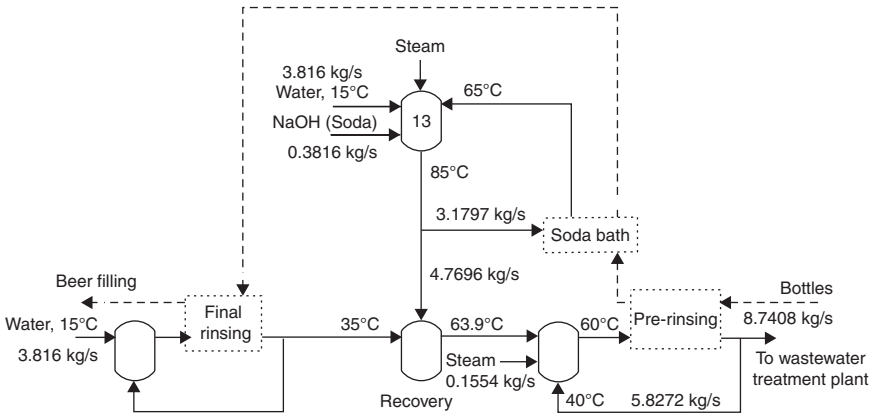

27.6 Brewing process: Cleaning in place section.

Washing: The washing system (Fig. 27.6) mainly aims at preparing the packaging materials (mainly bottles and kegs) before filling them with beer. This process is considered as a continuous operation. The bottles are successively pre-rinsed, then washed with soda and rinsed in successive baths again, before being filled with beer. The temperature of the baths is maintained by steam injection. The final rinsing is done with clear water at 15°C. Water of the final bath rinsing is recuperated and sent to the pre-rinsing bath, recovering heat from the bottles that are cooled down in the last bath.

It is assumed that the amount of water used for the third rinsing cycle is about 20% of the amount of beer produced. The fraction of NaOH/water for the bath rinse to supply water is equal to 1/10. The whole cleaning system proceeds at atmospheric pressure. Details on the temperature set points and the energy losses in the different baths are given on Fig. 27.6.

The utility system includes the following subsections:

Hot utility system: The process heat is supplied conventionally by steam produced in a boiler. Hot water is also used in the process. It is stored in an intermediate hot water tank, which also serves as a heat recovery system.

Refrigeration system: Cooling requirements are supplied by distributing cold glycol–water mixture that is produced in an ammonia refrigeration cycle.

27.2.2 Time Average Approach

The beer production is described a priori as a succession of batch reactors. However, in industrial plants, although the processing operations are batch, the overall process can be considered as a nearly constant process by realising the operation in different batch reactions that are operated with a certain dephasing. The heat recovery being made is possible by introducing hot water buffer tanks. It is therefore possible to apply

© Woodhead Publishing Limited, 2013

the time average approach (Linnhoff *et al.*, 1988) to represent the process operation by replacing the instantaneous flows or power by the mean energy needed per unit flow multiplied by the mean unit flow per product flow (Equation [27.1]).

$$\dot{m}_s\,[\mathrm{kg/s}] = m_s\,[\mathrm{kg/kg\,product}] \cdot \tilde{\dot{M}}_p\,[\mathrm{kg\,product/s}] \qquad [27.1]$$

where the mean flow of product flow is calculated by Equation [27.2]

$$\tilde{\dot{M}}_{\mathrm{product}}\left[\mathrm{kg_{product}/s}\right] = \frac{\dot{M}\left[\mathrm{kg_{product}/y}\right]}{t_p\,[\mathrm{s/y}]} \qquad [27.2]$$

In the following, all the flows and power that will be presented will refer to mean flows and power.

27.2.3 Inventory of Flows Entering and Leaving the System Boundaries

Following the definition of the system (Fig. 27.1), the first step is the identification of the flows entering and leaving. The flows entering the system are the raw materials (water, corn, malt (barley) and hops), the energy (natural gas in the boiler and electricity), the support materials (water, soda, etc.) and the packaging materials. The cleaning of bottles requires water and soda as input flows. The waste water leaves the cleaning system. The total water required at the third rinsing is 20% of the total beer produced, and is the same for the bath rinsing step as well. The amount of soda is 10% of the water added to the bath rinse. It leaves the system as part of the waste water flow. The streams leaving the system are the products (bottled beer) and the waste streams. The bio-waste of husk (dregs) accounts for 30% of the initial malt added. In addition, evaporated water and CO_2 from the fermentation leaves the system and is released into the environment.

Figure 27.7 summarises the major flows entering and leaving the system. Table 27.1 gives the specific major flows in units of bottled beer produced.

27.2.4 Energy Conversion and Distribution System

A boiler is used to produce the steam, thus natural gas is burned as primary fuel to generate the heat and convert the water into steam. Electricity is also required in small amounts for the pumping power for the water in the boiler unit. The waste stream from the boiler is the flue gases, which exhaust at 200°C in the chimney. The overall boiler efficiency is 89%, accounting for 2% of radiation losses and 9% in the flue gases.

© Woodhead Publishing Limited, 2013

Table 27.1 Inlet and outlet flows of the process

Input		
Malt	0.135	kg/kg
Corn	0.0115	kg/kg
Water	1.029	kg/kg
Demineralised water	.051	kg/kg
Cleaning water	0.391	kg/kg
Soda	0.02	kg/kg
Natural gas	748.9	kJ_{LHV}/kg
Electricity	69.3	kJ e/kg
Cooling water	9.47	kg/kg
Output		
Beer	1.0	kg/kg
Brewing dregs	0.0397	kg/kg
Waste water	0.458	kg/kg
Vapour	0.081	kg/kg
CO_2	0.0373	kg/kg

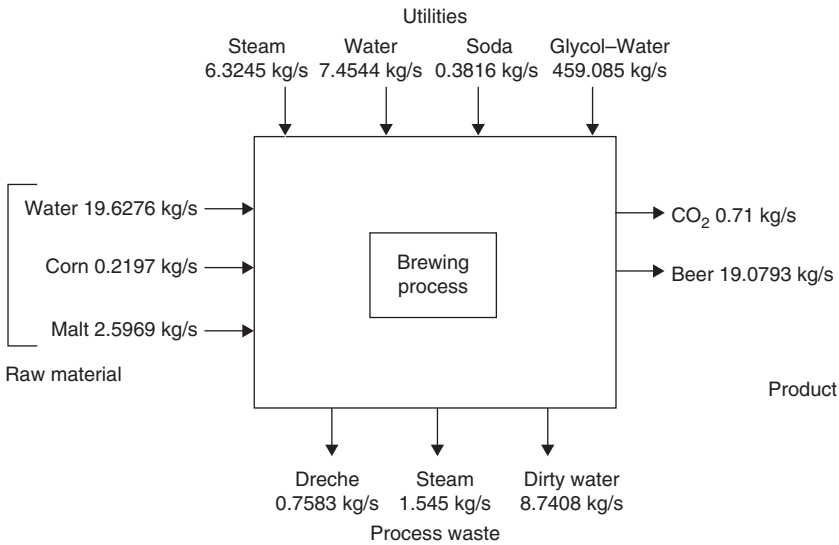

27.7 Block flow diagram representation of the brewing process.

In most conventional bottle-cleaning systems, some steam is directly injected to heat up the water. This will require make-up water (demineralised water) to be added to compensate the losses.

Glycol–water is produced by a refrigeration unit, which consumes electricity as resource to drive its compressor. In nominal operation there is no requirement for make-up glycol–water unless there is leakage in the

© Woodhead Publishing Limited, 2013

Table 27.2 Current energy bill

Description	Specific cost	Flows	Operating cost
Electricity	0.136 €/kWh	1,322 kWe	1,470.9 k€/y
Natural gas	0.048 €/kWh	17,062 kW_{LHV}	6,699.2 k€/y
Water	0.07 €/m3	0.31 m^3/s	630.0 k€/y
Demineralised water	1.0 €/m3	0.001 m^3/s	35.0 k€/y

Table 27.3 Current utility requirements with no heat recovery

Utilities	Requirements
Hot utility	17,062.0 kW_{LHV}
Cold utility	7,555.9 kW
Electricity	1,322.2 kWe

system. The refrigeration unit works with ammonia as the refrigerant fluid in our case.

Defining the Energy Bill

With no internal heat recovery, the conventional brewing process consumes 17,062 kW_{LHV} of primary energy in form of lower heating value of natural gas. This corresponds, therefore, to a heat supply to the process of 15,252.51 kW. The cooling load is of 7,555.9 kW, which is provided by the refrigeration unit, whereas 1,322.2 kW of electricity is required to drive the necessary pump and compressor. We find the natural gas consumption as 0.3595 kg/s, which results in a natural gas bill of 6,699.2 k€/y. The electricity cost, in this case, is 1,470.9 k€/y. The net yearly operating cost, including water and demineralised water, is 8,837.1 k€/y (see Table 27.2).

27.2.5 Defining the Process Heat-Transfer Requirements

The definition of the heat-transfer requirement of the process aims at analysis of the role of heat transfer in each of the process unit operations. The unit operations in the Flowsheet are therefore analysed with regard to their role in the beer-production recipe. From this analysis, one has then defined the heat-transfer requirement to be used for Process Integration, i.e. define the enthalpy–temperature profile of the heat-transfer demand including the corresponding ΔT_{min} contribution.

For defining the heat-transfer requirement, the main take-home messages are:

© Woodhead Publishing Limited, 2013

Process unit analysis: analyse the role of the process unit operation and understand what are the inlet and output flows, and what are the principles of the unit operation, in order to identify the role of energy (i.e. heat and electricity) in the operation.

Hot stream definition: the goal is to cool down the hot streams with the highest possible temperature. This means looking at the process unit operation, and trying to define a process unit scheme that maximises the temperature of the fluids that will enter to be cooled in a heat exchange operation.

Cold stream definition: when heat is required, the goal is to define the minimum temperature at which the heat has to be supplied.

Non-isothermal mixing are heat exchangers: The non-isothermal mixing of Fig. 27.8, defines two heat-transfer requirements, one hot stream from 80°C to the mixing temperature, and one cold stream from 15°C to the mixing temperature (31.25°C). If the Pinch Point temperature is 40°C (i.e. 45°C for the hot stream), total amount of 140 kW over the 195 kW of the heat exchange in the mixing could be recovered for streams heating Above the Pinch while the same amount would be recovered from the hot streams Below the Pinch to heat up the corresponding cold stream in the mixer. In such a case, the mixer is a heat exchanger that transfers 140 kW across the Pinch.

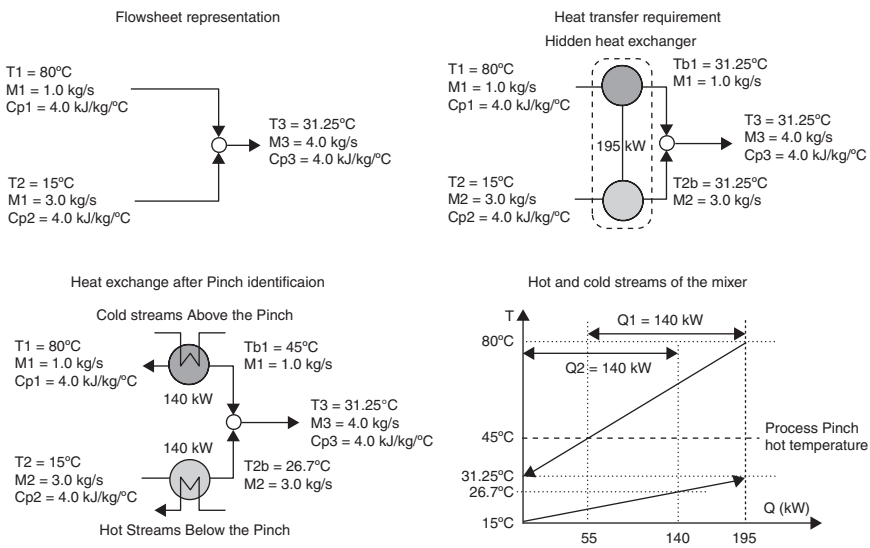

27.8 Non-isothermal mixing heat transfer requirement and heat recovery if the Pinch Temperature is at 45°C for the hot streams.

© Woodhead Publishing Limited, 2013

It is therefore important, at the level of the targeting stage, to define all the non-isothermal mixing as heat exchangers and to decide, once the Pinch Points are identified, if non-isothermal mixing can still be realised or if part of the heat exchange has to be realised first in heat exchangers before mixing. In the given example, the final configuration would be that described in Fig. 27.8.

Let us analyse the process requirement of the first unit (MAK) on the Process Flowsheet. Referring to Fig. 27.9, there exist several ways of defining the heat-transfer requirements of the unit. First, it has to be observed that the heat requirement of the unit is in fact hidden in the hot water tank that supplies the MAK unit with hot water. The hot water tank is not really related to the process; it really serves as an intermediate stream for the

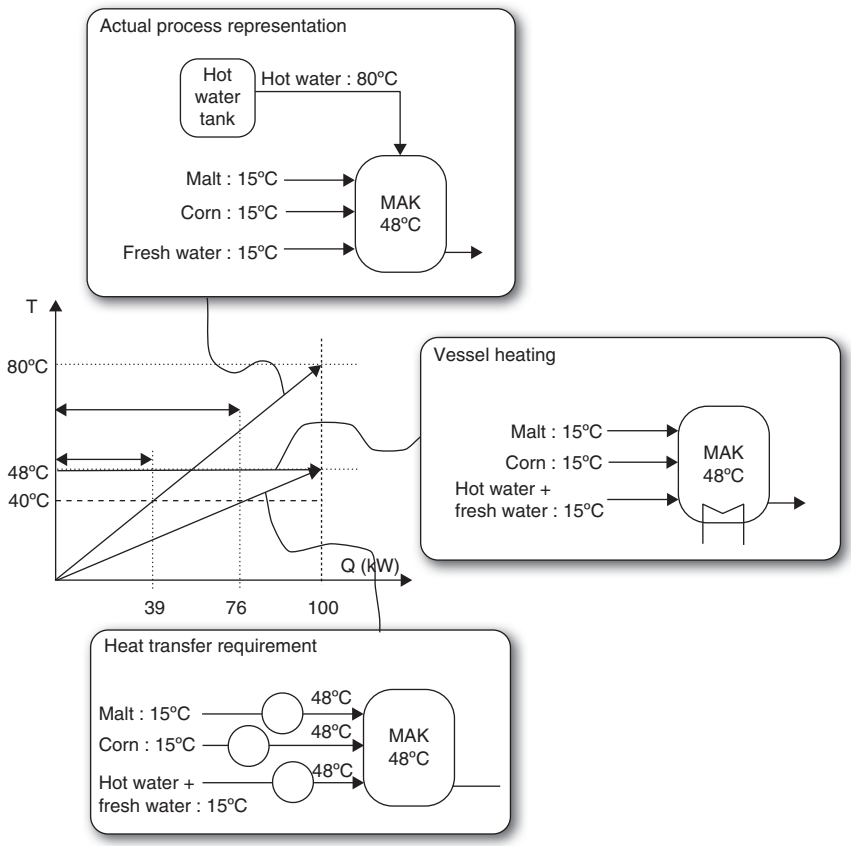

27.9 Process unit: heat-transfer requirement analysis, heat recovery if the Pinch Point is at 40°C.

© Woodhead Publishing Limited, 2013

Table 27.4 Exergy demand of 100 kW heating for the different heat requirement of the same unit operation (MAK), possible heat recovery if the Pinch is at 40°C

Heat-transfer requirements	Exergy (kW)	Heat at 40°C (kW)
Hot water from 15°C to 80°C	11.40	38.46
Vessel heating at 48°C	11.84	0.00
Heat feed streams from 15°C to 48°C	6.97	75.76

process. The requirement of the MAK unit has therefore to be related to the injection of hot water, which defines the way the MAK requirement is satisfied today.

However, an alternative way of defining the requirement could be to decide to heat the vessel after mixing the ingredients, or better, to preheat the streams entering the vessels to a temperature of 48°C. In order to calculate the respective heat loads of the different streams, one has to first consider that the total amount of water is fixed; therefore, the water flow is the flow of the fresh water plus the flow of hot water. In this situation, the heat loads of the three heat-transfer requirements will be the same, but the defined cold streams will be different.

The solution with feed preheating is the one with the lowest exergy requirement (see Table 27.4), and also with the highest possible level for heat recovery. This is explained in Fig. 27.9 and illustrated where the Process Pinch Point is at 40°C. The heat recovery potential is in fact much higher when one defines the requirement taking into account the feed preheating. The feed preheating would, however, require a heat exchange between the corn, malt and water mixture and another process stream. Considering that this counter-current heat exchange could be difficult to realise, we have decided that only the water will be heated to a temperature, such that the mixture reaches the required 48°C.

The same kind of analysis is implemented for the different process unit operations.

27.2.6 Analysing the Streams Leaving the Systems

The streams leaving the system have to reach their system's boundary state. For the products, they have to be brought to their 'ideal' distribution state. The flows released to the environment have to reach a state that is in equilibrium with the environment. This can be done by heat exchange, and therefore defines a heat recovery opportunity. When setting up the heat recovery target, it is important to list and analyse all the heat exchange opportunities that are available from the streams leaving the system. In order to maximise the heat recovery, the enthalpy–temperature profile will be established following the rules presented above for the process streams, and defining as

© Woodhead Publishing Limited, 2013

a target the conditions that are the closest to the environment conditions. The target state is however a *soft* target, since it does not necessarily have to be reached.

For the waste streams, it is important to examine if the waste treatment system is part of the system boundaries or not.

1. Beer – Beer leaves the system as the final product and will be stored to be filled later in the beer bottles.
2. Flue gases – Flue gases exhaust from the chimney of the boiler system (Steam Cycle) at almost 200°C. It is possible to treat these gases to cool down to optimal temperature to preheat the fresh air going to the burner. This in turn increases the exergy level of the hot gases in the burner and thus reducing the consumption of natural gas for the same amount of steam production.
3. Steam Condensate – Flash Vessel is used to improve the efficiency of condensation of the condensate return in the boiler system. This steam exhaust is usually lost and not recovered.
4. Husk (Dreche) – Malt waste in the form of husk is extracted during the filtration of mash before boiling process. The amount is approximately 30% by mass of the initially added barley. In our case it is around 0.7583 kg/s or 2.73 t/h. This husk is usually given to animals, losing the possibility of converting this into methane (biogas) through the biomethanation process.
5. Steam evaporation at WOK – 10% by mass of the working wort is evaporated during the boiling and energy is recovered from this vapour by cooling it down to the ambient temperature.
6. Trub – 0.2% by mass of wort is lost during the centrifuge step to finally remove any proteins from the wort.
7. Dirty water – A significant amount of dirty water leaves the bottle-cleaning system. This water includes soda, dirt and impurities absorbed during the process, and is usually sent to the water treatment plant to be used for other purposes.
8. Water – CIP – A part of water heated to 80°C in the hot section goes out of the system to be used for cleaning the tanks and other devices. This energy is not recoverable, and is lost in the cleaning necessary for maintaining the hygiene at the production line.

27.2.7 Overall Process Requirement Definition

The hot and cold streams defined for the whole process are given in Table 27.5. We give here some hints on the hot and cold streams definitions for the different sections.

© Woodhead Publishing Limited, 2013

Table 27.5 List of streams in brewing process

Process Unit	Name – Process	$\dot{M}$(kg/s)	T_{in} (°C)	T_{target} (°C)	$\dot{Q}$(kW)	$\Delta T_{min}/2$
Hot Section 1	Water – MAK	2.4415	15	51.5	369.9	2
	MAK – Heating	2.9971	48	65	188.6	2
	Water – MAT	4.9652	15	54.5	823.6	2
	MAT – Heating	7.2982	48	65	420.1	2
Hot Section 2	MAT+MAK	10.2953	65	75	368.4	2
	Water – Filter	5.9130	15	80	1,608.9	2
	CIP	6.767	15	80	1,841.1	2
	WOK – Boiling	15.4500	78	105	1,662.9	2
	WOK – Evaporation	15.4500	105	105	3,319.8	2
	Vapour – Recovery	1.5450	105	100	17.2	1
	Vapour – Recovery	1.5450	100	100	3,487.9	
	Vapour – Recovery	1.5450	100	25	482.8	2
Hot Section 3	Centrifuge	1.3890	52	80	857.9	2
	Wort – Cooling	15.2634	102.5	10	5,434.6	2
Cold Section 1	Fermentation	15.2634	10	10	534.8	2
Cold Section 2	Cooling	15.2634	10	6	233.8	2
	Maturing	15.2634	6	6	425.5	2
Cold Section 3	Chilling	15.2634	6	1	714.5	2
	Chillage	15.2634	1	1	427.7	2
Cold Section 4	Beer preheating	15.26	1	15	822.05	2
	Pasteurisation heating	19.0793	15	80	4,854.05	2
	Pasteurisation cooling	19.0793	70	5	4,858.4	2
Cleaning	Soda Bath Temperature	3.1797	65	85	251.9	2
	Pre-rinse Bath Temperature	5.8272	40	60	472.8	2
	Soda make-up	0.3816	15	85	39.8	2
	Water to soda tank	3.816	15	85	1,287.1	2
	Pre-rinse make-up	0.1554	15	60	29.3	2
	Final Rinse Water make-up	3.816	35	60	399.34	2
	Soda Bath Rinse – Out	4.7696	85	60	472.7	2
	Pre-rinse – Out	8.7408	40	20	713.7	2

MAT and MAK tanks: the water is preheated to heat up the corn and malt streams and reach the required temperature in the different tanks. It is also assumed that the first preheating to 102°C is not necessary and that a temperature of 75°C has to be reached.

Evaporation in the launter tun: The evaporation takes place at 105°C. The vapour condensation is considered as a hot stream with a condensation at 100°C considering pure vapour. After condensation the liquid is still sub-cooled to reach the 25°C target temperature. This is a *soft* temperature.

© Woodhead Publishing Limited, 2013

Centrifuge: A water make-up is added and has to be heated to 80°C.

CIP: Hot water used for Cleaning In Place is produced at 80°C. It is assumed that after its usage the hot water cannot be recovered and is sent cold to the water treatment plant.

Trub: Trub could be added as a hot stream if heat exchange can be realised with the solid flow. The flow is however small when compared to the major flow.

Fermentation: The feed is first cooled down to the fermentation temperature, and then the temperature is maintained. Note that we consider the temperature in the tank, and not the temperature of the glycol–water mixture used to maintain the temperature in the tank.

Maturation: The flow is first cooled in a heat exchanger before reaching the maturation temperature.

Water dilution: This is a non-isothermal mixer. First, beer is preheated from 1°C to 15°C before being mixed with the diluting water. This preserves the cooling recovery capacity of the cold beer.

Bottle cleaning: The steam heating is replaced by the corresponding heat-transfer requirement. We consider a heat exchanger to control the bath tank temperature. The water make-up flow rate includes the water injected as steam in order to preserve the water balance. The make-up flows are preheated to the corresponding tank temperature. When water flows from one tank to another, isothermal mixing at the receiving tank is considered. This is done by introducing the corresponding heat exchanges. The hot water leaving the bottle-cleaning system and going to the treatment plant is cooled down to 20°C. The heat exchange requirement in the bottle-cleaning system is represented on Fig. 27.10.

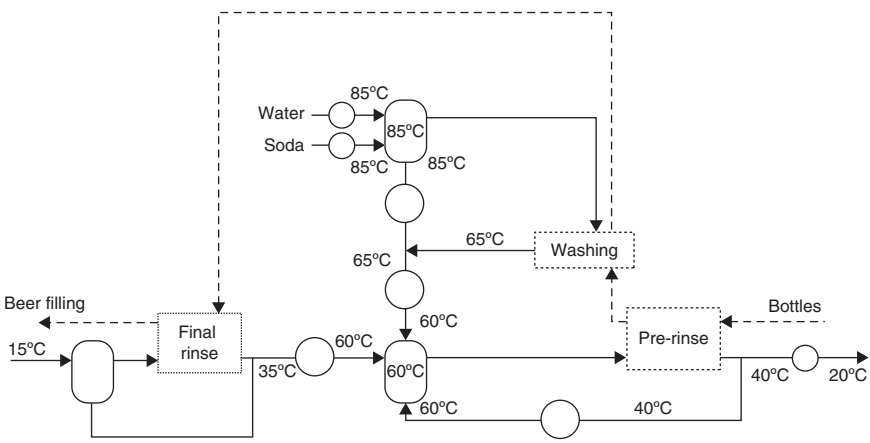

27.10 Heat-transfer requirement of the bottle-cleaning section.

© Woodhead Publishing Limited, 2013

27.3 Calculating Maximum Heat Recovery in the System

Assuming a ΔT_{min} contribution of 2°C for each liquid stream (i.e. an overall ΔT_{min} of 4°C), we calculate the maximum heat recovery between the hot and cold streams of the process. We also plot the Composite Curves and Grand Composite Curve of the process (Figs 27.11 and 27.12). We obtain by balance the minimum energy requirements (MER) for the brewing process, considering the heating, cooling and refrigeration requirements (Table 27.6). For the refrigeration requirement, we consider the fresh water as defining the cooling water temperature. From our analysis, the Pinch Point is at the ambient temperature. This means that the overall cooling requirement is fact to be realised below the ambient temperature, and has to be realised using a refrigeration cycle.

The current energy requirements are found to be 15,185.18 kW_{LHV} for the heating load and 7,555.9 kW for the refrigeration load to be compared with the minimum target values of 4,904.0 and 3,089.1 kW of refrigeration load. The energy savings correspond therefore to 67.71% of savings for the hot utility and 57.57% of savings for the refrigeration load.

27.3.1 Identification of the Penalising Heat Exchangers and the Heat Recovery Potentials

The penalising heat exchangers are heat exchangers that transfer heat across the Pinch Point. The definition of the penalising heat exchangers has however to be completed by the existence of Pseudo-Pinch Point as the one created by the heat recovery of the evaporated vapour.

One major penalty is created by the refrigeration system that cools down the beer product after pasteurisation. This is a heat exchanger crossing the Pinch Point. The heat recovery penalty is 3,957.9 kW, i.e. 38.50%. This saving is realised both Above the Pinch i.e. reduction of the heating requirement, and Below the Pinch, i.e. reduction of the refrigeration requirement where it accounts for 88.61% of the savings.

Table 27.6 Minimum heating and cooling requirement target for the process

Minimum requirement	Amount (kW)
Heating	4,904.0
Cooling	0
Refrigeration	3,089.1

© Woodhead Publishing Limited, 2013

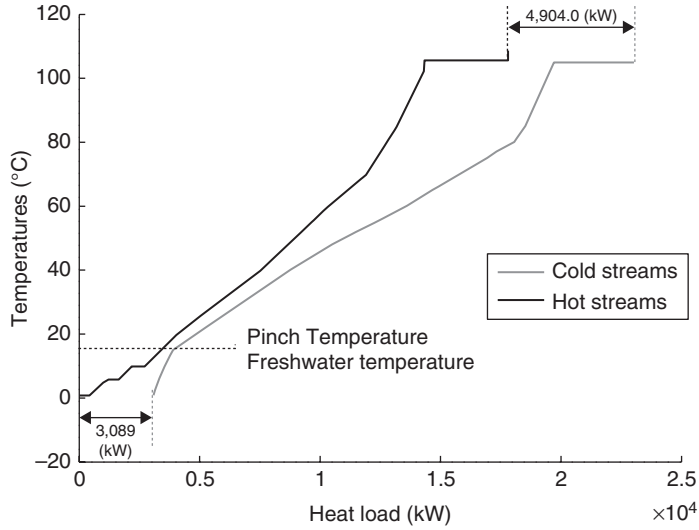

27.11 Hot and Cold Composite Curves of the process.

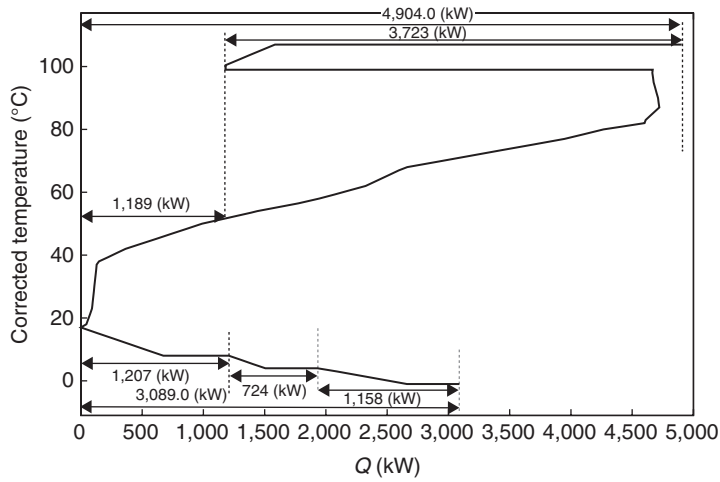

27.12 Grand Composite Curve of the brewing process.

The additional saving comes from heat recovery from evaporation and the bottle-cleaning system. Considering that the Pinch Point is created by the freshwater input temperature, the overall amount of heat available could be recovered in the process, leading to an additional saving of 4,701.6 kW explaining 45.7% of the energy penalty.

© Woodhead Publishing Limited, 2013

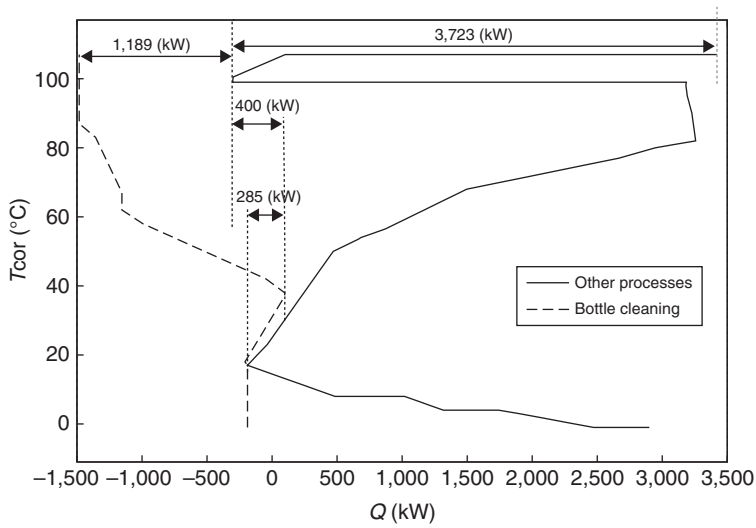

27.13 Integrated Composite Curve of the bottle-cleaning section.

It is also interesting to analyse the integration between sections. For this analysis, the Integrated Composite Curve representation is interesting. As an example, Fig. 27.13 shows the Integrated Composite Curve of the bottle-cleaning section. One can see from this analysis that the minimum heat requirement can be divided into two major parts that could be solved dependently one from the other: the process hot section that receives 3,723 kW of the high temperature heat, and 1,189 kW sent to the bottle-cleaning subsystem. 285 kW will be recovered from the waste heat of the bottle-cleaning system to preheat the streams of the other sections, while the 400 kW will be supplied from the higher temperature waste heat from the hot section of the bottle-cleaning section.

From analysis of the Grand Composite Curve and the Integrated Composite Curve, it is also important to notice that most of the steam used in heat exchangers or steam injection to supply heat to the process at a temperature below 96°C will have probably been changed into heat recovery heat exchangers.

27.4 Defining the Energy Conversion System

Before designing the heat recovery Heat Exchanger Network (HEN) system, it is important to first analyse the integration of the energy conversion system.

Conventionally, a boiler is used to provide steam for the heating requirements, and a glycol–water system powered by a refrigeration unit is used to provide the refrigeration requirements. It is, however, important to analyse

© Woodhead Publishing Limited, 2013

also the possibility of integrating heat pumps and cogeneration units in order to reduce the energy bill of the process.

27.4.1 Grand Composite Analysis

The analysis of the Grand Composite Curve (Fig. 27.12) already gives some indications of the possible energy conversion opportunities.

For temperature Above the Pinch, the heat requirement can be divided into two different zones:

- Above 105°C: 3,723 kW has to be supplied to the process, mainly for the beer evaporation above 105°C.
- From 20°C to 60°C: 1,189 kW can be supplied, mainly for water preheating. This could indicate an opportunity for working with a lower temperature in the boiler chimney, realising flue gas water condensation for preheating process water. From this analysis it can also be concluded that air preheating would not be a valid option for the recovery boiler. Introducing condensation in the boiler and considering cooling down the gas to 40°C could increase the boiler efficiency to 104% based on the lower heating value of the natural gas, leading therefore to a consumption of 4.715.4 kW_{LHV} or a gas bill reduction of 72.4%.

Below the Pinch, the overall amount of refrigeration has to be supplied by a single refrigeration cycle. In the present situation, the refrigeration cycle is working with a Coefficient of Performance (COP) of 5.80 kW_{cold}/kWe. This leads to a cost of 0.023 €/kW h_{cold}. Assuming that the efficiency of the refrigeration cycle will not be affected by the reduction of the demand, the expected electricity consumption for the refrigeration cycle can be estimated as 532.42 kW.

From the analysis of the Grand Composite Curve, the refrigeration demand can be divided into three parts:

- From ambient (19°C) to fermentation (10°C): This corresponds to 1,207 kW or 39.07% of the demand.
- From fermentation (10°C) to maturation (6°C): This corresponds to 724 kW or 23.44% of the demand.
- From maturation (6°C) to the lowest temperature (1°C): Corresponds to the rest of the supply, i.e. 1,158 kW (37.49%).

Staging the supply of the refrigeration would allow increasing the efficiency of the refrigeration system, and therefore reducing the price of supplying

© Woodhead Publishing Limited, 2013

the refrigeration load. It is possible to approximate the impact of staging the refrigeration load by using the concept of the Carnot Factor. For a refrigeration load $\dot{Q}_c$ at a temperature T_{cold} supplied to a source with a temperature T_{amb}, the theoretical mechanical power $\dot{E}_{ref}$ required is calculated by Equation [27.3]. Knowing the present consumption, one could calculate an efficiency η by Equation [27.4] and consider that this efficiency will stay constant. The new consumption can therefore be calculated by Equation [27.5]. Table 27.7 gives the estimated mechanical power for the three levels identified. In the calculation, we have considered a temperature difference of 9°C between the refrigeration requirement and the supply considering the possible use of an intermediate fluid.

$$\dot{E}_c(T_c) = -\dot{Q}(T_c)\cdot\left(1-\frac{T_{amb}}{T_c}\right) \quad [27.3]$$

$$\eta = \frac{\dot{E}_c(T_{ref})}{\dot{W}_c(T_{ref})} \quad [27.4]$$

$$\dot{W}_c(T_c) = \frac{-\dot{Q}(T_c)\cdot\left(1-\left(T_{amb}/T_c\right)\right)}{\eta} \quad [27.5]$$

Using the approximation of the exergy efficiency, one could approximate the mechanical power required to 449.8 kW. The staging corresponds to an expected refrigeration efficiency increase of 15.51% and a new COP of 6.9 kW_{cold}/kW e.

This would also reduce accordingly the use of cooling water by 0.12 m^3/s, which corresponds to a reduction of 0.60%.

With this first analysis, it is therefore possible to estimate the new energy bill after heat recovery and integration with the present energy conversion system, see Table 27.8.

It could be, however, assumed at this stage that the heat of the refrigeration cycle is directly sent to the cooling water and not reused in the process.

Table 27.7 Expected mechanical power for the refrigeration loads with a reference temperature of 25°C (298 K)

Temperature (°C)	Load (kW)	$\dot{W}(T = -8°C)$	$\dot{W}(T)$
10	1,207.0	208.0	146.3
6	724.0	124.8	103.9
1	1,158.0	199.6	199.6
Total	3,089.0	532.4	449.8

© Woodhead Publishing Limited, 2013

Table 27.8 Estimated new energy bill after heat recovery

	Annual bill (k€/y)	%ref
Natural gas	1,851.45	28
Electricity	500.44	34
Water	251.12	40
Total	2,603.01	29

27.4.2 Defining the Possible Energy Conversion Technologies

Existing Energy Conversion Systems

Steam boiler: A boiler is used to produce steam and thus to provide the heat requirements of the brewing process. A detailed diagram is given in Fig. 27.14. Steam is produced at a temperature of 193°C and a pressure of 8.5 bar; it is then expended to 6 bar in the distribution system. The condensates return at 3 bars in saturated conditions. It is then flashed to a pressure of 1.5 bar in a deaeration tank, where it is mixed with the demineralised water make-up required to compensate the steam used in direct injections in the process. A pump (efficiency 90%) is necessary to raise the pressure of the returned condensate before it enters into the burner for heat transfer.

Refrigeration cycle: The refrigeration needs are supplied by an ammonia refrigeration cycle (Fig. 27.15) operating between 3.2 bar (–8°C) and 10 bar (25°C). The compressor isentropic efficiency is 85%. The cycle is cooled using cooling water and supplies a glycol–water distribution loop operating between –5°C and –1°C.

Alternative Energy Conversion Units

Cogeneration engine: A cogeneration engine could be used to replace the boiler system. Internal combustion engines have an attractive electrical efficiency, and it is possible to recover heat from both exhaust gases and cooling water. Table 27.9 shows the characteristics of a typical cogeneration engine using natural gas as fuel.

According to the optimal placement of a cogeneration unit, the hot streams of the cogeneration unit should be Above the Pinch Point. From the analysis of the Grand Composite Curve, however, one may expect problems in integrating the cogeneration unit since the temperature of the water cooling system is not high enough to supply the evaporation heat load in

© Woodhead Publishing Limited, 2013

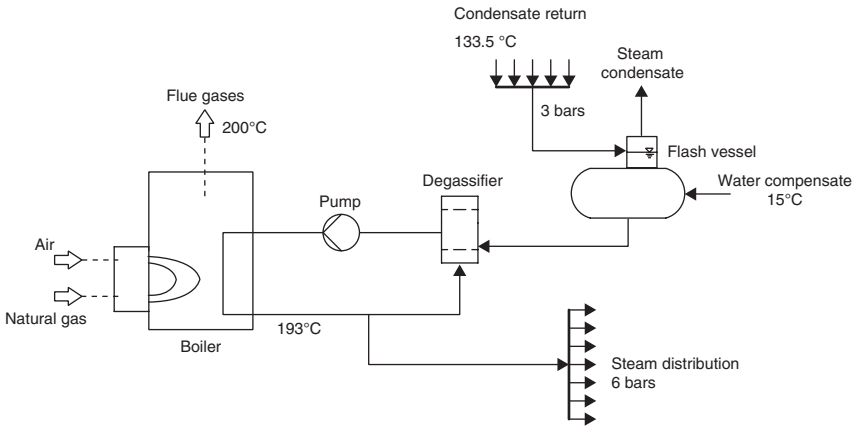

27.14 Steam distribution system of the process.

the process. However, based on the Grand Composite Curve analysis, it could also be suggested to use water condensation in the recovery boiler in order to supply the low temperature heat.

Waste treatment and energy conversion: The husk leaving the process is hot and is rich in carbon and hydrogen species. The husk has a lower heating value of approximately 14.3 MJ/kg and that can be converted into a mixture of CH_4 and CO_2 by bio-methanation in anaerobic conditions. This reaction generally requires a specific operating temperature of 35°C, which defines a new cold stream in the process.

Based on the report published by the French agency ADEME (ADEME, 2011), 75 Nm^3 of bio-methane with a lower heating value of 35.7 MJ/Nm^3 can be recovered from 1 t of husk, which represents 22,430 t of husk for this brewery study, resulting in 1,674,781 m^3 of possible methane production. With proper calculations, by using the lower heating value of methane, we may produce 16,608 MWh_{LHV}/y or an available mean power of 2,030.3 kW. This production requires about 4% (81.2 kWe) of lower heating value as electricity for the bio-methane production, as well as 20% (406.1 kW) as heat to maintain the temperature in the methanation vessel. This defines a cold stream to be added in the list of the streams to be heated. The heat available in the husk is at 75°C, to be cooled down to 35°C, and this makes a heat load of 54.8 kW (i.e. $0.762 \times 1.8 \times (75 - 35)$). If the bio-methane produced is used in a cogeneration unit for Combined Heat and Power production, we may expect an electrical efficiency of 34% and a thermal efficiency of 52%. Table 27.10 defines the resulting hot and cold streams of the bio-methane production and its combustion in a gas engine.

© Woodhead Publishing Limited, 2013

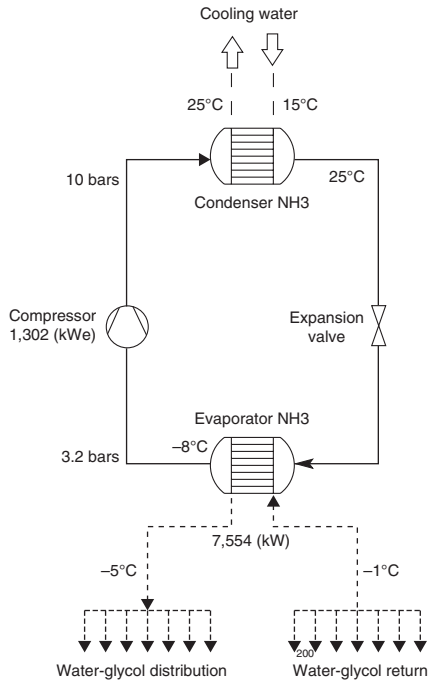

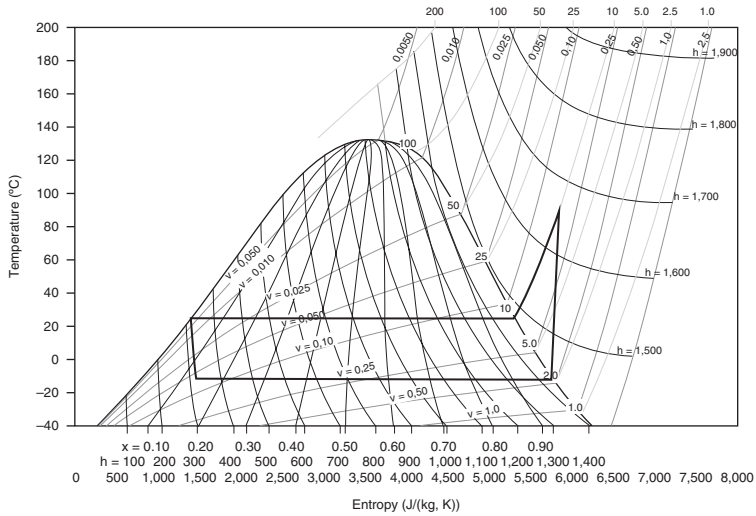

27.15 Ammonia cycle for producing the glycol–water cold loop.

© Woodhead Publishing Limited, 2013

Table 27.9 Cogeneration unit characteristics based on GE-Jenbacher data, power range: 500–1100 kW (www.gejenbacher.com)

Description				Power (kW)	Efficiency (%)
$\dot{M}_{f\,uel}$ (kWe LHV)				2,605	
$\dot{W}_e$ (kWe)				1,063	40.8
Without water condensation in the flue gases					
	T_{in} (°C)	T_{out} (°C)	$\Delta T_{min}/2$	Power (kW)	Efficiency (%)
$\dot{Q}_{Gas}$ (kW)	470	120	15	537	21.0
$\dot{Q}_{Cooling}$ (kW)	87	80	2	653	25.0
$\dot{Q}_{th}$ (kW)				1,190	46.0
With water condensation in the flue gases					
	T_{in} (°C)	T_{out} (°C)	$\Delta T_{min}/2$	Power (kW)	Efficiency (%)
$\dot{Q}_{Cooling}$ (kW)	87	80	5	653	25.07
$\dot{Q}_{Gas}$(kW)	470	60	15	632	24.26
$\dot{Q}_{Gas}$(kW)	60	40	15	209	8.02
$\dot{Q}_{th}$ (kW)				1,494	57.35

Table 27.10 Cogeneration unit based on the bio-methane produced on the process husk

Description				Power (kW)	Efficiency (%)
$\dot{M}_{f\,uel}$ (kWe_{LHV})				2,030.3	
$\dot{W}_e$ (kWe)				609.1	30.0
	T_{in} (°C)	T_{out} (°C)	$\Delta T_{min}/2$	Power (kW)	Efficiency (%)
$\dot{Q}_{Cooling}$ (kW)	87	80	5	424.1	20.89
$\dot{Q}_{Gas}$ (kW)	470	90	15	631.7	31.11
$\dot{Q}_{Gas}$ (kW)	34	35	2	351.2	17.30

27.4.3 Heat Pumping

Refrigeration Cycles Integration

As the Pinch Point is also at the ambient temperature, the hot stream of the refrigeration cycle can also be used to supply heat to the process. The operating conditions of the refrigeration cycle have therefore to by adjusted, not only for the evaporation temperature but also for the condensation temperature. Therefore, we have to optimise the operating conditions of the refrigeration cycle. As the refrigeration system is using a glycol–water mixture to distribute the cold to the process, the solution will be to reuse the existing system and to reorganise the glycol–water distribution system with three different temperature levels.

The operating conditions will change the amount of heat that can be recovered, and therefore affect the flow of the other refrigeration cycles to be used.

© Woodhead Publishing Limited, 2013

Table 27.11 New operating conditions for the three refrigeration cycles

	Evaporation (°C)	Condensation (°C)	$\dot{Q}_c$ (kW)	$\dot{W}_{mec}$ (kW)
Conditions 1	1.0	50.0	1,000.0	355.1
Conditions 2	–3.0	38.3	1,000.0	312.6
Conditions 3	–8.0	26.7	1,000.0	276.6

The final operating conditions considered for the refrigeration cycle are given in Table 27.11. It would be still possible to optimise the operating conditions of the cycles if needed.

Mechanical Vapour Recompression

The theory of the heat pump integration recommends the integration of the heat pump to raise heat from Below to Above the Pinch Point. If, from the Grand Composite Curve analysis, the mechanical vapour recompression appears not to be interesting, it will be shown that the mechanical vapour recompression is justified when the energy conversion system integration is considered. In fact, the heat pumping effect of the refrigeration cycle will introduce utility Pinch Points that will justify the use of the mechanical vapour recompression. The mechanical vapour recompression will also help the integration of the cogeneration engine, since the heat of the engine cooling water is available below the high temperature Pinch Point.

The mechanical vapour recompression system is described in Fig. 27.16. (See also Table 27.12.) It should be noted that only part of the recovered vapour will be compressed, the rest of the flow being recovered is without recompression since it has already reached the required temperature level. It should be mentioned that the representation of the mechanical vapour recompression is identical to a close cycle. This means that one can always visualise the evaporation heat load and the exchange with the condensing vapour. In reality, there will be no heat exchanger at the evaporation temperature, the evaporation being directly replaced by a reduction of the condensation heat load.

It also has to be highlighted that, for the two streams (recompressed and not), the condensed water is cooled down to the system limits.

27.4.4 Mathematical Formulations

From the analysis of the Grand Composite Curve and the proposed set of energy conversion units, we can conclude that there will be more than one option for supplying the requirement of the process. In addition, one can

© Woodhead Publishing Limited, 2013

Table 27.12 Operating conditions for the mechanical vapour recompression

	Evaporation	Condensation	Max$\dot{Q}_c$	Max$\dot{W}_{mec}$	COP$^{\cdot}$
	(°C)	(°C)	(kW)	(kW)	
MVR 1	98.0	109.0	3,434.2	150.9	23.8

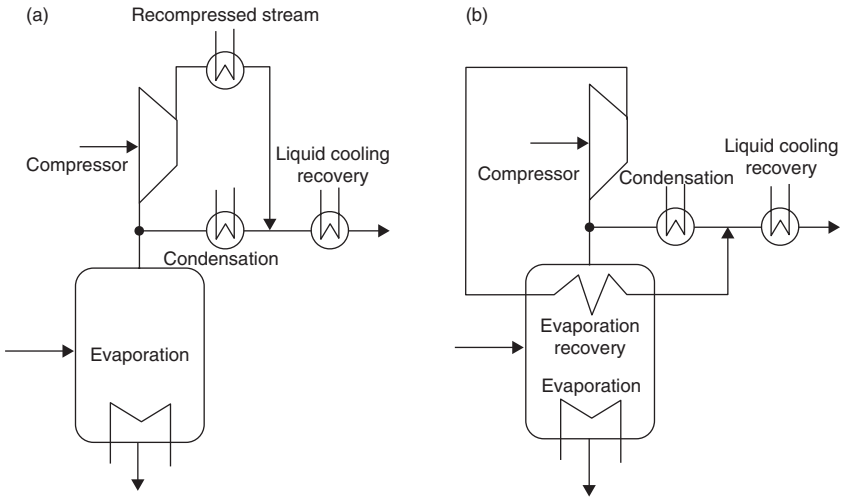

27.16 Mechanical vapour recompression scheme for vapour recovery: (a) scheme for external use of the recompressed stream and (b) scheme for internal use of the recompressed stream.

also see that the different energy conversion systems will be interconnected or interrelated.

When looking at the energy conversion units, one can see that each is related to hot and cold streams, as well as to a cost or resource consumption and to mechanical power consumption or production. At the difference with the process streams, the flows in the utility systems have to be optimised in order to minimise the cost of supplying the energy requirement.

Following the theory of Process Integration, this means maximising the flow of the cheapest utility first. If this works for simple systems, this is not anymore the case for the system under study, since both hot and cold streams of the refrigeration cycles are used and the Combined Heat and Power production units will interact and/or compete with the heat pumps and the mechanical vapour recompression.

It is therefore easier to calculate the flows by using mathematical programming techniques. The Mixed Integer Linear Programming (MILP) formulation proposed by Marechal and Kalitventzeff (1998b) solves the

© Woodhead Publishing Limited, 2013

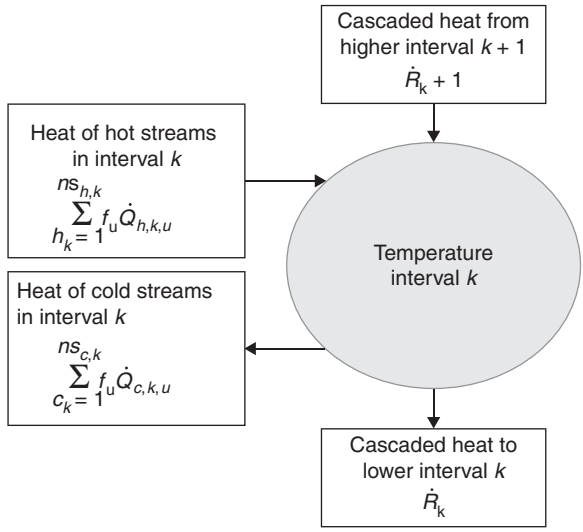

27.17 Graphical Heat Cascade representation for MILP formulation without heat exchange restrictions.

Heat Cascade and calculates the maximum heat recovery, together with the optimal integration of energy conversion units, by minimising the operating cost (Equation [27.6]) of supplying the heat and cold requirements of the process while satisfying the Heat Cascade constraints (Equation [27.7]), as illustrated in Fig. 27.17. Introducing the electricity balances for import (Equation [27.9]) and export (Equation [27.9]), the CHP production is, therefore, optimised considering the possibility or not of exporting electricity to the grid. In the formulation, the bold text corresponds to variables of the problem to be defined by the optimisation algorithm, while normal text refers to problem parameters that will not be affected by the optimisation procedure.

When temperatures are fixed, the problem is a linear programming problem, since the objective function and the constraints are all linear with respect to the problem variables. The use of integer variables allows engineers to select the best utility system and to propose more than only the best selection.

Solving the MILP problem will calculate the best flows in the system, considering the possible interactions between the process streams and the utility system, but also considering the heat exchange interactions between two utility flows.

As this is a linear problem, the optimal solution is identified by the activation of inequality constraints. In our case, two major categories can be activated:

© Woodhead Publishing Limited, 2013

The Pinch Points correspond to the activation of $\dot{R}_k \geq 0$ constraints and will define Pinch Points between the Hot and Cold Composite Curves.

The maximum flow corresponds to the maximum usage allowed for a utility stream.

It has to be highlighted that, due to the Heat Cascade constraints (Equation [27.8]) it is assumed that the proposed utility system is chosen with the appropriate conditions to satisfy the process requirement. As a consequence no 'magic' heating or cooling duty will be added to the system and the resulting Hot and Cold Composite Curves will be balanced.

$$\min_{\dot{E}_{\text{el}}^{-},\dot{E}_{\text{el}}^{+},f_u,\dot{R}_k,f_u} F_{\text{obj}} = \sum_{f=1}^{nf}\left(c_f^{+}\sum_{u=1}^{nu} f_u \dot{E}_{f,u}^{+}\right) + c_{\text{el}}^{+}\dot{\text{E}}_{\text{el}}^{+} - c_{\text{el}}^{-}\dot{\text{E}}_{\text{el}}^{-} + \sum_{u=1}^{nu} f_u c_u \qquad [27.6]$$

$$\sum_{h_k=1}^{ns_{h,k}} f_u \dot{Q}_{h,k,u} - \sum_{c_k=1}^{ns_{c,k}} f_u \dot{Q}_{c,k,u} + \dot{\boldsymbol{R}}_{\boldsymbol{k+1}} - \dot{\boldsymbol{R}}_{\boldsymbol{k}} = 0 \quad \forall k = 1,\ldots,nk \qquad [27.7]$$

$$\dot{\boldsymbol{R}}_{\mathbf{1}} = 0 \;\; \dot{\boldsymbol{R}}_{\boldsymbol{nk+1}} = 0 \quad \dot{\boldsymbol{R}}_{\boldsymbol{k}} \geq 0 \;\; \forall k = 2,\ldots,nk \qquad [27.8]$$

$$\dot{E}_{\text{el,process}} + \sum_{u=1}^{nu} f_u \dot{E}_{\text{el},u}^{+} + \dot{\boldsymbol{E}}_{\text{el}}^{+} - \sum_{u=1}^{nu} f_u \dot{E}_{\text{el},u}^{-} \geq 0 \qquad [27.9]$$

$$\dot{E}_{\text{el,process}} + \sum_{u=1}^{nu} f_u \dot{E}_{\text{el},u}^{+} + \dot{\boldsymbol{E}}_{\text{el}}^{+} - \dot{E}_{\text{el}}^{-} - \sum_{u=1}^{nu} f_u \dot{E}_{\text{el},u}^{-} = 0 \qquad [27.10]$$

$$\dot{E}_{\text{el}}^{+} \geq 0 \quad \dot{E}_{\text{el}}^{-} \geq 0 \qquad [27.11]$$

$$y_u \cdot f_u^{\min} \leq f_u \leq y_u \cdot f_u^{\max} \qquad [27.12]$$

Based on a formulation originally presented by Papoulias *et al.* (1983), the MILP formulation presented here can be easily extended to introduce additional constraints, such as restricted matches (Becker and Maréchal, 2012a) or multi-period problems (Marechal and Kalitventzeff, 2003). It can also be used to solve combined heat and water problems (Marechal and Kalitventzeff, 2005) as well as to optimise the operating conditions of complex systems, such as integrated steam networks (Marechal and Kalitventzeff, 1999) or site scale problems (Marechal and Kalitventzeff, 1998a).

© Woodhead Publishing Limited, 2013

Comparison of Energy Conversion System

In this section we compare different options for the supply of heat to the process. The following scenarios for integration of energy conversion units are considered.

Scenario A Boiler + Refrigeration
Scenario B Boiler + Heat pumping from the refrigeration cycle
Scenario C Condensation boiler + Refrigeration
Scenario D Condensation boiler + Heat pumping from refrigeration cycle
Scenario E Condensation boiler + Heat pumping from refrigeration cycle and mechanical vapour recompression
Scenario F Cogeneration engine + Heat pumping from the refrigeration cycle
Scenario G Cogeneration biogas engine and natural gas + Heat pumping from the refrigeration cycle
Scenario H Cogeneration biogas engine and natural gas + Heat pumping from the refrigeration cycle and mechanical vapour recompression

Table 27.13 presents the results of the energy conversion system integration including the heat recovery options identified by the Process Integration analysis.

Table 27.14 compares the energy consumption results of the different scenarios.

Primary energy is calculated by considering an efficiency of 56% for the electricity production (this is the efficiency of a natural gas combined cycle) and accounting only for fossil fuel (i.e. the biogas produced from the waste is not accounted as a primary energy resource). In this table, the scenario S0 refers to the present situation without heat recovery.

Table 27.13 Detailed results (power of the energy conversion system in kW)

Case	frg1	frg2	frg3	MVR	Cog	Bcog	combcond	comb
SA	215.7	153.8	173.0	0.0	–0.0	–0.0	0.0	4,726.1
SB	368.1	224.0	208.4	0.0	–0.0	–0.0	0.0	3,804.4
SC	215.7	153.8	173.0	0.0	–0.0	–0.0	4,234.9	0.0
SD	346.4	211.9	202.3	0.0	–0.0	–0.0	3,784.4	0.0
SE	531.6	289.6	237.7	69.0	–0.0	–0.0	1,676.8	0.0
SF	531.6	289.6	237.7	0.0	6,272.1	-0.0	0.0	0.0
SG	531.6	289.6	237.7	0.0	5,120.3	609.1	0.0	0.0
SH	480.0	244.1	312.5	107.1	1,353.4	–0.0	0.0	0.0
SI	486.5	265.9	289.6	101.3	455.9	609.1	0.0	0.0

© Woodhead Publishing Limited, 2013

Table 27.14 Energy consumption of solutions

Case	Nat.gas (kW)	Cool. water (kW)	Elec. out (kWe)	Elec. in (kWe)	Primary energy (kW)	% (%)
S0	17,062.0	0.0	8,878.0	1,322.2	19,423.0	100.0
SA	4,726.1	3,141.6	0.0	579.7	5,761.3	29.7
SB	3,804.4	2,539.0	0.0	834.2	5,294.2	27.3
SC	4,234.9	3,141.6	0.0	579.7	5,270.1	27.1
SD	3,784.4	2,890.3	0.0	797.4	5,208.5	26.8
SE	1,676.8	1,061.2	0.0	1,150.0	3,730.3	19.2
SF	15,680.1	8,063.3	5,058.3	0.0	6,647.4	34.2
SG	12,800.8	7,148.4	4,530.3	0.0	4,710.9	24.3
SH	3,383.4	1,232.3	172.2	0.0	3,076.0	15.8
SI	1,139.7	674.6	0.0	107.3	1,331.3	6.9

Table 27.15 Total cost calculation including investment

Case	Nat.Gas (k€/y)	Elec. (k€/y)	Opex (k€/y)	Maint. (k€/y)	Inv. (k€)	Total (k€/y)	% (%)
S0	6,699.2	1,405.8	8,105.0	0.0	0.0	8,105.0	100.0
SA	1,855.7	616.5	2,472.1	0.0	0.0	2,472.1	30.5
SB	1,493.8	887.1	2,380.9	0.0	0.0	2,380.9	29.4
SC	1,662.8	616.5	2,279.3	0.0	0.0	2,279.3	28.1
SD	1,485.9	848.0	2,333.9	0.0	0.0	2,333.9	28.8
SE	658.4	1,222.9	1,881.3	1.0	75.9	1,889.1	23.3
SF	6,156.7	–5,379.0	777.6	94.1	6,899.3	1,488.0	18.4
SG	5,026.1	–4,817.5	208.5	85.9	6,302.3	857.4	10.6
SH	1,328.5	–183.1	1,145.4	21.9	1,606.5	1,310.8	16.2
SI	447.5	114.1	561.6	17.5	1,283.0	693.7	8.6

Table 27.15 presents the overall results obtained for the different scenarios. For electricity, only the electricity needed by the energy conversion system is considered, not the electricity needed by the process itself.

For calculating the operating cost, the yearly operation time is considered and it does not distinguish between selling or purchasing electricity. The values of Table 27.16 are considered to estimate the investment. Only cogeneration and mechanical vapour recompression are considered for the investment, and calculations have not been considered for the other units or for the investment of the heat recovery heat exchangers. It could be mentioned that the reuse of the existing refrigeration system should be analysed in more detail to confirm that the new compression ratio can be realised with the existing system. The operation with different operating temperature in the refrigeration implies the reorganisation of the glycol–water system adding more tanks and defining a new operating strategy. It also has to be mentioned that staging the heat recovery from the refrigeration cycle,

© Woodhead Publishing Limited, 2013

Table 27.16 Data for the investment estimation

Cogeneration	1.100	(k€/kWe)
Cogeneration maintenance	0.015	(€/kWhe)
Mechanical vapour recompression	$4.000*(\dot{E}_{el})^{0.9}$	(k€)
Mechanical vapour recompression maintenance	0.02	(€/kWhe)
Estimated lifetime of equipment	15	(y)
Interest rate	6	(%)

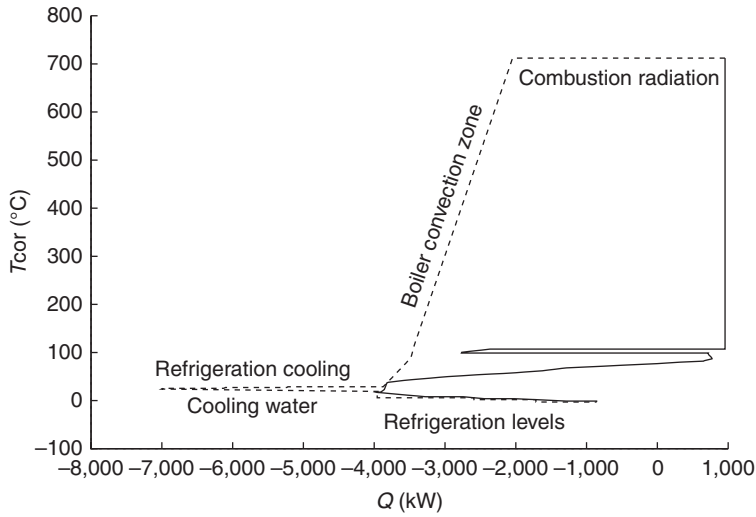

27.18 Integrated Composite Curves of energy conversion system for scenario A.

profiting from the heat pumping effect, will mean retrofitting the hot water recovery system, introducing one hot water storage tank per Utility Pinch Point introduced in the system. This requires the development of a more detailed simulation model.

Given below some comments on the different scenarios.

Scenarios A and B – Boiler + Refrigeration

These two scenarios allow showing the benefit of the heat recovery from the refrigeration cycle. By increasing the temperature level of the refrigeration cycle, one can see that 922.0 $kW_{LH\,V}$ can be saved with the heat pumping solution. The additional mechanical power consumed is 254.5 kWe, which features an overall COP of 3.6.

The Integrated Composite Curves of the energy conversion system for these two solutions are compared on Figs 27.18 and 27.19.

© Woodhead Publishing Limited, 2013

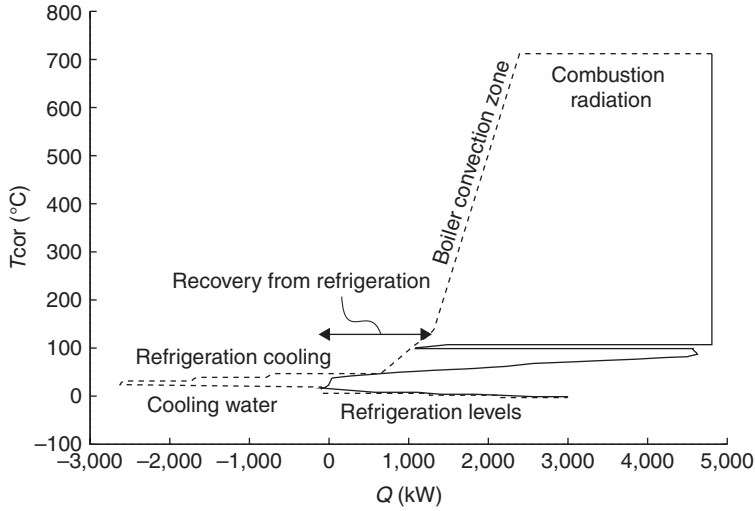

27.19 Integrated Composite Curves of energy conversion system for scenario B.

Scenarios C and D – Condensing Boiler + Refrigeration

Introducing a condensing boiler could save 491.2 kW or 10.39% of the natural gas consumption in the minimum energy requirement conditions. By increasing the temperature level of the refrigeration cycle, one can see that 451.0 kW_{LHV} can be saved by the heat pumping solution. The additional mechanical power consumed is 217.7 kWe, which features an overall COP of 2.1. It is interesting to note that the saving from the condensing boiler is no longer significant, and that most of the condensing heat is finally released in the cooling system.

The analysis shows, therefore, that although a real benefit can be observed from the condensing boiler integration, the benefit is set to zero when the heat pumping from the refrigeration system is considered. The difference between scenario B and scenario C is explained by a small reduction of the heat pumping temperature in the refrigeration cycle, which leads to an increase in the efficiency of the refrigeration cycle. The Integrated Composite Curves of the energy conversion system for these two solutions are compared on Figs 27.20 and 27.21.

Scenario E – Condensing Boiler, Refrigeration and Mechanical Vapour Recompression

When mechanical vapour recompression is introduced, the Utility Pinch Point observed in scenarios B and D is moved in order to reduce the flow of natural gas. The use of mechanical vapour recompression is optimised,

© Woodhead Publishing Limited, 2013

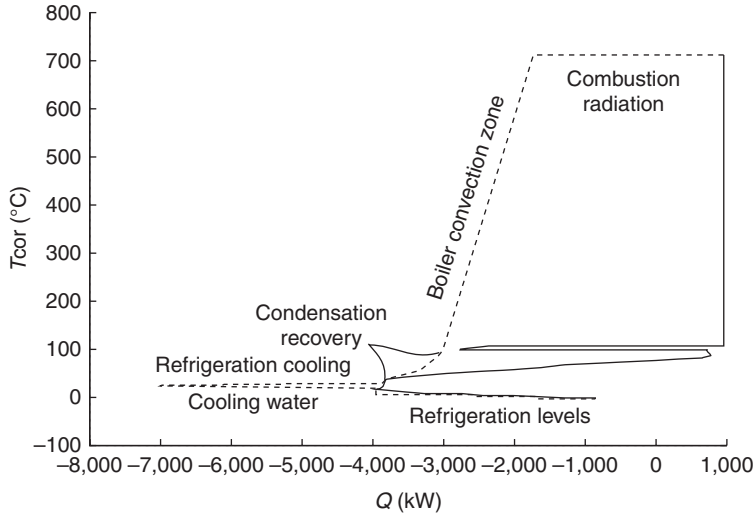

27.20 Integrated Composite Curves of energy conversion system for scenario C.

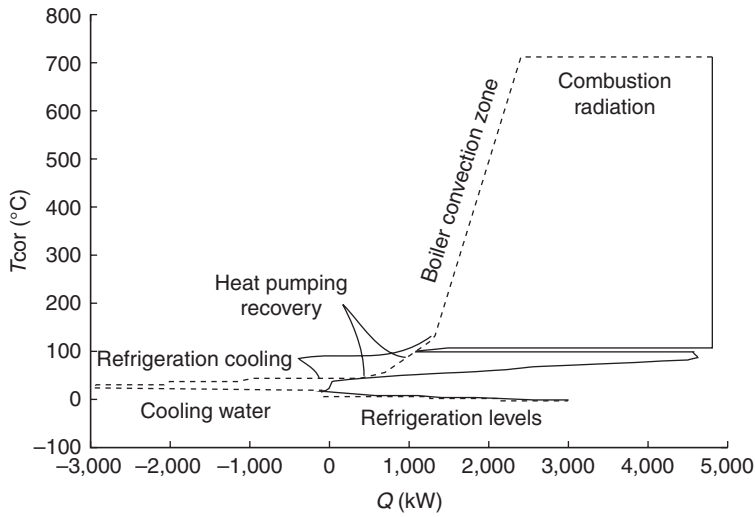

27.21 Integrated Composite Curves of energy conversion system for scenario D.

together with the temperature of the refrigeration cycle heat recovery, to profit from the heat pumping effect (Fig. 27.22). The natural gas saving corresponds to 2,559.0 kW or 60.42% of the natural gas consumption in the minimum energy requirement conditions. This is obtained with an increase

© Woodhead Publishing Limited, 2013

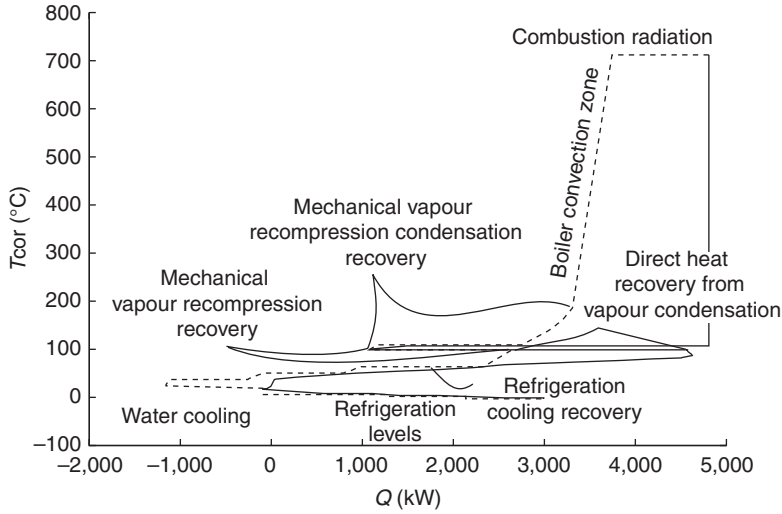

27.22 Integrated Composite Curves of energy conversion system for scenario E.

of 570.3 kWe spent in the refrigeration cycles and in the mechanical vapour recompression. The COP of this scenario is of 4.49 when compared with the solution using the condensing boiler with heat pumping.

Scenarios F and G – Cogeneration and Refrigeration

In scenarios F and G, we compare the cogeneration systems, with and without biogas production. From Figs 27.23 and 27.24, it can be seen that the system is not favourable for a cogeneration unit, mainly because the heat load of the engine cooling is only partly used to satisfy the process heat load. There is also a competition with the refrigeration cycles, which cannot be used anymore as a heat pump.

The system becomes, however, a net electricity producer. When compared with scenario A, it can calculate the marginal efficiency of the electricity production by Equation [27.13]. For scenario F, a marginal efficiency of the electricity production of 51.47% can be obtained. The efficiency can also be observed when considering the difference in the cooling water usage that increases from 3,141.6 to 8,063.3 kW (i.e. 4,921.7 kW).

The biogas is used to reduce the amount of natural gas consumed and contributes also to the production of mechanical power.

$$\eta_{\text{marg},i} = \frac{\dot{E}_i - \dot{E}_{\text{SA}}}{\text{L}\dot{\text{H}}\text{V}_{\text{Si}} - \text{L}\dot{\text{H}}\text{V}_{\text{SA}}} \qquad [27.13]$$

© Woodhead Publishing Limited, 2013

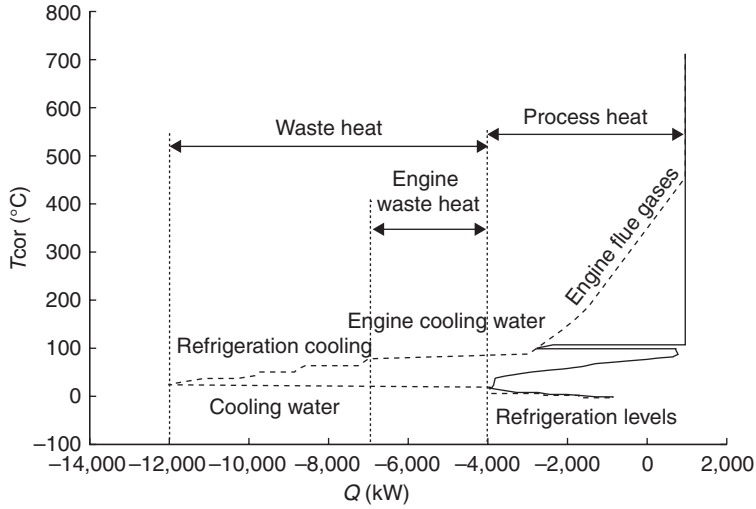

27.23 Integrated Composite Curves of energy conversion system for scenario F.

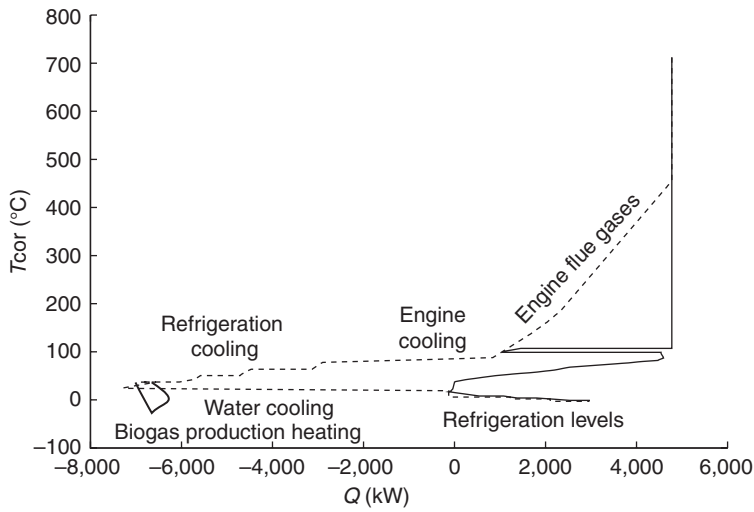

27.24 Integrated Composite Curves of energy conversion system for scenario G.

Scenarios H and I – Cogeneration, Refrigeration and Mechanical Vapour Recompression

Scenarios H and I consider, in addition, the use of mechanical vapour recompression. Changing the temperature level of the vapour recovery allows one to see the big advantage of doing the recompression. Without using the

© Woodhead Publishing Limited, 2013

biogas, the solution obtained corresponds to net production of mechanical power while reducing the natural gas consumption by 28.42%. The marginal efficiency cannot be calculated anymore, except if scenario E is taken as a reference. In this case, the marginal efficiency of the electricity production is of 77.46%, much higher than could be obtained without mechanical vapour recompression.

In both scenarios, mechanical vapour recompression involves 70.97% of the vapour available. The remaining vapour is directly used to heat up process streams.

From the investment point of view, the engine of scenario H is 4.6 times smaller than in scenario F without mechanical vapour recompression.

Scenarios H and I are those representing the lowest primary energy consumption. Compared with the starting point, i.e. 17,062 kW_{LHV} and 1,322 kWe corresponding to 19,422.7 kW, the primary energy saving corresponds to 84.16% of the present consumption. When considering the use of the biogas produced from the waste streams, the savings are even more attractive, with a value of 93.15%.

From the primary energy point of view, it should be realised that the solution with combustion and mechanical vapour recompression (scenario E) features similar results with a saving corresponding to 80.79%.

Considering the price of electricity and natural gas, it should be realised that the solution with the lowest operating cost is the one with a maximum production of electricity. The operating cost difference has, however, to compensate the investment of a bigger engine.

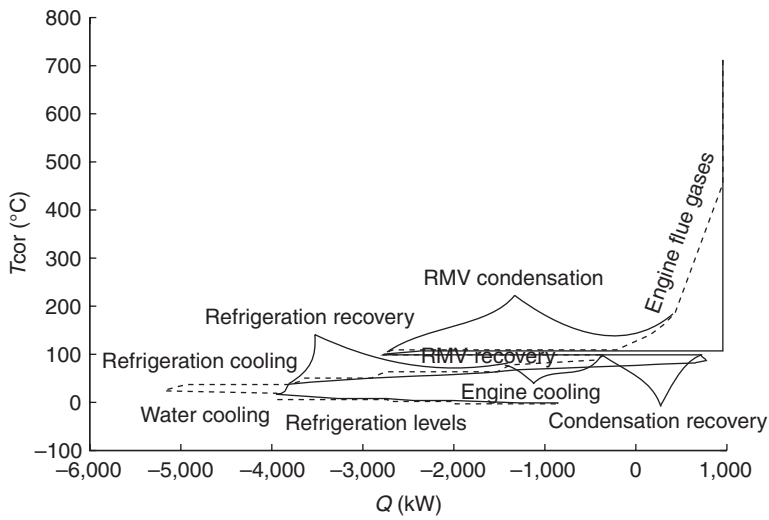

27.25 Integrated Composite Curves of energy conversion system for scenario H.

© Woodhead Publishing Limited, 2013

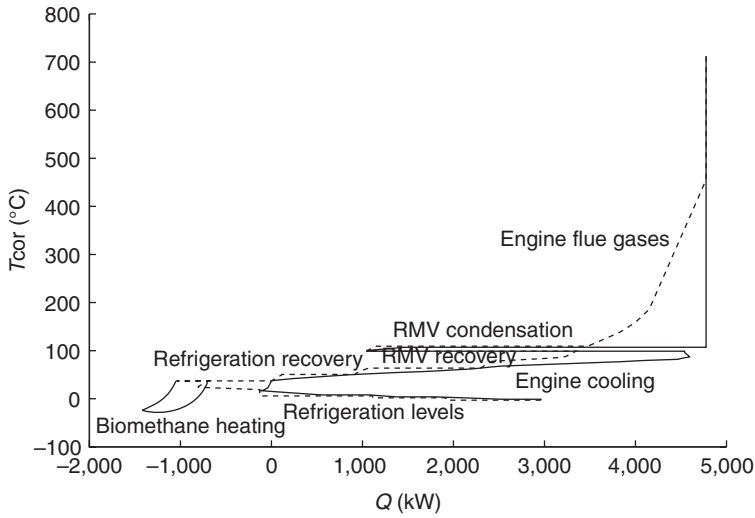

27.26 Integrated Composite Curves of energy conversion system for scenario I.

The Integrated Composite Curves of the two scenarios are given on Figs 27.25 and 27.26.

27.5 Conclusion

As a result of the energy conversion system integration, the complete list of streams is defined and can be used to design the HEN design (the resulting list of hot and cold streams is given in the Annex). Before starting the HEN design, however, the list of streams has to be analysed again, and in particular the streams related to the use of hot water identified. Indeed, the needs of the units first have to be defined, in order to define the hot and cold streams requirement, once the energy target is set and the Process and Utility Pinch Points are identified; the list of streams to be considered in the HEN has to be defined by analysing the use of hot water in the system.

The first step in this analysis would be to identify the conditions of the water tanks to be considered in the system. From this first analysis the water usage network has to be designed to yield a smaller number of streams to be finally considered for the HEN design. This approach could be performed by a simple examination, or by applying mathematical programming models considering multi-period operation (Becker and Maréchal, 2012b) and combined Mass and Heat Integration (Renard *et al*., 2012).

© Woodhead Publishing Limited, 2013

27.5.1 List of Streams for the HEN Design

Name	Temp: in (C)	Heat load (kW)	Temp: out (C)	DTmin/2 (K)	Unit
A	15.00	369.90	51.50	–2.00	MAK
B	48.00	188.60	65.00	–2.00	MAK
C	15.00	823.60	54.50	–2.00	MAK
D	48.00	420.10	65.00	–2.00	MAK
E	65.00	368.40	75.00	–2.00	MATMAK
F	15.00	3,450.4	80.00	–2.00	MATMAK
G	78.00	1,662.9	105.00	–2.00	MATMAK
H	105.00	3,319.8	105.00	–2.00	MATMAK
I	105.00	–17.200	100.00	10.00	RECOV
J	100.00	–3,487.9	100.00	1.00	RECOV
K	100.00	–482.80	25.00	2.00	RECOV
L	52.00	857.90	80.00	–2.00	MATMAK
M	102.50	–5,434.6	10.00	2.00	MATMAK
N	10.00	–534.80	10.00	2.00	FERM
O	10.00	–233.80	6.00	2.00	FERM
P	6.00	–425.50	6.00	2.00	FERM
Q	6.00	–714.50	1.00	2.00	FERM
R	1.00	–427.70	1.00	2.00	FERM
S	1.00	822.05	15.00	–2.00	FERM
T	15.00	4,854.0	80.00	–2.00	FERM
U	70.00	–4,858.4	5.00	2.00	FERM
V	65.00	251.90	85.00	–2.00	CIP
W	40.00	472.80	60.00	–2.00	CIP
X	15.00	1,326.9	85.00	–2.00	CIP
Y	15.00	29.300	60.00	–2.00	CIP
Z	35.00	399.34	60.00	–2.00	CIP
AA	85.00	–472.70	60.00	2.00	CIP
AB	40.00	–713.70	20.00	2.00	CIP
E1	470.00	–271.10	58.00	15.00	ENG
E1C	58.00	–89.835	40.00	15.00	ENG
E2	90.00	–280.06	80.00	2.00	ENG
BE1	87.00	–424.06	80.00	2.00	BENG
BE2	470.00	–631.71	90.00	15.00	BENG
BE3	35.00	351.22	35.00	–2.00	BENG
FRG1–	65.00	–62.913	55.00	1.85	FRG1
	65.00	–1229.2	65.00	1.16	FRG1
	190.85	–436.07	65.00	5.00	FRG1
FRG1_	1.00	1,241.6	1.00	–5.00	FRG1
FRG2–	51.67	–37.352	41.67	1.85	FRG2
	51.67	–802.01	51.67	1.16	FRG2
	166.55	–231.13	51.67	5.00	FRG2
FRG2_	–3.00	804.57	–3.00	–5.00	FRG2
FRG3–	38.33	–44.886	28.33	1.85	FRG3
	38.33	–1,042.7	38.33	1.16	FRG3
	142.18	–245.28	38.33	5.00	FRG3
FRG3_	–8.00	1,043.3	–8.00	–5.00	FRG3

© Woodhead Publishing Limited, 2013

Name	Temp: in (C)	Heat load (kW)	Temp: out (C)	DTmin/2 (K)	Unit
RMV–	110.00	–4.4050	109.00	1.36	RMV
	110.00	–2,322.2	110.00	0.85	RMV
	148.56	–81.933	110.00	3.67	RMV
RMV_	98.00	2,307.2	98.00	–1.00	RMV
COOLW	17.00	674.62	22.00	–2.00	COOLW

27.6 Sources of Further Information

Useful information concerning the data collection and other application of Process Integration techniques in the food processing industry can be found in *Handbook of Water and Energy Management in Food Processing* (Klemeš *et al.*, 2008).

For further information on exergy and its application in industrial energy systems, refer to the book *Thermodynamic and Energy System Analysis* (Borel and Favrat, 2010).

In the book, *Computer Aided Process and Product* (Puigjaner and Heyen, 2006), further information can be found on computer-aided methods for process engineering, in particular concerning data reconciliation methods and the application of MILP techniques for the integration of utility systems in processes.

Most of the theoretical concepts used in this chapter are explained in detail in this handbook. However, the chapters of the UNESCO Encyclopaedia of Life Support Systems (Marechal, 2008) can also be useful. In particular, the chapter Pinch Analysis (3.19.1.7) gives a summary of the Process Integration techniques, while the chapter Improving Process Performances Using Pinch Analysis (3.19.1.8) gives a summary of how Pinch based methods can be used to improve the energy efficiency of a process and how energy conversion techniques can be integrated in an optimal way. This chapter also explains in more detail the combined use of Pinch and Exergy Analysis.

27.7 References

ADEME (2011). Methanization at the farm – practical guide Technical Report Editor ADEME (France), (in French) <www2.ademe.fr> accessed 06.07.2013.

Becker, H., Maréchal, F. (2012a). Energy integration of industrial sites with heat exchange restrictions. *Computers and Chemical Engineering*, **37**, 104–118.

Becker, H., Maréchal, F. (2012b). Targeting industrial heat pump integration in multiperiod problems. *Computer Aided Chemical Engineering*, 2012, 415–419.

Borel, L., Favrat, D. (2010). *Thermodynamic and Energy System Analysis*. EPFL Press, Lausanne, Switzerland 2010, Chapters 3.2 to 3.3. 109–113.

© Woodhead Publishing Limited, 2013

Klemeš, J., Smith, R., Kim, J-K. (eds) (2008). *Handbook of Water and Energy Management in Food Processing*. Woodhead Publishing Ltd, Cambridge, UK.

Linnhoff, B., Ashton, G., Obeng, E. (1988). Process integration of batch processes. *IChemE Symposium Series*, **109**, 221–237.

Marechal, F. (2008). Chapter 3.19.1.7, 3.19.1.8, UNESCO encyclopaedia of life support systems, In: Frangopoulos Ch and Tsatsaronis G., EOLSS Publishers Co Ltd, Oxford, UK.

Marechal, F., Kalitventzeff, B. (1998a). Energy integration of industrial sites: tools, methodology and application. *Applied Thermal Engineering*, **18**(11), 921–933.

Marechal, F., Kalitventzeff, B. (1998b). Process integration: selection of the optimal utility system. *Computers and Chemical Engineering*, **22**(1), S149–S156.

Marechal, F., Kalitventzeff, B. (1999). Targeting the optimal integration of steam networks. *Computers and Chemical Engineering*, **23**, s133–s136.

Marechal, F., Kalitventzeff, B. (2003). Targeting the integration of multi-period utility systems for site scale process integration. *Applied Thermal Engineering*, **23**, 1763–1784.

Marechal, F., Kalitventzeff, B. (2006). Computer aided process and product engineering CAPE. In: *Utilities Integration (Energy, Water)*, Luis Puigjaner and Georges Heyen (eds). Wiley – VCH Verlag GmbH and Co. KGaA-Germany, 327–379.

Papoulias, S. A., Grossmann, I. E. (1983). A structural optimization approach in process synthesis – I. Utility systems. *Computers and Chemical Engineering*, **7**(6), 695–706.

Renard, L., Périn-levasseur, Z., Salgueiro, L., Savulescu, L. (2012). Combined heat and mass integration: a benchmarking case study. 22nd European Symposium on Computer Aided Process Engineering (ESCAPE 22) (June), 17–20.

Puigjaner, L., Heyen, G. (eds) (2005). *Computer Aided Process and Product Engineering – CAPE*. Wiley–VCH Verlag GmbH and Co. KGaA- Germany.

27.8 Appendix A: Complementary Tables

Table A.1 Specific heat capacity of material streams

Material stream	Specific heat capacity – Cp (kJ/kg K)
Water	4.18
MAK	3.75
MAT	3.43
MAT + MAK	3.52
Soda (NaOH)	1.49
Sprouted barley / corn	1.8

Table A.2 Operating conditions boiler

Description	Value
LHV natural gas	47,460 (kJ/kg)
Cost natural gas	0.048 (€/kWh)
Boiler efficiency	89(%)

© Woodhead Publishing Limited, 2013

Table A.3 $\Delta T_{min}/2$ for streams

Streams	$\Delta T_{min}/2$
Liquid	2
Liquid–vapour	1
Gas	4

Table A.4 Brewing operation data

Description	Value
Operation time	8,180 h/y
Daily operation time	24 h
Plant lifetime	12 y
Maintenance time	10 d/y
Failure time	5%
Interest rate	5%
Beer production (68.7 t/h)	561,000.85 t/y

Table A.5 Timeline of the batch processes in the brewery (hot part)

Stream	Process	Start time (min)	End time (min)	Total time (min)
MAK	Heating 15–65°C	0	60	60
MAT	Heating 15–65°C	0	60	60
MAT + MAK	Heating 65–75°C	60	130	70
Filtrate	Filter	130	250	120
WOK	Evaporation	250	320	70
Wort	Centrifuge	320	380	60
Wort	Cooling	380	420	40

Table A.6 Timeline of the batch processes in the brewery (cold and cleaning parts)

Stream	Process	Total time
Wort	Fermentation @ 10°C	14 d
Wort + yeast	Maturing @ 6°C	10 d
Beer chilling	Chillage @ 1°C	6–7 h
Beer	Filtration + dilution + pasteurisation	2 h
Bottle cleaning	Bottle cleaning	Continuous

27.9 Appendix B: Nomenclature

c_{el}^{+} purchase cost of electricity (MU/kJ)
c_{el}^{-} selling price of electricity (MU/kJ)
$\dot{E}_{el,process}$ electricity consumed by the process (kW)

© Woodhead Publishing Limited, 2013

$\dot{E}^{+}_{\mathrm{el}}$	overall electricity purchased for the process (kW)
$\dot{E}^{-}_{\mathrm{el}}$	overall electricity exported from the process (kW)
c^{+}_{f}	fuel price (MU/kJ)
$\dot{E}^{+}_{f,u}$	nominal energy (or heating value) delivered to unit u by the fuel (e.g. natural gas) (kW)
$\dot{E}_{\mathrm{el},u}$	nominal electricity demand (+) or excess (−) of unit u (kW)
c_u	nominal operating cost per hour of unit u (excluding the fuel and electricity cost of unit u)
C_u	fixed cost related to the use of unit u
f_u	level of usage of unit u. This is a multiplication factor that is applied to all streams and flows of the unit u
$f_u^{\min}$	minimum level of usage of unit u
$f_u^{\max}$	maximum level of usage of unit u
y_u	integer variable defining the use ($y_u = 1$) or not ($y_u = 0$) of unit u
$\dot{Q}_{h/c,k,u}$	nominal heat load of hot or cold stream h/c in temperature interval k and belonging to unit u
$\dot{R}_k$	cascaded heat from the temperature interval k to the lower temperature intervals

© Woodhead Publishing Limited, 2013

28

Applications of Process Integration Methodologies in Dairy and Cheese Production

MARTIN JOHN ATKINS and MICHAEL R. W. WALMSLEY,
University of Waikato, New Zealand

DOI: 10.1533/9780857097255.5.864

Abstract: This chapter provides a brief introduction to the dairy industry, before outlining specific issues in applying contemporary Process Integration techniques to the dairy industry. Selected published case studies will also be reviewed, in order to illustrate the quantum of benefits that have been achieved from utilising Process Integration techniques. Finally, future developments that are needed to improve Process Integration in the dairy industry will be outlined.

Key words: Process Integration, Pinch Analysis, dairy processing.

28.1 Introduction

The dairy industry produces a wide variety of products from milk, using a range of different processing techniques. Internationally, approximately 60% of milk produced is used for fluid-milk products, 25% for cheese and whey products, while the remaining 15% is used for butter, milk concentrate, milk-powder products, and cream (Xu and Flapper, 2011); however, the product mix is very country specific, depending on the size of the domestic market relative to the milk production capacity of the country. Only around 7% of global milk production enters world trade, with the remainder being consumed domestically (Blayney *et al.,* 2006). For a good introduction to the various processes and processing equipment used in the production of dairy products, see the *Dairy Processing Handbook* (Tetra Pak, 2003).

The size and composition of dairy processing facilities is also highly varied, depending on both the product mix and the intended market. For example, large dairy exporting countries, such as New Zealand and the Netherlands, are dominated by large multi-product dairy factories, while dairy factories that process fluid-milk for town supply are often an order of magnitude smaller and supply only the local domestic market. In 2000, there were 710

© Woodhead Publishing Limited, 2013

dairy factories in France, each processing an average of 31,900 t/y of milk, whereas in the Netherlands there were only 15 dairy factories, each processing an average of 555,600 t/y of milk (Ramírez *et al.,* 2006). The trend internationally, especially in developed nations, is toward fewer and larger dairy factories.

The dairy industry, like the food industry in general, has a number of important process and product requirements, such as hygiene, product safety, nutritional value, and product quality. These factors provide a number of important industry-specific constraints on the application of traditional Process Integration techniques. The non-continuous nature of the operation of most dairy plants makes the application of traditional Process Integration techniques (e.g. Pinch Analysis) difficult, and consequently Novel Pinch Analysis methods for improved integration have been developed.

A number of factors affect the amount of energy and water required in the processing of dairy products, including the type of processing, the technical standards of the dairy factory, and efficient operation of the plant (i.e. good housekeeping). Some processes used in the production of dairy products are inherently more energy intensive than others; however, there is a large variation in Specific Energy Consumption (SEC) reported internationally, with only some of the variation being explained by the age and scale of the processing plant. For example, the range of SEC for the processing of fluid-milk products ranged from 0.2 to 6.0 MJ/kg milk in the USA, and 0.3 to 12.6 MJ/kg milk in Europe (Xu *et al*., 2009). Water use is also highly varied, although somewhat product dependent, with water consumption for European dairy processers ranging from 0.2 to 11 L of water per L of milk (Daufin *et al*., 2001).

The complex interactions between water and energy use are particularly relevant to the dairy industry, and therefore much of the recent progress in Process Integration is focused on developing methodologies that combine Heat Integration and Mass/Water Integration (Savulescu and Kim, 2008). The concurrent design and synthesis of both heat exchanger and water networks is a complex task, due to the co-dependence between the two. The other challenge is the drive to reduce water consumption, especially hot water use, which can affect the ability to utilise low-grade waste heat by simply heating water for cleaning (Dalsgård, 2002).

The fuel mix used in dairy processing is still predominantly fossil fuel based, mainly natural gas or coal, although electrical energy may be from renewable sources depending on the source of generation. CHP is also used at some dairy factories. There is further potential for fuel switching (mainly from coal to natural gas) although biomass is also beginning to be considered as a viable option in some cases. Dairy processes are typically characterised by low Pinch Temperatures (<100°C), which suits the integration of solar thermal energy to provide a portion of the thermal demand

© Woodhead Publishing Limited, 2013

(Atkins *et al.,* 2010a); however, the economics are not yet favourable for the widespread integration of renewable energy for process heat.

In this chapter, issues specific to the dairy industry in applying contemporary Process Integration techniques will be outlined. Selected published case studies will also be reviewed, in order to illustrate the quantum of benefits that has been achieved from utilising Process Integration techniques. Finally, future developments that are needed to improve Process Integration in the dairy industry will be outlined.

28.2 Application of Process Integration Methodologies

There are a number of issues to consider when applying Process Integration methodologies to the dairy and cheese industry. Some of these issues will be outlined and discussed in this section. These include the use of non-/semi-continuous and batch operations, zone targeting and integration, the integration of evaporators and heat pumps, constraints on heat exchange and temperature driving forces of different streams, and Mass Integration and water minimisation.

28.2.1 Non-/Semi-continuous and Batch Operation

One of the strengths of the Process Integration approach is the establishment of rigorous targets that are both meaningful and achievable. These targets are also a property of the system (i.e. stream data), and therefore independent of any HEN solution. The designer then has an opportunity to compare the performance of any proposed HEN, or an existing HEN in a retrofit situation, to these targets. There are two main challenges with targeting and integration in the dairy industry: (a) multiple individual processes operating independently on a single site, and (b) the non-/semi-continuous and batch operation of processes due to process or the required cleaning regimes.

A common view is that the greatest opportunity for large gains in efficiency and increased heat recovery lie in increasing Total Site Integration. Many processing plants have imbalances between heat sources and heat sink requirements and, therefore, the surplus heat from one plant can theoretically be used to supply the heat deficit of another plant. The achievement of system integration between plants is usually accompanied by complexities, and is difficult to achieve in practice, mainly because plants do not always operate simultaneously, which leads to operational and scheduling problems. One of the main causes for non-/semi-continuous operation in the dairy industry is the need for regular cleaning.

© Woodhead Publishing Limited, 2013

Cleaning of process equipment – Cleaning in Place (CIP) – is vital to ensure product safety and hygiene, and the length of time between washes is of critical importance to production rates, product safety, and energy and water consumption. Run times between CIP of equipment vary from several hours to several weeks, depending on the process and processing equipment being used. For example, a typical milk pasteurising process may run for between 6 and 12 h between washes, and a large spray dryer may operate for 4 weeks before a drying-chamber clean. The tendency is toward extending run times where allowable. Some plants also have the ability to parallel process where there may be multiple processing lines in operation and one is cleaned or on standby.

Where there are multiple individual processes onsite, cleaning schedules are usually determined by production considerations, and therefore there is no scheduled planning of CIPs between processes to improve energy efficiency. As a result, integrating processes is difficult because of the different cleaning schedules (which can be on an ad hoc basis) and the fact that process streams may not coincide with each other. There is also the difficulty, in directly exchanging heat between streams in different processes, due to the location and proximity of the streams on site.

Variability in operations can also be introduced due to seasonal milk supply changes, especially where pastoral grazing of stock is predominant. Seasonal flow of milk can vary dramatically depending on climate, economics of production, farming practices, and land use. Peak flows of milk can be much higher than at the shoulders of the season, with many plants operating for only relatively short periods of time to handle peak milk production. This is more of an issue in countries such as New Zealand where most dairy cows are grazed on pasture and the quantity of milk produced varies during the year with peak milk production typically occurring in late spring.

Process Integration methods developed for Batch Processes may be used to some extent, especially when the process is a pure Batch Process. The time-slice model can also be applied to individual plants with some success (Kemp and Deakin, 1989a, 1989b), and the large requirement for hot water for cleaning provides a convenient storage option. But depending on the number of individual plants on site and total Number of Streams (NoS), the number of combinations of operating states can become extremely large, making the TSM approach difficult (Atkins *et al.*, 2010b).

28.2.2 Zone Targeting and Integration

Before the merits of inter-plant heat transfer are considered, the potential for integration on an individual process level should be examined. There are often significant and worthwhile heat recovery or demand reduction opportunities within an individual plant or process. These local or zonal

© Woodhead Publishing Limited, 2013

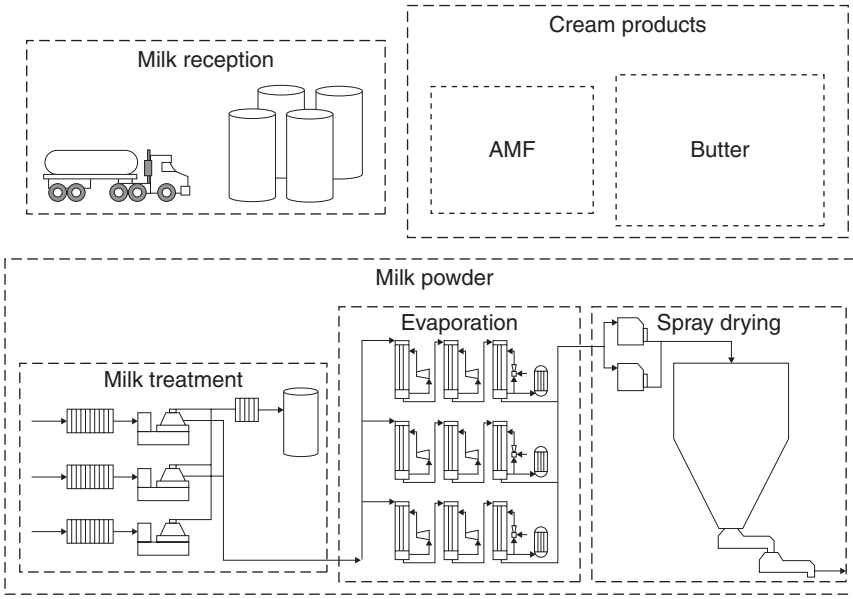

28.1 Simplified schematic of a dairy factory.

integration projects usually have a lower threshold to overcome in order to be economic and acceptable. Another advantage of integrating a zone is that the challenge of non-continuous operation is reduced. For example, consider the simplified dairy factory illustrated in Fig. 28.1, with milk reception, a cream products plant, and milk-powder plant.

Cream products use cream from milk treatment in the milk-powder plant, which produces both AMF and butter, and operates for 12/d including CIP. The milk-powder plant operates continuously for 24 h, with two evaporator and milk treatment lines operating while one is cleaned before being left on standby.

One of the initial actions is to determine the best way to analyse the various plants and processes. A traditional Total Site a Analysis could be conducted focusing on CHP options and heat exchange via the utility system – although in this case, this type of integration would not be feasible, due to the non-continuous operation of the different plants and the temperatures of the various streams.

A shortcoming of this approach is that it assumes that all of the heat sink and source streams from all individual plants are available to match with other source or sink streams in spite of practical considerations. For example, consider a heat source located in milk treatment and a feasible match within AMF. Using the traditional steady state or Total Site a Approach for targeting, it would be assumed that these two streams together could

© Woodhead Publishing Limited, 2013

be matched for heat exchange without consideration of the availability or proximity of these streams in relation to each other. Furthermore, if AMF only operated for a limited duration each year then the situation would be entirely unrealistic. The merits of an indirect heat recovery loop could be considered, although the local integration potential and relative heat balances of the individual plants should be considered first.

An alternate approach is to consider the processes or plants individually (i.e. cream products, milk-powder) or individual zones within the process. For example the milk-powder plant can be considered as an individual plant/process or as three separate zones: milk treatment, evaporation, and spray drying. Factors such as availability, run times, production schedule, and the nature of the process become important when deciding what constitutes a zone, or if several zones should be considered together for integration. The milk treatment zone is operated more or less independently of the rest of the milk-powder plant, and a high level of integration can be obtained, due to the very small temperature driving forces that are able to be used and the nature of the milk treatment process.

Finally, indirect heat exchange via a heat recovery loop with thermal storage can be used to integrate processes or zones developed by (Ahmad and Hui, 1991; Hui and Ahmad, 1994a, 1994b) This approach was further developed by (Atkins *et al.*, 2010b, 2012). If thermal storage is used and correctly sized, some of the issues with non-continuous operation can to a certain extent be overcome. Heat recovery within a zone or process should be considered first, and the merits of integrating streams indirectly should be considered on a case-by-case basis. See the relevant chapter in this volume for information on the design and integration of heat recovery loops in non-/semi-continuous processes.

28.2.3 Integration of Evaporators and Heat Pumps

Many dairy processes use evaporators to concentrate process streams, often before drying, with multi-effect falling-film tubular evaporators being most common. Mechanical Vapour Recompression (MVR) and Thermo-Vapour Recompression (TVR) are also commonly used and should follow the Appropriate Placement Principle if possible (Townsend and Linnhoff, 1983)– although constraints on the evaporator operating temperatures and pressures may cause this to be violated. A simplified schematic of a multi-effect evaporator with two MVR and one TVR effects is illustrated in Fig. 28.2.

The traditional Process Integration method for examining the integration of evaporators is to examine the thermodynamic profile of the evaporator against the background process (Smith and Jones, 1990). While this approach can provide insight to the process, it is often the case that there exists a relatively small range of temperatures and pressures at which evaporators may operate, due

© Woodhead Publishing Limited, 2013

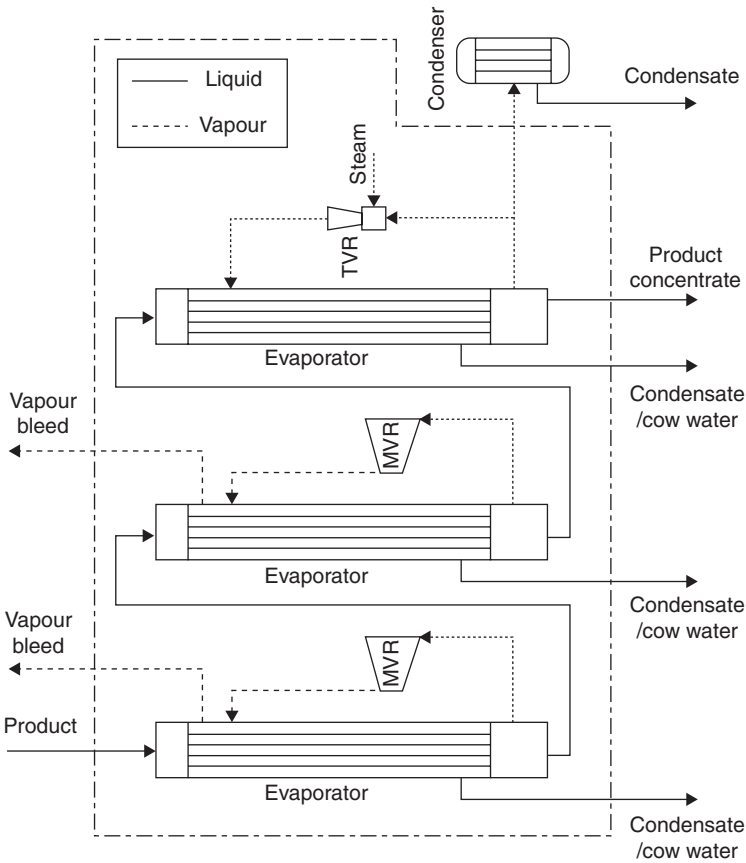

28.2 Simplified schematic of a multi-effect evaporator including two MVR and one TVR effects.

to the thermal sensitivity of the product and operability of the equipment. The highest temperature an evaporator effect would operate when concentrating milk is usually around 70°C, due to the tendency of salts to deposit, and the denaturing of proteins (Westergaard, 2004). As a result, there is seldom opportunity to alter the thermodynamic profile of evaporators to improve integration with the background process, especially in retrofit situations.

That is not to say that there are no opportunities to include evaporators in Process Integration studies, as there are other evaporator streams such as condensers and condensate (often called cow water) that may be a source of waste heat and can be utilised by the process. When conducting a Process Integration study involving evaporators that are constrained due to product constraints, the following streams can still be included in the analysis without having to alter the thermodynamic profile of the evaporators:

© Woodhead Publishing Limited, 2013

- Inlet product stream
- Product concentrate
- Condensate/cow water
- Vapour to condensers
- Vapour bleed streams.

Vapour bleeding is sometimes used as a heat source to heat process streams (usually the incoming process stream to the evaporator). It occurs where a small amount of vapour from the shell side of the calandria is used, thereby reducing the amount of vapour available to be used in the next effect for evaporation and to increase the overall net energy input into the dryer (Robertson and Baldwin, 1993). Robertson and Baldwin (1993) used Pinch Techniques to examine a milk-powder plant and concluded that, although the evaporators were well integrated, minor changes and the use of vapour bleeding to preheat various process streams could reduce the energy use by 6–10%. Westphalen and Wolf Maciel (2000a, 2000b) developed an algorithm based on Pinch Analysis for optimising the fraction of vapour bleed used for heating.

Vapour bleed can be a useful technique although care should be taken as there are often other heat sources that are not used (e.g. the condenser), which may be more suitable. Furthermore, where vapour bleeding is employed, there will be an overall increase in energy use of the evaporator. Robertson and Baldwin (1993) derived an equation to predict the increase in steam consumption due to vapour bleeding for a multi-effect evaporator with a TVR on the first effect. Care should be taken when determining what effect vapour should be bled from because, if the vapour is taken from an effect at a higher temperature than is needed, then there will be an increased energy penalty in the consumption of live steam or power in the case of an MVR.

There are often excellent opportunities for integrating heat pumps in the dairy industry, due to characteristically low Pinch Temperatures and a large amount of low-grade waste heat available. The Appropriate Placement Principle should be followed (Townsend and Linnhoff, 1983) and there may be merit in considering multi-stage compression in some cases (Kapustenko *et al*., 2008). Optimisation methods have been developed for integrating heat pumps, and these methods have been successfully applied to the dairy industry (Becker *et al*., 2011, 2012).

28.2.4 Heat Exchange Constraints

Perhaps the biggest constraint in the food-processing industry is that of hygiene and product safety, with other concerns such as energy efficiency

© Woodhead Publishing Limited, 2013

remaining subservient issues. While it is possible to improve the heat recovery in many cases by increased heat transfer area, the possible savings need to be compared to any penalty incurred by reduced times between cleaning cycles due to increased biofouling of heat exchangers or other process equipment.

One major concern in the processing of milk products is that of thermophilic bacteria or thermophiles that are able to grow between 40°C and 65°C. For example, thermophiles grow in regeneration heat exchangers, such as those used in milk treatment areas, and evaporators (Scott *et al.*, 2007). While thermophile growth is unavoidable at these conditions, special attention may be needed to avoid promoting thermophile growth by examining internal temperature profiles of heat exchangers, or shear rate acting at the heat exchanger wall, and also the flow arrangement of heat exchangers.

Plate Heat Exchangers (PHE) are commonly used in the dairy industry and can easily reach temperature differences in the order of 1°C, which can result internal temperature profiles that may magnify this problem. The selection of greater ΔT_{min} values may therefore be warranted where it is known in advance that thermophile growth or biofouling will be a concern. It has even been suggested that more use of direct steam injection for product heating could be used as a substitute for PHE (Brooks and Flint, 2008). Energy use would increase, but the increased costs could be offset by potential decrease of downgraded product.

Typically, when stream temperatures are shifted for the Problem Table calculation, each stream is shifted by a global $\Delta T_{min}/2$. This adjustment is fine where all the streams have approximately the same heat transfer coefficients; however, if there are streams, such as gases, that have low heat transfer coefficients, this approach may yield misleading energy and heat exchanger area targets. To overcome this situation a ΔT_{min} contribution can be used where the stream is shifted by ΔT_{cont} instead of the usual $\Delta T_{min}/2$ (Kemp, 2007). Conversely, if streams have high heat transfer coefficients, such as boiling or condensing streams, then a lower ΔT_{cont} can be assigned to those streams.

The ΔT_{cont} approach is useful in Process Integration analysis in the dairy industry, because of the use of hot air for drying and other streams with low heat transfer coefficients. For example, if the global ΔT_{min} was 5°C and a ΔT_{cont} of 15°C was assigned to the gas streams then for a standard stream/gas match the ΔT_{min} would be 5/2 + 15 = 17.5°C and for a gas/gas match the ΔT_{min} would be 15 + 15 = 30°C.

28.2.5 Mass Integration and Water Minimisation

There is large potential for water reduction in the processing of dairy products, and many water reduction methods and strategies have been

© Woodhead Publishing Limited, 2013

employed previously. The main focus to date has been regeneration technologies, such as ultrafiltration, to remove contaminants from process waste water for reuse in the process (Akoum *et al.*, 2004; Vourch *et al.*, 2008). Very few studies have been reported that use Process Integration methodologies to focus on water reduction specifically in the dairy industry (Peng *et al.*, 2001), although large reductions in fresh water consumption of 60% have been found (Peng *et al.*, 2001). Many of the freshwater reduction opportunities include reusing hot waste water or evaporator condensate in the CIP process as a pre-rinse, which can reduce both water use and the need for hot utility. This practice is used at some large dairy factories in New Zealand and offers significant energy and water savings (French, 2003), although there is opportunity for the practice to become more widespread. It has been suggested that the temperature of waste streams, such as hot evaporator condensate, could be upgraded via the use of solar thermal energy (Atkins *et al.*, 2010b). There still remains much opportunity for the application of Process Integration techniques that focus on Mass Integration and water minimisation to be applied successfully to the dairy industry.

28.3 Selected Case Studies

There have been numerous published studies that apply various Process Integration methods to the dairy industry. Three of these studies have been selected to illustrate some of the variety of uses of Process Integration methods and the quantum of savings that have been demonstrated in the dairy industry.

28.3.1 Case Study 1 – Integration of Different Dairy Processes

An early application of Pinch Analysis to the dairy industry was reported by Lovell-Smith and Baldwin (1988), who examined the Minimum Energy Consumption (MEC) required by typical milk-powder, casein, and butter operations. Stream specific ΔT_{min} contributions were used based on typical temperature differences found throughout the industry at the time. Energy targets were compared to typical energy usage for similar plants operating in New Zealand at the time, and savings between 12% and 81% were identified. The authors also note that further savings could be realised if individual plants were combined in the analysis. For example, MEC could be decreased by 30% if the butter and casein plant were integrated and 12% if the butter and milk-powder plant were combined.

© Woodhead Publishing Limited, 2013

The placement of thermocompressors (TVR) in the multi-effect evaporator was also examined to determine its effect on the minimum required energy targets, and also if current thermocompressors were appropriately placed in relation to the Pinch Temperature (Townsend and Linnhoff, 1983). The required hot utility for the milk-powder plant was reduced by 27% and the Pinch Temperature was unchanged at 56°C when thermocompressors were included. Although there were large savings identified, the issues of impracticable HEN, the non-continuous operation of processes, and economics were cited as major obstacles to the implementation of many of the opportunities. However, the use of MVR in combination with thermocompressors is now widespread and is considered industry standard in the New Zealand dairy industry.

28.3.2 Case Study 2 – Integration of Heat Pumps in Cheese Production

The importance of examining the utility system, especially the refrigeration system of dairy factories, and cheese plants in particular, is illustrated by a study by Kapustenko and co-workers (Kapustenko *et al.*, 2008). The ammonia refrigeration unit of a cheese plant was examined for how waste heat from this unit could be most effectively utilised, including the option of additional compression of the refrigerant to increase the amount of heat recovered.

Initially, a single stage compression system was examined and waste heat was used to preheat demineraliser make-up water. The ammonia was compressed to 12 bar and both superheat (at 114°C) and part of the latent heat at 28°C were used to preheat the sink, as shown by the Composite Curves shown in Fig. 28.3a. A ΔT_{min} of 2°C was chosen as an acceptable Minimum Driving Force, due to the use of compact PHE. As can be seen in Fig. 28.3a, the amount of heat recovery was limited by the heat sink and so an additional heat sink (process water) was included, and an additional 417.1 kW of heat could be recovered while meeting the ΔT_{min} constraint. The Composite Curves for this case are shown in Fig. 28.3b. It is apparent from the Composite Curves that the amount of heat recovery is limited by the condensation temperature of the ammonia, which coincides with the Pinch Temperature (28°C). One option to improve the situation is to split the ammonia stream and apply additional compression, thereby increasing the condensation temperature and allowing the cold composite to shift more to the left and take greater advantage of the available heat.

The authors used a specially developed software package to determine the optimal split ratio of the refrigerant and pressure of the additional

© Woodhead Publishing Limited, 2013

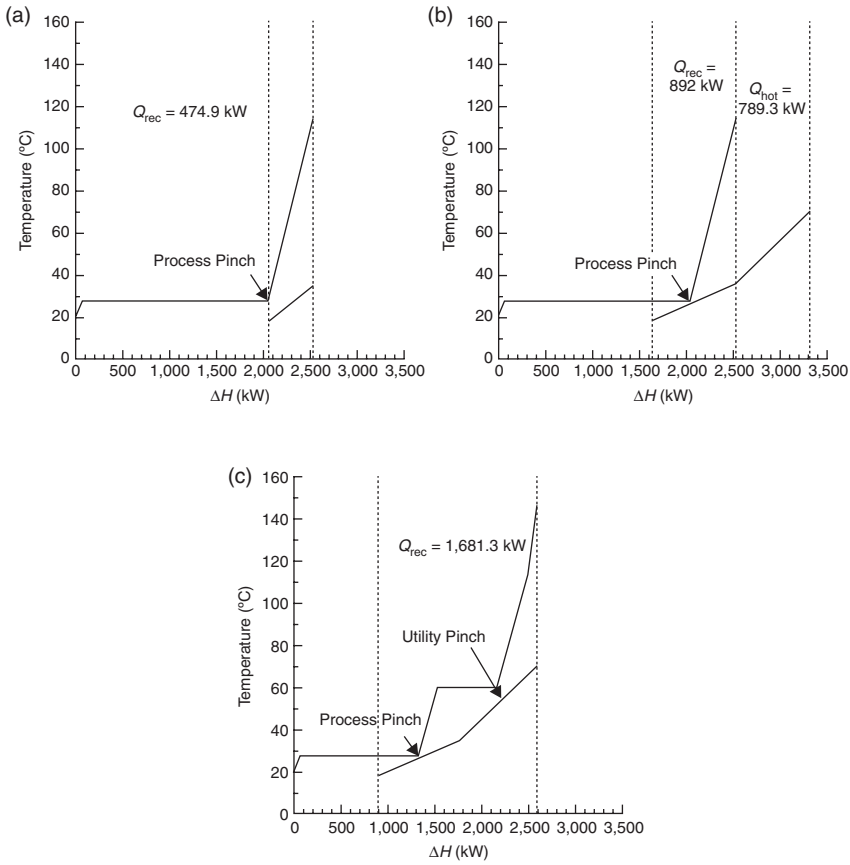

28.3 Composite Curves for (a) the existing process, (b) the inclusion of process water without additional compression, and (c) integrated process with additional compression. (After Kapustenko *et al.*, 2008.)

compression. Heat recovery could be increased a further 789.2 kW if 37% of the refrigerant were compressed from 12 to 26 bar and the new condensation temperature corresponded to 60°C. A Utility Pinch is also created as a result of the new condensing temperature, which creates three separate regions where heat cannot be transferred across the two Pinch Temperatures. The Composite Curves for this final case are shown in Fig. 28.3c and the stream data are given in Table 28.1.

The economics of the various schemes were compared, and both schemes were favourable with a payback of around 10 months. Although the secondary compression system required two additional compressors, consumed an

© Woodhead Publishing Limited, 2013

Table 28.1 Stream data for Composite Curves in Fig. 28.3c

Stream no.	Stream name	Type	TS (°C)	TT (°C)	CP (kW/°C)	ΔH (kW)
1.1	Cooling of gaseous ammonia	Hot	114	28	3.533	303.88
1.2	Condensation of ammonia	Hot	28	28	–	1,245.96
1.3	Cooling of liquid ammonia	Hot	28	20	5.164	41.31
2.1	Cooling of gaseous ammonia	Hot	146	60	2.738	235.50
2.2	Condensation of ammonia	Hot	60	60	–	631.72
2.3	Cooling of liquid ammonia	Hot	60	20	3.161	126.45
3	Demineraliser make-up water	Cold	18	35	27.933	474.87
4	Process water	Cold	18	70	23.200	1,206.40

From Kapustenko *et al.* (2008).

extra 60 kW of power, and needed two additional heat exchangers, the extra capital and operational expenditure was offset by the larger energy savings.

This case study is an excellent example of applying Process Integration techniques to a specific subset of streams or zones, and where possible considering process or utility modifications that significantly improve heat recovery and the integration of the process and utility system. Furthermore, it demonstrates the importance of including the heating and cooling requirements of the various utility systems in the analysis. Low-grade waste heat from refrigeration units, air compressors, unreturned boiler condensate and the like can usually be utilised due to the characteristic low Pinch Temperature of most dairy processes.

28.3.3 Case Study 3 – Milk-Powder Plant

A detailed study of the integration of a milk-powder plant was conducted by Atkins *et al.* (2011). The main objective of the study was to examine several methods of integrating the spray dryer exhaust into an existing drying plant via indirect heat recovery using a water loop. A major energy requirement in milk-powder production is the heating of the inlet air to the spray dryer from ambient to around 200°C. For a spray dryer producing 23 t/h of product, the air heater duty alone is around 21 MW. Most of this energy is lost in the exhaust air, which is typically at around 75–90°C. The schematic of the milk-powder plant with spray dryer exhaust heat recovery (excluding milk treatment and standardisation) is shown in Fig. 28.4. A Grid Diagram of the HEN for the powder plant including exhaust heat recovery is shown in Fig. 28.5.

The obvious selection of a suitable match for the dryer exhaust is the dryer inlet air; however, due to the larger driving force needed for indirect air-to-air heat exchange, there was only a 13% reduction in hot utility for this case.

© Woodhead Publishing Limited, 2013

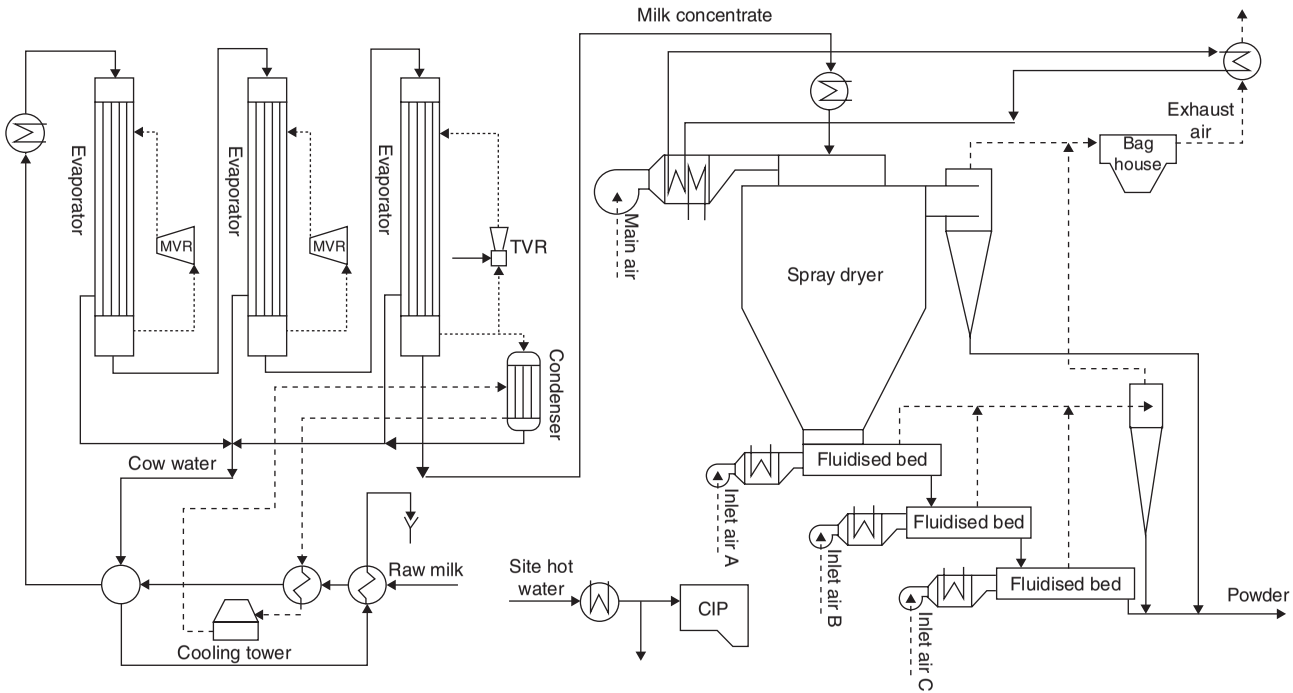

28.4 Schematic of a typical milk powder plant including an example of a coupled loop heat exchanger from the exhaust to the dryer inlet air. (From Atkins *et al.*, 2011.)

© Woodhead Publishing Limited, 2013

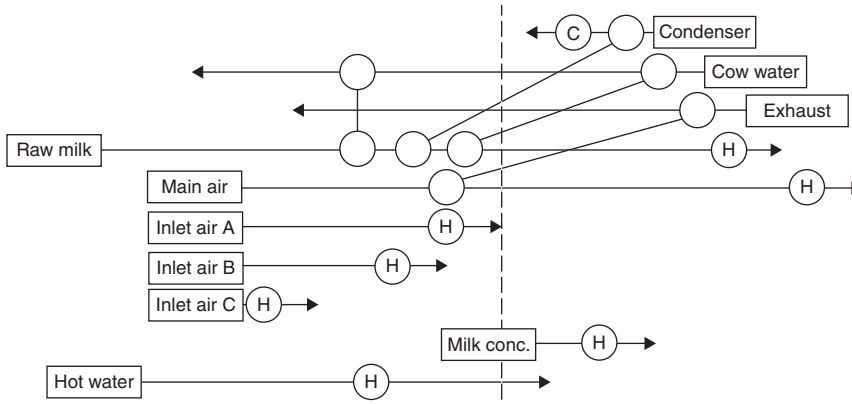

28.5 Grid Diagram of the HEN including exhaust heat recovery for the milk-powder plant shown in Fig. 28.4.

The amount of heat recovery possible from the exhaust varied depending on the heat sinks selected and also on the design and configuration of the exhaust heat exchanger, average face velocity, and mass flow rate of the water loop. Modelling the performance of the actual heat exchangers and water loop was important to maximise heat recovery and to give some realistic values of temperature driving forces within the heat exchangers.

One of the main obstacles to heat recovery of the dryer exhaust air was the problem of particulate fouling on the exhaust heat exchanger surface. In order to minimise particle deposition, internal conditions in the exhaust heat exchanger should avoid the so-called particle sticky region. The level of heat recovery would thereby be compromised, and care needs to be taken to consider the other effects of heat exchange, such as fouling and condensation. Therefore, at the targeting stage the engineer may need to be aware of the trade-off between heat recovery, increased pressure drop due to fouling, and selection of reasonable target temperatures for the exhaust stream, which are considered soft data. An exhaust target temperature could be selected, based on the powder properties, to avoid or minimise fouling, but at the same time this would limit the amount of heat recovery. An analogous situation may be that the limiting temperature for heat recovery from flue gas is often the Acid Dew Point (Smith, 2005).

The authors conclude that the economic feasibility of dryer exhaust heat recovery is highly dependent on the site energy cost and the primary fuel source, and there can be a large variation of energy cost between plants; however, for sites with moderate to high thermal energy cost, exhaust heat recovery can be economically attractive with simple paybacks in the order of 2–5 y.

© Woodhead Publishing Limited, 2013

28.4 Future Trends

There are number of important areas of Process Integration where methodological development would benefit the dairy industry and food-processing industry in general. Some of these important areas will be briefly outlined in this section.

The dairy, food, and beverage industries have been identified as the principal industrial sectors that could benefit from the use of renewable energy for process heat, in particular solar thermal energy (Kalogirou, 2004; IEA, 2008). There have been several studies that have examined the potential for integrating solar thermal for process heat (Atkins *et al*., 2010a; Quijera *et al*., 2011) and absorption refrigeration (Tora and El-Halwagi, 2010). One of the developing areas in Process Integration is methods to integrate renewables given the variable nature of the supply. The task is complex, and is complicated further where the demand is also variable, such as in the dairy and food-processing industry. Methods are emerging for integrating renewables (Varbanov and Klemeš, 2010), Process Integration and optimisation is comprehensively deal with in Klemeš *et al*., 2011. Nemet and Klemeš, 2011) covered PI with heat storage for solar sources of heat. However it is still the need for good case studies and methodological refinement for particular situations.

The dairy and food-processing industries are characterised by a high degree of interaction between water and energy use, and there have been different methods proposed that attempt to combine Heat Integration and Mass Integration or water minimisation (Savulescu and Kim, 2008). Despite methods being proposed, to date there have been no published studies of these methods being applied to actual problems in the dairy or food industries. The slow uptake may be due to several reasons, such as the complexity of the methods, but the lack of published industry-specific examples and case studies is a major obstacle for industry in taking up and applying these advanced methods. Although they may be understood and applied within academia, most dairy processers use consultants and equipment suppliers for efficiency projects, and so the real challenge is getting these bodies to understand and apply these advanced methodologies.

28.5 Sources of Further Information

A good overview of energy and water reduction strategies for the food and beverage sector, including dairy processing, is presented by Klemeš *et al*. (2008). A good introduction to the several processes and unit operations found in the dairy industry is the Dairy Processing Handbook (Tetra Pak, 2003), and for milk-powder production specifically, see Milk-Powder Technology (Westergaard, 2004). For a more detailed treatment of dairy science and technology, see Walstra *et al*. (2005). The International Dairy

© Woodhead Publishing Limited, 2013

Federation is also a permanent source of important and accessible information on issues relating to dairy processing, including energy and water usage. Two useful publications are Reduction of Greenhouse Gas Emissions at Farm and Manufacturing Levels (IDF, 2007) and Energy Use in Dairy Processing (IDF, 2005a, 2005b). To ensure reliable and accurate Process Integration studies it is important that the physical properties of dairy products are accounted for, which are extensively documented by Middleton (1996).

28.6 References

Ahmad, A., Hui, D. C. W. (1991). Heat recovery between areas of integrity. *Computers and Chemical Engineering*, **15**(12), 809–832.

Akoum, O., Jaffrin, M. Y., Ding, L. H., Frappart, M. (2004). Treatment of dairy process waters using a vibrating filtration system and NF and RO membranes. *Journal of Membrane Science*, **235**(1–2), 111–122.

Atkins, M. J., Walmsley, M. R. W., Morrison, A. (2010a). Integration of solar thermal for improved energy efficiency in low-temperature-pinch industrial processes. *Energy*, **35**(5), 1867–1873.

Atkins, M. J., Walmsley, M. R. W., Neale, J. R. (2010b). The challenge of integrating non-continuous processes – milk powder plant case study. *Journal of Cleaner Production*, **18**(9), 927–934.

Atkins, M. J., Walmsley, M. R. W., Neale, J. R. (2011). Integrating heat recovery from milk powder spray dryer exhausts in the dairy industry. *Applied Thermal Engineering*, **31**, 2101–2106.

Atkins, M. J., Walmsley, M. R. W., Neale, J. R. (2012). Process integration between individual plants at a large dairy factory by the application of heat recovery loops and transient stream analysis. *Journal of Cleaner Production*, **34**, 21–28. DOI:10.1016/j.jclepro.2012.01.026.

Balannec, B., Gésan-Guiziou, G., Chaufer, B., Rabiller-Baudry, M., Daufin, G. (2002). Treatment of dairy process waters by membrane operations for water reuse and milk constituents concentration. *Desalination*, **147**(1–3), 89–94.

Becker, H., Maréchal, F., Vullermoz, A. (2011). Process integration and opportunities for heat pumps in industrial processes. *International Journal of Thermodynamics*, **14**(2), 59–70.

Becker, H., Vullermoz, A., Maréchal, F. (2012). Heat pump integration in a cheese factory. *Applied Thermal Engineering*, **43**, 118–127. DOI:10.1016/j.applthermaleng.2011.11.050.

Blayney, D., Gehlhar, M., Bolling, C. H., Jones, K., Langley, S., Normile, M. A., Somwaru, A. (2006). U.S. Dairy at a Global Crossroads. United States Department of Agriculture, Economic Research Report Number 28.

Brooks, J. D., Flint, S. H. (2008). Biofilms in the food industry: problems and potential solutions. *International Journal of Food Science Technology,* **43**, 2163–2176.

Dalsgård, H. (2002). Simplification of process integration in medium-size industry. PhD thesis, Department of Mechanical Engineering, Technical University of Denmark.

Daufin, G., Escudier, J. -P., Carrère, H., Bérot, S., Fillaudeau, L., Decloux, M. (2001). Recent and emerging applications of membrane processes in the food dairy industry. *Trans IChemE*, **79C**, 89–102.

© Woodhead Publishing Limited, 2013

French, C. (2003). Energy and water integration in dairy processes: a practical methodology. Masters of Engineering Thesis, Department of Chemical and Process Engineering, University of Canterbury, Christchurch, New Zealand.

Hui, D. C. W., Ahmad, A. (1994a). Minimum cost heat recovery between separate plant regions. *Computers and Chemical Engineering*, **18**(8), 711–728.

Hui, D. C. W., Ahmad, A. (1994b). Total site heat integration using the utility system. *Computers and Chemical Engineering*, **18**(8), 729–742.

International Dairy Federation. (IDF) (2005a). *Energy Use in Dairy Processing*. Bulletin of the International Dairy Federation 401/2005, Brussels, Belgium.

International Dairy Federation. (IDF) (2007). *Reduction of Greenhouse Gas Emissions at Farm and Manufacturing Levels*, Bulletin of the International Dairy Federation 422/2007, Brussels.

International Energy Agency (IEA) (2008). *Potential for solar heat in industrial processes*, available at: www.iea-shc.org/publications/downloads/task33-Potential_for_Solar_Heat_in_Industrial_Processes.pdf [accessed 24.02.12]

Kalogirou, S. (2004). Solar thermal collectors and applications. *Progress in Energy and Combustion Science*, **30**, 231–295.

Kapustenko, P. O., Ulyev, L. M., Boldyryev S. A., Garev, A. O. (2008). Integration of a heat pump into the heat supply system of a cheese production plant. *Energy*, **33**, 882–889.

Kemp, I. C. (2007). (authors of the first edition Linnhoff, B., Townsend, D. W., Boland, D., Hewitt, G. F., Thomas, B. E. A., Guy, A. R., Marsland, R) *Pinch analysis and process integration. A User Guide on Process Integration for Efficient Use of Energy.* Elsevier, Amsterdam, The Netherlands.

Kemp, I. C., Deakin, A. W. (1989a). The cascade analysis for energy and process integration of batch processes. Part 1. Calculation of energy targets. *Chemical Engineering Research and Design*, **67**, 495–509.

Kemp, I. C., Deakin, A. W. (1989b). The cascade analysis for energy and process integration of batch processes. Part 2. Network design and process scheduling. *Chemical Engineering Research and Design*, **67**, 510–516.

Klemeš, J., Friedler, F., Kim, J. K. (2011). *Sustainability in the Process Industry: Integration and Optimization*. McGraw-Hill, New York, USA.

Klemeš, J., Smith, R., Kim, J. K. (2008), *Handbook of Water and Energy Management in Food Processing.* Woodhead Publishing Ltd, Cambridge, UK.

Lovell-Smith, J. E. R., Baldwin, A. J. (1988). Energy saving opportunities in a dairy manufacturing plant. *New Zealand Journal of Dairy Science and Technology*, **23**, 61–74.

Middleton, J. (1996), *Physical Properties of Dairy Products*, 3rd ed. MAF Quality Management, Minisitry of Agriculture, Auckland, New Zealand.

Nemet, A., Klemeš, J. (2011). Optimising the temperature of heat storage to serve processes with varying supply and demand – captured solar energy curve. *Chemical Engineering Transactions*, **25**, 605–610.

Peng, S. F., Farid, M., Wilks, T. (2001). Application of water pinch analysis to a dairy plant. *Acta Horticulturae*, **566**, 199–203.

Quijera, J. A., Alriols, M. G., Labidi, J. (2011). Integration of a solar thermal system in a dairy process. *Renewable Energy*, **36**, 1843–1853.

Ramírez, C. A., Patel, M., Blok, K. (2006). From fluid milk to milk powder: energy use and energy efficiency in the European dairy industry. *Energy*, **31**, 1984–2004.

© Woodhead Publishing Limited, 2013

Refstrup, E. (2000). Evaporation and drying technology developments. *International Journal of Dairy Technology,* **53**, 163–167.

Robertson, L. J., Baldwin, A. J. (1993). Process integration study of a powder plant. *Journal of Dairy Research*, **60**(3), 327–338.

Savulescu, L., Kim, J. (2008). Novel methods for combined energy and water minimisation in the food industry. In: Klemeš, J., Smith, R., Kim, J. K. (eds), *Handbook of Water and Energy Management in Food Processing.* Woodhead Publishing Ltd, Cambridge, UK, pp. 304–331.

Scott, S. A., Brook, J. D., Rakonjac, J., Walker, K. M. R., Flint, S. H. (2007). The formation of thermophilic spores during the manufacture of whole milk powder. *International Journal of Dairy Technology*, **60**(2), 109–117.

Smith, R. (2005), *Chemical Process – Design and Integration*. Wiley, Chichester, UK.

Smith, R., Jones, P. S. (1990). The optimal design of integrated evaporation systems. *Journal of Heat Recovery System CHP*, **10**, 341–368.

Tetra Pak. (2003), *Dairy Processing Handbook,* 2nd ed. Tetra Pak Processing Systems, Lund, Sweden.

Tora, E. A., El-Halwagi, M. M. (2010). Integration of solar energy into absorption refrigerators and industrial processes. *Chemical Engineering and Technology*, **33**(9), 1495–1505.

Townsend, D. W., Linnhoff, B. (1983). Heat and power networks in process design: Part I: Criteria for placement of heat engines and heat pumps in process networks. *AIChE Journal*, **29**(5), 742–748.

Varbanov, P. S., Klemeš, J. J. (2010). Total sites integrating renewables with extended heat transfer and recovery. *Heat Transfer Engineering*, **31**(9), 733–741.

Vourch, M. Balannec, B., Chaufer, B., Dorange, G. (2008). Treatment of dairy wastewater by reverse osmosis for water reuse. *Desalination*, **219**(1–3), 190–202.

Walstra, P., Wouters, J. T. M., Geurts, T. J. (2005), *Dariy Science and Technology*, 2nd ed. CRC Press, Boca Raton, FL, USA.

Westergaard, V. (2004), *Milk Powder Technology Evaporation and Spray Drying*. Niro A/S, Copenhagen, Demark,.

Westphalen, D. L., Wolf Maciel, M. R. (2000a). Optimization of bleed streams in evaporation systems based on pinch analysis: new approach. *Computer Aided Chemical Engineering*, **8**, 997–1002.

Westphalen, D. L., Wolf Maciel, M. R. (2000b). Pinch analysis of evaporation systems. *Brazilian Journal of Chemical Engineering*, **17**(4–7), 525–538.

Xu, F., Flapper, J. (2011). Reduce energy use and greenhouse gas emissions from global dairy processing facilities. *Energy Policy*, **39**(1), 234–247.

Xu, F., Flapper, J., Kramer, K. J. (2009). Characterization of energy use and performance of global cheese processing. *Energy*, **34**(11), 1993–2000.

© Woodhead Publishing Limited, 2013

29

Applications of Process Integration Methodologies in Beet Sugar Plants

KRZYSZTOF URBANIEC, MIROSŁAW GRABOWSKI and JACEK WERNIK, Warsaw University of Technology, Plock Campus, Poland

DOI: 10.1533/9780857097255.5.883

Abstract: This chapter discusses the applications of Process Integration methods to the design of energy systems, and water and wastewater systems, of beet sugar plants. Characteristic features of conventional sugar plants based on purification of raw beet juice and evaporating crystallisation are reviewed, the design of plant retrofit aimed at improvements in energy and water use is discussed, and case studies are presented. A concept of the sugar production process based on cooling crystallisation of raw beet juice is then outlined, and the design of an energy system and a water and wastewater system for a conceptual beet sugar plant employing the new process is discussed.

Key words: beet sugar plant, Process Integration, energy use in sugar production, water use in sugar production, retrofit design.

29.1 Introduction

In the 1980s and 1990s, the world output of sugar tended to exceed the demand, causing a surplus situation and low prices in the world sugar market so that investments in new sugar factories were rare. In the subsequent decade, however, world sugar stocks were gradually reduced, falling to their lowest level in 20 years in 2010–11. In view of steadily growing global demand for sugar, its price is expected to remain on a relatively high plateau over the coming years (OECD-FAO, 2011). Manufacturers tend, therefore, to increase the production volume, through new investments but mainly by retrofit of existing sugar factories, taking advantage also of advances in sugar technology and environment protection technologies.

A sugar factory retrofit typically includes improvements in the factory's energy system to decrease energy consumption, thus reducing the economic uncertainty associated with the increasing trend in fuel prices and cutting down emission charges. Apart from that, factory reconstruction measures aimed at reducing water consumption and wastewater discharge are often

© Woodhead Publishing Limited, 2013

required, to satisfy increasingly stringent environmental regulations and cut down discharge permission fees.

A retrofit strategy that is of particular interest to sugar factory operators involves reducing energy consumption by improving heat recovery, and reducing water consumption by optimal use of the throughput of existing wastewater treatment. This may create opportunities to increase the sugar output while avoiding costly investments in the utility systems. Several alternative designs with varying capital and operating costs are usually produced, and the final retrofit design is selected from these alternatives so as to balance the cost of investment against the value of the attainable reduction of the Operating Cost.

29.2 Sugar Production from Sugar Beet

In 2010, the world output of sugar was about 160 Mt, of which c.20% was produced from sugar beet (Bruhns *et al.*, 2012). Sugar beet is a renewable material which cannot be stored for a long period, and therefore processing is carried out seasonally in factories preferably located close to the beet growing areas.

A high water content in the raw material – about three-quarters of the material mass – is the cause of the high energy intensity of sugar production. In Table 29.1, an indicative material balance of a beet sugar factory is shown. In order to obtain crystalline sugar with a negligible water content, water

Table 29.1 Raw material and products in the material balance of a beet sugar factory

		Content (%)			Amount per 100 kg beet (kg)			
		Water	Sucrose	Non-sugars	Total	Water	Sucrose	Non-sugars
Raw material	Sugar beet				100.0	76.0	18.0	6.0
Products	Sugar	0	100	0	15.5	0	15.5	0
	Molasses	20	48	32	3.1	0.6	1.5	1.0
	Dried pulp	10	10	80	6.0	0.6	0.6	4.8
Remaining balance	Freshwater supplied			25.2	25.2			
	Sucrose lost			0.4			0.4	
	Waste sludge separated			0.2				0.2
	Water separated			100.0	100.0			

Source: Adapted from Bruhns and Lorenz (2006).

© Woodhead Publishing Limited, 2013

must be separated thermally with the minimum energy expenditure determined by its specific heat of evaporation – 2,258 kJ or 627 kWh/kg of water (at atmospheric pressure). Since the early days of industrial sugar production, rational energy use has been a major concern for sugar technologists, leading to the application of energy-saving technologies such as multi-stage evaporation and complex Heat Exchanger Networks (HENs) for heat recovery.

The sugar industry is a major water user and wastewater producer, mainly because large water streams are needed for hydraulic transport and cleaning of soil-contaminated raw material. A large beet sugar factory, processing 10,000 t of beet/d, may require 2,500–4,000 m^3 freshwater per day and discharge an even larger stream of wastewater that may also include water liberated from the beet processed. Water-saving measures, such as water reuse, regeneration and recycle, are therefore well known and widely applied in the sugar industry.

29.3 Identification of Opportunities to Improve Energy and Water Use in Sugar Plants

The sugar manufacturing process includes the following main stages:

1. Raw material pre-processing to remove foreign matter and facilitate sucrose drawing from vegetable tissue.
2. Disintegration of vegetable tissue and sucrose drawing in juice.
3. Juice purification to reduce its content of non-sugars.
4. Evaporation to remove excess water, thus concentrating the juice.
5. Crystallisation of sugar from concentrated juice.

The usual arrangement of energy flows in a beet sugar factory is shown in Fig. 29.1. Leaving aside pulp drying, with its separate energy flow, the energy system can be divided into four subsystems: power station, multi-stage evaporator, process heating subsystem including a HEN and water cooling circuit.

The operating principle of the power station is that of combined generation of heat and power in a steam cycle employing a boiler and a back-pressure turbine. Steam from the turbine exhaust is the hot utility supplied to the evaporator and, if necessary, to other pieces of process equipment.

In the evaporator subsystem, vapours and condensates are generated at various temperature levels, which correspond to the individual evaporation stages. Vapours and condensates are the carriers of medium temperature heat to be used in the process heating subsystem, which includes an extractor, a set of evaporating crystallisers and a HEN. Crystallisation vapours are the carriers of low temperature heat that can only partly be recovered (by

© Woodhead Publishing Limited, 2013

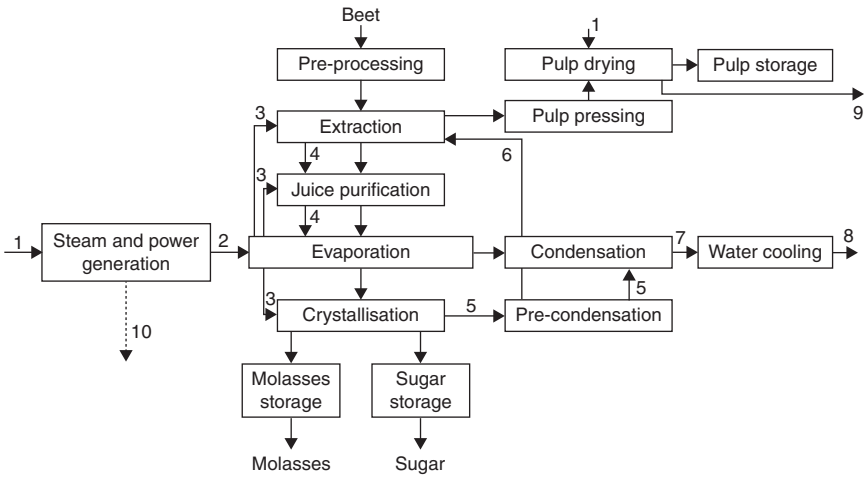

29.1 Scheme of material and energy flows in a beet sugar factory: 1 – fuel, 2 – steam, 3 – heating vapours, 4 – hot juice, 5 – vapours from crystallisation, 6 – hot water, 7 – cooling water from condensers, 8 – waste heat, 9 – drying gas discharge, 10 – power.

pre-condensation), while its remaining part is discharged to the cooling circuit where incoming vapours are condensed in a mixing condenser supplied with cooling water. Warm water from the condenser outlet is directed to cooling towers or cooling ponds that make heat dissipation to the environment possible; atmospheric air is the cold utility.

The cooling circuit is both a part of the energy system and a part of the water and wastewater system of the sugar factory. In direct contact between water and atmospheric air, some water is lost by evaporation but the loss is more than off-set by the inflow of condensing vapours and warm condensates, so that continuous draining of water from the cooling circuit is needed.

The water and wastewater system includes two more subsystems as schematically shown in Fig. 29.2:

- Main water and wastewater circuit, including hydraulic beet transport, beet washer and water-regeneration equipment.
- Water circuit in the power station and sugar manufacturing plant.

In the main circuit supplied with freshwater and water drained off from the cooling circuit, the soil-containing beet is removed by hydraulic transport from the reception area and delivered to the cleaning equipment. The clean beet is conveyed to the sugar manufacturing plant, while the soil in mixture with water flows to the regeneration equipment where contaminants

© Woodhead Publishing Limited, 2013

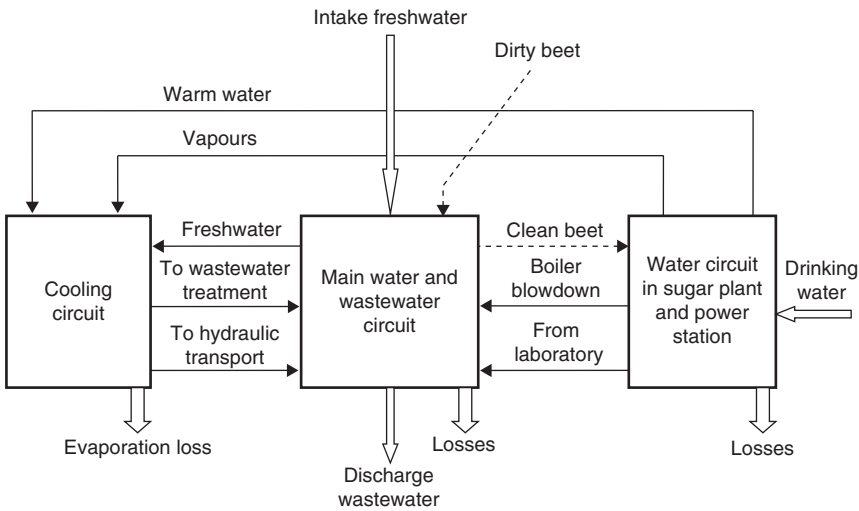

29.2 Subsystems of the water and wastewater system in a beet sugar factory.

are separated so that water can partially be recycled to the main circuit. The surplus of regenerated water is discharged from the main circuit to a receiving body, and the separated contaminants are discharged as sludge to a storage area.

The water circuit in the power station and sugar manufacturing plant is supplied mainly with a large stream of water contained in clean beet entering the manufacturing process. In this process, water is liberated from beet and transformed into vapours and warm condensates that are subsequently supplied to the cooling circuit. In addition, a small amount of wastewater is discharged to the main circuit, and a certain amount of water is carried away from the factory in by-products and waste sludge.

Although the links between water use and energy use in a sugar factory are obvious, all the major water-using and regeneration operations in the main circuit can be regarded as isothermal. It is therefore possible to consider water and energy problems separately, that is, to solve the energy minimisation problem first and then use the results as input data to the subsequent water minimisation.

29.4 Reduction of Energy Consumption

A wealth of knowledge has been acquired from numerous cases of energy system retrofit carried out in the European sugar industry. In the following subsections, experience from the applications of Heat Integration to sugar factory retrofit is summarised.

© Woodhead Publishing Limited, 2013

29.4.1 Problem Statement

In a typical problem of energy system retrofit in a beet sugar factory, given are parameters of the extraction, juice purification and sugar crystallisation processes, that is, a set of hot streams and a set of cold streams with their supply and target temperature, heat capacity flow rates and heat transfer coefficients are defined. Given also are data on:

- inlet and outlet conditions of the multi-stage evaporation process;
- existing process equipment units, including evaporators, heat exchangers and other heat receivers, as well as their connections;
- costs for additional heat transfer area in the evaporator and in the HEN;
- current use of utilities and availability of utilities (for heating and cooling).

The retrofit objective is to increase the energy system throughput to a predetermined value while minimising the total cost comprising investment and operating cost. Investments in the utility systems should be avoided, but in the evaporation subsystem changes in the evaporator structure including addition of new evaporator units can be considered. In the process heating subsystem, structural changes in the HEN and changes in the allocation of heating duties to individual exchangers and other heat receivers are allowed. However, changes in vapour flows extracted from evaporation to process heating should not lead to juice concentration at evaporator outlet being increased above a predetermined value.

Typical schemes of energy systems in beet sugar factories can be found elsewhere (van der Poel *et al*., 1998). In general, a system comprising 5–7 evaporation stages and 30–40 heat receivers is difficult to design, owing to many degrees of freedom in the design decision. However, the cost of evaporator retrofit is usually so high and local constraints (such as available space and access routes for new equipment units) are so stringent that acceptable structural options of the evaporator are few and rather easy to identify. The optimum option can be selected by exhaustive search employing targeting and evaluation of targeting results. As shown schematically in Fig. 29.3a, once the cost-effective retrofit concept has been selected, it becomes possible to redesign the evaporator and the process heating subsystem including HEN.

29.4.2 Energy Targeting and Retrofit design

As the established targeting approach is based on the assumption of fixed process conditions, it cannot properly reflect the energy improvement potential associated with interactions between evaporation and process

© Woodhead Publishing Limited, 2013

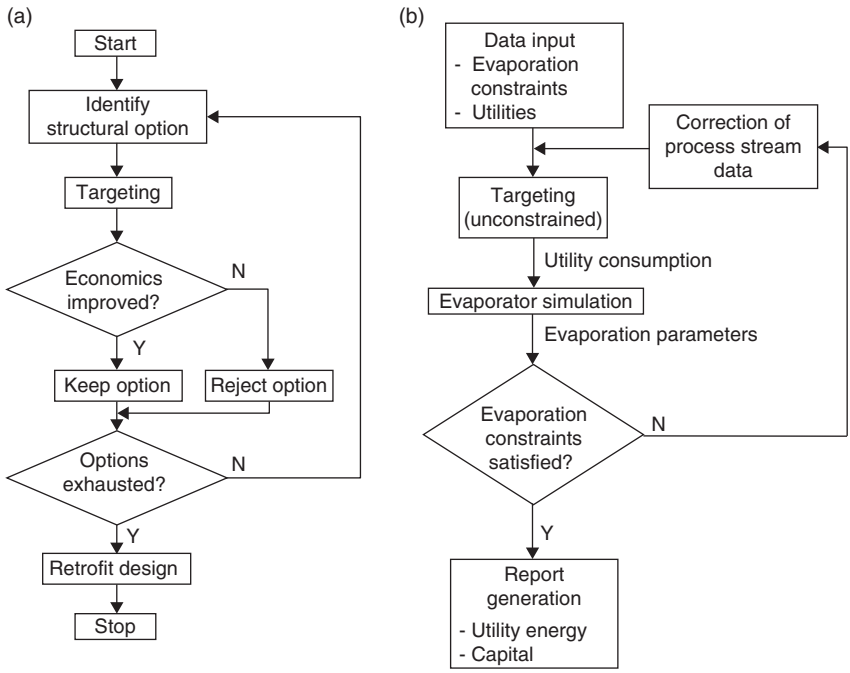

29.3 Block diagrams of the Retrofit design procedure (a) and its targeting step (b).

heating. To improve heat recovery in a sugar factory, it is necessary to modify vapour generation in the individual evaporation stages while adjusting allocation of vapours to various heating operations. Energy consumption and process changes need thus to be considered simultaneously, necessitating an extension of the established approach. In the procedure developed by Urbaniec *et al.* (2000), the thermal system is broken down into the evaporator and the process heating equipment. If targeting is restricted to the process excluding evaporation, then vapours generated in the evaporator – except last effect vapour – are regarded as utilities, while last stage vapour is regarded as a process stream. As a consequence, the results of restricted targeting include utility consumption, that is, flowrates of vapours extracted from the individual evaporator stages. These vapour flowrates has not to violate the constraints of evaporation capacities dependent on the heat transfer surfaces of the existing evaporator stages and total evaporation being not greater than the available water amount, determined by inlet and outlet values of juice concentration. One can establish whether or not the constraints are satisfied by simulating the evaporation process with the flowrates of the extracted vapours set equal to the values obtained by

© Woodhead Publishing Limited, 2013

targeting. If the process turns out to be not realisable, corrections should be introduced in the process streams.

The extended targeting problem, transformed into a problem of targeting under constraints, can be solved iteratively using a conventional targeting algorithm combined with an evaporator simulator, as schematically shown in Fig. 29.3b. Corrections of process stream data are usually limited to the flowrates of last stage vapour and condensate. Starting from initial flowrate values that are later changed depending on the results of the evaporator simulation, correct targets are typically obtained in a few steps.

Once the extended targeting problem has been solved, redesigning the evaporator is straightforward because evaporation loads in the individual stages are known and thus new evaporator units can be sized along with condensate tanks, piping, etc., providing also a starting point for the retrofit of the process heating subsystem. As the decisions on extractor and crystalliser heating have already been taken at the targeting stage, attention can now be focused on the HEN, for which the retrofit problem can be conveniently solved using one of the methods described in the literature. In the Network Pinch approach (Assante and Zhu, 1997), the design task is broken down into a search for topology changes, called the diagnosis stage, followed by an evaluation stage and a cost optimisation stage. Promising HEN modifications selected from the diagnosis stage are assessed in terms of their impacts on implementation cost (piping, foundation, etc.), operability and safety. Any options found to be impractical are removed and the remaining options are cost-optimised together with the existing HEN to give the final HEN retrofit design.

29.4.3 Case Study – Energy

The sugar factory to be retrofitted has a processing capacity of 4,800 t beet per day and the specific fuel consumption is about 3.40 kg oil equivalent (at 41 MJ/kg) per 100 kg beet. Extraction of sugar from sliced beet takes place in a trough-type extractor, which requires heating with vapour at a temperature not lower than 110°C. Juice evaporation is carried out in five Robert-type (natural circulation) evaporator units arranged in five stages, as schematically shown in Fig. 29.4a, and the final juice concentration is 66 kg/100 kg. Sugar is crystallised in three stages using batch-type, natural circulation evaporating crystallisers, which require heating with vapour at a temperature not lower than 120°C. Juice and syrup heating is carried out in a Heat Exchanger Network, which includes seven shell-and-tube and seven plate-type units.

The retrofit is primarily aimed at increasing the processing capacity to 7,000 t beet per day, and secondary aims are increased sugar yield, improved sugar quality and reduced specific energy consumption. In the

© Woodhead Publishing Limited, 2013

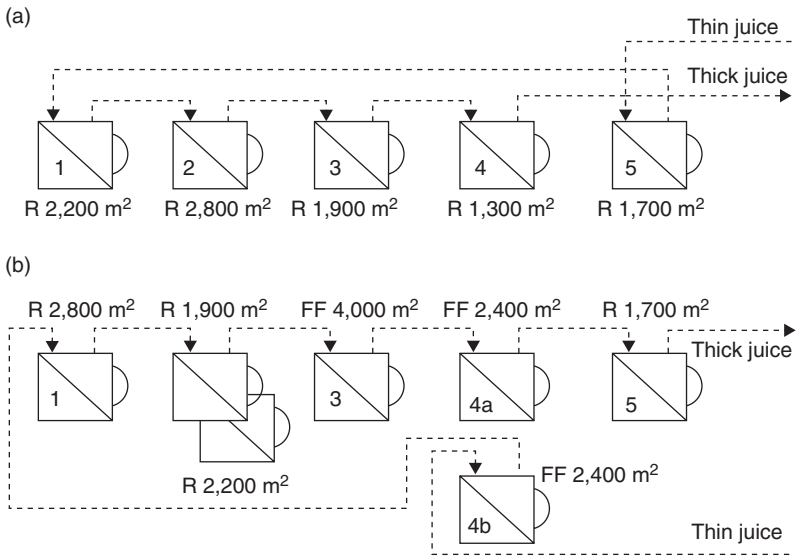

29.4 Evaporator schemes: (a) existing arrangement (processing capacity 4,800 t/d beet), (b) retrofit proposal (7,000 t/d beet). Juice flows are indicated by arrows, steam and vapour flows are omitted. Types of evaporator units: R – Robert, FF – falling film.

sugar manufacturing plant, debottlenecking, selective process changes and improved heat recovery are needed. By taking advantage of the capacity margin of the existing power station and improved energy efficiency of the sugar manufacturing plant, it should be possible to avoid power station extension.

To facilitate a reduction in the energy intensity, the concentration of juice supplied from evaporation to crystallisation will be increased to 70 kg/100 kg and the crystallisers will be reconstructed to make heating with vapour at 105–106°C possible. In order to satisfy the changed needs of the crystallisation section and eliminate a critical bottleneck, the evaporator should be extended. By properly combining the evaporator extension with the HEN retrofit, an improvement in heat recovery can be achieved, resulting in a reduced specific energy demand.

Three options for evaporator structure, listed below in order of increasing energy efficiency, are considered as acceptable with respect to the required space and estimated investment cost.

(a) Forward-feed, four-stage arrangement and crystalliser heating with 2nd vapour (least expensive option considered as a reference).
(b) Forward-feed, five stages and crystalliser heating with 3rd vapour.

© Woodhead Publishing Limited, 2013

(c) Five stages with backward-feed pre-evaporator in the 4th stage supplying vapour to crystalliser heating, and forward-feed arrangement of the remaining stages.

Regarding HEN retrofit, it is assumed that all the existing plate heat exchangers will remain in use. Shell-and-tube units can be replaced by new plate units, except for one or two HEN nodes in which the value of the Minimum Allowed Temperature Difference is less important.

For each of the three evaporator options, energy and capital targets that describe retrofit concepts for the entire energy system were determined using the procedure outlined above. A summary of targeting results obtained for ΔT_{min} = 2°C (optimum value corresponding to the minimum total cost) is given in Table 29.2. The most cost-effective reconstructed evaporator station (option c) includes four existing Robert-type units (heat transfer areas 2,800, 2,200, 1,900 and 1,700 m^2) and three new falling film units (heat transfer areas 4,000 m^2 and twice 2,400 m^2). The proposed evaporator arrangement is schematically shown in Fig. 29.4b.

Using evaporator simulation results that are a part of the solution of the extended targeting problem, process stream and utility data were extracted for the HEN retrofit problem. The optimally retrofitted network is represented as a Grid Diagram in Fig. 29.5. It should include seven existing and seven new plate heat exchangers, and an existing shell-and-tube unit. Of the existing plate units, one should have its heat transfer surface reduced, another one should be re-piped and three units should have their heat transfer surfaces extended. The combined heat transfer area of existing plate units, after adjustments, was estimated at 1,100 m^2, and that of the new units was 650 m^2. The duty of the existing shell-and-tube unit (300 m^2) should be changed.

The expected results of the sugar factory retrofit are summarised in Table 29.3. The reduction of specific fuel consumption is estimated at 29%, and makes it possible to increase the processing capability without extending the power station. The payback period of 3.5 years reflects the combined effect of increased sugar output and reduced specific energy consumption.

Table 29.2 Solutions of the extended targeting problem, three options of evaporator structure

Structural option	a	b	c
Number of evaporation stages	4	5	5*
Crystalliser heating from stage no.	2	3	4
Estimated cost, 10^3 USD/y			
Investment**	313	387	411
Energy	1,990	1,640	1,500
Total	2,303	2,027	1,911

* With pre-evaporation in the 4th stage; ** depreciation period 6 years.

© Woodhead Publishing Limited, 2013

Table 29.3 Expected results of sugar factory retrofit (oe – oil equivalent 41 MJ/kg)

Parameter, unit	Attained	Value proposed
Beet processing capacity, t/d	4,824	7,000
Material mass during 85 d of beet campaign		
beet processed, t	410,040	595,000
sugar produced, t	50,640	80,400
fuel consumed, toe	13,948	14,436
Specific fuel consumption, kg oe per 100 kg beet	3.40	2.43
Simple payback period, y	–	3.5

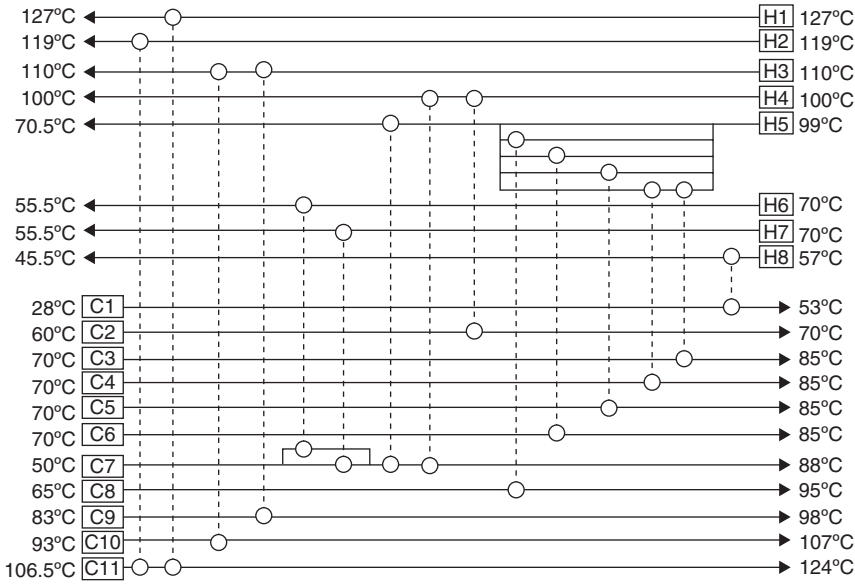

29.5 Grid Diagram representation of the retrofitted HEN. Hot streams H1–H4 represent vapours generated in stages 1–4 and H5 represents condensates collected from stages 2 to 5 of the evaporator. H6 to H8 represent water carrying low-temperature heat. Cold streams C1 to C11 represent process media arranged in the order of increasing target temperature.

29.5 Reduction of Water Consumption

Sugar industry has been quite successful in adapting to regulatory restrictions on freshwater use and wastewater discharge. In the following subsections, studies on the application of water targeting methods for the improvement of water and wastewater systems of sugar plants are summarised.

© Woodhead Publishing Limited, 2013

29.5.1 Problem Statement

The consumption of freshwater in the factory is determined by the functioning of the main water and wastewater circuit, schematically shown in Fig. 29.6, and its interaction with the other two circuits. (The flowrate values given in the scheme are expressed in kg per 100 kg beet, and thus are independent of the beet processing capacity of the factory.) The main circuit comprises the so-called fluming circuit, to which impurities are supplied during hydraulic transport of soil-containing beet. As the beet is delivered to the cleaning equipment, most soil remains in flume water that is subsequently regenerated by sedimentation in the settling tank. The sediments may be additionally treated in filter presses (not shown in the scheme); after that, wet beet soil is discharged from the factory.

A part of the stream of water regenerated in the settling tank is recycled to the beet washer and further to the fluming circuit, but another part is supplied for further regeneration to the wastewater treatment plant. The resulting deficit of flume water is compensated for by the intake of moderately contaminated water from the kiln-gas scrubber and the beet washer, and other components of the water and wastewater circuit ('other effluents' and 'condenser water' in Fig. 29.6).

The wastewater treatment plant makes it possible to regenerate contaminated water supplied from the fluming circuit and the cooling circuit while also satisfying requirements imposed on the quality of wastewater to be discharged from the factory. Following the degradation of contaminants and sludge separation, a part of the stream of regenerated water is recycled to the

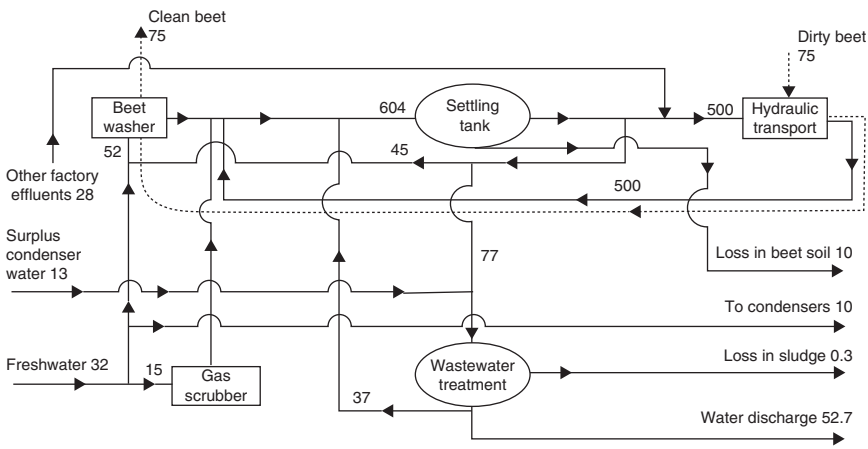

29.6 Simplified scheme of the main water and wastewater circuit (values of water flowrate given in kg/100 kg beet).

© Woodhead Publishing Limited, 2013

factory for reuse in the fluming circuit, and the remaining part is discharged as wastewater to a receiving body.

In a typical retrofit problem, a set of water-using and water-regeneration operations in the main circuit, and the parameters of each operation is given. Constraints may be imposed on changes in the circuit structure. Data are also given on:

- content of impurities in freshwater,
- soil content in beet,
- water content in sludges separated and removed from the circuit,
- allowable content of impurities in the regenerated water discharged from the circuit.

A possible retrofit objective is to minimise freshwater consumption by low-cost investments aimed at optimum use of the regeneration operations. Allowable structural changes in the circuit under consideration include closing pipe connections, or establishing new ones, between circuit components. Apart from that, water flowrates in feasible connections can be modified. A more advanced problem is to minimise the annual cost of water management comprising investment and operating costs, with less stringent structural constraints.

29.5.2 Water Targeting and Retrofit Design

Details of the structure of the main water and wastewater circuit may depend on the characteristics of sugar manufacturing process, and in particular its energy consumption. If the energy efficiency is not very high, necessitating the discharge of a large amount of waste heat from the cooling circuit to the atmosphere, then the vapour stream discharged from the sugar manufacturing plant to condensers in the cooling circuit is rather large, leading to a corresponding evaporation loss from the cooling towers. The loss must be compensated for by the supply of freshwater to be mixed with cooling water returned from the cooling towers to the condensers.

For a complete evaluation of the quality of water used in a sugar factory, about 15 contaminants including Suspended Matter (SM) and Chemical Oxygen Demand (COD) should be taken into account (Tomaszewska, 1998). It is, however, agreed that a quick evaluation can be based on the concentrations of SM and COD only. It is worth noting that if only one impurity is considered then its build-up and degradation can easily be analysed using graphical techniques, and the structure of the main water and wastewater circuit can be optimised by the inspection of feasible options. If more impurity components are considered, then the application of mathematical modelling and mathematical optimisation techniques becomes indispensable.

© Woodhead Publishing Limited, 2013

To evaluate the attainable reduction of water consumption, the Water Pinch approach can be used Wang and Smith (1994) and later extended by Kuo and Smith (1998) – see also Chapter 10. Prior to carrying out engineering calculations, it is necessary to describe the functioning of components of the main circuit by determining the values of indices expressing the build-up of impurities in water-using operations and the degradation of impurities in water-regeneration operations. By analysing the combined effect of all the operations at given impurity content in freshwater taken in and wastewater discharged, Water Pinch makes it possible to evaluate the water consumption at optimum utilisation of circuit components. Both circuit structure, that is, the set of connections between its sources and sinks, and the water flowrates in these connections can be optimised. Depending on the objective function, the results make it possible to identify opportunities to save water, or to reduce the annual cost of water management.

29.5.3 Case Study – Water

The main circuit presented above, operated in a sugar factory processing 10,000 t beet/d, should be retrofitted to minimise the consumption of freshwater. Restricting the attention to SM and COD as the only indices of contaminant concentration, the retrofit conditions for water management are summarised in Table 29.4.

The optimisation of water flowrates for minimum freshwater consumption was carried out using the regeneration–recycle option of the Water Pinch approach (Kuo and Smith, 1998). The values of design parameters given in Table 29.4, and the values of water flowrates given in Fig. 29.6, were used as input data.

Two sets of structural constraints were taken into consideration. At first, it was assumed that, similar to the existing system, recycled wastewater could only be used in the fluming circuit. Nevertheless, in the optimised scheme, with water flowrates within the circuit shown in Fig. 29.7, the regenerated wastewater is not recycled at all. The intake of freshwater is reduced to 20.3 kg per 100 kg beet.

As the second step aimed at a better understanding of the water-saving potential, the structural constraints were relaxed by assuming free use of recycled wastewater. This has led to a theoretically optimal but impracticable scheme in which recycled wastewater would be supplied to the beet washer and kiln-gas scrubber, and further to the fluming circuit. The intake of freshwater would then be reduced to 18.0 kg per 100 kg beet.

A summary of optimisation results including changes in the system structure, and a comparison between the initial and optimal values of key water flowrates, are shown in Table 29.5. As can be seen, in both cases of modification of the water and wastewater circuit the water consumption can be

© Woodhead Publishing Limited, 2013

Table 29.4 Operating parameters of the water and wastewater system in a sugar factory

Concentration of contaminants in freshwater, ppm	
SM	65
COD	130
Soil content in beet, %	8
Share of soil amount transferred to water, %	
In fluming circuit	0.90
In beet washer	0.10
Concentration of contaminants in surplus condenser water, ppm	
SM	100
COD	200
Concentration of contaminants in other factory effluents, ppm	
SM	100
COD	200
Ratio of contaminant reduction in the settling tank	
SM	0.98
COD	0.095
Water content in sludge removed, %	
From settling tank	80
From wastewater treatment plant	50
Allowable concentration of contaminants in water discharged, ppm	
SM	30
COD	80

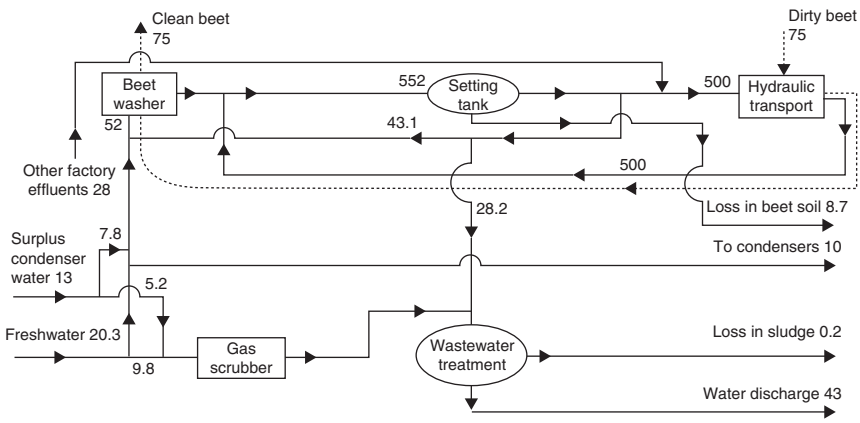

29.7 Simplified scheme of the main water and wastewater circuit optimised for minimum consumption of freshwater (values of water flowrate given in kg/100 kg beet).

reduced (37% and 44% relative to the existing system). Apparently, the structural constraint forbidding the recycle of regenerated wastewater is not critical because, by relaxing it, only a small improvement in freshwater consumption is obtained. The main point is that a significant water saving can

© Woodhead Publishing Limited, 2013

Table 29.5 Results of water minimisation

Source	Sink	Water flow, kg per 100 kg beet		
		Reference (existing system)	Recycle of regenerated water to system parts outside fluming circuit	
			No	Yes
Freshwater supply		32	20.3	18
Beet washer	Settling tank	52	52	52
Gas scrubber	Settling tank	15	≠	≠
Gas scrubber	Wastewater treatment	≠15	14	
Hydraulic transport	Settling tank	500	500	506
Settling tank	Beet washer	45	43.1	41
Settling tank	Hydraulic transport	472	472	465
Settling tank	Wastewater treatment	77	28.2	43.3
Surplus condenser water	Wastewater treatment	13	≠	≠
Surplus condenser water	Beet washer	≠	7.8	≠
Surplus condenser water	Gas scrubber	≠	5.2	≠
Wastewater treatment	Settling tank	37	≠	≠
Wastewater treatment	Beet washer	≠	≠	10
Wastewater treatment	Gas scrubber	≠	≠	7
	Water discharge	52.7	43	39.8

≠ denotes no connection between source and sink.

be achieved at nearly unchanged water flowrates through the settling tank and wastewater treatment plant. This implies that the performance of the water and wastewater circuit could be improved through low-cost investments restricted to new piping connections thus avoiding changes in the existing water-regeneration equipment.

29.6 Energy and Water Use in Sugar Production Directly from Raw Beet Juice

Apart from the conventional beet sugar technology, proposals for alternative sugar manufacturing processes are known. In this context, the role of Process Integration is to enable the optimisation of new processes with respect to energy and water use.

© Woodhead Publishing Limited, 2013

29.6.1 Background

An alternative concept of the sugar manufacturing process, based on evaporation of raw beet juice and subsequent cooling crystallisation of sugar from concentrated raw juice, has been developed and tested by Italian researchers (Vaccari *et al*., 2005a). Contrary to conventional sugar manufacturing, it does not include calco-carbonic juice purification, and evaporating crystallisation of sugar from concentrated juice is replaced by cooling crystallisation. The alternative process can therefore be simpler, more environment-friendly and less energy intensive than the conventional one (Vaccari *et al*., 2005b). Such features make it suitable for applications in small factories (processing capacity in the order of 1,000 t beet/d) located close to beet growing areas. By reducing the beet transportation radius, thus decreasing the cost of beet supply, small sugar plants based on the alternative process potentially gain further competitive advantage over large plants (processing capacity in the order of 10,000 t beet/d), which dominate the picture of the contemporary beet sugar industry.

A simplified Process Flowsheet is shown in Fig. 29.8. Cleaned and sliced beet is supplied to a trough extractor, where raw juice is produced. Maximum temperature in the extractor is 76–78°C, but it requires heating with steam at saturation temperatures above 100°C. The concentration of solids in raw juice is about 15 kg/100 kg, and the juice temperature at extractor outlet is about 30°C. The juice is then screened to remove beet particles, heated up to 70°C, micro-filtered to remove high-molecular impurities and softened in an ion-exchange station.

Further processing takes place in a backward-feed (counter-current), multi-stage evaporator in which temperatures in the consecutive stages increase in the direction of juice flow. The temperature of 80–85°C required for the subsequent crystallisation step is attained at the evaporator outlet, where the juice concentration is about 70 kg/100 kg. After mixing with sugar recycled from the crystallisation subsystem, the juice attains a solids concentration of 74 kg/100 kg, which is increased in an additional evaporator body to its final value of about 86 kg/100 kg. These concentration values should be regarded as constraints imposed on the evaporation process.

The concentrated raw juice is mixed with seed crystals and supplied to the first cooling crystalliser. The temperature is slowly decreased to about 40°C, causing sugar crystals to grow. By centrifuging the crystal slurry at the crystalliser outlet, white sugar is separated from the first run-off syrup. Two more crystallisation stages provide lower grade sugars that are recycled, while molasses is discharged from the last stage.

The energy demand and water demand of the alternative process were preliminarily studied for a sugar plant with the processing capability of 1,000 t beet/d. Process Integration is a family of tools well suited for studies

© Woodhead Publishing Limited, 2013

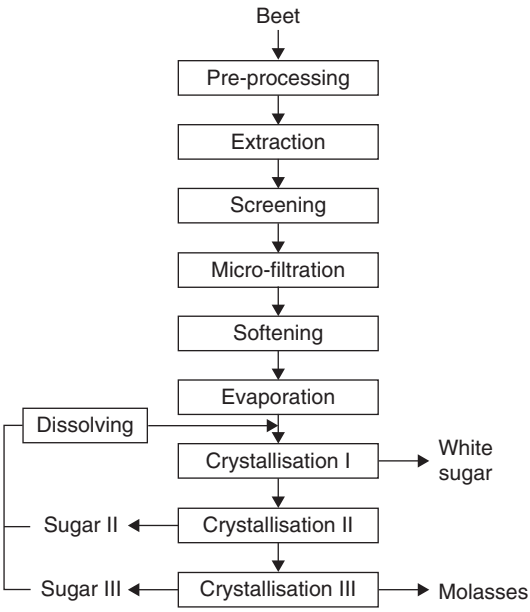

29.8 Simplified flowsheet of the alternative sugar manufacturing process.

carried out prior to the detailed plant design, that is, when a set of possible engineering solutions needs to be quickly screened to identify the most promising ones that deserve in-depth evaluation.

29.6.2 Energy Use

Heat in 1.2 bar steam generated in the power station is supplied to the extraction and evaporation, as schematically shown in Fig. 29.9. Vapour and hot condensate generated in the evaporator, as well as other hot process streams, are the carriers of heat that can partly be recovered in a Heat Exchanger Network. Excess vapour is condensed, and waste heat is transferred to cooling water and subsequently discharged from the process via cooling towers installed in the water circuit, to the atmospheric air.

The energy flow in steam supplied to evaporation is transformed into multiple energy flows in vapours and condensates that leave the evaporation. As raw juice must be evaporated in the temperature range 40–85°C, low temperatures of vapours and condensates limit the possibilities of heat recovery. Considerable energy-saving potential can, however, be found in the evaporator scheme and the use of vapour recompression. The scheme shown in Fig. 29.9 includes a backward-feed, four-stage evaporator for combined concentration of raw juice (in four bodies) and syrups supplied to

© Woodhead Publishing Limited, 2013

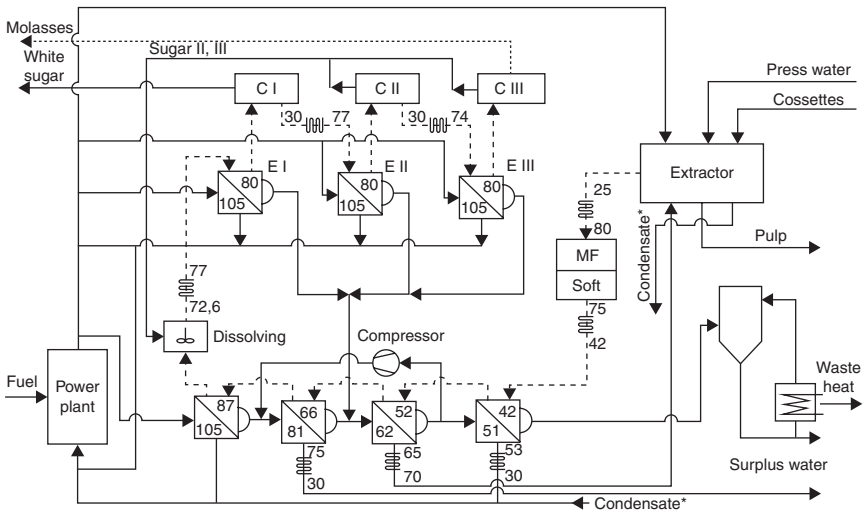

29.9 Example of thermal scheme of a sugar factory employing the alternative process. Thick lines – steam or vapour connections; MF – microfiltration; Soft – softening; E I, E II, E III – evaporator bodies for concentration of syrups; C I, C II, C III – crystallisers. Symbolic coils indicate heating or cooling requirements (not indicated: crystalliser cooling). Temperature values are given in °C.

crystallisation (in three more bodies connected with the first stage), and a compressor that raises the pressure of third vapour to that of first vapour.

In the following, it is assumed that the power station is fuelled with natural gas, which makes it possible to choose between various options of Combined Heat and Power generation. Commonly used in the sugar industry is a steam cycle, that includes a boiler supplying steam to a back-pressure turbine coupled with an electric generator and, from the turbine exhaust, to the process. In order to increase the flexibility of the power station with respect to the ratio of power to heat supplied, a part of the flow of boiler steam can bypass the turbine via a throttling valve, as indicated by asterisk in Fig. 29.10a. A low-investment power station for a small factory would include a boiler operated at steam parameters 25 bar and 400°C, and a turbine operated at a back-pressure of 1.2 bar.

Another possible solution of the power station is one based on a gas turbine. Its advantage is that for equal amount of heat supplied, it can generate more power than the pure steam cycle. The gas turbine drives an electric generator, and the exhaust gas at about 500°C flows to a heat recovery boiler, which supplies saturated steam at 1.2 bar (105°C) to the process. In order to increase the flexibility of the power station with respect to the ratio of power to heat generated, the boiler can be equipped with additional firing as indicated by asterisk in Fig. 29.10b.

© Woodhead Publishing Limited, 2013

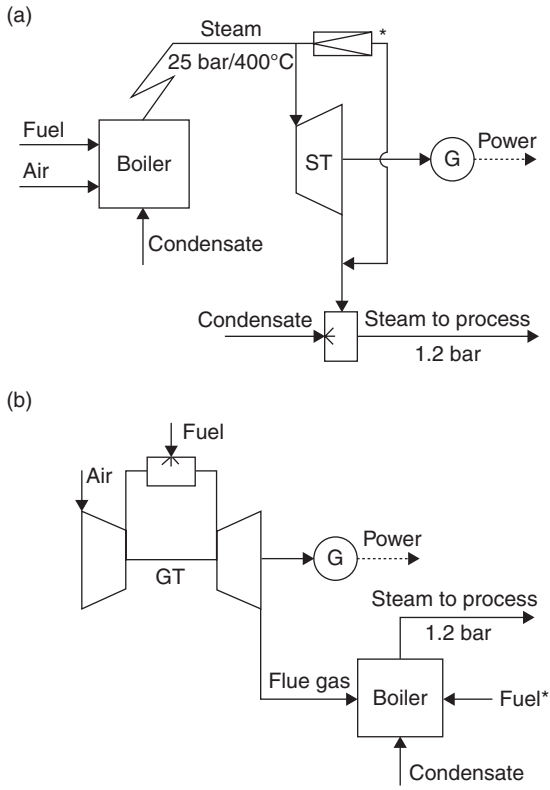

29.10 Options of the power station: (a) steam cycle, (b) gas turbine cycle. ST – steam turbine; G – power generator; GT – gas turbine.

Ideally, while supplying the necessary steam flow to the process, the power station should generate as much power as is needed for driving factory equipment, including possibly a vapour compressor (no power export or import). As the power consumed by the compressor drive depends on the vapour flowrate, this is a constraint to be observed when optimising vapour flowrates in the evaporation subsystem. The required value of juice concentration at the evaporator outlet (70 kg/100 kg, see Section 29.6.1) is reflected by another constraint. For any evaporator scheme which may include a vapour recompression circuit, process-to-process heat recovery in the HEN should be maximised. The constraints mentioned above can be regarded as a system of equations in several unknown variables, their number depending on the evaporator scheme. By calculating the values of unknown variables, vapour flowrates in the evaporation subsystem are determined and, together with the resulting condensate flowrates, are included in the set of process data on which targeting is based.

© Woodhead Publishing Limited, 2013

Table 29.6 Sugar factory data assumed for the energy studies

Processing capacity	1,000 t beet/d
Power consumption excl. vapour compressor	
Specific	18.5 kWh/t beet
Total	771 kW
Fuel	Natural gas
Efficiency values	
Vapour compressor, internal	0.70
Vapour compressor, mechanical	0.95
Steam boiler	0.94
Steam turbine	0.695
Gas turbine	0.208
Heat recovery boiler	0.80

The targeting procedure to be adopted for the novel process is similar to that developed for the conventional process and described in Section 29.4.2. It is started with process stream data that include estimated flowrate values. Targeting results are subsequently introduced as coefficients into the equation system reflecting juice concentration and power generation constraints. After solving the equation system, it becomes possible to improve the initial estimates. Usually, two or three iterative steps are sufficient to arrive at a solution determining hot utility consumption, which can be recalculated as fuel consumption.

Using the approach explained above, minimum energy consumption was analysed for a white sugar factory processing 1,000 t beet/t. Factory data including characteristic indices of two types of power station equipment are given in Table 29.6. Regarding the thermal system, the use of plate-type evaporator bodies and plate heat exchangers of known heat transfer characteristics was assumed. Evaporator schemes featuring three, four and five stages, optionally including a vapour recompression circuit, were considered. In Fig. 29.11, sample Composite Curves are shown for the process featuring four-stage evaporation with vapour recompression over stages 2 and 3, at Minimum Allowed Temperature Difference in the HEN $T_{min} = 5°C$. (Being predetermined by process requirements, the heat supply to extraction is constant and therefore not represented in the Composite Curves.)

Restricting the attention to a specific power station type, for each evaporator scheme and a definite temperature distribution between individual evaporation stages as well as a specific value of T_{min} in the HEN, targeting generates unique values of:

- minimum consumption of hot utility,
- if applicable, power consumption in the vapour compressor,
- total heat transfer area in the evaporator,
- total heat transfer area in the HEN.

© Woodhead Publishing Limited, 2013

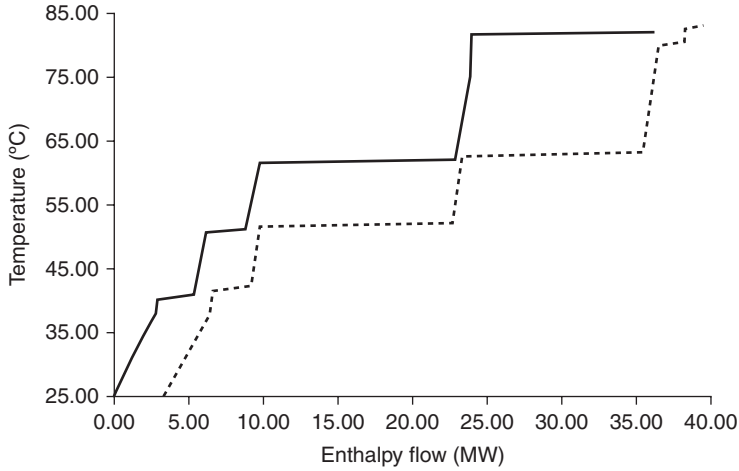

29.11 Composite Curves for the alternative process including four-stage evaporation with vapour compression (factory processing 1,000 t/d beet, Minimum Temperature Difference 5°C).

This makes it possible to calculate the combined heat transfer area of the evaporator bodies and heat exchangers, and the total energy input including hot utility and compression power. After investigating all the evaporator options and sufficiently many versions of realistic temperature distribution, Pareto-optimal options of the thermal system can be identified as ones characterised by both small heat transfer area and low energy consumption, and from them the most suitable option can be selected.

By carrying out the selection procedure for the two power station types under consideration, two suitable options of the energy system (i.e., power station together with the thermal system) can be pointed out and compared with each other, as shown in Table 29.7. Option 1, featuring a gas turbine based power station and evaporator with vapour recompression, is the most energy-efficient and has the advantage of smallest heat transfer area. However, as it includes a large and very costly compressor, the steam turbine based power station featuring an evaporator with vapour recompression (option 2) is also an interesting alternative. It is more energy intensive and the necessary heat transfer area is larger, but its compressor is smaller and less costly than that needed for option 1.

29.6.3 Water Use

The water and wastewater system under consideration, and its subsystems are schematically shown in Fig. 29.12. The over-all operating principle is

© Woodhead Publishing Limited, 2013

Table 29.7 Comparison of two optimised options of the energy system

Option		Heat transfer area (m^2)			Compressor power demand (kW)	Specific energy demand (kWh/t beet)
		Total	Evaporator	Heat exchangers		
1	Gas turbine	1,520	1,080	440	1,380	145
2	Steam turbine	1,900	1,190	715	500	194

Note: Vapour compression included in both options.

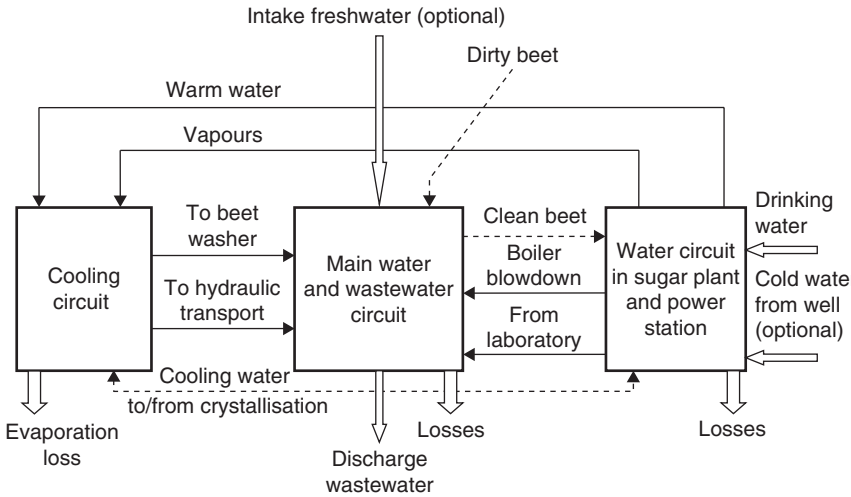

29.12 Subsystems of the water and wastewater system in a sugar factory employing the alternative process.

similar to that of the water and wastewater systems applied in conventional sugar manufacturing and discussed in Section 29.3.

The differences relative to the corresponding system of a conventional sugar factory can be found mainly in the water circuit of the sugar manufacturing plant and the power station. While sugar crystallisation in the conventional process is essentially carried out by evaporating water from supersaturated syrups (massecuites) at about 80°C, the novel process employs massecuite cooling only (from about 80°C to about 30°C). The crystallisers must therefore be continuously supplied with cooling water at a temperature not higher than 20°C. Water returned from crystallisers is brought back to cooling towers in the barometric circuit, where its temperature should be decreased below 20°C. If this condition cannot be satisfied,

© Woodhead Publishing Limited, 2013

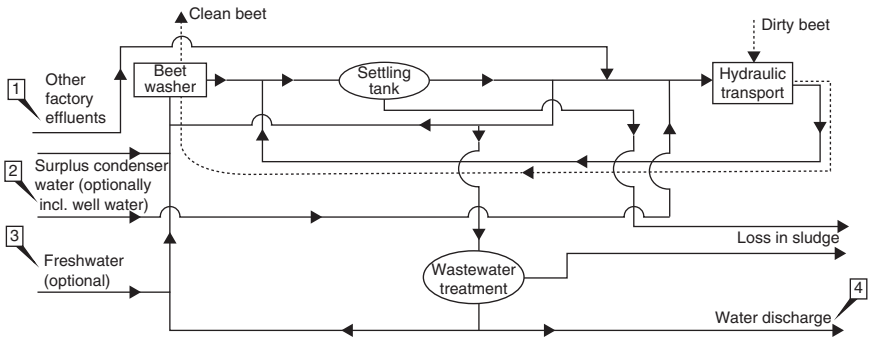

29.13 Scheme of the main water and wastewater circuit. 1 – from the circuit in the sugar plant and power station, 2 – from the barometric circuit, 3 – from an external source, 4 – to a recipient.

then it is necessary to provide an additional stream of cold water from an external source – for example, a well – to the massecuite cooling.

As regards the barometric circuit and the main circuit, their functions are identical to those of the corresponding circuits in a conventional sugar factory. In the main circuit, schematically shown in Fig. 29.13, the key water-using operation is the hydraulic transport (fluming) of dirty beet from the storage to the sugar manufacturing plant. At known operating conditions (soil content in incoming beet, allowable concentration of contaminants in regenerated wastewater, etc.), the structure of the connections between the operations of water use and water-regeneration, together with the associated water flowrates, can be optimised for minimum water consumption.

The results of energy studies on the alternative process reviewed in Section 29.6.1 indicate that water liberated from beet in the sugar manufacturing plant can be partly recycled to the process, but the rest must be discharged, either as surplus condensate loaded with Volatile Organic Compounds (VOC), or as vapour to be condensed in the barometric circuit. The resulting flowrate of water to be subsequently discharged to the main water and wastewater circuit correlates with energy consumption in the sugar manufacturing plant.

Another conclusion to be drawn from the energy studies is that the choice of energy system for a sugar factory employing the alternative process cannot be based on energy efficiency alone, as the investment costs of different system options are widely different. Depending on factory location and economic parameters, various options of the energy system will be applied, and therefore water consumption is studied by considering a set of cases of different energy consumption.

As regards the subsystems of the water and wastewater system, the attention can be restricted to the main water and wastewater circuit. Using the

© Woodhead Publishing Limited, 2013

approach described in Section 29.5, its operating conditions are summarised in Table 29.8. The flowrates of water leaving the circuit in sugar manufacturing plant and power station, and the barometric circuit, can be determined from the mass and energy balance of the factory. From the energy studies discussed in Section 29.6.2, the balance data are available for a set of energy system options with differentiated energy efficiency. In the following, two options are considered: (1) power station based on a steam turbine, evaporator station with vapour recompression; energy consumption is comparable with that of an advanced conventional sugar factory; (2) power station based on gas turbine, evaporator station with vapour recompression; energy consumption is lower than that attainable in conventional sugar factories.

The possibility of an energy system being operated at weather conditions that affect the temperature of cooling water returned from cooling towers is taken into account by varying it between 20°C and 30°C. At 20°C it is possible to carry out sugar crystallisation using only water circulated in the cooling circuit. At higher temperatures it is necessary to supply well-water (assumed temperature 5°C) to the low temperature sections of crystallisers. 10 kg of well-water per 100 kg is needed when the temperature of cooling water reaches 30°C; higher temperatures are unlikely in the European climate and therefore are not considered.

The operating conditions summarised in Table 29.8, together with the water flowrates determined from mass and energy balances of the sugar manufacturing plant, constitute the main part of data needed for the optimisation of water use in the main water and wastewater circuit using Water Pinch. In order to solve the minimisation problem for a specific set of input data, it is necessary to define the allowable structures of the circuit under consideration and to specify a starting point for the numerical search procedure. This is achieved by specifying the circuit components and the constraints imposed on their connections, and setting up a feasible (non-optimal) water balance. Assuming the circuit includes the components shown in Fig. 29.13, sample constraints and associated data on water-using operations (corresponding to energy system option A and cooling water temperature of 30°C) are given in Table 29.9.

The results of water minimisation obtained for the data specified above are shown in Fig. 29.14. The intake of freshwater to the main water and wastewater circuit is zero, meaning that the combined flowrate of water discharged from the barometric circuit, and the circuit in the sugar manufacturing plant and the power station, are sufficiently large to satisfy the needs of the main circuit.

A summary of results obtained for two energy system options at cooling water temperature ranging from 20°C to 30°C is given in Table 29.10. As can be seen, in both cases the intake of freshwater can be avoided, implying that in steady state it is possible to operate the entire water and wastewater

© Woodhead Publishing Limited, 2013

Table 29.8 Operating parameters of the water and wastewater system in a sugar factory

Concentration of contaminants in freshwater, ppm	
SM	30
COD	30
Concentration of contaminants in surplus condenser water and other factory effluents, ppm	
SM	100
COD	200
Soil content in beet, %	8
Share of soil transferred to water	
In hydraulic transport	0.90
In beet washer	0.10
Ratio of contaminant reduction in the settling tank	
SM	0.86
COD	0.08
Water content in sludge removed, %	
From settling tank	80
From wastewater treatment	40
Allowable concentration of contaminants in regenerated wastewater, ppm	
SM	50
COD	150

Table 29.9 Example of structural constraints and data on water-using operations

Source	Sink	Connection
Freshwater	Beet washer	Possible
Settling tank	Wastewater treatment	Possible
Settling tank	Discharge	Forbidden
Wastewater treatment	Hydraulic transport	Forbidden
Wastewater treatment	Discharge	Possible
Beet washer	Hydraulic transport	Forbidden
Beet washer	Discharge	Forbidden
Hydraulic transport	Discharge	Forbidden
Hydraulic transport	Beet washer	Forbidden
Other factory effluents	Hydraulic transport	Possible

Operation	Limiting flow (kg/100 kg beet)	SM at inlet (ppm)	SM at outlet (ppm)	COD at inlet (ppm)	COD at outlet (ppm)
Beet washing	157	975	6,058	1,890	3,138
Hydraulic transport	689	1,475	11,925	2,821	3,139

Other data: flow of surplus condenser water to the main circuit 22 kg/100 kg beet, this including well-water 10 kg/100 kg beet.

© Woodhead Publishing Limited, 2013

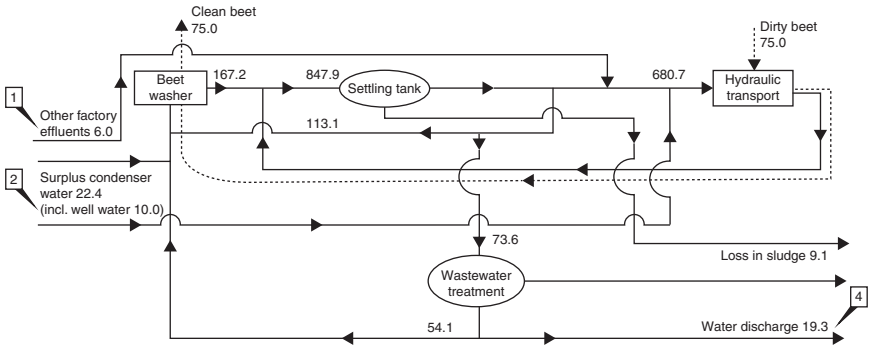

29.14 Optimum water flowrates (kg/100 kg beet) in the main water and wastewater circuit operated at parameters specified in Table 29.8 (Option B) of the energy system, cooling water temperature 30°C. The factory is supplied with well-water at a temperature of 5°C only. 1 – from the circuit in the sugar plant and power station, 2 – from the barometric circuit, 4 – to a recipient.

system using only water liberated from the beet. Actually, a certain amount of freshwater may be needed at the factory start-up, when it is necessary to operate beet fluming and washing, and initiate to extraction while still waiting for beet juice to be supplied to evaporation.

29.7 Future Trends

Using the established sugar production process, about 60% of the beet mass entering the process is directly disposed of mainly as wastewater or evaporated water. About 14% is transformed into final product (sugar), about 4% to sugar-containing co-product (molasses), and the rest to fibrous co-product – pressed pulp. In the subsequent upgrading of by-products, there are different options with varying associated added value, ranging from fertilisers and compost, energy recovery (biogas, bioethanol, or beet pulp directly used as fuel), animal feed (feed yeast grown on molasses, pressed pulp, dried pulp), to high-added value biochemicals and ingredients for human diet (bakery yeast, citric acid, dietary sweeteners, dietary fibre).

A trend, gaining in importance over recent decades, is to deviate from the established process route by using a part of the stream of sucrose-containing juice for direct processing to biofuels – mainly bioethanol. Practised today in numerous cane sugar factories of South America and some beet sugar factories of Europe, bioethanol production is expected to expand because large-scale use of ethanol as a transportation fuel already is a reality in a number of countries, and has been planned for coming years in the USA and EU. Apart from that, a new situation has been created in the European sugar

© Woodhead Publishing Limited, 2013

Table 29.10 Results of water minimisation for two options of the energy system and cooling water temperatures between 20°C and 30°C

Input information			Results					
Energy-system option	Cooling water temperature (°C)	Surplus from barom. circuit	Intake freshwater	To fluming	To beet washing	To settling tank	To treatment	Discharge
A) Steam turbine and vapour compression (steam 26.4 kg/100 kg b)	30.0	27.6	0	719	150	870	74.3	23.7
	26.6	24.1	0	720	171	890	74.4	19.9
	23.3	21.1	0	720	208	928	74.4	16.5
	20.0	18.0	0	708	200	909	70.0	13.7
B) Gas turbine and vapour compression (steam 15.1 kg/100 kg b)	30.0	22.4	0	680	167	848	73.6	19.3
	26.6	18.6	0	708	200	909	71.0	14.2
	23.3	15.7	0	709	198	907	70.9	11.4
	20.0	12.7	0	733	201	918	73.3	8.8

Flowrates in kg per 100 kg beet (constant flowrates not shown in the table: inflow from the circuit in sugar plant and power station 6.0; loss in sludges 9.1).

© Woodhead Publishing Limited, 2013

sector that, until recently, has been protected by price regulation and custom barriers making it uneconomic to import cane sugar produced in other continents. Over the period 2005–14 the European Commission has been be implementing a market reform aimed at the reduction of sugar price, admission of sugar imported mainly from least developed countries, and restructuring of the European sectors of sugar beet growing and processing for improved competitiveness in a global environment. Accordingly, beet sugar manufacturers are cutting down their costs by concentrating production to larger factories and seeking sources of additional income through investments in new equipment and new production lines. In the period 2005–11, the number of sugar factories in the EU dropped from 213 to 106, while the average beet processing capacity was increased from c.7000 to 8300 t/d and the number of beet ethanol plants reached 21 (CEFS, 2011).

The expansion of co-product upgrading, production of bioethanol and, in the long run also, production of other biofuels such as biobutanol and biohydrogen is accompanied by the need to adapt to increasingly stringent environmental regulations (CEFS/CIBE, 2010). In the foreseeable future, this will stimulate demand for efficient engineering tools to optimise the use of energy and water in the beet sugar industry. Sugar plants that are interconnected with other production facilities such as ethanol distilleries, and/or provide heating for surrounding civic settlements, can be regarded as industrial clusters. The potential for energy-saving measures and reduction of CO_2 emissions in such clusters can be evaluated using Total Site Methodology (Dhole and Linnhoff, 1993) extended by (Klemeš *et al*., 1997).

29.8 Sources of Further Information and Advice

The reliability of engineering calculations relating to energy and water use in sugar factories depends on the availability of data on physicochemical properties of raw materials, intermediates and products or coproducts. These can be found in books published in recent decades, including Baloh and Wittwer (1995) and Bubnik *et al*. (1995). As a source of more material data, but mainly as a handbook for quick reference on various aspects of beet sugar manufacturing including energy and water use, one can mention van der Poel, Schiweck and Schwartz (1998). Books devoted to beet sugar manufacturing in general were published by Bia (1992) and more recently by Asadi (2008), and with focus on energy use by Urbaniec (1989) and later by Baloh (1991).

As a general reference on process design and Process Integration, Smith (2005) can be mentioned. Discussions on Process Integration in the broader context of sustainability issues are presented by Klemeš *et al*. (2010) and next year by El-Halwagi (2011). A book edited by Waldron (2007) deals with energy, waste and wastewater aspects. Another book, edited by Klemeš, Smith and Kim (2008), is focused on energy and water management in food

© Woodhead Publishing Limited, 2013

processing and includes a chapter (Urbaniec and Klemeš, 2008) on energy and water in sugar manufacture. Urbaniec, Zalewski and Klemeš (2000) presented applications of Process Integration methods to energy use, and Urbaniec and Wernik (2002) to water use, in sugar factories.

The EU-funded project, TOSSIE, has been carried out in the period 2006–08 to review prospects of improving the beet sugar manufacturing technology and reducing the environmental impact of sugar factories in Europe. The results of project work are reviewed by Bruhns *et al*. (2010). Comprehensive guides for energy and water saving are in the Best Available Techniques Reference Document (BREF) in the Food, Drink, and Milk Industries (Institute for Prospective Technological Studies, 2006).

29.9 References

Asadi, M. (2007). *Beet-Sugar Handbook.* Wiley, Hoboken, USA.

Assante, N. D. K., Zhu, X. X. (1997). An automated and interactive approach for heat exchanger retrofit. *Trans IChemE,* **75**, 349–360.

Baloh, T. (1991). *Energy Economy in the Sugar Industry (in German).* Bartens, Berlin, Germany.

Baloh, T., Wittwer, E. (1995). *Energy Manual for Sugar Factories.* Bartens, Berlin, Germany.

Bia, O. (1992). *Technology and Equipment of the Sugar Industry* (in Italian). Eridania Béghin Say, Genoa, Italy.

Bruhns, J., Baron, O., Maier, K. (eds) (2012). *Sugar Economy Europe 2012.* Berlin, Germany, Bartens.

Bruhns, M., Lorenz, F. (2006). Rational energy use in sugar-industry processes – efficiency increase through process integration (in German). *VDI Berichte Fortschrittliche Energiewandlung und–anwendung*, N1924.

Bruhns, M., Glavič, P., Jensen, A. S., Narodoslawsky, M., Pezzi, G., Urbaniec, K., Vaccari, G. (2010). Research for a sustainable European sugar sector. *Sugar Industry/Zuckerindustrie,* **135**, 487–495.

Bubnik, Z., Kadlec, P., Urban, D., Bruhns, M. (1995). *Sugar Technologists Manual.* Bartens, Berlin, Germany.

CEFS. (2011). Sugar Statistics 2011. Available from: www.cefs.org (accessed 5 March 2012).

CEFS/CIBE. (2010). *The EU Beet and Sugar Sector: A Model of Environmental Sustainability.* Available from: www.cefs.org (accessed 5 March 2012).

Dhole, V. R., Linnhoff, B. (1993). Total site targets for fuel, co-generation, emissions, and cooling. *Computers & Chemical Engineering*, **17**, S101–S109.

El-Halwagi, M. M. (2011). *Sustainable Design Through Process Integration: Fundamentals and Applications to Industrial Pollution Prevention, Resource Conservation, and Profitability Enhancement.* Butterworth-Heinemann, Waltham, USA.

Institute for Prospective Technological Studies, European Commission, Joint Research Centre. (2006). *Integrated Pollution Prevention and Control Reference*

© Woodhead Publishing Limited, 2013

Document on Best Available Techniques in the Food, Drink and Milk Industries. <eippcb.jrc.es/reference/fdm.html> (accessed 3 March 2012).

Klemeš, J., Dhole, V. R., Raissi, K., Perry, S. J., Puigjaner, L. (1997). Targeting and design methodology for reduction of fuel, power and CO_2 on total sites. *Applied Thermal Engineering*, **17**, 993–1003.

Klemeš, J., Friedler, F., Bulatov, I., Varbanov, P. (2010). *Sustainability in the Process Industry: Integration and Optimisation.* McGraw-Hill, New York, USA.

Klemeš, J., Smith, R., Kim, J.-K. (eds) (2008). *Handbook of Water and Energy Management in Food Processing.* Woodhead Publishing, Cambridge, UK.

Kuo, W. C. J., Smith, R. (1998). Designing for the interactions between water use and effluent treatment. *Trans IChemE,* **76**(part A), 287–301.

OECD-FAO. (2011). *Agricultural Outlook 2011–2020, Chapter 6 Sugar*. <www.oecd.org/dataoecd/2/37/48184295.pdf> (accessed 14 February 2012).

Smith, R. (2005). *Chemical Process Design and Integration.* John Wiley & Sons, Chichester, UK.

Tomaszewska, A. (1998). *Environment-friendly Water and Wastewater Management in Sugar factories, Part I: Water Management in the Sugar Industry* (in Polish). Fundacja Rozwoj SGGW, Warszawa, Poland.

Urbaniec, K. (1989). *Modern Energy Economy in Beet Sugar Factories.* Elsevier, Amsterdam, the Netherlands.

Urbaniec, K., Klemeš, J. (2008). Water and energy management in the sugar industry. In: Klemeš, J., Smith, R., J.-K. Kim (eds.), *Handbook of Water and Energy Management in Food Processing.* Woodhead Publishing, Cambridge, UK.

Urbaniec, K., Wernik, J. (2002). Identification of opportunities to save water in a beet sugar factory. *Sugar Industry/Zuckerindustrie,* **127**, 439–443.

Urbaniec, K., Zalewski, P., Klemeš, J. (2000). Applications of process integration methods to retrofit design for Polish sugar factories. *Sugar Industry/Zuckerindustrie,* **125**, 439–443.

Urbaniec, K., Zalewski, P., Zhu, X. X. (2000). A decomposition approach for retrofit design of energy systems in the sugar industry. *Applied Thermal Engineering*, **20**, 1431–1442.

van der Poel, P. W., Schiweck, H., Schwartz, T. (eds) (1998). *Sugar Technology.* Bartens, Berlin, Germany.

Vaccari, G., Sgualdino, G., Tamburini, E., Pezzi, G., Citterio, P., Verardi, R., Urbaniec, K. (2005a). New eco-friendly proposal for the crystallization of beet raw juice. *Journal of Cleaner Production*, **13**, 1447–1460.

Vaccari, G., Tamburini, E., Sgualdino, G., Urbaniec, K., Klemeš, J. (2005b). Overview of the environmental problems in beet sugar processing: possible solutions. *Journal of Cleaner Production*, **13**, 499–507.

Waldron, K. (ed.) (2007). *Waste Management and Co-product Recovery in Food Processing*. Woodhead Publishing, Cambridge, UK.

Wang, Y. P., Smith, R. (1994). Wastewater minimisation. *Chemical Engineering Science,* **49**, 981–1006.

© Woodhead Publishing Limited, 2013

30

Application of Process Integration Techniques for the Efficient Use of Energy in a Urea Fertiliser Plant: A Case Study

MARTÍN PICÓN-NÚÑEZ, University of Guanajuato, México

DOI: 10.1533/9780857097255.5.914

Abstract: This chapter presents a practical application of Process Integration (PI) techniques for the efficient use of energy in a fertiliser plant. The case under study is the CO_2 stripping process for the production of urea in an existing plant in Mexico. The retrofit analysis of an existing process can take two possible forms of action: the modification of the existing heat recovery structure for increased heat recovery, and the identification of the appropriate changes to operating conditions for more efficient energy utilisation. In this chapter we show that the practical information obtained through the application of PI techniques brings about unseen opportunities for avoiding unnecessary energy waste.

Key words: urea production, Process Retrofit, energy efficiency, Combined Heat and Power.

30.1 Introduction

Urea is the most important nitrogen-based fertiliser in use in the world. There are a number of available technologies for its production, and the main difference between them consists in the way reactants are separated from urea and recycled back to the process. Overall, the production of urea is based on the chemical reaction between ammonia and carbon dioxide at high pressure and temperature to produce ammonium carbamate, which after dehydration gives urea and water according to the following reactions:

$$2NH_3 + CO_2 \Rightarrow NH_2COONH_4 \quad [30.1]$$

$$NH_2COONH_4 \Rightarrow NH_2CONH_2 + H_2O \quad [30.2]$$

© Woodhead Publishing Limited, 2013

The reaction between NH_3 and CO_2 is highly exothermic and rapidly proceeds to completion; however, the reaction of dehydration of carbamate is endothermic and slow. The reaction conversion is reported on a CO_2 basis, and is normally in the range of 50–80%. Conversion increases with temperature and with the NH_3/CO_2 ratio, and decreases as the H_2O/CO_2 ratio increases.

Modern urea technology has been the result of the development of more efficient ways of separating urea from the other constituents, on improving the recovery of excess NH_3, and improving the decomposition of carbamate for recycle. Other aspects of technology development are those related to the use of materials of construction able to withstand the highly corrosive nature of the carbamate solution, and the synthesis of more energy efficient processes. A block diagram that summarises the main steps in the production of urea, presented by the European Fertilizer Manufacturers' Association (2000), is shown in Fig. 30.1.

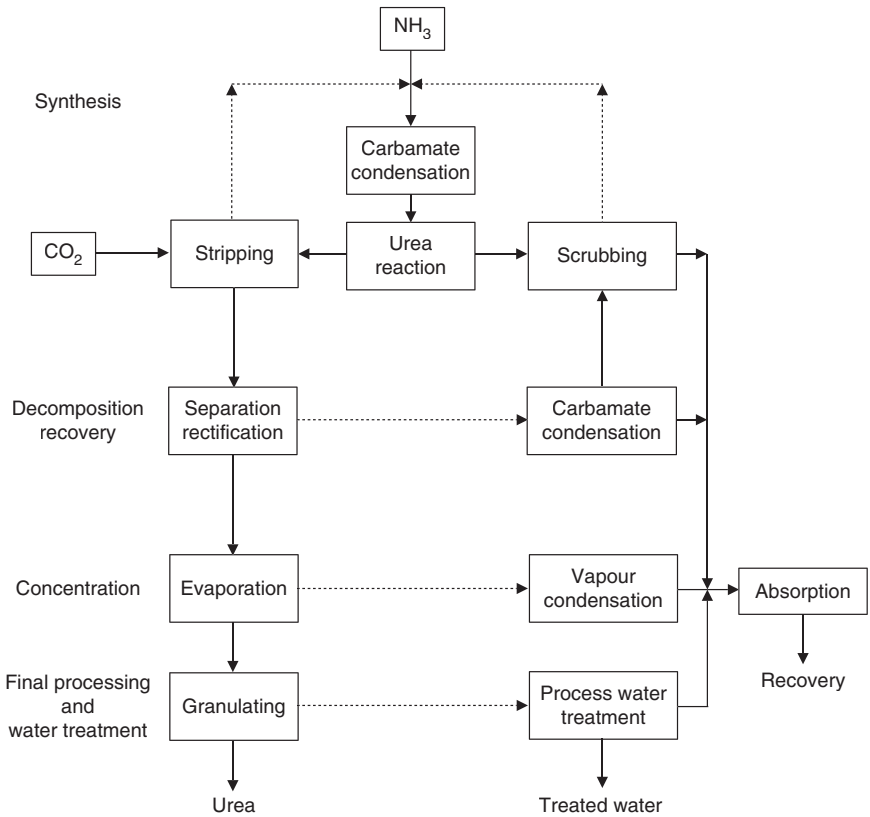

30.1 Block diagram of the urea production process (European Fertilizer Manufacturers' Association, 2000).

© Woodhead Publishing Limited, 2013

30.2 Process Description

Most of the production of urea in the world is obtained from one of the two main commercial production processes. These technologies are characterised by the application of a stripping process, either with the use of CO_2 or with the use of NH_3 as the stripping agent (Dentea *et al.*, 1988). In the CO_2 stripping process, the raw material, NH_3 and CO_2, react at high pressure (14 MPa) and high temperature (180°C) to produce ammonium carbamate at a molar ratio NH_3/CO_2 of 3. A conversion of around 60% for CO_2 and 41% for NH_3 are typically reached. The reactor effluent, with the unconverted NH_3 and CO_2, undergoes a stripping operation. This stripping step is carried out by putting the urea solution counter-currently into contact with fresh CO_2 at the reactor pressure. NH_3 and CO_2 being stripped-off are partially condensed and recycled back to the reactor. During this condensation stage, a large amount of heat is rejected. Such energy is taken advantage of by raising medium pressure steam at 0.784 MPa (8 kg/cm^2), which is recovered and used elsewhere in the process. The complete flowsheet diagram of the process under study is shown in Fig. 30.2. The urea solution produced, after the reaction steps that take place in R-1, E-1, E-2 and E-3, proceeds through a concentration stage that involves the following pieces of equipment: T-7, T-4, T-2, D-6 and D-7. After concentration, urea is sent to a prilling device located at the top of a prilling tower; liquid drops are spread down the cooling tower and cooled using ambient air that is forced counter-currently up the tower. The final solid product is then sent to storage. Part of the reactor effluent undergoes a series of purification steps (T-1, D-5 and T-5) in which NH_3 and CO_2 are separated and recycled back to the reaction section.

The compression of CO_2 to the required operating pressure is achieved by means of a turbo-compressor, which takes mechanical energy from a steam turbine that operates with superheated steam; part of this steam is expanded within the turbine and extracted for heating purposes. So the thermal energy demanded by the process is supplied by means of steam. Four steam mains are used in the plant, namely: very high pressure (VHP): 5.88 MPa (60 kg/cm^2); high pressure (HP): 2.35 MPa (24 kg/cm^2); medium pressure (MP): 0.784 MPa (8 kg/cm^2) and low pressure (LP) steam: 0.343 MPa (3.5 kg/cm^2). VHP steam is used to run a cogeneration system that produces the power for the operation of the CO_2 compressor. HP steam is extracted from the turbine for servicing the heating needs of the process; MP steam is raised at the carbamate condenser (E-2); and LP steam is used for heating purposes and for running the vacuum ejector systems. The cooling load of the process is removed through the use of a water recirculating cooling system with a counter-current cooling tower.

© Woodhead Publishing Limited, 2013

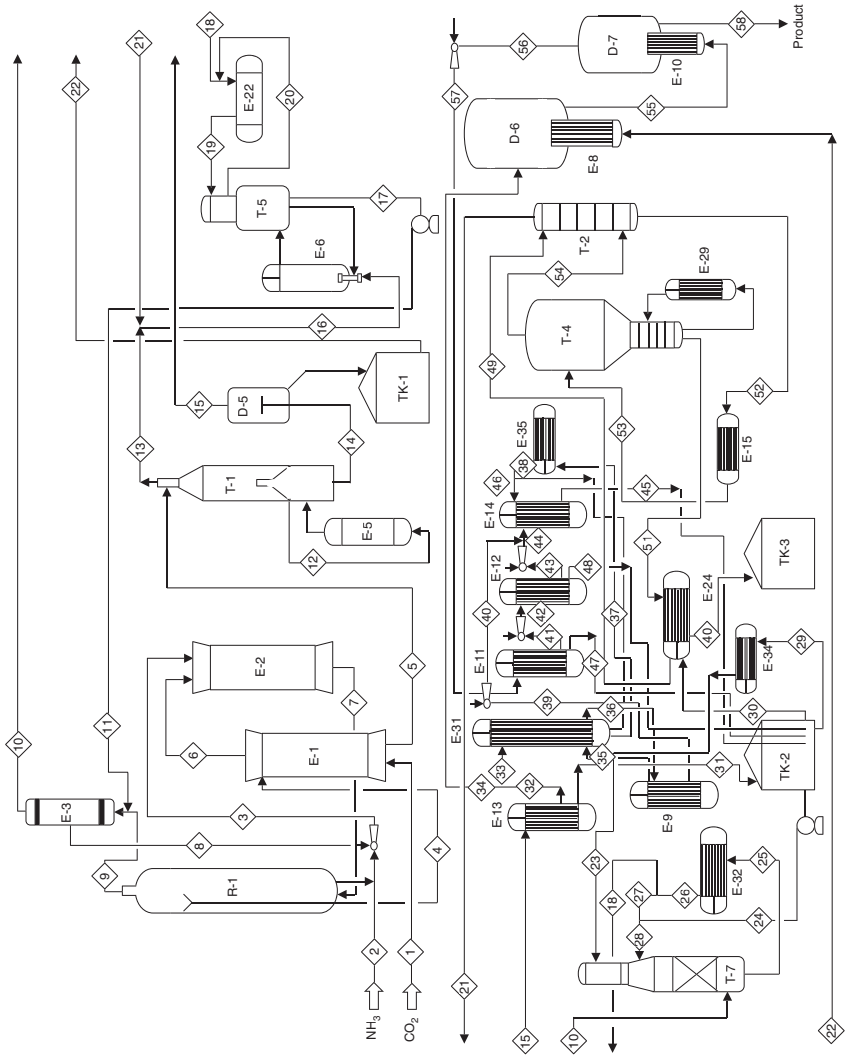

30.2 Flowsheet of the urea production process (CO_2 stripping).

© Woodhead Publishing Limited, 2013

30.2.1 Energy Consumption and Process Data

Pinch principles are a straightforward and simple way of determining the minimum energy consumption of a process; they have been explained in Chapters 4 and 5. A basic parameter for quantifying the external heating and cooling requirements of a process is the minimum temperature approach available for heat transfer. The way calculations are performed presumes that all streams, whether hot or cold, take part in the same heat recovery structure. In a real plant, this is not necessarily the case, for there are situations where independent systems are formed, each with its own minimum temperature approach. In the case under study, Pinch Analysis principles are used, and it is assumed that an overall system is formed with all process streams present and a single minimum temperature approach applies for the whole plant.

For a nominal production of 1,000 t/d of urea, and from the design conditions, the process operates with a minimum temperature approach for heat transfer (ΔT_{min}) of 6°C. From the energy balance of the process, this ΔT_{min} is located on exchanger E-34. The design data of exchanger E-34 is shown in Fig. 30.3. Given a minimum ΔT_{min} of 6°C and applying the Problem Table Algorithm (Linnhoff *et al.*, 1994) and see also Chapter 2, for the determination of the minimum utility requirements, the theoretical minimum energy consumption of the plant under design conditions is: $Q_{h\ min}$ = 21.5 MW. Knowledge of this value is an important starting point in the determination of opportunities for energy reduction. If the theoretical energy consumption is compared to the actual energy consumption reported by the utility plant, we then have an idea of the potential for energy saving. In a practical application of Pinch principles for energy efficiency, it is crucial that the real operating conditions be known and the study be based on them.

Field determination of operating data, such as mass flowrates, composition, inlet and outlet temperatures, operating pressures and pressure drops, is a process that involves either direct reading or the calculation of the desired variables from known data. For the urea process under consideration, the

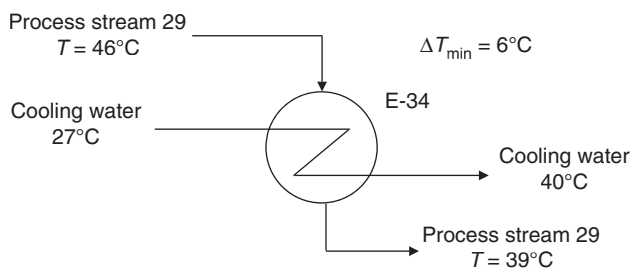

30.3 Minimum ΔT for heat transfer for design conditions.

© Woodhead Publishing Limited, 2013

Table 30.1 Real process data for a production rate of 1000 t/d

Stream (in HEN)	Type	Description (No. flow-sheet)	T_s (°C)	T_T (°C)	CP (kW/°C)	ΔH (MW)
C1	Cold	Stream 2 (NH_3)	8	165	35.52	5.58
C2	Cold	Stream 3	164	165	37.39	0.04
H3	Hot	Stream 6	178	165	23.07	0.30
C4	Cold	Stream 1	130	172	9.31	0.39
C5	Cold	Stream 11	76	146.5	18.26	1.18
H6	Hot	Stream 9	170	146.5	5.04	0.12
C7	Cold	Stripping (E-101)	172	172	–	20.62
H8	Hot	Carbamate condenser (E-102)	165	165	–	26.90
H9	Hot	Scrubber (E-103)	146.5	146.5	–	4.69
C10	Cold	Stream 12 Evaporator of T-101 (E-105)	115	127.4	223.20	2.77
C11	Cold	Stream 12 Evaporator of T-101 (E-105)	127.4	127.4	–	4.83
H12	Hot	Stream 16 E-106	106	70	232.44	8.37
H13	Hot	Stream 20 and 18 E-122	82	58	10.12	0.24
C14	Cold	Stream 22 a D-106	98	130	44.41	1.42
C15	Cold	Stream 22 a D-106 (E-108)	130	130	–	11.33
C16	Cold	Stream 55 a D-107	130	140	22.59	0.23
C17	Cold	Stream 55 a D-107 (E-110)	140	140	–	1.68
H18	Hot	Stream 25 E-132	104	55	26.95	1.32
H19	Hot	Stream 29 E-134	48	40	1.84	0.01
C20	Cold	Stream 52 E-115	142	180	43.61	1.66
C21	Cold	Evaporator (E-129)	141	141	–	1.20
H22	Hot	Stream 51 E-124	141	77	26.32	1.68
C23	Cold	Stream 30 E-124	48	102	31.20	1.68
H24	Hot	Stream 15 E-113	94	76.6	26.08	0.45
H25	Hot	Stream 15 E-113	76.6	42.6	13.11	0.45
H26	Hot	Stream 35 and 38 E-109	67	58.3	24.01	0.21
H27	Hot	Stream 35 and 38 E-109	58.3	41	12.07	0.21
H28	Hot	Stream 33 E-131	132	67	208.67	13.56
C29	Cold	Stream 36 E-131	36	55	713.86	13.56
H30	Hot	Stream 57 E-111	60	55.3	261.41	1.23
H31	Hot	Stream 57 E-111	55.3	46	132.11	1.23
H32	Hot	Stream 42 E-112	82	72.3	39.74	0.39
H33	Hot	Stream 42 E-112	72.3	53	19.97	0.39
H34	Hot	Stream 44 E-114	93	86	39.53	0.20
H35	Hot	Stream 44 E-114	86	72	13.95	0.20

final data collected for a production of approximately 1,000 t/d are shown in Table 30.1.

The data in Table 30.1 are deliberately presented in a way that is typically used for Energy Integration studies using Pinch principles. The first column refers to the name the stream takes when presented on a Grid Diagram. In the second column of the table, the streams are classified depending on whether

© Woodhead Publishing Limited, 2013

Table 30.2 Heat exchanger specifications and design data

Exchanger	Area (m^2)	No. tube passes	T_S (°C)		T_T (°c)		Q (MW)
			Hot	Cold	Hot	Cold	
E-1	754	1	214	183	214	150	21.42
E-2	1,056	1	170	147.5	170	149	2.40
E-3	35	1	183	80	160	90	1.51
E-5	300	1	143	111	143	135	4.64
E-6	340	4	109	40	72	50	7.45
E-8	385	1	143	89	143	130	12.1
E-9	195	6	66	26.7	42	41	2.16
E-10	50	1	170	130	170	134	1.81
E-11	457	6	134	26.7	42	38.7	4.49
E-12	72	4	106	26.7	43.3	42	1.55
E-13	105	4	92	26.7	43.3	42	2.17
E-14	12	4	115	26.7	43.3	42	0.38
E-15	18.4	1	214	141	214	191	1.59
E-22	4.13	1	52	26.7	45	42	0.15
E-24	21.7	1	138	42	105	70	8.72
E-29	68.5	1	175	138	175	138	1.65
E-31	500	4	130	37.8	66	51.1	8.96
E-32	25.1	2	87	26.7	42	37.7	0.65
E-34	4	1	46	26.7	39	40	0.12
E-35	51	1	147	52	147	73.3	4.18

they need to be cooled (hot streams) or to be heated (cold streams). The third column links the stream to its reference number as it appears on the process flowsheet diagram (Fig. 30.2) and presents useful information for the construction of the heat recovery network on a Grid Diagram. The following columns provide the supply and target temperatures: the CP, which represents the product between the heat capacity and the mass flowrate, and finally the last column shows the total stream enthalpy change. Heat exchanger operating data have also been collected and are shown in Tables 30.2 and 30.3. Most of the information on heat exchangers is available from the specification sheet provided by the supplier, and other information has to be determined from data measured on site. Measured and calculated data for the case of coolers and condensers have also been collected. These are shown in Table 30.4.

30.2.2 Energy Targets for Minimum Temperature Approach for Heat Transfer (ΔT_{min}) in the Existing Process

The construction of the Composite Curves (for the definition see Chapter 2) constitutes the principal element for determining the possible

© Woodhead Publishing Limited, 2013

Table 30.3 Type of heat exchanger and application

Exchanger name	Type of service	Utility
E-1	Heating	HP steam
E-2	Cooling	MP steam raising
E-3	Cooling	Cooling water
E-5	Heat recovery	Through LP steam
E-4*	Cooling	Cooling water
E-6	Cooling	Cooling water
E-8	Heat recovery	Through LP steam
E-9	Cooling	Cooling water
E-10	Heating	MP steam
E-11	Cooling	Cooling water
E-12	Cooling	Cooling water
E-13	Cooling	Cooling water
E-14	Cooling	Cooling water
E-15	Heating	MP steam
E-17	Cooling	Cooling water
E-22	Cooling	Cooling water
E-24	Heat recovery	Process-to-process
E-29	Heating	MP steam
E-31	Heat recovery	Process-to-process
E-34	Cooling	Cooling water
E-35	Cooling	Cooling water

* Not shown in the process flowsheet. Plate-and-frame unit.

Table 30.4 Measured and calculated cooling water mass flowrate in coolers and condensers

Exchanger	Cooling water flowrate (m^3/h)
E-4	164.6
E-7	1,200.0
E-9	89.9
E-11	222.6
E-12	55.3
E-13	78.1
E-14	14.0
E-17	655.6
E-19	132.6
E-20	93.5
E-21	120.2
E-22	13.0
E-32	45.5
E-34	2.1
Total:	2,887.0

Cooling water is available at 27°C.

© Woodhead Publishing Limited, 2013

options for process modifications that lead to improved energy efficiency. Their construction proceeds after the appropriate process data have been gathered. In the case of grass-roots designs, once the process flowsheet and the heat and mass balance for a given throughput have been specified, the required data can be extracted. The same procedure applies in the case of existing processes. The data to be extracted include the identification of the hot and cold streams; hot streams are those that has to reject heat in order to reduce their temperature to a given target, and cold streams are those that must absorb heat for their temperature to be increased. Other basic stream data to be extracted include the following: mass flowrates (m), specific heat capacity (C_P), supply temperature (T_S) and target temperature (T_T).

There are some principles that have to be taken into consideration during the gathering of data from the flowsheet, and mass and energy balances. Streams are first identified as hot and cold streams; their supply and target temperatures correspond to those existing between the major pieces of equipment. In the case of mixing points, the main consideration is that streams must mix isothermally; that is, the streams participating in the process has to be separately taken from their supply temperature to the final mixing target temperature. Care should be taken in cases where phase change occurs; in such situations, if it applies, it is advisable to separate the stream into two sections – the section where sensible heat transfer takes place, and the section where phase change takes place (Smith, 2005). Reactors can also be represented on the Composite Curves (see Chapter 2). In such a case, the heat evolved during the reaction is removed via a secondary fluid, for instance steam, which may be taken as a process stream for the representation of the reactor. Considering the process flowsheet of Fig. 30.2, the extracted data is shown in Table 30.1. Analysis of the real operating data reveals that the minimum temperature approach for heat transfer is 12°C (the value for the design condition is 6°C as mentioned earlier) and is located around exchanger E-5 (Fig. 30.4). The Composite Curves for a $\Delta T_{\min}$ of 12°C along with the main pieces of equipment are shown in Fig. 30.5. The energy targets for $\Delta T_{\min}$= 12°C are: $Q_{h\min}$= 26.50 MW and $Q_{c\min}$= 20.35 MW.

The steam balance of the plant indicates that a large amount of LP steam does not find application on site and is finally condensed for the recovery of the treated water. The utility exchanger that carries out the duty is exchanger E-17. The mass balance around this exchanger is shown in Fig. 30.6. As seen from this diagram, 8 t/h of LP steam at 0.343 MPa (3.5 kg/cm^2) is wasted. Later on it will be shown how this situation can be avoided, with consequent benefits in terms of improved energy efficiency and savings in operating cost.

© Woodhead Publishing Limited, 2013

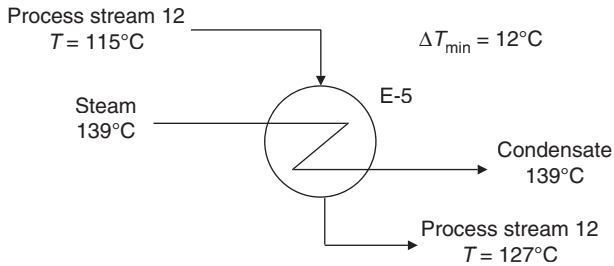

30.4 Localisation of the exchanger that operates with the Minimum Temperature Difference for heat transfer for real operating conditions (12°C).

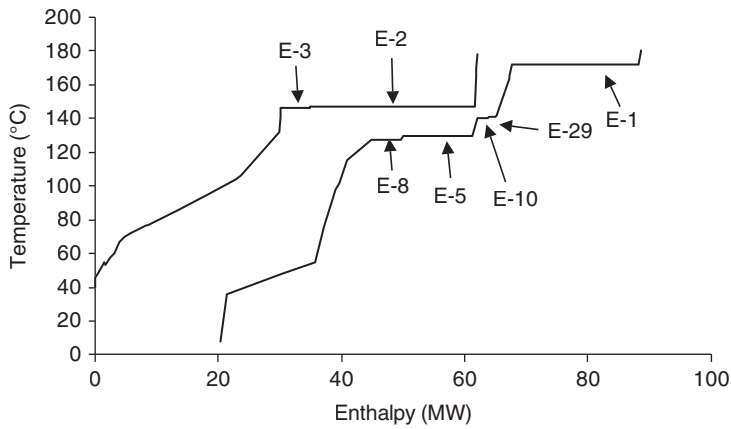

30.5 Process Composite Curves for ΔT_{min} = 12°C.

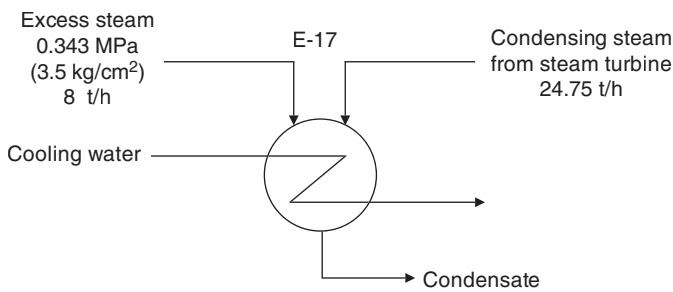

30.6 Utility exchanger (E-17) for the condensation of surplus steam.

© Woodhead Publishing Limited, 2013

30.2.3 Heat Recovery Network

The network of heat exchangers, coolers and heaters that carries out the duty of recovering heat and supplying the minimum external heating and cooling is graphically represented by means of a Grid Diagram, in which hot streams are shown as straight lines going from right to left drawn on top of the cold streams, which run in the opposite direction. Utility exchangers are symbolised by circles with the notation H or C for heaters and coolers, whereas process-to-process heat recovery exchangers are illustrated as two circles linked by a vertical straight line. Derived from the process diagram of Fig. 30.2, the actual HEN structure of the plant is extracted and presented in the Grid Diagram (Fig. 30.7).

From the network structure of Fig. 30.7, we see that there is little energy recovery within the process and a large amount of energy is either taken or eliminated through external utilities. The former situation gives rise to the existence of independent energy systems. A close look at the network structure of Fig. 30.7 reveals that a further subdivision can be identified: the Process-to-Process Heat Recovery Network, the heating network and the cooling network. These three substructures are linked to each other, but their analyses are conducted separately.

30.3 Opportunities for the Reduction of Energy Consumption

The opportunities for reducing the energy consumption of the process are divided into two main categories: those related to the changes in operating conditions in relation to the cogeneration system, and those related to increasing energy recovery. These options are analysed in the following sections.

30.3.1 Cogeneration System

As already mentioned, the process for the production of urea takes place at high temperature (185°) and pressure (14 MPa). The thermal duty of the process is approximately 26.50 MW and the power consumption is around 5 MW. The heat/power ratio is 5.3, which confirms that the process is an ideal candidate for the integration of a combined heat-and-power system operated with a steam turbine (Eastop and Croft, 1995). For the nominal production of 1,000 t/d of urea, the design operating conditions of the turbine are shown in Fig. 30.8.

For the specified production rate, the current plant power requirement for the operation of the CO_2 compressor is 5.92 MW. This power

© Woodhead Publishing Limited, 2013

© Woodhead Publishing Limited, 2013

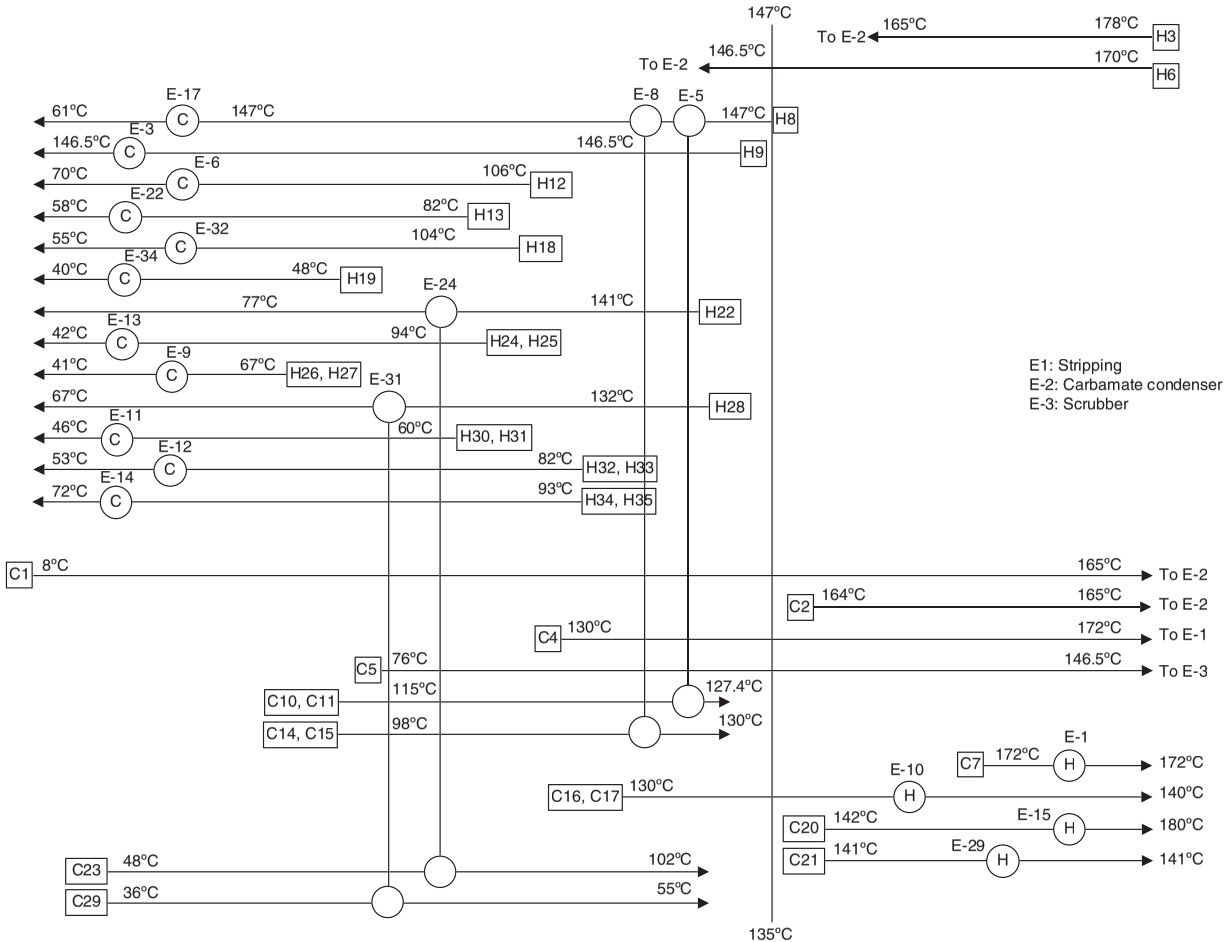

30.7 HEN structure of existing plant (ΔT_{min} = 12°C).

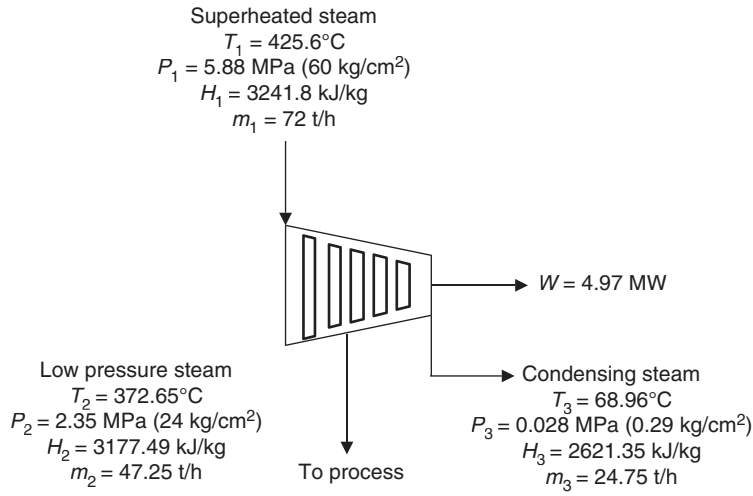

30.8 Design condition of steam turbine.

is supplied by a back-pressure steam turbine, which is fed with 72 kg/h of superheated steam at 5.88 MPa (60 kg/cm^2); 47.25 t/h of MP steam at 2.35 MPa (24 kg/cm^2) is extracted in order to supply the process heating duty; the rest of the steam is exhausted and condensed in the surface condenser E-17. The turbine surface condenser operates with cooling water and receives exhausted steam from the turbine, and unused LP steam at 0.343 MPa (3.5 kg/cm^2). Figure 30.9 shows a Grand Composite Curve (see Chapters 2 and 4) and the actual operation of the cogeneration system.

Further investigation to determinate the reason why there is a substantial difference between the nominal power consumption (5 MW) and the actual power consumption (5.92 MW) for the production rate of 1,000 t/d led to the following finding: under design conditions, process specification establishes that the CO_2 feed stream must enter the compressor at a maximum temperature of 32°C. However, the current CO_2 compressor feed temperature fluctuates between 45°C and 50°C. This situation had been common over the years, and operators and production managers went without realising the detrimental effect that this unattended situation had brought upon the energy consumption. The correction of this temperature not only results in an instant saving of power (15.5%) but also, as less power is produced, less HP steam is extracted. Since the HP extraction steam has now been reduced to 43.76 t/h, the new energy balance around the turbine for a power production of 5 MW indicates that the superheated feed steam is now reduced to 64.05 t/h. This represents a saving of 7.95 t/h (11.04%). Figure 30.10 shows the modified operating conditions.

© Woodhead Publishing Limited, 2013

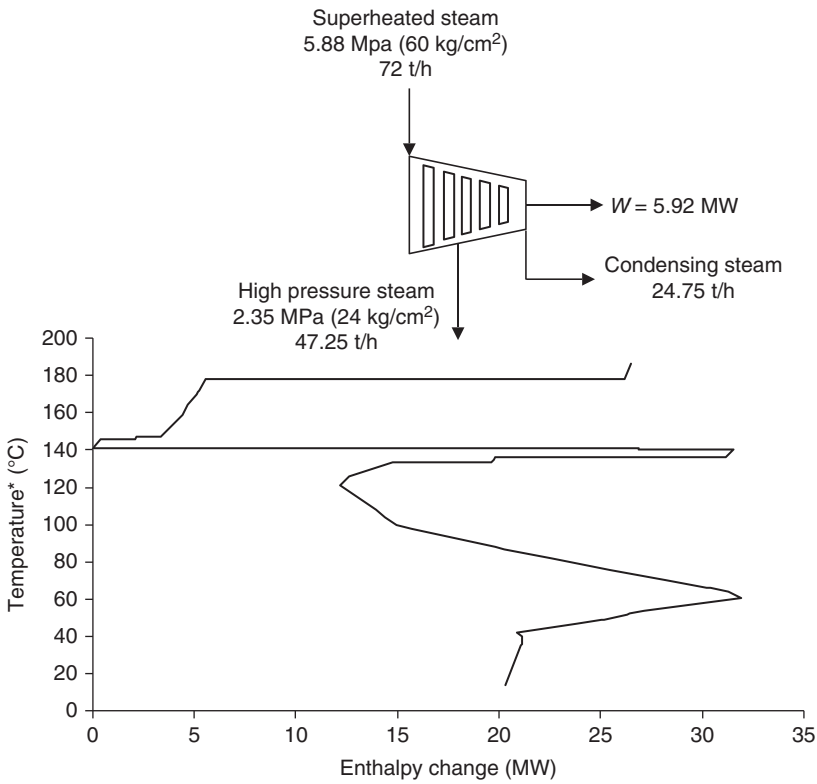

30.9 Grand Composite Curve and the actual operation of the cogeneration system. Representation of the turbine mass and energy balance on the Grand Composite Curve for actual operating conditions.

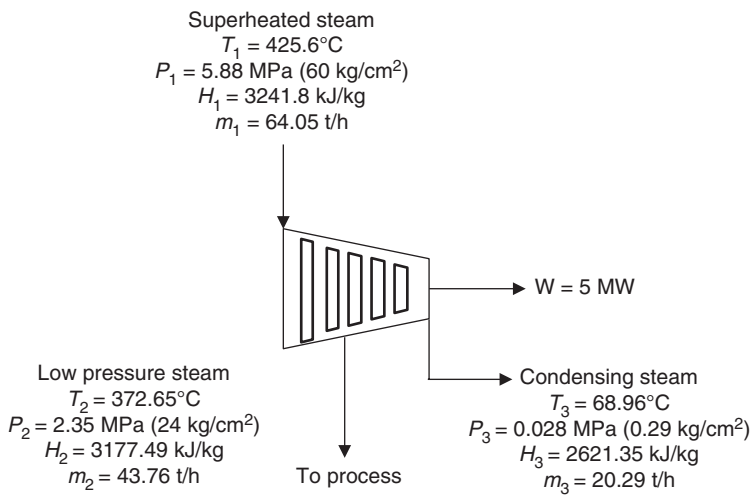

30.10 Modified operating conditions of steam turbine.

© Woodhead Publishing Limited, 2013

30.3.2 Improving Energy Recovery

Changing Operating Conditions

From real operating data, it is found that the minimum temperature approach for heat transfer in the process is 12°C, and it occurs at exchanger E-5. The conceptual information that the Composite Curves give can be interpreted in the following way: at current operating conditions the minimum external energy consumption is $Q_{h\,\min}$= 26.50 MW, and the minimum external cooling is $Q_{c\,\min}$= 20.35 MW. Increasing heat recovery so that the minimum temperature approach reduces to 6°C, the external heating load would be 23.14 MW and the cooling load 16.98 MW. For these conditions, there is a potential for reducing the external heating load to 3.34 MW (12.6%). Figure 30.11, shows the Composite Curve of the process for a $\Delta T_{\min}$ of 6°C, where it can be seen that the heat load of exchangers E-10 and E-29, which were originally supplied using MP steam, obtained from the expansion of HP steam to MP steam (Fig. 30.5), can now be served using LP steam.

Part of the MP steam is used to run the ejector system and eventually LP steam is recovered and sent to the LP steam mains. A large amount of LP steam (8 t/h) does not find application in the plant and its heat content is lost through condensation at a surface condenser E-17 (Fig. 30.6). In order to avoid this energy loss, MP steam can be substituted by LP steam in some of the process sinks such as E-10 and E-29, whose heat duty is 1.81 and 1.65 MW. The preceding discussion states that the energy demand of the process could be reduced by a total of 3.46 MW. The impact of this reduction upon the production of VHP steam can be obtained from an

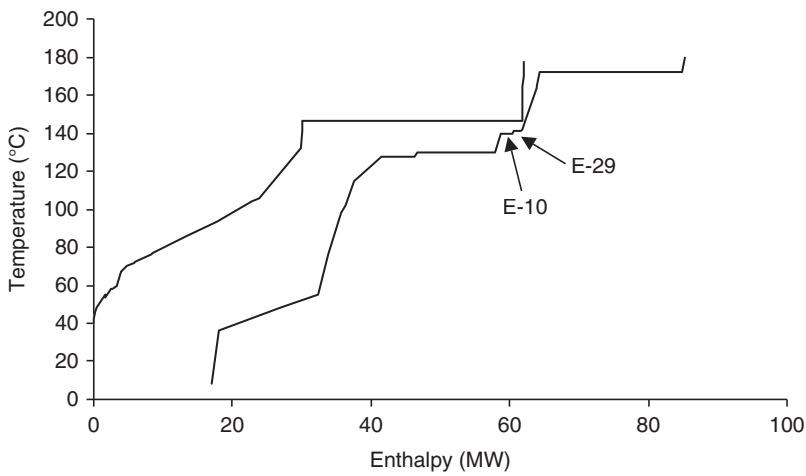

30.11 Increased heat recovery seen through the Composite Curves. $\Delta T_{\min}$ = 6°C.

© Woodhead Publishing Limited, 2013

© Woodhead Publishing Limited, 2013

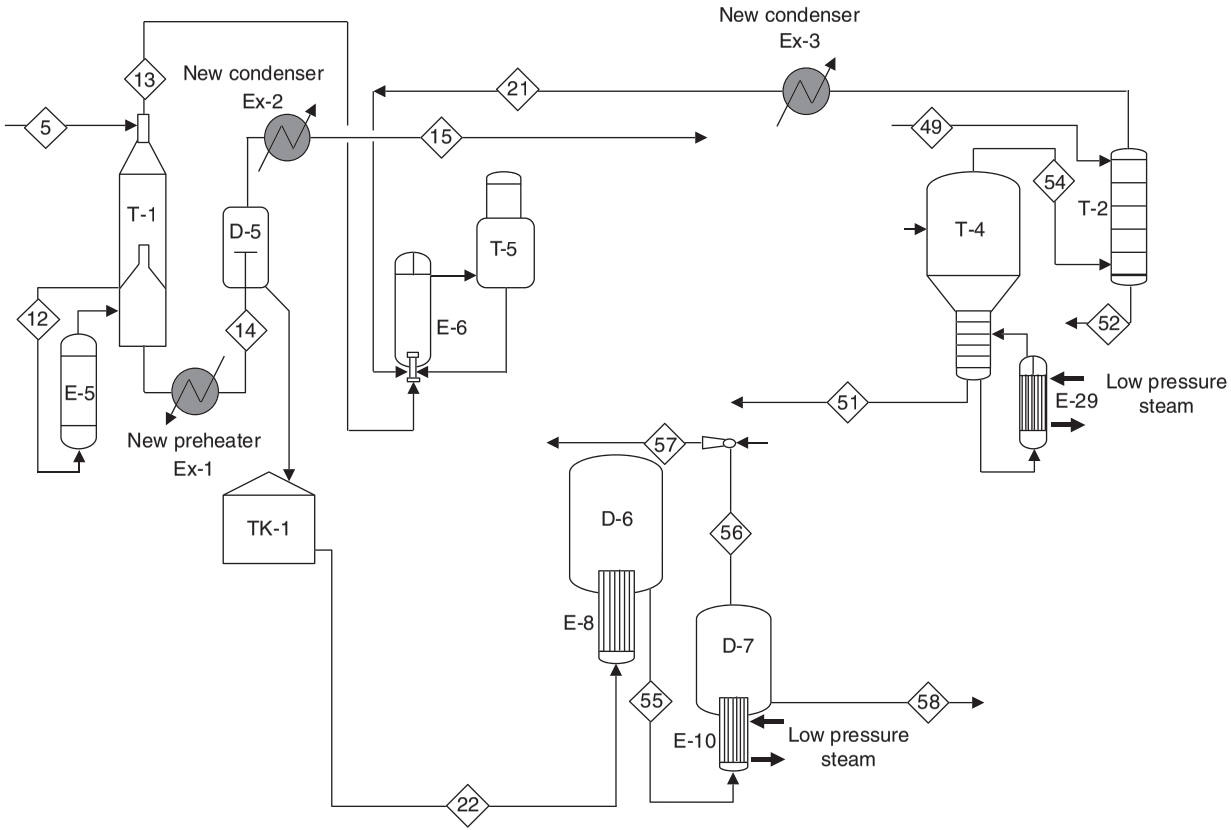

30.12 Installation of additional heat transfer area through exchangers Ex-1, Ex-2 and Ex-3, for the process to maintain its operability during the substitution of MP steam for LP steam on exchanger E-10 and E-29.

energy balance around the steam turbine giving a saving of 2.94 t/h. This represents a further saving of 4%.

The implementation of the substitution of MP for LP steam to run exchangers E-10 and E-29 is not straightforward, and requires further understanding of the operation. In the case of exchanger E-10, for the same heat transfer area installed, the use of steam at 147°C instead of 170°C brings about a reduction in the heat load being transferred from 1.9 MW to 0.76 MW. Analysis of the operation of the process indicates that the most efficient way of installing additional exchanger area is placing it between tower T-1 and flash tank D-5 (preheater Ex-1), as shown in Fig. 30.12. This implementation is likely to reduce the efficiency of the separation in flash tank D-5, due to the lower heat transfer driving force. This situation can be avoided by increasing the vacuum conditions in the system by the installation of an additional condenser after D-5 (Ex-2), as shown in Fig. 30.12.

The operation of E-29 with LP steam will be accomplished by the installation of a second condenser (Ex-3) after column T-2. The situation that arises is similar to the case of E-10 where the temperature driving force is reduced; the reduction in driving force is accompanied by a reduction in the heat load transferred. So, in order to restore the driving force without having to increase the exchanger surface area, vacuum is created by means of a new condenser.

With the preceding modifications, 5.27 t/h of LP steam find an application within the process. The consequence of this is that the surface condenser E-17 reduces its cooling load in two ways: by the reduction of the exhaust steam from the turbine, and by reducing the amount of unused 0.343 MPa (3.5 kg/cm^2) steam. This represents a reduction of 5.34 MW in the cooling load of E-17 and a saving of 16.43 m^3/h of cooling water that otherwise would be lost to ambient, due to evaporation and cooling tower blow-down.

Increasing Energy Recovery

Analysis of the heat recovery network reveals important energy reduction opportunities through increased heat recovery. These options are analysed, first from the thermal point of view, and then considering practical implications.

(a) ***CO_2 feed stream.*** Raw CO_2 is fed to stripper E-1 at a temperature of 130°C after passing the compression stage. HP steam is consumed for the stripping process to take place, and for raising the system temperature to 172°C. The amount of energy absorbed in E-1 for increasing the CO_2 temperature is 0.39 MW; if this amount of energy could be recovered from elsewhere, the heat load on the stripper could be reduced by 1.8%. Figure 30.13 shows a heat recovery option that consists in matching streams H3 and H4 with stream C4 (CO_2).

From the heat recovery network structure point of view, streams H3, H6 and C4, form a separate system from the rest of the heat recovery network.

© Woodhead Publishing Limited, 2013

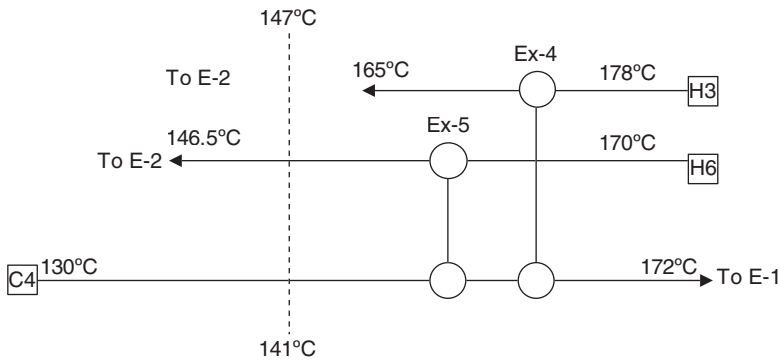

30.13 Reduction of the heat load on exchangers E-1 and E-2 by heat recovery from streams H3 and H6 through exchangers Ex-4 and Ex-5 for the preheating of the CO_2 stream (C4).

This new structure brings about some benefits; for instance, the amount of LP steam that otherwise is produced in E-2, which in the case of not finding further application is condensed in exchanger E-17, is reduced by 0.66 t/h, with consequent reduction in cooling load.

From the practical point of view, there are some limitations to the new heat recovery structure of Fig 30.13. After a detailed analysis, the plant lay-out modifications necessary to use stream H6 in this new structure make the project infeasible, since considerable piping would be required; also, lack of nearby physical space for installing exchanger Ex-5 limit the use of stream H6. More importantly, there are operating limitations to the use of stream H3, since the removal of heat from its gaseous composition (CO_2 and NH_3) can result in condensation with the consequent reaction to carbamate, which may cause blockage of the heat exchanger.

(b) ***NH_3 feed stream.*** Ammonia enters the process at a temperature of 8°C and is then heated to the condenser temperature of 165°C (E-2). The large cooling capability of the NH_3 stream (H1) could be taken advantage of in order to reduce the process total cooling load. Such an action would cause the heat released in the condenser E-2 to be removed through the raising of more MP steam. For a case where more MP production is justifiable, then the following heat recovery structure can be considered: cooling water through exchangers E-4, E-9 and E-13 can be replaced by the cold ammonia stream as shown in Fig. 30.14. This arrangement removes 1.65 MW of heat from streams H24, H25, H26, H27, H34 and H35, which is equivalent to the raising of 2.78 t/h of steam at E-2. From the operative point of view, there is a risk of crystallisation inside the condensers due to the low temperature of ammonia.

Another option would be to use the NH_3 stream to fully supply the cooling needs of exchanger E-4 (cooling circuit of E-3). The heat load in this application is 3.44 MW, which represents an increase of 5.83 t/h of steam

© Woodhead Publishing Limited, 2013

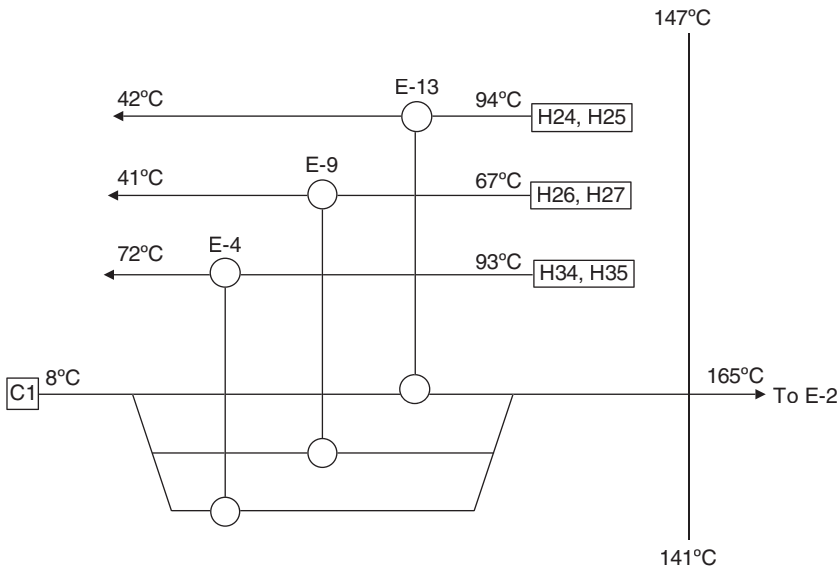

30.14 Use of the NH_3 (C1) stream to reduce the cooling loads on streams (H24, H25, H26, H27, H34 and H35) through exchangers E-4, E-9 and E-13.

raised at E-2. However, since exchanger E-4 is a plate-and-frame unit it would not be suitable, since the high operating pressure of ammonia surpasses the maximum pressure this exchanger technology can withstand. A shell-and-tube exchanger should be used instead.

The final network structure for a ΔT_{min} of 6°C that includes the modification presented in Fig. 30.12 is shown in Fig. 30.15. It is worth noting that the nomenclature used for exchangers E-10 and E-29 in the diagram correspond to a heater application. Even though it is actually an exchanger being operated by steam, this is steam raised within the same process, so it can be considered as an indirect process-to-process heat recovery. Exchangers Ex-1, Ex-2 and Ex-3 have been included in the diagram. A summary of the savings obtained with the modifications to the process are shown in Table 30.5.

30.4 Conclusion

This chapter has sought to give the reader some elements for the practical application of PI principles for the efficient use of energy in processing plants. Knowledge of PI principles is fundamental for a successful application of retrofit studies in real plants; however, equally important is the knowledge of the process itself, which in most applications might render infeasible but some attractive proposals for energy saving. In this chapter it has also been shown that through the proper application of PI tools the

© Woodhead Publishing Limited, 2013

Table 30.5 Summary of energy and capital savings

Substitution of MP steam by LP steam in exchangers E-10 and E-29			
Utility	Mass flowrate (t/h)	Heat load (MW)	Savings (USD/y)
VHP steam	2.94	3.105	88,200.0
Cooling water	6.3	2.045	14,253.0
Correction of CO_2 compressor inlet temperature			
VHP steam	5.01	5.291	150,295.0
Cooling water	10.134	3.289	22,923.3
Total:			275,671.3

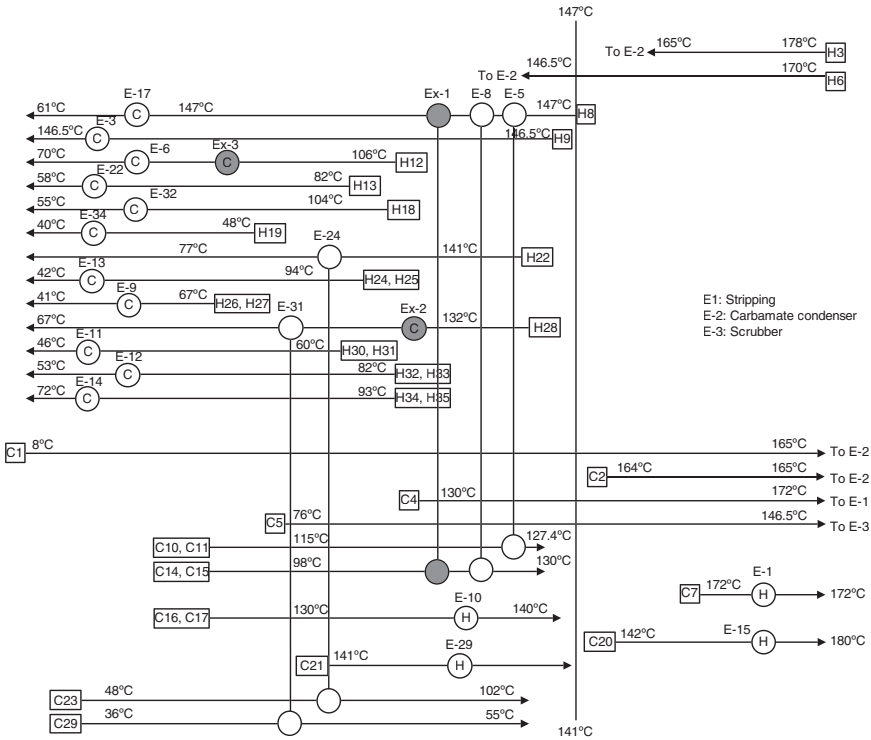

30.15 Modified heat recovery network for increased heat recovery. $\Delta T_{min} = 6°C$.

practitioner is able to identify unseen operating mistakes that lead to energy and water waste, with corresponding economic and environmental effects. Modern urea plants consider energy efficiency as one of the design objectives. The process studied in this chapter, although a highly integrated process, has shown some areas of improvement for future urea plants.

© Woodhead Publishing Limited, 2013

30.5 Sources of Further Information

Given that in many energy intensive processes, a large proportion of the total production cost is dominated by the amount of energy expenditure, and that a large potential for energy savings exists in the processing industry, the development of simple and yet effective technologies for the retrofit of existing processes is of paramount importance.

Since the concept of the Process Pinch became known to the industrial sector, and examples of its application were published, it has become one of the most important and effective means of analysing existing processes, leading to the achievement of real and practical energy savings through process modifications. For instance, Spriggs and Ashton (1986) have reported the application of Pinch Analysis to a wide range of industrial processes and the savings achieved.

More recently, applications of Pinch Analysis for the reduction of energy expenditure in process plants have been published for various cases; for instance, in the case of ethylbenzene production (Yoon *et al*., 2007) savings of upto 5.8% with minimum HEN structural changes have been reported. Feng *et al*. (2011) analysed petrochemical processes such as aniline and aromatic plants. They introduced a different approach for the definition of Heat Integration boundaries within the plant; this approach simplifies the retrofit study of these processes, achieving energy savings also with minimum changes. Applications to the case of ammonia plants were reported by Panjeshahi *et al*. (2008). Energy savings in the cold part of the plant where refrigeration is used were shown to be as high as 15%. In their work, both the heat recovery network and the utility system are analysed; for the latter, exergy analysis that applies to below ambient situations for the reduction of power expenditure was employed. Other processes where Pinch and exergy Analysis have simultaneously been used is the pulp and paper industry (Brown *et al*., 2005).

Jegla *et al*. (2000) developed techniques for the retrofit of furnaces in refineries based on the optimisation of the stack temperature and air preheating system. Al-Riyami *et al*. (2001) developed studies for the retrofit of a fluid catalytic cracking (FCC) unit in an oil refinery. Process data for 23 hot streams and 11 cold streams were obtained through process simulation. Optimised Heat Exchanger Network structures were obtained, to be used later as the basis for retrofitting the existing one. As in most cases, it is shown that energy savings can only be achieved if investment is made in additional heat recovery surface area.

Most of the work done on retrofit of existing process looks at the heat recovery network and seeks to increase energy recovery by minimising structural changes. Piacentino (2011) presents an automated approach for achieving increased energy recovery at minimum changes. Asante and Zhu

© Woodhead Publishing Limited, 2013

(1997) developed a retrofit approach based on thermodynamics and practical engineering; they found that a heat recovery network is thermodynamically limited by certain exchangers, where the temperature approach for heat recovery tends to zero as the heat recovery increases. They termed these 'Pinching Matches' since they become a bottleneck for heat recovery. They propose a systematic search that seeks to eliminate this type of matches with the minimum number of changes. Further improvements of this work are described by Smith *et al*. (2010).

Other types of process, such as sugar production, have also been subject to Pinch Analysis studies. The work reported by Urbaniec *et al*. (2000) involves the study of multi-effect evaporators, heat exchangers and the power plant. The approach considers the separation of the process into two distinct parts: the evaporation section, where vapours and condensates are generated, and the process heating subsystem.

The integration of large industrial complexes is an extremely difficult and complex task; however, Matsuda *et al*. (2009) carried out a study like this in Japan. They used the concept of Total Site Pinch Technology, which was combined with the use of R-curve analysis and Site Source–Sink Profile analysis.

Graphical approaches for the retrofit of Heat Exchanger Networks have also been developed. For instance, Norman and Berntsson (2009) developed an approach where heaters and coolers are used as the basis for the identification of potential cost effective heat recovery network revamping projects.

From the exposition above, it can be seen that there is not a single approach that serves well in every retrofit situation, given the distinct nature and the wide variety of production plants across the world. Better and more powerful tools for the analysis of existing processes are yet to be developed, and most of them will be process specific. At this stage, however, it is important to stress the importance of combining practical process knowledge with Pinch Analysis theory for a complete and sound application. Experienced engineers and technology experts need to work hand in hand, so that the results can have the impact predicted by theory.

30.6 References

Al-Riyami, B. A., Klemeš, J., Perry, S. (2001). Heat integration retrofit analysis of a heat exchanger network of a fluid catalytic cracking plant. *Applied Thermal Engineering*, **21** (13–14), 1449–1487.

Asante, N. D. K., Zhu, X. X. (1997). An automated and interactive approach for heat exchanger network retrofit. *Chemical Engineering Research and Design*, **75** (3), 349–360.

Brown, D., Maréchal, F., Paris, J. (2005). A dual representation for targeting process retrofit, application to a pulp and paper process. *Applied Thermal Engineering*, **25** (7), 1067–1082.

© Woodhead Publishing Limited, 2013

Dentea M., Pieruccia S., Sogaroa A., Carlonib G., Rigollib E. (1998). Simulation program for urea plants. *Computers and Chemical Engineering*, **12** (5), 389–400.

European Fertilizer Manufacturers' Association. (2000). Production of Urea and Urea Ammonium Nitrate, Booklet No. 5, Brussels, Belgium.

Eastop T. D., Croft D. R. (1995). *Energy Efficiency*. Longman Group, Ltd, Essex, England.

Feng, X., Pu, J., Yang, J., Chu K. H. (2011). Energy recovery in petrochemical complexes through heat integration retrofit analysis. *Applied Energy*, **88** (5), 1965–1982.

Jegla, Z., Stehlík, P., Kohoutek, J. (2000). Plant energy saving through efficient retrofit of furnaces. *Applied Thermal Engineering*, **20** (15–16), 1545–1560.

Kemp I. (2007). *Pinch Analysis and Process Integration* (authors of the first edition: Linnhoff, B., Townsend, D. W., Boland, D., Hewitt, G. F., Thomas, B. E. A., Guy, A. R., Marsland, R. (1982 and 1994), *A User Guide on Process Integration for the Efficient Use of Energy*. IChemE, Rugby, UK) 2nd ed. Elsevier, Amsterdam, The Netherlands.

Linnhoff, B., Townsend, D. W., Boland, D., Hewitt, G. F., Thomas, B. E. A., Guy, A. R., Marsland, R. (1982 and 1994). *A User Guide on Process Integration for the Efficient Use of Energy*. IChemE, Rugby, UK.

Matsuda, K., Hirochi, Y., Tatsumi, H., Shire, T. (2009). Applying heat integration total site based pinch technology to a large industrial area in Japan to further improve performance of highly efficient process plants. *Energy*, **34** (10), 1687–1692.

Nordman, R., Berntsson, T. (2009). Use of advanced composite curves for assessing cost-effective HEN retrofit II. Case studies. *Applied Thermal Engineering*, **29** (2–3), 282–289.

Panjeshahi, M. H., Langeroudi, E. G., Tahouni, N. (2008). Retrofit of ammonia plant for improving energy efficiency original. *Energy*, **33** (1), 46–64.

Piacentino, A. (2011). Thermal analysis and new insights to support decision making in retrofit and relaxation of heat exchanger networks. *Applied Thermal Engineering*, **31** (16), 3479–3499.

Smith R. (2005). *Chemical Process Design and Integration*. John Wiley & Sons, Ltd, UK.

Smith, S., Jobson, M., Chen, L. (2010). Recent development in the retrofit of heat exchanger networks. *Applied Thermal Engineering*, **30** (16), 2281–2289.

Spriggs, H. D., Ashton, G. (1986). Divers applications of pinch technology within the process industries. Proceedings from the Eighth Annual Industrial Energy Technology Conference, Houston TX, USA, paper: ESL-IE-86-06-72, 448–452.

Urbaniec, U., Zalewski, P., Zhu, X. X. (2000). A decomposition approach for retrofit design of energy systems in the sugar industry. *Applied Thermal Engineering*, **20** (15–16), 1431–1442.

Yoon, S. G., Lee, J., Park S. (2007). Heat integration analysis for an industrial ethylbenzene plant using pinch analysis. *Applied Thermal Engineering*, **27** (5–6), 886–893.

30.7 Appendix: Nomenclature

C_p	heat capacity, kJ/kg °C
CP	heat capacity mass flowrate, kW/°C
HEN	heat recovery network

© Woodhead Publishing Limited, 2013

HP	high pressure steam, kPa
LP	low pressure steam, kPa
m	mass flowrate, t/h
MP	medium pressure steam, kPa
$Q_{h\min}$	minimum external heating load, MW
$Q_{c\min}$	minimum external cooling load, MW
T_S	supply temperature, °C
T_T	target temperature, °C
$\Delta T_{\min}$	minimum temperature approach for heat transfer, °C
VHP	VHP steam, kPa

© Woodhead Publishing Limited, 2013

31

Process Integration for Energy Saving in Buildings and Building Complexes

PETRO O. KAPUSTENKO and OLGA P. ARSENYEVA,
National Technical University –
Kharkiv Polytechnical Institute, Ukraine

DOI: 10.1533/9780857097255.5.938

Abstract: This chapter discusses the possibilities offered by implementing Process Integration for the efficient use of energy in buildings and building complexes. In many countries buildings account for about 40% of the total energy demand and 36% of the total greenhouse gas emissions, and are hence considered both consumers and producers of energy. Buildings can be categorised as industrial, residential, or commercial/public, with a further category for building complexes. A description of the Total Site Analysis (TSA) method is provided, with specific reference to its application to District Energy (DE) systems and integration procedures. Recently studied practical examples of the implementation of this type of system are also presented and analysed.

Key words: Process Integration, buildings, energy efficiency, District Energy system, renewable energy sources.

31.1 Introduction

The primary goal for all energy production today is to satisfy consumer requirements; an important part of this is comfortable conditions and adequate services in homes, offices, workshops and so on, which are situated in a variety of building types. Depending on the climatic conditions, the percentage of a country's total energy requirement that is needed to maintain a comfortable temperature inside buildings can be as high as 40–45%. Any shortage in energy supply results in electricity switch-offs, most commonly during summer in hot climates (as a result of increased use of air conditioning and refrigeration), or during winter in colder climates (as a result of increased use of heating).

Maintaining favourable living conditions for the population involves both heating up and cooling down the building interior. The task of keeping a building at the optimum temperature is very similar to the task of the process industry, with different cold and hot streams inside the building and in

© Woodhead Publishing Limited, 2013

the immediate and more distant surroundings. To minimise the consumption and cost of utilities, the correct energy source and energy levels are required, and energy recuperation between the streams must be maximised. Pinch Technology and Process Integration are valuable tools in this respect, and have provided good results in process industries. Of course, just as at the refinery, for example, the first task is to ensure that losses into the environment are at the lowest economically viable levels, and optimal thermal insulation and equipment design must be chosen. Once these steps have been carried out, the full Process Integration methodology can be implemented.

31.2 Buildings as Consumers and Producers of Energy

There are approximately 200 million buildings in the 27 member states of the EU alone, accounting for about 40% of a country's final energy demand and 36% of the total greenhouse gas emissions (Eurostat, 2011; EC Directive 2010/31/EU). About two-thirds of these buildings are classified as residential, with commercial and public buildings accounting for the remaining one-third (estimated by Balaras *et al*., 2005). Similar energy usage patterns are observed in the US, where commercial and public buildings account for 45% of energy use according to the USDE (2011), as well as in all OECD countries (IEA, 2011).

Around 65% of the energy used in buildings is for heating, cooling and hot water preparation. According to Zeng *et al*. (2011), space heating or cooling accounts for around 15% of the total energy consumption in China, and this figure is increasing. Hong (2009) estimates that the building sector in China is expected to contribute 40% of the total energy savings target for the period 2000–2020. Considering that in 2008 the above countries consumed 54% of the total energy produced worldwide, according to the USDE (2011), the importance of effective energy usage in buildings cannot be overstated.

Figure 31.1 shows the three main building categories: industrial, residential, and public and commercial. In industrial buildings (workshops, offices and utility buildings), the energy demand for space heating, hot water and air conditioning can be considerable, depending on the climatic conditions and industry type. This energy consumption can be integrated with the waste heat of industrial processes, providing significant energy savings, and must be included in any assessment of Total Site Process Integration, as shown by Klemeš *et al*. (2010). However, many food industries in Eastern Europe and Russia use ammonia refrigeration units that discharge heat in summer, but at the same time rely on gas or coal-fired boilers to heat water. Kapustenko *et al*. (2008) used Pinch Analysis to show that, with a relatively minor retrofit and moderate investment, it can be beneficial, providing payback in less than a year.

© Woodhead Publishing Limited, 2013

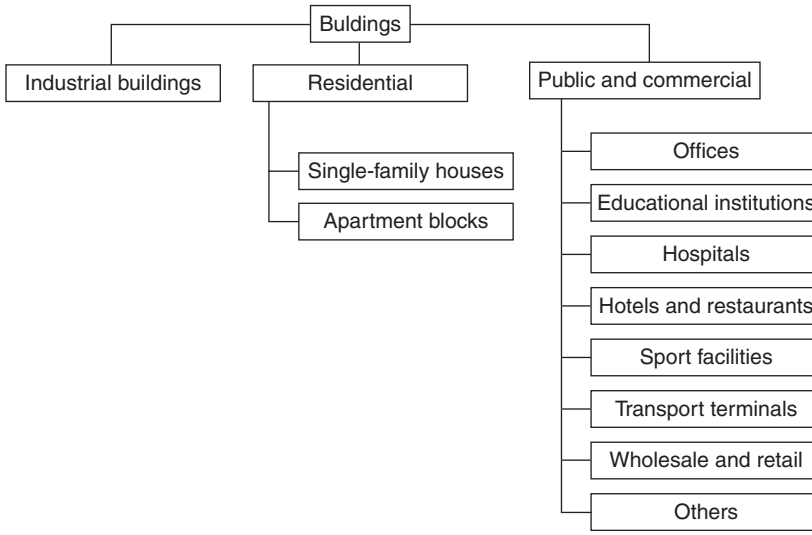

31.1 Classification of buildings by their purpose.

Energy consumption in residential buildings in the EU averages 150–230 kWh/m^2 per year according to Balaras *et al*. (2005). In Eastern Europe this rises to 250–400 kWh/m^2, and is frequently around two times higher than Western European consumption. In Northern European countries, on the other hand, well-insulated low-energy buildings can have an annual consumption of as little as 60–80 kWh/m^2. According to the Danish Environmental Protection Agency, residential energy use per capita is subject to significant variation among European countries: in Southern Europe (Portugal, Spain, Greece), for example, this varies between 150 and 350 kWh/capita, while values of 500–700 kWh/capita are common in most countries in Northwest Europe and in Scandinavia. Levels in most EU countries are fairly steady, fluctuating from year to year with the weather, but in some Southern European countries, such as Greece and Spain, residential energy use has shown a steady increase over the last decade (Eurostat, 2011).

An individual family house, or even a medium size apartment block that does not use renewable energy, a Combined Heat and Power (CHP) system or a heat pump does not offer a great deal of scope for Process Integration. Given the relatively limited number of possible options in this respect, computer modelling software is often the best way to identify the optimal solution. Several types of building energy simulation software are currently available, and are described and analysed in a number of studies, including: Kanagaraj and Mahalingam's (2011) work on strategies for the design of energy-efficient office buildings; Yiqun *et al*.'s (2008) study of the energy modelling of office buildings; the investigation into energy retrofitting of

© Woodhead Publishing Limited, 2013

historical buildings by Ascione *et al*. (2011); Poirazis *et al*.'s (2008) study energy simulations for glazed office buildings; and work on calibrating whole building energy models by Raftery *et al*. (2011). Some of these studies present simplified energy-analysis tools that only provide data on the annual energy usage of buildings, but some use more detailed models that provide a simulation of the energy consumption of a building on an hourly basis. Some authors, such as Fesanghary *et al*. (2012) and earlier Diakaki *et al*. (2008), use multi-objective optimisation to improve the energy efficiency and environmental performance of buildings.

The optimisation of energy consumption in buildings is currently a major priority in the energy policy, not only of the EU but also worldwide. The construction and adoption of buildings with very low or even close to zero energy consumption is widely promoted; in these low-energy buildings, as much as 80% of the operational cost can be saved through integrated design solutions.

Molin *et al*. (2011) studied the concept of super-insulated houses, which were first planned in the late 1970s as a reaction to the oil crisis. The first passive houses were developed in Germany in the 1990s, with the first house built in 1991; they are now more widely built across Northern Europe and also, more recently, in the USA. The first passive houses in Sweden were completed in 2001 in the area of Lindes, just outside Gothenburg. The resulting annual energy demand for space heating in these houses was about 13 kWh/m^2. Marszal *et al*. (2011) analysed the concept of the Zero Energy Building (ZEB), which is no longer perceived as a prospect for the distant future but as a realistic solution for the mitigation of CO_2 emissions and the reduction of energy consumption in the building sector. Goals for the implementation of ZEBs have been discussed at the international level, for example in the Energy Independence and Security Act of 2007 in the US (EISA 2007) and in the DIRECTIVE 2010/31/EU on the Energy Performance of Buildings in the EU. Thiers and Peuportier (2012) discussed a related concept, 'positive energy building' (PEB), which combines energy savings with energy recovery from local renewable resources, such as solar radiation, wind, biomass or environmental heat from the environment. This system allows energy to be saved through the combination of a high level of insulation, heat recovery from extracted air, extremely airtight construction and the use of efficient equipment.

Energy regulations and energy certification programs are basic tools for the improvement of energy efficiency in buildings. They set energy efficiency requirements for the design and construction of new buildings and retrofitting of existing buildings (in the form of both extensions and renovations) and aim at minimising final energy consumption. Perez-Lombard *et al*. (2011) summarised the history, scope and development of building energy codes in different countries and defined a hierarchy of energy efficiency

© Woodhead Publishing Limited, 2013

requirements. Compliance with the section of the building energy codes dealing with Heat, Ventilation and Air Conditioning (HVAC) systems is the most important factor in ensuring that a building is energy efficient. Energy efficiency standards should also include a life cycle primary energy perspective, as discussed by Dodoo *et al*. (2011). A literature review of papers on energy-efficient building services can be found in Luck (2012).

The following measures for improving energy efficiency in buildings were proposed by Diakaki *et al*. (2008):

- Improvement of the building envelope (improvement of insulation, selection of optimal building colour and shape, installation of heat-insulating doors and windows, increase of thermal mass, etc.).
- Reduction of the heating and cooling loads (exploitation of the principles of bioclimatic architecture, incorporation of passive heating and cooling techniques, control of solar gains, mirror glazing, etc.).
- Use of 'intelligent' energy management, i.e. advanced sensors, energy control (zone heating and cooling) and monitoring systems.
- Use of renewable energy sources (solar thermal systems, geothermal energy, hybrid systems, etc.).
- Improvement of the indoor comfort conditions in parallel with minimisation of the energy requirements (increase of the ventilation rate, use of mechanical ventilation with heat recovery, improvement of boilers and air conditioning, efficient use of multi-functional equipment such as integrated water heating with space cooling, etc.).

In Process Integration terminology, the first three measures correspond to reactor and separation systems on the Onion Diagram, while the last two represent heat recovery and utilities systems. As mentioned previously, Process Integration technology is more beneficial in situations with more variables, where more heat exchanging streams and utilities are involved. There is even more room for improvement when a number of buildings are integrated in a building complex with a common energy supply and distribution system, or in large multipurpose buildings where a number of different services are involved.

31.3 Commercial and Public Buildings and Building Complexes

As mentioned previously, in OECD countries commercial and public buildings are responsible for up to 45% of the energy consumed in the buildings sector (see USDE (2011) for the US data). Most of these buildings contain a number of appliances that consume or generate energy, and many are situated in complexes such as universities, hospitals or hotels, where several

© Woodhead Publishing Limited, 2013

buildings are situated close to one an other and are under the same ownership. This makes them ideal candidates for energy improvements in the form of integrating CHP systems, combined cooling, heating and power (CCHP) systems, heat pumps (HP) and renewable sources of energy into their energy systems.

Medrano *et al*. (2008) investigated the potential for the implementation of distributed generation (DG) in commercial buildings in California. Using the computer program eQUEST, the hourly energy consumption of four types of commercial building was analysed, including office buildings, which account for 19% of the total energy consumption of commercial buildings in the USA (USDE 2011); hospitals, accounting for 8%, and education buildings, accounting for 11%. The results are presented in Figs 31.2 and 31.3.

The data clearly show that the energy demands in the buildings studied are not steady, but fluctuate over time. These variations differ significantly

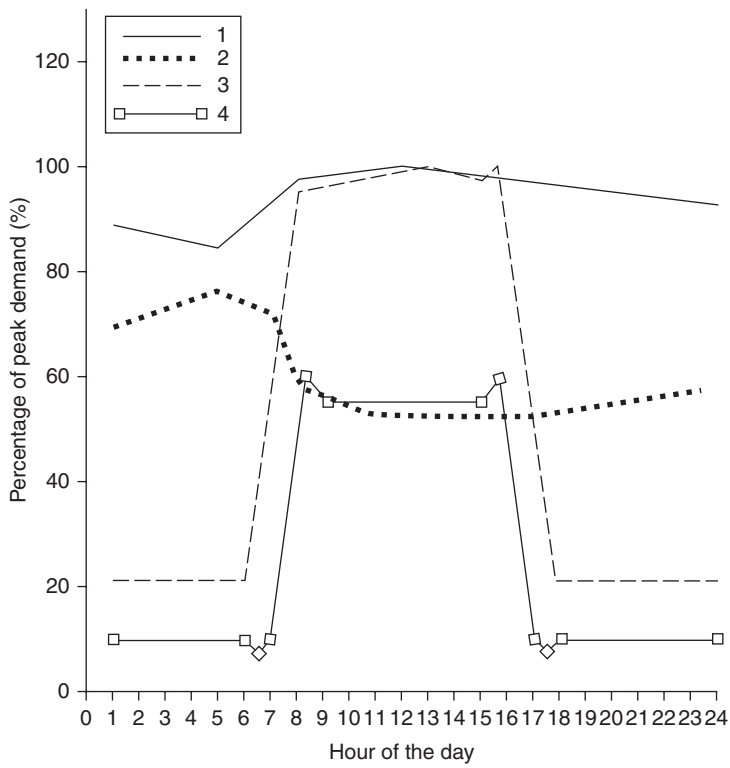

31.2 Example of electric power and natural gas hourly profiles (after Medrano *et al*. (2008)). Hospital (1 – electricity, 2 – gas) and medium office building (3 – electricity, 4 – gas).

© Woodhead Publishing Limited, 2013

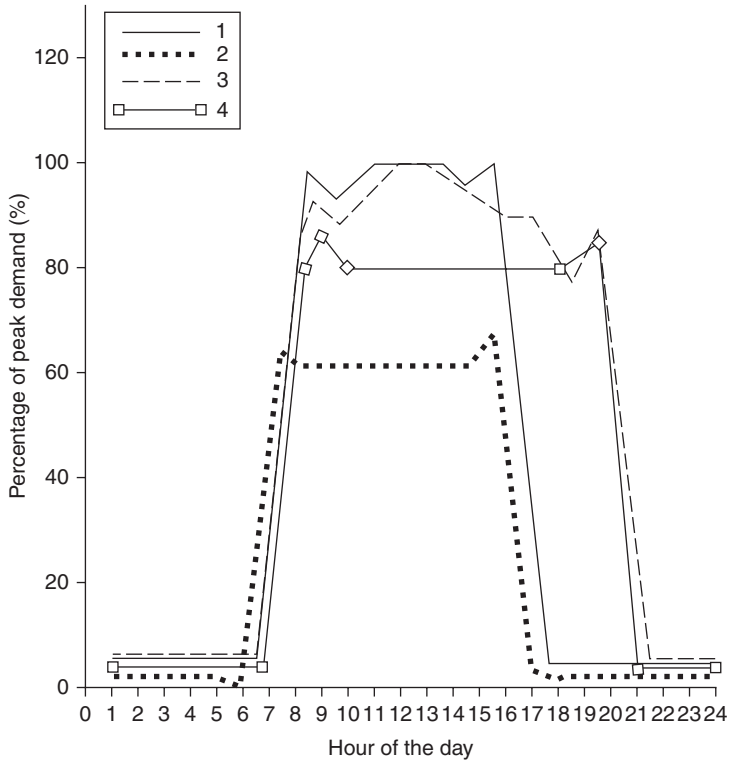

31.3 Example of electric power and natural gas hourly profiles (after Medrano *et al*. (2008)). Small office building (1 – electricity, 2 – gas) and college (3 – electricity, 4 – gas).

between buildings, and can also change with the time of year and climate conditions. In most cases these fluctuations are dependent on the energy load of the buildings; Fig. 31.4 shows a typical hourly distribution of the hot water supply in a residential apartment building.

Pinch Technology was originally developed for use in continuous steady state processes. When the energy demand of a building complex is not subject to particularly significant variation, the traditional steady Pinch Analysis can be used as an approximation. For example, Herrera *et al*. (2003) carried out a Pinch Analysis for the energy retrofit of a hospital in Mexico and reported a potential energy saving of 38%. The climatic conditions in Mexico mean that significant fluctuations in the energy demand due to marked differences in temperature do not occur (see Figs 31.2 and 31.3), which might explain the accurate results obtained using this method.

However, in buildings with a highly fluctuating energy demand, a more rigorous procedure is required. Kemp and Macdonald (1987) originally

© Woodhead Publishing Limited, 2013

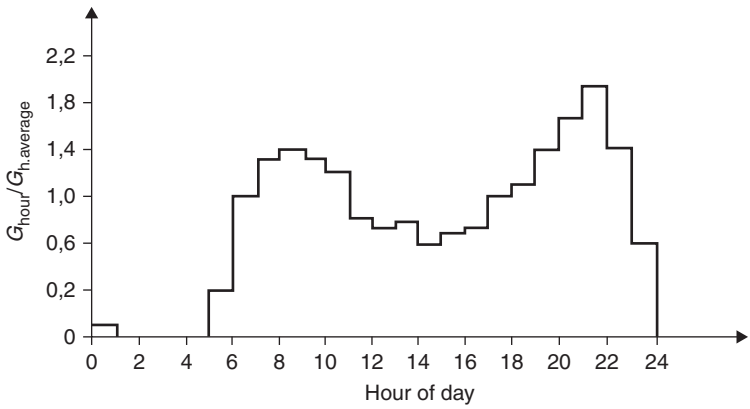

31.4 Hourly distribution of tap hot water demand in residential apartments building according to Tovazhnyanskyy *et al*. (2007, p. 119).

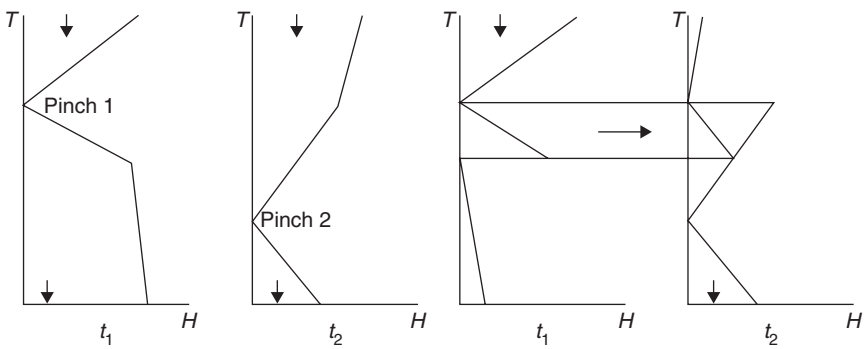

31.5 Heat transfer between time intervals by energy storage (after Kemp (1990)).

proposed Cascade Analysis, an extension of Pinch Analysis for Batch Processes, for this purpose. This method treats the energy process in a building as a 24 h cyclic Batch Process. The cycle is divided into time intervals, during which the process can be treated as continuous. For each time interval, called a cascade, targets are established for hot and cold utilities together with the local (instantaneous) Pinch Temperature. The individual cascades can then be presented in the same table, and their Composite Curves presented side by side on a graph. For example, Fig. 31.5 shows Composite Curves for two cascades (Kemp, 1990). When two processes in different time intervals have different Pinch Temperatures, heat can be recovered from one process Below the Pinch and transferred to another Above its Pinch. The amount of heat to be transferred can be calculated using the heat cascades for the two

© Woodhead Publishing Limited, 2013

processes. The heat can be stored for the duration of the time interval of the first process and released at the time interval of the second process, as shown in Fig. 31.5. Another option, which does not rely on heat storage, is to reschedule the process operations.

31.3.1 Building Complex Case Study

Kemp (1990, 2007) presented a case study in which Cascade Analysis was used in the energy retrofit of a hospital made up of a complex of buildings including a main building with wards, operating theatres, administrative offices, and other general departments, and also a boiler house, laundry and incinerator situated about 1 km away. The original energy demand of the hot utilities in the complex is presented in Fig. 31.6. After rescheduling the operation of the incinerator operation according to the results of the Cascade Analysis, a change in demand was observed, as shown in Fig. 31.7. As a result, different capital investments and payback period options for the energy retrofit were estimated, and are displayed in Table 31.1.

The case study shows that Process Integration methodology is useful in the energy analysis of buildings and building complexes. Process Integration can offer a number of benefits in the efficiency of utility systems, particularly through rescheduling the operations of different appliances, and can offer energy savings in the form of heat recuperation, especially if CHP systems can be integrated into the project.

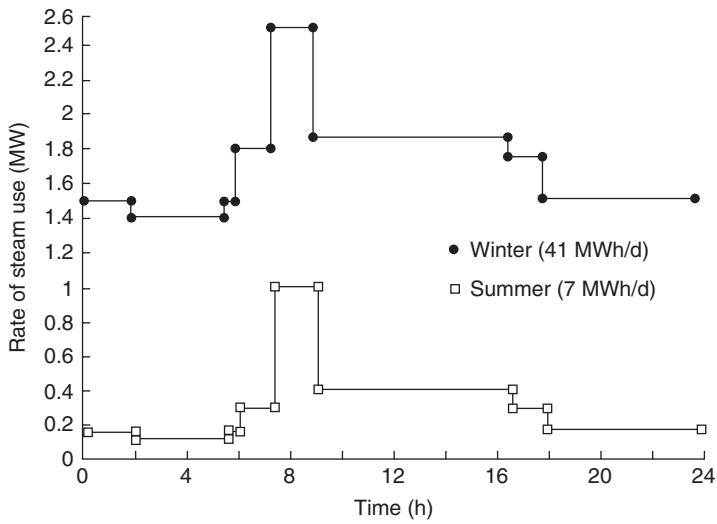

31.6 Variations of hot utility requirement during day, with original scheduling for case study of Kemp (1990).

© Woodhead Publishing Limited, 2013

Table 31.1 Options of energy retrofit for case study by Kemp (1990)

Project description	Savings (£/y)	Capital cost (£)	Payback time (y)
Incinerator heat recovery	14,000	15,000	1.1
With rescheduling	20,000	15,000	0.8
Other heat recovery projects	33,000	16,500	5.0
CHP with diesel engines	87,000	150,000	1.7
Standby generator conversion	100,000	500,000	5.0
New engine	187,000	650,000	3.5
Total for diesel CHP projects	250,000	900,000	3.6
CHP with gas turbine			

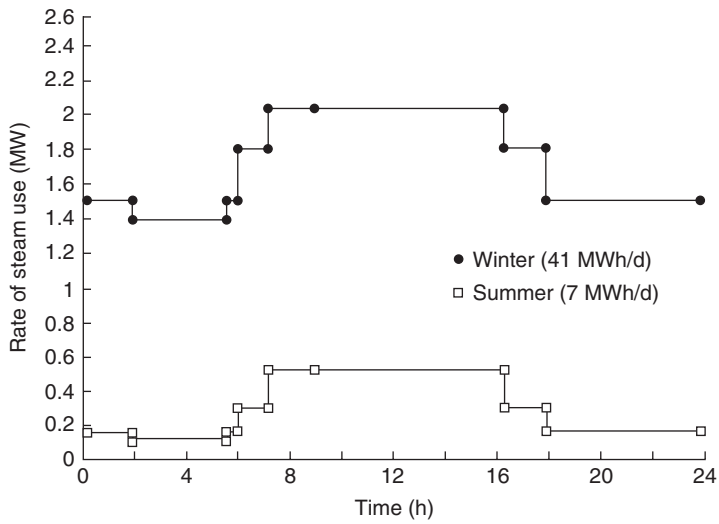

31.7 Variations of hot utility requirement during day after rescheduling of incinerator operations for case study of Kemp (1990).

31.4 District Energy (DE) Systems and Total Site Analysis (TSA)

Another aspect of Process Integration concerns those cases where buildings and their complexes, together with other generation facilities and consumers of energy, are constituent parts of a more complex energy system, through which they can receive and/or discharge energy. In many modern cities the energy supply and distribution for complexes of residential, public and commercial buildings is provided by District Heating systems or more generally DE systems, which offer promising opportunities for Process Integration.

© Woodhead Publishing Limited, 2013

31.4.1 District Energy Systems

To maintain the required energy balance in buildings or building complexes, a supply of both hot and cold utilities is required, which can be generated locally by local boilers, refrigerators and air conditioners. In these cases the options for Process Integration methodology are limited to those described in the previous section. In urban areas, where buildings of different kinds are situated in close proximity to one another, the supply of utilities can be provided, from a centralised distribution network, in the form of steam, hot water or chilled water. This is achieved through DE systems, which today represent the most energy-efficient means of supplying utilities in densely populated areas.

DE began as a system for heat supply, known as District Heating (DH). It can trace its roots as far back as the popular hot water-heated baths and greenhouses of ancient Rome, and systems of this sort have been used in Europe since the fourteenth century (Rezaie, 2012). The US Naval Academy constructed the first DH system on its Annapolis campus in 1853, and New York's commercial DH system was built in 1877. There are now approximately 700 DE systems functioning in the USA, according to the International Energy Agency (IEA, 2011). Northern European countries are the main users of DE systems. For instance, Sweden has installed a 40 TWh DH system, which supplied more than half of the heating capacity of the country in 2000 (Gebremedhin, 2003), while Denmark has more than 400 DH networks (Fruergaard *et al*., 2010). The percentage of homes relying on a DH system is around 65% in countries such as Latvia, Lithuania and Ukraine.

DE systems produce steam, hot water or chilled water, which is then piped underground to individual buildings for space heating, domestic hot water heating and air conditioning (IEA, 2012). Individual buildings served by a DE system do not require their own boilers or furnaces, chillers or air conditioners. The benefits offered by DE systems include:

- Improved energy efficiency: steam, hot water or chilled water arrives at a building ready to use. In addition, DE systems can use the 'reject heat' that results from burning fuel to produce electricity at a power plant. This CHP or 'cogeneration' system can produce heating and cooling as well as electricity for customers. A CHP system may have double the fuel efficiency of an electric generation plant and can also lower the emissions typically associated with conventional fossil-fuel powered electricity production.
- Enhanced environmental protection: the less energy is used, the less SO_2 and CO_2 and other emissions are expelled into the environment.
- Fuel flexibility.

© Woodhead Publishing Limited, 2013

- Ease of operation and maintenance.
- Reliability.
- Comfort and convenience.
- Decreased building capital cost.
- Improved architectural design flexibility.

31.4.2 Heat Integration in the Optimisation of DE Systems

A DE system consists of a number of heat producing and generating units, which can be regarded as analogous to an industrial enterprise in a given location. All these producers and consumers of heat energy are indirectly connected by heat agents moving through a system of pipes. To examine the indirect integration at the site level, a graphical method was introduced by Dhole and Linnhoff (1993), known as Site Source and Sink Profiles. These are generated based on the Grand Composite Curves (GCC) of the individual processes. Based on the hypothesis that the non-monotonic parts (pockets) of the GCCs represent the areas with the most scope for intra-process heat transfer, Dhole and Linnhoff (1993) proposed that these pockets should be eliminated from the process GCCs. In indirect integration, an intermediate fluid receives heat from one process and transfers it to a sink of another process. In the years following Dhole and Linnhoff's initial study, the TSA methodology was developed, as described in detail in Chapter 6 of this book.

Girardin *et al*. (2010) presented the principles of Pinch Analysis and Energy Integration applied to the development of an efficient DE system based on the Geographical Information System (GIS) framework. Taking the Geneva area as an example, authors classified buildings into eight different categories – residential, administrative, commercial, industrial, education, healthcare, tourism, etc. – further split into ten divisions according to the year of construction or renovation, leading to a total of 80 categories. For each category, the annual energy consumption for heating, hot water production, cooling and electricity was determined on the basis of a statistical analysis of the buildings. Based on these data, the building requirement model evaluated the heating and cooling loads as a function of the outdoor temperature.

An inventory of the available energy resources was also stored in the GIS database, to provide information on the availability of endogenous resources (lake and surface water, underground water, geothermal heat) or waste heat (waste water treatment plants or industries). Information on solar irradiation was combined with the available roof surface area and orientation, in order to estimate the solar potential in the area, and the available biomass

© Woodhead Publishing Limited, 2013

and potential wind energy were also taken into account. In addition, hot/cold distribution system costs were estimated based on the heat and power density in the different areas, allowing a comparison of centralised and decentralised polygeneration options, such as the integration of CHP systems and/or HPs. For each of these measurements, the year was divided into three periods: summer, mid-season, and winter. Process Integration methodology (Marechal and Kalitventzeff, 1998) was then applied, and heat–temperature Composite Curves were computed based on the list of buildings present in the area.

Figure 31.8 displays these heat–temperature Composite Curves for the district of Geneva. The dotted curves correspond to the targeted heat demand for 2030, based on a specific refurbishment and urban development scenario. Once the Composite Curves have been computed, Process Integration techniques may be used to estimate the optimal integration of the energy conversion technologies. This is particularly useful when the integration of CHP systems, HPs or polygeneration systems is considered. Together with the resources database, the calculation of the Composite Curves of an area in each period of the year corresponds to the structuring phase of the optimal design of DH systems as described by Weber *et al.* (2006).

The Composite Curves allowed the optimal supply temperatures to be identified for the DH system in the Geneva area. In order to maximise the efficiency of the system and to avoid having to base the network size on the

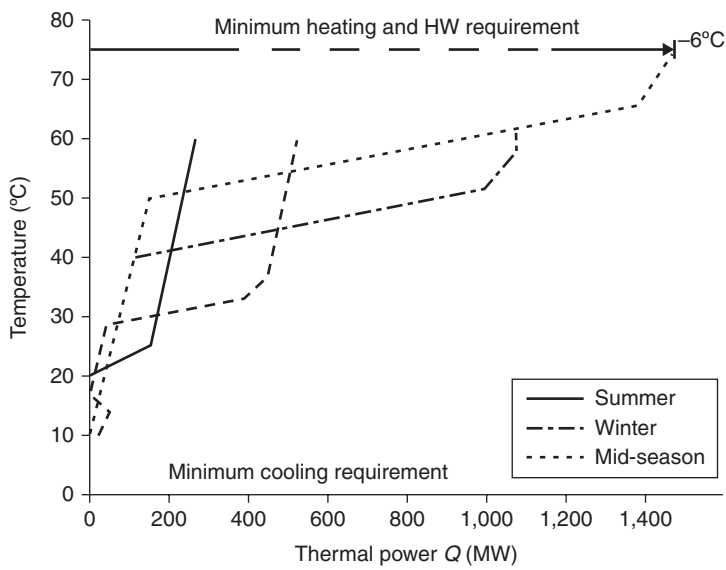

31.8 Composite Curves of the Geneva area: actual state and 2030 predictions (after Girardin *et al.*, 2010).

© Woodhead Publishing Limited, 2013

highest required temperature in a zone, decentralised HPs were judged to be a good option for local increases in the temperature of the distributed heat. The optimal heat distribution temperature can then be established on the basis of a combination of centralised and decentralised HPs. The results suggested that a combined cycle gas turbine and heat pump system was the best option for the DE system in Geneva. The advantages of this method have been confirmed by the improvement in energy consumption and generation levels, and by reduction in CO_2 emissions.

For the large scale integration of complex energy systems such as cities, Becker and Marechal (2011) proposed the use of a method that they had originally developed for industrial sites with some heat exchange restrictions. Using this method, which works on the principle of Total Site Integration, each district or location can be considered as a separate sub-system that requires heat transfer units to connect them and allow heat transfer: these units are the heating/cooling systems. Becker and Marechal (2011) formulate the problem as a Mixed Integer Linear Programming (MILP) problem, taking into account not only restricted matches but also the optimal integration of intermediate heat transfer units and the energy conversion system, such as HP and CHP. A mathematical formula is drawn up to enable the selection of optimal heat transfer technologies. For solutions avoiding the energy penalty, the Composite Curves of optimal heat transfer units must be embedded between the new hot and cold envelope Composite Curves. If the time average method is applied, non-simultaneous operations can be considered in different sub-systems in which direct heat exchange is not possible. To illustrate the application of this method, Becker and Marechal (2011) examine a dryer process in a paper production plant. However, in order for this method to be used for the implementation of DE systems in cities, further modifications are necessary.

31.5 The Use of Industrial Waste Heat

In Northern European countries such as Sweden, DH is well-established and covers more than 40% of the total heat demand for apartment blocks, detached houses and other buildings (Holmgren and Gebremedhin, 2004). Heat supplies from various sources have been extensively employed (Holmgren, 2006), and can also be used for the development and retrofit of new and existing DE systems. It has been shown that special attention should be paid to the integration of DE systems with the industrial sector, which plays a dual role, being in some cases a supplier of waste heat and in others a consumer. Of the total energy supply of 60 TWh used to produce DH, which heated buildings and tap water during 2004, –6 TWh originated from industrial excess heat (Klugman *et al*., 2009) and DH consumption within the industrial sector was 4.6 TWh (Holmgren and Gebremedhin,

© Woodhead Publishing Limited, 2013

2004). An analysis of the potential use of low-grade thermal energy from the process industry in the UK is presented by Ammar *et al*. (2012).

The integration of energy in the industrial sector is a task ideally suited to Process Integration TSA, but there has been rather limited work in the literature on the integration of waste heat with DH networks. The technical, economic and environmental feasibility of the integration of waste heat from the pharmaceutical industry using a DH network was evaluated by Ajah *et al*. (2007, 2008). They investigated the possibility of upgrading low-grade heat using chemical and mechanical HPs. Holmgren (2006) studied the impact of the integration of waste heat from industries, and waste incineration into the DH network. The waste heat from industry covered approximately 15% of the overall heat demand. However, these studies did not take into account the part load performance of the CHP system and the boiler.

Svensson *et al*. (2008) presented a method for evaluating the usage of the excess heat in a pulp mill to supply heat for a DH system; the application of the method is illustrated in Johnsson *et al*. (2008). They evaluated the various options involving the integration of new energy-efficient technologies, including process-integrated evaporation and drying, that were identified by Axelsson *et al*. (2006), with the aim of increasing the surplus energy from the pulp mill. This surplus heat can be either integrated within the process or exported. The study investigated the techno-economic impact of the integration of excess heat with a DH system. However, as shown by Kapil *et al*. (2012), the model proposed by Svensson *et al*. (2008), like previous works, does not account for the part load performance of CHP and boilers.

Kapil *et al*. (2012) proposed a new Heat Integration methodology that accounts for the fact that the integration of waste heat from a process site using a DH network reduces the heat produced by the DH itself. This decrease in energy production reduces the heat load on the CHP and the boilers, which then operate under partial load conditions. Partial load operation can also be caused by, for example, seasonal changes in heat load and electricity production. The economic feasibility of the integrated system is determined to a great extent by the part load performance in DH systems, which must therefore be evaluated in order to optimise the operational costs.

Depending on the relative cost of electricity and heat, power production, heat consumption and part load performance can affect one another. The electricity can be either imported or exported to the grid, depending on whether the DH produces a deficit or a surplus of electricity. The heat supplied by the DH system may include waste heat from industry, which is not available during shutdowns. Therefore, the DH supply should allow for additional capacity in order to maintain a continuous supply of heat during these shutdown periods. If heat demand is low, the CHP and boiler can operate at part load, once again confirming the importance of evaluating the part load performance of the generation equipment.

© Woodhead Publishing Limited, 2013

Kapil *et al*.'s (2012) proposed approach consists in applying TSA to an industrial site, modifying the Source and Sink Composite Curves according to the DH requirement for the supply line temperature. This method allows the identification of the industrial waste heat potential, which can be utilised by the DH system. The next step is mathematical modelling, taking into account variations in DH heat demand and the part load performance of the energy generating equipment. With the use of linear models, the optimisation problem is modelled as an MILP problem, with the operating energy cost as an objective function. The model can also accommodate the variability of Total Site Profiles in different seasons, but this feature is not used in the case studies presented in this work.

The two case studies presented by Kapil *et al*. (2012) are both somewhat hypothetical in nature but nevertheless provide a detailed description of the methodology. The authors used the Total Site data from a case study of industrial site utility systems and associated site-wide energy use presented in a previous study. The data are then integrated with (1) the DH network of Linköping city, described by Rolfsman (2004); and (2) a large hospital complex studied by Perry *et al*. (2008). The Composite Curves for the industrial site studied in the original work are shown in Fig. 31.9.

For the first case study the amount of low-grade heat available for DH at a temperature higher than 105°C is 62.11 MW. The temperature of 105°C corresponds to a supply temperature of 90°C and a minimum approach temperature of 15°C. A Site Source Profile below 105°C is shifted by 62.11

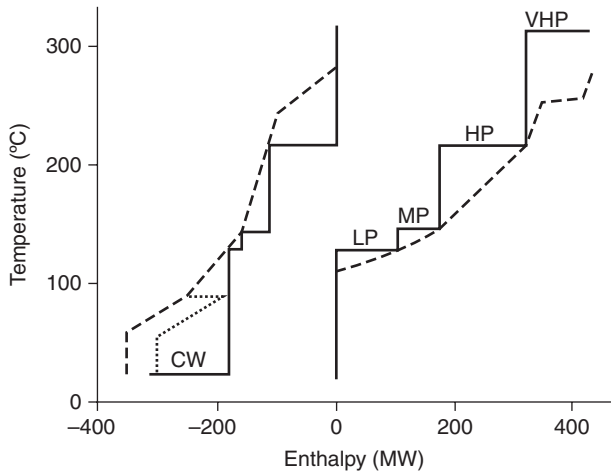

31.9 Site Source and Sink Composite Curve (dashed lines) and low grade heat available from the site profiles (dotted line) for DH (Kapil *et al.*, 2012). Solid lines show site steam composites: VHP – very high pressure steam; HP – high pressure; MP – medium pressure; LP – low pressure; CW - cooling water.

© Woodhead Publishing Limited, 2013

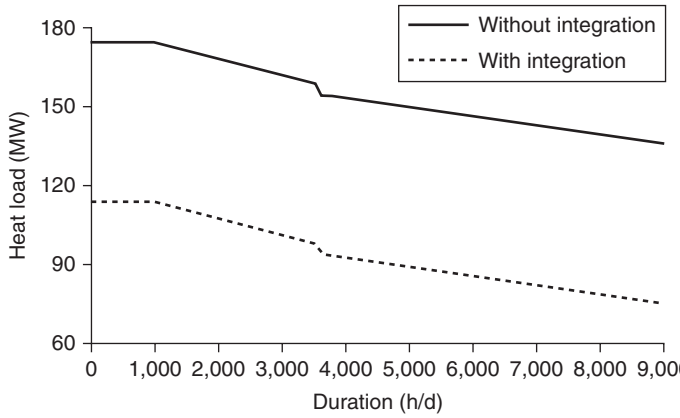

31.10 Heat supply with and without integration of waste heat for case study 1 of paper by Kapil *et al*. (2012).

MW to account for the extraction of low-grade energy, and hence the cooling water (CW) requirement for the Total Site decreases by 62.11 MW. The calculated optimised heat supply lines, with and without integration of waste heat, are presented in Fig. 31.10. It is clear that a significant reduction in the amount of heat required from the DH generation equipment is achieved. From an environmental point of view this leads to a considerable reduction in CO_2 emissions, a fact which is not discussed in Kapil *et al*. (2012).

However, there are economic disadvantages associated with this method: the revenue for the DH system is generated by selling electricity to the grid and heat to DH consumers, and from the consumption of waste through incineration, while the system expenditure is composed of fuel (oil and coal). The integration of waste heat with DH decreases the thermal load. This, in turn, reduces the part load on the CHP units, which leads to a decrease in annual electricity production. Electricity revenue consequently falls from 56.5 to 49.26 M$/y. There is also a decrease in the utilisation of waste fuel to produce steam from the boiler. Therefore, after integration of waste heat from industry, the overall annual operating energy revenue from the DH system falls from $202.53 to $193.26 M/y. This shows that, for any optimised DH system already in use which has installed generating capacities, a detailed analysis should be carried out before any decisions are made regarding Industrial Waste Heat Integration. Although beneficial for the environment, thanks to the reduction in CO_2 emissions, renovation is not always cost-effective, and can also create problems with the utilisation of municipal waste.

Thollander *et al*. (2010) used an example of a DH system in Sweden to analyse the factors influencing collaborations between DH and industry, and also reviewed previous studies in this field. Despite the complexity of

© Woodhead Publishing Limited, 2013

all the technological and economic aspects of the system, they came to the conclusion that establishing effective collaboration between industry and DH has more to do with the individuals and organisations involved in the relationship than with the technology used.

The importance of energy collaboration between different companies in achieving improvements in energy efficiency is emphasised in a paper by Hackl *et al*. (2011), who analysed Sweden's largest chemical cluster using the TSA method. The methodology allows the investigation of different options for the delivery of waste heat from one process to another using a common utility system, and can also provide the basis for Heat Integration within a larger geographical area, which may include building complexes, offices and residences, in addition to industrial sites. The accuracy of the method is limited by the fact that it assumes that the processes within the cluster are all running at steady state, and that all the processes are running simultaneously. Changes in loads and temperatures depending on factors such as the production rate, maintenance or changes in the product are therefore not considered, and neither is the part-time operation of DH generating equipment.

The work of Kapil *et al*. (2012) shows that Process Integration technology is a valuable tool for estimation of energy targets when integrating complex energy systems, including DH networks. However, the best results can be achieved by combining this methodology with computer modelling and the MILP optimisation technique. Special attention should be paid to the retrofit of DE systems that have already been optimised by other methods, or on the basis of different models, for the optimisation of municipal energy systems; see, for example, Rolfsman (2004). The DH system used in Linköping, discussed above, was optimised during its development in a number of ways, using the technologies available at the time. One of these techniques is described in Rolfsman (2004), who used the MILP approach to analyse the optimisation of home insulation, fuels and generating equipment in Linköping for the year 1996. At that time the city had 130,000 inhabitants, with a requirement of about 1 TWh of DH.

By 2007 the population of Linköping had grown to 140,000 inhabitants, and the heat requirement increased to 1.7 TWh, with a projected demand of 1.9 TWh in 2025, according to Difs *et al*. (2010). So now the hypothetical industrial waste heat from the paper mill, as studied by Kapil *et al*. (2012), would prove extremely useful. Since this type of heat resource is not available for the area of Linköping, Difs *et al*. (2010) considered an alternative valuable renewable energy source, namely biomass gasification. For this purpose a model of the DH system was constructed using the energy system optimisation tool MIND (Method for analysis of industrial energy systems). The analysis examined the profitability for the DH supplier, as well as consequences for global CO_2 emissions, both in the short-term (up to 2012) and

© Woodhead Publishing Limited, 2013

the medium term (up to 2025). The Linköping case study clearly shows the importance of correctly predicting future energy demands, particularly in a growing city.

The MIND method, which is based on MILP, and its coordination with Pinch Technology in an iterative procedure, is described in more detail by Bengtsson *et al*. (2002). The MIND method and Pinch Technology work on two different system levels, so their coordination provides improved information for undertaking changes to the process. The methodology is in line with that proposed by Kapil *et al*. (2012) and with all industrial Process Integration approaches that involve close interaction with process simulation software. The study also emphasises the need for new developments in the Process Integration technique when it is employed for the integration of various energy sources, especially renewables, into the energy systems of buildings.

31.6 Renewable Energy for Buildings

The need to minimise fossil-fuel consumption and environmental hazards from CO_2 and greenhouse gas emissions is recognised worldwide. The EC DIRECTIVE 2010/31/EU reaffirms the commitment to the EU-wide development of energy from renewable sources by endorsing a mandatory target of a 20% share of energy from renewable sources by 2020. Directive 2009/28/EC establishes a common framework for the promotion of energy from renewable non-fossil sources, namely wind, solar, aerothermal, geothermal, hydrothermal and ocean energy, hydropower, biomass, landfill gas, sewage treatment plant gas and biogases.

Lund *et al*. (2010) analysed different scenarios for the development of energy systems in Denmark up to 2060 with the aim of finally achieving 100% renewable energy system (100% RES). The research, based on the GIS method, has shown that a substantial reduction in fuel demands and CO_2 emissions as well as cost can be achieved by raising the percentage of heating in Denmark supplied by DH from 46% up to 70%. They identified the main potential sources of renewable energy in that area as biomass, HPs for upgrading low-grade heat, waste incineration and the use of waste heat from industry, with further prospects for solar energy, geothermal heating and biogas production.

Sperling and Moller (2012) also emphasised the role of DH in the potential for achieving a 100% RES system in Denmark. They reported a study into the 'Energy City' project in Frederikshaven, which aims to establish a 100% RES system by 2015. Using the EnergyPLAN model (Lund, 2010b) the study investigated different scenarios for the development of the town's energy system. Their conclusion is that the implementation of 100% RES in general, particularly the redesign of DH systems, will involve detailed, strategic energy planning by municipalities and local utility providers at the

© Woodhead Publishing Limited, 2013

level of individual DH networks. Building and maintaining municipal heat atlases is one way to tackle this problem and to revive a more strategically oriented method for municipal heat planning.

Of the renewable energy sources, geothermal energy has been in use the longest with DH systems, having been used in the continuous operation of Chaudes-Aigues thermal station in France since the fourteenth century (Rezaie, 2012). A comprehensive review of the direct utilisation of geothermal energy was carried out by Lund *et al*. (2011). The total amount of directly utilised geothermal energy in 2010 was 117,778 GWh, with Iceland, China, Turkey, France and Russia making the greatest direct use of this type of energy. In addition to direct utilisation worldwide, a further 67,246 GWh was used for electricity generation in 2010 (Bertani, 2012).

A systematic methodology for the optimal design of geothermal energy systems involving a Process Integration procedure was proposed by Gerber and Marechal (2012). The method requires that the potential resources for the area are known, based on previous geological data. To represent the seasonal variations of the demand in energy, the yearly operation is divided into four periods corresponding to different average ambient temperatures. Then the resources and demand profiles are integrated using Process Integration techniques and an MILP problem is solved to minimise the operating cost of the system for each single period. Based on the results of the Process Integration step, indicators of thermo-economic performance are calculated for each period and then combined to obtain the yearly overall performance of the system. Using a multi-objective optimisation strategy all the clusters corresponding to the potential combinations of resources and technologies are evaluated, and a Pareto curve calculated for each. The results obtained using this methodology demonstrate the potential for the exploitation of deep geothermal resources and their integration in urban energy systems for CHP production.

Biomass is another important source of renewable energy. According to the estimation of Haberl *et al*. (2011) for different scenarios up to 2050, the gross bioenergy potential ranges from 64 to 161 EJ/y, depending on climate impact, yields and diet, while the dependency on cropland expansion is weak. They concluded that the food requirements of a growing population, and in particular the feed required for livestock, strongly influence the potential of bioenergy. Integrated approaches are required to optimise food and bioenergy supply. A number of researchers have investigated and assessed different options for biomass usage in DH systems; see for example Fahlén (2009). The use of this renewable source of energy opens up the possibility of retrofitting existing fossil-fuel heating plants; see for example Kalina (2010).

A review of the state-of-the-art in solar-based and ground source-based renewable energy systems, with optimum performances to reduce

© Woodhead Publishing Limited, 2013

conventional energy usage in sustainable buildings, is presented in Shi *et al*. (2012). As shown in the study by Faninger (2000), overcoming the mismatch between solar-energy supply and energy demand requires the implementation of thermal storage in a solar system. Biomass is proposed as an optimal form of seasonal storage for solar energy and an attractive auxiliary fuel for solar heating systems. A case study of a single family low-energy house has shown that in solar-assisted heating systems the annual solar share for space heating and hot water can reach 36.5%. Up to August 1998, 12 solar-assisted biomass DH plants with a collector area of 225–1,250 m^2 were in operation in Austria. The solar share for space heating and hot water preparation is only about 14% of the annual average, but the solar share for hot water preparation outside the heating season is more than 80%.

A procedure for regional renewable energy and resource planning was proposed by Lam *et al*. (2011). Using Regional Energy Cascade Analysis, their proposed method estimates the energy target within regional supply chains and provides results for energy exchange flows between zones, the quantity of energy required to be imported/exported, and the locations of the demands. The study shows that the renewable resources are usually available on a smaller scale and distributed over a given area. Their availability (with the exception of biomass and geothermal energy) is usually well below maximal values, and varies significantly with time and location. The energy demands (heating, cooling and power) of the sites under consideration vary significantly with time of the day and period of the year. As a result, optimising energy conversion systems using renewable resources is more complex than when using just fossil fuels. One way of levelling out the inherent variations and efficiently satisfying demands is to combine the supply and demand streams of the individual users in larger systems as in the Total Sites system, which may serve industrial plants as well as buildings. An extension of this system has been developed by Perry *et al*. (2008), who added residential and service-building processes to the traditional scope of Total Sites, allowing low-grade industrial heat and renewable sources of energy to be utilised. This enables the application of the Total Site Integration strategy to local communities involving a number of smaller-scale entities and is referred to as the Locally Integrated Energy Sector.

Examining the combination of systems at the local level, Varbanov and Klemeš (2011) proposed a methodology that takes into account variation in demand and availability of renewables, and simultaneously maximises heat recovery. It is based on Total Site Integration and allows Heat Storage possibilities to be considered. For temporal variations dynamic modelling elements and concepts very similar to those used for Batch Processes are introduced, including terms such as horizon and time slice (interval).

The time variations of energy demands have been studied in both industrial and residential contexts. Data relating to the variation in the energy

© Woodhead Publishing Limited, 2013

consumption of commercial buildings provided by Medrano *et al*. (2008) is a useful example (see Figs 31.2 and 31.3), as is the data relating to hot tap water consumption in residential apartment blocks (Tovazhnyanskyy *et al*., 2007) shown in Fig. 31.4. There are two types of trends: hourly variations during each day, and seasonal variations during the year. For the hourly variations (Fig. 31.4) there are nearly steady periods during the usual office hours and two consumption peak intervals in the morning and in the evening. The seasonal variations are relatively smooth, with more substantial space heating demands from October until April in both studies. Demand variations are mostly predictable. However, there are differences between the patterns observed for residential and commercial buildings, industrial sites and farms.

Varbanov and Klemeš (2011) assessed the overall availability of renewables and their variability over time. Some values were found to be close to those of fossil fuels: for example, geothermal energy varies little over time; while biomass can be well stored for continuous energy generation. Biomass supply varies according to the season and the availability of biowaste. However, sufficient storage could be made available. The availability of other renewable sources such as wind and solar can vary more rapidly, changing by the hour or even in a matter of minutes. These types of variation require an extension of the Total Site methodology to account for the fact that the changes have different time horizons. For biomass, the Time Slices needed would have a duration in the order of months, or weeks as a minimum. For wind and solar energy, the time slice durations will obviously be much shorter (Nemet *et al*., 2011). The procedure is based on optimising the load-levels and selecting items from a discrete superset of candidate time boundaries (Nemet *et al*., 2012).

To establish an efficient procedure for the dynamic energy targeting of Total Sites, the various heat sources and sinks on the site are assessed. The heating and cooling demands of individual processes that remain after internal Heat Integration are used to create the Heat Source Profile and the Heat Sink Profile for an industrial site. When utilities are placed against targeting profiles, it is necessary to account for the generation of each utility carrier from process heat sources or its consumption by process heat sinks. The potential for utility generation is represented by the Site Source Composite Curve and the potential for consumption by the Site Sink Composite Curve (Klemeš *et al*., 2010). When the process energy generated for a certain utility becomes insufficient to cover the demand, the two curves can be displaced and part of the demand for the current utility are left to be covered by a different utility at a higher temperature. Then, some of the low pressure steam generated should be used to cover the hot water requirement. Further up the temperature scale, the remaining unused low pressure steam generated from the

© Woodhead Publishing Limited, 2013

process is, in turn, insufficient to cover demand and some medium pressure steam from the site boilers is used to make up the shortfall. This utilisation of higher temperature utilities to satisfy lower temperature utility requirements is known as utility cascading. Varbanov and Klemeš (2011) proposed a concise representation of utility cascading, with more comprehensive diagrams providing views of complete systems, coining the term 'utility interval'.

Integrating the renewables requires a new kind of Total Sites system that is able to take into account the distributed availability of the renewables and the need to maximise the reuse of any available waste heat in a given area. This requires minimising the transportation of the energy and limiting the scale of the capture facilities. As a result, some of the processes to be integrated have lower temperature heating demands, which can be satisfied with hot water. Hot water is a non-isothermal utility that must be adequately represented by the targeting methodology.

To handle the variability observed, a piecewise approximation of the demands is used. The site integration parameters are represented in a piecewise constant, revealing the need to set up a time horizon for the model and to further partition it into Time Slices (Nemet *et al*., 2011). Total Site Targeting is performed within each time slice. One important feature is that some Time Slices may have a heat excess that can be transferred to later Time Slices or lower temperatures. This type of heat transfer from an earlier time slice to a later one is implemented using heat storage. Energy storage is a complicated issue (Verda and Colella, 2011), which could in part be solved by Heat Integration methodology, which can provide targets to be achieved.

Varbanov and Klemeš (2011) proposed the following overall procedure for Targeting Total Sites with temporal variations and renewables.

(i) Analyse the temporal variations in the heating and cooling demands of the site processes (plants, buildings, farms) and partition the modelling horizon into Time Slices.
(ii) Assume initially that no heat is stored before the first time slice for all utility types.
Steps (iii) and (iv) are performed for each Time Slice:
(iii) Obtain the Heat Integration targets for each process unit.
(iv) Obtain the Total Site Utility Targets using the Total Site Heat Cascade, Total Site Profiles and Site Composite Curves.
(v) For cyclic operation, the heat transfer flow from the time slice in the Total Site Heat Cascade should be fed (recycled) to the first Time Slice. At this point, a reiteration of step (iv) is needed until the values of the heat transfers to the first time slice become equal to or sufficiently close to those of the heat transfers from the last Time Slice.

© Woodhead Publishing Limited, 2013

(vi) Identify the target for energy storage capacity for each utility type using the heat transfer flows between the Time Slices in the Total Site Heat Cascade. For each utility type the heat storage capacity will be equal to the largest heat transfer flow between Time Slices.
The procedure is illustrated in Varbanov and Klemeš (2011) using a case study.

31.7 Conclusion

Buildings are among the principal consumers of energy. A reduction in their energy consumption will lead to savings in fossil-fuel usage and a significant drop in greenhouse gases and CO_2 emissions.

Pinch Analysis and Process Integration methodology proved to be useful in improving energy efficiency in buildings.

The application of Process Integration must be carried out in combination with computer modelling and MILP.

Process Integration can be most successfully implemented in building complexes and DE systems.

To achieve best results heat exchangers with enhanced heat transfer should be used. PHEs have proved to be both reliable and efficient in this respect.

Further developments in Process Integration methodology are required to optimise its use in increasing the energy efficiency of buildings, particularly with regard to the integration of renewable energy sources and waste heat from the industrial sector.

31.8 Sources of Further Information and Advice

The importance of reducing the energy consumption of buildings and building complexes has been recognised in many countries worldwide, who have in turn adopted a selection of appropriate policies. Useful information on these policies with regard to the member states of the EU can be found in the DIRECTIVE 2010/31/EU on the Energy Performance of Buildings, which is representative of many similar directives elsewhere. A detailed description of the construction and use of low-energy buildings with minimal energy losses and maximal use of renewable energy sources can be found in the very useful handbook by Harvey (2006). Process Design and Process Integration are covered in detail in books authored by Smith (2005) and Kemp (2007); also recommended for Russian-speaking readers is the title by Smith *et al*. (2000). Klemeš *et al*. (2010) discusses these issues in a broader context of sustainability. Finally, useful discussions of recent developments and trends in DE systems and the use of renewable energy sources can be found in papers by Kapil *et al*. (2011) and Nemet *et al*. (2012).

© Woodhead Publishing Limited, 2013

31.9 References

Ajah, A. N., Mesbah, A., Grievink, J., Herder, P. M., Falcao, P. W., Wennekes, S. (2008). On the robustness, effectiveness and reliability of chemical and mechanical heat pumps for low-temperature heat source district heating: A comparative simulation-based analysis and evaluation. *Energy*, **33**, 908–929.

Ajah, A. N., Patil, A. C., Herder, P. M., Grievink, J. (2007). Integrated conceptual design of a robust and reliable waste-heat district heating system. *Applied Thermal Engineering*, **27**, 1158–1164.

Ammar, Y., Joyce, S., Norman, R., Wang, Y., Roskilly, A. P. (2012). Low grade thermal energy sources and uses from the process industry in the UK. *Applied Energy*, **89**, 3–20.

Ascione, F., de Rossi, F., Vanoli, P. G. (2011). Energy retrofit of historical buildings: theoretical and experimental investigations for the modelling of reliable performance scenarios. *Energy and Buildings*, **43**, 1925–1936.

Axelsson, E., Olsson, M. R., Berntsson, T. (2006). Heat integration opportunities in average Scandinavian kraft pulp mills: pinch analyses of model mills. *Nordic Pulp and Paper Research Journal*, **21**(4), 466–75.

Balaras, C. A., Droutsa, K., Dascalaki, E., Kontoyiannidis, S. (2005). Heating energy consumption and resulting environmental impact of European apartment buildings. *Energy and Buildings*, **37**, 429–442.

Becker, H., Maréchal, F. (2011). Energy integration of industrial sites with heat exchange restrictions. *Computers and Chemical Engineering*, **37**, 104–118, doi:10.1016/j.compchemeng.2011.09.014

Bengtsson, C., Karlsson, M., Berntsson, T., Söderström, M. (2002). Co-ordination of pinch technology and the MIND method – applied to a Swedish board mill. *Applied Thermal Engineering*, **22**, 133–144.

Bertani, R. (2012). Geothermal power generation in the world 2005–2010 update report. *Geothermics*, **41**, 1–29.

Dhole, V. R., Linnhoff, B. (1993). Total site targets for fuel, co-generation, emissions, and cooling. *Computers and Chemical Engineering*, **17**(suppl.), 101–109.

Diakaki, C., Grigoroudis, E., Kolokotsa, D. (2008). Towards a multi-objective optimisation approach for improving energy efficiency in buildings. *Energy and Buildings*, **40**, 1747–1754.

Difs, K., Wetterlund, E., Trygg, L., Söderström, M. (2010). Biomass gasification opportunities in a district heating system. *Biomass and Bioenergy*, **34**, 637–651.

Directive 2010/31/EU of the European Parliament and of the Council of 19 May 2010 on the energy performance of buildings. *Official Journal of the European Union*, 18.6.2010, Brussels, Belgium.

Dodoo, A., Gustavsson, L., Sathre, R. (2011). Building energy-efficiency standards in a life cycle primary energy perspective. *Energy and Buildings*, **43**, 1589–1597.

Eurostat. (2011). Eurostat regional yearbook 2011. Available from: <ec.europa.eu/energy/publications/statistics/> Accessed 20 January 2012.

Fesanghary, M., Asadi, S., Geem, Z. W. (2012). Design of low-emission and energy-efficient residential buildings using multi-objective optimisation algorithm. *Building and Environment*, **49**, 245–250.

Fahlén E, Ahlgren, E. O. (2009). Assessment of integration of different biomass gasification alternatives in a district-heating system. *Energy*, **34**, 2184–2195.

Faninger, G. (2000). Combined solar-biomass district heating in Austria. *Solar Energy*, **69**(6), 425–435.

© Woodhead Publishing Limited, 2013

Fruergaard, T., Christensen, T. H., Astrup, T. (2010). Energy recovery from waste incineration: assessing the importance of district heating networks. *Waste Management*, **30**, 1264–1272.

Gebremedhin, A. (2003). The role of a paper mill in a merged district heating system. *Applied Thermal Engineering*, **23**, 769–78.

Gerber, L., Maréchal F (2012). Defining optimal configurations of geothermal systems using process design and process integration techniques. *Applied Thermal Engineering*, **43**, 29–41.

Girardin, L., Marechal, F., Dubuis, M., Calame-Darbellay, N., Favrat, D. (2010). EnerGis: a geographical information based system for the evaluation of integrated energy conversion systems in urban areas. *Energy*, **35**, 830–840.

Haberl, H., Erb, K.-H., Krausmann, F., Bondeau, A., Lauk, C., Muller, C., Plutzar, C., Steinberger, J. K. (2011). Global bioenergy potentials from agricultural land in 2050: sensitivity to climate change, diets and yields. *Biomass and Bioenergy*, **35**, 4753–4769.

Hackl, R., Andersson, E., Harvey, S. (2011). Targeting for energy efficiency and improved energy collaboration between different companies using total site analysis (TSA). *Energy*, **36**, 4609–4615.

Harvey, L. D. D. (2006). *A Handbook on Low-energy Buildings and District Energy Systems: Fundamentals, Techniques, and Examples*. Earthscan (James and James), London, UK.

Herrera, A., Islas, J., Arriola, A. (2003). Pinch technology application in a hospital. *Applied Thermal Engineering*, **23**, 127–139.

Holmgren, K. (2006). Role of a district-heating network as a user of waste-heat supply from various sources – the case of Goteborg. *Applied Energy*, **83**, 1351–1367.

Holmgren, K., Gebremedhin, A. (2004). Modelling a district heating system: introduction of waste incineration, policy instruments and co-operation with an industry. *Energy Policy*, **32**, 1807–1817.

Hong, T. (2009). A close look at the China design standard for energy efficiency of public buildings. *Energy and Buildings*, **41**, 426–435.

IEA. (2011). (International Energy Agency). Energy Balances of OECD Countries – 2011 Edition, Paris.

IEA. (2012). International Energy Agency. Available from <www.iea-dhc.org/> Accessed 20 January 2012.

Jönsson J, Svensson, I. L., Berntsson, T., Moshfegh, B. (2008). Excess heat from kraft pulpmills: trade-offs between internal and external use in the case of Sweden. Part 2: results for future energy market scenarios. *Energy Policy*, **36**(11), 4186–97.

Kalina, J. (2010). Retrofitting of municipal coal fired heating plant with integrated biomass gasification gas turbine based cogeneration block. *Energy Conversion and Management*, **51**, 1085–1092.

Kanagaraj, G., Mahalingam, A. (2011). Designing energy efficient commercial buildings – a systems framework. *Energy and Buildings*, **43**, 2329–2343.

Kapil, A., Bulatov, I., Smith, R., Kim, J.-K. (2012). Process integration of low grade heat in process industry with district heating networks. *Energy*, **44**, 11–19.

Kapustenko, P. O., Ulyev, L. M., Boldyryev, S. A., Garev, A. O. (2008). Integration of a heat pump into the heat supply system of a cheese production plant. *Energy*, **33**, 882–889.

Kemp, I. C. (1990). Applications of the time-dependent cascade analysis in process integration. *Heat Recovery Systems and CHP*, **10**(4), 423–435.

© Woodhead Publishing Limited, 2013

Kemp, I. C. (2007). *Pinch Analysis and Process Integration. A User Guide on Process Integration for Efficient Use of Energy*. Elsevier, Amsterdam, The Netherlands. (authors of the first edition: Linnhoff, B., Townsend, D. W., Boland, D., Hewitt, G. F., Thomas, B. E. A., Guy, A. R., Marsland, R. H. (1982 and 1994). *A User Guide on Process Integration for the Efficient Use of Energy.* IchemE, Rugby, UK).

Kemp, I. C., MacDonald, E. K. (1987). Energy and process integration in continuous and batch processes. *IChemE Symposium Series*, **105**, 185–200.

Klemeš, J., Friedler, F., Bulatov, I., Varbanov, P. (2010). *Sustainability in the Process Industry: Integration and Optimisation*. McGraw Hill Companies Inc., New York, USA.

Klugman, S., Karlsson, M., Moshfegh, B. (2009). A Swedish integrated pulp and paper mill – energy optimisation and local heat cooperation. *Energy Policy*, **37**, 2514–2524.

Lam, H. L., Varbanov, P. S., Klemeš, J. J. (2011). Regional renewable energy and resource planning. *Applied Energy*, **88**, 545–550.

Luck, K. (2012). Energy efficient building services for tempering performance-oriented interior spaces – a literature review. *Journal of Cleaner Production*, **22**, 1–10.

Lund, H. (2010). *EnergyPLAN – advanced energy systems analysis computer model – documentation version 8.0*. Aalborg, Aalborg University. <energy.plan.aau.dk/EnergyPLAN-Version8-February2010.pdf> accessed 26.02.12.

Lund, H., Möller B., Mathiesen, B. V., Dyrelund, A. (2010). The role of district heating in future renewable energy systems. *Energy*, **35**, 1381–1390.

Lund, J. W., Freeston, D. H., Boyd, T. L. (2011). Direct utilization of geothermal energy 2010 worldwide review. *Geothermics*, **40**, 159–180.

Marechal, F., Kalitventzeff, B. (1998). Energy integration of industrial sites: tools, methodology and application. *Applied Thermal Engineering*, **18**, 921–933.

Marszal, A. J., Heiselberg, P., Bourrelle, J. S., Musall, E., Voss, K., Sartori, I., Napolitano, A. (2011). Zero Energy Building – a review of definitions and calculation methodologies. *Energy and Buildings*, **43**, 971–979.

Medrano, M., Brouwer, J., McDonell, V., Mauzey, J., Samuelsen, S. (2008). Integration of distributed generation systems into generic types of commercial buildings in California. *Energy and Buildings*, **40**, 537–548.

Molin, A., Rohdin, P., Moshfegh, B. (2011). Investigation of energy performance of newly built low-energy buildings in Sweden. *Energy and Buildings*, **43**, 2822–2831.

Nemet, A., Klemeš, J. J., Varbanov, P. S. (2011). Methodology for maximising the use of renewables with variable availability. *Computer Aided Chemical Engineering*, **28**, 1944–1948.

Nemet, A., Klemeš, J. J., Varbanov, P. S., Kravanja, Z. (2012). Methodology for maximising the use of renewables with variable availability. *Energy*, **44**(1), 29–37.

Pérez-Lombard, L., Ortiz, J., Coronel, J. F., Maestre, I. R. (2011). A review of HVAC systems requirements in building energy regulations. *Energy and Buildings*, **43**, 255–268.

Perry, S., Klemeš J., Bulatov, I. (2008). Integrating waste and renewable energy to reduce the carbon footprint of locally integrated energy sectors. *Energy*, **33**(10), 1489–97.

© Woodhead Publishing Limited, 2013

Poirazis, H., Blomsterberg, E., Wall, M. (2008). Energy simulations for glazed office buildings in Sweden. *Energy and Buildings*, **40**, 1161–1170.

Raftery, P., Keane, M., Costa, A. (2011). Calibrating whole building energy models: detailed case study using hourly measured data. *Energy and Buildings*, **43**, 3666–3679.

Rezaie, B., Rosen, M. A. (2012). District heating and cooling: review of technology and potential enhancements. *Applied Energy*, **93**, 2–10.

Rolfsman, B. (2004). Optimal supply and demand investments in municipal energy systems. *Energy Conversion and Management*, **45**(4), 595–611.

Shi, L., Chew, M. Y. L. (2012). A review on sustainable design of renewable energy systems. *Renewable and Sustainable Energy Reviews*, **16**, 192–207.

Smith, R. (2005), *Chemical Process Design and Integration*. Wiley and Sons Ltd, Chichester, UK.

Smith, R., Klemeš, J., Tovazhnyanskyy, L. L., Kapustenko, P. O., Ulyev, L. M. (2000). *Foundations of Heat Processes Integration.* Kharkiv, NTU KhPI, Ukraine (In Russian).

Sperling, K., Möller, B. (2012). End-use energy savings and district heating expansion in a local renewable energy system – a short-term perspective. *Applied Energy*, **92**, 831–842.

Svensson, I. L., Jönsson, J., Berntsson, T., Moshfegh, B. (2008). Excess heat from kraft pulp mills: trade-offs between internal and external use in the case of Sweden part 1: methodology. *Energy Policy*, **36**(11), 4178–4185.

Thiers, S., Peuportier, B. (2012). Energy and environmental assessment of two high energy performance residential buildings. *Building and Environment*, **51**, 276–284.

Thollander, P., Svensson, I. L., Trygg, L. (2010). Analyzing variables for district heating collaborations between energy utilities and industries. *Energy*, **35**, 3649–3656.

Tovazshnyanskyy, L. L., Kapustenko, P. O., Khavin, G. L., Arsenyeva, O. P. (2007). *Plate Heat Exchangers in Heat Supply.* Kharkiv, NTU KhPI, Ukraine (in Russian).

USDE. (2011). 2010 Buildings Energy Data Book. D&R International, Ltd. Available from: <buildingsdatabook.eren.doe.gov/docs> Accessed 20 January 2012.

Varbanov, P. S., Klemeš, J. J. (2011). Integration and management of renewables into Total Sites with variable supply and demand. *Computers and Chemical Engineering*, **35**, 1815–1826.

Verda, V., Colella, F. (2011). Primary energy savings through thermal storage in district heating networks. *Energy*, **36**, 4278–4286.

Weber, C., Heckl, I., Friedler, F., Marechal, F., Favrat, D. (2006). Network synthesis for a district energy system: a step towards sustainability. *Computer Aided Chemical Engineering*, **21**, 1869–1874.

Yiqun, P. Y., Rongxin, Y., Huang, Z. (2008). Energy modeling of two office buildings with data center for green building design. *Energy and Buildings*, **40**, 1145–1152.

Zeng, R., Wang, X., Di, H., Jiang, F., Zhang, Y. (2011). New concepts and approach for developing energy efficient buildings: ideal specific heat for building internal thermal mass. *Energy and Buildings*, **43**, 1081–1090.

© Woodhead Publishing Limited, 2013

32

Heat Transfer Enhancement in Heat Exchanger Networks

ROBIN SMITH, MING PAN and IGOR BULATOV,
The University of Manchester, UK

DOI: 10.1533/9780857097255.5.966

Abstract: Heat transfer can be intensified in shell-and-tube heat exchangers for improved heat transfer performance. Such intensification has been widely studied from the point of view of individual heat exchangers (HEs). The use of heat transfer enhancement in Process Integration has many benefits. First, enhanced heat exchangers require less heat transfer area for a given heat duty because of higher heat transfer coefficients. Second, the heat transfer capacity for the given HE can be increased without changing physical size of the exchanger. Third, the use of enhancement can reduce pumping requirement in some cases, as enhanced HE can achieve higher overall heat transfer coefficients with lower velocities, which may lead to lower friction losses. Using enhancement techniques has practical advantages in Heat Exchanger Network (HEN) retrofit, as it can avoid modification of the network structure. The implementation of enhancement is a relatively simple task that can be easily achieved within a normal maintenance period, allowing production losses to be kept to a minimum level and no civil engineering requirement. This chapter provides an introduction to the enhancement methods of commercial shell-and-tube heat exchangers and their engineering application. The key aspects of enhancing shell-and-tube heat exchangers in HEN retrofit are presented and illustrated with examples involving both energy saving and fouling considerations.

Key words: Heat Exchanger Network (HEN), retrofit, Heat Integration, heat transfer enhancement, energy saving, shell-and-tube heat exchanger, optimisation, fouling.

32.1 Introduction to Shell-and-Tube Heat Exchangers

Shell-and-tube heat exchangers are the most widely used type in the process industries. Consideration here will be restricted to this type. For the simulation of shell-and-tube exchangers, the most commonly used methods include the Bell-Delaware method (Taborek, 1988), the simplified Tinker method (ESDU Ltd., 1984) and the Wills-Johnston method (Wills and Johnston, 1984). These have only addressed liquid phase heat transfer

© Woodhead Publishing Limited, 2013

so far. In this chapter, consideration will be restricted to heat exchange between streams in the liquid phase. For other phases (e.g. condensation), more information can be found in the following literature. Cavallini *et al*. (2003) reviewed the most recent thermal designs of condensers for the air conditioning and refrigeration industry, where both in tube and bundle condensation are considered, related to the use of plain and enhanced surfaces. Allen and Gosselin (2008) presented a model for estimating the total cost of shell-and-tube heat exchangers with condensation in tubes or in the shell, as well as a designing strategy for minimising this cost. Serth (2007) stated that a boiling fluid consisting of a two-phase mixture of vapour and liquid is more complex than single-phase flow, and special methods are needed to calculate the pressure drop in equipment handling boiling fluids.

To predict HE performances, it is necessary to calculate the overall heat transfer coefficient and pressure drop for both fluids. Understanding of fluid behaviour on the tube-side is relatively straightforward. Well-known correlations, such as the Colburn correlation (Bhatti and Shah, 1987), the Dittus-Boelter correlation (Bhatti and Shah, 1987) and the Plain Tube Pressure Drop method (Serth, 2007) are sufficiently accurate for tube-side calculations. The methods commonly used for shell-side calculations include the Bell-Delaware method (Taborek, 1988), the Developed Delaware method (Gnielinski *et al*., 1998), the Chart method (Ayub, 2005), the simple Delaware method (Kern and Kraus, 1972), the simplified Tinker method (ESDU Ltd., 1984) and the Wills-Johnston method (Wills and Johnston, 1984). However, those methods for the shell-side often result in significantly different heat transfer coefficients and pressure drops, compared with commercial software (e.g. HTRI®). Thus, a new simulation model (Wang *et al*., 2012) has been developed to respond to this fundamental need for a more reliable model for estimating the performance of shell-and-tube exchangers.

32.1.1 Modelling of Shell-and-Tube Heat Exchangers

In the new model (Wang *et al*., 2012), heat transfer coefficients and pressure drops of the tube-side are calculated firstly, and then improved models of the Chart method (Ayub, 2005) and the simple Delaware method (Kern and Kraus, 1972) are used for shell-side calculations. Figure 32.1 describes the geometric details of shell-and-tube heat exchangers, where L is the tube length, B is the baffle spacing, B_{in} is the inlet baffle spacing, B_{out} is the outlet baffle spacing, n_b is the baffle number, D_{no} is the shell-side nozzle diameter, D_{ni} is the tube-side nozzle diameter, P_T is the tube pitch, D_s is the shell diameter, D_i is the tube inner diameter, D_0 is the tube outer diameter, L_{sb} is the shell-bundle clearance, n_t is the tube number, Bc is the baffle cut and n_p is the tube passes.

© Woodhead Publishing Limited, 2013

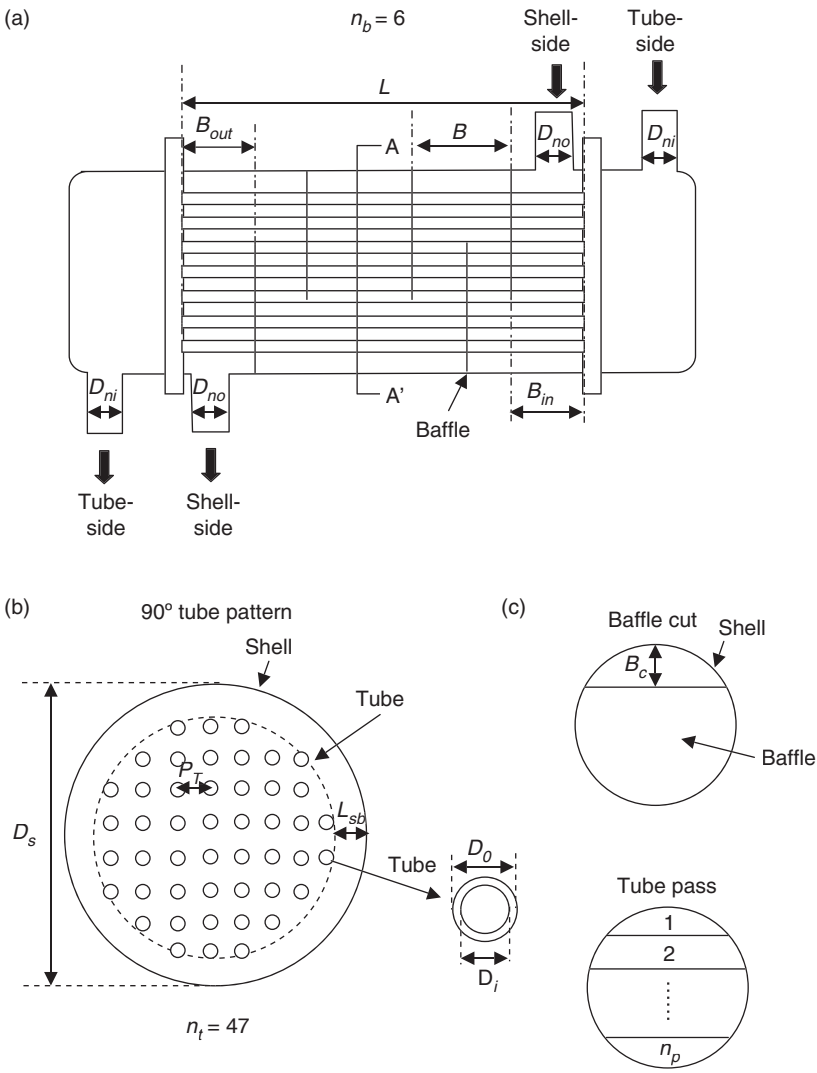

32.1 Geometry specifics of shell-and-tube heat exchanger (Wang *et al*., 2012). (a) Shell-and-tube heat exchanger; (b) A-A′ (tube bundle) and (c) A-A′ (baffle cut and tube pass). L: tube length, B: baffle spacing, B_{in}: inlet baffle spacing, B_{out}: outlet baffle spacing, n_b: baffle number, D_{no}: shell-side nozzle diameter, D_{ni}: tube-side nozzle diameter, P_T: tube pitch, D_s: shell diameter, D_i: tube inner diameter, D_0: tube outer diameter, L_{sb}: Shell-bundle clearance, n_t: tube number, B_c: baffle cut, n_p: tub.

© Woodhead Publishing Limited, 2013

Tube-Side Heat Transfer Coefficient

To calculate the tube-side heat transfer coefficient, the velocity (v_i), Reynolds number (Re_i) and Prandtl number (Pr_i) of the tube-side need to be obtained first, as in Equations [32.1]–[32.3], where D_i is the tube inner diameter; $\overline{m}_i$ is the mass flowrate of tube-side fluid; n_p and n_t are the numbers of tube passes and tubes, respectively. For tube-side fluid properties, specific heat capacity (C_{pi}), viscosity (μ_i), fluid density (ρ_i) and thermal conductivity (k_i) are evaluated at the average bulk fluid temperature.

$$v_i = \frac{\overline{m}_i (n_p / n_t)}{p_i (\pi D_i^2 / 4)} \quad [32.1]$$

$$\mathrm{Re}_i = \frac{D_i v_i \rho_i}{\mu_i} \quad [32.2]$$

$$\mathrm{Pr}_i = \frac{C_{pi} \mu_i}{k_i} \quad [32.3]$$

Equation [32.4] shows the correlation of the tube-side Nusselt number (Nu_i) based on the Dittus-Boelter correlation (Bhatti and Shah, 1987), in which some of the original parameters for cooling have been updated, and L is tube length.

$$\mathrm{Nu}_i = \begin{cases} 0.024\,\mathrm{Re}_i^{0.8}\,\mathrm{Pr}_i^{0.4} & \text{for heating} \\ 0.023\,\mathrm{Re}_i^{0.8}\,\mathrm{Pr}_i^{0.4} & \text{for cooling} \end{cases} \cdot \mathrm{Re}_i \geq 10^4 \quad [32.4]$$

$$\mathrm{Nu}_i = 0.116\left(\mathrm{Re}_i^{2/3} - 125\right)\mathrm{Pr}_i^{1/3}\left[1 + \left(\frac{D_i}{L}\right)^{2/3}\right] \cdot 2{,}100 < \mathrm{Re}_i < 10^4 \quad [32.5]$$

$$\mathrm{Nu}_i = 1.86\left[\mathrm{Re}_i\,\mathrm{Pr}_i\left(\frac{D_i}{L}\right)\right]^{1/3} \cdot \mathrm{Re}_i \leq 2{,}100 \quad [32.6]$$

Then, the tube-side heat transfer coefficient (h_i) can be calculated:

$$h_i = \left(\frac{k_i}{D_i}\right) \times \mathrm{Nu}_i \quad [32.7]$$

© Woodhead Publishing Limited, 2013

Tube-Side Pressure Drop

There are three major elements to the tube-side pressure drop. These are the pressure drop due to fluid friction in the tube straight sections (ΔP_{fi}), the pressure drop due to the tube entrance, exit and return losses (ΔP_r) and the pressure drop in the nozzles (ΔP_{ni}).

The pressure drop due to friction loss (ΔP_{fi}) is based on the Darcy friction factor (f_i) (Serth, 2007), where g_c is the unit conversion factor, which is equal to 1.0 kg·m/(N·s^2).

$$f_i = 0.4137\,\text{Re}_i^{-0.2585} \quad \text{Re}_i \geq 3{,}000 \tag{32.8}$$

$$f_i = \frac{64}{\text{Re}_i} \cdot \text{Re}_i < 3{,}000 \tag{32.9}$$

$$\Delta P_{\text{fl}} = \frac{n_p f_i L \rho_i v_i^2}{2 g_c D_i} \tag{32.10}$$

Equations [32.11]–[32.13] present the pressure drop related to the tube entrance, exit and return losses (ΔP_r) (Serth, 2007). α_r is the number of velocity heads allocated for minor losses.

$$\alpha_r = 2n_p - 1.5 \text{ for turbulent flow} \tag{32.11}$$

$$\alpha_r = 3.25n_p - 1.5 \text{ for laminar flow} \tag{32.12}$$

$$\Delta P_r = \frac{0.5\alpha_r \rho_i v_i^2}{g_c} \tag{32.13}$$

To estimate the pressure drop in the nozzles (ΔP_{ni}), the inlet and outlet nozzles should be considered separately, as shown in Equations [32.14]–[32.21] (Serth, 2007).

$$v_{\text{ni,inlet}} = \frac{\overline{m}i}{\rho_i \left(\pi D_{\text{ni,inlet}}^2 / 4\right)} \tag{32.14}$$

$$\text{Re}_{\text{ni,inlet}} = \frac{D_{\text{ni,inlet}} v_{\text{ni,inlet}} \rho_i}{\mu_i} \tag{32.15}$$

© Woodhead Publishing Limited, 2013

$$\Delta P_{\mathrm{ni,inlet}} = \frac{0.375 N_S \rho_i v_{\mathrm{ni,inlet}}^2}{g_c} \text{ for turbulent flow} \quad [32.16]$$

$$\Delta P_{\mathrm{ni,inlet}} = \frac{0.75 N_S \rho_i v_{\mathrm{ni,inlet}}^2}{g_c} \text{ for laminar flow} \quad [32.17]$$

where $v_{\mathrm{ni,inlet}}$ is the velocity of inlet nozzle on the tube-side, $D_{\mathrm{ni,inlet}}$ is the inner diameter of the inlet nozzle on the tube-side, N_S is the number of shell passes and $\Delta P_{\mathrm{ni,inlet}}$ is the pressure drop of the inlet nozzle on the tube-side.

$$v_{\mathrm{ni,outlet}} = \frac{\overline{m}i}{\rho_i \left(\pi D_{\mathrm{ni,outlet}}^2 / 4\right)} \quad [32.18]$$

$$\mathrm{Re}_{\mathrm{ni,outlet}} = \frac{D_{\mathrm{ni,outlet}} v_{\mathrm{ni,outlet}} \rho_i}{\mu_i} \quad [32.19]$$

$$\Delta P_{\mathrm{ni,outlet}} = \frac{0.375 N_S \rho_i v_{\mathrm{ni,outlet}}^2}{g_c} \text{ for turbulent flow} \quad [32.20]$$

$$\Delta P_{\mathrm{ni,outlet}} = \frac{0.75 N_S \rho_i v_{\mathrm{ni,outlet}}^2}{g_c} \text{ for laminar flow} \quad [32.21]$$

where $v_{\mathrm{ni,outlet}}$ is the velocity of the outlet nozzle on the tube-side, $D_{\mathrm{ni,outlet}}$ is the inner diameter of the outlet nozzle on the tube-side and $\Delta P_{\mathrm{ni,outlet}}$ is the pressure drop of the outlet nozzle on the tube-side.

The pressure drop in the nozzles (ΔP_{ni}) is given by:

$$\Delta P_{\mathrm{ni}} = \Delta P_{\mathrm{ni,inlet}} + \Delta P_{\mathrm{ni,outlet}} \quad [32.22]$$

Based on Equations [32.8]–[32.22], the overall tube-side pressure drop (ΔP_i) is obtained.

$$\Delta P_i = \Delta P_{\mathrm{fi}} + \Delta P_r + \Delta P_{\mathrm{ni}} \quad [32.23]$$

Shell-Side Heat Transfer Coefficient

Ayub (2005) proposed a chart method to calculate the shell-side heat transfer coefficient in a single segmental shell-and-tube heat exchanger.

© Woodhead Publishing Limited, 2013

This method was based on a graphical representation of a wide range of actual exchanger data. The author also demonstrated that the results from this method agreed well with HTRI® (Ayub, 2005). However, as shell-side heat transfer coefficient information is only presented in a chart without numerical correlations, the chart method cannot be readily applied in a mathematical simulation and optimisation studies. Therefore, Equations [32.32] and [32.33], are set up in this section, based on the chart presented by Ayub (2005). As shown in Ayub's work, the shell-side heat transfer coefficient (h_0) can be calculated from:

$$h_0 = \frac{F_s F_p F_L k_0^{2/3} (C_{p0}\mu_0)^{1/3}}{UC_1 \times D_0} \quad [32.24]$$

$$F_p = 0.85 \quad [32.25]$$

$$F_L = 0.90 \quad [32.26]$$

where D_0 is the tube outer diameter, and UC_1 is the unit conversion factor converting British units to SI units, which is equal to 16.11. Shell-side fluid properties, specific heat capacity (C_{p0}), viscosity (μ_0), fluid density (ρ_0) and thermal conductivity (k_0) are evaluated at the average bulk fluid temperature.

The factor F_z is defined as:

$$F_z = \frac{\rho_0 D_0 v_{h0}}{\mu_0 \times UC_2} \quad [32.27]$$

$$v_{ho} = \frac{\overline{m}_0}{\rho_0 S_{hm}} \quad [32.28]$$

where $\overline{m}_0$ is the mass flow rate for the shell-side fluid; v_{h0} is the velocity of the shell-side fluid used for calculating the heat transfer coefficient; UC_2 is the unit conversion factor for converting British units to SI units and equals 124.1251; and S_{hm} is the shell-side cross-flow area for calculating v_{h0}.

S_{hm} of 90° tube layout angle is calculated as:

$$D_{\text{otl}} = D_s - L_{sb} \quad [32.29]$$

$$N_{PT,90°} = \text{even}\left\lceil \frac{D_{\text{otl}} - D_0}{P_T} \right\rceil \quad [32.30]$$

© Woodhead Publishing Limited, 2013

$$S_{hm,90^\circ} = B\left[\frac{D_s - N_{PT,90^\circ}P_T - D_0}{2} + N_{PT,90^\circ}(P_T - D_0)\right] \quad [32.31]$$

where the function even$\lceil X \rceil$ returns the largest even number not larger than X, L_{sb} is the diameter clearance between the shell and the tube bundle, D_{otl} is bundle outer diameter, P_T is tube pitch and B is central baffle spacing.

The relationship of factors F_s, F_z and baffle cut (B_c) is given in the chart proposed by Ayub (2005), in which F_s is the function of F_z and B_c. The correlations of F_s, B_c and F_z are formulated as:

$$F_s = -9.2223F_z^2 + 76.78F_z + 17.793, \cdot F_z \le 2 \quad [32.32]$$

$$F_s = 34.4783F_z^{0.6633}B_c^{-0.5053}, \cdot 2 < F_z \le 1{,}000 \quad [32.33]$$

Shell-Side Pressure Drop

The simplified Delaware method (Kern and Kraus, 1972) uses fewer empirical equations, but provides accurate results (Serth, 2007), compared to other methods, for a wide operating range of the shell-side diameter and the flow velocity. The simplified Delaware method (Kern and Kraus, 1972) is a relatively simple method, but only suitable for 20% baffle cut scenarios. In this section, new additional correlations of the shell-side cross-flow area (Equations [32.35] and [32.36]) and the relationships between pressure drop and baffle cut (Equations [32.45]–[32.47]) are added to guarantee that the simplified Delaware method can be used for larger baffle cuts. The shell-side pressure drop consists of the pressure drop due to fluid friction in the straight section of shell (ΔP_{f0}) and the pressure drop in the nozzles (ΔP_{n0}).

Equation [32.34] is based on the simplified Delaware method, which presents the pressure drop in one central baffle spacing when the baffle cut is 20% ($\Delta P_{fb,20\%Bc}$).

$$\Delta P_{fb,20\%Bc} = \frac{f_0 D_s \rho_0 v_{p0}^2}{2g_c D_e} \quad [32.34]$$

where f_0 is shell-side friction factor, D_e is equivalent diameter and v_{p0} is the velocity of shell-side fluid used for calculating the pressure drop.

Similar to the estimation of the shell-side heat transfer, v_{p0} depends on S_{pm} (the shell-side cross-flow area) when calculating the pressure drop and S_{pm} also varies with different tube layout angles:

© Woodhead Publishing Limited, 2013

For 90° tube layout angle:

$$S_{\mathrm{pm},90^\circ} = B\left[\frac{D_s - D_{\mathrm{otl}}}{2} + \frac{D_{\mathrm{otl}} - D_0}{P_T}(P_T - D_0)\right] \cdot D_s \le 0.7\mathrm{m} \quad [32.35]$$

$$S_{\mathrm{pm},90^\circ} = B\left[D_s - D_{\mathrm{otl}} + \frac{D_{\mathrm{otl}} - D_0}{P_T}(P_T - D_0)\right] D_s > 0.7\,\mathrm{m} \quad [32.36]$$

Then, the velocity of the shell-side fluid (v_{p0}) can be calculated as:

$$v_{p0} = \frac{\overline{m}_0}{\rho_0 S_{\mathrm{pm}}} \quad [32.37]$$

Equations [32.38]–[32.42] present the equivalent diameter (D_e), related Reynolds number (Re_0) and friction factors.

$$D_e = \frac{4(P_T^2 - \pi D_0^2/4)}{\pi D_0} \text{ for square pitch} \quad [32.38]$$

$$\mathrm{Re}_0 = \frac{D_e \rho_0 v_{p0}}{\mu_0} \quad [32.39]$$

$$f_0 = 144\left[f_1 - 1.25\left(1 - \frac{B}{D_s}\right)(f_1 - f_2)\right] \quad [32.40]$$

$$f_1 = (0.0076 + 0.00653543 D_s)\,\mathrm{Re}_0^{-0.125} \cdot D_s = 0.7 \quad \text{if} \quad D_s \ge 0.7\,\mathrm{m} \quad [32.41]$$

$$f_2 = (0.0016 + 2.2835 \times 10^{-3} D_s)\,\mathrm{Re}_0^{-0.157}, D_s = 0.59 \text{ if } D_s \ge 0.59\,\mathrm{m} \quad [32.42]$$

The pressure drop in the straight section of the shell with 20% baffle cut ($\Delta P_{f0,20\%Bc}$) can be determined in Equations [32.43] and [32.44].

$$\Delta P_{f\,0,20\%Bc} = (n_b - 1)\Delta P_{fb} + R_s \Delta P_{fb} \quad [32.43]$$

$$R_s = \left(\frac{B}{B_{\mathrm{in}}}\right)^{1.8} + \left(\frac{B}{B_{\mathrm{out}}}\right)^{1.8} \quad [32.44]$$

© Woodhead Publishing Limited, 2013

where R_s is the correction factor for unequal baffle spacing, B is the central baffle spacing, B_{in} and B_{out} are the inlet and outlet baffle spacings, respectively.

To consider the pressure drop in the straight section with different baffle cuts (ΔP_{f0}), new correlations are proposed in Equations [32.45]–[32.47].

$$\Delta P_{f0} = \Delta P_{f0,20\%Bc}\left(\frac{B_c}{20\%}\right)^{-0.26765}, 20\% < B_c \le 30\% \quad [32.45]$$

$$\Delta P_{f0} = \Delta P_{f0,20\%Bc}\left(\frac{B_c}{20\%}\right)^{-0.36106}, 30\% \le B_c < 40\% \quad [32.46]$$

$$\Delta P_{f0} = \Delta P_{f0,20\%Bc}\left(\frac{B_c}{20\%}\right)^{-0.58171}, 40\% \le B_c \le 50\% \quad [32.47]$$

The pressure drop in the shell-side nozzles can be determined in the same correlations as for calculating the pressure drops in the tube-side nozzles (Serth, 2007).

$$v_{n0,\text{inlet}} = \frac{\overline{m}_0}{\rho_0\left(\pi D_{n0,\text{inlet}}^2/4\right)} \quad [32.48]$$

$$\text{Re}_{n0,\text{inlet}} = \frac{D_{n0,\text{inlet}} v_{n0,\text{inlet}} \rho_0}{\mu_0} \quad [32.49]$$

$$\Delta P_{n0,\text{inlet}} = \frac{0375 N_s \rho_0 v_{n0,\text{inlet}}^2}{g_c} \text{ for turbulent flow} \quad [32.50]$$

$$\Delta P_{n0,\text{inlet}} = \frac{075 N_s \rho_0 v_{n0,\text{inlet}}^2}{g_c} \text{ for laminar flow} \quad [32.51]$$

where $v_{n0,\text{inlet}}$ is the velocity of inlet nozzle on the shell-side, $D_{n0,\text{inlet}}$ is the inner diameter of the inlet nozzle on the shell-side, N_S is the number of shell passes and $\Delta P_{n0,\text{inlet}}$ is the pressure drop of the inlet nozzle on the shell-side.

$$v_{n0,\text{outlet}} = \frac{\overline{m}_0}{\rho_0\left(\pi D_{n0,\text{outlet}}^2/4\right)} \quad [32.52]$$

© Woodhead Publishing Limited, 2013

$$\mathrm{Re}_{n0,\mathrm{outlet}} = \frac{D_{n0,\mathrm{outlet}} v_{n0,\mathrm{inlet}} \rho_0}{\mu_0} \quad [32.53]$$

$$\Delta P_{n0,\mathrm{outlet}} = \frac{0.375 N_s \rho_0 v_{n0,\mathrm{outlet}}^2}{g_c} \text{ for turbulent flow} \quad [32.54]$$

$$\Delta P_{n0,\mathrm{outlet}} = \frac{0.75 N_s \rho_0 v_{n0,\mathrm{outlet}}^2}{g_c} \text{ for laminar flow} \quad [32.55]$$

where $v_{n0,\mathrm{outlet}}$ is the velocity of the outlet nozzle on the shell-side, $D_{n0,\mathrm{outlet}}$ is the inner diameter of the outlet nozzle on the shell-side and $\Delta P_{n0,\mathrm{outlet}}$ is the pressure drop of the outlet nozzle on the shell-side.

The pressure drop in the nozzles (ΔP_{n0}) can be presented as:

$$\Delta P_{n0} = \Delta P_{n0,\mathrm{inlet}} + \Delta P_{n0,\mathrm{outlet}} \quad [32.56]$$

Based on the above equations, the shell-side pressure drop (ΔP_0) is obtained.

$$P_0 = \Delta P_{f0} + \Delta P_{n0} \quad [32.57]$$

U, *Logarithmic Mean Temperature Difference (LMTD),* F_T *and* A

The overall heat transfer coefficient (U) can be calculated with Equation [32.58], where k_{tube} is tube conductivity, R_{Di} and R_{D0} are the fouling resistances of the tube-side and shell-side.

$$U = \left[\frac{D_0}{h_i D_i} + \frac{D_0 \ln\left(D_0/D_i\right)}{2k_{\mathrm{tube}}} + \frac{1}{h_0} + \frac{R_{D_i} D_0}{D_i} + R_{D0} \right]^{-1} \quad [32.58]$$

Before the LMTD is considered, the outlet temperature of the shell-side ($T_{0,\mathrm{outlet}}$) is set as an initial estimated value, and then this will be iterated and updated accordingly. The outlet temperature of the tube-side ($T_{i,\mathrm{outlet}}$) can be calculated based on energy balances.

$$\overline{m}_0 C_{p0} (T_{0,\mathrm{outlet}} - T_{0,\mathrm{inlet}}) = \overline{m}_i C_{pi} (T_{i,\mathrm{outlet}} - T_{i,\mathrm{inlet}}) \quad [32.59]$$

© Woodhead Publishing Limited, 2013

where $T_{0,\text{inlet}}$ is the inlet temperature of the shell-side and $T_{i,\text{inlet}}$ is the inlet temperature of the tube-side.

LMTD is the mean temperature difference between the two fluid streams, which is given in Equation [32.60].

$$\text{LMTD} = \frac{\left|T_{0,\text{inlet}} - T_{i,\text{outlet}}\right| - \left|T_{0,\text{outlet}} - T_{i,\text{inlet}}\right|}{\ln\left(\left|T_{0,\text{inlet}} - T_{i,\text{outlet}}\right| / \left|T_{0,\text{outlet}} - T_{i,\text{inlet}}\right|\right)} \quad [32.60]$$

In multi-tube-pass heat exchangers, the flow pattern includes both counter and co-current flows and, therefore, the mean temperature difference is not equal to the logarithmic mean when tube passes are more than one, and the correction factor of *LMTD* (F_T) is used (Serth, 2007).

$$R = \frac{T_{0,\text{inlet}} - T_{0,\text{outlet}}}{T_{i,\text{outlet}} - T_{i,\text{inlet}}} \quad [32.61]$$

$$P = \frac{T_{i,\text{outlet}} - T_{i,\text{inlet}}}{T_{0,\text{inlet}} - T_{i,\text{inlet}}} \quad [32.62]$$

For $R \neq 1$:

$$\alpha = \left(\frac{1 - RP}{1 - P}\right)^{1/N,} \quad [32.63]$$

$$S = \frac{\alpha - 1}{\alpha - R} \quad [32.64]$$

$$F_T = \frac{\sqrt{R^2 + 1}\ln\left((1 - S)/(1 - RS)\right)}{(R - 1)\ln\left[2 - S\left(R + 1 - \sqrt{R^2 + 1}\right)/2 - S\left(R + 1 + \sqrt{R^2 + 1}\right)\right]} \quad [32.65]$$

For $R = 1$:

$$S = \frac{P}{N_s - (N_s - 1)P} \quad [32.66]$$

$$F_T = \frac{S\sqrt{2}}{(1 - S)\ln\left[2 - S\left(2 - \sqrt{2}\right)/2 - S\left(2 + \sqrt{2}\right)\right]} \quad [32.67]$$

© Woodhead Publishing Limited, 2013

Based on the above calculation, the overall heat transfer area can be determined in two ways. One is based on the geometry of the HE (A) and the other is based on the overall heat transfer coefficient (A'). They are presented in Equations [32.68] and [32.69].

$$A = n_t \pi D_0 L_{\text{eff}} \quad [32.68]$$

where L_{eff} is the tube effective length.

$$A' = \frac{\overline{m}_0 C_{p0} \left| T_{0,\text{inlet}} - T_{i,\text{outlet}} \right|}{U \times F_T \times \text{LMTD}} \sum_{i=1}^{n} X_i Y_i \quad [32.69]$$

Iteration

Since the outlet temperature of the shell-side ($T_{0,\text{outlet}}$) is assumed, the overall heat transfer area based on this temperature (A') will not be the same as the overall heat transfer area based on the HE geometry (A). For this reason, an iteration loop from Equations [32.59]–[32.69] is proposed, to find a suitable outlet temperatures of shell-side until the values of A and A' are converged. This usually converges in a few iterations.

32.1.2 Comparison of Different Heat Exchanger Models

The new heat exchanger model (M4) (Wang *et al.*, 2012) is compared with three models, namely, the Bell-Delaware (Taborek, 1988), the simplified Tinker (ESDU Ltd., 1984) and the Wills-Johnston (Wills and Johnston, 1984), and two commercial software packages, namely, HTRI® and HEXTRAN® (Wang *et al.*, 2012). The details of the methods used in the models are presented in Table 32.1. Table 32.2 shows the stream properties and the geometry details of practical heat exchangers.

As shown in Table 32.3, the stream temperatures, heat transfer coefficients and pressure drops calculated from Model M4 are similar to values obtained by HTRI® and HEXTRAN®. The three models considered in this paper (M1, M2 and M3) may give significantly different results, compared with HTRI® and HEXTRAN®.

As shown in the tube-side results from the developed model, HTRI® and HEXTRAN®, the major difference is in the heat transfer coefficients. Model M4 and HTRI® method usually gives higher values than does HEXTRAN®, which uses the Colburn correlation (i.e. Nu = 0.023 $\text{Re}^{0.8}$ $\text{Pr}^{1/3}$) (Bhatti and Shah, 1987) to calculate the tube-side heat transfer coefficient. Compared with Equation [32.73], the Colburn correlation uses a smaller factor to

© Woodhead Publishing Limited, 2013

Table 32.1 Modelling methods of shell-and-tube heat exchanger

	Tube-side		Shell-side	
Model	Heat transfer method	Pressure drop method	Heat transfer method	Pressure drop method
M1	Colburn correlation (Bhatti and Shah, 1987)	Plain tube pressure drop (Serth, 2007)	Bell-Delaware (Taborek, 1988)	Bell-Delaware (Taborek, 1988)
M2	Dittus-Boelter correlation (Bhatti and Shah, 1987)	Plain tube pressure drop (Serth, 2007)	Developed Bell-Delaware (Gnielinski *et al.*, 1998)	Simplified Tinker (ESDU Ltd., 1984)
M3	Dittus-Boelter correlation (Bhatti and Shah, 1987)	Plain tube pressure drop (Serth, 2007)	Developed Bell-Delaware (Gnielinski *et al.*, 1998)	Wills-Johnston (Wills and Johnston, 1984)
M4	Modified Dittus-Boelter correlation (Wang *et al.*, 2012)	Plain tube pressure drop (Serth, 2007)	Modified Chart (Wang *et al.*, 2012)	Modified simple Delaware (Wang *et al.*, 2012)

calculate the Nusselt number (Nu_i). For calculating pressure drop, the plain tube pressure drop method (Serth, 2007) is used. The values predicted by the proposed model have reasonably good agreement with those from HTRI® and HEXTRAN®.

In the shell-side calculations, Model M4 and HTRI® give similar values. HEXTRAN® uses different correlations for the heat transfer coefficient and friction factor of an ideal tube bank, while HTRI® includes a large number of empirical parameters for heat transfer and flow resistance, with many adjustable parameters. The HTRI® model can provide a good representation of the experimental data for shell-side heat transfer and pressure drop (Serth, 2007).

32.2 Heat Transfer Enhancement Techniques

Heat transfer enhancement generally means an increase of the heat transfer coefficient. The goal of enhancement is to reduce the size and cost of heat exchanger equipment, or to increase the heat duty for a given size heat exchanger. Based on the geometry characteristics of shell-and-tube exchangers, the intensification techniques are categorised into tube-side and shell-side. Tube-side enhancement devices provide an important

© Woodhead Publishing Limited, 2013

Table 32.2 Stream data and geometry of a heat exchanger example

	Shell-side	Tube-side
Streams		
Specific heat C_P (J/kg·K)	2,470	2,052
Thermal conductivity k (W/m·K)	0.137	0.133
Viscosity μ (mPa·s)	0.40	3.60
Density ρ (kg/m^3)	785	850
Flow rate m_i (kg/s)	5.675	18.917
Inlet temperature T_{in} (°C)	200.0	38.0
Fouling resistance (m^2·K/W)	0.00035	0.00053
Geometry of heat exchanger		
Tube pitch PT (m)	0.03175	
Number of tubes n_t	124	
Number of tube passes n_p	4	
Tube length L (m)	4.27	
Tube effective length L_{eff} (m)	4.17	
Tube conductivity k_{tube} (W/m·K)	51.91	
Tube pattern (tube layout angle)	90°	
Tube inner diameter D_i (m)	0.0212	
Tube outer diameter D_0 (m)	0.0254	
Shell inner diameter D_s (m)	0.489	
Number of baffles n_b	41	
Baffle spacing B (m)	0.0978	
Inlet baffle spacing B_{in} (m)	0.127	
Outlet baffle spacing B_{out} (m)	0.127	
Baffle cut B_c	20%	
Inner diameter of tube-side inlet nozzle $D_{i,inlet}$ (m)	0.1023	
Inner diameter of tube-side outlet nozzle $D_{i,outlet}$ (m)	0.1023	
Inner diameter of shell-side inlet nozzle $D_{0,inlet}$ (m)	0.0779	
Inner diameter of shell-side outlet nozzle $D_{0,outlet}$ (m)	0.0779	
Shell-bundle diametric clearance L_{sb} (m)	0.059	

Table 32.3 Modelling results of the heat exchanger example

	Tube-side temperature (°C)	Shell-side temperature (°C)	Tube-side pressure drop (kPa)	Shell-side pressure drop (kPa)	Tube-side heat transfer coefficient (W/(m^2·K))	Shell-side heat transfer coefficient (W/(m^2·K))	Overall heat transfer coefficient U (W/(m^2·K))
Example 1							
M1	38~69	200~115	70.0	7.1	885.0	901.1	286.3
M2	38~72	200~105	70.0	10.5	1,207.1	1,400.7	365.5
M3	38~73	200~104	70.0	8.9	1,207.1	1,583.2	376.8
M4	38~73	200~104	70.0	12.1	1,207.1	1,508.9	372.5
HTRI	38~72	200~105	71.2	12.5	1,299.3	1,473.5	380.4
HEXTRAN	38~70	200~112	69.6	14.7	886.2	1,274.5	315.7

© Woodhead Publishing Limited, 2013

toolset in heat transfer augmentation, especially for shell-and-tube heat exchangers with plain tubes. The tube-side enhancement techniques are classified as those requiring additional devices (e.g. twisted-tape inserts and coiled-wire inserts), and special tube geometries (e.g. internally finned tubes). For shell-side enhancement, externally finned tubes are intended to extend and roughen the tube surface on the shell-side, and helical baffles can improve shell-side heat transfer coefficient with low pressure drop.

32.2.1 Tube-Side Enhancement Techniques

Two types of approach have been widely adopted for tube-side heat transfer intensification: tube inserts and internal fins. In this section, twisted-tape (TT) inserts are first introduced, followed by coiled-wire (CW) inserts and internal fins, as illustrated in Fig. 32.2.

Twisted-Tape Inserts

TT is one of the most commonly used forms of tube-side heat transfer enhancement. This is mainly due to its low cost, ease of installation and low maintenance. The geometric features characterising this type of insert are the twist pitch (H), tape thickness (δ) and tape width (w). Usually the tape width is assumed to be the same as the tube inside diameter. The performance of twisted tapes is often described by the dimensionless twist ratio (y).

$$y = \frac{H}{D_i} \qquad [32.70]$$

Laminar Flow

Manglik and Bergles (1993) proposed correlations to describe the performance of TTs, for fully developed laminar flow and constant wall temperature. The enhanced $Nu_{t,l}$ correlation is presented as follows:

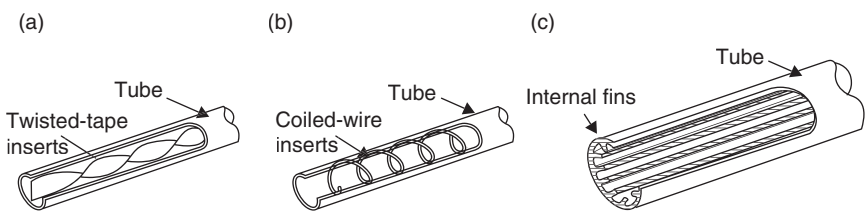

32.2 Illustrations of tube-side enhancement techniques (TT inserts, CW inserts and internal fins) (Pan *et al.*, 2013). (a) Twisted-tape inserts; (b) coiled-wire inserts and (c) internal fins.

© Woodhead Publishing Limited, 2013

$$Nu_{t,l} = 4.612\left\{\left[\left(1+0.0951Gz^{0.894}\right)^{2.5} + 6.413\times10^{-9}\left(Sw.Pr^{0.391}\right)^{3.385}\right]^{2} + 2.132\times10^{-14}\left(\mathrm{Re}_{ax}\cdot Ra\right)^{2.23}\right\}^{0.1}\left(\frac{\mu_b}{\mu_w}\right)^{0.14} \quad [32.71]$$

The Swirl number (Sw) is defined as:

$$Sw = \frac{\mathrm{Re}_{sw}}{\sqrt{y}} \quad [32.72]$$

where Re_{Sw} is the Reynolds number based on the swirl velocity. The equation to calculate the swirl velocity (v_s) is:

$$v_s = v_a(1+\tan a)^{0.5} \quad [32.73]$$

where:

$$\tan a = \frac{\pi D_i}{2H} = \frac{\pi}{2y} \quad [32.74]$$

The axial velocity is defined in terms of the mass flow rate (M) and the axial flow cross-sectional area (A_c).

$$v_a = \frac{M}{\rho_i A_c} \quad [32.75]$$

$$A_c = \frac{\pi D_i^2}{4} - \delta D_i \quad [32.76]$$

The correlation proposed by Manglik and Bergles (1993) to estimate pressure drop by means of the Fanning friction factor, is given by:

$$f_{t,l} = \left[15.767\left[\frac{\pi+2-\left(2\delta/D^i\right)}{\pi-\left(4\delta/D^i\right)}\right]^2\left(1+10^{-6}Sw^{255}\right)^{1/6}\right]\mathrm{Re}_{sw}^{-1} \quad [32.77]$$

The proposed correlations are based on data for water and ethylene glycol and were tested for $300 \le Re \le 30{,}000$. The authors reported average uncertainties in $Nu_{t,l}$ and $f_{t,l}$ of ± 4.1% and ± 4.5%.

© Woodhead Publishing Limited, 2013

Turbulent Flow

Manglik and Bergles (1993) also developed correlations to describe the performance of twisted tapes in fully developed turbulent flow, with constant wall temperature and constant heat flux. These correlations are based on the same experimental data used in the laminar region. Equation [32.78] calculates the enhancement of the heat transfer coefficient through the Nusselt number ($Nu_{t,t}$).

$$Nu_{t,t} = 0.023 Re^{0.8} Pr^{0.4} \left(\frac{\pi}{\pi - \left(4\delta / D^i\right)} \right)^{0.8} \left(\frac{\pi + 2 - \left(2\delta / D^i\right)}{\pi - \left(4\delta / D^i\right)} \right)^{0.2} \left(1 + 0.769 / y\right) \times \phi \quad [32.78]$$

For liquids, the correction factor for fluid property variation (ϕ) is defined in Equation [32.79]. For heating, $m = 0.18$, and for cooling, $m = 0.3$.

$$\phi = \left(\frac{\mu_b}{\mu_w} \right)^m \quad [32.79]$$

Equation [32.80] is used for gases, with $n = 0.45$ for heating and $n = 0.15$ for cooling.

$$\phi = \left(\frac{T_b}{T_w} \right)^n \quad [32.80]$$

Equation [32.81] presents the correlation to predict the Fanning friction factor in the turbulent region.

$$f_{t,t} = \frac{0.079}{Re^{0.25}} \left(\frac{\pi}{\pi - \left(4\delta / D^i\right)} \right)^{1.75} \left(\frac{\pi + 2 - \left(2\delta / D^i\right)}{\pi - \left(4\delta / D^i\right)} \right)^{1.25} \left(1 + \frac{2.752}{y^{1.29}} \right) \quad [32.81]$$

Transition Flow

Abu-Khader (2006) proposed a correlation to estimate the performance in transition flow. The author defined the transition regime within the boundaries of $Sw > 1{,}400$ and $Re \leq 10{,}000$. This method consists of a linear interpolation between the Nusselt number in laminar flow and in turbulent flow, as described by Equation [32.82].

$$Nu_{t,tr} = Nu_{t,t} - \left[\frac{10^4 - Re}{10^4 - Re_{sw=1,400}} \right] \left(Nu_{t,t} - Nu_{t,t} \right) \quad [32.82]$$

© Woodhead Publishing Limited, 2013

where:

$$Re_{sw=1,400} = \frac{1,400\sqrt{y} \times \left(\pi - \left(4\delta / D^{i}\right)\right)}{\left[1 + \left(\pi / 2y\right)^{2}\right]^{1/2} \pi} \quad [32.83]$$

The laminar flow Nusselt number ($Nu_{t,l}$) is calculated at Sw = 1,400 and the turbulent flow Nusselt number ($Nu_{t,t}$) at Re = 10,000.

The Fanning friction factor was presented in Equation [32.84]. This expression is particularly suitable for the transition region, because the friction factor data for tubes with TT inserts do not exhibit the discontinuity in the transition region that is characteristic of empty tube flows (Abu-Khader, 2006).

$$f_{t,tr} = \left(f_{t,t}^{10} + f_{t,t}^{10}\right)^{0.1} \quad [32.84]$$

Coiled-Wire Inserts

The geometry of helically coiled wires is characterised by the helical pitch (p), the wire diameter (w) and the helix angle (α). García *et al.* (2005) explained the effect of wire coils on the flow pattern. They stated that this type of insert could act as a swirl flow generator or a turbulence promoter. If the wire coil acts as a swirl flow generator, a rotating flow at the edge of the tube is formed. This helical flow continues throughout the length of the tube and causes a centrifugal effect. The heat transfer augmentation mechanism is caused by the centrifugal forces, which create a flow pattern that moves the heated fluid from the boundary layer towards the tube axis. If the wire coil acts as a turbulence promoter, the separation and reattachment mechanisms increase the turbulence level. Whenever wire coils are in contact with the tube wall, they are considered to act as integral roughness disturbing the existing laminar sub-layer.

Laminar Flow

The correlations proposed by Uttarwar and Raja Rao (1985) were used to simulate the performance of wire coils in laminar flow. The enhancement of the tube-side heat transfer coefficient was determined using Equation [32.85]:

$$Nu_{c,i} = 1.65 \tan \alpha Re_{Dk}^{m} Pr^{0.35} \left(\frac{\mu_b}{\mu_w}\right)^{0.14} \quad [32.85]$$

where

$$m = 10.25(\tan \alpha)^{-0.38} \quad [32.86]$$

© Woodhead Publishing Limited, 2013

$$\tan\alpha = \frac{\pi D_i}{2p} \quad [32.87]$$

$$D_h = \frac{LD_i^2 - L_{wc}t^2}{LD_i - L_{wc}t} \quad [32.88]$$

$$L_{wc} = \frac{\pi D_i L}{p} \quad [32.89]$$

Equation [32.85] was verified in laminar flow ($30 \leq Re_{Dk} \leq 675$) for oil heating ($300 \leq Pr \leq 675$). The ranges of the insert geometries tested were $0.08 \leq w/D_i \leq 0.13$ and $32° \leq w/D_i \leq 61°$. The reported deviations of $Nu_{c,l}$ were ± 7.5%.

Uttarwar and Raja Rao (1985) found that the Fanning friction factor ($f_{c,l}$), defined in terms of the hydraulic diameter, was only 5–8% higher than that of the smooth tube. Thus, the authors did not develop a friction factor correlation. Moreover, studies carried out by Wang and Sundén (2002) used values 6.5% higher than that of the smooth tube. Hence, the correlation used to determine the pressure drop for laminar flow was that of the smooth tube (Equation [32.90]), taking into account a 6.5% increase.

$$f_{c,i} = (1 + 0.065)\frac{16}{Re} \quad [32.90]$$

Turbulent Flow

García *et al*. (2005) proposed the following correlations to determine the enhanced Nusselt number and Fanning friction factor for wire coils within the turbulent region.

$$Nu_{e,t} = 0.132\left(\frac{p}{D_i}\right)^{-0.372} Re^{0.72} Pr^{0.37} \quad [32.91]$$

$$f_{e,t} = 9.35\left(\frac{p}{w}\right)^{-1.16} Re^{-0.217} \quad [32.92]$$

Equation [32.91] correlates 95% of the experimental data used by García *et al*. (2005) within a deviation of 9%, for $1{,}700 \leq Re \leq 80{,}000$. Their results showed a deviation of 8% for 95% of the friction factor experimental data in the region of $2{,}000 \leq Re \leq 30{,}000$. At higher Reynolds ($30{,}000 \leq Re \leq 80{,}000$), the use of this equation over-predicted the experimental values.

© Woodhead Publishing Limited, 2013

Internal Fins

Internally finned tubes constitute the most popular form of passive enhancement. The enhancement geometry used for this study is the helical fin. The geometric variables that describe a helical fin are the fin height (e), the helix angle (α), the fin pitch (p), the number of fins (N_f) and the fin width (t). The fin height is the distance measured from the internal wall of the tube to the top of the fin. The helix angle is the angle that the fin forms with the tube axis. The fin pitch is the distance between the centres of two fins measured in the axial direction. The number of fins refers to how many stars can be counted around the circumference of the tube. Finally, the fin width is the thickness of the fin (Zdaniuk *et al.*, 2008).

Laminar Flow

Watkinson *et al.* (1975) proposed correlations to simulate the performance of internally finned tubes within the laminar region. These are based on data for single-phase oil in horizontal tubes at approximately uniform wall temperature.

For helical fin tubes, the enhancement of the tube-side heat transfer coefficient was described using Equation [32.93].

$$Nu_{if,t} = 19.2\left(\frac{t}{p}\right)^{0.5} Re_{Dk}^{0.26} Pr^{1/3} \left(\frac{D_h}{L}\right)^{1/3} \left(\frac{\mu_b}{\mu_w}\right)^{1/3} \phi_e \qquad [32.93]$$

where:

$$\phi_e = \frac{2.25\left(1 + 0.01 Gr_{Dk}^{1/2}\right)}{\log Re_{Dk}} \qquad [32.94]$$

Fin pitch (p) can be determined as follows:

$$p = \frac{\pi D_i}{N_f \tan \alpha} \qquad [32.95]$$

The Grashof (Gr_{Dk}) and Reynolds (Re_{Dk}) numbers are both evaluated using the hydraulic diameter (D_k). For internally finned tubes, it is defined as four times the cross-sectional area of the finned tube divided by its perimeter (Huq *et al.*, 1998).

$$D_k = 4\left(\frac{0.25\pi D_i^2 - N_f \cdot e \cdot t}{\pi D_i + 2N_f \cdot e}\right) \qquad [32.96]$$

© Woodhead Publishing Limited, 2013

$$Gr_{Dk} = \frac{g\rho^2 D_k^2 \beta \Delta T_{iw}}{\mu^2} \quad [32.97]$$

The tube-side temperature difference between the wall and the bulk phase (ΔT_{iw}) is:

$$\Delta T_{iw} = |T_{ib} - T_{iw}| \quad [32.98]$$

The bulk phase temperature (T_{ib}) was approximated by a mean average between the inlet and outlet temperature of the fluid.

$$T_{ib} = \frac{T_{i,\text{in}} + T_{i,\text{out}}}{2} \quad [32.99]$$

The mean wall temperature (T_{iw}) was calculated based on the ratio of the enhanced overall heat transfer coefficient (U_e) to the enhanced tube-side heat transfer coefficient (h_e):

$$T_{iw} = T_b + \frac{U_e}{h_e}(T_{ob} - T_{ib}) \quad [32.100]$$

Watkinson *et al*. (1975) also proposed a correlation for single-phase fluids to calculate the enhanced Fanning friction factor ($f_{if,l}$) for fully developed flow within the laminar region.

$$f_{if,i} = \frac{16.4}{Re_{Dk}}\left(\frac{D_h}{D_i}\right)^{1.4} \quad [32.101]$$

Turbulent Flow

Jensen and Vlakancic (1999) developed physically based and generally applicable correlations that describe the performance of micro-fin tubes within the turbulent region. The general form of the correlation that predicts the enhancement ratio of the Nusselt number is:

$$\frac{Nu_{if,t}}{Nu} = \left(\frac{l_{csw}}{D_i}\right)^{-1/2}\left(\frac{0.25\pi D_i^2}{0.25\pi D_i^2 - N_f \cdot e \cdot t}\right)^{0.8} func(\text{geometry}) \quad [32.102]$$

For $e/D_i \leq 0.02$:

$$\left(\frac{l_{csw}}{D_i}\right) = \left[1 - 1.577 P_{\text{modified}}^{0.64}\left(\frac{2e}{D_i}\right)^{0.53}\left[\left(\frac{\pi}{N_f} - \frac{t}{D_i}\right)\cos\alpha\right]^{0.28}\right] \quad [32.103]$$

© Woodhead Publishing Limited, 2013

For $0.02 < e/D_i \leq 0.03$:

$$\left(\frac{l_{csw}}{D_i}\right) = \left[1 - 0.994 P_{\text{modified}}^{0.89} \left(\frac{2e}{D_i}\right)^{0.44} \left[\left(\frac{\pi}{N_f} - \frac{t}{D_i}\right)\cos\alpha\right]^{0.41}\right] \quad [32.104]$$

$$func(\text{geometry}) = \left(\frac{SA_{\text{actual}}}{SA_i}\right)\left(1 - 0.059 P_{\text{modified}}^{-0.31} \left[\left(\frac{\pi}{N_f} - \frac{t}{D_i}\right)\cos\alpha\right]^{-0.66}\right) \quad [32.105]$$

where:

$$P_{\text{modified}} = N_f \frac{\sin\alpha}{\pi} \quad [32.106]$$

$$SA_{\text{actual}} = L\left(\pi D_i + 2N_f e\right) \quad [32.107]$$

$$SA_n = L\pi D_i \quad [32.108]$$

Jensen and Vlakancic (1999) correlated the pressure drop data into a Blasius form for the Fanning friction factor:

$$\frac{f_{if,t}}{f} = \left(\frac{l_{csw}}{D_i}\right)^{-1.25} \left(\frac{0.25\pi D_i^2}{0.25\pi D_i^2 - N_f \cdot e \cdot t}\right)^{1.75} \quad [32.109]$$

32.2.2 Shell-Side Enhancement Techniques

Two types of shell-side intensification techniques, helical baffles and externally fined tubes, are addressed in this section. Figure 32.3 shows their geometry characteristics in details.

Helical Baffles

A recent empirical study was carried out by Zhang *et al.* (2009) to introduce new correlations for the prediction of shell-side heat transfer coefficient. According to Zhang *et al.* (2009), the shell-side heat transfer coefficient depends on the value of the associated Nusselt number (Nu_s).

The shell-side heat transfer coefficient (h_s) is therefore calculated as:

$$h_s = \left(\frac{k_s}{D_0}\right) Nu_s \quad [32.110]$$

© Woodhead Publishing Limited, 2013

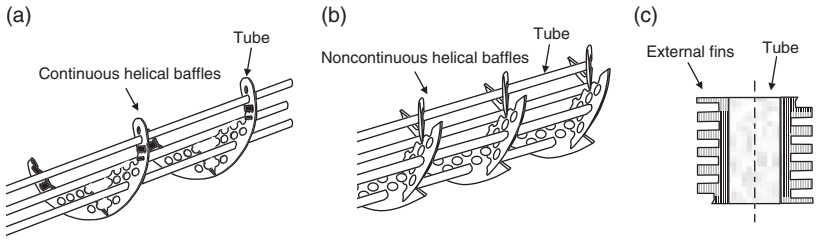

32.3 Illustrations of shell-side enhancement techniques (helical baffles and external fins) (Pan *et al.*, 2013). (a) Continuous helical baffles; (b) Non-continuous helical baffles and (c) external fins.

where, k_s is shell-side fluid thermal conductivity and D_0 is tube outer diameter.

It is clearly seen that the shell-side heat transfer coefficient (h_s) is directly proportional to Nusselt number (Nu_s) which is formulated as follows:

$$Nu_s = ARe_s^B Pr_s^{1/3} \quad [32.111]$$

where, Re and Pr are the shell-side fluid Reynolds and Prandtl numbers, A and B are constants.

The values of A and B depend on the helical angle (β) of the baffle as presented by Zhang *et al*. (2009) in Table 32.4.

The Prandtl number (Pr_s) is calculated as:

$$Pr_s = \frac{Cp_s \mu_s}{k_s} \quad [32.112]$$

where Cp_s, μ_s and k_s are the specific heat capacity, dynamic viscosity and thermal conductivity of the shell-side fluid.

The Reynolds number (Re_s) is related to the shell-side velocity (u_s), the tube outer diameter (D_0) and the shell-side kinematic viscosity (v_s), as shown in Equation [32.113].

$$Re_s = \frac{u_s D_0}{v_s} \quad [32.113]$$

$$u_s = \frac{q_s}{S} \quad [32.114]$$

where, q_s is the volumetric flowrate and S is the cross-flow area of the shell-side.

© Woodhead Publishing Limited, 2013

Table 32.4 Values of constants A and B for different baffle arrangements

Baffle type	A	B
Segmental baffles	0.706	0.474
Helical baffles with $\beta = 20°$	0.275	0.542
Helical baffles with $\beta = 30°$	0.365	0.516
Helical baffles with $\beta = 40°$	0.455	0.488
Helical baffles with $\beta = 50°$	0.326	0.512

Source: Zhang *et al*. (2009).

The cross-flow area at the shell centre-line of the helical baffle (S) is determined by:

$$S = 0.5B\left[D_s - D_1 + \frac{D_1 - D_0}{P_t}\left(P_t - D_0\right)\right] \quad [32.115]$$

where B is the baffle spacing/helical pitch, D_s is the shell inner diameter, D_1 is the tube bundle circumscribed circle ($D_1 = D_s - L_{sb}$, L_{sb} is shell-bundle diametric clearance) and P_t is the tube pitch.

According to Zhang *et al*. (2009), the helical pitch correlation for the continuous helical baffle differs from the non-continuous structure. For the continuous helical baffles, B is determined by:

$$B = B_{\text{segmental}} \quad [32.116]$$

For the non-continuous helical baffles, the helical pitch is calculated as:

$$B = \sqrt{2}D_s \tan\beta \quad [32.117]$$

To calculate the shell-side friction factor, Zhang *et al*. (2009) proposed a correlation that is capable of predicting the friction factor for the shell-side, based on the shell-side fluid Reynolds number. The correlation and its associated constants are described below.

$$f_s = C\,Re_s^D \quad [32.118]$$

The constants C and D in Equation [32.118] change with the type of baffle accordingly, as shown in Table 32.5.

External Fins

There are three different tube diameters that are arranged inside-to-outside. These are the finned tube inner diameter (D_i), the root tube diameter

© Woodhead Publishing Limited, 2013

Table 32.5 Values of constants *C* and *D* for different baffle arrangements

Baffle type	A	B
Segmental baffles	25.1	−0.692
Helical baffles with $\beta = 20°$	11.0	−0.715
Helical baffles with $\beta = 30°$	13.5	−0.774
Helical baffles with $\beta = 40°$	34.7	−0.806
Helical baffles with $\beta = 50°$	47.9	−0.849

Source: Zhang *et al*. (2009).

(D_r) and the finned tube outer diameter (D_o). The related fin height (b) can thus be obtained as $b = (D_o - D_r)/2$. To evaluate the exchanger performance with external fins, various coefficients and parameters must be obtained, such as the heat transfer coefficient, the associated pressure drop, the heat transfer area and the efficiency of the fins. In this section, the well-established model of predicting external fins performance in a shell-and-tube heat exchanger is presented based on the models described by Serth (2007).

In Serth's model (Serth, 2007), to determine the shell-side heat transfer Coefficient (h_s) and pressure drop (ΔP_s), the tube clearance (C') and the equivalent tube diameter (D_e) must be calculated first with a known value of the effective root tube diameter (D_r'). The effective root tube diameter is usually obtained by taking the total volume introduced by the fins into consideration, and adding it up as an encircling cylinder to the original tube volume. The effective root tube diameter is therefore calculated by the following Equations [32.119]–[32.121]:

$$C' = P_t - D_r' \qquad [32.119]$$

$$D_e = \frac{4\beta P_t^2 - \pi D_r'^2}{\pi D_r'} \qquad [32.120]$$

$$D_r' = \left[D_r^2 + 4 n_f b \tau (D_r + b) \right]^{0.5} \qquad [32.121]$$

where P_t is the tube pitch and β is the pitch factor ($\beta = 1$ for square pitch, and $\beta = 0.86$ for triangular pitch), D_r is the root tube diameter, n_f is the number of fins per unit length (fin density), τ is the fin thickness and b is the fin height.

Subsequently, the Reynolds number (Re_s) of shell-and-tube heat exchanger with externally finned tubes is calculated. In Equation

© Woodhead Publishing Limited, 2013

[32.122], G is the shell-side mass flux and μ_s is the shell-side dynamic viscosity.

$$Re_s = \frac{G \times D_e}{\mu_s} \quad [32.122]$$

Thus, the shell-side fluid heat transfer coefficient (h_s) is determined as:

$$h_s = jH \times Pr_s^{1/3} \left(\frac{k_s}{De} \right) \quad [32.123]$$

$$jH = 0.5 \left(1 + \frac{B}{D_s} \right) \left(0.08 Re_s^{0.6821} + 0.7 Re_s^{0.1772} \right) \quad [32.124]$$

where Pr_s is the shell-side Prandtl number, k_s is the shell-side thermal conductivity, B is the baffles spacing and D_s is the shell-side diameter.

In this work, the model used to calculate the level of pressure drop achieved in the shell-side when external fins are introduced has been discussed by Serth (2007). First, the shell-side friction factor is calculated using Equations [32.125] and [32.126].

$$f_1 = \left(0.0076 + 0.000166 D_s \right) Re_s^{-0.123} \quad [32.125]$$

$$f_2 = \left(0.0016 + 5.8 \times 10^{-5} D_s \right) Re_s^{-0.157} \quad [32.126]$$

The shell-side friction factor (f_s) is:

$$f_s = 144 \left[f_1 - 1.25 \left(1 - \frac{B}{D_s} \right) \left(f_1 - f_2 \right) \right] \quad [32.127]$$

The total heat transfer area of an externally finned tube exchanger is represented by the sum of the surface area of all fins introduced to the exchanger (A_{fins}) and the prime surface area remaining (A_{prime}) (Serth, 2007).

$$A_{\text{total}} = A_{\text{fins}} + A_{\text{prime}} \quad [32.128]$$

$$A_{\text{fins}} = 2 n_f L \pi \left(r_{2c}^2 - r_1^2 \right) \quad [32.129]$$

$$A_{\text{prime}} = 2 \pi r_1 \left(L - n_f L \tau \right) \quad [32.130]$$

© Woodhead Publishing Limited, 2013

$$r_{2c} = r_2 + \frac{\tau}{2} \quad [32.131]$$

where r_2 is the outer radius of the fin tube and r_1 is the external radius of the root tube.

32.2.3 Example

In this section, the intensification techniques reviewed in this chapter are evaluated through a practical exchanger design problem. Based on this, exchanger area, capital cost and pressure drop under different intensification combination are compared, demonstrating the validity and efficiency of the adopted techniques. Table 32.6 presents the exchanger geometry and stream property detail of the case study. The capital costs of implementing the intensification techniques are shown in Table 32.7.

Table 32.6 Stream data and geometry of a shell-and-tube exchanger

		Shell-side	Tube-side
Streams	Specific heat C_P (J/kg·K)	2,470	2,052
	Thermal conductivity k (W/m·K)	0.137	0.133
	Viscosity μ (mPa·s)	0.40	3.60
	Density ρ (kg/m^3)	785	850
	Flow rate m_i (kg/s)	5.675	18.917
	Inlet temperature T_{in} (°C)	200.0	38.0
	Fouling resistance (m^2·K/W)	0.00035	0.00053
Geometry of HE	Tube pitch PT (m)	0.03175	
	Number of tubes n_t	124	
	Number of tube passes n_p	4	
	Tube conductivity k_{tube} (W/m·K)	51.91	
	Tube pattern (tube layout angle)	90°	
	Tube inner diameter D_i (m)	0.0212	
	Tube outer diameter D_0 (m)	0.0254	
	Shell inner diameter D_s (m)	0.489	
	Number of baffles n_b	41	
	Baffle spacing B (m)	0.0978	
	Inlet baffle spacing B_{in} (m)	0.127	
	Outlet baffle spacing B_{out} (m)	0.127	
	Baffle cut B_c	20%	
	Inner diameter of tube-side nozzle (m)	0.1023	
	Inner diameter of shell-side inlet nozzle (m)	0.0779	
	Shell-bundle diametric clearance L_{sb} (m)	0.059	

© Woodhead Publishing Limited, 2013

Table 32.7 Capital costs of exchanger design techniques

Design techniques	Cost = $(K_0 + \Sigma K_i) \times$ (Exchanger Area)$^{0.8}$ ($)
Tube-side (intensification)	
Twisted-tape inserts (TT)	$K_1 = 1.0$
Coiled-wire inserts (CW)	$K_2 = 1.5$
Internal fins (IF)	$K_3 = 10.0$
Shell-side (intensification)	
Helical baffles (HB)	$K_4 = 2.0$
External fins (EF)	$K_6 = 10.0$
Plain tubes – single segmental baffles (PT-SSB)	$K_0 = 20.0$

Table 32.8 shows the exchanger details with different intensification techniques. It can be found that the tube-insert techniques increase the tube-side heat transfer coefficients, reduce pressure drops due to the requirement of less exchanger length (namely smaller exchanger area), and thus lead to lower capital cost, such as TT-SSB (twisted-tape: –1.3% of ΔP_i and –2.8% of capital cost) and CW-SSB (coiled-wire: –11.4% of ΔP_i and –2.8% of capital cost); helical baffles need to increase shell-side pressure drop to achieve heat transfer intensification, thus higher capital cost may result, e.g. PT-HB (helical baffles: +60.7% of ΔP_0 and +8.4% of capital cost); as fin tubes commonly increase the tube surface area, more heat can be exchanged in the smaller exchanger (the total heat transfer area is much larger than the geometry area), and consequently less capital cost is required, e.g. IF-SSB (internal fins: 59.8% of $A_{\text{exchanger}}/A_{\text{total}}$ and –7.1% of capital cost) and PT-EF (external fins: 39.9% of $A_{\text{exchanger}}/A_{\text{total}}$ and –14.0% of capital cost). In order to find the optimal exchanger design for Example 1, the combination of intensification techniques is proposed: CW-EF (coiled-wire inserts on the tube side with external fins on the shell-side: –54.5% of ΔP_i, –53.2% of ΔP_0, 39.9% of $A_{\text{exchanger}}/A_{\text{total}}$ and –16.6% of capital cost).

Internal and external tube fins, TT inserts, CW inserts and helical baffles are widely used in the process industries. However, most intensification techniques not only enhance heat transfer performance but also increase pressure drops, resulting in high capital cost requirements. In this section, the overview of detailed models for the adopted intensification techniques is presented, and the given models are utilised to adjust exchanger geometry for mitigating unit vibration. From the example, the performances of the intensified techniques addressed are investigated, and the high efficiency HEs with combining intensification techniques (up to 62.3% and 61.9% reductions of ΔP_i and ΔP_0, and up to 15.4% increase of heat transfer) are able to achieve significant economic benefits for exchanger design (up to 16.6% reduction of capital cost).

© Woodhead Publishing Limited, 2013

Table 32.8 Comparison of different exchanger design techniques

Designed exchangers	Tube-side			Shell-side			U (W/m²·°C)	Area (m²)		Cost ($)
	Type	Performance		Type	Performance					
		h_i (W/m²·°C)	ΔP_i (kPa)		h_0 (W/m²·°C)	ΔP_0 (kPa)		Total	Exchanger	
PT-SSB	Plain tube	1,207.22	70.03	Single segmental baffles	1,508.42	12.13	372.49	41.22	41.22	392
TT-SSB	Twisted tapes	1,605.55	69.10	Single segmental baffles	1,508.42	11.02	410.10	37.44	37.44	381
CW-SSB	Coiled wires	1,766.98	62.08	Single segmental baffles	1,508.42	10.71	421.90	36.39	36.39	381
IF-SSB	Internal fins	1,551.95	39.36	Single segmental baffles	1,508.42	6.66	405.82	37.83	22.62	364
PT-HB	Plain tube	1,207.22	68.86	Helical baffles	1,619.03	19.49	378.84	40.53	40.53	425
PT-EF	Plain tube	1,207.22	34.98	External fins	746.49	6.26	297.49	51.61	20.59	337
TT-HB	Twisted tapes	1,605.55	67.82	Helical baffles	1,619.03	17.67	417.83	36.75	36.75	411
TT-EF	Twisted tapes	1,605.55	35.22	External fins	746.49	5.81	321.00	47.83	19.08	328
CW-HB	Coiled wires	1,766.98	60.90	Helical baffles	1,619.03	17.17	430.08	35.70	35.70	410
CW-EF	Coiled wires	1,766.98	31.84	External fins	746.49	5.68	328.18	46.79	18.67	327
IF-HB	Internal fins	1,551.95	38.64	Helical baffles	1,619.03	10.68	413.38	37.14	22.21	382
IF-EF	Internal fins	1,551.95	26.40	External fins	746.49	4.62	318.36	48.23	15.17	352

© Woodhead Publishing Limited, 2013

32.3 Heat Transfer Enhancement in Heat Exchanger Network Retrofit

Heat transfer intensification is an effective technique for improving energy recovery in HENs by enhancing heat transfer without any network topology modifications. Retrofitting HENs has been widely studied in the process industries in the last few decades, because of increasing concerns about how energy is utilised and recovered in the existing HENs. Conventional retrofit approaches to improve HEN heat recovery mostly involve adding more exchanger area, installing new exchangers, rearranging heat recovery matches and repiping streams. Although these approaches can achieve energy savings in retrofit, most require considerable capital investment for the retrofit associated with configurational changes or structural modification for the existing heat exchanging arrangement. More importantly, the overall heat transfer coefficients of the existing exchangers might change if the heat recovery arrangement is changed. For example, a different stream might be matched in retrofit, and this should be considered during the retrofit study. Recently, heat transfer intensification has been more widely adopted in the process industries as an efficient technique for retrofitting the HEN. By implementing enhancement techniques for existing exchangers, higher heat transfer coefficients can be achieved, leading to more heat exchange in the existing matches. Thus, the overall energy recovery of the HEN can be improved, even though no topology modification is considered (Pan *et al.*, 2011a). Heat transfer intensification has practical advantages in HEN retrofit, as it can avoid physical modification of the exchanger itself, and it can be easily implemented with much lower investment cost.

32.3.1 Sensitivity Tables for Network Response

HEN retrofit problems generally need to consider reduction in the use of utilities, the number of HEs to be enhanced, the enhancement details of each HE and the pressure drop constraints. As there are a large number of potential exchanger enhancement options in a HEN, estimating the efficiency of all these options is not straightforward. Moreover, safety and operability play an important role in the decision for retrofitting. These factors are qualitative in nature, and although they cannot be expressed explicitly, they have to be traded off against other design requirements. To solve complex and large-scale problems, solution strategies can benefit from early screening using exchanger sensitivity tables.

Sensitivity tables presented by Kotjabasakis and Linnhoff (1986) can be used to quantify the impact of heat transfer intensity on the utility consumption of the HEN. Sensitivity tables are based on a simple heat transfer equation ($Q = U \cdot A \cdot LMTD$), in which only stream data and network structure are needed.

© Woodhead Publishing Limited, 2013

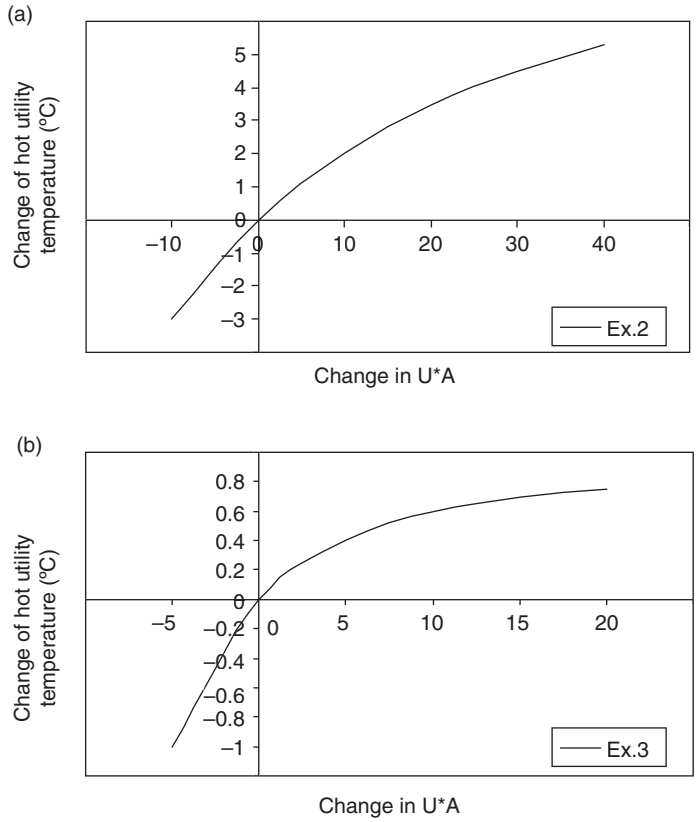

32.4 Sensitivity graphs of (a) Exchanger 2 and (b) Exchanger 3 (Wang *et al.,* 2012).

Assume that the inlet temperature of the hot utility (HU) in a HEN is the response parameter, the change of temperatures for the utility exchangers related to the utility path will be known when the UA value (heat transfer coefficient, U, multiplied by area, A) of exchangers is changed. The best candidate exchanger for enhancement can be found if its response parameter has high sensitivity. As shown in Fig. 32.4, exchanger 2 is a good candidate, since with 25% increment of UA value, the inlet temperature of the hot utility increase is almost 4°C. By contrast, exchanger 3 is not a good candidate because, with 25% increment of UA value, the inlet temperature of the utility increases only slightly. Sensitivity Analysis is the key basis of the proposed work, which can help to identify the exchangers with a large energy saving potential.

To explain why a high sensitivity exchanger can be a good candidate, Fig. 32.5 is used to show the maximum heat recovery in a HE, where the

© Woodhead Publishing Limited, 2013

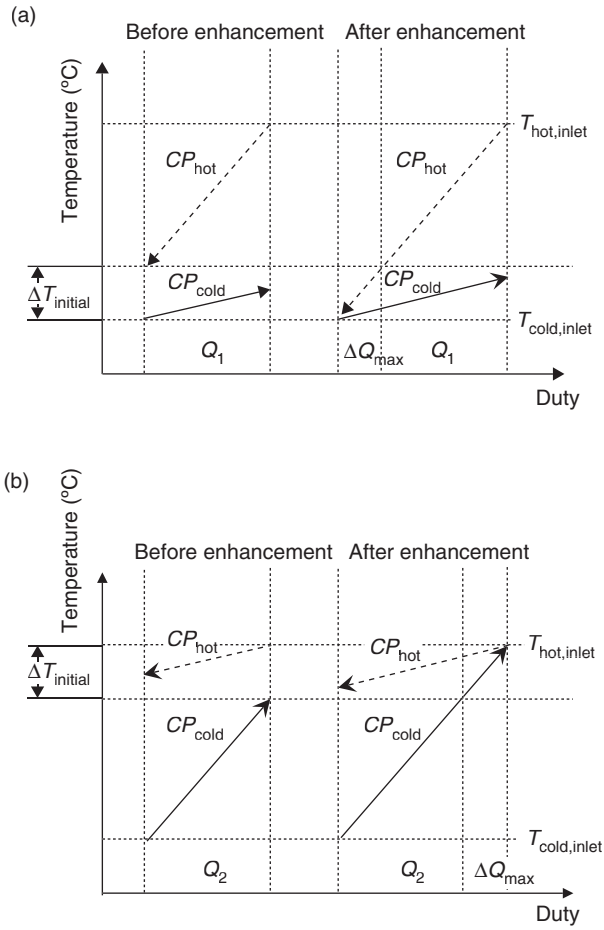

32.5 Maximum heat recovery in a HE (Wang *et al.*, 2012): (a) $CP_{hot} < CP_{cold}$, $\Delta Q_{max} = \Delta T_{initial}\ CP_{hot}$ and (b) $CP_{hot} > CP_{cold}$, $\Delta Q_{max} = \Delta T_{initial}\ CP_{cold}$.

red line indicates the hot stream, and the blue line indicates the cold stream. In the figure, the slope of line is the reciprocal value of CP (heat-flow capacity, which is the product of heat capacity and flow rate) for each stream, and the equation of maximum heat recovery in an exchanger is given as: $\Delta Q_{max} = \Delta T_{initial} CP_{min}$, where ΔQ_{max} is the maximum heat recovery, $\Delta T_{initial}$ is the initial temperature difference between the inlet of high CP stream and the outlet of low CP stream and CP_{min} is the CP value of the stream that has lower CP in the exchanger. Based on this, the energy saving depends on CP_{min} and $\Delta T_{initial}$. If a HE on the utility path is enhanced, then for the exchanges between the enhanced one and utility exchanger, the heat transfer is reduced, due to small heat transfer driving force. In other words, the

© Woodhead Publishing Limited, 2013

exchanger with a large CP_{min} and $\Delta T_{initial}$, and close to utility exchanger, can be a high sensitivity HE.

The objective of this methodology is to find the best candidate exchanger for enhancement. Good candidates can be easily identified. Although a systematic way to distinguish which exchangers are good for enhancement has been proposed, the proposed method is based on heuristics, which requires judgement. Application of optimisation techniques would allow a more systematic approach.

32.3.2 Mathematical Optimisation Method for Network Retrofit

In general, there are two groups of design methods used for HEN retrofit: manual design, based on Pinch Analysis, and automated design, using mathematical programming techniques. Early studies were mainly based on the use of graphical interpretation of the energy recovery characteristics. In a more recent alternative, mathematical programming methods have been developed as an effective way to optimise the HEN for retrofit scenarios. Due to the non-linearity of LMTD, HEN retrofit problems are usually formulated as an MINLP model or a combined NLP–MILP model.

Most research conducted so far has assumed constant heat transfer coefficients for the exchangers during the study of HEN retrofit. However, when the streams involved in a particular exchanger are rearranged, which is widely adopted in the existing design methods, the overall heat transfer coefficients of these exchangers should reflect the changes of their streams involved. This drawback may lead to unrealistic solutions if the assumption of constant heat transfer coefficient is maintained. Employing intensified heat transfer units to the existing exchangers without network topology modifications can be an effective way to avoid some of the drawbacks. Thus, in this section, a novel optimisation method (Pan *et al.*, 2012) is introduced for improving the energy recovery of HENs without topology modification through heat transfer enhancement. In this approach, a new MILP model has been built to effectively reduce the computational difficulties for HEN retrofit problems, and a robust optimisation strategy using two iteration loops has been proposed to systematically identify optimal heat recovery systems.

Model of Network Retrofit with Heat Transfer Enhancement

The modelling of HENs with enhancement includes various equations related to heat transfer between streams. Equations for calculating the LMTD are non-linear but treated as fixed parameters by fixing stream temperature for the heat exchange and the LMTD is sequentially updated with an iterative procedure (Pan *et al.*, 2012).

© Woodhead Publishing Limited, 2013

Initial LMTD

The initial LMTD ($LMTD'$) can be calculated with stream temperatures (HTI'_{ex}, HTO'_{ex}, CTI'_{ex} and CTO'_{ex}) that are fixed initially, as shown in Equation [32.132], where EX is the set of all exchangers, HTI'_{ex} and HTO'_{ex} are the inlet and outlet initial temperatures, respectively, of the hot stream in exchanger ex, while CTI'_{ex} and CTO'_{ex} are the inlet and outlet initial temperatures, respectively, of the cold stream in exchanger ex.

$$LMTD'_{ex} = \frac{(HTI' - CTO') - (HTO'_{ex} - CTI'_{ex})}{\mathrm{In}[(\mathrm{HTI}'_{ex} - CTO'_{ex}) / (HTO'_{ex} - CTI'_{ex})]}, \ \forall ex \in EX \qquad [32.132]$$

Intensified Heat Transfer

In this paper, clean exchangers are assumed, and the calculations of their overall heat transfer coefficients are simplified as follows:

$$DU_{ex} = DTU_{ex} + DSU_{ex}, \ \forall ex \in EX \qquad [32.133]$$

where DTU_{ex}, DSU_{ex} and DU_{ex} are the reciprocal values of tube-side, shell-side and the overall heat transfer coefficient for exchanger ex.

Based on Equation [32.133], the overall heat transfer coefficient of each exchanger (U_{ex}) is obtained:

$$U_{ex} = \frac{1}{DU_{ex}}, \quad \forall ex \in EX \qquad [32.134]$$

Note that Equation [32.134] is non-linear. To linearise the non-linear term, first order Taylor series expansions are utilised, as presented in Equations [32.135]–[32.137]. U'_{ex} and DU'_{ex} are the initial values of U_{ex} and DU_{ex}. Positive variables, AU_{ex} and BU_{ex} are remainder terms, and should be very small. This is formulated in the objective function.

$$U_{ex} = U'_{ex} + (-1) \times (DU'_{ex})^{-2} \times (DU_{ex} - DU'_{ex}), \quad \forall ex \in EX \qquad [32.135]$$

$$AU_{ex} \geq U_{ex} - U'_{ex}, \quad \forall ex \in EX \qquad [32.136]$$

$$BU_{ex} \geq U'_{ex} - U_{ex}, \quad \forall ex \in EX \qquad [32.137]$$

To select suitable exchangers for intensification, two sets of binary variables are proposed:

© Woodhead Publishing Limited, 2013

$ETEX_{ex.ti} = 1$, if the *ti*th type of tube-side intensification is implemented in exchanger *ex*; otherwise, it is 0.

$ESEX_{ex.si} = 1$, if the *si*th type of shell-side intensification is implemented in exchanger *ex*; otherwise, it is 0.

In this section, the types of tube-side intensification addressed include non-intensification, TT inserts, CW inserts, internal fins, the combination of TT and internal fins, and the combination of CW and internal fins. While for shell-side intensification, non-intensification, helical baffles, external fins, and the combination of helical baffles and external fins are considered. Equations [32.138] and [32.139], and Equations [32.140] and [32.141] restrict the tube-side and shell-side heat transfer coefficients with or without intensification.

$$DTU_{ex} \le MINDTU_{ex,ti} \times ETEX_{ex,ti},\ \forall ex \in EX,\ ti \in TI \qquad [32.138]$$

$$DTU_{ex} \le MAXDTU_{ex,ti} \times ETEX_{ex,ti},\ \forall ex \in EX,\ ti \in TI \qquad [32.139]$$

$$DSU_{ex} \le MINDSU_{ex,si} \times ESEX_{ex,si},\ \forall ex \in EX,\ si \in SI \qquad [32.140]$$

$$DSU_{ex} \le MAXDSU_{ex,si} \times ESEX_{ex,si},\ \forall ex \in EX,\ si \in SI \qquad [32.141]$$

where *TI* and *SI* are the sets of all types of tube-side and shell-side intensification, $MAXDTU_{ex,ti}$ and $MINDTU_{ex,ti}$ are the upper and lower bounds of the reciprocal value of tube-side heat transfer coefficients if the *ti*th type of tube-side intensification is implemented in exchanger *ex*, while $MAXDSU_{ex,si}$ and $MINDSU_{ex,si}$ are the upper and lower bounds of the reciprocal value of shell-side heat transfer coefficients if the *si*th type of shell-side intensification is implemented in exchanger *ex*.

In addition, only one type of intensification can be implemented in tube-side and shell-side in an exchanger, as shown in Equations [32.142] and [32.143].

$$\sum_{ti \in TI} ETEX_{ex,ti} = 1,\ \forall ex \in EX \qquad [32.142]$$

$$\sum_{si \in SI} ESEX_{ex,si} = 1,\ \forall ex \in EX \qquad [32.143]$$

© Woodhead Publishing Limited, 2013

Stream Temperature Constraints

Equations [32.144]–[32.146] represent the constraints regulating the stream temperatures in the inlet and outlet of the whole network, where *CS* and *HS* are the sets of all cold streams and hot streams; $EX^i_{cs,}$ $EX^o_{cs,}$ EX^i_{hs} and EX^o_{hs} describe the sets of all exchangers located in the network inlet or outlet; CMF_{ex} and HMF_{ex} are flow fractions of cold and hot streams in exchanger *ex,* which presents the flow fractions of parallel exchangers (if single exchanger is used, its flow fraction is equal to 1), with the restriction that the stream outlet temperature must be equal to the network target temperature ($CSTO_{cs}$ or $HSTO_{hs}$); $CSTI_{cs}$ and $CSTO_{cs}$ are inlet and outlet temperatures of cold stream *cs* in the whole network, while $HSTI_{hs}$ and $HSTO_{hs}$ are inlet and outlet temperatures of hot stream *hs* in the whole network, CTI_{ex} is inlet temperature of cold stream in HE *ex*, and HTI_{ex} is inlet temperature of hot stream in exchanger *ex*.

$$CTI_{ex} = CSTI_{cs}, \ \forall ex \in EX^i_{cs}, \ cs \in CS \quad [32.144]$$

$$\sum_{ex \in EX^o_{cs}} (CMF_{ex} \times CTO_{ex}) = CSTO_{cs}, \ cs \in CS \quad [32.145]$$

$$HTI_{ex} = HSTI_{hs}, \ \forall_{ex} \in EX^i_{hs}, \ hs \in HS \quad [32.146]$$

$$\sum_{ex \in EX^o_{hs}} (HMF_{ex} \times HTO_{ex}) = HSTO_{hs}, \ hs \in HS \quad [32.147]$$

Equations [32.148] and [32.149] restrict the Minimum Temperature Difference approach ($\Delta T_{\min}$) in each exchanger, where HTO_{ex} is outlet temperature of the hot stream in exchanger *ex* and CTO_{ex} is the outlet temperature of the cold stream in exchanger *ex*.

$$HTI_{ex} \geq CTO_{ex} + \Delta T_{\min}, \ \forall ex \in EX \quad [32.148]$$

$$HTO_{ex} \geq CTI_{ex} + \Delta T_{\min}, \ \forall ex \in EX \quad [32.149]$$

Heat Transfer Differences

In Equations [32.150] and [32.151], the heat transfer in each exchanger is estimated based on $LMTD'_{ex}$, thus there might be some differences for energy exchange between streams and exchangers. HBA_{ex} and HBB_{ex} are positive variables, and represent these differences. For the energy balance between streams and exchangers, HBA_{ex} and HBB_{ex} should be small and

© Woodhead Publishing Limited, 2013

the objective function has been formulated to minimise the sum of these infeasibilities in energy balances. In addition, $HFCP_{ex}$ and $CFCP_{ex}$ are heat-flow capacities (the multiplication between heat capacity and flow rate) of the hot stream and the cold stream in exchanger *ex*, and EXA_{ex} is heat transfer area of exchanger *ex*.

$$HBA_{ex} \geq HFCP_{ex} \times (HTI_{ex} - HTO_{ex}) - EXA_{ex} \times U_{ex} \times LMT D'_{ex}, \quad \forall ex \in EX \qquad [32.150]$$

$$HBB_{ex} \geq EXA_{ex} \times U_{ex} \times LMTD'_{ex} - HFCP_{ex} \times (HTI_{ex} - HTO_{ex}), \quad \forall ex \in EX \qquad [32.151]$$

Energy Balance Differences

Due to the energy balance in HEs, the heat duties of the cold stream and the hot stream should be the same. However, the different arrangement of heat transfer through intensification may lead to heat duty differences between the cold stream and the hot stream in the exchangers. Equations [32.152] and [32.153] are proposed to describe differences in energy balances, and the variables, AEB_{ex} and BEB_{ex}, are positive and should be small.

$$AEB_{ex} \geq HFCP_{ex} \times (HTI_{ex} - HTO_{ex}) - CFCP_{ex} \times (CTI_{ex} - CTO_{ex}), \quad \forall ex \in EX \qquad [32.152]$$

$$BEB_{ex} \geq CFCP_{ex} \times (CTI_{ex} - CTO_{ex}) - HFCP_{ex} \times (HTI_{ex} - HTO_{ex}), \quad \forall ex \in EX \qquad [32.153]$$

Variable Differences

Since the heat transfer coefficients in some exchangers change, differences between initial stream temperatures and updated stream temperatures exist, which are represented in Equations [32.154] and [32.155] using positive variables $DAHTI_{ex}$ and $DBHTI_{ex}$.

$$DAHTI_{ex} \geq HTI_{ex} - HTI'_{ex}, \quad \forall ex \in EX \qquad [32.154]$$

$$DBHTI_{ex} \geq HTI'_{ex} - HTI_{ex}, \quad \forall ex \in EX \qquad [32.155]$$

Meanwhile, differences between the initial and updated temperatures for the hot stream outlet ($DAHTO_{ex}$ and $DBHTO_{ex}$), and the cold stream inlet

© Woodhead Publishing Limited, 2013

and outlet ($DACTI_{ex}$, $DBCTI_{ex}$, $DACTO_{ex}$ and $DBCTO_{ex}$) are formulated in the same way.

$$DAHTO_{ex} \geq HTO_{ex} - HTI'_{ex}, \ \forall ex \in EX \quad [32.156]$$

$$DBHTO_{ex} \geq HTO'_{ex} - HTI_{ex}, \ \forall ex \in EX \quad [32.157]$$

$$DACTI_{ex} \geq CTI_{ex} - CTI'_{ex}, \ \forall ex \in EX \quad [32.158]$$

$$DBCTI_{ex} \geq CTI'_{ex} - CTI_{ex}, \ \forall ex \in EX \quad [32.159]$$

$$DACTO_{ex} \geq CTO_{ex} - CTO'_{ex}, \ \forall ex \in EX \quad [32.160]$$

$$DBCTO_{ex} \geq CTO'_{ex} - CTO_{ex}, \ \forall ex \in EX \quad [32.161]$$

In Equation [32.134], calculating the overall heat transfer coefficient, initial values, U'_{ex} and DU'_{ex} have been used for linearisation. Thus, the differences between the initial and updated values of the heat transfer coefficient must also be considered. AU_{ex} and BU_{ex} are positive variables and represent the differences for U_{ex}, while positive variables, ADU_{ex} and BDU_{ex} represent the differences for DU_{ex}.

$$AU_{ex} \geq U_{ex} - U'_{ex}, \ \forall ex \in EX \quad [32.162]$$

$$BU_{ex} \geq U'_{ex} - U_{ex}, \ \forall ex \in EX \quad [32.163]$$

$$ADU_{ex} \geq DU_{ex} - DU'_{ex}, \ \forall ex \in EX \quad [32.164]$$

$$BDU_{ex} \geq DU'_{ex} - DU_{ex}, \ \forall ex \in EX \quad [32.165]$$

Energy Saving

Equation [32.166] presents energy saving (QS) achieved in the HEN, where EX_{hu} and EX_{cu} are the set of all exchangers consuming hot and cold utilities; $OCTI_{ex}$ and $OHTI_{ex}$ are the inlet temperatures of the cold stream and the hot stream in exchanger ex in the original HEN.

$$QS = \sum_{ex \in EX_{hu}} \left[CFCP_{ex} \times (CTI_{ex} - OCTI_{ex}) \right] + \sum_{ex \in EX_{cu}} \left[HFCP_{ex} \times (OHTI_{ex} - HTI_{ex}) \right] \quad [32.166]$$

© Woodhead Publishing Limited, 2013

Objective Function

The objective of the new MILP-based method is to minimise the summation of the differences in energy balances, heat transfer and the variables with the restriction of an estimated energy saving value (QS'), as shown in Equations [32.167] and [32.168].

$$QS \geq QS' \qquad [32.167]$$

$$\begin{aligned} Obj = & \sum_{e \in EX} \left(DACTI_{ex} + DBCTI_{ex} + DACTO_{ex} + DBCTO_{ex} + AU_{ex} + BU_{ex} \right) \\ & + \sum_{e \in EX} \left(DAHTI_{ex} + DBHTI_{ex} + DAHTO_{ex} + DBHTO_{ex} + ADU_{ex} + BDU_{ex} \right) \\ & + \sum_{e \in EX} \left(HBA_{ex} + HBB_{ex} + AEB_{ex} + BEB_{ex} \right) \end{aligned} \qquad [32.168]$$

The new MILP optimisation framework model consists of an objective function given in Equation [32.168] and the model constraints given in Equations [32.132] and [32.133], and from Equations [32.135]–[32.167]. Contrary to conventional retrofit models, the model proposed is able to find a feasible retrofit solution for achieving a certain energy saving in Equation [32.167], which requires an iterative loop to update the initial values of the model variables, and to solve the updated model repeatedly until the objective value in Equation [32.168] is close to 0. Once a feasible retrofit solution is found, the estimated value in Equation [32.167] will increase gradually in another iteration loop to find the maximum energy saving for all potential retrofit solutions. These two iteration loops are introduced in detail in the next sub-section.

Iteration Algorithm for Optimisation

The MILP model presented in the sub-section, 'Model of network retrofit with heat transfer enhancement' is proposed to find a feasible solution for HEN retrofit with a certain energy saving or retrofit profit. To obtain the feasible or optimal solution, two iteration loops are to be executed as follows. The first loop (Loop 1) is used to solve repeatedly the MILP model and to obtain a feasible solution for HEN retrofit with a certain energy saving (an estimated value QS' in Equation [32.167]). The second loop (Loop 2) successively seeks the maximum value of QS, and interacts with the first loop (Loop 1) for finding the solution based on QS.

- *The first iteration loop (Loop 1)*

  Step 1: Input initial stream temperatures and estimated energy saving (QS).

© Woodhead Publishing Limited, 2013

Step 2: Calculate $LMTD'_{ex}$ based on the initial stream temperatures.
Step 3: Solve an MILP model to minimise an objective value.
Step 4: Obtain the new streams temperatures (HTI_{ex}, HTO_{ex}, CTI_{ex} and CTO_{ex}) from the MILP model.
Step 5: Calculate $LMTD_{ex}$ with the new stream temperatures. If $LMTD_{ex}$ is infeasible with new stream temperatures, $LMTD'_{ex}$ is used for $LMTD_{ex}$.
Step 6: Calculate the difference between $LMTD$ and $LMTD'_{ex}$.
Step 7: Obtain the differences in energy balances, heat transfers, stream temperatures and heat transfer coefficients.
Step 8: If the summation of differences given in Step 6 and Step 7 is small enough, terminate the procedure; otherwise, update the new $LMTD''_{ex}$ as $LMTD''_{ex} = (LMTD'_{ex} + LMTD_{ex})/2$, new U''_{ex} as $U''_{ex} = (U'_{ex} + 1/DU_{ex})/2$, and execute from Step 2 to Step 7 iteratively.

The details of Loop 1 are shown in Fig. 32.6.

- *The second iteration loop (Loop 2)*

When Loop 1 finds the solution for HEN retrofit under the initial estimated energy saving (QS'), Loop 2 will gradually increase the value of QS', and execute Loop 1 until the maximum value is found. The procedure of finding the maximum QS includes:

Step 1: Estimate initial energy saving (QS').
Step 2: Execute Loop 1 to test this estimated value (QS').
Step 3: If the assumed QS' is too large, the objective value in Equation [32.136] cannot be small enough to be repeated in Loop 1 (i.e. infeasible in Loop 1). Then the value of QS' is reduced by half, and return to Step 2 until the objective value in Equation [32.167] becomes close to 0 (i.e. feasible in Loop 1).
Step 4: Set the feasible QS' and the minimum infeasible QS' from Step 3 or from Step 7.
Step 5: Calculate the average value of the feasible QS' (Step 4) and the minimum infeasible QS' (Step 4). A new QS' is obtained from: 0.5× [feasible QS' (Step 4) + minimum infeasible QS' (Step 4)].
Step 6: Check the feasibility of the QS' set in Step 5 in Loop 1.
Step 7: If the QS' tested in Step 6 is infeasible in Loop 1, find a new QS'': $QS'' = 0.5\times$[feasible QS' (Step 4) + infeasible QS' (Step 5)], and back to Step 6 until the new QS'' is feasible in Loop 1.

© Woodhead Publishing Limited, 2013

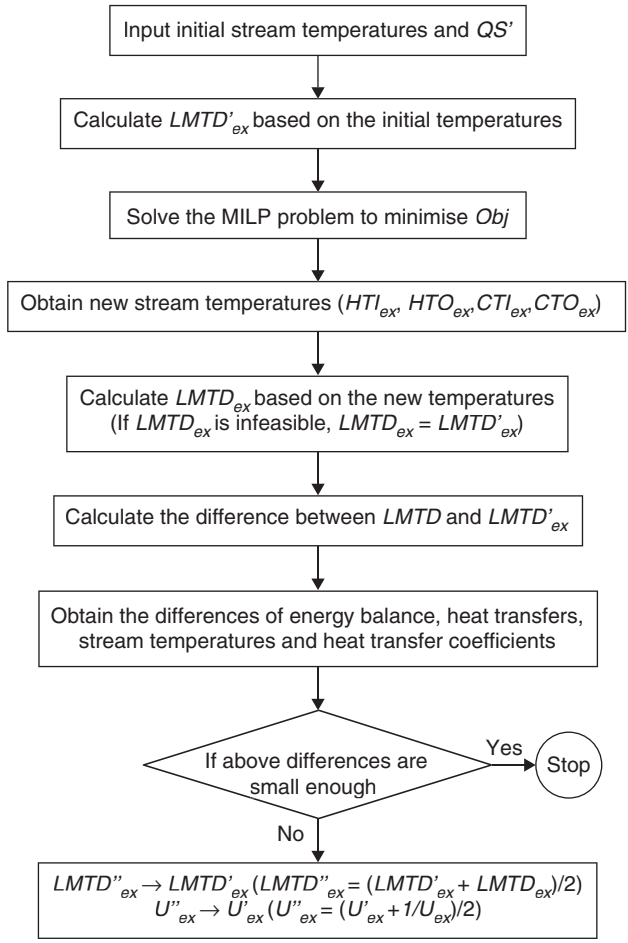

32.6 The procedure of Loop 1 (Pan *et al.*, 2012).

Step 8: Go back to Step 4 and set the feasible *QS'* obtained from Step 7. Repeat Step 4 to Step 7 to find the maximum feasible *QS'*.

Figure 32.7 describes the detailed procedure of Loop 2. An illustration for finding each feasible *QS* is presented in Fig. 32.8, in which the feasible *QS'* in the 2nd iteration of Loop 2 is very close to the maximum value. Based on Figs 32.7 and 32.8, it can be noted that if Loop 1 can find a feasible solution under the initial assumed value (*QS'*), this value can increase, and Loop 1 is executed to find whether there is a feasible solution for the lager *QS'*. Otherwise, the iteration is terminated.

© Woodhead Publishing Limited, 2013

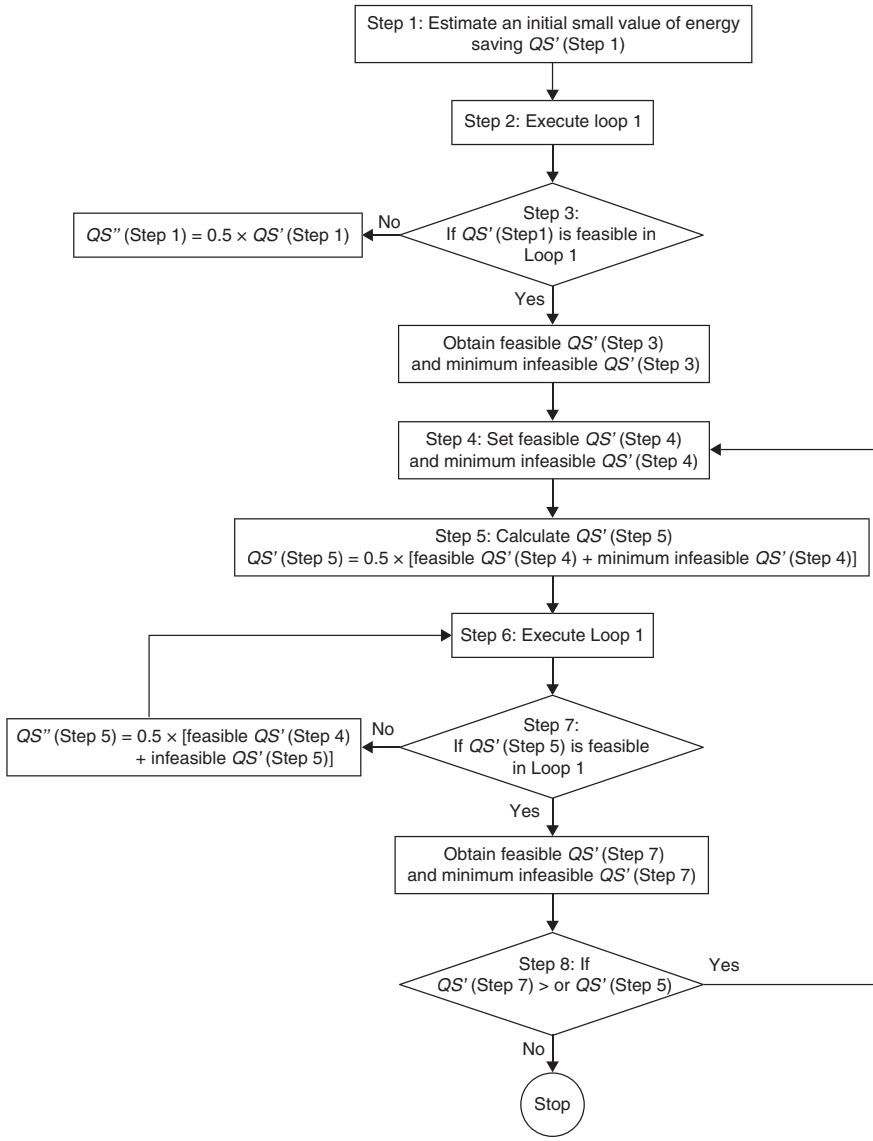

32.7 The procedure of Loop 2 (Pan *et al.*, 2012).

32.3.3 Example

Figure 32.9 presents an existing preheat train for a crude-oil distillation column in a refinery plant. The retrofit objective is to reduce the

© Woodhead Publishing Limited, 2013

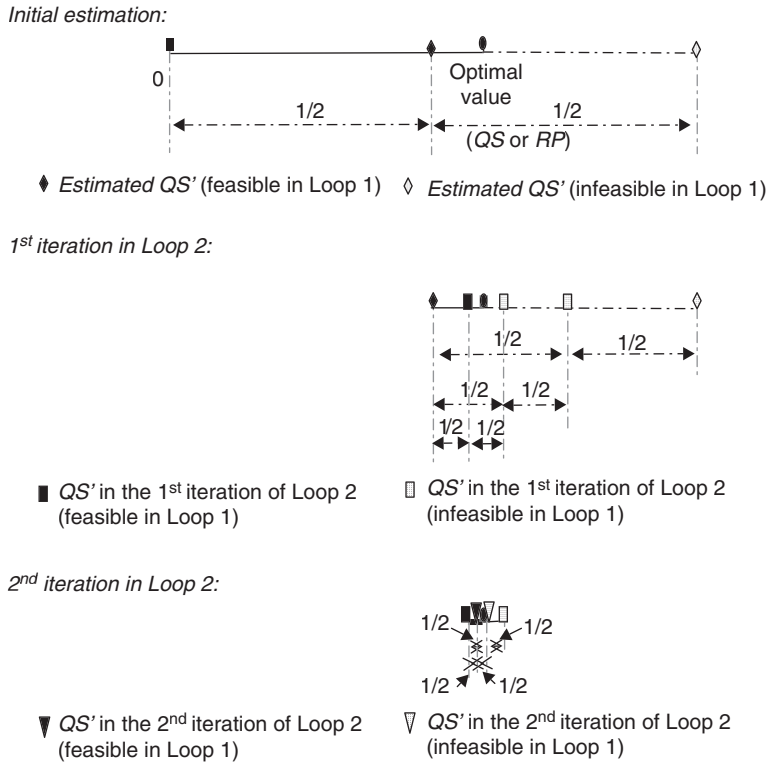

32.8 An illustration for estimating *QS'* in Loop 2 (Pan *et al.*, 2012).

HU consumption. This means reducing the heat duty of HE 30 (target exchanger). The stream data and initial exchanger data can be found in Tables 32.9 and 32.10. The Minimum Temperature Difference approaches ($\Delta T_{\min}$) before and after heat transfer intensification are 19ºC and 5ºC. To evaluate the enhancement methods, different intensified techniques are taken into account in detail, and the economic benefits of the proposed approach are illustrated.

The detailed types of intensification include: tube-side (TT inserts, CW inserts, internal fins, the combination of TT and internal fins, and the combination of CW and internal fins), and shell-side (helical baffles, external fins, and the combination of helical baffles and external fins). Based on the literature review in Section 32.3, the enhancement level and capital cost of each type of intensification are assumed, and presented in Table 32.11, where the retrofit cost of one exchanger is equal to the fixed charge (A) plus the sum of retrofit costs related to exchanger area ($\sum$(B×Area)).

© Woodhead Publishing Limited, 2013

© Woodhead Publishing Limited, 2013

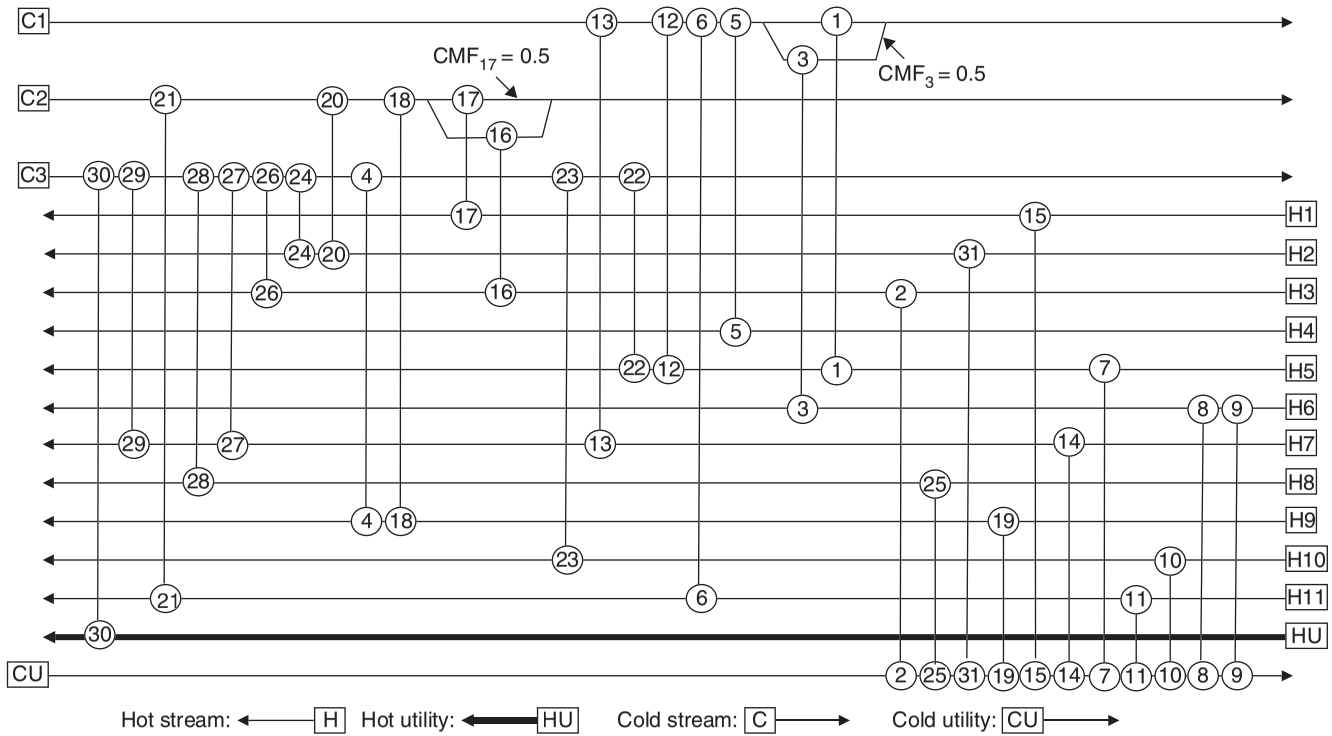

32.9 An exchanger network of existing preheat train for a crude-oil distillation column in a refinery plant (Pan *et al.*, 2012).

© Woodhead Publishing Limited, 2013

Table 32.9 Stream details in the HEN

Stream	C1	C2	C3	H1	H2	H3	H4	H5	H6	H7	H8	H9	H10	H11	HU	CU
FCP (kW/°C)	323	358.5	474	14.2	181.5	113	100	22.2	39.5	28	176	24.5	25	69.6	93	9,652.5
T_{in} (°C)	33.5	91.34	151	335	253.2	294	212	213	174	364	290	284	240	179	1,500	12.45
T_{out} (°C)	95.6	157.3	352	69.4	116.1	130	156	61.7	43.3	65.6	211	65.6	57.8	69.3		

FCP: heat-flow capacities (the multiplication between heat capacity and flow rate); T_{in}, T_{out}: stream temperatures in HEN inlet and outlet.

Table 32.10 Exchanger details of original HEN

EXs	HTI_{ex} (°C)	HTO_{ex} (°C)	CTI_{ex} (°C)	CTO_{ex} (°C)	$LMTD_{ex}$ (°C)	EXA_{ex} (m^2)	Duty (kW)	h_i (kW/m^2·°C)	h_0 (kW/m^2·°C)	U_{ex} (kW/m^2·°C)	Max available U_{ex} (kW/m^2·°C)
1	117.2	66.3	33.5	40.5	51.7	175.0	1,130.8	0.250	0.250	0.125	0.213
2	131.2	130.0	14.2	14.2	116.4	11.7	139.8	0.202	0.202	0.101	0.172
3	174.4	76.7	33.5	57.5	74.0	116.7	3,860.3	0.894	0.894	0.447	0.760
4	284.2	174.7	156.7	162.4	54.3	175.0	2,682.0	0.565	0.565	0.282	0.480
5	212.4	156.1	49.0	66.5	125.5	100.0	5,633.4	0.898	0.898	0.449	0.763
6	174.4	85.7	66.5	85.6	45.5	650.0	6,176.5	0.418	0.418	0.209	0.355
7	66.3	61.7	13.0	13.0	50.9	20.0	102.4	0.205	0.205	0.102	0.174
8	76.7	62.2	12.5	12.6	56.6	30.0	571.6	0.672	0.672	0.336	0.571
9	62.2	43.3	12.5	12.5	39.5	55.6	745.4	0.678	0.678	0.339	0.576
10	171.1	57.8	12.6	12.9	90.2	277.8	2,832.8	0.226	0.226	0.113	0.192
11	85.7	69.3	12.9	13.0	64.2	55.6	1,141.5	0.639	0.639	0.320	0.543
12	169.1	117.2	85.6	89.2	52.1	22.2	1,150.6	1.989	1.989	0.994	1.690
13	221.1	147.2	89.2	95.6	87.5	38.1	2,069.2	1.243	1.243	0.622	1.057
14	147.2	65.6	13.0	13.2	87.0	85.7	2,285.9	0.613	0.613	0.307	0.521
15	109.3	69.4	13.2	13.3	74.3	42.9	566.6	0.354	0.354	0.177	0.300
16	198.4	131.2	91.3	133.7	51.3	128.6	7,586.7	2.300	2.300	1.150	1.955
17	335.4	109.3	91.3	109.2	82.2	207.7	3,210.1	0.376	0.376	0.188	0.319
18	174.7	139.7	121.5	123.9	31.8	207.7	858.6	0.260	0.260	0.130	0.221
19	139.7	65.6	13.3	13.5	83.9	138.5	1,816.1	0.313	0.313	0.156	0.266
20	206.2	141.9	123.9	156.4	31.2	1,384.6	11,684.2	0.540	0.540	0.270	0.459
21	178.7	174.4	156.4	157.3	19.7	27.7	296.2	1.088	1.088	0.544	0.925
22	212.7	169.1	151.1	153.1	34.7	83.1	968.6	0.671	0.671	0.336	0.570

© Woodhead Publishing Limited, 2013

23	240.1	171.1	153.1	156.7	42.6	41.5	1,724.4	1.947	1.947	0.974	1.655
24	253.2	206.2	162.4	180.4	57.1	1,038.5	8,525.4	0.288	0.288	0.144	0.244
25	222.7	210.9	14.0	14.2	202.7	66.7	2,085.1	0.309	0.309	0.154	0.262
26	293.7	198.4	180.4	203.1	44.9	300.0	10,771.6	1.599	1.599	0.799	1.359
27	249.0	221.1	203.1	204.7	29.2	233.3	780.5	0.229	0.229	0.115	0.195
28	290.4	222.7	204.7	229.9	35.1	1,020.0	11,903.4	0.666	0.666	0.333	0.566
29	364.3	249.0	229.9	236.7	57.1	240.0	3,228.0	0.471	0.471	0.235	0.400
30	1,500.0	912.5	236.7	351.9	891.2	180.0	54,633.2	0.681	0.681	0.341	0.579
31	141.9	116.1	13.5	14.0	114.8	60.0	4,683.1	1.362	1.362	0.681	1.157

EXs: exchangers; HTI_{ex} and HTO_{ex}: inlet and outlet temperatures of Hot streams in exchanger *ex*; CTI_{ex} and CTO_{ex}: inlet and outlet temperatures of cold streams in exchanger *ex*; $LMTD_{ex}$: logarithmic mean temperature difference in exchanger *ex*; EXA_{ex}: heat transfer area of exchanger *ex*; h_i and h_0: tube-side and shell-side heat transfer coefficient; U_{ex}: overall heat transfer coefficient of exchanger *ex*.

© Woodhead Publishing Limited, 2013

Table 32.11 Enhancement level and capital cost of each type of intensification, and the cost of adding more heat transfer area

Intensification techniques	Intensification: Cost = $A + \sum (B \times \text{Area})$ (\$) Adding area: Cost = $A + B \times \Delta\text{Area}$ (\$)		Max times of intensification
	A	*B*	
Tube-side			
TT inserts	1,000	25	1.20
CW inserts		30	1.40
Internal fins		35	1.73
TT inserts and internal fins		50	1.88
CW inserts and internal fins		55	2.00
Shell-side			
Helical baffles		30	1.15
External fins		35	1.65
Helical baffles and external fins		55	1.75
Adding more heat transfer area	3,460	200	

Table 32.12 shows the retrofit details obtained from the new method. It can be found that, according to the operational constraints of exchangers (Max available U_{ex} in Table 32.10) and intensified techniques (Table 32.11), the optimal solution includes the single technique implementation (e.g. TT inserts in exchanger 20, internal fins in exchanger 23, helical baffles in exchanger 3 and external fins in exchanger 12), and the combination of both tube-side and shell-side intensification (e.g. in exchanger 29, CW inserts and internal fins are used simultaneously in tube-side, while in shell-side, external fins are implemented). The retrofitted HEN can achieve 4.28% energy saving, and requires lower retrofit costs compared with the adding-area method (186,000 US$ vs 237,666 US$).

Implementation of intensified heat transfer is an efficient way to increase energy recovery in a HEN. The reported design approach is able to give realistic and practical solutions for the debottlenecking of HENs, as detailed intensified techniques are systematically applied. This leads to substantial capital saving, as no structural modifications in the heat recovery system configuration are considered. The example shows that, based on the new approach, greater energy saving can be achieved (4.28%) at lower capital cost (22% of reduction, compared with the case where adding exchanger areas is considered).

© Woodhead Publishing Limited, 2013

Table 32.12 Exchanger details of optimal retrofitted HEN

EXs	HTI_{ex} (°C)	HTO_{ex} (°C)	CTI_{ex} (°C)	CTO_{ex} (°C)	$LMTD_{ex}$ (°C)	EXA_{ex} (m^2)	Duty (kW)	h_i (kW/ m^2·°C)	h_0 (kW/ m^2 °C)	U_{ex} (kW/m^2 °C)	Intensified techniques		Retrofit cost ($)	
											Tube-side	Shell-side	IHT	AHTA
1	114.3	65.2	33.5	40.3	49.9	175.0	1,090	0.250	0.250	0.125				
2	130.2	130.0	14.0	14.0	116.2	11.7	27	0.202	0.023	0.021				
3	174.4	76.6	33.5	57.5	74.0	116.7	3,864	0.794	1.028	0.448		HB	3,500	3,500
4	284.2	174.9	156.8	162.5	54.3	175.0	2,679	0.563	0.563	0.282				
5	212.4	156.1	48.9	66.3	125.6	100.0	5,633	0.896	0.897	0.448				
6	174.6	85.7	66.3	85.5	45.6	650.0	6,187	0.418	0.417	0.209				
7	65.2	61.7	13.0	13.0	50.4	20.0	78	0.202	0.125	0.077				
8	76.6	62.1	12.5	12.6	56.5	30.0	571	0.672	0.673	0.336				
9	62.1	43.3	12.5	12.5	39.5	55.6	743	0.677	0.678	0.339				
10	169.2	57.8	12.6	12.9	89.6	277.8	2,786	0.226	0.222	0.112				
11	85.7	69.3	12.9	13.0	64.2	55.6	1,139	0.639	0.638	0.319				
12	169.7	114.3	85.5	89.3	50.2	22.2	1,229	1.658	3.280	1.101		EF	778	3,939
13	218.4	146.3	89.3	95.6	85.7	38.1	2,018	1.232	1.242	0.618				
14	146.3	65.6	13.0	13.2	86.7	85.7	2,261	0.604	0.613	0.304				
15	109.3	69.4	13.2	13.3	74.4	42.9	567	0.356	0.357	0.178	TT	HB	2,357	3,533
16	184.1	130.2	91.3	125.3	48.2	128.6	6,086	2.299	1.716	0.983				
17	335.4	109.3	91.3	109.2	82.3	207.7	3,210	0.376	0.376	0.188				
18	174.9	138.9	117.3	119.7	35.8	207.7	882	0.260	0.219	0.119				
19	138.9	65.6	13.3	13.5	83.6	138.5	1,796	0.312	0.309	0.155				
20	212.0	139.4	119.7	156.5	34.6	1,384.6	13,170	0.561	0.540	0.275	TT		34,615	8,659
21	178.7	174.6	156.5	157.3	19.7	27.7	288	1.087	1.027	0.528				
22	212.7	169.7	151.1	153.1	35.2	83.1	955	0.635	0.671	0.326				

(*Continued*)

© Woodhead Publishing Limited, 2013

Table 32.12 Continued

EXs	HTI_{ex} (°C)	HTO_{ex} (°C)	CTI_{ex} (°C)	CTO_{ex} (°C)	$LMTD_{ex}$ (°C)	EXA_{ex} (m^2)	Duty (kW)	h_i (kW/m^2·°C)	h_0 (kW/m^2 °C)	U_{ex} (kW/m^2 °C)	Intensified techniques		Retrofit cost ($)	
											Tube-side	Shell-side	IHT	AHTA
23	240.1	169.2	153.1	156.8	40.9	41.5	1,772	3.367	1.510	1.042	IF		1,454	4,046
24	253.2	212.0	162.5	178.2	61.4	1,038.5	7,481	0.198	0.288	0.117				
25	213.3	210.9	13.9	14.0	198.2	66.7	424	0.308	0.036	0.032				
26	293.7	184.1	178.2	204.4	30.6	300.0	12,385	2.604	2.792	1.347	IF	HB and EF	26,997	44,600
27	239.3	218.4	204.4	205.6	22.4	233.3	587	0.229	0.220	0.112				
28	290.4	213.3	205.6	234.2	24.4	1,020.0	13,565	1.252	0.966	0.545	TT and IF	EF	86,700	133,636
29	364.3	239.3	234.2	241.6	37.0	240.0	3,498	0.940	0.678	0.394	CW and IF	EF	21,600	35,753
30	1,500.0	937.7	241.6	351.9	903.3	180.0	52,296	0.609	0.681	0.322				
31	139.4	116.1	13.5	13.9	113.7	60.0	4,242	1.359	1.146	0.622				

EX$_s$: exchangers; *HTI*$_{ex}$ and *HTO*$_{ex}$: inlet and outlet temperatures of hot streams in exchanger *ex*; *CTI*$_{ex}$ and *CTO*$_{ex}$: inlet and outlet temperatures of cold streams in exchanger *ex*; *LMTD*$_{ex}$: logarithmic mean temperature difference in exchanger *ex*; *EXA*$_{ex}$: heat transfer area of exchanger *ex*; h_i and h_0: tube-side and shell-side heat transfer coefficient; U_{ex}: overall heat transfer coefficient of exchanger *ex*; *CW*: coiled-wire inserts; *TT*: twisted-tape inserts; *IF*: internal fins; *HB*: helical baffles; *EF*: external fins; IHT: intensified heat transfer; AHTA: adding heat transfer area.

© Woodhead Publishing Limited, 2013

32.4 Heat Transfer Enhancement in Heat Exchanger Network Retrofit with Fouling Consideration

Fouling of Heat Exchangers (HEs) is a chronic problem in the process industry, and costs billions of dollars every year. It has been studied extensively by researchers around the world. An extremely large number of academic and industrial studies of the problem have been reported in the literature. Fouling is concerned with the formation of unwanted material on heat transfer surfaces. Fouling creates a chronic operational problem that involves energy recovery and environmental issues. The problems manifest as loss (or reduction) in production, increased energy consumption, increased pressure losses, antifouling chemical cost, cleaning cost, and so on.

According to Yang *et al*. (2011), fouling of the HE depends on two major operational parameters: the wall shear stress and the surface temperature. The use of tube inserts, one type of enhancement technique, has been shown to be effective in mitigating crude-oil fouling while at the same time enhancing heat transfer, as there will be axial and radial distributions of local shear stress in the tube-side with the introduction of inserts (Ritchie and Droegemueller, 2008). In this section, the fouling model of tube inserts is introduced, and combined in the optimisation approach of HEN retrofit (proposed in Section 32.3.2). Moreover, an industrial study is carried out to demonstrate the validity and efficiency of the enhancement techniques in HEN retrofit scenarios.

32.4.1 Fouling Deposition with Tube Inserts

Based on the work proposed by Yang *et al*. (2009), fouling on a HE surface can be described in two steps. In the first step (induction period), the active fouling species adheres to the heat transfer surface and gradually covers it from a fractional coverage of $\theta = 0$ to total coverage at θ_{max}. This pre-conditioning layer is very thin, though not necessarily a single molecular layer, and so the increase in fouling resistance R_f is negligible. Changes in surface roughness are ignored. In the second step (fouling period), the fouling layer may start to grow immediately on the covered/pre-conditioned surface, when it may be assumed that the growth rate is proportional to θ. The overall rate of fouling resistance growth can therefore be expressed as:

$$\frac{dR_f}{dt} = \theta R_f' \qquad [32.169]$$

where R'_f is the form of established fouling rate expression, and the simple threshold model (Polley *et al*., 2007) is utilised in this report:

© Woodhead Publishing Limited, 2013

$$R'_f = \alpha Re^{-0.8} Pr^{-0.33} \exp\left(\frac{-E}{R.T_w}\right) - \gamma Re^{0.8} \quad [32.170]$$

$$Re_e = 1.8526Re - 0.3945 \quad [32.171]$$

In Equations [32.170] and [32.171], α and γ are constants, Re and Re_e are the Reynolds numbers before and after heat transfer enhancement, Pr is the Prandlt number, E is activation energy or apparent activation energy, R is universal gas constant and T_w is the tube wall temperature.

Yang *et al*. (2009) also proposed a second-order growth rate (θ_g) on fractional surface coverage (θ):

$$\frac{\mathrm{d}\theta_g}{\mathrm{d}t} = k_1\theta(1-\theta) \quad [32.172]$$

Equation [32.172] shows that in the early stage of surface pre-conditioning, active species can be captured and adhered to the surface. Meanwhile, the particles that stick to the surface act as seeds, attracting more foulant around them, such that fouling proceeds in a micro-growth manner.

Based on the concept of removal or release from the surface, as in adsorption science, the removal rate (θ_r) of the surface coverage is assumed to be proportional to the surface coverage, as shown in Equation [32.173].

$$\frac{\mathrm{d}\theta_r}{\mathrm{d}t} = k_2\theta \quad [32.173]$$

The net growth rate of θ by combining Equations [32.172] and [32.173] is:

$$\frac{\mathrm{d}\theta}{\mathrm{d}t} = k_1\theta(1-\theta) - k_2\theta \quad [32.174]$$

Thus, integrating Equation [32.174] gives the fractional surface coverage (θ):

$$\theta = \frac{k_1 - k_2}{k_1} \times \frac{1}{1 + c \times e^{-(k_1 - k_2)t}} \quad [32.175]$$

where c is constant, t presents time, and k_1 and k_2 are lumped growth rate and removal rate constants.

$$k_1 = A_i exp\left(\frac{-E}{R \cdot T_w}\right) \quad [32.176]$$

$$k_2 = r \times u^{0.8} \quad [32.177]$$

© Woodhead Publishing Limited, 2013

In Equations [32.176] and [32.177], A_i and r are constants, T_w is the tube wall temperature, R is the universal gas constant, E is the activation energy and u is the flow velocity.

Compared with the induction time when the growth of θ reaches its maximum at 0.5 θ_{max}, the fouling time is much longer (normally several months vs several days), and thus the induction time may be negligible in the whole operational period and the overall rate of fouling resistance growth in Equation [32.169] can be simplified as:

$$\frac{dR_f}{dt} = \theta_{max} R'_f \qquad [32.178]$$

According to Equation [32.175], θ_{max} is given by:

$$\theta_{max} = \frac{k_1 - k_2}{k_1} \qquad [32.179]$$

Integrating Equation [32.178], the fouling resistance at operational time t can be estimated as:

$$R_f = \theta_{max} \times R'_f \times t \qquad [32.180]$$

The HEN retrofit procedure addressed in this section is to change the heat transfer coefficients of HEs on the tube-side by implementing tube-insert intensification with constant heat transfer area, which provides energy savings without any topology modifications. In addition, the heat transfer area, stream flowrates and heat capacities in each exchanger are maintained constant during the HEN retrofit. Therefore, the fouling resistance formulations can be combined with the optimisation approach (proposed in Section 32.3.2) for HEN retrofit. Only two types of non-linear terms are generated in the proposed model: the LMTD and the fouling resistance (R_f).

By contrast with the assumption of calculating the overall heat transfer coefficient (U) in Section 32.4.2, this section considers more details for the U calculation:

$$\frac{AD_{ex}}{A_{ex}} DUD_{ex} = \frac{OD_{ex}}{ID_{ex}} DTUD_{ex} + \frac{OD_{ex} ln(OD_{ex} / ID_{ex})}{2k_{tube}} + DSUD_{ex} + TRF + SRF_{ex} \qquad [32.181]$$

where $DTUD_{ex}$, $DSUD_{ex}$ and DUD_{ex} are the reciprocal values of the tube-side, shell-side and overall designed heat transfer coefficients for exchanger ex, respectively, AD_{ex} and A_{ex} are the designed and required area of exchanger

© Woodhead Publishing Limited, 2013

ex, OD_{ex} and ID_{ex} are the outer and inner tube diameters of exchanger ex, k_{tube} is the tube conductivity, and TRF_{ex} and SRF_{ex} are the tube-side and shell-side fouling resistances.

To resolve the computational difficulties related to those non-linear terms, the iterative procedures mentioned in Section 32.3.2 are utilised to find the optimal solutions for implementing enhancement in a HEN retrofit with fouling considerations.

32.4.2 Example

The example introduced in Section 32.3.3 is used to illustrate the effect of tube-insert techniques on fouling in a HEN retrofit (Fig. 32.9). The retrofit objective is to reduce the hot utility (HU) consumption, that is, to reduce the heat duty of HE 30 (target exchanger). The stream data and initial exchanger data can be found in Tables 32.9 and 32.13. Moreover, the heat-flow capacities of the HU and cold utility (CU) are 93 kW/ºC and 9652.5 kW/ºC, the inlet temperatures of the HU and CU are 1,500ºC and 12.45ºC, the Minimum Temperature Difference approaches ($\Delta T_{\min}$) before and after heat transfer intensification are 19ºC and 5ºC, respectively, and the minimum time from the beginning to when the exchanger is required for cleaning is 3.1 months (HE 28). To evaluate the fouling effect, two stages are followed in this section. In the first stage, only heat transfer enhancement is considered in the exchangers. In the second stage, tube-side enhancement and fouling deposition are taken into account in detail, and the economic benefits of the proposed approach are evaluated. The cost parameters used in this study are $FCOSTIHT_{ex}$ = 2,000 ($), $COSTA_{ex}$ = 10 ($/m^2), $COSTU_{ex}$ = 5,000 (US$), CCU = 0 (US$/kW·y) and CHU = 100 (US$/kW·y).

Retrofitting HEN without Consideration of Fouling

In this stage, tube-insert techniques are implemented to maximise HEN retrofit profit without addressing fouling deposition. It is assumed that the shell-side heat transfer coefficient and the shell-side fouling resistance are constant during the retrofit. Based on the proposed method, the optimal solution for HEN retrofit with enhancement is obtained. The details of the optimal retrofitted HEN are shown in Table 32.14.

In the retrofit solution, 14 exchangers are selected for heat transfer enhancement, and about $168 k of retrofit profit is achieved with a saving of 6.75% of HU consumption. However, some exchangers need cleaning more frequently (1.9 months in HE 24, 2.0 h in HE 4, 2.3 months in exchanger 28, 2.5 months in exchanger 29 and 2.6 months in exchanger 22), compared with the minimum time of 3.1 months (HE 28) in the original scenario.

© Woodhead Publishing Limited, 2013

Table 32.13 Exchanger details of original HEN (fouling consideration)

EX	Shell-side temperature (°C)		Tube-side temperature (°C)		LMTD (°C)	Wall temperature (°C)	Duty (kW)	h_i (kW/m²·°C)		h_0 (kW/m²·°C)		U (kW/m²·°C)		Area (m²)		Operating time (month)
	In	Out	In	Out				Designed	Required	Designed	Required	Designed	Required	Designed	Required	
1	117.2	66.3	33.5	40.5	51.7	56.7	1,130.8	0.263	0.263	0.375	0.375	0.125	0.125	192.5	175.0	9.4
2	131.2	130.0	14.2	14.2	116.4	55.4	139.8	0.208	0.208	0.304	0.304	0.101	0.101	12.8	11.7	7.1
3	174.4	76.7	33.5	57.5	74.0	76.2	3,860.3	0.521	0.521	0.671	0.671	0.224	0.224	256.7	233.3	11.9
4	284.2	174.7	156.7	162.4	54.3	187.5	2,682.0	0.703	0.703	0.847	0.847	0.282	0.282	192.5	175.0	3.5
5	212.4	156.1	49.0	66.5	125.5	94.1	5,633.4	0.453	0.453	0.898	0.898	0.224	0.224	220.0	200.0	5.4
6	174.4	85.7	66.5	85.6	45.5	96.5	6,176.5	0.479	0.479	0.627	0.627	0.209	0.209	715.0	650.0	5.2
7	66.3	61.7	13.0	13.0	50.9	31.1	102.4	0.211	0.211	0.307	0.307	0.102	0.102	22.0	20.0	8.8
8	76.7	62.2	12.5	12.6	56.6	36.1	571.6	0.893	0.893	1.008	1.008	0.336	0.336	33.0	30.0	5.7
9	62.2	43.3	12.5	12.5	39.5	29.2	745.4	0.903	0.903	1.017	1.017	0.339	0.339	61.1	55.6	4.5
10	171.1	57.8	12.6	12.9	90.2	49.0	2,832.8	0.235	0.235	0.339	0.339	0.113	0.113	305.6	277.8	15.3
11	85.7	69.3	12.9	13.0	64.2	39.4	1,141.5	0.832	0.832	0.959	0.959	0.320	0.320	61.1	55.6	9.6
12	169.1	117.2	85.6	89.2	52.1	107.1	1,150.6	0.204	0.204	0.298	0.298	0.099	0.099	244.5	222.2	7.2
13	221.1	147.2	89.2	95.6	87.5	126.7	2,069.2	0.411	0.411	0.552	0.552	0.184	0.184	141.4	128.6	12.7
14	147.2	65.6	13.0	13.2	87.0	51.0	2,285.9	0.786	0.786	0.920	0.920	0.307	0.307	94.3	85.7	6.0
15	109.3	69.4	13.2	13.3	74.3	41.6	566.6	0.392	0.392	0.530	0.530	0.177	0.177	47.1	42.9	8.0
16	198.4	131.2	91.3	133.7	51.3	134.3	7,586.7	0.927	0.927	1.035	1.035	0.345	0.345	471.5	428.6	7.9
17	335.4	109.3	91.3	109.2	82.2	146.0	3,210.1	0.422	0.422	0.564	0.564	0.188	0.188	228.5	207.7	9.9
18	174.7	139.7	121.5	123.9	31.8	135.1	858.6	0.275	0.275	0.390	0.390	0.130	0.130	228.5	207.7	12.1
19	139.7	65.6	13.3	13.5	83.9	46.1	1,816.1	0.340	0.340	0.469	0.469	0.156	0.156	152.3	138.5	13.2
20	206.2	141.9	123.9	156.4	31.2	153.6	11,684.2	0.663	0.663	0.810	0.810	0.270	0.270	1,523.1	1,384.6	5.4

(*Continued*)

© Woodhead Publishing Limited, 2013

Table 32.13 Continued

EX	Shell-side temperature (°C)		Tube-side temperature (°C)		LMTD (°C)	Wall temperature (°C)	Duty (kW)	h_i (kW/m^2·°C)		h_0 (kW/m^2·°C)		U (kW/m^2·°C)		Area (m^2)		Operating time (month)
	In	Out	In	Out				Designed	Required	Designed	Required	Designed	Required	Designed	Required	
21	178.7	174.4	156.4	157.3	19.7	164.4	296.2	0.504	0.504	0.653	0.653	0.218	0.218	76.2	69.2	4.9
22	212.7	169.1	151.1	153.1	34.7	167.4	968.6	0.658	0.658	0.805	0.805	0.268	0.268	114.2	103.8	3.6
23	240.1	171.1	153.1	156.7	42.6	175.3	1,724.4	0.736	0.736	0.876	0.876	0.292	0.292	152.3	138.5	4.7
24	253.2	206.2	162.4	180.4	57.1	192.6	8,525.4	0.308	0.308	0.431	0.431	0.144	0.144	1,142.3	1,038.5	3.4
25	222.7	210.9	14.0	14.2	202.7	88.4	2,085.1	0.335	0.335	0.463	0.463	0.154	0.154	73.3	66.7	10.0
26	293.7	198.4	180.4	203.1	44.9	214.6	10,771.6	0.984	0.984	1.079	1.079	0.360	0.360	733.3	666.6	4.3
27	249.0	221.1	203.1	204.7	29.2	215.0	780.5	0.239	0.239	0.344	0.344	0.115	0.115	256.6	233.3	4.3
28	290.4	222.7	204.7	229.9	35.1	233.5	11,903.4	0.881	0.881	0.998	0.998	0.333	0.333	1,122.0	1,020.0	3.1
29	364.3	249.0	229.9	236.7	57.1	261.6	3,228.0	0.556	0.556	0.706	0.706	0.235	0.235	264.0	240.0	4.2
30	1,500.0	912.5	236.7	351.9	891.2	673.7	54,633.2	0.910	0.910	1.022	1.022	0.341	0.341	198.0	180.0	15.7
31	141.9	116.1	13.5	14.0	114.8	55.5	4,683.1	0.290	0.290	0.408	0.408	0.136	0.136	330.0	300.0	5.3

© Woodhead Publishing Limited, 2013

Table 32.14 Exchanger details of retrofitted HEN with maximum retrofit profit (fouling consideration)

EX	Shell-side temperature (°C)		Tube-side temperature (°C)		LMTD (°C)	Wall Temperature (°C)	Duty (kW)	Cost ($)	h_i (kW/m^2·°C)		h_0 (kW/m^2·°C)		U (kW/m^2· °C)		Area (m^2)		Operating time (month)
	In	Out	In	Out					Designed	Required	Designed	Required	Designed	Required	Designed	Required	
1	113.1	65.7	33.5	55.7	49.9	55.7	1,053.4	0	0.263	0.248	0.375	0.375	0.125	0.121	192.5	175.0	13.9
2	130.1	130.0	13.8	55.0	116.2	55.0	13.3	0	0.208	0.011	0.304	0.304	0.101	0.008	12.8	11.7	881.8
3	174.4	76.7	33.5	76.2	74.0	76.2	3,860.2	0	0.521	0.521	0.671	0.671	0.224	0.223	256.7	233.3	11.9
4	284.2	163.1	157.8	207.6	36.8	207.6	2,966.9	12,080	3.069	3.069	0.847	0.847	0.460	0.460	192.5	175.0	2.0
5	212.4	156.1	48.7	93.9	125.8	93.9	5,633.4	0	0.453	0.452	0.898	0.898	0.224	0.224	220.0	200.0	5.5
6	171.7	85.3	66.2	95.6	44.7	95.6	6,009.5	0	0.479	0.470	0.627	0.627	0.209	0.207	715.0	650.0	6.1
7	65.7	61.7	13.0	30.9	50.7	30.9	88.9	0	0.211	0.162	0.307	0.307	0.102	0.087	22.0	20.0	26.5
8	76.7	62.2	12.5	36.2	56.6	36.2	572.9	7,337	0.896	0.896	1.008	1.008	0.337	0.337	33.0	30.0	9.6
9	62.2	43.3	12.5	29.2	39.5	29.2	744.1	0	0.903	0.902	1.017	1.017	0.339	0.339	61.1	55.6	4.5
10	160.1	57.8	12.6	47.1	86.4	47.1	2,556.8	0	0.235	0.214	0.339	0.339	0.113	0.107	305.6	277.8	29.0
11	85.3	69.3	12.9	39.3	64.1	39.3	1,115.7	0	0.832	0.802	0.959	0.959	0.320	0.314	61.1	55.6	11.6
12	158.9	113.1	84.8	104.0	46.4	104.0	1,015.7	0	0.204	0.201	0.298	0.298	0.099	0.099	244.5	222.2	9.1
13	214.4	126.9	88.0	136.8	71.6	136.8	2,448.7	10,648	0.918	0.918	0.552	0.552	0.266	0.266	141.4	128.6	10.0
14	126.9	65.6	13.0	46.8	79.3	46.8	1,717.5	0	0.786	0.547	0.920	0.920	0.307	0.253	94.3	85.7	25.9
15	96.3	69.4	13.2	39.1	68.8	39.1	382.0	0	0.392	0.240	0.530	0.530	0.177	0.130	47.1	42.9	46.5
16	209.6	130.1	91.3	143.6	52.1	143.6	8,985.3	12,546	1.337	1.337	1.035	1.035	0.402	0.402	471.5	428.6	8.1
17	335.4	96.3	91.3	169.9	57.8	169.9	3,394.7	11,806	1.059	1.059	0.564	0.564	0.283	0.283	228.5	207.7	5.0
18	163.1	130.9	125.9	141.7	15.4	141.7	789.6	13,766	1.375	1.375	0.390	0.390	0.246	0.246	228.5	207.7	8.3
19	130.9	65.6	13.2	44.4	80.6	44.4	1,600.2	0	0.340	0.292	0.469	0.469	0.156	0.143	152.3	138.5	29.7
20	189.0	134.0	128.1	156.9	15.8	156.9	9,977.2	25,664	3.313	3.313	0.810	0.810	0.456	0.456	1,523.1	1,384.6	4.8

(*Continued*)

© Woodhead Publishing Limited, 2013

Table 32.14 Continued

EX	Shell-side temperature (°C)		Tube-side temperature (°C)		LMTD (°C)	Wall Temperature (°C)	Duty (kW)	Cost ($)	h_i (kW/m^2·°C)		h_0 (kW/m^2·°C)		U (kW/m^2· °C)		Area (m^2)		Operating time (month)
	In	Out	In	Out					Designed	Required	Designed	Required	Designed	Required	Designed	Required	
21	178.7	171.7	155.9	170.6	18.5	170.6	489.1	11,559	2.518	2.518	0.653	0.653	0.383	0.383	76.2	69.2	3.8
22	212.7	158.9	151.1	177.9	25.4	177.9	1,194.5	11,589	3.293	3.293	0.805	0.805	0.454	0.454	114.2	103.8	2.6
23	240.1	160.1	153.6	189.9	29.8	189.9	2,000.4	11,813	3.676	3.676	0.876	0.876	0.484	0.484	152.3	138.5	3.1
24	253.2	189.0	164.1	209.5	41.7	209.5	11,653.0	22,791	1.543	1.543	0.431	0.431	0.269	0.269	1,142.3	1,038.5	1.9
25	217.9	210.9	13.7	87.3	200.6	87.3	1,229.7	0	0.335	0.154	0.463	0.463	0.154	0.092	73.3	66.7	88.6
26	293.7	209.6	188.6	221.0	45.8	221.0	9,499.5	0	0.984	0.734	1.079	1.079	0.360	0.311	733.3	666.6	10.0
27	242.2	214.4	208.7	223.3	15.2	223.3	780.8	14,168	1.189	1.189	0.344	0.344	0.220	0.220	256.6	233.3	3.0
28	290.4	217.9	210.3	247.4	23.4	247.4	12,758.8	21,258	4.404	4.404	0.998	0.998	0.535	0.535	1,122.0	1,020.0	2.3
29	364.3	242.2	237.2	286.0	36.1	286.0	3,416.6	13,007	2.318	2.318	0.706	0.706	0.394	0.394	264.0	240.0	2.5
30	1,500.0	952.2	244.4	684.2	910.2	684.2	50,946.7	0	0.910	0.756	1.022	1.022	0.341	0.311	198.0	180.0	29.6
31	134.0	116.1	13.4	53.9	111.3	53.9	3,262.5	0	0.290	0.174	0.408	0.408	0.136	0.098	330.0	300.0	30.6

© Woodhead Publishing Limited, 2013

Table 32.15 Exchanger details of retrofitted HEN with operating time longer than 8 months (fouling consideration)

EX	Shell-side temperature (°C)		Tube-side temperature (°C)		LMTD (°C)	Wall temperature (°C)	Duty (kW)	Cost ($)	h_i (kW/m²·°C)		h_0 (kW/m²·°C)		U (kW/m²·°C)		Area (m²)		Operating time (month)
	In	Out	In	Out					Designed	Required	Designed	Required	Designed	Required	Designed	Required	
1	115.7	66.4	33.5	40.3	51.2	56.4	1,095.9	0	0.263	0.253	0.375	0.375	0.125	0.122	192.5	175.0	12.0
2	130.9	130.0	13.9	13.9	116.5	55.2	97.9	0	0.208	0.124	0.304	0.304	0.101	0.071	12.8	11.7	40.1
3	174.4	76.7	33.5	57.5	74.0	76.2	3,860.5	0	0.521	0.521	0.671	0.671	0.224	0.224	256.7	233.3	11.9
4	284.2	179.7	157.5	162.9	58.4	188.8	2,559.4	0	0.703	0.561	0.847	0.847	0.282	0.251	192.5	175.0	8.0
5	212.4	156.1	48.9	66.3	125.6	94.1	5,633.4	9,210	0.455	0.452	0.898	0.898	0.225	0.224	220.0	200.0	9.2
6	174.7	83.3	66.3	86.1	43.3	98.8	6,357.3	14,712	0.588	0.555	0.627	0.627	0.232	0.226	715.0	650.0	9.3
7	66.4	61.7	13.0	13.0	51.0	31.1	104.5	0	0.211	0.214	0.307	0.307	0.102	0.103	22.0	20.0	8.0
8	76.7	60.7	12.5	12.6	55.7	40.2	631.1	8,064	1.227	1.155	1.008	1.008	0.386	0.376	33.0	30.0	8.2
9	60.7	43.3	12.5	12.5	38.9	28.9	685.7	0	0.903	0.789	1.017	1.017	0.339	0.317	61.1	55.6	8.0
10	162.5	57.8	12.6	12.9	87.3	47.5	2,619.2	0	0.236	0.219	0.339	0.339	0.113	0.108	305.6	277.8	25.3
11	83.3	69.3	12.9	13.0	63.1	38.9	975.8	0	0.832	0.634	0.959	0.959	0.320	0.278	61.1	55.6	26.3
12	162.1	115.7	86.1	89.2	48.1	105.8	1,028.9	0	0.204	0.194	0.298	0.298	0.099	0.096	244.5	222.2	10.4
13	216.1	143.1	89.2	95.6	82.7	126.9	2,044.8	8,678	0.452	0.445	0.552	0.552	0.194	0.192	141.4	128.6	21.5
14	143.1	65.6	13.0	13.2	85.5	50.1	2,170.1	0	0.786	0.733	0.920	0.920	0.307	0.296	94.3	85.7	8.8
15	102.4	69.4	13.2	13.2	71.4	40.2	467.8	0	0.392	0.304	0.530	0.530	0.177	0.152	47.1	42.9	24.4
16	194.4	130.9	91.3	131.4	50.4	137.4	7,179.8	12,544	1.335	0.858	1.035	1.035	0.402	0.333	471.5	428.6	33.4
17	335.4	102.4	91.3	109.8	71.1	159.5	3,308.8	10,700	0.698	0.593	0.564	0.564	0.241	0.224	228.5	207.7	15.0

(*Continued*)

© Woodhead Publishing Limited, 2013

Table 32.15 Continued

EX	Shell-side temperature (°C)		Tube-side temperature (°C)		LMTD (°C)	Wall temperature (°C)	Duty (kW)	Cost ($)	h_i (kW/m²·°C)		h_0 (kW/m²·°C)		U (kW/m²·°C)		Area (m²)		Operating time (month)
	In	Out	In	Out					Designed	Required	Designed	Required	Designed	Required	Designed	Required	
18	179.7	128.5	120.6	124.1	24.5	146.9	1,254.2	14,153	1.667	1.376	0.390	0.390	0.257	0.246	228.5	207.7	9.7
19	128.5	65.6	13.2	13.4	79.6	44.0	1,543.0	0	0.340	0.282	0.469	0.469	0.156	0.140	152.3	138.5	34.4
20	196.0	132.0	124.1	156.5	19.7	158.5	11,611.8	25,663	3.311	2.356	0.810	0.810	0.456	0.426	1,523.1	1,384.6	8.0
21	178.7	174.7	156.5	157.3	19.8	164.4	281.1	0	0.504	0.454	0.653	0.653	0.218	0.205	76.2	69.2	8.0
22	212.7	162.1	151.1	153.4	28.7	179.1	1,123.1	11,588	3.289	1.509	0.805	0.805	0.453	0.377	114.2	103.8	8.0
23	240.1	162.5	153.4	157.5	33.3	190.8	1,938.1	11,813	3.676	1.901	0.876	0.876	0.484	0.420	152.3	138.5	8.0
24	253.2	196.0	162.9	184.8	48.6	211.5	10,377.4	22,789	1.541	0.636	0.431	0.431	0.269	0.205	1,142.3	1,038.5	8.0
25	221.4	210.9	13.7	13.9	202.3	87.9	1,848.4	0	0.335	0.274	0.463	0.463	0.154	0.137	73.3	66.7	24.5
26	293.7	194.4	184.8	208.5	34.6	233.9	11,220.4	17,212	4.926	2.283	1.079	1.079	0.567	0.486	733.3	666.6	8.1
27	243.9	216.1	208.5	210.1	17.6	224.5	778.9	14,176	1.193	0.705	0.344	0.344	0.220	0.190	256.6	233.3	8.0
28	290.4	221.4	210.1	235.7	27.5	248.6	12,140.1	21,258	4.405	1.725	0.998	0.998	0.535	0.433	1,122.0	1,020.0	8.0
29	364.3	243.9	235.7	242.8	42.0	288.4	3,369.8	13,302	2.762	1.263	0.706	0.706	0.408	0.334	264.0	240.0	8.0
30	1,500.0	944.0	242.8	351.9	906.3	682.1	51,709.8	0	0.910	0.785	1.022	1.022	0.341	0.317	198.0	180.0	26.7
31	132.0	116.1	13.4	13.7	110.3	53.6	2,903.5	0	0.290	0.149	0.408	0.408	0.136	0.088	330.0	300.0	41.5

© Woodhead Publishing Limited, 2013

Retrofitting HEN with Consideration of Fouling

In this stage, tube-side fouling deposition and intensification are considered simultaneously to improve energy saving in the whole network in order to minimise the retrofit cost. It is noted that the minimum time that an exchanger is required for cleaning is 3.1 months in the original network. To increase the operational time of the whole process, the proposed method is utilised to obtain the optimal solution under the constraint of $minT_{ex} \geq 8$ months. The details of optimally retrofitted HENs are shown in Table 32.15. Even though the retrofit profits of the new solutions are not as high as the previous solution in Section 33.5.2.1 ($76 kUS ($minT_{ex}$ = 8 months) *vs* $168 kUS ($minT_{ex}$ = 1.9 months)), the operational times of the exchangers are significantly longer. This can save substantial capital investment, because of potential production losses during unit cleaning process.

The proposed design approach is able to give realistic and practical solutions for the debottlenecking of the HEN as detailed intensified techniques are systematically applied. This leads to substantial capital saving, as no structural modification in the heat recovery system configuration is required. The example shows that, based on the new approach, greater energy saving can be achieved (5.35% of reduction) with significantly longer operational times (3.1–8 months).

32.5 Sources of Further Information

There are various sources of information on intensifying heat transfer to improve heat recovery in retrofitted HENs. This section includes the most important sources of information from conferences, journals, service providers and projects.

Conferences

- Process Integration, Modelling and Optimisation for Energy Saving and Pollution Reduction (PRES), organised annually since 1998, <www.conferencepres.com>
- European Symposium on Computer Aided Process Engineering (ESCAPE), organised annually since 1992, <www.cape-wp.eu>
- Dubrovnik Conference on Sustainable Development of Energy, Water and Environment Systems (SDEWES), organised annually since 2002, <www.sdewes.fsb.hr>
- International conference of Heat Exchanger Fouling and Cleaning, organised every two years since 2003, www.heatexchanger-fouling.com

© Woodhead Publishing Limited, 2013

Journals

- *AIChE Journal*, <www.aiche.org/publications/journals/aiche-journal>
- *Applied Thermal Engineering*, <www.journals.elsevier.com/applied-thermal-engineering/>
- *ASME Journal of Heat Transfer*, <asmedl.org/HeatTransfer>
- *Chemical Engineering Science*, <www.journals.elsevier.com/chemical-engineering-science/>
- *Chemical Engineering Transactions*, <www.aidic.it/cet>
- *Computer Aided Chemical Engineering*, <www.elsevier.com/wps/find / bookdescription.cws_home/BS_CCE/description>
- *Computer and Chemical Engineering*, <www.journals.elsevier.com/computers-and-chemical-engineering//>
- *Energy*, <www.journals.elsevier.com/energy/>
- *Heat Transfer Engineering*, <www.tandfonline.com/loi/uhte20>
- *Industrial & Engineering Chemistry Research*, <pubs.acs.org/journal/iecred>
- *International Communications in Heat and Mass Transfer*, <www. journals.elsevier.com/international-communications-in-heat-and-mass-transfer/>
- *International Journal of Heat and Mass Transfer*, <www.journals. elsevier.com/international-journal-of-heat-and-mass-transfer/>

Service Providers

- Centre for Process Integration, School of Chemical Engineering and Analytfical Scfience, The , Manchešter, M13 9PL, United Kingdom, <www.ceas.manchester.ac.uk/research/centres/centre forprocessintegration/>, contact person: Robin Smith
- Process Integration Limited, One Central Park, Northampton Road, Manchester, M40 5BP, United Kingdom, <www.proint.org>, contact person: Robin Smith
- Cal Gavin Limited, Minerva Mill Technology Centre, Station Road, Alcester, Warwickshire, B49 5ET, United Kingdom, <www.calgavin.com/>
- Group of Advanced Materials and Porous Solids, Department of Chemical Engineering, University of Bath, Bath, BA2 7AY, United Kingdom, <www.bath.ac.uk/chem-eng/research/materials/index.html>, contact person: Barry Crittenden
- Centre for Process Integration and Intensification (CPI^2), Research Institute of Chemical and Process Engineering, Faculty of Information Technology; University of Pannonia, Egyetem u. 10, Veszprém, H-8200, Hungary, < cpi.uni-pannon.hu/>, contact person: Jiří Klemeš

© Woodhead Publishing Limited, 2013

Projects

- 'Intensified Heat Transfer for Energy Saving in Process Industries', EP/G060274/1 EPSRC-PROJECT, The , Manchester, United Kingdom, <*gow.epsrc.ac.uk/NGBOViewGrant.aspx*?GrantRef=EP/G060274/1>, 09 November 2009–08 November 2011
- INTHEAT, 'Intensified Heat Transfer Technologies for Enhanced Heat Recovery', Grant Agreement No. 262205, EC FP7 project, Process Integration Limited, Manchester, United Kingdom, <intheat.dcs.uni-pannon.hu/>, 1 December 2010–30 September 2012.

32.6 Nomenclature

$\Delta T_{\min}$	Minimum Temperature Difference approach (°C)
ΔP	total pressure drop (kPa)
ΔP_f	pressure drop due to fluid friction in straight sections (kPa)
$\Delta P_{f0,20\%Bc}$	pressure drop in straight section of shell with 20% baffle cut (kPa)
$\Delta P_{fb,20\%Bc}$	pressure drop in one central baffle spacing when baffle cut is 20% (kPa)
ΔP_n	pressure drop in nozzles (kPa)
ΔP_r	pressure drop due to tube entrance, exit and return losses (kPa)
μ	viscosity (mPa·s)
0	shell-side
A	pre-exponential factor in Arrhenius expression (m^2·K/kJ)
A	overall heat transfer area based on the geometry of HE (m^2)
A'	overall heat transfer area based on the overall heat transfer coefficient (m^2)
AD_{ex}	designed area of exchanger *ex* (m^2)
ADU_{ex}	positive variable, differences between initial and updated values of DU_{ex} (kW/m^2 °C)$^{-1}$
AEB_{ex}	positive variable, energy balance differences between hot stream and cold stream in exchanger *ex* (kW)
A_{ex}	required area of exchanger *ex* (m^2)
AU_{ex}	remainder term for calculating the difference between U_{ex} and U'_{ex} (kW/m^2 °C)
B	central baffle spacing (m)
B_c	baffle cut
BDU_{ex}	positive variable, differences between initial and updated values of DU_{ex} (kW/m^2 °C)$^{-1}$

© Woodhead Publishing Limited, 2013

BEB_{ex}	positive variable, energy balance differences between hot stream and cold stream in exchanger *ex* (kW)
B_{in}	inlet baffle spacing (m)
B_{out}	outlet baffle spacing (m)
BU_{ex}	remainder term for calculating the difference between U_{ex} and U'_{ex} (kW/m^2 °C)
$CFCP_{ex}$	heat-flow capacities (the multiplication between heat capacity and flow rate) of cold stream in exchanger *ex* (kW/ °C)
CMF_{ex}	flow fraction of cold stream in exchanger *ex*
C_p	specific heat capacity (J/kg·K)
CP_{min}	CP value of the stream that has lower CP in the exchanger (J/kg·K or J/kg °C)
cs	Cold Stream
CS	set of all cold streams
$CSTI_{cs}$	network inlet temperatures of cold stream *cs* (°C)
$CSTO_{cs}$	network outlet temperatures of cold stream *cs* (°C)
CTI'_{ex}	initial inlet temperatures of cold streams in exchanger *ex* (°C)
CTI_{ex}	inlet temperatures of cold stream in exchanger *ex* (°C)
CTO'_{ex}	initial outlet temperatures of cold streams in exchanger *ex* (°C)
CTO_{ex}	outlet temperatures of cold stream in exchanger *ex* (°C)
D_0	tube outer diameter (m)
$DACTI_{ex}$	positive variable, differences between initial and updated temperatures for cold stream inlet (°C)
$DACTO_{ex}$	positive variable, differences between initial and updated temperatures for cold stream outlet (°C)
$DAHTI_{ex}$	positive variable, differences between initial and updated temperatures for hot stream inlet (°C)
$DAHTO_{ex}$	positive variable, differences between initial and updated temperatures for hot stream outlet (°C)
$DBCTI_{ex}$	positive variable, differences between initial and updated temperatures for cold stream inlet (°C)
$DBCTO_{ex}$	positive variable, differences between initial and updated temperatures for cold stream outlet (°C)
$DBHTI_{ex}$	positive variable, differences between initial and updated temperatures for hot stream inlet (°C)
$DBHTO_{ex}$	positive variable, differences between initial and updated temperatures for hot stream outlet (°C)
D_e	equivalent diameter (m)
D_i	tube inner diameter (m)
D_n	nozzle inner diameter (m)
D_{otl}	bundle outer diameter (m)

© Woodhead Publishing Limited, 2013

DSU_{ex}	reciprocal value of shell-side heat transfer coefficient for exchanger *ex* $(kW/m^2\ °C)^{-1}$
DTU_{ex}	reciprocal value of tube-side heat transfer coefficient for exchanger *ex* $(kW/m^2\ °C)^{-1}$
DU'_{ex}	initial value of DU_{ex} $(kW/m^2\ °C)^{-1}$
DU_{ex}	reciprocal value of the overall heat transfer coefficient for exchanger *ex* $(kW/m^2\ °C)^{-1}$
E	activation energy or apparent activation energy (kJ/mol)
$ESEX_{ex.si}$	1 if the *si*th type of shell-side intensification is implemented in exchanger *ex*; otherwise, it is 0
$ETEX_{ex.ti}$	1 if the *ti*th type of tube-side intensification is implemented in exchanger *ex*; otherwise, it is 0
Ex	exchanger
EX	set of all exchangers
HEN	Heat Exchanger Network
HE	heat exchanger
EXA_{ex}	heat transfer area of exchanger *ex* (m^2)
EX_{cu}	set of all exchangers consuming cold utilities
EX_{hu}	set of all exchangers consuming hot utilities
EX_{ics}	set of all exchangers located in the network inlet cold streams
EX_{ihs}	set of all exchangers located in the network inlet hot streams
EX_{ocs}	set of all exchangers located in the network outlet cold streams
EX_{ohs}	set of all exchangers located in the network outlet hot streams
f_0	shell-side friction factor
f_i	Darcy friction factor
F_L	leakage factor
F_p	tube pitch factor
F_s	shell-side geometry factor
FT	correction factor of $LMTD$
F_z	Reynolds number in shell-side for heat transfer coefficient
g_c	unit conversion factor, 1.0 $kg\cdot m/(N\cdot s^2)$
h	heat transfer coefficient $(W/(m^2\cdot K)$ or $W/(m^2\cdot °C))$
HBA_{ex}	positive variable, heat transfer differences between streams and exchanger in exchanger *ex* (kW)
HBB_{ex}	positive variable, heat transfer differences between streams and exchanger in exchanger *ex* (kW)
$HFCP_{ex}$	heat-flow capacities (the multiplication between heat capacity and flow rate) of hot stream in exchanger *ex* (kW/°C)
HMF_{ex}	flow fraction of hot stream in exchanger *ex*
hs	hot stream

© Woodhead Publishing Limited, 2013

HS	set of all hot streams
$HSTI_{hs}$	network inlet temperatures of hot stream *hs* (°C)
$HSTO_{hs}$	network outlet temperatures of hot stream *hs* (°C)
HTI'_{ex}	initial inlet temperatures of hot streams in exchanger *ex* (°C)
HTI_{ex}	inlet temperatures of hot stream in exchanger *ex* (°C)
HTO'_{ex}	initial outlet temperatures of hot streams in exchanger *ex* (°C)
HTO_{ex}	outlet temperatures of hot stream in exchanger *ex* (°C)
i	tube-side
ID_{ex}	inner tube diameter of exchanger *ex* (m)
inlet	inlet
k	thermal conductivity (W/m·K or W/m·°C)
$k1$	rate constant in induction period model (s^{-1})
$k2$	removal rate constant in induction period (s^{-1})
k_{tube}	tube conductivity (W/m·K or W/m·°C)
L	tube length (m)
L_{eff}	tube effective length (m)
$LMTD$	logarithmic mean temperature difference (°C)
$LMTD'$	initial logarithmic mean temperature difference in exchanger *ex* (°C)
L_{sb}	diameter clearance between shell-and-tube bundle (m)
m	mass flow rate (kg/s)
M	a sufficiently large positive number
$MAXDSU_{ex,si}$	upper bound of the reciprocal value of shell-side heat transfer coefficients with the *si*th type of shell-side intensification $(kW/m^2\ °C)^{-1}$
$MAXDTU_{ex,ti}$	upper bound of the reciprocal value of tube-side heat transfer coefficients with the *ti*th type of tube-side intensification $(kW/m^2\ °C)^{-1}$
$MINDSU_{ex,si}$	lower bound of the reciprocal value of shell-side heat transfer coefficients with the *si*th type of shell-side intensification $(kW/m^2\ °C)^{-1}$
$MINDTU_{ex,ti}$	lower bound of the reciprocal value of tube-side heat transfer coefficients with the *ti*th type of tube-side intensification $(kW/m^2\ °C)^{-1}$
n	nozzle
n_p	tube passes
N_{PT}	number of tubes in the centre of shell
N_S	number of shell passes
n_t	number of tubes
Nu	Nusselt number
Obj	objective value

© Woodhead Publishing Limited, 2013

OD_{ex}	outer tube diameter of exchanger *ex* (m)
outlet	outlet
Pr	Prandtl number
P_T	tube pitch (m)
QS	energy saving in HEN (kW)
QS'	estimated value of energy saving (kW)
R	universal gas constant (kJ/(mol·K))
R_D	fouling resistances (m^2·K/W or m^2·°C/W)
Re	Reynolds number
R_f	fouling resistance (m^2·K/W or m^2·°C/W)
R_s	correction factor for unequal baffle spacing
S_{hm}	shell-side cross-flow area for heat transfer coefficient (m^2)
SI	sets of all types of shell-side intensification
si	type of shell-side intensification
S_{pm}	shell-side cross-flow area for pressure drop (m^2)
SRF_{ex}	shell-side fouling resistance (m^2·K/W or m^2·°C/W)
t	time (s)
T	temperature (°C)
TI	sets of all types of tube-side intensification
ti	type of tube-side intensification
TRF_{ex}	tube-side fouling resistance (m^2·K/W or m^2·°C/W)
u	velocity (ms^{-1})
U	overall heat transfer coefficient (W/(m^2·K) or W/(m^2·°C))
U'_{ex}	initial value of U_{ex} (kW/m^2 °C)
U_{ex}	the overall heat transfer coefficient for exchanger *ex* (kW/m^2 °C)$^{-1}$
v	flow velocity (m/s)
α	dimensioned constant in fouling model
α_r	number of velocity heads allocated for minor losses
β	constant in fouling model
γ	dimensioned constant in fouling model
ΔQ_{max}	maximum heat recovery (kW)
$\Delta T_{initial}$	initial temperature difference between the inlet of high CP stream and the outlet of low CP stream (°C)
θ	fractional surface coverage
ρ	density (kg/m^3)

32.7 References

Abu-Khader, M. (2006). Further understanding of twisted tape effects as tube insert for heat transfer enhancement. *Heat Mass Transfer*, **43**, 123–134. DOI: 10.1007/s00231–006–0097–7.

© Woodhead Publishing Limited, 2013

Ahmad, S., Polley, G. T. (1990). Debottlenecking of heat exchanger networks. *Heat Recovery Systems & CHP*, **10**(4), 369–385. DOI: 10.1016/0890–4332(90)90087-Z.

Allen, B., Gosselin, L. (2008). Optimal geometry and flow arrangement for minimising the cost of shell-and-tube condensers, *International Journal of Energy Research*, **32**, 958–969. DOI: 10.1002/er.1398.

Asante, N. D. K., Zhu, X. X. (1996). An automated approach for heat exchanger network retrofit featuring minimal topology modification. *Computers and Chemical Engineering*, **20**, S7-S12. DOI: 10.1016/0098–1354(96)00013–0.

Asante, N. D. K., Zhu, X. X. (1997). An automated and interactive approach for heat exchanger network retrofit. *Trans IChemE*, **75**(A), 349–360. DOI: 10.1205/026387697523660.

Athier, G., Floquet, P., Pibouleau, L., Domenech, S. (1998). A mixed method for retrofitting heat-exchanger networks. *Computers and Chemical Engineering*, **22**, S505–S511. DOI: 10.1016/S0098–1354(98)00094–5.

Ayub, Z. H. (2005). A new chart method for evaluating single-phase shell-side heat transfer coefficient in a single segmental shell-and-tube heat exchanger. *Applied Thermal Engineering*, **25**, 2412–2420. DOI: 10.1016/j.applthermaleng.2004.12.015.

Bhatti, M. S., Shah, R. K. (1987). Turbulent and transition convective heat transfer in ducts. In *Handbook of Single-Phase Convective Heat Transfer*, Kakac, S., Shah, R. K., Aung, W. (eds), Wiley, New York, 4–1–4–166. DOI: 10.1080/07373938908916581.

Bochenek, R., Jezowski, J. M. (2006). Genetic algorithms approach for retrofitting heat exchanger network with standard heat exchangers. *Computer Aided Chemical Engineering*, **21**, 871–876. DOI: 10.1016/S1570–7946(06)80155–0.

Briones, V., Kokossis, A. (1996). A new approach for optimal retrofit of heat exchanger networks. *Computers and Chemical Engineering*, **20**, S43–S48. DOI: 10.1016/0098–1354(96)00018-X.

Cavallini, A., Censi, G., Del Col, D., Doretti, L., Longo, G. A., Rossetto, L., Zilio, C. (2003). Condensation inside and outside smooth and enhanced tubes-a review of recent research. *Refrigeration*, **26**, 373–392. DOI: 10.1016/S0140–7007(02)00150–0.

Ciric, A. R., Floudas, C. A. (1990). A comprehensive optimisation model of the heat exchanger network retrofit problem. *Heat Recovery Systems & CHP*, **10**(4), 407–422. DOI: 10.1016/0890–4332(90)90090–7.

Ciric, A. R., Floudas, C. A. (1989). A retrofit approach for heat exchanger networks. *Computers and Chemical Engineering*, **13**(6), 703–715. DOI: 10.1016/0098–1354(89)80008–0.

Crittenden, B. D., Kolaczkowski, S. T., Takemoto T. (1993). Use of in-tube inserts to reduce fouling from crude oils. *AIChE Symp Series*, **89**(295), 300–307.

ESDU Ltd. (1984). *Baffled Shell-and-tube Heat Exchangers; Flow Distribution, Pressure Drop and Heat Transfer Coefficient on the Shell-side.* ESDU International Ltd, London, UK.

Frausto-Hernandez, S., Rico-Ramirez, V., Jimenez-Gutierrez, A., Hernandez-Castro, S. (2003). MINLP synthesis of heat exchanger networks considering pressure drop effects. *Computers and Chemical Engineering*, **27**, 1143–1152. DOI: 10.1016/S0098–1354(03)00042–5.

© Woodhead Publishing Limited, 2013

García, A., Vicente, P., Viedma, A.(2005). Experimental study of heat transfer enhancement with wire coil inserts in laminar-transition-turbulent regimes at different Prandtl numbers. *International Journal of Heat Mass Transfer*, **48**, 4640–4651. DOI: 10.1016/j.ijheatmasstransfer.2005.04.024.

Gnielinski, A., Zukauskas, A., Skrinska, A. (1983). *Heat Exchanger Design Handbook*. Hemisphere Publishing Corp., New York, USA.

Huq, M., Aziz-ul Huq, A., Rahman, M. (1998). Experimental measurements of heat transfer in an internally finned tube. *International Communications in Heat and Mass Transfer*, **25**(5), 619–630. DOI: 10.1016/S0735–1933(98) 00049–9.

Jensen, M., Vlakancic, A. (1999). Experimental investigation of turbulent heat transfer and fluid flow in internally finned tubes. *International Communications in Heat and Mass Transfer*, **42**, 1343–1351. DOI: 10.1016/S0017–9310(98)00243–9.

Kern, D. Q., Kraus, A. D. (1972). *Extended Surface Heat Transfer.* McGraw-Hill, New York, USA.

Kotjabasakis, E., Linnhoff, B. (1986). Sensitivity tables for the design of flexible processes (1)-how much contingency in heat exchanger networks is cost-effective. *Chemical Engineering Research and Design*, **64**(a), 197–211.

Kovac Kralj, A., Glavibvc, P. (1995). Retrofit of complex and energy intensive processes. *Computers and Chemical Engineering*, **19**(12), 1255–1270. DOI: 10.1016/0098–1354(94)00121–9.

Krueger, A. W, Pouponnot, F. (2009). Heat exchanger performance enhancement through the use of tube inserts in refineries and chemical plants – successful application examples: Spirelf, Turbotal and Fixotal systems. Proc. Eurotherm Conference on Fouling and Cleaning in Heat Exchangers, Schladming, Austria, pp. 400–406.

Manglik, R., Bergles, A. (1993). Heat transfer and pressure drop correlations for twisted-tape inserts in isothermal tubes. Part 1: laminar flows. *ASME Journal of Heat Transfer*, **115**, 881–889. DOI: 10.1115/1.2911383.

Nguyen, D. Q., Barbaro, A., Vipanurat, N., Bagajewicz, M. J. (2010). All-at-once and step-wise detailed retrofit of heat exchanger networks using an MILP model. *Industrial and Engineering Chemistry Research*, **49**, 6080–6103. DOI: 10.1021/ie901235c.

Pan, M., Bulatov, I., Smith, R., Kim, J. K. (2011a). Improving energy recovery in heat exchanger network with intensified tube-side heat transfer. *Chemical Engineering Transactions*, **25**, 375–380. DOI: 10.3303/CET1125063.

Pan, M., Bulatov, I., Smith, R., Kim, J. K. (2011b). Novel optimisation method for retrofitting heat exchanger networks with intensified heat transfer. *Computer Aided Chemical Engineering*, **29**, 1864–1868. DOI: 10.1016/B978–0–444–54298–4.50151–3.

Pan, M., Bulatov, I., Smith, R., Kim, J. K. (2012). Novel MILP-based iterative method for the retrofit of heat exchanger networks with intensified heat transfer. *Computers and Chemical Engineering*, **42**, 263–276. DOI: 10.1016/j.compchemeng.2012.02.002.

Pan, M., Bulatov, I., Smith, R., Kim, J. K. (2013). Optimisation for the retrofit of large scale heat exchanger networks with different intensified heat transfer techniques. *Applied Thermal Engineering*, 53(2) 373–386.

© Woodhead Publishing Limited, 2013

Polley, G. T., Wilson, D. I., Pugh, S. J., Petitjean, E. (2007). Extraction of crude oil fouling model parameters from plant exchanger monitoring. *Heat Transfer Engineering*, **28**, 185–192. DOI: 10.1080/01457630601064447.

Ponce-Ortega, J. M., Jimenez-Gutierrez, A., Grossmann, I. E. (2008). Simultaneous retrofit and heat integration of chemical processes. *Industrial and Engineering Chemistry Research*, **47**, 5512–5528. DOI: 10.1021/ie071182\+.

Ritchie, J. M., Droegemueller, P. (2008). Application of tube inserts in heat exchangers: benefits of tube inserts. In *Heat Exchanger Design Handbook*, Hewitt, G. F. (ed.), Begell House, Redding, CT, Section 3.21.2, 2008.

Serth, R. W. (ed.) (2007). Design of shell-and-tube heat exchangers. In *Handbook of Process Heat Transfer Principles and Applications*, Elsevier Ltd, Oxford, UK, 187–244.

Sorsak, A., Kravanja, Z. (2004). MINLP retrofit of heat exchanger networks comprising different exchanger types. *Computers and Chemical Engineering*, **28**, 235–251. DOI: 10.1016/S0098–1354(03)00167–4.

Taborek, J. (1988). Vol.3: Shell-and-tube heat exchangers. In *Heat Exchanger Design Handbook*, Schlunder, E. U, Bell, K. J., Hewitt, G. F., Schmidt, F. W., Spalding, D. B., Taborek, J., Zukauskas, A., Gnielinski, V. (eds), Hemisphere Publishing Corp., New York, USA, 3.3.1–3.3.5.

Uttarwar, S., Raja Rao, M. (1985). Augmentation of laminar flow heat transfer in tubes by means of coiled wire inserts. *ASME Journal of Heat Transfer*, **107**, 930–935. DOI: 10.1115/1.3247523.

Varbanov, P. S., Klemeš, J. (2000). Rules for paths construction for HENs debottlenecking. *Applied Thermal Engineering*, **20**(15–16), 1409–1420. DOI: 10.1016/S1359–4311(00)00015–6.

Wang, L., Sundén, B. (2002). Performance comparison of some tube inserts. *International Communications in Heat and Mass Transfer,* **29**(1), 45–56. DOI: 10.1016/S0735–1933(01)00323–2.

Wang, Y., Pan, M., Bulatov, I., Smith, R., Kim, J. K. (2012). Application of intensified heat transfer for the retrofit of heat exchanger network. *Applied Energy*, **89**, 45–59. DOI: 10.1016/j.apenergy.2011.03.019.

Watkinson, A., Miletti, D., Kubanek, G. (1975). Heat transfer and pressure drop of internally finned tubes in laminar flow. *ASME Paper*, 75-HT-41.

Wills, A., Bott, T.R., Gibbard, I. J. (2000). The control of biofilms in tubes using wire-wound inserts. *Canadian Journal of Chemical Engineering*, **78**, 61–64. DOI: 10.1002/cjce.5450780110.

Wills, M. J. N., Johnston D. (1984). A new and accurate hand calculation method for shell-side pressure drop and flow distribution, Proceedings on 22nd National Heat Transfer Conference, American Society of Mechanical Engineers, **36**, 67–79.

Yang, M., O'Meara, A., Crittenden, B. D. (2011). Determination of crude oil fouling thresholds. Proceedings of International Conference of Heat Exchanger Fouling and Cleaning, Greece, 1–6.

Yang, M., Young, A., Niyetkaliyev, A., Crittenden, B. D. (2009). Modelling of fouling induction period. Proceedings of Conference on Heat Exchanger Fouling and Cleaning VIII., Schladming, Austria: www.heatexchanger-fouling.com, 69–75.

© Woodhead Publishing Limited, 2013

Yee, T. F., Grossmann, I. E. (1990). Optimisation models for heat integration-II, heat exchanger network synthesis. *Computers and Chemical Engineering*, **14**, 1165–1184. DOI: 10.1016/0098–1354(90)85010–8.

Zdaniuk, G., Chamra, L., Mago, P. (2008). Experimental determination of heat transfer and friction in helically-finned tubes. *Experimental Thermal and Fluid Science*, **32**, 761–775. DOI: 10.1016/j.expthermflusci.2007.09.006.

Zhang, J. F., Li, B., Huang, W. J., Lei, Y. G., He, Y. L., Tao, W. Q. (2009). Experimental performance comparison of shell-side heat transfer for shell-and-tube heat exchangers with middle-overlapped helical baffles and segmental baffles. *Chemical Engineering Science*, **64**, 1643–1653. DOI: 10.1016/j.ces.2008.12.018.

© Woodhead Publishing Limited, 2013

33

Applications of Pinch Analysis in the Design of Isolated Energy Systems

SANTANU BANDYOPADHYAY,
Indian Institute of Technology, Bombay, India

DOI: 10.1533/9780857097255.5.1038

Abstract: This chapter extends the applicability of Pinch Analysis to the design of isolated energy systems. Isolated energy systems serve the energy need of a location by converting nearby primary energy sources, and such systems are independent of the nationwide energy supply chain. The concept is illustrated with various applications.

Key words: Pinch Analysis, isolated energy systems, renewable energy systems, design space.

33.1 Introduction

Sustainable energy systems can provide energy services to the present generation without compromising similar levels of energy services for the future generations (Manish *et al*., 2006). A sustainable energy system by itself does not ensure overall sustainable development, as several other parameters need to be considered. However, as the energy service is one of the most critical parameters affecting the quality of life, the sustainability of future energy systems is an important prerequisite for overall sustainable development. Major components towards developing a sustainable energy system are improved energy efficiency and appropriate utilisation of the renewable energy sources. An isolated energy system serves the energy demands of a location by providing energy near its point of utilisation. The term 'isolated' essentially signifies that these energy systems are self-contained, and not connected with the larger nationwide energy system directly. For example, isolated energy systems, independent of the national grid, are employed for remote electrification. These isolated energy systems form a subset of the distributed generation and distribution system and include small generation units, typically with the capacity of about 10–250 kW (Willis and Scott, 2000). It has been estimated that more than 1,500 million people around the world have no access to electricity as of 2005 (International Energy Agency, 2006). The vast majority of them are from Sub-Saharan Africa and South

© Woodhead Publishing Limited, 2013

Asia, where electrification rates are only 25.8% and 51.8% (International Energy Agency, 2006). To provide electricity to such remote areas, decentralised electricity generation using renewable energy technologies, such as wind electric generators, photovoltaic systems, etc., may be employed in combination with biomass-based traditional energy systems. Not only electrical systems, as similarly isolated energy system can also meet the thermal demand. Electric geysers/heaters are used in households to generate hot water and, on the other hand, conventional boilers or furnaces are used in process industries for their low temperature process applications. Scarcity of fossil fuels and increase in electricity cost calls for utilisation of solar thermal systems for these applications as isolated energy systems. The advantages of such systems are negligible fuel cost, non-polluting, modularity, and ease of extensibility. Disadvantages are associated with the high unpredictability, as well as low energy density (kW/m^2), of different renewable resources, along with high initial capital investment for such a system.

Renewable energy resources are intermittent, with daily and seasonal variations. Additionally, the power available from renewable sources is stochastic in nature. This leads to a mismatch between the collection and conversion of different renewable energy sources with the energy demands. Therefore, it is often necessary to use an energy storage system for reliable energy supply. The excess energy, when available, is stored in a storage device (such as a battery for electrical energy, or storage tank for thermal energy), and supplied to demand when required. In the case of small conventional isolated energy systems, fluctuations in energy demand forces the energy generation system to operate in part-load conditions. For such scenarios, it is also important to provide an energy storage system to improve the performance of the overall system. Examples of some of the isolated energy systems (Royle *et al*., 1994) are:

- Solar photovoltaic system for electrifying small load,
- Wind-battery system for remote electrification,
- Solar thermal system for providing thermal energy to household and low temperature process applications, etc.

The performance of an isolated energy system depends upon proper sizing of the overall system. The size of a system able to supply the required energy demand can be determined by simulating the entire system using the resource and the demand data. Optimisation of the entire system may be performed to arrive at a sizing which satisfies certain cost and reliability criteria. Techniques of Pinch Analysis can also be applied to design and optimisation of isolated renewable energy systems. This chapter illustrates the successful applications of Pinch Analysis principles to design isolated energy systems.

© Woodhead Publishing Limited, 2013

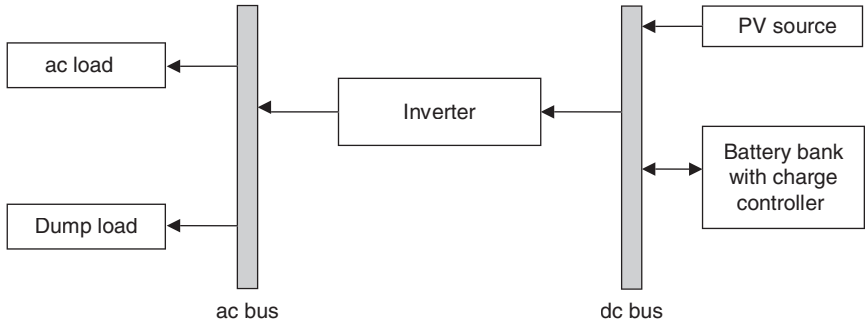

33.1 Schematic of an isolated photovoltaic-battery system for remote electrification.

33.2 Isolated Energy Systems: Descriptions and Models

An isolated energy system typically consists of an energy conversion device, an energy delivery sub-system, an energy storage sub-system and interlinking between these subsystems. For example, an isolated energy system with solar photovoltaic (PV) conversion device will consists of photovoltaic modules, battery bank, electrical loads, charge controller and inverter. The schematic configuration of such an isolated photovoltaic array-battery system is shown in Fig. 33.1 (Arun *et al.*, 2009a). At some times, the battery may be fully charged and the net power produced by the sources is greater than the demand. This excess power is dumped using the dump load. The dump load may be connected either to the dc or the ac bus. In reality, dump loads are not installed for some stand-alone renewable energy systems, e.g., photovoltaic-battery systems. In such cases, it mathematically represents excess power, which is not really generated as the charge regulator disconnects the generator from the respective bus.

In a generic isolated energy system, photovoltaic power generation modules can be replaced by, or complemented with, other renewable-based energy conversion devices or small diesel-based generators. Based on the nature of electricity generation, it may be connected either to the alternating current (ac) bus or the direct current (dc) bus. Accordingly, the inverter may be replaced by a bi-directional converter to convert ac to dc or dc to ac. The schematic of such a generalised isolated energy system, involving multiple generators, is shown in Fig. 33.2 (Sreeraj *et al.*, 2010).

The generalised system (see Fig. 33.2), consists of n power sources, where the first m sources (i.e., 1st to mth) are connected to the ac bus, and the remaining $n–m$ sources (i.e., $m + 1$th to nth) are connected to the dc bus. Let

© Woodhead Publishing Limited, 2013

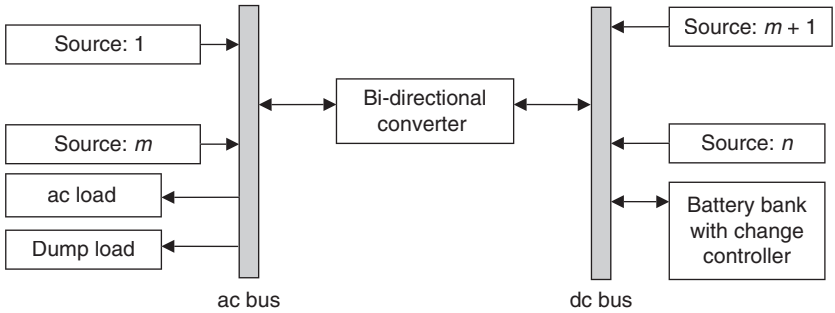

33.2 Schematic of an isolated system incorporating multiple sources.

$P_j(t)$ represent the power generated by the jth source. The net power available at the dc bus may be represented as follows:

$$P_{\text{gen}}(t) = \sum_{j=m+1}^{n} P_j(t) + \eta_i(t) \sum_{j=1}^{m} P_j(t) \qquad [33.1]$$

where $\eta_i(t)$ represents the efficiency associated with the bi-directional converter. The cumulative energy generated by all the sources may be represented as:

$$P_{\text{gen},C}(t) = \int_0^t P_{\text{gen}}(\lambda)\mathrm{d}\lambda \qquad [33.2]$$

Let $D(t)$ be the power required by the load. The cumulative energy required by the load at the dc bus may be represented as:

$$D_C(t) = \int_0^t \frac{D(\lambda)}{\eta_i(\lambda)}\mathrm{d}\lambda \qquad [33.3]$$

Cumulative Energy Generated and the Cumulative Energy Required may be plotted on a time vs energy axis. These curves are equivalent to the Composite Curves of Pinch Analysis. Typical Composite Curves, Supply Composite Curve and Demand Composite Curve, are plotted in Fig. 33.3 (Bandyopadhyay, 2011a). It may be noted that the energy is equivalent to the heat transfer, and time is equivalent to the temperature of the Composite Curves of Pinch Analysis. However, instead of the y-axis, time is plotted as the x-axis in Fig. 33.3. Energy generated in renewable generators can be supplied to supply the load demand. Energy generated during or before the demand can be supplied; energy generated after the demand cannot be supplied to the demand.

In general, the Energy Supply Composite Curve has to lie above the Energy Demand Composite Curve. To fulfil this condition, the Energy

© Woodhead Publishing Limited, 2013

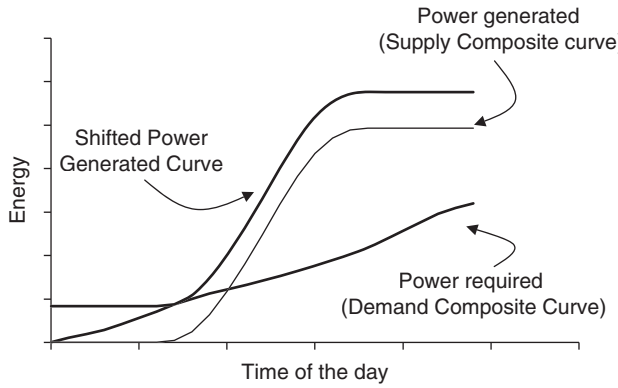

33.3 A typical Energy Supply Composite and Energy Demand Composite Curves.

Supply Composite Curve may be shifted upwards, till it touches and lies completely above the Demand Composite Curve. The shifted Energy Supply Composite Curve is also shown in Fig. 33.3. Physically, such a shifting can be achieved by incorporating initial battery storage.

It may be noted that there are losses during charging and discharging of the battery. Because of these losses, Composite Curve representations are not very useful. A Grand Composite Curve (GCC) equivalent may be plotted to analyse such isolated energy systems (Bandyopadhyay, 2011a).

The net power available to charge the battery ($P_{\text{net}}(t)$) is the sum of the power generated by the sources connected to the dc bus and the power available from the ac bus.

$$P_{\text{net}}(t) = \sum_{j=m+1}^{n} P_j(t) + \left(\sum_{j=1}^{m} P_j(t) - D(t) \right) f_i(t) \qquad [33.4]$$

The term inside the bracket is the net power generated at the ac bus, and f_i represents the efficiency associated with the bi-directional converter (η_i). The net power generated at the ac bus, which is the difference between power generated by the various power sources and the load demand, can be either positive (i.e., excess power is generated) or negative (i.e., demand exceeds supply). Accordingly, the power flows either from ac bus to dc bus or vice versa. The power loss in the bi-directional converter is accounted for by the factor, f_i and is given as follows:

$$\begin{aligned} f_i(t) &= \eta_i \quad \text{when} \quad \sum_{j=1}^{m} P_j(t) \geq D(t) \\ &= \frac{1}{\eta_i} \quad \text{otherwise} \end{aligned} \qquad [33.5]$$

© Woodhead Publishing Limited, 2013

It may be possible that during some time intervals, the total energy that can be produced by all the generators is greater than the sum of the energy demand and that can be stored in the battery. As mentioned earlier, this excess energy has to be dumped ($P_{du}(t)$) or a lower amount of energy has to be produced by the power sources. Therefore, the energy transfer across the battery bank ($dQ_B(t)/dt$) is proportional to the net power available at the dc bus. It may be noted that $P_{du}(t)$ is a non-negative variable.

$$\frac{dQ_B(t)}{dt} = \left(P_{net}(t) - P_{du}(t)\right) f(t) \qquad [33.6]$$

where $f(t)$ represents the efficiencies associated with the charging (η_c) and discharging processes (η_d) of the battery.

$$\begin{aligned} f(t) &= \eta_c \quad \text{when} \quad P_{net} \geq 0 \\ &= \frac{1}{\eta_d} \quad \text{when} \quad P_{net} < 0 \end{aligned} \qquad [33.7]$$

The change in stored energy in the battery, over a small time period of Δt, may be approximately expressed as follows:

$$Q_B(t+\Delta t) = Q_B(t) + \left(\sum_{j=1+m}^{n} P_j(t) + \left(\sum_{j=1}^{m} P_j(t) - D(t) \right) f_i(t) - P_{du}(t) \right) f(t)\Delta t \qquad [33.8]$$

33.3 Grand Composite Curve and Storage Sizing

The graphical representation of storage requirement, as a function of time, is equivalent to the GCC, see Chapter 2 *Basic terminology*, in Heat Exchanger Networks (HENs). In HENs, heat is transferred from hot streams (sources) to cold streams (demands), with temperature being the driving force (quality). Principles of Pinch Analysis can be applied to generalised source–sink problems with generalised flow variables and associated quality attributes (Sahu and Bandyopadhyay, 2011). Similarly, in the case of an isolated energy system, the energy generator is the source, and energy requirement is the demand. The time is the directional quality for an isolated energy system. Energy has to be generated at or before its demand; it cannot be generated after the demand. In this sense, time plays the directional quality. This is similar to the pressure that plays a directional quality for a co-generation system (Bandyopadhyay *et al.*, 2010).

As the power available from the source and the power required for the load, as functions of time, are known, Equation [33.8] may be solved to find the stored energy at the end of each time-step over the time horizon by

© Woodhead Publishing Limited, 2013

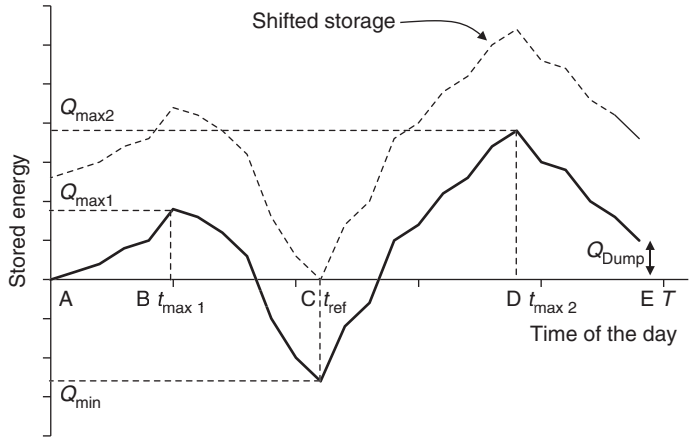

33.4 Typical variation of stored energy level, representing GCC for an isolated energy system.

initially assuming zero dump energy ($P_{du} = 0$). For finding the minimum battery capacity, the stored energy level is determined for a hypothetical battery with an initial zero state (i.e., $Q_B\,(t = 0) = 0$). Equation [33.8] can be simplified by incorporating the assumptions of zero dump energy and zero initial battery state:

$$Q_B(t+\Delta t) = Q_B(t) + \left(\sum_{j=1+m}^{n} P_j(t) + \left(\sum_{j=1}^{m} P_j(t) - D(t) \right) f_i(t) \right) f(t)\Delta t \qquad [33.9]$$

A typical variation of stored energy in the battery is shown in Fig. 33.4. This is equivalent to the GCC representation. Point 'A' in Fig. 33.4 depicts the zero initial stored energy condition.

Furthermore, the repeatability of the battery state of energy over the time horizon, T, can be ensured through the following equation:

$$Q_B(t=0) = Q_B(t=T) \qquad [33.10]$$

The repeatability condition implies that there is no net energy supplied to or drawn from the battery bank over the time horizon. It is assumed that the load is recurring in the same pattern after time T. Therefore, starting with zero initial state of charge, the energy to be dumped is indicated by the stored energy level at the end of the time horizon, $Q_B\,(t = T)$. The power availability and the load at each time-step are repeated in the next cycles, and if the initial state of charge of the battery is not equal to the final, the battery charge will either accumulate or deplete over the time and thereby

© Woodhead Publishing Limited, 2013

cannot ensure the sustainability of the energy system. Therefore, the energy to be dumped can be expressed as:

$$Q_{\text{Dump}} = Q_B(t = T) - Q_B(t = 0) \quad [33.11]$$

The final stored energy at the end of the time horizon is represented by 'E' in Fig. 33.4. If the final stored energy level, at the end of the time horizon, is negative, i.e., if $Q_B\ (t = T) < 0$, then the power sources are insufficient to meet the load. Starting from zero energy level, positive stored energy at the end of the time horizon is necessary for meeting the demand, incorporating various system losses. However, in such a case, energy to be dumped can be determined using Equation [33.11] to satisfy repeatability condition Equation [33.10].

It may be noted that in an actual system, the battery charge level is always non-negative. This is represented by the following constraint.

$$Q_B(t) \geq 0 \quad \forall t \quad [33.12]$$

Figure 33.4 shows the variation of stored energy during the entire time horizon, T. Let Q_{min} be the minimum stored energy, occurring at t_{ref} (point 'C' in Fig. 33.4). To ensure the non-negativity of the stored energy [33.12], the system should start with at least Q_{min} of stored energy. Therefore, the minimum energy level of the stored energy indicates the minimum initial energy level. After shifting the entire GCC vertically with the minimum initial energy, it is going to touch the time axis at this point. This indicates the bottleneck for the storage requirement. Using the terminology of Pinch Analysis, we may call it the Pinch Point (t_{ref}). The vertically shifted storage curve is also shown in Fig. 33.4. However, as the entire curve is shifted vertically by a constant amount (Q_{min}), and the minimum battery requirement depends on the change in stored energy level, the original curve is being considered in the following section to determine the minimum battery requirement.

From the GCC (i.e., Fig. 33.4), it may be noted that Q_{max1} is the maximum stored energy before t_{ref} and Q_{max2} is the maximum stored energy level after t_{ref}. They occur at t_{max1} (point 'B' in Fig. 33.4) and t_{max2} (point 'D' in Fig. 33.4), respectively. Energy stored till the Pinch Point is extremely crucial in satisfying load up to that time. Any energy dumped during this time interval would increase the initial storage requirement. This observation is equivalent to the Golden Rule of Pinch Analysis – in terms of Pinch Analysis of resource allocation networks, no waste generation Below the Pinch Point.

As no energy is allowed to dump before Pinch Point (point 'C' in Fig. 33.4), the extra energy generated by the generator, if any, has to be dumped at an appropriate time interval. This ensures that Equation

© Woodhead Publishing Limited, 2013

[33.10] is satisfied. This is done to reduce the required battery capacity to its minimum value. The excess energy, $Q_B\,(t = T)$ can be dumped at various instants to reduce the peak of the stored energy of the hypothetical battery, keeping the minimum of the stored energy of the battery to occur at reference time itself.

The peak of the stored energy level that occurs after t_{ref}, i.e., Q_{max2}, can be reduced by dumping the excess energy between t_{ref} and t_{max2}, and hence, the peak of the energy stored by the actual battery after t_{ref} can be lowered by an amount equal to the dumped energy. This is because of the excess energy $Q_B\,(t = T)$ that is available between t_{ref} and t_{max2}. On the other hand, the peak of the stored energy level that occurs before t_{ref}, i.e., Q_{max1}, cannot be reduced as there is no excess energy between t_{max1} and t_{ref}. The energy stored in an actual battery cannot be negative Equation [33.12], and a real battery should not be discharged beyond a certain limit. Discharging the battery beyond the specified minimum limit will affect the life of the battery. Typically, a battery is allowed to be discharged till its depth of discharge (X). Combining these, the minimum battery capacity (B) required can be determined as (Sreeraj *et al.*, 2010):

$$B = \max\left(\frac{(Q_{max1} - Q_{min}}{X}, \frac{(Q_{max2} - Q_{min} - Q_B(t = T))}{X}\right) \text{ where } Q_B(t = T) \geq 0 \qquad [33.13]$$

33.4 Design Space

For various values of generator size, the minimum storage requirement can be determined using the GCC of the system. A diagram of different energy generator sizes and the corresponding minimum battery sizes represents the sizing curve of the system. Any point above the sizing curve represents a feasible design option and may be called a design space. The concept of design space has its roots in the work of Poddar and Polley (1996), who have applied it for optimising heat exchangers. Subsequently, Muralikrishna and Shenoy (2000) used the concept to obtain minimum area and cost targets in heat exchanger design. The design space approach has been applied to various fields; e.g., identifying optimum storage volume and collector area combination for solar water heating system for residential applications (Kulkarni *et al.*, 2007), for industrial applications (Kulkarni *et al.*, 2008), as well as water heating systems with optimised water replenishment (Kulkarni *et al.*, 2009), and optimum sizing of generator and storage system in various cases of isolated power systems – in particular: photovoltaic-battery (Arun *et al.*, 2009a), diesel-battery (Arun *et al.* 2008) and wind-battery (Roy *et al.*, 2009). On the basis of time series simulation of the isolated energy systems, subject to different design and

© Woodhead Publishing Limited, 2013

operating constraints, the design space can be identified on a generator size vs storage requirement diagram.

Initially, the minimum generator rating for which Equation [33.10] is satisfied is searched. It may be observed from Equation [33.11] that the dump energy for the minimum generator rating is identical to zero. The simulations to obtain the minimum storage capacity are carried out for different values of the generator rating, higher than the minimum generator rating. For a photovoltaic system, array area ($A > A_{\min}$) represents the size of the generator rating. Initially, the minimum array area ($A_{\min}$) for the entire system is determined. For each value of array area ($A > A_{\min}$) considered, the corresponding minimum battery bank capacity is obtained from the GCC of the system (Equation [33.13]). The combinations of the different array areas and the corresponding minimum storage capacities may be plotted on an array area (or array rating) vs battery bank capacity diagram, which is defined as the sizing curve of the system. The sizing curve represents the minimum storage capacity required for a given array rating. The sizing curve divides the entire space into feasible and infeasible regions. The region above the sizing curve represents the feasible region, as any combination of array area and battery capacity represents a feasible design option. The entire feasible region, including the sizing curve, is the design space for a given problem. Steps involved in generating the design space are summarised in Fig. 33.5. A typical design space is shown in Fig. 33.6.

33.4.1 System Optimisation

The set of all configurations which can meet the load forms the design space, and it can be used to select the optimum configuration based on the specified objective. The objective function, used in this chapter, is the minimum Cost of Energy (COE). The COE depends upon the capital cost, operation and maintenance cost and the amount of energy delivered. COE is represented as:

$$\mathrm{COE} = \frac{\sum_i C_{0i}\mathrm{CRF}_i + \mathrm{AOM}}{E} \qquad [33.14]$$

where C_{0i} is the capital cost of the ith system component corresponding to different power sources (photovoltaic module, wind turbine, etc.) battery bank, inverter and balance of system. AOM is the annual operating and maintenance cost and E is the amount of energy delivered to meet the demand. The Capital Recovery Factor (CRF) is a function of life (n) and the discount rate (d). Steps involved in determining the optimum system configuration from the sizing curve and design space is also highlighted in Fig. 33.5.

© Woodhead Publishing Limited, 2013

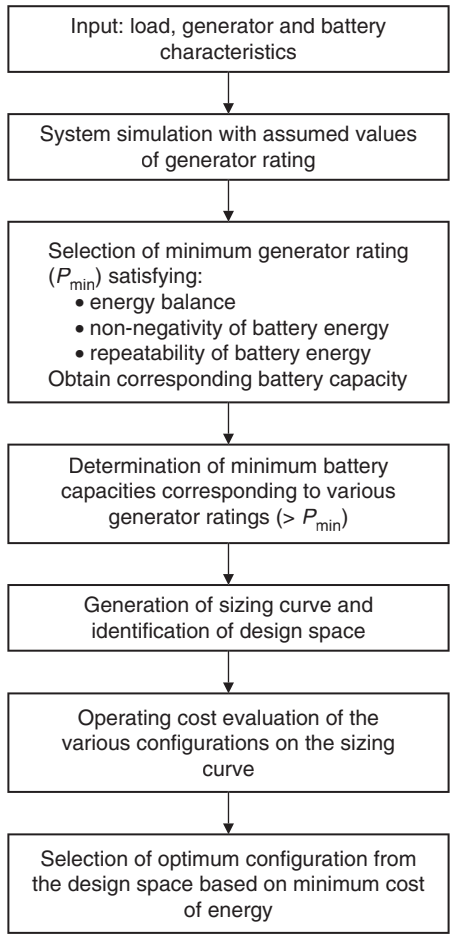

33.5 Steps involved in generating the design space and system optimisation.

33.5 Illustrative Applications

Applicability of the described methodology is demonstrated through various systems. Though the underlying methodology remains same, various energy conversion devices and associate storage options offer additional constraints. Some of the applications are discussed briefly in this section.

33.5.1 Photovoltaic-Battery System

Many methods, from simple correlations to detailed mathematical models, have been proposed for optimising the photovoltaic-battery system. Broadly,

© Woodhead Publishing Limited, 2013

these methods can be grouped into deterministic and stochastic approaches. In the deterministic approach, the uncertainty associated with the solar insolation is not considered, and an independent design of the photovoltaic array and battery bank are obtained (Egido and Lorenzo, 1992). A simple method to size a stand-alone PV system has been proposed by Bhuiyan and Asgar (2003). On the other hand, probabilistic approaches to sizing a photovoltaic system need to account for the effect of solar insolation variability in the system design (Bucciarelli, 1984). A Pinch Analysis-based methodology, to optimally size a photovoltaic system, is also proposed. Sizing of a photovoltaic-battery system involves the determination of the array rating (in terms of the array area or the peak power, W_p) required, and the capacity of the battery bank.

The power generated by the photovoltaic array at any given time t is given by:

$$P(t) = \eta_0 A I_T(t) \quad [33.15]$$

where η_0 is the photovoltaic system efficiency, A is the total array area (m^2) and I_T the total instantaneous radiation incident on the array (W/m^2). The efficiency of a photovoltaic array depends on the construction material, cell configuration, processing technology, operating temperature, solar insolation, operating current and voltage of the array, etc. For simplicity, the effect of ambient temperature on the power production from the photovoltaic array has not been explicitly included in the model. Solar radiation incident on the array, maintained at an inclination (β), is calculated using the following equation (Sukhatme and Nayak, 2008):

$$I_T = (I_g - I_d) r_b + I_d \left(\frac{1 + \cos\beta}{2} \right) + I_g \left(\frac{1 - \cos\beta}{2} \right) r \quad [33.16]$$

where I_g is the global solar radiation (W/m^2), I_d is the diffuse radiation (W/m^2), r_b is the tilt factor and r is the ground reflectance. The typical sizing curve and design space for an isolated photovoltaic-battery system is shown in Fig. 33.6.

33.5.2 Wind-Battery System

Sizing a wind-battery system involves considering the interaction between the availability of wind and the electrical demand subject to different design constraints (Notton *et al.*, 2001). Parametric investigations for wind-battery system have been reported by Kaldellis (2004). The power output of a wind turbine (P_w) is expressed as a function of wind velocity at hub height (v), the rotor area (A) and air density (ρ) as below:

© Woodhead Publishing Limited, 2013

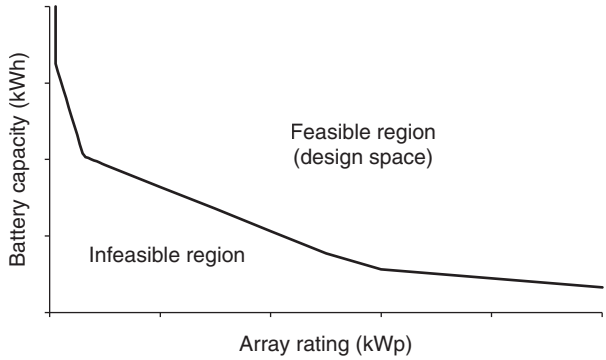

33.6 Typical Sizing Curve and design space for an isolated photovoltaic-battery system.

$$P_w = \frac{1}{2}\rho A v^3 C_p \eta_0 \qquad [33.17]$$

where C_p is the power coefficient of the wind turbine and η_0 is the overall efficiency of the electro-mechanical subsystems. However, the power generated from a turbine at a given wind speed and rotor area will depend upon the power coefficient, which is a complex function of other turbine design parameters. Hence, to obtain the power generated from a wind turbine at a given wind velocity, it is desirable to have a mathematical model of the power generated at different wind speeds. Such a model is known as the power curve model for the wind turbine. The following form of power curve model was proposed by Powell (1981):

$$P_w = \begin{cases} P_r \dfrac{v^k - v_c^k}{v_r^k - v_c^k} & \text{for} \quad v_c < v < v_r \\ p_r & \text{for} \quad v_r < v < v_f \\ 0 & \text{otherwise} \end{cases} \qquad [33.18]$$

Here, P_r is the rated electrical power (W), v_c is cut-in wind speed (m/s), v_f is cut-off wind speed (m/s), v_r is the rated wind speed (m/s) and k is the Weibull shape parameter (Powell, 1981). The value of the shape parameter varies from 1.5 to 3 for different wind regimes. Empirical models relating the power output to the machine parameters, such as rated (v_r), cut-in (v_c) as well as cut-off (v_f) wind velocities, rated power (P_r) and parameters characterising the wind regime of the site, can also be applied for system sizing (Yang *et al.*, 2007). Alternatively, the power output from a wind machine may also be computed by separately modelling the wind turbine

© Woodhead Publishing Limited, 2013

rotor blades, the transmission system (if any) and the electrical generator, and integrating them (Roy *et al.*, 2009). The power coefficient (C_p) vs tip-speed ratio (λ) characteristic of the wind rotor can be modelled using advanced theories such as the Blade Element Momentum (BEM) methodology (Wilson and Lissaman, 1974), vortex wake models (Afjeh and Keith, 1986), Navier–Stokes equations (Xu and Sankar, 2005), etc.

The wind speed data are generally available at a specified meteorological mast height (H_i). To generate wind data at turbine hub height (H) the following model proposed by Justus (1978) is used:

$$v = v_i \left(\frac{H}{H_i} \right)^z \qquad [33.19]$$

where v is the wind speed at turbine hub height H and v_i is wind speed at reference height H_i. In Equation [33.19], z is the power law exponent (taken as 1/7 for open land). Along with this shaft work transfer model and model of the electrical generator should also be considered.

Similar to the sizing of a photovoltaic-battery system, sizing of a wind generator battery system involves the determination of the generator required and the capacity of the battery bank. In the case of a wind-battery system, the interdependence of the system design variables may be highlighted on a rotor diameter vs rated power diagram. It may be noted that there can be many feasible alternatives for the rotor diameter, given a rating of the generator. When battery capacity is chosen as an optimisation variable, the minimum diameter required for a given generator rating can be determined. The locus of the minimum diameter for different rated power may be plotted on a rotor diameter vs rated power diagram. A typical physical design space for wind-battery system is shown in Fig. 33.7. The hub height of the wind machine is specified and is the same for all combinations of generator rating and rotor diameter. Consequently, the utilisable rotor diameter is limited to a maximum value, and is shown by the maximum diameter limit line in Fig. 33.7. The minimum generator rating limit is represented by the vertical line labelled as the minimum rated power limit (Fig. 33.7). The closed space bounded by the minimum diameter curve, the maximum diameter limit and the minimum rated power, indicates the physical limits of designing the wind turbine system and is called the physical design space for the overall system. Any point within the physical design space will be a feasible solution to the design problem, whereas a point lying outside the boundaries prescribed by the physical design space will not be able to meet the load, thus leading to an infeasible system. Constant battery capacity lines are also shown within the physical design space. The storage size, the generator size as well as the rotor blade diameter, are correlated simultaneously through the physical design space representation.

© Woodhead Publishing Limited, 2013

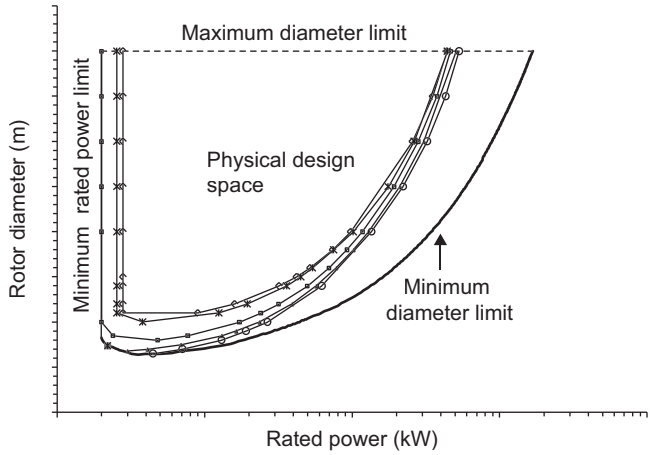

33.7 Physical design space for wind-battery system.

33.5.3 Solar Thermal Systems

A number of design methods for solar water heating systems have been proposed in the literature. These methods can be broadly classified into two categories, namely, correlation-based methods and simulation-based methods. Methods based on utilisability (Duffie and Beckman, 1991), *F* chart (Klein *et al*., 1976), $\bar{\phi}$-*F* chart (Klein and Beckman, 1979), etc. are prominent examples of correlation-based methods. Different simulation programs such as TRNSYS (Klein *et al*., 1975), SOLCHIPS (Lund and Peltola, 1992), etc. have been used to design solar hot water systems through a detailed simulation approach. The design space methodology to design a solar thermal system was introduced by Kulkarni *et al*. (2007).

Storage tank temperature (T_{st}) is an important parameter, which influences the system size and performance. The energy balance of a well-mixed storage tank can be expressed as:

$$\left(\rho C_p V_{st}\right)\frac{dT_{st}}{dt} = A_c\left[I_T F_R(\tau\alpha) - F_R U_L(T_{st} - T_a)\right]^{+} - q_{Ls} - U_{st}A_{st}.(T_{st} - T_a) \quad [33.20]$$

There are two additional constraints to be satisfied for an isolated solar thermal system. The temperature of the storage tank during load has to be greater than the desired load temperature.

$$T_{st} \geq T_L \quad [33.21]$$

© Woodhead Publishing Limited, 2013

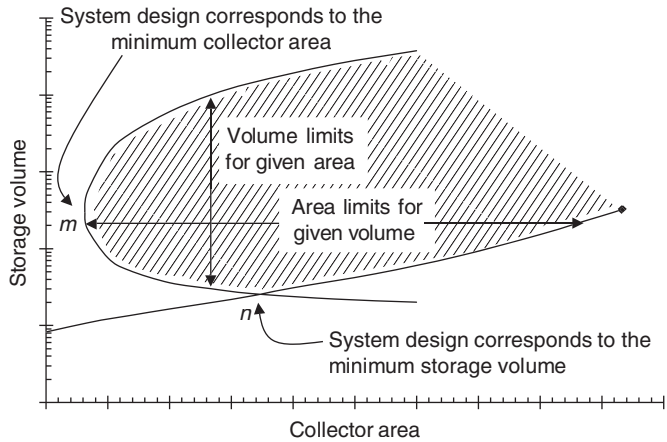

33.8 Design space of a thermal system.

On the other hand, the storage tank temperature has to be always less than the boiling temperature of working fluid.

$$T_{st} \leq T_{sat} \qquad [33.22]$$

A typical design space for solar thermal system is shown in Fig. 33.8.

33.6 Sources of Further Information and Advice

Optimal sizing is important to achieve sustainable energy systems. Applications of the discussed methodology are demonstrated through examples of solar photovoltaic-battery systems, wind-battery systems and solar thermal systems. Other applications include diesel-battery systems (Arun *et al*., 2008), renewable-based hybrid energy systems (Sreeraj, 2010), conventional-renewable hybrid systems (Arun *et al*., 2010), etc. Current and future state-of-the-art development in Wind-PV hybrid energy systems is reviewed by Nema *et al*. (2009). A co-generation system, based on solar energy to supply simultaneously electrical as well as thermal energy, can be effectively designed using a solar photovoltaic-thermal based system (Kumar and Rosen, 2011). Such a system can also be designed using the principles of Pinch Analysis (Krishna Priya and Bandyopadhyay, 2011).

Renewable energy sources are highly probabilistic in nature. It is important to include uncertainty of various renewable energy resources in appropriately sizing the isolated energy system. Various methodologies have been proposed to incorporate resource uncertainty in the design stage (Egido and Lorenzo, 1992). Various methodologies for designing a solar thermal system with stochastic techniques are discussed by Sharma

© Woodhead Publishing Limited, 2013

and Siddhartha (2012). Chance-constrained programming is a useful tool, applicable for studying mathematical models with random variables. This approach was introduced by Charnes and Cooper (1959), based on the concept of constraints in the mathematical model complying with specified values of probability. The chance-constrained programming approach can be incorporated in the framework to design isolated energy systems with resource uncertainty (Bandyopadhyay, 2011b). Applications of the chance-constrained programming-based design space methodology include: design of a diesel-battery system with demand uncertainty (Arun *et al*., 2009b), a photovoltaic-battery system with solar radiation uncertainty (Arun *et al*., 2009a), a wind-battery system with wind availability uncertainty (Roy *et al*., 2010), a hybrid renewable energy system with resource uncertainty (Sreeraj *et al*., 2010), etc. It may be interesting to note that the design space need not be convex when uncertainties are incorporated (Roy *et al*., 2011). Future research is directed towards improving design of isolated energy systems while incorporating various levels of uncertainties.

33.7 References

Afjeh, A. A., Keith T. G. Jr (1986). A vortex lifting line method for the analysis of horizontal axis wind turbines. *Trans ASME, Journal of Solar Energy Engineering*, **108**, 303–309.

Arun, P., Banerjee, R., Bandyopadhyay, S. (2008). Optimum sizing of battery integrated diesel generator for remote electrification through design-space approach. *Energy*, **33**, 1155–1168.

Arun, P., Banerjee, R., Bandyopadhyay, S. (2009a). Optimum sizing of photovoltaic battery systems incorporating uncertainty through design space approach. *Solar Energy*, **83**(7), 1013–1025.

Arun, P., Banerjee, R., Bandyopadhyay, S. (2009b). Optimum design of battery integrated diesel generator systems incorporating demand uncertainty. *Industrial & Engineering Chemistry Research*, **48**(10), 4908–4916.

Arun P., Banerjee, R., Bandyopadhyay, S. (2010). Optimum design of diesel generator integrated photovoltaic-battery system. *Energy & Fuels*, **24**(12), 6565–6575.

Bandyopadhyay, S. (2011a). Design and optimization of isolated energy systems through pinch analysis. *Asia-Pacific Journal of Chemical Engineering*, **6**(3), 518–526.

Bandyopadhyay, S. (2011b). Design of renewable energy systems incorporating uncertainties through pinch analysis. Computer Aided Chemical Engineering 29, 1994–1998.

Bandyopadhyay, S., Varghese, J., Bansal, V. (2010). Targeting for cogeneration potential through total site integration. *Applied Thermal Engineering*, **30**(1), 6–14.

Bhuiyan, M. M. H., Asgar, A. M. (2003). Sizing of a stand-alone photovoltaic power system at Dhaka. *Renewable Energy*, **28**(6), 929–938.

Bucciarelli, L. L. Jr (1984). Estimating loss-of-power probabilities of standalone photovoltaic solar energy systems. *Solar Energy*, **32**(2), 205–209.

© Woodhead Publishing Limited, 2013

Charnes, A., Cooper, W. W. (1959). Chance-constrained programming. *Management Science*, **6**, 73–79.

Duffie, J. A., Beckman, W. A. (1991). *Solar Engineering of Thermal Processes*, 2nd ed. John Wiley and Sons, New York, USA.

Egido, M., Lorenzo, E. (1992). The sizing of standalone PV-systems: a review and a proposed new method. *Solar Energy Materials and Solar Cells*, **26**, 51–69.

International Energy Agency. (2006). *World Energy Outlook*, 2nd ed. IEA Publications.

Justus, C. G. (1978). Wind energy statistics for large arrays of wind turbines (New England and central US regions). *Solar Energy*, **20**(5), 379–386.

Kaldellis, J. K. (2004). Parametric investigation concerning dimensions of a stand-alone wind-power system. *Applied Energy*, **77**, 35–50.

Klein, S. A., Beckman, W. A. (1979). A general design method for closed loop solar energy systems. *Solar Energy*, **22**, 269–282.

Klein, S. A., Beckman, W. A., Duffie, J. A. (1976). A design procedure for solar heating systems. *Solar Energy*, **18**, 113–127.

Klein, S. A., Cooper, P. I., Freeman, T. L., Beekman, D. L., Beckman, W. A., Duffie, J. A. (1975). A method of simulation of solar processes and its application. *Solar Energy*, **17**, 29–37.

Krishna Priya, G. S., Bandyopadhyay, S. (2011). Optimum sizing of standalone photovoltaic thermal (PVT) systems using design space approach. Paper presented in the 31st Annual PAASE Meeting and Symposium, Manila, Philippines, June 15–18.

Kulkarni, G. N., Kedare, S. B., Bandyopadhyay, S. (2007). Determination of design space and optimization of solar water heating systems. *Solar Energy*, **81**(8), 958–968.

Kulkarni, G. N., Kedare, S. B., Bandyopadhyay, S. (2008). Design of solar thermal systems utilizing pressurized hot water storage for industrial applications. *Solar Energy*, **82**, 686–699.

Kulkarni, G. N., Kedare, S. B., Bandyopadhyay, S. (2009). Optimization of solar water heating systems through water replenishment. *Energy Conversion & Management*, **50**, 837–846.

Kumar, R., Rosen, M. A. (2011). A critical review of photovoltaic-thermal solar collectors for air heating. *Applied Energy*, **88**(11), 3603–3614.

Lund, P. D. and Peltola S. S. (1992). SOLCHIPS – a fast pre-design and optimization tool for solar heating with seasonal storage. *Solar Energy*, **48**, 291–300.

Manish, S., Pillai, I. R., Banerjee, R. (2006). Sustainability analysis of renewables for climate change mitigation. *Energy for Sustainable Development*, **10**(4), 25–36.

Muralikrishna, K., Shenoy, U. V. (2000). Heat exchanger design targets for minimum area and cost. *Chemical Engineering Research and Design*, **78A**, 161–167.

Nema, P., Nema, R. K., Rangnekar, S. (2009). A current and future state of art development of hybrid energy system using wind and PV-solar: A review. *Renewable and Sustainable Energy Reviews*, **13**(8), 2096–2103.

Notton G., Muselli M., Poggi P., Louche L. (2001). Decentralized wind energy systems providing small electrical loads in remote areas. *International Journal of Energy Research*, **25**, 141–164.

Poddar T. K., Polley, G. T. (1996). Heat exchanger design through parameter plotting. *Chemical Engineering Research and Design*, **74A**, 849–852.

© Woodhead Publishing Limited, 2013

Powell, W. R. (1981). An analytical expression for the average power output of a wind machine. *Solar Energy*, **26**(1), 77–80.

Roy, A., Kedare, S. B., Bandyopadhyay, S. (2009). Application of design space methodology for optimum sizing of wind–battery systems. *Applied Energy*, **86**(12), 2690–2703.

Roy, A., Kedare, S. B., Bandyopadhyay, S. (2010). Optimum sizing of wind-battery systems incorporating resource uncertainty. *Applied Energy*, **87**(8), 2712–2727.

Roy, A., Kedare, S. B., Bandyopadhyay, S. (2011). On the existence of non-convexities in the design space of isolated wind-battery systems. *Wind Engineering*, **35**(2), 221–244.

Royle, S., Robinson, J., McCrea, A. (1994). Renewable energy in Northern Ireland. *Geography*, **79**(3), 232–245.

Sahu, G. C., Bandyopadhyay, S. (2011). Holistic approach for resource conservation. *Chemical Engineering World*, December, 104–108.

Sharma, N., Siddhartha, V. (2012). Stochastic techniques used for optimization in solar systems: A review. *Renewable and Sustainable Energy Reviews*, **16**(3), 1399–1411.

Sreeraj, E. S., Chatterjee, K., Bandyopadhyay, S. (2010). Design of isolated renewable hybrid power systems. *Solar Energy*, **84**(7), 1124–1136.

Sukhatme, S. P., Nayak, J. K. (2008). *Solar Energy: Principles of Thermal Collections and Storage*, 3rd ed. Tata-McGraw Hill, New Delhi, India.

Willis, H. L., Scott, W. G. (2000). *Distributed Power Generation Planning and Evaluation.* Marcel Dekker Inc., New York, USA.

Wilson, R. E., Lissaman, P. B. S. (1974). *Applied Aerodynamics of Wind Power Machines*. Oregon State University, Corvallis, USA.

Xu, G., Sankar, L. N. (2000). Computational study of horizontal axis wind turbines. *Journal of Transactions on ASME: Journal of Solar Energy Engineering*, **122**, 35–39.

Yang, H., Lu, L., Zhou, W. (2007). A novel optimization sizing model for hybrid solar-wind power generation system. *Solar Energy*, **81**, 76–84.

© Woodhead Publishing Limited, 2013

34

Software Tools for Heat Integration

IGOR BULATOV, The University of Manchester, UK

DOI: 10.1533/9780857097255.6.1059

Abstract: Complexity of problems of Process Integration, modelling and optimisation in chemical engineering requires the application of computers and dedicated software. Software packages have been widely used for process simulation, integration and optimisation for both design and retrofit. A variety of efficient tools are available, but the problem for the user is that each software developer focuses on their product advantages. This chapter provides an overview based on experience and applications of Process Integration software tools. Software tools described in this section are Aspen Energy Analyzer, CDU-int, CRYO-int, DIST-int, HEAT-int, HEXTRAN, Site-int, Spreadsheet Based tool, SPRINT, STAR, SuperTarget and WORK.

Key words: Heat Integration, software tools, Heat Exchanger Network (HEN) design and retrofit, utility system design and retrofit.

34.1 Heat Integration Software Tools

A number of Heat Integration tools has been developed in recent decades. Though this is not a comprehensive list of the software tools that exist worldwide, it provides quite a wide range of tools available in the market and academia.

34.1.1 Aspen Energy

Aspen Energy Analyzer (Aspentech, 2012), aligned with flowsheet simulators such as Aspen HYSYS® and Aspen Plus®, provides an easy environment to perform optimal Heat Exchanger Network (HEN) design and Pinch Analysis. Aspen Energy Analyzer is a core element of AspenTech's aspenONE® Engineering applications. Aspen Energy Analyzer's main features are that it:

- calculates targets for energy and capital investment;
- enables the development of improved Heat Integration projects, significantly reducing operating, capital and design costs, and minimising energy-related emissions;

© Woodhead Publishing Limited, 2013

- provides tools for performing process optimisation;
- provides both graphical and algorithmic methods.

With the large number of design alternatives available, it is likely that a seemingly obvious solution obtained by inspection may be far from optimal. The task of developing an optimal heat-integrated design (based on capital and operating cost) can be complex. The solution is to identify the best options without spending prohibitive amounts of resources in doing so. Aspen Energy Analyzer helps maximise the reuse of heating and cooling duties within the system, with an optimal HEN. The duties that are not satisfied by heat recovery then require external utilities. This approach minimises the external utility requirements, saving energy and capital at a lower environmental impact.

34.1.2 CDU-int

CDU-int (PIL, 2012) designs heat-integrated crude oil distillation systems.

The design of crude oil distillation processes has been traditionally carried out in two steps. First, the design is established for the distillation system. Second, the Heat Integration arrangements are designed. Good design practice would explore the interactions between the design of the distillation column and the design of the HEN. However, even best practice in traditional design approaches has many shortcomings. What is needed is a novel approach that allows the distillation and Heat Integration arrangements to be designed and optimised simultaneously. In retrofit, improving the design for increased energy efficiency, or for increased throughput, brings special challenges. The use of existing equipment must be maximised whilst identifying cost-effective design changes. Changes to operating conditions throughout the system, column internals and heat exchange arrangements must be optimised simultaneously.

CDU-int has capabilities that distinguish it from other software packages for modelling crude oil distillation, which allow design and operation changes to both the crude oil distillation and to the HEN to be considered simultaneously. New semi-rigorous models for the distillation have been developed and have been coupled with the design of the HEN. This allows the distillation and heat recovery system to be designed and optimised simultaneously. The Heat Integration is considered down to the level of individual matches, rather than using targets for the heat recovery. This is necessary if the interactions through features such as the pump-around matches are to be considered adequately. Retrofit can be controlled to restrict the number of modifications. Product qualities can be defined in terms of the bulk properties, and can be either maintained to specified values or manipulated in the optimisation. If required, the quantities of the various products can

© Woodhead Publishing Limited, 2013

be manipulated, along with the energy consumption, as part of the optimisation to increase the overall profit, rather than simply reducing operating cost.

CDU-int main functionalities are to:

- optimise the operating conditions of existing crude oil distillation systems to reduce energy consumption or to increase profit without capital investment;
- modify the design of an existing column or the design of the HEN or both in a controlled way to reduce energy consumption;
- modify the design of an existing column, the product flowrates and quality, and the design of the HEN simultaneously to increase profit;
- explore different distillation configurations in the design of existing units, such as the introduction of pre-flash or pre-fractionator units;
- optimise column pressures;
- explore changes to the design of existing HENs for increased heat recovery or increased throughput;
- optimise the configuration of new crude oil distillation systems.

Both retrofit and new design can be considered. Changes to the operation and design of existing HENs can be explored. Individual matches are considered and changes to the network can be controlled so that the complexity of either retrofit or new design can be controlled.

Crude oil distillation can be modelled using new semi-rigorous modelling techniques. These new models produce predictions of distillation performance that hardly differ from the predictions of rigorous modelling techniques. However, these new models for the first time provide the ability to explore changes to the configurations of the column automatically. Bulk properties can not only be predicted with accuracy, but can also be controlled.

CDU-int can be used to screen different distillation configurations, such as pre-flash, pre-fractionator and progressive distillation arrangements. The software can be used to identify the most appropriate arrangement. Column pressures can be optimised simultaneously with configuration. When screening such arrangements, Heat Integration is considered simultaneously.

An interesting unique facility of CDU-int is that it allows all aspects of the design and operation at steady state to be explored by simultaneously accounting for the distillation columns and the HEN. The simplest application might call for the operation of the existing design to be optimised for reduced operating cost or increased profit. Existing designs can be modified keeping control over the complexity of the retrofit. New designs can be explored to identify novel new designs.

Professional tool with customer service and continuing tool updates.

© Woodhead Publishing Limited, 2013

34.1.3 CRYO-int

CRYO-int (PIL, 2012) simulates, optimises and synthesises complex refrigeration systems for low temperature gas processing.

CRYO-int is used for the design of low temperature (sub-ambient) processes. Low temperature processes require heat rejection to refrigeration systems. The result is that the operating cost for such processes are usually dominated by the cost of power to run the refrigeration system. For large-scale systems and very low temperatures, multiple levels of refrigeration, cascaded systems and mixed refrigerants are used. Such complex refrigeration systems can be analysed using CRYO-int. One of the fundamental problems with mixed refrigerants is the choice of refrigerant composition. CRYO-int can be used to optimise refrigerant composition.

CRYO-int main functionalities:

- target minimum shaft power for low temperature cooling duties;
- optimise the number and temperatures of refrigeration levels;
- target minimum shaft power for cascade refrigeration systems;
- target minimum shaft power for mixed refrigerant systems;
- determine the optimum composition for mixed refrigeration systems;
- simulate and optimise complex refrigeration designs;
- design and optimise of LNG liquefaction systems.

CRYO-int can target minimum shaft power for simple and complex refrigeration cycles. Targets are based on rigorous thermodynamic calculations and have high accuracy when compared with rigorous simulation.

CRYO-int allows simulation of simple and complex refrigeration systems. These may have multiple heat levels and multiple compressors. Physical properties are represented by equations of state. Designs can be optimised for minimum power consumption or minimum cost.

CRYO-int allows the design (synthesis) of complex refrigeration systems.

When using multiple refrigeration levels, there are often trade-offs between the temperature of the levels and their load. As the temperature of each level is adjusted, it not only affects its own shaft power requirement, but that of the other levels also. Multiple levels of refrigeration must be optimised simultaneously.

CRYO-int can optimise the composition of mixed refrigerants to minimise shaft power requirements. This is achieved by optimising the composition of the refrigerant to match the cooling profile.

CRYO-int allows LNG liquefaction cycles to be simulated and optimised.

The software provides visual representation of the shaft power losses in refrigeration cycles. This provides the designer with insights that could not be obtained otherwise.

Professional tool with customer service and continuing tool updates.

© Woodhead Publishing Limited, 2013

34.1.4 DIST-int

DIST-int is another PIL (2011) software tool, aimed at designing integrated distillation systems.

Distillation operations consume a significant proportion of the energy of most processing sites. DIST-int enables the most appropriate distillation configuration and its Heat Integration arrangement to be designed for minimum energy consumption or minimum total cost. This requires the selection of the type of column to be used, the sequence of the columns, the operating pressure of the columns and Heat Integration arrangement. Distillation columns can be simple (using one feed, producing two products with a single reboiler and single condenser) or complex (pre-fractionators, side-strippers, side-rectifiers, dividing wall or partitioned, dephlegmators). DIST-int can select the most appropriate type of column to be used, the sequence of the columns, the operating pressure and the Heat Integration matches simultaneously. Heat pumping can also be included. For low temperature (sub-ambient) distillation, the additional problem is that the refrigeration system needs also to be designed simultaneously, along with everything else. The refrigeration system might involve multiple stages, cascade systems or use mixed refrigerants.

DIST-int main functionalities:

- minimise energy consumption for a fixed column configuration through pressure optimisation and Heat Integration;
- determine the best configuration of energy-integrated simple and complex column arrangements;
- simultaneously optimise column pressures for heat-integrated distillation configurations;
- select Heat Integration matches;
- identify heat pumping opportunities,
- simultaneously optimise selection of column type, sequence, operating pressure of the columns, Heat Integration matches and heat pumping opportunities;
- for sub-ambient distillation systems, simultaneous design of the refrigeration system;
- screen refrigeration system designs for sub-ambient distillation systems, including multiple levels, cascade systems and mixed refrigerants.

Minimising the energy cost of distillation systems requires the heat recovery opportunities to be maximised. DIST-int can optimise the pressure and Heat Integration matches for a fixed distillation configuration to minimise energy cost. Column pressures can be constrained to operate within bounds to allow retrofit studies and to allow practical constraints in new designs to be included.

© Woodhead Publishing Limited, 2013

DIST-int can be used to screen sequences of simple and complex columns. Software can be used to identify the most appropriate arrangement of simple and complex columns. Column pressures are optimised simultaneously with configuration. Optimisation can be based on energy consumption or utility costs or total cost.

DIST-int can be used to select the type of column to be used, the sequence of the columns, the operating pressure and the Heat Integration matches simultaneously. This facility within DIST-int allows novel distillation system designs to be identified. The Energy Integration implications of any given design can be considered within DIST-int. DIST-int can export data to HEAT-int. The facilities within DIST-int allow novel distillation system designs to be identified, and the interactions between the design of the distillation system and the utility system servicing it to be examined, together with the sensitivity of the design to changes in feedstock, etc.

Rather than recovering heat to reduce energy cost, heat pumping schemes can be applied. Various heat pumping schemes are possible. HEAT-int has the facility of allowing heat pumping around a given column or between columns. Such schemes are identified whilst considering all other issues simultaneously.

Low temperature (sub-ambient distillation) requires a refrigeration system also to be specified. This cannot be done in isolation from the rest of the design if the best results are to be obtained, but has to be designed simultaneously with all other features of the system. The objective of such designs is usually to minimise the power consumption. In addition to all the degrees of freedom that need to be optimised for above ambient designs, the refrigeration system offers many other options, including multiple levels, cascade systems and mixed refrigerants.

This is a professional tool, with customer service and continuing tool updates.

34.1.5 HEAT-int

HEAT-int (2011) is a product of Process Integration Ltd. This program is used to improve the energy performance of individual processes on a site. HEAT-int is a next-generation development of SPRINT software (by a related team of developers) to a commercial standard, and it provides more user-friendly interface features. HEAT-int is used to improve the energy performance of individual processes on a site. Energy targets can be set based on thermodynamic principles. HEAT-int can be used to optimise the choice of utilities for an individual process. Once options have been explored using targets, HEAT-int can design the appropriate HEN design automatically for the choice of utilities and level of heat recovery made. Both retrofit and new design can be carried out interactively or automatically. If design is carried

© Woodhead Publishing Limited, 2013

out automatically, the designer maintains control over network complexity. HEAT-int carries out network optimisation. Because of the interactions between HEAT-int and SITE-int, both programs are linked by common data structures and files.

HEAT-int main functionalities are to:

- target minimum energy consumption;
- optimise the load of utilities for individual processes;
- carry out interactive network design;
- automatically design new HENs;
- automatically retrofit HENs with control of the number of modifications;
- simulate HENs using simple models;
- optimise HENs;
- explore HEN operability;
- interface with SITE-int, CDU-int and DIST-int (see below).

HEAT-int sets energy targets and optimises the selection of utilities for individual processes.

The tools include the Composite Curves, the Grand Composite Curve and the Problem Table. These tools allow the designer to predict hot and cold utility targets for individual processes. HEAT-int automatically places the optimal mix of utilities against the Grand Composite Curve. In addition to providing energy-based targets for the process, the program can also target for the surface area of the heat exchangers (HEs) and the minimum number of HE units and shells. Combining these targets allows total cost targets to be predicted ahead of design.

An interactive design grid allows the process designer to manipulate the design of existing and new HENs manually.

New design can be carried out automatically. To avoid automatic design creating structures that are over-complex, HEAT-int allows the designer to keep control over the resulting network complexity.

HEAT-int offers flexibility in the approach to HEN retrofit. One approach identifies bottlenecks in the existing network that limit energy recovery. Structural changes can then be made to overcome the bottlenecks. The structural changes made are resequencing (change of location of an existing exchanger on the same streams), repiping (change of location allowing the streams to change), adding a new exchanger and introducing a stream split. HEAT-int finds the best structural modifications, but leaves the designer in control of the number of modifications. An alternative approach allows multiple modifications to be identified according to the retrofit economic criterion.

For a given network structure HEAT-int will calculate the intermediate network temperatures and HE performances using simple HE models.

© Woodhead Publishing Limited, 2013

The software has different simulation modes, that are dependent on the data specified and the options selected. HEs can be specified by either heat duty or heat transfer area.

HEAT-int can automatically adjust the degrees of freedom in the network to achieve minimum total annualised cost for both retrofit and new design. The optimisation reduces the network cost by trading off the utility cost against capital cost.

The program can also determine the best network modifications to deal with different operating cases.

This is a professional tool with customer service and continuing tool updates.

34.1.6 HEXTRAN

HEXTRAN (2012) is a steady-state simulator that provides a view of heat transfer systems. It helps to design new systems, monitor current systems, optimise existing operations, as well as prevent or solve heat transfer problems. The program rigorously simulates integrated processes and allows the engineer to monitor the performance of individual exchangers or an entire heat transfer network. It also offers informative post-processing displays, and plots results from network targeting, Grand Composite Curves and zone analysis exercises. HEXTRAN is efficient in all types of design and operational analysis work, such as individual exchanger and network designs, Pinch Analysis, exchanger zone analysis, split flow, area pay-out and cleaning cycle optimisations.

HEXTRAN simulates actual performance and can make the difference between profit and loss:

- improved process heat transfer, product yield and quality;
- increased energy efficiency and significantly reduced operating cost;
- increased plant flexibility and throughput;
- optimised cleaning schedule for exchangers;
- optimal antifouling selection and usage;
- improved process designs and revamps.

The HEXTRAN process heat transfer simulator offers features that enable the engineer to evaluate complex design, operational and retrofit situations:

- enables the design of both simple and complex heat transfer systems, resulting in cost-effective, flexible processes;
- allows retrofitting existing equipment and revamp HENs to yield optimum performance;

© Woodhead Publishing Limited, 2013

- enables the identification of cleaning incentives and the prediction of future performance.

34.1.7 Optimal Audit ©

Optimal Audit © is computer software developed by PROSPECT, Universiti Teknologi Malaysia for the rapid and efficient calculation of energy-efficient facilities as well as for monitoring gas emissions and wastewater quality (see Fig. 34.1). It is a Microsoft Windows-based program that was developed to automate and, rapidly as well as efficiently, to assist plants and buildings to perform:

- energy consumption trend analysis;
- benchmarking to identify current energy usage status;
- boiler energy analysis;
- electrical maximum demand analysis;
- electrical tariff analysis;
- power generation efficiency;
- equipment efficiency analysis (e.g. motor, pumps);
- gas emission monitoring;
- wastewater discharge monitoring.

It is designed to assist engineers to perform a general plant energy audit.

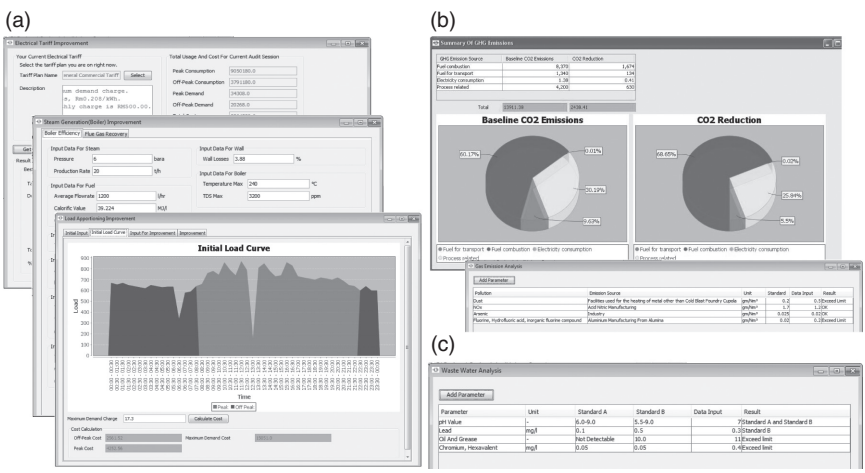

34.1 Optimal Audit featuring 3-in-1 capability for (a) energy, (b) gas emissions and (c) wastewater analysis.

© Woodhead Publishing Limited, 2013

34.1.8 Optimal Heat ©

Optimal Heat © is a computer software package developed by Process Systems Engineering Centre (PROSPECT), Universiti Teknologi Malaysia for the retrofit of heat recovery network to reduce energy in chemical process plants. It is a Microsoft Windows-based programme that was developed to automate, and rapidly and efficiently assist the design and retrofit of a HEN. It also enables the rapid determination of the minimum hot and cold utility requirements for a process, and the improvement of HEN structure for a process plant to achieve the minimum hot and cold utility consumptions. In addition, Optimal Heat can also automatically generate the optimal utility combination for a given process and allow the automatic and semi-automatic design of a HEN to achieve the energy targets.

Optimal Heat was developed based on the synergistic combination of three key techniques to reduce the hot and cold utility consumption, namely Pinch Analysis, MATRIX and Path Optimisation. The software implements the established principles of Pinch Analysis for a new plant. It also includes the features of the new MATRIX technique proposed by Lim (2002) for the retrofit of existing processes to reduce the hot and cold utility usage. The MATRIX technique is a new methodology aimed at improving heat recovery by *MA*ximising the *T*otal *R*euse of the e*X*isting heat recovery network area (MATRIX). The advantage of this technique is its ability to improve the existing design to optimal or near optimal heat recovery with minimal changes on the existing process structure, and hence, requiring the minimal capital investment. The third technique being implemented is path optimisation technique that is used to evolve a HEN and maximise heat recovery from an existing process.

The key features of the Optimal Heat software are as follows:

- The minimum hot and cold utility demands, or the energy target, are determined by the software based on the Pinch Analysis technique. The maximum heat recovery potential and the Pinch Temperatures for a process are shown on the Composite Curves (CC) Diagram.
- The multiple utility design allows more utility cost savings. The software automatically determines the heat load for various levels of utilities. Then, it prioritises the use of the cheaper utility in order to maximise utility cost savings. Figure 34.2 shows a sample of Balanced Grand Composite Curve generated from Optimal Heat software.
- The software automatically generates the Grid Diagram for HEN Design. Hot and cold streams are matched based on the Pinch Design rules. Optimal Heat also adds an optional feature for users to manually perform HEN Design (see Fig. 34.3). This provides the flexibility for the designers to override the basic Pinch Design rules.

© Woodhead Publishing Limited, 2013

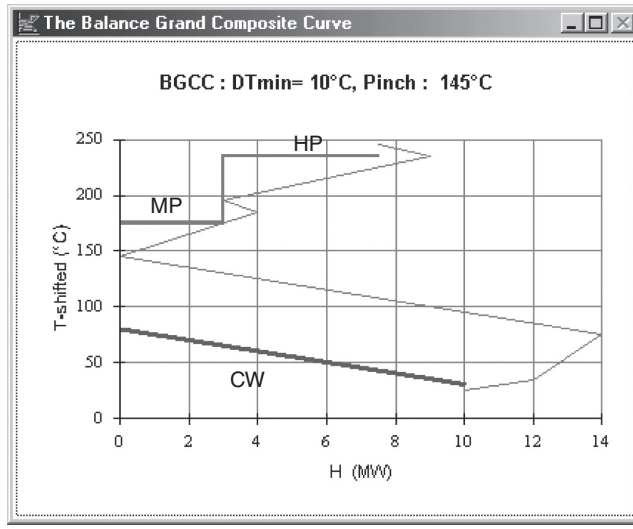

34.2 Balanced Grand Composite Curve.

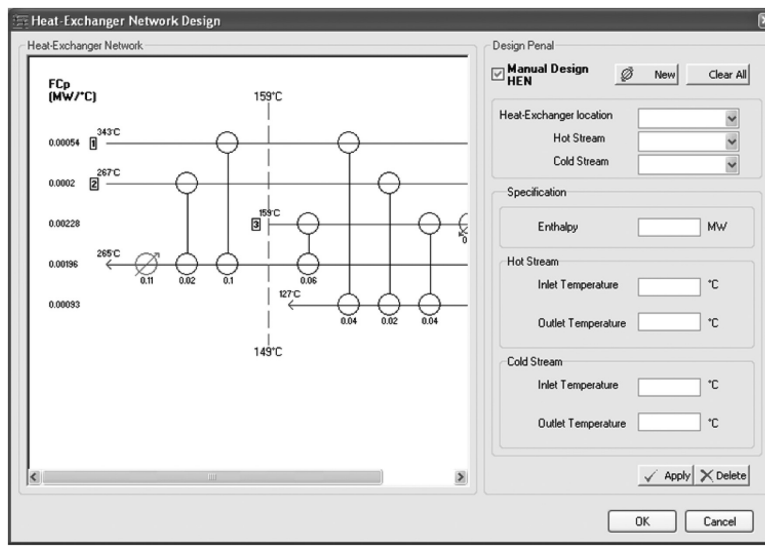

34.3 Auto and manual HEN Design.

- Software also generates a plot of the exergy block diagram (EBD) based on the MATRIX technique (see Fig. 34.4). The EBD can provide key insights for exergy analysis of an existing network. It can be used to assist the designer to graphically and effectively generate surgical network revamp.

© Woodhead Publishing Limited, 2013

Table 34.1 Match-Matrix for HEN retrofit screening

	H1 (503.8)	H2 (1,369.9)	H3 (196.1)	H4 (185.4)	H5 (921.7)	H6 (438.6)
C1 (503.8)		✓		✓		
C2 (438.6)						✓
C3 (1,764.9)					✓	
C4 (921.7)			✓			
C5 (196.1)	✓					

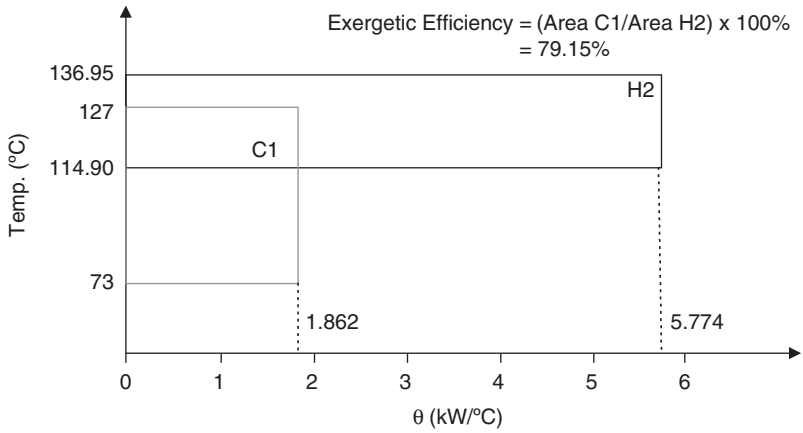

34.4 EBD for exergetic efficiency analysis.

- Optimal Heat automatically generates the Match-Matrix for retrofit design (Table 34.1). The software lists out all the possible matches in a Matrix and eliminates the infeasible matches. Designers can use the Match-Matrix to match the hot and cold streams and obtain the retrofitted network design for an existing process.
- The software also performs Network Evolution in the final stage of the retrofit. This module provides an algorithm to determine the most cost-effective path and the optimal heat load shift for performing energy relaxation. Figure 34.5 shows the Path Optimisation Curve.

34.1.9 SITE-int

Like HEAT-int, SITE-int (2012) is a product of Process Integration Ltd. SITE-int is a state-of-the-art software package for the design, optimisation and integration of site utility systems in process industries. Site utility systems provide the heating, cooling and power requirements for the processes on manufacturing sites.

© Woodhead Publishing Limited, 2013

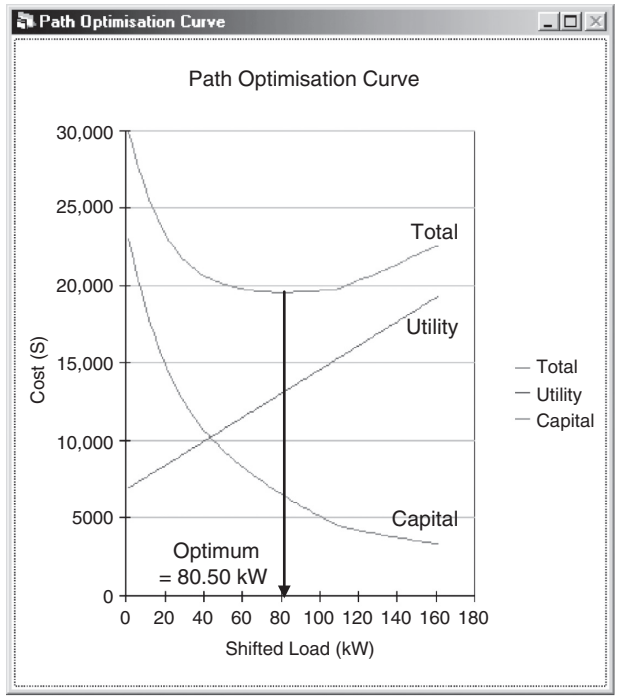

34.5 Path optimisation diagram for palm oil refinery retrofit project.

For all but the smallest manufacturing sites, the steam and co-generation systems are extremely complex. Steam boilers, steam turbines, gas turbines, heat recovery steam generators, fired heaters and steam headers with different pressures provide a complex pattern of energy supply and power generation. Complex interactions occur within the utility system, between the individual processes and the utility system, and between the different processes through the utility system. The key to reducing energy cost for a site is first to model it and optimise it. This can provide immediate cost savings. Only in this way can the saving potential for the existing utility system be evaluated. Even further, it allows the potential to improve still further to be identified through modifying the system.

SITE-int main functionalities:

- models and optimise site utility systems;
- minimises operating cost for existing systems without modification;
- targets co-generation potential;
- optimises site steam pressures and loads;
- minimises energy cost for the site by modifying the system;

© Woodhead Publishing Limited, 2013

- determins the true benefit from saving energy in the individual processes;
- reduces greenhouse gas emissions from the site.

Utility systems usually have significant redundancy in place to allow the site to respond to changes in the operation across the site. However, this redundancy presents opportunities to improve performance by managing its operation more effectively. To exploit this requires a simulation model of the site. The model has to account for part-load performance of items such as boilers, steam turbines, gas turbines and heat recovery steam generators.

SITE-int has regression and data reconciliation functions to create part-load models of the components of utility systems from plant operating data.

A given utility system configuration incorporates important degrees of freedom for optimisation. Multiple boilers with different efficiencies and different fuels, multiple steam turbines with different efficiencies and gas turbine heat recovery steam generators provide options for steam generation at different costs. Different paths for the heat flow through the system can all be exploited for significant cost reduction. SITE-int has a utility system optimisation facility that allows existing utility systems to be optimised across a number of operating cases.

SITE-int can develop temperature–enthalpy profiles of the site. Such profiles provide a single picture representing the heating and cooling requirements across the entire site. This allows targets to be set for fuel consumption in the boilers, co-generation potential and energy cost. The match between the requirements of the individual processes and the site steam generation and steam use allows the potential to swap between different steam levels to be identified, with potential to increase co-generation and decrease cost.

SITE-int allows the fuel requirements of the utility system to be predicted. These can then be related to the emissions of greenhouse gases. Thus, the emissions can be predicted and the site optimised to reduce emissions, taking into account all operating cost.

This is a professional tool with customer service and continuing tool updates.

34.1.10 Spreadsheet Based Tool for Heat Integration

The advent of Pinch Analysis provides a comprehensive as well as systematic approach to maximise plant energy efficiency as well as other utilities. The Pinch technique is amenable for use with commercial spreadsheets. It displays multiple cells that together make up a grid consisting of rows and columns, each cell containing either alphanumeric text or numeric values.

© Woodhead Publishing Limited, 2013

Kemp (2007) has introduced a Microsoft Excel ® spreadsheet for Pinch Analysis, targeting calculations and plots. The main features in this spreadsheet are:

- input of stream data;
- calculation of CC, Problem Table, energy targets and Pinch Temperature;
- plotting of CC and GCC;
- plotting stream population over temperature range and basic Grid Diagram;
- tables and graphical plots of variation of energy and Pinch Temperature over a range of ΔT_{min}.

Area and cost targeting are not in spreadsheet as the considerable extra complexity, the frequent lack of suitable data on HE coefficients and the flat nature of most cost–ΔT_{min} plots. Topology can still be identified from the graphs of utility use and Pinch Temperature against ΔT_{min} (Kemp, 2007).

34.1.11 SPRINT

The SPRINT software package was first developed at UMIST (now The). It fiš ušed for the dešfign of the energy šyštemš for individual processes (SPRINT, 2012). SPRINT is an energy targeting and optimisation tool for the choice of utilities for an individual process. Its other functionality is to provide an automated HEN design for the set of utilities chosen. The important thing is that, though both new design and retrofit can be carried out automatically, the designer keeps full control over network complexity. In retrofit, modifications can be chosen automatically, the designer can then choose one at a time such that the minimum number of modifications is made, and the final decision is left to the designer. Another SPRINT function is that it can carry out network optimisation.

SPRINT and STAR (another software tool developed at The University of Manchester, see below) can interact between each other: common data structures link both programs so that each can use the same files and no manual data transfer between the packages is required.

SPRINT main functionalities:

- optimisation of choice and load of utilities for individual processes;
- automatic design of new HENs;
- automatic retrofit design of HENs with minimum number of modifications;
- automatic design for multiple utilities (new design and retrofit);
- interactive network design;
- simulation of networks using simple models;

© Woodhead Publishing Limited, 2013

- targeting minimum energy consumption;
- optimisation of networks;
- network operability.

The user can set up and edit the network structure through an interactive graphical editor (see Fig. 34.6). This editor allows easy modification of the network by using a series of graphical tools. For the given network structure the program will calculate the intermediate network temperatures and HE performances. The program has various simulation modes which are dependent on the data specified and the options selected. HEs can be specified by either heat duty or heat transfer area.

New design is carried out automatically, but within a framework where the designer keeps full control over network complexity. Automatic design can create structures, which involve impractical arrangements of stream splitting which the designer has to then evolve to a practical design. SPRINT also allows the designer to keep full control over the complexity of stream splitting arrangements.

SPRINT can automatically adjust the degrees of freedom in the network to achieve minimum total annualised cost for both new design and retrofit. The optimisation process reduces the network cost by trading off the utility cost against capital cost. The program can also determine the best network modifications to deal with different operating cases.

This is a professional tool with customer service.

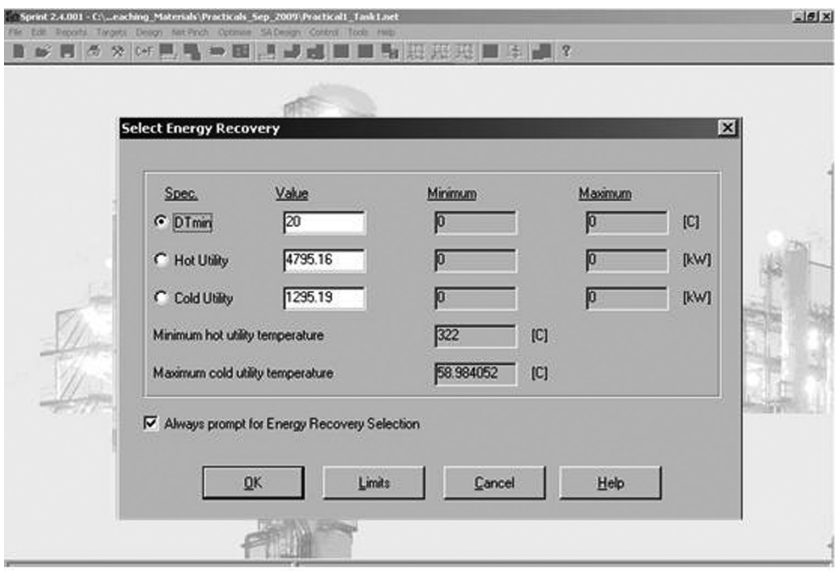

34.6 SPRINT software interface. (SPRINT, 2011.)

© Woodhead Publishing Limited, 2013

34.1.12 STAR

STAR (2012) is a software package for the design of site utility and co-generation systems. The interactions between the processes on the site and the steam system, steam turbines, gas turbines (with auxiliary firing options), boiler house, local fired heaters and cooling systems are all analysed using STAR. It can be used for reducing energy cost or planning infrastructure investment in situations where changes to operations on the site are anticipated or energy equipment needs to be replaced. The most effective capital investment strategy can be investigated. STAR can also be used to investigate the reduction of flue gas emissions to meet tighter environmental regulations. Several functionalities of STAR are given below:

Utility System Optimisation. A Utility system configuration incorporates important degrees of freedom for optimisation. The STAR graphical interface is shown in Fig. 34.7. Multiple boilers with different efficiencies and different fuels, multiple back pressure steam turbines, condensing turbines, gas turbine heat recovery steam generators and let-down valves provide optional heat flow paths that can all be exploited for significant cost reduction. STAR has a utility system optimisation facility that allows existing

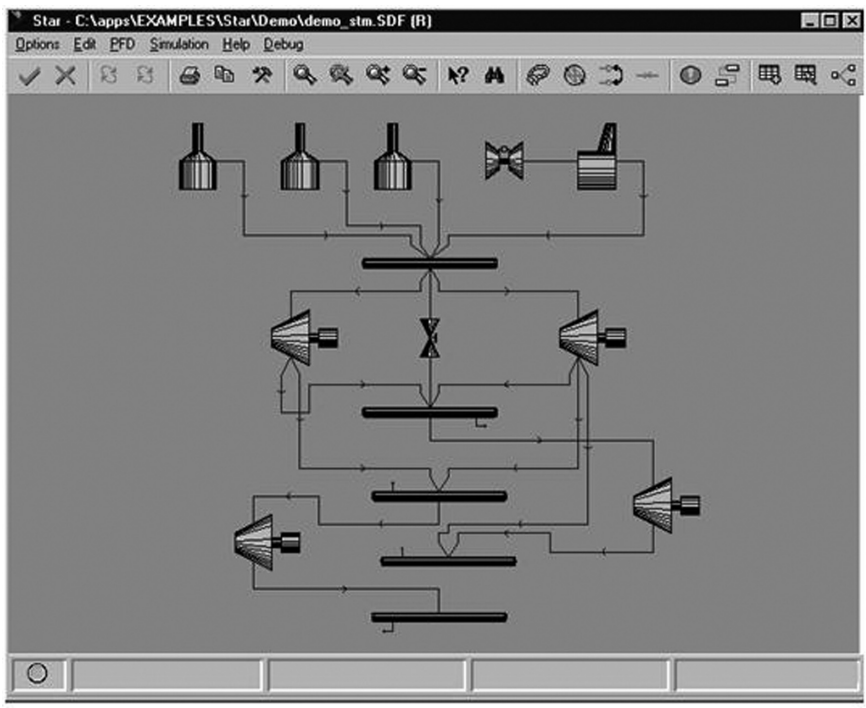

34.7 Interface of STAR. (STAR, 2012.)

© Woodhead Publishing Limited, 2013

Utility systems to be optimised. It can also be used to plan infrastructure debottlenecking and investment.

Top Level Analysis. For existing sites study, it is important to understand influence of the existing site infrastructure on the degrees of freedom to make changes and the economic consequences of any changes. STAR provides this in its Top Level Analysis so that the designer does not waste time pursuing changes which will be neither viable nor economic in the context of the overall site. The engineer thus no longer needs to analyse the multitude of options available for change; instead, he is directed to the few most attractive changes in the site.

Process Energy Targets. STAR is focused on the analysis of utility systems, but it also has tools available to set energy targets and select utilities for individual processes. Using these tools allows the picture of the Total Site to be built up from the individual processes within STAR. These tools include the Composite Curves (Fig. 34.8), the Grand Composite Curve, Balanced Grand Composite Curve, etc. (Fig. 34.9), and the Problem Table, that enable the engineer to predict hot and cold utility targets for individual processes.

Total Sites. Processes consume hot utilities but some also generate steam. Processes are usually linked to a common utility system involving multiple levels of steam and power generation. The generation of steam provides heat recovery through the steam system. The site imports or exports power

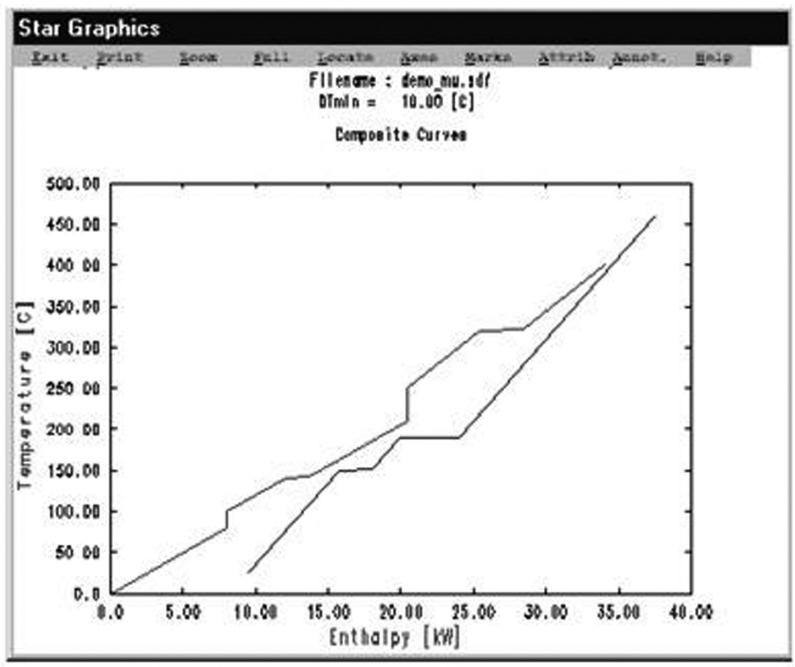

34.8 Star Graphics – Composite Curves.

© Woodhead Publishing Limited, 2013

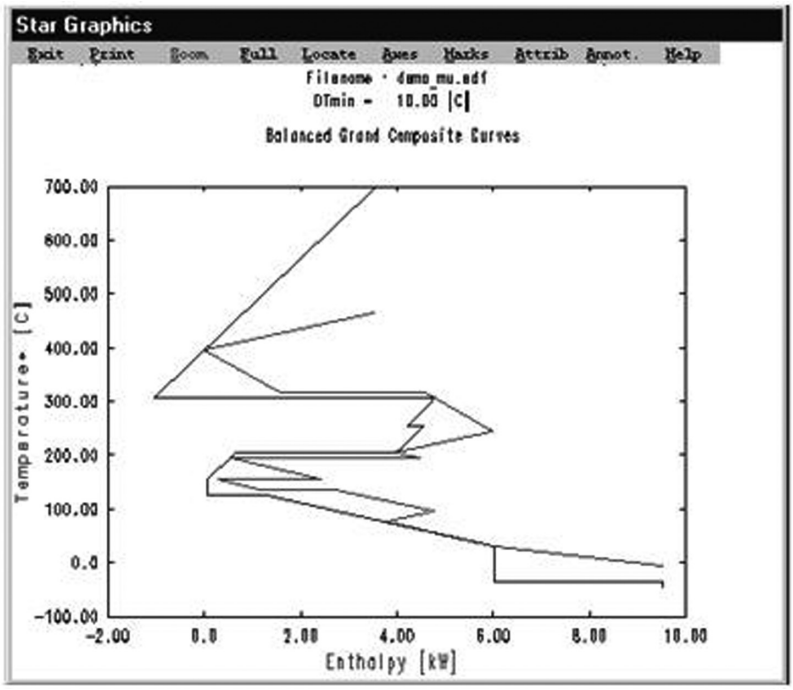

34.9 Star Graphics – Balanced Grand Composite Curves.

to balance the power generated. STAR can produce Total Site Profiles representing the heating and cooling requirements of the site (Fig. 34.10). This allows targets to be set for fuel consumption in the boilers, cogeneration potential and energy cost. Profiles can be based on either the full heat recovery data or more simply from the data for the utility exchangers only. The Total Site's co-generation potential can be targeted.

Boiler Systems and Steam Turbine System. STAR provides optimal targets the amount of steam generated for process use by boilers and gas turbines (with auxiliary firing options). Different gas turbine arrangements can be studied using a gas turbine model. Steam turbines are part of the utility system on most sites, and are used for power generation or as allocated drivers for process machines. STAR incorporates the design of steam turbine networks and analysis operability.

Emissions. Using STAR, the engineer can study various options to reduce emissions. By relating the energy requirements of the processes to the supply of utilities, it is possible to target for the amount of fuel required for the utility system. These targets can be combined with information on the fuel and type of combustion device to provide targets for CO_2, SO_x, NO_x and particulates.

This is a professional tool with customer service.

© Woodhead Publishing Limited, 2013

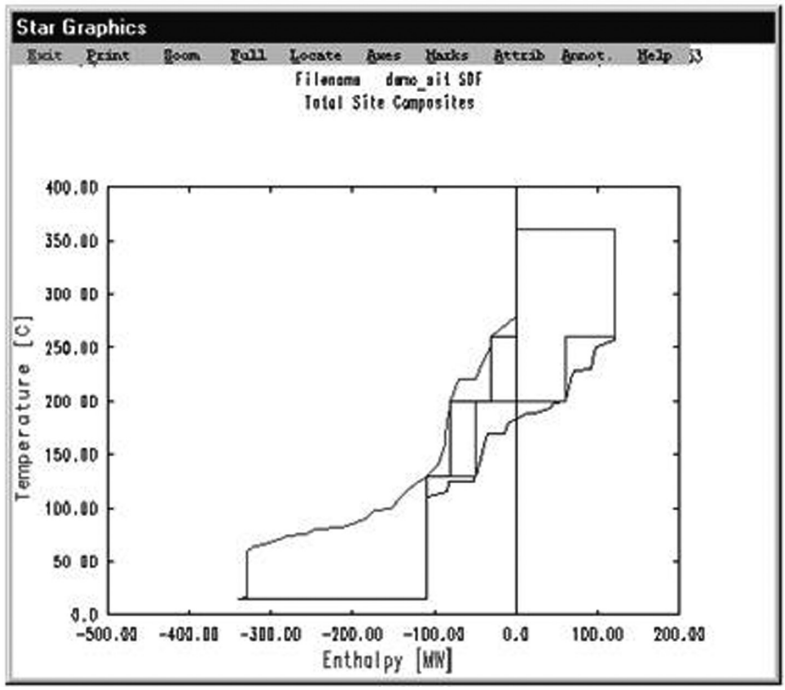

34.10 Total Site Profiles representing the heating and cooling requirements.

34.1.13 SuperTarget

SuperTarget was introduced in 1992 to help plants to improve Heat Integration in new design and retrofit projects reducing Operating cost and optimally targeting capital investment (KBC, 2012). SuperTarget offers the best economic performance target for heat recovery, and helps in designing the most effective HEN. Successive releases have built on the foundation of their predecessors, continuing to push back the boundaries of energy Pinch Analysis, whilst making step changes in ease-of-use through improved data handling, data transfer and increased automation. Still the preferred tool of energy Pinch experts worldwide, SuperTarget is also a tool for day-to-day application by novice or occasional users, and it makes Pinch Analysis a routine part of process design. SuperTarget has been designed to make it accessible to users with different levels of Pinch expertise. An intuitive user interface makes the technology accessible to novice or occasional users, advanced tools are available to more expert users, and many of the most time consuming tasks traditionally associated with Pinch Analysis have been fully or partially automated.

SuperTarget takes data directly from most popular process simulation programs through interfaces to Aspen Plus, HYSYS and PRO/II. It attempts an

© Woodhead Publishing Limited, 2013

automatic data extraction system which converts the raw process data into Pinch data where the user may override the extraction defaults if necessary. SuperTarget comprises three program modules – Process, Column and Site:

Process is the core program used for energy optimisation in a single process unit. Process is used for:

(i) Energy Targeting;
(ii) HEN Design;
(iii) Identifying the Potential for Economic Energy Savings;
(iv) Determining the Optimum Balance of Capital Investment and Operational Improvement.

Column carries out a thermal analysis of the heat distribution in distillation columns. Column is used for:

(i) Identifying heat load redistribution for lower utility costs or for heat exchange with process streams;
(ii) Automatically optimising the locations of each feed;
(iii) Successfully analysing even the most difficult columns, for example crude towers.

Site is used for Total Site™ heat and power targeting across a manufacturing site. Site helps plants:

(i) Identify Site-Wide Energy Targets;
(ii) Optimise Utility Levels and Placement;
(iii) Identify and Quantify Co-generation Potential;
(iv) Lower Emissions Through Reduced Fuel Consumption.

Professional tool with customer service and continuing tool updates.

34.1.14 WORK

Low temperature processes require heat rejection to refrigeration systems. The result is that the operating cost for such processes are usually dominated by the cost of power to run the refrigeration system. For large-scale systems, multiple levels of refrigeration, cascaded systems and mixed refrigerants are used. WORK (2012) is a software package used for the design of low temperature (sub-ambient) processes. Complex refrigeration systems can be analysed using WORK. Cascade and mixed refrigerant systems can be analysed. For mixed refrigerants, WORK can be used to optimise refrigerant composition. It provides:

- understanding complex refrigeration systems;
- targeting minimum shaft work for a low temperature cooling duties;

© Woodhead Publishing Limited, 2013

- optimising the number and temperatures of refrigeration levels;
- targeting minimum shaft work for cascade refrigeration systems;
- targeting minimum shaft work for mixed refrigerant systems;
- determining the optimum composition for mixed refrigeration systems.

Targeting Low Temperature Systems. WORK can target minimum shaft work for simple and complex refrigeration cycles. Targets are based on rigorous thermodynamic calculations and have high accuracy when compared with rigorous simulation. An example of refrigeration cycle report is shown in Fig. 34.11.

When using multiple refrigeration levels, usually trade-offs between the temperature of the levels and their load have to be considered. As the temperature of each level is adjusted, it not only affects its own shaft work requirement, but also that of the other levels. Multiple levels of refrigeration must be optimised simultaneously. WORK allows this to be done based on its high accuracy shaft work predictions.

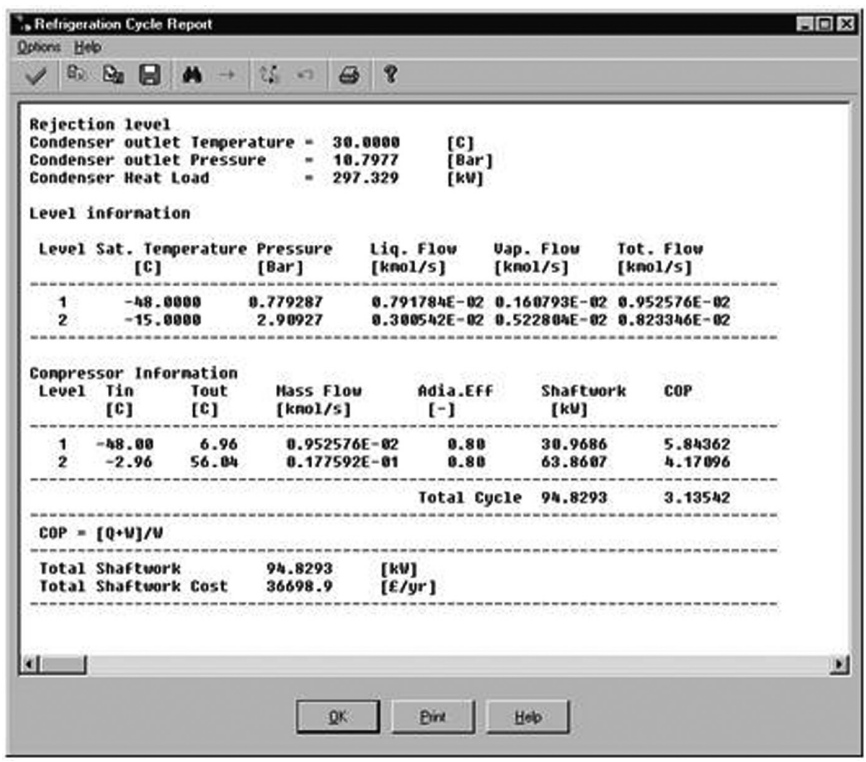

34.11 Refrigeration cycle report.

© Woodhead Publishing Limited, 2013

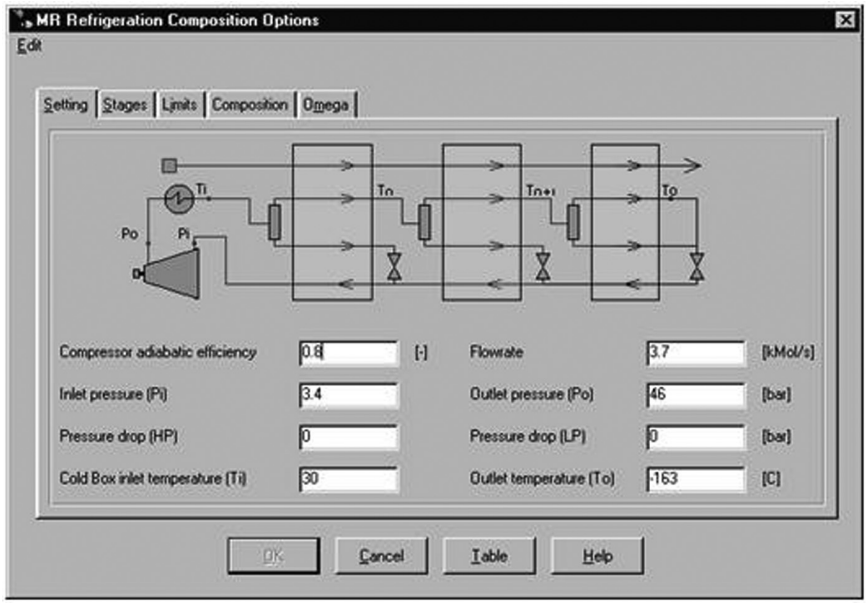

34.12 Refrigeration composition options.

Simulation of Refrigeration Systems. WORK allows simulation of simple and complex refrigeration systems (Fig. 34.12). These may have multiple heat levels and multiple compressors. The refrigerant heat loads and temperature levels can be optimised relative to the background process to minimise shaft work requirement.

Optimisation of Mixed Refrigeration Systems. WORK can optimise the composition of mixed refrigerants to minimise shaft work requirements. This is achieved by optimising the composition of the refrigerant to match the cooling profile (Fig. 34.13). WORK allows visual representation of the shaft work losses in refrigeration cycles. All aspects of the losses can be represented, including both mechanical and thermal losses.

34.2 Sources of Further Information and Advice

The software tools discussed in this chapter exploit basic to most advanced concepts of Process Integration. Developers often offer training and support to commercial software. Along with the support from the developers, in-built helpers and manuals, it is always a good idea to have some reference literature sources at hand. Below are some general reference books providing extensive information on Process Integration methods applied in the software tools described in this chapter:

© Woodhead Publishing Limited, 2013

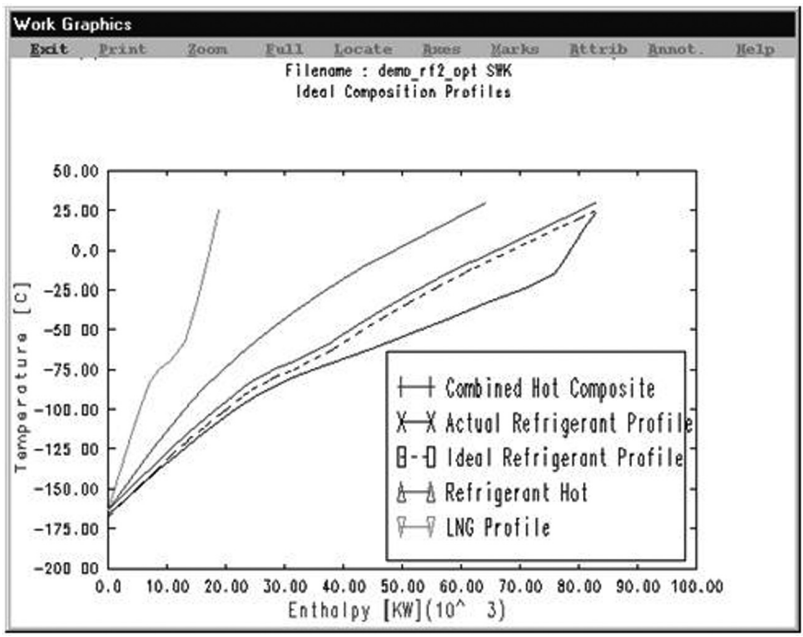

34.13 Ideal Composition Profiles.

Kemp (2007) – This book shows how to understand and optimise energy use in process industries. The book intended both for experienced and newly qualified engineers, as well as academics and students. Supported by downloadable software, the book explains how to extract the stream data necessary for a Pinch Analysis and describes the targeting process in depth, to design of HENs, hot and cold utility systems, Combined Heat and Power (CHP), refrigeration, and optimisation of system operating conditions. It provides tips and techniques for practical application. Several detailed case studies and other examples covering a wide range of industries, including buildings and other non-process situations are discussed.

Kim and Smith (2005) – A chapter on Pinch Design and Analysis in the Encyclopedia of Chemical Processing. Provides state-of-the-art information on the methods and practices related to Process Integration in chemical industries. It includes the design of key unit operations involved with chemical processes – design, unit operation, and integration of reactors and separation systems.

Klemeš *et al*. (2010) – This book provides an overview of the Process Integration and optimisation methodologies and their application to improving the energy efficiency of not only industrial, but also non-industrial energy users. An additional aim is to evaluate how these methodologies can be adapted to include the integration of waste and renewable energy sources.

© Woodhead Publishing Limited, 2013

Linnhoff *et al.* (1982) [revised edition in 1994] – The most well-known and perhaps most referenced book on Process Integration. This 'red book', authored by a team of founders of Process Integration technology led by Bodo Linnhoff, was updated for an extended second edition in 1994. Although it was published a long time ago, it remains an excellent source for teaching and learning about Heat Integration and several other Process Integration technology applications, providing the reader with a smooth and understandable learning path.

Smith (1995) and the second edition, Smith (2005) – This book deals with the design and integration of chemical processes, with the focus on conceptual issues that are fundamental to the design of the process. The text emphasises both the design and selection of the steps as individual operations and their integration. The design of utility systems is discussed in the text so that the interactions between processes and the utility system and interactions between different processes through the utility system can be exploited to maximise the performance of the site as a whole. The book also provides the engineer with an understanding of the limitations of the methods used in chemical process design. The book provides a practical guide to chemical process design and integration for undergraduate and postgraduate students of chemical engineering, practicing process designers and chemical engineers, and applied chemists working in process development. The text includes a number of examples and exercises in each chapter.

Wider process design context can be found for example in the following books:

El-Halwagi (2006) – The textbook presents a comprehensive treatment of the concepts, tools and applications of Process Integration. Emphasis is given to systematic ways of analysing process performance. Graphical, algebraic and mathematical procedures are presented in detail. In addition to covering the fundamentals of the subject, the book also includes numerous case studies and examples that illustrate how Process Integration is solving actual industrial problems.

Floudas (1995) – This book presents the theory and methods for nonlinear and mixed-integer optimisation, and their applications in the important area of process synthesis. As modern Process Integration tools become increasingly reliant on mathematical programming methods, it becomes a important for the process designer to understand those methods. Other topics include modelling issues in process synthesis, and optimisation-based approaches in the synthesis of heat recovery systems, distillation-based systems and reactor-based systems. The basics of convex analysis and non-linear optimisation are also covered and the elementary concepts of mixed-integer linear optimisation are introduced. All chapters have illustrations and geometrical interpretations of the material as well as suggested problems. The

© Woodhead Publishing Limited, 2013

book is a valuable source, as a textbook or a reference, for researchers and graduate students interested in continuous and discrete non-linear optimisation issues in engineering design, process synthesis, process operations, applied mathematics, operations research, industrial management and systems engineering.

Georgiadis and Pistikopoulos (2006) – The book considers overall Process Integration methods but it is the focus on complex distillation systems and higher level approach that makes it especially interesting. The authors describe application of techniques of process simulation, optimisation and control.

A number of ground-breaking papers that describe particular aspects of Process Integration have been published up to date. References to some of them are given in other parts of this handbook.

34.3 References

Aspen Energy Analyzer. <www.aspentech.com/products/aspen-hx-net.aspx> Assessed 10.08.2012.

CDU-int. <www.processint.com/chemical-industrial-software/cdu-int> Assessed 10.08.2012.

CRYO-int. <www.processint.com/chemical-industrial-software/cryo-int> Assessed 10.08.2012.

DIST-int. <www.processint.com/chemical-industrial-software/dist-int> Assessed 10.08.2012.

El-Halwagi, M. M. (2006). *Process Integration*. Academic Press, Amsterdam, The Netherlands.

Floudas, C. A. (1995). *Nonlinear and Mixed-integer Optimisation: Fundamentals and Applications*. Oxford University Press, Oxford, UK.

Gas Turbine World. (2001). *Handbook 2000–2001,* vol. 21. Pequot, Southport, CT, USA.

Georgiadis, M. C., Pistikopoulos, E. N. (2006). *Energy and Process Integration*. Begell House, Redding, CT, USA.

HEAT-int. <www.processint.com/chemical-industrial-software/heat-int> Assessed 10.08.2012.

HEXTRAN. <iom.invensys.com/AP/Pages/SimSci-Esscor_ProcessEngSuite_HEXTRAN.aspx> Assessed 10.08.2012.

Kemp, I. C. (2007). *Pinch Analysis and Process Integration. A User Guide on Process Integration for Efficient Use of Energy.* (authors of first edition Linnhoff, B., Townsend, D. W., Boland, D., Hewitt, G. F., Thomas, B. E. A., Guy, A. R., Marsland, R. H. (1982). IChemE, Rugby, UK) Elsevier, Amsterdam, The Netherlands.

Kim, J., Smith, R. (2005). Pinch design and analysis. In *Encyclopedia of Chemical Processing*. Marcel Dekker, New York, USA, 2165–2180.

Klemeš, J., Friedler, F., Bulatov, I., Varbanov, P. (2010). *Sustainability in the Process Industry: Integration and Optimisation*. McGraw-Hill, New York, USA, 384 ps.

Klemeš, J., Smith, R., Kim, J.-K. (eds) (2008). *Handbook of Water and Energy Management in Food Processing*. Woodhead Publishing Limited, Cambridge, England, ISBN 1 84569 195 4, 1029 ps.

© Woodhead Publishing Limited, 2013

Lam, H., Klemeš, J., Kravanja, Z., Varbanov, P. (2011). Software tools overview: process integration, modelling and optimisation for energy saving and pollution reduction. *Asia-Pacific Journal of Chemical Engineering*, **6**(5), 696–712, DOI:10.1002/apj.469.

Lim, F. Y. (2002). MATRIX – a new systematic technique for retrofit of heat exchanger network. MSc Dissertation, Universiti Teknologi Malaysia, Johor Bahru, Malaysia.

Linnhoff, B., Townsend, D. W., Boland, D., Hewitt, G. F., Thomas, B. E. A., Guy, A. R., Marsland, R. H. (1982). *A User Guide on Process Integration for the Efficient Use of Energy*. IChemE, Rugby, UK [revised edition published in 1994].

Manan, Z. A., Tan, Y. L., Foo, D. C. Y. (2004). Targeting the minimum water flowrate using water cascade analysis technique. *AIChE Journal*, **50**(12), 3169–3183. DOI: 10.1002/aic.10235.

Manan, Z. A., Tea, S. W., Wan Alwi, S. R. (2009). A new technique for simultaneous water and energy minimisation in process plant. *Chemical Engineering Research and Design*, **87**(11), 1509–1519. DOI: 10.1016/j.cherd.2009.04.013.

Optimal Audit © <www.cheme.utm.my/prospect/index.php/software/19?task= blogcategory> Assessed 10.08.2012.

Optimal Heat © <www.cheme.utm.my/prospect/index.php/heat-matrix> Assessed 10.08.2012.

Process Systems Engineering Centre (PROSPECT), Universiti Teknologi Malaysia, <www.cheme.utm.my/prospect> Assessed 01.08.2012.

Site-Int <www.processint.com/chemical-industrial-software/site-int> Assessed 10.08.2012.

Smith, R. (1995). *Chemical Process Design*. McGraw-Hill, New York, USA.

Smith, R. (2005). *Chemical Process Design and Integration.* Wiley, Chichester, UK.

Smith, R., Klemeš, J., Tovazhnyansky, L. L., Kapustenko, P. A., Uliev, L. M. (2000). *Foundations of Heat Processes Integration*. NTU KhPI, Kharkiv, Ukraine (in Russian).

SPRINT. <www.ceas.manchester.ac.uk/research/centres/centreforprocessintegration/software/packages/sprint/> Assessed 10.08.2012.

STAR. <www.ceas.manchester.ac.uk/research/centres/centreforprocessintegration/software/packages/star/> Assessed 10.08.2012.

SuperTarget. <www.kbcat.com/Software-Solutions/SuperTarget/> Assessed 10.08.2012.

WORK. <www.ceas.manchester.ac.uk/research/centres/centreforprocessintegration/software/packages/work/> assessed 10.08.2012.

© Woodhead Publishing Limited, 2013

35

Mass and Water Integration Software Tools

IGOR BULATOV, The University of Manchester, UK

DOI: 10.1533/9780857097255.6.1086

Abstract: Mass Integration studies were the next stage of Process Integration development. No wonder that following the pattern of Heat and Power Integration technology development, Mass Integration software tools soon appeared and became available for industry and academia. In this chapter, the following Mass Integration tools are described: Active learning in chemical engineering (ALChemE), H2-int, Hydrogen Pinch Spreadsheet Tool, HyNDT™, Mass Exchange Network (MEN), Optimal-Water©, RCNet, WATER, WaterTarget and Water/Target (Water Design).

Key words: water and wastewater minimisation, water networks, Mass Integration, hydrogen networks.

35.1 Mass and Water Integration Software Tools

Overall, there are less Mass and Water Integration software tools developed so far compared to Heat Integration. This might be due to the fact that Mass Integration research is a younger field of research than Heat Integration and that energy has always been in the limelight for industry and academia.

35.1.1 Active Learning in Chemical Engineering (ALChemE)

ALChemE (2012) is an educational tool used for training students at Texas A&M University. Along with a number of online educational exercises on chemical engineering topics, it includes System Synthesis and Process Integration case studies, which can be quite helpful in learning the principles of Mass Integration. The tool initially provides examples of Mass Integration processes, based on Sorin and Bedard (1999) and Jacob *et al*. (2002), and gives solutions to those problems. Then, exercise problems offer students a freshwater minimisation problem. ALChemE is still under construction and, when fully operational, will offer students online opportunity to develop in detail their Process Integration skills.

© Woodhead Publishing Limited, 2013

35.1.2 H2-int

H2-int (2012) improves the performance and design of refinery hydrogen networks. The worldwide trend towards the production of low sulphur and low aromatic gasoline and diesel, and the trend towards processing heavier crude oils, places increased demands on refinery hydrogen systems. Meeting the resulting increased demands for hydrogen can require significant capital investment in, for example, steam reformers and compression equipment. Yet, most refinery hydrogen systems are inefficient and have significant room for improvement. H2-int allows refiners to improve the performance of their hydrogen networks, both to reduce operating costs and to decrease capital investment, to meet the new demands. H2-int allows targets to be set for minimum hydrogen consumption. Targets can be set for hydrogen recovery and hydrogen plant production. Targets also give insights into the effective use of hydrogen purification units. The assessment of hydrogen resources can be presented in a simple, graphical manner, which gives the engineer insights into process design, sensitivity analysis and operations planning. These graphical targeting methods are complemented by detailed design methods for hydrogen distribution networks that allow practical complexities, such as compression costs and piping costs into the calculations. H2-int allows detailed analysis of all gas impurities to be carried out. This involves detailed physical property calculations within the consumer and producer units during optimisation.

H2-int main functionalities are to: (i) Target minimum hydrogen network consumption on the basis of hydrogen purity, (ii) Target minimum hydrogen network consumption, including complete analysis of the network impurity components, (iii) Minimise hydrogen demand through maximising hydrogen re-use, (iv) Analyse hydrogen purification options, (v) Select the optimum choice between multiple sources of hydrogen, (vi) Explore the trade-offs between hydrogen flowrate and purity, (vii) Design of hydrogen distribution networks, and (viii) Explore options for hydrogen recycle to hydrogen plants.

Hydrogen consumers require a specified flowrate of hydrogen with a specified partial pressure at their inlets. In many cases, there are gases leaving the consumers that contain significant amounts of hydrogen. H2-int can systematically analyse the potential for re-using hydrogen across a refinery based on lumping of the impurities as methane. This analysis is quick and simple, and gives a target for the minimum consumption of hydrogen that maintains the consumer demands. Maximising the recovery of hydrogen also means that losses to the fuel and flare systems are minimised. In this way, the use of available hydrogen can be maximised or the production of hydrogen in hydrogen plants minimised. Results are presented in a simple, graphical manner, providing the engineer with insights.

© Woodhead Publishing Limited, 2013

Whilst lumping of the impurities as methane is quick, simple and gives insights, it neglects important features of the details of the impurities, such as hydrogen sulphide. H2-int allows a target to be set based on a detailed consideration of all impurity components. This requires detailed physical property calculations in the producer and consumer units.

H2-int carries out the design of the distribution system automatically. The designer maintains control over the network complexity and can impose constraints, such as maximum and minimum flowrates, forbidden connections and compulsory connections. Distribution features and costs associated with pipework and compression are included in the design. Again, the design (synthesis) can be carried out either using lumped impurities or by a detailed analysis of the individual impurity components.

Often, there are several possible sources of fresh hydrogen available, for example, a hydrogen plant, catalytic reformers and imports from chemical plants, such as ethylene processes. Each source can have a different quality, pressure and cost. H2-int is able to select the best mix of supplies in order to satisfy the problem at a minimum cost.

The consumption of hydrogen can be decreased by the introduction of hydrogen purification units. The purification units would typically be pressure-swing adsorption or membrane units. The placement of these units within the network is critical. Fundamental principles dictate where such units must be placed to derive the maximum benefit for the network. Indeed, misplacement of the units can bring no benefit at all in terms of the overall network. H2-int allows the designer to determine the optimum type, size and placement of different purifier designs.

Hydrogen networks offer degrees of freedom that in some cases allow trade-offs between hydrogen purity and flowrate. Such opportunities arise from the mixing that takes place throughout the network. H2-int allows these trade-offs to be explored systematically.

35.1.3 Hydrogen Pinch Spreadsheet Tool

An automated Pinch spreadsheet based on Excel (Nelson and Liu, 2008) enables the user to quickly and accurately identify the hydrogen purity at the Pinch Point, and the minimum flowrates of hydrogen utilities, without an iterative graphical construction. The spreadsheet represents all streams with the same hydrogen purity separately as individual streams, can handle Multiple-Pinch problems easily, and is efficient in studying the quantitative effects of varying flowrates of hydrogen utilities and adding off-gas purification techniques. The tool is robust and can handle not only general Pinch problems but also Multiple-Pinch situations along with purifier placement.

© Woodhead Publishing Limited, 2013

35.1.4 Hydrogen Network Design Tool (HyNDT™)

HyNDT™ (Hydrogen Network Design Tool) (2012) is Technip's proprietary advanced refinery hydrogen management software system, which allows the refinery to establish an efficient, cost-effective and optimised hydrogen network architecture, including the underlying objective of minimising the refinery carbon footprint.

HyNDT™ is an optimisation tool that is structured around a virtual hydrogen management Console to obtain an overview of the refinery H_2 balance in order to identify and rank options to improve refinery hydrogen systems and to increase the efficiency and profitability of the refinery. HyNDT™ is based on advanced LP Modelling techniques that allow detection of the optimum hydrogen make-up to meet the demand of all process units connected to a data network by matching hydrogen sources with appropriate sinks.

HyNDT™ Console identifies producers and consumers of hydrogen in a refinery and then determines the best way to connect them so that hydrogen recovery is maximised. It enables shaping or reshaping new or existing refinery hydrogen systems by identifying potential hydrogen containing refinery off-gas (ROG) streams for purposes of hydrogen recovery, assessing the capacity of dedicated H_2 producers, and evaluating H_2 make-up quality for final users. It entails a comprehensive design methodology (H_2 Network Analysis), involving all the associated hydrogen distribution costs relevant to each H_2 recovery solution, in order to provide Capex/Opex evaluation for each prospective H_2 network solution.

35.1.5 Mass Exchange Network (MEN)

In his book, El-Halwagi (1997) provides a CD with two software tools: MEN software and optimisation software LINGO. MEN is a software tool developed for the design of waste recovery networks. It is based on algebraic and optimisation-based solutions for MEN synthesis problem. It can generate composition interval diagrams, tables of exchangeable loads and optimisation formulations for minimising the cost of Mass Separating Agents (MSAs). The user is required to enter supply and target composition, maximum MSA flowrate, solute distribution, cost and some other parameters for lean streams, and supply and target compositions and flowrates for rich streams. As a result, the software generates Composition Interval Diagrams, tables of exchangeable loads for rich and lean streams, and writes a LINGO input file for use with LINGO optimisation software. The LINGO optimiser enclosed in the CD is a student version (with a limited number of constraints and variables) of LINDO Systems Inc.

© Woodhead Publishing Limited, 2013

Table 35.1 Water Cascade Table (WCT)

Freshwater 2.0571 kg/s			Wastewater 8.1571 kg/s		
Conc, C (ppm)	dP	Sum F source (kg/s)	Total F (kg/s)	Cum. water flowrate (kg/s)	Cum. water surplus (kg/s)
				2.0571	
0		0.8	–0.4		
	0.00001			1.6571	
10			–5.8		0.00001657
	0.000004			–4.1429	
14		5	5		0
	0.000011			0.8571	
25		5.9	5.9		0.00000943
	0.000009			6.7571	
34		1.4	1.4		0.00007024
	0.999966			8.1571	
					8.15693576

35.1.6 Optimal-Water©

Optimal-Water© (2012) is a Microsoft Windows-based program that enables the rapid determination of the minimum water and energy requirements for a process, and the improvement of the water and heat recovery network structure for a process plant and for an urban system to achieve the minimum utility (freshwater and heat) consumption. Optimal-Water is developed by PROSPECT, Universiti Teknologi Malaysia. Optimal-Water has been tailored for the retrofit of water and heat recovery networks to reduce water and energy in chemical process plants and in urban water systems. Software was developed based on the synergistic combination of techniques to minimise energy, freshwater consumption as well as waste water generation.

The Water Cascade Analysis (WCA) by Manan *et al*. (2004) is one of the key features implemented by Optimal-Water to establish the true minimum freshwater and wastewater targets for continuous and semi-continuous water-using processes (Table. 35.1). WCA is a numerical technique that can quickly yield accurate minimum water targets and Pinch Point locations for a water network. Various options for water minimisation involving process changes, including water regeneration and equipment modifications, can be rapidly and systematically assessed using WCA. Problems involving Multiple Pinches can be handled more efficiently, accurately and with much less effort.

The software can also automatically propose a water network design to achieve maximum water recovery (shown in Fig. 35.1).

© Woodhead Publishing Limited, 2013

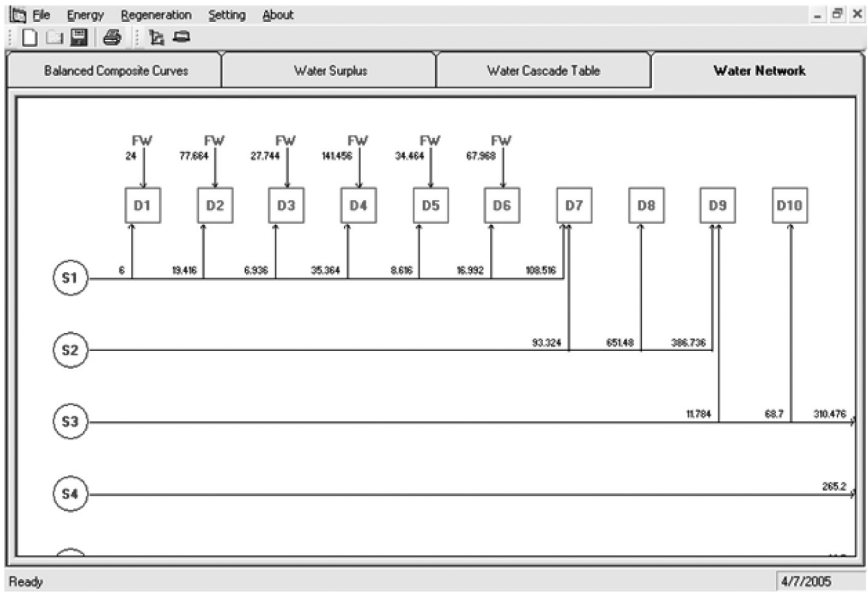

35.1 Water network diagram.

Software also incorporates the Source and Demand Heat Composite Curves, which is a graphical approach that simultaneously targets the minimum water and energy consumption of a water-using network – see Fig. 35.2 (Manan *et al*., 2009). The Source and Demand Heat Composite Curves provide key information on the state of a water-using network and allow water-using network design to be carried out graphically.

35.1.7 RCNet

RCNet (Foo, 2013) is a spreadsheet software based on Microsoft Excel for the synthesis of Resource Conversation Networks (RCN) for the efficient use of material resources (e.g., water, utility gases, solvents, etc.) in industrial plants. Software is an implementation of well-established Process Integration tools, namely Pinch Analysis and mathematical optimisation techniques. Pinch Analysis is used to determine minimum flowrate targets for fresh resource (freshwater, gas, etc.) and waste discharge (e.g. wastewater, purge gas, etc.), prior to detailed RCN design. To perform the targeting task, material cascade analysis is used. Next, a mathematical optimisation technique based on the superstructural model is used to design the RCN that achieves the flowrate targets.

The user may choose to calculate any of the following resource conservation problems: (i) water minimisation, (ii) gas recovery, or (iii) Property

© Woodhead Publishing Limited, 2013

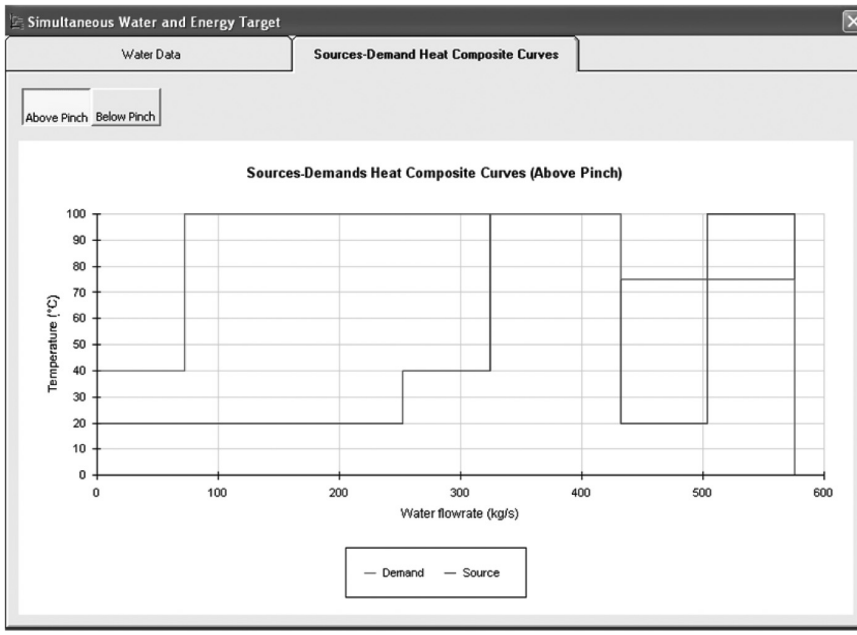

35.2 Source and Demand Heat Composite Curves for simultaneous determination of water and energy targets.

Integration. After selection of units and specifying limiting data, the software carries out the targeting stage and designs the water network that achieves the flowrate targets.

35.1.8 Water

WATER (2012) is a software package for the design of water systems in the process industries (Fig. 35.3). Water is used for a wide variety of operations in mass transfer and washing operations, steam systems, cooling systems, etc. Rising water cost, restrictions in water use and increased environmental awareness have driven designers towards more efficient water systems. WATER targets and designs for minimum water consumption through identification of re-use opportunities. Opportunities for regeneration of water for further re-use or recycling are identified. Effluent treatment systems are designed for minimum cost through design methods that lead to distributed systems. Water use, regeneration and effluent treatment networks are designed automatically, keeping the designer in full control of network complexity. Multiple contaminants are handled.

© Woodhead Publishing Limited, 2013

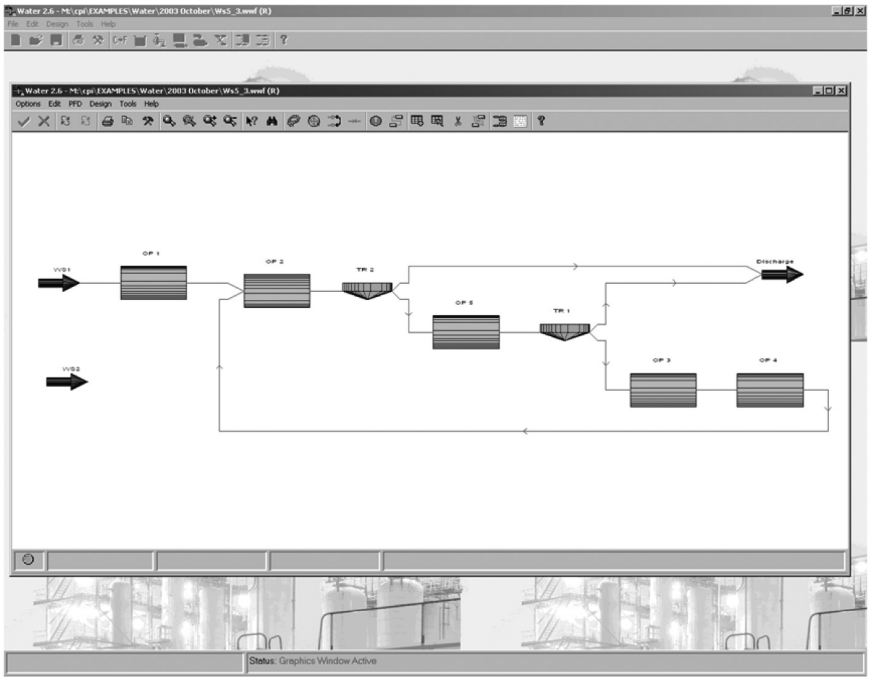

35.3 Graphical interface of WATER software. (WATER, 2012.)

Issues addressed by WATER include:

Water Minimisation: WATER allows freshwater to be minimised through the identification of re-use opportunities. Maximising re-use minimises consumption and minimises the volume of wastewater generated. The program works from knowledge of the constraints on water quality required by each operation. Constraints can be specified for multiple contaminants. Also, maximum and minimum flowrate constraints, forbidden matches and water losses/gains in individual operations can be specified.

Multiple Sources of Freshwater: It is often the case that there are a number of different sources of freshwater available with different qualities and different costs. WATER is able to optimise the use of different sources of freshwater.

Automatic Design of Water Re-Use Networks: WATER not only allows targets to be set for water re-use networks, but also designs the network automatically. All constraints relating to maximum and minimum flowrates, forbidden matches and water losses/gains in individual operations can be catered for. The designer also has control over the network complexity.

Regeneration of Water: Once the re-use of water has been maximised, further reduction can only be brought about by the regeneration of wastewater. The regeneration can be any reaction or separation process that removes

© Woodhead Publishing Limited, 2013

the contamination, which would otherwise prevent its further use. Once regenerated, the water can either be re-used or recycled. In regeneration re-use any water used by an operation is not allowed to re-enter the same operation. The water can enter the same operation many times. It is important to distinguish between these cases, as recycling can sometimes be undesirable. WATER allows regeneration re-use and regeneration–recycling to be examined and compared.

Automatic Design of Effluent Treatment Networks: Once water use has been minimised the resulting effluent must be disposed of at minimum cost, whilst meeting environmental discharge regulations. Effluents should be segregated for treatment where appropriate, and only mixed where appropriate. If this policy is adopted, the design becomes distributed rather than centralised. WATER can design effluent treatment networks automatically for minimum cost. The designer maintains control over network complexity and constraints relating to maximum and minimum flowrates, forbidden matches and water losses/gains in treatment operations.

Pipe-work and Sewer Costs in Network Design: Not only can WATER include capital cost associated with regeneration and treatment processes, but the cost of connecting operations associated with running new pipes and sewers can also be included. This cost is included with the freshwater cost and other capital cost in the overall trade-off. It is important to include pipework and sewer cost, as these have a profound influence over the network structure and complexity.

35.1.9 WaterTarget™

WaterTarget™ (2012) is a commercial software provided by KBC. It is a suite of software tools which assist the user to simultaneously consider opportunities for water re-use, regeneration and treatment.

- WaterTracker reconciles water and contaminant balances. This application compiles water network information using drag and drop drawing, drill-down detail, shortcut unit operation models and stream data editors.
- WaterPinch helps to determine optimum water networks and wastewater treatment strategies. The application has optimisation routines to minimise network operating costs subject to user specified constraints.

WaterTarget can help to reduce water consumption and wastewater generation and the plant's impact on the environment. At the same time, it can help to:

- Achieve environmental compliance,
- Avoid water supply or treatment bottlenecks,

© Woodhead Publishing Limited, 2013

- Reduce the capital cost of new supply or treatment facilities,
- Reduce the operating cost of water supply, treatment and discharge.

Together, these products provide a solution for identifying efficient and practical means of complying with environmental legislation or managing a restricted supply.

35.1.10 WaterTarget (Water Design)

WaterTarget software can be found on a CD in Mann and Liu (1999). Software generates freshwater use/wastewater targets, and suggests ways to achieve them. It can also help in isolating bottlenecks that limit water re-use, and in finding new re-use opportunities. The book that accompanies the CD describes water re-use and wastewater minimisation principles and practices. Downloadable from Virginia Polytechnic Institute and State University website, Water Design (2012) is a PC-based software tool sufficient for developing many aspects of Water Pinch Analysis and synthesis covered in Mann and Liu (1999).

35.2 Sources of Further Information and Advice

As can be seen from the review, there are fewer Water or Mass Integration software tools on the market compared to Heat Integration tools. Numerous tools dealing with water management, hydraulic issues, etc., are outside the scope of this review, which focuses entirely on Process Integration software.

It is worth mentioning a book by El-Halwagi (1997) that presents systematic techniques for cost-effective pollution prevention. Step-by-step procedures are presented that are widely applicable to the chemical, petrochemical, petroleum, pharmaceutical, food and metals industries. Various levels of complexity, from graphical methods to algebraic procedures and mathematical optimisation, numerous applications and case studies, and integrated software for optimising waste recovery systems, can be helpful for practising engineers, environmental scientists, plant managers, advanced undergraduate and graduate students, and researchers in the areas of pollution prevention and Process Integration. It shows the reader how to establish pollution–prevention targets for a process and then to develop implementable, cost-effective solutions. It contains step-by-step procedures that can be applied to environmental problems in a wide variety of process industries. It integrates pollution prevention with other process objectives. It includes a CD-ROM that contains software for design of waste recovery networks (MEN) and optimisation (LINGO).

© Woodhead Publishing Limited, 2013

From the most recent works, the book published by Foo (2013) deals in detail with Process Integration related to mass, water and property and it can be a source of valuable information.

An overview of the software tools, including the water and mass software, has been presented by Lam *et al*. (2011). This paper provides an overview of software tools based on long experience and applications in the area of Process Integration, modelling and optimisation. The first part reviews the current design practice and the development of supporting software tools. The Water and Mass Integration software tools are based on Water Pinch and Mass Pinch principles. These are discussed in detail in the literature sources recommended below. Along with papers with the insights of the technology, papers providing more general overview of the water or mass minimisation problems, case studies or closely related topics (e.g. Simultaneous Water and Heat Integration) are also provided. The list is by no means exhaustive – it just gives the reader an overview of technologies presented and key notions.

A useful review of water network design methods has been provided by Bagajewicz (2000). Other reviews of Mass Integration technology is given in Klemeš and Perry (2007) and Klemeš *et al.* (2008). More specific Water Pinch Technology applications are given e.g. in Doyle and Smith (1997). Capital cost aspects of MENs are discussed in detail in Fraser and Hallale (2000a, 2000b). Transition from graphical tools to automated design of total water systems is considered in Gunaratnam *et al.* (2005). In their work, Kim and Smith (2004) describe automated approach to design of discontinuous water systems. Batch process synthesis of water re-use/recycle and interception networks is given in Ng *et al.* (2008). Also batch process wastewater minimisation technique is discussed by Majozi (2005). An integrated design for a heat-and-water system is examined by Savulescu *et al.* (2005a, 2005b). Leewongtanawit (2005), in her work, also studied this topic and described it in a more concise way in Leewongtanawit and Kim (2008, 2009). There are numerous applications of Mass Integration technology, not only in refining and chemical plants but also in food industry (Thevendiraraj *et al.*, 2003). Among papers and other documents providing insights to Hydrogen Network Integration, those of Alves (1999) and Alves and Towler (2002) should be mentioned. Hallale and Liu (2001) discuss refinery hydrogen management aspects. Purifier selection aspects are discussed in Liu and Zhang (2004).

35.3 References

ALChemE (Active Learning in Chemical Engineering). (2012). <alcheme.tamu.edu> accessed 10.09.2012.

Alves J. (1999). Analysis and design of refinery hydrogen distribution systems. PhD thesis, UMIST, Manchester, UK.

© Woodhead Publishing Limited, 2013

Alves, J. J., Towler, G. P. (2002). Analysis of refinery hydrogen distribution systems. *Industry and Engineering Chemistry Research*, **41**, 5759–5769.

Bagajewicz, M. (2000). A review of recent design procedures for water networks in refineries and process plants. *Computers & Chemical Engineering*, **24**, 2093–2113.

Doyle, S. J., Smith. R. (1997). Targeting water reuse with multiple contaminants. *Trans. IChemE*, **75**(part B), 181–189.

El-Halwagi, M. (1997). *Pollution Prevention Through Process Integration Systematic Design Tools.* Academic Press, San Diego, California, USA. An imprint of Elsevier Science Publishing Co Inc., 334 p.

Foo, D. (2013). *Process Integration for Resource Conservation.* CRC Press, Boca Raton, FL, USA, Taylor & Francis Group, 606 pp. <www.crcpress.com/product/isbn/9781439860489> Accessed 10.09.2012.

Fraser, D. M., Hallale, N. (2000a). Capital and total cost targets for mass exchange networks: Part 1: simple capital cost models. *Computers & Chemical Engineering*, **23**(11–12),1661–1679.

Fraser, D. M., Hallale, N. (2000b). Capital and total cost targets for mass exchange networks: Part 2 detailed capital cost models. *Computers & Chemical Engineering*, **23**(11–12), 1681–1699.

Gunaratnam, M., Alva-Argбez, A., Kokossis A., Kim, J., Smith, R. (2005). Automated design of total water systems. *Industrial & Engineering Chemistry Research*, **44**(3), 588–599.

H2-int. <www.processint.com/chemical-industrial-software/h2-int> Accessed 10.08.2012.

Hallale, N., Liu, F. (2001). Refinery hydrogen management for clean fuels production. *Advances in Environmental Research*, **6**(1), 81–98.

HyNDT™. (2012). <technip.com/en/our-business/onshore/hydrogen-syngas> Accessed 26.09.2012.

Jacob, J., Kaipe, H., Couderc, F., Paris, J. (2002). Water network analysis in pulp and paper processes by pinch and linear programming techniques. *Chemical Engineering Communications*, **189**, 184–206.

Kim, J.-K., Smith, R. (2004). Automated design of discontinuous water systems. *Process Safety and Environmental Protection*, **82**(3), 238–248.

Klemeš, J., Perry, S. (2007). Process optimisation to minimise water use and wastage. In K. Waldron (ed.), *Waste Management and Co-product Recovery in Food Processing,* vol. 1. Woodhead, Cambridge, UK, pp. 90–118.

Klemeš, J., Smith, R., Kim, J.-K. (eds). (2008). *Handbook of Water and Energy Management in Food Processing*. Woodhead, Cambridge, UK.

Klemeš, J., Varbanov, P., Lam, H. L. (2009). Water footprint, water recycling and food industry supply chain. In K. Waldron (ed.), *Waste Management and Co-product Recovery in Food Processing,* vol. 2. Woodhead, Cambridge, UK, pp. 134–168.

Lam, H. L., Klemeš, J. J., Kravanja, Z., Varbanov, P. S. (2011). Software tools overview: process integration, modelling and optimisation for energy saving and pollution reduction. *Asia-Pacific Journal of Chemical Engineering*, **6**(5), 696–712.

Leewongtanawit, B. (2005). Heat-integrated water system design. PhD thesis, UMIST, Manchester, UK.

Leewongtanawit, B., Kim, J. (2008). Synthesis and optimisation of heat-integrated multiple-contaminant water systems. *Chemical Engineering and Processing*, **47**(4), 670–694.

© Woodhead Publishing Limited, 2013

Leewongtanawit, B., Kim, J. (2009). Improving energy recovery for water minimisation. *Energy*, **34**(7), 880–893.

Liu, F., Zhang, N. (2004). Strategy of purifier selection and integration in hydrogen networks. *Chemical Engineering Research and Design*, **82**(A10), 1315–1330.

Majozi, T. (2005). An effective technique for wastewater minimisation in batch processes. *Journal of Cleaner Production*, **13**, 1374–1380.

Manan, Z. A., Foo, C. Y., Tan, Y. L. (2004). Targeting the minimum water flow rate using water cascade analysis technique. *AIChE Journal*, **50**(12), 3169–3183.

Manan, Z. A., Tea, S. Y., Alwi, S. R. W. (2009). A new technique for simultaneous water and energy minimisation in process plant. *Chemical Engineering Research and Design*, **87**(11), 1509–1519.

Mann, J., Liu, Y. A. (1999). *Industrial Water Reuse and Wastewater Minimization*. McGraw-Hill Professional, New York, USA, 450 ps.

Nelson, A., Liu, Y. (2008). Hydrogen-Pinch analysis made easy. *Chemical Engineering*, June 2008, and <www.design.che.vt.edu/h2pinch/h2pinch.html> Accessed 16.09.2012.

Ng, D. K. S., Foo, D. C. Y., Rabie, A., El-Halwagi, M. M. (2008). Simultaneous synthesis of property-based water reuse/recycle and interception networks for batch processes. *AIChE Journal*, **54**(10), 2624–2632.

Optimal-Water©, <www.cheme.utm.my/PROSPECT/index.php/water-matrix> Accessed 10.08.2012.

Savulescu, L., Kim, J., Smith, R. (2005a). Studies on simultaneous energy and water minimisation – Part I: Systems with no water re-use. *Chemical Engineering Science*, **60**(12), 3279–3290.

Savulescu, L., Kim, J., Smith, R. (2005b). Studies on simultaneous energy and water minimisation – Part II: Systems with maximum re-use of water. *Chemical Engineering Science,* **60**(12), 3291–3308.

Sorin, M., Bédard, S. (1999). The global pinch point in water reuse networks. *Transactions of the Institution of Chemical Engineers (Part B)*, **77**, 305–308.

Thevendiraraj, S., Klemeš, J., Paz, D., Aso, G., Cardenas, J. (2003). Water and wastewater minimisation study of a citrus plant. *Resources, Conservation and Recycling*, **37**, 227–250.

WATER. (2012). Process Integration Software (Centre for Process Integration, School of Chemical Engineering and Analytical Science, The University of Manchester, U.K.). <www.ceas.manchester.ac.uk/research/centres/centreforprocessintegration/software/packages/water/> accessed 10.082012.

WaterTarget™. (2012). KBC software. <www.kbcat.com/Software-Solutions/WaterTarget/> Accessed 10.09.2012.

Water/Target (Water Design). (2012). <www.design.che.vt.edu/waterdesign/waterdesign.html> Accessed 16.09.2012.

© Woodhead Publishing Limited, 2013

36

Epilogue: The Importance of Problem Formulation and Data Extraction in Process Integration

JIŘÍ JAROMIR KLEMEŠ, University of Pannonia, Veszprém, Hungary

DOI: 10.1533/9780857097255.6.1099

Abstract: Process Integration (PI) is a powerful tool for designing and optimising processes in terms of efficiency in the use of energy, water and other resources, and also sustainability. It has been widely extended, and has become both a part of the curricula of most good engineering degree courses, as well as a routine tool for advanced design and optimisation in various industries. However, sometimes the comparative simplicity of the basic methodology is still misunderstood. Even PI has some potential pitfalls, related especially to the formulation of the problem and Data Extraction (DE). Regardless of the precision used, the results largely depend on solving the correct problem: it is therefore essential that the formulation reflects reality adequately and appropriate data have been extracted. An incorrect DE has been the reason for some less trained users' conclusions that PI did not work. When revisiting most of those problems, it becomes obvious that they were not due to problems with the PI methodology, but rather to user inexperience. In this chapter the editor of the handbook would like to stress correct problem formulation, and especially correct DE, as crucial issues.

36.1 Introduction: Process Integration – from its Roots to its Present Strong Position

Achieving savings in energy and water usage, thereby counteracting global warming and reducing greenhouse gas emissions, has become a major technological, societal, and political issue of significant strategic importance. Numerous studies have been carried out with the aim of improving the efficiency of energy supply and utilisation, while also reducing emissions of greenhouse gases, volatile organic compounds and other pollutants. As a response to these industrial and societal requirements, a number of new methodologies emerged during the 1970s. The most significant of these were (i) Process System Engineering (PSE) (Sargent, 1979), which was based on

© Woodhead Publishing Limited, 2013

a method known as 'flowsheeting'; and (ii) PI, the early development of which is covered in Chapter 1 of this handbook.

Both disciplines were developed with the help of dedicated conferences: for PSE, these include the European Symposium on Computer Aided Process Engineering (ESCAPE, 2013), facilitated by the European Federation of Chemical Engineering Working Party on Computer Aided Process Engineering (CAPE, 2013), and a number of PSE conferences (PSE, 2012) and in Asia (2013). Recently, however, the area of PSE also encompasses a number of PI topics.

There is a dedicated conference for PI – the Conference on Process Integration, Modelling and Optimisation for Energy Saving and Pollution Reduction (PRES, 2012), which has been supported by a number of chemical and chemical engineering societies, including the Czech Society of Chemical Engineering, the Hungarian Chemical Society, the Italian Association of Chemical Engineering, the Canadian Society for Chemical Engineering, and recently also by the Chemical Process and Energy Resources Institute – CERTH, Greece (PRES'13, 2013). Another dedicated conference, first organised in 1992, is the International Process Integration Jubilee Conference. There are also some other conferences, mainly dedicated to sustainability and cleaner, environmentally-friendly production, in which PI plays an important role, such as the Conference on Sustainable Development of Energy, Water and Environment Systems (SDEWES, 2013), which has a regular session entitled 'Energy and Water Efficiency for Sustainable Future: Knowledge Development and Transfer'. It is remarkable that PI has remained a topic of importance and interest to researchers for 35 years, and that recently it has even been an area of growth.

The major web sources – Google Scholar (2012) – GS, Web of Knowledge℠ and Web of Science℠ (Thompson Reuters, 2012), Scopus (2012) – SC and Scopus without self-citations – SCnet – list a considerable number of works. GS is taken as an example below. The figures in some cases include different usages of the same/similar terms, and a detailed check of such a large number of citations was not possible.

PI: about 55,100 works in GS

Pinch Technology/Methodology: 2,760 in GS plus several hundred additional hits for variations such as Pinch approach
Heat Integration: about 7,700 in GS
Water Integration: 1,170 in GS
Mass Integration: 2,100 in GS
Total Site: more than 10,000 in GS; however, some of these are not related to PI

© Woodhead Publishing Limited, 2013

Table 36.1 A selection of most cited publications related to PI

Reference	Google Scholar	Web of Knowledge℠ Web of Science℠	Scopus	Scopus without self-citations	Scopus without self-citations in 2012
Wang and Smith (1994)	766	568	560	556	43
Linnhoff *et al.* (1982, 1994) – book	759		357	354	29
Smith (2005) – book	725				
Linnhoff and Hindmarsh (1883)	638	425	388	388	44
El-Halwagi and Manousiouthakis (2004)	431		181 (in Wiley)		
El-Halwagi and Manousiouthakis (1989)	427	316	323	305	16
Linnhoff and Flower (1998)	423	308	232	231	22
El-Halwagi (1997) – book	361				
TF Yee, IE Grossmann (1990)	348	275	275	244	28
Kemp (2007) – book	228				
El-Halwagi *et al.* (2003)	220	179	194	181	27

More precise figures can be obtained for the number of citations received by major studies, and the results show a substantial interest in a number of key works. The data in Table 36.1 do not constitute a fully comprehensive overview, but are intended to demonstrate the on-going interest in PI and related further developments. It should be noted that the Scopus data does not include books from the other publishers; in fact, until comparatively recently this comprehensive database of peer-reviewed abstracts and citations did not record publications and references outside Elsevier. Google Scholar, on the other hand, covers all web sources, but these can also include sources that are not peer-reviewed or recognised scientific publications. Thompson Reuters ISI Web of Knowledge and Web of Science are again not providing the data for all publications, e.g. for all books. Figures were collected on 2 December 2012 and are still increasing.

36.2 Successful Applications of Process Integration

There have been numerous successful applications of PI technology; this section provides a short overview of the implementation of the methodology in selected industrial case studies. The discussion of each case is necessarily

© Woodhead Publishing Limited, 2013

condensed, due to limitations on space; further information is available in the relevant works cited.

The main fields in which PI methodology has been implemented have traditionally been the chemical, oil refining, and petrochemical industries. Some examples include: the retrofitting of the Heat Exchanger Network (HEN) of a fluid catalytic cracking (FCC) unit, consisting of a main column and a gas concentration section, by Al-Riyami *et al*. (2001); Seikova *et al*.'s (1999) study of retrofitting a crude-oil preheating system; the PI of sodium hypophosphate production by Tovazhnyansky *et al*. (2010); and Matsuda *et al*.'s (2010) study of energy saving in the reaction section of the hydrodesulphurisation process using self-heating recuperation technology.

Many studies have employed Pinch Technology (and the specifically Heat Integration Analysis) in the food processing industry. The thermodynamic profile of this industry differs significantly from that of the oil refining and petrochemical industries: it is characterised by process streams of relatively low temperature (normally 120–140°C), a small number of hot streams, elevation of food solutions at a low boiling point, and a considerable deposition of scale in evaporators and heat recovery systems. The processes also tend to operate on a seasonal basis. Case studies relating to energy efficiency in food processing have involved several different areas. Studies on the sugar industry can be found in Klemeš *et al*. (1999), also in Grabowski *et al*. (2001), and in more detail in Grabowski *et al*. (2002). Klemeš *et al*. (1998) also present a comprehensive study covering a sugar plant, a raw sunflower-oil plant, and a corn crystal glucose plant, while Ram and Banerjee (2003) carried out a study that analysed a sugar plant using Heat Integration (HI) methodology in a developing country. Heat Integration Analysis of a brewery, offering considerable energy savings, is examined in Hufendiek and Klemeš (1997). An early case study of a whisky distillery by Smith and Linnhoff (1988) was later used as an example of successful implementation (CADDET, 1994) and illustrates how HI can reduce energy use and increase energy efficiency; another study involving a whisky distillery can be found in Kemp (2007). Finally, Fritzson and Berntsson (2006) studied a Swedish slaughtering and meat processing plant.

In the UK, several case studies have been documented by the Department for the Environment, Transport and the Regions, including a study of a food processing factory (DETR, 1997) and of waste heat recovery (DETR, 1996). The waste heat recovery potential for the UK alone was assumed to be 8.3 PJ/y, which represented around £M 14 at the time, and equates to more than £M 30 at today's prices. It had been established that the pasteurisation process used in the dairy industry was already highly efficient in terms of heat recovery (up to 95%), but sterilisation was more energy intensive, with bottle sterilisation consuming 300–500 MJ/t. The Associated Dairies plant involved in the DETR study carried out several measures on

© Woodhead Publishing Limited, 2013

the basis of PI methodology and achieved considerable savings. The other food and drink processes reviewed by DETR (1996) were bakeries, breweries, the drying process in the production of flavourings and ingredients. A specific example is of a breadcrumb drying plant, in which an energy saving potential of about 30% was identified.

The study by Soh *et al*. (2011) is a good example of the implementation of PI methodology in another field, namely the pulp and paper industry. A further interesting application related to HI is an analysis of a mechanical pulp and paper mill by Ruohonen *et al*. (2010), who use the term 'Advanced Composite Curves'.

Pinch Technology is a vital subdivision of process engineering. Linnhoff March (today part of KBC Advanced Technologies) – see Chapter 1 – have carried out a number of case studies in the field, and listed over 400 clients worldwide already in 2002 (Linnhoff March – KBC Advanced Technologies 2002). The exact details of the projects in which they are involved are mostly confidential, but publicity information can be obtained from the company. Even today KBC Advanced Technologies stress that 'Pinch Technology is a vital subdivision of process engineering. Completing a process engineering project without a Pinch study leads to a less efficient design from the beginning' (KBC Advanced Technologies, 2012). They are also offering a 'Pinch Technology Introduction' (KBS Energy Services, 2012), following the progress made at The Inštfitute of Scfience and Technology (UMIST), now The , and Lfinnhoff March Ltd.

Total Sites have significantly increased in scope compared to the application of HI in individual processes. Varbanov *et al*. (2005) demonstrated the synthesis of a utility system (CHP network) of an industrial Total Site by applying a combination of targeting and mathematical programming techniques, while Herrera *et al*. (2003) studied a hospital complex Total Site that included an institute, a general hospital, a regional laundry centre, a sports centre, and some other public buildings. Recently, Bandyopadhyay *et al*. (2010) presented options for targeting co-generation potential by means of Total Site Integration.

36.3 Methods of Obtaining Credible High Integration HI Solutions

Traditional Pinch Analysis assesses the minimum practical energy needs for a process through a systematic design procedure involving five steps:

1. Collection of plant data.
2. Setting targets for minimum practical energy requirements.
3. Examination of process changes that contribute to meeting the target.
4. Establishing the minimum energy design that achieves the target.
5. Optimisation, allowing a trade-off between energy cost and capital cost.

© Woodhead Publishing Limited, 2013

The first issue is how to begin a PI study. Kemp (2007) summarised the steps involved, which had been further developed based on the authors' experience. The steps listed in this work relate to HI, but could equally apply to Mass/Water Integration. Klemeš and Varbanov (2010) created a workflow diagram to outline the procedure (Fig. 36.1).

36.4 Data Extraction

DE is a crucial step, which can be performed automatically from simulation data (Linnhoff and Akinradewo, 1998). Several software packages offer this option, such as SuperTarget™ (2012), but care is still needed in its implementation: software-run (automatic) DE can be likened to computerised translation between two languages. The finer details still require the judgement, experience, and even intuition of an expert engineer. Poor DE can easily lead to missed opportunities to improve the process design. If the DE accepts all the features of the existing flowsheet, then there will be no scope for improvement. Since 2000 the methodology has undergone further developments, with attempts to carry out automatic DE, but practical experiences, along with some basic rules, remain valuable. The answers to the following questions should be considered as the rules that should be followed:

1. When is a stream a stream?
2. How precise must the data be for specific steps?
3. How should considerable specific heat (Cp) changes and latent heat be handled?
4. What are the DE rules?
5. How should the heat loads, capacities and temperatures of an extracted stream be calculated?
6. How 'soft' are the data in the flowsheet/plant?
7. Where can data relating to the capital and running cost can be found?

36.4.1 When Is a Stream a Stream?

This is one of the key issues determining the correct setup of a problem. Streams that do not gain or provide heat should be disregarded. This rule considerably simplifies the problem. There are also some other streams that should not be included for PI purposes, for reasons of distance, safety, or product purity, or for operational reasons. When deciding which streams are to be extracted, the following question should be answered: when is a stream a stream?

© Woodhead Publishing Limited, 2013

© Woodhead Publishing Limited, 2013

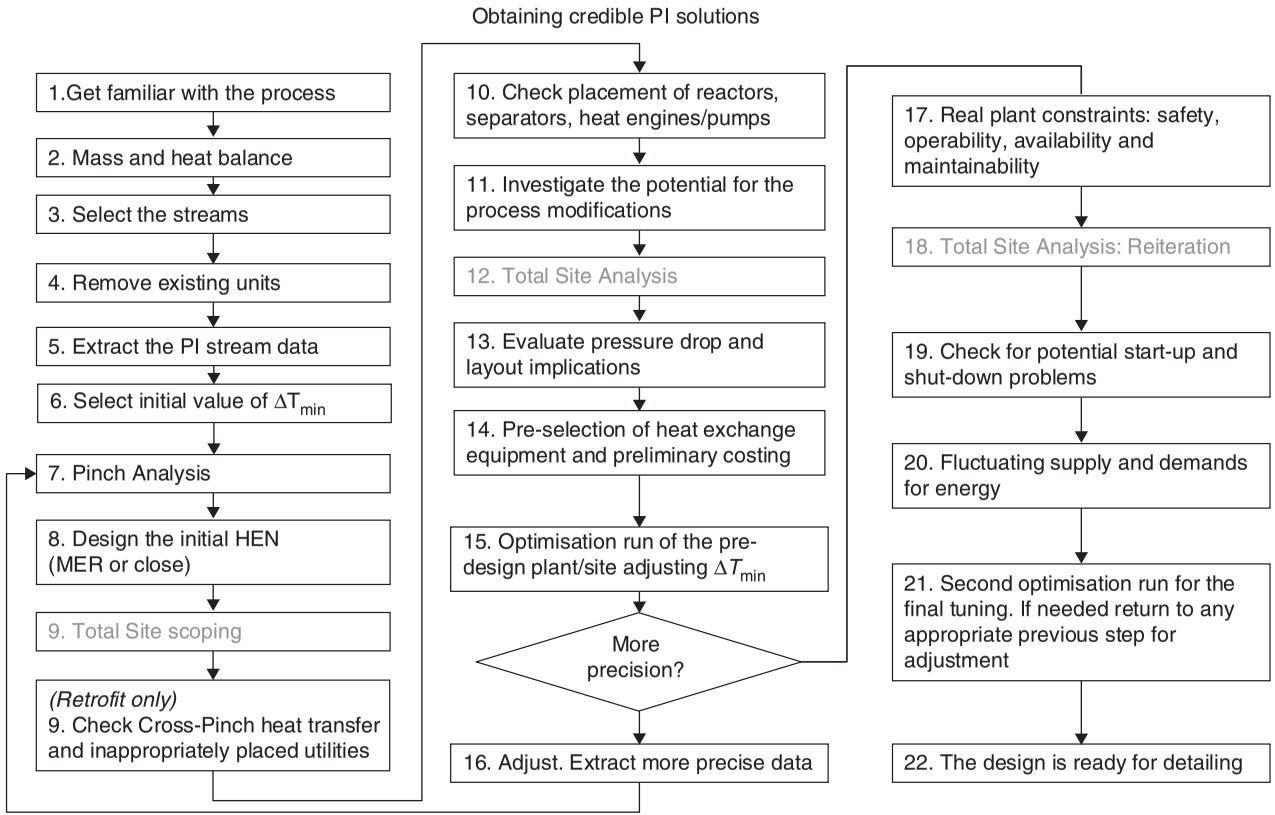

36.1 Workflow diagram of Process Integration study (after Klemeš and Varbanov, 2011).

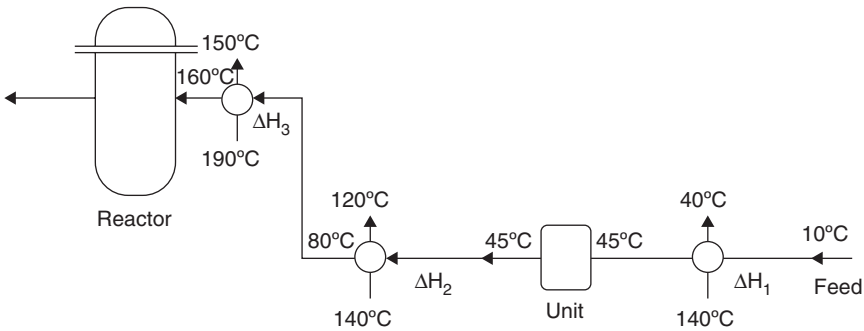

36.2 An example – a flowsheet fragment (after CPI, 2004).

Let us consider the example in Fig. 36.2, which was first introduced by Linnhoff *et al*. (1982) and is now used in many courses based on UMIST/The TEACHFING MATERfIALŠ (CPI, 2004), AŠ WELL AŠ, fIN MODfIfied form, in publications by Smith (2005) and later Kemp (2007). The figure shows part of a flowsheet, in which the feed stream is heated by a recuperating heat exchanger to 45°C before entering a processing unit. After leaving this unit, the stream is heated again by two heat exchangers and then enters a reactor. Operation of the reactor requires the feed stream to be at 160°C. The options for the number of streams we should extract are: (i) from 10°C to 160°C; (ii) from 10°C to 45°C and 45°C to 160°C; or (iii) from 10°C to 45°C, 45°C to 80°C and 80°C to 160°C.

If option (iii) is applied, the resulting design would be identical to the existing setup in Fig. 36.2, with three heat exchangers with identical heat duties. Critics of the PI technique concluded that no improvement was achieved through the use of this methodology in this case. Option (ii) offers a greater degree of freedom: the first heat exchanger would be the same as in the current flowsheet, but the rest of the design could be modified. The extraction of two streams would be suitable when the processing unit demands a feed temperature of close to 80°C. Option (i) would provide the greatest freedom and scope for improvement; however, the processing unit must be able to support a variable feed temperature, which could be anything between 10°C (the supply temperature) and 160°C (the target for the reactor).

If the processing unit is a filter, as assumed by Smith (2005), there would be a restriction on the filter supply temperature, as high temperatures could pose a problem for the filter. If, however, the processing unit is just storage, as assumed by Linnhoff *et al*. (2012), a different temperature restriction might apply. This simple example demonstrates that stream extraction cannot be fully automatic, but requires further assessment related to processing units and their performance.

© Woodhead Publishing Limited, 2013

36.4.2 How Precise Does the Data for Specific Steps Need to Be?

This question is posed very frequently, with many claiming that PI analysis cannot be carried out due to insufficiently precise data. PI starts with rough assumptions, which are then corrected over several rounds of analysis. PI and initial optimisation are more about screening and scoping than detailed design. The goal is to establish an answer to the question of what potential for energy saving exists, and in which direction the optimisation should proceed. A potential of around 15% is sufficient – the precise figure can be, for example, 13% or 17%, with no negative effects. In the regions close to the Pinch the data should be as precise as possible (Linnhoff *et al.*, 1982 and most later publications). At the start of the analysis, the designer might have only a vague idea of where, and at what temperature, the Pinch will occur. As stated above, DE has to start from rough assessments that are later corrected.

36.4.3 How Should Considerable Cp Changes and Latent Heat Be Handled?

Figure 36.2 clearly shows that phase changes are very likely to occur when the temperature rises from 10°C to 160°C; Cp also changes with the temperature, so using a constant value for Cp would be unrealistic. To address this problem, a segmentation technique was developed and has been used in STAR (2012), for example. Important parameters include the number of segments to define, and the temperatures with which they should start and end. Each segment increases the complexity, so segments should be kept to a minimum.

36.4.4 What Are the Data Extraction (DE) Rules?

Some DE rules were introduced very early by Linnhoff *et al.* (1982) and are now used in many courses based on UMIST teaching materials (e.g. CPI 2004); Smith (2005), Kemp (2007) and most recently Klemeš *et al.* (2010) all use a modified form of Linnhoff *et al.*'s original rules. Most are related to HI, but the principles can also be applied to Mass/Water Integration. Klemeš and Varbanov (2010) provided an overview of these rules, as follows:

1. *Non-isothermal Mixing.* The mixing of two or more streams with different temperatures represents a heat exchange, with a degradation of the higher temperature. It can also result in Cross-Pinch heat transfer.

© Woodhead Publishing Limited, 2013

2. *Heat Losses.* In most cases the heat losses are neglected. This is not correct for situations where streams are long or subject to very different temperatures. The solution is to introduce hypothetical coolers/heaters representing the losses.
3. *Extracting Utilities*. The utilities should never be extracted from the existing plant or flowsheet, as this would probably result in the same use of utilities as previously, thereby neglecting more efficient options such as the generation of utilities. It should be noted, however, that a steam is not always a utility, but is in some cases also used as a process stream, for example, as a stripping steam in separation columns.
4. *Generation of Utilities*. HI analysis using the Grand Composite Curve may indicate valuable options for using otherwise wasted heat or cold to generate utilities. A number of errors have been made as a result of simply matching the evaporation and condensation lines without allowing for the heat segments (preheating and superheating, steam vapour cooling, condensate sub-cooling).
5. *Extracting at the Effective Temperature*. In some cases a stream cannot be extracted directly as it is still required by a related process. A hot stream, for example, should be extracted at the temperature at which the heat becomes available. Smith (2005) presents a good example of this in the form of a reactor using a quench liquid.
6. *Forced and Prohibited Matches*. There may be matches in a HEN that should be either prohibited, for example due to contamination risk, or secured. Software tools usually offer this option; it can alternatively be achieved by an appropriate penalty/bonus in the objective function.
7. *Keeping Streams Separate Only when Necessary*. If streams can be merged, it may be possible to eliminate some heat exchanging units.

36.4.5 How Should the Heat Loads, Capacities and Temperatures of an Extracted Stream Be Calculated?

Once a stream has been extracted, the next problem is the calculation of the heat-related data. Common engineering practices can be used to take measurements during plant operation, followed by data reconciliation – see for example Klemeš *et al*. (1979) and later BELSIM (2003). Another option is to use a flowsheeting simulation model based on programs such as Aspen Plus® (2012) or Aspen HYSYS® (2012). These options are time consuming and at early stages in the design the process structure is likely to evolve. A simplified approach based on the extracted data can therefore be employed, and has been shown to be sufficient in the initial stages.

© Woodhead Publishing Limited, 2013

36.4.6 How 'Soft' Are the Data in a Flowsheet/Plant?

Inexperienced operators may attempt to perform the PI analysis based on the temperatures already shown in the Process Flow Diagram, an approach that often results in useful opportunities being overlooked. The best implementation of PI analysis involves questioning every temperature, and, following discussion with the plant designer/manager, establishing which temperatures are absolutely crucial ('hard' data) and which can be compromised ('soft' data). In practice, most data are soft to some respect, which can be advantageous. In particular, streams leaving the plant are usually characterised by soft data and are suitable for optimisation via the +/- principle. Data softness is related to changing conditions and to flexibility, operability, and resilience.

36.4.7 Where Can Data Relating to the Capital and Running Cost Be found?

The need to find costs data arises when the appropriate ΔT_{min} must be selected, as the optimum ΔT_{min} depends on economic parameters. Estimating capital cost is time consuming: approximation methods (such as that used by Taal *et al.*, 2003) can be used in the initial stage when little is known about the design and materials required or the temperature, pressure and composition of streams. The cost of equipment is subject to regional variation and may be related to market conditions, while operating cost is also difficult to estimate, as they are affected by labour and taxation, and are mainly a function of the cost of energy. A potential pitfall is using the current price of energy in the analysis; instead, the anticipated average energy price for the life span of the plant should be used, or, for retrofits, for the expected payback period. A number of studies have failed to follow this rule. The next problem is then where to find energy price projections for the next five to ten years, given that even the forecasts made by qualified institutions have not proved accurate. One possible approach is the use of scenarios and the targeting of the most flexible design, which would provide a balanced optimum for a variety of situations.

36.5 Integration of Renewables – Fluctuating Demand and Supply

The availability of renewables varies significantly with time and location, while the energy demands of sites is similarly subject to variation according to the time of the day and period of the year. An advanced variation on PI methodology considers time as another dimension to the problem,

© Woodhead Publishing Limited, 2013

and could be a potential solution. A basic methodology has previously been developed for the HI of batch processes, involving the Time Slice and Time Average Composite Curves (Kemp and Deakin, 1989), which were also revisited by Foo *et al*. (2008). A novel approach has involved extending the HI analysis to renewables – Perry *et al*. (2008), further developed by Varbanov and Klemeš (2011). Dealing with variation and fluctuation introduces an extra level of complexity to the DE problem. The key is the specification of the time intervals or Time Slices (Nemet *et al*., 2011).

36.6 Results Interpretation

After DE, the correct interpretation of the results is the most important step in PI analysis and optimisation. The results are usually presented in the form of a printout and, in most cases, by a Grid Diagram or Process Flow Diagram supported by tables. Many software tools offer an interface allowing the transfer of extracted data to minimise any misinterpretation.

The assessment of the results and the identification of possible further developments and corrections in the process technology is one of the most difficult aspects, and is dependent on issues of data uncertainty, data 'softness', flexibility, operability, controllability, safety, availability, and maintenance. It is advisable not to rely on one single solution, but to explore different scenarios related to various operating conditions and to test the sensitivity of the design. At this stage, a well-developed and graphically-supported user interface, even one based on interactive graphics, can prove very helpful.

36.7 Conclusion: Making It Happen

Even when a sustainable design has been drawn up with optimised parameters, it still has to be put into practice. This involves selling projects that may be considered unconventional by investors and contractors. This was a problem in the early stages of the development of the PI methodology; however, PI, and particularly HI, has since been proven to be a very powerful and efficient tool: it has gained in popularity, and decision makers have become more receptive to its implementation. Some of the pioneers of this research were the members of the 'PI Research Consortium' at UMIST, later The . In thfiš century the rapfid developmentš
in PI have spread to other areas of the world; alongside the traditional areas of Europe and America, Asia, and particularly South East Asian countries such as Malaysia, China, India, and the Philippines, are becoming major players in the field: see, for example, Wan Alwi *et al*. (2011) on Simultaneous

© Woodhead Publishing Limited, 2013

Energy and Water Minimisation; Wan Alwi and Manan (2010) on simultaneous targeting and design; Saw *et al*. (2011) on property-based resource conservation networks; Liew *et al*. (2012) on Total Site Sensitivity Analysis; and Wan Alwi (2012) on PI targeting method for hybrid power systems.

However, the close, smooth and continuous joint effort, and collaboration amongst the PI specialists, plant designers, plant management, and the owners/contractors is still a major issue. Without their help and full support none of the industrial implementation could be archived.

36.8 Sources of Further Information

Sources of further information have been provided in each chapter, covering the specific topic or group of topics addressed there. The introductory chapter lists the works covering the general aspects of PI, which fall into three categories: (i) textbooks, handbooks, and books providing a general overview, (ii) review papers, and (iii) websites.

A number of books have been published on the subject, all listed in Chapter 1, and some also in chapters dealing with specific topics. Most are of very high quality and are written by experts in the field who have either made a considerable contribution to the development of the methodology and/or possess long term experience and unique skills in the area. It should be noted, however, that the references listed naturally cover only the period up to the writing of the chapter in question; information on the newest developments can be found in the most recently published sources.

36.9 Acknowledgements

This handbook was developed thanks to the team at Woodhead Publishing Limited led by Mr Ian Borthwick and then Mrs Sarah Hughes. The handbook editor would like to express his thanks and enormous appreciation on behalf of all the contributors. Warm thanks and appreciation are also due to all the authors of the chapters, every one of whom have managed to find time in their extremely busy schedules to deliver very high quality and dedicated contributions. The editor is very happy that almost all of the authors who were invited to contribute were able to accept the invitation and complete their manuscripts.

Financial support from various EC co-financed projects has made editing this book possible. There is not sufficient space here to list all the EC, NATO, and national projects that have contributed to the development of PI from early 1990s onwards; however, the editor should mention the most recent projects, principally INTHEAT – Intensified Heat Transfer Technologies for Enhanced Heat Recovery, under Grant Agreement EC FP7 262205,

© Woodhead Publishing Limited, 2013

and EFENIS – Efficient Energy Integrated Solutions for Manufacturing Industries, under Grant Agreement ENER/FP7/296003/EFENIS – these and all others are gratefully acknowledged.

The Hungarian projects Társadalmi Megújulás Operatív Program (TÁMOP) 'Tudományos képzés műhelyeinek támogatása' TÁMOP-4.2.2/B-10/1–2010–0025 and TAMOP-4.2.2.A-11/1/ KONV-2012–0072 – 'Design and optimisation of modernisation and efficient operation of energy supply and utilisation systems using renewable energy sources and ICTs' have also been of great help in putting together this work; their contribution is much appreciated.

36.10 References

Al-Riyami, B.A., Klemeš, J., Perry, S. (2001). Heat integration retrofit analysis of a heat exchanger network of a fluid catalytic cracking plant. *Applied Thermal Engineering*, **21**, 1449–1487.

ASPEN ENERGY ANALYZER (2012). <www.aspentech.com/products/aspen-hx-net.aspx> (accessed 13 November 2012).

Aspen HYSYS®, V7.3. (2012). Conceptual design and performance improvement of processes <www.aspentech.com/hysys> (accessed 03/12/2012).

Aspen Plus®, V7.3.2. (2012). Conceptual design of chemical processes <aspentech.com/core/aspen-plus.aspx.com/core/aspen-plus.aspx> (accessed 03/12/2012).

Bandyopadhyay, S., Varghese, J., Bansal, V. (2010). Targeting for cogeneration potential through total site integration. *Applied Thermal Engineering*, **30**(1), 6–14.

BELSIM. (2003). *VALI III User Guide, 2003*. Belsim S.A., Liege, Belgium.

CADDET Centre for the Analysis and Dissemination of Demonstrated Energy Technologies. (1994). Integrated Heat Recovery in a Malt Whisky Distillery. Project No. UK-94–509.

CAPE. (2013). Working Party of Computer Aided Process Engineering of the European Federation of Chemical Engineering <www.cape-wp.eu> (accessed 10/02/2013).

CPI [Centre for Process Integration]. (2004). Heat integration and energy systems. MSc Course, UMIST, Manchester, UK.

DETR – Department of the Environment, Transport and the Regions. (1997). Van den Bergh Oils Ltd, Purfllet: The use of Pinch Analysis in a Food Processing Factory. Good Practice Case Study 355, 8 ps.

DETR – Department of the Environment, Transport and the Regions. (1996). David Reay & Associates and Osprey Environmental Technologies Ltd. Waste Heat Recovery in the Process Industry. 61 ps.

El-Halwagi, M. M. (2006). *Process Integration*. Academic Press, Amsterdam, The Netherlands.

El-Halwagi, M. M., Gabriel, F., Harell, D. (2003). Rigorous graphical targeting for resource conservation via material recycle/reuse networks. *Industrial and Engineering Chemistry Research*, **42**(19), 4319–4328.

El-Halwagi, M. M., Manousiouthakis, V. (1989). Synthesis of mass exchange networks. *AIChE Journal*, **35**(8), 1233–1244. ESCAPE 23, 23rd European Symposium on Computer Aided Process Engineering<escape23.fi> (accessed 15/04/2013).

© Woodhead Publishing Limited, 2013

Foo, D. C. Y., Chew, Y. H., Lee, C. T. (2008). Minimum units targeting and network evolution for batch heat exchanger network. *Applied Thermal Engineering*, **28**(16), 2089–2099.

Fritzson, A., Berntsson, T. (2006). Efficient energy use in a slaughter and meat processing plant – opportunities for process integration. *Journal of Food Engineering*, **76**(4), 594–604.

GOOGLE SCHOLAR. <scholar.google.co.uk> (accessed 2/12/2012).

Grabowski, M., Klemeš, J., Urbaniec, K., Vaccari, G., Wernik, J. (2002). Energy and water use in a sugar manufacturing process based on cooling crystallization of concentrated raw juice. (Energie- und Wasserbedarf bei der Zuckererzeugung mittels Kühlungskristallisation von eingedidicktem Rohsaft). *Zukerindisurie*, **127**(8), 604–609.

Grabowski, M., Klemeš, J., Urbaniec, K., Vaccari, G., Zhu, X. X. (2001). Minimum energy consumption in sugar production by cooling crystallisation of concentrated raw juice. *Applied Thermal Engineering*, **21**, 1319–1329.

Gundersen, T. (2000). A process integration primer – implementing agreement on process integration. International Energy Agency, SINTEF Energy Research, Trondheim, Norway.

Herrera, A., Islas, J., Arriola, A. (2003). Pinch technology application in a hospital. *Applied Thermal Engineering*, **23**, 127–139.

Hufendiek, K., Klemeš, J. (1997). Integration a brewery by pinch analysis. *Gospodarka Paliwami i Energią*, **45**(9), 22–25 *(in Polish)*.

International Process Integration Jubilee Conference. (2013). <www.chalmers.se/en/areas-of-advance/energy/Pages/default.aspx> (accessed 1/01/2013).

KBC Advanced Technologies. (2012). <www.kbcat.com/Consultancy-Solutions/Energy-Services/Pinch-Analysis> (accessed 17/11/2012).

KBC Energy Services. (2012). Pinch technology Introduction <www.kbcat.com/default/Documents/PinchIntro.pdf> (accessed 17/11/2012).

Kemp, I. C. (2007) (authors of the first edition Linnhoff, B., Townsend, D. W., Boland, D., Hewitt, G. F., Thomas, B. E. A., Guy, A. R., Marsland, R.). *Pinch Analysis and Process Integration. A User Guide on Process Integration for Efficient Use of Energy*. Elsevier, Amsterdam, The Netherlands.

Kemp, I. C., Deakin, A. W. (1989). The cascade analysis for energy and process integration of batch processes. *Chemical Engineering Research and Design*, **67**, 495–509.

Klemeš, J., Friedler, F., Bulatov, I., Varbanov, P. (2010). *Sustainability in the Process Industry: Integration and Optimization*. McGraw-Hill, New York, USA.

Klemeš, J., Kimenov, G., Nenov, N. (1998). Application of pinch-technology in food industry. CHISA'98 / 1st Conference PRES'98, Prague, Lecture F6.6 [136].

Klemeš, J., Lu□cha, J., Vašek, V. (1979). Resent extension and development of design integrated system DIS. *Computers & Chemical Engineering*, **3**(4), 357–361.

Klemeš, J., Smith, R., Kim, J.-K. (eds) (2008). *Handbook of Water and Energy Management in Food Processing*. Woodhead, Cambridge, UK.

Klemeš, J., Urbaniec, K., Zalewski, P. (1999). Retrofit design for polish sugar factories using process integration methods. PRES'99 Proceedings, Friedler, F., Klemeš, J. (eds), Hungarian Chemical Society, Budapest, 377–382.

Klemeš, J., Varbanov, P. S. (2011). Heat integration – history, recent developments and achievements. Fourth International Conference on Modeling, Simulation

© Woodhead Publishing Limited, 2013

and Applied Optimization, ICMSAO 2011, art. no. 5775642, <www.scopus.com/inward/record.url?eid=2-s2.0–79959665105&partnerID=40&md5=8c65ab8e76d06215a5db98722bb88b83>, (accessed 3/12/2012).

Klemeš, J., Varbanov, V. (2010). Process integration – successful implementation and possible pitfalls. *Chemical Engineering Transactions*, **21**, 1369–1374, DOI: 10.3303/CET1021229.

Liew, P. Y., Wan Alwi, S. R., Varbanov, P. S., Manan, Z. A., Klemeš, J. J. (2012). A numerical technique for total site sensitivity analysis. *Applied Thermal Engineering*, **40**, 397–408.

Linnhoff, B., Akinradewo, C. G. (1998). Automated interface between simulation and integration. CHISA 1998/1st Conference PRES 1998, Plenary lecture A3.0 [818].

Linnhoff, B., Flower, J.R., 1978, Synthesis of heat exchanger networks: I. Systematic generation of energy optimal networks. *AIChE Journal*, 24(4), 633–642.

Linnhoff, B., Hindmarsh, E. (1983). The pinch design method for heat exchanger networks. *Chemical Engineering Science*, **38**(5), 745–763.

Linnhoff, B., Townsend, D. W., Boland, D., Hewitt, G. F., Thomas, B. E. A., Guy, A. R., Marsland, R. H. (1982 [revised edition published in 1994]). *A User Guide on Process Integration for the Efficient Use of Energy*. IChemE, Rugby, UK.

Linnhoff March – KBC Advanced Technologies. (2002). <www.kbcat.com/default/documents/industry%20releases/linnhoff.pdf> (accessed 17/11/2012).

Manan, Z. A., Tea, S. Y., Alwi, S. R. W. (2009). A new technique for simultaneous water and energy minimisation in process plant. *Chemical Engineering Research and Design*, **87**(11), 1509–1519.

Matsuda, K., Kawazuishi, K., Hirochi, Y., Sato, R., Kansha, Y., Fushimi, C., Shikatani, Y., Kunikiyo, H., Tsutsumi, A., (2010). Advanced energy saving in the reaction section of the hydro-desulfurization process with self-heat recuperation technology. *Applied Thermal Engineering*, **30**(16), 2300–2305.

Nemet, A., Klemeš, J. J., Varbanov, P. S., 2011. Methodology for maximising the use of renewables with variable availability. *Computer Aided Chemical Engineering*, **29**(B), 1944–1948.

Perry, S., Klemeš, J., Bulatov, I. (2008). Integrating waste and renewable energy to reduce the carbon footprint of locally integrated energy sectors. *Energy*, **33**(10), 1489–1497.

PRES. (2012). International Conference on 'Process Integration, Modelling and Optimisation for Energy Savings and Pollution Reduction', 2012, <www.conferencepres.com> (accessed 3/12/2012).

PRES'13. (2013). 16th International Conference on 'Process Integration, Modelling and Optimisation for Energy Savings and Pollution Reduction', 2013, <pres13.cperi.certh.gr/index.php/en> (accessed 1/01/2013).

PSE 2012. (2012). 11th International Symposium on Process Systems Engineering, Singapore <www.pse2012.sg> (accessed 10 November 2012).

PSE ASIA 2013. (2013). Kuala Lumpur, Malaysia <www.cheme.utm.my/pseasia2013/> (accessed 1/01/2013).

Raghu Ram, J., Banerjee, R. (2003). Energy and cogeneration targeting for a sugar factory. *Applied Thermal Engineering*, **23**(12), 1567–1575.

Ruohonen, P., Ahtila, P. (2010). Analysis of a mechanical pulp and paper mill using advanced composite curves. *Applied Thermal Engineering*, **30**(6–7), 649–657.

© Woodhead Publishing Limited, 2013

Sargent, R. W. H. (1979). Flowsheeting. *Computers & Chemical Engineering*, **3**(1–4), 17–20.

Saw, S. Y., Lee, L., Lim, M. H., Foo, D. C. Y., Chew, I. M. L., Tan, R. R., Klemeš, J. J. (2011). An extended graphical targeting technique for direct reuse/recycle in concentration and property-based resource conservation networks. *Clean Technologies and Environmental Policy*, **13**(2), 347–357.

SDEWES – Eight Conferences on Sustainable Development of Energy, Water and Environment Systems. (2013). <www.dubrovnik2013.sdewes.org> (accessed 1 January 2013).

SCOPUS – Abstract and Citation Data Base of Peer – Reviewed Literature. (2012). Elsevier <www.scopus.com> (accessed 2 December 2012).

Seikova, I., Varbanov, P., Ivanova, E. (1999). Debottlenecking of a heat-integrated crude oil distillation system. In: Friedler, F., Klemeš, J. (eds). *Proceedings of PRES'99*. Hungarian Chemical Society, Budapest, pp. 583–588.

Shenoy, U. (1995). *Heat Exchanger Network Synthesis: Process Optimization by Energy and Resource Analysis*. Gulf Professional, Houston, TX, USA.

Smith, R. (2005). *Chemical Process Design and Integration*. Wiley, Chichester, UK.

Smith, R., Linnhoff, B. (1988). The design of separators in the context of overall processes. *Chemical Engineering Research and Design*, **66**(3), 195–228.

Soh, G. K., Wan Alwi, S. R., Manan, Z. A. (2011). A new graphical approach for simultaneous targeting and design of paper recycling network. Special Issue: *Resource Conservation, Asia Pacific Chemical Engineering Journal (APJ)*, **6**(5), 778–786.

STAR. (2012). Process integration software (Centre for Process Integration, School of Chemfical Engfineerfing and Analytfical Scfience, The , U.K.). <www.ceas.manchester.ac.uk/research/centres/centreforprocessintegration/software/packages/star> (accessed 18 November 2012)].

SuperTarget™. (2012). KBC energy and utilities software to optimise heat integration <www.kbcat.com/default/petrosim/2012%20Brochures/SuperTarget_web.pdf> (accessed 13 November 2012).

Taal, M., Bulatov, I., Klemeš, J., Stehlík, P. (2003). Cost estimation and energy price forecast for economic evaluation of retrofit projects. *Applied Thermal Engineering*, **23**, 1819–1835.

Thompson Reuters ISI, Web of Knowledge and Web of Science. (2012). <www.isiknowledge.com> (accessed 2 December 2012).

Tovazhnyansky, L., Kapustenko, P., Ulyev, L., Boldyryev, S., Arsenyeva, O. (2010). Process integration of sodium hypophosphite production. *Applied Thermal Engineering*, **30**(16), 2306–2314.

Varbanov, P., Perry, S., Klemeš, J., Smith, R. (2005). Synthesis of industrial utility systems: cost-effective de-carbonisation. *Applied Thermal Engineering*, **25**(7), 985–1001.

Varbanov, P. S., Klemeš, J. J. (2010). Total sites integrating renewables with extended heat transfer and recovery. *Heat Transfer Engineering*, **31**(9), 733–741.

Varbanov, P. S., Klemeš, J. J. (2011). Integration and management of renewables into Total Sites with variable supply and demand. *Computers and Chemical Engineering*, **35**(9), 1815–1826.

Wan Alwi, S. R., Ismail, A., Manan, Z. A., Bahiyah, Z. A. (2011). New graphical approach for simultaneous mass and energy minimisation. *Applied Thermal Engineering Journal*, **31**(6–7), 1021–1030.

© Woodhead Publishing Limited, 2013

Wan Alwi, S. R., Manan, Z. A. (2010). STEP – a new graphical tool for simultaneous targeting and design of heat exchanger network. *Chemical Engineering Journal*, **162**, 106–121.

Wan Alwi, S. R., Mohammad Rozali, N. E., Manan, Z. A., Klemeš, J. J. (2012). A process integration targeting method for hybrid power systems. *Energy*, **44**(1), 6–10.

Wang, Y. P., Smith, R. (1994). Wastewater minimisation. *Chemical Engineering Science*, **49**(7), 981–1006.

Yee, T. F., Grossmann, I. E. (1990). Simultaneous optimization models for heat integration – II. Heat exchanger network synthesis. *Computers and Chemical Engineering*, **14**(10), 1165–1184.

© Woodhead Publishing Limited, 2013

Index

Above the Pinch, 32–3
  positions relative to the heat recovery Pinch, 33
absorption heat pumps (AHP), 88
absorption units, 193–6
  principles of Heat Integration of absorption machines, 196
  single-effect absorption heat pumps configurations, 194
Acid Dew Point, 878
acid gas removal systems
  retrofit Mass Integration in petrochemical plants, 725–51
    hybrid approach, 741–4
    Mass Exchanger Network Synthesis (MENS), 727–34
    Pinch approach, 736–40
    solution equilibria, 744–6
    Venturi scrubber and ethanolamine absorber system, 734–6
Active Learning in Chemical Engineering (ALChemE), 1086
Actual Cooling Load Curve (ACLC), 784, 785
Actual Heat Load Curve (AHLC), 784, 785
Advanced Composite Curves (ACC), 783–6
  identifying HEN retrofit, 785–6
    ACCs, 787
    heater removal, 786
    release heater modification placed high in temperature, 786
    release heater modification placed low in temperature, 785
Agricultural-Land Footprint
  energy planning, 513–15
    EPCC solution, 514
    optimal energy allocation, 515
    source and sink data, 514
algebraic targeting approach, 362
ammonia, 914–5
  feed stream, 931–2
    reduction of cooling load, 932
annualisation factor, 33
ant colony, 104
appropriate placement, 33–4, 131–2
  placement of a steam turbine, 34
area efficiency, 34, 286
Aspen Energy Analyzer, 1059–60
Aspen HYSYS, 1059, 1108
Aspen Plus, 1059, 1108
aspenONE, 1059
atmospheric distillation unit (ADU), 542
attainable region (AR), 111
automated network design, 34, 301–3
  sequential frameworks for HEN synthesis, 303
Automated Targeting Model (ATM), 450
average aggregate inventory value, 573

backpressure turbine, 810
Balanced Composite Curves (BCC), 35, 267–8
batch formula, 35–6
batch operation, 866–7
batch processes, 35
  Heat Integration, 310–46
    graphical technique, 313–24
    industrial case study, 339–46
    mathematical technique, 324–35
    multipurpose batch facility, 335–9
Bath formula, 269
beet sugar plants
  energy and water use, 898–909

© Woodhead Publishing Limited, 2013

beet sugar plants (*cont.*)
energy use, 900–4
example of structural constraints and data on water-using operations, 908
operating parameters of water and wastewater system, 908
optimum water flowrates, 909
overview, 899–900
simplified flowsheet, 900
water use, 904–9
opportunities to improve energy and water use, 885–7
scheme of material and energy flows, 886
subsystems of water and wastewater system, 887
Process Integration, 883–912
sugar production from sugar beets, 884–5
raw material and products, 884
Bell-Delaware method, 966, 967, 978
Below the Pinch, 36
benchmarking, 779–80
binary variables, 327
bioethanol, 909
biofuel, 4
biological oxygen demand (BOD), 387
biomass, 957–8
biomass network
Regional Energy Surplus–Deficit Curves (RESDC), 578–81
schematic diagram, 581
bioprocesses
integration in pulp and paper mills, 793–4
black liquor
combustion in the recovery boiler, 772
heat balance, 773
evaporation, 769, 778
Blade Element Momentum (BEM) methodology, 1051
bleached-stock cleaning, 769
bleaching, 778
boiler feed water (BFW), 802
boiler systems, 1077
boiling, 822–3
bottle cleaning, 836
bottling, 823
brewing industry
batch processes timeline (cold and cleaning part), 862
batch processes timeline (hot part), 862
brewery process block flow diagram, 822
brewing operation data, 862
calculating maximum heat recovery, 837–9
ΔT_{min} /2 for streams, 862
energy conversion system, 839–58
industrial production system, 821
list of streams for Heat Exchanger Network Design, 859–60
operating condition boiler, 861
process flowsheet analysis, 823–36
Process Integration application, 820–63
specific heat capacity of material streams, 861
brown-stock washing, 777
buildings and building complexes
commercial, public buildings and building complexes, 942–7
example of electric power and natural gas hourly profiles, 943, 944
consumers and producers of energy, 939–42
classification of buildings by their purpose, 940
Process Integration for energy saving, 938–61

capital cost, 36
capital recovery factor (CRF), 1047
carbon dioxide, 916
feed stream, 930–1
heat recovery option for CO_2 preheating, 931
carbon emission networks (CEN)
energy planning, 556–8
data, 557
Limiting Composite Curve (LCC), 558
Unified Targeting Algorithm (UTA), 558

© Woodhead Publishing Limited, 2013

carbon emissions Pinch diagram, 510
Carbon Footprint (CFP), 43–4
Cascade analysis, 945
cash flow, 574
causticising, 770
CDU-int, 1060–1
  functionalities, 1061
centrifuge, 836
Chart method, 967
cheese production
  future trends, 879
  integration of heat pumps, 874–6
    Composite Curves, 875
    Stream Data Composite Curves, 876
  Process Integration applications, 864–79
  Process Integration methodologies, 866–73
    evaporators and heat pump integration, 869–71
    heat exchange constraints, 871–2
    Mass Integration and water minimisation, 872–3
    multi-effect evaporator with two MVR and one TVR effects, 870
    non-/semi-continuous and batch operation, 866–7
    simplified schematic of a dairy factory, 868
    zone targeting and integration, 867–9
chemical oxygen demand (COD), 387, 895
chillage, 823
circulated energy, 810
cleaning in place (CIP), 836, 867
closed-cycle compression machines, 191–2
  integration of compression heat pumps, 192
co-current flow system, 737–9
  construction Operating Lines, 738
  with fixed minimum composition difference, 738
coefficient of performance (COP), 38
  heat pump configuration, 39
cogeneration
  Process Integration techniques, 484–500
    Combined and Heat Power (CHP), 485–8
cogeneration engine, 842
  cogeneration unit based on the bio-methane produced on process husk, 845
  cogeneration unit characteristics based on GE-Jenbacher data, 845
cogeneration system, 924, 926–7
  actual operating condition and power production, 927
  design condition of steam turbine, 926
  modified operating conditions of steam turbine, 927
coiled-wire inserts, 984–5
  laminar flow, 984–5
  turbulent flow, 985
coke dry quench (CDQ) unit, 758
coke oven gas (COG) sweetening, 546–8
  data for MEN problem, 547
  GCC for MEN, 548
  UTA for MEN, 547
Colburn correlation, 967
Cold Composite Curve, 643, 648
cold process stream, 135
cold stream, 36, 278, 643–4, 831
Cold Utility Curve (CUC), 784
column, 1079
Column Grand Composite Curve (CGCC), 36–7
combined cross flow system, 737–9
  construction Operating Lines, 738
Combined Energy and Water Integration
  overview, 461–3
    schematic diagram, 462
  Process Integration, 461–80
  sequential, simultaneous, mathematical programming, 476–8
  state of the art methodology, 468–76
    Composite Curves with separate system for WEN, 470
    schematic diagram, 472
    single contaminant water-using system data, 470

© Woodhead Publishing Limited, 2013

Combined Energy and Water Integration (*cont.*)
Superimposed Mass-and-Energy Curves, 471
temperature *vs.* concentration diagram, 471
temperature *vs*. water type usage, 469
water path concept, 466–8
water-energy specifics and challenges, 463–6
energy-water system interactions, 466
water interactions within the layers of the Onion Diagram, 464
WEN – general problem, 465
Combined Heat and Power (CHP), 3, 36, 92–3, 485–8, 543, 800
advanced energy conversion cycles, 176–81
energy flows for heat machines, 178
optimum thermodynamic integration of a heat engine, 178
optimum thermodynamic integration of a heat pump, 179
principle of refrigeration, 180
benefits against conventional system, 486
heat/power needs of an existing specialty chemical batch plant, 487
Process Integration application to the synthesis of heat and power utility system, 168–98
Process Integration of heat engines, 181–90
total energy costs, 488
utility loads and temperature levels, 169–76
basic concepts, 170–1
district heating network delivery of excess process heat, 174–6
Heat Integration of a district heating system, 176
hot oil utility systems, 173–4
steam utility systems, 171–3
commercial/public buildings, 942–7
building complex case study, 946–7
hot utility requirement, 946
options of energy retrofit, 947
utility requirement after rescheduling of incinerator operations, 947
Composite Curve, 8, 37, 130, 140–1, 597, 813, 945, 950, 959
schematic diagram, 141
Composite Table Algorithm (CTA), 524–5, 563–4
vs. Unified Targeting Algorithm (UTA), 540–1
calculation of net flow, 541
composition interval diagrams, 1089
composition interval table (CIT), 524
concentration difference, 37–8
concentration of contaminant, 37
concentration *vs*. mass load diagram (CMD), 406, 408
conceptual design, 80
Conference on Process Integration, Modelling and Optimisation for Energy Saving and Pollution Reduction, 1100
Conference on Sustainable Development of Energy, Water and Environment Systems, 1100
contaminant mass flow, 38
continuous variables, 326
controllability indices-based anticipating sequential method, 106–7
cooking, 777
cooling, 823
cooling circuit, 886
cooling duty, 38
cooling system, 38
cooling water networks
retrofit, 394–5
targeting of cooling water flowrate, 396
cooling water system, 386
design for energy and water conservation in oil industry, 675–80
cold process stream data, 677
conventional design in typical oil refinery, 676

© Woodhead Publishing Limited, 2013

cooling tower design parameters, 680
cooling water feasible region, 678
design, 678–9
design parameters, 677
economic comparison of conventional method, 680
hot process stream data, 677
optimum design configuration, 680
performance parameters of water supply, 679
process description, 675–6
project objectives, 676–7
results, 679–80
targeting, 677–8
targeting the water supply condition, 679
Cost Effective Minimum Water Network (CEMWN), 368
cost of energy (COE), 1047
cost of goods sold, 574
CP tables, 38
Cross-Pinch heat transfer
Cross-Pinch heat exchanger, 39
crude distillation unit (CDU), 634–5
crude oil distillation, 1060–1
crude preheat trains, 157
cryogenic processes, 40
CRYO-int, 1062
Cumulative Demand Curve
Regional Energy Supply-Deficit Curves, 40
Cumulative Supply Curve, 40

dairy production
future trends, 879
integration of different diary processes, 873–4
milk-powder plant, 876–9
Process Integration applications, 864–79
Process Integration methodologies, 866–73
evaporators and heat pump integration, 869–71
heat exchange constraints, 871–2
Mass Integration and water minimisation, 872–3
multi-effect evaporator with two MVR and one TVR effects, 870
non-/semi-continuous and batch operation, 866–7
simplified schematic of a dairy factory, 868
zone targeting and integration, 867–9
Danish Environmental Protection Agency, 940
data extraction, 32, 40, 133, 134–8, 361
challenges, 136–8
data required for Heat Integration, 134–5
Process Integration, 1104, 1106–9
capital and running cost data, 1109
Cp changes and latent heat, 1107
data handling in flowsheet/plant, 1109
data precision, 1107
extraction of heat loads, capacities and temperatures, 1108
rules, 1107–8
stream, 1104, 1106
Total Site, 203–11
combined heat sink information or Site Sink Profile, 211
combined heat source information or Site Source Profile, 210
Grand Composite Curve for process A, 204
Grand Composite Curve for process A with stream segments, 207
Grand Composite Curve for process B, 205
Grand Composite Curve for process B with stream segments, 209
Grand Composite Curve with HP steam generation, 206
Problem Table for process A, 204
Problem Table for process B, 205
stream segment data extracted from process A, 208
stream segment data extracted from process B, 209
Total Site Profiles, 211

© Woodhead Publishing Limited, 2013

debottlenecking, 64, 84, 85, 264, 575
effluent thermal-treatment system in petrochemical plant, 693–9
base case of effluent thermal-treatment network, 695
construction of the Effluent Profile Composite Curve, 696
design, 697–8
economic comparison of the base case and proposed strategy, 699
Effluent Composite Curve modification, 698
effluent stream data, 694
feasible region for Feasible Water Supply Line, 696
final design of effluent cooling system, 699
new Pinch Point of Target Water Supply Line, 697
overall solution strategy flow chart, 695
performance conditions of effluent cooling system, 694
process description, 693–4
project objectives, 694
results, 698
targeted water supply of cooling tower, 699
targeting, 694–6
targeting cooling tower inlet supply condition, 697
DeNOx/DeDiox technology, 807
design evolution, 133–4, 159–65
design space, 1046–8
deterministic approach, 1049
Developed Delaware method, 967
dilution, 823
direct recycle, 431–3
direct reuse/outsourcing, 354
direct reuse/recycle, 444
disjunctive-genetic programming, 103
distillation columns, 1063
DIST-int, 1063–4
distributed cooling systems
design for effluent thermal treatment in oil industry, 687–93
cooling tower design parameters for conventional and ODEC design, 693
cost of conventional *vs.* ODEC design, 693
design, 689–90
effluent cooling systems, 688
Effluent Profile Composite Curve construction, 689
effluent stream data, 688
feasible boundaries, 689
feasible boundary water supply conditions, 691
Migrated Pinch Point, 690
optimum cooling tower design flowchart, 691
optimum effluent network of the ODEC, 691
overall cost, 692
process description, 687–8
project objectives, 688
results, 690–3
targeting, 688-9
water conservation opportunity with the ODEC, 693
water supply conditions with conventional and ODEC design, 692
distributed effluent treatment systems, 391–2
Effluent Composite Curve, 392
schematic diagram, 393
District Energy (DE) systems, 948–9
Heat Integration, 949–51
District Heating (DH), 948
Dittus-Boelter correlation, 967, 969
driving force (DF), 111
Driving Force Plot (DFP), 273–5, 641, 642
incomplete HEN, 274
dump load, 1040

EC Directive 2010/31/EU, 941, 956
effective temperature extraction, 1108
effluent, 687–99
Effluent Composite Curve, 41
effluent thermal treatment
debottlenecking in petrochemical plant, 693–9
distributed cooling systems in oil industry, 687–93

© Woodhead Publishing Limited, 2013

effluent treatment networks, 1094
electricity generation conversion factor, 807
electricity generation efficiency, 811
electricity grid, 41
emergy
  energy planning, 515–17
    EPCC solution, 517
    optimal energy allocation, 517
    source and sink data, 517
emission targeting, 43
emissions, 1077
end time, 42
energy bill
  current utility requirements with no heat recovery, 830
  schematic diagram, 830
energy-capital trade-off, 42
'Energy City' project, 956
Energy Composite Curves, 473
energy consumption, 4–6
  reduction, 887–93
    case study, 890–3
    energy targeting and retrofit design, 888–90
    expected results of sugar factory retrofit, 893
    Grid Diagram of retrofitted HEN, 893
    problem statement, 888
energy conversion system, 839–58
  boiler + refrigeration, 852–3
    Integrated Composite Curves of energy conversion system for scenario A, 852
    Integrated Composite Curves of energy conversion system for scenario B, 853
  cogeneration, refrigeration and Mechanical Vapour Recompression, 856–8
    Integrated Composite Curves of energy conversion system for scenario H, 857
    Integrated Composite Curves of energy conversion system for scenario I, 858
  cogeneration and refrigeration, 855–6
    Integrated Composite Curves of energy conversion system for scenario F, 856
    Integrated Composite Curves of energy conversion system for scenario G, 856
  comparison, 850–2
    data for investment estimation, 852
    energy consumption of solutions, 851
    power of the energy conversion system, 850
    total cost calculation of with investment, 851
  condensing boiler, refrigeration and Mechanical Vapour Recompression, 853–5
    Integrated Composite Curves of energy conversion system for scenario E, 855
  condensing boiler + refrigeration, 853
    Integrated Composite Curves of energy conversion system for scenario C, 854
    Integrated Composite Curves of energy conversion system for scenario D, 854
  grand composite analysis, 840–2
  heat pumping, 845–6
  mathematical formulations, 846–58
    Graphical Heat Cascade representation for MILP formula, 848
  technology, 842–5
energy cost, 60
energy crop biomass, 228
energy demand, 4–6
  characteristics, 228–32
    classification of users, 229
    energy system design and operation requirements, 231–2
    residential electricity demands, 230
    variability, 229–30
    variability types, 231
  extended Total Site methodology, 226–56
  Heat Cascades, 239–49
  process streams and utilities, 235–6

© Woodhead Publishing Limited, 2013

energy demand (*cont.*)
Solar Thermal Energy Integration into LIES, 250–6
thermal energy storage and integrated architecture, 232–5
Time Slices identification, 236–9
energy efficiency
existing mills, 777–83
Heat Integration, 781–3
key points, 777–9
overall methodology, 779–81, 780
Energy Footprint (EFP), 44
Energy Independence and Security Act (2007), 941
Energy Integration, 423
applications in oil refineries and petrochemical complexes, 633–701
effluent treatment and regeneration, 687–99
Heat and Power Integration, 634–67
design of multi-stream heat exchangers in petrochemical industries, 645–52
heat recovery improvement in aniline production unit, 655–62
low-temperature gas separation processes design, 662–7
retrofit of ammonia plant for improving energy efficiency, 652–5
retrofit of crude preheat train in an oil refinery, 634–40
retrofit of heat exchanger network in aromatics plant, 641–6
water and wastewater minimisation, 667–86
Energy Match Diagram (EMD), 470
energy planning
based on Agricultural-Land Footprint, 513–15
EPCC solution, 514
optimal energy allocation, 515
source and sink data, 514
based on emergy, 515–17
EPCC solution, 517
optimal energy allocation, 517
source and sink data, 517
based on inoperability, 517–19
EPCC solution, 518
optimal energy allocation, 519
source and sink data, 518
based on Water Footprint, 515
EPCC solution, 516
optimal energy allocation, 516
source and sink data, 515
carbon emission networks (CEN), 556–8
data, 557
Limiting Composite Curve (LCC), 558
Unified Targeting Algorithm (UTA), 558
energy quality
degradation, 773–4
heat degradation by process, 775
process water consumption reduction, 775
energy recovery, 804
improvement, 928–32
changing operating conditions, 928–30
Composite Curves, 928
energy and capital savings, 933
increasing energy recovery, 930–2
installation of additional heat transfer area, 929
modified Heat Recovery Network, 933
energy relaxation path, 54
energy saving
Process Integration in buildings and building complexes, 938–61
buildings as consumers and producers of energy, 939–42
commercial, public buildings and building complexes, 942–7
District Energy systems and Total Site Analysis, 947–51
renewable energy for buildings, 956–61
use of industrial waste heat, 951–6
energy-saving potential, 756
energy-saving projects
heavy chemical complex, 756–7
achievement of theoretical energy saving, 757
integration across two sites, 756–7

© Woodhead Publishing Limited, 2013

results of energy-saving studies, 756
steel plant, 761
cooler side, 761
heater side, 761
energy supply
characteristics, 228–32
classification of sources, 228
classification of users, 229
energy system design and operation requirements, 231–2
variability from renewable resources, 230–1
extended Total Site methodology, 226–56
Heat Cascades, 239–49
process streams and utilities, 235–6
Solar Thermal Energy Integration into LIES, 250–6
thermal energy storage and integrated architecture, 232–5
Time Slices identification, 236–9
energy targets
minimum temperature approach for heat transfer, 920, 922–3
exchanger localisation, 923
Process Composite Curves, 923
utility exchanger for condensation of surplus steam, 923
energy use, 900–4
comparison of two optimised options of energy system, 905
Composite Curves for alternative process, 904
power station options, 902
thermal scheme, 901
energy utilisation, 804–7
EnergyPLAN model, 956
enthalpy, 42–3
change, 43, 496
difference, 43
eQUEST, 943
essential match, 48
ethanolamine absorber system, 736, 740, 747–8
DEA system configuration, 737
MEA system configuration, 736
optimal system configuration using only MEA, 748
optimisation results, 748
options studied using hybrid approach, 748
European Symposium on Computer Aided Process Engineering (ESCAPE), 1100
evaporator subsystem, 885
options of evaporator structure, 892
schematic diagram, 891
Exchanger Minimum Approach Temperature Difference (EMATD), 784
exergy block diagram (EBD), 1069
Exergy Composite Curves, 43
Exergy Grand Composite Curves, 43
extended Total Site, 53
methodology for varying energy supply and demand, 226–56
characteristics, 228–32
Heat Cascades, 239–49
process streams and utilities, 235–6
Solar Thermal Energy Integration into LIES, 250–6
thermal energy storage and integrated architecture, 232–5
Time Slices identification, 236–9
external fins, 990–3
Extreme Cooling Load Curve (ECLC), 784, 785
Extreme Heat Load Curve (EHLC), 784, 785

Fanning friction factor, 983, 984, 985, 987
fermentation, 823, 836
filtration, 823
fin height, 986
fin pitch, 986
fixed contaminant, 402
fixed contaminant-load, 525, 527–9
fixed flow networks, 525–6, 527–9
fixed flowrate, 402
problem, 355
fixed load problem, 355
flowrate, 43
targeting, 457
flowsheeting, 1100
fluming circuit, 894
fossil fuels, 228

© Woodhead Publishing Limited, 2013

fouling
example, 1020–5
exchanger details of original HEN, 1021–2
exchanger details of retrofitted HEN with maximum retrofit profit, 1023–4
retrofitting HEN with consideration of fouling, 1025
retrofitting HEN without consideration of fouling, 1020–4
heat transfer enhancement in HEN retrofit, 1017–25
deposition with tube inserts, 1017–20
fouling factor, 44
freshwater cost, 60
freshwater sources, 1093
fuzzy optimisation, 104

gas networks, 550–8
gas turbine, 52–3, 901
gas turbine CHP, 183–6
energy consequence for process heating, 186
principles, 184
steam network CHP, combined, 187–8
GT introduction with steam distribution systems, 189
gas turbine-vapour compression systems, 489–94
energy recovery from hot exhaust gases, 489
operation of a gas turbine with an after-burner, 490
operation of a gas turbine with an economiser, 490
performance of three gas turbines at full and part load, 495
performance of various commercial gas turbines, 494
stream data for a gas recompression station, 493
technical specifications of some commercial gas turbines, 494
temperature profiles of different gas turbines, 491
generalised property cascade, 65
Geographical Information System (GIS), 949, 956
geothermal energy, 228
Glover transformation, 331–2
grand composite analysis, 840–2
mechanical power for refrigeration load, 841
new energy bill after recovery, 842
Grand Composite Curve (GCC), 30, 44, 131, 150–3, 168, 170, 316, 537, 544, 949, 1065
background process, 151
background process and distillation column, 152
cogeneration system, 927
construction, 45
construction for batch processes, 317–24
data for literature, 318
demand curve, 323
Q-time diagram for optimum sizing of the accumulator, 321
targeting temperature intervals, 319
targeting the minimum size of boiler capacity and size of accumulator, 324
targeting the optimum accumulator size, 322
targeting using Composite Curves, 319
temperature intervals, 318
utility demand pattern, 322
utility demand pattern in batch facility, 320
utility system for batch facility with accumulator, 320
isolated energy systems, 1043–6
variation of stored energy level, 1044
pocket, 62
Grashof number, 986
grassroots analysis
extended procedures, 264–73
Balanced Composite Curves, 268
heat exchanger details, 271–2
heat transfer area targets, 268–70
multiple utilities and utility Pinches, 264–8

© Woodhead Publishing Limited, 2013

simplified Heat Cascade and GCC, 266
steam contributions to ΔT_{min}, 272–3
stream and utility data, 265
three-way trade-off in heat recovery systems, 268
Total Annual Cost and ΔT_{min}, 270–1
utility selection, 266
grassroots design, 84–90, 132, 137–8
extended procedures, 273–81
Driving Force Plot (DFP), 273–5
Pinch Design Method (PDM) limitations, 279–81
Remaining Problem Analysis (RPA), 276–7
splitting streams, 277–9
extended procedures for grassroots analysis, 264–73
heat recovery systems analysis and design, 262–304
optimisation for heat exchanger network synthesis, 295–303
overview, 262–4
existing facility improvement, 263–4
improved methodologies, 263
greenhouse gas emissions, 939
Grid Diagram, 44–5, 144–6
HENS, 45
schematic diagram, 145
ground cold, 228
ground heat, 228

H2-int, 711, 1087–8
schematic diagram, 711
hard data, 41
heat capacity flowrate, 45, 135
Heat Cascade, 9, 45–6, 65, 131, 141–3
intermittent processes and sites, 244–5
Heat Cascade Cell for Total Site, 245
schematic diagram, 46, 142
Total Site targets evaluation in supply and demands, 239–49
heat storage model for Heat Integration, 245–7
heat storage operating policy and management, 247
non-isothermal heat sources and sinks accounting, 242–3
Total Site Heat Cascade, 248–9
Total Site Heat Cascade for building steam work superstructure, 240
Total Site Profile and cascading of utilities, 240–2
utility prioritisation, 248
variability handling, 244–5
heat engines, 46–7
Process Integration, 181–90
combined gas turbine and steam network CHP, 187–8
gas turbine CHP, 183–6
organic Rankine cycle CHP, 188–90
steam turbine CHP, 181–3
schematic diagram, 47
heat exchange constraints, 871–2
Heat Exchange Match, 48
heat exchanger, 46–7, 143–6, 271–2, 496, 837–9
Integrated Composite Curve of bottle-cleaning section, 839
measured and calculated cooling water mass flow in coolers and condensers, 921
specifications and design data, 920
types and applications, 921
types by flow arrangement, 47
water networks relations, 773–6
degradation of energy quality, 773–4
process water network, 774–6
Heat Exchanger Network (HEN), 7, 47, 89–90, 107, 108, 112, 129–66, 157, 263, 541–8
data for organics distillation problem, 542
design, 48, 607–10
combined HRL system Grid Diagram, 610
three-tank HRL system Grid Diagram, 608
two-tank HRL system Grid Diagram, 609
four-steam, 537–40
data problem, 538
Grand Composite Curve (GCC), 540

© Woodhead Publishing Limited, 2013

Heat Exchanger Network (HEN) (*cont.*)
Unified Targeting Algorithm (UTA), 539
GCC for organics distillation, 544
heat transfer enhancement, 966–1037
fouling considerations, 1017–25
HEN retrofit, 996–1016
shell-and-tube heat exchangers, 966–79
techniques, 979–95
optimisation for synthesis, 295–303
automated network design, 301–3
rigorous targeting methods, 296–301
transformation of MEN problem, 545–6
UTA for organics distillation, 543
Heat Exchanger Network (HEN) retrofit, 783
bridge analysis, 786–9
Kraft pulp mill, 788–9
principles, 786–8
Heat Exchanger Network Synthesis (HENS), 301
heat flow, 48
heat flux, 48
heat generation conversion factor, 807
Heat Integration, 3, 7, 28, 29, 49, 92, 96, 634–67, 781–3, 792–3, 960
application, 811–16
characteristics of cold and hot streams in the MSW incinerator, 812
Composite Curves, 814
lower temperatures of Composite Curves, 814
lowest temperatures of Composite Curves, 815
Problem Table, 813
batch processes, 310–46
data requirement, 134–5
District Energy (DE) systems optimisation, 949–51
Composite Curves of Geneva area, 950
energy savings screening in existing mills, 792–3
graphical technique, 313–24
GCC construction for batch processes, 317–24
GCC for batch processes, 317
heat flow representation and cold stream Composite Curve, 316
hot and cold external utilities targeting, 316
Hot Stream Composite Curve, 315
quantity of heat and representation of heat flow, 315
time as an intrinsic constraint and driving force interpretation, 314
heat savings, 793
concept of Process-Integrated evaporation, 794
heat storage model, 245–7
industrial case study, 339–46
accounted heat losses, 344
flowsheet, 340
heat loss consideration, 344–6
heat losses result, 345
heating/cooling requirements, 342
improvement in energy usage, 343
optimal schedule over shorter time horizon, 345
results, 343
scheduling data, 341
schematic diagram, 342
SSN, 340
state task network, 340
stoichiometric data, 341
temperature variation in heat storage vessel, 344, 346
mathematical technique, 324–35
mathematical model, 325–35
problem statement and objective, 324–5
methodological developments in existing mills, 783–9
multipurpose batch facility, 335–9
software tools, 1059–84
spreadsheet based tool, 1072–3
targets and Heat Exchanger Network Design, 129–66
data extraction, 134–8
design evolution, 159–65
network design, 153–9
performance targets, 138–46
process modifications, 146–53

© Woodhead Publishing Limited, 2013

stages of heat recovery system design, 132–4
trigeneration system, 488–500
gas turbine-vapour compression systems, 489–94
steam turbine-absorption systems, 494–50
Heat Integration analysis
brewery, 1102
pulp and paper industry, 1103
workflow diagram of Process Integration study, 1105
HEAT-int, 1064–6
main functionalities, 1065
heat-integrated process dynamics, 108
heat load, 48
distribution, 301–2
loop, 160
path, 161
heat losses, 246–7, 1108
accounting partially for heat deterioration, 247
heat pumps, 49, 845–6
advanced energy conversion cycles
energy flows for heat machines, 178
optimum thermodynamic integration of a heat engine, 178
optimum thermodynamic integration of a heat pump, 179
principle of refrigeration, 180
Process Integration, 190–6
advanced energy conversion cycles, 176–81
Process Integration application to the synthesis of heat and power utility system, 168–98
Process Integration of heat engines, 181–90
utility loads and temperature levels, 169–76
utility loads and temperature levels
basic concepts, 170–1
district heating network delivery of excess process heat, 174–6
Heat Integration of a district heating system, 176
hot oil utility systems, 173–4
steam utility systems, 171–3
heat recovery, 49
improvement in aniline production unit, 655–62
aniline plant process stream data, 658
aniline production plant, 657
design approach, 657
energy-saving potential, 660
final retrofitted configuration of aniline unit HEN, 662
final retrofitted configuration of nitrobenzene unit HEN, 661
HEN structure representation, 659
overall retrofit procedure, 660
process description, 655–6
project objectives, 657
results, 659–61
unreasonable Heat Exchange Matches of aniline plant, 661
targeting level, 284–8
energy savings *vs.* investment for the retrofit case, 287
energy-target plot for the retrofit case, 285
heat recovery loops (HRL)
application to semicontinuous plants, 600–12
Heat Exchanger Network Design, 607–10
sizing the heat storage tanks, 610–11
targeting for multi-plant sites, 601–7
variable-temperature heat storage system, 612
application to semicontinuous processes for Process Integration, 594–626
complex sample, 613–17
CC for streams with Storage Pinch, 616
CCs of streams left over after intra-plant integration, 614
maximum savings of steam candidates, 615
network for vertical integration, 619
options generated from removing the stream causing a Storage Pinch, 617

© Woodhead Publishing Limited, 2013

heat recovery loops (HRL) (*cont.*)
semi-continuous multi-plant integration method, 613
stream data after preliminary screening, 615
two-rank HRP options, 618
future trends, 626
indirect heat recovery systems, 595–600
semi-continuous multi-plant dairy factory, 618, 620–6
Heat Recovery Minimum Approach Temperature Difference (HRATD), 784
Heat Recovery Network, 924
structure of existing plant, 925
Heat Recovery Pinch, 33, 60–1, 130
heat recovery potential, 837–9
Integrated Composite Curve of bottle-cleaning section, 839
Heat Recovery Steam Generator (HRSG), 387, 802
heat recovery system, 807–11
design stages, 132–4
grassroots and retrofit design, 262–304
extended procedures for grassroots analysis, 264–73
extended procedures for grassroots design, 273–81
optimisation or heat exchanger network synthesis, 295–303
overview, 262–4
retrofit analysis and design, 281–95
three-way trade-off, 268
heat sink, 49–50, 66
schematic diagram, 50
Heat Sink Profile, 50, 235
heat source, 50, 330
heat storage, 51, 329–32, 333–4, 960
model for Heat Integration, 245–7
operating policy and management, 247
heat storage tanks (HST), 595–6
selection, 598–9
sizing, 610–11
cost optimisation, 611
modelling with oil as the intermediate fluid, 611
heat surplus diagram, 469–70
heat-transfer, 830–3
heat transfer area, 51, 268–70
target, 51
heat transfer coefficient, 51, 967, 976, 978, 984, 986, 988–9, 992, 999, 1001, 1004
shell-side, 971–3
tube-side, 969–70
heat transfer enhancement, 51–2
fouling considerations, 1017–25
example, 1020–5
fouling deposition with tube inserts, 1017–20
heat exchanger networks, 966–1037
shell-and-tube heat exchangers, 966–79
HEN retrofit, 996–1016
details of optimal retrofitted HEN, 1015–6
enhancement level and capital cost, 1014
example, 1008–16
exchanger details of original HEN, 1012–3
exchanger network of existing preheat train for a crude-oil distillation, 1010
mathematical optimisation method, 999–1008
sensitivity tables for network response, 996–9
stream details in the HEN, 1011
techniques, 979–95
capital costs of exchanger design techniques, 994
comparison of different exchanger design, 995
example, 993–7
shell-side enchancement techniques, 988–93
tube-side enchancement techniques, 981–8
heating duty, 52
heating load, 52
heavy chemical complex

© Woodhead Publishing Limited, 2013

case study, 753–7
energy-saving projects, 756–7
R-curve analysis, 753–4
results, 754–6
study basis, 753
Total Site Profile (TSP) analysis, 753
helical baffles, 988–90
values for different baffle arrangement, 990
helix angle, 986
HEXTRAN, 978–9, 1066–7
hierarchical approach, 82–4
layers interaction, 84
Hot Composite Curve, 643, 648
hot oil circuit, 52
hot oil utility systems, 173–4
assessment of the hot oil temperatures, 175
hot process stream, 135
hot stream, 52, 278, 643–4, 831
Hot Utility Curve (HUC), 784
hot utility system, 827
HPS Gen, 759–60
HTRI, 967, 972, 978–9
hybrid analysis, 741–4
rationale, 741–2
approach, 742
mathematical programming approach, 742
mathematical programming approach strengths and weaknesses, 742
Pinch Technology advantages and disadvantages, 741
Pinch Technology approach, 741
steps, 742–4
philosophy of the hybrid synthesis met, 743
hydrogen, 30, 705
Composite Curve to hydrogen surplus diagram, 708
Composite Curves, 707
Pinch spreadsheet, 1088
Hydrogen Network Design Tool (HyNDT), 1089
hydrogen networks, 550–8
Hydrogen Pinch, 29, 52, 130, 707–9
hydrogen surplus diagram, 708
hydrogen surplus diagram, 52
hydropower, 228
HyNDT, 711

imported energy, 810
indirect heat recovery systems, 595–600
heat recovery loop costing, 599–600
indirect Heat Integration system with storage, 596
operational considerations, 600
selection of intermediate fluid and heat storage tanks, 598–9
sizing heat exchangers, 599
targeting and design methods, 596–8
industrial and hazardous waste (IHW), 803–4
industrial and hazardous waste incinerators, 803–4
rotary kiln, 803
industrial waste heat
uses, 951–6
heat supply with and without integration of waste heat, 954
Site Source and Sink Composite Curve, 953
inlet-outlet pair
stream conversion, 531–2
schematic diagram, 532
inlet segment, 407
inoperability
energy planning, 517–19
EPCC solution, 518
optimal energy allocation, 519
source and sink data, 518
integrated design, 384
integrated energy efficiency, 754
integrated forest biorefinery, 794
integrated Grand Composite Curve, 170
integration architecture, 233–5
LIES, 235
typical industrial Total Site, 234
interaction analysis, 781
intermediate fluid tanks, 598–9
internal fins, 986–8
laminar flow, 986–7
turbulent flow, 987–8
internal water sources, 409

© Woodhead Publishing Limited, 2013

International Process Integration Jubilee Conference, 1100
inventory turnover, 573–4
isolated energy systems
  applications of Pinch Analysis, 1038–54
  descriptions and models, 1040–3
    Energy Supply Composite and Energy Demand Composite Curves, 1042
    schematic diagram, 1040
    schematic diagram of system with multiple sources, 1041
  design space, 1046–8
    system optimisation, 1047–8
  Grand Composite Curve and storage sizing, 1043–6
    variation of stored energy level, 1044
  illustrative applications, 1048–53
    photovoltaic-battery system, 1048–9
    solar thermal system, 1052–3
    wind-battery system, 1049–52
isothermal utilities, 30
iteration, 978
  algorithm for optimisation, 1005–8
    schematic diagram for estimating energy saving, 1009
    schematic diagram of procedure, 1007, 1008

knowledge-based method, 80
Kraft pulp
  mill, 788–9
    bridge structures, 791
    Grid Diagram, 789
    network table D1 with exchange capacities in kW of useful matches, 790
  process energy demands and sources, 767–73
    energy demands in Kraft pulp mills, 772
    heat and power balance, 770–3
    heat and power demands, 767–70
    process description, 767
    schematic diagram, 768

Land Footprint (LFP), 44
launter tun, 835
lautering, 822
lime kiln, 770
Limiting Composite Curve (LCC), 37, 361, 362–3, 404, 405, 411, 415–16, 418, 537, 564–5
  schematic diagram, 363
Limiting Inlet Concentration, 53
Limiting Inlet Profile, 408–9
Limiting Outlet Concentration, 53
Limiting Outlet Profile, 408–9
Limiting Water Flowrate, 53
Limiting Water Profile, 384, 385
Linear Programming (LP), 709–10
LINGO, 1089
load networks, 525
Locally Integrated Energy Sector (LIES), 53, 234, 242, 958
  Solar Thermal Energy Integration, 250–6
    configuration, 250
    heating and cooling demands for process A, 251
    heating and cooling demands for process B, 251
    heating and cooling demands for process C, 251
    heating and cooling demands for process D, 252
    site utility specifications, 252
    Time Slices, 252
    Total Site Heat Cascade for initial case, 255
    Total Site Heat Cascade for modified case, 256
    Total Site targets for TS 1, 253
    Total Site targets for TS 2, 253
    Total Site targets for TS 3, 254
Logarithmic Mean Temperature Difference (LMTD), 53–4, 976–8
  initial, 1000
  temperature differences at heat exchanger ends, 54
loops, 54–5
  schematic diagram, 55
low-pressure turbine expansion, 810–11
low-temperature gas separation processes design, 662–7

© Woodhead Publishing Limited, 2013

designs for the ethylene case study, 666
optimisation results for the ethylene case study, 665
problem data for a natural gas stream, 663
process description, 662–3
project objectives, 663-4
results, 665–7
specification of the available hot and cold utilities, 663
synthesis and optimisation, 664
synthesis and optimisation procedure, 664–5

MAK tank, 835
malting, 822
marginal steam price, 55
Mass and Water Integration software tools, 1086–96
mass exchange cascade diagram, 56
Mass Exchange Network (MEN), 56, 426–9, 541–8, 1089
data for COG sweetening problem, 547
GCC for COG sweetening, 548
Mass Exchange Pinch Diagram, 428
MEN Synthesis problem, 427
supertargeting, 429
transformation into equivalent HEN problem, 545–6
UTA for COG sweetening, 547
Mass Exchange Pinch Diagram, 56
mass exchanger, 56
Mass Exchanger Network Synthesis (MENS), 727–34
concentration-pickup, 728
DFP, 730
retrofit of existing systems, 731–4
impact diagram, 733
retrofit design for phenol problem, 733
retrofit path, 732
Savings–Investment Diagram, 732
supertargeting, 729
y–x Composite Curves, 729
*y–y** Composite Curve Plot, 729
mass flowrate, 56
Mass Integration, 29, 423, 872–3
mass load deficit case, 372
Mass Pinch, 10
mass separating agent (MSA), 56, 355, 426–8, 1089
mass transfer, 427
Mass Transfer Composite Curve, 739–40
cross flow system, 739
stages targeting for co-current systems, 740
mass-transfer-based operations, 358–9
MTB water-using operations, 359
transfer of species from a rich to lean stream, 359
massecuites, 905
MAT tank, 835
material cascade analysis, 451
material conservation networks (MCN)
direct recycle and Material Recycle Pinch diagram, 431–3
food-processing plant, 432
proposed recycle on Pinch diagram, 433
targets for minimum fresh usage, maximum direct recycle and minimum waste discharge, 431
Mass Exchange Networks, 426–9
overall targeting, 424–6
hierarchy of Mass Integration strategies, 426
material balance for the targeted species before Mass Integration, 424
procedure for identifying minimum fresh usage, 425
Process Integration, 422–37
property-based Material Recycle Pinch diagram, 433–7
Water-Pinch Analysis, 429–30
Material Recovery Pinch Diagram (MRPD), 510
Material Recycle Pinch diagram, 431–3
material regeneration, 444
mathematical model, 325–35
constraints, 328–33
solution algorithm for reformulation-linearisation technique, 333
heat loss considerations, 333–5
insulated heat storage vessel, 334
superstructure, 325

© Woodhead Publishing Limited, 2013

mathematical optimisation method, 999–1008
iteration algorithm for optimisation, 1005–8
model with heat transfer enhancement, 999–1005
energy balance differences, 1003
energy saving, 1004
heat transfer differences, 1002–3
initial LMTD, 1000
intensified heat transfer, 1000–1
objective function, 1005
stream temperature constraints, 1002
variable differences, 1003–4
mathematical optimisation technique, 1091
mathematical programming methods
design and retrofit, 709–11
MATRIX technique, 1068–9
maturation, 823, 836
maximal heat recovery, 49
Maximum Energy Recovery (MER), 32, 57, 133, 170, 270
developing initial design, 154–7
network, 156
maximum flow, 849
maximum heat exchanger (MHX), 312
maximum heat recovery, 837–9
Grand Composite Curve, 838
Hot and Cold Composite Curves, 838
minimum heating and cooling requirement, 837
Maximum Resource Recovery (MRR), 11
mechanical power, 66
Mechanical Vapour Recompression (MVR), 846, 869
heat pumps, 192–3
Heat Integration of compression heat pumps, 193
operating conditions, 847
scheme for vapour recovery, 847
mechanical work, 57
milk-powder plant, 876–9
Grid Diagram of heat exchanger network, 878
schematic diagram, 877
milling, 822
MIND (Method for analysis of industrial energy systems), 955–6
minimum allowed stack temperature, 57
minimum allowed temperature difference, 41
minimum energy consumption, 57–8, 903
sugar factory data for energy studies, 903
minimum external cooling, 57–8, 139–43, 149
minimum external heating, 57–8, 139–43, 149
minimum number of shells, 58
minimum number of units, 58
minimum temperature approach, 918
minimum utility targets, 361–8
Mixed Integer Linear Programming (MILP), 300, 312–13, 333, 476–8, 507, 597, 951, 953, 955–6
model, 999
objective function, 1005
Mixed Integer Non-Linear Programming (MINLP), 81, 86, 95, 302, 313, 331, 333, 476–8, 710
mixing, 823
modified linear quadratic regulator, 110
modules, 31
mono-objective GA, 103
MPS Gen, 759–60
multi-objective evolutionary strategy, 104
multi-objective GA, 103
multi-plant site, 601–7
comparison of time-averaged and design point heat flow rates, 602
Hot and Cold CC for two HSTs, 603
Hot CC and Cold CC with cross-plant heat recovery, 605
maximum and minimum hot and cold HST temperatures, 604
schematic illustration, 601
sink and source data for the HRL system, 602
two-tank HRL system for production state B, 607
two-tank HRL system with H2 stream removed, 606
Multi-Stream Heat Exchanger (MSHE), 58, 645–51

© Woodhead Publishing Limited, 2013

optimum design in petrochemical industries, 645–52
calculation procedure of fl ow length, 649
case study Composite Curve, 651
design approach, 649–50
Hot and Cold Composite Curve representation, 648
MSHE dimension, 652
number of sections corresponding to proposed design method, 651
pressure drop between conventional *vs.* optimum design approach, 652
process description, 645–8
process stream data, 649
project objectives, 649
results, 650–2
stream flow through the MSHE, 648
total area and TAC from optimum design *vs.* conventional method, 652
multiple attribute decision-making (MADM), 507
multiple feeds, 409–11
targeting for water-using process, 410
multiple Pinches, 58
multiple utilities, 58
multiple utility targeting, 58
multipurpose batch facility, 335–9
Heat Integration data, 337
heat losses, 338
heating/cooling requirements, 337
optimal schedule with heat losses, 338
results for literature sample, 339
scheduling data, 336, 337
SSN, 336
state task network, 335
variation in heat storage vessel temperature, 338
municipal solid waste incineration plants, 802–3
municipal solid waste (MSW), 800, 802–3

Navier–Stokes equations, 1051
Nearest Neighbour Algorithm (NNA), 451, 513
Network Allocation Diagram (NAD), 373
network design, 32, 133, 153–9
loops and paths, 161–5
alternative network, 164, 165
evolved networks, 162
three-way trade-off, 160–1
network diagnosis, 87
network evolution, 59, 87
Network Pinch, 54, 59, 294, 636, 890
network retrofit, 87
nitrogen network, 553–5
data for magnetic tape plant, 554
LCC for magnetic tape plant, 555
UTA for magnetic tape plant, 554
non-continuous operation, 866–7
non-dominated sorting genetic algorithm, 103
non-isothermal heat sources, 242–3
utility cascading with storage, 243
non-isothermal mixing, 59, 831–2, 1107
heat-transfer requirement and heat recovery, 831
non-isothermal utilities, 30
non-linear programming (NLP), 710
non-mass-transfer-based operations, 359–61
common types of NMTB water-using operations, 360
NMTB water-using operations, 360
number of streams, 59–60
Nusselt number, 969, 983, 984, 987

objective functions, 105–6
oil refineries
Energy and Water Integration applications, 633–701
effluent treatment and regeneration, 687–99
Heat and Power Integration, 634–67
water and wastewater minimisation, 667–86
oil refinery hydrogen network
future trends of hydrogen management, 718–22
interactions between hydrogen networks and energy systems, 720–2

© Woodhead Publishing Limited, 2013

oil refinery hydrogen network (*cont.*)
interactions between hydrogen recovery and light-ends recovery, 718, 720
saving and effective hydrogen utilisation, 722
industrial case study, 711–18
hydrogen surplus diagram, 713
operational optimisation, 712–15
revamping optimisation, 715–18
Process Integration, 705–23
hydrogen consumer with source and sink locations, 706
schematic diagram, 706
technology review, 706–11
mathematical programming methods for design and retrofit, 709–11
software development, 711
targeting for minimum hydrogen utility, 707–9
Onion Diagram, 60, 443–6
conventional Onion Diagram, 444
extended Onion Diagram, 445
overall framework of a TMN, 446
schemes for material recovery, 445
operating cost, 60, 574
operating unit, 30
operational optimisation, 712–15
comparison between base case and optimised case, 715
hydrogen network, 712, 714
reactor inlet conditions for major hydrogen consumers, 715
Optimal Audit, 1067
Optimal Heat, 1068–70
auto and manual HEN design, 1069
Balanced Grand Composite Curve, 1069
EBD for exergetic efficiency analysis, 1070
Match-Matrix for HEN retrofit screening, 1070
Optimal-Water, 1090–1
Source and Demand Heat Composite Curves, 1092
Water Cascade Table (WCT), 1090
water network diagram, 1091
organic distillation plant, 541–8
coke oven gas (COG) sweetening, 546–8
data for organics distillation problem, 542
GCC for organics distillation, 544
transformation of MEN problem into equivalent HEN problem, 545–6
UTA for organics distillation, 543
organic Rankine cycle CHP, 188–90
Heat Integration of an ORC for waste heat electricity production, 190
outlet segment, 407
oxygen network, 555–6
data, 556
Unified Targeting Algorithm (UTA), 556
Oxygen Pinch Analysis, 10, 29, 130

paper industry
energy efficiency in existing mills, 777–83
evolution of paper mills, 789, 791–4
heat exchanger and water networks relations, 773–6
methodological developments for Heat Integration in existing mills, 783–9
Process Integration applications, 765–97
steam and power demands for paper processes, 767
paper mills
evolution, 789, 791–4
bioprocesses, 793–4
increasing Heat Integration, 792–3
process improvements, 791–2
particle swarm, 103–4
particle swarm optimisation (PSO), 654
pasteurisation, 823
paths, 54–5
schematic diagram, 55
payback time, 60
Peng–Robinson equation, 665
performance targets, 133, 138–46
stream data, 139
supply and target temperature of process streams, 138
petrochemical plants

© Woodhead Publishing Limited, 2013

Energy and Water Integration applications, 633–701
effluent treatment and regeneration, 687–99
Heat and Power Integration, 634–67
water and wastewater minimisation, 667–86
retrofit Mass Integration of acid gas removal systems, 725–51
hybrid approach, 741–4
Mass Exchanger Network Synthesis (MENS), 727–34
Pinch approach, 736–40
solution equilibria, 744–6
Venturi scrubber and ethanolamine absorber system, 734–6
photovoltaic-battery system, 1048–9
typical sizing curve and design space, 1050
Pinch Analysis, 641, 736–40, 781–2, 939, 944, 956, 1068, 1072–3, 1091, 1102, 1103
applications in isolated energy systems design, 1038–54
descriptions and models, 1040–3
design space, 1046–8
Grand Composite Curve and storage sizing, 1043–6
illustrative applications, 1048–53
diverse quality measure for sustainable energy planning, 505–19
energy planning based on Agricultural-Land Footprint, 513–15
energy planning based on emergy, 515–17
energy planning based on inoperability, 517–19
energy planning based on Water Footprint, 515
ethanolamine absorber system, 740
generalised problem statement, 508–10
motivating sample, 509–10
source and sink data for motivating sample, 509
graphical targeting procedure, 510–13
EPCC showing initial infeasible solution for motivating sample, 512
EPCC showing optimal solution for motivating sample, 512
optimal energy allocation for motivating sample, 513
quality loads of sources in motivating sample, 510
Source Composite Curve in motivating sample, 511
Pinch violations in existing Kraft pulp mills, 782
Process-based Graphical Approach (PGA), 411–18
supply chain, 577–8
aggregate planning in supply chain, 577
concept, 579
demand and production composite curves, 578
targeting a single water-using process, 405–11
multiple feeds, 409–11
water gain, 407–9
water loss, 406–7
Venturi scrubber system, 737–40
water networks synthesis with water loss and gain, 401–19
Pinch Analysis derived Energy Integration, 99
Pinch Analysis derived Material Integration, 99
Pinch decomposition, 131
Pinch Design Algorithm, 32
Pinch Design Method (PDM), 131–2, 153–4, 279–81
Pinch exchangers, 153–4, 163
Pinch match, 59, 61
Pinch Point, 60–1, 179, 511–13, 849, 1045
Pinch principles, 918–20
design data of exchanger E-34, 918
process data for production rate of 1000t/d, 919
Pinch spreadsheet, 1088
Pinch technology, 90
Pinch Temperature, 60–1
pipe-work, 1094

© Woodhead Publishing Limited, 2013

plant life time, 61
Plus/Minus Principle, 9, 61–2, 131, 147–50
  Heat Cascade, 149
positive energy building (PEB), 941
post-benchmarking analysis, 781
power, 57
power boiler, 772
power curve model, 1050
Power Integration, 634–67
power station, 885
Prandtl number, 989, 992
pressure drop, 62, 967
  shell-side, 973–6
  tube-side, 970–1
Primary Energy Savings (PES), 805
primary resource, 30
probabilistic approach, 1049
Problem Table Algorithm (PTA), 8, 62–3, 524, 536
  vs. Unified Targeting Algorithm (UTA), 540–1
    calculation of net flow, 541
process, 1079
process analysis, 63
Process-based Graphical Approach (PGA), 411–18
  preliminary analysis, 411–12
    limiting data, 412
  targeting and design, 412–18
    optimal water network with reuse/recycling, 417
    synthesis of water network with reuse/recycling, 418
    targeting for water-using process and water source allocation, 413
    Water Supply Lines, 416
process control, 109–11
process design, 64
  advantages, challenges and drivers, 79–113
  grass root *vs.* retrofit design, 84–90
  overview, 79–84
  Process Integration, 443–57
    revised Onion Diagram, 443–6
    Total Material Network (TMN) models, 446–50
    water minimisation in water fabrication plant, 451–7
process energy targets, 1076
process flowsheet, 30, 63, 823–36
  cold section
    schematic diagram, 826
  energy conversion and distribution system, 828–30
  flow inventory, 828
    brewing process, 829
    inlet and outlet flows, 829
  hot section, 825–6
    schematic diagram, 825
  hot utility system, 827
  process heat-transfer requirements, 830–3
    exergy demand of 100 kW heating, 833
    process unit, 832
  process requirement, 834–6
    heat transfer requirements of bottle-cleaning section, 836
    streams in brewing process, 835
  refrigeration system, 827
  schematic diagram, 824
  stream analysis, 833–4
  time average approach, 827–8
  washing, 827
    cleaning in place section, 827
process heating subsystem, 885–6, 888
Process Integration, 3–20, 90–7, 109–11
  advantages, challenges and drivers, 79–113
  application in brewing industry, 820–63
    batch processes timeline (cold and cleaning part), 862
    batch processes timeline (hot part), 862
    brewery process block flow diagram, 822
    brewing operation data, 862
    calculating maximum heat recovery, 837–9
    $\Delta T_{min}/2$ for streams, 862
    energy conversion system, 839–58
    industrial production system, 821
    list of streams for Heat Exchanger Network Design, 859–60

© Woodhead Publishing Limited, 2013

operating condition boiler, 861
process flowsheet analysis, 823–36
specific heat capacity of material streams, 861
application to thermal processing of waste, 799–819
Heat Integration application, 811–16
MSW incinerator, 800
scope, 802
simplified process flowsheet, 801
TERMIZO plant energy efficiency analysis, 804–11
waste thermal processing plants types, 802–4
applications in cheese and dairy production, 864–79
case studies, 873–9
future trends, 879
methodologies, 866–73
applications in pulp and paper industry, 765–97
energy demands and sources in Kraft pulping process, 767–73
energy efficiency in existing mills, 777–83
evolution of pulp and paper mills, 789, 791–4, 796
heat exchanger and water networks relations, 773–6
methodological developments for Heat Integration in existing mills, 783–9
steam and power demands for paper processes, 767
steam and power demands for pulp processes, 766
world pulp production, 766
approach for supply chain development, 571–92, 576–84
beet sugar plants, 881–910
energy and water use, 898–909
future trends, 909–11
opportunities to improve energy and water use, 885–7
reduction of energy consumption, 887–93
reduction of water consumption, 893–8
sugar production from sugar beets, 884–5
centre of expertise, 12–20
academia and education sector, 16
centres of research, application and expertise, 17–20
contractors and consultancies, 16
courses and projects, 13–14
development and application, 15
PIRC membership benefits, 14
Process Integration Research Consortium members, 15
research consortium, 13
cleaner process design, 443–57
Combined Heat and Power (CHP), 485–8
Combined Energy and Water Integration, 461–80
overview, 461–3
sequential, simultaneous, mathematical programming, 476–8
state of the art methodology, 468–76
water-energy specifics and challenges, 463–6
water path concept, 466–8
Combined Heat and Power (CHP) and heat pumps, 168–98
advanced energy conversion cycles, 176–81
heat engines, 181–90
utility loads and temperature levels, 169–76
controllability, 106–11
efficient use of energy in a urea fertiliser plant, 914–37
process description, 916–24
reduction of energy consumption, 924–32
energy saving in buildings and building complexes, 938–61
buildings as consumers and producers of energy, 939–42
commercial, public buildings and building complexes, 942–7
District Energy systems and Total Site Analysis, 947–51

© Woodhead Publishing Limited, 2013

Process Integration (*cont.*)
renewable energy for buildings, 956–61
use of industrial waste heat, 951–6
future trends, 592
grass root *vs.* retrofit design, 84–90
Heat Integration for trigeneration system, 488–500
gas turbine-vapour compression systems, 489–94
steam turbine-absorption systems, 494–50
heat recovery loops application to semicontinuous processes, 594–626
application, 600–12
complex sample, 613–17
future trends, 626
indirect heat recovery systems, 595–600
semi-continuous multi-plant dairy factory, 618, 620–6
history, 7–12
development, 10–12
importance of problem formulation and data extraction, 1099–112
applications, 1101–3
cited publications, 1101
data extraction, 1104, 1106–9
integration of renewables, 1109–10
methods of obtaining HI solutions, 1103–4
overview, 1099–101
results interpretation, 1110
material conservation network, 422–37
direct recycle and Material Recycle Pinch diagram, 431–3
Mass Exchange Networks, 426–9
overall targeting, 424–6
property-based Material Recycle Pinch diagram, 433–7
Water-Pinch Analysis, 429–30
oil refinery hydrogen network, 705–23
future trends of hydrogen management, 718–22
industrial case study, 711–18
technology review, 706–11
optimisation, 102–6
overview, 3–7, 79–84
development of the world consumption of electricity, 5
development of the world consumption of natural gas, 6
development of the world consumption of oil, 5
global energy demand and consumption, 4–6
process intensification, 97
Regional Energy Clustering (REC), 584–6
Resource Management Curve (RMC), 586–91
revised Onion Diagram, 443–6
supply chain characteristics and performance measurement, 572–6
effects of PI on supply chains, 575–6
measuring supply chain performance, 572–4
quality *vs.* quantity of four PI applications, 576
supply chain design, 572
supply chain process, 573
supply chain development, 576–84
Pinch Analysis, 577–8
Regional Energy Surplus–Deficit Curves (RESDC) for biomass network, 578–81
Resource Management Curve (RMC), 581–4
techniques, 98–102
combined energy and material, 102
mathematical modelling of Energy Integration, 100
mathematical modelling of Material Integration, 100–1
Pinch Analysis derived Energy Integration, 99
Pinch Analysis derived Material Integration, 99
property based, 98–9
techniques for cogeneration and trigeneration systems, 484–500
terminology, 28–78
context, 29–30

© Woodhead Publishing Limited, 2013

drawing utility exchangers, 74
fundamental terms, 30–74
symbols for heaters and coolers, 74
Total Material Network (TMN) models, 446–50
under disturbances, 112–13
Unified Targeting Algorithm for diverse problems, 524–65
approach to diverse resource optimisation problems, 525–7
basis for unification, 527–32
hydrogen and gas networks, 550–8
organic distillation plant, 541–8
overview, 524–5
property-based material reuse networks, 558–61
specialty chemical plant, 548–50
targeting alternative approaches, 561–4
water minimisation in water fabrication plant, 451–7
Process Integration Research Consortium (PIRC), 12–14
process intensification, 63, 97
process modification, 32, 63, 133, 146–53, 367
Grand Composite Curve and correct integration, 150–3
Plus/Minus Principle and appropriate placement, 147–50
process optimisation, 102–6
advantages, challenges and drivers, 79–113
grass root *vs.* retrofit design, 84–90
objective functions shape topology, 105–6
overview, 79–84
process Pinch Point, 174
process retrofit, 64
process simulation, 91, 134
process stream, 31, 32, 63–4, 134, 235–6, 889–90
process stream branch, 64
process synthesis, 64
Process System Engineering (PSE), 1099–100
process temperature, 70–1
process unit analysis, 831
process utilities, 235–6
process water network, 774–6
flow rates of process water, 776
processing plant, 30
prohibited matches, 64
property-based Material Recycle Pinch diagram, 433–7
degreasing case study, 436
degreasing plant, 435
determining fresh usage target via ternary property-cluster diagram for the degreaser, 437
Property-Based Material-Reuse Pinch diagram, 434
property-based material reuse, 64–5
property-based material reuse networks, 558–61, 564
papermaking process, 559–61
data, 559
Limiting Composite Curve (LCC), 561
Unified Targeting Algorithm (UTA), 560
Property Cascade A (PCA), 11
Property Integration, 423
pulp bleaching, 768
pulp cooking, 768
pulp drying, 769
machine, 778
pulp industry
energy demands and sources in Kraft pulping process, 767–73
energy efficiency in existing mills, 777–83
evolution of pulp mills, 789, 791–4
heat exchanger and water networks relations, 773–6
methodological developments for Heat Integration in existing mills, 783–9
Process Integration applications, 765–97
steam and power demands for pulp processes, 766
world pulp production, 766
pulp mills
evolution, 789, 791–4
bioprocesses, 793–4
increasing Heat Integration, 792–3
process improvements, 791–2

© Woodhead Publishing Limited, 2013

pulp screening, 768
pulp washing, 768

RCNet, 1091–2
R-curve analysis, 753–4
  analysis for a heavy chemical complex, 755
  parameters for a heavy chemical complex, 756
  results, 754–6
recausticising, 778–9
recovery boiler, 769–70, 778
refinery hydrogen management, 705
refinery hydrogen network, 550–3
  data, 551
  Limiting Composite Curve (LCC), 553
  Unified Targeting Algorithm (UTA), 552
refrigerant, 497
refrigeration, 65
refrigeration cycle, 842
  ammonia cycle for producing the glycol-water cold loop, 844
  integration, 845–6
    operating conditions, 846
refrigeration system, 827, 1079–81
  optimisation, 1081
  simulation, 1081
regeneration reuse/recycling, 354
Regional Energy Cascade Analysis, 958
Regional Energy Clustering (REC), 12, 584–6
  cluster properties, 586
  optimal biomass exchange flows, 585
  optimised bioenergy exchange flows, 585
  regional data for demonstration case study, 585
  RESDC for the case study, 587
regional energy supply, 30
Regional Energy Surplus–Deficit Curves (RESDC)
  biomass network, 578–81
    schematic diagram, 581
Regional Resource Management Composite Curve, 65
Reid Vapour Pressure (RVP), 435
Remaining Problem Analysis (RPA), 276–7
renewable energy
  buildings, 956–61
  cascade, 65
renewable energy resources, 1039
  integration, 1109–10
resource, 29
resource conservation, 29, 31
Resource Conservation Cascade Diagram (RCCD), 450
resource deficit, 65
Resource Management Curve (RMC), 581–4, 586–91
  construction, 583
  data for construction, 587
  energy and land use management, 588
  modification if biomass production in cluster 2 is increase, 591
  modification if certain amount of energy is imported to fill demand of cluster 2, 590
  modification if energy demand in cluster 2 is reduced, 591
  modification if the surplus if a certain area in Zone 1 is used for other purpose, 589
  modification if the surplus if a certain area in Zone 4 is used for other purpose, 589
  modification if the surplus in Cluster 1 is exported to energy market, 588
  modification if the surplus in Cluster 1 is transferred to cluster 2, 590
resource recovery, 31
resource recovery network, 31
resource sink, 66
resource surplus, 66
resource utilisation profiles, 473
response surface methodology, 85
retrofit
  ammonia plant for improving energy efficiency, 652–5
    configuration of retrofitted HEN, 656
    design approach, 654–5
    existing configuration of HEN, 654
    HEN specifications, 655
    process description, 652–4

© Woodhead Publishing Limited, 2013

process stream data, 653
project objectives, 653–4
results, 655
utility consumption *vs.* corresponding cost, 655
crude preheat train in an oil refinery, 634–40
computational procedure for finding network Pinch, 637
design approach, 636–8
direction of modified network Pinch strategy, 638
flow sheet of a crude oil preheat train, 635
heat exchanger data, 639
HEN Grid Diagram, 636
modification options of crude oil preheat unit, 640
optimisation procedure for HEN, 638
payback plot of the crude preheat train, 640
process description, 634–5
process stream data, 635
project objectives, 635–6
results, 639–40
heat exchanger network in aromatics plant, 641–6
cost evaluation of retrofit scenarios, 647
design approach, 643–4
DFP of existing HEN, 645
heat total distribution with existing HEN, 646
HEN Grid Diagram, 643
maximised energy-saving retrofit scenarios, 647
payback Time of proposed retrofit scenarios, 647
process description, 641
project objectives, 641, 643
relaxation of maximum energy saving, 647
results, 644–5
schematic of aromatics plant, 642
temperature profiles of counter-current heat exchanger, 644
retrofit analysis, 281–95
retrofit design, 84–90, 132, 138
heat recovery systems analysis and design, 262–304
optimisation for heat exchanger network synthesis, 295–303
overview, 262–4
existing facility improvement, 263–4
retrofit analysis, 281–95
actions, 283–4
area-energy diagrams for heat recovery problems, 281
case summary, 294–5
challenges, 282–3
cheaper design, 292
existing HEN in Grid diagram, 289
expensive design, 291
methodology, 288–94
shifting of operating conditions, 291
targeting level of heat recovery, 284–8
Retrofit Design Approach (RDA), 85
retrofit Mass Integration
acid gas removal systems in petrochemical plants, 725–51
hybrid approach, 741–4
Mass Exchanger Network Synthesis (MENS), 727–34
Pinch approach, 736–40
solution equilibria, 744–6
Venturi scrubber and ethanolamine absorber system, 734–6
retrofit strategy, 884, 888
block diagrams of procedure and targeting step, 889
energy targeting and, 888–90
water targeting, 895–6
return of assets (ROA), 574
revamp design, 84
revamping optimisation, 715–18
base case-hydrogen surplus diagram, 718
base case-revamping design, 717
hydrogen surplus diagram, 720
optimised hydrogen network, 719
reactor inlet conditions for major hydrogen consumers, 721
results comparison, 721
Reynolds number, 649, 974, 986, 989

© Woodhead Publishing Limited, 2013

rigorous energy targeting, 296–9
  temperature intervals in extended Heat Cascade, 299
  temperature intervals in Heat Cascade, 296
rigorous heat transfer area targeting, 301
rigorous unit targeting, 299–300
robust control, 106–7
R-ratio, 754

Scandinavian Kraft mill, 770
  extracted data, 771
seasonal effects, 782
semi-continuous multi-plant dairy factory, 618, 620–6
  dairy factory with the six separate plants, 620
  effect of T_{hot} on average heat recovery, 624
  heat recovery opportunities, 623
  HRL and HEN design, 625
  impact of storage volume on average heat recovery, 624
  instantaneous total available heat flow rate of heat sources and sinks, 622
  network design options, 626
  representative operating schedule, 621
  stream data for potential streams on the HRL, 622
semicontinuous operation, 866–7
semicontinuous processes, 66
  heat recovery loops application for Process Integration, 594–626
    application, 600–12
    complex sample, 613–17
    future trends, 626
    indirect heat recovery systems, 595–600
    semi-continuous multi-plant dairy factory, 618, 620–6
sensitivity analysis, 66
sensitivity tables
  network response, 996–9
    maximum heat recovery in heat exchanger, 998
    sensitivity graphs, 997
Serth's model, 991
sewer cost, 1094
shaft work, 66
shell-and-tube heat exchangers, 966–79
  comparison of different heat exchanger models, 978–9
    modelling methods, 979
    modelling results, 980
    stream data and geometry, 980, 993
  modelling, 967–78
    geometry specifics, 968
shell-side enchancement techniques, 988–93
  schematic diagram, 989
Shifted Composite Curve, 66, 511
  schematic diagram, 67
shifted temperature, 70–1
short-term variations, 783
shuffled frog leaping algorithm, 104
simplified Delaware method, 973
simulated annealing, 103, 636
simulation, 1081
Sink Composite Curve, 67, 511
sinks, 242–3, 431
  utility cascading with storage, 243
site, 1079
Site Composite Curve, 67, 243
SITE-int, 1070–2
  path optimisation diagram for palm oil refinery retrofit project, 1071
Site Profiles, 753
Site Sink Composite Curves, 243
Site Sink Profile, 67
Site Source Profile, 67
  TSP, 68
Site Utility Composite Curves, 67
Site Utility Grand Composite curve (SUGCC), 218–22
  699.5 kW heat recovery and 1600 kW boiler steam supply, 221
  heat recovery and maximum boiler steam supply, 221
  maximum heat recovery, 219
soft data, 41
software development, 711
solar emjoule, 506
solar radiation, 228
solar thermal system, 1052–3
  design space, 1053

© Woodhead Publishing Limited, 2013

SOLCHIPS, 1052
solution equilibria, 744–6
  equilibrium relationships for MEA and DEA solutions, 745–6
    equilibrium functions for H_2S for each of the streams, 746
  fitting actual data for scrubber system, 744
Source Composite Curve, 68, 510, 511
Source/Demand Water Allocation Curves, 469–70
source elimination, 353
Source-Sink Allocation Composite Curves, 370–3
  flowrate and mass load deficit case, 373
  NAD, 374
  schematic diagram, 372
Source/Sink Composite Curves, 362, 366–8
  schematic diagram, 366
source-sink mapping diagram, 370
sources, 431
specialty chemical plant, 548–50
  data for water network, 549
  LCC for water network, 549
  UTA for water network, 549
specific energy consumption (SEC), 865
specific heat capacity, 68, 135, 492
splitting streams, 277–9
  heat exchange between cold and hot streams, 279
SPRINT, 1064, 1073–4
  software interface, 1074
stand-alone design, 383–4
STAR, 1075–8
  graphics-balanced Grand Composite Curves, 1077
  Graphics-Composite Curves, 1076
  software interface, 1075
  Total Site Profiles, 1078
starting time, 68
state sequence network (SSN), 313, 325
steam boiler, 842
  steam distribution system, 843
steam contributions, 272–3
steam cycle, 901
steam network CHP, 187–8
  GT introduction with steam distribution systems, 189
steam pressure drop, 62
steam turbine, 68–9, 916, 1077
  electricity production, 772–3
steam turbine-absorption systems, 494–50
  Grand Composite Curve, 498
  operating data for three commercial steam turbines, 499
  performance data of absorption system, 499
  trigeneration system, 495
  turbine performance parameters at part load, 500
  turbine performance parameters for 100% load, 499
steam turbine CHP, 181–3
  back pressure levels, 183
  heat recovery steam cycle with extraction and condensation, 184
  principles, 182
steam utility systems, 171–3
  graphical assessment of MP and LP steam loads, 173
  industrial steam network with a MP and LP headers, 172
steel plant
  case study, 757–61
    energy-saving projects, 761
    result of TSP analysis, 759–61
    study basis, 757–9
    utility conditions, 759
storage scope, 246
stream, 922, 1104, 1106
  flowsheet fragment, 1106
  separation, 1104
stream splitting, 68, 157–9, 161
  Below and Above Pinch, 158
superstructure, 69
SuperTarget, 1078–9, 1104
supertargeting, 69
supplementary fuel, 810
supply chain
  Process Integration, 571–92
    characteristics and performance measurement, 572–6
    development, 576–84
    future trends, 592

© Woodhead Publishing Limited, 2013

supply chain (*cont.*)
Regional Energy Clustering (REC), 584–6
Resource Management Curve (RMC), 586–91
supply temperature, 69
Surplus Composite Curve, 69
suspended matter (SM), 895
sustainable energy planning
Pinch Analysis using diverse quality measure, 505–19
energy planning based on Agricultural-Land Footprint, 513–15
energy planning based on emergy, 515–17
energy planning based on inoperability, 517–19
energy planning based on Water Footprint, 515
generalised problem statement, 508–10
graphical targeting procedure, 510–13
quality indices for energy streams, 508
Swirl number, 982
synthetic natural gas (SNG), 94
system optimisation, 1047–8
schematic diagram, 1048
systematic design, 80–1
Systematic Hierarchical Approach For Process Screening (SHARPS), 368

target energy
retrofit design, 888–90
target temperature, 70, 137
targeting, 32, 69–70
targeting Carbon Footprint reduction, 29
targeting of total sites, 959–61
targeting property-based material reuse, 29
targeting supply chains, 29
targets, 69–70
Temperature-Concentration Diagram, 471
temperature difference, 41
temperature-enthalpy, 8, 70
temperature lift, 70
TERMIZO plant, 804–11
energy utilisation, 804–7
balance data per ton of treated MSW and evaluated criteria, 808
criteria for evaluation of WTE units, 806
energy streams in a MSW incineration plant, 806
heat recovery system, 807–11
modifications on factor Pl_{ef}, 809
model scheme in W2E software, 805
Theoretical Cooling Load Curve (TCLC), 784
Theoretical Heat Load Curve (THLC), 784, 785
thermal energy storage, 232–3
storage types by temperature change, 233
Thermo-Vapour Recompression (TVR), 869
threshold problem, 71
time average approach, 827–8
Time Average Composite Curves, 71, 1110
Time Average Model (TAM), 71, 311–12, 597
Time Slice, 71, 1110
identification, 236–9
acceptance/rejection of the candidate time period boundary, 237
approximation of solar irradiation availability, 237
combination, 239
dependence of number of TSs (NTS), 238
different energy demands, 238
merging TS boundaries, 239
variable energy sources, 236–8
Time Slice Composite Curves, 71
Time Slice Model (TSM), 311, 597
Tinker method, 966, 978
top level analysis, 71, 1076
topology traps, 72
Total Annual Cost (TAC), 72, 270–1, 652
Total Material Network (TMN), 446–50
targeting procedure for a fixed flowrate TMN with inside based approach, 448

© Woodhead Publishing Limited, 2013

targeting procedure for a fixed-load TMN with inside based approach, 447
targeting procedure for a TMN with ATM, 450
targeting procedure for TMN with inside based approach, 449
total revenue, 574
Total Site, 29, 72
data extraction, 203–11
combined heat sink information or Site Sink Profile, 211
combined heat source information or Site Source Profile, 210
Grand Composite Curve for process A, 204
Grand Composite Curve for process A with stream segments, 207
Grand Composite Curve for process B, 205
Grand Composite Curve for process B with stream segments, 209
Grand Composite Curve with HP steam generation, 206
Problem Table for process A, 204
Problem Table for process B, 205
stream segment data extracted from process A, 208
stream segment data extracted from process B, 209
Total Site Profiles, 211
methodology, 201–23
overview, 201–2
integration of process heating and cooling demands, 202
Profiles and Composite Curves, 212–18
Site Utility Grand Composite Curve (SUGCC), 218–22
Total Site Analysis (TSA), 953, 955
and DE systems, 947–51
Total Site Composite Curves, 72, 212–18
LP steam generation, 218
minimum VHP demands from boilers and maximum heat recovery, 217
Source and Sink Profile maximum overlap and minimum VHP demands from boilers, 216
steam and cooling main information, 212
steam used and generated across Total Site, 213
Total Site Heat Cascade, 248–9
overall procedure, 248–9
TSs, 249
Total Site Integration, 9, 29, 93–4, 227
Total Site Pinch, 72
Total Site Process Integration, 939
Total Site Profiles (TSP), 30, 72, 212–18, 240–2
heavy chemical complex, 753
analysis for a heavy chemical complex, 755
results, 754
LP steam generation, 218
mapping of the heat cascading flows on Site Composite Curves, 241
potential steam heat recovery, 214
Source and Sink Profile maximum overlap and minimum VHP demands from boilers, 216
steam and cooling main information, 212
steam boilers providing VHP steam, 215
steam levels, 213
steam used and generated across Total Site, 213
steel plant, 759–61
current case, 760
schematic diagram, 760
targeting case, 760–1
VHP reduction to 1600 kW, 216
Total Sites, 1076–7, 1103
Total Sites approach
chemical industrial complex and steel plant, 752–62
case study of a heavy chemical complex, 753–7
case study of a steel plant, 757–61
trigeneration
Process Integration techniques, 484–500
Combined Heat and Power (CHP), 485–8
Heat Integration for trigeneration system, 488–500
TRNSYS, 1052
trub, 836

© Woodhead Publishing Limited, 2013

true minimum target, 356
tube-side enchancement techniques, 981–8
  schematic diagram, 981
twisted-tape inserts, 981–4
  laminar flow, 981–2
  transition flow, 983–4
  turbulent flow, 983
Two-Dimensional Grid Diagram (TDG), 473–4
tyre-to-fuel process, 374–8
  limiting water data, 376
  process after water recovery, 377
  schematic diagram, 375
  source/link allocation curve and NAD, 376

ultrapure water (UPW), 451
Unified Targeting Algorithm (UTA), 532–41, 563–4, 564–5
  alternative approaches to targeting, 561–4
    allocation network, 562–4
    exchange network, 561–2
  approach to diverse resource optimisation problems, 525–7
    analogues for application to diverse integration problems, 527
  basis for unification, 527–32
    allocation and exchange processes, 529–31
    conceptual representation of diverse network processes, 528
    fixed flow and fixed load processes, 527–9
    stream conversion to equivalent inlet-outlet pair, 531–2
  diverse Process Integration problems, 524–65
  four-steam HEN, 537–40
  Grand Composite Curve (GCC) and Limiting Composite Curve (LCC), 537
  hydrogen and gas networks, 550–8
  important aspect, 535–6
  main steps, 533–5
  organic distillation plant, 541–8
  overview, 524–5
  property-based material reuse networks, 558–61
  specialty chemical plant, 548–50
  vs. PTA and CTA, 540–1
    calculation of net flow, 541
unit operations, 31
urea fertiliser plant
  process description, 916–24
    energy consumption and process data, 918–20
    energy targets for minimum temperature approach for heat transfer, 920, 922–3
    flow sheet of production process, 917
    Heat Recovery Network, 924
  Process Integration for efficient use of energy, 914–37
    block diagram of urea production process, 915
  reduction of energy consumption, 924–32
    cogeneration system, 924, 926–7
    improving energy recovery, 928–32
utility, 32
  extraction, 1108
  generation, 1108
utility cascading, 240–2
  Heat Cascade cell for Total Site, 242
  without storage, 242
utility interval, 960
utility path, 72
Utility Pinch, 60–1, 73
Utility Pinch Point, 172, 267
utility system, 73
  optimisation, 1075–6

vacuum distillation unit (VDU), 542
variable-temperature heat storage system, 612
Venturi scrubber system, 734–5, 737–40, 746–7
  arrangement, 735
  Mass Transfer Composite Curve, 747
  stream flows and compositions, 735
  sulphur recovery system, 734
virtual water, 506
vortex wake models, 1051

© Woodhead Publishing Limited, 2013

waste biomass, 228
Waste Framework Directive 2008/98/EC, 804
waste thermal processing plants, 802–4
waste-to-energy (WTE), 800, 816
waste water-treatment plants (WWTP), 109
wastewater minimisation, 29, 667–86
  cooling water systems design, 675–80
  refinery, 668–75
    construction of Limiting Composite Curve, 671
    cooling system integrated ozone water treatment, 673
    design, 671–3
    Feasible Water Supply Line, 672
    limiting process water data, 670
    limiting profile of a single process, 671
    optimum configuration of water and wastewater system, 675
    performance parameters of base case, 669
    Pinch Point water specification, 674
    process description, 668
    project objectives, 668
    results, 673–5
    system for petroleum refinery, 668
    targeting, 669–71
    targeting result of water and wastewater system, 674
    targeting *vs.* design values of proposed strategy, 674
wastewater network, 86, 101, 103
wastewater treatment, 388
WATER, 1092–4
  graphical interface, 1093
water, 29
Water Cascade Analysis (WCA), 362, 363–6, 1090
  general structure of WCT, 364
  principle of water cascading, 364
water consumption
  reduction, 893–8
    case study, 896–8
    operating parameters of water and wastewater system, 897
    problem statement, 894–5
    results of water minimisation, 898
    scheme of main water and wastewater circuit, 894, 897
    water targeting and retrofit design, 895–6
Water Design, 1095
water dilution, 836
Water-Energy Network (WEN), 464–5
  optimisation, 475
  project implementation road map, 475
Water Footprint (WFP), 43–4
  energy planning, 515
    EPCC solution, 516
    optimal energy allocation, 516
    source and sink data, 515
water gain, 407–9
  graphical representation of water-using process, 408
water gain profile, 408
Water Integration, 95
  applications in oil refineries and petrochemical complexes, 633–701
  effluent treatment and regeneration, 687–99
  Heat and Power Integration, 634–67
    design of multi-stream heat exchangers in petrochemical industries, 645–52
    heat recovery improvement in aniline production unit, 655–62
    low-temperature gas separation processes design, 662–7
    retrofit of ammonia plant for improving energy efficiency, 652–5
    retrofit of crude preheat train in an oil refinery, 634–40
    retrofit of heat exchanger network in aromatics plant, 641–6
  water and wastewater minimisation, 667–86
water loss, 406–7
  graphical representation of water-using process, 407
water main concept, 474

© Woodhead Publishing Limited, 2013

water management
Water Pinch Analysis, 353–78
approaches, 353–5
steps, 357–74
tyre-to-fuel process, 374–8
Water Integration, 355–7
Water Management Hierarchy (WMH), 353–4
water minimisation, 667–86, 872–3, 1093
cooling water systems design, 675–80
future trends, 397–8
Process Integration for water systems, 388–97
distributed effluent treatment systems, 391–2
energy recovery for water networks, 397
retrofit of cooling water networks, 394–5
separate systems for combined water and energy savings, 398
simultaneous water and energy minimisation, 395–7
superstructure approach for the design of water networks, 394
total water systems optimisation, 392–4
Water Pinch Analysis, 389–91
refinery, 668–75
construction of Limiting Composite Curve, 671
cooling system integrated ozone water treatment, 673
design, 671–3
economical evaluation of the solution strategy, 675
Feasible Water Supply Line, 672
limiting process water data, 670
limiting profile of a single process, 671
optimum configuration of water and wastewater system, 675
performance parameters of base case, 669
Pinch Point water specification, 674
process description, 668
project objectives, 668
results, 673–5
system for petroleum refinery, 668
targeting, 669–71
targeting result of water and wastewater system, 674
targeting *vs.* design values of proposed strategy, 674
simultaneous energy in multiple contaminant systems in petrochemical plant, 680–6
combined water and energy balance, 681
cost evaluation of suggested modification scenarios, 685
design, 684
identification of non-isothermal mixing point, 683
modified configuration of water and wastewater network, 686
non-isothermal mixing area and separate systems in Composite Curve, 684
performance parameters of treatment unit, 682
process description, 680–2
project objectives, 682–3
results, 684–6
snapshot of water and wastewater targeting software, 685
targeting, 683–4
water and wastewater system, 681
water system specifications, 682
systematic design methods in process industries, 383–98
water fabrication plant, 451–7
data for wastewater streams, 454
limiting data, 453
material cascade analysis for flowrate targeting of UPW, 453
minimum flowrate targeting for wastewater treatment, 455
network design with NNA for UPW recovery scheme, 454
semi-conductor plant, 451–7
total water network for semi-conductor plant, 455, 456
Water Pinch Analysis, 353–78
approaches, 353–5
steps, 357–74
tyre-to-fuel process, 374–8
Water Integration, 355–7

© Woodhead Publishing Limited, 2013

water use, 386–8
cooling water system, 386
effluent treatment systems, 387–8
energy production systems, 387
water network, 73, 86, 103, 108, 113, 358–61, 548–50
data for specialty chemical plant, 549
heat exchanger relations, 773–6
degradation of energy quality, 773–4
process water network, 774–6
LCC for specialty chemical plant, 549
synthesis with water loss and gain via extended Pinch Analysis, 401–19
Process-based Graphical Approach (PGA), 411–18
targeting a single water-using process, 405–11
UTA for specialty chemical plant, 549
water network design, 95
water path concept, 466–8
water paths/water-saving paths, 467
Water Pinch Analysis, 60–1, 87, 429–30, 907
approaches for water management and minimisation, 353–5
categorisation of water reuse/recycling strategies, 355
WMH, 354
steps, 357–74
analysis of water network, 358–61
data extraction, 361
economic evaluation, 373
minimum utility targets setting, 361–8
water network design/retrofit, 368–73
tyre-to-fuel process, 374–8
water and wastewater minimisation, 389–91
targeting minimum water flowrate, 389, 390
Water Integration, 355–7
applications, 357
Pinch Analysis critical success factor, 356
significance, 356–7
water management and minimisation, 353–78
Water-Pinch diagram, 430
water pocket, 62
Water Pollution Footprint (WPFP), 44
water recycling, 73, 354
water regeneration, 73, 1093–4
water reuse, 74, 468
networks, 1093
water sink, 73
water sources, 73
water supply diagram, 362
Water Supply Line, 403, 414, 416, 418
water targeting
retrofit design, 895–6
water use, 904–9
results of water minimisation, 910
scheme of main water and wastewater circuit, 906
subsystem of water and wastewater system in sugar factory, 905
water-using operation, 74, 384–5, 402, 467, 478
WaterPinch, 1094
WaterTarget, 1094–5
WaterTracker, 1094
W2E software, 808
weeks of supply, 573
Wills-Johnston method, 966, 978
wind, 228
wind-battery system, 1049–52
physical design space, 1052
wood handling, 777
WORK, 1079–81
Ideal Composition Profiles, 1082
refrigeration composition options, 1081
refrigeration cycle report, 1080
work, 57
working capital, 574

Zero Energy Building (ZEB), 941
zone integration, 867–9
zone targeting, 74, 867–9

© Woodhead Publishing Limited, 2013